Association of Structural Engineers of Serbia

15th CONGRESS

ZLATIBOR, SEPTEMBER 6-8 2018

ASES INTERNATIONAL CONGRESS PROCEEDINGS

IN COOPERATION

SUPPORTED BY

Република Србија
Министарство
просвете, науке и
технолошког развоја

SPONSORS

CIP - Каталогизација у публикацији
Библиотека Матице српске, Нови Сад

624+69(082)

ASSOCIATION of Structural Engineers of Serbia. Congress (15 ; 2018 ; Zlatibor)
ASES International congress proceedings [Elektronski izvor] / Association of Structural Engineers of Serbia, 15th Congress, September 6-8th, 2018, Zlatibor ; [editors Đorđe Lađinović, Zlatko Marković, Boško Stevanović]. - Beograd : Društvo građevinskih konstruktera Srbije, 2018 (Novi Sad : Grafički centar - GRID, Fakultet tehničkih nauka Univerziteta). - 1 elektronski optički disk (CD-ROM) : tekst, slika ; 12 cm

Sistemski zahtevi: Nisu navedeni. - Nasl. sa naslovnog ekrana. - Tiraž 250. - Radovi na srp. i engl. jeziku. - Bibliografija.

ISBN 978-86-6022-070-9

a) Грађевинарство - Зборници
COBISS.SR-ID 325104647

Izdavač:	**Društvo građevinskih konstruktera Srbije** Beograd, Bulevar kralja Aleksandra 73/I
Urednici:	prof. dr **Đorđe Lađinović** prof. dr **Zlatko Marković** prof. dr **Boško Stevanović**
Tehnički urednik:	doc. dr **Jelena Dobrić**
Tehnička priprema:	asist. **Nina Gluhović** asist. **Marija Todorović**
Gafički dizajn:	asist. **Tijana Stevanović**
Dizajn korica:	asist. **Tijana Stevanović**
Štampa:	**Grafički centar – GRID** **Fakultet tehničkih nauka Univerziteta u Novom Sadu**
Tiraž:	**250 primeraka**
	Beograd, septembar 2018.

POVODOM TRIDESETOGODIŠNJICE POSTOJANJA
A ZA NAROČITE ZASLUGE I USPEHE POSTIGNUTE
U RAZVIJANJU I UNAPREĐENJU GRAĐEVINSKOG
KONSTRUKTERSTVA I DOPRINOS UZDIZANJU
STRUČNIH KADROVA

ukazom broj 38 od 29. aprila 1983. godine

PREDSEDNIŠTVO SFRJ

ODLIKOVALO JE

SAVEZ DRUŠTAVA GRAĐEVINSKIH
KONSTRUKTERA JUGOSLAVIJE

ORDENOM RADA SA SREBRNIM VENCEM

Organizacioni odbor Kongresa:

Predsedništvo DGKS:

prof. dr Đorđe Lađinović, predsednik,
Aleksandar Bojović, potpredsednik,
prof. dr Zlatko Marković, generalni sekretar,
prof. dr Boško Stevanović, sekretar,
prof. dr Dragoslav Stojić,
prof. dr Mira Petronijević,
prof. dr Snežana Marinković,
v. prof. dr Danijel Kukaras,
doc. dr Branko Milosavljević,
doc. dr Selimir Lelović,
Duško Tomić,
Goran Vukobratović,
Goran Tadić,
Đorđe Pavkov,
Lazar Marković,
Branko Knežević,
Gojko Grbić.

Naučni odbor Kongresa:

prof. dr György Balazs (Mađarska),
prof. dr Radu Banchila (Rumunija),
prof. dr Dubravka Bjegović (Hrvatska),
prof. dr František Wald (Češka Republika),
prof. dr Milan Veljković (Holandija),
v. prof. dr Mirjana Vukićević (Srbija),
prof. dr Tatjana Isaković (Slovenija),
prof. dr Miloš Knežević (Crna Gora),
prof. dr Đorđe Lađinović (Srbija),
prof. dr Asterios Liolios (Grčka),
prof. dr Jože Lopatič (Slovenija),
prof. dr Duško Lučić (Crna Gora),
prof. dr Snežana Marinković (Srbija),
prof. dr Zlatko Marković (Srbija),
prof. dr Goran Markovski (Makedonija),
doc. dr Branko Milosavljević (Srbija),
prof. dr Primož Može (Slovenija),
prof. dr Tihomir Nikolovski (Makedonija),
prof. dr Doncho Partov (Bugarska),
prof. dr Radenko Pejović (Crna Gora),
prof. dr Mira Petronijević (Srbija),
prof. dr Milenko Pržulj (Slovenija),
prof. dr Vlastimir Radonjanin (Srbija),

prof. dr Boško Stevanović (Srbija),
prof. dr Dragoslav Stojić (Srbija),
prof. dr David Fernández-Ordóñez (Španija),
prof. dr Radomir Folić (Srbija),
prof. dr Rüdiger Höffer (Nemačka),
prof. dr Meri Cvetkovska (Makedonija),
prof. dr Hugo Corres Peiretti (Španija).

KONGRES JE ORGANIZOVAN U SARADNJI SA:

GRAĐEVINSKIM FAKULTETOM UNIVERZITETA U BEOGRADU;
FAKULTETOM TEHNIČKIH NAUKA UNIVERZITETA U NOVOM SADU.

POKROVITELJ KONGRESA:

MINISTARSTVO PROSVETE, NAUKE I TEHNOLOŠKOG RAZVOJA

SPONZORI KONGRESA:

Platinasti sponzori:

PERI-OPLATE D.O.O. Šimanovci

ŠIRBEGOVIĆ Inženjering, Gračanica, BiH

Zlatni sponzori:

ADING D.O.O. Beograd

ARMONT SP D.O.O. Beograd

CRH (Srbija) D.O.O. Popovac

ENERGOPROJEKT HOLDING A.D. Beograd

MARTINI GRADNJA D.O.O. Inđija

PEIKKO SLOVAKIA S.R.O. Kráľová nad Váhom, Slovakia

PUT-INŽENJERING D.O.O. Niš

Srebrni sponzori:

CENROPROJEKT D.O.O. Beograd

DEL ING D.O.O. Beograd

ENERGOPROJEKT ENTEL A.D. Beograd

MAPEI SRB D.O.O. Beograd

PIRAMIDA D.O.O. Sremska Mitrovica

Bronzani sponzori:

ASA IBELIK D.O.O. Beograd

ASMEC CONSULTANTS D.O.O. Beograd

DNEC D.O.O. Beograd

EX BC D.O.O. Beograd

KOLAREVIĆ D.O.O. Pojate

METAL-CINKARA D.O.O. Inđija

SIKA SRBIJA D.O.O. Šimanovci

ŠIDPROJEKT D.O.O. Šid

DOSADAŠNJI KONGRESI, SIMPOZIJUMI I SAVETOVANJA

PRVO SAVETOVANJE
JUGOSLOVENSKIH INŽENJERA KONSTRUKTERA
ZAGREB, decembar 1953.

DRUGI KONGRES
JUGOSLOVENSKOG DRUŠTVA GRAĐEVINSKIH KONSTRUKTERA
OPATIJA, maj 1958.

Predsednik:	akademik, prof. dr h.c. Đorđe LAZAREVIĆ, dipl.inž.građ., Beograd
Sekretar:	prof. Zvonimir PAVLOVIĆ, dipl.inž.građ., Beograd

TREĆI KONGRES
JUGOSLOVENSKOG DRUŠTVA GRAĐEVINSKIH KONSTRUKTERA
SARAJEVO, septembar 1964.

Predsednik:	prof. dr Kruno TONKOVIĆ, dipl.inž.građ., Zagreb
Potpredsednik:	prof. Ljubomir JEVTOVIĆ, dipl.inž.građ., Beograd
Sekretar:	prof. Zvonimir PAVLOVIĆ, dipl.inž.građ., Beograd

ČETVRTI KONGRES
JUGOSLOVENSKOG DRUŠTVA GRAĐEVINSKIH KONSTRUKTERA
PORTOROŽ, jun 1969.

Predsednik:	akademik, prof. dr Milan ĐURIĆ, dipl.inž.građ., Beograd
Potpredsednik:	prof. Miloš MARINČEK, dipl.inž.građ., Ljubljana
Sekretar:	Stojan DINIĆ, dipl.inž.građ., Beograd

PETI KONGRES
JUGOSLOVENSKOG DRUŠTVA GRAĐEVINSKIH KONSTRUKTERA
BUDVA, septembar 1974.

Predsednik:	akademik, prof. dr Milan ĐURIĆ, dipl.inž.građ., Beograd
Potpredsednik:	prof. Miloš MARINČEK, dipl.inž.građ., Ljubljana
Sekretar:	Stojan DINIĆ, dipl.inž.građ., Beograd

SIMPOZIJUM
JUGOSLOVENSKOG DRUŠTVA GRAĐEVINSKIH KONSTRUKTERA
"GREŠKE, SANACIJE I ISKUSTVA U INVESTIRANJU, PROJEKTOVANJU, GRAĐENJU I EKSPLOATACIJI GRAĐEVINSKIH OBJEKATA"
CAVTAT, novembar 1976.

ŠESTI KONGRES
JUGOSLOVENSKOG DRUŠTVA GRAĐEVINSKIH KONSTRUKTERA
BLED, septembar 1978.

Predsednik:	akademik, prof. dr Nikola HAJDIN, dipl.inž.građ., Beograd
Potpredsednik:	prof. Milenko PRŽULJ, dipl.inž.građ., Sarajevo
Sekretar:	Stojan DINIĆ, dipl.inž.građ., Beograd
Sekretar za međunarodne veze:	prof. dr Života PERIŠIĆ, dipl.inž.građ., Beograd

SIMPOZIJUM
JUGOSLOVENSKOG DRUŠTVA GRAĐEVINSKIH KONSTRUKTERA I INSTITUTA ZA MATERIJALE I KONSTRUKCIJE GRAĐEVINSKOG FAKULTETA UNIVERZITETA U BEOGRADU
"INOVACIJE JUGOSLOVENSKIH PROPISA ZA BETONSKE, METALNE I SPREGNUTE KONSTRUKCIJE - ISKUSTVA I NOVA SAZNANJA"
TROGIR, maj 1980.

Na Skupštini održanoj maja 1980. u Trogiru, Jugoslovensko društvo građevinskih konstruktera je promenilo naziv u SAVEZ DRUŠTAVA GRAĐEVINSKIH KONSTRUKTERA JUGOSLAVIJE - SDGKJ. Na Skupštini je odlučeno da izvršni odbor, izabran na VI Kongresu na Bledu, u istom sastavu obavlja dužnosti PREDSEDNIŠTVA SDGKJ do sledećeg kongresa.

Za predsednika i potpredsednika SDGKJ sa jednogodišnjim mandatom izabrani su:

Predsednik:	akademik, prof. dr Nikola HAJDIN, dipl.inž.građ., Beograd
Potpredsednik:	prof. Milenko PRŽULJ, dipl.inž.građ., Sarajevo

a za predsednika i potpredsednika SDGKJ za naredni jednogodišnji mandat:

Predsednik:	prof. Milenko PRŽULJ, dipl.inž.građ., Sarajevo
Potpredsednik:	Marijan KOŠČAK, dipl.inž.građ., Zagreb

SEDMI KONGRES
SAVEZA DRUŠTAVA GRAĐEVINSKIH KONSTRUKTERA JUGOSLAVIJE
CAVTAT, april 1983.

Predsednik:	prof. Milenko PRŽULJ, dipl.inž.građ., Sarajevo
Potpredsednik:	prof. dr Stanko ŠRAM, dipl.inž.građ., Zagreb
Sekretar:	Stojan DINIĆ, dipl.inž.građ., Beograd
Sekretar za međunarodne veze:	prof. dr Života PERIŠIĆ, dipl.inž.građ., Beograd

SIMPOZIJUM '85
SAVEZA DRUŠTAVA GRAĐEVINSKIH KONSTRUKTERA JUGOSLAVIJE
DUBROVNIK, april 1985.

Na sednici Predsedništva SDGKJ, održanoj aprila 1985. u Dubrovniku odlučeno je da se predsedniku, potpredsedniku, sekretaru i sekretaru za međunarodne veze, izabranim na VII Kongresu SDGKJ u Cavtatu, produži mandat do sledećeg kongresa.

OSMI KONGRES
SAVEZA DRUŠTAVA GRAĐEVINSKIH KONSTRUKTERA JUGOSLAVIJE
CAVTAT, april 1987.

Predsednik:	prof. dr Života PERIŠIĆ, dipl.inž.građ., Beograd
Potpredsednik:	prof. dr Franci KRŽIĆ, dipl.inž.građ., Ljubljana
Sekretar:	Stojan DINIĆ, dipl.inž.građ., Beograd
Sekretar za međunarodne veze:	docent dr Jure RADIĆ, dipl.inž.građ., Zagreb

JUGOSLOVENSKO SAVETOVANJE O PRIMENI NOVOG PRAVILNIKA ZA BETON I ARMIRANI BETON BAB 87 ZAJEDNO SA JUDIMK, GRAĐEVINSKIM INSTITUTOM ZAGREB I GRAĐEVINSKIM FAKULTETOM BEOGRAD
DUBROVNIK, april 1989.

Na sednici Predsedništva SDGKJ održanoj aprila 1989. u Dubrovniku, ponovo su izabrani za sledeći dvogodišnji period

Predsednik:	prof. dr Života PERIŠIĆ, dipl.inž.građ., Beograd
Potpredsednik:	prof. dr Franci KRŽIĆ, dipl.inž.građ., Ljubljana
Sekretar:	Stojan DINIĆ, dipl.inž.građ., Beograd
Sekretar za međunarodne veze:	docent dr Jure RADIĆ, dipl.inž.građ., Zagreb

DEVETI KONGRES
SAVEZA DRUŠTAVA GRAĐEVINSKIH KONSTRUKTERA JUGOSLAVIJE
CAVTAT, april 1991.

Predsednik:	prof. dr Života PERIŠIĆ, dipl.inž.građ., Beograd
Potpredsednik:	prof. dr Franci KRŽIĆ, dipl.inž.građ., Ljubljana
Sekretar:	Stojan DINIĆ, dipl.inž.građ., Beograd
Sekretar za međunarodne veze:	docent dr Jure RADIĆ, dipl.inž.građ., Zagreb
Članovi predsedništva:	prof. Vukašin AČANSKI, dipl.inž.građ., Maribor
	prof. dr Vinko ČANDRLIĆ, dipl.inž.građ., Zagreb
	prof. dr Radomir FOLIĆ, dip.inž.građ., Novi Sad
	akademik, prof. dr Nikola HAJDIN, dipl.inž.građ., Beograd
	prof. Dravan IVANOV, dipl.inž.građ., Skoplje
	prof. Gojko NENADIĆ, dipl.inž.građ., Beograd
	prof. Milenko PRŽULJ, dipl.inž.građ., Sarajevo
	Vladimir STANKOVIĆ, dipl.inž.građ., Titograd
	Vidoje ZELENOVIĆ, dipl.inž.građ., Priština
	prof. dr Stanko ŠRAM, dipl.inž.građ., Zagreb
	mr Cvetan TANEVSKI, dipl.inž.građ., Skoplje
Članovi Nadzornog odbora:	Jovan BOŠKOV, dipl.inž.građ., Novi Sad
	prof. dr Boris KOLJOZOV, dipl.inž.građ., Skoplje
	Zvonimir SABLJAK, dipl.inž.građ., Novi Sad

Posle raspada SFRJ, Savez društava građevinskih konstruktera Jugoslavije - SDGKJ transformisao se u ***Jugoslovensko društvo građevinskih konstruktera - JDGK****, koje je nastavilo delatnost SDGKJ. Na Osnivačkoj skupštini, održanoj 1.12.1994. godine u Beogradu, usvojen je novi statut i imenovano predsedništvo u sastavu:*

Predsednik:	prof. dr Života PERIŠIĆ, dipl.inž.građ., Beograd
Potpredsednik:	prof. dr Radomir FOLIĆ, dipl.inž.građ., Novi Sad
Generalni sekretar:	Stojan DINIĆ, dipl.inž.građ., Beograd
Članovi predsedništva:	akademik prof. dr Nikola HAJDIN, dipl.inž.građ., Beograd
	prof. dr Milorad IVKOVIĆ, dipl.inž.građ., Beograd
	Miroslav BAJIĆ, dip.inž.građ., Novi Sad
	Veljko BELADA, dipl.inž.građ., Podgorica
	Vidoje ZELENOVIĆ, dipl.inž.građ., Priština
	prof. dr Mirko AĆIĆ, dipl.inž.građ., Beograd
	prof. dr Aleksandar PAKVOR, dipl.inž.građ., Beograd
	prof. dr Mihailo MURAVLJOV, dipl.inž.građ., Beograd

Jugoslovensko društvo građevinskih konstruktera, zajedno sa Građevinskim fakultetom u Beogradu i Saveznim zavodom za standardizaciju, organizovalo je dva jugoslovenska savetovanja:

PRVO JUGOSLOVENSKO SAVETOVANJE
EVROKODOVI I JUGOSLOVENSKO GRAĐEVINSKO KONSTRUKTERSTVO
BEOGRAD, jun 1995.

DRUGO JUGOSLOVENSKO SAVETOVANJE
EVROKODOVI I JUGOSLOVENSKO GRAĐEVINSKO KONSTRUKTERSTVO
BEOGRAD, april 1997.

DESETI KONGRES
JUGOSLOVENSKOG DRUŠTVA GRAĐEVINSKIH KONSTRUKTERA
VRNJAČKA BANJA, jun 1998.

Na Skupštini JDGK, održanoj juna 1998. u Vrnjačkoj Banji, izabrano je novo predsedništvo i nadzorni odbor JDGK, u sledećem sastavu:

Predsednik:	prof. dr Mirko AĆIĆ, dipl.inž.građ., Beograd
Potpredsednik:	prof. dr Radenko PEJOVIĆ, dipl.inž.građ., Podgorica
Generalni sekretar:	Stojan DINIĆ, dipl.inž.građ., Beograd
Sekretar:	Svetislav SIMOVIĆ, dipl.inž.građ., Beograd
Članovi predsedništva:	akademik prof. dr Nikola HAJDIN, dipl.inž.građ., Beograd
	prof. dr Milorad IVKOVIĆ , dipl.inž.građ., Beograd
	prof. dr Života PERIŠIĆ, dip.inž.građ., Beograd
	prof. dr Aleksandar PAKVOR, dipl.inž.građ., Beograd
	prof. dr Miodrag SEKULOVIĆ, dipl.inž.građ., Beograd
	prof. dr Arsenije VUJOVIĆ, dipl.inž.građ., Podgorica
	prof. dr Radomir FOLIĆ, dipl.inž.građ., Novi Sad
	prof. dr Živojin PRAŠČEVIĆ, dipl.inž.građ., Beograd
	prof. dr Dragan BUĐEVAC, dipl.inž.građ., Beograd
	prof. dr Milić MILIĆEVIĆ, dipl.inž.građ., Niš
	mr Vidoje ZELENOVIĆ, dipl.inž.građ., Gacko
	Veljko BELADA, dipl.inž.građ., Podgorica
	Ivan MAMUŽIĆ, dipl.inž.građ., Novi Sad
	Dragan VUKADINOVIĆ, dipl.inž.građ., Beograd
	Jožef KERMECI, dipl.inž.građ., Kanjiža
Članovi Nadzornog odbora:	prof. dr Dušan NAJDANOVIĆ, dipl.inž.građ., Beograd - predsednik
	prof. dr Mladen ULIĆEVIĆ, dipl.inž.građ., Podgorica
	Miroslav BAJIĆ, dipl.inž.građ., Novi Sad

Na istoj skupštini izabrani su za počasne članove JDGK:

akademik prof. dr Nikola HAJDIN, dipl.inž.građ., Beograd
prof. dr Milorad IVKOVIĆ , dipl.inž.građ., Beograd
prof. dr Tihomir NIKOLOVSKI, dipl.inž.građ., Skoplje

takođe je izabrano i 14 zaslužnih članova JDGK:

prof. dr Života PERIŠIĆ, dipl.inž.građ., Beograd
prof. dr Radomir FOLIĆ, dipl.inž.građ., Novi Sad
Ivan MAMUŽIĆ, dipl.inž.građ., Novi Sad
prof. dr Aleksandar PAKVOR, dipl.inž.građ., Beograd
prof. dr Mirko AĆIĆ, dipl.inž.građ., Beograd
Stojan DINIĆ, dipl.inž.građ., Beograd
mr Vidoje ZELENOVIĆ, dipl.inž.građ., Gacko
prof. dr Boško PETROVIĆ, dipl.inž.građ., Beograd
prof. dr Miroslav DEBELJKOVIĆ, dipl.inž.građ., Beograd
mr Branislav VOJINOVIĆ, dipl.inž.građ., Beograd
prof. dr Milić MILIĆEVIĆ, dipl.inž.građ., Niš
prof. dr Milan GOJKOVIĆ , dipl.inž.građ., Beograd
dr Vladimir STANKOVIĆ, dipl.inž.građ., Podgorica
Veljko BELADA, dipl.inž.građ., Podgorica

SIMPOZIJUM 2000.
JUGOSLOVENSKOG DRUŠTVA GRAĐEVINSKIH KONSTRUKTERA
VRNJAČKA BANJA, 1-3. novembar 2000.

Na Skupštini JDGK, održanoj 2. novembra 2000. u Vrnjačkoj Banji, predsedništvo JDGK je prošireno sa dva člana i njegov sastav čine:

Predsednik:	prof. dr Mirko AĆIĆ, dipl.inž.građ., Beograd
Potpredsednik:	prof. dr Radenko PEJOVIĆ, dipl.inž.građ., Podgorica
Generalni sekretar:	Stojan DINIĆ, dipl.inž.građ., Beograd
Sekretar:	Svetislav SIMOVIĆ, dipl.inž.građ., Beograd
Članovi predsedništva:	akademik, prof. dr Nikola HAJDIN, dipl.inž.građ., Beograd
	prof. dr Milorad IVKOVIĆ, dipl.inž.građ., Beograd
	prof. dr Života PERIŠIĆ, dipl.inž.građ., Beograd
	prof. dr Aleksandar PAKVOR, dipl.inž.građ., Beograd
	prof. dr Miodrag SEKULOVIĆ, dipl.inž.građ., Beograd
	prof. dr Arsenije VUJOVIĆ, dipl.inž.građ., Podgorica
	prof. dr Radomir FOLIĆ, dipl.inž.građ., Novi Sad
	prof. dr Živojin PRAŠČEVIĆ, dipl.inž.građ., Beograd
	prof. dr Dragan BUĐEVAC, dipl.inž.građ., Beograd

prof. dr Milić MILIĆEVIĆ, dipl.inž.građ., Niš
mr Vidoje ZELENOVIĆ, dipl.inž.građ., Banja Luka
Veljko BELADA, dipl.inž.građ., Podgorica
Ivan MAMUŽIĆ, dipl.inž.građ., Novi Sad
Dragan VUKADINOVIĆ, dipl.inž.građ., Beograd
Jožef KERMECI, dipl.inž.građ., Kanjiža

Članovi Nadzornog odbora:

prof. dr Dušan NAJDANOVIĆ, dipl.inž.građ., Beograd - predsednik
prof. dr Mladen ULIĆEVIĆ, dipl.inž.građ., Podgorica
Miroslav BAJIĆ, dipl.inž.građ., Novi Sad

Na istoj skupštini izabrani su za počasne članove JDGK:

prof. dr Sande ATANASOVSKI, dipl.inž.građ., Skoplje
prof. dr Dragan IVANOV, dipl.inž.građ., Skoplje
prof. dr Milenko PRŽULJ, dipl.inž.građ., Ljubljana
prof. dr Vukašin AČANSKI, dipl.inž.građ., Maribor
prof. dr Života PERIŠIĆ, dipl.inž.građ., Beograd
Stojan DINIĆ, dipl.inž.građ., Beograd

takođe je izabrano i 10 zaslužnih članova JDGK:

prof. Dimitrije ĆERTIĆ, dipl.inž.građ., Beograd
Predrag ŽELALIĆ, dipl.inž.građ., Beograd
prof. Gojko NENADIĆ, dipl.inž.građ., Beograd
Anđelko KOVAČEVIĆ, dipl.inž.građ., Beograd
prof. dr Živojin PRAŠČEVIĆ, dipl.inž.građ., Beograd
Miroslav BAJIĆ, dipl.inž.građ., Beograd
prof. dr Mihailo MURAVLJOV, dipl.inž.građ., Beograd
prof. dr Arsenije VUJOVIĆ, dipl.inž.građ., Podgorica
Lazar PRODANOVIĆ, dipl.inž.građ., Beograd
Johan SKLENA, dipl.inž.građ., Novi Sad

JEDANAESTI KONGRES
JUGOSLOVENSKOG DRUŠTVA GRAĐEVINSKIH KONSTRUKTERA
VRNJAČKA BANJA, 25-27. septembar 2002.

Na Skupštini JDGK, održanoj 24. septembra 2002. u Vrnjačkoj Banji, izabrano je novo predsedništvo i nadzorni odbor JDGK, u sledećem sastavu:

Predsednik: prof. dr Mirko AĆIĆ, dipl.inž.građ., Beograd
Potpredsednik: prof. dr Radenko PEJOVIĆ, dipl.inž.građ., Podgorica

Generalni sekretar:	Stojan DINIĆ, dipl.inž.građ., Beograd
Sekretar:	Svetislav SIMOVIĆ, dipl.inž.građ., Beograd
Članovi predsedništva:	prof. dr Života PERIŠIĆ, dipl.inž.građ., Beograd prof. dr Radomir FOLIĆ, dipl.inž.građ., Novi Sad prof. dr Arsenije VUJOVIĆ, dipl.inž.građ., Podgorica prof. dr Živojin PRAŠČEVIĆ, dipl.inž.građ., Beograd prof. dr Dragan BUĐEVAC, dipl.inž.građ., Beograd prof. dr Dušan NAJDANOVIĆ, dipl.inž.građ., Beograd prof. dr Đorđe VUKSANOVIĆ, dipl.inž.građ., Beograd prof. dr Mladen ULIĆEVIĆ, dipl.inž.građ., Podgorica prof. dr Dragoslav STOJIĆ, dipl.inž.građ., Niš mr Vidoje ZELENOVIĆ, dipl.inž.građ., Gacko Dragan VUKADINOVIĆ, dipl.inž.građ., Beograd Ivan MAMUŽIĆ, dipl.inž.građ., Novi Sad Jožef KERMECI, dipl.inž.građ., Kanjiža
Članovi Nadzornog odbora:	mr Dragana ČUKIĆ, dipl.inž.građ., Beograd mr Đorđe LAĐINOVIĆ, dipl.inž.građ., Novi Sad Igor ĐURANOVIĆ, dipl.inž.građ., Podgorica

Na istoj skupštini izabrani su za počasne članove JDGK:

prof. dr Stanko ŠRAM, dipl.inž.građ. - Hrvatska
prof. dr Miodrag VELKOV, dipl.inž.građ. - Makedonija
prof. dr Aleksandar PAKVOR, dipl.inž.građ., Beograd
prof. dr Miodrag SEKULOVIĆ, dipl.inž.građ., Beograd
Predrag ŽELALIĆ, dipl.inž.građ., Beograd
Veljko BELADA, dipl.inž.građ., Podgorica
mr Vladimir STANKOVIĆ, dipl.inž.građ., Podgorica

takođe je izabrano i 12 zaslužnih članova JDGK:

prof. dr Dušan NAJDANOVIĆ, dipl.inž.građ., Beograd
prof. dr Radenko PEJOVIĆ, dipl.inž.građ., Podgorica
prof. dr Mladen ULIĆEVIĆ, dipl.inž.građ., Podgorica
prof. dr Petar ČOLIĆ, dipl.inž.građ., Beograd
Dušan SIMOVIĆ, dipl.inž.građ., Beograd
Svetislav SIMOVIĆ, dipl.inž.građ., Beograd
Dragan VUKADINOVIĆ, dipl.inž.građ., Beograd
Boško TRIVIĆ, dipl.inž.građ., Beograd
Jožef KERMECI, dipl.inž.građ., Kanjiža
Vukan NJAGULJ, dipl.inž.građ., Beograd
Dragomir LUKIĆ, dipl.inž.građ., Beograd
Miroslav SUBOTIĆ, dipl.inž.građ., Beograd

SIMPOZIJUM 2004.
JUGOSLOVENSKOG DRUŠTVA GRAĐEVINSKIH KONSTRUKTERA
VRNJAČKA BANJA, 29. septembar - 1. oktobar 2004.

Predsednik:	prof. dr Mirko AĆIĆ, dipl.inž.građ., Beograd
Potpredsednik:	prof. dr Radenko PEJOVIĆ, dipl.inž.građ., Podgorica
Generalni sekretar:	Stojan DINIĆ, dipl.inž.građ., Beograd
Sekretar:	Svetislav SIMOVIĆ, dipl.inž.građ., Beograd
Članovi predsedništva:	prof. dr Života PERIŠIĆ, dipl.inž.građ., Beograd
	prof. dr Radomir FOLIĆ, dipl.inž.građ., Novi Sad
	prof. dr Arsenije VUJOVIĆ, dipl.inž.građ., Podgorica
	prof. dr Živojin PRAŠČEVIĆ, dipl.inž.građ., Beograd
	prof. dr Dragan BUĐEVAC, dipl.inž.građ., Beograd
	prof. dr Dušan NAJDANOVIĆ, dipl.inž.građ., Beograd
	prof. dr Đorđe VUKSANOVIĆ, dipl.inž.građ., Beograd
	prof. dr Mladen ULIĆEVIĆ, dipl.inž.građ., Podgorica
	prof. dr Dragoslav STOJIĆ, dipl.inž.građ., Niš
	prof. dr Petar ČOLIĆ, dipl.inž.građ., Beograd
	mr Vidoje ZELENOVIĆ, dipl.inž.građ., Gacko
	Dragan VUKADINOVIĆ, dipl.inž.građ., Beograd
	Ivan MAMUŽIĆ, dipl.inž.građ., Novi Sad
	Jožef KERMECI, dipl.inž.građ., Kanjiža
Članovi Nadzornog odbora:	mr Dragana ČUKIĆ, dipl.inž.građ., Beograd
	mr Đorđe LAĐINOVIĆ, dipl.inž.građ., Novi Sad
	Igor ĐURANOVIĆ, dipl.inž.građ., Podgorica

Na istoj skupštini izabrani su za počasne članove JDGK:

prof. dr Predrag GAVRILOVIĆ, dipl.inž.građ.
Saško STREZOVSKI, dipl.inž.građ.
prof. Gojko NENADIĆ, dipl.inž.građ.
prof. dr Mihajlo TRIFUNAC, dipl.inž.građ.
prof. dr Milija PAVLOVIĆ, dipl.inž.građ.
prof. dr David LLOJD SMITH, dipl.inž.građ.
prof. dr. Arsenije VUJOVIĆ, dipl.inž.građ.
prof. dr Vlado GOCEVSKI, dipl.inž.građ.
prof. dr Tomislav RADOJIČIĆ, dipl.inž.građ.
Ivan MAMUŽIĆ, dipl.inž.građ.

takođe je izabrano i 12 zaslužnih članova JDGK:

Jovo SMILJANIĆ, dipl.inž.građ.
Dragan MAJKIĆ, dipl.inž.građ.
Lajčo STIPIĆ, dipl.inž.građ.
prof. dr Milivoje STANKOVIĆ, dipl.inž.građ.
prof. dr Dragoljub DRENIĆ, dipl.inž.građ.
prof. dr Dušan PETKOVIĆ, dipl.inž.građ.
prof. dr Dragan BUĐEVAC, dipl.inž.građ.
mr Dragana ČUKIĆ, dipl.inž.građ.
mr Milan ĐOKOVIĆ, dipl.inž.građ.
prof. dr Božidar S. PAVIĆEVIĆ, dipl.inž.građ.
mr Radivoje MRDAK, dipl.inž.građ.
prof. dr Vojislav MIHAILOVIĆ, dipl.inž.građ.

DVANAESTI KONGRES
JUGOSLOVENSKOG DRUŠTVA GRAĐEVINSKIH KONSTRUKTERA
VRNJAČKA BANJA, 27-29. septembar 2006.

Na Skupštini JDGK, održanoj 27. septembra 2006. u Vrnjačkoj Banji, izabrano je novo predsedništvo i nadzorni odbor JDGK, u sledećem sastavu:

Predsednik:	prof. dr Dejan BAJIĆ, dipl.inž.građ., Beograd
Potpredsednik:	Svetislav SIMOVIĆ, dipl.inž.građ., Podgorica
Sekretar:	prof. dr Snežana MARINKOVIĆ, dipl.inž.građ., Beograd
Članovi predsedništva:	prof. dr Dušan NAJDANOVIĆ, dipl.inž.građ., Beograd
	prof. dr Đorđe VUKSANOVIĆ, dipl.inž.građ., Beograd
	prof. dr Dragoslav STOJIĆ, dipl.inž.građ., Niš
	prof. dr Radomir FOLIĆ, dipl.inž.građ., Novi Sad
	doc. dr Đorđe LAĐINOVIĆ, dipl.inž.građ., Novi Sad
	doc. dr Bratislav STIPANIĆ, dipl.inž.građ., Beograd
	doc. dr Aleksandar RISTOVSKI, dipl.inž.građ., Kosovska Mitrovica
	dr Zoran FLORIĆ, dipl.inž.građ., Novi Sad
	Ivan MAMUŽIĆ, dipl.inž.građ., Novi Sad
	Zoran FILIPOVIĆ, dipl.inž.građ., Beograd
	Branko KNEŽEVIĆ, dipl.inž.građ., Beograd
	Slobodan CVETKOVIĆ, dipl.inž.građ., Beograd
	Slobodan MITROVIĆ, dipl.inž.građ., Beograd
Članovi Nadzornog odbora:	mr Slobodan GRKOVIĆ, dipl.inž.građ., Subotica
	Gojko GRBIĆ, dipl.inž.građ., Loznica
	Miroslav MIHAJLOVIĆ, dipl.inž.građ., Paraćin

Na istoj skupštini izabrani su za počasne članove JDGK:

Prof. dr Mirka AĆIĆA, dipl.građ.inž.
Prof. dr Radomira FOLIĆA, dipl.građ.inž.
Prof. dr Radenka PEJOVIĆA, dipl.građ.inž.
Prof. dr Trifuna PASKALOVA , dipl.građ.inž.
Mr Vidoja ZELENOVIĆA, dipl.građ.inž.

takođe je izabrano i 5 zaslužnih članova JDGK:

Prof. dr Đorđe VUKSANOVIĆ, dipl.građ.inž.
Prof. dr Dejan BAJIĆ, dipl.građ.inž.
Prof. dr Dragoslav STOJIĆ, dipl.građ.inž.
Jožef BARNA , dipl.građ.inž.
Mr Predrag PAVLOVIĆ, dipl.građ.inž.

SIMPOZIJUM 2008.
DRUŠTVA GRAĐEVINSKIH KONSTRUKTERA SRBIJE
ZLATIBOR "ČIGOTA", 24-26. septembar 2008.

Predsednik: prof. dr Dejan BAJIĆ, dipl.inž.građ., Beograd
Potpredsednik: Svetislav SIMOVIĆ, dipl.inž.građ., Podgorica
Sekretar: prof. dr Snežana MARINKOVIĆ, dipl.inž.građ., Beograd

Nije bilo izbora za zaslužne i počasne članove društva.

TRINAESTI KONGRES
DRUŠTVA GRAĐEVINSKIH KONSTRUKTERA SRBIJE
ZLATIBOR "ČIGOTA", 22-24. septembar 2010.

Na Skupštini DGKS, održanoj 22. septembra 2010. na Zlatiboru izabrano je novo predsedništvo i nadzorni odbor DGKS, u sledećem sastavu:

Predsednik: prof. dr Miloš LAZOVIĆ, dipl.inž.građ., Beograd
Potpredsednik: Aleksandar BOJOVIĆ, dipl.inž.građ., Beograd
Sekretar: prof. dr Boško STEVANOVIĆ, dipl.inž.građ., Beograd
Članovi predsedništva: prof. dr Snežana MARINKOVIĆ, dipl.inž.građ., Beograd
prof. dr Đorđe VUKSANOVIĆ, dipl.inž.građ., Beograd
prof. dr Mihajlo ĐURĐEVIĆ, dipl.inž.građ., Beograd
prof. dr Đorđe LAĐINOVIĆ, dipl.inž.građ., Novi Sad
doc. dr Bratislav STIPANIĆ, dipl.inž.građ., Beograd
prof. dr Dragoslav STOJIĆ, dipl.inž.građ., Niš
mr Slobodan GRKOVIĆ, dipl.inž.građ., Subotica
prof. dr Aleksandar RISTOVSKI, dipl.inž.građ., Kos.Mitrovica
Gojko GRBIĆ, dipl.inž.građ., Loznica

dr Zoran FLORIĆ, dipl.inž.građ., Novi Sad
Đorđe PAVKOV, dipl.inž.građ., Novi Sad
Svetislav SIMOVIĆ, dipl.inž.građ., Beograd
Goran VUKOBRATOVIĆ, dipl.inž.građ., Novi Sad
Branko KNEŽEVIĆ, dipl.inž.građ., Beograd

Članovi Nadzornog odbora: Miroslav MIHAJLOVIĆ, dipl.inž.građ., Paraćin
prof. dr Zlatko MARKOVIĆ, dipl.inž.građ., Beograd
Aleksandar TRAJKOVIĆ, dipl.inž.građ., Beograd

Na istoj skupštini izabran je 1 počasni član DGKS:

Prof. dr Mirko AĆIĆ, dipl.inž.građ.

SIMPOZIJUM 2012.
DRUŠTVA GRAĐEVINSKIH KONSTRUKTERA SRBIJE
VRNJAČKA BANJA, 19-21. septembar 2012.

Predsednik: prof. dr Miloš LAZOVIĆ, dipl.inž.građ., Beograd
Potpredsednik: Aleksandar BOJOVIĆ, dipl.inž.građ., Beograd
Sekretar: prof. dr Boško STEVANOVIĆ, dipl.inž.građ., Beograd

Nije bilo izbora za zaslužne i počasne članove društva.

ČETRNAESTI KONGRES
DRUŠTVA GRAĐEVINSKIH KONSTRUKTERA SRBIJE
NOVI SAD, 24-26. septembar 2014.

Na Skupštini DGKS, održanoj 24. septembra 2014. u Novom Sadu izabrano je novo predsedništvo i nadzorni odbor DGKS, u sledećem sastavu:

Predsednik prof. dr Đorđe LAĐINOVIĆ, dipl.inž.građ., Novi Sad
Potpredsednik: Aleksandar BOJOVIĆ, dipl.inž.građ., Beograd
Generalni sekretar: prof. dr Zlatko MARKOVIĆ, dipl.inž.građ., Beograd
Sekretar: prof. dr Boško STEVANOVIĆ, dipl.inž.građ., Beograd
Članovi predsedništva: prof. dr Snežana MARINKOVIĆ, dipl.inž.građ., Beograd
prof. dr Mira PETRONIJEVIĆ, dipl.inž.građ., Beograd
doc. dr Selimir LELOVIĆ, dipl.inž.građ., Beograd
mr Branko MILOSAVLJEVIĆ, dipl.inž.građ., Beograd
prof. dr Dragoslav STOJIĆ, dipl.inž.građ., Niš
prof. dr Danijel KUKARAS, dipl.inž.građ., Subotica
Branko KNEŽEVIĆ, dipl.inž.građ., Beograd

Đorđe PAVKOV, dipl.inž.građ., Novi Sad
Goran VUKOBRATOVIĆ, dipl.inž.građ., Novi Sad
Gojko GRBIĆ, dipl.inž.građ., Loznica
Lazar MARKOVIĆ, dipl.inž.građ., Subotica
Aleksandar ŽIVANOVIĆ, dipl.inž.građ., Beograd
Goran TADIĆ, dipl.inž.građ., Beograd

Članovi Nadzornog odbora: Ivan IGNJATOVIĆ, dipl.inž.građ., predsednik, Beograd
prof. dr Dejan DIVAC, dipl.inž.građ., Beograd
Zoran KOVRLIJA, dipl.inž.građ., Beograd

Nije bilo izbora za zaslužne i počasne članove društva.

ČETRNAESTI KONGRES
DRUŠTVA GRAĐEVINSKIH KONSTRUKTERA SRBIJE
BEOGRAD, 02. decembar 2016.

Na Skupštini DGKS, održanoj 02. decembra 2016. u Beogradu izmenjen je sastav predsedništva DGKS. Umesto Aleksandra Živanovića, dipl.inž.građ. izabran je Duško Tomić, dipl.inž.građ. (Energoprojekt Visokogradnja).

PETNAESTI KONGRES
DRUŠTVA GRAĐEVINSKIH KONSTRUKTERA SRBIJE
BEOGRAD, 01. decembar 2017.

Na Skupštini DGKS, održanoj 01. decembra 2017. u Beogradu izmenjen je sastav nadzornog odbora DGKS. Umesto prof. dr Dejana Divca, dipl.inž.građ. i Zorana Kovrlije, dipl.inž.građ. izabrani su doc. dr Predrag Blagojević, dipl.inž.građ. (Građevinsko-arhitektonski fakultet, Niš) i Vojin Zajić, dipl.inž.građ. (STRABAG, Beograd).

PRIZNANJA
SAVEZA DRUŠTAVA GRAĐEVINSKIH KONSTRUKTERA
JUGOSLAVIJE

ZA ŽIVOTNO DELO

U GRAĐEVINSKOM KONSTRUKTERSTVU

„Priznanje Saveza društava građevinskih konstruktera Jugoslavije za životno delo u građevinskom konstrukterstvu je najviše priznanje koje Predsedništvo SDGKJ dodeljuje svojim istaknutim članovima za izuzetan doprinos koji su dogogodišnjim radom i rezultatima dali razvoju našeg građevinskog konstrukterstva i napretku Socijalističke Federativne Republike Jugoslavije.“

Priznanje je ustanovljeno 1989. godine.

Dobitnici priznanja SDGKJ za životno delo u građevinskom konstrukterstvu su:

1989.

ĐORĐE LAZAREVIĆ
akademik SANU, profesor dr h.c.,
diplomirani građevinski inženjer,
prvi predsednik Jugoslovenskog društva građevinskih konstruktera, od 1958. do 1964.

KRUNISLAV TONKOVIĆ
profesor dr,
diplomirani građevinski inženjer,
drugi predsednik Jugoslovenskog društva građevinskih konstruktera, od 1964. do 1969.

BRANKO ŽEŽELJ
akademik SANU, profesor,
diplomirani građevinski inženjer

1990.

NIKOLA HAJDIN
akademik SANU, profesor dr,
diplomirani građevinski inženjer,
predsednik Jugoslovenskog društva građevinskih konstruktera, od 1978. do 1981.

MILORAD IVKOVIĆ
profesor dr,
diplomirani građevinski inženjer

STANKO ŠRAM
profesor dr,
diplomirani građevinski inženjer

1991.

STOJAN DINIĆ
diplomirani građevinski inženjer,
sekretar i generalni sekretar SDGKJ od 1969.

ZLATKO KOSTRENČIĆ
profesor dr,
diplomirani građevinski inženjer,

FRANCI KRŽIĆ
profesor dr,
diplomirani građevinski inženjer,
potpredsednik SDGKJ od 1987.

PETAR SERAFIMOV
akademik MANU, profesor dr,
diplomirani građevinski inženjer

Od 1991. do 1998. godine nisu dodeljivana priznanja za životno delo.

Jugoslovensko društvo građevinskih konstruktera je 1998. godine donelo odluku o nastavljanju dodeljivanja priznanja JDGK za žitovno delo u građevinskom konstrukterstvu.

PRIZNANJA
JUGOSLOVENSKOG DRUŠTVA GRAĐEVINSKIH KONSTRUKTERA

ZA ŽIVOTNO DELO
U GRAĐEVINSKOM KONSTRUKTERSTVU

„Priznanje Jugoslovenskog društva građevinskih konstruktera za životno delo u građevinskom konstrukterstvu je najviše priznanje koje Predsedništvo JDGK dodeljuje svojim istaknutim članovima za izuzetan doprinos koji su dogogodišnjim radom i rezultatima dali razvoju našeg građevinskog konstrukterstva.“

Dobitnici priznanja JDGK za životno delo u građevinskom konstrukterstvu su:

1998.

GOJKO NENADIĆ
profesor,
diplomirani građevinski inženjer

ŽIVOTA PERIŠIĆ
profesor dr,
diplomirani građevinski inženjer,
predsednik SDGKJ/JDGK od 1987. do 1998.

2000.

BOŠKO PETROVIĆ
akademik SANU, profesor dr,
diplomirani građevinski inženjer

MILAN GOJKOVIĆ
profesor dr,
diplomirani građevinski inženjer

BOŽIDAR S. PAVIĆEVIĆ
diplomirani građevinski inženjer

2002.

MIRKO AĆIĆ
profesor dr,
diplomirani građevinski inženjer
predsednik JDGK od 1998.

RADOMIR FOLIĆ
profesor dr,
diplomirani građevinski inženjer

ARSENIJE VUJOVIĆ
profesor dr,
diplomirani građevinski inženjer

DIMITRIJE ĆERTIĆ
profesor,
diplomirani građevinski inženjer

2004.

MIROSLAV DEBELJKOVIĆ
profesor,
diplomirani građevinski inženjer

ALEKSANDAR PAKVOR
profesor dr,
diplomirani građevinski inženjer

PREDRAG ŽELALIĆ
diplomirani građevinski inženjer

2006.

MOMIR KRASTAVČEVIĆ
profesor,
diplomirani građevinski inženjer

PRIZNANJA
DRUŠTVA GRAĐEVINSKIH KONSTRUKTERA SRBIJE

ZA ŽIVOTNO DELO

U GRAĐEVINSKOM KONSTRUKTERSTVU

„Priznanje Društva građevinskih konstruktera Srbije za životno delo u građevinskom konstrukterstvu je najviše priznanje koje Predsedništvo DGKS dodeljuje svojim istaknutim članovima za izuzetan doprinos koji su dogogodišnjim radom i rezultatima dali razvoju našeg građevinskog konstrukterstva.“

Dobitnici priznanja DGKS za životno delo u građevinskom konstrukterstvu su:

2008.

MIHAILO MURAVLJOV
profesor,
diplomirani građevinski inženjer

2010.

DANILO DRAGOJEVIĆ
diplomirani građevinski inženjer

VUKAN NJAGULJ
diplomirani građevinski inženjer

2012.

LJUBOMIR VLAJIĆ
profesor,
diplomirani građevinski inženjer

2014.

ŠERIF DUNICA
profesor,
diplomirani građevinski inženjer

2016.

VANJA ALENDAR
diplomirani građevinski inženjer

SLOBODAN CVETKOVIĆ
diplomirani građevinski inženjer

2018.

DEJAN BAJIĆ
profesor,
diplomirani građevinski inženjer

PRIZNANJA
SAVEZA DRUŠTAVA GRAĐEVINSKIH KONSTRUKTERA
JUGOSLAVIJE

ZA NAJBOLJA OSTVARENJA
U GRAĐEVINSKOM KONSTRUKTERSTVU

„U cilju podsticanja stvaralaštva, boljeg vrednovanja postignutih rezultata i najznačajnijih dostignuća našeg građevinskog konstrukterstva, Predsedništvo SDGKJ je početkom 1986. godine ustanovilo posebna godišnja stručna i društvena priznanja za najbolja ostvarenja u građevinskom konstrukterstvu u republikama i pokrajinama i u Jugoslaviji. Republička i pokrajinska društva građevinskih konstruktera dodeljuju svoja priznanja za najbolja ostvarenja u republikama i pokrajinama a Predsedništvo SDGKJ dodeljuje Jugoslovensko priznanje SDGKJ najboljem ostvarenju izabranom u konkurenciji ostvarenja koja su u toj godini dobila republička i pokrajinska priznanja.“

Priznanja su prvi put dodeljena za konstrukterska ostvarenja u 1986. godini.

Jugoslovenska priznanja SDGKJ za najbolja ostvarenja u građevinskom konstrukterstvu dobila su sledeća ostvarenja:

1986.

KONSTRUKCIJA NOVOG HANGARA JUGOSLOVENSKOG AEROTRANSPORTA NA AERODROMU BEOGRAD

Odgovorni projektanti konstrukcije:
profesor dr Milorad Ivković, dipl.inž.građ.
profesor dr Života Perišić, dipl.inž.građ.
profesor dr Mirko Aćić, dipl.inž.građ.
profesor dr Aleksandar Pakvor, dipl.inž.građ.

Graditelji konstrukcije:
Živadin Mijailović, dipl.inž.građ.
Višeslav Milosavljević, dipl.inž.građ.

1987.

PROJEKAT KONSTRUKCIJE KOMPLEKSA "CIBONA" U ZAGREBU

profesor dr Milutin Anđelić, dipl.inž.građ.

1988.

Naučnoistraživački rad:

POPREČNA RASPODELA OPTEREĆENJA KOD MOSTOVA SA VEĆIM BROJEM GLAVNIH NOSAČA U POPREČNOM PRESEKKU

asistent dr Zoran Desovski, dipl.inž.građ.

1989.

TEHNIČKO-TEHNOLOŠKO UNAPREĐENJE GRAĐEVINSKOG KONSTRUKTERSTVA NA IZGRADNJI HRAMA SVETOG SAVE NA VRAČARU U BEOGRADU PRIMENOM METODA TEŠKE GRAĐEVINSKE MONTAŽE, SPECIJALNE TEHNOLOŠKE PODIZNE OPREME, KAO I NOVIH KONSTRUKTIVNIH REŠENJA

Vojislav Marisavljević, dipl.inž.građ.
Dušan Arbajter, dipl.inž.građ.
Milutin Marjanović, dipl.inž.građ.
Dragan Kocić, dipl.inž.građ.
mr Milan Matović, dipl.inž.građ.

1990.

HIDROELEKTRANA "VIŠEGRAD"

Mira Pavlica, dipl.inž.građ.
Fevzija Beganović, dipl.inž.građ.
Mirza Pašić, dipl.inž.građ.
Vladimir Vujošević, dipl.inž.građ.

PRIZNANJA
JUGOSLOVENSKOG DRUŠTVA GRAĐEVINSKIH KONSTRUKTERA

ZA NAJBOLJA OSTVARENJA
U GRAĐEVINSKOM KONSTRUKTERSTVU

„U cilju podsticanja stvaralaštva, boljeg vrednovanja postignutih rezultata i najznačajnijih dostignuća našeg građevinskog konstrukterstva, Jugoslovensko društvo građevinskih konstruktera je ustanovilo posebna godišnja priznanja za najbolja ostvarenja u građevinskom konstrukterstvu u SR Jugoslaviji. Priznanja se dodeljuju za oblast projektovanja i/ili građenja konstrukcija objekata i za oblast nauke i tehnologije u građevinskom konstrukterstvu.“

Priznanja JDGK za najbolja ostvarenja u građevinskom konstrukterstvu dobila su sledeća ostvarenja:

1994.

Za projektovanje i izvođenje konstrukcije objekta:

PODZEMNO ŽELEZNIČKO STAJALIŠTE "VUKOV SPOMENIK"

SAOBRAĆAJNI INSTITUT - CIP
Odgovorni projektanti konstrukcije:
dr Branislav Popović, dipl.inž.građ.
Miloje Kandić, dipl.inž.građ.
Aleksandar Mojsić, dipl.inž.građ.

ENERGOPROJEKT HOLDING
Graditelji konstrukcije:
mr Dragan Gojgić, dipl.inž.građ.
Stanimir Mandić, dipl.inž.građ.
Vladimir Đurić, dipl.inž.građ.
Boško Grubić, dipl.inž.građ.

1996. i 1997.

Iz oblasti projektovanja i izvođenja konstrukcija:

IZVOĐENJE KONSTRUKCIJE DVORANE ZA MALE SPORTOVE FAKULTETA FIZIČKE KULTURE U BEOGRADU

Živorad Dimitrijević, dipl.inž.građ.

IZGRADNJA KOMPLEKSA ZA PROIZVODNJU LAB/LABS U KIRIŠU U RUSIJI

Svetislav Simović, dipl.inž.građ.
Nikola Lujić, dipl.inž.građ.
Novica Kostić, dipl.inž.građ.

Iz oblasti nauke i tehnologije u građevinskom konstrukterstvu:

STRATEŠKO-TEHNOLOŠKI PROJEKAT „UVOĐENJE EVROKODOVA ZA KONSTRUKCIJE U GRAĐEVINSKO KONSTRUKTERSTVO SRBIJE“

Rukovodilac projekta:
prof. dr Života Perišić, dipl.inž.građ.

Rukovodioci potprojekta:
prof. dr Aleksandar Pakvor, dipl.inž.građ.
v.prof. dr Dragan Buđevac, dipl.inž.građ.
prof. dr Dragoslav Stojić, dipl.inž.građ.
prof. dr Milić Milićević, dipl.inž.građ.
prof. dr Mihailo Muravljov, dipl.inž.građ.
prof. dr Petar Anagnosti, dipl.inž.građ.
prof. dr Radomir Folić, dipl.inž.građ.

1998. i 1999.

Iz oblasti projektovanja i izvođenja konstrukcija:

SPORTSKA DVORANA - BEOGRADSKA ARENA

Autori krovne konstrukcije:
prof. dr Milorad Ivković, dipl.inž.građ.
prof. dr Života Perišić, dipl.inž.građ.

prof. dr Mirko Aćić, dipl.inž.građ.
prof. dr Aleksandar Pakvor, dipl.inž.građ.

Projektanti krovne konstrukcije:
Vanja Alendar, dipl.inž.građ., viši stručni saradnik
asis. mr Snežana Marinković, dipl.inž.građ.
Odgovorni projektant:
Savo Formentunović, dipl.inž.građ.

Saradnik na projektu krovne konstrukcije:
Bojan Tepavčević, dipl.inž.građ.

Graditelji konstrukcije:
Živorad Dimitrijević, dipl.inž.građ.
mr Miilan Đoković, dipl.inž.građ.

MOST NA OBILAZNICI AUTOPUTA U BEOGRADU (OSTRUŽNICA) PREKO REKE SAVE

Projektanti:
Za čeličnu konstrukciju
Slobodan Cvetković, dipl.inž.građ.
Danilo Dragojević, dipl.inž.građ.
Za prilazne konstrukcije
Ivanka Kopčalić, dipl.inž.građ.
Stanislav Mojsilović, dipl.inž.građ.

Izvođači:
Za čeličnu konstrukciju
Stanoje Petković, dipl.inž.građ.
Branko Knežević, dipl.inž.građ.
Siniša Bruski, dipl.inž.građ.
Za betonskku konstrukciju
Miroslav Havram, dipl.inž.građ.
Mihajlo Tadić, dipl.inž.građ.
Ranko Petrović, dipl.inž.građ.

MOST NA BARŽAMA PREKO DUNAVA U NOVOM SADU

Radomir Lukić, dipl.inž.građ.
VUKAN Njagulj, dipl.inž.građ.
Đorđe Denčić, dipl.inž.građ.
Miško Gunjača, dipl.inž.građ.
mr Radomir Potić, dipl.inž.građ.

Iz oblasti nauke:

DOKTORSKA DISERTACIJA „PRILOG ANALIZI STABILNOSTI TANKOZIDNIH NOSAČA“

dr Duško Lučić, dipl.inž.građ.

MONOGRAFIJA "METALNE KONSTRUKCIJE"

Autori:
prof. dr Dragan Buđevac, dipl.inž.građ.
asis. mr Zlatko Marković, dipl.inž.građ.
asis. mr Dragana Bogavac, dipl.inž.građ.
asis. mr Dragoslav Tošić, dipl.inž.građ.

2000. i 2001.

Iz oblasti projektovanja i izvođenja konstrukcija:

PROJEKTOVANJE I IZGRADNJA MOSTA PREKO DUNAVA U NOVOM SADU "PETROVARADINSKA DUGA"

Projektanti mosta:
prof. Gojko Nenadić, dipl.inž.građ.
mr Ljiljana Đukić, dipl.inž.građ.

Projektant donjeg stroja:
Vukan Njagulj, dipl.inž.građ.

Projektant montaže:
Dragomir Lukić, dipl.inž.građ.
Miško Gunjača, dipl.inž.građ.

Šef montaže:
Branko Knežević, dipl.inž.građ.

PROJEKAT KONSTRUKCIJE POSLOVNOG OBJEKTA "ZEPTER" INTERNATIONAL - VARŠAVA

Autori:
doc. dr Miroslav Bešević, dipl.inž.građ.
prof. dr Dejan Bajić, dipl.inž.građ.
prof. dr Dragan Buđevac, dipl.inž.građ.

PROJEKTOVANJE I IZGRADNJA MOSTA PREKO REKE VELIKE MORAVE NA DESNOJ TRACI AUTOPUTA E70 KROZ MESTO MIJATOVAC

Projektant mosta:
Vukan Njagulj, dipl.inž.građ.

Projektant montaže:
Miroslav Havran, dipl.inž.građ.

Rukovodilac radova:
Mihajlo Tadić, dipl.inž.građ.

Iz oblasti nauke:

DOKTORSKA DISERTACIJA „GRANIČNA NOSIVOST PRI PROBIJANJU MONTAŽNIH PRETHODNO NAPREGNUTIH PLOČA U OBLASTI IVIČNIH STUBOVA“

dr Snežana Marinković, dipl.inž.građ.

DOKTORSKA DISERTACIJA „UTICAJ VREMENSKIH DEFORMACIJA NA GRANIČNA STANJA ARMIRANOBETONSKIH PLOČA NAPREGNUTIH U SVOJOJ RAVNI“

dr Pero Vujović, dipl.inž.građ.

2002. i 2003.

Iz oblasti projektovanja i izvođenja konstrukcija:

MOST "UNION BRIDGE" PREKO REKE MORAČE U PODGORICI

Autor idejnog rešenja i odgovorni projektant mosta:
mr Željka Radovanović, dipl.inž.građ.

Odgovorni projektant mosta:
dr Pero Vujović, dipl.inž.građ.

Iz oblasti nauke:

DOKTORSKA DISERTACIJA „IZBOČAVANJE LIMENIH NOSAČA POD DEJSTVOM LOKALNOG OPTEREĆENJA“

dr Nenad Marković, dipl.inž.građ.

DOKTORSKA DISERTACIJA „PRILOG ANALIZI VITKIH ARMIRANOBETONSKIH ELEMENATA SA KOSIM SAVIJANJEM“

dr Radomir Zejak, dipl.inž.građ.

DOKTORSKA DISERTACIJA „VIŠEKRITERIJUMSKA ANALIZA SEIZMIČKE OTPORNOSTI KONSTRUKCIJA ARMIRANOBETONSKIH ZGRADA“

dr Đorđe Lađinović, dipl.inž.građ.

2004. i 2005.

Iz oblasti projektovanja i izvođenja konstrukcija:

SANACIJA, REKONSTRUKCIJA, ADAPTACIJA I DOGRADNJA KONSTRUKCIJE P.C. UŠĆE U NOVOM BEOGRADU, NAKON BOMBARDOVANJA 1999. GODINE

Projektanti:
prof. dr Ljubomir Vlajić, dipl.inž.građ.
mr Predrag Blagojević, dipl.inž.građ.
mr Slobodan Grković, dipl.inž.građ.

iz oblasti nauke:

MAGISTARSKA TEZA „PRILOG UTVRĐIVANJU SEIZMIČKE POUZDANOSTI IZVEDENIH ARMIRANO BETONSKIH OBJEKATA“

mr Nataša STOJANOVIĆ, dipl.inž.građ.

2006. i 2007.

Iz oblasti projektovanja i izvođenja konstrukcija:

PROJEKAT DRUMSKOG MOSTA PREKO REKE VISLE U PLOCKU - IZVEDENO STANJE

Projektanti:
akademik prof. dr Nikola Hajdin, dipl.inž.građ.
doc. dr Bratislav Stipanić, dipl.inž.građ.

PUENTE DUARTE REHABILITATION PROJECT IN SANTO DOMINGO

Projektanti:
Slobodan Cvetkovic, dipl.inž.građ.
Stanislav Kolundzija, dipl.inž.građ.
prof. dr Branislav Kolundzija, dipl.inž.građ.

Iz oblasti nauke:

PRILOG REŠENJU PROBLEMA STABILNOSTI DVOPOJASNIH LANČANIČNIH SISTEMA

Dragan Kostić, dipl.inž.građ.

2008. i 2009.

Iz oblasti projektovanja i izvođenja konstrukcija:

NOVI TORANJ NA AVALI. KONSTRUKCIJA TORNJA

prof. dr Šerif Dunica, dipl.inž.građ.
Branislav Životić, dipl.inž.građ.
Aleksandar Bojović, dipl.inž.građ.

SPECIFIČNOSTI IZVOĐENJA OBNOVE TV TORNJA "AVALA"

Goran Milovanović, dipl.inž.građ.
Zoran Mišković, dipl.inž.građ.

Iz oblasti nauke:

PRERASPODELA UTICAJA KOD NAKNADNO KONTINUIRANIH SPREGNUTIH ARMIRANOBETONSKIH NOSAČA TOKOM VREMENA

Snežana Mašović, dipl.inž.građ.

PRORAČUN VITKIH DVOOSNO SAVIJANIH AB STUBOVA

Zoran Brujić, dipl.inž.građ.

2010. i 2011.

Iz oblasti nauke:

DOKTORSKA DISERTACIJA „EKSPERIMENTALNO–TEORIJSKA ANALIZA GRANIČNIH STANJA ARMIRANOBETONSKIH LINIJSKIH NOSAČA OJAČANIH SPREZANJEM SA NSM VLAKNASTIM KOMPOZITIMA“

dr Slobodan Ranković, dipl.inž.građ.

2012. i 2013.

Iz oblasti projektovanja i izvođenja konstrukcija:

NASTAJANJE I RAZRADA IDEJNOG REŠENJA I GRAĐENJE RASKLOPNOG MOSTA „PORT MILENA“

Projektanti:
Goran Tadić, dipl.inž.građ.
Duško Bobera, dipl.inž.građ.
Zoran Luković, dipl.inž.građ.

Iz oblasti nauke:

PONAŠANJE GRUPE ELASTIČNIH MOŽDANIKA KOD SPREGNUTIH NOSAČA OD ČELIKA I BETONA

dr Milan Spremić, dipl.inž.građ.

GRANIČNA NOSIVOST ARMIRANOBETONSKIH GREDNIH NOSAČA OD BETONA SA RECIKLIRANIM AGREGATOM

dr Ivan Ignjatović, dipl.inž.građ.

2014. i 2015.

Iz oblasti nauke:

DOKTORSKA DISERTACIJA „PONAŠANJA CENTRIČNO PRITISNUTIH ELEMENATA SLOŽENOG PRESEKA OD NERĐAJUĆEG ČELIKA“

dr Jelena Dobrić, dipl.inž.građ.

DOKTORSKA DISERTACIJA „NELINEARNA STATIČKA I DINAMIČKA ANALIZA OKVIRNIH ZGRADA PREMA PERFORMANSAMA“

dr Mladen Ćosić, dipl.inž.građ.

DOKTORSKA DISERTACIJA „NOSIVOST ZAVRTNJEVA KAO SREDSTVA ZA SPREZANJE U PREFABRIKOVANIM SPREGNUTIM KONSTRUKCIJAMA OD ČELIKA I BETONA“

dr Marko Pavlović, dipl.inž.građ.

Iz oblasti projektovanja i izvođenja konstrukcija:

ČELIČNA KONSTRUKCIJA ŽELEZNIČKOG MOSTA PREKO VELIKE MORAVE U ĆUPRIJI

SAOBRAĆAJNI INSTITUT - CIP
Projektanti:
Siniša Mihajlović, dipl.inž.građ.
Milorad Markovi, dipl.inž.građ.
Biljana Čolić, dipl.inž.građ.
Dejan Srejić, dipl.inž.građ.
prof. dr Šerif Dunica, dipl.inž.građ.
Marina Pešić, dipl.inž.građ.
Branislav Dašić, dipl.inž.građ.

ATLETSKA DVORANA "GENERAL JOVAN MIŠKOVIĆ" U BEOGRADU

CENTROPROJEKT D.O.O.
Projektanti:
prof dr Zlatko Marković, dipl.inž.građ.
Milomir Živanović, dipl.inž.građ.
doc. dr Jelena Dobrić, dipl.inž.građ.
prof. dr Dragan Buđevac, dipl.inž.građ.

2016. i 2017.

Iz oblasti nauke:

DOKTORSKA DISERTACIJA „PONAŠANJE AKSIJALNO PRITISNUTIH SPREGNUTIH STUBOVA PRI EKSPLOATACIONOM I GRANIČNOM OPTEREĆENJU “

dr Aleksandar Landović, dipl.inž.građ.

DOKTORSKA DISERTACIJA „EKSPERIMENTALNO ISTRAŽIVANJE GRANIČNE NOSIVOSTI OSLONAČKE VEZE OŠUPLJENIH MONTAŽNIH PLOČA“

dr Veljko Koković, dipl.inž.građ, prof dr Dejan Bajić, dipl.inž.građ.

DOKTORSKA DISERTACIJA „NELINEARNA ANALIZA LAMINATNIH KOMPOZITNIH PLOČA I LJUSKI SA DELAMINACIJAMA PRIMENOM MKE“

dr Miroslav Marijanović, dipl.inž.građ.

Iz oblasti projektovanja i izvođenja konstrukcija:

POSLOVNI KOMPLEKS “SIRIUS” U BLOKU 43 NA NOVOM BEOGRADU

STRABAG
Projektanti:
Vladimir Stefanović, dipl.inž.građ.
Igor Petrović, dipl.inž.građ.

PROJEKAT KONSTRUKCIJE POSLOVNOG OBJEKTA U RAJIĆEVOJ

MAŠINOPROJEKAT
Projektanti:
Aleksandar Trajković, dipl.inž.građ.
Ivana Leposavić, dipl.inž.građ.
Tanja Karlaš, dipl.inž.građ.
Vladimir Trajković, dipl.inž.građ.
Bojana Žarković, dipl.inž.građ.
Nenad Nedeljić, dipl.inž.građ.

CONTENTS

PRIZNANJE ZA ŽIVOTNO DELO U GRAĐEVINSKOM KONSTRUKTERSTVU DEJANU BAJIĆU, DIPL. INŽ……..... 2

P-1 *Igor Petrović, Vladimir Stefanović* - POSLOVNI KOMPLEKS "SIRIUS" U BLOKU 43 NA NOVOM BEOGRADU…….. 6

P-2 *Aleksandar Trajković, Ivana Leposavić* - PROJEKAT KONSTRUKCIJE POSLOVNOG OBJEKTA U RAJIĆEVOJ…….. 16

P-3 *Aleksandar Landović* - BEHAVIOR OF AXIALLY COMPRESSED COMPOSITE COLUMNS FOR EXPLOITATION AND ULTIMATE LOADS……..... 25

P-4 *Veljko Koković, Dejan Bajić* - EXPERIMENTAL STUDY ON ULTIMATE CAPACITY OF HCS WITH RESTRAINED SUPPORT CONNECTION…. 35

P-5 *Miroslav Marjanović* - NONLINEAR ANALYSIS OF LAMINATED COMPOSITE PLATES AND SHELLS WITH DELAMINATIONS USING FINITE ELEMENT METHOD…… 46

U-1 *Hugo Corres Peirreti, Freddy Ariñez Fernández, Julio Sánchez Delgado* - FIB MODEL CODE 2020 - CONTENT AND ONGOING PROCESS……... 58

U-2 *František Wald, Marta Kuříková, Lukáš Gödrich, Lubomír Šabatka, Jaromír Kabeláč, Drahoš Kojala* - MULTI LEVEL MEMBER AND CONNECTION DESIGN……. 73

U-3 *David Fernández-Ordóñez Hernández* - CONCRETE PREFABRICATION - LESSONS FROM THE PAST AND ADVANCES FOR THE FUTURE…. 85

U-4 *Milenko Pržulj* - SAVREMENE KONCEPCIJE I KONSTRUKCIJE SPREGNUTIH MOSTOVA……. 97

U-5 *Meri Cvetkovska, Milivoje Milanović, Cvetanka Chifliganec* - FIRE RESISTANCE OF REINFORCED CONCRETE AND STEEL-CONCRETE COMPOSITE STRUCTURES……... 123

S-43 *Bratislav Stipanić* - FACTORS OF IMPORTANCE FOR DURABILITY OF BRIDGES…… 144

S-44 *Srđan Živković, Lela Mitić, Marko Milošević, Nenad Golubović, Matej Kosovel* - THE IMPROVEMENT OF CONSTRUCION SOLUTION FOR PREFABRICATED REINFORCED CONCRETE ELEMENTS CONNECTIONS……... 154

S-45 *Miroslav Marjanović, Mira Petronijević* - PUSHOVER ANALYSIS OF BRIDGES INCLUDING SOIL-STRUCTURE INTERACTION EFFECTS.. 166

S-46 *Kemal Edip, Vlatko Šešov, Julijana Bojadžieva, Toni Kitanovski, Jordanka Čaneva, Dejan Ivanovski* - EFFECTS OF SOIL MODELLING IN SSI PROBLEMS…….. 176

S-47 *Ivan Milićević, Svetlana Nikolić-Brzev* - SEISMIC RETROFITTING OF RC FRAME BUILDINGS BY ADDING NEW RC SHEAR WALLS…… 182

S-48 *Aleksandra Radujković, Igor Džolev, Đorđe Lađinović* - THE CHORD ROTATION CAPACITY OF REINFORCED CONCRETE COLUMNS UNDER MONOTONIC LOADING…… 194

S-49 *Marija M. Janakieska, Kiril Gramatikov, Manja K. Kuzman* - ARCHITECTS' PERCEPTIONS OF ENGINEERED WOOD PRODUCTS IN MACEDONIA……. 202

S-50 *Ksenija Janković, Dragan Bojović, Marko Stojanović, Iva Despotović, Ljiljana Lončar* - CONCRETE PAVING BLOCKS AND FLAGS MADE WITH RECYCLED AGGREGATE FROM PRECAST ELEMENTSTHE… 212

S-51 *Nikola Tošić, Snežana Marinković, Jorge de Brito, Nenad Pecić, Ivan Ignjatović* - LONG-TERM PROPERTIES OF GREEN CONCRETE: TESTING AT THE MATERIAL AND STRUCTURAL LEVEL……... 218

S-52 *Dubravka Bjegović, Nina Štirmer, Ana Baričević* - CONCRETE USED IN LNG STORAGE TANKS……. 228

S-53 *Ksenija Janković, Marko Stojanović, Dragan Bojović, Ljiljana Lončar* - THE INFLUENCE OF POLYPROPYLENE FIBERS ON THE MECHANICAL PROPERTIES OF SHOTCRETE FOR SLOPES……. 237

S-54 *Dragan Nikolić, Snežana Mitrović, Goran Ćirović* - ESTIMATION STRENGTH PROPERTIES OF UHPC…… 245

S-55 *Bojan Milošević, Slobodan Ranković, Žarko Petrović, Marina Mijalković* - OVERVIEW OF EXPERIMENTAL EXAMINATION OF LINEAR GIRDERS MADE OF SELF-COMPACTING CONCRETE……... 255

S-56 *Aleksandar Savić, Marina Aškrabić, Brankica Kovačević, Danijela Pavlović* - PROPERTIES OF SCC MIXTURES WITH COARSE RECYCLED AGGREGATES…… 265

S-57 *Živko P. Cuckić, Vesna Ž. Cuckić, Olga Cuckić* - AUTONOMOUS LOAD-BEARING FRAMEWORK TECHNOLOGY……. 275

S-58 *Mirjana Malešev, Slobodan Šupić, Vlastimir Radonjanin, Mirjana Laban, Miroslava Radeka* - ECO BUILD - SUSTAINABLE USE OF WASTE MATERIALS FROM BIOMASS COMBUSTION……. 282

S-59 *Žarko Lazić, Lev Zaretsky, Gordana Broćeta, Marina Latinović* - HIGH BOND 10-WIRE STRAND…….. 290

S-60 *Aleksandar Radević, Jelena Dragaš, Vedran Carević, Dimitrije Zakić, Mladen Mladenović* - THE INFLUENCE OF DIFFERENT CURING CONDITIONS ON CEMENT AND HIGH VOLUME FLY ASH CONCRETE PROPERTIES……. 300

S-61 *Franc Sinur, Aljoša Šajna, Teja Török Resnik, Jakob Šušteršič* - CONCRETE CONTAINER FOR DISPOSAL OF LOW AND INTERMEDIATE LEVEL RADIOACTIVE WASTE…… 310

S-62 *Zlatko Zafirovski, Milorad Jovanovski, Vasko Gacevski* - TECHNICAL MEASURES FOR THE REHABILITATION IN THE HYDROTECHNICAL TUNNEL ON SASKA RIVER – M. KAMENICA… 319

S-63 *Liljana Dimevska, Meri Cvetkovska, Ana Trombeva Gavriloska, Marijana Lazarevska* - RESIDENTIAL BUILDINGS ANALYSIS ACCORDING TO THEIR ARHITECTURAL AND THERMAL CHARACTERISTICS…… 327

S-64 *Marija Docevska, Leart Taravari, Jose Campos e Matos, Goran Markovski* - QUALITY CONTROL PLAN OF ARCH CONCRETE BRIDGES……... 339

S-65 *Srđan Živković, Marko Milošević* - DIAGNOSTICS OF THE STATE OF STEEL BRIDGE OVER MLAVA RIVER…….. 350

S-66 *Slobodan Cvetković, Ninoslav Milenković* - HERMANOS PATINO BRIDGE IN SANTIAGO DE LOS CABALLEROS – BRIDGE REHABILITATION……. 360

S-67 *Vlastimir Radonjanin, Mirjana Malešev, Ivan Lukić, Slobodan Šupić, Vesna Bulatović, Olivera Bukvić* - ASSESSMENT OF RC STRUCTURE OF PART OF THE "TV-CENTER" RTV ON MISELUK IN NOVI SAD…… 369

S-68 *Miloš Knežević, Ivana Tešović, Duško Lučić, Zlatko Zafirovski, Mladen Muhadinović* - REHABILITATION OF THE RAILWAY TRACK VIRPAZAR-BAR, IN THE TUNNEL “SOZINA“ IN MONTENEGRO…... 379

S-69 *Doncho Partov, Petar Grekov, Vesselin Kantchev* - SURVEY OF THE BURIED REINFORCED CONCRETE ARCH BRIDGE AND ITS APPLICATION IN BULGARIA……..... 389

S-70 *Dunja Radovanović, Nenad Fric* - HOT-DIP GALVANIZING OF STEEL STRUCTURES – POSSIBILITIES AND LIMITATIONS…….. 401

S-71 *Dunja Radovanović, Nenad Fric* - STEEL STRUCTURE CORROSION PROTECTION SYSTEMS ACCORDING TO THE EN ISO 12944 STANDARDS……..... 410

S-72 *Nikola Tošić, Andrija Radović, Bogdan Šakić, Snežana Marinković* - LONG-TERM DEFLECTIONS OF GREEN CONCRETE BEAMS: ANALYTICAL AND NUMERICAL CALCULATIONS……... 420

S-73 *Slobodan Ranković, Bojan Milošević, Žarko Petrović, Marina Mijalković* - TESTING OF HOLLOWED PRESTRESSED ELEMENTS FOR FLOOR SLABS…….. 430

S-74 *Anka Starčev-Ćurčin, Andrija Rašeta, Mirjana Malešev, Danijel Kukaras, Đorđe Lađinović, Miloš Šešlija* - STRENGTH ASSESSMENT OF THE REINFORCED CONCRETE WALL DESIGNED BY STRUT-AND-TIE METHOD…….. 438

S-75 *Svetlana Kostić, Biljana Deretić-Stojanović* - TWO NUMERICAL MODELS FOR NONLINEAR ANALYSIS OF CFT COULUMNS……... 446

S-76 *Nikola Ivanović, Jelena Dobrić, Milan Spremić, Nina Gluhović, Jovana Milovanović* - NON-LINEAR LATERAL BUCKLING ANALYSIS OF ALUMINIUM ALLOY CHANNEL BEAMS…….. 456

S-77 *Todor Vacev, Miloš Milić, Stepa Paunović, Ivan Nešović, Andrija Zorić* - APPLICATION OF NONLINEAR FEA ON LAMINATE STRUCTURES IN CASE OF A WATER TANK V=100 m^3……..... 465

S-78 *Koce Todorov, Ljupčo Lazarov* - STRENGTH, STIFFNESS AND DUCTILITY OF MASONRY INFILLED FRAMES UNDER LATERAL LOADS……..... 475

S-79 *Stefan Kondić, Jelena Dobrić, Nina Gluhović* - DESIGN OF PEDESTRIAN BRIDGE ACCORDING TO EUROCODE 9……... 485

S-80 *Fidan Salihu, Meri Cvetkovska, Ana Trombeva Gavriloska, Milivoje Milanović* - COMPARATIVE ANALYSIS ON FIRE RESISTANCE OF ONE WAY CONTINUOUS RC SLABS ACCORDING TO EC2 AND FEM……... 496

S-81 *Jagoda Kruškonja, Jelena Dobrić, Nina Gluhović* - RESISTANCE AND SERVICEABILITY ANALYSIS OF STEEL FOOTBRIDGE STRUCTURE ACCORDING TO EUROCODE……..... 506

S-82 *Marina Rakočević* - AN INFLUENCE OF THE NUMBER OF LAYERS AND THE THICKNESS OF PLATE ON STRESS-STRAIN STATE IN A LAYERWISE PLATE THEORY……. 516

S-83 *Ana Trombeva-Gavriloska, Marijana Lazarevska, Meri Cvetkovska, Miloš Knežević* - BOND STRESS DISTRIBUTION ALONG CFRP STRENGTHENED RC BEAM…… 522

S-84 *Igor Gjorgjiev, Marija Vitanova* - DAMPING IDENTIFICATION FOR NEW HIGHWAY BRIDGES TESTED UNDER DYNAMIC LOADING…. 530

S-85 *Igor Gjorgjiev, Borjan Petreski, Vlado Micov* - EXPERIMENTAL STUDY OF BEAM-TO-COLUMN CONNECTION FOR PREFABRICATED RC STRUCTURE……..... 541

S-86 *Ilda Kovačević, Sanin Džidić* - POSSIBILITIES FOR PRODUCTION OF HIGH-STRENGTH CONCRETE (HSC) IN BOSNIA AND HERZEGOVINA…….. 549

S-87 *Marija Todorović, Boško Stevanović, Ivan Glišović, Tijana Stevanović* - END-NOTCHED GLULAM BEAMS REINFORCED WITH SCREWS…... 563

S-88 *Dragan Manojlović, Tatjana Kočetov Mišulić, Aleksandra Radujković* - WEIGHTED RESIDUAL METHOD IN ANALYSIS OF TIMBER CONCRETE COMPOSITE SYSTEM……..... 573

S-89 *Vladimir Živaljević, Mitar Đogo, Dušan Kovačević* - FEM ANALYSIS OF THE DYNAMIC TEST BY LOAD OF THE PILE……..... 583

S-90 *Doncho Partov, V. K. Kantchev, Ch. P. Stoyanov* - ANALYSIS OF THE RELAXATION OF A BENDING MOMENT OVER THE SUPPORT IN A CONTINUOUS COMPOSITE BEAM USING INTEGRAL EQUATIONS OF VOLTERRA……... 593

S-91 *Isidora Jakovljević, Saša Kovačević, Nenad Marković* - BUCKLING OF PLATES AND PLATE GIRDERS SUBJECTED TO PATCH LOAD……... 608

S-92 *Isidora Jakovljević, Zlatko Marković, Jelena Dobrić* - NUMERICAL EVALUATION OF FLEXURAL BUCKING OF HOT-FINISHED AND COLD-FORMED EHS COLUMNS……..... 618

S-93 *Nina Gluhović, Milan Spremić, Zlatko Marković* - RECENT RESEARCH ON DUCTILITY OF PERFORATED SHEAR CONNCTORS…….. 627

S-94 *Aljoša Filipović, Jelena Dobrić, Zlatko Marković, Dragan Buđevac, Nenad Fric* - EXPERIMENTAL INVESTIGATION OF COMPRESSED STAINLESS STEEL ANGLE COLUMNS…….. 635

S-95 *Vlastimir Radonjanin, Mirjana Laban, Mirjana Malešev, Slobodan Šupić* - IMPROVING WESTERN BALKANS' RESILIENCE TO HAZARDS BY BUILDING CAPACITY IN HIGHER EDUCATION……. 645

S-96 *Ranko Babić, Lidija Babić, Radomir Folić* - NEW DESIGN OF TUNNEL HOODS FOR HIGH SPEED TRAINS……. 655

S-97 *Predrag Popović* - LESSONS LEARNED FROM MAJOR BRIDGE COLLAPSES…… 664

DGKS AWARDS

FOR THE LIFETIME ACHIEVEMENT IN 2018 YEARS

PRIZNANJE ZA ŽIVOTNO DELO U GRAĐEVINSKOM KONSTRUKTERSTVU DEJANU BAJIĆU, DIPL.INŽ.

Dejan Bajić je rodjen 02.04.1950. godine u Beogradu, gde je završio osnovnu školu i gimnaziju sa odličnim uspehom. Za pokazani uspeh iz matematike i fizike tokom gimnazijskog školovanja nagradjen je diplomom "Mihajlo Petrović Alas".

Na Gradjevinski fakultet u Beogradu upisao se školske 1968/69 godine. Diplomirao je februara 1974. godine, na Odseku za konstrukcije, sa prosečnom ocenom tokom studija 8,75. Diplomski rad iz predmeta Betonske konstrukcije odbranio je sa ocenom 10,0. Poslediplomske studije, Odsek za konstrukcije, upisao je školske 1974/75. godine i položio sve predvidjene ispite sa maksimalnom ocenom 10,0.

Magistarski rad "Analiza deformacija elemenata armiranobetonskih konstrukcija pod dejstvom kratkotrajnog eksploatacionog opterećenja" odbranio je 11.05.1982 godine na Gradjevinskom fakultetu u Beogradu.

Doktorsku disertaciju "Prilog nelinearnoj analizi armiranobetonskih linijskih elemenata" odbranio je 27.12.1985. godine, takodje na Gradjevinskom fakultetu u Beogradu, pred komisijom: prof. N. Hajdin, prof. M. Ivković, prof. M. Aćić.

Odmah po diplomiranju, zaposlio se u Zavodu za Betonske konstrukcije Gradjevinskog fakulteta, kao stručni saradnik. Za asistenta pripravnika na grupaciji predmeta Betonske konstrukcije izabran je 30.05.1975. godine. U zvanje asistenta izabran je 31.3.1983. godine, a u zvanje docenta 25.11.1986. U zvanje vanrednog profesora izabran je 16.04.1992. godine, a u zvanje redovnog profesora na grupaciji predmeta Betonske konstrukcije 10.10.2001. godine.

Svoj radni vek proveo je na Gradjevinskom fakultetu. Penzionisan je 01.10.2015. godine.

Rad na Gradjevinskom fakultetu Univerziteta u Beogradu

Tokom zaposlenja držao je predavanja i vežbe iz grupacije predmeta Betonske konstrukcije i Betonski mostovi na svim Odsecima fakulteta. Držao je i vežbe na Gradjevinskom odseku Fakulteta tehničkih nauka u Novom Sadu, kao i predavanja iz premeta Betonski mostovi na Gradjevinskom fakultetu u Subotici. Na poslediplomskim studijama držao je deo predavanja iz predmeta Teorija plastičnosti.

Ističe se njegovo angažovanje u radu sa studentima pri izradi Diplomskih zadataka. Na predmetima Betonski mostovi i Betonske konstrukcije kod profesora Bajića je u roku od dvadeset godina diplomiralo preko 700 studenata. Takodje je bio više puta mentor i član Komisija za odbranu magistarskih radova i doktorskih disertacija.

Tokom nastavne delatnosti napisao je knjigu Armirani beton 3 - Elementi armiranobetonskih konstrukcija (sa prof. Živoradom Radosavljevićem), koja je doživela više izdanja. Takodje je u saradnji sa saradnicima (Drago Ostojić i Snežana Marinković) napisao dve zbirke ispitnih zadataka iz betonskih konstrukcija za Odsek za konstrukcije i Odsek za hidrotehniku. Ima učešće u izradi 3 monografije.

Ima objavljeno 65 radova u zbornicima i časopisima u zamlji i inostranstvu.

Učestvovao je u izradi više naučno - istraživačkih tema na Gradjevinskom fakultetu u Beogradu.
Prof.Bajić je bio dugogodišnji šef katedre za Betonske konstrukcije, bio je Prodekan Gradjevinskog fakulteta i Predsednik Jugoslovenskog društva gradjevinskih konstruktera (2006 -2010 god.). Bio je jedan od ispitivača za polaganje stručnog ispita pri Savezu inženjera i tehničara. Bio je duže vreme član Republičke revizione komisije.

Stručni rad na Gradjevinskom fakultetu

Naročito se ističe njegovo učešće (samostalno ili sa saradnicima) u izradi Idejnih i Glavnih projekata konstrukcija. Isprojektovao ih je 140, od kojih je 78 uspešno izvedeno.
Ima uradjeno preko 670 revizija objekata (mostova, rezervoara, zgrada, silosa, hala).
Pojavio se u nekoliko konkursa za mostovskle konstrukcije, bilo kao učesnik ili kao član žirija (novi most Beška, most na Adi).
Dobitnik je priznanja Jugoslovenskog društva gradjevinskih konstruktera za najbolje ostvarenje za 2000. i 2001. godinu za Projekat konstrukcije poslovnog objekta ZEPTER u Varšavi (sa prof Miroslavom Beševićem i prof. Draganom Budjevcem).

Učešće kao autora ili koautora u važnijim izvedenim glavnim projektima:

- Glavni projekat konstrukcije zgrade Srpskog narodnog pozorišta u Novom Sadu (sa M.Aćićem i D.Najdanovićem),
- Idejni i glavni projekat konstrukcije za šest hangara za helikoptere aerodroma u Kuvajtu (sa G.Nenadićem, M.Ivkovićem i M. Djurdjevićem),
- Glavni projekat konstrukcije objekta Privredno-sportskog centra MEJDAN u Tuzli, sa velikom i malom dvoranom univerzalne namene (sa A.Pakvorom, D.Najdanovićem i S.Cvetkovićem),
- Idejni i glavni statički proračun konstrukcije sinhrolifta i dokova ALAJ-BEG, Izmir, Turska (sa A.Babovićem, Ž.Perićićem, A.Pakvorom i D.Najdanovićem)
- Idejni i glavni projekat konstrukcije skladišta Robne kuće BEOGRAD, površine 100x160m (sa M.Ivkovićem, M.Aćićem i D.Najdanovićem).
- Glavni projekat konstrukcije poslovne zgrade AEROINŽENJERING-a na Novom Beogradu (sa R.Obradovićem, V.Alendarom i S.Brčićem),
- Glavni projekat konstrukcije zadnjeg kalkanskog rama hangara na Surčinu (sa M.Ivkovićem i B.Horvatovićem),
- Glavni projekat vodotornja PROGAR zapremine 2800 m3 u Boljevcima kod Beograda (sa V.Alendarom, D.Najdanovićem i J.Pregerom),
- Glavni projekat konstrukcije potpornih zidova na ulasku i izlasku iz tunela Lipik i Železnik, od montažnih armiranobetonskih elemenata (sa Z,Arsićem),
- Glavni projekat rekonstrukcije galerije ATELJE-a 212 u Beogradu,
- Glavni projekat konstrukcije sportskog centra "ADA" u Pljevljima (sa V.Matovićem i A.Pavićem),
- Glavni projekat konstrukcije poslovnog objekta u Nušićevoj ulici (sa M.Lazovićem),
- Glavni projekat rekonstrukcije sportske dvorane "Borac" u Čačku (sa G.Nenadićem i D.Budjevcem),
- Glavni projekat konstrukcije sportske dvorane u Dimitrovgradu (sa G.Nenadićem),

- Glavni projekat konstrukcije poslovno - stambenog objekta u ulici Požeškoj br.56-60 u Beogradu, površine oko 6500 m2 (sa B.Milosavljevićem i M.Stojanovićem)
- Tehničko rešenje ojačanja postojeće armiranobetonske konstrukcije nadstrešnice na autobuskom stajalištu „Zeleni venac" radi prihvatanja povećanog opterećenja (sa M.Muravljovom),
- Glavni projekat konstrukcije poslovnog objekta ZEPTER u Vrašavi (Poljska) sa M.Beševićem i D.Budjevcem,
- Glavni projekat konstrukcije nadogradnje zgrade Fakulteta tehničkih nauka u Novom Sadu (sa B.Stevanovićem i N.Stojanović),
- Glavni projekat konstrukcije stambeno-poslovnog objekta u ulici Strahinića Bana br.21 u Beogradu, površine 3800 m2(sa B.Milosavljevićem i M.Stojanovićem)
- Glavni projekat konstrukcije stambeno-poslovnog objekta u ulici Begejskoj u Beogradu, površine 6000 m2(sa S.Marinković, M.Stojanovićem i B.Gligićem),
- Glavni projekat konstrukcije sportske dvorane u Smederevu (sa G.Nenadićem i M.Stojanovićem),
- Statički proračun konstrukcije mosta KOGLJAHERBRUCKE, Austrija - kontinualni prednapregnuti ram, raspona 26+35+35+26 m (sa M.Lazovićem, B.Milosavljevićem, M.Stojanovićem, D.Pecom i B.Tepavčevićem),
- Glavni projekat adaptacije i rekonstrukcije objekta pozorišta "Madlenianum" u Zemunu (sa M.Muravljovom),
- Glavni projekat konstrukcije poslovno - stambenog objekta u uglu ulica Golsvortijeve i Hadži Djerine u Beogradu (sa S.Marinković i V.Majstorović)
- Glavni projekat konstrukcije objekta "METALS BANKA" u Novom Sadu (sa B.Gligićem, B.Milosavljevićem i M.Stojanovićem),
- Glavni projekat konstrukcije hotelsko - poslovnog objekta (Ivanijum) u Balkanskoj br.18 u Beogradu (sa M.Lazovićem i M.Stojanovićem),
- Glavni projekat konstrukcije poslovnog objekta (trgovina i ugostiteljstvo) hotel "Centar", Novi Sad, na uglu Jevrejske i Uspenske ulice (sa I.Ignjatovićem).

Važnije tehničke kontrole:

- Tehnička kontrola mosta preko Drine Pavlovića ćuprija,
- Tehnička kontrola konstrukcije objekta ZEPTER u ulici Kralja Petra u Beogradu,
- Tehnička kontrola Glavnog projekta konstrukcije novog Jugoslovenskog dramskog pozorišta u Beogradu,
- Tehnička kontrola konstrukcija mosta Zemun - Borča (sa M.Muravljovom).

Prof.dr Dejan Bajić, diplomirani inženjer gradjevinarstva, je nesumnjivo jedan od naših najistaknutijih konstruktera u oblasti betonskih konstrukcija. Ime Dejana Bajića ostaće upamćeno medju njegovim studentima, kao i u široj gradjevinskoj struci.

P1 – P5

DGKS AWARDS

FOR THE BEST PROFESSIONAL AND SCIENTIFIC ACHIEVEMENTS IN 2016 AND 2017 YEAR

ДГКС Друштво грађевинских конструктера Србије
ASES Association of Structural Engineers of Serbia
P-1
15. KONGRES
6-8. 9. 2018. Zlatibor

Igor Petrović[1], *Vladimir Stefanović*[2]

POSLOVNI KOMPLEKS "SIRIUS" U BLOKU 43 NA NOVOM BEOGRADU

Rezime:

Austrijska kompanija "Strabag" je u sastavu poslovnog kompleksa „Sirius" izgradila preko 26.000 m2 poslovnog prostora vrhunskog kvaliteta prema najsavremenijim standardima. Spratnost objekta je 2PO+P+8. Bruto površine nadzemnog dela iznose oko 18.500 m2, a garaža oko 7.800 m2. Konstruktivni armirano-betonski sistem čine međuspratne konstrukcije direktno oslonjene na stubove i zidove stepenišnih i liftovskih jezgara. U garažnom delu po obodu objekta je izvedena zaštitna konstrukcija u vidu dijafragme koja istovremeno vrši oslonačku funkciju za nadzemni deo objekta. Objekat je fundiran na temeljnoj ploči oslonjenoj na naglavne grede, šipove i dijafragme. Vrlo uspešno je primenjen sistem „Bela kada" (koncept koji omogućava vodo-zaptivenost podzemnih delova konstrukcije).

Ključne reči: poslovni objekat, armirano–betonska konstrukcija, garaža, dijafragma, bela kada

BUSINESS COMPLEX "SIRIUS" IN BLOCK 43, NEW BELGRADE

Summary:

Austrian company "Strabag" was general Contractor on the business complex "Sirius" which consists of 26,000 m2 of office space of top quality according to the most modern standards. Levels are 2UG+GF+8. The gross area of the above-ground part is about 18,500 m2, and the garage is about 7,800 m2. The constructive reinforced-concrete system consists of flat slabs directly supported by the columns and walls of the staircase and lift cores. A protective structure in the form of a diaphragm wall is performed in the garage around the perimeter of the building, which simultaneously performs the support function for the above-ground part of the building. Foundation structure consists of foundation slab supported by cap beams, piles and diaphragm walls. The "White tank" system (concept that ensures water-tightness of underground structures) was successfully implemented.

Key words: office building, reinforced-concrete structure, garage, diaphragm wall, white tank

[1] *Diplomirani inženjer građevine, Inženjer gradilišta, Strabag d.o.o., Milutina Milankovića 3b, igor.petrovic@strabag.com*
[2] *Diplomirani inženjer građevine, Rukovodilac projekta, Strabag d.o.o., Milutina Milankovića 3b, vladimir.stefanovic@strabag.com*

1. OPIS KONSTRUKCIJE OBJEKTA

Noseća konstrukcija objekta je armirano-betonska. "Sirius" se sastoji od dve nadzemne zgrade (A i B) sa osam spratova koje su povezane zajedničkom garažom na dva nivoa.

1.1. OBJEKAT "A"

Konstrukciju objekta "A" čine armirano-betonske ploče debljine d=26 cm, oslonjene direktno na stubove i zidove d=20 cm i d=25 cm.

Po obimu objekta su izvedene fasadne/parapetne grede dimenzija 20/128 cm koje se oslanjaju na fasadne stubove 40/40 cm na osnom rastojanju od 2.70 m.

U okviru stepenišnih jezgara, za vertikalnu komunikaciju kroz objekat, izvedena su stepeništa kao kose armirano-betonske ploče d=18 cm.

Bruto površina tipske osnove iznosi 1190 m2.

1.2. OBJEKAT "B"

Konstrukciju objekta "B" čine armirano-betonske ploče debljine d=22 cm, oslonjene direktno na stubove i zidove d=20 cm i d=25 cm. Srednji stubovi su dimenzija 55/55 cm a fasadni 40/40 cm na osnom rastojanju od 2.70 m.

Po obimu objekta su izvedene fasadne/parapetne grede dimenzija 20/124 cm koje se oslanjaju na fasadne stubove.

U okviru stepenišnih jezgara, za vertikalnu komunikaciju kroz objekat, izvedena su stepeništa kao kose armirano-betonske ploče d=18 cm.

Bruto površina tipske osnove iznosi 740 m2.

1.3. GARAŽA

Konstrukciju garaže čine armirano-betonske ploče debljine d=28 cm, oslonjene direktno ili preko kapitela d=56 cm na stubove i zidove d=20 cm i d=25 cm. Po spoljnom obimu objekta ploča -1 je oslonjena na armirano-betonsku dijafragmu d=60 cm. Za povezivanje dva nivoa garaže su izvedene dve rampe kao kose betonske ploče d=28 cm koje se bočno oslanjaju na betonske zidove.

U okviru stepenišnih jezgara, za vertikalnu komunikaciju kroz objekat, izvedena su stepeništa kao kose armirano-betonske ploče d=18 cm.

Armirano-betonska ploča prizemlja je debljine d=28 cm, oslonjena direktno ili preko kapitela (d=60 cm) na stubove i armirano-betonske zidove jezgara d=25 cm i d=20 cm.

Bruto površina jedne osnove iznosi 3900 m2.

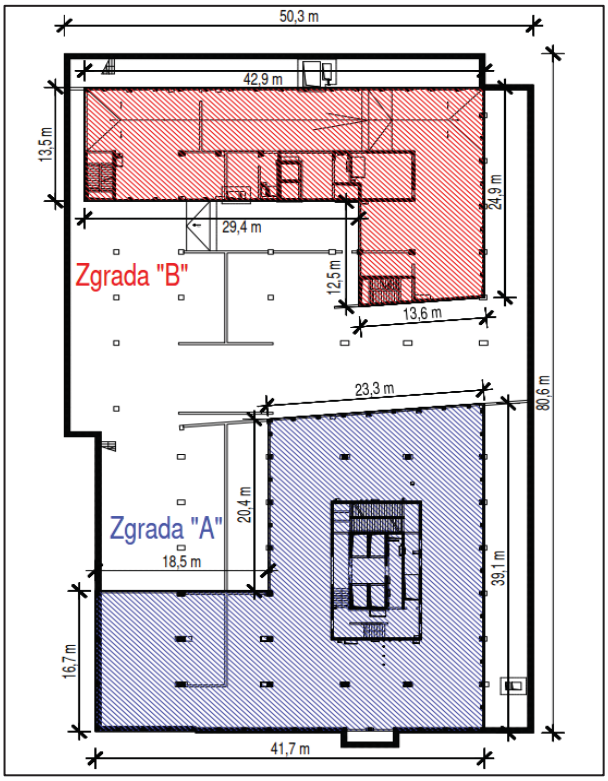

Slika 1 – Osnova garaže sa pozicijama zgrada "A" i "B"

Slika 2 – Izgled Siriusa "danas"

2. FUNDIRANJE OBJEKTA

Objekat je fundiran u geotehničkom profilu koji je karakterističan za celu teritoriju Novog Beograda. Na površini je nasip od refuliranog peska debljine do 3.0 m ispod kojeg zaleže peskovita prašina. Na dubinama većim od 14.0 m se nalaze jezerski sediment (šljunkovi).

2.1. OPIS TEMELJNE KONSTRUKCIJE

Temeljna konstrukcija objekta je fundirana na CFA šipovima φ 600 mm. Baze šipova su formirane u sloju aluvijalno jezerskih sedimenata. Usvojena je dozvoljena nosivost 1500 kN za CFA šipove prečnika φ 600 mm.

Potreban broj i raspored šipova određen je na osnovu uticaja od stubova i zidova objekta. Usvojeno je ukupno 337 (tristatridesetsedam) CFA šipova.

Preko šipova su izvedene podužne i poprečne naglavne grede. Podužne i poprečne naglavne grede su raspoređene tako da se ose stubova i zidova poklapaju sa osama naglavnih greda. Naglavne grede su dimenzija b/d=100/100 cm. Iznad podužnih i poprečnih naglavnih greda nalazi se temeljna ploča, debljine 55 cm. Temeljna ploča je kontinualnom izolacijom odvojena od naglavnih greda.

Slika 2 – Tehnologija izvođenja CFA šipova

3. ZAŠTITNA KONSTRUKCIJA – DIJAFRAGMA

Obezbeđenje iskopa temeljne jame je izvedeno uz pomoć zaštitne obimne konstrukcije od kontinualnih "zidova u tlu"- dijafragmi. Usled položaja podzemne građevinske linije kao i zahteva investitora za maksimalnom zauzetošću podzemnih etaža, odlučeno je da zaštitna konstrukcija bude stalnog karaktera tj. sastavni deo konstrukcije objekta bez dodatnih unutrašnjih zidova do same dijafragme.

3.1. OPIS ZAŠTITNE KONSTRUKCIJE

Razmatrano je nekoliko varijantnih rešenja potporne konstrukcije i izvedeno je najpovoljnije rešenje uzimajući u obzir postojeću situaciju na terenu kao i predviđeni način i dubinu fundiranja novoprojektovanog objekta.

Kruna dijafragme iznosi 74.09 mnv sa strane prema bulevaru Milutina Milankovića, dok se na ostalim stranama nalaziti na koti 71.59 mnv. Radni plato se formirao na koti 74.09 mnv prema ulici Milutina Milankovića, odnosno na ostalim stranama 71.59 mnv kako bi se pri izradi uvodnica i iskopu rovova dijafragmi olakšala kontrola iskopa i montaža koševa armature. Da bi se uradio široki iskop za formiranje radnog platoa po obimu temeljne jame je izvedena privremena škarpa. Ova škarpa se radila u nagibu 1,75H : 1V obzirom da je reč o privremenom rešenju i relativno plitkom iskopu.

Preko izvedenih lamela vertikalnog zida izvedene su vezne grede dimenzija 60x100 cm, odnosno 60x60 cm čiji je zadatak da ove pojedinačne lamele poveže u jedinstvenu konstruktivnu celinu.

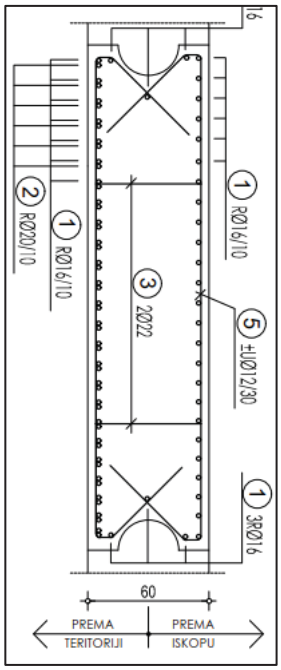

Slika 3 – Plan armature tipske lamele

Slika 4 – Betoniranje dijafragme

3.2. RAZUPIRANJE DIJAFRAGME

Da bi se sprečila velika horizontalna pomeranja, koja se pojavljuju u varijanti računskog modela konzolne podgrade, izrađena je konstrukcija od čeličnih profila za preuzimanje horizontalnih sila.

Primenjena su tri tipa razupiranja zaštitne konstrukcije. Prvi tip je čelični sklop koji se postavlja u horizontalnoj ravni u visini naglavne grede a vezuju se za anker ploče koje su na predhodno fiksirane za naglavne grede i dijafragme, na delu prema bulevaru Milutina Milankovića gde je viša dijafragma. Montirane su čelične šavne cevi Ø406.4 x 12 mm i Ø609.6 x 14.2 mm. Podvlake prema lamelama dijafragmi su urađene od profila HEB (IPB) 400 i 2xHEB (IPB) 400. Drugi tip razupiranja su dva ugaona razupirača koji se postavljaju u horizontalnoj ravni u visini naglavne grede dijafragmi a vezuju se zavarivanjem za anker ploče koje su predhodno fiksirane za naglavne grede (Slike 5 i 6). Za razupirače su usvojene čelične šavne cevi Ø406.4 x 12 mm i Ø406.4 x 14.2 mm (Slika 7). Za razupirač koji je postavljen u horizontalnoj ravni u visini naglavne grede dijafragmi prema Železničkoj stanici je izvedena čelična šavna cev Ø273 x 8 mm.

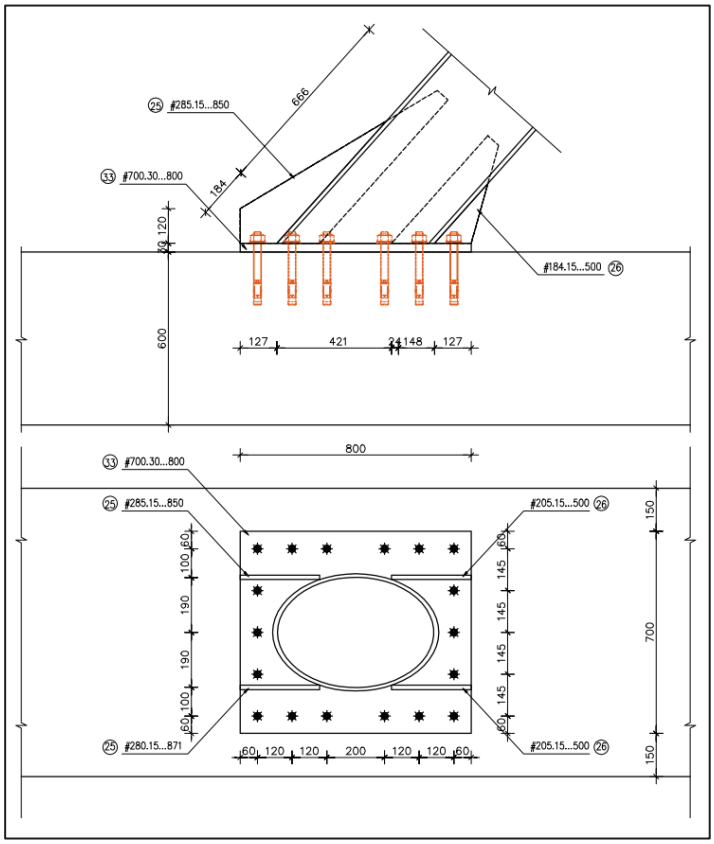

Slika 5 – Detalj veze čelične konstrukcije za razupiranje i naglavne grede

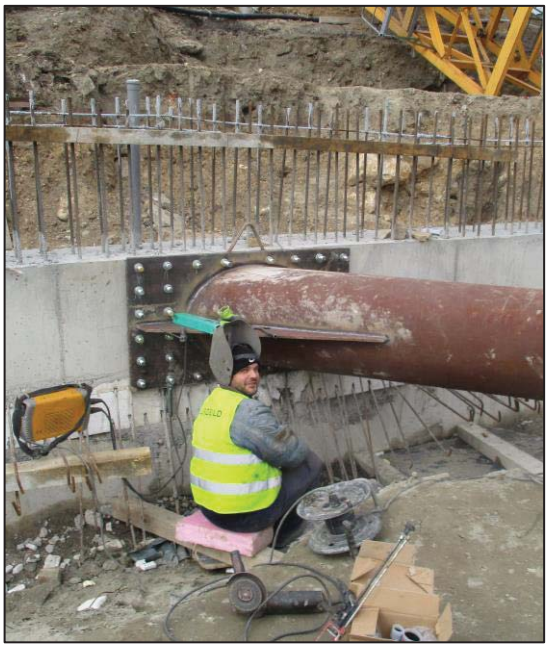

Slika 6 – Veza horizontalnog razupirača i naglavne grede dijafragme

Slika 7 – Razuporna konstrukcija dijafragme

4. BELA KADA

Vrlo uspešno je primenjen sistem „Bela kada“, tj. koncept za izvođenje podzemnog dela armirano-betonske konstukcije kojim je obezbeđena otpornost objekata na uticaje aktivnog hidrostatičkog pritiska prodora vode preko ugradnje vodonepropusnog betona i adekvatnih detalja izolacije. Izvedeni system je obuhvatio dobar kvalitet, ugradnju i negu betona i odgovarajući tretman prekida betoniranja. Izvršena je ugradnja kvalitetnog betona sa visokim vodootpornim svojstvima ka i pravilan izbor tehnologije proizvodnje, ugradnje i nege svežeg betona.

Sistem „Bela kada“ je postignut kombinacijom više različitih & kompatibilnih tehnoloških postupaka / detalja hidroizolacije.

4.1. DETALJ SPOJA DVE SUSEDNE LAMELE DIJAFRAGME

Rupe ϕ 56 mm su naknadno bušene na spojevima dve susedne lamele dijafragme i injektirane bentonitskom smešom pod velikim pritiskom.

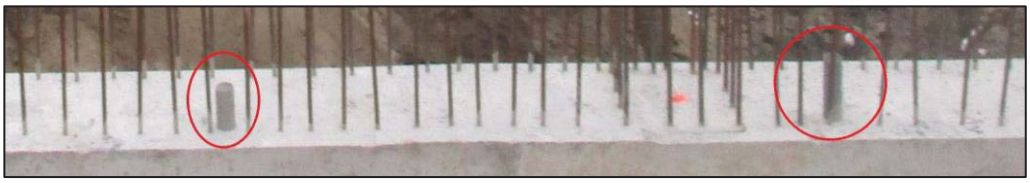

Slika 8 – Plastične cevi ostavljane u naglavnim gredama kao vođice za naknadno bušenje spoja lamela dijafragmi

4.2. DETALJ IZOLACIJE TEMELJNE PLOČE, SPOJA TEMELJNE PLOČE I DIJAFRAGME KAO I DETALJ PREKIDA BETONIRANJA TEMELJNE PLOČE

Izolacija temeljne ploče je izvedena u vidu bentonitske membrane položene na sloj mršavog betona.

Spoj temeljne ploče i dijafragme je rešen postavljanjem bubreće trake i creva za injektiranje (za slučaj naknadnog injektiranja).

Prekidi betoniranja temeljne ploče su izolovani korišćenjem Waterbar traka (Slika 10).

4.3. DETALJ SPOJA DIJAFRAGME, NAGLAVNE GREDE I PLOČE NIVOA -1 KAO I DETALJ SPOJA NAGLAVNE GREDE I OBODNOG ZIDA

Spoj naglavne grede i dijafragme je rešen postavljanjem bubreće trake i creva za injektiranje (za slučaj naknadnog injektiranja).

Ploča prizemlja, obodni zid iznad naglavne grede i naglavna greda su izolovani kontinualno sa spoljne strane „crnom“ izolacijom i adekvatnom zaštitom iste (Slika 9).

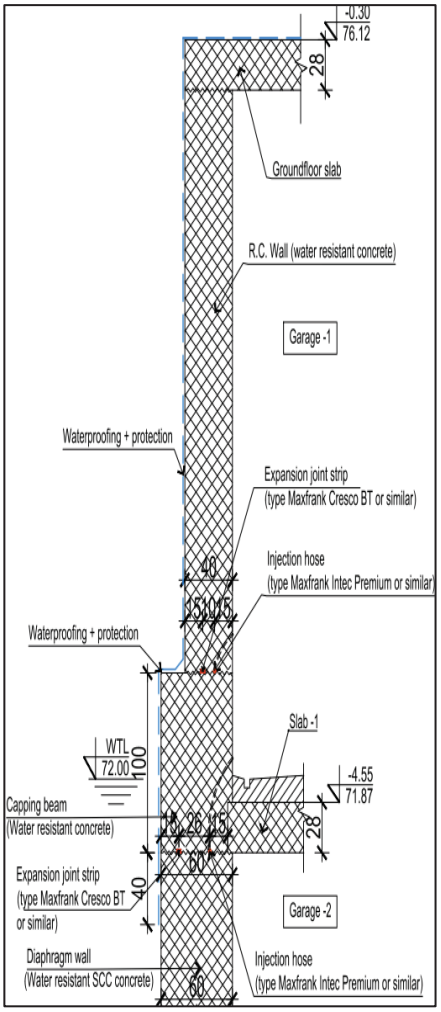

Slika 9 – Detalj spoja dijafragme, naglavne grede i ploče nivoa -1

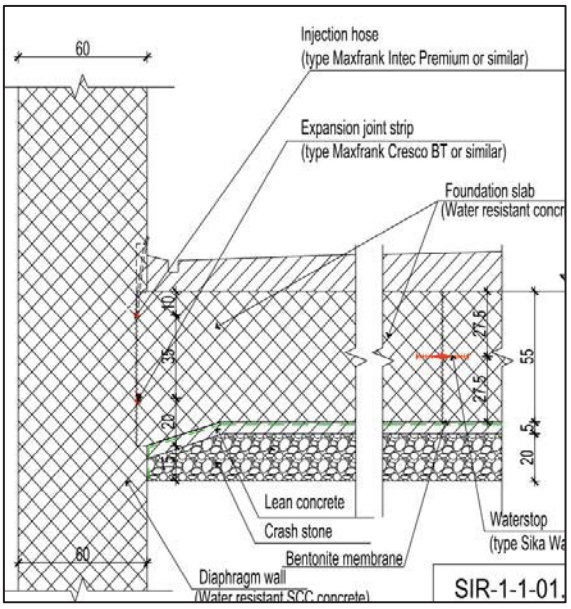

Slika 10 – Detalj izolacije temeljne ploče i spoja temeljne ploče i dijafragme

LITERATURA

[1] GEOTECHNICAL ENGINEERING OFFICE / Civil Enginering and Development Department / The Government of the Hong Kong / Special Administrative Region : Foundation design and construction. GEO PUBLICATION No. 1/2006, Hong Kong 2006.

[2] R.S. Narayanan, C.H. Goodchild : Concrete Basements. MPA The Concrete Centre, Surrey 2012.

[3] Implenia Spezialtiefbau GmbH : DIAPHRAGM WALLS, CUT-OFF WALLS AND SLURRY WALLS. Mannheim 2013.

[4] Ing. Erwin Girsch : Richtlinien Dichte Schlitzwände und Bohrpfähle. Wien 2013.

[5] Stevan Stevanović : Fundiranje 1. Naučna knjiga, Beograd 2010.

[6] The Institution of Structural Engineers : Standard Method of Detailing Structural Concrete. The Institution of Structural Engineers, London 2006.

[7] Dejan Bajić, Živorad Radosavljević : Armirani beton 3. IRO Građevinska knjiga. Beograd 1988.

ДГКС Друштво грађевинских конструктера Србије
ASES Association of Structural Engineers of Serbia
P-2
15. KONGRES
6-8. 9. 2018. Zlatibor

Aleksandar Trajković[1], Ivana Leposavić[2]

PROJEKAT KONSTRUKCIJE POSLOVNOG OBJEKTA U RAJIĆEVOJ

Rezime:

Kompleks u Rajićevoj nalazi se u najužem istorijskom jezgru Beograda, između ulica Knez Mihailove, Uzun Mirkove, Kralja Petra, Rajićeve i Tadeuša Košćuška.
Ceo kompleks je bruto površine oko 58.000m² (oko 29.200m² podzemno, oko 28.800m² nadzemno). Sastoji od tri glavne celine: podzemne, troetažne garaže koja se prostire ispod celog kompleksa, poslovnog (trgovinskog) dela koji se sastoji od tržnog centra sa 72 lokala i hotelskog dela sa 125 soba koji nije predmet ovog opisa ali se spominje zbog boljeg sagledavanja. U ovom radu je dat prikaz projektovanja konstrukcije garaža i tržnog centra.

Ključne reči: tržni centar,armirano-betonska konstrukcija,čelična konstrukcija

STRUCTURAL DESIGN OF COMMERCIAL BUILDING IN RAJICEVA STREET

Summary:

Complex on Rajiceva Street occupies a central location in the historic district of Belgrade, bordered by Knez Mihailova, Uzun Mirkova, Kralja Petra, Rajiceva and Tadeusa Koscuska Streets.
The complex overall has the gross area of around 58.000m² (approx. 29.200m² below grade and approx. 28.800m² above grade plane). It consists of three main units: underground parking garage, extending underneath the entire complex; business (mercantile) part, comprising a mall with 72 leasable spaces; and a hotel part with 125 room, which is not covered herein, but is mentioned for better understanding of the matter. This paper offers an overview of the parking garage and mall design process.

Key words: shopping mall, reinforced concrete structure, steel structure.

[1] dipl.inž.građ., glavni inženjer struke, SAM PROJEKT BIRO d.o.o., Šumatovačka 27, Beograd.
[2] dipl.inž.građ., vodeći projektant, Mašinoprojekt Kopring a.d., Dobrinjska 8a, Beograd.

1. UVOD

Poslovni kompleks u Rajićevoj nalazi se u najužem istorijskom jezgru Beograda, između ulica Knez Mihailove, Uzun Mirkove, Kralja Petra, Rajićeve i Tadeuša Košćuška.

Ceo kompleks je bruto površine oko 58.000 m² (oko 29.200 m² podzemno, oko 28.800 m² nadzemno). Sastoji od tri glavne celine: podzemne, troetažne garaže koja se prostire ispod celog kompleksa, poslovnog (trgovinskog) dela koji se sastoji od tržnog centra sa 72 lokala i hotelskog dela sa 125 soba koji nije predmet ovog opisa.

Rad na ovom projektu započet je u septembru 2006. godine. Građevinska dozvola je dobijena 2009. godine i Investitor je počeo sa radovima na pobijanju šipova radi zaštite susednih objekata. U periodu 2012-2014. godine dolazi do prekida radova. Krajem 2014. godine projekat se ponovo pokreće, radi se izmena projektne dokumentacije zbog dodatnih zahteva Investitora i počinju radovi na izgradnji objekta.

Investitor poslovnog kompleksa je Izraelska kompanija A.B.D.

Projekat je uradio Masinoprojekt Kopring.

Autori su akademik Milan Lojanica i profesor Vladimir Lojanica a odgovorni projektant arhitekture je Sonja Pešterac, d.i.a.

Odgovorni projekanti konstrukcije su Aleksandar Trajkovic, d.i.g. i Ivana Leposavic, d.i.g., Projektanti konstrukcije koji su učestvovali na ovom projektu su Tanja Karlaš, d.i.g., Nenad Nedeljić, d.i.g., Vladimir Trajković, d.i.g., Bojana Žarković, d.i.g.

Objekat je izvela kompanija STRABAG sa kooperantima.

Na projektu konstrukcije učrstvovalo je više projektanata nego što je pomenuto. Prvi Idejni projekat iz 2006. radila je Ranka Jovanović,d.i.g. pa je nastavio Aleksandar Hadži Antić,d.i.g. koji je kao odgovorni projektant bio na ovom projektu do sredine 2014, Marko Milovanović,d.i.g., Mirko Minić,d.i.g., Marko Radović,d.i.g. i Srbobran Stanbolić,d.i.g.

2. ARMIRANO-BETONSKA KONSTRUKCIJA

Konstrukcija objekta je kombinovana armiranobetonska i čelična konstrukcija.

Objekat je nepravilnih osnova, razigrane geometrije i očigledno komplikovan, a sve zbog multifunkcionalnih zahteva korisnika objedinjenih sa arhitektonskim oblikovanjem. Osnovni raster armiranobetonske konstrukcije je 8.0x8.0 m sa varijacijama rastera od 4.0x8.0 m, do 12.0x8.0 m.. Spratne visine su 4.5 m i 5.0m, a visina od prizemlja do prvog sprata poslovnog dela je 5.3 m. Objekat je sa velikim brojem denivelacija armiranobetonskih tavanica po etažama. Denivelacije su uslovljene arhitektonskim i funkcionalnim zahtevima, a konstrukteri su izasli u susret tim zahtevima. Pojedine armiranobetonske tavanice su oslonjene tako što su faktički obešene o zidove ili grede. Zbog obezbeđivanja uslova oslanjanja čeličnih delova konstrukcije na armiranobetonski deo konstrukcije, kao i konstrukcije za nošenje fasada, postoji veliki broj ugradbenih elemenata. Objekat obiluje erkerima i konzolnim ispustima.

Kompletna nadzemna armiranobetonska konstrukcija izvedena je od betona marke MB40. Podzemne armiranobetonske tavanice suterena, nivoa P1 i P2 su izvedene od betona MB30. Armiranobetonski zidovi podzemnih etaza izvedeni su od betona marke MB30 i MB40. Svi podzemni stubovi su MB40. Kompletna konstrukcija je livena na licu mesta.

Podzemni deo objekta je građen unutar konstrukcije koja je izvedena kao zaštita iskopa temeljne jame i susednih objekata. Ova konstrukcija se sastoji od zavese armiranobetonskih šipova. Izmedju šipova je izvedena armiranobetonska zid zavesa koja je podloga za hidroizolaciju. Time je definisana spoljna kontura konstrukcije kompleksa.

Podzemni deo je projektovan bez dilatacija.

Slika 1 – Objekat u izgradnji

Objekat je građen tako što je izvršen široki iskop unutar zavese šipova. Zbog velike dubine ukopavanja i odluke da se radi široki iskop do kote fundiranja, šipovi su prihvaćeni sa tri reda geotehničkih sidara, u visinama koje odgovaraju približno visinama tavanica podzemnih etaža. Izradom vertikalne i horizontalne konstrukcije odozdo na gore sukcesivno su ukidani nizovi geotehnickih sidara.

Deo konstrukcije uz biblioteku grada Beograda je povezan sa redosledom izvođenja radova na zaštiti iskopa temeljne jame i susednih objekata. Ovde je zaštita iskopa i susednih objekata izvedena po metodi top-down. Zbog toga je konstrukcija ovog dela objekta prošla kroz dve faze. Prva faza bila je izrada privremenih oslonaca, čeličnih stubova koji su ugrađeni u prethodno izvedene šipove, preko kojih se betonirao deo ploče suterena. Ova ploča razupire konstrukciju zaštite iskopa i susednih objekta. Iskopom na dole formirao se prostor za izvođenje donjih armiranobetonskih tavanica – razupora zaštitne konstrukcije. Završetkom temeljne ploče počelo je izvođenje vertikalnih elemenata konstrukcije i završetka delova tavanica koji su ostali neizbetonirani zbog tehnoloških potreba. Time su konstrukcije tavanica dobile konačne oslonce, a privremeni oslonci su se uklonili.

Konstrukciju podzemnih etaža formira horizontalna konstrukcija armiranobetonskih ploča i kapitela, i vertikalna konstrukcija stubova i zidova. Debljina armiranobetonskih ploča je 22.0 cm, sa kapitelima debljine 45.0 cm. Položaji i veličine kapitela definisani su proračunom, uz uslov da deformacije konstrukcije budu u granicama propisom dozvoljenih vrednosti. Dimenzije armiranobetonskih stubova i zidova definisane su u skladu sa propisima (uslov duktilnosti preseka za seizmičke uticaje).

Slika 2 – Konstrukcija podzemne etaže

Nadzemni deo konstrukcije sastoji se od armiranobetonske konstrukcije Poslovno-trgovačkog-komercijalnog dela i čelične konstrukcije. Hotelski deo II i komercijalni deo su odvojeni klasičnom dilatacijom ostvarenom udvojenim zidovima. Udvojeni zidovi su formirani od prizemlja pa na gore – ka krovu.

U podzemnim delovima objekta oni su objedinjeni u jedan jedinstveni masivan stub.

Vertikalni noseći elementi su AB stubovi i AB zidovi. Armirano-betonski zidovi su na svim mestima gde su locirana stepeništa i liftovi, ali su locirani i na mestima gde je bilo moguće da budu postavljeni u odnosu na arhitektonsko rešenje. Armirano-betonski stubovi su različitog poprečnog preseka. Od izduženih dimenzija 80x170; 80x120; 80x100; 80x160 u donjim etažama, pa do kvadratnog poprečnog preseka 80x80; 90x90 i 70x70 ili 40x40. Druga vrsta stubova su stubovi kružnog poprečnog preseka Ø50; Ø60 Ø70 i Ø80. Izduženi stubovi su oblikovani tako da su njihovi krajevi polukružni - u oplati od polovina cevi odgovarajućeg prečnika, a između su sa paralelnim ravnim stranicama.

Sve međuspratne AB konstrukcije su AB ploče, sa kapitelima radi osiguranja od proboja ili sa gredama iznad stubova. Debljina armiranobetonskih tavanica je od 22.0 cm do 27.0 cm, zavisno od raspona, uslova oslanjanja ploča i opterećenja. Konstrukcija je formirana tako da

udovolji zahtevima funkcija delova kompleksa, a da omogući stabilnost i upotrebljivost u svim fazama izgradnje.Horizontalna stabilnost je obezbeđena kombinacijom AB zidova i jezgara i AB ramova.

Objekat je fundiran u sloju laporovitih glina.Temeljna konstrukcija je armiranobetonska ploča sa kapitelima. Debljina temeljne armiranobetonske ploče je 80.0 cm i 90 cm. Zadebljanja ploče u vidu kontrakapitela su formirana ispod stubova. Debljina kapitela je 120.0 cm i 150.0 cm. Kapiteli su formirani od gornje ivice temeljne ploče na dole. Dimenzije kapitela su određene iz uslova nosivosti preseka i obezbeđenja sigurnosti na probijanje usled opterećenja od stubova, a da obezbeđenje probijanja bude bez dodatne armature.

Temeljna konstrukcija je izvedena na prethodno pripremljenoj podlozi. Duž cele površine iskopa uklonjena je intenzivnije izmenjena zona lapora, a potom zaštićen otvoreni iskop od spoljnih uticaja izradom tampon-sloja u skladu sa geotehničkim elaboratom. Ovaj tampon je istovremeno i deo horizontalne drenaže ispod objekta.

Kako je geološkim i geotehničkim istragama utvrđeno prisustvo podzemne vode na lokaciji, to je bilo neophodno da se izvede drenažni sistem. Izvedena je trajna drenaža i ispumpavanje vode tokom celog veka eksploatacije objekta. Drenažni sistem se sastoji od vertikalne i horizontalne drenaže. Vertikalna drenaža prihvata podzemne vode i sprovodi ih do horizontalne drenaže formirane ispod temeljne konstrukcije.

Iskustvo projektanata stečeno tokom izgradnje ovog komleksa, i sličnih objekata, je doprinos realizaciji objekata u centralnim gradskim jezgrima, među postojećim objektima starosti više decenija. Naime, zaštita iskopa temeljnih jama i susednih objekata primenom geotehničkih sidara zahteva veoma stroge uslove izvođenja sidara i ograničenje horizontalnih pomeranja na minimalne mere. Prisustvo objekata velike starosti, izvedenih od opeke, nedostatak elemenata za ukrućenje konstrukcije, sa mnogo intervencija kojima su neplanski i nestručno rušeni noseći zidovi, uz minimalna pomeranja zaštitnih konstrukcija izazivaju velika oštećenja na objektima u blizini konture iskopa temeljne jame.

Iskustvo pokazuje da se primena tehnologije top-down u ovim zonama pojavljuje kao sigurna metoda koja, pravilnim dirigovanjem faza rada, obezbedjuje stabilnost susednih objekata. To je poklazano i radovima u zoni biblioteke grada Beograda.

Slika 3 – Zaštitna konstrukcija

3. ČELIČNA KONSTRUKCIJA

Na objektu „Tržnog centra u Rajićevoj“ imamo osnovnu noseću čeličnu konstrukciju na "Pjaceti" koja se svojom površinom, značajem, rasponima i kompleksnošću izvođenja, izdvojila kao zasebna noseća celina. Međutim i manje celine sa nosećom čeličnom konstrukcijom pripadaju vrlo zahtevnim objektima predviđenim da prate arhitektonske zahteve funkcionalnosti, trajnosti i estetike.

Multifunkcionalna gradska pjaceta zamišljena je kao proširenje Knez Mihajlove ulice pre njenog ulivanja u Kalemegdan. Na tom delu projektovana je višeetažna (4 etaže) noseća čelična konstrukcija terasa i restorana(slika 4) ukupne površine oko 2500m2. Primarni podni nosači projektovani su od zavarenih sandučastih i I profila a sekundarni od valjanih I profila, raspona od 8 do 16m. Zbog ograničene međuspratne visine drugog sprata, određen broj greda raspona 16m okačen je za konstrukciju trećeg sprata tako da je za ove grede u fazi montaže bilo neophodno postaviti privremene oslonce. Pod je armirano betonska ploča livena na licu mesta preko nosećeg TR lima. Stubovi su spregnuti,kružnog preseka.

Slika 4 – Konstrukcija terasa pjacete u izgradnji

Pasarela (slike 5 i 6) je pešački višeetažni most koji spaja hotelsku kulu i komercijalni deo, raspona 16m na koti +18.21 i raspona 23.50m na kotama +21.17 i +23.94 a širine 2m. Glavnu noseću konstrukciju čine rešetkasti nosači visine jednog sprata, L=16m. Dijagonalna ispuna projektovana je od HOP kutijastih profila kao i vertikale koje imaju i funkciju nošenja staklene fasade. Na ovu rešetkastu konstrukciju oslanjaju se ramovi koji formiraju sledeću etažu, povezani horizontalnim krovnim spregom celom dužinom. Krajnji ramovi su portalni. Ležišta mosta su čelična. Raspored pokretnih oslonaca u oba pravca,pokretnih u podužnom pravcu i nepokretnih je usvojen tako da horizontalna seizmička pomeranja dve dilataciono nezavisne ab konstrukcije ne utiču na konstrukciju mosta. Pod je armirano betonska ploča livena na licu mesta preko nosećeg TR lima na sva tri nivoa.

Slika 5 – Pasarela u izgradnji

Slika 6 – Pasarela u eksploataciji

Konstrukciju za nošenje velike lanterne (slike 7 i 10) na koti +15.3 iznad glavnog hola, ukupne površine oko 1000 m2, čine grede koje formiraju „šahovska polja 4x4m“projektovane od valjanih I profila. Glavni nosači su raspona 16m na jednom delu a na drugom 10m i oslanjaju se na AB konstrukciju jednim krajem a drugim na stubove dimenzija Ø 457, visine do 15m. Kako se konstrukcijom lanterne na koti +15.3 spajaju tri konstruktivne dilatacione celine i to hotelska kula K1, hotelska kula K2 i komercijalno-tržni centar, predviđena je dilatacija na tom mestu udvajanjem krovne rigle i fasadnog stuba i predviđen sistem pokretnih oslonaca. Udvojena krovna rigla je prema arhitektonskim zahtevima vizuelno identična ostalim gredama (slika 9). Čelični stubovi (slika 7) na koti +15.3 osim što su oslonci nosačima lanterne istovremeno bočno pridržavaju fasadnu konstrukciju, visine 15m, formiranu od čeličnih stubova i greda ukupne tražene debljine 20cm.

Slika 7 – Kružni stubovi

Slika 8 – Fasada i lanterna

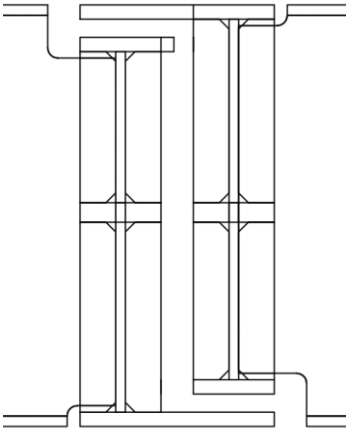

Slika 9 – Dtalj na dilataciji

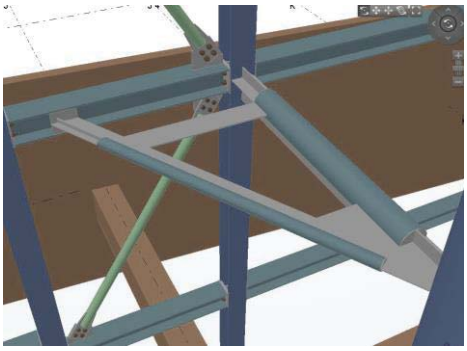

Slika 10 – Lanterna u eksploataciji *Slika 11 – Detalj veze fasade i stuba*

Vidne veze i oblici mnogih sekundarnih konstrukcija na ovom objektu morali su da budu usklađeni sa arhitektonskim predlozima i nacrtima zbog važnosti izgleda prostora(detalj veze stuba koji nosi lanternu i fasade prikazan je na slici 11)

Konstrukcija zvona prema Ulici Kralja Petra (slike 12 i 13) je ramovskog tipa, locirana na dva nivoa. Ova konstrukcija ima funkciju nošenja fasade i krovnog pokrivača kao i nošenja galerije-podesta za kretanje pešaka na koti +19,8. Sastoji se od 22 glavna nosača ramovskog tipa od kote +15.3 do kote 24.12 koji su međusobno povezani fasadnim riglama na kotama +19.80 i +24.12. Rigla na koti +19.8 je u isto vreme jedan od dva podužna nosača podesta za kretanje pešaka. Konstrukcija je kompletno obložena staklom a izvedena je od HOP kutijastog profila.

Slika 12 – Konstrukcija "zvona" *Slika 13–enterijer"zvona"*

Ostale čelične konstrukcije (slika 7) su: noseća konstrukcija eskalatora(slika 14a), podesta(slika 14b), nadstrešnica(slika 14c), pešačkih mostova raspona do 15m(slika 14d), stepeništa, lanterni, panoramskih liftova, konstrukcije za nošenje staklenih fasada(slika 14e) i konstrukcija za nošenje reklama(slika 14f) . Ukupan utrošak čelika S235 JRG2 na ovom objektu je oko 900 t.

a)

b)

c)

d)

e)

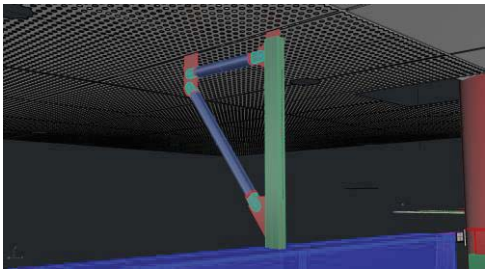

f)

Slika 14 – Ostale čelične konstrukcije

ДГКС Друштво грађевинских конструктера Србије
ASES Association of Structural Engineers of Serbia
P-3
15. KONGRES
6-8. 9. 2018. Zlatibor

Aleksandar Landović[1]

PONAŠANJE AKSIJALNO PRITISNUTIH SPREGNUTIH STUBOVA PRI EKSPLOATACIONOM I GRANIČNOM OPTEREĆENJU

Rezime:

U ovom radu dat je sažet prikaz eksperimentalnih i računskih istraživanja ponašanja centrično pritisnutih stubova spregnutog preseka od čelika i betona pri eksploatacionom i graničnom opterećenju. Istraživanja su sprovedena na Građevinskom fakultetu u Subotici, a publikovana su u okviru doktorske disertacije „Analiza ponašanja aksijalno pritisnutih spregnutih štapova pri eksploatacionom i graničnom opterećenju“. Glavni cilj istraživanja bio je utvrđivanje efikasnosti metoda za ojačavanje stubova usvojenim metodama, kao i formulisanje principa njihovog proračuna.

Ključne reči: spregnut presek, ojačavanje, eksperiment, nosivost.

BEHAVIOR OF AXIALLY COMPRESSED COMPOSITE COLUMNS FOR EXPLOITATION AND ULTIMATE LOADS

Summary:

This paper presents brief overview of experimental and numerical research of behaviour of axially loaded columns with composite section made from steel and concrete in exploitation and ultimate load state. The research was carried out at Faculty of Civil Engineering in Subotica and was published in PhD thesis “Analysis of behaviour of axially compressed composite bars for exploitation and ultimate load”. The main aim of research was determining the efficiency of method used for strengthening columns, also objective was formulating principles for their calculation.

Key words: Composite section, strengthening, experiment, resistance.

[1] *PhD, MSc, BSc, CE. assistant professor, University of Novi Sad, Faculty of Civil engineering Subotica, landovic@gf.uns.ac.rs*

1. INTRODUCTION

Large number of civil engineering structures are made from concrete. Many of those structures are old, damaged and deteriorated or their usage has been altered. Over the time, especially for bridges, degradation processes on reinforced concrete elements caused by increased traffic load took place. New seismic codes with increased demand caused some older structures to have inadequate seismic resistance. In some extreme cases, it is necessary to strengthen a structure during construction because of certain oversights within design and/or construction. Restructuring, adaptation and building extension often demands overall number of stories to be increased what, in turn, increases axial forces within columns. In all those cases it is often necessary to strengthen load bearing elements, e.g. columns. Eurocodes for composite structures of steel and concrete EN 1994-1-1 [1] and for concrete structures EN 1992-1 [2] does not provide explicit recommendations for design of strengthened columns. In that context, an extensive experimental and numerical research addressing the load carrying capacity of strengthened concrete columns was conducted at the Faculty of Civil Engineering in Subotica during long period from 2005 to 2016.

This paper presents three methods for strengthening of squared cross section reinforced concrete columns. First method is using of steel tube which is placed over the whole height of columns with empty space being filled up with fine-grain concrete or special concrete mixtures. Second method of strengthening is making of concrete jacket and using steel angles connected to each other by connecting plates forming steel cage around RC column. Third method of strengthening included tightening of the cross placed prestressed bolts. The investigation included experimental tests of all materials and column specimens in order to generate data for the key aspects of used methods for strengthening columns. After the main experimental study a numerical analysis was carried out to investigate influence of individual parts of built up composite cross section. The main aim of this research was determining the efficiency of method used for strengthening columns and formulating the principles for their calculation. All results of presented research are fully reported in [3] while partial results were presented [4], [5] and [6]. Prior to this research strengthening columns with steel tubes were used in [7] and [8].

2. EXPERIMENTAL PROGRAM

2.1 TEST SPECIMENS

Experimental analysis of presented problem was performed on a basic model of reinforced concrete column which was strengthened with mentioned three methods. A total of 26 stub axially compressed columns, including 21 strengthened specimens and 5 plain reinforced concrete specimens, were tested. Column models with their dimensions corresponds to real structure with aspect ratio of 1 by 3.3, e.g. 3.3 times smaller than real column. Models without the strengthening, and models that were strengthened, had square cross section with dimensions 12/12cm and height of 90cm. All column specimens were made of class C35/45 concrete. Main reinforcements were 8 bars of Ø6mm and stirrups of Ø4mm. Stirrups were

spaced 3cm at the top and the bottom 20cm of the column length and spaced 6cm in the middle. Steel of reinforcement had average yield strength of 550MPa and tensile strength of 650MPa.

Strengthening by first method was conducted with a premade reinforced concrete column placed into a steel tube while remaining space was filled with concrete (see Figure 1). Concrete of infill was varied in three different compressive strength quality. Classes of concrete were C20/25 (specimen B21), C40/50 (specimen B41) and C70/85 (specimen P01). The tubes used for strengthening were manufactured from mild steel sheet (3 mm in thickness), with the plate cut from the sheet, folded into a circular shape and then welded with a single bevel butt weld. Average yield strength, tensile strength and modulus of elasticity were experimentally determined to be 230 MPa, 340 MPa and 210 GPa, respectively. Tubes were 900mm long (same as concrete columns) with outside diameter of 194mm. Ratio of outer diameter and wall thickness of 65 was chosen so that limit conditions, for circular tubes filled with concrete, as defined by EC 4, ACI 318 and AISC 360 standards, were met.

Strengthening by second method was achieved simultaneously using steel angles, steel plates and concrete jacket. It was conducted with a reinforced concrete column placed into a premade steel cage with remaining space filled with class C60/75 concrete (see Figure 1). Distance between horizontal steel strips was varied in two cases. Steel cage was formed with four 30×3mm angles and seven (specimen L01) or nine (specimen L51) steel ≠90×40×3mm plates.

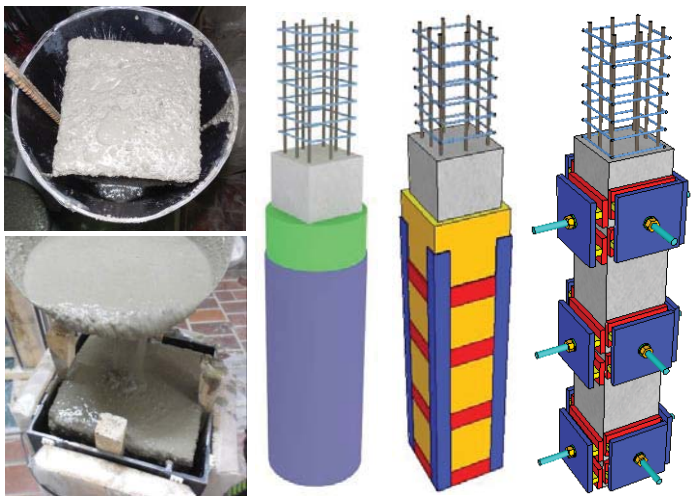

Figure 1 Concreting of infill an a schematic view of the strengthened column

Strengthening the columns by third method was achieved by tightening of the cross placed prestressed bolts. Number of bolts and their spaces were varied in two cases. Specimens with 3 pair of bolts (specimen V31) and four pair of bolts (specimen V41). All bolts were made from high strength 10.9 steel and tightened with force of P=50kN.

2.2 TEST SETUP

Experimental research included registering two types of deformation, namely measuring local deformation, e.g. strains, and measuring global deformation or column - shortening. Strain gauges were used to measure the variation of strains at section located in the middle of model height and were placed symmetrically due to longitudinal column axis (Figure 2). Four strain gauges were placed on RC column before fill concreting. Two displacement transducers were used to measure the axial deformation.

Figure 2 - Column models before experiment.

In all tested columns registering and analysis included: changes in stress and deformation state for all parts of the composite cross section, ultimate strength, shape of global deformation in failure, engagement of the individual parts of composite cross section. In RC models, beside

ultimate force and deformation, registering included value of the force at which cracking of concrete started, fracture development and propagation. The specimens were loaded continuously until failure. The concentric load was applied on the strengthened specimens through a steel bearing plates so that only central column was directly loaded.

3. EXPERIMENTAL RESULTS AND SPECIMEN BEHAVIOR

3.1 COLUMNS WITHOUT STRENGTHENING

For the purpose of comparisons, 5 plain reinforced concrete specimens subject to axially compression were also tested. All columns of this group showed very similar behavior. Figure 3 shows the measured load versus strains or displacement curves of tested plain reinforced concrete specimens. Column models showed almost full linear behavior during whole loading process until failure. This behavior is typical for axially compressed columns made from high grade concrete.

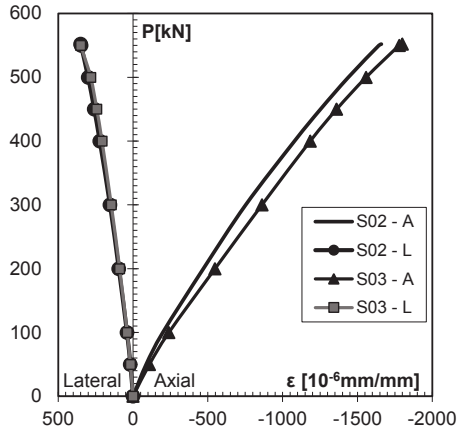

Figure 3. Measured load versus deformation of plain reinforced concrete specimens

For a plain reinforced concrete specimens first longitudinal cracks were detected at the ends of columns at loading of 90% of ultimate force. Failure of the RC columns occurred as a result of cracking and crushing of the concrete at the location of load application. Cracking on all specimens started at both ends of the column, but pronounced crack development in failure was registered at one end only (see Figure 7). Mean ultimate load force of unstrengthened columns determined during experimental testing is presented in Table 1.

3.2 STRENGTHENED COLUMNS

Testing of all strengthened models have been conducted according to similar experiment program phases as for unstrengthen models so that results could be directly compared. In that way direct assessment of successfulness of method for strengthening RC columns was possible and also, it was possible to cross compare strengthened models so influence of varying

parameters was evaluated. On following diagrams, deformation of unstrengthened column model (S02) is also presented for easier comparison with strengthened specimens.

Figure 4 shows diagram of dependence of compression axial force to the longitudinal and the lateral strains on specimens strengthened with steel tubes. In domain of exploitation loads, or up to 50% of crushing load, behavior of all parts of composite cross section is almost linear. Pronounced nonlinear increase of deformation in relation to increase of loading was registered for forces above the 80% of crushing load. Full composite action of all section parts is preserved for loads up to 25% of ultimate load. Ultimate load forces of strengthened columns registered during experimental testing are listed in table 1. When comparing behavior in exploitation loads domain, which corresponds to forces up to P=800kN, it can be noticed that difference between all strengthened models is relatively low.

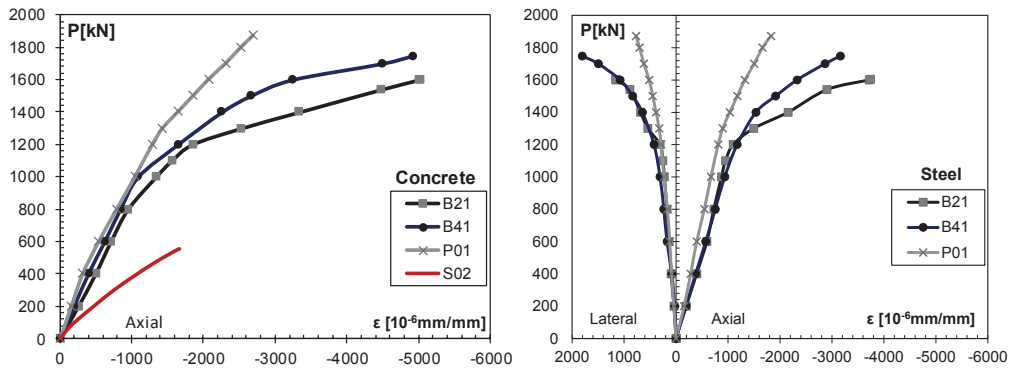

Figure 4. - Load (P) versus strain (ε) relationships for specimens strengthened by steel tubes.

Behavior of specimens strengthened with concrete jacket and steel cage is presented on Figure 5.

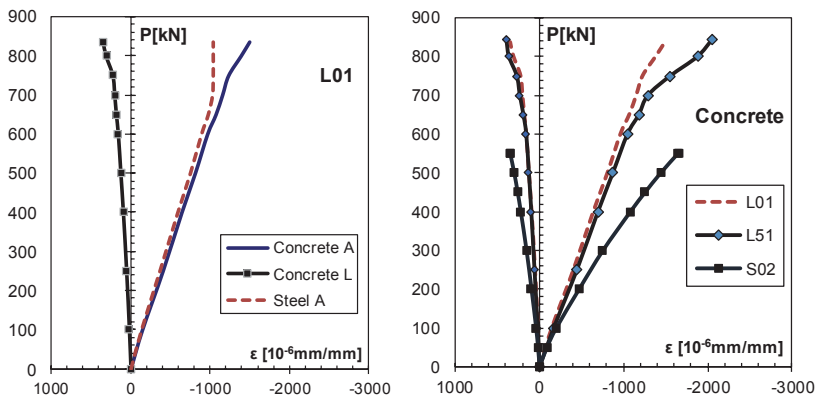

Figure 5. – Behavior of specimens strengthened by steel cages and concrete jacket.

Linear behavior of all section parts is maintained up to force of 700kN. That force corresponds with ultimate tensile stress in concrete jacket. After reaching those stress levels pronounced cracking of concrete was registered and composite action of cross section was disrupted. The difference between the two types of strengthened models (L01 and L51) is relatively small and both groups have noticeable linear response in domain of exploitation load states.

Behavior of specimens strengthened with prestressed high strength bolts is presented on Figure 6. The difference between the two specimens with different number of bolts (V31 and V41) is relatively small. Comparing these two models with unstrengthened specimen (S02), difference in behavior is only noticed in ultimate loads and strains. In domain of exploitation states all three types of columns have the same response. Model testing of these types of columns was limited by size factor and potential of this strengthening method wasn't fully achieved.

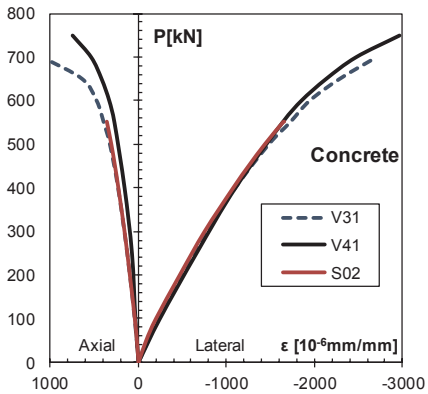

Figure 6 – Behavior of specimens strengthened by lateral prestressing

Mean value of ultimate load forces for all tested specimens registered during experiment are presented in table 1. The coefficient *ks* which represents increasing of the strength for the strengthened specimens is also given.

Table 1 – Ultimate load forces of column models

	Unstreng. specim.	*Tube 1 C20/25*	*Tube 2 C40/50*	*Tube 3 C70/85*	*Cage e=15cm*	*Cage e=10cm*	*Bolts 3 pairs*	*Bolts 4 pairs*
Pu[kN]	*592.0*	*1600.0*	*1709.3*	*1864.0*	*838.0*	*856.0*	*709.3*	*759.0*
ks [-]	*–*	*2.70*	*2.90*	*3.20*	*1.42*	*1.45*	*1.20*	*1.28*

Figure 7 shows the ends of the column specimens after the completed test.

Figure 7 - Comparisons of the failure modes of strengthened and unstrenthened columns

4. NUMERICAL ANALYSIS

After experimental part of research numerical analysis was performed in order to obtain a relevant data for preparing and defining the principles for calculation of the strengthened columns. An extensive numerical analysis by finite element method was performed in the software Ansys. A static, non-linear analysis was applied. In the first phase of analysis simulation of experimental testing was conducted. This analysis included all the significant parameters such as: non-linear stress-strain relationship, boundary conditions at the ends of the elements and contact conditions between the individual elements of the model. All material properties used in numerical analysis were experimentally determined on standard material specimens. Every part of cross section was modeled by appropriate finite element. Steel, concrete and rebar were modeled by Solid185, Solid65 and Link180, respectively.

The failure pattern observed during the experiment is accurately fitted by damaged shape of the FE model. A high coincidence of the ultimate load, longitudinal and lateral strains as well as lateral deflection and cracking of concrete in comparison to the experiment was achieved. Diagrams on Figure 8 and 9 presents' state of force to lateral and longitudinal strains obtained from numerical analysis compared to the experimental results. In order to determine the range of structural performance and to investigate the effects of variation of key individual parameters, multiple parametric studies have been created.

Reliable experimental and numerical analysis have provided the necessary data for the definition of expressions for determining the ultimate strength of all strengthened column models. In the second phase a calculation recommendations are defined separately for all of the analyzed members. Behavior of column models in the domain of exploitation load states is mainly linear with full composite action across cross section which justifies the use of linear elastic theory in calculation of stresses and deformations.

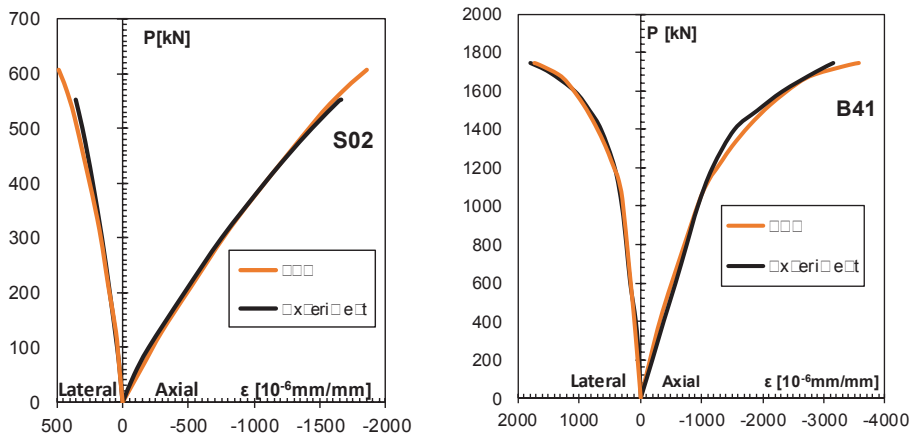

Figure 8 – Validation of numerical and experimental results

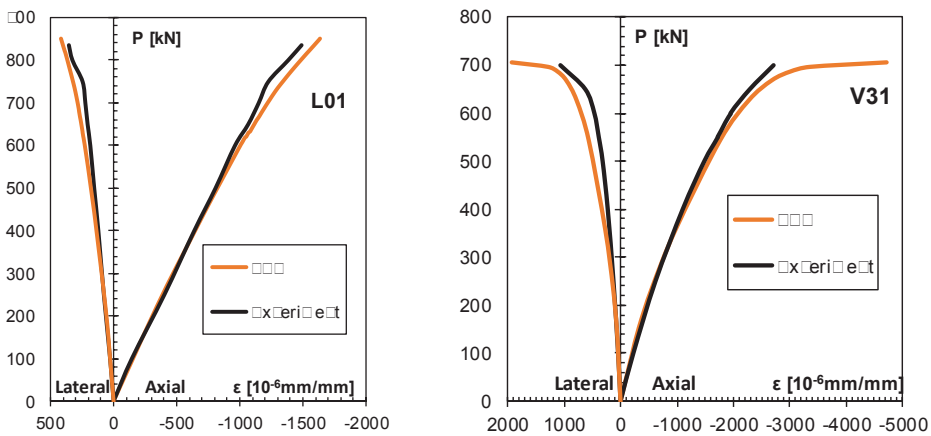

Figure 9 – Validation of numerical and experimental results

5. CONCLUSIONS

In this paper, the experimental and numerical investigation of the composite column made from steel and concrete has been briefly presented. Experimental results largely depend on assumptions made prior to design and forming of test samples what implies that conclusions refer to exactly defined boundaries. According to results obtained through experimental and numerical model analysis of samples following conclusion are drawn:

- Reinforced concrete columns from the control group have almost linear stress/strain relationship all the way to the failure. Columns strengthened with steel tubes exhibits

considerably more ductile behavior and are capable of withstanding larger deformations relative to classical reinforced concrete columns and columns strengthened with concrete jacket and steel cage.

- Difference between strains of reinforced concrete core column and steel tube, or steel cage, in the domain of exploitation load states, are relatively small, what implies that a composite action of the cross section is preserved.
- Stress-strain analysis revealed that whole cross section in composite columns is engaged for load carrying even though load is applied on central concrete column only.
- Behavior of column models in the domain of exploitation load states is mainly linear with full composite action across cross section which justifies the use of linear elastic theory in calculation of stresses and deformations.
- Columns strengthened with prestressed high strength steel bolts are capable of withstanding larger deformations compared to plain reinforced concrete columns. Full potential of this strengthening method is to be tested on real size specimens.

REFERENCES

[1] Eurocode 4, EN 1994-1:2004: Design of composite steel and concrete structures Part 1-1 – General rules and rules for buildings, European Committee for Standardization, 2004.

[2] Eurocode 2, EN 1992-1-1:2004: Design of concrete structures Part 1-1 – General rules and rules for buildings, European Committee for Standardization, 2004.

[3] Landović A.: Analysis of behavior of axially compressed composite bars for exploitation and ultimate loads, PhD Thesis University of Novi Sad, Faculty of Civil Engineering Subotica; June 2016.

[4] Landović A., Bešević M.: Analysis of behavior of the RC column strengthened with concrete jacket and steel angles, Simpozijum of Association of structural engineers of Serbia, Zlatibor, 15.-17. Sept. 2016, Proceedings, pp. 433-438, (In Serbian).

[5] Vlajić LJ., Landović A.: Analysis of methods for strengthening reinforced concrete columns coupled with steel tubes, 13th Congress of Association of structural engineers of Serbia, Zlatibor, 22.-24. Sept. 2010, Proceedings, pp. 284-291, (In Serbian).

[6] Vlajić Lj., Landović A.: Jedan primer sanacije centrično pritisnutih AB stubova na osnovu eksperimentalno-teorijske analize modelskih ispitivanja, Zbornik radova Građevinskog fakulteta Br.25 – Specijalno izdanje, Međunarodna konferencija Savremena dostignuća u građevinarstvu, Subotica, 2014.

[7] Vlajić Lj., Landović A.: Strengthening of reinforced concrete columns coupled with steel tubes, Materials and structures, Vol. 53, Iss. 4, 2010, pp. 39-49.

[8] Vlajić Lj., Vranjevac V., Lukić P.: Sanacija AB stubova na prilaznim konstrukcijama "Pančevačkog mosta" oštećenih dejstvom požara 2011.g.; Osmo naučno-stručno međunarodno savetovanje "Ocena stanja, održavanje i sanacija građevinskih objekata i naselja", Zbornik radova, Borsko jezero, 2013. str. 189-196.

ДГКС Друштво грађевинских конструктера Србије
ASES Association of Structural Engineers of Serbia
P-4
15. KONGRES
6-8. 9. 2018. Zlatibor

Veljko Koković[1], *Dejan Bajić* [2]

EKSPERIMENTALNO ISTRAŽIVANJE GRANIČNE NOSIVOSTI OSLONAČKE VEZE OŠUPLJENIH MONTAŽNIH PLOČA

Rezime:

Prethodno napregnute ošupljene montažne ploče se najčešće koriste kao međuspratne konstrukcije stambenih i poslovnih objekata. Uobičajeno nazivane "savršenim prefabrikatima", ošupljene ploče se tradicionalno projektuju kao elementi statičkog sistema proste grede. Međutim, ploče je moguće projektovati i kao kontinualne elemente za dejstvo dodatnog stalnog i korisnog opterećenja. Takođe, uspostavljanjem kontinuiteta ploče je moguće osloniti indirektno, bez kratkog elementa. U ovom radu je prikazano eksperimentalno istraživanje nosivosti kontinualizovanih ošupljenih ploča. Smičući lom je zabeležen na svim ispitanim uzorcima. U radu je prikazan zabeležen odgovor sistema i ukazano je na uticaj veze betona ugrađenih u različito vreme.

Ključne reči: prethodno napregnute montažne ošupljene ploče, kontinuitet, smičući lom, veza prianjanja betona ugrađenih u različito vreme, princip širenja formiranih prslina

EXPERIMENTAL STUDY ON ULTIMATE CAPACITY OF HCS WITH RESTRAINED SUPPORT CONNECTION

Summary:

Precast prestressed hollow core slabs are extensively used as suspended floors in residential and commercial buildings. Usually called "superior precast elements", HCS are traditionally designed and constructed as simple beams. However, HCS could be designed as continuous for superimposed and live loads. Additionally, end rotation restraint can be utilized to avoid the wall or beam ledge, in which case the HCS are indirectly supported. This paper presents an extensive experimental program consisting of load-testing ten large scale beams, composed from prefabricated hollow core slab elements and in-situ concrete. The tests were designed to investigate the hogging moment region of a continuous system. The flexural shear failure was recorded on all specimens. The observations show the behavior of the system and indicate the interface influence on shear strength of continuous composite HCS.

Key words: Hollow core slabs, support continuity, shear flexure, concrete to concrete bond, crack kinematics

---

[1] *Assistant professor, PhD, University of Belgrade, Faculty of Civil Engineering, Serbia*
[2] *Professor, PhD, University of Belgrade, Faculty of Civil Engineering, Serbia*

1.1. INTRODUCTION

The precast concrete industry is a dynamic and innovative branch of the construction industry thanks to cost efficiency based on the automated production process of concrete elements and short construction time. Moreover, this branch has the largest number of innovations in terms of new materials and load bearing capacity efficiency of structural elements. As a typical product of the precast concrete industry, hollow core slabs (HCS) make 50% of the market share of the commercial and residential floor structures.

Hollow core slabs (HCS) are precast concrete elements produced from the long line prestressed slab, up to 140 m in length. Production of HCS consists of saw cutting the hardened concrete, which is slip-formed or extruded over the straight prestressed strands. Because of the specific production process which disables incorporation of protruding reinforcement, the connection between adjoining slabs and between the slabs and the supporting structure can be made only over the in-situ concrete grouted in joints or cores. Additional site works are necessary in case of designed structural topping or tying system for prevention of progressive collapse. To fulfill the simple beam design assumption, the free rotation of the slabs' ends is ensured by the proper detailing of the connections [1].

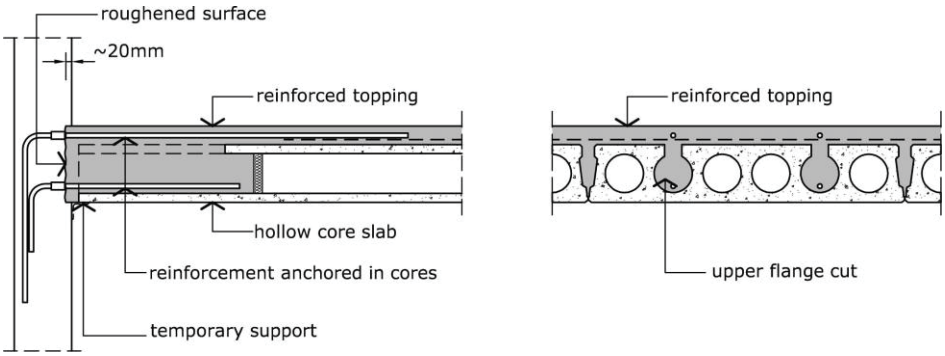

Figure 1: Indirect support detail

Intended continuity that can lower costs and bring structural benefits such as lowering deflection and improving the fire resistance was usually not considered by the provisions in the past. The major reason for that is the fact that the HCS are reinforced only with bottom prestressed strands. However, lack of analysis and design recommendations did not limited contracting engineers to use the continuous HCS system in past, probably relying on in-house tests. Research articles that discuss the efficiency of the continuity system were rare [2]–[4] and the first set of design rules and construction details was published in FIB Bulletin 6 [5], in 2000. Furthermore, the Bulletin presents an interesting possibility of the indirect support of precast hollow core slabs, the case in which the concrete cast in cores transfers the moment and shear. Figure 1 presents usual detail of indirect HCS support on RC wall. However, design recommendations that are given in the FIB Bulletin are mostly theoretical – adopted failure mechanisms were not recorded in experimental research [6], [7].

2. EXPERIMENTAL PROGRAM

Full-scale tests of simply supported beams were carried out in order to investigate the behavior and load capacity of a composite continuous hollow core slabs. Conducted three-point bending tests simulated the hogging bending region of the continuous HCS, Figure 1a. The experimental research consisted of loading up to failure of 10 composite beams, made of prefabricated HCS and cast in situ reinforced concrete topping. Shear span of the specimens equaled to five times the depth of the composite section, and referring to supports, the specimens were cantilevered to provide the constant prestress force over the shear span. An overview of research is summarized in the following sections, with more detailed information presented in these [8].

Specimens were formed of two hollow core slab elements with the depth of 260 or 350 mm and 80 mm cast-in-situ topping. The width of the specimens was 360 mm, because the 360 mm wide HCS element was obtained by the longitudinal cutting of the 1200 mm wide HCS. The upper flange of the HCS was additionally cut on the length that ranged from 350 to 1350 mm, ensuring the filling of cores with cast in situ concrete and indirect support of the HCS. In the middle of the specimen, the distance of the HCS elements was 300 or 160 mm, for the specimens with the indirect and direct support. The gap between the HCS elements was filled with cast-in-situ concrete, Figure 2b.

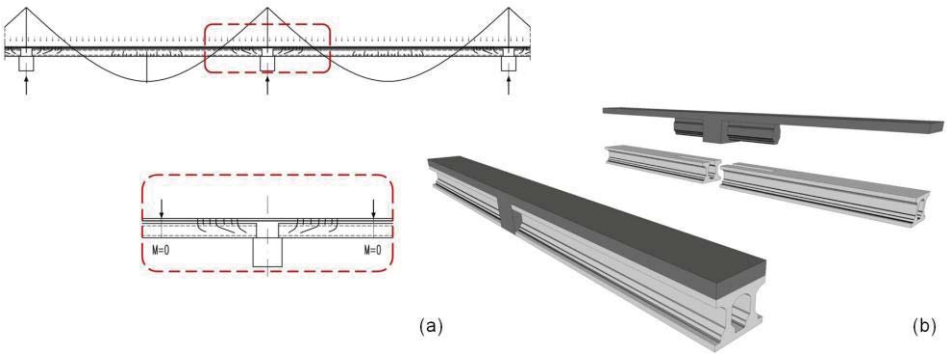

Figure 2: Continuous HCS and simple beam model (a); 3D view of the specimen

The supports of the specimens were provided over the 100 mm wide steel plates, while the load was applied over the steel profile. The connection of steel profile and specimen was provided through the reinforcement protruded from middle, cast-in-situ part of the specimen. The continuity of the HCS elements was provided over the topping reinforcement, determined to avoid flexural failure. Ten specimens were tested in two series – the first consisted of three pairs of identical specimens, while the second consisted of unique specimens. Test setup and geometry of specimens are illustrated in Figure 3.

2.1. TESTING AND INSTRUMENTATION

Tested composite beams were simply supported and subjected to three-point bending tests. Displacements, loads and strains at critical locations were measured during the testing. The layout of test set-up and measuring equipment is presented in Figure 3 (b).

Vertical displacements were measured by linear variable differential transformers (LVDTs) in four cross-sections; at the quarters of the beam span and in two cross-sections in the middle of the beam. The horizontal displacement of the specimen was measured at the roller support. The width and sliding of the vertical crack at the joint of the HCS and middle in-situ concrete was measured by LVDTs. Shear deformations were measured by LVDTs placed in "X" configuration – eight LVDTs were placed at 45°, measuring the four square regions. The value of applied force was continuously measured by a loading cell placed between a steel profile and a hydraulic jack mounted on a testing frame.

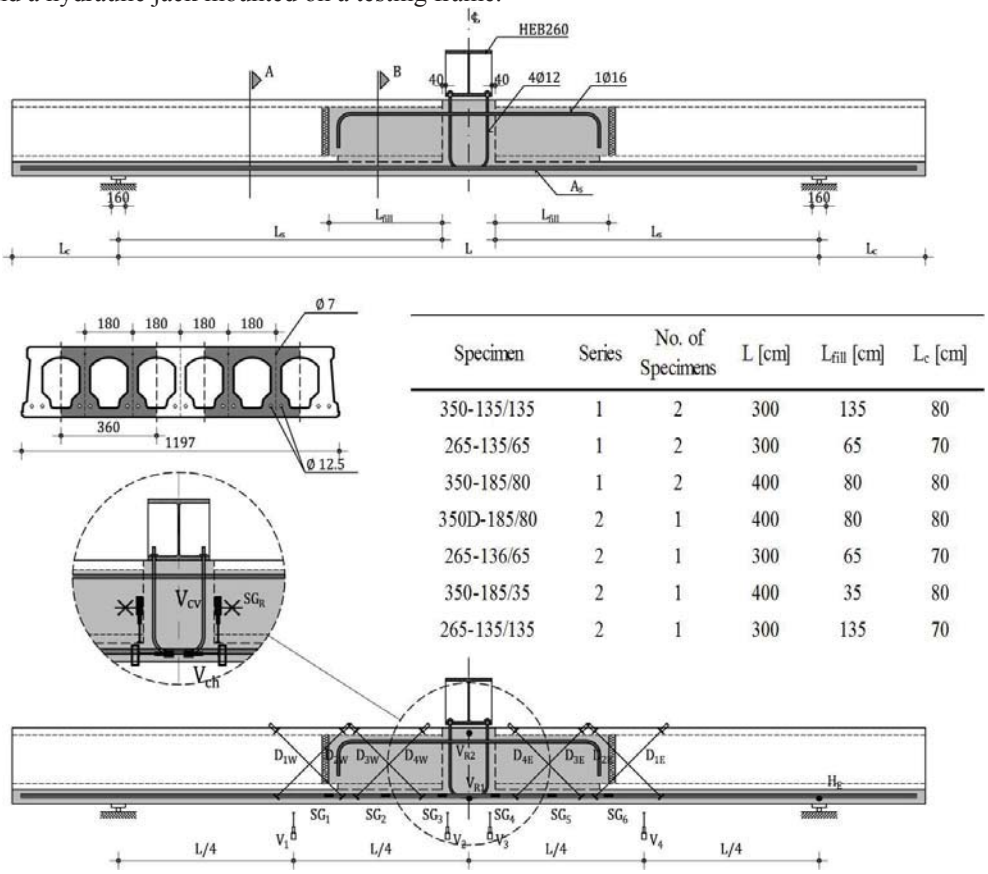

Specimen	Series	No. of Specimens	L [cm]	L_{fill} [cm]	L_c [cm]
350-135/135	1	2	300	135	80
265-135/65	1	2	300	65	70
350-185/80	1	2	400	80	80
350D-185/80	2	1	400	80	80
265-136/65	2	1	300	65	70
350-185/35	2	1	400	35	80
265-135/135	2	1	300	135	70

Figure 3: Geometry of the specimens: (a) reinforcement and support condition details; (b) specimen test setup and instrumentation used

The longitudinal reinforcement was instrumented with strain gauges in six cross-sections, placed on the two side bars in each of the cross-sections. The strains in HCS element webs were measured with the strain gauges forming rosettes.

Together with the displacement measurement of the predefined points using the point-wise sensors in the south beam face, the north surface of the specimens was observed by digital

cameras. Digital Image Correlation is used to track the surface displacement of the beam and to calculate a crack width and sliding.

The index of the specimens is given in the following form HxD-y/z, where x stands for the height of a hollow core element; y stands for the length of the shear span and z stands for the length of the filled void measured from the cast-in-situ mid-span joint of the specimen. D is for the direct support of the hollow core slab element.

3. EXPERIMENTAL RESULTS

Recorded failure of all specimens should be defined as flexural shear failure, Figure 4. For the beams of the second series flexural shear failure is recorded at lower load levels than expected, according to the test results of the first series. Concrete-to-concrete interface bond of the second series specimens proved inadequate.

Figure 4: Specimen 350-185/80-1 after failure

Observed failure mode of all specimens was flexural shear failure. All recorded cracks were bending cracks that propagated into a web of the HCS element, where rotated in the direction of loading point. The critical shear cracks (the crack at which the specimen failure is recorded) was the last recorded flexural crack with rotated part that coincide with the direct strut (line connecting support and loading point). In addition, a difference between critical shear crack and all other previously formed flexural shear cracks was crack propagation along the tension reinforcement, which resulted in the highest rate of widening. In the specimens of the second series, a horizontal part of critical shear crack was spreading along the interface of concrete cast in different times. However, the effect on crack width was the same.

3.1. FLEXURAL SHEAR FAILURE

Typical diagrams showing the load vs. vertical displacement and load vs. shear strain are shown on Figure 5. The measured shear deformation quantifies the effect of shear cracks on

beam deformation – development of critical shear crack at load of 190 kN is visible on diagram as change of curve slope. Ultimate shear strength of all specimens corresponds to recorded shear deformation value that ranged from 0.7 to 1 mm/m. The similar values were reported for the beams with the rectangular cross sections, independently of the beam height [9].

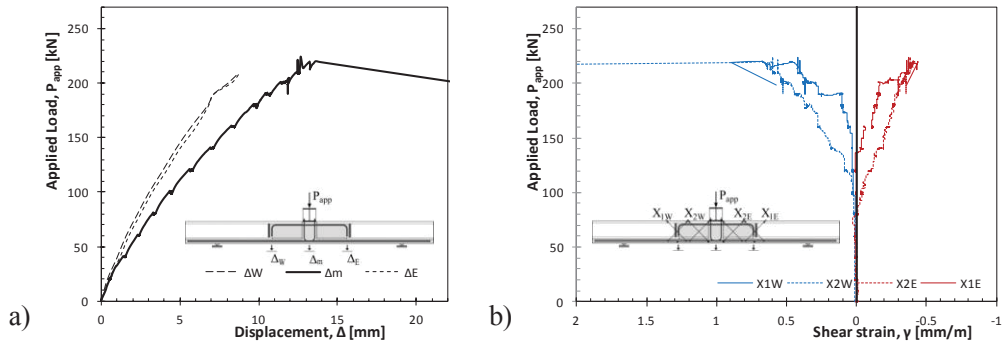

Figure 5: Applied load vs. deflection and measured shear strain – Specimen 350-185/80-1 after failure

Figure 6 presents the ratio of recorded and predicted shear load. Prediction values for specimens where the critical shear crack was recorded on part with filled core of the specimen are calculated based on the effective beam width according to FIB [5].

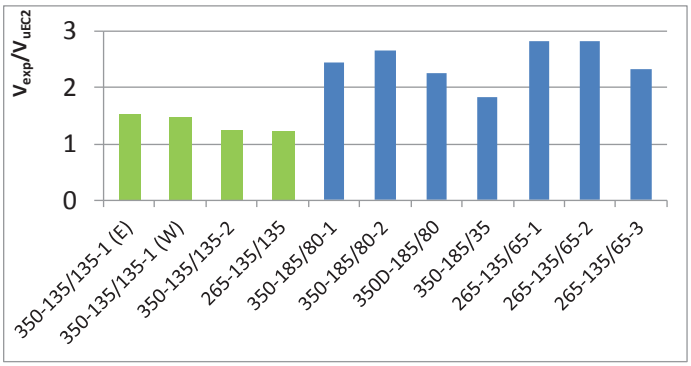

Figure 6: Applied load vs. deflection and measured shear strain – Specimen 350-185/80-1 after failure

As can be seen, prediction conservatism depends on the length of filled core. The mean ratio of recorded failure shear force and prediction is 1.3 for specimens with filled core, and higher than 2 for specimens with limited filling of the core with cast-in-situ concrete. Similar results for specimens with un-filled cores were reported in the experimental researches of the other authors [3], [4]. According to the FIB model [5], ratio of ultimate shear strength of beams with filled and un-filled cores should correspond to the ratio of the web widths, which is

approximately equal to 2. However, a ratio of recorded values is significantly lower – the mean value equals 1.1 for beams H265 and 1.2 for beams H350, which suggests that the effect of core concreting on shear strength is lower than assumed. The possible explanation is the recorded shape of critical crack.

3.2. EFFECT OF CAST IN-SITU CONCRETE INSIDE THE CORE

According to design principles and calculation models presented in [5], filling the cores of HCS element increases the shear strength capacity and allows the indirect supporting of HCS elements. In the case of inadequate strength, the in-situ concrete should be reinforced with shear reinforcement. Also, to avoid horizontal splitting of the HCS webs, principal concrete stress should be limited.

All recorded cracks had the origin from bending cracks. Cracks developed on the filled parts of the composite beams had the same pattern on HCS webs and in-situ concrete inside the cores, while the relative displacement between the concrete cast in different time was not noticed. The impact of local separation caused by in-situ concrete shrinkage has not been observed. The first bending crack formed at the joint between the HCS element and middle in-situ concrete. The measured width and sliding of this vertical crack developed along the smooth side surface of the HCS suggests that the vertical reaction at the end of indirectly supported HCS element was transferred by shear friction across vertical cracks.

3.3. SHEAR ON THE INTERFACE OF CONCRETE CAST IN DIFFERENT TIMES

The upper surface of HCS elements was roughened with brooms during the production process. The measured macro texture depth, R_t, ranged from 0.3 to 0.5 mm, which correspond to horizontal shear strength of 0.74 and 1.01 MPa, in the case of the first and second series specimens [10]. After conducted load tests, the topping bond strength was measured by a "pull-off" test, where the measured values ranged from 1.5 to 2.0 MPa. However, despite the similar recorded values of bond strength, topping bond should be classified as complete and poor according to pull-off surfaces, for the beams of the first and second series, respectively. In the case of the second series specimens, 100% of the fracture is observed at interface, Figure 7. The HCS upper surface of the first series specimens was no treated before casting, while bonding agent was used in the second series specimens.

Figure 7: Failure surface of first and second series topping

3.4. ANALYSIS OF SHEAR CRACK KINEMATICS AND SHEAR TRANSFER THROUGH THE CRACK

Digital images of painted surface of the specimen taken during the testing are correlated, resulting in a displacement of the field of view. Location and shape of the cracks was determined as the DIC information discontinuity. Figure 8 shows the crack development through the pictures of maximal principal strain calculated from measured displacements.

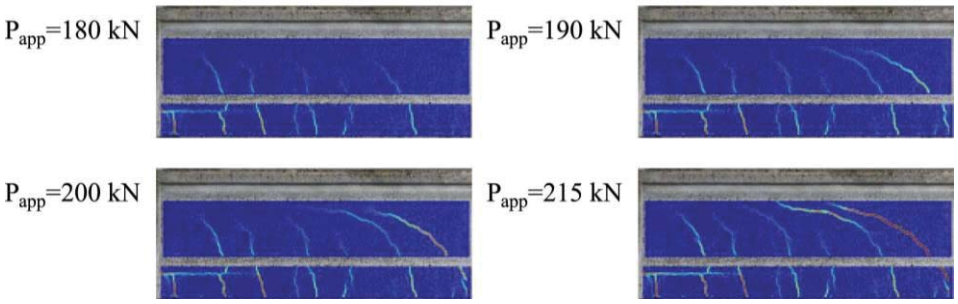

Figure 8: Cracks development on west side of specimen 350-185/80-1

The shear failure of 350-185/80-1 specimen was recorded immediately after the crack developed outside the filled part of the beam, Figure 9. The crack was observed after the load reached to 190 kN, and the delaminating branch was recorded when the load reached 200 kN. Shear failure was recorded at load of 219.9 kN. Constant rate of crack widening in regard to further loading indicated that delaminating branch occurred when the crack appeared. In other words, at load of 200 kN, the delaminating branch crack only propagated to the specimen's surface, when it was observed. Measured relative displacement of un-cracked parts of the specimen between developed cracks can be described according to the principle of rotation around a crack tip.

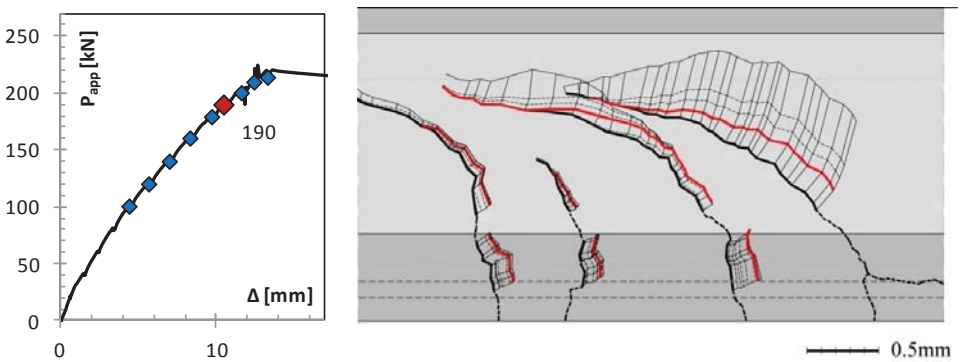

Figure 9: Cracks development and relative crack displacement on west side of specimen 350-185/80-1

Determined crack pattern was approximated with polygonal line and crack kinematics was calculated as a differential displacement of surrounding un-cracked surfaces. Based on principles given in u [11], computer software was written for data analysis. Calculation result is componential displacements – in the direction of crack (Δ) and in the direction perpendicular to it (ω).

In the dependence of crack relative displacements, stresses on cracks faces are estimated using the dilatancy models. The aggregate interlock relation [12] and Rough crack model [13] have been chosen since the solutions are given in the closed form. Shear and normal stress in relation to crack width are shown in Figure 10. A part of the shear force transferred through the crack was calculated as the sum of the stress along the crack area.

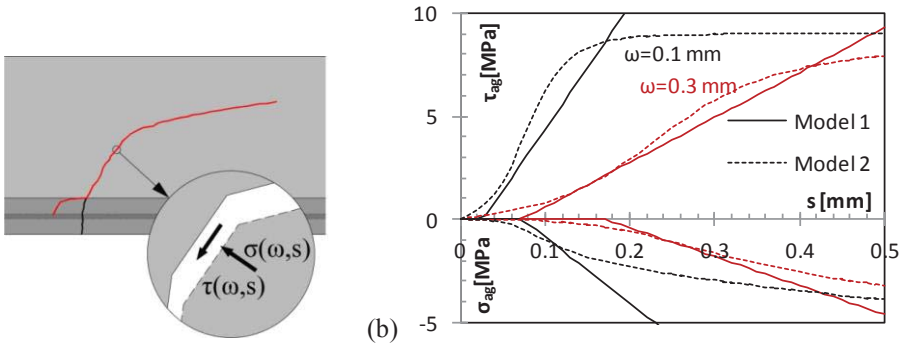

Figure 10: Crack stress (a) and comparison of used crack dilatancy models (b)

Obtained participation of the crack friction mechanism is in accordance with measurements of the other authors. The force value that is transferred through the certain crack depends on its geometry, angle of primary crack branch and the length of the secondary branch. In case of tested specimens, shear is mostly transferred through the flange of a composite beam, which is the obvious reason for the prediction conservatism.

4. CONCLUSIONS

This paper presents an extensive experimental program consisting of load-testing ten large scale beams, composed from prefabricated hollow core slabs and in-situ concrete. The tests were designed to investigate the hogging moment region of a continuous system. The main conclusions are listed below:

- The flexural shear failure was recorded on all specimens. The observed pattern of critical shear cracks differed among the specimens. In the most of beams, a failure crack was the last developed bending crack, with a secondary branch propagating along the direct strut.
- The mean ratio of recorded failure shear force and prediction are 1.3 and 2.4 for the specimens with the cores of the HCS concreted over the whole length of the shear span and specimens with the limited length of the filling, respectively.
- The mean ratio of recorded ultimate load between filled and voided beams equals 1.1 for beams H265 and 1.2 for beams H350.

- Vertical reaction at the end of indirectly supported HCS was transferred by shear friction across vertical cracks.
- The integral part of all critical shear cracks was delaminating branch that propagated along the tension reinforcement or along the horizontal interface in the case of the second series specimens. The HCS upper surface of the first series specimens was no treated before casting, while a bonding agent was used in the second series specimens.
- A basic difference between critical shear crack and all other previously formed cracks was in the rate of widening in regard to the load application.
- Cracks developed on the filled parts of the composite beams had the same pattern on HCS webs and in-situ concrete inside the cores. Relative displacement at the vertical interface of the concrete cast in different time was not noticed.
- Based on measured crack relative displacements, the contribution of the aggregate interlock equals to 60 to 80% of the shear strength. Shear is mostly transferred through the lower flange of a composite beam, which is the obvious reason for the prediction conservatism.

REFERENCES

[1] FIP Commission on Prefabrication, Precast prestressed hollow core slabs. FIP Recommendations, Thomas Telford, London, 1988.

[2] I. Rosenthal, "Full Scale Test of Continuous Prestressed Hollow Core Slab," PCI J., vol. 23, no. 3, pp. 74–81, 1978.

[3] K.-H. Tan, L.-X. Zheng, and P. Paramasivam, "Designing hollow-core slabs for continuity," PCI J., vol. 41, no. 1, pp. 82–91, 1996.

[4] M. Grzybowski and B. Westerberg, Prestressed Concrete Hollow Core Slabs Subjected to Negative Moment. Royal Institute of Technology, Publication TRITA-BRO-9107, Stockholm, Sweden, 1991.

[5] FIB Commission 6 Prefabrication, "Special design considerations for precast prestressed hollow core floors," CEB - FIP Guide to Good Practice, fib Bulletin No.6, Lausanne, Switzerland, 2000.

[6] F. Levi and P. G. Debernardi, "Prove di continuità longitudinale di solai di tipo alveolare privi di cappa di completamento," La Prefabbricazione, vol. 4, pp. 221–236, 1986.

[7] C. Bosco and P. G. Debernardi, "Indagine sulla continuità strutturale di solai alveolari prodotti col metodo Slipform," L'EDILIZIA, vol. 11, pp. 745–752, 1990.

[8] V. Koković, "Granična nosivost oslonačke veze ošupljenih montažnih betonskih ploča," doktorska disertacija, University of Belgrade, 2016.

[9] E. G. Sherwood, One-way shear behaviour of large, lightly-reinforced concrete beams and slabs. PhD thesis, Department of Civil Engineering, University of Toronto, Toronto, ON, Canada, 2007.

[10] prEN 1992-1-1, Eurocode 2, Design of Concrete Structures, Part 1.1: General Rules and Rules for Buildings. European Committee for Standardization, CEN, Brussels, Belgium, 2004.

[11] R. Vaz Rodrigues, Shear strength of reinforced concrete bridge deck slabs. Thèse EPFL, n° 3739, Lausanne, Switzerland, 2007.

[12] J. C. Walraven and H. W. Reinhardt, "Theory and experiments on the mechanical behaviour of cracks in plain and reinforced concrete subjected to shear loading," HERON, vol. 26, no. 1A, pp. 5–68, 1981.

[13] P. G. Gambarova and C. Karakoç, "A new approach to the analysis of the confinement role in regularly cracked concrete elements," in Transactions of the 7. International conference on structural mechanics in reactor technology. Vol. H, 1983, pp. 251–261.

ДГКС Друштво грађевинских конструктера Србије
ASES Association of Structural Engineers of Serbia
P-5
15. KONGRES
6-8. 9. 2018. Zlatibor

Miroslav Marjanović[1]

NELINEARNA ANALIZA LAMINATNIH KOMPOZITNIH PLOČA I LJUSKI SA DELAMINACIJAMA PRIMENOM MKE

Rezime:

Cilj disertacije bio je razvoj efikasnog proračunskog modela zasnovanog na Redijevoj Opštoj slojevitoj teoriji ploča (GLPT), koji je u stanju da opiše kinematiku delaminacije pri dinamičkom opterećenju. GLPT je predstavljala osnovu za razvoj poboljšanih slojevitih konačnih elemenata, koji su primenjeni u numeričkom rešenju različitih strukturnih problema. Geometrijska nelinearnost je uzeta u obzir na osnovu von Kármán-ovih pretpostavki. Prikazan je nelinearni "node-to-node" kontaktni algoritam koji zanemaruje uticaj trenja i sprečava međusobno preklapanje slojeva u zoni delaminacije. Energetski kriterijum, zasnovan na Tehnici virtuelnog zatvaranja prsline, je primenjen da bi se predvidelo širenje delaminacije. Faze Pre- i Post-processing-a su sprovedene primenom GiD Pre/Post Processor-a. Teoretska razmatranja su potvrđena kroz mnoštvo primera, za savijanje, slobodne vibracije, izbočavanje i dinamičku analizu kompozitnih i sendvič ploča i ljuski sa delaminacijom.

Ključne reči: kompozitna ploča/ljuska; delaminacija; GLPT; savijanje; vibracije; izbočavanje

NONLINEAR ANALYSIS OF LAMINATED COMPOSITE PLATES AND SHELLS WITH DELAMINATIONS USING FEM

Summary:

The aim of the dissertation was to develop the efficient computational tool based on the Generalized Laminated Plate Theory (GLPT) of Reddy, capable to describe the delamination kinematics in dynamic loading environment. GLPT became the basis for the development of enriched layered finite elements, applied in the numerical solution of several structural problems. The geometric nonlinearity is taken into account upon the von Kármán assumptions. The node-to-node nonlinear frictionless contact algorithm which prevents the layer overlapping in the delaminated zone of the plate is introduced. In addition, energy criterion based on the Virtual Crack Closing Technique is applied to predict a delamination growth. Pre- and post-processing phases are performed using the GiD Pre/Post Processor. Theoretical considerations are validated through the variety of examples for bending, free vibration, buckling and transient analysis of delaminated composite and sandwich plates and shells.

Key words: composite plate/shell; delamination; GLPT; bending; free vibrations; buckling

[1] *Assistant Professor, PhD, University of Belgrade, Faculty of Civil Engineering, mmarjanovic@grf.bg.ac.rs*

1. INTRODUCTION

Composite materials (see Fig. 1) attract the increasing attention in the various engineering disciplines. They play an important role in the design and construction of aircrafts, wind turbines, ships, cars and many other parts in mechanical and civil engineering. These materials have an excellent fatigue and corrosion resistance properties, as well as high stiffness-to-weight and strength-to-weight ratios. Examples are carbon-fiber, glass-fiber, or fiber-reinforced polymers (FRP). It is well-known that FRP-strengthening of the reinforced-concrete or wooden beams and slabs give excellent structural results, low time required and moderate cost. FRP bridge decks (Fig. 2, left) comprise sandwich profiles, spanning transversely or longitudinally between supporting elements (such as steel beams) or suspended from tension cables. The lightweight, stay-in-place formwork made of an FRP sandwich panel is also used for the construction of concrete and composite steel-concrete bridge decking (Fig. 2, right).

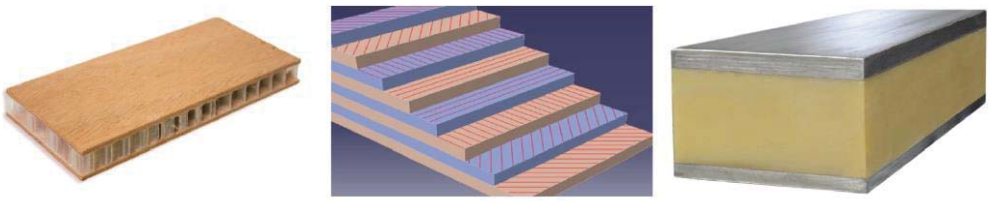

Figure 1 - Different types of laminar composites: honeycomb sandwich plate (left), laminated composite plate (middle) and soft-core sandwich panel (right)

Another type of plate structures relevant for the numerical model discussed in the dissertation are sandwich panels, i.e. structural members made of two stiff orthotropic faces separated by an isotropic core (Fig.1, right). In civil engineering, the soft-core sandwich panels are used as light roof and wall panels usually designed to provide the thermal isolation of the buildings. It is of the great importance that the bond between the face sheets and the soft-core in sandwich panel remain intact for the panel to perform on the appropriate level.

Figure 2 – Wolf Trap pedestrian bridge with FRP composite decking in Virginia, USA (left) and Uyllander Bridge in Amsterdam (right)

However, the significant shear stresses produced between the layers of the composite plate may cause *delamination*, which is the most common type of damage. It may also result from different fabrication induced faults in the joining of plies. Once significant damage occurs at

the ply level, the kinematic and material description of the problem must be changed before further analysis can proceed. An overview of delamination problems can be found in [1].

As the laminated composite plates are used for primary or secondary components of different engineering structures (generally loaded with transient loads), it is of the great importance to understand their fundamental dynamic properties, such as natural frequencies and mode shapes. This requires the adequate computational models able to consider the delamination of plates in dynamic loading environments, in order to predict the transient response of the delaminated structure.

1.1. GENERALIZED LAMINATED PLATE THEORY

The structural response of laminated composite plates (Fig. 3, left) can be accurately determined by the use of relatively simple Equivalent-Single-Layer (ESL) laminate theories, especially for the laminates with high length-to-thickness ratios [2]. However, in the case of thicker structural components, these theories are not adequate since they give too stiff response because of the simplifications associated with the classical plate kinematics. Due to the considerably different material characteristics of the adjacent layers within a laminate, discontinuities in transverse shear strains at the interfaces between layers may be significant - this phenomenon is not accounted for in ESL theories. Another problem that arises is inability of the ESL theories to consider the local damage effects (matrix cracking, delamination, free edge effects etc.).

The above limitations motivated the author to consider Reddy's Generalized Laminated Plate Theory (GLPT) [3] in the derivation of the numerical model, because the layerwise discontinuous displacement field (Fig. 3, right) of the GLPT is able to capture the relative displacements between the adjacent layers in the delaminated zone. To accurately predict the buckling phenomena due to significant in-plane forces acting on the laminate, the geometric nonlinearity is taken into account using the von Kármán's nonlinear plate kinematics [4].

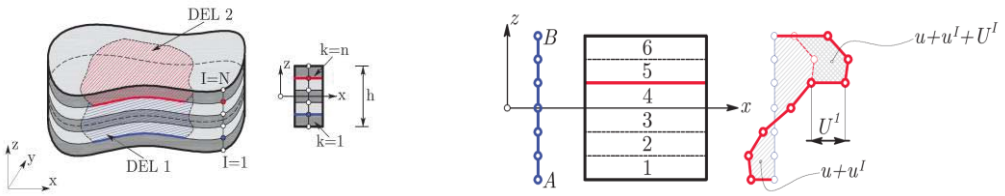

Figure 3 – Typical laminated composite plate with two delaminations (left) and assumed layerwise displacement field of the GLPT (right)

2. FINITE ELEMENT MODEL

Analytical solution of the GLPT exists only for the relatively simple plate geometries, loading types and boundary conditions. However, for the analysis of structural elements of arbitrary shape, loading, boundary conditions, as well as for the analysis of laminated composite plates with delaminations of arbitrary shape and arbitrary positioned within a structural element, numerical solution is required. The Euler-Lagrange differential equations of motion of the GLPT define the "strong" formulation of the geometrically nonlinear problem of

the laminated composite plate. These governing equations served as a basis for the development of a numerical (FE) solution. The primary variables of the problem are translational components of the mid-plane (u, v, w), relative displacements in numerical layers through the plate thickness (u^I, v^I, I=1,2,…,N) and delamination openings in three orthogonal directions (U^I, V^I, W^I, $I=1,2,\ldots, ND$). The typical layered finite element is shown in Fig. 4. The layerwise discontinuous displacement field of the GLPT is shown in Fig. 3, right.

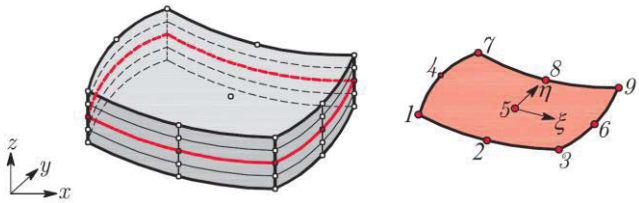

Figure 4 –Typical layered finite element with nine nodes (quadratic interpolation)

3. CONTACT ALGORITHM

The node-to-node nonlinear frictionless contact algorithm is proposed in the dissertation. The aim is to prevent the layer overlapping in the delaminated zone of the composite plate, during its motion in transient loading environment. The contact condition is iteratively enforced in every solution step, until the convergence criterion is satisfied (see Fig. 5).

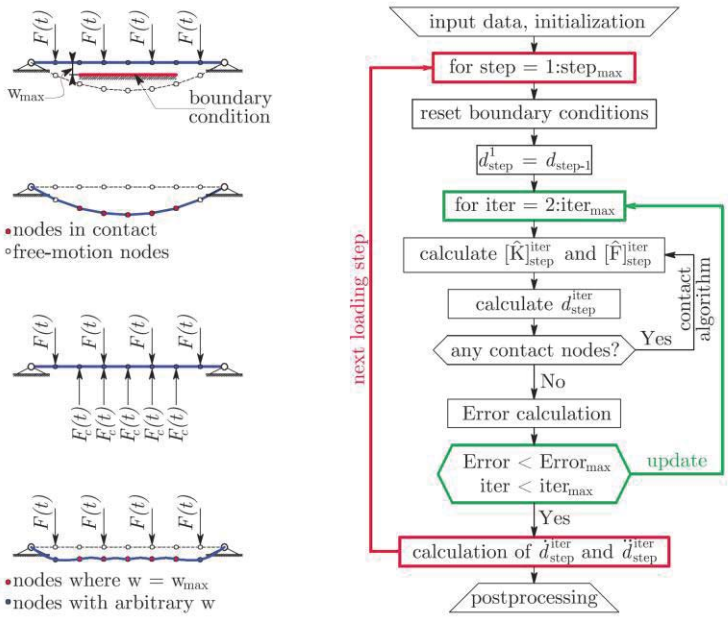

Figure 5 – Contact algorithm to prevent overlapping in delaminated interfaces (left) and the flowchart of the program (right)

After the global equilibrium in the current step is satisfied, the next time step is computed where the contact status is again checked. The advantage of the proposed method is that it can be implemented easily into the geometrically nonlinear transient analysis algorithm. The efficiency of the contact algorithm is illustrated in the paper already published by author in [5].

4. DELAMINATION PROPAGATION

The energy dissipated during the delamination propagation per unit of a newly created delaminated area is called Strain Energy Release Rate (SERR), which can be calculated using the direct or indirect methods that have been developed over years. Within this dissertation, the deformation field obtained from the numerical solution of the GLPT is used to predict three Strain Energy Release Rate components G_i, which are further compared with the interlaminar fracture toughness, using the fracture criteria along the crack boundary.

The algorithm for tracking the moving delamination front is presented as the extension of the method proposed by Xie et al. [6, 7], which was restricted to the structured FE meshes. The displacement field obtained from FE calculation is used for the computation of G_i using the Virtual Crack Closure Technique. The method requires the calculation of the delamination opening behind the crack front, the nodal forces along the front and the virtually closed area in front of the existing delamination. To predict the delamination growth the calculated components are compared with the inter-laminar fracture toughness. The direction in which delamination will grow is described by the vector normal to the delamination front, which components are accurately calculated in this study unlike the majority of the models from the literature (Fig. 6, left). The virtually closed area is determined using 6 control points for every node along the delamination front. After that, the forces along the delamination front, the delamination openings behind the front and finally G_i components are calculated in the region of the virtually closed area. A mixed-mode fracture criterion is applied next in all considered nodes. The algorithm is repeated until there are no more propagating nodes in the current step of the analysis. Subsequently, the analysis continues with the next time or loading increment. Some basics of the proposed algorithm are published by author in [8].

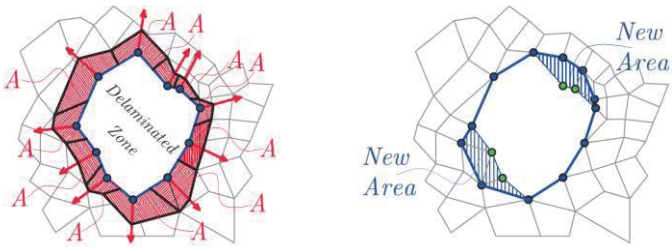

Figure 6 – Non-overlapping virtually closed areas along the delamination front (left) and the generation of new delaminated zones after the propagating nodes are identified (right)

5. ANALYSIS OF LAMINATED COMPOSITE SHELLS

In this part of the dissertation, the possibility to represent the continuously curved shell surfaces using the assembly of small flat triangular finite elements (Fig. 7) is presented. The same assumptions as used in the analysis of plates (regarding the transverse distribution of strains and stresses) are valid in the consideration of shells. Some properties of the vector algebra are used for the transformation of the coordinates and characteristic element matrices.

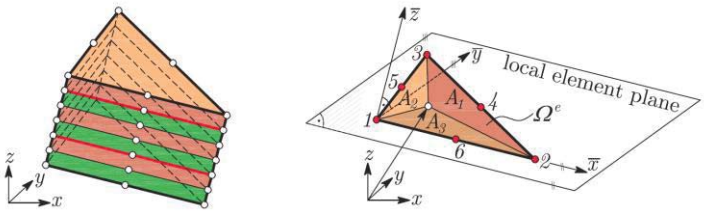

Figure 7 – Triangular layered element for the modeling of composite shells

However, in the proposed formulation the difficulty arises if all the elements meeting in a node are co-planar. This situation will arise for shallow shell structures, at (folded) shell segments and at straight boundaries of developable surfaces. The proposed model is applied in the free vibration analysis of laminated composite shells. The part of the presented results is already published by Marjanović and Vuksanović in [9].

6. OBJECT-ORIENTED COMPUTER PROGRAM

Performance and memory efficiency are two crucial requirements for the finite element programs. Therefore, the code should be well organized to increase the flexibility and reduce its maintenance cost. It should be extendable to new formulations, algorithms and concepts. The solution process in the FEM can be split into several steps:

1. Pre-Processing - geometry definition (points, lines, surfaces, volumes), definition of attributes or conditions (BC, loads...), their assignment to the geometrical entities and finally generation of the finite element mesh,
2. Simulation - Calculation in solver,
3. Post-processing - Visualization of the results.

All these steps must be carried out carefully, and must be easy for the user to perform. Within this dissertation, the pre- and post-processing phases are performed using the GiD Pre/Post Processor developed in CIMNE, Barcelona, which algorithm is shown in Fig. 8.

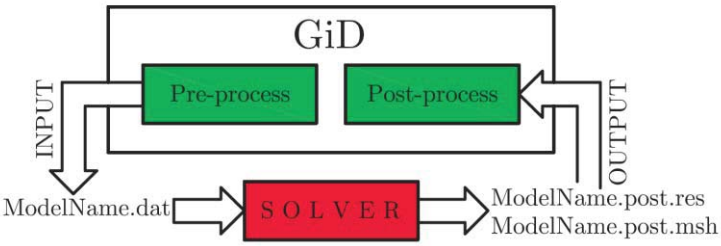

Figure 8 – The algorithm of the GiD-based finite element program

The graphical interface used for all simulations in this dissertation is illustrated in Fig. 9.

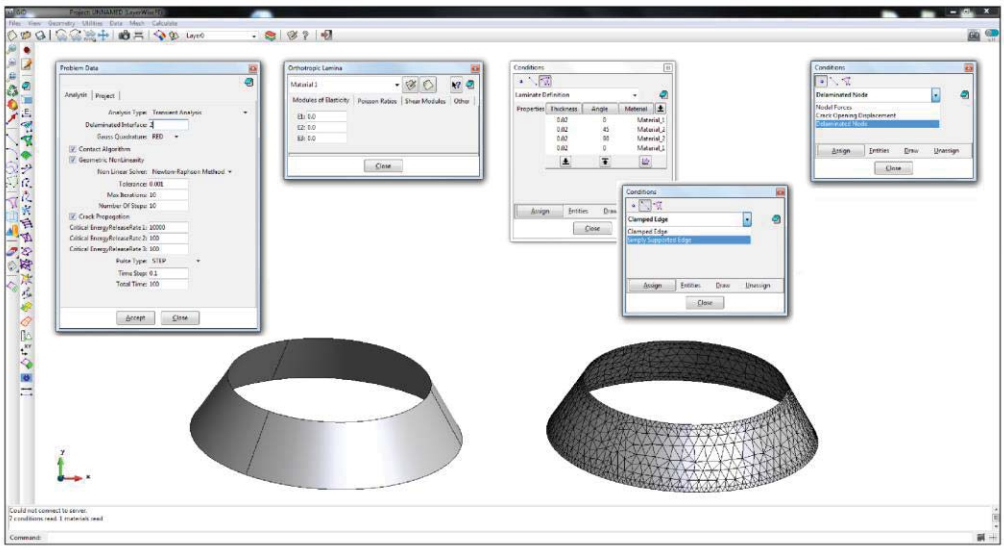

Figure 9 – Graphical interface in GiD for the assignment of problem data (left), materials (center) and conditions (right). Geometric domain of the conical shell / meshed model (below)

7. CONCLUSIONS

In the thesis, family of triangular and quadrilateral layered finite elements with varying levels of interpolation, capable to incorporate the independent motion of adjacent delaminated interfaces are recalled based upon the Generalized Laminated Plate Theory of Reddy. The numerical model is extended for the analysis of free vibration response of composite shells, using simple geometrical considerations. Due to some simplifications of the shell kinematics, the limitations of the model are highlighted in this study. Geometrical nonlinearity is accounted based upon the von Kármán assumptions. Inter-laminar penetration between delaminated layers has not been enabled by activating the contact conditions between the individual layers.

A novel delamination propagation algorithm has been implemented based on the Virtual Crack Closure Technique, to allow for the change of the previously imposed delaminated zone during the static and dynamic motion of the plate. The proposed models have been verified and their accuracy is demonstrated using the variety of benchmark examples. The accuracy is proved both for the intact and delaminated composite plates. The differences between the models considering stationary and propagating delamination have been highlighted.

From the number of numerical analyses, the following conclusions are drawn:

- The simplifications regarding the transverse shear deformation in the ESL theories cause the underestimation of the transverse deflections and the overestimation of the fundamental frequencies of laminated composite plates, when compared to the GLPT.
- When the delamination is present, the influence of the transverse shear deformation is higher for the plates with highly constrained boundaries. Reduced integration is necessary in thin plate situation to prevent the shear locking.
- Transverse shear deformation severely influences the fundamental dynamic characteristics of cylindrical and conical laminated composite shells, both for the thin and thick shell situation. This influence is higher for the shells with the higher level of orthotropy, as well as for the higher modes of oscillation.
- The proposed model is capable to accurately predict the fundamental frequencies of intact laminated composite plates of different shapes, even by using the quadrilateral elements for approximation of the circular plate geometry. Slightly better performance of quadratic elements is detected in the prediction of higher modes of vibration.
- The reduction of the fundamental frequency of the laminated composite plates caused by the presence of the delamination is more pronounced for higher modes. The position of the embedded delamination through the plate thickness plays an important role by significantly reducing the global fundamental frequency of the delaminated plate (both composite and sandwich) for mid-plane delamination, and otherwise having a marginal effect when near-surface delamination is employed.
- For composite shell structures, the mesh refinement, as expected, reduces the natural frequencies of the CC cross-ply cylindrical and conical shells, with the convergence to the exact solution both for the structured and unstructured mesh and shell thicknesses varying from thin to thick situation.
- Because of the geometry idealization using the at triangular FEs for the generation of curved surfaces, a stiffer response then expected is obtained in the case of conical shells.
- When the delamination is present within a shell structure the natural frequency is reduced severely after the increase of the delaminated area above 12% of the shell area. For the numerical models with highly constrained boundaries, the influence of the delamination area on natural frequencies is higher.
- The proposed model accurately predicts the critical buckling load of laminated composite plates, in comparison with the existing close form and 3D elasticity solutions. The accuracy is proven even for the coarse mesh, leading to the reduced computational cost. It is documented that the delaminated area up to the 6% of the plate area does not reduce the critical buckling load. When the delamination position within a plate is considered, near-surface delamination has smaller influence to the results, because the intact rest of the plate is stiff enough to hold the majority of the critical buckling

loading. The similar trend is observed for the uniaxially compressed sandwich plates, having in mind that thin delaminated layer will buckle independently from the rest of the plate.

- The activation of the contact algorithm during the transient analysis of laminated composite plates showed to have only a minor effect in linear analysis. However, in the geometrically nonlinear analysis the delamination has a considerable influence. Changing the position of delamination in the geometrically nonlinear analysis is not affecting the transient response if the contact algorithm is not activated, in contrary with the case when contact algorithm is activated.
- Transient analysis of delaminated plates showed that when a small delamination area is present within a laminate only a marginal increase of the amplitude and the period of oscillations is observed in linear analysis. However, in the case of geometrically nonlinear transient analysis the period of oscillations is slightly reduced because of the added bending stiffness of the plate, as expected. For the larger size of the delaminated area the amplitudes and the period of oscillations of the laminate are significantly increased due to the significant stiffness degradation. Changing the position of the delamination zone through the plate thickness does not have a large effect on the frequency of the oscillations in the linear analysis.
- The sandwich plates are highly vulnerable to embedded delamination between the soft-core and rigid face sheets when subjected to exponential blast pulse loading. The global amplitudes of the intact rest of the plate are increased because of the splitting. The crack opening displacements are small in the linear and slightly higher in the geometrically nonlinear analysis. On the other hand, if the delamination occurs within the rigid face sheet, the global amplitudes of the intact rest of the plate are nearly the same as for the intact late, because the undamaged part has the more or less the same bending stiffness as the intact plate. When the delamination area is small the face-core debonding is negligible. The CODs are slightly higher in the geometrically nonlinear transient analysis. After increase of the delaminated area, however, the global linear plate motion significantly changes and becomes more complex, with increased amplitudes due to the reduction of the plate stiffness. In the geometrically nonlinear response of the sandwich plates the added bending stiffness leads to a reduction of the crack opening displacements as compared to the linear case. The highest amplitudes and crack opening displacements are reached at the end of blast pulse and start of free vibration phase.
- Incorporation of the delamination propagation algorithm severely influences the transient response of the delaminated plate. In the moment of delamination extension the response of the delaminated layer is changed considerably leading to the reduction of the frequency because of the stiffness degradation and increase of the amplitudes. The general trend of the delamination extension is independent of the mesh density, but the final shape of the delamination is mesh-dependent by means of creation of smooth delamination front for fine mesh and polygon-shaped front for coarse mesh. The considerable change in the transient response of delaminated plates occurs nearly in the same time point regardless of the mesh density. The mesh refinement results in the lower amplitudes of oscillations of the delaminated segment, with higher frequencies, due to the fact that fine mesh allows for smooth step-by-step change in the delaminated zone, which is a robust and elegant, but also a very simple approximation of the real

behavior of the delaminated structure. The mesh dependence is caused by a node-to-node delamination propagation algorithm, which implies two main approximations: (1) the node-to-node approximation of a virtually closed area A and, (2) the node-to-node approximation of the movement of the delamination front.

- On the other hand, when static bending analysis of laminated plates is performed with activated delamination propagation algorithm, it has been found that linear finite elements result in the slightly higher values of the calculated reaction force in the displacement-control analysis of the DCB, in comparison with the quadratic elements. The distribution of the G_I along the plate width calculated using the linear elements is nearly constant in contrast with the quadratic elements for which the distribution is curved. The mesh refinement in width direction does not significantly influence the G_I distribution, while the reduction of the displacement increment leads to the convergence of numerical solution.

ACKNOWLEDGMENTS

The work on this thesis was advised by Prof. Dr. Djordje Vuksanović, who suddenly passed away during the final stage of writing of the dissertation. The author would like to dedicate this work to a memory of him.

The co-advisory of Prof. Dr.techn. Günther Meschke (Ruhr Universität Bochum, Lehrstuhl für Statik und Dynamik) is gratefully acknowledged.

The work on this thesis was supported by the Government of the Republic of Serbia - Ministry of Education, Science and Technological Development, under the Project TR-36048. The financial support has been also provided through the SEEFORM project financed by DAAD.
The full license of MATLAB software was provided through this project. The full license of GiD software was provided by the Institute of Structural Mechanics, Ruhr University Bochum.

REFERENCES

[1] Bolotin V. V.: Delaminations in composite structures: its origin, buckling, growth and stability, Composites Part B: Engineering, 27, 1996, 129-145.

[2] Vuksanović Dj., Ćetković M.: Bending , free vibrations and buckling of laminated composite and sandwich plates using a layerwise displacement model, Composite Structures, 88, 2009, 219-227.

[3] Barbero E. J., Reddy J. N.: Modeling of Delamination in Composite Laminates using a Layer-Wise Plate Theory, International Journal of Solids and Structures, 28(3), 1991, 373-388.

[4] von Kármán T.: Festigkeits Versuche unter allseitigem Druck, Verhandlungen der Deutchen Ingenieurwesen, 55, 1911, 1749-1757.

[5] Marjanović M., Vuksanović Dj., Meschke G.: Geometrically nonlinear transient analysis of delaminated composite and sandwich plates using a layerwise displacement model with contact conditions, Composite Structures, 122, 2015, 67-81.

[6] Xie D., Biggers S. B.: Strain energy release rate calculation for a moving delamination front of arbitrary shape based on the virtual crack closure technique. Part I: Formulation and validation, Engineering Fracture Mechanics, 73(6), 2006, 771-785.

[7] Xie D., Biggers S. B.: Strain energy release rate calculation for a moving delamination front of arbitrary shape based on the virtual crack closure technique. Part II: Sensitivity study on modeling details, Engineering Fracture Mechanics, 73(6), 2006, 786-801.

[8] Marjanović M., Meschke G., Vuksanović Dj.: A finite element model for propagating delamination in laminated composite plates based on the virtual crack closure method, Composite Structures, 150, 2016, 8-19.

[9] Marjanović M., Vuksanović Dj.: Free vibrations of laminated composite shells using the rotation-free plate elements based on Reddy's layerwise discontinuous displacement model, Composite Structures, 159, 2016, 320-332.

U1 – U5

OPENING LECTURES

ДГКС Друштво грађевинских конструктера Србије
ASES Association of Structural Engineers of Serbia
U-1
15. KONGRES
6-8. 9. 2018. Zlatibor

Hugo Corres Peiretti[1], *Freddy Ariñez Fernández*[2], *Julio Sánchez Delgado*[3]

fib MODEL CODE 2020. SADRŽAJ I TEKUĆI PROCES.

Rezime:

Model Propisa je jedan od najznačajnijih dokumenata izdatih od strane *fib*-a. Prvo izdanje objavljeno je 1970. godine. Od tada, *fib* je publikovao nova izdanja 1978., 1990, i najnovije, 2010. godine. Modeli propisa su referentna literatura i uticali su na izdavanje nacionalnih i regionalnih pravilnika. Ovaj rad prikazuje sadržaj novog Modela Propisa 2020 i tekući rad na njegovoj pripremi.

Ključne reči: konstrukcijski beton, nove i postojeće konstrukcije, pravilnici, sigurnosni koncept, materijali, upravljanje konstrukcijama tokom upotrebnog veka

fib MODEL CODE 2020. CONTENT AND ONGOING PROCESS.

Summary:

Model Code is one of the most important documents produced by *fib*. The first edition was published in 1970. Since then, *fib* has published new and updated editions in 1978, 1990 and, the most recent one, in 2010. All of these documents have been reference documents that have influenced the production of National and Regional Codes.This paper shows the content of the new Model Code 2020 and the ongoing work for its preparation

Key words: structural concrete, new and existing structures, codes, safety format, materials, design, management of structures during the service life

[1] *PhD, President, International Federation for Structural Concrete (fib), hcp@fhecor.es*
[2] *PhD, Structural Engineer, FHECOR*
[3] *MSc, Structural Engineer, FHECOR*

1. INTRODUCTION

Model Code is one of the most important documents produced by *fib*. The first edition was published in 1970. Since then, *fib* has published new and updated editions in 1978, 1990 and, the most recent one, in 2010. All of these documents have been reference documents that have influenced the production of National and Regional Codes. Model Code 1978 had a strong influence on the previous version of Eurocode 2; Model Code 1990 had the same strong influence on the current version of Eurocode 2 and Model Code 2010 similarly guides the preparatory work CEN has started for the new editions of the Eurocodes. Model Codes have always been an important reference for researchers, designers and constructors.

Some years ago, the *fib* started the process to produce a new updated edition to be published in 2020. This new Model Code intends to approach, at the same level, new and existing structures. It will present more general and more rational models, removing any trace of previous empirical design rules (MC2010 was an important step forward, but further steps are possible and needed). It will be an operational model code and oriented towards practical needs. It will recognize the needs of engineering communities around the world. MC 2020 has to be a real International Code.

This paper shows the content of the new Model Code 2020 and the ongoing work for its preparation.

2. MAIN IDEAS/GOALS OF THE NEW MC 2020

1.1. MC 2020 WILL BE A SINGLE, MERGED STRUCTURAL CODE FOR NEW AND EXISTING STRUCTURES.

There were many different approaches for codes to be able to cover existing structures. A good summary of the evolutions of codes for existing structures was presented by Dr Steve Danton [1], at the first workshop to discuss the content of the new MC 2020 held in The Hague in June 2015.

The first approach/generation was to use the codes developed for new structures and apply them to existing structures. The result was not good because it failed to recognise the differences between design and assessment. Typically, the results obtained with this approach were conservative for assessment works, because it did not adequately take into account actual material properties, structural detailing and tolerances.

The second approach/generation was to write codes for existing structures. The result was also not good enough because there were cases of duplication of content, omission of content and it presented problems in the case of interventions (modification of existing structures).

The new approach, and what is often called the new generation of codes, is to develop a single, merged code structural code for both new and existing structures. And this is exactly what we decided to do for the new MC 2020.

The principles for the development of a unified Model Code will be: General provisions / models common for design, assessment and interventions. Provisions / models have to be general to be applied for the different problems we have to solve. General provisions / models

capable of taking into account actual material properties, structural detailing and tolerances that may be found on existing structures.

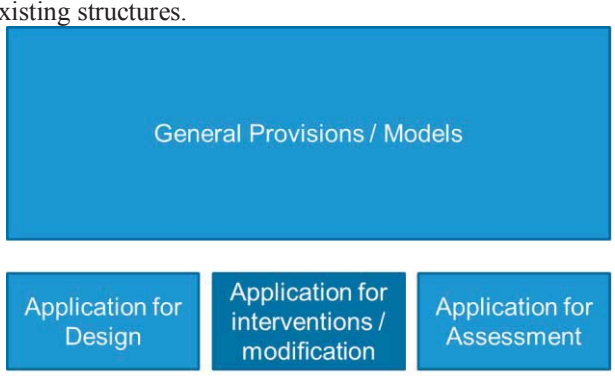

Figure 1 - New generation of structural codes for new and existing structures. Figure presented by Dr. Steve Denton at the first workshop on Model Code 2020, held at The Hague on June 2015 [1]

1.2. MC2020 HAS TO PRESENT GENERAL AND MORE RATIONAL MODELS, REMOVING ANY TRACE FROM PREVIOUS EMPIRICAL DESIGN RULES.

MC2010 was an important step forward in removing empirical design rules leaving space for general and rational models. This criterion has to be expanded in the new MC 2020.

Figure 2 shows the differences in using a general rational with an empirical rule for bending of a reinforced concrete section.

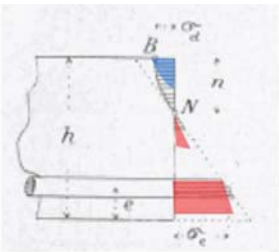

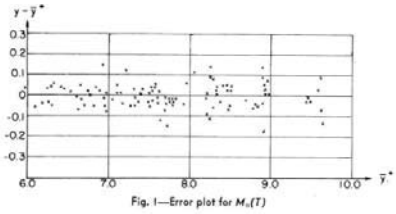

$$M_R = 0.431 \cdot b \cdot d^2 \cdot \rho^{0.75} \cdot f_y^{0.9} \cdot f_c^{0.1} \text{ (psi, in)}$$

Ritter, W., 1899, *Die Bauweise Hennebique*, Schweizerische Bauzeitung, Zurich

Courtesy of Aurelio Muttoni

Zsutty T.C., *Ultimate Strength Behaviour Study by* ***Regression Analysis of Beam Test Data***, ACI Structural Journal, May 1963

Figure 2 - Mechanical models vs. empirical equations, the case of bending. Figure presented by Prof Aurelio Muttoni at the first workshop on Model Code 2020, held at The Hague on June 2015 [2]

Ritter proposed in 1899 the model which is still used in *fib*, see Figure 3 taken from MC 2010. This general approach allows considering: axial force, different cross-section shapes, several reinforcement layers, prestressing, different concrete types, different types of loads (fire, seismic loads, etc.). In addition, the model can be easily adapted to a wide variety of cases (different types of concrete, non-metallic reinforcement, sections subjected to different types of deterioration, etc.). This model may be used to consider the different situations we have in the design of new structures and in the assessment and interventions in existing structures. In comparison, the empirical formula proposed by Zsutty in 1963 is only valid for the conditions for which was developed.

Figure 7.3-1 shows the possible range of strain distributions for concrete, reinforcing steel and prestressing steel. In the figure, the following limits are shown:

A = reinforcing strain limit;

B = concrete compression limit; and

C = concrete pure compression strain limit.

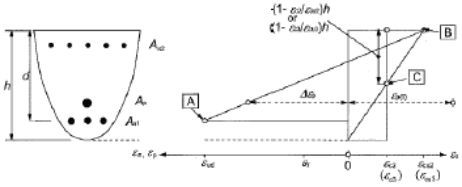

Figure 7.3-1: Possible strain distributions in the ultimate limit state.

7.3.2 Bending with and without axial force

7.3.2.1 Beams, columns and slabs

This sub-clause applies to undisturbed areas of beams, slabs and similar types of members for which sections remain approximately plane before and after loading. The discontinuity regions of beams and other members, where plane sections do not remain plane, may be designed and detailed according to sub-clause 7.3.6.

When determining the ultimate bending resistance of reinforced or prestressed concrete cross-sections, the following assumptions are made:

- plane sections remain plane;
- the strain in bonded reinforcement or bonded prestressing tendons, whether in tension or in compression, is the same as that in the surrounding concrete;
- the tensile strength of the concrete is ignored;
- the stresses in the concrete are derived from stress-strain relations for the design of cross-sections as given in sub-clause 7.2.3.1.5;
- the stresses in the reinforcing and prestressing steel are derived from the design curves in sub-clause 7.2.3.2 and 7.2.3.3; and
- the initial strain in the prestressing tendons is taken into account when

Figure 3 - fib MC 2010 model for bending [3].

Figure 4 shows how the same *fib* model may be used for assessment of existing structures or for design of new structures or interventions.

The top part of the figure shows different types of concretes that can be found in existing and in new structures, including new types of concrete: FRC, UHPFRC, Green Concretes, Tailor-made concretes, etc. In order to use the model for all of the different concretes it is only necessary to have the correct constitutive equations for the different cases. The bottom part of the figure shows the constitutive equations currently available in MC 2010 for concretes with different compressive strengths.

MC 2010 was drafted to take into account different types of actions, in addition to static actions, such as for example, seismic actions, fire and many others. This same philosophy was preserved in MC 2020, adopting models, like the one shown in Figure 4, where different types of actions can be represented only by considering the pertinent constitutive equations. Figure 5 shows the constitutive equations proposed by MC 2010 to represent the behavior of confined concrete for seismic actions, or concrete subjected to different temperatures, to consider the influence of fire.

The assessment of existing structure requires setting forth criteria to estimate representative characteristics of concrete. Thus, we must define the right experimental test campaign in order to obtain results that are actually representative of the structure.

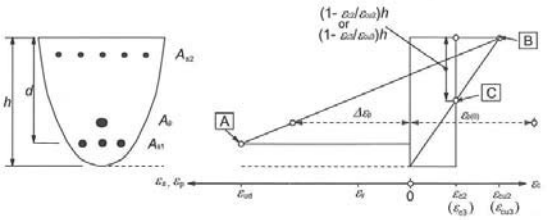

			EXISTING CONCRETE			
fck	17	20	90	120	150	250
			DESIGN CONCRETE			
fck	17	20	90	120	150	250
			FIBRE REINFORCED CONCRETE (FRC)			
fck	17	20	90	120	150	250
					UHPFRC	
fck	17	20	90	120	150	250

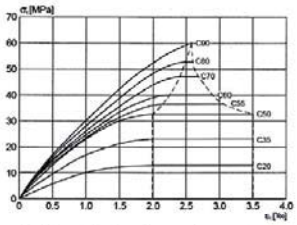

Figure 7.2-7: Design stress strain relations for various concrete strength classes (parabola-rectangle) for $\gamma_c = 1.5$

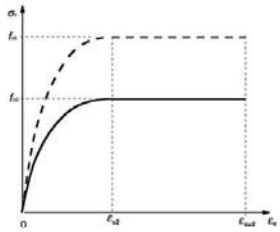

Figure 7.2-9: Parabola-rectangle diagram for concrete in compression

Figure 4 - fib Model Code 2010 model for bending extended for assessment of existing structures or for design of new structures or interventions on existing structures. Constitutive equations for concretes with different compressive strengths.

Likewise, we also need more and better models, than the ones currently available in MC 2010, in order to represent the effect of different types of deteriorations in the bearing capacity of concrete.

In the case of reinforcing and prestressing steel it is possible setting forth constitutive equations that represent the situations found in the assessment, design and intervention of structure, both for static actions and other actions that may be found in the structures. In fact, MC 2010 has already established many of these equations, see Figures 6 and 7.

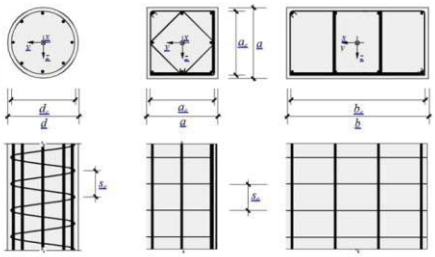

fib MC 2010 Figure 7.2-13: Compression members with confining reinforcement

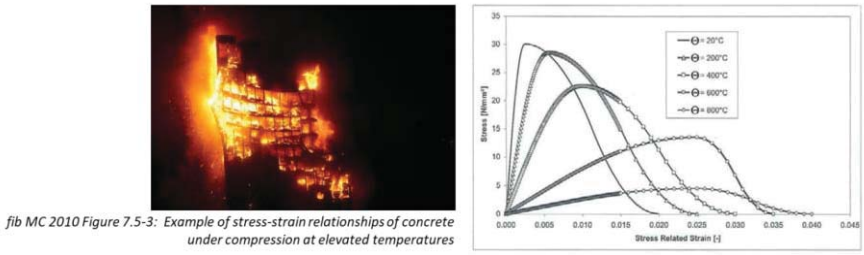

Figure 5 - fib Model Code 2010 model for bending extended for the assessment of existing structures or for the design of new structures or interventions on existing structures. Constitutive equations for confined concrete and concrete subjected to different temperatures.

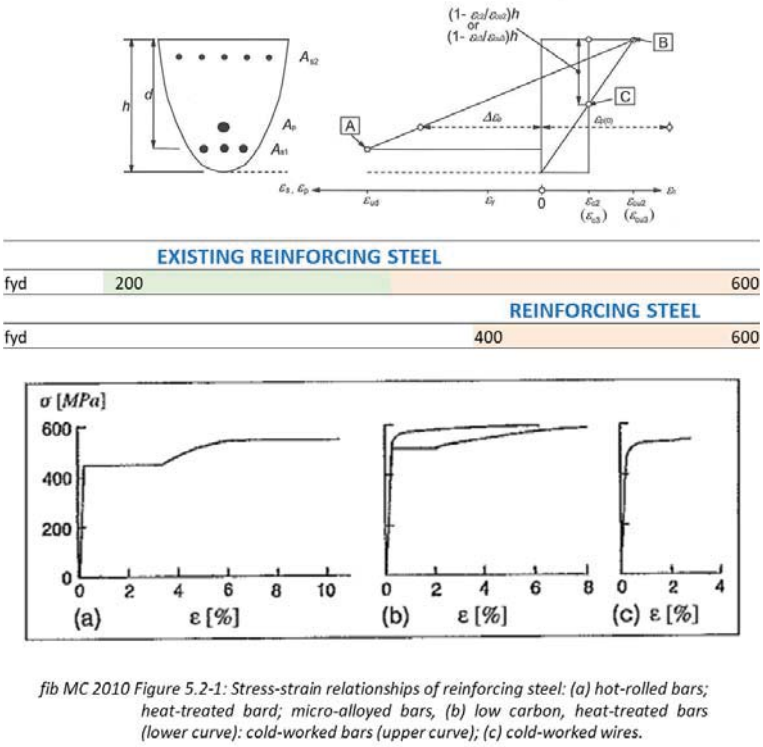

Figure 6 - fib MC 2010 model for bending extended for assessment of existing structures or for design of new structures or interventions on existing structures. Constitutive equations for reinforcing steel.

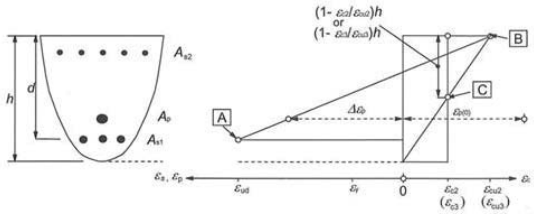

EXISTING PRESTRESSING STEEL			
fyp	1700	2000	2500
PRESTRESSING STEEL			
fyp	1700	2000	2500

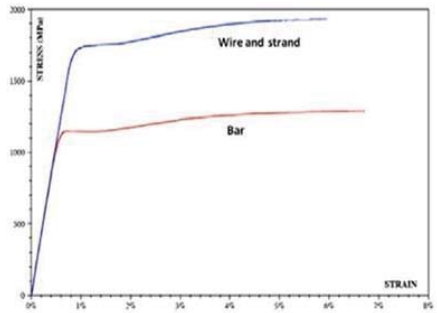

fib MC 2010 Figure 5.3-1: Typical stress-strain diagrams for prestressing steel

Figure 7 - fib MC 2010 model for bending extended for assessment of existing structures or for design of new structures or interventions on existing structures. Constitutive equations for prestressing steel.

The same model can be used to represent non-metallic reinforcement, used lately in new structures and in retrofitting existing structures. For this type of material it will be necessary to revise the safety formats in order to define material safety factors that take into account the brittleness of these materials as well as other specific uncertainties.

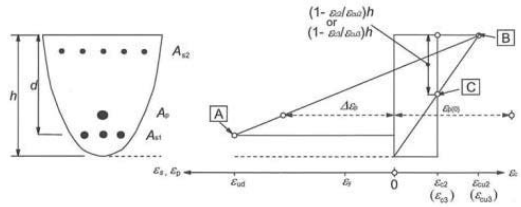

NON-METALLIC REINFORCEMENT / FRP			
fck	1000		2500

	CFRP	GFRP	AFRP
Tensile strength f_f [MPa]	600-3000	400-1600	600-2500
Modulus of elasticity E_f [GPa]	80-500	30-60	30-125
Ultimate strain ε_{fu} [%]	0.5-1.8	1.2-3.7	1.8-4.0

fib MC 2010 Table 5.5-1:Tensile properties of FRP reinforcement

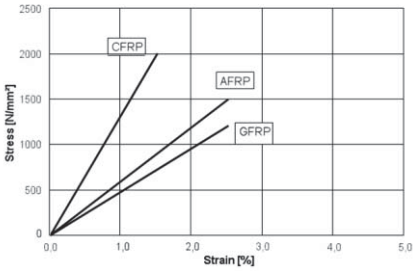

fib MC 2010 Figure 5.5-1: Stress-strain diagram of non-metallic reinforcement in the principal fibre direction

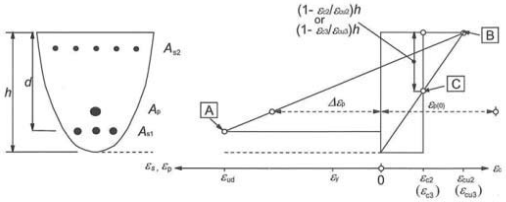

Figure 8 - fib MC 2010 model for bending extended for assessment of existing structures or for design of new structures or interventions on existing structures. Use of non-metallic reinforcement.

The same *fib* model for normal stresses is capable of estimating the resistance of a reinforced section. In this case, it is necessary to elaborate a system to represent the tensional state in section under the loads, generally permanent loads, applied prior to the design forces. This can be materialized with a preliminary strain in all of the materials of the cross-section. Afterwards, taking into account the initial stress state, additional factored loads can be applied to the structure for a given combination.

Figure 9 shows a cross-section a) with dimensions of 0.30x0.50 and C25 concrete and 4 rebars with a diameter of 16 mm of B500B steel and a cover of 0.05 m. It also shows b) the section affected by a corrosion process of the reinforcing steel, showing how the concrete cover was lost as well as 80% of the original rebar area. Finally, it shows c) a section where the concrete cover was replaced and a steel plate with dimensions of 200x20 mm2 was added.

The original section had ULS strength of 142 kNm, as shown in Figure 10. The damaged section has ULS strength of 117 kNm, as shown in Figure 11. It is clear that the resisting capacity of the structure was reduced. Figure 12 shows the tensional state of the damaged section for permanent load forces. Finally, Figure 13 shows the ULS strength of the reinforced section, considering a preliminary deformation that corresponds to the permanent load forces on section b). The efficiency of the reinforcement can be strongly conditioned by the tensional state of the section prior the application of the reinforcement as well as its corresponding design loads.

The *fib* model for normal stresses is capable of taking into account all of the different situations that occur in a section for the design of a new structure, for the assessment of an existing structure and for the evaluation of the bearing strength of possible interventions.

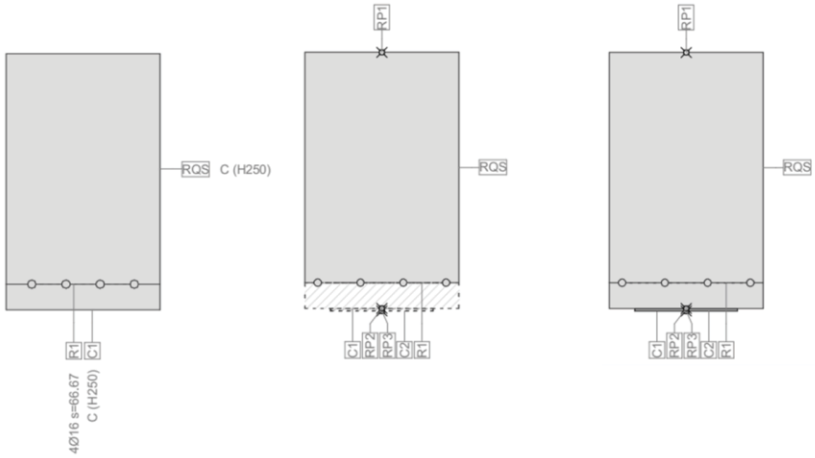

Figure 9 - a) Original cross-section design b) Deteriorated cross-section, for a reinforcing steel corrosion process. C) Reinforced cross-section, where the part of the missing cover was replaced and a steel plate was added to the bottom face.

Nevertheless, it will be necessary in the new MC 2020 to adequately describe the process to take into account the tensional state of the section before considering the designed reinforcement. It will also be necessary to clarify how to deal with the ULS safety of the loads on the structure, generally, permanent loads, before the application of the reinforcement. For new structures, load factors are applied at once because, in this case, the initial deformations are not taken into account. For reinforcements and retrofitting of existing structures, we first take into account the tensional state under the loads that act prior the execution of the reinforcement, possibly with characteristics values and, afterwards, at the ULS, these loads will be considered with their corresponding safety factor, which was not considered at the initial state.

The analysis proposed in this paper corresponds to normal stress models. It is still necessary to carry out a detailed work to adapt the available models for other forces such as shear, punching shear and torsion, in order for these models to consider all of the situations described above.

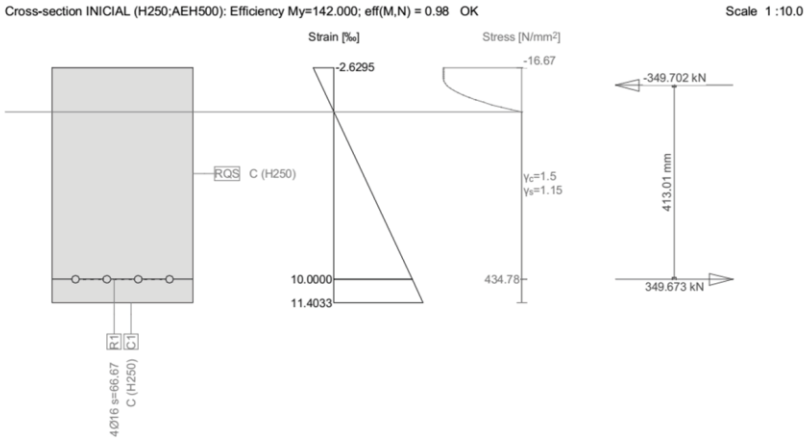

Action forces / Efficiency: eff(M,N) = 0.98 OK

No.	AP	P	Bending and axial force N [kN]	M_y [kNm]	M_z [kNm]	eff(M,N) [-]	Shear forces and torsion V_y [kN]	V_z [kN]	T [kNm]	eff(V,T) [-]	Complete CS eff(M,N,V,T) [-]
1	AP4		0	142.000	-	0.98					

- : Calculation with uniaxial bending (neutral axis is horizontal)!!

Figure 10 - ULS strength of the original design of the cross-section.

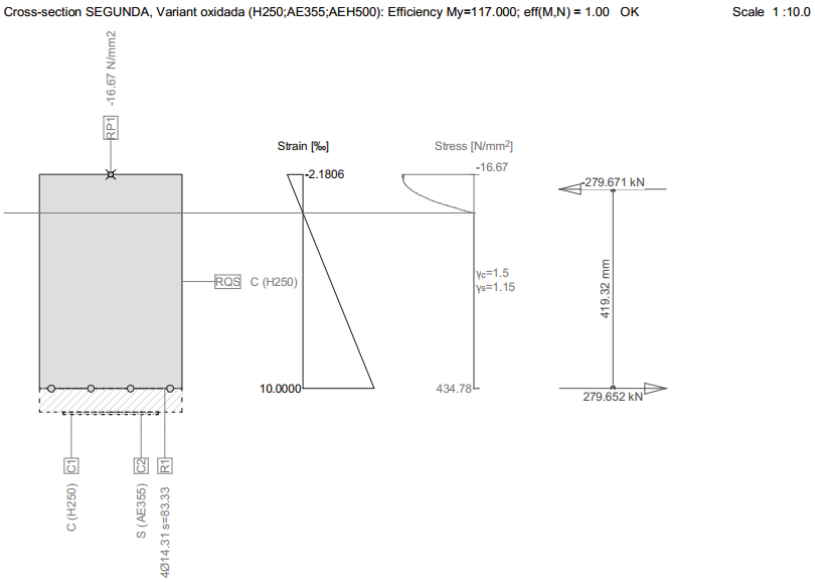

Action forces / Efficiency: eff(M,N) = 1.00 OK

No.	AP	P	Bending and axial force N [kN]	M_y [kNm]	M_z [kNm]	eff(M,N) [-]	Shear forces and torsion V_y [kN]	V_z [kN]	T [kNm]	eff(V,T) [-]	Complete CS eff(M,N,V,T) [-]
1	AP4		0	117.000	-	1.00					

- : Calculation with uniaxial bending (neutral axis is horizontal)!!

Figure 11 - ULS strength of the cross-section after it was damaged by corrosion.

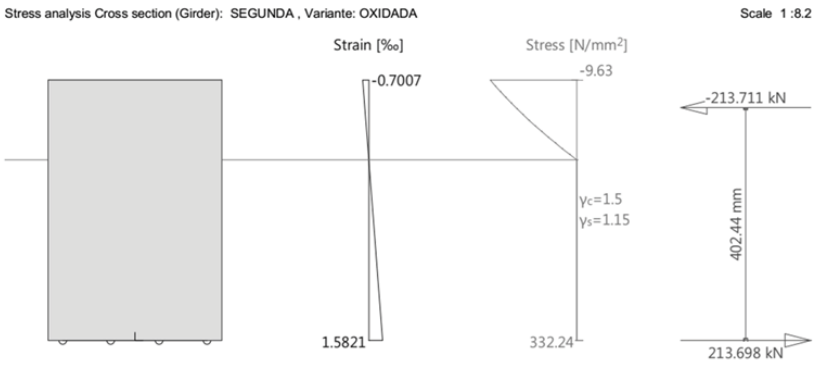

Action forces / Loading history - calculation with loading steps, (in-)active parts,

No.	AP	P	Bending and axial force N [kN]	M_y [kNm]	M_z [kNm]	Shear forces and torsion V_y [kN]	V_z [kN]	T [kNm]	Remarks -
1 2	AP4		0	86.000	0				Set inactiv

1 : Set inactiv: C2,C1

Figure 12 - Tensional state of the cross-section subjected to the bending moment that corresponds to the permanent load.

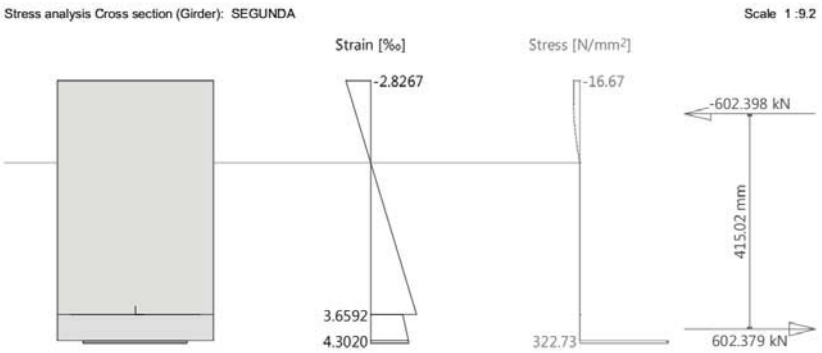

Action forces / Loading history - calculation with loading steps, (in-)active parts,

No.	AP	P	Bending and axial force N [kN]	M_y [kNm]	M_z [kNm]	Shear forces and torsion V_y [kN]	V_z [kN]	T [kNm]	Remarks -
1 2	AP4		0	86.000	-				Set inactiv
3 4	AP4		0	164.000	-				Set activ

Figure 13 - ULS strength of the reinforced section, considering the tensional state of the cross-section for permanent loads, prior the reinforcement installation.

1.3. MODEL CODE 2020 WILL BE AN OPERATIONAL MODEL CODE AND ORIENTED TOWARDS PRACTICAL NEEDS.

The evolution of codes has grown in content and pages. In addition, modern codes generate the false impression that all problems in structural engineering are solved, when it is manifestly evident that each time that we face a structural engineering problem we show how little we really know and how much we need to research, see Figure 14. Research is an ever-increasing field in structural concrete but it is often not focused on practical problems.

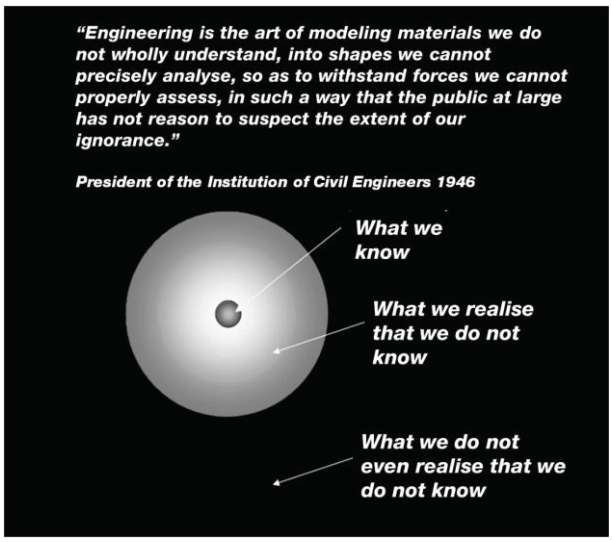

Figure 14 - Words of the president of the Institution of Civil Engineers in England in 1946.

The new MC 2020 must be an example of trend change. How to solve this enormous challenge?

Traditionally, MC's have been drafted using the right part for principles and application rules and the left part for comments. The rules must be clear, general and coherent with the content in other parts of the document. The comments should be very specific and above all, referenced to other documents that support the proposed rules and even that show more specific application aspects of these rules. It has always been desired for the models and rules in Model Codes to be explained in background documents. The current goal is to publish the background documents in the bulletings, as in the recent Bulletin 80 [4] on safety formats for existing structures, or in the Structural Concrete Journal of the *fib*. All effort on this matter will save explanations in the code text and it will help for a better comprehension of the considered principles and rules.

The new MC 2020 has the ambition to have indications on what is currently unknown and therefore is susceptible to be studied. It is possible that this document can also help to coordinate research efforts towards necessary subjects.

MC 2010 introduced the concept of different approximation levels. This a very intelligent way to use complex models with different approximation levels to allow the use of the same conceptual base and, depending on the required precision level, the use of simplifications in determined initial design levels or the total capacity of the models when the problem requires it, see Figure 15.

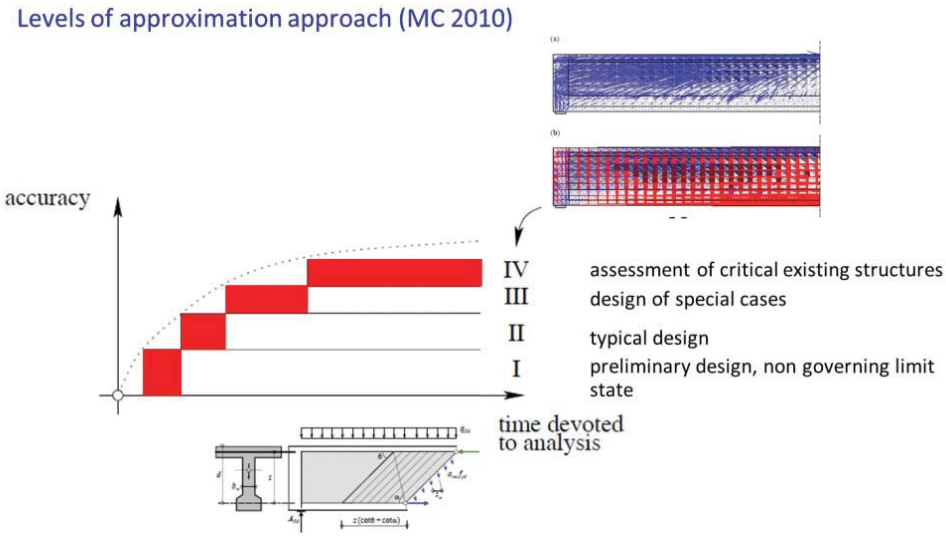

Figure 15 - Different levels of Aproximations. Figure presented by Prof Aurelio Muttoni at the first workshop on Model Code 2020, held at The Hague on June 2015 [2]

1.4. MODEL CODE 2020 WILL RECOGNIZE THE NEEDS OF ENGINEERING COMMUNITIES AROUND THE WORLD. MC 2020 HAS TO BE A REAL INTERNATIONAL CODE.

From an open perspective there is no justification that structural engineering can be so different from some countries to others. Although, it is acceptable to think that there may be different environmental, or action or specific constraints in each region.

In reality there are very different problems to solve, very different traditions to solve them and very distinct social and economic conditions to approach them.

The *fib* the International Federation for Structural Concrete has set forth the need to collect information on this diversity and gather information on the needs of different regions. Therefore, it has programmed workshops in different continents that present the evolution of MC 2020 at the same time that local experts in different areas present their respective points of view and specific needs. This labor results in a more international character of the new MC 2020.

Figure 16 - fib Model Code 2020 Workshops in different continents.

3. FINAL CONSIDERATIONS

The new version of MC 2020 has a solid starting point, MC 2010. It is a thorough document that shows many of the ideas that are needed in the new version and only require more or less development.

There has been a great discussion on what was needed for the future. The established criteria promise a MC 2020 that without a doubt will become a major reference in the future of structural engineer, just as it has happened with the previous versions. A MC for new and existing structures that aims for a single and consistent approach of problems. A MC that proposes, depending on the available knowledge, general and physical models that can be used indistinctly for new and existing structures. A MC that is practice-oriented. Finally, an international MC that represents the aspirations of *fib* that really is an international association formed by 45 countries from all of the continents.

It must a document that shows a new trend in the preparation of codes that has gradually become overwhelming.

The new MC must, in addition, serve to identify different fields where current knowledge is insufficient in order to, as much as possible, lead research in the direction where it is most needed.

REFERENCES

[1] Danton; S. Presentation made at the first workshop on Model Code 2020, held at The Hague on June 2015.

[2] Muttoni; A. Presentation made at the first workshop on Model Code 2020, held at The Hague on June 2015.

[3] *fib*. Model Code for Concrete Structures 2010. 28 Octuber 2013. ISBN:9783433030615

[4] *fib* Bulletin No. 80. Partial factor methods for existing concrete structures. 2016. Pages: 129. ISBN: 978-2-88394-120-5

ДГКС Друштво грађевинских конструктера Србије
ASES Association of Structural Engineers of Serbia
U-2
15. KONGRES
6-8. 9. 2018. Zlatibor

František Wald[1], Marta Kuříková[2], Lukáš Gödrich [3], Lubomír Šabatka[4], Jaromír Kabeláč [5], Drahoš Kojala[6]

NAPREDNA "MULTI LEVEL" METODA PRORAČUNA ELEMENATA I VEZA

Rezime:

Globalna analiza čeličnih konstrukcija je sprovedena koristeći Metodu Konačnih elemenata bez primene tradicionalnih procedura. Nova generacija Evrokodova nakon 2021. godine obuhvatiće deo EN 1993-1-14:2021 - Proračun čeličnih konstrukcija metodom konačnih elemenata. Proračun elementa je određen proračunom veza. Uticaj krutosti na savijanje je najednostavniji primer. To je izazov za svakog inženjera od prvih sistematičnih testova sprovedenih 1917. godine. Ovaj rad prikazuje napredan proračun veze, njegovu validaciju i verifikaciju, te kako će proračun elemenata koji uključuje veze biti tertian u budućnosti.

Ključne reči: čelične konstrukcije, proračun veze, компонентalna метода, метода коначних елемената

MULTI LEVEL MEMBER AND CONNECTION DESIGN

Summary:

The global analysis of steel structures is carried out by Finite Element Analyses (FEA) and all the traditional procedures are not used any more. In new generation of structural steel Eurocodes after 2021 will be organised the knowledge in volume EN 1993-1-14:2021 Design of steel structures by finite element method. The member design is influenced by joint design. The sensitivity to bending stiffness is the simplest example. It is challenge for engineer from first systematic tests in 1917. In this contribution is shown the advanced design of joint and its Validation and Verification and how the member design including joints will be treated in next future.

Key words: steel structures, connection design, component method, finite element method

[1] *Prof. Ing., CSc, Czech Technical University in Prague, rantisek.wald@fsv.cvut.cz*
[2] *Ing., PhD., Czech Technical University in Prague, marta.kurejkova@fsv.cvut.cz*
[3] *Ing., PhD., Czech Technical University in Prague, lukas.godrich@fsv.cvut.cz*
[4] *Ing., IDEA RS, sabatka@idea-rs.com*
[5] *Ing., IDEA RS, kabelac@idea-rs.com*
[6] *Ing., IDEA RS, drahoskojala@idea-rs.com*

1. INTRODUCTION

Experimental evidence and curve fitting procedures were and still are used for safe and economical design of connections [1]. Based on analytical models of resistance of connectors, as welds, bolds, and plates, and the estimated lever arm of internal forces is predicted resistance of connection. Zoetemeijer [2] was the first who equipped this model with estimation of stiffness and deformation capacity. The elastic stiffness was improved in the work of Steenhius, see [3]. Basic description of components behaviour in major structural steel connections was prepared by Jaspart for beam to column connections [4] and by Wald et al for column bases [5]. Method implemented in the current European structural standard for the steel and composite connections [6] and is applied in majority of software for structural steel in Europe. The idea was generalised by da Silva [7] for 3D behaviour including nonlinear parts of behaviour. Procedure starts with decomposition of a joint to components followed by their description in terms of normal/shear force deformation behaviour. After that, components are grouped to examine joint moment-rotational behaviour and classification/representation in a spring/shear model and application in global analyses. Advantage of this often called Component Method (CM) is integration of current experimental and analytical knowledge of connections components behaviour, bolts, welds and plates. This provides very accurate prediction of behaviour in elastic and ultimate level of loading. Verification of the model is possible using simplified calculation. Disadvantage of CM is that experimental evaluation of internal forces distribution is available only for limited number of the open section joint configurations. In temporary scientific papers, description of atypical components is either not present or has low validity and description of background materials. The CM is not developed and standardised for hand calculation but for preparation of design tables or software tools. For hollow section connections is still used curve fitting procedures based on mechanical and numerical experiments with its low quality of prediction and big restrictions, see for example Ch. 7 of EN1993-1-8:2006 [6].

2. VALIDATION AND VERIFICATION

FEA´s for connections are used from 70s of last century as research-oriented FEA (RFEA). Their ability to express real behaviour of connections is making numerical experiments a valid alternative to testing and source of additional information about local stresses. Material model for FEA uses true strain stress-strain diagram. Validation and Verification (V&V) process of models is integral part of the procedure, see e.g. [8], and the FEA studied are based on the researcher's own experiments. During preparation of CM for EN 1998-1-3:2006 were deeply modelled all basic components, see [9]. Special attention was given to modelling of the T stub, which represents the end plate connections beam to column joints, beam splices and column bases. Last generation of FEA models of connections is utilised in studies focussed to application of high strength steel in the connections [10].

V&V of the FEA design models (DFEA) of steel connections design is native part of its preparation, see [11]. The detailed procedure for verification of CBFEM and its application in design tool IDEA RS Connections was prepared, see [12]. The procedure consists

of preparation of Benchmark studies for used components, e.g. bolts, welds, slender plates in compression, anchor bolts, and concrete block in compression. Three different types of welded connections were selected for benchmark studies, connections loaded in shear, in bending, and welded to flexible plate. For bolted connections are prepared benchmark studies for T-stub in tension, the splices in shear and the generally loaded end plate connection, see Figure 1. For slender plate in compression is studied the triangular haunch in compression, the slender stiffener of column web and the plate in compression between bolts. For hollow section joints are studied the welded joints between CHS or RHS members and RHS/CHS diagonals welded to the open section chords in shape of T, K and TT joints. For column bases are prepared verifications for T stubs in tension and compression and for the generally loaded columns of open and hollow sections. Benchmark study consist of description of selected joint, results of CBFEM and CM, differences described in term of global behaviour on the force-deformation/rotation curve, and verification of initial stiffness, resistance, deformation capacity. At the end of each Benchmark study is prepared a Benchmark case to allow the user to check his results. In some cases, gives the CBFEM method higher resistance, initial stiffness or deformation capacity. Advanced FEM model from the bricks element validated on own or from literature experiments is used in these cases, to get proper results. CBFEM is approved by this procedure.

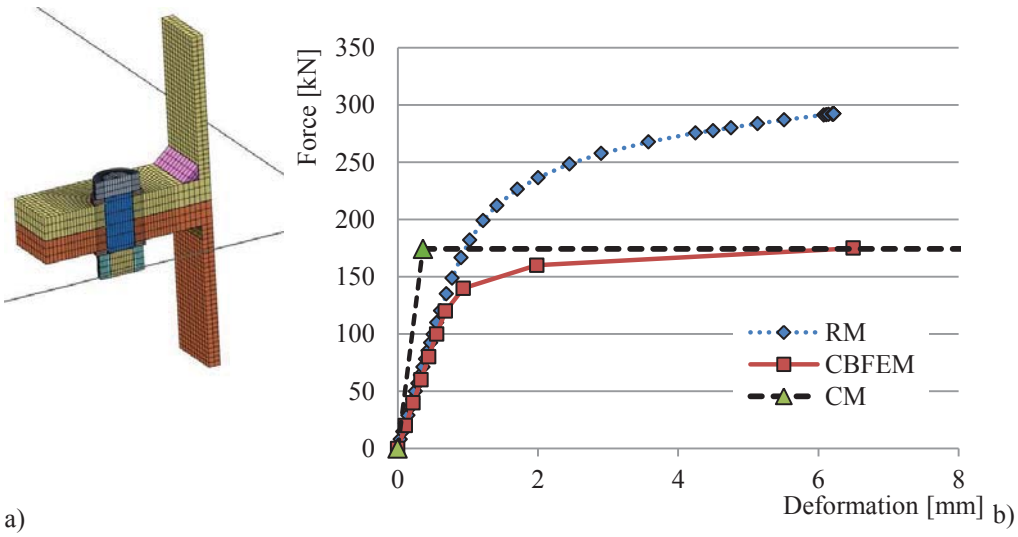

Figure 1 - The bolted T stub in tension a) mesh for research FEM, b) force-deformation diagram

The research FEA of the bolted T stubs in tension was prepared Midas FEA code, see Figure 1a, and validated on experiments [13]. T-stub of steel S235, with flange thickness t_f = 20 mm, web thickness t_w = 20 mm, flange width b_f = 300 mm, length b = 100 mm, double fillet weld a_w = 10 mm, bolts 2 x M24 8.8 with pitch w = 165 mm was modelled and selected for sensitivity study. The research FEM using the true stress true stain material diagram represents the experimental behaviour was used for verification of the CBFEM model of T stub, see

Figure 1b. For thin plates gives CM unrealistic low value due to neglecting of membrane action of end plates, see Figure 2. For regular plates predict CM higher resistance by neglecting the shear and bending interaction on deformed endplate. For very thick plates is for CM calculated the limit of deformation capacity separately and its estimation may not fit into shear and tension interaction in bolt. The sensitivity study of flange thickness width and material quality, bolt size, pitch and material quality, shows good prediction resistance by CBFEM on asked design level. Summary of verification of CBFEM to CM for the bolted T stub in tension is presented in Figure 3, where are recapitulated the studies for bolt size, material and pitches, the flange thickness and width. The results show that the difference of the two calculation methods is mostly up to 10 %. In cases with CBFEM/CM > 1,1 accuracy of CBFEM was verified by the results of RM which gives highest resistance in all selected cases.

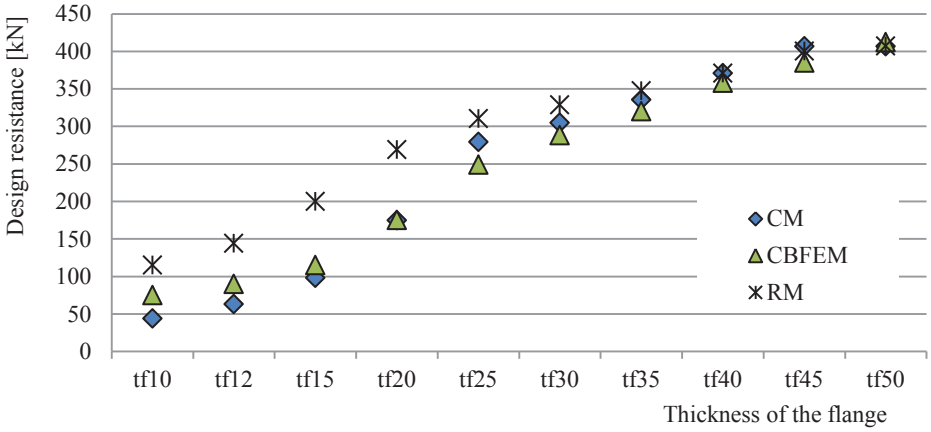

Figure 2 - Sensitivity study of flange thickness

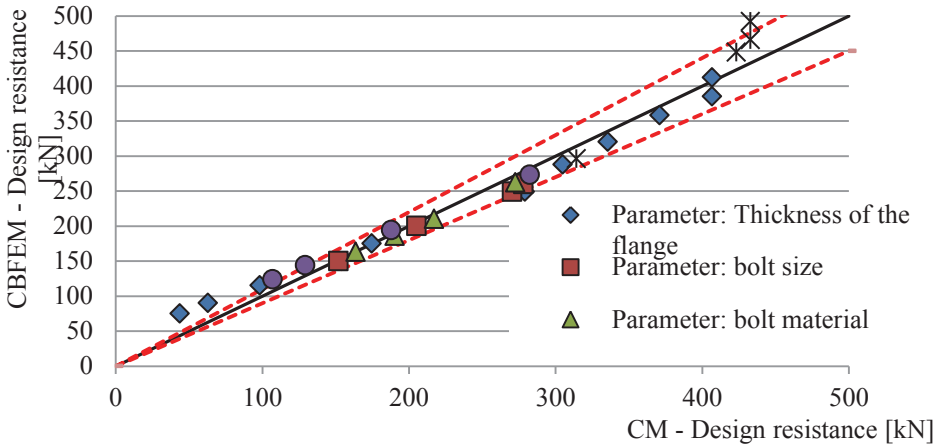

Figure 3 - Summary of verification of CBFEM to CM for the bolted T stub in tension

Experimental investigation of three samples of the generally loaded end plate joints was performed [13]. End plates were welded on two RHS 250 x 150 x 16 beams of different lengths 2000 mm and 1000 mm. The beams and plates were designed from S355, with measured values of $f_{y,m}$ = 410 MPa and $f_{u,m}$ = 582 MPa. The end plates P10 – 400 x 300 were connected by M20 8.8 bolts, with the vertical distances 35 – 230 – 100 – 35 mm and horizontal ones 30 – 240 – 30 mm. The beam with connection 500 mm from its centre was loaded in its centre through P20 by hydraulic jack, see Figure 4. The configuration creates in the connection shear forces and bending moments. The results of the contact imprints on paper placed between the end plates is included on right side of the Figure 1b. The inclination of the specimens varied from 0°; 30° till 45°. The test set up with 0° inclination is documented at Figure 5.

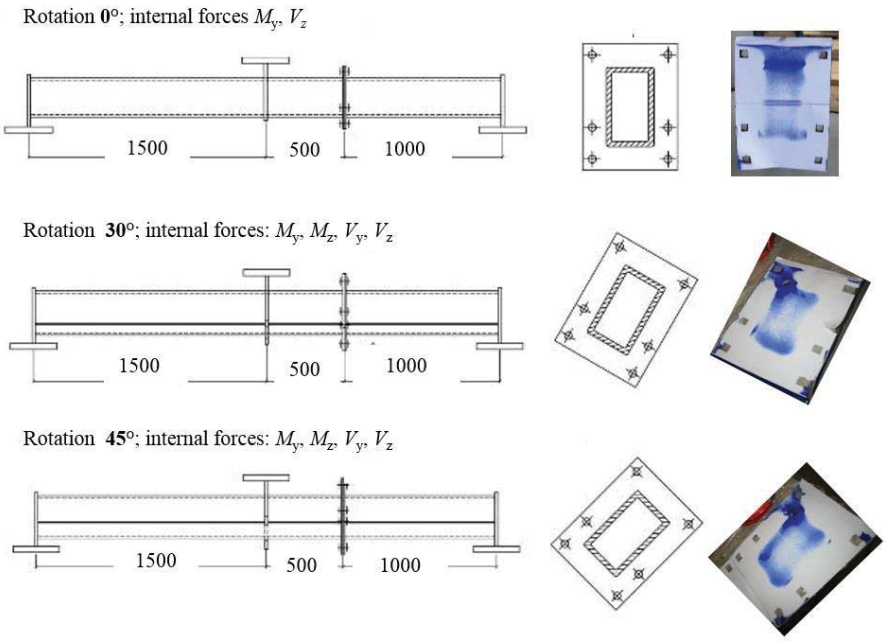

Figure 4 - Position of the beam splice joins on beam, inclination and contact imprints

Figure 5 - The test sample with 0° inclination

Connections were designed according to EN 1993-1-8:2006 [6]. Four components are guiding the behaviour the fillet welds, the beam flange in compression and in tension, the end plate in bending and the bolts in tension. Effective lengths for circular and noncircular failures are considered according to EN 1993-1-8:2006 cl. 6.2.6. Three modes of collapse according to cl. 6.2.4.1 are considered. Bolts are designed according to cl. 3.6.1. Design resistance considers punching shear resistance and rupture of the bolt. For component method is in EN1993-1-8:2006 recommended a linear interaction. The quadratic interaction curve according to [14] is included in verification study.

Samples 30° and 45° with strong axis bending moment were chosen to present of the global behaviour described by moment-rotation diagram, see Figs 6 and 7. CM with quadratic interaction gives higher initial stiffness compared to CBFEM and experimental data. In all cases are resistances by CM and CBFEM similar and corresponds to asked characteristic design level. Experimentally measured resistance is higher including hardening of the materials after reaching yield strength. Resistance calculated by CBFEM was compared with the results of CM and experimental results, see Figure 8. CM with linear interaction gives conservative values of resistance. CM with quadratic interaction gives the highest resistances, which are to experimental results still rather conservative. CBFEM gives similar results as CM with quadratic interaction. The verification of the prediction of the resistance of the CBFEM to CM for inclination of°0° and changing the end plate thickness is presented in Figure 9 and Table 1. The verification of the prediction of the resistance of the CBFEM to CM for inclination of°0° and changing the bolt material is presented in Table 2. The results show good agreement between both models.

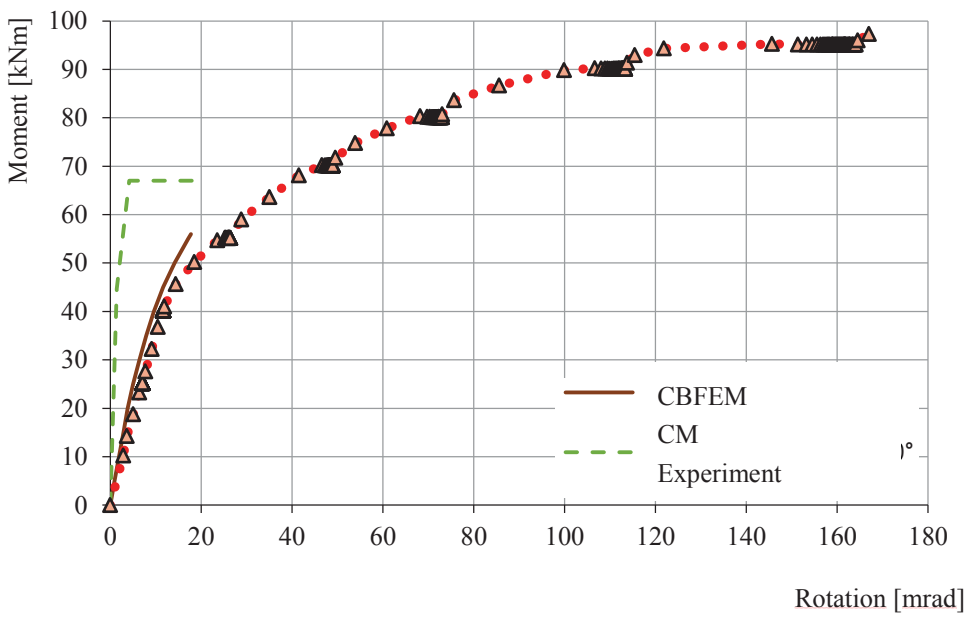

Figure 6 - Validation of moment rotational curve of numerical model (CBFEM) and analytical model (CM) to experiments for inclination 30°

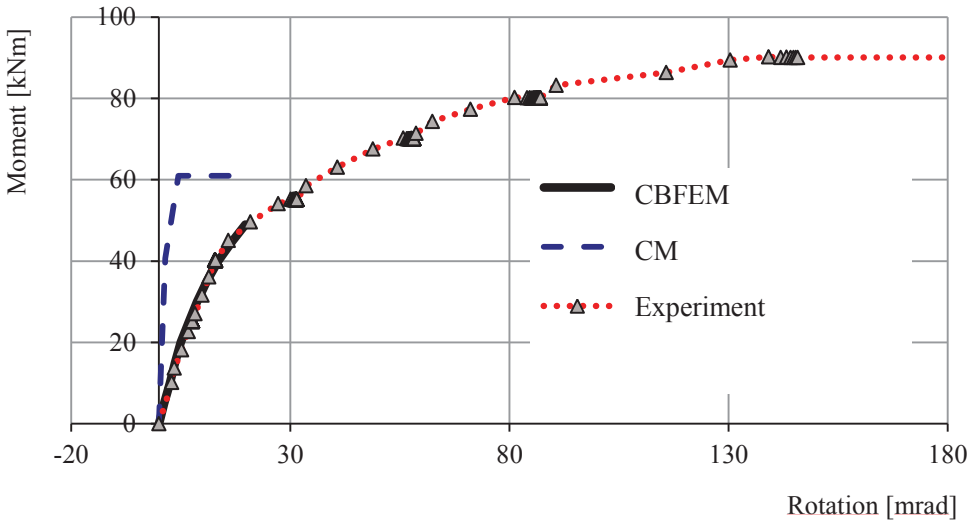

Figure 7 - Validation of moment rotational curve of numerical model (CBFEM) and analytical model (CM) to experiments for inclination 45°

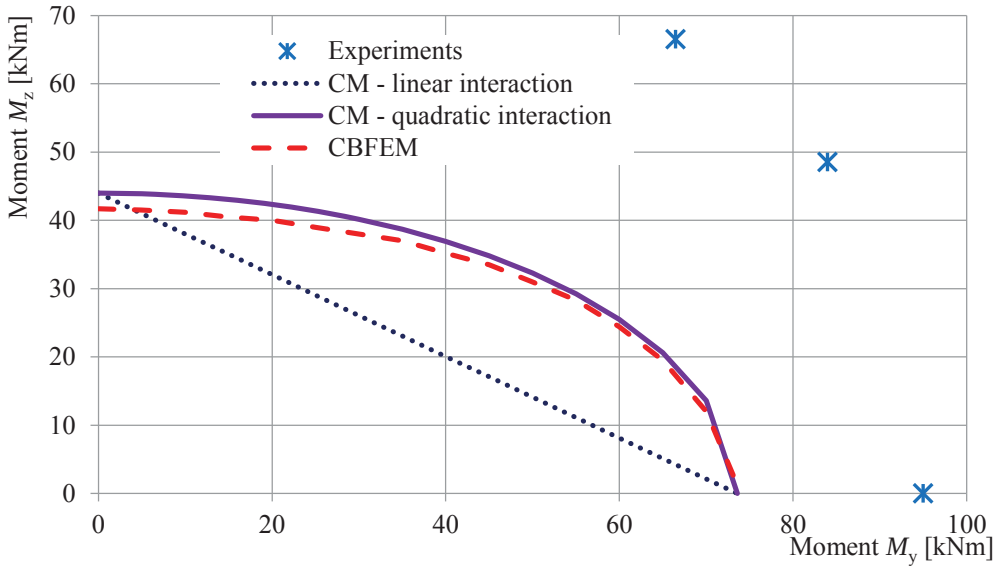

Figure 8 - Validation of resistances for numerical model (CBFEM) and analytical model (CM) to experiments

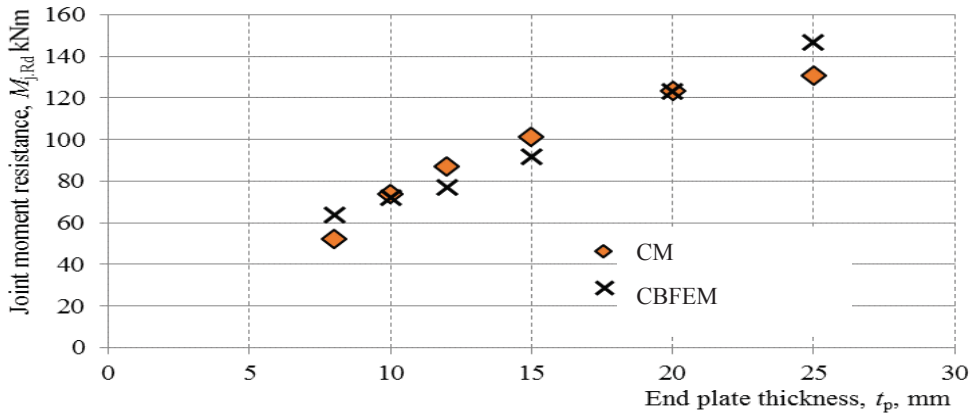

Figure 9 - Verification of numerical model (CBFEM) to analytical model (CM) for the end plate thickness

Table 1 – Verification of numerical model (CBFEM) to analytical model (CM) for the end plate thickness

Parameter	Numerical model, CBFEM		Analytical model, CM		Ration CBFEM/ CM
End plate thickness, f_p, mm	Bending resistance, kNm	Decisive component	Bending resistance, kNm	Decisive component	
8	64	End plate in bending	52	End plate in bending	1,22
10	72	End plate in bending	74	End plate in bending	0,98
12	77	End plate in bending	87	End plate in bending	0,88
15	92	End plate in bending	101	End plate in bending	0,91
20	123	End plate in bending	124	End plate in bending	1,00
25	147	Bolts in tension	131	Bolts in tension	1,12

Table 2 – Verification of numerical model (CBFEM) to analytical model (CM) for inclination of°0° and bolts 8.8

Parameter	Numerical model, CBFEM		Analytical model, CM		Ration CBFEM /CM
Bolt class	Bending resistance kNm	Decisive component	Bending resistance kNm	Decisive component	
4.8	49	End plate in bending	48	End plate in bending	1,01
5.8	50	End plate in bending	56	End plate in bending	0,89
6.8	55	End plate in bending	64	End plate in bending	0,86
8.8	72	End plate in bending	74	End plate in bending	0,98
10.9	75	End plate in bending	79	End plate in bending	0,94

3. MEMBER BEHAVIOUR INCLUDING CONNECTIONS

The discrete evaluation of members may be based on the same procedure as for joints. For joints it is expected no recalculation of global analyses due to design is necessary. For members the iterative procedure is obvious to reach a satisfactory result. It the first step are solved the internal forces and deformations in the 3D FEM with 1D elements with global imperfections, Geometrically Non-linear Elastic Analysis with Imperfections, on the structure with selected cross-sections of members, see Figure 10a. Selected member with its internal force is then analysed by FEM using 3D Geometrically and Materially Non-linear Analysis with Imperfections including joints, see Figure 10b. It allows to introduce buckling of member in both planes and lateral torsional buckling. The member is checked according to ULS and SLS and the cross-sections are modified, see EN 1993-1-1:2005 [15]. The structure with modified member is recalculated by 3D FEM with global imperfections. The procedure is repeated to achieve a satisfactory accuracy in prediction.

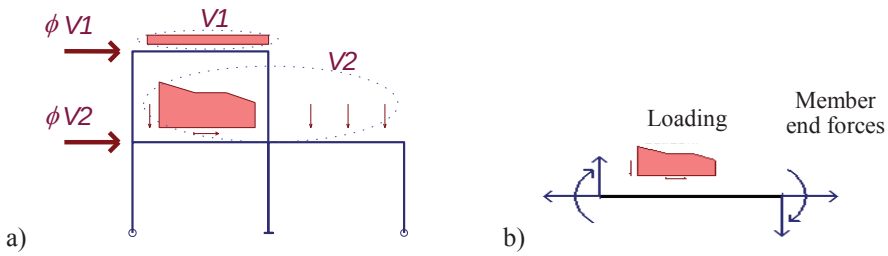

Figure 10 - a) Sketch of Geometrically non-linear elastic global analysis with imperfections with separate member and joint
a) Geometrically and Materially Non-linear Analysis with Imperfections

Geometrically non-linear elastic global analysis with imperfections a) is equipped with separate member and joint Geometrically and Materially Non-linear Analysis with Imperfections.

$$k_b = S_{j,ini} L_b / (I_b E) \quad (1)$$

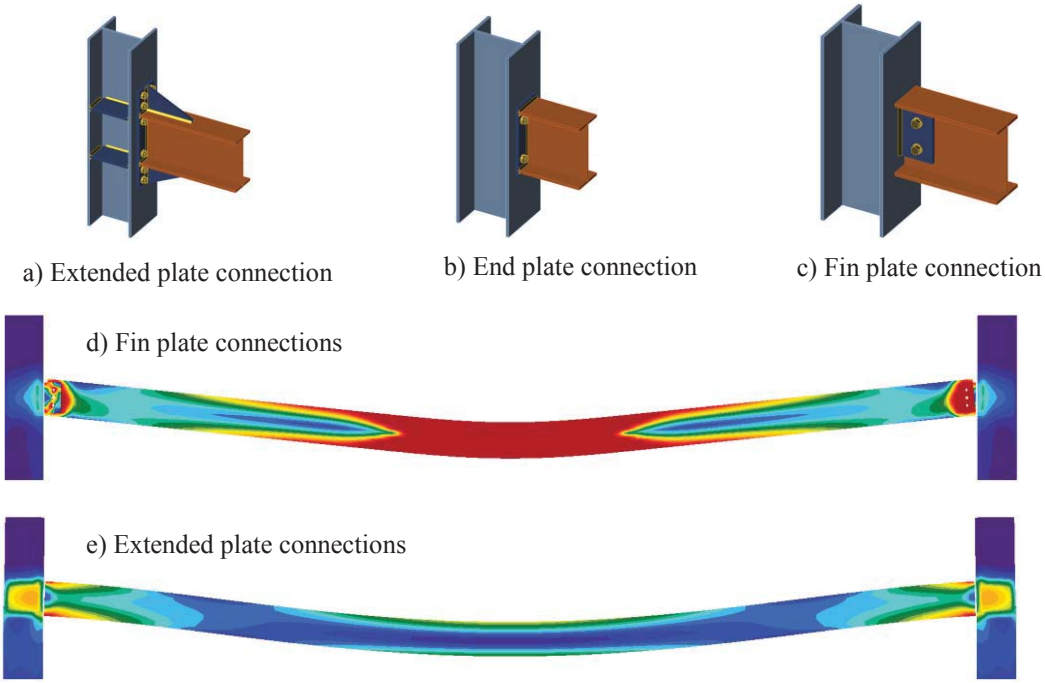

Figure 11 -a) Extended end plate, b) End plate connection, c) Fin plate connection, d) Von Misses' stresses along the beams with fin plate and e) with extended plate connections, Idea Member [17]

The influence of joint stiffness k_b to beam of cross-section IPE 330 is shown in Figure 12. There are three areas of the stiffness classification of the joint according to EN 1993-1-8:2006 [6] hinged joints $k_b < 0{,}5$ and rigid one $k_b > 25$. The beam is designed for the bending moment at ULS and deflection at SLS. The limits of accuracy in prediction are expected to be 5 % for ULS and 20% for SLS.

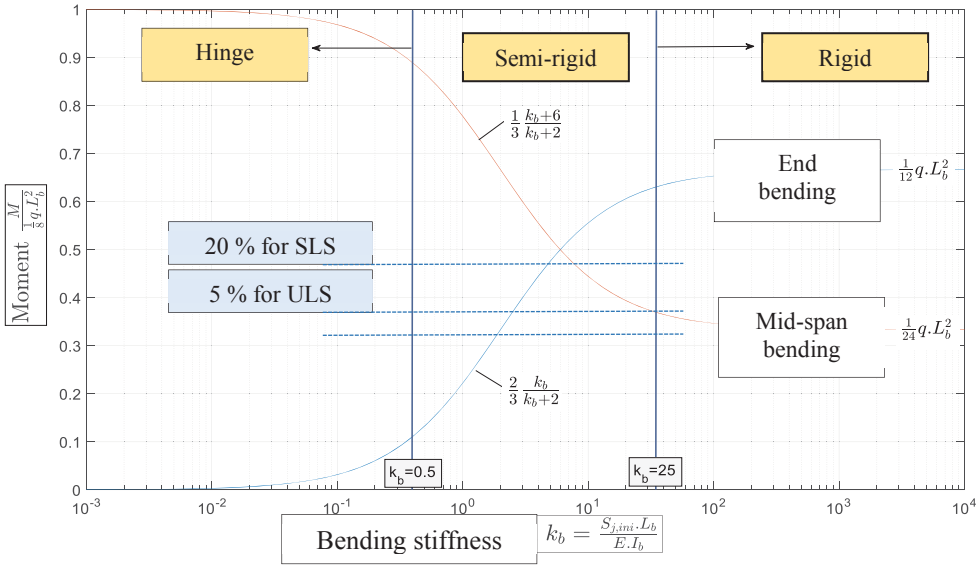

Figure 12 - Influence of the relative bending stiffness of the joint in logarithmic scale to the relative mid span bending moment

4. SUMMARY AND ACKNOWLEDGMENT

The presented results show the good accuracy of CBFEM verified to CM and to advanced calculations/experiments in cases where the CBFEM gives higher stiffness, resistance, or deformation capacity, see [12].

The member 3D analyses including connections allows prediction of behaviour of complex member, with haunches, openings etc., including connection and loading.

The work was prepared under the R&D project MERLION II supported by Technology Agency of the Czech Republic, project No TH02020301.

REFERENCES

[1] Wald F., Gödrich L., Šabatka L., Kabeláč J., Navrátil J., "Component Based Finite Element Model of Structural Connections", *12th International Conference on Steel, Space and Composite Structures*. Singapore, pp. 337-344, 2014.

[2] Zoetemeijer P., "*Summary of the Researches on Bolted Beam-to-Column Connections*". Report 6-85-7, University of Technology, Delft, 1985.

[3] Steenhuis M., Gresnigt N., Weynand K., "Pre-Design of Semi-Rigid Joints in Steel Frames", *Proceedings of the Second State of the Art Workshop on Semi-Rigid*

Behaviour of Civil Engineering Structural Connections, COST C1, Prague, pp.131-140, 1994.

[4] Jaspart J.P., "Design of structural joints in building frames", *Progress in Structural Engineering and Materials*, 4, pp.18–34, 2002.

[5] Wald F., Sokol Z., Steenhuis M. and Jaspart, J.P., "Component Method for Steel Column Bases", *Heron* 53, pp. 3-20, 2008.

[6] EN1993-1-8, Eurocode 3: Design of steel structures - Part 1-8: Design of joints, CEN, Brussels, 2006.

[7] Da Silva Simoes L., "Towards a consistent design approach for steel joints under generalized loading", Journal of Constructional Steel Research, 64, pp. 1059-1075, 2008

[8] Bursi O. S .and Jaspart J. P. Calibration of a Finite Element Model for Isolated Bolted End-Plate Steel Connections, *Journal of Constructional Steel Research,* 44/3, pp. 225-262, 1997.

[9] Virdi K. S. et al, "*Numerical Simulation of Semi. Rigid Connections by the Finite Element Method*", Report of Working Group 6 Numerical, Simulation COST C1, Brussels Luxembourg, 1999.

[10] Girao Coelho A. , Rotation capacity of partial strength steel joints with three-dimensional finite element approach, *Computers & Structures*, 116, pp. 88-97, 2013

[11] Wald F., Kwasniewski L., Gödrich L., Kurejková M., "Validation and verification procedures for connection design in steel structures", *12th International Conference on Steel, Space and Composite Structures*. Singapore, pp. 111-120, 2014.

[12] Wald F., Gödrich L., Šabatka L., Kabeláč J., Navrátil J., "Component Based Finite Element Model of Structural Connections", *12th International Conference on Steel, Space and Composite Structures*. Singapore, pp. 337-344, 2014 .

[13] Gödrich L., Wald F., Sokol Z., "Advanced Modelling of End Plate", *Eurosteel 2014,* Naples, pp. 287-288, 2014.

[14] Neumann N., "Design model for combined in-plane and out-of-plane bending of steel joints connecting H or I sections", *Eurosteel 2014*, Naples, pp. 2050-2056, 2014

[15] EN 1993-1-1, Eurocode 3: Design of steel structures- Part 1-1: General rules and rules for buildings, CEN, Brussels, 2005.

[16] *IDEA Member*, Brno, 2018, https://www.ideastatica.com/.

[17] Baniotopoulos, C. C., Wald F., The Paramount Role of Joints into the Reliable Response of Structures, From the Classic Pinned and Rigid Joints to the Notion of Semi-rigidity, NATO series, Springer, 2000.

ДГКС Друштво грађевинских конструктера Србије
ASES Association of Structural Engineers of Serbia
U-3
15. KONGRES
6-8. 9. 2018. Zlatibor

David Fernández-Ordóñez Hernández [1]

PREFABRIKOVANI BETON - LEKCIJE IZ PROŠLOSTI I BUDUĆI NAPREDAK

Rezime:

Prefabrikacija betonskih elemenata evoluirala je od svojih početaka, donoseći mnoge prednosti industrijalizacije. Današnja prefabrikacija u poređenju sa tradicionalnim građenjem ima niz prednosti. Jedini način da se industrijalizuje građenje je da se izmesti deo rada sa gradilišta u postrojenja za prefabrikaciju. Prefabrikacija podrazumeva racionalne i efikasne procese proizvodnje, obučene radnike, sistematizaciju operacija koje se ponavljaju i nižu cenu rada po m^2 kao rezultat automatizovane proizvodnje. Automatizacija procesa se već koristi u oblastima kao što su pripremanje armature, montaža ploča, betoniranje i obrada završne površine betona.

Ključne reči: Prefabrikacija, Istorija industrijalizovanog građenja, Montaža, Prednaprezanje

CONCRETE PREFABRICATION - LESSONS FROM THE PAST AND ADVANCES FOR THE FUTURE

Summary:

Prefabrication in concrete has evolved in depth and breadth from its beginnings, bringing many of the advantages of industrialisation to construction, while solving some of the problems that arose in the early years. Today prefabrication, compared to traditional construction methods, and concrete as a material, feature a number of beneficial characteristics. Precast elements are factory made products. The only way to industrialise the construction industry is to shift work from temporary construction sites to modern permanent facilities. Factory production entails rational and efficient manufacturing processes, skilled workers, systematisation of repetitive tasks, and lower labour costs per m^2 as a result of automated production. Factory products are process-based and lean manufacturing principles are deployed. Automation is gradually being implemented in factories and is already in place in areas such as the preparation of reinforcing steel, mould assembly, concrete casting, and surface finishing on architectural concrete.

Key words: Prefabrication, Industrialised Construction, Precast History, Prestressing

[1] *PhD, Secretary General, International Federation for Structural Concrete (fib), secretary.general@fib-international.org*

"All... must be built with due reference to durability, convenience, and beauty. Durability will be assured when foundations are carried down to the solid ground and materials wisely and liberally selected; convenience, when the arrangement of the apartments is faultless and presents no hindrance to use, and when each class of building is assigned to its suitable and appropriate exposure; and beauty, when the appearance of the work is pleasing and in good taste, and when its members are in due proportion according to correct principles of symmetry."

Vitruvius

1. INTRODUCTION - INDUSTRIALISED CONSTRUCTION

The origin of prefabrication, i.e., the application of industrial processes to construction, can be traced back to the early eighteenth century. The Industrial Revolution, with the advent of new materials such as steel and glass, had a huge impact on architecture and prefabrication. In some cases architectural design underwent fundamental change, giving rise to new styles solidly rooted in industrial processes. (1, 2)

Prefabrication in concrete has evolved in depth and breadth from its beginnings, bringing many of the advantages of industrialisation to construction, while solving some of the problems that arose in the early years. Today prefabrication, compared to traditional construction methods, and concrete as a material, feature a number of beneficial characteristics. The inherent advantages in such industrialised construction are described below. (3)

Precast elements are factory made products. The only way to industrialise the construction industry is to shift work from temporary construction sites to modern permanent facilities. Factory production entails rational and efficient manufacturing processes, skilled workers, systematisation of repetitive tasks, and lower labour costs per m² as a result of automated production. Factory products are process-based and lean manufacturing principles are deployed. Automation is gradually being implemented in factories and is already in place in areas such as the preparation of reinforcing steel, mould assembly, concrete casting, and surface finishing on architectural concrete. And other stages in the process are sure to follow.

The *fib* has recently published in its Bulletin 74, "Planning and design handbook on precast building structures", a thorough description of the advanced possibilities that prefabrication in concrete offers for the new challenges in the building industry. (4)

2. ADVANCES IN PREFABRICATION

After over half a century of experimentation, Europe has generated all manner of prefabricated construction components. Building construction solutions have evolved on the back of constant improvements in technique and the fruitful collaboration among architects, engineers, designers and builders. From the outset, prefabrication exhibited an amazing capacity to provide new technical and creative solutions to architectural and building construction problems, Figure 1.

Prestressing is commonly used in prefabrication. The technique not only delivers all the advantages of prestressed concrete from the construction standpoint, but also economises on

manufacturing costs because of the low labour input and the absence of the expensive anchorage devices needed for post-tensioning.

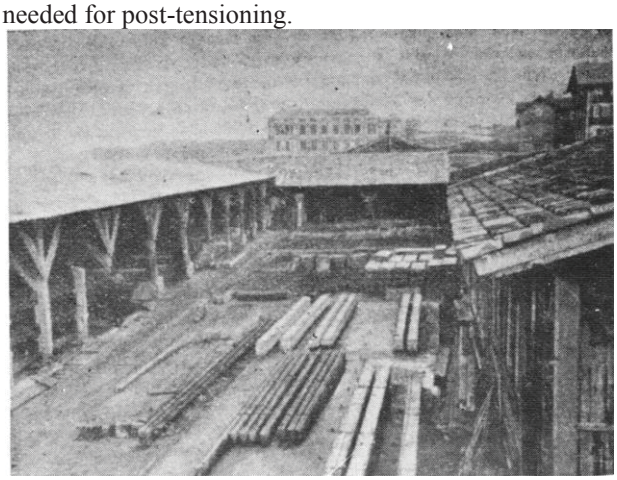

Figure 1 - Coignet factory

The history of prefabrication with prestressed elements in Europe covers over 50 years of ongoing progress in technique and substantial improvements in material quality, component design and the construction or production process. Production control was viewed as essential from the outset. The most advanced construction materials available at any given time were used in prefabrication.

Prestressing steel has always been characterised by a high elastic modulus. Only high early age compressive strength concrete was used, to be able to introduce prestressing forces early in the manufacturing process. Thanks to these features and to strict production and performance control, precast manufacturers are able to produce elements with much more slender cross-sections than can be made in situ. From the very start, then, prefabrication has required rigorous quality control of materials, processes and worksite assembly, Figure 2.

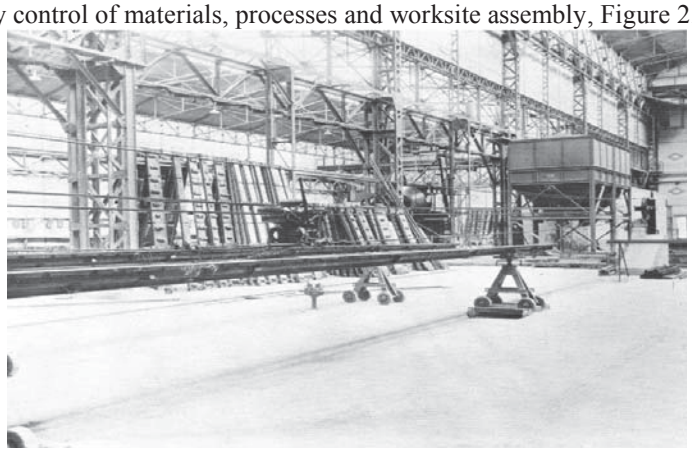

Figure 2 - Prestressed elements Factory at Montargis

The use of higher quality materials has delivered better structural behaviour and longer durability of components. Structures made of high performance concrete produced in plants with strict manufacturing controls in place exhibit higher resistance to external attack than observed for in situ concrete structures.

Prefabrication has always been, and still is, the means for introducing new technical developments in construction practice, including innovative quality systems that have led to the application of quality certifications for construction-related activities.

From the start, prefabricated production control has always deployed the most reliable procedures. Before analytical and numerical calculation methods were regarded to ensure sufficient safety, physical trials were conducted to verify the technical viability of precast products and their related structures, Figures 3 and 4.

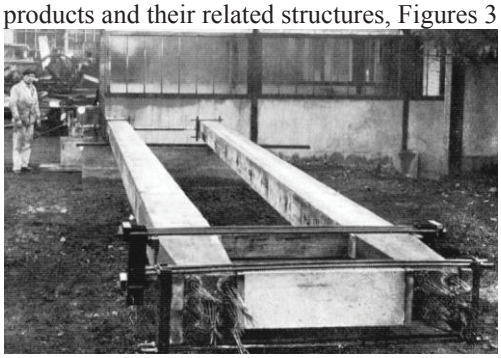

Figure 3 - Conducting tests on precast prestressed poles

Figure 4 - Tests on precast prestressed beams

The first bridges would be the precursors to the very complex, large span, precast, structurally continuous bridges built today. Initially, all beams were verified by load tests run at the plant to determine whether the experimental deflection was consistent with the design value, Figure 5. (5)

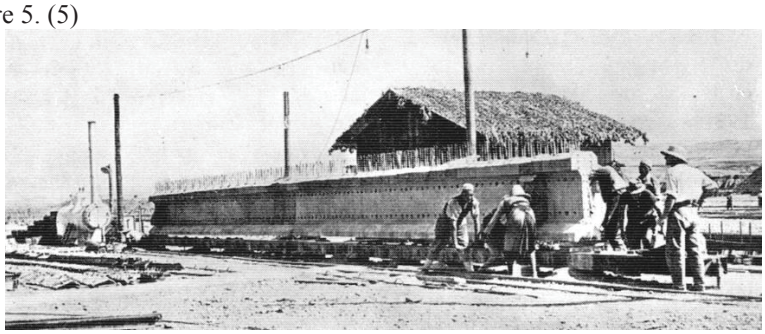

Figure 5 - Precast prestressed beam on Portes de Fer Bridge

Another important reason why the prefabrication industry developed in Europe was large-scale output capacity for both structural members and other precast elements that were quickly introduced starting in 1945.

In the late nineteen forties and early nineteen fifties beams were the key structural members in all manner of deck slabs. They could be supplemented with concrete blocks or other

components in solutions widely used at the time and still applied today. They could likewise be used in other members. These beams were designed to bear large live loads and could be supplemented with an in situ concrete slab, Figure 6. (6)

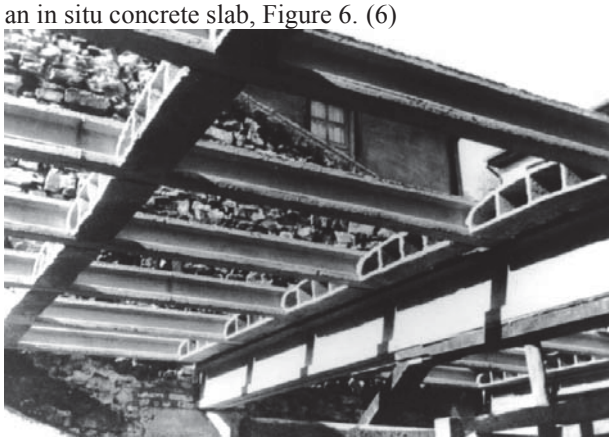

Figure 6 - Prestressed beams used with the (at the time) new concrete blocks

In the earliest plants, prestressing benches and hoisting and transport machinery were small-scale facilities, which limited the prestressing forces that could be induced and the size of the products that could be cast. Then Hollow core slabs were developed at the same time in the USA and in Europe, Figure 7.

Beginning in the late nineteen forties, a wide range of prestressed poles for electric power lines were also developed and manufactured in Europe, much as Freyssinet had done at his Montargis factory from the nineteen twenties onward.

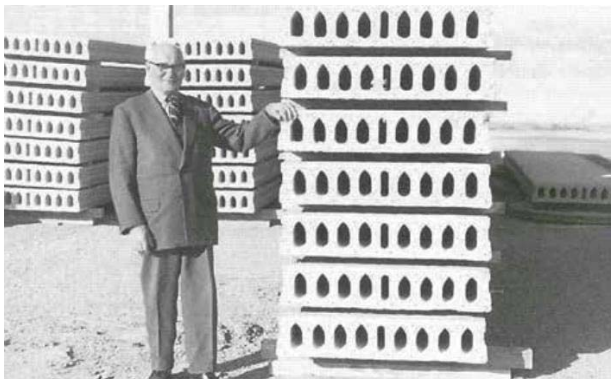

Figure 7 - Hollow core slabs

By the end of nineteen fifties flat or surface members such as prestressed and double-T slabs began to be developed to preclude the need for blocks in combination with beams. Both prestressed hollow core and solid slabs were produced. These slabs were used either as the entire deck floor, which rested on joists or stronger beam-type members, or as the precast bottom of a deck slab, over which a concrete top was poured on site. Self-supporting precast slabs constituted yet another application. Once this technology was mastered, larger

prefabricated members for roofs on large industrial buildings also began to be built. (7, 8, 9, 10,11)

The simple design of precast prestressed beams was no obstacle, however, to their more imaginative use in all manner of complex structures. One common application was pointed roofs in industrial buildings, where the joints were made in situ to ensure structural continuity, perhaps an early version of the complex continuous portal frame structures built today.

Prefabricated trusses were likewise designed and built at the time. They consisted of precast elements connected and assembled in situ. The joints between these elements constituted the key factor in the design and construction of the entire structure. The original design for such industrial buildings called for small joists, which gradually evolved into the use of larger, higher capacity and higher performance beams, Figure 8.

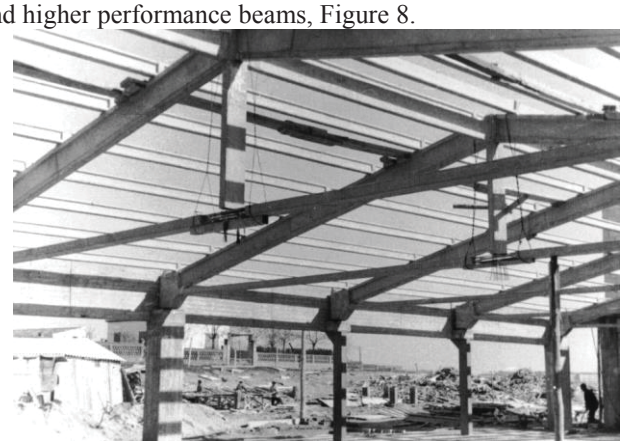

Figure 8 - Precast truss roof system

By the nineteen sixties, when prefabrication had become a consolidated building procedure, prefabrication programmes for fully or partially prefabricated buildings began to appear. Fully prefabricated industrial buildings involving many kinds of members (columns, beams, girders, purlins and enclosure panels) soon dotted industrial estates and similar areas, Figure 9.

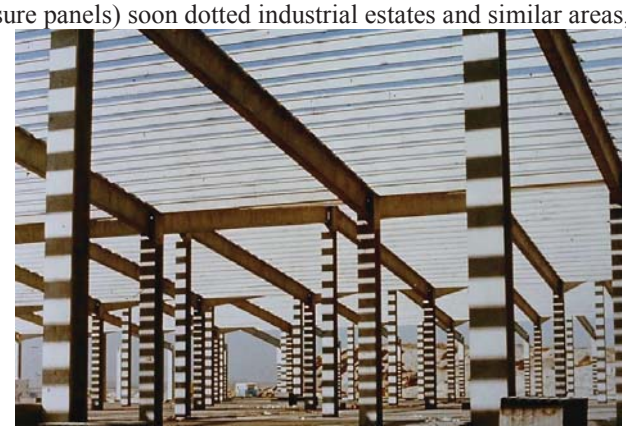

Figure 9 - Industrial building

As prefabrication makes optimal use of materials, its potential for savings is much greater than in cast-in-situ construction. Structural performance and durability are also enhanced through design, modern manufacturing equipment and carefully planned working procedures, Figure 10. (12, 13, 14, 15, 16, 17)

Figure 10 - Precast distribution centre. Internal view

Architectural freedom is needed to create new building designs. Architectural design is no longer subject to the inflexible concrete elements of yesteryear and almost any building can be adapted to the builder's or the architect's requirements. Architectural grace and variety need not clash with increased efficiency. Gone are the days when industrialisation meant large numbers of identical units. On the contrary, efficient production can be combined with skilled workmanship, allowing for modern architectural design at no extra cost. In today's society, building appearance and finishes may largely determine construction procedures. Precast concrete elements accommodate a wide variety of finishes, ranging from carefully moulded surfaces to high quality architectural concrete. The use of beams and columns with special shapes and high quality finishes can afford architects considerable creative freedom and range of expression, Figures 11 and 12. (18)

Figure 11 - Precast commercial centre

Figure 12 - Precast concrete panels for a commercial centre

Precast concrete offers considerable scope for improving structural efficiency. Longer spans and shallower construction depths can be obtained by using precast prestressed concrete

for beams and floors. The major benefit for building structures lies in improved structural efficiency, for more slender components optimise the use of materials. The greatest comparative advantage is attained with vertical members, especially load bearing columns, whose bearing capacity rises by 100 to 150 % when the concrete strength is increased from 30 to 90 N/mm², Figure 13. (19, 20, 21)

Figure 13 - Precast building for offices

3. TRENDS IN PREFABRICATION

The use of precast concrete in construction is widely regarded as an economic, durable, environmentally friendly, structurally sound and architecturally versatile form of construction. The precast concrete industry is continuously making efforts to keep on line with the demands of modern society: economy, efficiency, technical performance, safety, labour circumstances and environmental friendliness.

The evolution of building construction and civil engineering works during the next decades will undoubtedly be influenced by the developments in information processing, global communication, industrialization and automation. These are already certain to be implemented in prefabrication. However, when looking into the efficiency of present building processes, there must be a smoother transition from the design of the construction to its completion. The only way to move forward from the traditional labour intensive methods to the modern approach of prefabrication is to apply an industrial philosophy throughout the entire building process. (22, 23, 24)

Sustainability is a major issue in any industrial activity today. In the building industry, prefabrication is able to provide the best approach to this end. In fact, the whole life-cycle can be better controlled. Industrialized production of elements allows for saving materials and energy when constructing. In all phases, time, waste, noise and dust, in a whole environmental impact, are reduced.

Prefabrication of concrete structures is an industrialized process with a large potential for the future. It is often considered by uninitiated designers as a variant execution technique of

cast in-situ construction, where the notion of prefabrication means that parts of the construction are precast in specialized plants, to be assembled afterwards on site in such a way that the initial concept of cast in-situ structures is obtained again. This viewpoint is false. Every construction system has its own characteristics which to a greater or lesser extent influence the structural lay-out, span and width, stability system, etc. For the best results a design should, from the very outset, respect the specific and particular demands of the intended structure, Figures 14 and 15.

Figure 14 - Precast tall building for offices

Figure 15 - Precast tall building with special design

The design of the building is not fixed by rigid concrete elements and almost every building can be adapted to the requirements of the builder or the architect. There is no contradiction between architectural elegance and variety on the one hand and increased efficiency on the other. The days are gone when industrialization meant large numbers of identical units; on the contrary, an efficient production process can be combined with skilled workmanship, which permits a modern architectural design without extra costs.

Certain types of buildings are frequently required to be adaptable to the user's needs. This is especially the case with offices. The most suitable solution to this effect is to create a large free internal space without any restriction to possible subdivisions with partition walls. Precast concrete has many more assets than are mentioned above, and excessive repetition of products

or long design and manufacture periods are no longer found in contemporary practice. On the contrary, thanks to modern production techniques and computer aided manufacture in combination with Building Information Modelling (BIM), flexibility combined with short delivery times has become a major commercial advantage of prefabrication.

Today structure accounts for only a small portion of total building construction and maintenance costs. M&E services can be integrated into the construction system. Another major advantage is that precast structures can be designed to specific building facility needs. Prefabrication also provides certain advantages with respect to M&E services. The thermal mass of concrete has been efficiently used to store thermal energy in hollow core floors, for instance, leading to substantial savings in heating costs. Even today, most construction activities continue to place a heavy burden on the environment in terms of energy demand, use of resources, pollution, noise and waste production.

Precast concrete is linked to the most advanced techniques in construction and also to the most sustainable uses and processes. The future in construction will be intimately linked to industrialization and prefabrication. The installation of building services can be integrated into the building system. A major advantage is that the precast structure can be designed according to the specific needs of the building equipment. Elements can be provided with a variety of holes, fixings can be cast in the units, and a lot of additional means are available on site after erection of the precast building, Figure 16.

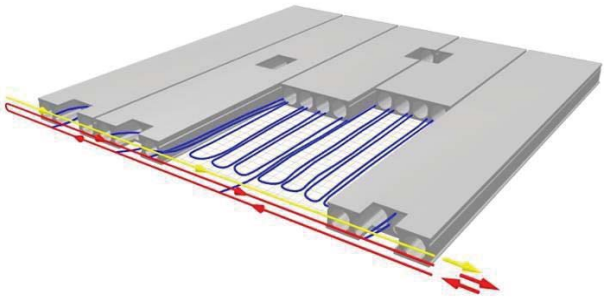

Figure 16 - Services inside precast elements

Therefore, the latest generation of precast concrete buildings has evolved over the past 30 years into buildings of high specification. Architectural structural precast concrete elements are being used on an increasing number of prestigious commercial buildings, and steelwork, timber, plastics and masonry are being combined for the holistic benefit of the entire building process.

Designers are becoming more aware of the high quality finishes possible in prefabricated units, and changes are now being made to the way that the traditional precast structures are conceived and designed. The construction industry is calling for multi-functional design, where the optimum use of all the elements forming the building must be maximised. Precasting cannot be ignored any longer at the initial study of buildings, either for the total structure or for parts of it.

REFERENCES

[1] Evolución de la prefabricación para la edificación en España. Medio siglo de experiencia. M. Burón y D. Fernández-Ordóñez. Informes de la Construcción, Vol 48 nº 448, marzo/abril 1997.

[2] Eugène Freyssinet. J.A. Fernández Ordóñez. 2C Ediciones. Barcelona. 1978

[3] "Arquitectura y Represión. Seminario de Prefabricación". J.A. Fernández Ordóñez. Cuadernos para el Diálogo. 1973

[4] L´art de l´ingénieur, constructeur, entrepreneur, inventeur. A. Picon. Centre Georges Pompidou, Le Moniteur. 1997

[5] "Pensar la Ingeniería. Antología de Textos de José Antonio Fernández Ordóñez". J.R. Navarro Vera. Colegio de Ingenieros de Caminos, Canales y Puertos y Fundación Juanelo Turriano, Madrid, 2009

[6] "Prefabrication for Affordable Housing. State of the Art Report". Bull 60. *Fib* Commission 6 Prefabrication. DCC. Germany. 2011

[7] *fib* Bulletin 6: Guide to good practice "Special design considerations for precast prestresssed hollow core floors", ISBN 2-88394-046-0, 2000

[8] *fib* TG 6.1 Design recommendations "Precast prestressed hollow core floors" in preparation. Publication foreseen for 2019

[9] FIP Guide to good practice, "Shear at the interface of precast and in situ concrete"; January 1982, ISBN 0 907862 02 0

[10] FIP Recommendations "Precast prestressed hollow core floors" - FIP Commission on Prefabrication, Thomas Telford 1988 - ISBN 0 7277 1375 2

[11] FIP Guide to good practice: "Quality assurance of hollow core slabs" - FIP Commission on prefabrication, July 1992, SETO, ISBN 1 8747266 8

[12] *fib* Bulletin 19: State-of-art Report "Precast Concrete in Mixed Construction", 2002

[13] FIP Guide to good practice "Composite floor structures" - FIP Commission on Prefabrication, SETO 1998, ISBN 1 874266 38 7

[14] *fib* bulletin 41: "Treatment of imperfections in precast concrete structural elements", 2007, ISBN 978-2-88394-081-9

[15] *fib* Bulletin 43: Guide to good practice "Structural connections for precast concrete buildings", fib Commission on Prefabrication, February 2008.

[16] *fib* Bulletin 46: State of art report "Fire design of concrete structures - structural behaviour and assessment", ISBN 978-2-88394-086-4, July 2008

[17] *fib* Bulletin 63: Guide to good practice "Design of precast concrete structures against accidental actions", ISBN 978-2-88394-103-8

[18] *fib* TG 6.11: Guide to good practice "Precast insulated sandwich panels"

[19] *fib* Bulletin 74: "Planning and design handbook on precast building structures". Manual - textbook (ISBN 978-2-88394-114-4, September 2014)

[20] *fib* Bulletin 78. "Precast-concrete buildings in seismic areas". State-of-the-art report (ISBN 978-2-88394-118-2, March 2016)

[21] FIP: "Planning and Design Handbook on precast building structures" - FIP Commission on Prefabrication, SETO Ltd 1994, ISBN 1 874266 11 5

[22] CEB-FIP Model Code for Concrete Structures, Paris Bulletin d'information du CEB Nr 124/125, Volume II, April 1978.

[23] CEB-FIP Model Code for concrete structures 1990, London, Thomas Telford, 1991

[24] *fib* Model Code for concrete structures 2010, Berlin, Ernst&Sohn, 2013

ДГКС Друштво грађевинских конструктера Србије
ASES Association of Structural Engineers of Serbia
U-4
15. KONGRES
6-8. 9. 2018. Zlatibor

Milenko Pržulj[1]

SAVREMENE KONCEPCIJE I KONSTRUKCIJE SPREGNUTIH MOSTOVA

Rezime:
Razvoj teorije i prakse sprezanja čelika i betona u posljednjim decenijama ponovo je učinio konkurentnim čelik kao materijal za mostove svih raspona i sistema. U većem broju evropskih razvijenih zemalja u toku je novi zamah u primjeni spregnutih konstrukcija u mostogradnji uz izraženu kreativnost i inovativnost. Sprezanje čelika i betona najviše se primjenjuje za gredne mostove a zadnjih decenija i za okvirne sisteme kao integralne konstrukcije. Sprezanje je u prednosti i za nadlučne konstrukcije lukova velikih raspona i za mostove sa kosim zategama.
Na primjerima aktuelnih izgrađenih spregnutih mostova iz naše prakse i u svijetu ukazuje se na nove koncepcije, konstruktivna rješenja i uslove, kada su spregnute konstrukcije u prednosti.

Ključne riječi: koncepcije, gredni, okvirni – integralni, lučni i zavješeni spregnuti mostovi

STATE-OF-THE-ART CONCEPTIONS AND DESIGNS OF COMPOSITE BRIDGES

Summary:
By the development the theory and practice in composite steel and concrete structures in last decades, steel has been competitive as material for bridges of all spans and systems. In most European countries, there is a new upswing in the composite bridge construction, accompanied by a creativeness and inventiveness. Composite steel and concrete structures have been predominantly introduced to beam bridges; during recent decades, however, to frame and integral bridges as well. Such structures are also advantageous to the decks of large-span arch bridges as well as to the cable-stayed bridges. Using examples of the actual constructed composite bridges from our practice as well as worldwide, new conceptions and schemes, design solutions and circumstances are indicated which make composite steel and concrete structures advantageous.

Key words: conception, composite beam bridges, composite frame and integral bridges, composite arch bridges, composite cable – stayed bridges

[1]*prof. dr. Milenko Pržulj, konzultant za mostove i konstrukcije (Povšetova 29, 1000 Ljubljana, milenko.przulj@siol.net)*

1 UVOD

Savremene tehnologije omogućuju sprezanje različitih materiala. Sprezanje u širem smislu je konstruktivno i funkcionalno objedinjavanje dva ili više materijala različitih osobina u jedinstven spregnut presjek. U nizu mogućih sprezanja različitih materiala u graditeljstvu imaju praktičnu primjenu sprezanje čelika i betona, sprezanje betona različite starosti i kvaliteta i sprezanje betona i drveta.

U definisanju osnovnih osobina čelika i betona realna je konstatacija:

- čelik je dobar material za mostove jer se, pored ostalog, može pouzdano i sigurno zaštititi od uticaja agresivne sredine;
- beton je dobar material za mostove, ali se još uvijek ne može garantovati njegova trajnija zaštita od uticaja agresivne sredine.

Beton bez pomoći čelika u smislu armiranja, prednaprezanja ili sprezanja ne može preuzeti napone zatezanja. Prevaziđene su zablude i predubjeđenja, da samo kod čeličnih mostova treba računati sa troškovima održavanja.

Razvoj spregnutih konstrukcija se odvija u dva pravca:

- razvoj teorije spregnutih konstrukcija i eksperimentalnih istraživanja
- razvoj i unapređenje prakse konstruisanja, projektovanja i postupaka građenja spregnutih konstrukcija u mostogradnji.

Kod projektovanja i izgradnje mostova sprezanje čelika i betona najčešće se primjenjuje za rasponske konstrukcije grednih sistema mostova. Pored grednih sistema sve više se primjenjuje sprezanje okvirnih, lučnih i zavješenih mostova.

Za projektovanje i izgradnju spregnutih mostova, pored poznavanja teoretskih osnova i propisa potrebno je poznavati postupke radioničke izrade, načina spajanja, posebno zavarivanje i montaže čeličnih konstrukcija. Namjena članka je, da pored ostalog, animira investitore, projektante i izvođače za veću primjenu spregnutih konstrukcija.

Materiali za betonske mostove imaju velike prirodne rezerve, cijena rada je niža, tako da je beton u prednosti za manje i srednje mostove.

Spregnuti mostovi su u prednosti za pojedinačne mostove srednjih raspona, jer omogućavaju brzu izgradnju bez angažovanja veće opreme i rada na gradilištu. Za veće mostove samo varijantna rješenja omogućavaju objektivan i racionalan izbor. Spregnuti mostovi se brže grade, lakše rekonstruišu, zamjenjuju i recikliraju.

2 KRATAK PRIKAZ RAZVOJA SPREGNUTIH MOSTOVA

Prije stotinu godina počela je upotreba betona za kolovozne ploče putnih i željezničkih mostova. U početku beton je imao funkciju ispune između čeličnih nosača ili koritastih limova. Od dvadeset do trideset godina prošlog stoleća beton kao ispuna zamjenjen je nosivom armirano betonskom pločom koja se oslanjaja na čelične nosače.

Značajna istraživanja sudjelovanja armirano betonskih ploča i čeličnih nosača su bila od 1920–1940 godine. Prvi pisani članci o spregnutim nosačima su se pojavili na kongresu međunarodnog društva za mostove i konstrukcije u Parizu 1932 godine.

Značajan podsticaj za razvoj spregnutih mostova imali su rezultati probnog opterećenja i sa tim povezana istraživanja na mostu preko rijeke Save u Zagrebu 1939. godine. Most nije bio projektovan i dimenzioniran kao spregnuta konstrukcija. Izmjereni naponi i deformacije pri probnom opterećenju su pokazala veliki stepen sprezanja.

Prvi propisi za spregnute konstrukcije su se pojavili između 1940 i 1955 godine. Na našim prostorima korišten je »DIN 1078 – Verbung Träger Strassenbrücken. Prvi pravilnik o spregnutim konstrucijama u Jugoslaviji usvojen je 1970. godine. Prva primjena spregnutih konstrukcija u Jugoslaviji bila je 1955. godine za kolovoznu ploču čeličnog rešetkastog mosta preko rijeke Save u Bosanskoj Gradiški. Šestdeset godina upotrebe spregnutih konstrukcija za mostove obogatila je načine, konstruktivna rješenja i statičko dinamičku analizu sprezanja čelika i betona.

Savremene spregnute konstrukcije, čelik-beton i evropski propisi »Eurocode 4 – Design of composite steel and concrete structures« obuhvataju sva tri osnovna konstruktivna elemenata: nosače, ploče i stubove.

Razvoj teorije i prakse spajanja čeličnih konstrukcija zavarivanjem i visoko vrijednim vijcima omogućuju nove funkcionalne i skladne oblike presjeka, radioničkih i montažnih nastavaka i olakšavaju izradu i montažu.

Za sprezanje čeličnih nosača i armiranih betonskih ploča koriste se elastični i kruti moždanici raznih oblika. Podjela je zasnovana prema načinu preuzimanja napona smicanju. U savremenoj praksi najviše se koriste elastični moždanici u vidu čepova.

Cijena izgradnje armirano betonskih ploča utiče na konkurentnost spregnutih mostova. Pokušaji da se AB ploče grade kao montažne, što je bilo primjenjeno na izgradnji velikih viadukata u Švajcarskoj i nekim drugim mostovima u periodu od 1960 – 1980 godine, pokazalo je nedostatke u smanjenoj trajnosti, pa se ne preporučuje za nove mostove. Na smanjenje cijene izrade AB ploča može se uticati preko tehnologije izgradnje sa primjenom pomičnih oplata koji kao oslonac koriste čelične nosače. Tanje AB ploče debljine 18 – 20 cm karakteristične za prve decenije primjene spregnutih mostova, sada su radi trajnosti i većih pokretnih opterećenja debele 22 – 30 cm.

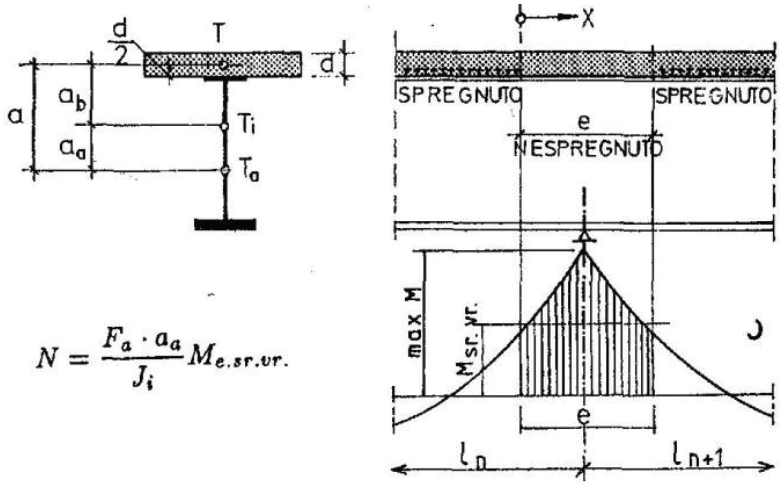

Slika 1: Skica diskontinualnog sprezanja nad srednjim stubovima

Kod sprezanja čelika i betona razlikujemo kruto, elastično i diskontinualno sprezanje. Kod krutog sprezanja nema pomaka na spoju AB ploče i čeličnog nosača. Kod elastičnog sprezanja omogućena su pomjeranja na spoju AB ploče i čeličnog nosača što smanjuje uzdužne i smičuće sile u presjecima, a momenti se povećavaju skladno sa krutosti presjeka. Smanjenje uzdužnih sila lakše je postići primjenjem diskontinualnog sprezanja. Na dijelovima nosača sa najvećim momentima presjeci se ne sprežu. Kolovozna AB ploča se na tim mjestima ne prekida. Na tim dijelovima nosača nema smičućih sila između AB ploča i čeličnih nosača, a uzdužna sila je konstantna. Momente preuzima čelični dio spregnutih presjeka (slika 1).

Reološki uticaji od skupljanja i tečenja betona kao i uticaji temperature ne utiču na povećanje sile, jer se ukupna smičuća sila preuzima na krajevima nosača gdje postoji sprezanje. U savremenoj praksi projektovanja spregnutih mostova primjenjuje se diskontinualno sprezanje pa se time izbegava primjena uzdužnih kablova za prednaprezanje kolovoznih AB ploča radi preuzimanja zatežućih napona. Povećana potrošnja čelika kompenzira se sa jednostavnijom i bržom izgradnjom.

Po obimu sprezanja razlikujemo sprezanje presjeka samo za pokretno opterećenje, tako da čelični nosač preuzima cijelu vlastitu težinu i težinu betona, bez privremenih oslonaca pod čeličnim nosačima postavljenim prije betoniranja. Sprezanje za ukupno stalno i pokretno opterećenje podrazumjeva da je čelični nosač poduprt pred betoniranjem AB ploče. Sprezanje se može kombinovati i sa predhodnim ili naknadnim prednaprezanjem čeličnih nosača i (ili) AB ploča.

U prvim decenijama primjene sprezanja, sprezani su samo punostjeni čelični nosači. U poslednjih trideset godina uspješno se sprežu i rešetkasti čelični nosači. U pogledu statičkih sistema u početku su se sprezali gredni sistemi sa jednim ili više diskontinualnih ili kontinualnih sistema. U savremenoj praksi sprezanje čelika i betona se primjenjuje i za okvirne, lučne i zavješene sisteme mostova. U našoj i evropskoj praksi za rasponske konstrukcije putnih mostova širine 8 – 14 m najčešće projektovani poprečni presjeci imaju dva glavna nosača (slika 2):

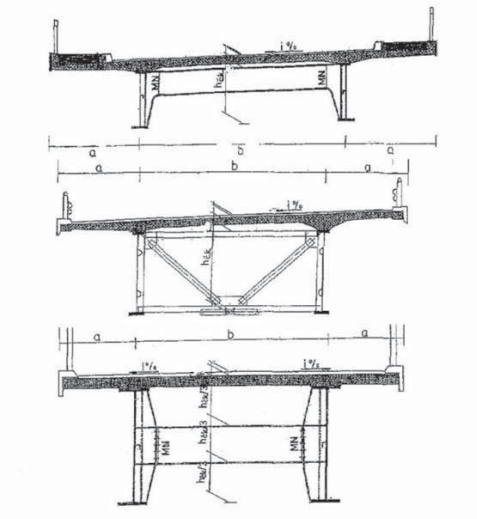

Slika 2: Variantna rješenja poprečnih presjeka mostova sa dva punostjena glavna nosača

Razmak između nosača i raspon konzola potrebno je pravilno uravnotežiti, tako da je b >= 2a.

Visina, položaj, presjek, način spajanja poprečnih nosača sa glavnim nosačima, kao i razmak poprečnih nosača zavisi od više parametara (statički sistem, veličina raspona, oblik presjeka i visina glavnih nosača, način betoniranja AB ploče, radionička izrada i montaža).

Za mostove velikih raspona, posebno za mostove u krivini racionalni su pravokutni ili trapezni sandučasti presjeci (slika 3). Pri konstruisanju sandučastih presjeka neophodno je uvažavati i tehnologiju radioničke izrade, transporta i montaže.

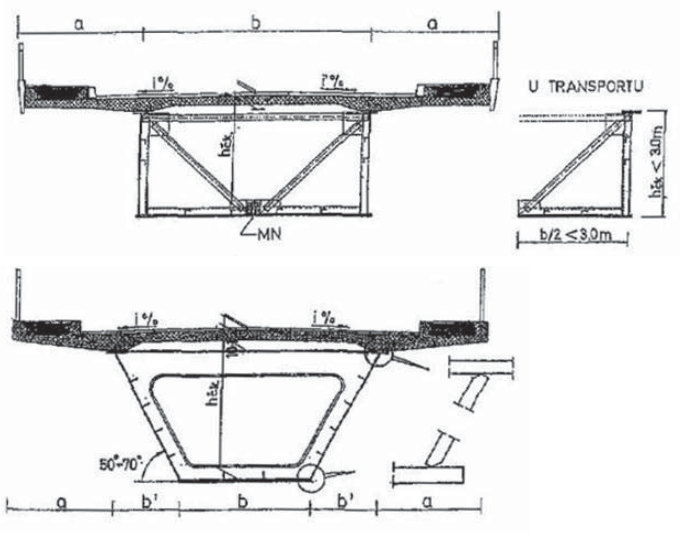

Slika 3: Sandučasti presjeci za mostove većih raspona

Za spregnute mostove većih raspona i veće širine na autoputevima moguće su vrlo različite koncepcije sandučastih poprečnih presjeka (slika 4). Ograničena širina sandučastog presjeka radi transporta i montaže upućuje na velike dužine konzola, koje je racionalno poduprijeti sa kosim potporama.

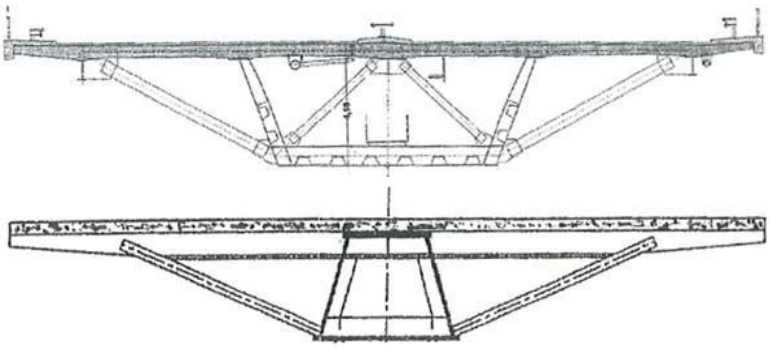

Slika 4: Poprečni presjeci mostova većih širina na autoputevima

Dalji razvoj spregnutih mostova ide u pravcu sve veće primjene prostornih rešetkastih cijevnih nosača koji se preko specialno oblikovanog gornjeg a često i donjeg pojasa sprežu sa AB pločama (slika 5).

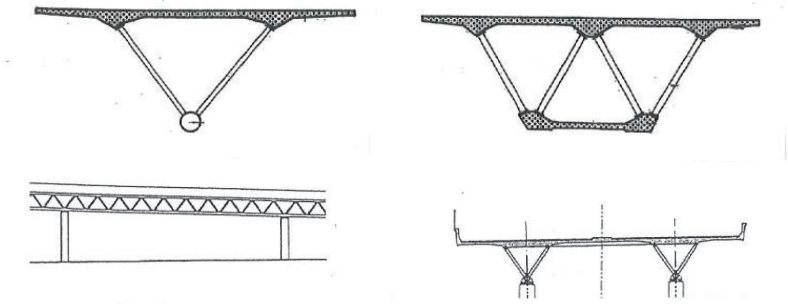

Slika 5: Sheme prostornih spregnutih rešetkastih nosača za mostove

U Švajcarskoj su izgrađeni autoputni dolinski viadukti dužine cca 1000 m sa rasponima 40–50 m, koji su na raspisu Investitora bili najuspješniji. Pored ekonomičnosti viadukti se lijepo prilagođavaju prirodnom ambijentu, djeluju lagano i transparentno (slika 6).

Slika 6: Viadukti sa rešetkastim spregnutim prostornim nosačem

U savremenoj praksi projektovanja spregnutih mostova čelik - beton karakteristična su tri trenda:

- dvojno sprezanje
- okvirne integralne spregnute konstrukcije
- hibridni (mješani) mostovi

Kod spregnutih mostova velikih raspona primjenjuju se dvojno spregnuti presjeci. Betonska ploča u sastavu donjeg pritisnutog pojasa sandučastog presjeka smanjuje potrošnju čelika u zoni pritiska i povećava krutost presjeka.

Pri projektovanju dvojno spregnutih mostova otvaraju se neka pitanja u izboru odgovarajućih statičkih modela, proračunu, konstruiranju i granicama ekonomičnosti.

Ta pitanja se prije svega odnose na:

- Tok smičućih napona između čeličnog sandučastog nosača i betonske donje ploče.
- Djelotvornost površinskog sprezanja između donje čelične i betonske ploče.
- Sudjelovanje moždanika i poprečnih ukrućenja pri prenosu smičućih sila u donju betonsku ploču.

- Unos sile u donju ploču na krajevima ploče.
- Predpostavke sudjelujuće visine i širine debelih betonskih ploča.
- Zamor visoko opterećenih moždanika.
- Uticaj pojedinačnih visokih smičućih napona krute betonske ploče na raspored statičkih količina.
- Ekonomična rješenja da se pritisak na oplatu i vlastita težina svježeg betona prenesu na čelične vertikalne limove i donju ploču.
- Konstruktivna rješenja i ekonomičnost upotrebe betonskih poprečnih nosača nad osloncima.

Najbitniji rezultati nekih aktuelnih istraživanja

- Za dvojno sprezanje su povoljnije konstrukcije sa promjenljivom visinom.
- Potrebno je izbjegavati nagle promjene poprečnog presjeka.
- Na krajevima donje ploče su nastupila velika opterećenja moždanika.
- Prenos sile u donju ploču se koncentriše u zonama vertikalnih limova.
- Ako je u vertikalnim limovima raspoređeno više redova moždanika možemo pojednostavljeno pretpostaviti, da uvođenje sile u donju ploču ide isključivo preko moždanika u vertikalnim limovima i u njihovoj blizini.
- Poprečna ojačanja vertikalnih limova i donjeg pojasa preuzimaju značajan dio smičućih napona i tako rasterećuju moždanike.
- Sile iz čeličnog poprečnog presjeka u donju betonsku ploču se prenose sa smičućim i nateznim silama u moždanicima.

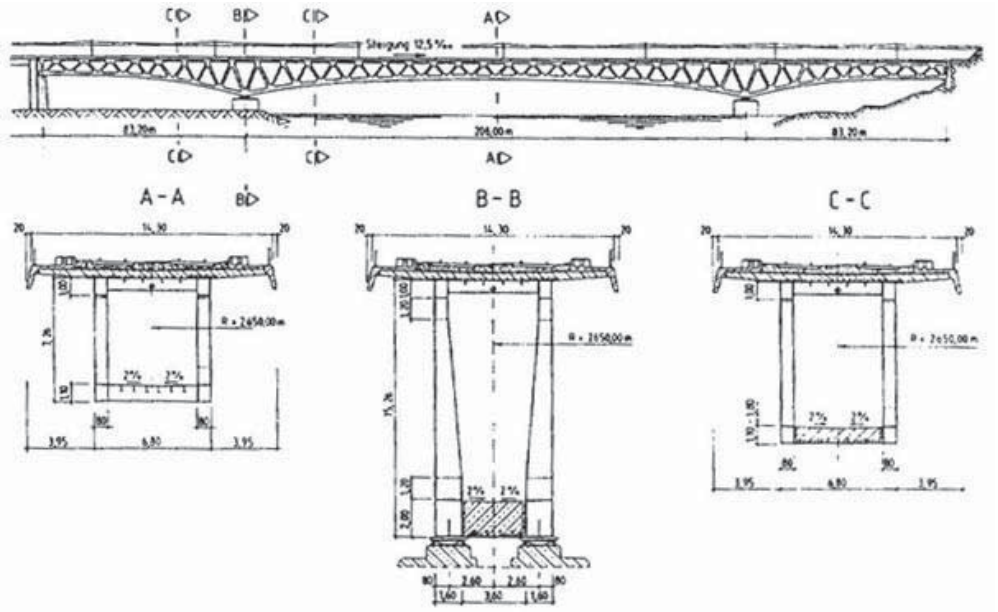

Slika 7: Spregnuta rešetkasta konstrukcija željezničkog mosta u Njemačkoj

Na novim brzim željeznicama u Njemačkoj izgrađeno je više mostova sa spregnutom rešetkastom konstrukcijom. Izuzetnu pozornost izaziva rješenje mosta preko rijeke Main kod Nantenbacha za dupli kolosjek, koji je dovršen 1993. godine. Dva glavna kontinualna rešetkasta nosača sa tri raspona, promjenljive visine od 8,5 do 16,5 m imaju rekordan srednji raspon od 208 m (sl. 7). Spregnuta su oba pojasa rešetkastog nosača izuzev srednje (zategnute) zone donjeg pojasa. Glavni raspon izgrađen je konzolnim postupkom, što je prirodno obzirom na odnos raspona i profil prepreke.

3 GREDNI SPREGNUTI MOSTOVI

Sprezanje čelika i betona se najviše primjenjuje pri projektovanju putnih i željezničkih mostova grednih sistema. Racionalne veličine raspona ovise od morfologije, prvenstveno visine - dubine prepreke, uslova temeljenja, namjene mosta, statičkog sistema, načina montaže i odnosa tržišnih cijena u funkciji vremena i lokacije. Na primjerima projektovanih i izgrađenih mostova iz savremene prakse moguće je uvjerljivo i pregledno prikazati praktičnu primjenu savremenih trendova razvoja spregnutih konstrukcija mostova.

Most preko rijeke Neretve kod Jablanice (8)

Za razliku od ranije izgrađenih mostova sa kontinualnim spregnuto-prednapregnutim kostrukcijama kod kojih je kablovima ostvareno kontinualo sprezanje, putni most preko rijeke Neretve ima kontinualnu konstrukciju sa diskontinualnim sprezanjem (slika 8).

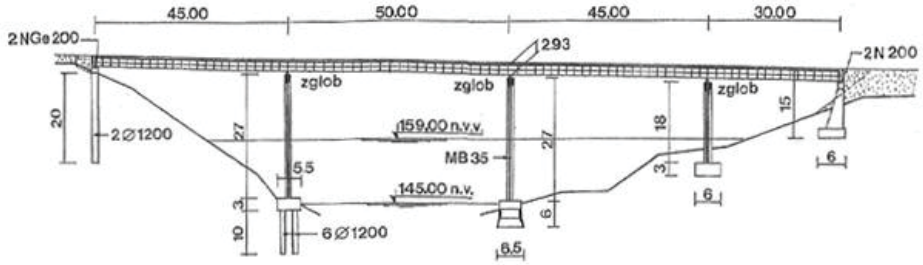

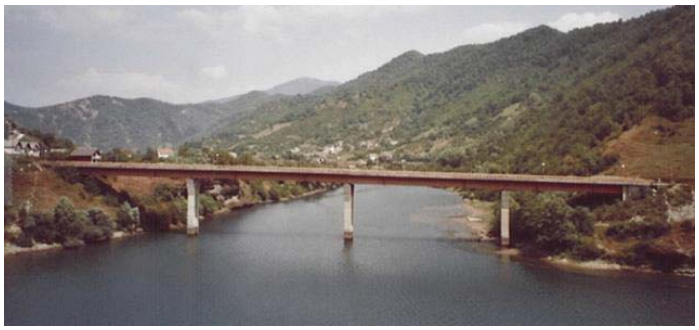

Slika 8: Putni spregnuti most na r. Neretvi sa diskontinualnim sprezanjem

Most je izgrađen 1985. godine za samo 6 mjeseci kao ekonomičnije rješenje u odnosu na varijantu sa konstrukcijom od prednapregnutog betona. Visina mosta iznad terena čine

neekonomičnu izradu privremenih oslonaca za montažu i sprezanje vlastite težine. U zonama pozitivnih momenata izvršeno je sprezanje čeličnog nosača, dok se u zonama negativnih momenata sprezanje ne može obezbijediti bez dodatnog prednaprezanja kablovima. Da bi se izbjeglo prednaprezanje, ojačani čelični nosač iznad oslonaca prima uticaje bez sadejstva armirano-betonske ploče. Ekonomska opravdanost takve koncepcije je pojednostavljenje montaže, skraćenje vremena građenja, eliminisanje nepovoljnih dopunskih utjecaja od prednaprezanja, te smanjenje uticaja u vremenu t = tn od skupljanja i tečenja betona uz nešto veću potrošnju čelika. Betoniranjem kolovozne ploče po fazama, prvo u poljima a zatim nad osloncima, uticano je na smanjenje napona zatezanja u betonu.

Most preko rijeke Save u Orešju (10)

Glavna konstrukcija mosta raspona 85+134+85 projektovana je kao kontinualna dvojno spregnuta-prednapregnuta konstrukcija promjenljive visine do 5,80 m nad riječnim stubovima do 3.00 m u sredini mosta.

Izgrađena je – montirana sa po dva pomoćna oslonca u krajnjim poljima i slobodnom konzolnom gradnjom srednjeg raspona uz sukcesivno betoniranje donje odnosno gornje ploče i prednaprezanje.

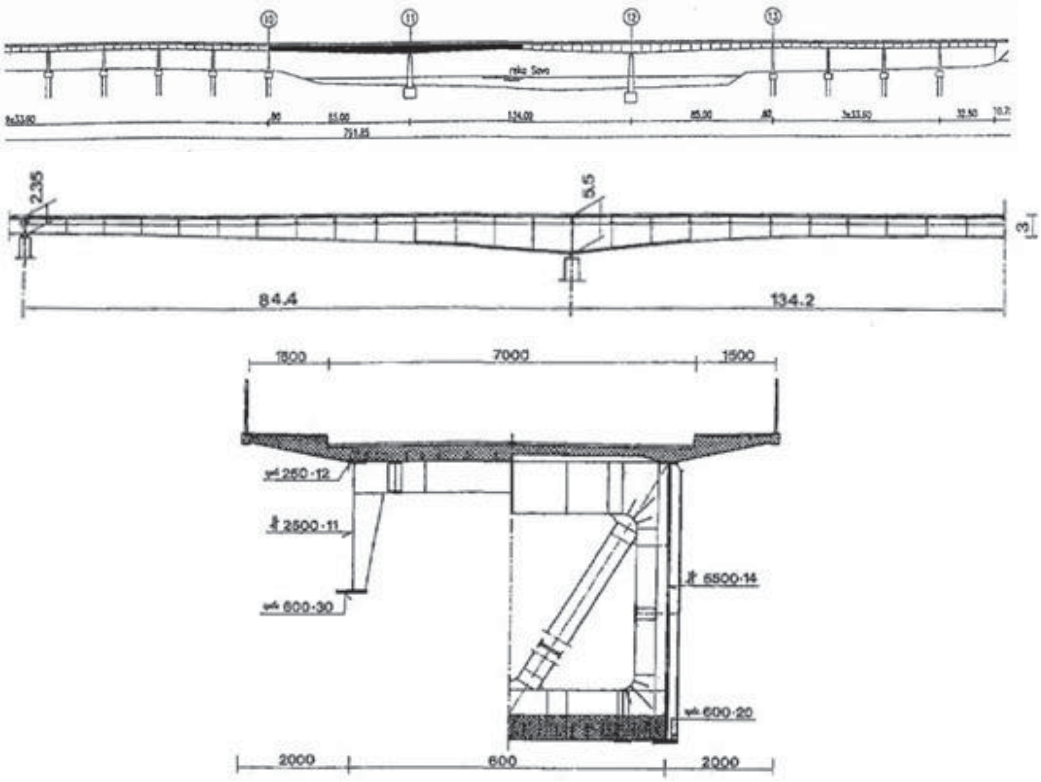

Slika 9: Dispozicija dvojno spregnutog putnog mosta na r. Savi u Orašju

Prema našim saznanjima ovo je bila prva primjena dvojnog sprezanja i otvorila je put za nove mogućnosti kombinacije čelika i betona u mostogradnji. U vrijeme projektovanja mosta od 1966 – 1968 godine kao i danas konkurentnost čeličnih mostova i za ove raspone bila je manja u odnosu na mostove od prednapregnutog betona. Iz ove okolnosti proizišla je ideja i realizacija dvojnog sprezanja uz maksimalno smanjenje učešća čelika i povećanje učešća betona u spregnutom presjeku mosta (slika 9).

Most preko Jablaničkog jezera (15)

Kontinualna spregnuta rasponska konstrukcija mosta ima 11 uravnoteženih simetričnih raspona 32,00+39,50+7x55,00+39,50+32,00=528,00 m. Konstrukcija mosta slijedi geometriju ceste na mostu i prilagođava se krivinama i proširenjima na krajnjim dijelovima mosta.

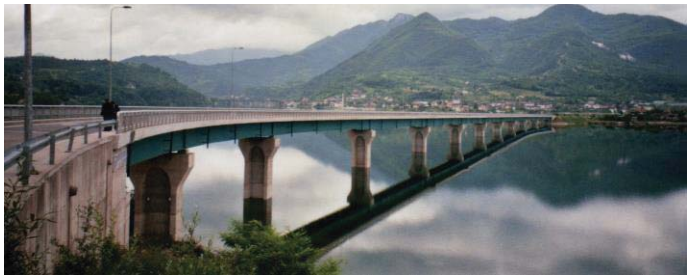

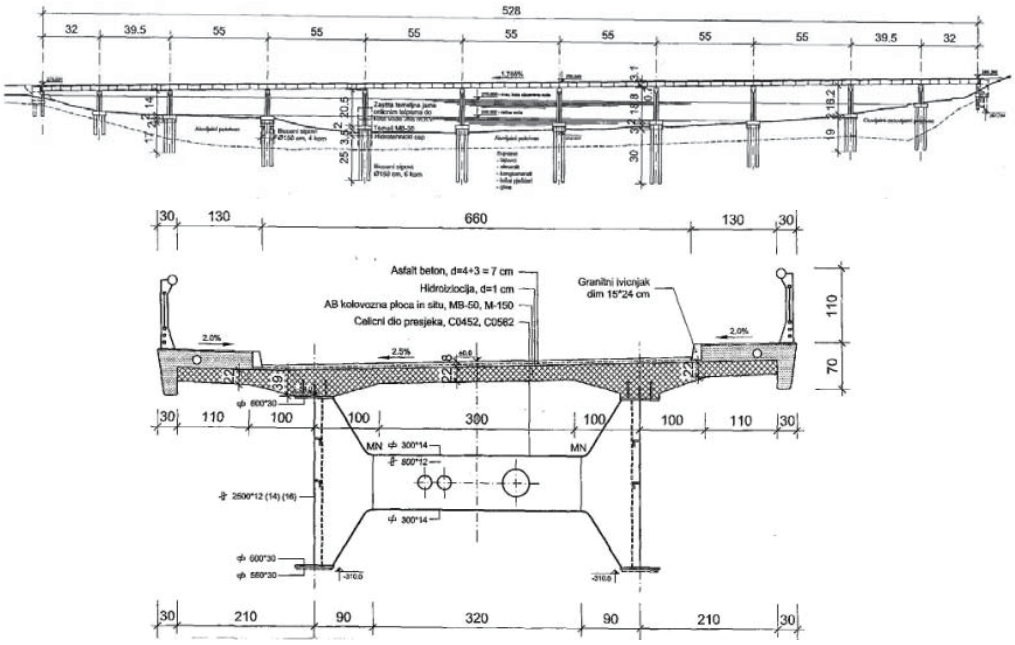

Slika 10: Izgled, uzdužni i poprečni presjek putnog spregnutog mosta preko Jablaničkog jezera

Raspon od 55,00 m na većem dijelu mosta je optimalan za kontinualne spregnute konstrukcije sa diskontinualnim sprezanjem bez primjene kablova za prednaprezanje armirane betonske ploče na dijelovima iznad srednjih stubova. Raspon od 55.00 m je limitni za montažu čeličnog roštilja rasponske konstrukcije navlačenjem bez pomoćnih oslonaca i bez privremenog zavješenja. Ovako pojednostavljena tehnologija ugradnje i montaže opravdava nešto povećanu potrošnju čelika za čeličnu konstrukciju što potvrđuje savremena praksa u Švajcarskoj i drugim razvijenim državama.

Cjelokupna tehnologija izgradnje mosta koncipirana je na maksimalnom korištenju jezera promenljivog nivoa i radne plovne platforme sa koje se buše šipovi, postavljaju talpe zagata, betoniraju temelji i stubovi, montira čelična konstrukcija i betonira kolovozna ploča.

Zadržali smo uobičajeni koncept poprečnog presjeka mosta sa dva glavna nosača i otvorenim presjekom bez sprezanja poprečnih nosača koji je vrlo racionalan i prisutan je u evropskoj i našoj praksi (slika 10).

Pješački most preko rijeke Drave u Ptuju (16)

Most je lijep primjer savremene spregnute kontinualne rešetkaste konstrukcije izgrađene 1997. godine. Čelična rešetkasta prostorna konstrukcija mosta visine 1,23 m izrađena je od cijevi u zavarenoj izvedbi. Čelična konstrukcija preuzima težinu svježeg betona, a spregnuti presjek težinu opreme i korisno opterećenje pješaka (slika 11).

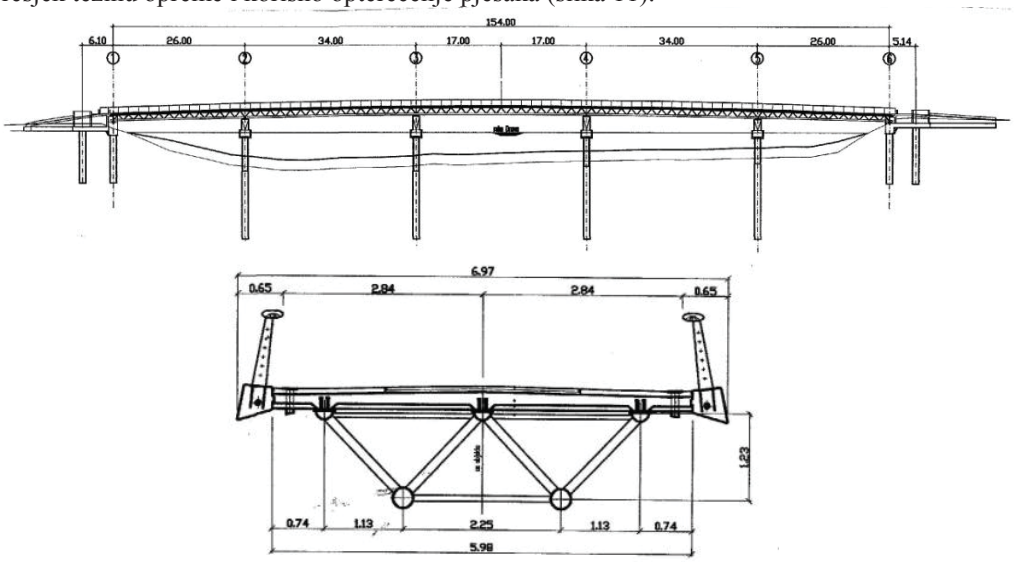

Slika 11: Spregnuti pješačko biciklistički most preko r. Drave na Ptuju

Novi viadukti na autoputevima u Njemačkoj (12)

U poslednjim godinama na autoputevima u Njemačkoj izgrađeni su vrlo lijepi savremeni viadukti sa spregnutim rasponskim konstrukcijama. Viadukt Talbrücke Ruchenbach na A 71 dužine 1000 m ima raspona od 50 – 105 m i premoštava dolinu dubine do 60 m (slika 12).

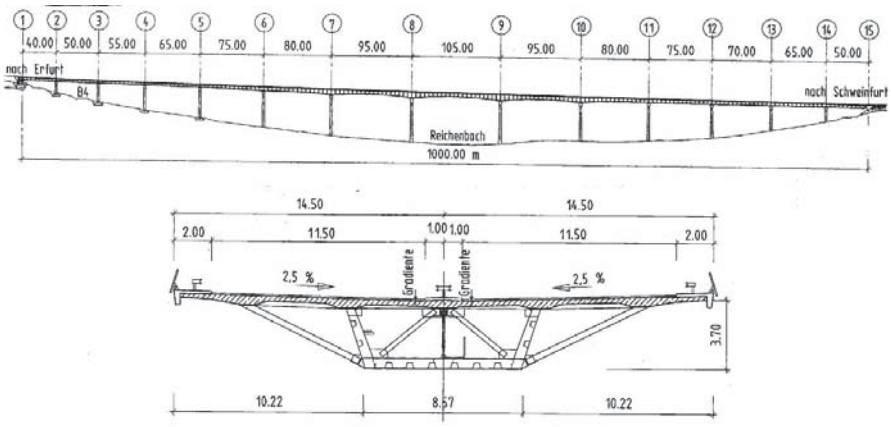

Slika 12: Spregnuta konstrukcija viadukta na autoputu u Njemačkoj

Poprečni presjek rasponske konstrukcije je jedinstven, širine 29 m za oba kolovoza. Visina sandučastog nosača je na dijelu većih raspona promjenljiva od 3,70 – 6,50 m. Trapezni nosač širine 8,57 m ima sa bočnih strana kose potpore tako da se kolovozna AB ploča poprečno oslanja na četiri oslonca.

Ploča je betonirana na licu mjesta pomoću unificirane prenosne oplate. Montaža čelične konstrukcije je kombinovana navlačenjem uz pomoć kljuna na manjim rasponima i kombinovana na dijelu velikih raspona. Sandučasti trapezni presjek rasponske konstrukcije relativno male širine omogućuje male širine visokih stubova i lijep izgled viadukta (slika 13). Potrošnja konstruktivnog čelika je 222 kg/m2 a cijena viadukta bila je 1056 EUR/m2.

Slika 13: Izgled viadukta Talbrücke Ruchenbach

Viadukt Mirna (13)

Viadukt Mirna na istarskoj brzoj cesti »Y« u Hrvatskoj premoštava široku dolinu rijeke Mirne na visini 15-40 m. Spregnuta rasponska konstrukcija ukupne dužine 1355 m ima 22 raspona sa tipičnim rasponom 66,50 m. Pored ostalog teško i skupo temeljenje na čeličnim

zabijenim šipovima velike dužine dalo je prednost znatno lakšoj spregnutoj konstrukciji. Poprečni presjek viadukta za jedan kolovoz brze ceste je konstruisan iz dva glavna nosača konstantne visine 2,75 m na razmaku 5,50 m sa konzolama 2,30 m.

Pojasevi nosača su širine 700 i 800 mm debljine 30 – 35 mm. Poprečni nosači su nespregnuti, postavljeni u sredini visine glavnih nosača. Glavni nosači su na različitim visinama sa čime se postiže poprečni nagib AB ploče. Interesantna su rješenja opreme viadukta (slika 14).

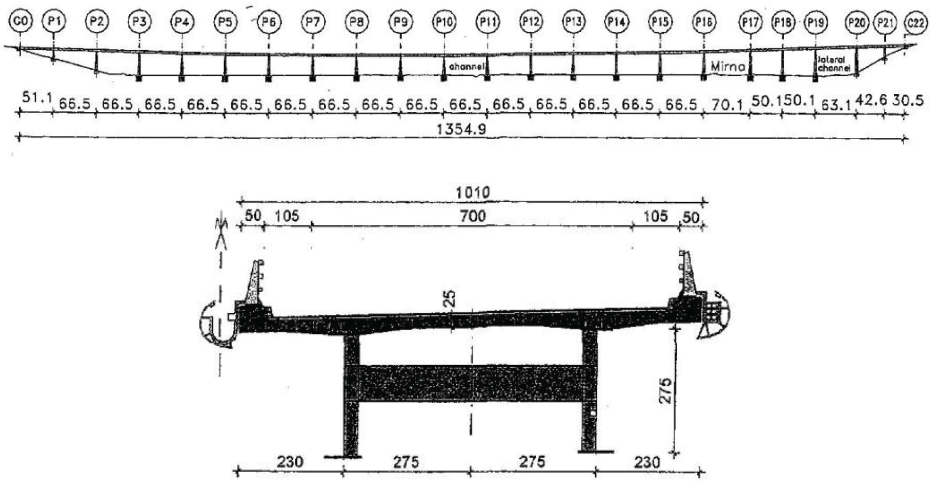

Slika 14: Uzdužni i poprečni presjek viadukta Mirna na Istarskoj brzoj cesti

Montaža čelične konstrukcije viadukta navlačenjem sa kljunom od obala prema sredini je jednostavna i brza. Izgled viadukta pokazuje dobro uklapanje u okolinu (slika 15).

Slika 15: Montaža čelične konstrukcije i izgled viadukta Mirna

4 SPREGNUTI INTEGRALNI PUTNI MOSTOVI STATIČKOG SISTEMA UPETE GREDE

Za putne mostove i nadvožnjake primjenjuju se spregnute okvirne – integralne konstrukcije sa jednim rasponom od 25 do 50 (60) m, koje eleminišu nedostatke spregnutih mostova statičkog sistema proste grede.

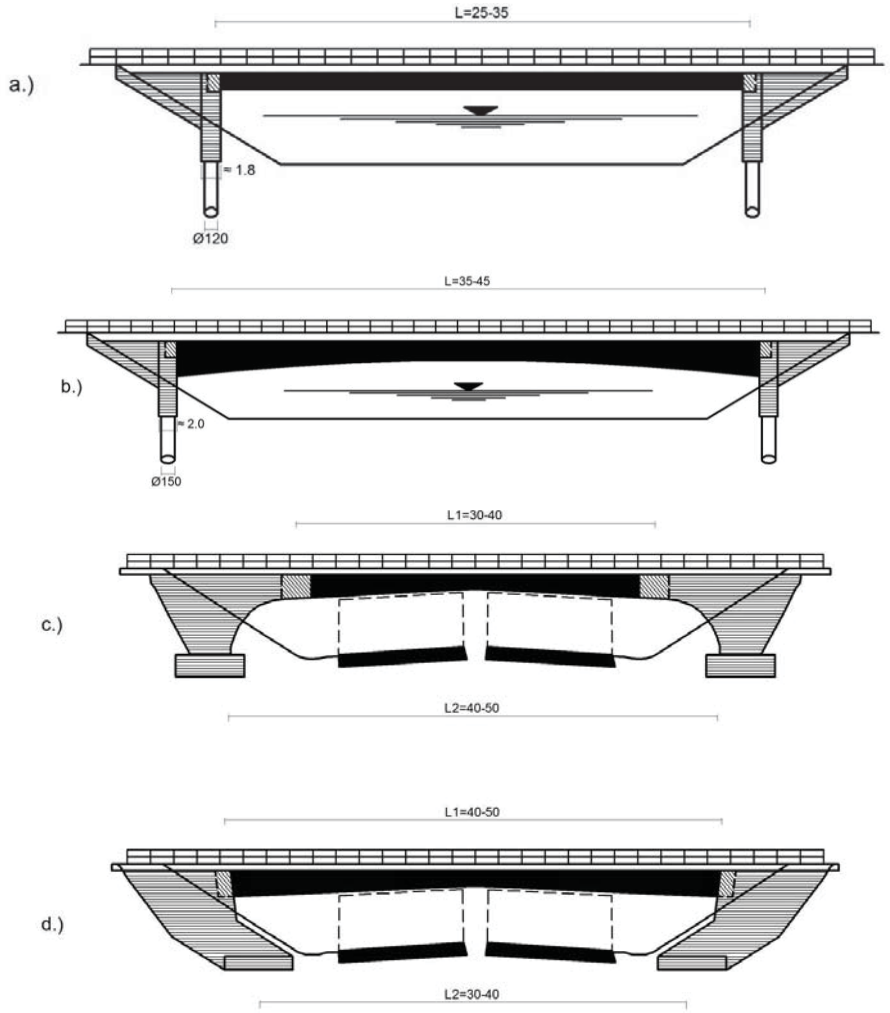

a) Čelična konstrukcija konstantne visine
b) Čelična konstrukcija promjenjive visine
c) Obalni stubovi konzolno konstruisani za veće raspone
d) Obalni stubovi koso konstruisani da omoguće veće raspone

Slika 16: Uzdužni presjeci integralnih spregnutih okvirnih putnih mostova u jednom rasponu

Za premošćenje kanala i manjih rijeka gdje nisu poželjni međuoslonci brzo i ekonomično se može izgraditi integralna spregnuta konstrukcija. Za raspone do 30 m rasponska konstrukcija je konstantne visine l/20 – l/30, a za veće raspone promjenljive visine u polju l/30 a na osloncima l/20 sa paraboličnim intradosom. Krajevi rasponske konstrukcije su na dužini 1,0–1,5 m kruto povezani sa vrhom elastičnih krajnjih stubova. Do uvođenja u praksu integralnih konstrukcija projektovani su spregnuti mostovi sistema proste grede. Oslonačke zone ovih mostova, ležišta, dilatacije, krajevi konstrukcije i vrhovi stubova imali su znatna oštećenja od slane vode sa kolovoza. Integralna okvirna konstrukcija nema te nedostatke i lakše se održava. Prednost pred betonskim integralnim mostovima je primjena za veće raspone, lakša montaža rasponske konstrukcije i građenje bez skele i uticaja na vodni tok i druge prepreke u profilu koji se premoštava.

Prema našim informacijama u našoj i evropskoj praksi nisu još izgrađeni cestni kontinualni integralni mostovi. U toku je razvoj primjene integralnih spregnutih konstrukcija za željezničke mostove.

Na slici 16 pokazani su mogući uzdužni presjeci integralnih spregnutim mostova u jednom rasponu.

Rasponska čelična konstrukcija konstantne visine za raspone 25 do 35 m (slika 16a) lakša je za radioničku izradu i montažu uz nešto veću potrošnju čelika.

Rasponska čelična konstrukcija promjenjive visine omogućuje veće raspone od 35 – 45 (50 m) (slika 16b) parabolični intrados daje lakoću mostu. Transport i montaža su nešto složeniji.

Obalni stubovi su od bušenih šipova Ø 120 ili 150 sa stenama debljine 1,5 do 2 m i omogućuju uklještenje čelične konstrukcije i elastično ponašanje konstrukcije u eksploataciji. Integralne konstrukcije c) i d) sa specifičnim konstrukcijom obalnih stubova omogućuje veće raspone i manje elastično ponašanje. Suženjem presjeka prema temelju i pliće temeljenje povećavaju elastično ponašanje stubova.

Poprečni presjeci spregnutih integralnih mostova zavisni su od veličine raspona i širine. Preporučuju se dva (za široke mostove i više) zavarena sandučasta nosača konstantne ili promjenjive visine iznad kojih se na licu mjesta betonira i spreže kolovozna ploča.

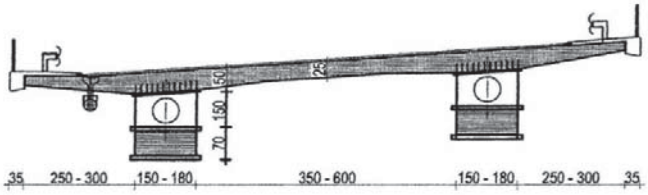

Slika 17: Karakterističan presjek spregnutih integralnih mostova širine 10 do 14 m

Nosači sandučastog presjeka su zahtjevniji u radioničkoj izradi ali su stabilniji u transportu i montaži. Za uklještenje sandučastih presjeka nisu potrebne poprečne veze i spregovi jer oblik nosača i kruta veza sa opornicima daje jim potrebnu torzionu krutost. Kolovozna ploča je deblja od 25 – 40 cm sa naglašenim vutama i konzolama.

Statička analiza integralnih mostova

Jedan od razloga za nedovoljnu primjenu integralnih mostova je težnja projektanata za jasnim aplikativnim statičkim sistemima grednih mostova. Savremena računska oprema i programi koji se zasnivaju na teoriji konačnih elemenata omogućuju egzaktniju i brzu analizu integralnih mostova na prostornom 3D modelu. Integralni i konvencionalni mostovi se međusobno razlikuju po načinu preuzimanja uticaja od promjene temperature, reologije betona i deformacija. Kod konvencionalnih mostova horizontalne deformacije su slobodne, a kod integralnih mostova su djelomično spriječene kontaktom sa tlom i nasipom. Interakcija most – temeljna tla i nasip je od bitnog značaja za ponašanje konstrukcije pri preuzimanju uticaja i deformacija posebno pri preuzimanju deformacija od parazitnih uticaja. Statičku analizu pojedinih nosivih dijelova integralne konstrukcije nije moguće obrađivati odvojeno jer je nosiva konstrukcija integralna sa kompleksnim interaktivnim djelovanjem rasponske konstrukcije, obalnih stubova sa krilnim zidovima, srednjih stubova, temelja (šipova), temeljnog tla i trupa puta.

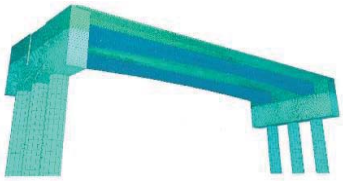

Slika 18: Model spregnute integralne okvirne konstrukcije mosta

Veličina parazitnih dejstava zavisi od geometrije objekta od odnosa krutosti između rasponske konstrukcije i stubova i od krutosti temeljnog tla. Kod monolitne – krute povezanosti rasponske konstrukcije sa obalnim stubovima posebno je značajna realna ocjena krutosti temeljnog tla. Pri projektovanju integralnih mostova je neophodna veća saradnja projektanta sa geomehaničarom nego kod projektovanja konvekcionalnih mostova. Najbolji način da se izbjegne rizik nepravilne procjene krutosti tla je da se statičke veličine i deformacije integralne konstrukcije sračunaju za dvije krajnje vrijednosti karakteristika temeljnog tla. Ocjena realne krutosti tla i promjene njene vrijednosti po dubini je objektivno vrlo teška. Ako na primjer za integralni most uzmemo niske vrijednosti koeficijenata krutosti tla, dobiju se za oko 15 % veće vrijednosti momenata i deformacija u sredini rasponske konstrukcije.

Za visoke vrijednosti koeficijenata krutosti tla dobiju se za oko 10 do 15 % veće vrijednosti momenata na spoju rasponske konstrukcije i stubova. Sa manjim dodatkom armature ili kablova treba preuzeti ekstremne uticaje za oba slučaja.

Usidrenja krajeva čelične konstrukcije u opornike i prelaz sa integralne konstrukcije na nasip

Kod mostova na glavnim putevima i autoputevima prelaz sa konstrukcije na nasip je podsredstvom prelazne ploče i asfaltne dilatacije. Kod mostova dužine do 60 m potrebna su dodatna rješenja na nasipu i oslonačke zone prelazne ploče. Nasip se ojačava sa geomrežama. Između nasipa i zidova opornika ugrađuje se sloj stiropora debljine 5 – 10 cm zavisno od raspona koji omogućuje deformacije spregute rasponske konstrukcije. Geomreže smanjuju potiske nasipa na obalne stubove a stiropor omogućuje manje deformacije. Moguća sleganja tla

iza opornika neutrališe prelazna ploča koja se na konstrukcije opornika oslanja preko neoprenskih ležišta.

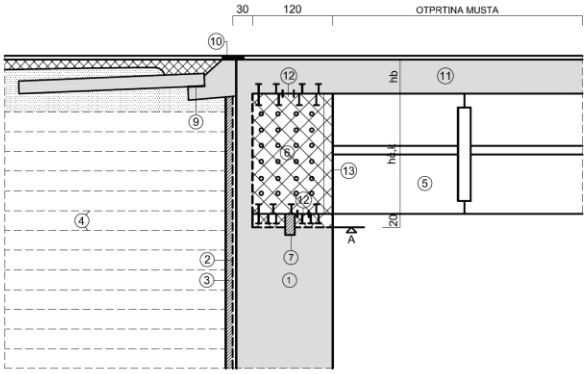

1) stena opornika
2) bitumenski premaz
3) stiropor 5 – 10 cm
4) nasip iz kamenitog materijala ojačanoj geomrežama
5) čelična konstrukcija
6) ubetonirani dio čelične konstrukcije
7) privremeni oslonac čelične konstrukcije
8) čepasti moždanici Ø 19 dužine 150 na razmaku 30 – 60 cm
9) neoprensko ležište
10) asfaltna dilatacija
11) kolovozna AB ploča
12) otvori Ø 200 za prolaz betona i vibratora
13) unutranja čelična zavjesa sprečava prolaz betona u sandučasti čelični presjek

Slika 19: Detalj usidrenja krajeva čelične konstrukcije u opornike i prelaz sa integralne konstrukcije na nasip

Integralni spregnuti most preko rijeke Ljubljanice u Ljubljani

Za izgradnju gradskog mosta preko rijeke Ljubljanice u Ljubljani projektovana je integralna spregnuta rasponska konstrukcija raspona 36 m (otvora 34,3 m) širine mosta 14 m.

Rasponska konstrukcija ima dva čelična nosača sandučastog presjeka promjenjive visine od 1,80 m pri uklještenju do 1 m u sredini raspona i širine 1,8 m. Most istovremeno služi i za prelaz većeg broja instalacija pa su na krajevima predviđene komore.

Obalni stubovi mosta su temeljeni na po tri šipa Ø 150 cm na koje se nastavlja betonski zid širine 1,7 m i visine 6 m. Obalni stubovi na šipovima su dovoljno elastični što omogućuje deformacije okvirne konstrukcije mosta. Iza zidova obalnih stubova predviđen je sloj stiropora debljine 10 cm a nasip je ojačan geomrežama koje smanjuju pritisak tla na konstrukciju mosta.

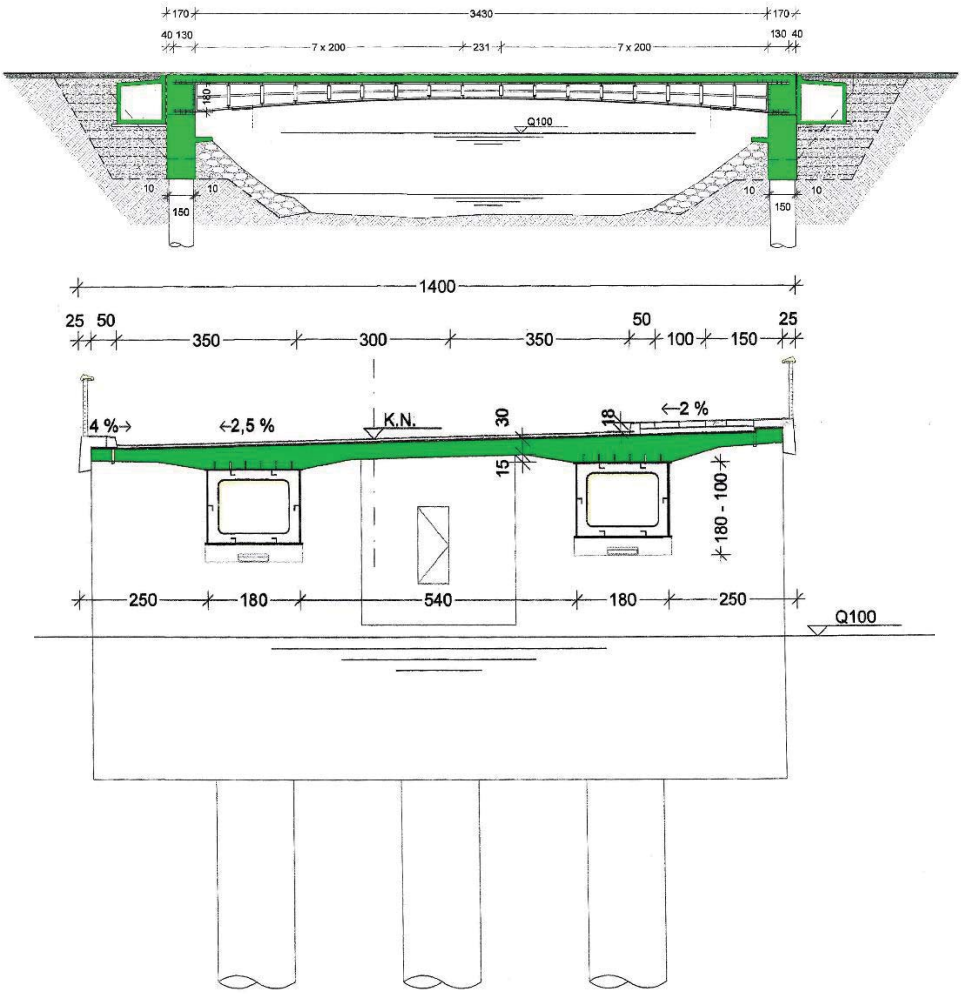

Slika 20: Uzdužni i poprečni presjek spregnutog integralnog mosta na r. Ljubljanici u Ljubljani raspona 36 m

Spregnuta integralna konstrukcija nadvožnjaka preko autoputa

Za izgradnju nadvožnjaka iznad autoputeva i drugih saobračajnica u eksploataciji spregnute integralne konstrukcije omogućuju rješenja sa jednim većim rasponom uz minimalno remećenje i prekide saobraćaja.

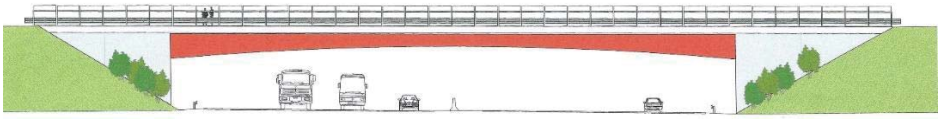

Slika 21: Izgled nadvožnjaka

Na slici 22 je uzdužni i poprečni presjek nadvoza na magistralnom putu koji koso pod uglom od 58° premoštava oba koilovoza autputa ukpne pravokutne širine 40,50 m. Izgradnja stuba u razdelnom pojasu autputa nedovoljne širine nije bila prihvatljiva radi ometanja intenzivnog saobraćaja.

Nadvoz je projektovan i konstruisan kao kosa, spregnuta, integralna, ramovska konstrukcija raspona 57,17 m ukupne širine 12,40 m. Dva glavna čelična nosača sandučastog presjeka su promjenljive visine od 1,10 m u sredini raspona do 2,40 m pri uklještenju u obalne stubove. Širina nosača je konstantna 1,5 m. Čelični nosači su na dužini 1,5 m ubetonirani – uklješteni u obalne stubove podobnom rješenju datom na slici 19.

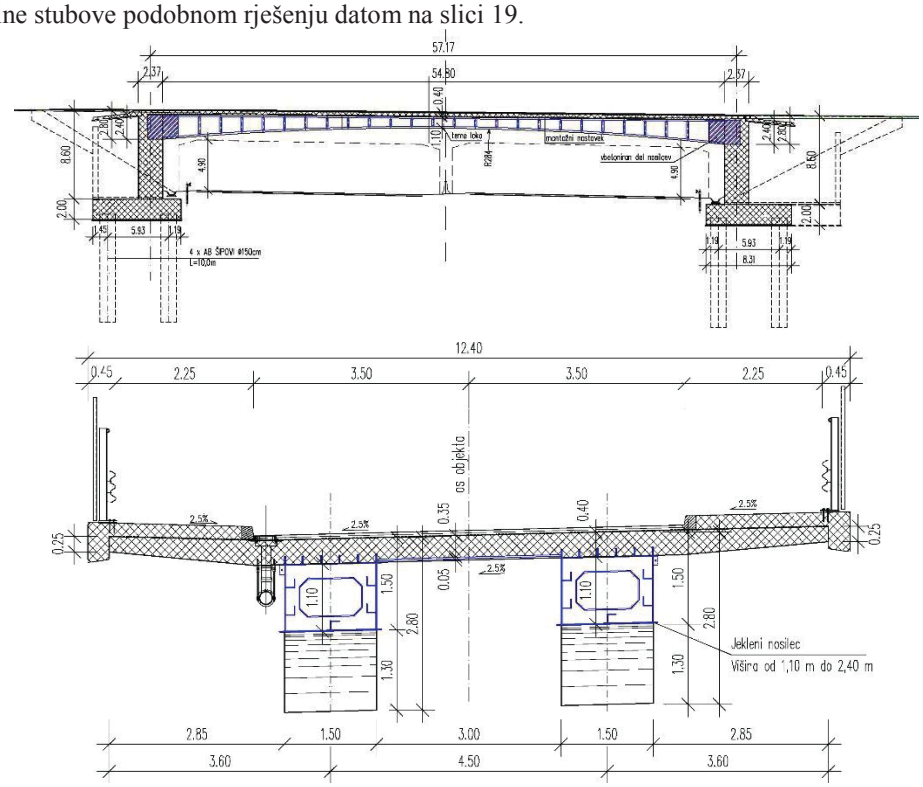

Slika 22: Uzdužni i poprečni presjek integralnog spregnutog nadvoza raspona 57,17 m

5 LUČNI MOSTOVI SA SPREGNUTIM PRESJEKOM LUKOVA ILI NADLUČNE KONSTRUKCIJE

Prije 10 – 15 godina lučni mostovi su se gradili iz betona ili od čelika. Betonski lučni mostovi su imali širok spektar raspona od 50 do rekordnih 390 m na mostu za otok Krk. Čelični lučni mostovi su dostigli najveći raspon od 518 m koji je izgrađen 1976. godine u SAD.

Lučni spregnuti mostovi izgrađeni u Kini (11)

Poslednjih godina u Kini je izgrađeno 14 velikih lučnih mostova raspona od 130 do rekordnih 425 m. Zajednična karakteristika svih ovih mostova je, da imaju presjeke lukova iz čelika i betona kao spregnuti ili obbetonirani presjeci. Čelični dio presjeka služi kao skela (i oplata) za betonski dio presjeka. Oprema za montažu čeličnih dijelova je minimalna i čine je samo zatege. Čelični presjeci lukova su kombinacija jedne ili više cijevi raznih dijametara i debljine zidova koja se po montaži ispunjavaju betonom – sprežu. Ovdje se na najbolji način koristi saznanje, da su za pritisnute spregnute elemente najracionalni kružni presjeci ispunjeni betonom. Za kompletan utisak bila bi interesantna komparativna analiza lukova izgrađenih po ovom konceptu sa spregnutim presjekom i armirano betonskih lukova, kakvi su se gradili u Europi.

Most Wanxian – Yangtze širine 24 m ima rekordan raspon luka 420 m (slika 23).

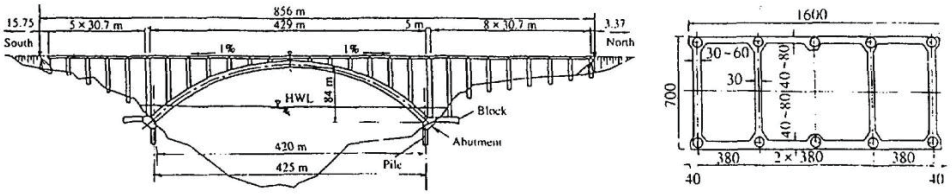

Slika 23: Lučni spregnuti most Wanxian – Yangtze raspona luka 420 m u Kini

Čelični dio presjeka lukova formiran je kao prostorna rešetkasta konstrukcija od 10 čeličnih cijevi na razmaku 6,45 po visini i 4 x 3,8 m po širini (slika 24). Segmenti dužine 15,2 m montiraju se dizalicama sa plovne platforme i pridržavaju kosim zategama. Nakon kompletiranja čelične konstrukcije lukova cijevi se ispunjavaju betonom i kao spregnuti presjek preuzimaju težinu betonskog dijela presjeka.

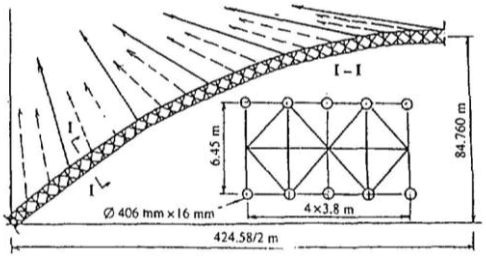

Slika 24: Dio čelične konstrukcije luka

Most Skradin na dijelu autoputa Zadar-Šibenik (14)

Za teške i duboke prirodne prepreke i lučne mostove velikih raspona jedinstven most za oba kolovoza autoputa ukupne širine 21 m (bez zaustavnih traka) je smisleno i racionalno rješenje (slika 25). Nad betonskim lukom sandučastog dvočeličkog presjeka raspona 204 m izgrađena je spregnuta nadlučna konstrukcija sa 12 raspona 4x32+3x28+3x32+28+24=360 m. Konstrukciju čine dva nosača sandučastog presjeka 1200/1700 mm sa konzolama 7,60 m i jakim poprečnim nosačima na razmaku 4,00 m. Sandučasti presjek ima potrebnu torzijsku krutost za konzole naglašenih raspona. Na krajevima konzola su rubni povezujući nosači I presjeka visine 400 mm.

Prednosti spregnute nadlučne konstrucije je manja težina a time i manje opterećenje i dimenzije presjeka luka, jednostavna i brza izgradnja. Komparativna analiza mosta Skradin i mosta Maslenica sličnih raspona lukova pokazuje prednosti rješenja sa spregnutim nadlučnim konstrukcijama.

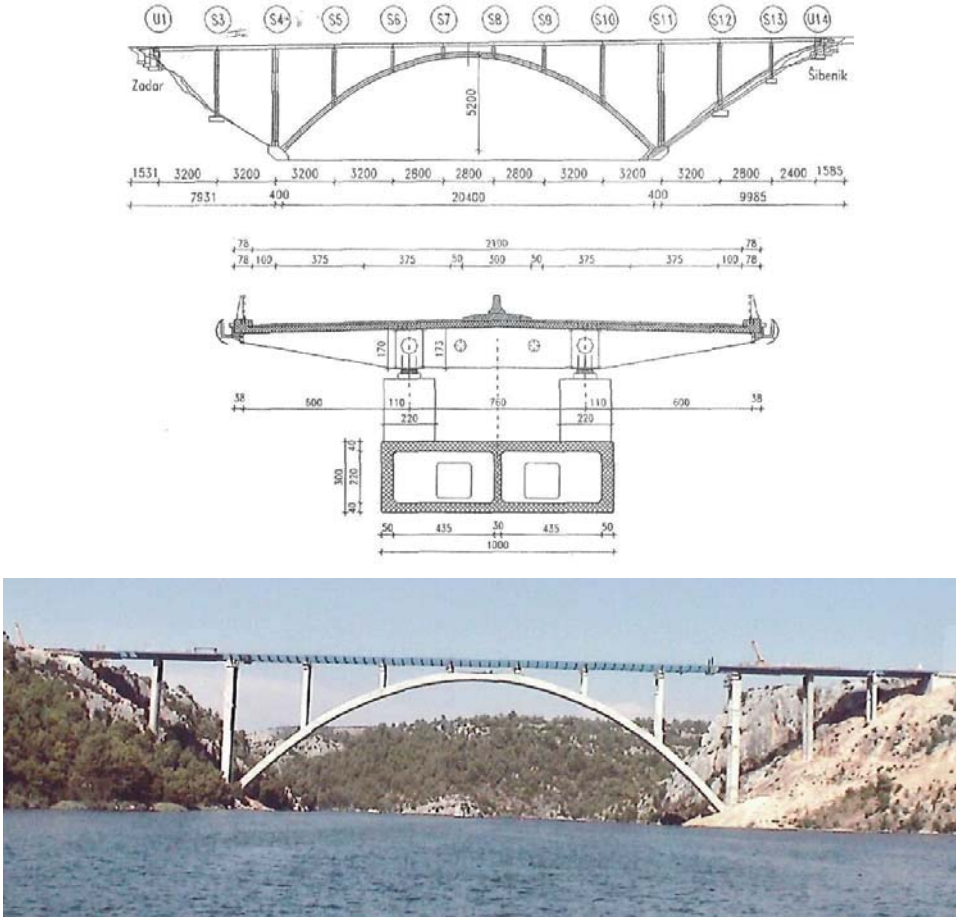

Slika 25: Uzdužni i poprečni presjek i izgled mosta Skradin na autoputu Zadar - Šibenik

Lučni most sa cjelovito spregnutom konstrukcijom

Na slici 26 prikazana je koncepcija putnog lučnog mosta sa cjelovito spregnutom konstrukcijom. Dvozglobni cijevni lukovi raspona 103 m sa presjekom cijevi 1600/20 mm na razmaku 6,0 m spojeni su poprečnim nosačima na mjestima stubova nadlučne konstrukcije. Po montaži cijevi se ispune betonom i kao spregnuti presjek preuzimaju težinu nadlučne konstrukcije i saobraćajnog opterećenja. Stubovi nad lučnom konstrukcijom su dvozglobne cijevi 600/7 mm ispunjene i spregnute sa betonom. Spregnuta nadlučna konstrukcija sa 8 raspona po 17,50 m je uobičajenog presjeka sa dva glavna nosača.

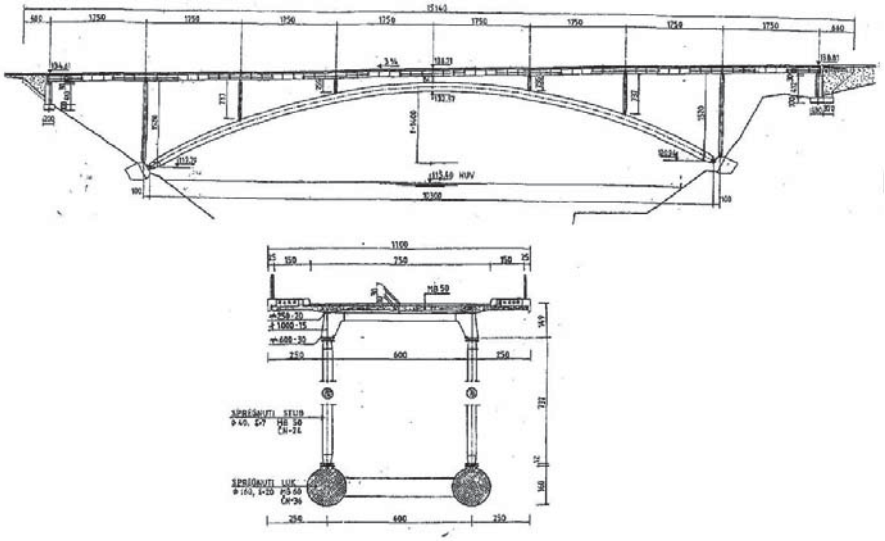

Slika 26: Konstrukcija cjelovito spregnutog lučnom mosta

Lučni most preko jezera Gazivode kod Kosovske Mitrovice

Čelični rešetkasti dvozglobni lukovi raspona 200 m imaju obješenu spregnutu rasponsku konstrukciju. Prednosti spregnute konstrukcije je manja cijena u odnosu na čeličnu ortotropnu konstrukciju a znatno manja težina, a time i potrošnja čelika za lukove u odnosu na betonsku konstrukciju (slika 27).

Slika 27: Izgled lučnog mosta raspona 200 m preko jezera Gazivode

6 SPREGNUTE RASPONSKE KONSTRUKCIJE NA MOSTOVIMA SA KOSIM ZATEGAMA

U intenzivnom razvoju i izgradnji mostova sa kosim zategama, karakteristično za zadnje decenije (zavješeni – zauzdani mostovi) spregnute rasponske konstrukcije su konkurentne za raspone od 200 – 400 m. Za raspone do 200 m konkurentan je beton, a za raspon preko 400 m čelik sa ortotropnom pločom. Prednosti spregnute konstrukcije je manja težina u odnosu na beton, a niža cijena u odnosu na čelik, brza je i relativno jednostavna izgradnja.

Glavni dio mosta preko Dubrovačke rijeke je obješen sa kosim zategama raspona 244+80,7 (slika 28). Ima spregnutu rasponsku konstrukciju sa dva čelična I nosača visine 2 m i AB pločom debljine 25 cm.

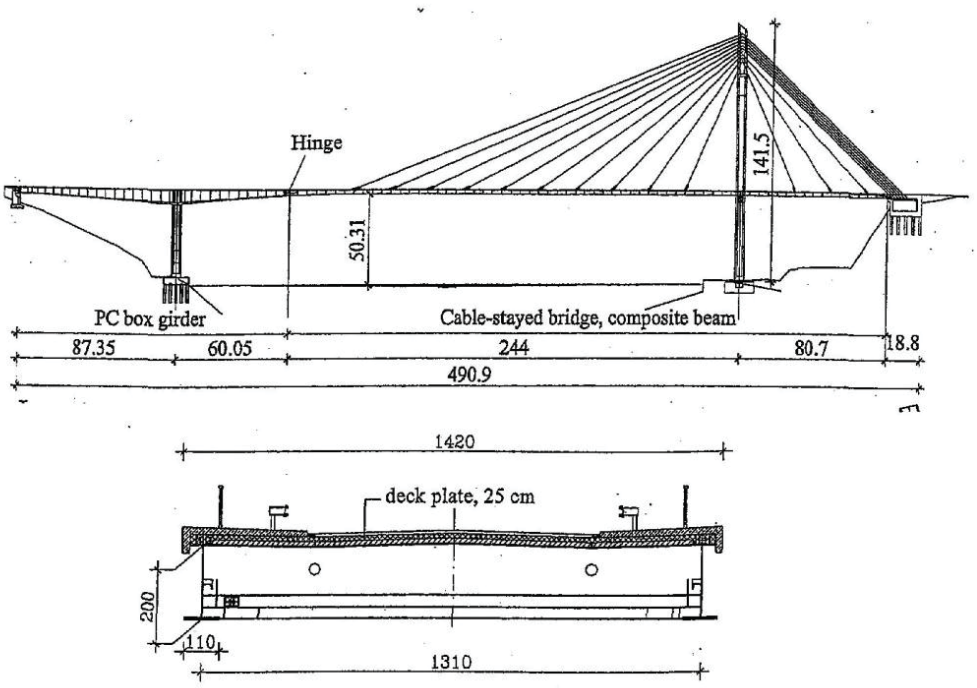

Slika 28: Uzdužni i poprečni presjek mosta sa kosim zategama preko Dubrovačke rijeke

Za most preko Jablaničkog jezera projektovana je i varijanta sa kosim zategama raspona 93+202+93 sa spregnutom rasponskom konstrukcijom (slika 29). Rasponska konstrukcija ima dva čelična zavarena glavna nosača visine 1600 mm na razmaku 8,00 m, jake poprečne nosače na mjestima zavješenja i AB ploču debljine 22 cm spregnutu sa glavnim nosačima. Namjena varijantnog rješenja bila je da se smanji broj stubova koji se temelje na šipovima u dubokoj vodi jezera. I pored smanjenja cijene temeljenja i manjeg broja stubova u dubokoj vodi jezera, varijanta sa kosim zategama bila je skuplja za 15 % radi značajnog udjela cijene zatega i pilona.

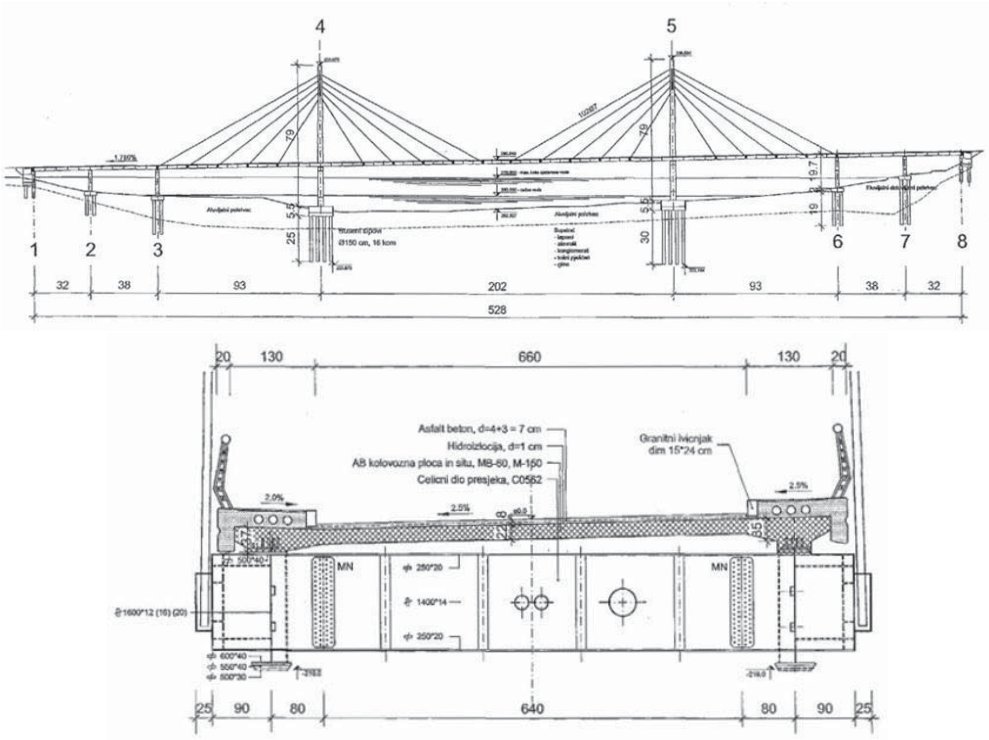

Slika 29: Uzdužni i poprečni presjek mosta sa kosim zategama i spregnutom gredom preko Jablaničkog jezera

Zaključna razmatranja

- Sve dok se inžinjeri u ulozi investitora, projektanata ili graditelja unapred opredeljuju i specijaliziraju za materiale a ne za objekte, beton kao material masovnije upotrebe bit će u prednosti i u mostogradnji. Inžinjer treba da realizuje najpodobniju konstrukciju, a material bira prema osobenosti prepreke i uslovima tržišta.
- Material za betonske konstrukcije ima velike prirodne resurse, a cijena rada je niža. Beton je u prednosti kod manjih i srednjih mostova, posebno kod izgradnje skupine objekata na novim saobraćajnicama.
- Čelik u vidu spregnutog presjeka je u prednosti kod pojedinačnih mostova srednjih raspona, jer omogućuje brzu izgradnju bez učešća veće opreme i rada za gradilišta.
- Za veće mostove samo varijantna, konkurentna rješenja daju pravo na prednost pojedinim materialima ili sistemima.
- Ako neka sredina želi održati konkurentnost materiala, mora brinuti da oba materiala imaju šansu za kontinuitet u poslu i čuvanje stručnih ljudi i referenci.

- Zahvaljujući prednostima koje pružaju spregnute konstrukcije može se s sigurnošću očekivati njihov značaj, razvoj i primjena u budućnosti uz sve oštriju konkurenciju sa AB prednapregnutim mostovima.
- Izgledna mogućnost ekonomskog poboljšanja kod mostova većih raspona sa dvojnim sprezanjem čine spregnute konstrukcije najekonomičnijim i za raspone preko 150m.
- Spregnute konstrukcije sa pločom kao krovom iznad čelične konstrukcije uz pravilnu odvodnju, izolaciju i dobru antikorozivnu zaštitu nemaju oštečenja ni posle 30 godina eksploatacije, pa je to njihova prednost u odnosu na konstrukciju od betona.
- U većem broju evropskih država primjetan je novi zamah u primjeni spregnutih konstrukcija u mostogradnji uz izraženu inovativnost. Bila mi je želja da u ovom radu ukažem na taj zamah kao animirajući podsticaj za konstruktore mostova sa ovih prostora.
- Čelične spregnute konstrukcije se jednostavnije saniraju, obnavljaju i zamjenjuju.
- Izgradnja spregnute konstrukcije manje remeti prirodni ili urbani ambijent.
- I dalje ostaju otvorena stručna pitanja poboljšanja tehnologije betoniranja kolovoznih ploča, prednaprezanja i optimalizacija debljine i oblika vertikalnih limova i pojaseva.

LITERATURA:

[1] N. Hajdin: Različite mogućnosti sprezanja betona i čelika u mostogradnji, Spregnute konstrukcije, specialno izdanje časopisa Izgradnja, Beograd 1972

[2] N. Hajdin:; Einige Beispiele der Kombination von Stahl und Beton im Brückenbau, Schweizer Architekt und Ingenieur 103 (1985)

[3] F. Nather: Stahlbrücken mit Doppelverbund in Deutschland, Bauingenieur 72 (1997) 131-141 Springer-vdi Verlag 1997

[4] F. Nather: Verbundbrücken–Stand der Technik–Perspektive für Zukunft, Stahlbau '90

[5] R. Saul, W. Zellner: Railway Bridge with double Composite Action Across River Main, IABSE Symposium, Leningrad 1991

[6] R. Saul, W. Zellner: Combined Highway-Railway Bridge with Double Composite Action, IABSE Symposium, Leningrad 1991

[7] F. Kržić: Jeklene konstrukcije, Gradbena fakulteta Ljubljana (1997)

[8] M. Pržulj: Spregnute konstrukcije, univerzitetni učbenik, Građevinska knjiga, Beograd, 1989

[9] M. Pržulj: Savremeni oblici sprezanja čelika i betona u mostogradnji, Građevinar br. 41, Zagreb, 1989

[10] M. Pržulj: Composite Steel and concrete structures Applications in Bridges, 7th International Symposium, Ohrid, oktobar 1997

[11] Structural Engineering International 2/97, 3/97, 3/2007, Zürich, IABSE

[12] Brücken und tunnel der Bundesfernstrassen 2004, Deutscher Bundes Verlag

[13] Z. Šavor, G. Hrelja, N. Mujkanović, Design and Construction of Mirna Viaduct, International conference on Bridges, Dubrovnik 2006

[14] Z. Šavor, G. Hrelja, N. Mujkanović, Most preko kanjona reke Krke kod Skradina, Zlatni sabor HDGK 1953-2003, Zagreb 2003

[15] M. Pržulj, Z. Hadžihasanović, M. Kamenica: Projekt mosta preko Jablaničkog jezera, Građevinar br. 58, 02/2006

[16] International symposium Composite Steel and Concrete Structures, Slovenian Metal Processing Association, Ljubljana, september 2004

ДГКС Друштво грађевинских конструктера Србије
ASES Association of Structural Engineers of Serbia
U-5
15. KONGRES
6-8. 9. 2018. Zlatibor

Meri Cvetkovska[1], *Milivoje Milanović*[2], *Cvetanka Chifliganec* [3]

POŽARNA OTPORNOST ARMIRANOBETONSKIH I SPREGNUTIH KONSTRUKCIJA OD ČELIKA I BETONA

Rezime:

Razumevanje ponašanja i odgovora konstrukcija u požaru je od posebnog značaja za projektovanje konstrukcija za dejstvo požara. Evrokodovi tretiraju požar kao incidentno opterećenje konstrukcija, pa konstruktivni elementi moraju biti dimenzionisani da izdrže požar tokom propisanog vremenskog perioda. Mnogi faktori utiču na požarnu otpornost konstrukcija. Ovaj rad je fokusiran na požarnu otpornost i ponašanje različitih armiranobetonskih i spregnutih konstrukcija od čelika i betona i ramovskih konstrukcija. Kroz nekoliko primera biće prikazan i diskutovan uticaj požara na raspodelu temperature unutar konstruktivnih elemenata, uticaj na momente savijanja i deformacije elemenata i na globalno ponašanje cele konstrukcije.

Ključne reči: požar, prenos toplote, statička analiza, AB konstrukcije, spregnute konstrukcije

FIRE RESISTANCE OF REINFORCED CONCRETE AND STEEL-CONCRETE COMPOSITE STRUCTURES

Summary:

Understanding the performance and the response of the structures in fire is of a particular importance for structural fire design. According to Eurocodes, fire is treated as accidental load on structures and structural elements have to be designed to withstand fire during the prescribed period of time. Fire induced temperatures cause reduction of the load-bearing characteristics of the constitutive materials of the structural elements and this effect directly reflects on the reduction of their bearing capacity. Stresses and strains caused by temperature additionally reduce the fire resistance of structures. This research is focused on the fire resistance and the behavior of different types of reinforced concrete and steel-concrete composite elements and frame structures. By several case studies the influence of the fire on temperature distribution within the structural elements, the fire resistance of the whole structure, the bending moments and deformations of elements are presented and discussed.

Key words: fire, heat transfer, stress-strain analysis, RC structures, composite structures

[1]*Prof. PhD, Faculty of Civil Engineering, University "Ss. Cyril and Methodius", Macedonia, cvetkovska@gf.ukim.edu.mk*
[2] *Assist.prof., PhD, State University in Novi Pazar, Department of Civil Engineering, Srbija, milanovicnp@gmail.com*
[3] *Assist. Msc, Faculty of Civil Engineering, UKIM, Macedonia, c.chifliganec@gf.ukim.edu.mk*

1. INTRODUCTION

Nowadays the regulations in many countries require that the structures have to fulfil not only the basic requirements regarding the structures' bearing capacity, stability and serviceability, but also requirements concerning the fire safety of structures, as: the load bearing resistance of the construction can be assumed for a specified time period of fire exposure; the generation and spread of fire and smoke within the works are limited; the spread of fire to neighbouring construction works is limited; the occupants can leave the works or can be rescued by other means; the safety of rescue teams is taken into consideration [1,2,3].

Generally, fire resistance is ability of a structure, a part of a structure or a member to fulfill its required functions (load bearing function and/or fire separating function) for a specified load level, for a specified fire exposure and for a specified period of time [1]. The behavior of a member, as well as of the entire structure, in case of fire depends on many factors, such as: the fire exposure, i.e. the intensity and duration of the fire action, the position of the elements in relation to the fire compartment, i.e. the fire scenario, the structural system and support conditions, the distribution and intensity of the existing loads, the size and shape of the elements, as well as the temperature dependence of the thermal and mechanical characteristics of the constitutive materials.

In Balkan countries, where lack of technical standards and codes in the field of fire safety of buildings exists, raising awareness for necessity of assessing the fire resistance of structures is especially important. Nowadays, in practice, only single structural elements are analyzed by using simplified calculation methods, while worldwide, the global structural response of buildings in fire conditions is accurately determined with proper use of advanced calculation methods.

The nonlinear numerical analyses of different types of structural elements and frame structures are presented in this paper. The analysis are conducted with the computer programs specialized for structural fire analysis: SAFIR [4] and FIRE [4]. The numerical analysis of structure exposed to fire consists of two steps. The first step involves determining the temperature distribution in the cross section of the fire exposed structural members, referred to as 'thermal analysis'. The second step of the analysis, termed as 'stress-strain analysis', determines the response of the structure due to static and thermal loading.

2. THERMAL AND STRESS-STRAIN ANALYSIS

The time dependent temperature field in the cross section of the elements exposed to fire depends on: intensity of the fire and the time of fire exposure; position of the element with respect to the flames; element geometry; conduction coefficients and the specific heats of the materials; the processes of heat transfer by convection and radiation.

While the nonlinear and transient temperature field is determined, the following assumptions are made:

- A fire is modeled by a single valued gas temperature history;
- Temperature dependent material properties are known (recommended in Eurocodes);
- In most cases two dimensional heat transfer is assumed;

- No contact resistance to heat transmission at the interface between two different materials (usually steel and concrete) occurred;
- The easier heat penetration, while cracks appeared, or some parts of the cross section crushed, is neglected.

The stress-strain analysis of structures exposed to fire have to take under consideration the following aspects:

- changes in the mechanical properties of the materials due to temperature changes,
- the degradation of the elements cross-sections due to the occurrence of cracks and crushing of concrete,
- increased effects of creep and shrinkage of materials,
- restrained thermal dilatations in the longitudinal directions and within the cross-sections.

The solution method is nonlinear direct stiffness procedure coupled with time step integration. Within a given time step an iterative approach is used to find a deformed shape resulting in equilibrium between internal stresses and external loadings. The internal stresses are function of: current deformed shape; current temperature distribution; prior response and thermal history.

In each time step on the basis of defined temperature field, the deformed shape of the structure is defined as function of the intensity of the external loads and internal forces. The calculation goes on until the failure of the whole structure happens.

This research is focused on the fire resistance and the behavior of different types of reinforced concrete and steel-concrete composite elements and frame structures. By several case studies the influence of the fire on temperature distribution within the structural elements, the fire resistance of the whole structure, the bending moments and deformations of elements are presented and discussed.

3. CASE STUDY 1: FIRE RESISTANCE OF RC COLUMNS

The columns as structural elements have an important role in preventing loss of global stability of structures under fire. If these elements do not suffer failure, damages shall be of a local character, which shall enable evacuation and efficient extinguishing of the fire.

The fire resistance of centrically loaded RC columns depends on: shape and dimensions of the cross section; concrete cover thickness; type of aggregate; steel ratio, intensity of the axial force, as well as the fire scenario [5], but the dominant effects have the shape and dimensions of the cross section and the intensity of the axial force.

The set of columns with height h=3m, with same cross-sectional area of 900cm^2, same percentage of reinforcement of 1% and different column's side ratios: 30x30cm, 25x36cm, 20x45cm and 60x15cm (RC wall) were analyzed. The columns were exposed to ISO834 standard fire from all sides and all over the height. All columns were fixed at the bottom side and pin-ended on the other side and such support conditions were chosen to enable free expansion in longitudinal direction. As a result of the column's height and the dimensions of the cross sections, small slenderness ratios were achieved. In such case the support conditions had a negligible impact on the fire resistance of the columns and were not varied in this study. Siliceous aggregate concrete was used and the compressive strength at ambient temperature

was f_c(20°C)=30MPa. The yield strength of the reinforcing bars at ambient temperature was taken to be f_y(20°C)=400MPa.

In order to define the influence of the load level on the fire resistance of the columns, the intensity of the axial compressive force was varied. The load coefficient α was defined as ratio between the applied axial force and the ultimate axial force of the column at ambient temperature. The load coefficient α was varied between α=0.1 and α=0.4.

Numerically achieved results for the temperature distribution in the cross sections of two types of columns, from the set of analyzed columns, for two characteristic moments, are presented on Figure 1 and Figure 2.

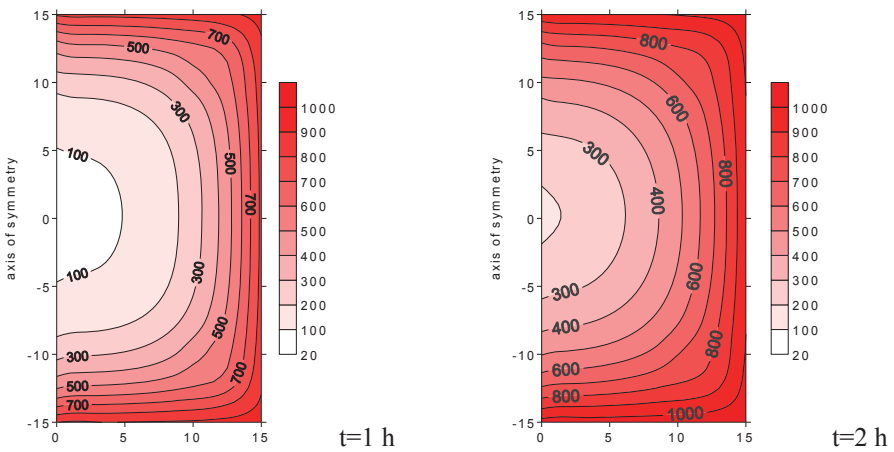

Figure 1- Temperature distribution in the cross section of the column with dimensions 30x30 cm, for two characteristic moments

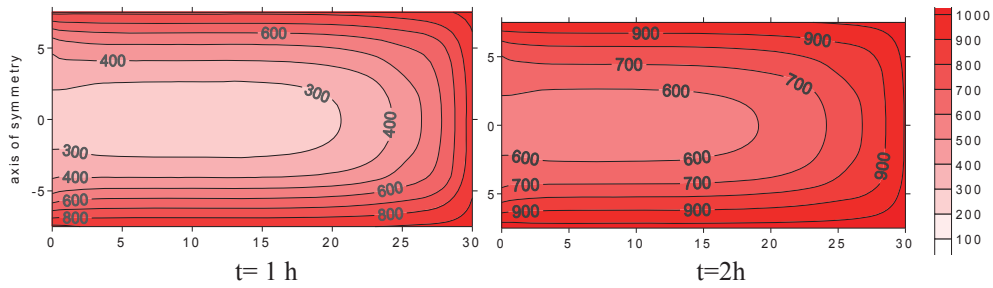

Figure 2- Temperature distribution in the cross section of the column with dimensions 15x60 cm (RC wall), for two characteristic moments

By comparison of the isotherms in the cross sections it could be found out that in case when the ratio between the two sides of the cross section is higher (for example 15x60cm), the temperature penetrates dipper in a shorter time period and the average temperature of the cross section is higher than in case when the ratio is less or equal to one (case of column 30x30cm). This results with higher reduction of material properties and reduction of the bearing capacity of the column. Consequently, the column has lower fire resistance.

As part of the analysis, besides the shape and the dimensions of the cross sections of the fire exposed columns, the intensity of the axial force was varied too. The load coefficient α was involved as ratio between the applied axial force and the ultimate axial force of the column at ambient temperature. The load coefficient α was varied between α=0.1 and α=0.4. This enabled comparison of the fire resistance of the analyzed set of columns with different shapes and sizes, for different load levels.

Numerically achieved results for the stresses in the concrete part of the cross sections of the two types of analyzed columns, for load coefficient α=0.35 and for two characteristic moments, are presented on Figure 3 and Figure 4.

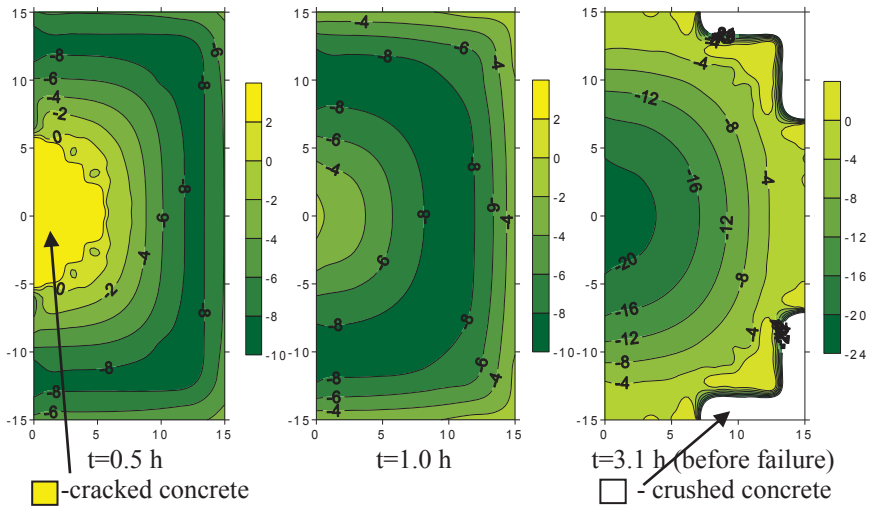

Figure 3- Time redistribution of stresses in the cross section of centrically loaded RC column with dimensions 30x30 cm, exposed to fire from all sides, (load ratio α = 0.25)

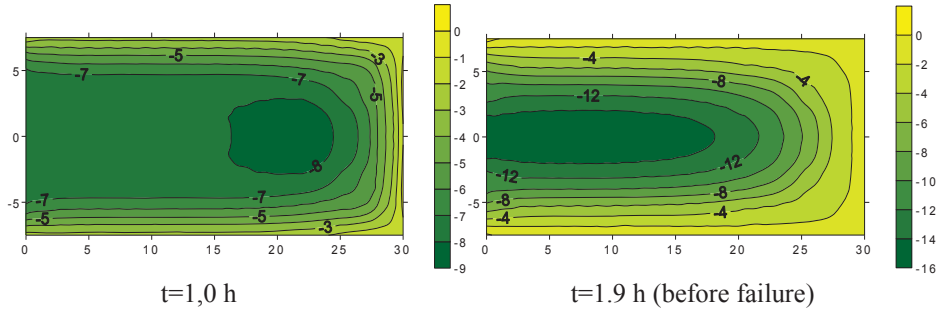

Figure 4 - Time redistribution of stresses in the cross section of centrically loaded RC column with dimensions 15x60 cm (RC wall), exposed to fire from all sides, (α = 0.25)

At first moments of fire expose, because of the high temperature differences between the surface layers and inner layers and because free thermal expansion is not allowed, the concrete core cracks. This effect happens when load coefficient is less than 0.3 and is not so much

expressed when the ratio between the two sids of the cross section is higher. For example, in case of column 15x60cm (Figure 4) this effect doesn't appear for load coefficient higher than 0.2. After a time high temperatures penetrates dipper into the cross section, mechanical properties of steel and concrete are reduced and the effect of the axial force becomes dominant, so cracks are closed.

For the analyzed set of columns, the fire resistance curves as function of the shape of the cross-section and the intensity of the axial compressive force were constructed (Figure 5). These curves indicate that the highest fire resistance achieves the column with lowest ratio between the two sides of the cross section. The reason for that is the lowest average temperature of the column's cross section.

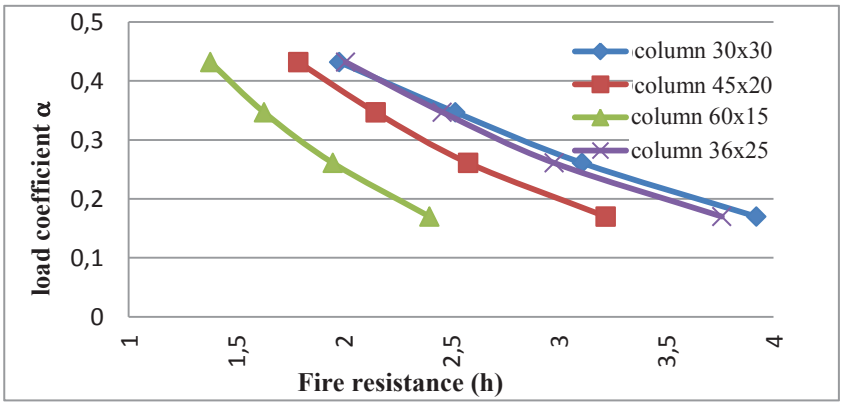

Figure 5 – Fire resistance curves for centrically loaded RC columns exposed to fire from all sides, as function of the shape of the cross section and the load coefficient α

The total axial dilatation of the columns as result of the total thermal elongation and the negative axial dilatation caused by the compressive axial force, for all four RC columns exposed to fire from all four sides and for the load coefficient α=0.35, are presented on Figure 6.

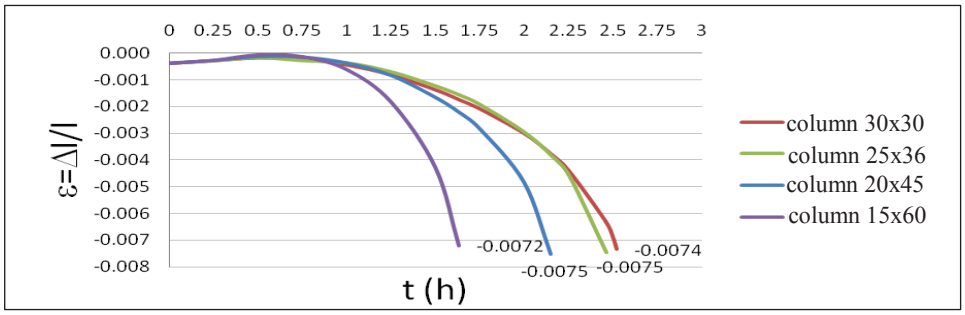

Figure 6 – Axial dilatation of the centrically loaded RC columns exposed to fire from all sides, for load coefficient α=0.35, as function of the shape of the cross section

If we analyze the total axial dilatation of the columns as function of the intensity of the axial force and the time of fire exposure, it can be noticed that for all four shapes of cross sections at the beginning of the heating process the positive dilatations caused by temperature are dominant. The negative dilatations caused by the axial force decrease with tendency to become positive, which is case for load coefficients less than 0.3. After a time the average temperatures of the column's cross sections become higher, the mechanical characteristics of the steel and concrete are reduced, the negative dilatations are dominant again and significantly larger than the positive dilatations caused by temperature. As a result of that, the columns fail in compression. The most sensitive is the cross section with dimensions 15x60 cm (due to a higher average temperature), and the best behavior shows the cross section with dimensions 30x30cm.

4. CASE STUDY 2: FIRE RESISTANCE OF STEEL-CONCRETE COMPOSITE COLUMNS

Due to the thermal mass of concrete, steel-concrete composite columns have higher fire resistance than steel columns and it looks like the composite columns were developed to improve the fire resistance of steel columns. In practice, the most often used composite columns are: fully encased steel sections FES; partially encased steel sections PES and concrete filled tubular sections CFS. The concrete covers the steel section and protects it from intensive heating, i.e. acts like insulation to the steel section. In case of partially encased steel sections, the flanges of the steel section are directly exposed to fire and the effect of concrete as a "heat shield" is less. In case of concrete filled tubular sections the steel section is direct exposed to high temperatures while the concrete core remains cold and behaves as 'heat sink'. In such case stresses are redistributed to the relatively cool concrete core and the fire resistance is much higher than in case of steel columns without concrete core.

The load-bearing capacity of the column cross section can be determined from the interaction curve "bending moment-axial force". At elevated temperatures the stress-strain characteristics of concrete and steel become non-linear and deteriorate rapidly [3]. This effect directly reflects on the reduction of the axial force and the bending moment that could be accepted by the column cross section, respectively the interaction curve of the column cross section is reduced.

Four different types of columns were analyzed in this paper [6,7], three of which were steel concrete composite columns with different cross sections (fully encased steel sections FES, partially encased steel sections PES and concrete filled tubular sections CFS), while the fourth one was a reinforced concrete column which had been taken for comparison, so as to draw the necessary conclusions for the advantage of the steel concrete composite columns over the reinforced concrete columns of the same size and the same initial loads.

The criterion for dimensioning the columns was the design value of the plastic resistance to axial compression and for all four cross sections the value is close to 5500 KN. From the aspect of the heat transfer and the temperature distribution in the cross section of the columns, the dimensions of the three types of composite sections are almost the same, and only the RC cross section has bigger dimensions.

The “bending moment-axial force" interaction curves for all four types of columns were constructed as function of the time period of standard fire exposure ISO 834 and conclusions about the fire resistance of the columns were drawn. For this purpose the computer program SAFIR [10] was used. Thermal and mechanical properties of steel, concrete and reinforcement were adopted according to the recommendations given in Eurocode 4, part 1-2 [3].

The cross sections of all four composite columns are presented in Figure 7. Cross section temperature fields and average temperatures are presented in Figure 8.

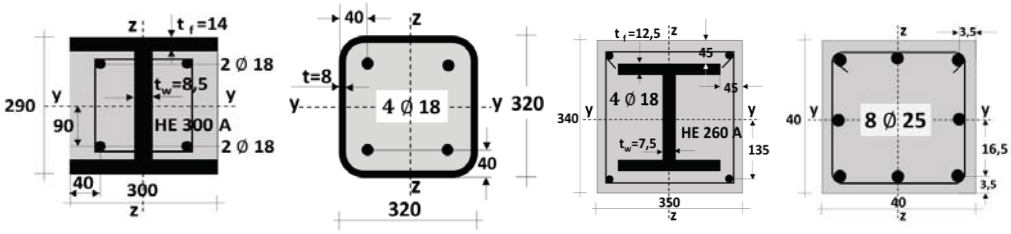

Figure 7 - Cross section geometry of the columns: PES – partially encased steel profile; CFS – concrete field hollow section; TES – totally encased steel section and RC section

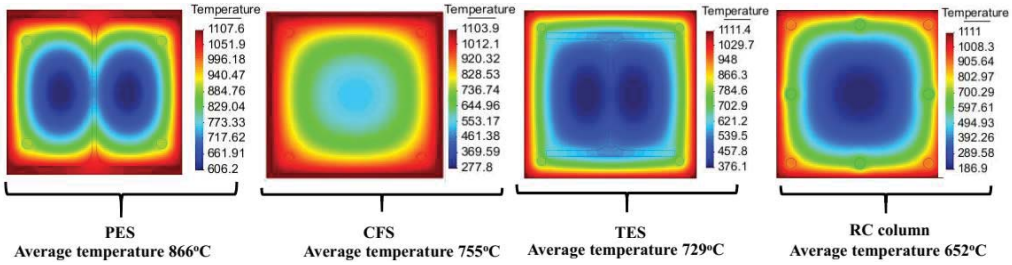

Figure 8 – Temperature distribution and average temperatures of the cross sections: PES, CFS, TES and RC column, at moment t=180 min

The “bending moment-axial force" interaction curves for all four types of columns were constructed as function of the time period of standard fire exposure according to the simplified procedure recommended in EN 1994-1-2. In Figure 9 temperature dependent interaction curves only for the strong axis are presented. In case of fire, highest fire resistance has the totally encased section while the partly encased section and the concrete filled hollow section have lower fire resistance. The steel profiles significantly increase the initial bearing capacity of the partly encased sections and the concrete filled hollow sections, but, because of the peripheral position of the steel it is heated to high temperatures in relatively short time period and the reduction of the mechanical properties of steel is caused, which results in lower fire resistance. The steel profile of the totally encased section is in the interior of the section and it is protected by the concrete that has a low thermal conductivity, which provides the steel to stay cold for a longer period of time and keep its mechanical properties which provides higher fire resistance. Additional disadvantage of the partly encased section is the proportional participation of the steel section which is higher than the one in the concrete hollow section; therefore, the partly encased section has higher ultimate strength for service conditions.

The changes in average temperatures of the cross sections are crucial for the analysis. For a defined heating period, the design values of the plastic resistances of the composite sections to compressive normal force $N_{pl,Rd,T}$ are presented as a percentage of the design values of the plastic resistances to compressive normal force $N_{pl,Rd,20^{o}C}$ at room temperature, Figure 10.

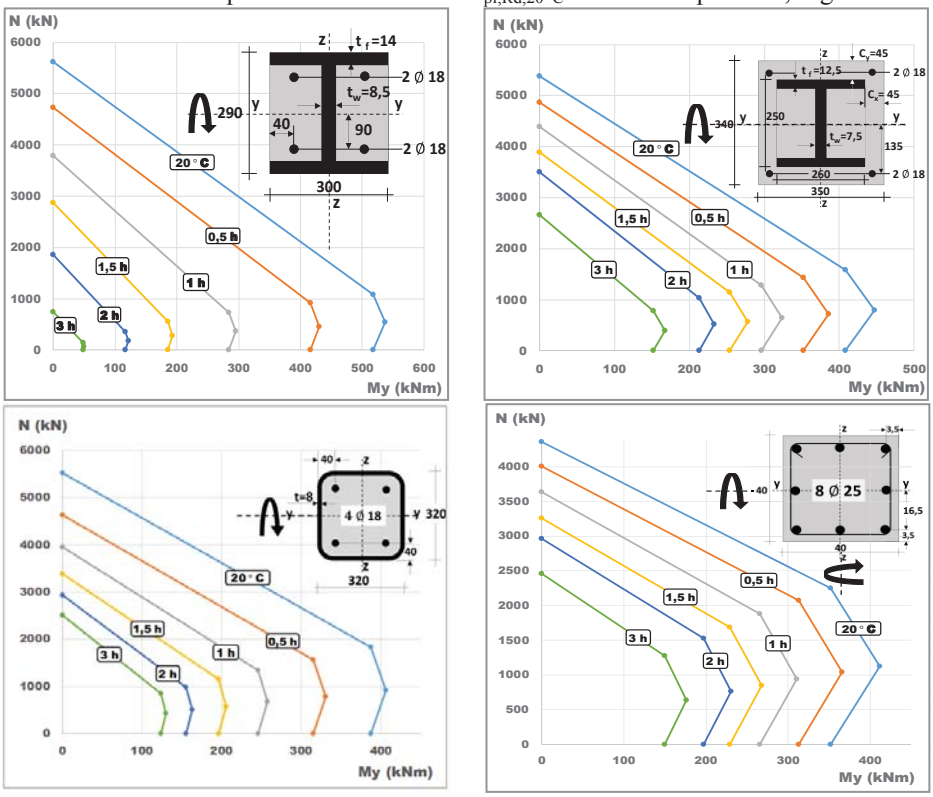

Figure 9 – M-N Interaction curves of composite cross sections, for bending moments about the strong axis, at different moments of fire exposure

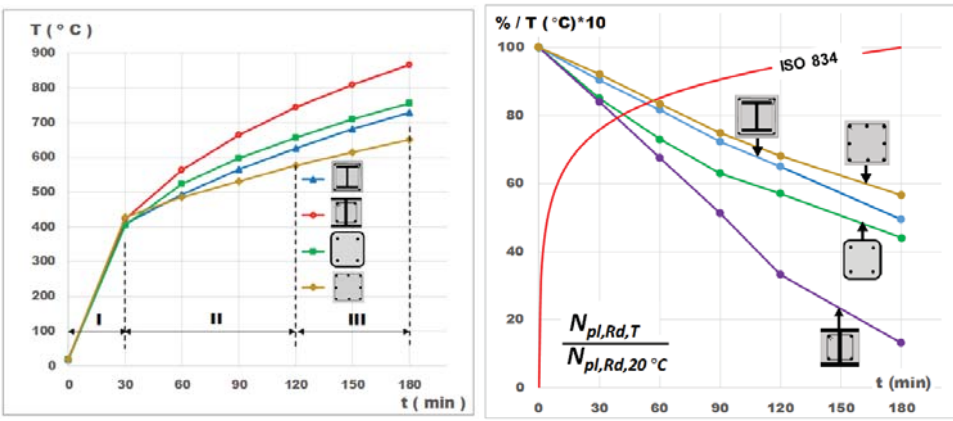

Figure 10 – Average temperature and axial force bearing capacity of the columns for different moments of fire action

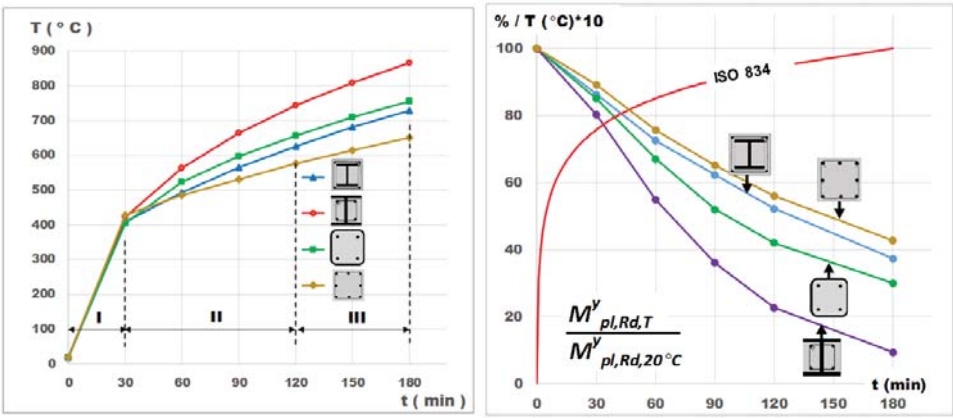

Figure 11 – Average temperature and bending moment bearing capacity about the strong axis for different moments of fire action

The diagrams in Figure 11 present the design values of the plastic resistance moments, about the strong axis of the different types of composite cross sections, $M_{pl,Rd,T}$ as a percentage of the design values of the plastic resistance moments $M_{pl,Rd,\,20oC}$ at room temperature.

The rise of temperature in the composite column cross sections, as a result of fire action, decreases the bearing capacity of the cross sections for axial compression force and biaxial bending. The drop in the bearing capacity depends on the type of the cross section, the heating time, fire scenario etc.

The biggest loss of the M – N bearing capacity is in the cross sections where the steel profile (element) is directly exposed to heating, as for PES-partially encased sections. In sections, where the steel element (profile) is protected with a concrete lining (TES section) there is a minimal drop in the M–N bearing capacity. Concrete, which is characterized by low

thermal conductivity, prevents rapid penetration of the temperature into the steel element and the reinforcement and provides better behavior of the column. From the same reason the reinforced concrete column has highest fire resistance and lowest reduction of the bearing capacity.

The average temperature diagrams for the analyzed types of composite column cross sections, given in Figure 10a, show very clearly the penetration of the temperature into the cross section for specific heating intervals. The shape of the curves is very similar to the diagrams presenting the loss of bearing capacity of the cross sections for axial compressive force (Figure 10b) and the loss of bearing capacity on the bending moments (Figure 11).

5. CASE STUDY 3: FIRE RESISTANCE OF RC FRAME STRUCTURE

This research was focused on the fire resistance and the behavior of fire exposed reinforced concrete frame structure [8]. In general, fire location is hard to be predicted and therefore the determination of the worst fire scenario, which has to be considered in the structural fire design, is very challenging. Different fire scenarios mean different locations of the fire, aiming to create worst but still realistic fire conditions. For this research the fire compartment was assumed to be one or two spans of same floor, or the whole floor.

For the purpose of this research twelve different fire scenarios were considered and the heating regime was defined with the standard temperature-time curve ISO-834. All fire scenarios were analyzed for two different load ratios ($q/q_u \approx 0.6$ and $q/q_u \approx 0.8$). The internal forces, displacements and failure modes were defined and comparison of results was made.

The three-bay three-storey RC frame, analyzed in this paper, is shown in Figure 12. The structure is made of concrete with siliceous aggregate, with a compressive strength f_c=30 MPa and reinforcing bars with a yield strength f_y=400 MPa. The RC structure is designed for load combination that includes seismic action, according to the national standards. The cross sections of all beams are 0.35x0.45 m^2 and the column sections are 0.40x0.40 m^2. The concrete cover thickness of all cross-sections is a=2 cm. Uniformly distributed load of 50 kN/m (for $q/q_u \approx 0.6$) and 67 kN/m (for $q/q_u \approx 0.8$), including self weight, is applied. Geometry, support conditions, reinforcement details and numeration of: bays, beams, columns and joints, are shown in Fig. 12.

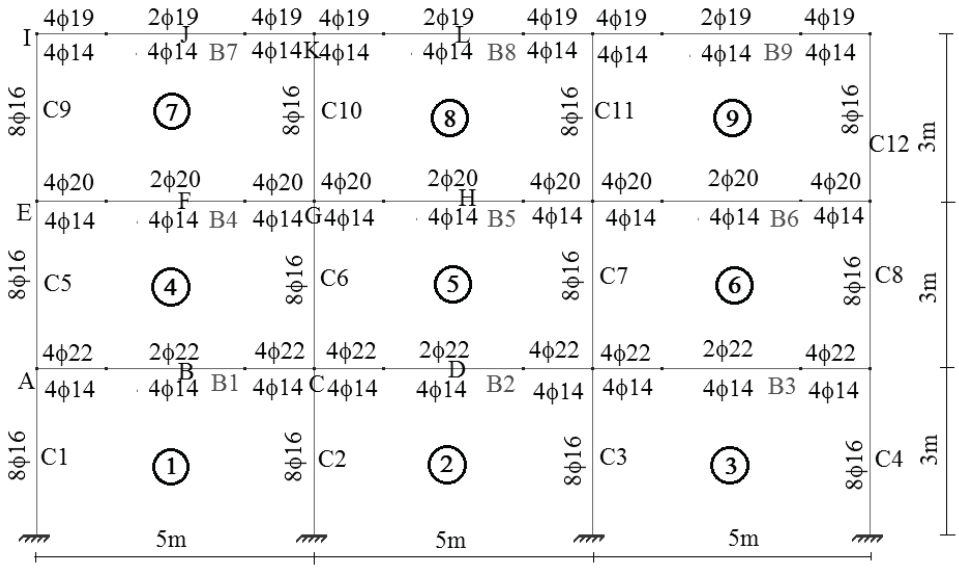

Figure 12 - Frame geometry, support conditions, reinforcement, numeration of: beams, columns, joints and bays

The material models for concrete and steel are the constitutive models given in Eurocode 1992-1-2 and Eurocode 1993-1-2, respectively. The 2D numerical analyses were conducted for temperature raise according to Standard fire curve ISO-834. Top compartment beams were assumed to be fire exposed on three sides (bottom, left and right side) and the bottom compartment beams were assumed to be fire exposed only on the top side. Outer compartment columns were heated only on one side and middle compartment columns were heated on two sides.

The fire resistance for each analyzed fire scenario was calculated for two different load ratios and the results are presented in Table 1. In programme SAFIR there is no deflection criterion for defining the failure point, therefore the calculation goes on until the failure of the whole structure happens.

Table 1- Fire scenarios and corresponding fire resistances of the frame

Fire scenario	Spans involved in fire scenario	Fire resistance for q/q_u=0.6	Fire resistance for q/q_u=0.8
I	1, 2, 3	215.97 min = 3.60 hours	138.43 min = 2.31 hours
II	4, 5, 6	178.01 min = 2.97 hours	116.4 min = 1.93 hours
III	7, 8, 9	126.92 min = 2.12 hours	75.21 min = 1.25 hours
IV	1, 2	215.92 min = 3.6 hours	138.45 min = 2.31 hours
V	1	215.68 min = 3.59 hours	137.23 min = 2.29 hours

Continuation of Table 1- Fire scenarios and corresponding fire resistances of the frame

VI	2	No failure before 5 hours	200.08 min = 3.33 hours
VII	4, 5	177.27 min = 2.95 hours	116.22 min = 1.94 hours
VIII	4	179.29 min = 2.99 hours	116.97 min = 1.95 hours
IX	5	249.24 min = 4.15 hours	151.20 min = 2.52 hours
X	7, 8	127.84 min = 2.13 hours	75.97 min = 1.27 hours
XI	7	125.87 min = 2.10 hour	75.10 min = 1.25 hours
XII	8	149.49 min = 2.49 hours	92.86 min = 1.55 hours

As expected, the frame with higher value for the load ratio reaches lower fire resistance. The higher the position of the fire compartment is the lower the fire resistance of the frame is. All fire scenarios involving some or all spans of the top floor result with lower fire resistance in comparison to the corresponding fire scenario at the lower storeys.

There is a negligible difference in the fire resistance of the frame in the case of a whole floor fire compartment and when the fire compartment involves only the outer span or both, the outer and the central span of the same floor. Exception to this conclusion is the case when the fire compartment comprises only the middle span of the floor. The fire resistance in this case is significantly higher than in case of other possible fire scenarios for the same floor, for reasons being explained in the sections below.

During the first minutes of the fire action, large thermal expansions of the fire exposed beams occur. Depending on the fire scenario these thermal elongations are more or less restrained by the adjacent bays.

In the top beams of the fire compartment, in the heated parts of the cross-sections, these restraints result in high compressive forces that act as prestressing forces. The compressive axial force reduces the positive mid-span bending moment and delays the moment when yielding of reinforcement will occur, so it has a positive effect on the fire resistance of the frame [8]. When fire occurs only in the outer span of a floor, free outward expansion is allowed and the induced axial force is smaller and has a bit smaller effect. After the initial rapid increase of the compressive axial force, later in the ongoing fire process, the top beams experience reduction of compression due to heat penetration deeper in the cross sections, thus resulting in lower temperature differences but higher thermal elongations in comparison to the bottom beams (beams B7 and B8 in fire scenario X – Fig. 13). Exceptions are the top beams in the cases when the fire compartments comprise only the middle span of a floor. In such cases the compression force increases in time (example, beam B8 in fire scenario XII - Fig. 13). This is the main reason why in the cases of fire scenarios with fire in the middle span of the floor only (fire scenarios VI, IX and XII) the fire resistances are much higher compared to the cases when the fire is located in the outer span or spread through the whole floor. In all possible fire scenarios of a particular floor there are no significant differences in the evolution of the axial forces in the fire exposed top beams (either outer span or middle span beams).

In the bottom beams of the fire compartments, the initial tensile forces, developed as a result of the mechanical loading, fast convert into compressive axial forces. Because these

beams are only heated from the top side and the main part of the cross-section is cold, small thermal elongations occur. Later in the ongoing fire process, the bigger the restraints of the cold and stiff adjacent frame elements are, the bigger the induced compressive axial forces are i.e. for the bottom beams of the fire compartments there is a difference in the evolution of axial forces in the outer and the middle span beams (beams B4 and B5 in fire scenario X - Fig. 13).

All columns experience minor changes of axial forces due to the fire exposure.

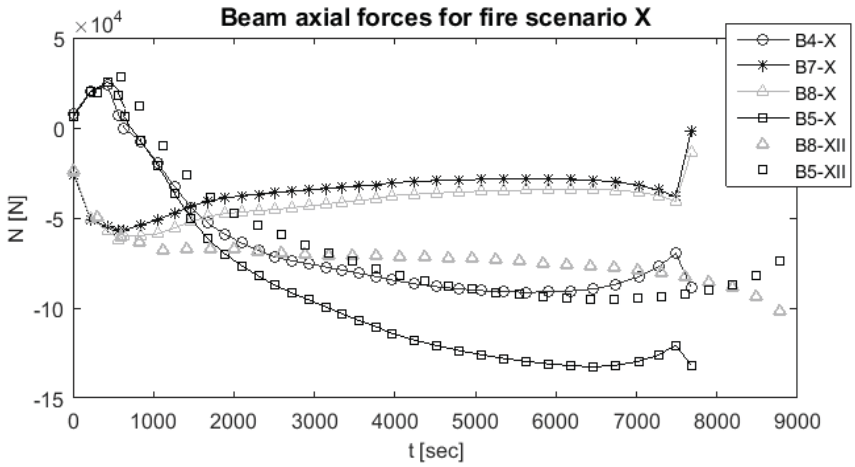

Figure 13 - Time dependent axial forces in beams in fire scenario X and XII

All top beams of a fire compartment (fire exposed on the bottom and on both sides) tend to lift up during the first minutes of the fire exposure because of the high temperature differences in the cross-sections and the pressure in the lower heated parts of the beam cross sections. The negative bending moments at the ends of these beams decrease and the positive mid-span bending moments tend to become negative i.e. redistribution of moments occurs [8]. The time when major redistribution occurs depends on the fire scenario and the dimensions of the cross sections. Later, the temperature penetrates deeper in the cross sections, the temperature differences between the bottom and the top sides become smaller and the bending moment diagrams tend to return to the shape as for the moment t=0 sec, but never reach the initial shapes (Figure 14).

The lateral displacements at the top levels of the fire compartments and the deflections of characteristic beams at the moment of failure, for some of the analysed fire scenarios, are presented in Table 2.

a) b)

Figure 14 - Bending moment diagrams for different time of the fire analysis, in fire scenario III a) t=24 sec b) t=126.92 min

As expected, the comparison of the lateral displacements at the top levels of the fire compartments in fire scenarios I, II and III, which represent whole floor fire compartments, lead to conclusion that the higher the floor is the bigger the lateral displacements are. When the fire compartment involves the outer and the middle span, the lateral displacement has its largest value and almost always the outer beam deflection has its smallest value. When the fire compartment involves the outer span only, the lateral displacement has its smallest value and almost always the outer beam deflection has its highest value. Where the fire compartment comprises only the middle span of a particular floor, the lateral displacements at the level of the top beams are smallest because of the cold and stiff outer spans of the frame.

Table 2 - Deformations and displacements in characteristic joints of the frame

Fire scenario	Deformation at the moment of failure	Horizontal displacement of joints	Vertical displacement of joints
I	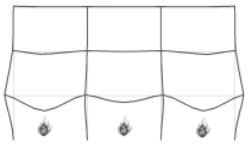	Δx_A=-5.98 cm	Δy_B = -10.37 cm Δy_D = -4.65 cm
II	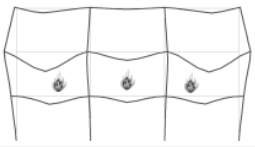	Δx_E= -8 cm	Δy_F = -13.04 cm Δy_B = -5.47 cm Δy_H = -5.45 cm Δy_D = -4.09 cm
III	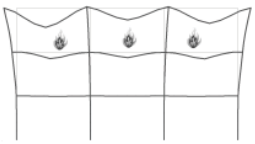	Δx_I= -8.58 cm	Δy_J = -13.01 cm Δy_F = -4.41 cm Δy_L = -7.85 cm Δy_H = -3.82 cm

Continuation of Table 2 - Deformations and displacements in characteristic joints of the frame

IV	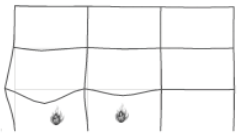	Δx_A= -6.72 cm	Δy_B = -10.15 cm Δy_D = -4.39 cm
V	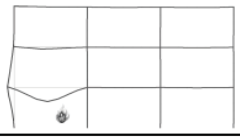	Δx_A=-4.44 cm	Δy_B=-10.62 cm
X	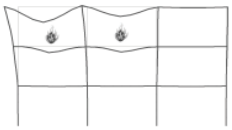	Δx_I=-9.86 cm	Δy_J=-11.51 cm Δy_F=-4.61 cm Δy_L=-7.11 cm Δy_H=-4.09 cm
XI	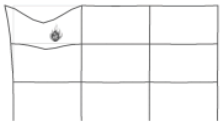	Δx_I=-6.20 cm	Δy_J=-13.60 cm Δy_F=-4.31 cm
XII	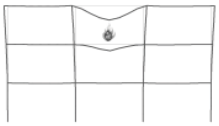	Δx_I=-2.5 cm	Δy_L=-11.13 cm Δy_H=-4.89 cm

6. CASE STUDY 4: FIRE RESISTANCE OF STEEL-CONCRETE COMPOSITE FRAME STRUCTURES

Two frames with different support conditions (horizontally restrained and non-restrained) with three types of beam cross-sections are analyzed in this case study: steel profile coupled with RC slab, partially encased steel section coupled with RC slab and, in practice the most common case, previous two types of beams with ceiling construction made of 30 mm thick plasterboard.

The analyzed two storey two span frame structures are shown in Figures 15 [9]. The fire scenario involves the both spans of the ground floor. The different types of cross sections of the steel-concrete composite beams are given in Figures 16 and 17.

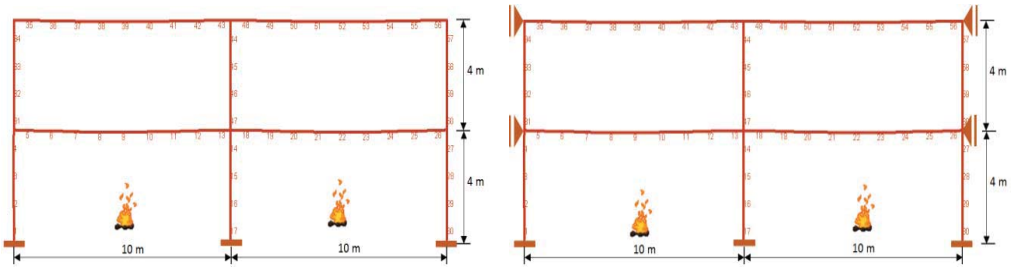

Figure 15 – Geometry and fire scenario for the horizontally non-restrained and restrained frame structure

The cross sections in the middle of the span are presented in Figures 16b and 16d and at the supports in Figures 16a and 16c. All columns are with same cross section - partially encased profile HE 360 A, without additional reinforcement. The ceiling construction (in Figure 17) consists of a plasterboard with a thickness of 30 mm. The frames are exposed to ISO 834 standard fire. The material characteristics are according to EC3 and EC4.

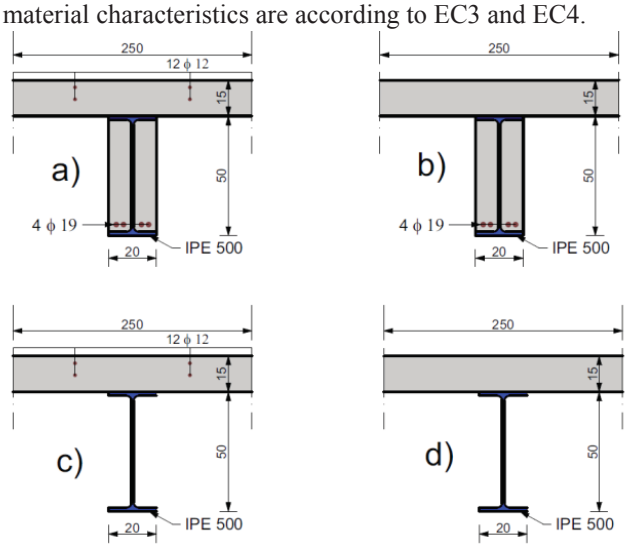

Figure 16 - Beam cross sections: partially encased steel profile and free steel profile

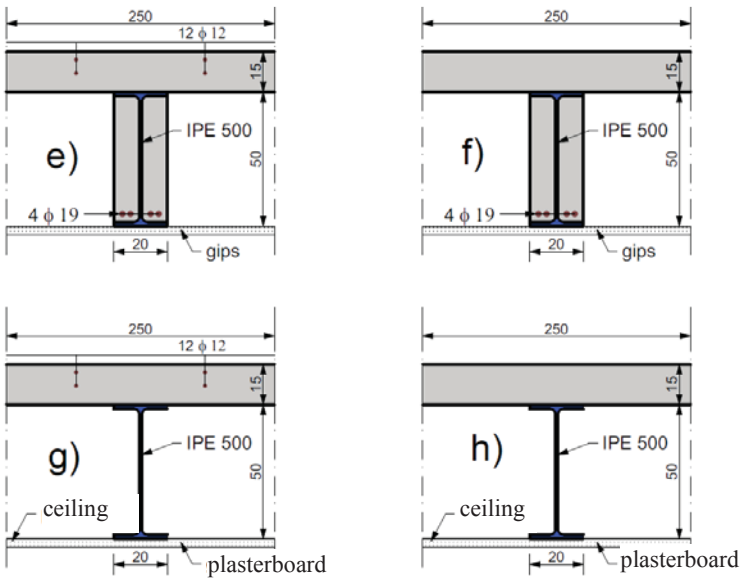

Figure 17 - Beam cross sections: partially encased steel profile and free steel profile with ceiling construction

Frames with the following types of cross-sections were considered:

- unprotected steel profile in a horizontally unrestrained frame - 1
- partially encased steel section PES in a horizontally unrestrained frame-2
- steel profile with plasterboard ceiling in a horizontally unrestrained frame -3
- PES with plasterboard ceiling in horizontally unrestrained frame - 4
- steel profile with plasterboard ceiling in a horizontally restrained frame - 5
- PES with plasterboard ceiling in a horizontally restrained frame - 6

The loss of load bearing capacity of the elements or exceeding the deflection criterion were adopted as basic criterion for failure of the element or the frame structure as a whole. The max. deflection in case of fire was limited to L / 30.

Deflections of certain types of fire exposed composite beams above the ground floor are presented in Figure 18a. Only the beam with an unprotected steel profile (type-1) reaches the limit deflection. All other types of beam cross-sections failed due to loss of bearing capacity without reaching the limit value of the deflection. Beam type-2, partially encased steel section, as a result of concrete participation, has a significantly higher bearing capacity and less deformation than beam type-1. All other types of beams (with ceiling construction made of plasterboard as insulation) even after two hours of heating do not collapsed.

Time dependent axial forces in beams with different cross-sections are presented in Figure 18b. In the horizontally restrained frame significant growth of the axial force is noticed and higher fire resistance is achieved.

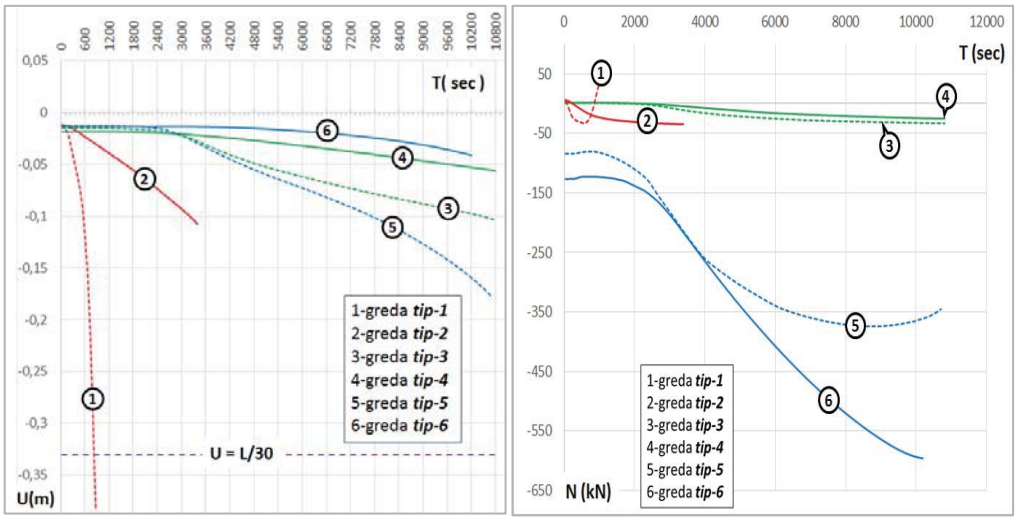

a) b)

Figure 18- Deflections at the middle of the spans and axial forces in beams with different types of cross sections

7. CONCLUSIONS

In the past, the design of structures was made with respect to the: dead loads, imposed loads, wind, snow and in seismic regions the seismic action. Fire as an action on structures was not considered. Nowadays, fire as an incidental action on structures is increasingly explored. As a consequence of many fire incidents, where parts or whole buildings collapsed, the engineers started to change the logic. Treating fire only through architectural and urban design recommendations and fire protecting elements with isolation materials was not enough. There was a necessity for understanding the behavior of: construction materials, structural elements, assemblies and whole structures, under fire exposure. Nowadays, there are many advanced computer programs, based on the finite element method, that successfully incorporate the lows of thermodynamics, fluid mechanics, statics etc. Parallel to the development of these programs, in order to verify its accuracy, many experimental studies were conducted. There were fire experiments on single element types and on whole structures, especially made for the experimental purposes.

In Balkan countries, where lack of technical standards and codes in the field of fire safety of buildings exists, raising awareness for necessity of assessing the fire resistance of structures is especially important.

REFERENCES

[1] EN 1991-1-2: Eurocode 1: Actions on structures - Part 1-2: General actions - Actions on structures exposed to fire, 2002.

[2] EN 1992-1-2: Eurocode 2: Design of concrete structures - Part 1-2: General rules. Structural fire design, 2004.

[3] EN 1994-1-2: Eurocode 4: Design of composite steel and concrete structures – Part 1-2: General rules. Structural fire design, 2005.

[4] SAFIR-Computer program, University of Liege, Belgium, 2014.

[5] Cvetkovska M. (2002). Nonlinear stress strain behavior of RC elements and RC frames exposed to fire. PhD. Thesis, Ss. Cyril and Methodius – Skopje, R. Macedonia.

[6] M.Milanović, M. Cvetkovska , P. Knežević. Load-bearing capacity of fire exposed composite columns. Journal Građevinar (67) 12/2015

[7] M. Milanovic, M.Cvetkovska. Interaction diagrams axial force-bending moment for fire exposed steel-concrete composite sections, Applications of Structural Fire Engineering, pp. , 2017.

[8] Meri Cvetkovska, Milos Knezevic, Qiang Xu, Cvetanka Chifliganec, Marijana Lazarevska, Ana Trombeva Gavriloska, Fire scenario influence on fire resistance of reinforced concrete frame structure, Procedia Engineering-ELSEVIER, Vol. 211, 2018, pp 28-35

[9] Milivoje Milanović, Meri Cvetkovska, Cvetanka Chifliganec, Petar Knežević. Fire reistance of steel- concrete composite frames as function of types of cross sections. 12th International scientific and professional conference on contemporary theory and practice in construction, pp.91-98, Banja Luka 2016

ДГКС ASES

S43 – S96

PROCEEDINGS OF INTERNATIONAL CONGRESS

ДГКС Друштво грађевинских конструктера Србије
ASES Association of Structural Engineers of Serbia
S-43
15. KONGRES
6-8. 9. 2018. Zlatibor

Bratislav Stipanić[1]

FAKTORI OD ZNAČAJA ZA TRAJNOST MOSTOVA

Rezime:

U radu su razmatrani faktori od značaja za trajnost mostova koji treba treba da se respektuju prilikom projektovanja, izgradnje i održavanja u cilju realizacije predviđene eksploatacije mosta tokom njegovog predviđenog veka trajanja. Prikazano je sledećih deset faktora od značaja za trajnost mostova: saobraćaj na mostu, lokacija mosta, materijal konstrukcije mosta, konstrukcijski tip mosta, konstrukcijski detalji, kolovoz na mostu, oprema na mostu, fundiranje mosta, incidentna - izuzetna dejstva i održavanje mosta. Posebno su razmatrani oni sadržaji koji se odnose na trajnost mostova kod sledećih konstrukcijskih Evrokodova: Osnove proračuna konstrukcija (EN1990), Projektovanje betonskih konstrukcija (EN 1992) i Projektovanje čeličnih konstrukcija (EN 1993).

Ključne reči: mostovi, trajnost, betonski mostovi, čelični mostovi, održavanje mostova

FACTORS OF IMPORTANCE FOR DURABILITY OF BRIDGES

Summary:

The paper treates the relevant factors for durability of bridges that should be respected in design, construction and maintenance in order to realize an appropriate bridge service use during its foreseen working life. Ten relevant factors that affect the durability of bridges are listed as follows: traffic on the bridge, location of the bridge, construction material, structural type of the bridge, structural detailing, carriageway, equipment, foundation, accidental actions and bridge maintenance. The contents related to bridge durability are particularly considered, as cited in the following structural Eurocodes: Basis of structural design (EN 1990), Design of concrete structures (EN 1992) and Design of steel structures (EN 1993).

Key words: bridges, durability, concrete bridges, steel bridges, bridge maintenance

[1] *dr Bratislav Stipanić, e-mail: stipanic.bratislav@gmail.com*

1. DURABILITY OF BRIDGES AND DESIGN

1.1. INTRODUCTION

During all stages of design (design solution proposal, concept design, preliminary design, and final design) special attention should be payed to bridge durability. The factors of importance for bridge durability should be taken into account in bridge design.

The set of European norms EN titled Structural Eurocodes treats the design of bridges, with respect to bridge durability, mostly in the following documents:

EN 1990 Eurocode: Basis of structural design

EN 1991 Eurocode 1: Action on structures, Part 2: Traffic loads on bridges

EN 1992 Eurocode 2: Design of concrete structures, Part 1-1: General rules and rules for buildings, Part 2: Concrete bridges

EN 1993 Eurocode 3: Design of steel structures, Part 1-1: General rules and rules for buildings, Part 2: Steel bridges

EN 1994 Eurocode 4: Design of composite steel and concrete structures, Part 1-1: General rules and rules for buildings, Part 2: General rules and rules for bridges

EN 1997 Eurocode 7: Geotechnical design

EN 1998 Eurocode 8: Design of structures for earthquake resistance, Part 2: Bridges.

The Eurocodes serve as reference documents to the following purposes:

- as a means to prove compliance od building and civil engineering works with the essential requirements for the safety, serviceability and durability;
- as a basis for specifying contracts for construction works related engineering services;
- as a framework for drawing up harmonised technical specifications for construction products (ENs and ETAs).

1.2. BASIS OF STRUCTURAL DESIGN

EN 1990, as basis of structural design, establishes principles and requirements for the safety, serviceability & durability of structures, describes the basis for their design & verification and gives the guidelines for related aspects of structural reliability.

EN 1990 is applicable not only for new structures, but as well it is applicable for the structural appraisal of existing construction, in developing the design of repairs and alterations or in assessimng changes of use.

The General assumptions defined in EN 1990 (Basis of structural design) are the following:

- the choice of the structural system and the design of structure is made by appropriately qualified and experienced personnnel;
- execution is carried out by personnel having the appropriate skill and experience;
- adequate supervision and quality control is provided during execution of the work, i.e. in design offices, factories, plants and on site;
- the construction materials and products are used as specified in Eurocodes or in the relevant execution standards, or reference material or product specifications;
- the structure will be adequately maintained;
- the structure will be used in accordance with the design assumptions.

The Basic requirements are given in EN 1990 as follows.

1. A structure shall be designed and executed in such way that it will, during its intended life, with appropriate degrees of reliability and in an economical way: sustain all actions and influences likely to occur during execution and use, and remain fit for the use for which it is required.
2. A structure shall be designed to have adequate: structural resistance, serviceability and durability.
3. In the case of fire, the structural resistance shall be adequate fro the required period of time.
4. A structure shall be designed and executed in such way that it will not be damaged by events such as: explosion, impact and the consequences of human errors - to an extent disproportionate to the original cause.
5. Potential damage shall be avoided or limited by appropriate choice of one or more of the following:
   - avoiding, eliminating, or reducing the hazards to which the structure can be subjected;
   - selecting a structural form which has low sensitivity to the hazards considered;
   - selecting a structural form and design that can survive adequately the accidental removal of an individual member or a limited part of the structure, or the occurence of acceptable localised damage;
   - avoiding as far as possible structural system that can collapse without warning;
   - tying the structural members together.
6. The basic requirements ahould be met: by the choice of the suitable materials, by appropirate design and detailing, and by specifying control procedures for design, production, execution, and use relevant to the particular project.

The Reliability management is considered in EN 1990 as follows.

1. The reliability required for the structures shall be achieved: by design in accordance with Eurocodes and by appropriate execution & quality management measures.
2. Different choice of reliability may be adopted for structural resistance and for serviceability.
3. The choice of the levels of reliability for particular structure should take the account of the relevant factors, including:
   - the possible cause and/or mode of attaing limit state;
   - the possible consequences of failure in terms of risk of life, injury, potential economic losses;
   - public aversion to failure;
   - the expense and procedures necessary to reduce the risk of failure.
4. The levels of reliability that apply to aparticular structure may be specified in one of the following ways: by the classification of the structure as a whole and by the classification of its components.
5. The levels of reliability relating to structural resistance and serviceability can be achieved by suitable combinations of:
   a) preventive and protective measures (e.g. implementation of safety barriers, active nad passive protetctive measures against fire, protection against risks of corrosion such as painting or cathodic protection);

b) measures relating to design calculations;
c) measures relating to quality management;
d) measure aimed to reduce errors in design and execution of the structure, and gross human errors;
e) other measures relating to the following other design matters:
   - the basic requirements;
   - the degree of robustness (structural integrity)
   - durability, including the choice of design working life;
   - the extent and quality of preliminary investigations of soil and possible evironmental influences;
   - the accuracy of the mechanical models used;
   - the detailing;
f) efficient execution;
g) adequate inspection and maintenance according to procedures specified in the project documentation.

6. The measures to prevent potential causes of failure and/or reduce their consequences may, in appropriate circumstances, be interchanged to a limited extent provided that the required reliability levels are maintained.

The indicative Design working life is specified in EN 1990 by Table 1.

Table 1 – Indicative design working life (according to EN 1990)

Design working life category	Indicative design working life (years)	Examples
1	10	1 Temporary structures
2	10 to 25	Replaceable structural parts, e.g. bearings
3	15 to 30	Agricultural and similar structures
4	50	Building structures and other common structures
5	100	Monumental building structures, **bridges**, and other civil engineering structures

The Durability is treated in EN 1990 as follows.

1. The structure shall be designed such as deterioration over its design working life does not impair the performance of thel structure below that intended, having due regard to its environment ant the anticipated level of maintenance.
2. In order to achieve an adequately durable structure, the following should be taken into account:
   - the intended or foreseeable use of the structure;
   - the required design criteria;
   - the expected environmental conditions;
   - the composition, properties and performance of the materials and products;
   - the properties of the soil;
   - the choice of the structural system;

- the quality of wokmanship and the level of control;
- the particular protective measures;
- the intended maintenance during the design working life.

3. The environmental conditions shall be defined at the design stage so that their significance can be assesed in relation to durability and adequate provisions can be made for protection of the materials used in the structure.
4. The degree of any deterioration can be estimated on the basis of calculations, experimental investigations, experience from earlier constructions, or a combination of these considerations.

In order to provide a structure that corresponds to the requirements and to the assumptions made in design, appropriate Quality management measures should be in place. These measures comprise:

- definition of the reliability requirements,
- organization measures and
- controls at the stages of design execution, use and maintenance.

1.3. DESIGN OF CONCRETE BRIDGES

The bridge durability, especialy environmental conditions and concrete cover to reinforcement, is particularly treated by EN 1992: Design of concrete structures – Part 2 (Concrete bridges).

The durability, including concrete cover to reinforcement, is considered by EN 1992: Design of concrete structures – Part 1 (General rules and rules for buildings) as follows.

The Corrosion protection of steel reinforcement depends on density, quality and thickness of concrete cover and cracking. The cover density and quality is achieved by controlling the maximum water/cement rationand minimum cement content and may be related to a minimum class of concrete.

The exposure conditions are chemical and phisical conditions to which the structure is exposed in addition to the mechanical actions.

The Environmental conditions are classified as:

1. No risk of corrosion attack /class XO/
2. Corrosion induced by carbonation (4 classes of environment: dry or permanently wet /XC1/, wet & rarely dry /XC2/, moderate humidity /XC3/, cyclic wet & dry /XC4/)
3. Corrosion induced by chlorides (3 classes of environment: moderate humidity /XD1/, wet & rarely dry /XD2/, cyclic wet & dry /XD3/)
4. Corrosion induced by chlorides from sea water (3 classes of evironment: exposed to airborne salt but not in direct contact waith sea water /XS1/, permanently submerged /XS2/ and tidal, splash & spray zones /XS3/)
5. Freeze/Thraw attack (3 classes of environment: slightly aggressive chemical environment /XA1/, moderately agressive chemical environment /XA2/, highly agressive chemical environment /XA3/).

In addition to the above conditions, particular forms of agressive or indirect action should be considered including:

- chemical attack arising from: the use of the structure, solutions of acids or sulfate salts, chlorides contained in concrete and alki-aggregate reactions;

- physical attack arising from: temperature change, abrasion and water penetration.

Water penetration or the posibility of leakage from the carriageway into the inside of voided structures should be considered in design.

Where de-icing salt is used, all exposed concrete surfaces within *x* of the carriageway horizontally or within *y* above the carriageway, should be considered as beeing directly affected by de-icing salts.

Requirements for durability shall be included when considering the following: structural conception, material selection, construction details, execution, quality control, inspection, verifications and special masures (e.g. use of stainless steel, coatings, cathodic protection).

Concrete cover is the distance between the surface and the reinforcement closest to the nearest concret surface (including links and stirrups and surface reinfocement when relevant) and the nearest concrete surface. The nominal concrete cover shall be specified in the drawings. It is defined as a minimum cover plus an allowance in design for deviation.

Minimum concrete cover shall be provided in order to ensure:

- the safe transmission of bond forces,
- the protection of the steel against corrosion,
- an adequate fire resistance.

Where a concrete surface is subject to abrasion caused by ice or solid transportation in running water the cover should be increase by a minimum 10 mm.

1.4. DESIGN OF STEEL BRIDGES

The working life, durability and robustness are particularly treated for steel bridges by EN 1993: Design of steel structures – Part 2: Steel bridges design, while EN 1993-1 Design of steel structures (General rules and rules for buildings) considers the design working life, durability and robustness for steel structures as follows.

Depending upon the type of action affecting durability and the design working life of steel structures shall be:

- designed against corrosion by means of: suitable surface protection, the use of weathering steel or the use of stainless steel;
- detailed for sufficient fatigue life;
- designed for wearing;
- designed for accidental action;
- inspected and maintained.

The design working life should be taken as the period for which a bridge is required to be used for its intended prupose, taking into account anticipated maintenance but ont major repair. A design working life of a premanent birdge of 100 years is recommended. For temporaray brdige the design working life may be stated in the project spoecifications.

To ensure durability, bridges and their components should be designed to minimise damage or be protected from exessive deformation, deterioration, fatigue and accidental actions that are expected during the design working life.

The structural parts of a bridge to which gardrails or parapets are connected, should be designed to ensure that plastic derformations of the guardrails or parapets can occur without damaging the structure.

The components that cannot be designed with sufficient reliability to achieve the total design working life of the bridge should be replaceable. These may include: stays, cables & hangers; bearings; expansion joints; drainage devices; guardrails & parapets; asphalt layer & other surface protection; wind shields; noise barriers.

Under the title «robustness and structural integrity» in structural Eurocode EN 1993 it is defined as follows. The design of the bridge should ensure that when the damage of a component due to accidental actions occurs, the remaining structure can sustain at least the accidental load combination with reasonable means. The effects of coorrosion or fatigue of components and material should be taken into account by appropriate detailing.

The structural parts susceptible to corrosion, mechanical wear or fatigue should be designed that inspection, maintenance and reconstruction can be carried out satisfactorily and access is available for in-service inspection and maintenance.

For those elements that cannot be inspected fatigue checks should be carried out and an appropriate corrosion allowance should be provided.

Bridges shall be designed for fatigue for the duration of their design working life.

The required fatigue life of the structure and its components should be attained by the:

- fatigue design of details and with the serviceability checks;
- structural detailing for orthotropic steel decks;
- appropriate material choice;
- appropriate fabrication (conforming to EN 1090).

2. FACTORS AFFECTING ON DURABILITY OF BRIDGES

2.1. INTRODUCTION

Ten main factors of importance for durability of bridges are the following ones:

- Traffic
- Location
- Construction material
- Structural type
- Detailing
- Carriageway
- Equipment
- Foundation
- Accidental actions
- Maintainance.

2.2. TRAFFIC

As it is well known the bridges are civil engineering structures that carry the traffic lines over the natural or artificial obstacles. Moreover, as well, it can be industrial-, cable- or pipe-lines.

Therefore the traffic on the bridge may be:

- roadway traffic
- railway traffic

- pedestrian and/or cycle traffic,

or some mixture of them.

The durability of the bridges largely depends on the frequency, quantity, quality and dynamic effects of traffic loads. Thus EN 1991 defines the appropriate load models for actual roadway, railway and pedestrian/cycle traffic on the bridges.

2.3. LOCATION

The location of the bridge includes all environmental conditions where the bridge is located, such as:

- obstactle where across the bridge is located (river, channel, lake, strait, valey, traffic line, urban parts, etc.)
- terrain, ground and soil conditions (topography and geotechnical conditions)
- climate actions (wind, temperature, raifalls, snowfalls, water streams, ice actions etc.)
- seismic actions (seismic activity of the ground).

Durability of the bridges is very much affected by all above cited environmental conditions determined by the bridge location.

2.4. CONSTRUCTION MATERIAL

Depending on the material which from can be constructed, the bridges can be classified as:

- concrete bridges
- steel bridges
- composite (concrete-steel) bridges
- wooden bridges
- masonary (stone) bridges.

The modern bridges are mainly constructed as concrete, steel and composite bridges.

The wooden bridges are nowdays built as pedestrian/cycle bridges or some temporary bridges only.

The masonary (stone) bridges are nowdays the bridges from the past (historical importance), or rarely the bridges for some very short spans.

The choice of construction materials results mainly from bridge spans, traffic and location; that it is connected with economical, architectural and durability reasons as well.

2.5. STRUCTURAL TYPE

The bridges can be constructed as the following structural types:

- beam bridges
- frame bridges
- arch bridges
- cable-stayed bridges
- suspension bridges.

The design application of particular type of bridge structural system mainly depends on the bridge spans, but it is affected by location, traffic, architectural, economical and durability reasons, as well.

Generally, the beam bridges (depending on construction materials) have some common durability issues. Particular issues are present for the durabiity of the specific structural parts of more complex bridge structural systems, as cable-stayed and suspension bridges.

2.6. STRUCTURAL DETAILING

The bridge durability is affected very much by structural detailing, such as:

- details of carriageway structure
- details of main girders and cross beams (including connections)
- support details (over the piers and abutments)
- details of connections
- details related to: prestressing cables, tendons, suspenders, suspension cables, stay cables.

2.7. CARRIAGEWAY

The applied technical solutions of the carriageway (including its equipment) affect largely the bridge durability, such as:

- asphalt pavement
- waterproofing
- drainage
- safety barriers
- guardrails, parapets & kerbs
- footways.

2.8. EQUIPMENT

The appropriate choice of the bridge equipment has the significant importance for bridge durability, such as:

- bearings
- expansion joints
- instalation devices.

2.9. FOUNDATIONS

The appropriate choice of the foundation types is significantly important for bridge durability.

The choice depends mainly on the soil conditions and actions on bridge.

The settlements of the bridge within the allowable limits shall be enabled by foundation.

2.10. ACCIDENTAL ACTIONS

The bridges should be either protected by accidental actions or calculated for these actions. Neverthless, unexpected large accidental actions directly endager the durability of the bridges.

Accidental actions on the bridge can be classified as:

- collisions from vehicules or vessels
- huricaine & tornado winds

- earthquakes
- ground actions (settlements, slidings, vulcain activities etc.)
- waterflow actions due to havy rain & floods
- fire actions
- terorism and war actions.

2.11. MAINTENANCE

In order to enable the required bridge durability during bridge service life, the following activities related to maintenance should be realized:

- bridge inspection by trial load
- bridge maintenance: control inspection, regular & preventive maintenance, rehabilitation (if needed) and urgent maintenance (if needed)
- bridge monitoring
- bridge managing.

2.12. CONCLUSION

The above cited factors, relevant for bridge durability, shall be treated during design, construction and maintenance in order to realize an appropriate service use of the bridge during its foreseen working life.

The quality management measures should be in place during design, execution, use and maintenance.

REFERENCES

[1] EN 1990:2002 Eurocode: Basis of structural design, CEN, Brussels, 2002

[2] EN 1991:2003 Eurocode 1: Action on structures, Part 2: Traffic loads on bridges, CEN, Brussels, 2003

[3] EN 1992-1-1:2004 Eurocode 2: Design of concrete structures - Part 1.1: General rules and rules for buildings, CEN, Brussels, 2004

[4] EN 1992-2:2005 Eurocode 2: Design of concrete structures - Part 2: Concrete bridges – Design and detailing rules, CEN, Brussels, 2004

[5] EN 19931-1:2005 Eurocode 3: Design of steel structures - Part 1.1: General rules and rules for buildings, CEN, Brussels, 2005

[6] EN 1993-2:2006Eurocode 3: Design of steel structures - Part 2: Steel bridges, CEN, Brussels, 2006

ДГКС Друштво грађевинских конструктера Србије
ASES Association of Structural Engineers of Serbia
S-44
15. KONGRES
6-8. 9. 2018. Zlatibor

Srđan Živković[1], Lela Mitić[2], Marko Milošević[3], Nenad Golubović[4], Matej Kosovel[5]

POBOLJŠANJE KONSTRUKCIONOG REŠENJA VEZA KOD PREFABRIKOVANIH ARMIRANO BETONSKIH ELEMENATA

Rezime:

Projektovanje i građenje objekata u seizmičkim aktivnim područjima ima svoje specifičnosti. Naša zemlja je tek nakon razornog zemljotresa u Skoplju usvojila Privremene tehničke propise za građenje u seizmičkim područjima. Pri projektovanju se odnedavno kod nas koristi i Evrokod 8. Sa potrebom izgradnje objekata u IX seizmičkoj zoni, javljaju se problemi u ostvarivanju veza glavnih i sekundarnih nosača, kao i prenosa seizmičkih sila. U radu je prikazano poboljšanje rešenje veza prefabrikovanih armirano betonskih elemenata za primenu u IX seizmičkoj zoni, primenom savremenih naučnih metoda, na praktičan, ekonomičan i pouzdan način.

Key words: prefabrikovani armirano betonski elementi, IX seizmička zona

THE IMPROVEMENT OF CONSTRUCION SOLUTION FOR PREFABRICATED REINFORCED CONCRETE ELEMENTS CONNECTIONS

Summary:

Designing and construction at seismic areas is very specific. Our country only acknowledged Temporary technical regulations for construction at seismic areas after devastating earthquake in Skopje. The use of Eurocode 8 in designing has recently began in Serbia. With increased need for building objects within IX seismic area additional problems for achievement of connections among main and secondary beams occur as well as with seismic forces transfer. In this paper is given the solution for improvement of prefabricated reinforced concrete elements connections for use at IX seismic zone, by use of modern scientific methods in practical, economical and reliable way.

Key words: prefabricated reinforced concrete elements, IX seismic zone

[1]*Assistant professor, PhD, Faculty of Civil Engineering and Architecture – University of Niš, srdjan.zivkovic@gaf.ni.ac.rs*
[2] *Graduate civil engineer, Put Inženjering d.o.o., Niš, miticl@putinzenjering.com*
[3] *PhD student, Master in Civil Engineering, Innovation Center University of Niš, Faculty of Civil Engineering and Architecture – University of Niš, marko.milosevic@gaf.ni.ac.rs, marko.milosevic.mat@gmail.com*
[4] *Master in Civil Engineering, Put Inženjering d.o.o., Niš, golubovicn@putinzenjering.com*
[5] *Univ.dipl.inž.grad., Corus Inženirji d.o.o., Ajdovščina, Slovenia, matej.kosovel@corusinzenirji.si*

1. INTRODUCTION

Designing and construction at seismic areas is very specific. Our country only acknowledged Temporary technical regulations for construction at seismic areas after devastating earthquake in Skopje (1963, moment magnitude of 6,1 which equals 6,9 when compared to Richter's scale). The territory of Republic of Serbia belongs to the group of seismic areas (there are 3 characteristic seismic zones: VII, VIII and IX zones according to MCS). On the present day The rule book on technical regulations for high-rise buildings construction at seismic areas, which has been elected in 1981. is in effect. The use of Eurocode 8 or SRPS EN 1998-1:2015 "Design of structures for earthquake resistance – Part 1: General rules, seismic actions and rules for buildings" in design has recently began in Serbia and for its complete use it is necessary to have The national annex.

Technical regulations that are currently in effect don't comprehensively process the construction connections at prefabricated reinforced concrete elements. The objects that are built within prefabricated reinforced concrete system are mainly located at VII and VIII seismic MCS area. However, with increased need for building objects within IX seismic area additional problems for achievement of connections among main and secondary beams of roof construction occur, as well as problems related to transfer of seismic forces from roof and intermediate floor constructions to piles, ground and foundation. Hence, the existing solutions cannot be applied to object construction at zone IX.

Improvement of existing construction connections for use at zone IX, with utilization of modern day scientific methods has solved the connection problem in practical, economical and reliable way, hence the safety and functionality of existing products have been increased.

2. REVIEW OF APPLIED TECHNICAL REGULATIONS

Applied technical regulations:

- SRPS EN 1990 – Basis of structural design;
- SRPS EN 1991-1-1:2012 – Actions on structures– Part 1-1: General actions – Densities, self-weight, imposed loads for buildings;
- SRPS EN 1991-1-1/NA:2015 – Actions on structures – Part 1-1: General actions – Densities, self-weight, imposed loads for buildings – National Annex;
- SRPS EN 1991-1-3:2012 – Actions on structures – Part 1-3: General actions – Snow loads;
- SRPS EN 1991-1-3/NA:2017 – Actions on structures – Part 1-3: General actions – Snow loads – National Annex;
- SRPS EN 1991-1-4:2012 – Actions on structures – Part 1-4: General actions – Wind actions;
- SRPS EN 1991-1-4/NA:2017 – Actions on structures – Part 1-4: General actions – Wind actions – National Annex;
- SRPS EN 1992-1-1:2015 – Design of concrete structures – Part 1-1: General rules and rules for buildings;

- SRPS EN 1992-1-1/NA:2015 – Design of concrete structures – Part 1-1: General rules and rules for buildings – National annex; General rules for the structural design of buildings and civil engineering works in reinforced and prestressed concrete made with normal and lightweight aggregates, plain or lightly reinforced concrete and precast concrete for the design of reinforced concrete components with unbonded tendons.
- SRPS EN 1993-1-1:2012/A1:2017 – Design of steel structures – Part 1.1: General rules and rules for buildings – Change 1;
- SRPS EN 1993-1-1/NA:2013 – Design of steel structures – Part 1.1: General rules and rules for – National annex; Eurocode 3, part 1-1 gives generic detailed strength rules which are applicable to steel structures in general.
- SRPS EN 1998-1:2015 (en) – Design of structures for earthquake resistance – Part 1: General rules, seismic actions and rules for buildings; Complementary to Eurocodes 1 to 7 and 9. Additional provisions for the structural design of buildings and civil engineering works to be constructed in seismic regions where risk to life and/or risk of structural damage are required to be reduced. General requirements and rules for assessment of seismic actions and combinations with other actions. General rules for earthquake resistant design of buildings and specific rules for buildings and elements constructed with each of the various structural materials.
- SRPS EN 1997 – Geotechnical design.

3. LIMIT-STATES CONDITIONS AND THE LIST OF REQUESTS

Limit-state conditions have been defined in order to solve the connection problems in a practical, economical and reliable way, so that the certainty, functionality and sustainability of existent prefabricated reinforced concrete beams are increased [1], hence, the construction of objects in seismic zone IX is enabled. This is how the use of existent prefabricated system is enabled at the locations where there are strict conditions in terms of seismic soil activity.

Imput data for Seismic calculation – Modal analysis
According to SRPS EN 1998-1:2015 (en) – Design of structures for earthquake resistance – Part 1: General rules, seismic actions and rules for buildings.

- Soil category: B – deposits of very dense sand, gravel or very rigid clay, at least a few dozen meters thick, with increase of mechanical characteristic that occurs with increase of depth.
- Middle value of transversal seismic waves travel speed:

$$V_{s,30} = 360 - 800\ m/sec \tag{1}$$

- Number of impacts at 30 cm:

$$N_{SPT} > 50\ impacts/30\ cm \tag{2}$$

- Non-drained shearing firmness:

$$C_u > 250\ kPa \tag{3}$$

- Level of importance: II – ordinary buildings that belong to no other category:

$$\gamma_I = 1{,}0 \tag{4}$$

- Calculated soil acceleration:

$$a_g = 2{,}25\ m/sec^2 \tag{5}$$

Accidental eccentricity of floor mass: $e_i = \pm 0{,}050 \times L_i$.

Table 1 – Spectrum types [2]

Faktorji smeri potresa:					
Obtežni primer	Kot α[°]	k,α	k,α+90°	kz	Faktor O.
Edx	0	1.000	0.300	0.000	1.500
Edy	90	1.000	0.300	0.000	1.500

Tip spektra				
Obtežni primer	S	Tb	Tc	Td
Edx	1.200	0.150	0.500	2.000
Edy	1.200	0.150	0.500	2.000

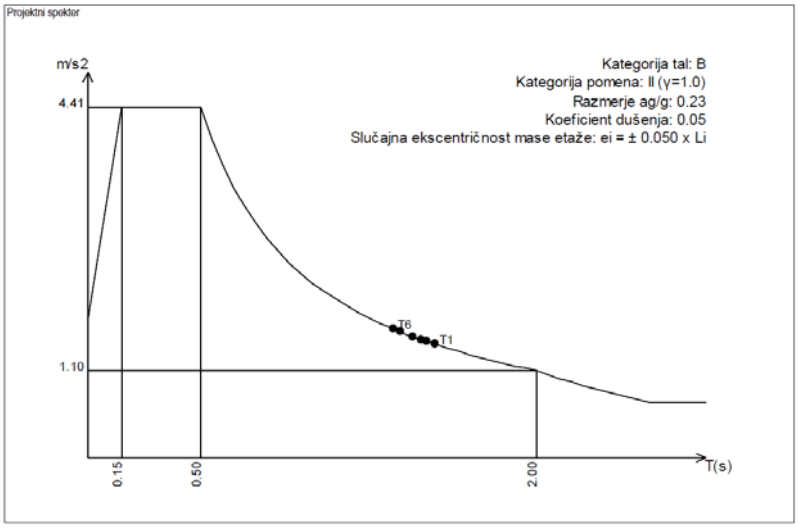

Figure 1 – Project spectrum [2]

4. ANALYSIS AND SOLUTION OPTIMISATION

Mathematical model of typical connection [1], came out of stress field analysis and deformations on seismic effects of construction solutions for secondary and primary beams connections, that are given in figures 2 and 3 at zone IX of seismic activity.

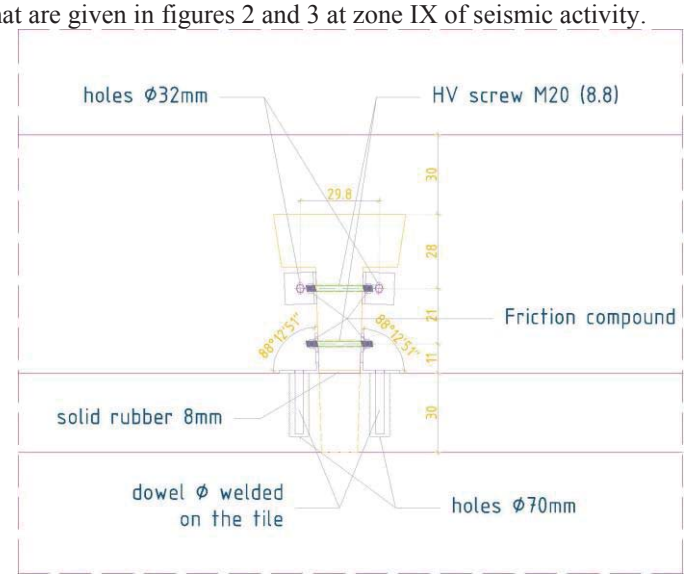

Figure 2 – Detail of secondary and primary beams connection – longitudinal section

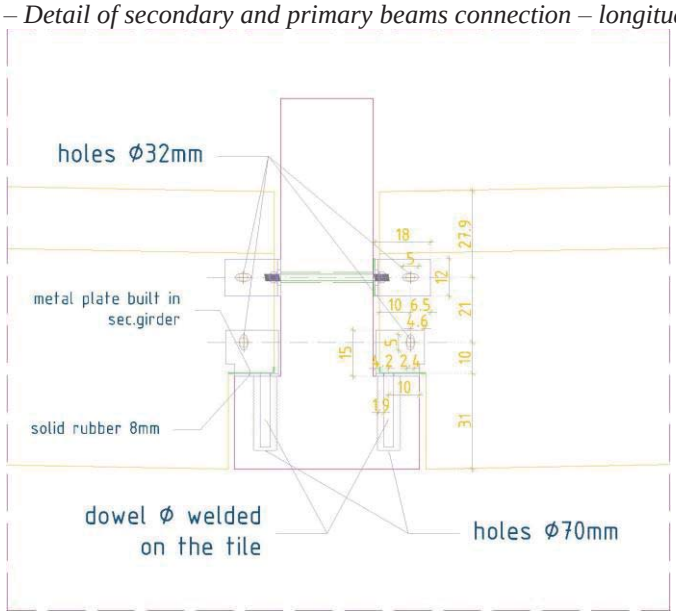

Figure 3 – Detail of secondary and primary beams connection – transversal section

4.1. IMPUT DATA

4.1.1. Calculated values of effects

Ultimate limit state: ⟹ C category – connections resistant to slipping at ultimate limit state. Seismic forces for ultimate limit state according to EN 1998 are in the range of:

$N_{Ed} = 50\ kN\ \div 310\ kN.$

4.1.2. Primary plate material

S 235, $t \leq 40\ mm.$

4.1.3. Characteristics of screw bolts

Preloaded high-ranking screw bolts – HV screw bolts
Bolt class: 8.8 and 10.9
M12 ÷ M36 HV with complete tightening force

4.1.4. Connection load capacity

Distribution of seismic effects at screw bolts:

$$F_{gornji,Ed} = N_{Ed} \cdot \frac{15{,}7\ cm}{21\ cm} \tag{6}$$

$$F_{donji,Ed} = N_{Ed} \cdot \frac{5{,}3\ cm}{21\ cm} \tag{7}$$

Screw bolts at oval holes with opening axis parallel to direction of load transfer: $k_s = 0{,}76;$

Number of frictions surfaces: $n = 2.$

4.2. FOR ULS– CATEGORY C

4.2.1. Calculated load capacity of HV screw bolts on slipping

$$F_{s,Rd} = \frac{k_s \cdot n \cdot \mu}{\gamma_{M3}} \cdot F_{p,C} \tag{8}$$

$$F_{s,Rd} = \frac{0{,}76 \cdot 2 \cdot 0{,}593}{1{,}25} \cdot F_{p,C} = 0{,}72 \cdot F_{p,C} \tag{9}$$

$$\frac{F_{gornji,Ed}}{F_{s,Rd}} \leq 1{,}0 \tag{10}$$

4.2.2. Load capacity of HV screw bolts at pressure by hole wrap

$$k_1 = \min\left(2{,}8 \cdot \frac{e_2}{d_0} 1{,}7; 2{,}5\right) = 2{,}5 \tag{11}$$

$$\alpha_d = \frac{e_1}{3 \cdot d_0} = \frac{64\ mm}{3 \cdot 24\ mm} = 0{,}89 \rightarrow \alpha_b = min(\alpha_d\ ; \frac{f_{ub}}{f_u}\ ; 1{,}0) = 0{,}89 \tag{12}$$

$$t = \min\left(2 \cdot t_v ; t_1\right) = 20mm \tag{13}$$

$$F_{b,Rd} = \frac{k_1 \cdot \alpha_b \cdot f_u \cdot d \cdot t}{\gamma_{M2}} \tag{14}$$

$$F'_{b,Rd} = \frac{2{,}5 \cdot 0{,}89 \cdot f_u \cdot 2{,}0 \cdot d}{1{,}25} \cdot f_u = 3{,}56 f_u d \tag{15}$$

$$\frac{F_{gornji,Ed}}{F'_{b,Rd}} \leq 1{,}0 \tag{16}$$

4.2.3. Control of load capacity of connection elements

Primary element - plates: ≠120×10 mm

Gross cross-section:

$$N_{pl,Rd} = \frac{A \cdot f_y}{\gamma_{M0}} = 564kN \tag{17}$$

Net cross-section:

$$N_{pl,Rd} = \frac{0{,}9 \cdot A_{neto} \cdot f_u}{\gamma_{M2}} = 497{,}66kN \tag{18}$$

$$F_{gornji,Ed} \leq N_{pl,Rd} = \min\left(N_{pl,Rd,bruto} ; N_{pl,Rd,neto}\right) \tag{19}$$

For HV screw bolts with complete tightening force the underlay tiles have been applied in order to bring the surfaces into parallel position, according to SRPS M. B2.030, thickness s = 4 mm and diameter D_{min} (at both sides).

Tensile screw nut has been determined by SRPS M. B2.629 diameter e_{min}, thickness m_{min}..

4.3. SECONDARY AND PRIMARY BEAMS TYPICAL CONNECTION OPTIMIZATION

Optimization of typical connection has been conducted by analysis of mathematical solution model. The analysis has been conducted by two entering parameters, Md and bolt class of HV screw bolts, while exiting variable N_{Ed} presents the limit load capacity for given values Md and HV. Thereby, the accepted values are, for:

$$HV\ 8.8 \rightarrow f_{ub} = 80\ \ kN/cm^2 \tag{20}$$

$$HV\ 10.9 \rightarrow f_{ub} = 100\ \ kN/cm^2 \tag{21}$$

and

$$Md \in \{M12, M16, M20, M22, M24, M27, M30, M36\} \tag{22}$$

In accordance with previously introduced labels for given variable values Md and HV unambiguously have been determined the values of:

$$\begin{cases} d, d_0 \\ A, A_s \\ k_1, \alpha_d, \alpha_b \\ F_{p,c}, F_{s,Rd}, F_{b,Rd}, F'_{b,Rb} \end{cases} \tag{23}$$

It is assumed that the intensity of force N_{Ed} isn't limited from above, i.e. that its limit is set in the range of $N_{Ed} = 50\ kN\ \div 310\ kN$. This assumption gives the possibility of use of given mathematical model on other problems, which optimizes the model.

4.3.1 Model simulation

Model has been software realized[6] and numerically tested. The solution algorithm is given in *Figure 4*.

```
As=[0.84 1.57 2.45 3.03 3.53 4.59 5.61 8.17];
A=[1.13 2.01 3.14 3.80 4.52 5.473 7.07 10.18];
d=[12 16 20 22 24 27 30 36];
d0=[13 18 22 24 26 30 33 39];
HV=[8.8 10.9];
fub=[80 100];
for i=1:8
  k1=min(165.2/d(i)-1.7,2.5);
  alphab=min(21.333/d(i),1);
  for j=1:2
    Ned1=0;
    U1=true;
    U2=true;
    FsRd=0.5048*As(i)*fub(j);
    alphab=min(alphab,fub(j)/36);
    FbRd=k1*alphab*115.2;
    while (U1 && U2)
      Fgornje=Ned1*0.7476;
      U1=Fgornje/FsRd ≤1;
      U2=Fgornje/FbRd ≤1;
      Ned1=Ned1+1;
    end
    Ned(i,j)=Ned1-1;
  end
end
```

Figure 4 – The solution algorithm

[6]*The author of software solution is Bogdan Đorđević, master mathematician, Research intern at Scientific-mathematical faculty of University of Nis, bogdan.djordjevic@pmf.edu.rs.*

Algorithm results table review is given in Table 2. Chart display of algorithm results is given in figure 5, while figure 6 shows tape diagram in order to more easily compare the values of N_{Ed}.

Table 2 – Limit values of N_{Ed} (kN)

M_d	$HV\ 8.8$	$HV\ 10.9$
M12	*46*	*57*
M16	*85*	*107*
M20	*133*	*166*
M22	*164*	*205*
M24	*191*	*239*
M27	*248*	*305*
M30	*274*	*274*
M36	*229*	*229*

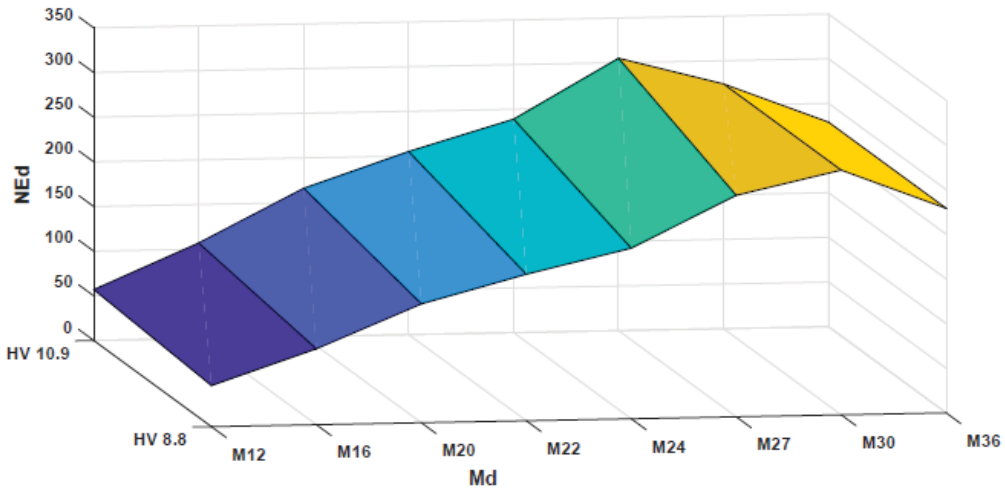

Figure 5 – Chart display of limit load capacity of N_{Ed} (kN)

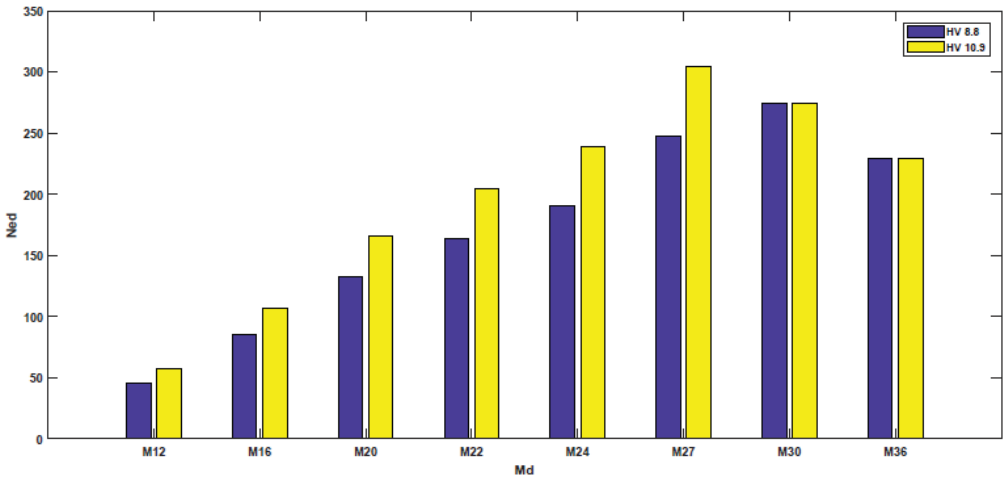

Figure 6 – Tape diagram of limit load capacity of N_{Ed} (kN)

Limit load capacity of connection elements is satisfied for applied construction solution given in figures 2 and 3, depending on seismic effect intensity. The lowest value of limit load capacity $N_{pl,Rd}$ is reached when $d_0 = 39\ mm$ and it amounts $N_{pl,Rd} = 419{,}904\ kN$, which is significantly higher than limit force due to seismic effect, for given conditions N_{Ed}.

It is also noticeable that with increase of screw bolts diameter at M30 and M36 the limit load capacity decreases. The decrease of load capacity which occurs with increase of diameter is the consequence of construction connection solution, namely, too little distance among utmost screw bolts and plate edge, equation (11) and (12), which means that limit state occurs due to crush that happens because of too small distance between external bolt and the edge of plate.

In figures (figure 7, 8 i 9) are given construction solutions for improvement of prefabricated secondary and primary beams connections, which have been conducted by „Put Inženjering“ d.o.o. from Niš [1], at object Logistični center on Območju LT9, Brnik, Slovenia [2].

Figure 7 – Performed roof construction of the object

Figure 8 – Performed primary and secondary beams connection

Figure 9 – Performed primary and secondary beams connection

REFERENCES

[1] Put Inženjering, doo, Niš: Tehnička dokumentacija: Armirano betonski montažni sistem, Steel Concrete Construction, 2018.

[2] Corus Inženirji d.o.o., Ajdovščina, Slovenia: Final Design – Logistični center na Območju LT9, Brnik, 2017.

[3] SRPS EN 1993-1-1:2012/A1:2017 – Design of steel structures – Part 1-3: General rules and rules for buildings.

[4] SRPS EN 1993-1-1:/NA:2013 – National Annex.

[5] SRPS EN 1998-1:2015– Design of structures for earthquake resistance – Part 1: General rules, seismic actions and rules for buildings.

ДГКС Друштво грађевинских конструктера Србије
ASES Association of Structural Engineers of Serbia
S-45
15. KONGRES
6-8. 9. 2018. Zlatibor

Miroslav Marjanović[1], *Mira Petronijević*[2]

PUSHOVER ANALIZA MOSTOVA SA UTICAJEM INTERAKCIJE TLA I KONSTRUKCIJE

Rezime:

Rad se bavi uticajem interakcije tla i konstrukcije na kapacitet pomeranja AB mosta fundiranog na plitkim temeljima. Kapacitet pomeranja u poprečnom pravcu određen je primenom multi modalne pushover analize. Ciljno pomeranje je određeno primenom N2 metode. Uticaj tla je uzet u obzir zadavanjem opruga odgovarajuće krutosti prema NEHPR. Razmatrana su dva tipa tla prema EN1998-1. Analiza je sprovedena primenom programa SAP2000 za slučaj kruto i fleksibilno oslonjene konstrukcije. Data je analiza dobijenih rezultata.

Ključne reči: AB most; pushover analiza; plitak temelj; interakcija tla i konstrukcije.

PUSHOVER ANALYSIS OF BRIDGES INCLUDING SOIL-STRUCTURE INTERACTION EFFECTS

Summary:

This paper deals with the effects of soil-structure interaction (SSI) on the displacement capacity of multi-span RC bridge founded on shallow foundations. Modal pushover analyses are carried out in transverse direction. Target displacement of the monitoring point is calculated using N2 method. The SSI is considered through boundary springs according to NEHPR. Two different soil properties are considered according to EN1998-1. Analyses are carried out using SAP2000, considering fixed- and flexible-base models. The obtained results are discussed.

Key words: RC bridge; pushover analysis; shallow foundation; soil-structure interaction.

[1] *Professor, PhD, University of Belgrade, Faculty of Civil Engineering, pmira@grf.bg.ac.rs*
[2] *Assistant Professor, PhD, University of Belgrade, Faculty of Civil Engineering, mmarjanovic@grf.bg.ac.rs*

1. INTRODUCTION

The increasing attention in earthquake analysis of bridges in the last years is associated with the collapse of bridges that have occurred in areas with high seismicity. EU has adopted standards EN 1998-1 [1] and EN 1998-2 [2] that recognized the need for reliable estimation of the nonlinear seismic response of bridges. EN 1998-2 prescribes two nonlinear methods for the analysis and design of earthquake resistant bridges: (a) the nonlinear response-history analysis (NRHA) and (b) the nonlinear static pushover analysis (SPA). NRHA including the SSI effects is complex and time consuming, since it requires the discretization of the bridge superstructure and a large volume of the surrounding soil. Therefore, the SPA has been extended to the SSI problem [3] as less demanding procedure. Standard pushover analysis (SPA), developed and used for the seismic assessment of buildings, is performed subjecting the structure to the monotonically increasing lateral forces with invariant distribution until a target displacement is reached. Both, the force distribution and assessment of target displacement are based on the assumption that the response is controlled by a fundamental mode which remains unchanged. The SPA has been extended to regular bridge analysis [3]. For irregular bridges, multi-modal pushover analysis (MPA) [4] and extended multi-modal pushover (EMPA) have been developed [5]. The detailed investigation of the effectiveness of both approaches in bridge analysis is presented in [5]. The main conclusion of this investigation is that SPA methods are accurate enough for regular bridge configurations, where the effective modal mass of the fundamental mode is at least 80% of the total mass, while the advantages of the MPA become evident when irregular bridges are considered.

In the conventional bridge analysis, SSI is usually neglected due to the prevailing view that the SSI has beneficial effect on the seismic response of structures. Mylonakis and Gazetas [6] have shown that this view is an oversimplification which sometimes may lead to the unsafe design of bridges. However, very limited investigations have focused on the soil-structure interaction effects on pushover analysis of bridges.

The purpose of this study is to investigate the effects of SSI on the displacement capacity of a typical bridge structure founded on shallow foundations. Modal pushover analyses are carried out in the transverse direction, taking into account three different scenarios related to different soil properties below the foundations: (1) fixed-base structure, (2) structure founded on soft rock (soil type B according to EN1998-1) or (3) firm send and limestone (soil type C). SSI is considered through boundary springs using the appropriate dynamic foundation stiffness. The peak ground acceleration is $a_g = 0.30$ g.

Results of the multi-modal pushover analysis (MPA) in transverse direction are presented and the influence of SSI and higher modes on transverse displacements, base shear and plastic hinge formation are discussed.

2. MULTI MODAL PUSHOVER ANALYSIS

The multi-modal pushover analysis (MPA) is proposed by Chopra and Goel (2002) in order to take into account higher modes of vibration in determining the displacement capacity of high raise buildings. Paraskeva et al. [4] extended MPA to seismic assessment of bridges.

According to EN 1998-2, only inelastic behavior is allowed in the piers. The pushover analyses are carried out separately for each significant mode n, and the contributions from individual modes to the calculated response quantities (displacements, drifts, etc.) are combined using an appropriate combination rule (SRSS). The basic steps are summarized below:

1. Compute the natural periods and mode shapes of the bridge. Select n natural periods T_n and mode shapes ϕ_n of the bridge, to account for 80-90% of the effective modal mass in the considered, lateral, direction.

2. Chose the appropriate monitoring point (MP) for tracking the displacement in the considered direction and calculating the inelastic displacement demands. In the paper, the MP is taken as the resultant of modal load pattern of the first transverse mode [5]:

$$x^* = \left(\sum_{j=1}^{N} x_j m_j \phi_{jn} \right) / \left(\sum_{j=1}^{N} m_j \phi_{jn} \right) \tag{1}$$

   where:

   x_j is the distance of the jth mass m_j from a selected point of the MDOF system,
   ϕ_{jn} is the value of ϕ_n at the location of m_j.

3. Carry out pushover analysis for each mode n by applying the modal force distribution $s_n^*=\mathbf{m}\phi_n$ (where $\mathbf{m}$ is the mass matrix of the structure), in order to obtain modal pushover curves V_{bn} - u_{rn} (base shear vs. displacement of the monitoring point).

4. Idealize modal pushover curves for each mode n by bilinear curves using the equal energy absorption rule.

5. Convert idealized pushover curve of the MDOF system to the capacity curve of an equivalent SDOF system, in *ADRS* format (S_{an}-S_{dn}), using modal conversion parameters:

$$S_{an} = \frac{V_{bn}}{M_n^*}, \qquad S_{dn} = \frac{u_{rn}}{\Gamma_n \phi_{rn}} \tag{2}$$

   where, S_{an} is spectral acceleration, S_{dn} is spectral displacement, ϕ_{rn} is the value of the ϕ_n at the selected monitoring point, $M_n^* = L_n \Gamma_n$ is the effective modal mass, $L_n = \phi_n^T \mathbf{m} \mathbf{1}$, $\Gamma_n = L_n / M_n$ is the modal participation factor and $M_n = \phi_n^T \mathbf{m} \phi_n$ is the generalized mass for mode n.

6. From the capacity curve obtained in (5), extract the spectral displacement and spectral acceleration at yielding point ($S_{dy,n}$ and $S_{ay,n}$, respectively), for each mode n.

7. Calculate elastic vibration period of the equivalent SDOF system T_n^* for each mode n:

$$T_n^* = 2\pi \sqrt{\frac{S_{dy,n}}{S_{ay,n}}} = 2\pi \sqrt{\frac{M_n^* S_{dy,n}}{V_{by,n}}} \tag{3}$$

where $V_{by,n}$ is base shear at yielding point.

8. Transform the demand spectrum into the ADRS format $S_a(g)$-S_d, where:

$$S_d = \frac{T^2}{(2\pi)^2} S_a(g) \tag{4}$$

9. Calculate the spectral target displacement, $S_{de,n}$, of the equivalent SDOF system with known period T_n^* and infinite elastic behavior using the following equation:

$$S_{de,n} = S_{ae}(T_n^*)\left(\frac{T_n^*}{2\pi}\right)^2 \tag{5}$$

where $S_{ae}(T_n^*)$ is spectral acceleration obtained for period T_n^*.

10. Calculate the inelastic displacement demand $S_{d,n}$ of the equivalent SDOF system in the nth mode using the procedure based on the N2 method adopted in EN 1998-1. For:

a) $T_n^* \geq T_C$ (medium and long period range)

$$S_{d,n} = S_{de,n} \tag{6}$$

b) $T_n^* < T_C$ (short period range)

$$S_{d,n} = \frac{S_{de,n}}{q_u}\left[1 + (q_u - 1)\frac{T_C}{T_n^*}\right] \geq S_{de,n} \tag{7}$$

where q_u is the ratio between the spectral acceleration (base force) in the equivalent SDOF with unlimited elastic behavior $S_{ae}(T_n^*)$ and spectral acceleration (base force) at yielding point $S_{ay,n}$, in the nth mode:

$$q_u = \frac{S_{ae}(T_n^*)}{S_{ay,n}} \tag{8}$$

11. Convert the inelastic displacement demands $S_{d,n}$ at the monitoring point and corresponding base shears of the actual bridge, for each individual mode n, from the inelastic SDOF system to the MDOF system, according to:

$$\begin{aligned} u_{rn} &= S_{d,n}\Gamma_n\phi_n \\ V_{rn} &= S_{a,n}\Gamma_n L_n = S_{a,n}M_n^* \end{aligned} \qquad n = 1, 2, \ldots, N \tag{9}$$

where u_{rn} is the modal displacement demand along the actual bridge deck, V_{rn} is the

base shear, $S_{d,n}$ is the spectral displacement demand of the SDOF system at the location of monitoring point and $S_{a,n}$ is the spectral acceleration of the SDOF system at the location of the monitoring point.

12. Total value of any response quantity r is determined by combining the peak modal responses r_n from individual modes using SRSS combination rule $r = \left(\sum_i^n r_i\right)^{1/2}$.

3. DESCRIPTION OF STUDIED BRIDGE STRUCTURE

The Nišava Bridge is a seven-span continuous bridge structure of 232.2m total length (21.6+5×37.8+21.6), curved-in-plan, with radius of curvature R=540m and longitudinal slope of 1.82%, (Fig. 1a). The idealized bridge deck cross section is presented in Fig. 1b. The deck is supported by six RC piers P_1-P_6 of unequal clear heights: P_1=17.14m, P_2=17.51m, P_3=16.82m, P_4=16.11m, P_5=16.07m, P_6=9.95m, and equal rectangular hollow cross section. The piers and are founded on prismatic footings. The inner piers (P_2-P_5) are monolithically connected to the deck, while for the outer piers (P_1 and P_6) a bearing type connection is adopted allowing the movement only in the tangential direction. The rotation about longitudinal and transverse axis is unrestrained in all connections. The deck is resting on piers over "Neotopf" bearings.

The bridge was designed according to Serbian regulations as an object of high importance, for VII seismic zone (PGA of 0.1g) and soil type I (equivalent to the soil type B of EN1998-1). The adopted damping in transverse direction is ξ_i=7%. The reinforcement detailing according to Serbian regulations leads to the high amount of confinement of the joints [7], thus the structure is designed as a ductile, allowing plastic hinge formation at the end of the piers. The adopted reinforcement is shown in Fig. 1c.

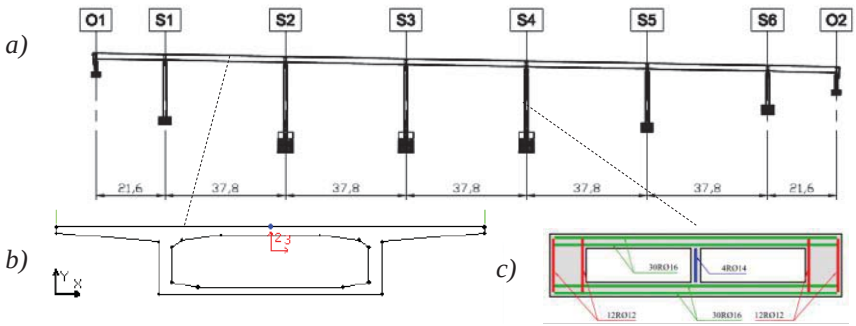

Figure 1 - a) Bridge layout; b) Idealized bridge deck cross section; c) pier cross section with adopted reinforcement

4. NUMERICAL MODEL

The considered structure is modelled in SAP2000. The material properties of RC members and steel reinforcement are given in Table 1. The deck is supposed to remain in the elastic range. The torsional rigidity is reduced to 50%. The reinforcement of the piers is assigned using the Section Designer tool of SAP2000. Bending rigidity of the piers is reduced to 50%.

Mass of the structure is generated from the self-weight (Q_G = 51441.2kN), additional dead loadings ($Q_{\Delta G}$ = 11038.8kN) and traffic loading (Q_T = 2104.6kN), according to EN 1998-2.

To investigate the influence of SSI, three different scenarios are analysed: (1) fixed-base structure, (2) flexible-base structure on a soil type B and (3) flexible-base structure on a soil type C. The soil properties are provided in Table 2. Abutments A1-A2 are modelled as nonlinear springs (K_z = 1800000kN/m, K_{long} = 4644kN/m) and appropriate gap elements (K_{gap} = 1000kN/m, d_{gap} = 5cm).

Table 1 – Material properties of RC members

Element	Material	E [GPa]	ν	γ [kN/m^3]	f_c' [MPa]	f_y [MPa]	f_u [MPa]
Beam	C30/37	31.5	0.2	25.0	23.00	-	-
Pier	C35/45	35.0	0.2	25.0	27.75	-	-
Rebar	RA 400/500	210.0	0.3	78.5	-	400	500

Increase of the shear deformation during the earthquake decreases shear modulus and increases damping in the soil. The ratio of effective shear modulus G and shear modulus G_0, associated with small strains is calculated according to [8] for the considered soil types and a_g=0.30g and presented in Table 3. The designed spectral accelerations, S_{DS} = $S_e(T)=2.5a_g(g)S\ \eta$, are taken according to EN1998-1 [1]. The change of damping due to foundation-soil interaction is calculated using FEMA 440 [9]. The result shows that there is neither increase of damping and therefore, nor spectrum reduction.

Table 2 – Soil properties in three considered scenarios

Scenario	Soil	Soil type	G_0 [kN/m^2]	ρ [t/m^3]	ν [-]
1	Rock	B	-	-	-
2	Soft rock	B	300000	2.20	0.20
3	Firm sand and limestone	C	90000	2.00	0.35

Table 3 – G/G_0 ratios for various site classes [9]

Soil	Site class	S_{DS} / 2.5 [10]			Considered bridge structure				
		≤0.1	0.4	≥0.8	η	S	S_{DS} / 2.5	G/G_0	G [kN/m^2]
Soft rock	B	1.00	0.95	0.90	1	1.20	0.360g	0.957	287100
Clay	C	0.95	0.75	0.60	1	1.15	0.345g	0.787	70830

Foundation impedance is the complex function which depends on the frequency of vibrations, geometry of the soil-foundation contact surface and the soil properties. The components of the dynamic stiffness are calculated according to Pais and Kausel [8] as:

$$K_{i,d} = \alpha_i K_i \quad \wedge \quad K_{ii,d} = \alpha_i K_i, \quad i = x, y, z \tag{9}$$

where:

K_i, i=x,y,z are translational static stiffnesses of the foundation,

K_{ii}, $i=x,y,z$ are rotational static stiffnesses of the foundation,
α_i and α_{ii}, $i=x,y,z$ are frequency-dependent dynamic stiffness coefficients.

Having in mind that the earthquake loading is generally of a low frequency, for the practical purpose, without the loss of accuracy, $\alpha_{ij}=1$ can be adopted. The static stiffnesses of the foundation, which depend on the effective shear modulus G, Poisson's ratio ν and foundation dimensions $B \times L$ [8], are provided in Table 4.

Table 4 – Dimensions and stiffnesses of foundation for soil types B and C

Soil	$L \times B$	G	ν	K_x	K_y	K_z	K_{xx}	K_{yy}	K_{zz}
	[m]	[MPa]	[-]	[MN/m]			[MNm/m]		
B	3.75×2.00	287.1	0.20	4028	4251	4712	19516	49169	54843
C	5.00×3.00	70.8	0.35	1529	1598	2009	18038	38173	36161

5. RESULTS OF THE MULTIMODAL PUSHOVER ANALYSIS

The bridge is assessed using the MPA [4] in transverse direction. The properties of the elastic response spectra are as follows: Type 1, a_g = 0.30 g, soil types B and C according to EN1998 [1] (as shown in Fig. 3). The required dynamic properties (periods T_n and modes ϕ_n) are determined using the standard eigenvalue analyses in SAP2000. Mode shapes are illustrated in Fig. 2. In the MPA, only transverse modes which modal mass participation factors are higher than 2% are considered [5]. The lowest obtained mode is the longitudinal one in all scenarios. Five transverse modes, which account for the 84.5-87.8% of the total mass in the transverse direction, are considered. The slight non-symmetry of mode shapes originates from the different height of columns, indicates that the stiffness of the substructure is not equally distributed along the bridge.

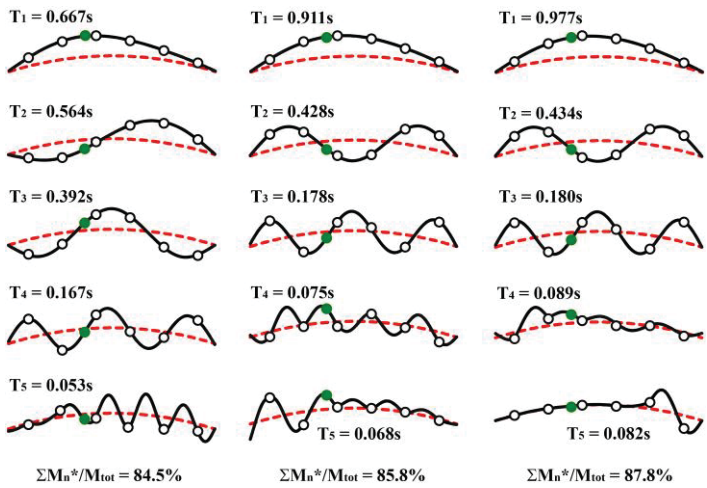

Figure 2 - Mode shapes ϕ_i in transverse direction for the fixed-base model (left), soil B (middle) and soil C (right); white bullets=pier locations P_i, green bullet=monitoring point MP

The pushover analyses are carried out separately for each significant mode. The inelastic behaviour in the piers is modelled using the software built-in P-M2-M3 plastic hinges, according to FEMA 356 [10]. The gravity loads are applied before each pushover analysis, and P-Δ effects are included.

Fig. 3 illustrates the procedure for obtaining the inelastic displacement demands for three considered scenarios. Two considered elastic response spectra are plotted, along with the capacity curves for the first three transverse modes (4th and 5th transverse modes are omitted for the sake of simplicity).

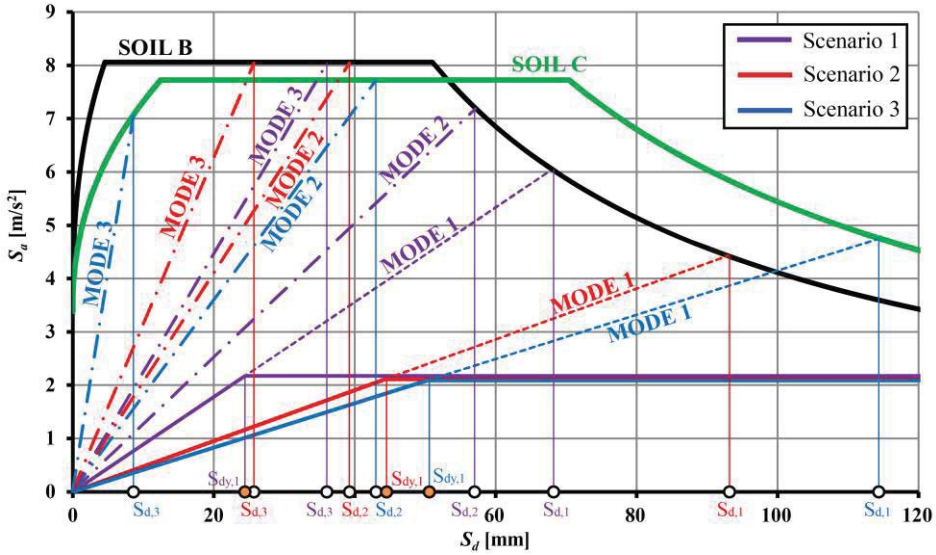

Figure 3 - Black and green lines: elastic response spectra for soils B and C (a_g=0.30g, ξ_i=7%). Capacity curves for three considered scenarios, corresponding to the first 3 transverse modes

The capacity curves corresponding to higher transverse modes are linear, which means that ductility demand $\mu = 1$, i.e. the structure remains elastic in the higher modes. In addition, for the first transverse mode in all three scenarios, $T_1^* > T_C$ and therefore $S_{d,1} = S_{de,1}$, according to [11]. Thus only the elastic spectra have been plotted in Fig. 3.

Fig. 4a illustrates the total transverse inelastic displacements u_r for three considered scenarios (obtained using the SRSS combination), in comparison with the displacement u_1 obtained only by considering the first transverse mode. It is evident that the first transverse mode contributed to the final response significantly in all scenarios. Target displacement in the monitoring point MP for three considered scenarios are: $u_{MP,1}$ = 133.36mm, $u_{MP,2}$=173.48mm and $u_{MP,3}$=212.75mm (obtained using SRSS combination). The corresponding ductility demands are μ_1=2.767, μ_2=2.099 and μ_3=2.266. The total base shear forces are V_{b1} = 25624kN, V_{b2} = 25538kN and V_{b3} = 25439kN. The base shear modal contributions are presented in Fig. 5.

Finally, for the determination of plastic hinge distribution along the structure, the bridge is pushed using the modal force distribution of the first transverse mode (which have the

highest contribution to the overall response), to the value of peak displacement $u_{MP,i}$ in each scenario *i*. The formation of plastic hinges is shown in Fig. 4b.

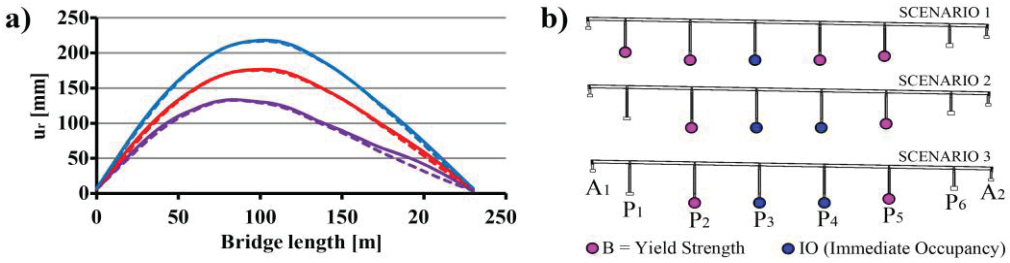

Figure 4 - a) Transverse inelastic displacements u_r for three considered scenarios (solid lines – SRSS combination, dashed lines –first transverse mode), b) plastic hinge distribution along the structure for the scenarios 1-3

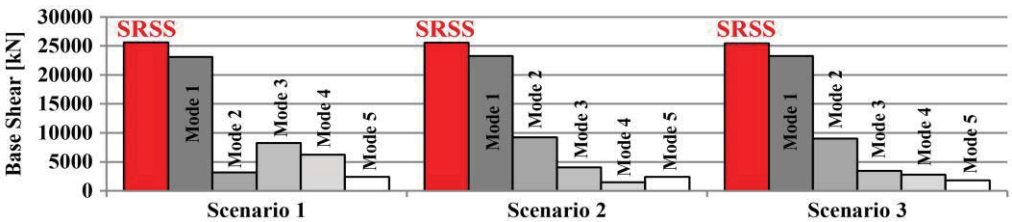

Figure 5 - Base shear modal contributions for the scenarios 1-3 and the corresponding values of base shear for the SRSS combination

6. CONCLUSIONS

In the paper, the multimodal pushover analysis including the effects of SSI of the RC Nišava Bridge has been presented. The seismic demands of the structure have been calculated, considering five dominant transverse modes. The overall bridge performance showed the following:

1. Neither local nor global failure occurred, even under seismic actions that three times exceed the design level,
2. A significant overstrength of the bridge is found due to the partial safety factors used in the design, minimum reinforcement due to the Serbian code requirements and application of conservative code provisions related to the longitudinal bar buckling,
3. The fundamental transverse mode shape contributes to the final response significantly, both for the transverse displacements and base shear,
4. The SSI increased target displacement of the monitoring point from 30% (scenario 2) to 59.9% (scenario 3) in comparison with the fixed-base.
5. The SSI reduced the ductility demand, from 24% in scenario 2 to 18% in scenario 3.
6. The effect of SSI on the total base shear is negligible.
7. In the fixed-base model, plastic hinges have been formed in piers P1-P5, while the SSI leaded to the plastic hinge formation only in piers P2-P5.

ACKNOWLEDGMENTS

The financial support of the Ministry of Education, Science and Technological Development, Republic of Serbia, through the projects TR-36043 and TR-36048, is gratefully acknowledged. The authors express their gratitude to the bridge design team [12] for providing the technical details of the structure.

REFERENCES

[1] EN 1998-1 - Design of structures for earthquake resistance - Part 1: General rules, seismic actions and rules for buildings. CEN, Brussels, Belgium, 2006.

[2] EN 1998-2 - Design of structures for earthquake resistance - Part 2: Bridges. CEN, Brussels, Belgium, 2006.

[3] Pinho, R., Casatotti, C., Antoniou, S.: A comparison of single-run pushover analysis techniques for seismic assessment of bridges, Earthquake Engineering and Structural Dynamics, 36, 2007, 1347–1326.

[4] Paraskeva, T.S., Kappos, A.J., Sextos, A.G.: Extension of modal pushover analysis to seismic assessment of bridges, Earthquake Engineering and Structural Dynamics, 35, 2006, 1269–1293.

[5] Paraskeva, T.S., Kappos, A.J.: Further development of a multimodal pushover analysis procedure for seismic assessment of bridges, Earthquake Engineering and Structural Dynamics, 39, 2010, 211-222.

[6] Mylonakis, G., Gazetas, G.: Seismic soil-structure-interaction: beneficial or detrimental?, Journal of Earthquake Engineering, 4 (3), 2000, 277-301.

[7] Petronijević, M., Marjanović, M., Milojević, D.: Pushover analysis for seismic assessment of RC Nišava bridge. 16th European Conference on Earthquake Engineering – 16ECEE, Thessaloniki, Greece, 2018, paper 10906.

[8] NIST GCR 12-917-21: Soil-Structure Interaction for Building Structures, U.S. Department of Commerce, 2012.

[9] FEMA 440: Improvement of Nonlinear Static Seismic Analysis Procedures, Federal Emergency Management Agency, Washington, DC, USA, 2005.

[10] "FEMA 356: Prestandard and commentary for the Seismic Rehabilitation of Buildings", Federal Emergency Management Agency, Washington, DC, USA, 2000.

[11] Fajfar, P., Gašperšič, P., Drobnič, D.: A simplified nonlinear method for seismic damage analysis of structures. International Workshop: Seismic Design Methodologies for the Next Generation of Codes, Bled, Slovenia, 1997, 183–194.

[12] Ličina, Ž., Kovrlija, Z.: Main Design of Nišava Bridge. Institute of Transportation CIP, Belgrade, Serbia, 2010.

ДГКС Друштво грађевинских конструктера Србије
ASES Association of Structural Engineers of Serbia
S-46
15. KONGRES
6-8. 9. 2018. Zlatibor

Kemal Edip[1], Vlatko Šešov[2], Julijana Bojadžieva[3], Toni Kitanovski[4], Jordanka Čaneva[5], Dejan Ivanovski[6]

EFEKTI MODELIRANJA TLA U PROBLEMIMA INTERAKCIJE TLA I KONSTRUCKIJE

Rezime:

Pri simulaciji seizmičke interakcije strukture tla, zemljišni medijum se obično uzima u obzir kao širok region gde se konstruktivni odnosi obično smatraju elastičnim. Samo u domenu malih deformacija, linerano modeliranje tla otkriva inicijalnu stvarnu simulaciju fenomena tla. Prema tome, treba se koristiti nelinerano materijalno modeliranje zemljišta.

Ključne reči: interakcija tlo - konstrukcija, modeliranje materijala

EFFECTS OF SOIL MODELLING IN SSI PROBLEMS

Summary:

Simulation of seismic interaction of soil-structure, the soil medium is usually taken into account as a wide region in which constitutive relations are usually considered to be elastic. Only in domain of small deformation the linear soil modeling reveals initially real simulation of the soil phenomena. Thus, nonlinear material modeling of soil should be used in simulation problems.

Key words: interaction soil – construction, material modeling

[1] *Assist. Prof. PhD, Institute for Earthquake Engineering and Engineering Seismology, University "Ss. Cyril and Methodius", Skopje, Republic of Macedonia, kemal@pluto.iziis.ukim.edu.mk*
[2] *Prof. PhD, Institute for Earthquake Engineering and Engineering Seismology, University "Ss. Cyril and Methodius", Skopje, Republic of Macedonia, vlatko@pluto.iziis.ukim.edu.mk*
[3] *Assist. Prof. PhD, Institute for Earthquake Engineering and Engineering Seismology, University "Ss. Cyril and Methodius", Skopje, Republic of Macedonia, jule@pluto.iziis.ukim.edu.mk*
[4] *MSc, Institute for Earthquake Engineering and Engineering Seismology, University "Ss. Cyril and Methodius", Skopje, Republic of Macedonia, tonik@pluto.iziis.ukim.edu.mk*
[5] *MSc,Institute for Earthquake Engineering and Engineering Seismology, University "Ss. Cyril and Methodius", Skopje, Republic of Macedonia, dance@pluto.iziis.ukim.edu.mk,*
[6] *Institute for Earthquake Engineering and Engineering Seismology, University "Ss. Cyril and Methodius", Skopje, Republic of Macedonia, ivanovski@pluto.iziis.ukim.edu.mk*

1. INTRODUCTION

The constitutive modeling of soil media has been an important topic in the field of soil structure interaction. In the past decades many attempts have been performed to develop constitutive models for modeling of soil media. Two major classes are available in the literature: linear elastic models and non linear elastic model in which stress strain relations deviate from linearity. It is of special attention to deal also with failure envelope where its description plays a crucial role in soil simulation. The aim of this study is to present the newly implemented material models in finite element software ANSYS for simulation of soil medium in soil-structure interaction problems. Although in numerical calculations constitutive models are the most difficult and tricky part of the problem, there are some elementary features of the soil behavior which should be taken into consideration in most cases. The constitutive models are usually classified with respect to their mathematical parameters. For more detailed explanation the reader can refer to the following publications [1,2]. Although the classification of the material models is useful for scientists it is still confusing for the wider professional public. At the end the engineers are the users of the constitutive models for modeling properly the particular tasks. Therefore, model evaluation appears more useful for users of constitutive models in geotechnical engineering. Laboratory experiments of soil specimens are used for testing of constitutive models and checking for some basic soil features such as nonlinearity, irreversibility, failure criteria, deformation history etc.

As given in the work of Herle [3] it is quite impossible to consider all features by using only single material model. In the work of Chi and Kuchwaha [4] a non linear finite element model has been developed to study the soil failure by using the hyperbolic stress strain model. Experiments conducted by Rowe and Peaker [5] show that both deformation mode and magnitude affect the distribution of earth pressure. Building upon the pioneering works of Drucker-- and Prager [6] on soil plasticity the trend has been to develop more precise and correct elastoplastic models for simulation of real materials. In the work of Loret and Prevost [7] different parameters are considered in solutions for the Drucker-- Prager elasto plastic material models. On the other hand development of von Mises [8] elastic plastic equations has enabled considerable improvement in simulation of soil materials.

2. MODELLING OF SOIL MEDIUM

In the finite element context of integration of material models, the constitutive equations are carried out at integration points. The incremental analysis is done and the solution is assumed to be known at the start of the increments. Knowing the strain increment $\Delta\varepsilon$ it is possible to calculate the stress at the end of the increment. In general the integration of the elasto-plastic models presents a challenging numerical problem since the plastic strain is defined as a rate after the material behavior has changed at the yield point.

In this work in numerical modeling the soil in the soil structure interaction problem is modeled as a non linear medium using the Drucker-- Prager and Bilinear Isotropic (BISO) material models. In order to complete the investigation an elastic model of soil is also simulated for completeness of the comparison.

The frame structure is exposed to earthquake acceleration and the results compared accordingly. Then the non linear material models are compared with elastic soil medium and

the results are discussed consequently. For more detailed explanation of the material models the reader is referred to [7, 9]. The calibration of the non linear material models for Bilinear and Drucker-- Prager material laws is done according to the work of Kodama and Komiyo [10].

The Biliniear Isotropic material model (BISO) uses the von Mises yield criteria coupled with an isotropic work hardening assumption. The material behavior is described by a bilinear stress-strain curve starting at the origin with positive stress and strain values. The initial slope of the curve is taken as the elastic modulus of the material. At the specified yield stress the curve continues along the second slope defined by the tangent modulus. The tangent modulus cannot be less than zero nor greater than the elastic modulus [11].

On the other hand the Drucker-Prager model uses the outer cone approximation to the Mohr-Coulomb law. The amount of dilatancy can be controlled with the dilatancy angle. If the dilatancy angle is equal to the friction angle, the flow rule is associative [11].

The soil medium is presented as a two dimensional model composed of four layers resting on bedrock. In Table 1 the soil layers properties are tabulated in a way that the bottom layers are characterized with better soil characteristics.

Table 1 - Material parameters in finite element analysis

Soil medium	Layer number	Thickness (m)	Density (kg/m^3)	Elastic Modulus (kPa)	Friction angle (deg)	Uniaxial yield stress (kPa)
Elastic	1	3	1.1	2000		
	2	7	1.3	2200		
	3	6	1.5	2400		
	4	14	2	2600		
Drucker-- Prager	1	3	1.1	2000	35	
	2	7	1.3	2200	35	
	3	6	1.5	2400	35	
	4	14	2	2600	35	
Von Mises	1	3	1.1	2000		0.1
	2	7	1.3	2200		0.1
	3	6	1.5	2400		0.1
	4	14	2	2600		0.1

The soil is discretized using eight nodded plane strain elements PLANE82. The dynamic analysis is performed by transient analysis using the step by step method. The proportional viscous damping matrix is taken to be proportional to mass and stiffness matrix (Rayleigh damping). The Rayleigh damping factors, alpha and beta are calculated such that the critical damping is 5% for first two modes. The bottom boundary of the soil model is fixed while side boundaries are simulated as viscous boundaries.

3. SOIL STRUCTURE INTERACTION SYSTEM

In order to show the influence of the soil material modelling to the structural response a comparison of three different cases has been performed. First the soil medium is simulated as

an elastic material model. Then the same soil medium is simulated as nonlinear by considering the Drucker-- Prager and BISO material models. In order to have a bigger range of results the frame is considered as one, three and five storey frames. The frame structural elements are idealized as two dimensional elastic beam elements BEAM3 having three degrees of freedom at each node, translations in the nodal x and y directions and rotation about the nodal z axis. The behaviour of the frame structure is supposed as elastic and is modelled using two parameters, the modulus of elasticity $E=3.15x10^7$ kPa and Poisson's ration n=0.2. The bay length of the frame is taken to be 4.0 m and storey height of 3.0 m. Section of beams is 40 x 50 cm while the column section is 50 x 50cm. A mass of 11 tons is assigned on each node to simulate the real structural behaviour (total 44 tons per floor). For all RC frames the beam and column sections, floor masses and number of bays are kept constant in all cases. The only parameter that is altered is the storey number.

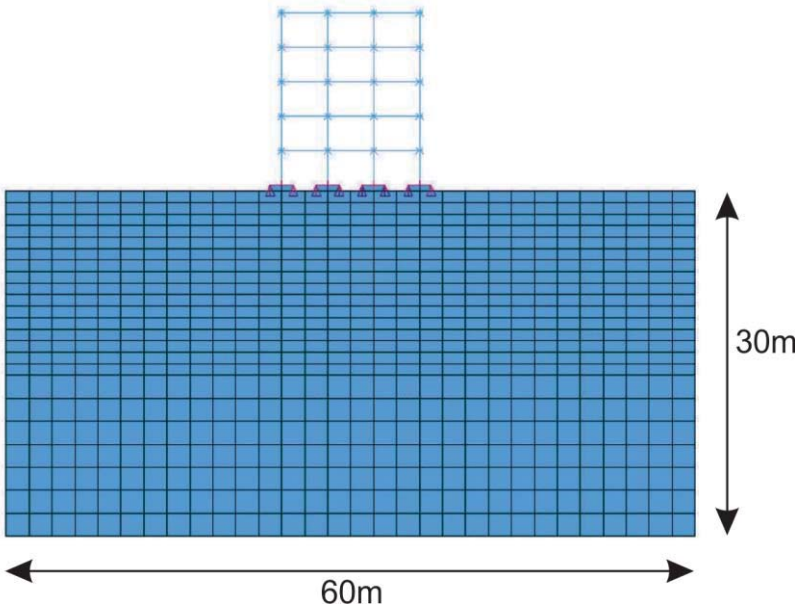

Figure 2 - Coupled Soil structure system of a five storey frame

Finite element modelling of the coupled soil-structure system is performed by the software ANSYS [11] as shown in Figure 2. The effect of soil-structure interaction is carried out with the acceleration time history of the El Centro earthquake with a scaled peak ground acceleration of 0.25g. The foundation where the structure is supported is taken to be 8 nodded plane element having two degrees of freedom in each node, translations in the nodal x and y directions. The moment transfer capability between the column and the footing is created by using a constraint equation where the rotation of the beam is transferred as force couples to the plane element. In Table 2 below the difference in the structural response is given.

Table 2 - Structural values from the analysis of the frame structures

No. of Storey	Soil Medium	Max. acceleration at top of Str. (m/s²)	Max. displacement at top of Str. (mm)	Max. moment at top of Str. (kNm)
1	Elastic	2.54	9.44	28.5
	Drucker- Prager	2.77	9.33	25.6
	BISO	2.79	9.39	31.7
3	Elastic	2.60	4.89	2.02
	Drucker- Prager	2.60	4.08	4.03
	BISO	2.68	4.66	4.40
5	Elastic	2.55	5.67	2.75
	Drucker- Prager	2.60	5.57	5.49
	BISO	2.61	6.87	5.79

According to the acceleration values of the Table 2 the maximum acceleration at the top of structure is considerably big when using linear elastic material model. This illustrates that in soil medium analysis usage of elastic material model is not realistical and should be considered carefully. On the other hand, in using Drucker-Prager material model the maximum structural moment at top of structure has smaller values when compared with elastic material model. In moment comparison the usage of BISO model has similar values with the Drucker-Prager model although the deviation of the results is observed. When comparing the horizontal displacement at the top of structures it can be stated that in all cases of frames considered the Drucker-Prager model predicts the smallest values. In comparison of maximum acceleration values at the top of structures it can be concluded that the elastic material model has the smallest values while the usage of Drucker-Prager and BISO models vary accordingly. Thus it can be stated that in simulation of soil medium by non linear material models the calibration of the parameters with experimental results has to be performed previously.

4. CONCLUSION

It is to be stated that in the literature there are many examples where behavior of real geotechnical structures are compared. Although, relatively little attention has been given to effects of material modeling on the results from analysis. The major advantage of the proposed model is that the description of the soil model is both linear and non-linear which allows basic mechanical responses to be predicted in a correct manner. Moreover, all parameters used in the model have explicit physical meanings and can be calibrated through laboratory tests. On the other hand the main limitations of the model is that due to linear effects the predictability using linear material model can cause over prediction of the critical strength at high deformation values. The best algorithm of soil modeling is the one that combines computational efficiency with acceptable accuracy. Since analytical solution is not always available all elastoplastic models are implemented with some negligible error.

REFERENCES

[1] Darve, F., *Incrementally non-linear constitutive relationships.* Geomaterials, Constitutive Equations and Modelling, 1990: p. 213-238.

[2] Cambou, B. and C. Di Prisco, *Constitutive modelling of geomaterials*2000: Hermes Science Publications.

[3] Herle, I., *„On basic features of constitutive models for geomaterials".* Journal of Theoretical and Applied Mechanics, 2008. 38(1-2): p. 61-80.

[4] Chi, L. and R. Kushwaha, *A non-linear 3-D finite element analysis of soil failure with tillage tools.* Journal of Terramechanics, 1990. 27(4): p. 343-366.

[5] Rowe, P. and K. Peaker, *Passive earth pressure measurements.* Geotechnique, 1965. 15(1): p. 57-78.

[6] Drucker--, D., W. Prager, and H. Greenberg, *Extended limit design theorems for continuous media.* Quart. Appl. Math, 1952. 9(4): p. 381-389.

[7] Loret, B. and J.H. Prevost, *Accurate numerical solutions for Drucker---Prager elastic-plastic models.* Computer Methods in Applied Mechanics and Engineering, 1986. 54(3): p. 259-277.

[8] Krieg, R. and D. Krieg, *Accuracies of numerical solution methods for the elastic-perfectly plastic model.* ASME, Transactions, Series J-Journal of Pressure Vessel Technology, 1977. 99: p. 510-515.

[9] Nyssen, C., *An efficient and accurate iterative method, allowing large incremental steps, to solve elasto-plastic problems.* Computers & Structures, 1981. 13(1–3): p. 63-71.

[10] Kodama, N. and K. Komiya, *Model Experiment and Numerical Modelling of Dynamic Soil-Structure Interaction*, in *Materials with Complex Behaviour*, A. Öchsner, L.F.M. Silva, and H. Altenbach, Editors. 2010, Springer Berlin Heidelberg. p. 269-276.

[11] ANSYS. *Fem Software*. 2006

ДГКС Друштво грађевинских конструктера Србије
ASES Association of Structural Engineers of Serbia
S-47
15. KONGRES
6-8. 9. 2018. Zlatibor

Ivan Milićević[1], *Svetlana Nikolić-Brzev*[2]

SEIZMIČKO OJAČANJE AB RAMOVSKIH KONSTRUKCIJA KONSTRUISANJEM NOVIH AB ZIDOVA

Rezime:

Većina starijih postojećih AB konstrukcija u oblastima umerene i visoke seizmičnosti je osetljiva na dejstvo zemljotresa. Ove konstrukcije često ne ispunjavaju zahteve savremenih seizmičkih propisa, strožije u odnosu na zahteve starih propisa. Ojačanje u vidu konstruisanja novih AB zidova je efikasan način smanjenja seizmičkih zahteva koje elementi postojeće konstrukcije moraju da ispune, što naročito važi kod ramovskih AB konstrukcija. U radu je analizirana postojeća ramovska AB konstrukcija škole, locirane u oblasti visokog seizmičkog hazarda u Centralnoj Aziji. Objekat je projektovan i izveden 60-ih godina XX veka. Primenom linearne i pushover analize utvrđeno je da postojeća konstrukcija ne ispunjava zahteve pri dejstvu zemljotresa propisanog inteziteta. Ojačanje konstrukcije ostvareno je konstruisanjem novih AB zidova a njegova efikasnost je potvrđena rezultatima linearne i pushover analize.

Ključne reči: ramovske AB konstrukcije, seizmičko ojačanje, pushover analiza, AB zidovi

SEISMIC RETROFITTING OF RC FRAME BUILDINGS BY ADDING NEW RC SHEAR WALLS

Summary:

The majority of older existing RC buildings in regions of moderate and high seismicity are vulnerable to earthquake effects. They often do not meet current seismic codes requirements which are more stringent compared to the older codes. Addition of new RC shear walls is an effective retrofit strategy for the reduction of seismic demands on the existing members, especially in case of RC frame structures. The paper presents a case study of an existing school building located in high seismic hazard zone in Central Asia. The building is a bare RC frame structure, designed and constructed in 1960s. The seismic assessment via linear elastic and pushover analysis showed that the structure is deficient for code-prescribed earthquake intensity. A feasible retrofit scheme in the form of new RC shear walls has been developed and its effectivness was verified via linear elastic and pushover analysis.

Key words: RC *frame* buildings, seismic retrofitting, pushover analysis, RC shear walls

[1] *Teaching Assistant, MSc Civ. Eng., University of Belgrade, Faculty of Civil Engineering, ivanm@imk.grf.bg.ac.rs*
[2] *Prof. Dr., consulting structural/earthquake engineer, Belgrade, Serbia, and Adjunct Professor, University of British Columbia, Vancouver, Canada, svetlana.brzev@gmail.com*

1. INTRODUCTION

Many older reinforced concrete (RC) existing buildings are vulnerable to earthquake effects due to inadequate design, construction and/or detailing practices, which may lead to damage or even collapse in major earthquakes. These older buildings often do not meet the current seismic design code requirements. Contemporary seismic codes contain more stringent requirements in terms of design provisions and seismic hazard levels compared to the older codes. It is also true that the knowledge regarding detailing and construction practices for some building typologies, e.g. RC frame buildings, has evolved over the last few decades.

In general, the seismic assessment of existing buildings can be performed using linear elastic and nonlinear seismic analysis procedures. The assessment via linear elastic procedures commonly implies force-based assessment – comparison of member capacity-to-demand ratios and verification of lateral drift restrictions. Elastic seismic demand is determined using either an equivalent static or a modal analysis. It is modified (reduced) using force reduction factor to account for inelastic structural behaviour under seismic actions. This concept is still applied in some design codes without any restrictions regarding detailing of members for local ductility to justify it. Since uncertainty regarding seismic behaviour of older RC buildings is very high, contemporary seismic codes in Europe and USA (e.g. [1], [2]) have taken one of the following approaches to address this uncertainty: (1) by using an appropriate force reduction factor for the structure when all members comply with the code requirements for local ductility, (2) by using the minimum code-prescribed force reduction factor regardless of the available ductility capacity at the local level, or (3) employ linear and nonlinear seismic analysis procedures for performance-based assessment. The third approach has been used by design practitioners over the last few decades (Brzev and Sherstobitoff [3], Mpampatsikos et al. [4], Fardis et al. [5]), because it gives a better understanding of inelastic behaviour and possible failure mechanisms of the building. In addition, the existing buildings often cannot meet the ductility and/or strength requirements associated with first two approaches.

When seismic safety of an existing building is deemed deficient, an appropriate retrofitting scheme can be applied to enhance its seismic performance and meet the requirements of modern seismic codes. This could be achieved by enhancing strength, stiffness and/or ductility of the existing building (Thermou and Elnashai [6], Fardis [7]). The retrofit strategy highly depends on whether the building is deficient at the local or the global level. The enhancement of ductility capacity at the local level can be achieved by jacketing, which consists of applying RC/steel/FRP overlays at critical zones of structural members (beams/colums) with inadequate detailing (e.g. widely spaced transverse reinforcement or insufficient lap splicing). In this case, the modification of the overall stiffness and strength is insignificant and hence the displacement demands are not changed as a result of the retrofit. However, if the existing structure is characterized by low ductility, the above-mentioned strategy is often either deemed ineffective or prohibitively expensive. This is particularly true for flexible structures such as RC frame buildings. The reduction of the global deformation demands in such buildings can be achieved through stiffness and strength enhancement by adding a new seismic-force-resisting system (e.g. new RC shear walls, moment frames, or steel bracings) or installation of seismic dampers, reduction of mass, etc. The application of these techniques for seismic retrofitting of semi-burried RC water reservoirs is described in (Nikolic-Brzev and Sherstobitoff [8]).

Addition of new RC shear walls is a relatively simple and cost-effective technique for seismic retrofitting of RC frame buildings. The wall location depends on the specific building configuration and architectural plan. Usually, the walls are added at the perimeter because of their ability to enhance torsional rigidity of the structure, easier construction access and facilitation of the new foundation system, without compromising the interior architectural form of the building. For example, exterior walls can either be placed parallel to the façade (outside of the frame gridlines, Kaplan et al. [9]) or integrated with the existing frame members through partial or full infilling (Fardis et al. [5]). The latter technique can also be applied to the interior walls, which are commonly used if the goal is to preserve the exterior appearance of the building or to avoid the overloading of the perimeter wall foundations. The main construction challenges associated with this retrofit technique are: connection between the new walls and the existing frame structure, and the construction of the new wall foundation.

The primary objective of the retrofit is to ensure integral connection between a new wall and the existing structure. When RC shear walls are placed in the plane of the existing frame, it is necessary to ensure continuity of vertical wall reinforcement by providing holes in the beams and/or slabs at each floor level. A connection between the new wall and the existing columns can be achieved using horizontal steel anchors (dowels), provided that the existing columns were detailed to act as boundary elements. Alternatively, new shear walls can be separated by gaps from the adjacent columns, to avoid the need to provide horizontal dowels. The results of experimental studies on RC frames which were converted into RC shear walls using different connections between RC walls and adjacent frame members are presented in (Biskinis and Fardis [10]). It was concluded that infilled RC walls and monolithic RC walls can be designed using similar approach. The foundation for new RC wall must be designed to resist the overturning moments and shear forces at the base of the wall, which may be high in some cases. Whenever possible, new wall foundations should be integrated with the existing adjacent column foundations. When the gravity loads are low, the overturning moments could cause the uplift before development of wall plastic hinges. In such cases, soil anchors are needed. Alternatively, uplift may be allowed to minimize the size and the cost of wall foundations; this might reduce the demands on the wall itself but is likely going to increase the demands on the rest of the structure (Fardis et al. [5]).

This paper presents a case study of an existing RC school building located in high seismic hazard zone in Central Asia. The building is a 2-storey bare frame structure designed according to the Soviet Union's design codes valid at the time of its construction (1960s). Seismic evaluation has shown that the building does not meet the current seismic code requirements, hence seismic retrofit is required. A feasible retrofit scheme in the form of new RC shear walls has been developed. Both linear elastic modal analysis and nonlinear static analysis have been performed for the existing and the retrofitted structure, and the results have been discussed.

2. BUILDING DESCRIPTION

The two-storey RC school building is located in a Central Asian country which was a part of the former Soviet Union at the time of construction (1960s). Central Asia has been recognized as one of the highest earthquake hazard regions in the world. It is expected that the building was designed according to Russian codes SNiP II-B.1-62: Code for Concrete and Reinforced Concrete Structures (issued in 1962) and seismic code SNiP II.A-12.62: The

Construction in Seismic Areas. There have been several updates of seismic design codes since the construction date. Seismic evaluation discussed in the paper was performed according to the current codes.

The school consists of several building blocks which are separated by seismic gaps and act as independent structures. A typical building block is shown in Fig. 1a. The plan dimensions of the building are: 33 m length by 12 m width, and the overall height is 7.42 m. The lateral-force-resisting system in both directions is RC moment frame comprised of 0.25 by 0.45 m beams and 0.40 m square columns. The reinforcement detailing of columns and beams is shown in Fig. 1b. Based on the original construction drawings, normative concrete compressive strength and reinforcement yield stress were taken as 14.5 MPa (B25) and 400 MPa (A400), respectively. All columns are supported by isolated footings. Pinned base conditions were considered for the linear and nonlinear seismic analyses. The soil category III (corresponding to soft soil conditions) and seismic intensity higher than 9 (I > 9) were assumed according to СНиП КР 20-02:2009 [11]. It was also assumed that exterior walls and partitions are isolated from the structure (there is no interaction).

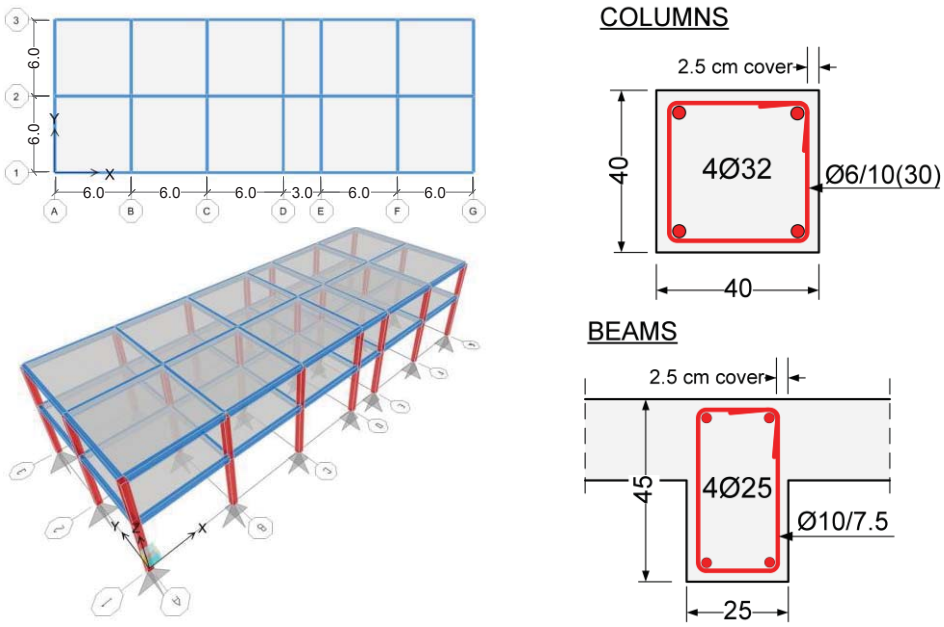

a) **b)**

Figure 1 – Two-storey RC frame building: a) An isometric view and plan of 3-D numerical model , and b) cross-sectional dimensions and reinforcement details for columns and beams

3. SEISMIC ASSESMENT OF THE EXISTING BUILDING

Since the structure is regular both in plan and in elevation, both linear elastic response spectrum analysis and nonlinear static analyses were used for the seismic assessment of typical 2-D frames. Initially, linear elastic modal analysis according to СНиП КР 20-02:2009 [11] was

performed to evaluate the seismic safety in terms of seismic Capacity/Demand (C/D) ratios of structural members and lateral deformability of the structure. The pushover analysis was consequently performed to assess the inelastic deformation demands and failure mechanisms.

3.1 LINEAR ELASTIC RESPONSE SPECTRUM ANALYSIS

Linear elastic response spectrum analysis, referred to as "Spectral Method" according to [11], was used to perform the linear seismic analysis of the existing structure. Modal analysis was carried out to obtain the dynamic characteristics of the building, which are further used in the Spectral Method. The results showed that the structure is predominantly influenced by the first translational mode, since more than 90% of the total modal mass is associated with the first mode in both orthogonal directions. For that reason, seismic response of the structure was considered separately in X and Y direction. Torsional effects were neglected. The reduction factor of the elastic seismic force for RC frames was taken as 3.3 [11]. Fig. 2 shows the code-prescribed acceleration response spectra [11], where spectral accelerations are shown as a fraction of gravity acceleration (A/g). It can be seen that the maximum design spectral accelerations are extremely high (more than $0.5g$).

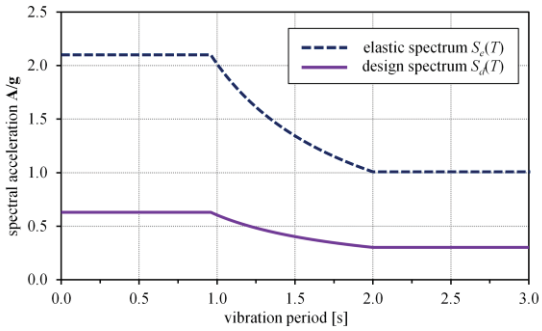

Figure 2 – Elastic and design acceleration response spectra for the seismic analysis

The results of linear elastic seismic analysis are presented in Table 1. It can be seen that the structure is rather flexible, because the fundamental vibration period is on the order of 1.15 sec, however the spectral accelerations are very high due to soft soil conditions (see Fig. 2). Note that the ratio of design seismic force (V) and the total seismic weight (W = 13342 kN) is above 0.5. Elastic inter-storey and total drift ratios were calculated by multiplying drift ratios from the analysis by the reduction factor of 3.3 (according to the "equal displacement" rule). Inter-storey drift ratios at roof level, $\Delta_{e,roof}$, and level 1, $\Delta_{e,1}$, were compared to the code limit (2.0%) [11]. Evidently, the existing structure is significantly deficient in providing global seismic safety for the code level earthquake. It should be noted that, for soil category III and seismic intensity I > 9, the current seismic code [11] restricts the fundamental period of new buildings to maximum 0.4 sec, which the existing building clearly violates.

The C/D ratios were determined for critical columns and beams (as shown in Table 2). Member capacities (resistances) were calculated according to the Limit States Design Method, defined in the current code [12]. Frame 1 and Frame C shown in Fig. 1a were considered as typical frames in X and Y directions, respectively. It can be concluded from Table 2 that the key structural members have inadequate flexural and shear resistance against seismic load.

Table 1 – Fundamental periods, base shear and drift ratios for the existing structure

Direction	***Fundamental period [sec]***	***Base shear [kN]***	$\Delta_{e,1}$ ***[%]***	$\Delta_{e,roof}$ ***[%]***	$\Delta_{e,total}$ ***[%]***
X direction	*1.115*	*7042 (0.53W)*	*12.48*	*2.40*	*8.00*
Y direction	*1.153*	*6720 (0.50W)*	*12.77*	*2.79*	*8.33*

Table 2 – Summary of C/D ratios at critical locations of the existing RC columns and beams

Structural member	***X direction (Frame 1)***		***Y direction (Frame C)***	
	Bending	***Shear***	***Bending***	***Shear***
Interior column	*0.21*	*0.77*	*0.19*	*0.68*
Exterior column	*0.18*	*0.94*	*0.16*	*0.83*
Beam	*0.18*	*0.46*	*0.15*	*0.89*

3.2 NONLINEAR STATIC (PUSHOVER) ANALYSIS

Nonlinear static (pushover) analysis was performed for 2-D representative frames in each direction – Frame 1 and Frame C, as mentioned above. Since local seismic codes don't contain guidelines for the performance-based assessment of existing structures, the analysis was performed according to the general principles set by ASCE 41-13[2].

Properties of the numerical model (geometry, cross-sections and materials) were the same as for linear analysis. Flexural plastic hinges were concentrated at the ends of beam and column spans. Chord rotations of flexural plastic hinges were calculated from basic principles of mechanics and are deemed conservative compared to the corresponding values from [2]. Constant axial forces due to gravity load were considered for determining column hinge properties, but the magnitude varied for specific hinges depending on their location (floor level). Due to non-ductile detailing of transverse reinforcement in columns, the confinement effects were neglected for determination of column hinge rotation capacity. Shear hinges were defined based on force-based characteristics by anticipating a brittle shear failure. Moment and shear capacities of hinges were determined according to the Limit States Design Method from [12], using nominal values of concrete and steel strengths. It should be noted that ASCE 41-13 [2] recommends mean strength values for evaluation of ductile structural components, but based on the detailing of the existing beams and columns they were classified as non-ductile. For performance-based evaluation each plastic hinge is associated with the three performance levels, as per ASCE 41-13 [2]: Immediate Occupancy (IO), Life Safety (LS), and Collapse Prevention (CP). These performance levels were identified for flexural hinges through chord rotations at yielding (IO performance), 70% of the rotation corresponding to the ultimate moment capacity (LS performance) and 100% rotation at the ultimate moment capacity for the CP performance, which is followed by a significant loss of the lateral force capacity. Numerical models (2-D frames) were subjected to unidirectional static analysis with incremental increase of displacement at control node (at the roof level). Lateral load pattern was proportional to the shape of the fundamental vibration mode for the 2-D frame under consideration. P-Δ effects were also considered in the analysis.

Seismic displacement demands in terms of total drift ratio corresponding to the building height H = 7.42 m, were calculated based on the target displacements determined from [2]:

$$\Delta_t = d_t / H = \left(C_0 \times C_1 \times C_2 \times S_e(T) \frac{T_e^2}{4\pi^2} g \right) / H \tag{1}$$

where the values of C_1 and C_2 modification factors were set to 1.0, while C_0 (transformation of SDOF to MDOF system) was calculated as 1.07 in both directions. The effective fundamental periods T_e in both directions were equal to corresponding values from Table 1, and were used to calculate the elastic spectral accelerations, according to Fig. 2. The final values of total (target) drifts in X and Y directions were $\Delta_{t,x}$ = 8.06% and $\Delta_{t,y}$ = 8.33%, respectively. Note that the target drifts are similar to the total drifts obtained from linear elastic analysis (see Table 1).

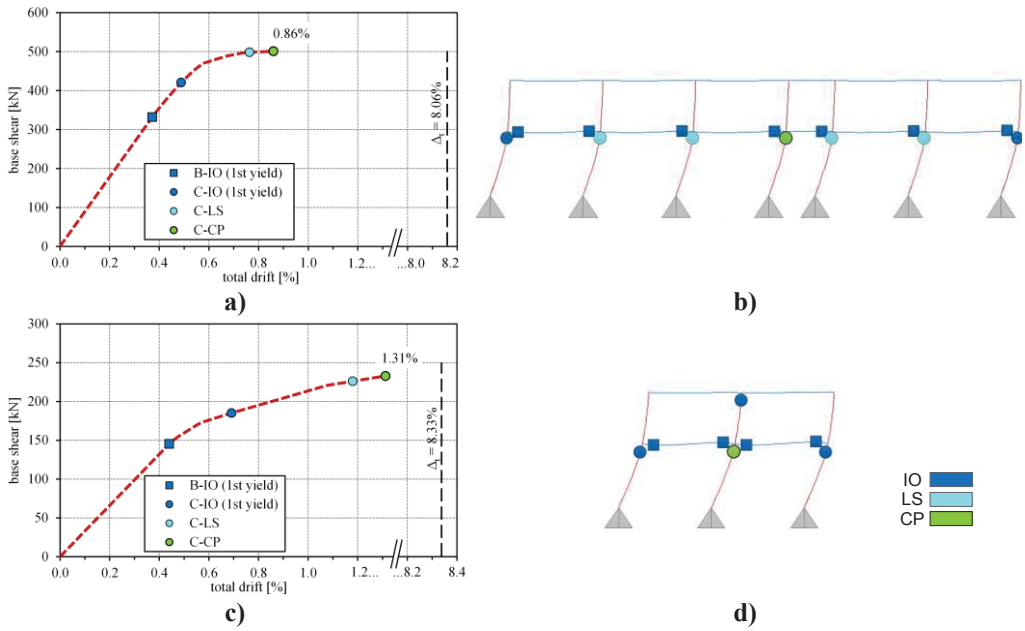

Figure 3 – Pushover analysis results for the existing building: a) pushover curve for Frame 1, b) deformed shape for Frame 1 at the onset of collapse, c) pushover curve for Frame C, and d) deformed shape for Frame C at the onset of collapse

It can be seen from the pushover curves shown in Figs. 3a and 3c that the existing structure has very low deformation capacity. It is expected that the collapse in longitudinal (X) direction may occur at 0.86% drift and a very limited displacement ductility, as illustrated by Fig. 1a. The frames in transverse (Y) direction have shown a larger drift potential, since the collapse is expected at 1.31% drift, and the structure has more significant displacement ductility, as shown in Fig. 1c. For a satisfactory seismic performance, the structure should demonstrate Life Safety (LS) performance at the target displacement/drift corresponding to a code-level earthquake. However, the analysis results show that the existing structure is expected to collapse (corresponding to CP level) at displacement/drift levels which are a fraction of the target displacements/drifts for the design earthquake intensity. The deformed shape of Frame 1 prior to collapse (see Fig. 3b) indicates a possible undesirable soft-storey mechanism at the ground

floor level. At that stage, flexural plastic hinges at the top of ground floor columns are characterized by high rotations corresponding to LS or CP performance levels. However, flexural plastic hinges in the beams are at IO performance level. It is noteworthy that shear failure is not anticipated (this is consistent with the results of linear analysis).

4. ADDITION OF NEW RC SHEAR WALLS AS A SEISMIC RETROFIT SCHEME

Since the analysis results have shown that the existing structure does not comply with the requirements of the current seismic code [11], a seismic retrofit scheme was developed by providing new RC shear walls at critical locations in the building. The aim of the retrofit was to reduce the seismic displacement demands on the existing members by increasing global lateral stiffness, to increase lateral load-resisting capacity, and to prevent the formation of a soft-storey failure mechanism. The wall layout was selected such that the walls are constructed at the building perimeter to minimize the disruption of occupants during the construction. An additional interior wall was provided to control the flexural demand on the foundation (which could be a potential issue in a layout with exterior walls only). The final retrofit scheme was selected so that architectural function of the building was not compromised. Fig. 4 shows a typical floor plan which illustrates layout of new RC shear walls.

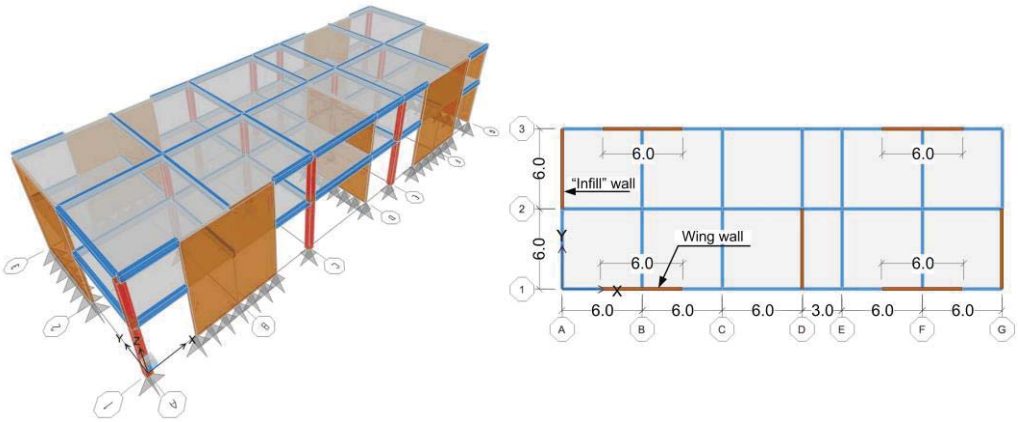

Figure 4 – Retrofitted frame building with added RC shear walls

Another retrofit objective was to minimize the length of added RC shear walls whenever possible. New RC shear walls in X direction were constructed in the form of wing walls, in the form of two shorter (3 m long) walls placed on each side of the existing columns. In Y direction, new 6 m-long RC shear walls were constructed in line of the existing frame bays, between the adjacent RC columns. All RC shear walls were 0.2 m thick. Concrete grade B30 and steel grade A400 reinforcement were used for the wall design according to [12]. The walls were reinforced with ±Ø16/20 vertical and ±Ø16/30 horizontal reinforcement. Wall design was performed based on the seismic demand from linear elastic analysis according to [11]. The continuity of vertical reinforcement up the the building height was achieved by drilling holes through the existing RC beams. To ensure monolithic behaviour, the connection between added

wing walls (in X direction) and existing RC columns was achieved by providing horizontal dowels anchored into the existing columns. Since the existing columns couldn't be used as boundary elements of new walls due to poor detailing, walls in Y direction were separated by a 20 mm gap at each end. The foundation of new shear walls was constructed by connecting the new wall footing and the isolated footings of the adjacent existing RC columns.

4.1 LINEAR ELASTIC RESPONSE SPECTRUM ANALYSIS

Numerical model of the retrofitted structure is similar to the model used for the analysis of existing structure, except that new shear walls were added at specified locations (see Fig. 4). Shear walls were modelled as 2-D plate elements. The same assumptions were used in the analysis as for the existing structure. The reduction factor of the elastic seismic force for RC walls according to code is 3.3 (the same as for RC frames). The results of linear elastic response spectrum seismic analysis are presented in Table 3. The C/D values for critical columns and beams are presented in Table 4. Note that the base shear-to-seismic weight (V/W) ratios for the retrofitted and the existing structure are similar. It can be seen that the retrofit was effective in reducing the displacements in both directions, and the displacement limit of 2.0% [11] has been met. In addition, all existing members have satisfied the strength criterions (values of C/D ratios are higher than 1.0). In conclusion, seismic retrofit scheme using new RC shear walls is fully effective in controlling lateral displacements/drifts and enhancing lateral load resistance of the building.

Table 3 – Fundamental periods, base shear and drift ratios for the retrofitted structure

Direction	***Fundamental period [sec]***	***Base shear [kN]***	$\Delta_{e,1}$ ***[%]***	$\Delta_{e,roof}$ ***[%]***	$\Delta_{e,total}$ ***[%]***
X direction	*0.122*	*7279 (0.55W)*	*0.11*	*0.13*	*0.12*
Y direction	*0.143*	*7560 (0.57W)*	*0.15*	*0.19*	*0.17*

Table 4 – Summary of C/D ratios at critical locations of columns and beams

Structural member	***X direction (Frame 1)***		***Y direction (Frame C)***	
	Bending	***Shear***	***Bending***	***Shear***
Interior column	*3.16*	*4.63*	*12.24*	*49.40*
Exterior column	*3.94*	*7.51*	*10.22*	*45.35*
Beam	*2.62*	*3.63*	*3.50*	*17.19*

4.2 NONLINEAR STATIC (PUSHOVER) ANALYSIS

Nonlinear static analysis was performed for three 2-D frames: Frame 1 and Frames C and D. Note that Frame D was considered for nonlinear analysis because it contains a RC shear wall, as shown in Fig. 4. An equivalent 2-D frame method was used for modelling RC shear walls. An RC shear wall was modelled as an equivalent wide column with cross-sectional dimensions corresponding to the wall section. Stiff horizontal beam elements were added to simulate the effect of wall-to-slab interaction in addition to beam elements simulating the actual beams in the existing RC frames. To simulate the effect of rigid diaphragms, additional rigid links with pinned end connections were used to connect Frames C and D.

Plastic hinges for the existing beam and column sections remained unchanged (see Section 3.2). Plastic hinge characteristics for the RC shear wall sections were developed for bending with constant (gravity) axial force and shear. Chord rotations for flexural plastic hinges were calculated from the basic principles of mechanics. The performance levels (IO, LS, and CP) were characterized by the same rotation levels as described for beam and column hinges. Flexural hinges were located at the middle of the adopted plastic hinge length, which was taken equal to 50% of wall length. The wall shear hinge characteristics (shear capacity versus interstorey drift) were determined according to [2]. IO, LS and CP levels, expressed in terms of interstorey drift, were associated with the first attainment of shear resistance, the onset of significant strength degradation, and 70% of total deformation capacity, respectively. The moment and shear capacities for RC shear walls were determined according to [12].

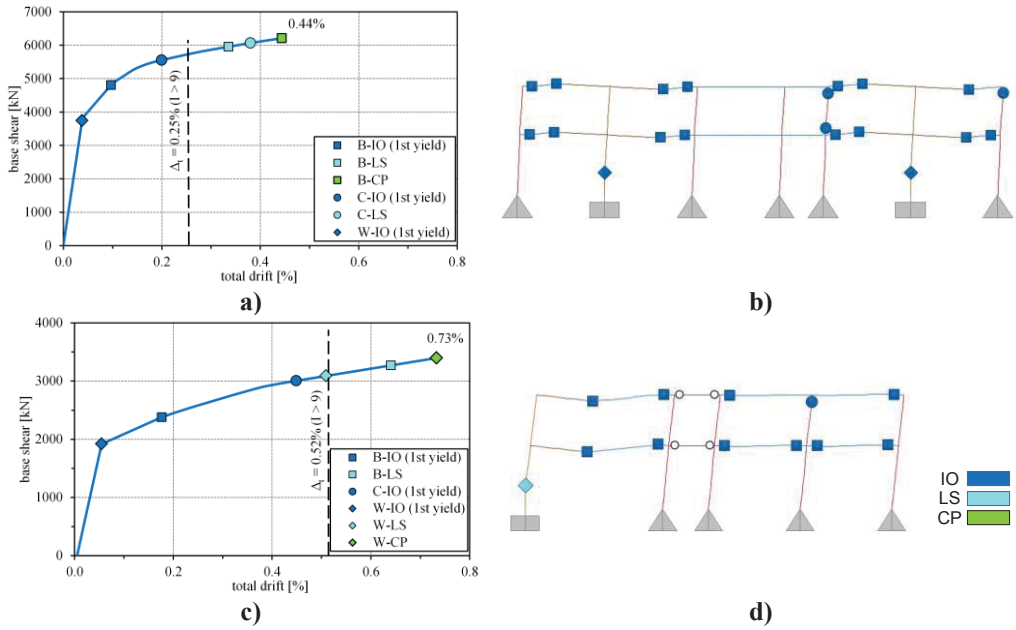

Figure 5 – Pushover analysis results for the retrofitted building: a) pushover curve for Frame 1, b) deformed shape of Frame 1 at the target displacement, c) pushover curve for Frames C&D, and d) deformed shape for Frames C&D at the target displacement

The models were subjected to nonlinear static analysis using "modal load pattern". *P-Δ* effects were also considered. Target drifts were determined from Eq. 1 [2]. The product of all modification factors ($C_0 \times C_1 \times C_2$) in X and Y directions was equal to 2.35 and 3.59 and corresponding total (target) drifts were $\Delta_{t,x}$ = 0.25% and $\Delta_{t,y}$ = 0.52%. The corresponding values of the elastic total drifts from Table 3 are lower due to fact that code [11] applies "equal displacement" rule in all cases, regardless of the value of structure's fundamental period.

Fig. 5 shows capacity curves and deformed shapes from pushover analysis of 2-D frames in X and Y directions. The retrofitted structure shows a ductile behaviour. Wall flexural hinges in Y direction experience rotations corresponding to LS performance level while hinges of all other members experience IO performance level at the attainment of corresponding target

displacement (see Figs. 5b and 5d). Shear failure of all members is prevented at all performance levels. The failure mechanism of the structure in X direction is governed by high flexural rotations at the ends of 3 m long beams (Fig. 5a), while in Y direction flexural failure of the wall prevails (Fig. 5c).

5. DISCUSSION AND CONCLUSIONS

Based on the seismic assessment of the existing building via linear elastic and nonlinear analyses it can be concluded that the existing structure is expected to fail at the code-level earthquake. The seismic demands and capacities of the existing and retrofitted structure are compared in Fig. 6, in Acceleration vs Displacement Response Spectrum (ADRS) format. The demand and capacity curves obtained from nonlinear analysis are expressed in terms of normalized spectral acceleration (expressed as a fraction of *g*) versus spectral displacements.

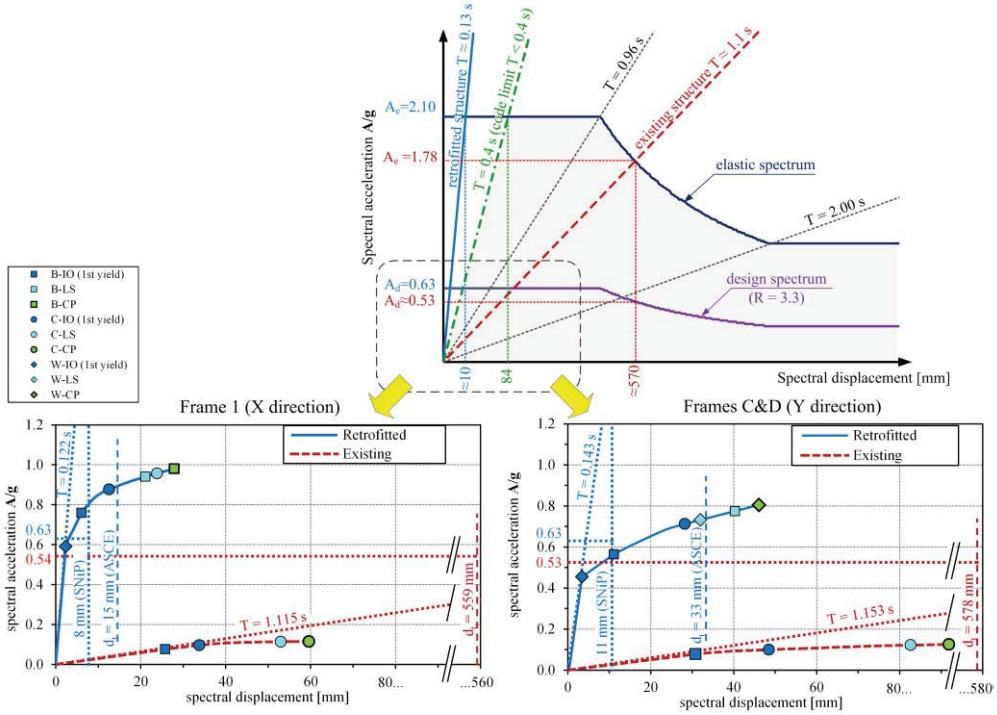

Figure 6 – Existing vs retrofitted building: pushover analysis results in ADRS format

It can be seen from the schematic ADRS diagram that high displacement demands for the existing structure are due to its high flexibility (fundamental period of 1.15 sec). The current seismic code [11] contains provisions for controlling the seismic demands for new buildings by restricting the inter-storey drift ratio to 2% and the fundamental period to 0.4 sec for structures constructed at soft soil sites (see Fig 6). However, the existing structure does not comply with these restrictions nor has the necessary ductility potential deemed necessary given extremely high seismic demand.

The addition of new RC shear walls changes the overall seismic response of the building. A significant increase in global lateral stiffness and strength of the retrofitted structure compared to the existing one can be observed (fundamental period has dropped from 1.1 to 0.15 sec, see Fig. 6). The seismic demands in terms of target displacements are substantially reduced and the formation of a soft-storey mechanism is prevented. There is an apparent overstrength of the retrofitted structure compared to the inelastic acceleration A_d = 0.63g, due to the same amount and distribution of vertical reinforcement in new shear walls as well as the overstrength of the existing members (see Table 4). Nevertheless, the retrofitted structure is expected to undergo inelastic behavior under seismic action and attain the (desirable) LS performance level.

ACKNOWLEDGMENTS

The research described in this paper was supported by the Serbian Ministry of Education, Science and Technological Development through the TR-36048 project.

REFERENCES

[1] EN 1998-3: Design of structures for earthquake resistance - Part 3: Assessment and retrofitting of buildings. Comite Europeen de Normalisation, Brusells, 2005.

[2] ASCE/SEI 41-13: Seismic evaluation and retrofit of existing buildings. American Society of Civil Engineers, Reston, VA, 2014.

[3] Brzev S. and Sherstobitoff J.: Performance-based seismic evaluation of concrete reservoir structures. Proceedings of the 13th World Conference on Earthquake Eng., Canada, 2004, Paper No. 1823.

[4] Mpampatsikos V., Nascimbene R. amd Petrini L.: A Critical Review of the R.C. Frame Existing Building Assessment Procedure According to Eurocode 8 and Italian Seismic Code, Journal of Earthquake Engineering, 12(S1), 2008, 52-82.

[5] Fardis M., Schetakis A. and Strepelias E.: RC buildings retrofitted by converting frame bays into RC walls, Bull. Earthquake Eng., 11, 2013, 1541-1561.

[6] Thermou G. E. and Elnashai A. S.: Seismic retrofit schemes for RC structures and local–global consequences, Prog. Structural Engineering Materials, 8, 2006, 1-15.

[7] Fardis M.: Seismic design, assessment and retrofitting of concrete buildings: Based on EN‑Eurocode 8, Springer, Dordrecht, 2009.

[8] Nikolic-Brzev, S. and Sherstobitoff, J.: Seismic upgrade techniques for concrete reservoirs - a Canadian experience, Proceedings of the Sixth US National Conference on Earthquake Engineering, Seattle, 1998, Paper 225.

[9] Kaplan H., Yilmaz S., Cetinkaya N. and Atimtay E.: Seismic Strengthening of RC Structures with Exterior Shear Walls, Sadhana 36(1), 2011, 17-34.

[10] Biskinis D. and Fardis M.: Strength, stiffness and cyclic deformation capacity of RC frames converted into walls by infilling with RC, Bull. Earthquake Eng., 14, 2016, 769-803

[11] СНиП КР 20-02:2009: Сейсмостойкое строительство. Нормы проектирования (Earthquake engineering design standard). Государственное Агентство По Архитектуре И Строительству При Правительстве Кыргызской Республики, Bishkek, Kyrgyz Republic, 2009, (in Russian).

[12] СП 63.13330.2012. Бетонные и железобетонные конструкции (Concrete and reinforced concrete structures – Design requirements), Russia, 2011, (in Russian).

ДГКС Друштво грађевинских конструктера Србије
ASES Association of Structural Engineers of Serbia
S-48
15. KONGRES

Aleksandra Radujković[1], *Igor Džolev*[2], *Đorđe Lađinović* [3]

KAPACITET OBRTANJA TETIVE ARMIRANOBETONSKIH STUBOVA ZA MONOTONO OPTEREĆENJE

Rezime:

Odredbe EN 1998-3 propisuju da se kapacitet deformacije elemenata verifikuje u pogledu rotacije tetive. Postoje razlike u ponašanju AB elemenata usled dejstva cikličnog i monotonog opterećenja. U radu su procenjene vrednosti granične rotacije tetive stubova usled monotono rastućeg opterećenja i upoređene sa kapacitetom dobijenim za ciklično opterećenje (prema EN 1998-3) i za monotono opterećenje. Nelinearne analize su sprovedene pomoću programa OpenSees sa nelinearnim elementima uzimajući u obzir raspodeljenu i koncentrisanu plastičnost.

Ključne reči:rotacija tetive, monotono opterećenje, smičući raspon

THE CHORD ROTATION CAPACITY OF REINFORCED CONCRETE COLUMNS UNDER MONOTONIC LOADING

Summary:

The provisions of EN 1998-3 prescribe that the deformation capacity of elements is verified in terms of the chord rotation. There are differences regarding the behavior of RC elements under cyclic and monotonic loading.In this paper, the ultimate chord rotation of the columns,under monotonically increasing loads, has been assessed and compared with the appropriate capacity obtained for cyclic loading (according to EN 1998-3) and monotonic loading.Nonlinear analyses were conducted using the OpenSees software framework with nonlinear beam column element taking into account distributed and concentrated plasticity.

Key words: chord rotation, monotonic loading, shear span

[1]*Ass. Prof.,PhD, Faculty of Technical Sciences, University of Novi Sad, leksa@uns.ac.rs*
[2]*Ass., MSc, PhD student, Faculty of Technical Sciences, University of Novi Sad, idzolev@uns.ac.rs*
[3]*Full Prof., PhD, Faculty of Technical Sciences, University of Novi Sad, ladjin@uns.ac.rs*

1. INTRODUCTION

EN 1998-3 [1] provides a set of rules that represent displacement based approach for assessment of existing and new buildings. Seismic assessment is determined by checking that the corresponding capacities are not exceededby the demands.Comparison of estimated demand and capacity depends on the type of structural element. For ductile element, seismic demand and capacity are expressed in terms of deformation, whereas for brittle element,in terms of force. In Annex A EN 1998-3, capacity models for assessment of reinforced concrete (RC) structures under cyclic loading are given. The demands on both ductile and brittle elements are obtained from nonlinear method of analysis (static or dynamic). Although nonlinear time-history analysis is the most accurate procedure for estimating seismic demands, the application of nonlinear static analysis is generally considered more appropriate in engineering practice.

There are differences between the behavior of RC element under cyclic and monotonic loading. These differences are due to different mechanical behavior of confined concrete and reinforcement and have been observed in a large number of experimental researches [2]. It was found that both the degree and the extent of concrete damage were more severe under cyclic loading compared with monotonic loading. The deformation capacities under monotonic loading are significantly larger than in cyclic loading. Based on experimental results, the expression for determining the capacity of chord rotation was proposed, which takes into account the loading type [3]. Also, for the determination of the plastic hinge length and the ultimate strain of confined concrete, different expressions are used for monotonic and cyclic loading.

One of the most important parameters for member deformation capacity is shear-span ratio. In ordinary regular plane frames, columns normally have shear span ratios greater than 2.5 and beams around 3. For such values of the shear span ratio, the inelastic behavior and the ultimate deformation of frame members are due to flexure and are inherently ductile (provided that all members are designed not to fail in shear before they yield in flexure at the end sections).

In this paper, reinforced concrete columns loaded with monotonically increasing loads in order to determine the ultimate values of the chord rotation,are analyzed. These values are compared with the chord rotation capacity determined according to EN 1998-3, as well as with the corresponding capacity that takes into account the loading type.

2. MODELING PROCEDURE FOR NONLINEAR ANALYSIS

Nonlinear analysis method represents the reference method for displacement-based seismic assessment. The model for nonlinear analysis should include the nonlinear force-deformation relation of the structural components. The use of the finite element method for nonlinear analysis offers a number of elements for modeling beams and columns with distributed or concentrated inelasticity. The inelastic behavior is defined at the cross-section level, preferably by using the fiber model. Distributed plasticity elements allow for the plastic hinges to be formed at any location along the element length. Concentrated inelasticity elements are designed to include plasticity at their member ends, and these elements range from simple one-

or two-component models, to more sophisticated elements with fiber modeling at predetermined plastic hinge lengths [4].

Numerous empirical equations,which are based on experimental data, have been proposed for the prediction of the plastic hinge length, L_{pl}. The same empirical expression for L_{pl} cannot fit both the monotonic and the cyclic data. Taking into account the loading type, the plastic hinge length can be determined on the basis of the following expressions [5]:

$$L_{pl,mon} = h\left(1.1 + 0.04\min\left(9, \frac{L_v}{h}\right)\right) \tag{1}$$

$$L_{pl,cy} = 0.2h\left(1 + \frac{1}{3}\min\left(9, \frac{L_v}{h}\right)\right) \tag{2}$$

or according to the research of Panagiotakos and Fardis [6]:

$$L_{pl,mon} = 0.18L_v + 0.021a_{sl}d_{bl}f_y \tag{3}$$

$$L_{pl,cy} = 0.12L_v + 0.014a_{sl}d_{bl}f_y \tag{4}$$

where:

L_v is the moment/shear ratio at the end section,

h is the depth of the cross-section,

d_{bl} is the diameter of the lapped bars and

f_y is the mean value of the yield strength of the lapped bars in MPa and

a_{sl} is the coefficient that equals 1 if the slippage of the longitudinal bars from its anchorage zone beyond the section of maximum moment is possible, or 0 if it is not.

Eq. (3) and (4) indicate that L_{pl} of reinforced concrete members under monotonic loading is 1.5 times larger than in case of cyclic loading.

Plastic hinge length can be specified with widely used Pauley and Priestley equation:

$$L_{pl} = 0.08L + 0.022d_{bl}f_y \tag{5}$$

where:

L is the length of member.

In EN 1998-3, two expressions for determining the plastic hinge length are given, depending on the concrete confinement models (according to EN 1992-1 and EN 1998-3), both for the case of cyclic loading L_{pl} may be calculated for the confined concrete models according to EN 1998-3, from the following expression:

$$L_{pl} = \frac{L_v}{30} + 0.2h + 0.11\frac{d_{bl}f_y}{\sqrt{f_c}} \tag{6}$$

where:

$f_c$isconcrete compressive strength in MPa.

Eq. (1) and (2) are the best among the possible simple expressions, since L_{pl} is given as a function of the shear span ratio (L_v/h) and the cross-section depth. The longitudinal bar

properties are included in Eq. (3), (4), (5) and (6) in order to take into account the additional rotation of the plastic hinge due to slippage.

3. CAPACITY MODELS ACCORDING TO EN 1998-3

The ultimate deformation of RC section or member is conventionally identified as the post-ultimate strength point of the lateral load-deformation response, where any increase in the imposed deformations cannot increase the resisting force above 80% of the ultimate strength [5]. A section will reach the ultimate condition whenthe ultimate elongation in the tensile reinforcement is reached, or when the ultimate strain inthe extreme compressed concrete fibers is reached.

The primary deformation measure in EN 1998-3 is the chord rotation θ of a member over the shear span. This measure captures the behavior of the member as a whole, relates readily to more global measures of seismic response, such as story drifts, while at the same time,it can point to failure at the local level [6].The chord rotation is defined as the angle between the tangent to the axis at the yielding end and a chord that connects that end with the end of the shear spanL_v. The chord rotation is also equal to the element drift ratio, i.e. the deflection at the end of the shear span with respect to the tangent to the axis at the yielding end, divided by the shear span.

The values of ultimate chord rotation θ_{um} can be obtained from theoretical assumptions or based on experimental results. Pure empirical expression was developed by Panagiotakos and Fardis (2001) [6] for shear span ratios in range 2–6.5. They noticed that for the shear span ratio greater than 6, empirical expression overpredicts θ_{um}, as the lack of inclined cracking for such values of the shear span ratio reduces overall deformations. Almost equivalent expression was obtained on the basis of large database of test results, by Biskins (2007) and Biskins and Fardis (2004, 2007). [3] This expression refers to chord rotation of members with rectangular compression zone and detailing for earthquake resistance, in case of flexure controlled failure:

$$\theta_{um} = a_{st}\left(1-0.43a_{cy}\right)\left(1+\frac{a_{sl}}{2}\right)\left(1-0.42a_{w,r}\right)\left(1-\frac{2}{7}a_{w,nr}\right)\cdot$$
$$\cdot 0,3^{\nu}\cdot\left[\frac{\max\left(0,01;\omega'\right)}{\max\left(0,01;\omega\right)}\cdot f_c\right]^{0,225}\cdot\left(\min\left(9;\frac{L_v}{h}\right)\right)^{0,35}\cdot 25^{\left(\alpha\cdot\rho_{sx}\cdot\frac{f_{yw}}{f_c}\right)}\cdot 1,25^{100\cdot\rho_d} \tag{7}$$

where:

a_{st} is the coefficient dependent on the steel type, 0.0185 for ductile hot rolled or heat-treated steel and 0.015 for cold-worked steel,

a_{cy} is the zero-one variable for the type of loading, 0 for monotonic and 1 for cyclic loading,

$a_{w,r}$ is the zero-one variable for rectangular walls, 1 for rectangular walls and 0 otherwise,

$a_{w,nr}$ is the zero-one variable for non-rectangular walls, 1 for walls with T-, H-, U- or hollow rectangular section and 0 for other members,

$\nu = N/bhf_c$ where b is width of compression zone and N is the axial force,

ω, ω' are mechanical reinforcement ratios of tension and compression longitudinal reinforcement, respectively

α is effectiveness factor for confinement by transverse reinforcement,
ρ_{sx} is ratio of transverse steel parallel to the loading direction, and
ρ_d is steel ratio of diagonal reinforcement in each diagonal direction.

An increase of shear span ratio results in an increase in capacity of ultimate chord rotation (as well as the plastic hinge length), but only upto certain values, and this is taken into account in Eq. (7).

Depending on the type of steel, slipping of longitudinal bars and in case of cyclic loading, this expression was adopted in EN 1998-3 as the total ultimate chord rotation capacity:

$$\theta_{um} = \frac{1}{\gamma_{el}} 0,016 \cdot 0,3^{\nu} \cdot \left[\frac{\max(0,01;\omega')}{\max(0,01;\omega)} \cdot f_c \right]^{0,225} \cdot \left(\frac{L_v}{h} \right)^{0,35} \cdot 25^{\left(\alpha \cdot \rho_{sx} \cdot \frac{f_{yw}}{f_c}\right)} \cdot 1,25^{100 \cdot \rho_d} \tag{8}$$

where:

γ_{el} is 1.5 for primary seismic members and 1.0 for secondary ones. Value $\gamma_{el} = 1.0$ corresponds to mean values, and for $\gamma_{el} = 1.5$ that equation is conservative for primary seismic members.

According to Eq. (6) and (7), chord rotation capacity is 1.75 time greater in case of monotonic loading in relation to cyclic loading.

Member deformation capacity depends on its geometric and mechanical properties. In increasing this capacity, the shear-span ratio seems to be the most important, as well as the ratio of compression-to-tension reinforcement and concrete strength f_c. The amount of confining reinforcement is less important [6].

4. NUMERICAL EXAMPLES

In this paper, reinforced concrete columns, 3 m high, with cross-sectional dimensions 40 x 40 cm, were analyzed, in order to estimate the ultimate value of the chord rotation due to monotonically increasing horizontal force. Concrete grade C30/37 and steel type C500 were specified for the columns.The four columns generated for the study have different longitudinal or transverse reinforcement, Fig.1. For all RC columns,the adopted axial load value was 0.2 and shear span ratio was 7.5 (belonging to a group of ductile members).

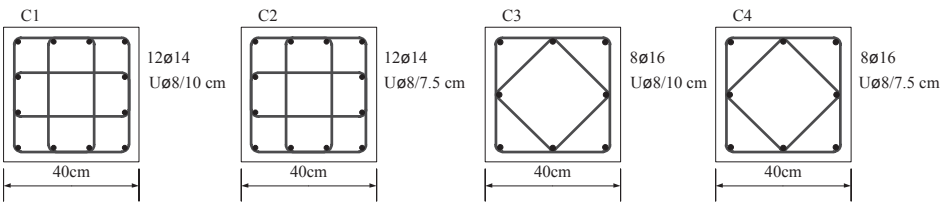

Figure 1 - Cross sectional dimensions of reinforced concrete columns specimens

The values of ultimate chord rotation capacity and plastic hinge lengthfor these columnswere obtained for cyclic loading according to EN 1998-3 (Eq. 8 and Eq. 6).In case of monotonic loading, the values of ultimate chord rotation capacity and plastic hinge length were determined based on Eq. 7 and Eq. 1.Table 1shows values of ultimate chord rotation. For

specimens C1 and C2, L_{pl} = 32 cm and for specimens C3 and C4, L_{pl} = 34 cm, for cyclic loading (C). In case of monotonic loading (M) for all models L_{pl} = 56 cm. The expression given in Eq. 5 does not take into account the type of load, andthe terms in Eq. 3 and Eq. 4 would produce higher values of the plastic hinge lengths in both load cases and they will not be taken into account in further analysis.

Table 1 – Ultimate chord rotation

	C1	C2	C3	C4
$\theta_{um,cyc}$	0.035	0.037	0.033	0.035
$\theta_{um,mon}$	0.061	0.065	0.057	0.061

Columns were modelled with force-based non-linear beam column element using OpenSees. [7]. A distributed and lumped plasticity models were used in the analysis of each specimen, taking into account different L_{pl} for each model. In the distributed plasticity model (DP), the number of integration points was chosen, and therefore, the locations, as well as the weights coefficients,were specified. The tip when choosing the number of integrating points is that the length of the part at the end of the element corresponds to the length of the plastic hinges. Gauss-Lobatto integration rule was assumed, and cases with 4 (approximately corresponding plastic hinge length for cyclic load) and 3 (approximately corresponding plastic hinge length for monotonic load) integration points were considered. In the concentrated plasticity model (CP), based on modified Gauss-Radau quadrature, with six integration points, plastic hinge length were exactly specified at the element ends. For each column, four models were analyzed, including two models of plasticity and two lengths of the plastic hinge (DP-C, DP-M, CP-C and CP-M).

In each integration point, cross section was presented with fiber model, which was defined with three kinds of fibers: unconfined concrete (cover), confined concrete (core) and reinforcement. The concrete was modelled by the uniaxial material Concrete01, steel was modelled by the uniaxial material Steel02. The stress-strain curves for concrete and steel for column C1 are shown in Fig.2. The strength of confined concrete, the strain that corresponds to this strength and the ultimate strain of the extreme fiber of the compression zone were adopted according to EN 1998-3 Annex A. Geometric nonlinearity was taken into account through the P-Δ effect.

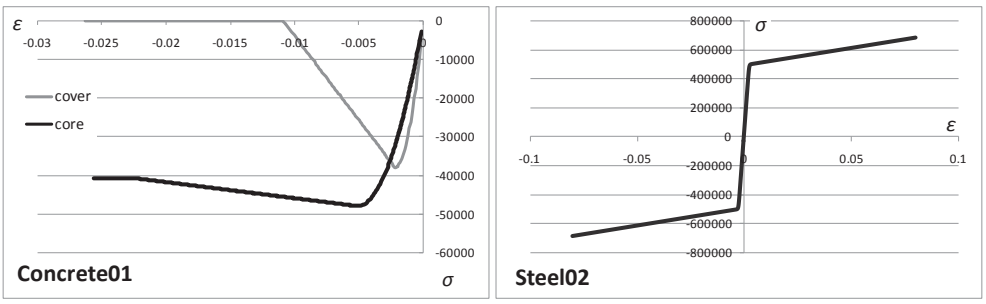

Figure 2 - Stress-strain curves for concrete and steelfor column C1

The ultimate chord rotation for different models of considered columns was estimated for global ultimate limit state reached at 20% drop of the lateral resistance in force displacement curve. Fig. 3 shows force-displacement curves and moment-chord rotation curves for different models of column C1. The dots, marked on curves, present the ultimate values. For other column specimens, force-displacement and moment-chord rotation curves are very similar. Force-displacement response primarily depends on the plastic hinge length. CP-M is the model with the greatest plastic hingelength and such model can perform ductile behavior.

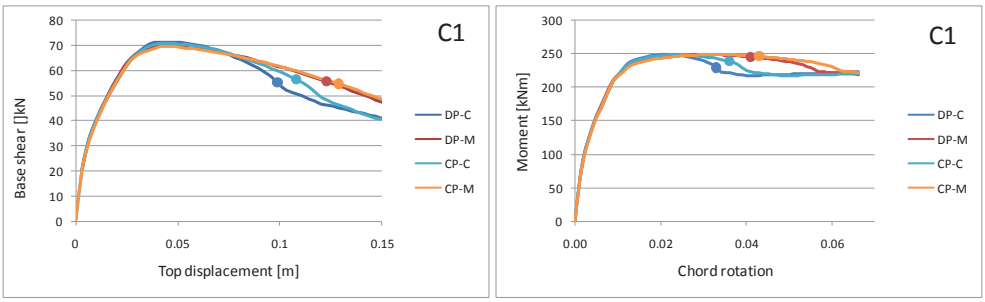

Figure 3 - Force-displacement and moment-chord rotation curves for different models of column C1

Figure 4 shows the estimated values of the ultimate chord rotation for different models of column specimens. There is no significant difference in these values between the columns being considered. Models with larger plastic hinge lengths (calculated from the expression for monotonic load) give higher values of estimated ultimate chord rotations. Except for the DP-C model, all estimated values are greater than the capacity of the ultimate chord rotation according to EN 1998-3, i.e. for cyclic loads. All estimated values are lesst han the capacity calculated on the basis of the monotonic load expression.

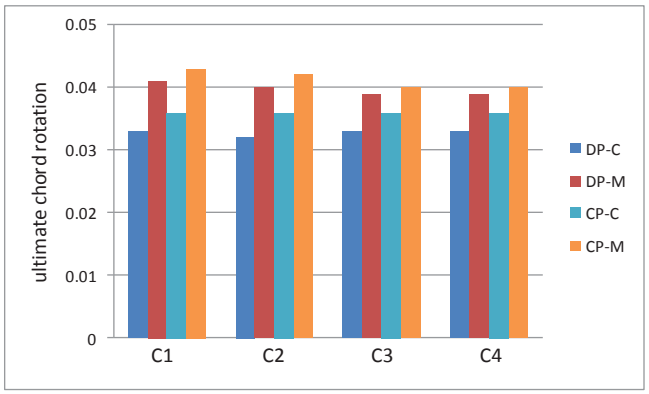

Figure 4 - Estimated values of θ_{um} for different models of column specimens

5. CONCLUSION

The provisions of Eurocode 8 part 3 prescribe that the deformation capacity of the elements is verified in terms of the chord rotation. In the paper, the estimated ultimate chord rotation of the column specimen, under monotonically increasing loads, has been compared with the appropriate capacity obtained forcyclic loading (EN 1998-3) and monotonic loading. All estimated values are less than the capacity calculated on the basis of the monotonic load expression. The reason for this can be twofold: a) as mentioned above, empirical expressions overestimate the value of θ_{um} in case when the shear span ratio is greater than 6 (for observed columns $L_v / h = 7.5$), b) the estimated capacity was determined based on the ultimate state of the element, and in doing so, the ultimate strains of the tensile reinforcement and/or the concrete extreme compression fibers were not reached, because the P-Δ effect had a significant influence on the nonlinear response of the column. Except for model with the lowest plastic hinge length, all estimated values are greater than the capacity of the ultimate chord rotation according to EN 1998-3, i.e. for cyclic loads. This observation corresponds to the above-mentioned fact that larger deformations occurrather due to monotonic than cyclic load. Determination of the chord rotation capacity of elements according on EN 1998-3 is questionable, when applying nonlinear static analysis, because the calculated capacities would be less than expected in a monotonically increasing load, but would certainly be conservative.

ACKNOWLEDGMENTS

The work has been done within the scientific research project TR 36043 "Development and application of a comprehensive approach to the design of new and safety assessment of existing structures for seismic risk reduction in Serbia", which is funded by the Ministry of Science of Serbia.

REFERENCES

[1] EN 1998-3:2005.: Design of Structures for Earthquake Resistance - Part 3: Assessment and Retrofitting of Buildings, CEN, Brussels, Belgium, 2005

[2] Yuan F., Wu Y-F.: Effect of load cycling on plastic hinge length in RC columns, Engineering Structures, Volume 147, 2017, 90-102.

[3] Fardis, M. N.: Seismic Design, Assessment and Retrofitting of Concrete Buildings, Geotechical, Geological and Earthquake Engineering, volume 8, Springer, Dordrecht, 2009.

[4] Scott M., Fenves G.: Plastic Hinge Integration Methods for Force-Based Beam-Column Elements, Journal of Structural Engineering, 132(2), 2006, 244-252

[5] Biskins, D. E., Fardis, M. N.: Deformations of Concrete Members at Yielding and Ultimate under Monotonic or Cyclic Loading (Including Repaired and Retrofitted Members), Report No. SEE 2009-01, Department of Civil Engineering, University of Patras, 2009

[6] Panagiotakos, T. B., Fardis, M. N.: Deformations of Reinforced Concrete Members at Yielding and Ultimate, ACI Structural Journal 98(2), 2001, 135-148

[7] Mazzoni, S., McKenna, F., Scott, M., Fenves, G. L. "OpenSees Command Language Manual." PEER Center, University of California, Berkeley, USA, 2007

ДГКС Друштво грађевинских конструктера Србије
ASES Association of Structural Engineers of Serbia
S-49
15. KONGRES
6-8. 9. 2018. Zlatibor

Marija M. Janakieska[1], Kiril Gramatikov[2], Manja K. Kuzman[3]

PROIZVODI NA BAZI DRVETA SA STANOVIŠTA ARHITEKATA U MAKEDONIJI

Rezime:

Drvna industrija u Republici Makedoniji ima dugu tradiciju pravljenja širokog spektra proizvoda. Danas se drvo uglavnom koristi za stambene objekte i krovne konstrukcije manjeg raspona; mada postoji izvesno interesovanje za primenu drveta na fasadama i u enterijeru zgrada. U ovoj studiji upoređujemo stavove i svest arhitekata o upotrebi EWP-a u Makedoniji. Studija je zasnovana na uzorku od 91 inženjera arhitekture koji su učestvovali u *online* anketi. Rezultati pokazuju da postoji pozitivan stav vezan za korišćenje drveta uopšte, pri čemu većina ispitanika veruje da će se obim njegove upotrebe u budućnosti povećati. Ovi podaci mogu ukazati na tržišne mogućnosti i mogu identifikovati prepreke za primenu EWP-a.

Ključne reči: EWPs, arhitekte, drvene konstrukcije, specifikacija materijala, Makedonija

ARCHITECTS' PERCEPTIONS OF ENGINEERED WOOD PRODUCTS IN MACEDONIA

Summary:

Wood industries in the Republic of Macedonia have a long tradition in producing a wide range of goods. Nowadays, wood is mainly being used for residential houses and limited roof constructions; although there has been certain interest in using wood on the facades or as an interior application in buildings. In this study, we compare architect attitudes and awareness regarding the usage of EWPs in Macedonia. It is based on a sample of 91 architects using on-line surveys. Results suggest that there is a positive perception regarding the usage of wood in general, with the majority of respondents believing that its usage will increase in future. These findings can implicate market opportunities and can identify barriers to EWPs adoption.

Keywords: EWPs, architects, timber construction, material specification, Macedonia

[1] *PhD candidate, Faculty of Civil Engineering, Department on Concrete and Timber Structures, University "Sts. Cyril & Methodius", Skopje, Macedonia, e-mail:marija_mls@hotmail.com*
[2] *Professor PhD, Faculty of Civil Engineering, Department on Concrete and Timber Structures, University "Sts. Cyril & Methodius", Skopje, Macedonia, e-mail: gramatikov@gf.ukim.edu.mk*
[3] *Assoc. Prof. PhD, University of Ljubljana, Department of Wood Science and Technology, Biotechnical Faculty, Jamnikarjeva 101, 1001 Ljubljana, Slovenia, e-mail: manja.kuzman@bf.uni-lj.si*

1. INTRODUCTION

Growing environmental awareness presents one of the most important advantages for wood being used as a construction material, where the choice is motivated by the fact that wood is a renewable material and that its use reduces CO_2 emissions - provided that the raw material is harvested in forests where sustainable forestry is practiced including replanting and adoption of management plans [1]. The introduction of new products in the construction sector, however generally meets up scepticism, hesitation, low awareness, and high uncertainty in the marketplace; therefore, the communication of information is vital to market success [2-4]. There are demand stimulants: efficiency improvements in existing buildings and renovations; improved specialized training; efforts to make the sector more attractive in terms of research and innovation; and a greater active uptake of new technologies.

In Europe, the wood products sector plays a pivotal role in the development of a sustainable society, where economic, environmental, social and cultural aspects of using natural resources are taken into account [5]. In this context, wood-based products are also the most preferred building materials in terms of energy-efficient construction [6, 7].

Many building material selection choices are guided by a desire to minimize their negative impacts, either on the occupants or on the environment [8]. To specifiers such as architects, new materials present both opportunities and risks. While opportunities derive from new or improved technical performance or aesthetic qualities, risks lie in the lack of design or manufacturing experiences [9].

1.1. ENGINEERED WOOD PRODUCTS (EWPs)

In the past two decades, a new class of structural wood products has been developed to form the basis for a range of building solutions that are increasingly functional, based on a combination of performance and sustainability characteristics. This has been possible because of the new industrial processes that provide increased dimensions and superior engineering properties for structural products that can use manufacturing residues and lower-grade and smaller diameter trees as feedstock. The result is a category of products broadly known as EWPs which are increasingly be adopted in architectural design and building applications [10, 11].

To date, the literature is lacking in studies that specifically examine a comprehensive understanding of architect perceptions related to EWPs. As such, we selected architects as the key target group in this research effort as they are key decision makers in the selection of materials in the construction sector.

The construction industry is the consumer of EWPs. Some of the key products in this family of materials are shown in Table 1.

In Macedonia, the wood sector has a very long tradition and has always been an important segment of country economy. To get a better picture of the importance of the forest sector, some additional information regarding relevant forestry statistics are presented in Table 2.

Table 1 –Selected Engineered wood products (EWPs)

GLT Glulam-glued laminated timber	**CLT** Cross-laminated timber	**PSL** Parallel strand lumber	**LSL** Laminated strand lumber
LVL Laminated veneer lumber	**SWP** Solid wood panel	**PW** Plywood	**LDF/MDF/HDF** Low/medium/high-density fiberboard
VP Veneered particleboard	**PB** Particleboard	**OSB** Oriented strand board	**LS** Light sandwich (honeycomb) panels
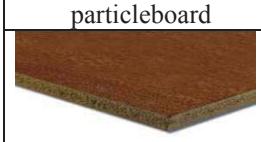			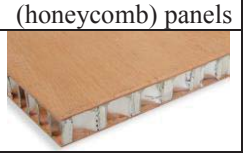

Table 2 – Macedonia – Selected Forestry Data, 2015 (Government Statistics)

Surface area of forested land (ha)	$1.09 \cdot 10^6$
Forested area (%)	42%
Number of naturally occurring tree species	319
Growing stock (m^3)	$75.94 \cdot 10^6$
Annual growth of growing stock (m^3forest)	$1.62 \cdot 10^6$
Annual harvest (m^3 forest)	$1.09 \cdot 10^6$
Hardwoods (m^3)	-
Softwoods (m^3) **Sawn wood**	-
Consumption Per Capita (m^3/y)	0.1

Unfortunately, in the last 2-3 decades the Republic of Macedonia has experienced many economic and social changes that either directly or indirectly influenced the wood industry sector. In Macedonia, wood is often used only for small residential houses, or limited roof construction or canopies; although there has been recent interest in using wood on the facades of buildings and in the interior applications due to demand for enhanced aesthetic appearance. Macedonian architects are trying to implement wood in their designs, but only as a decorative material with the most used constructive material being concrete. Table 3 identifies the key differences in wood-based construction in Macedonia.

Table 3 – Wood-based Construction Macedonia

Share of detached houses in residential construction [%]	n.a
Market share of wood in detached houses [%]	2-5
Market share of wood in multi-story construction [%]	-
Maximum number of floors allowed from wood, with sprinklers, in 2014	3
Key wood construction techniques	Timber panel Traditional timber-frame Massive-timber
Organizations promoting wood at national levels	University "Ss. Cyril and Methodius", Faculty of Civil Engineering – Skopje; Building companies
Sawn wood consumption per capita [m^3/y]	0.1

We suggest that the absence of comprehensive promotion of the wood sector can be significantly explained by the lack of understanding by the aforementioned members of the wood value chain from the forest to building construction. In this research, we test the level of understanding, awareness, and potential use of EWPs technologies for structural and non-structural building applications from the perspectives of architects, an area that has not previously been researched to any significant degree.

2. THE STUDY

2.1. OBJECTIVES

The overarching goal of this study is to identify architects` perceptions regarding potential advantages/benefits and disadvantages/challenges in specifying EWPs. Based on these perceptions, we hope to identify communication mechanisms and messaging to increase architect understanding of EWPs. Changing specifier preferences regarding the positive attributes of EWPs may greatly affect the market structures for wood products that, in turn, impact demand, supply, opportunities for manufacturers, increasing employment, and overall local, regional, and national economic development.

2.2. METHODS

A survey questionnaire was constructed and developed by an international group of architects as a part of a larger survey. The study methods included a two-stage survey; in the first stage, personal interviews were conducted, and then, based on input from these in-person interviews, the second stage an exploratory web-based survey was designed. The survey questionnaire was in English.

The target population of the survey included practicing architects' members of Chamber of Certified Architects and Certified Engineers of the Republic of Macedonia. Respondent data were collected through the on-line survey (the instrument was programmed in 1ka, a free web

survey software developed by the Centre for Social Informatics at Faculty of Social Sciences, University of Ljubljana); random sampling of these association populations was used. Based upon similar studies [12, 13, 14, 15] a response rate of 15-35% is considered adequate for analytical purposes for business/corporate surveys. Taking into account an expected response rate within this range and a sampling error of 10% [16] we sent out 320 questionnaires. In Macedonia, the survey process took place from late May 2017 to mid-June 2017. Two e-mail survey reminders followed the initial mailing. The first reminder was sent one week after the original mailing and the second two weeks after the first reminder. We received 91 responses. Taking into account non-deliverables (e.g., invalid emails addresses or out-of-business firms); the response rates was 28%.

The questionnaire was divided into four parts. The first part contained questions about general perceptions and familiarity of architects with EWPs. The second part covered questions regarding their specifications of non-load and load-bearing systems, followed by the third part with questions on information sources and information needs of architects. The last part included demographic questions about respondent gender, country, profession and experience.

When ranking the familiarity and characteristics of EWPs, the Modified Borda Count was used. In this case, each respondent has to choose 5 (or 3) top options and rank these options in order of familiarity. Likert-type response scales, ranging from not important (1) to important (3), were used when asking about the importance of different ways of getting information about EWPs.

3. RESULTS AND DISCUSSION

About 90% of all respondents work with architecture, followed by 5% of respondents working with building construction, while the remainder work in project management, interior design and structural engineering. Respondents had an average of 5-15 years of experience, 38% men and 62% women.

3.1. GERERAL PERCEPTIONS AND FAMILIARITY OF EWPs

From the list provided, including photos, respondents were asked to identify which EWPs they were most familiar with; the possible selection products are listed in Table 4. The cells reflecting a percentage higher than 80% are coloured orange. In general, the overall familiarity with EWPs is relatively high.

The most common EWPs familiarity in Macedonia are structural GLT, SWP, PW, OSB – over 90% respondents from Macedonia note familiarity with these products. CLT, PB, and VP are also well known by respondents, less known are PSL, LVL and LSL. Respondents also selected the five most familiar EWPs. We used a method called the Modified Borda count, where the most familiar EWPs gets 5 points, the second most familiar 4 points… and the fifth most familiar, 1 point. The EWPs with the highest sum of points was placed first. As seen in Table 5, the first five ranked EWPs are coloured orange. In Macedonia OSB is ranked first, followed PW and GLT.

Table 4 – Respondent familiarity with EWPs

	GLT	CLT	PSL	LSL	SWP	LVL	PW	LDF/ MDF / HDF	VP	PB	OSB	LS
No	6	18	25	37	6	23	7	13	17	18	3	40
	6.60 %	19.80 %	27.50 %	40.70 %	6.60 %	25.30 %	7.70 %	14.30 %	18.70 %	19.80 %	3.30 %	44.00 %
Yes	85	73	66	54	85	68	84	78	74	73	88	51
	93.40 %	80.20 %	72.50 %	59.30 %	93.40 %	74.70 %	92.30 %	85.70 %	81.30 %	80.20 %	96.70 %	56.00 %

Table 5 – Respondent familiarity with Top 5 Ranked EWPs

	GLT	CLT	PSL	LSL	SWP	LVL	PW	LDF/ MDF /HDF	VP	PB	OSB	LS
points	254	49,5	45,8	42,1	237,7	112,3	286,8	107,4	98,7	43,6	292,9	74,8
ranks	3	11	12	14	4	5	2	6	8	13	1	10

Respondents were asked if they think there has been an increased use of new EWPs in the last 5 years. 35% think that the use has increased, while more than 50% think it remained the same.

Further on, respondents were asked to identify their clients' perceptions of EWPs. Their responses suggest that clients in Macedonia generally want to have more information about EWPs. Additionally, around 5% from Macedonia believe that their clients are not interested in EWPs.

3.2. USE OF EWPs IN NON-LOAD AND LOAD – BEARING SYSTEMS

Respondents were also asked to select building components where they specify/use EWPs in non-load bearing systems such as roofing, windows, flooring, exterior/interior surfaces and stairs (Figure 1). EWPs were ranked highest for interiors, followed by flooring. Use of EWPs in exterior surfaces and windows was low – respondents ranked them last.

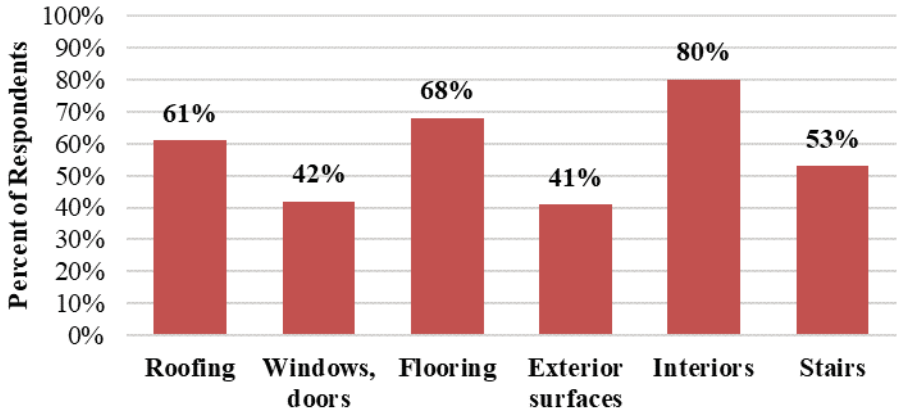

Figure 1 - Respondent specification/use of EWPs in non-load bearing systems

In addition, interest in the most frequently used load-bearing systems among architects in Macedonia (Figure 2). Over 40% of the respondents indicated in the first place light frame followed by the engineering frame system. The results show the share of log construction is also quite high in Macedonia.

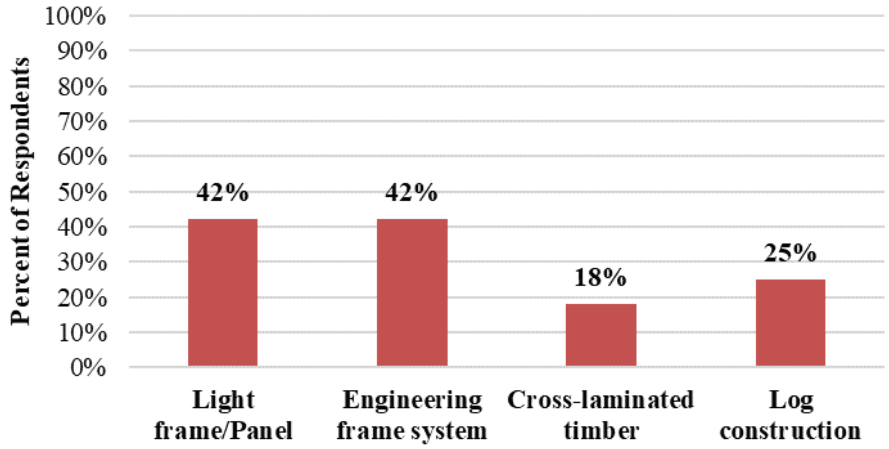

Figure 2 - The specification/use of EWPs in load bearing systems

Respondents were next asked to select the type of building where they use the most EWPs (Figure 3). They reported the most usage with residential buildings (70%). However, less than 30% Macedonian respondents used/specified EWPs with mixed-use buildings.

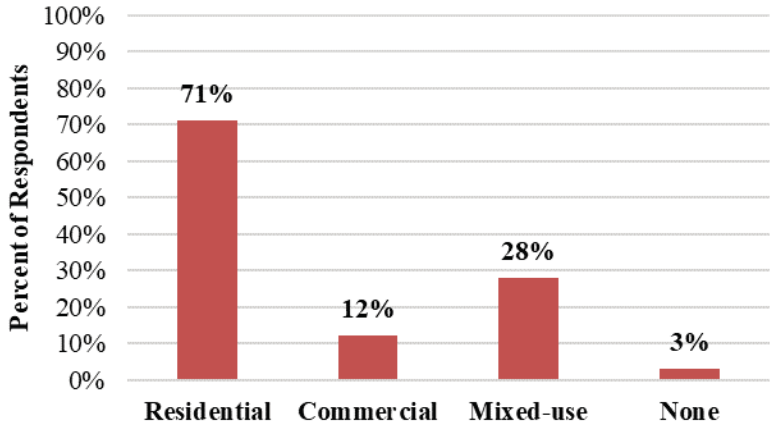

Figure 3 - Usage/Specification of EWPs in different types of buildings

3.3. INFORMATION SOURCES AND NEEDS OF ARCHITECTS / PROMOTIONAL METHODS

Given the importance of learning about products on the job, respondents were queried about various methods of obtaining information to support their firms and profession. The respondents were asked to select a number from 1 to 3, where 1 reflected the information source was not important, while 2=somewhat important, and 3=very important. Average response values by country are shown in Figure 4. The most important informational tool is the Internet, followed by building companies and EWPs manufacturers.

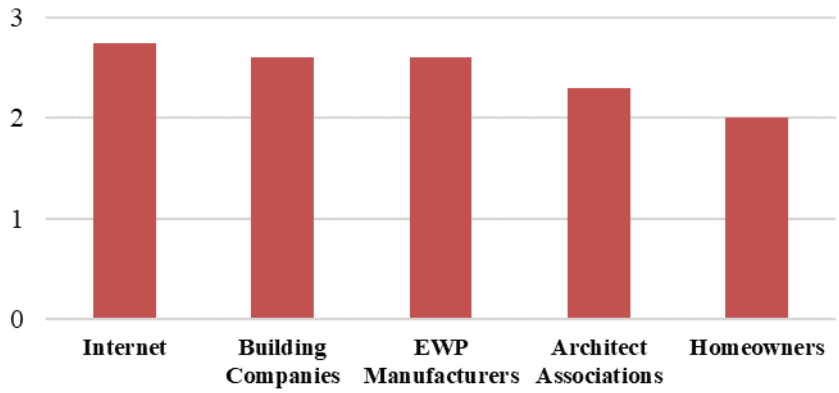

Figure 4 - Importance of various information sources: 1-Not important and 3- Important

Respondents were also asked about the effectiveness of various information sources in terms of learning about wood and wood products relative to architectural applications. It was noted that obtaining information through technical specifications was the top rated preference,

followed by contact with manufacturers, visits to building sites and visits to completed structures.

4. CONCLUSION AND DISCUSSIONS

The objective of this study was to better understand architects' perception of EWPs and identify factors that positively contribute to the likelihood EWPs usage/specification could increase in Macedonia. An online survey was conducted to collect data from over 91 respondents.

The results show that there is a positive perception in terms of familiarity with different EWPs in Macedonia. The most common applications are structural (GLT, SWP, PW, OSB). In terms of architects' opinion on whether there has been increased use of new EWPs in the last 5 years, in Macedonia they think that it has remained the same - a finding in line with architect's experiences in timber building. There is in general a lack of knowledge of the principles of design options in using timber for structural performance. Most architects reported building residential buildings in wood, but that an era of multi-story buildings is coming in the future. The second research aimed to characterize information sources used by architects as well as the perceived value of these sources- the internet is clearly the leading source of information.

The third objective was to characterize the information needs of architects. Respondents first note a need for more technical information to understand the potential of EWPs, followed by visits to buildings sites and visits to build objects. Architects could be good advocators for an increased use of EWPs but increased efforts must be placed to increase their knowledge. Demonstration projects are vital to show the various actors teamwork with EWPs in practice; e.g. collaboration among representatives of the wood industry, architects, builders and housing associations, to better understand the technical and the business potential of wood as a multi-purpose building material.

Using the information obtained in this study will contribute to an understanding of the probability that innovative bio-based building materials with minimal environmental impact are chosen in residential and non-residential buildings, as well as high-rise buildings, and to a greater understanding of the drivers of and barriers to increased use. Change is difficult – the barriers to wood are complex and the building industry is both averse to risk and slowed by inertia – but with the right focus, the wood industry can make a difference, while using EWPs can create new business opportunities for the construction industry by using validated material solutions and design tools. As the authors believe that the increased use of EWPs may be an important element of a more sustainable future built environment, more information about use and perceptions is needed.

REFERENCES

[1] M.H. Ramage, H. Burridge, M. Busse-Wicher, G. Fereday, T. Reynolds, D.U. Shah, G. Wu, L. Yu, P. Fleming, D. Densley-Tingley: The wood from the trees: The use of timber in construction, Renewable and Sustainable Energy Reviews 68, 2017, 333-359.

[2] P. Malaval, Stratégie et gestion de la marque industrielle: Produits et services business to business, Publ. Union 1998.

[3] F. Robichaud, R. Kozak, A. Richelieu, Wood use in nonresidential construction: A case for communication with architects, Forest Products Journal 59(1/2), 2009, 57-65.

[4] E. Hansen, E. Nybakk, When innovativeness determines market orientation: the forest sector and the Great Recession, BioProducts Business 1(1), 2016, 1-12.

[5] O. Høibø, E. Hansen, E. Nybakk, Building material preferences with a focus on wood in urban housing: durability and environmental impacts, Canadian Journal of Forest Research 45(11), 2015, 1617-1627.

[6] M. Kitek Kuzman, D. Sandberg, A new Era for Multi-Storey Timber Buildings in Europe'In: 70th FPS International convention June 27-29, Portland, US, 2016.

[7] M. Kitek Kuzman, D. Sandberg, Comparison of timber-house technologies and initiatives supporting use of timber in Slovenia and in Sweden-the state of the art, iForest-Biogeosciences and Forestry 10(6), 2017, 930-938.

[8] A. Sinha, R. Gupta, A. Kutnar, Sustainable Development and Green Buildings, Wood Industry/Drvna Industrija 64(1), 2013, 45-53.

[9] M.F. Ashby, K. Johnson, Materials and design: the art and science of material selection in product design, Elsevier, Oxford, 2002.

[10] K. Jones, J. Stegemann, J. Sykes, P. Winslow, Adoption of unconventional approaches in construction: The case of cross-laminated timber, Construction and Building Materials 125, 2016, 690-702.

[11] D. Sandberg, Additives in Wood Products—Today and Future Development, Environmental Impacts of Traditional and Innovative Forest-based Bioproducts, Springer, 2016, pp. 105-172.

[12] R.A. Kozak, D.H. Cohen, Architects and structural engineers: An examination of wood design and use in nonresidential construction, Forest products journal 49(4), 1999, 37.

[13] J. O'Connor, R. Kozak, C. Gaston, D. Fell, Wood use in nonresidential buildings: opportunities and barriers, Forest products journal 54(3), 2004, 19-28.

[14] K. Hemström, K. Mahapatra, L. Gustavsson, Perceptions, attitudes and interest of Swedish architects towards the use of wood frames in multi-storey buildings, Resources, conservation and recycling 55(11), 2011, 1013-1021.

[15] D.T. Damery, P. Fisette, Decision making in the purchase of siding: A survey of architects, contractors, and homeowners in the US northeast, Forest Products Journal 51(7/8), 2001, 29-36.

[16] D.A. Dillman, Mail and Internet surveys: The tailored design method--2007 Update with new Internet, visual, and mixed-mode guide, John Wiley & Sons 2011.

ДГКС Друштво грађевинских конструктера Србије
ASES Association of Structural Engineers of Serbia
S-50
15. KONGRES
6-8. 9. 2018.Zlatibor

Ksenija Janković[1], Dragan Bojović[2], Marko Stojanović[3], Iva Despotović[4], Ljiljana Lončar[5]

BETONSKI BLOKOVI I PLOČE ZA POPLOČAVANJE SA RECIKLIRANIM AGREGATOM IZ PREFABRIKACIJE

Rezime:

U ovom radu je prikazana mogućnost korišćenja recikliranog agregata iz betonskih blokova i ivičnjaka u proizvodnji betonskih elemenata za trotoare. Eksperimentalni rad uključuje nekoliko vrsta betona napravljenih sa različitim količinama cementa i recikliranog agregata od betona. Na osnovu rezultata ispitivanja pretpostavljeno je da je moguće izraditi betonske blokove i ploče u skladu sa evropskim standardima. Rezultati pokazuju da se zamenom prirodnog agregata, agregatom od drobljenog betona mogu proizvesti betonski elementi koji ispunjavaju zahtjeve EN 1338 i EN 1339, ali klasa zavisi od procenta zamene prirodnog agregata recikliranim.

Ključnereči:agregat od recikliranog betona, blokovi za popločavanje, ploče za popločavanje

CONCRETE PAVING BLOCKS AND FLAGS MADE WITH RECYCLED AGGREGATE FROM PRECAST ELEMENTS

Summary:

The possibility of using recycled aggregate from precast paving blocks and curbs in the production of concrete elements for the pedestrian areas is shown in this paper. Experimental work has included few types of concrete made with different amounts of cement and recycled concrete aggregate. Based on the testing results it was assumed that it is possible to produce the concrete paving blocks and flags comply with European standards. The results show that replacing natural aggregate with crushed concrete aggregate produces concrete elements which meet the requirements of EN 1338 and EN 1339, but class depends of percent of replacement natural aggregate by recycled.

Key words: recycled concrete aggregate, paving blocks, paving flags

[1]*PhD, principal research fellow, IMS Institute, Bul. vojvode Mišića 43,Belgrade, ksenija.jankovic@institutims.rs*
[2]*PhD,research assistant, IMS Institute,Bulevar vojvode Mišića 43,Belgrade, e-mail: dragan.bojovic@institutims.rs*
[3]*MSc,research assistant, IMS Institute,Bulevar vojovde Mišića 43,Belgrade, e-mail: marko.stojanovic@institutims.rs*
[4]*PhD, Research Associate, Belgrade University College of Apllied Studies in Civil Engineering and Geodesy, Hajduk Stankova 2, Beograd, ivickad@gmail.com*
[5]*BScCE,profess. adviser, IMS Institute,Bulevar vojvode Mišića 43,Belgrade, e-mail: ljiljana.loncar@institutims.rs*

1. INTRODUCTION

One common means for achieving a more environmentally-friendly concrete is crushing concrete to produce coarse aggregate for the production of new concrete. In this way the consumption of natural resources as well as the disposal of waste concrete in landfills is reduced. As the matter of fact, the use of recycled-aggregate concrete is becoming increasingly interesting in civil construction as regards to sustainable development. Many studies show that it is possible to use crushed concrete as coarse aggregate, which has already been accounted for in the regulations of many countries [1].

Research showed that up to 30% coarse or 20% fine recycled concrete-derived aggregate had no effect on the concrete strength [2]. Concrete made with recycled aggregate (RA) or recycled concrete aggregate (RCA) also needs to be tested in order to confirm that it has adequate freeze–thaw and sulphate resistance for its intended use. The maximum strength class of concrete made with RCA should not be more than C50 [2].

Results of the investigation of Poon et al. show that the production of non-structural precast concrete blocks is possible with low grade recycled aggregate [3]. By combining recycled aggregate of brick and concrete (50:50%) it is possible to produce concrete for paving for pedestrian areas and (25:75%) for traffic [4].

In the production of precast concrete elements there are some mistakes in production which result in products that do not have certain required properties. Such products cannot be used and they most often end up at the landfill. One of the ways to reduce the formation of landfills is recycling. By crushing concrete aggregate from the concretes obtained, which can be used as a component material in the production of concrete after being fractionated.

Comparing previous test results of concrete paving blocks and flags made of ordinary concrete and properties of concrete with recycled concrete as aggregate it can be concluded that this kind of concrete can be used for the production of elements for pedestrian areas [5].

The aim of this paper is application of recycled concrete in the production of paving elements. Some properties of concrete made with different replacement level of natural aggregate by recycled concrete (25 and 100%), such as compressive strength, water absorption, density, were done. Testing results of concrete paving flags and blocks according to EN 1338 and EN 1339 were presented.

2. EXPERIMENTAL WORK

Two referent types of concrete with crushed aggregate were prepared (Table 2). Recycled aggregate concrete were designed in such a way that coarse aggregate (fractions 4/8 and 8/16 mm) was replaced with 25 and 100% recycled concrete aggregate.

Concrete were made using CEM II/B-S 42.5 N.

The recycled aggregate was obtained by crushing damaged prefabricated elements made of concrete consistency S1, a class of strength C 35/45. After the crushing, concrete was separated into fractions 0/4 mm, 4/8 mm and 8/16 mm. Particle size distribution is shown in Table 1.

Table 1 – Particle size distribution

Fraction mm	Sieve size (mm)									
	0.125	0.25	0.5	1	2	4	8	16	31.5	45
0/4	9.8	17.2	29.5	51.9	86.9	99.9	100.0	100.0	100.0	100.0
4/8				0.2	0.2	1.0	94.0	100.0	100.0	100.0
8/16				0.1	0.1	0.1	2.4	94.2	100.0	100.0

Table 2 - Concrete mix proportion

Concrete mixture	C1	C2
Cement [kg/m3]	330	320
Water-cement ratio W/C	0.40	0.40
Aggregate-cement mix ratio A/C	5.7272	6.0469

Workability is not important for precast elements, so required consistency measured by slump test was 1.0 cm. Water to cement ratio depends on percentage and fractions which were replaced by recycled concrete aggregate.

Concrete paving blocks and flags were made in steel moulds. Blocks and flags were produced in two layers. Facing layer is consist of quartz sand and cement. For blocks base layer concrete mixtures C1 and for flags mixtures C2 were used. Dimensions of blocks were 20x30x8 cm and 30x30x6 cm for flags.

The effective water-cement ratio is the same for all types concrete, but due to the increased absorption of water in the recycled aggregate, the amount of water increased from 3-15% depending on the mixtures used and the amount of recycled aggregate.

3. RESULTS AND DISCUSSION

3.1. CONCRETE PROPERTIES

The consistency of the fresh concrete was class S1 according to standard SRPS ISO 4103/1997.

The samples for testing concrete compressive strength were made. Concrete was compacted with vibration in metal cube-shaped molds with an edge length of d = 150 mm, and the samples were cured in water at a temperature of + 20 ° C until they were tested according to SRPS EN 12390-2 standard.

Testing of concrete compressive strength at the age of 3, 7, 14 and 28 days was carried out according to SRPS EN 12390-3 standard. Bulk density of hardened concrete was tested according to SRPS EN 12390-7 standard and ranged from 2350 to 2400 kg/m^3. The results of the testing are shown in Figures 1-2.

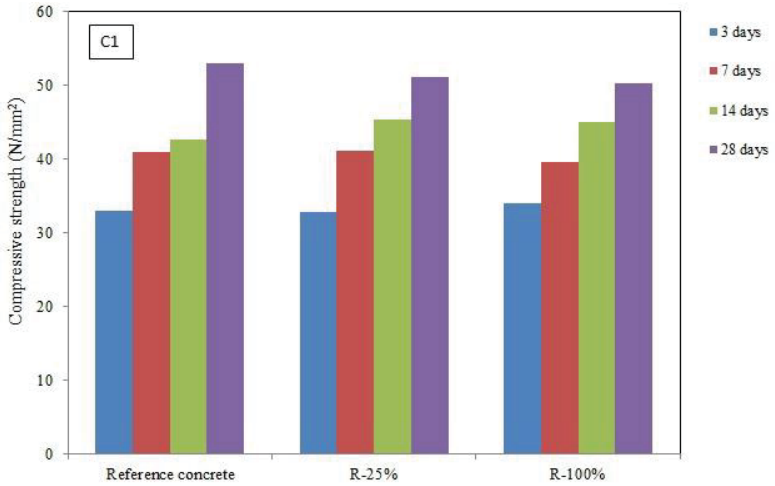

Figure 1 - Compressive strength of concrete C1

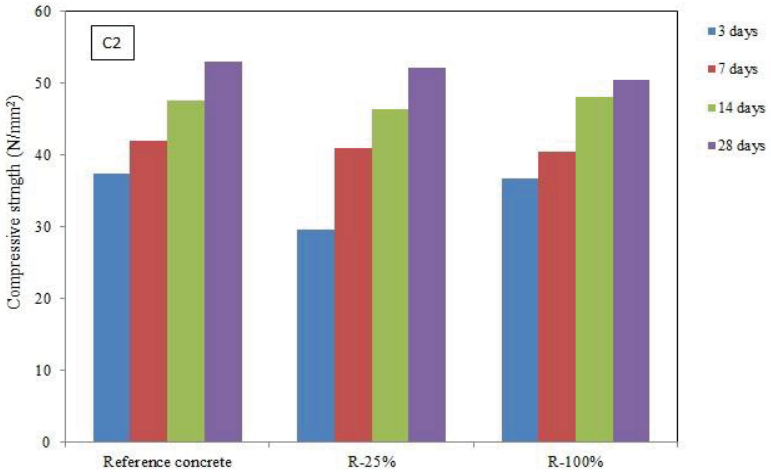

Figure 2 - Compressive strength of concrete C2

Water absorption of aggregate reflects to amount of water necessary to provide concrete with same consistency, i.e. for concrete with greater amount of recycled aggregate the required amount of water is greater. Properties of concrete depend of the quality of recycled aggregate. In this case, concrete which was used for the production of recycled aggregate had compressive strength class C 35/45. That is the reason why concrete with recycled aggregate had compressive strength which is not significantly different compared to reference concrete. All concrete types also satisfied compressive strength class C 35/45. For samples with 100% recycled coarse aggregate decrease of strength was 4%, while for samples with 25% recycled coarse aggregate decrease was only 2%.

3.2. CONCRETE PAVING BLOCKS AND FLAGS

Concrete paving blocks and flags were tested in terms of the following properties [6-7]:

- Weather resistance,
- Tensile splitting strength for blocks, bending strength for flags,
- Abrasion resistance.

Weather resistance is determined by tests for freeze – thaw resistance with de-icing salt and for water absorption. Abrasion resistance is determined by the Wide Wheel Abrasion test, or as an alternative by the Böhme test.

All types of concrete products had a water absorption of less than 6% and a loss of mass after the freeze / thaw cycle ≤ 1.0 kg/m^2 and meet the requirements for both Class 2 and Class 3 resistance to weather resistance.

For all types of concrete elements, the volume loss was ≤ 18 cm^3/50 cm^2 per Bohme test and met the wear resistance class 4.

The minimum tensile splitting strength for concrete paving blocks 20x30x8 cm according to EN 1338 was from 3.1 MPa to 3.6 MPa, and the characteristic tensile strength T ranging from 3.7 to 4.2 MPa, depending on the percentage a coarse natural aggregate replaced by a recycled concrete aggregate, 100% or 25%. Accordingly, all types of blocks met the standard criteria, since the characteristic tensile splitting strength T was greater than 3.6 MPa and a minimum ≥ 2.9 MPa.

The minimum tensile strength of the concrete paving flags 30x30x6 cm according to EN 1339 was 3.3 MPa and 3.8 MPa, and the mean 3.6 MPa and 4.4 MPa, depending on which percentage of the natural aggregate was replaced by the recycled concrete aggregate, 100 % or 25%. Accordingly, tile flags with 100% recycled large aggregate have met the criteria for bending strength class 1 according to EN 1339, since their minimum strength was greater than 2.8 MPa and the mean strengths greater than 3.5 MPa. The flags with 25% recycled coarse aggregate have met the criteria for bending strength class 2 according to EN 1339, since their minimum strength was greater than 3.2 MPa and a mean of 4.0 MPa.

4. CONCLUSIONS

The possibilities of using recycled concrete as aggregate for production concrete paving blocks and flags are presented in this paper. From the investigation results the following can be concluded:

- The concrete density decreased as the percent of recycled brick aggregate increased.
- The compressive and tensile splitting strength of concrete blocks and bending strength of paving flags decreased as the percent of recycled brick aggregate increased.
- Water absorption of the paving blocks and flags not exceeded the limit of 6%.
- Mass loss for all type of concrete blocks and flags after freeze/thaw test was≤ 1.0 kg/m^2, so it satisfied the requirements for the best class for weather resistance according to the European standards.
- Abrasion resistance of paving elements satisfy the requirements of the European standards
- It was possible to use up to 100% of recycled concrete as coarse aggregate to prepare concrete paving blocks which meet the requirements of EN 1338.

- The production of concrete paving flags is possible with recycled concrete as aggregate. The quality of elements depend of replacement level of natural aggregate. It is possible to get paving flags, according to EN 1339, bending strength Class 1 with 100% recycled concrete as aggregate and Class 2 for bending strength with replacement levels up to 25%.

Based on the obtained results it can be concluded that the use of aggregate from recycled concrete is possible. Concrete made with this type of aggregate can be used for the production of elements for pedestrian areas and various non-structural elements. In this way, the environment is protected, and the waste produced in its own production is re-used as a component material for concrete.

ACKNOWLEDGMENTS

We thank the company "BINIS", Banja Luka, which has enabled the realization of the experimental part of the paper.

The work reported in this paper is a part of the investigation within the research project TR 36017 "Utilization of by-products and recycled waste materials in concrete composites in the scope of sustainable construction development in Serbia: investigation and environmental assessment of possible applications" supported by the Ministry of Education, Science and Technological Development, Republic of Serbia. This support is gratefully acknowledged.

REFERENCES

[1] V. Corinaldesi, Mechanical and elastic behaviour of concretes made of recycled-concrete coarse aggregates, Construction and BuildingMaterials 2010: 24: 1616–1620.

[2] Soutsos M. N., Tang K., Millard S.G. Concrete building blocks made with recycled demolition aggregate, Construction and Building Materials 2011; 25: 726-735.

[3] Poon C.S., Kou S.C., Wan H.W., Etxeberria, Properties of concrete blocks prepared with low grade recycled aggregate, Waste Management 2009; 29: 2369-2377.

[4] Poon C.S., Chan D. Paving blocks made with recycled concrete aggregate and crushed clay brick, Construction and Building Materials 2006; 20: 69-577.

[5] Jankovic K., Loncar Lj.,Kacarevic Z., Romakov Z., Bojovic, D. Some experience of testing concrete blocks and kerbs according to EN and JUS, Proceedings of the international scientific-professional meeting "Civil engineering – science and practice", Žabljak, Serbia and Montenegro, 2006., Vol. 2, p. 539-544

[6] SRPS EN 1338:2012 Concrete paving blocks – Requirements and test methods, CEN

[7] SRPS EN 1339:2008, SRPS EN 1339:2008/AC: 2014 Concrete paving flags – Requirements and test methods, CEN

ДГКС Друштво грађевинских конструктера Србије
ASES Association of Structural Engineers of Serbia
S-51
15. KONGRES
6-8. 9. 2018. Zlatibor

Nikola Tošić[1], Snežana Marinković[2], Jorge de Brito[3], Nenad Pecić[4], Ivan Ignjatović[5]

DUGOTRAJNA SVOJSTVA ZELENIH BETONA: ISPITIVANJA NA NIVOU MATERIJALA I KONSTRUKTIVNIH ELEMENATA

Rezime:

Ekološki problemi koji nastaju usled proizvodnje betona se jedino mogu rešiti kroz upotrebu zelenih betona – betona sa recikliranim i otpadnim materijalima. Ovaj rad ima za cilj da predstavi rezultate ispitivanja dugotrajnih svojstava betona sa recikliranim agregateom, proizvedenog sa 100% krupnog agregata od recikliranog betona, betona sa velikim sadržajem letećeg pepela u kome leteći pepeo klase F čini 50% ukupnog vezivnog materijala i uporednog betona sa prirodnim agregatom. Za ove tri betonske mešavine je tokom 700 dana ispitano skupljanje i tečenje na betonskim prizmama kao i ugibi, dilatacije i prsline na armiranobetonskim prostim gredama tokom 700 dana pod opterećenjem. Rezultati ukazuju da se zeleni betoni mogu uspešno koristiti u konstrukcijske svrhe.

Ključne reči: reciklirani agregat, leteći pepeo, greda, skupljanje, tečenje, ugib

LONG-TERM PROPERTIES OF GREEN CONCRETE: TESTING AT THE MATERIAL AND STRUCTURAL LEVEL

Summary:

The environmental problems posed by the production of concrete can be solved namely by using green concrete produced with recycled and waste materials. This study intends to present results on the long-term properties of concrete produced with 100% coarse recycled concrete aggregate and concrete produced with 50% of class F fly ash in total cementitious materials and compare them with a companion natural aggregate concrete. The three concrete mixes were tested at the material level where shrinkage and creep were tested for 700 days on concrete prisms, and at the structural level where deflections, strains, and cracks of simply supported reinforced beams were tested under sustained load for 700 days. The results show that green concrete can be successfully used as structural concrete.

Key words: recycled concrete aggregate, fly ash, beam, shrinkage, creep, deflection

[1] *PhD, Teaching assistant, University of Belgrade, Faculty of Civil Engineering, ntosic@imk.grf.bg.ac.rs*
[2] *PhD, Full professor, University of Belgrade, Faculty of Civil Engineering, sneska@imk.grf.bg.ac.rs*
[3] *PhD, Full professor, Instituto Superior Técnico ,University of Lisbon, jb@civil.ist.utl.pt*
[4] *PhD, Assistant professor, University of Belgrade, Faculty of Civil Engineering, ivani@imk.grf.bg.ac.rs*
[5] *PhD, Assistant professor, University of Belgrade, Faculty of Civil Engineering, peca@imk.grf.bg.ac.rs*

1. INTRODUCTION

Modern Society and its rapid development in the twentieth century cannot be imagined without concrete, the most-produced material in the world [1]. However, the fact that it is produced in the amount of approximately 20 billion tons annually [2] causes significant impact on the environment. One of the main effects of concrete production is the depletion of natural resources, whether for the production of cement, in the amount of over 4 billion tons annually [3] (also causing significant CO_2 emissions), or natural river and crushed stone aggregates, in the amount of over 15 billion tons annually [4]. A second important impact is the construction and demolition waste (CDW) generated from building activities. According to Eurostat, the construction sector in Europe is responsible for generating 820 million tons of CDW annually [5], which is over 45% of the total amount waste generated. Within CDW, waste concrete is the major component, mostly being disposed of in landfills.

The only way to address these problems in the future is to search for sustainable alternatives to traditional concrete. The research community has been focusing on the use of waste and recycled materials in so-called green concrete, i.e. concrete with a lower environmental impact compared with traditional natural aggregate (cement) concrete (NAC).

One such solution is the use of recycled concrete aggregates (RCA) in the production of new concrete, called recycled aggregate concrete (RAC). RCA is obtained by recycling concrete waste in mobile or stationary recycling facilities, using a single- or multiple-stage crushing and sieving process, technologically similar to the production of crushed stone aggregates [6]. The product of concrete recycling, RCA, is a two-phase material consisting of natural aggregate (NA) particles and a certain amount of attached residual mortar from the parent concrete. This residual mortar has a significant effect on RCA properties, decreasing its density and increasing its porosity and water absorption [7].

Another approach in green concrete design is the reduction of cement use, typically through its replacement with certain industrial by-products with cementitious properties, e.g. fly ash, blast furnace slag. In countries such as Serbia, which still rely heavily on coal for the production of electricity [8], fly ash is the most promising option. One option is to use it in the production of so-called high-volume fly ash concrete (HVFAC) in which fly ash constitutes more than 50% of the total cementitious materials [8].

Both RAC and HVFAC have been studied extensively in previous years, but mostly at the level of short-term mechanical properties, and now increasingly, at the level of durability-related properties [9,10]. However, at the material level, significant knowledge is still lacking in the area of long-term properties of RAC and HVFAC, i.e. shrinkage and creep. Previous research has concluded that because RCA is usually weaker than NA, it provides less restraint for shrinkage and creep; hence, these properties are usually inferior in RAC compared with a companion NAC produced with the same effective water-cement (w/c) ratio. In the case of HVFAC, the effect of fly ash on shrinkage and creep is typically positive due to the smaller amount of cement paste. Both shrinkage and creep are found to be lower in HVFAC compared with a companion NAC [10]. Nonetheless, more research is needed in this area in order to integrate these types of concrete into standards and codes.

Unfortunately, even in the low amounts that they are used today, RAC and HVFAC are mostly relegated to non-structural use, which leads to down-cycling. The full potential of both

types of concrete can only be achieved if they are used in reinforced concrete, which makes up the majority of concrete produced in developed countries [1]. There is already a sufficiently large body of literature studying the structural behaviour of RAC and HVFAC. However, these studies focus almost exclusively on the short-term behaviour of reinforced RAC and HVFAC members and structures [11–14]. Research on the long-term behaviour of reinforced RAC and HVFAC members under sustained loads is still missing, namely the deflections of such members. This is especially important since serviceability models are not as reliable as ultimate state models [15]. Unfortunately, because of the difficulties associated with carrying out sustained load tests on beams, only a few experiments exist for RAC [16,17] and none for HVFAC.

With that in mind, the aim of this experimental program was to comparatively study the long-term properties of NAC, RAC, and HVFAC on the material and structural level. For this purpose, three concrete mixes were designed: NAC, RAC with 100% coarse RCA and HVFAC with 50% of fly ash in total cementitious materials. From the mixes, specimens were cast for testing basic mechanical properties as well as shrinkage and creep behaviour, and six simply supported reinforced concrete beams were produced for testing the long-term structural behaviour of these types of concrete under sustained load.

2. MATERIALS AND METHODS

2.1 MATERIALS

As NA in this study, river sand and gravel from the Danube were used in three particle sizes: I (0/4 mm) as sand, and II (4/8 mm) and III (8/16 mm) as gravel. RCA was produced by demolishing and crushing a 40 years old bridge near Belgrade. It was sieved into two coarse particle sizes: II (4/8 mm) and III (8/16 mm).

For the aggregates, oven-dry (OD) and saturated-surface dry (SSD) densities were determined according to EN 1097-6 [18]. The water absorption of the aggregates after 24 h was also tested according to the same standard, but for RCA it was also determined after 30 min. The results are presented in Table 1. As expected, the results show higher water absorption and lower density of RCA compared with NA. Also importantly, approximately 85% of the RCA's water absorption occurs within the first 30 min, which has important implications on mix design. According to these results, the RCA can be classified as class B-I according to Silva et al. [7], which is a somewhat lower quality for recycled aggregates from unmixed concrete waste; however, they can still be used in the production of structural RAC.

The fly ash was obtained from the power plant Nikola Tesla B in Obrenovac. Tests showed that it had a mean particle size of 8.53 μm and a specific density of 2075 kg/m^3. Its chemical composition, showed it having CaO, SiO_2, Al_2O_3 and Fe_2O_3 contents of 7.62%, 58.24%, 20.23% and 5.33%, respectively. It was classified as low-calcium or class F according to ASTM C618-12a [19]. For cement, a CEM II/A-M(S-L) 42.5R cement with a specific density of 3150 kg/m^3 was used, produced by Lafarge Beočin, Serbia.

For longitudinal reinforcement in beams, Ø10 mm ribbed bars grade B500C with a yield stress of f_y =574–600 MPa were used.

Table 1 – Properties of NA and RCA

Aggregate	OD density (kg/m^3)	SSD density (kg/m^3)	Water absorption	
			30 min (%)	24 h (%)
NA I	2570	2600	–	1.20
NA II	2550	2580	–	1.24
NA III	2590	2620	–	1.04
RCA II	2390	2480	3.01	3.67
RCA III	2360	2550	3.55	4.05

2.2 CONCRETE MIXES

The three concrete mixes prepared in this study (NAC, RAC and HVFAC) were designed for a target compressive strength of 35 MPa on a 100 mm cube after 28 days and a slump of 100–150 mm. The mix proportions are provided in Table 2. In the case of RAC, there was a need for including additional water to compensate for the 30 min absorption (this value was chosen since it represents typical transport duration for ready-mixed concrete in Belgrade).

Table 2 – Mix proportions

Mix	Cement	Water	Fly ash	NA (kg/m^3)		RCA
	kg/m^3	kg/m^3	kg/m^3	sand	gravel	kg/m^3
NAC	285	175	–	815	996	–
RAC	285	175 + 21.5	–	767	–	937
HVFAC	200	195	200	810	810	–

2.3 TEST SETUP

For testing the mechanical and long-term properties of the three concrete mixes, different specimens were cast. For testing compressive strength (f_c), splitting tensile strength ($f_{ct,sp}$), flexural tensile strength ($f_{ct,fl}$) and modulus of elasticity (E_{cm}), 100 mm cubes, Ø150/150 mm cylinders, 120 x 120 x 360 mm prisms and Ø150/300 mm cylinders were used, respectively. Each property was obtained as an average of three measurements.

For testing shrinkage and creep, 120 x 120 x 360 mm prisms were used, which were cured for 24 h after which they were demoulded and moved to a laboratory for 700 days at a temperature of 22±3 °C and a relative humidity (RH) of 50±15%. Both shrinkage and creep were measured by gluing steel pins on the concrete surface of prisms and using a mechanical strain gauge with a 100 mm base to perform measurements. While shrinkage was tested for all three mixes, creep was tested only on RAC and HVFAC specimens loaded after 7 and 28 days

(RAC7, RAC28, HVFAC7, and HVFAC28). The creep specimens were loaded in steel frames (Figure 1) to different stress-to-strength at loading age ratios, $\sigma_c/f_{cm}(t_0)$: 0.60 for specimens RAC7 and HVFAC7 and 0.45 for specimens RAC28 and HVFAC28 and tested for 700 days. This meant that all specimens would exhibit non-linear creep, typically assumed to begin above $\sigma_c/f_{cm}(t_0)$ ratios of 0.4–0.5 [20], i.e. the relationship between creep strain and stress becomes non-linear. While these stress levels are high, they are still plausible in practice and codes such as Eurocode 2 and the *fib* Model Code 2010 have provisions for these cases [21,22].

Finally, from the three concrete mixes, six simply supported, 3.2 m-span beams were cast, i.e. two beams from each concrete mix. The beams had a 160 x 200 mm cross-section and were reinforced with 2Ø10 mm bars as tensile reinforcement (with an effective depth of 169 mm) and 2Ø6 mm bars as compressive reinforcement. Of the two beams cast from each mix, one was loaded after 7 days and the other after 28 days and the load was maintained for 700 days (the beams are labelled NAC7, NAC28, RAC7, RAC28, HVFAC7, and HVFAC28). All of the beams were loaded in four-point bending in thirds of their span. Identical $\sigma_c/f_{cm}(t_0)$ ratios were adopted as for the creep specimens: 0.60 for beams loaded after 7 days and 0.45 for beams loaded after 28 days. All of the beams were cured for 24 h and during the experiment were kept under identical laboratory conditions as the shrinkage and creep specimens.

The deflections of the beams were measured using mechanical dial indicators: first measurements were performed before loading and the initial deflection was measured 5 min after applying the load; after that, measurements were carried out at increasing intervals for 700 days after loading. Cracking was observed visually using a crack gauge. As an example, one of the beams is shown in Figure 1.

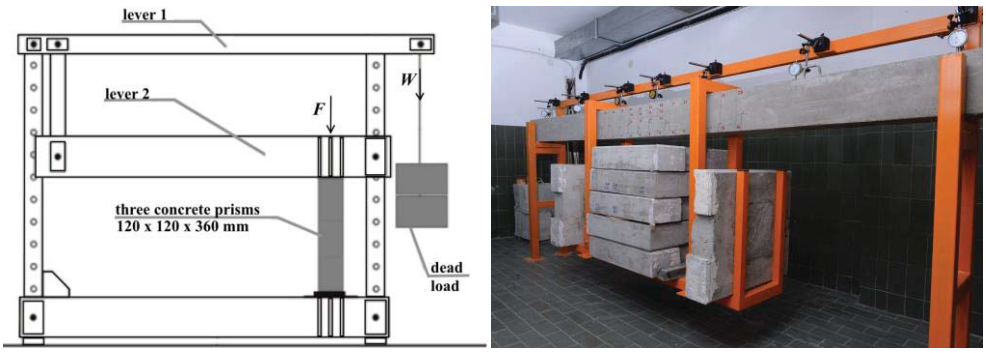

Figure 1 – Schematic of steel frames for testing creep (left) and test setup for reinforced concrete beams (right)

3. RESULTS AND DISCUSSION

3.1 MECHANICAL PROPERTIES

The fresh and hardened state properties of the mixes are given in Table 3. The workability of the mixes shows that, without a superplasticizer, it was difficult to control the slump of RAC and HVFAC. NAC and RAC also achieved a slightly larger 28-day compressive strength than

the target 35 MPa, whereas HVFAC was around 15% below the target. The curing regime of only one day wet curing probably had a significant effect on the compressive strength development of HVFAC. As for the modulus of elasticity and splitting tensile strength, they do not show any visible trends or correlations.

Table 3 – Fresh and hardened properties of the mixes

Mix	Slump	$f_{cm,cube}$ (MPa)		E_{cm} (GPa)		$f_{ct,sp}$ (MPa)	
	(mm)	7 days	28 days	7 days	28 days	7 days	28 days
NAC	115	32.9	40.7	30.1	32.2	2.0	2.4
RAC	140	32.2	37.4	26.2	30.8	2.0	2.5
HVFAC	70	21.8	30.1	25.2	28.7	1.2	2.1

3.2 SHRINKAGE AND CREEP

The measured shrinkage strains are presented in Figure 2. After 700 days, RAC had the largest shrinkage strain of –0.807‰ followed by NAC with –0.677‰ and HVFAC with –0.633‰. The shrinkage of RAC was 19% greater than that of NAC while the shrinkage of HVFAC was 7% smaller than that of NAC. The observed differences between the mixes are expected while the somewhat erratic evolution of measurements is the consequence of the seasonal variation in RH in the laboratory. Also, very importantly, a levelling-off of the shrinkage measurements is observed around 450–500 days for all mixes, pointing towards a potential end of drying, as is theoretically expected.

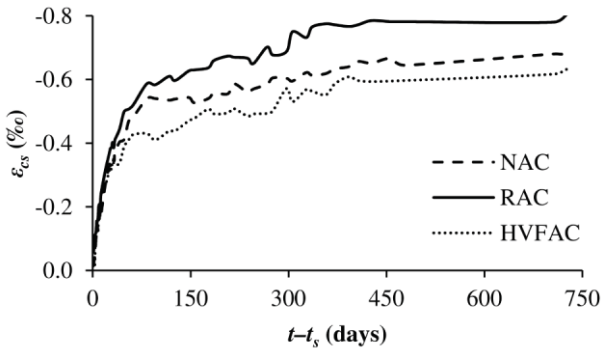

Figure 2 – Shrinkage strain measurements

As stated in the previous section, creep was measured only on RAC and HVFAC specimens. The time evolution of the stress-dependent strain, $\varepsilon_{c\sigma}$, is shown in Figure 3. For both RAC and HVFAC, the lines for specimens loaded at 7 and 28 days are parallel. In other words, a significant effect of creep non-linearity or of loading age cannot be detected. Furthermore, the experimental creep coefficient, φ_{exp} (ratio of creep strain to initial strain), was 2.50 and 2.69 for RAC7 and RAC28, respectively, and 1.78 and 1.75 for HVFAC7 and

HVFAC28, respectively. Again, there is no evidence of an effect of creep non-linearity or loading age, even to the contrary, the creep coefficient of RAC28 is higher than that of RAC7. The only noticeable thing is the significantly higher creep of RAC compared with HVFAC.

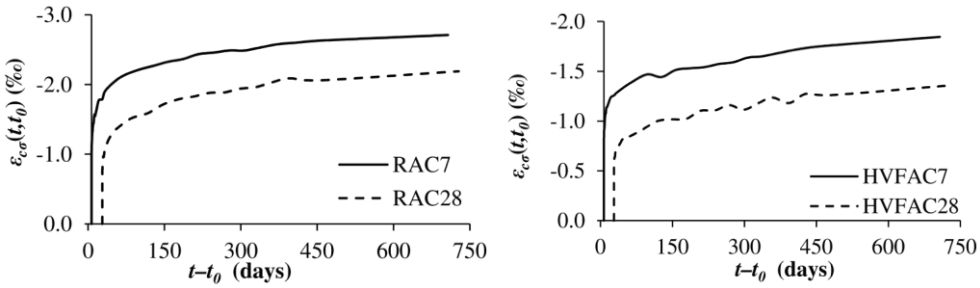

Figure 3 – Stress-dependent strain measurements

3.3 BEAM DEFLECTIONS AND CRACKING

To achieve the target $\sigma_c/f_{cm}(t_0)$ ratios in the beams, the mechanical properties were measured on the day of the loading and then the load was calculated for each beam. Because of the different mechanical properties of the mixes and different loading ages, the applied loads were different for each beam. Table 4 presents the ratios of the applied bending moment M_{Ed} to the cracking and ultimate bending moments M_{cr} and M_{Rd}, respectively. NAC and RAC beams were loaded to similar M_{Ed}/M_{Rd} ratios (0.44–0.55), relatively typical for service load levels. These ratios are smaller for HVFAC beams since HVFAC had a lower compressive strength compared with NAC and RAC.

Mid-span deflection measurements are also given in Table 4 where $a(t_0)$ represents the initial deflection measured 5 min after loading and a(700) represents the deflection measured 700 days after loading. The last column in Table 4 represents the ratio of 700-day-to-initial deflection $a(700)/a(t_0)$. For all six beams, this value lies in a very narrow range of 2.11–2.49. The time development of this 'normalized' deflection is shown in Figure 4.

Table 4 – Beam loads and deflections

Beam	***M_{Ed} (kNm)***	***M_{Ed}/M_{cr}***	***M_{Ed}/M_{Rd}***	***$a(t_0)$ (mm)***	***a(700) (mm)***	***$a(t_0)/a(700)$***
NAC7	***7.63***	***3.33***	***0.53***	***9.17***	***19.34***	***2.11***
NAC28	***6.84***	***2.49***	***0.48***	***8.11***	***17.22***	***2.12***
RAC7	***7.86***	***3.65***	***0.55***	***10.89***	***23.24***	***2.13***
RAC28	***6.36***	***2.45***	***0.44***	***6.23***	***15.52***	***2.49***
HVFAC7	***5.49***	***3.27***	***0.39***	***6.13***	***13.05***	***2.13***
HVFAC28	***5.35***	***2.59***	***0.38***	***4.04***	***9.48***	***2.20***

For beams of the same concrete mix loaded at different ages, there is no effect of loading age and stress level that can be observed. At the same time, differences in the development of normalized deflections are negligible between beams of different concrete mixes even though they exhibit different shrinkage and creep behaviour at the material level. This is possibly because of high load levels applied, which lead to pronounced cracking in the beams and a small height of the compressed zone, thus reducing the effects of shrinkage and creep.

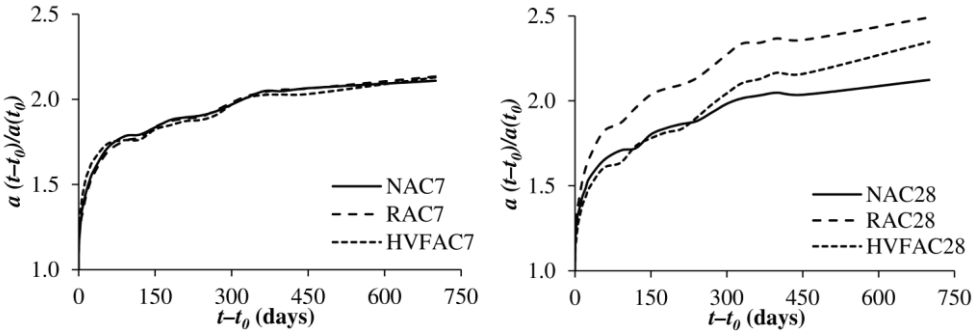

Figure 4 – Time evolution of normalized deflections

Finally, the results of crack spacing, s_m, and crack width, w_m, measurements 5 min and 450 days after loading are shown in Table 5. NAC and RAC beams can be seen to have similar crack spacing and width (comparing beams loaded at the same age), while HVFAC beams show larger crack spacing and smaller crack widths, as expected from similar load levels of NAC and RAC and lower load level of HVFAC beams.

Table 5 – Crack spacing and crack width measurements

Beam	5 min after loading		450 days after loading	
	s_m (mm)	w_m (mm)	s_m (mm)	w_m (mm)
NAC7	135	0.05	115	0.15
NAC28	120	0.15	110	0.20
RAC7	100	0.08	100	0.15
RAC28	125	0.08	105	0.10
HVFAC7	145	0.08	125	0.15
HVFAC28	155	0.05	130	0.08

4. CONCLUSIONS

This paper presented results from an experimental programme testing the long-term behaviour of NAC, RAC and HVFAC at the material (shrinkage and creep) and structural level

(deflections and cracking). Based on the obtained results on concrete specimens and reinforced concrete beams, the following conclusions can be drawn:

- NAC and RAC produced with the same effective *w/c* ratio had a similar 28-day compressive strength (within 10%), whereas HVFAC in which fly ash comprised 50% of total cementitious materials had almost 30% lower 28-day compressive strength, mostly because of the effect of one day of wet curing;
- RAC had the largest shrinkage after 700 days, 19% larger compared with NAC and HVFAC had the smallest shrinkage strain, 7% smaller compared with NAC;
- Creep tested on RAC and HVFAC specimens did not exhibit pronounced effects of creep non-linearity or loading age with creep coefficients of specimens from the same concrete but loaded at different ages being within 8%. Additionally, RAC exhibited significantly larger creep deformations than HVFAC;
- After 700 days under sustained load, all six beams in the experiment had similar normalized deflections (ratios of final-to-initial deflection), in the range of 2.11–2.49. There was no apparent effect of creep non-linearity or loading age on the time evolution of normalized deflections.

ACKNOWLEDGEMENTS

The work reported in this paper is funded under grant TR 36017 by the Ministry for Education, Science and Technology, Republic of Serbia and grant 451-03-1924/2016-09/3 funded jointly by the Ministry for Education, Science and Technology, Republic of Serbia and the Foundation for Science and Technology, Republic of Portugal.

REFERENCES

[1] K.L. Scrivener, J.M. Vanderley, E.M. Gartner, Eco-efficient cements: Potential, economically viable solutions for a low-CO2, cement based materials industry, Paris, 2016.

[2] WBCSD, The Cement Sustainability Initiative, World Bus. Counc. Sustain. Dev. (2009). http://www.wbcsdcement.org/pdf/CSIRecyclingConcrete-FullReport.pdf (accessed July 7, 2016).

[3] USGS, Minerals Yearbook, US Geol. Surv. (2015). minerals.usgs.gov/minerals/pubs/commodity/cement/mcs-2015-cement.pdf (accessed July 7, 2016).

[4] W.H. Langer, L.J. Drew, J.J. Sachs, Aggregate and the Environment, Alexandria, VA, 2004. www.agiweb.org/environment/publications/aggregate.pdf.

[5] Eurostat, Generation of waste by waste category, hazardousness and NACE Rev. 2 activity, Brussels, 2017.

[6] I. Ignjatović, N. Tošić, S. Marinković, Tehnološki i ekonomski aspekt proizvodnje agregata od recikliranog betona u Srbiji, in: Građevinski Mater. u Savrem. Graditelj., DIMK Srbije, Belgrade, 2015: pp. 1–8.

[7] R.V. Silva, J. de Brito, R.K. Dhir, Properties and composition of recycled aggregates from construction and demolition waste suitable for concrete production, Constr.

Build. Mater. 65 (2014) 201–217. doi:10.1016/j.conbuildmat.2014.04.117.

[8] J. Dragaš, I. Ignjatović, N. Tošić, S. Marinković, Mechanical and time-dependent properties of high-volume fly ash concrete for structural use, Mag. Concr. Res. 68 (2016) 632–645.

[9] R.V. Silva, Use of recycled aggregates from construction and demolition waste in the production of structural concrete, Universidade de Lisboa, 2015.

[10] A.M. Rashad, A brief on high-volume Class F fly ash as cement replacement - A guide for Civil Engineer, Int. J. Sustain. Built Environ. 4 (2015) 278–306. doi:10.1016/j.ijsbe.2015.10.002.

[11] J. Xiao, C.Q. Wang, J. Li, M. Tawana, Shake-table model tests on recycled aggregate concrete frame structure, ACI Struct. J. 109 (2012) 777–786.

[12] A.B. Ajdukiewicz, A.T. Kliszczewicz, Comparative tests of beams and columns made of recycled aggregate concrete and natural aggregate concrete, J. Adv. Concr. Technol. 5 (2007) 259–273. doi:10.3151/jact.5.259.

[13] J. Pacheco, J. de Brito, D. Soares, Destructive horizontal load tests of full-scale recycled aggregate concrete structures, ACI Struct. J. 112 (2015) 815–826.

[14] M. Arezoumandi, J.S. Volz, C.A. Ortega, J.J. Myers, Effect of total cementitious content on shear strength of high-volume fly ash concrete beams, Mater. Des. 46 (2013) 301–309. doi:10.1016/j.matdes.2012.10.031.

[15] A.W. Beeby, S. Narayanan, Designer's guide to Eurocode 2: Design of concrete structures, Thomas Telford, London, 2005.

[16] A.M. Knaack, Y.C. Kurama, Sustained service load behavior of concrete beams with recycled concrete aggregates, ACI Struct. J. 112 (2015) 565–578. doi:10.14359/51687799.

[17] S. Seara-Paz, B. González-Fonteboa, F. Martínez-Abella, D. Carro-Lopez, Long-term flexural performance of reinforced concrete beams with recycled coarse aggregates, Constr. Build. Mater. 176 (2018) 593–607.

[18] EN 1097-6, Tests for mechanical and physical properties of aggregates - Part 6: Determination of particle density and water absorption, CEN, Brussels, 2000.

[19] ASTM-C618-12a, Standard specification for coal fly ash and raw or calcined natural pozzolan for use in concrete, ASTM International, West Conshohocken, PA, 2012.

[20] Z.P. Bažant, M. Jirasek, Creep and hygrothermal effects in concrete structures, Springer, Dordrecht, 2018.

[21] EN 1992-1-1, Eurocode 2: Design of concrete structures - Part 1-1: General rules and rules for buildings, CEN, Brussels, 2004.

[22] FIB, fib Model Code for Concrete Structures 2010, International Federation for Structural Concrete (fib), Lausanne, 2013. doi:10.1002/9783433604090.

ДГКС Друштво грађевинских конструктера Србије
ASES Association of Structural Engineers of Serbia
S-52
15. KONGRES
6-8. 9. 2018. Zlatibor

Dubravka Bjegović[1], *Nina Štirmer*[2], *Ana Baričević*[3]

BETON U LNG REZERVOARIMA

Rezime:

LNG rezervoari su posebne konstrukcije koje se koriste za skladištenje ukapljenog prirodnog plina. Obzirom da se transportiraju velike količine LNG-a, veoma je važno imati siguran prostor za njegovo skladištenje. Iskustvo je pokazalo da se za izgradnju LNG rezervoara može uspješno primjenjivati beton. Pri tome ipak posebnu pažnju treba posvetiti svojstvima građevinskih materijala kako bi se osiguralo da ne dođe do pojave pukotina. To također znači da projektiranje i ispravno održavanje LNG rezervoara zahtijeva odlično znanje o toplinsko-mehaničkim svojstvima i svojstvima propusnosti betona pri ekstremno niskim temperaturama, tzv. kriogenim temperaturama. U ovom radu dan je pregled referentnih radova s postojećim znanjima o toplinsko-mehaničkim svojstvima i svojstvima propusnosti betona pri vrlo niskim temperaturama.

Key words: LNG rezervoar, beton, kriogene temperature, toplinsko-mehanička svojstva

CONCRETE USED IN LNG STORAGE TANKS

Summary:

LNG storage tanks are special structures used for storage of liquefied natural gas. Since large quantities of LNG are transported it is increasingly important to have safe storage facilities. Experience has showed that concrete can be successfully used for construction of LNG storage tanks. However, special care should be taken since the properties of construction materials used must assure that no damage will occur. It also means that the design and proper maintenance of LNG storage tanks require excellent knowledge of the thermo-mechanical and permeability properties of concrete at extremely low temperatures, the so-called cryogenic temperatures. This paper presents a review of reference papers outlining the current knowledge on thermo-mechanical and permeability properties of concrete at very low temperatures.

Key words: LNG tank, concrete, cryogenic temperatures, thermo-mechanical properties

[1] *Prof. emerita, University of Zagreb Faculty of civil engineering, Department of materials, dubravka@grad.hr*
[2] *Prof., University of Zagreb Faculty of civil engineering, Department of materials, ninab@grad.hr*
[3] *Assistant prof. University of Zagreb Faculty of civil engineering, Department of materials, abaricevic@grad.hr*

1. INTRODUCTION

Natural gas (NG) is a natural resource for which the global demand has considerably increased in recent years. While the share of coal and oil in energy production is forecast to dramatically decrease by 2030, the share of NG is predicted to reach 25.9% of the world's energy usage [1]. The demand for the world primary energy is expected to grow by 1.6% per annum in the period between 2010–2030. In order to meet this requirement, energy production will need to be increased by 39%. Liquefied natural gas (LNG) is natural gas under atmospheric or increased pressure and cooled to very low temperatures so that it converts to liquid form. When natural gas is cooled to -161˚C it becomes a clear, odorless and colorless liquid. When natural gas is liquefied, it shrinks more than 600 times in volume. Since LNG takes up about 1/600th the volume of natural gas in the gaseous state, it is suitable for worldwide transport on tankers. A terminal for liquified gas is a facility for filling or emptying tankers which transport this energent. After being received at the terminal LNG is usually transported into insulated tanks specially constructed for LNG storage. These tanks must maintain the low temperature of the liquid and minimise the quantity of evaporated gas. Every tank has the equipment that ensures its proper and safe operation. According to [2-4] the types of on shore LNG storage tanks could be designed as follows:

- Single containment tank,
- Double containment tank,
- Full containment tank,
- Membrane tank,
- In-ground tank and
- Composite concrete cryogenic tank (C3T).

The Statistics portal for the 1st quarter of 2017 [5] on storage tank capacity for liquefied natural gas worldwide, by country (in million cubic meters), is shown in Figure 1 and the data from 2015 [6] on the number of LNG tanks per country, are presented in Figure 2.

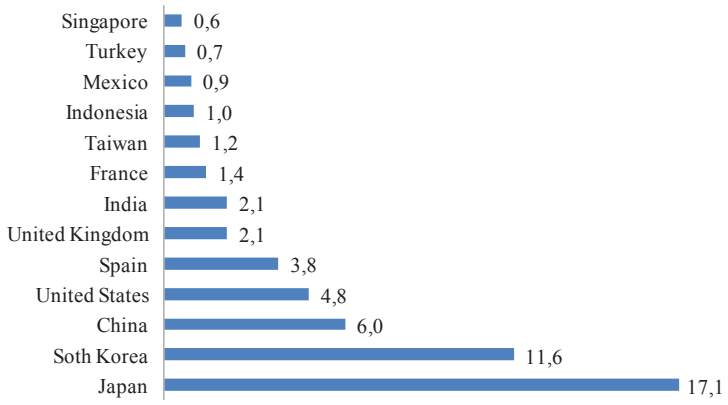

Figure 1 - Storage tank capacity for LNG worldwide in million cubic meters [5], [6]

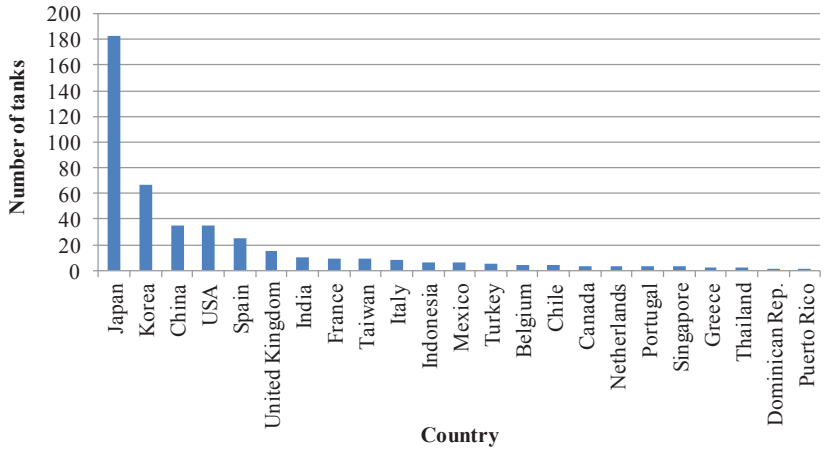

Figure 2 - Number of LNG tanks per country

Global data show that Japan, with 183 tanks, has currently the highest number of LNG storage tanks, followed by Korea with 67, China and the USA with 35, and in Europe the first is Spain with 25 tanks and UK with 10.

Experience has showed that concrete can be successfully used for construction of LNG storage tanks for each solution. However, special care should be taken since the characteristics of construction materials used must ensure that no damage will occur. It also means that the design and proper maintenance of LNG storage tanks requires excellent knowledge of thermo-mechanical and permeability properties of concrete at extremely low temperatures, the so-called cryogenic temperatures. The tank will be exposed to the cooling cycle when the tank is filled and/or when the steel plate is damaged which may cause the gas to leak and come into contact with the insulation but also with the outer concrete plate and thus cause the thermal shock for the outer concrete plate, [7-9]. For this reason, the knowledge of thermo-mechanical and permeability properties of concrete at extremely low temperatures is crucial both when designing and using the tanks.

2. THERMO-MECHANICAL PROPERTIES OF CONCRETE

Thermo-mechanical properties of concrete presented in the paper are thermal deformation and thermal conductivity, and mechanical properties are strength and modulus of elasticity. Hereinafter described are the properties of concrete at cryogenic temperature and suggestions for calculating its mechanical properties.

2.1 MECHANICAL PROPERTIES

At temperatures ranging from -10°C to -196°C, mechanical properties, such as compressive strength, tensile strength, stress-to-strain relationship, modulus of elasticity, and bond strength of concrete and reinforcement, are decreased if the temperature is lowered [10-12]. However, it needs to be said that, if concrete reaches normal temperature after being cooled and/or exposed

to temperature cycles and temperature shocks, mechanical properties are degraded or decreased [11].

2.1.1 Compressive strength

The increase of compressive strength under the influence of extremely low temperature can be calculated. According to fib Model Code 2010 [14], it can be described with the following expression for 0° ≥ T ≥ -170°C, for a single temperature drop:

$$\Delta f_{cm} = 12m\left[1 - \left(\frac{T+170}{170}\right)^2\right] \quad (1)$$

where:
Δf_{cm} is the gain in the compressive strength (MPa)
m is the moisture content in % by mass
T is the temperature (°C)

2.1.2 Tensile strength

The tensile splitting strength of concrete $f_{c,split}(\theta)$ is determined according to the expression shown in fib Model Code 2010 [14]:

$$f_{c,split}(\theta, mc) = C \cdot f_c(\theta, mc)^{0.67} \quad (2)$$

where
$f_c(\theta, mc)$ is the compressive strength of concrete on the cylinder at the observed temperature and humidity
C coefficient which varies from 0.3 (for naturally dry concrete) and 0.56 (for water saturated concrete).
According to EN 1992-3:2013 [15], the tensile strength f_{ctx} can be calculated from the expression:

$$f_{ctx} = \alpha \cdot {f_{ckT}}^{2/3} \quad (3)$$

where:
α is the coefficient which takes into account the moisture content in concrete, and the values are stated in Table 1 (EN 1992-3:2013):

Table 1 – The coefficient α

Tensile strength	***Saturated concrete***	***Dry concrete***
f_{ctm}	***0.47***	***0.30***
$f_{ctk0,05}$	***0.27***	***0.21***
$f_{ctk0,95}$	***0.95***	***0.39***

2.1.3 Modulus of elasticity

The modulus of elasticity of concrete is increased by lowering temperature, but the increase is not as significant as with compression strength. In [14] the data given say that the elasticity module is increased 1.7 times if concrete is exposed to -190°C, and [7] states possible increases of 1.15 for dry concrete, 1.5 for sealed concrete and 1.8 for water saturated concrete.

According to Kazmierczak [16], significant increases of the value of the modulus of elasticity are recorded at temperatures -165°C as follows:

a) For dry concrete $E_c(T = -165°C) \approx 1.15 \cdot E_c(T = 20°C)$
b) For sealed concrete $E_c(T = -165°C) \approx 1.5 \cdot E_c(T = 20°C)$
c) For saturated concrete $E_c(T = -165°C) \approx 1.8 \cdot E_c(T = 20°C)$

However, the test results show that there are significant deviations resulting from the conditions of placing concrete but also from environment aggression. The static modulus of elasticity can be calculated according to Krstulovic-Opara [13], by the following expression:

$$E_c(T) = E_c(T = 20°C) \cdot \left(1 + 0.5 \cdot \frac{20°C - T}{185°C}\right) \tag{4}$$

and the dynamic modulus of elasticity by the expression:

$$E_{c,dynamic}\,(T) = [\alpha \cdot f_c(T, mc) + \beta] \cdot 10^3 \tag{5}$$

2.2 THERMAL PROPERTIES

2.2.1 Thermal deformation

Thermal stresses in concrete are the function of differential thermal deformations, which depend on the coefficient of thermal deformation of components and on the modulus of elasticity at extremely low temperatures (ELT). The thermal deformation and the coefficient of thermal deformation of concrete at ELT are the functions of the type of aggregate and temperature [13]. The thermal deformations of concrete are increased by the increased water-cement ratio, and by the effects of load and ELT on concrete, and by the increased moisture in concrete. The coefficient of thermal deformation is decreased if the temperature is lowered, approximately by 10% for dry concrete [14], and for wet concrete it varies, depending on the humidity level of concrete [13].

2.2.2 Thermal conductivity

Thermal conductivity is the property of construction materials to conduct heat. The value of thermal conductivity λ is extremely variable, even in the same material. It depends on the density and porosity, chemical composition of the material, the humidity content in the material and on the temperature of the material. In a very dry concrete exposed to cryogenic temperature the changes in thermal conductivity are small, while the thermal conductivity is increased in a wet concrete [13].

3. PERMEABILITY PROPERTIES

Permeability of concrete is an essential property in LNG tanks, because, if gas leaks through the damaged steel part of the container, it can come into contact with concrete through which gas is not to pass. The designed values for internal permeability of concrete are within the range of 10^{-18} m^2 to 10^{-20} m^2.

Testings conducted on a few types of concrete [12] indicate that at lowered temperature the permeability of concrete is decreased, and the best results in impermeability have the concretes with limestone aggregate [17, 18].

4. EXISTING CODES AND STANDARDS

For the design and construction of LNG tanks the construction industry adheres to the international network of codes and standards which specifies safe technologies, materials and designs for the construction of an import terminal. The codes and standards enable the industry to implement generally approved technologies and ensure a high level of safety. The development and implementation of these codes and standards promote sharing the state-of the-art technologies and research around the world. Some of the standards, mainly European and American, are widely used worldwide [2, 19-23]. Figure 3 [2] shows a global presentation of how the codes and standards compare.

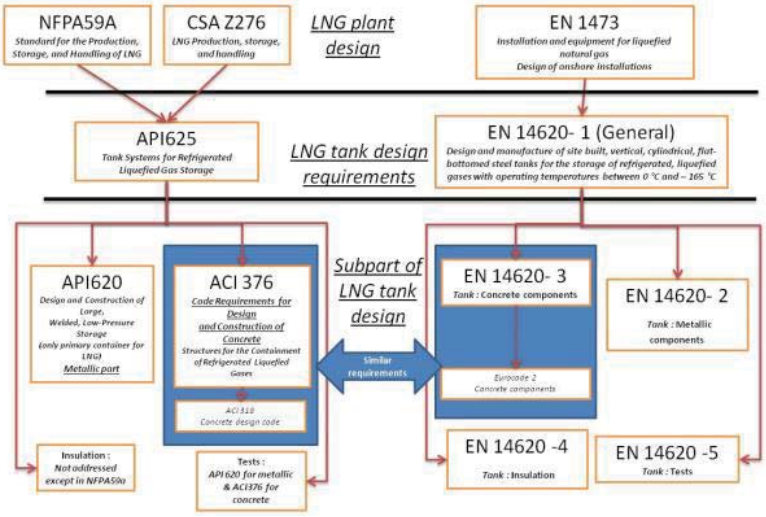

Figure 3 - Presentation of how American and European codes and standards compare [2]

The stability and tightness of a concrete outer tank has to be guaranteed by the appropriate design under cryogenic conditions, too. The relevant codes provide a lot of formal regulations, but give no precise indications for analytical procedures and criteria which have to be applied in the design. In [24], Roetzer and Baumann deal with the behavior of reinforced and prestressed concrete sections in direct contact with LNG, considering thermal strains and

consecutive crack formation. Mechanical models, which have to be clear and simple, are also discussed.

5. CONCLUSION

The mechanical properties of concrete are increased when concrete is exposed to extremely low temperatures. The thermal deformation and the coefficient of thermal deformation at ELT are the functions of the type of aggregate and temperature. The coefficient of thermal deformation is decreased at lowered temperature by approx. 10% for dry concrete, and for wet concrete it varies, depending on the level of moisture in concrete. Thermal deformations of concrete are increased by the water-cement ratio, by the effects of load and ELT on concrete, and by the increased humidity of concrete. Thermal permeability is linearly increased by approx. 40% to -170°C, and the coefficient of thermal deformation is increased by 20%. The lowered temperature decreases the gas impermeability of concrete, and it is controlled by the type of aggregate and the humidity of concrete. The outline of codes and standards is also given.

REFERENCES

[1] Agarwal, R., Rainey, T. J., Ashrafur Rahman, S. M., Steinberg, T., Perrons, R. K. Brown, R. J.: LNG Regasification Terminals: The Role of Geography and Meteorology on Technology Choices, Energies 2017, 10, 2152; 19 pp., doi:10.3390/en10122152

[2] NFPA59A TASK FORCE, To recommend requirements for Membrane tank systems, https://www.nfpa.org/Assets/files/AboutTheCodes/59A/NFPA59A_Membrane Tank Report_Supplemental Material to TIA.pdf

[3] Kimberly Hoyle, Composite Concrete Cryogenic Tank (C3 T): A Precast Concrete Alternative for LNG Storage, http://www.gastechnology.org/Training/Documents/LNG17-proceedings/8-6-Kimberly_Hoyle.pdf

[4] In Ground LNG Storage Tanks, http://www.netdecheck.com/en/lngtech/ug-tank/index.html

[5] LNG storage tank capacity worldwide by country 2017, https://www.statista.com/statistics/723079/lng-global-storage-tank-capacity-by-country/

[6] Retail LNG Handbook, Retail LNG & The Role of LNG Import Terminals, 2015., GIIGNL, International Group of Liquefied Natural Gas Importers, 106 pp

[7] Roetzer, J., Baumann, T.: Outer Concrete Containment of LNG -Tanks – Design agains Thermal Shock, https://www.scribd.com/document/262876142/LNG-Thermal-Shock

[8] Hjorteset, K., Wernli, M., LaNier, M. W., Hoyle, K. A., Oliver, W. H.: Development of large-scale precast, prestressed concrete liquefied natural gas storage tanks, http://www.abam.com/sites/default/files/techpapers/DevelopmentofLarge-ScalePrecast,PrestressedConcreteLiquefiedNaturalGasStorageTanks.pdf

[9] LNG Terminal, S- Tank Engineering, http://www.s-tank.com/eng/products/pro05.htm

[10] Dahmani, L., Khenane, A., Kaci, S.: Behavior of the reinforced concrete at cryogenic temperatures, Cryogenics 47 (2007) 517–525

[11] Van der Veen J. C., Properties of concrete at very low temperatures. A survey of the literature, Report No. 25–87–2. Delft University of Technology, 1987. 124 pp

[12] Kogbara, R. B., Iyengar, S. R., Grasley, Z., Zollinger, D. G.: A review of concrete properties at cryogenic temperatures: Towards direct LNG containment, Article in Construction and Building Materials, October 2013 DOI: 10.1016/j.conbuildmat.2013.04.025

[13] Krstulovic-Opara, N.: Liquefied Natural Gas Storage: Material Behavior of Concrete at Cryogenic Temperatures, ACI Materials Journal / V. 104, No. 3, May-June 2007., Title no. 104-M3, 297-306, plus Appendix 33-53.

[14] fib Model Code 2010, 2013. fib Model Code for Concrete Structures, Fédération internationale du béton/ International Federation for Structural Concrete (fib), Switzerland

[15] EN 1992-2-3, 2013. Eurocode 2: Design of concrete structures – Part 3: Liquid retaining and containment structures

[16] Kazmierczak, S.: Selected Issues of Prestressed Concrete Containment Tanks for the Storage of Liquefied gases design in Accordance with EN 14620, Technical Transactions, Civil Engineering, 3-B/2015, DOI: 10.4467/2353737XCT.15.166.4341, 101-113.

[17] Kogbara, R. B., Parsaei, B., Iyengar, S. R., Grasley, Z., Masad, E. A.. Zollinger, D. G.: Evaluating damage of crygenic concrete using acustic emission sensors and permeability testing, Proc. SPIE 9061, Sensors and Smart Structures Technologies for Civil, Mechanical, and Aerospace Systems 2014, 90613B (April 10, 2014); doi:10.1117/12.2045708

[18] Kogbara, R. B., Iyengar, S. R., Grasley, Z. C., Rahman, S., Masad, E. A., Zollinger, D. G.: Relating damage evolution of concrete cooled to cryogenic temperatures to permeability, Cryogenics 64 (2014) 21–28

[19] Mokhatab, S., Mak, J. Y., Valappil, J. V., Wood, D. A.: Handbook of Liquefied Natural Gas, Elsevier, 2014, ISBN 13: 978-0-12-404585-9

[20] Managing LNG Risks – Operational Integrity, Regulations, Codes, and Industry Organisations, LNG Information Paper No. 4, https://giignl.org/sites/default/files/PUBLIC_AREA/About_LNG/4_LNG_Basics/lng_4_-_operational_integrity_7_3_09-aacomments-aug09.pdf

[21] LNG Information Paper No. 1-7, – Industry Safeguard Systems, Basic Properties of LNG - Engineering.com

[22] Hanskat, C. S.: Design and Construction of Concrete Tanks for Refrigerated Liquefied Gas Containment, Part 1, ACI Spring 2012 Convention March 18 – 21, Dallas, TX, https://www.concrete.org/portals/0/files/pdf/webinars/hanskat.pdf

[23] LNG Information Paper No. 4, Managing LNG Risks – Operational Integrity, Regulations, Codes, and Industry Organisations,

https://giignl.org/sites/default/files/PUBLIC_AREA/About_LNG/4_LNG_Basics/lng_4_-_operational_integrity_7_3_09-aacomments-aug09.pdf,

[24] Roetzer, J., Baumann, T.: Outer concrete containments of LNG-tanks – Design against thermal shock, Tailor Made Concrete Structures – Walraven & Stoelhorst (eds)© 2008 Taylor & Francis Group, London, ISBN 978-0-415-47535-8

ДГКС Друштво грађевинских конструктера Србије
ASES Association of Structural Engineers of Serbia
S-53
15. KONGRES
6-8. 9. 2018.Zlatibor

Ksenija Janković[1], Marko Stojanović[2], Dragan Bojović[3], Ljiljana Lončar[4]

UTICAJ POLIPROPILENSKIH VLAKANA NA MEHANIČKA SVOJSTVA MLAZNIH BETONA ZA OBLAGANJE KOSINA

Rezime:

U ovom radu je prikazana mogućnost korišćenja polipropilenskih vlakana u mlaznom betonu koji bi se koristio za oblaganje kosina. Ispitivani su mlazni betony sa različitim sadržajem polipropilenskih vlakana i poređeni sa referentnim uzorcima spravljenim bez vlakana. Ploče od mlaznog betona su ispitivane na probijanje, a čvrstoće pri pritisku i pri zatezanju cepanjem su određene na kockama u starosti od 28 dana. Mlazni betoni sa sadržajem 5 kg/m3 polipropilenskih vlakana su imali najpovoljnija mehanička svojstva.

Ključne reči: mlazni beton, poplipropilensaka vlakna energija apsorpcije, čvrstoća

THE INFLUENCE OF POLYPROPYLENE FIBERS ON THE MECHANICAL PROPERTIES OF SHOTCRETE FOR SLOPES

Summary:

This paper presents the possibility of the use of polypropylene fibers in shotcrete which would be used for coating slopes. Shotcrete mixes with different content of polypropylene fibers were tested and compared with referent shotcrete without fibers. Puncture testing was performed on shotcrete slabs, while compressive and tensile splitting strength were testing on cubes at 28 days of age. Obtained results for shotcrete containing 5 kg/m^3 polypropylene fibers show the best mechanical properties.

Key words: shotcrete, polypropylene fiber, reinforcement, energy absorption, strength

[1]*PhD, principal research fellow, IMS Institute, Bulevar vojvode Mišića 43, Belgrade, ksenija.jankovic@institutims.rs*
[2]*MSc,research assistant, IMS Institute,Bulevar vojovde Mišića 43,Belgrade, e-mail: marko.stojanovic@institutims.rs*
[3]*PhD,research assistant, IMS Institute,Bulevar vojvode Mišića 43,Belgrade, e-mail: dragan.bojovic@institutims.rs*
[4]*BScCE,profess. adviser, IMS Institute,Bulevar vojvode Mišića 43,Belgrade, e-mail: ljiljana.loncar@institutims.rs*

1. INTRODUCTION

Applying fresh concrete mass through a hose and pneumatically projected at high velocity to a horizontal, sloping or vertical surface, rock surface (in the cavity, tunnel, slope, etc.) is called "shotcrete" or "sprayed concrete". This procedure is very widely used, since the built-in concrete is distinguished by high physical-mechanical properties (bulk density, strength, surface adhesion, waterproofness, frost resistance) as well as satisfactory durability [1].

Shotcrete has been used for more than 50 years as a protective coating of wall masses, soil surfaces that are prone to collapsing. Before 1990, only a few research papers were published in scientific journals with information related to the mechanical properties of shotcrete, which raised awareness of the use of this material to the academic community as an opportunity to improve tunnel safety and stabilize the slopes [2].

Some of the main roles in designing this kind of material are to withstand the loads and deformationsthe ground can cause during the working life of the tunnels, maintaining adequate ground stability, protecting the workers and the equipment from falling rock masses [3, 4].

However, the adhesion between the rock and shotcrete is a complex issue. The properties and, therefore, the capacity and deformability of shotcrete, are stimulated by numerous factors such as: mechanical properties of the rocks, the stresses in the rock masses, the adhesion between the rock bolts and shotcrete and their mechanical properties and, among other things, the thickness of shotcrete layer [5, 6].

The basic objective of designing shotcrete is to create a self-supporting arc, consisting of shotcrete and other components for supporting the rock bolts, such as wall anchors, wire mesh and other structural reinforcement which is exposed to certain loads and deformations.

In particular, in tunnels located at great depths, the rock maintenance system should allow the permissible displacement of tunnel walls to prevent the collapse of tunnels. In this state, the relevant characteristics of the concrete shields are: its deformability at the maximum displacement and its strength during the displacement. In this case, during the tunnel design, it is not expected to accept tension around the tunnel, but it allows the deformation of the energy transfer from the rock to the shotcrete lining [7].

Shotcrete is often made with certain specific chemical additives, as well as with micro reinforcement (usually steel or synthetic fibers). Accelerated increase in shotcrete strength, its ability to easily apply to faceted surfaces without the need for formwork, and the ability to provide additional flexibility to the rock mass, make this process ideal for use in underground works, as well as in the field of rehabilitation.

As technology evolves, the application of new technologies in construction, where there are more and more applications of the so-called "fiber reinforced shotcrete" (FRS), is also being monitored. The main difference is that FRS concrete contains steel or synthetic fibers.

2. EXPERIMENTAL WORK

In this paper, three types of shotcrete were prepared, which were assembled with different polypropylene fibers and one control type without fibers.

The design of shotcrete which would be used for the stabilization of slopes in the Grdelička gorge within the project of construction of the E75 Motorway was designed with materials that were available to the concrete producer.

Shotcrete is made with materials that are available in Serbia. Portland cement with the addition of limestone CEM II / A-L 42.5 R, manufactured by CRH - Popovac, was used. The chemical, physical and mechanical properties of the cement are shown in Table 1.

Table 1 - Properties of cement CEM II / A-L 42.5R, CRH - Popovac

Chemical, %		*Physical*		*Mechanical*	
SiO_2	19.32	*Specific gravity, kg/m^3*	3110	*Compressive strength, N/mm^2*	
Al_2O_3	5.87				
Fe_2O_3	1.92	*Specific surface, cm^2/g*	3550	2 days	29.9
CaO	63.01			7 days	-
MgO	2.58	*Standard consistency, %*	27.8	28 days	53.4
Na_2O	0.22			*Flexural strength, N/mm^2*	
K_2O	0.51	*Setting time, min*		2 days	6.4
SO_3	2.45	*Initial*	215	7 days	-
Cl^-	0.010	*Final*	275	28 days	9.9

Natural, river, fractionated stone aggregate with the maximum grain size of 8 mm was used.

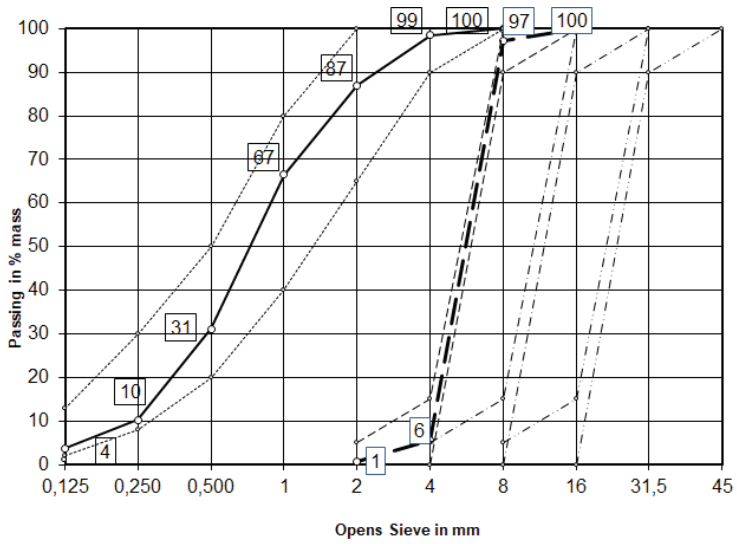

Figure 1 – Aggregate size distribution

The fine aggregate is a fraction of 0/4 mm while the coarse aggregate is a fraction of 4/8 mm. Specific gravity of fine and coarse aggregates were 2610 kg/m3 and 2650 kg/m3 respectively. In addition, the fine and coarse aggregate fineness modulus was 3.16 and 5.22, respectively. The aggregate size distribution (fractions 0/4 and 4/8 mm) are shown in Figure 1.

Polypropylene fibers "Master fiber 151" - BASF, were used in the research. The fibers were extruded from polyolefin polymer. The fiber properties are shown in Table 2.

Table 2 - Properties of the polypropylene fiber

Properties	*Values*
Material	*Polypropylene 100%*
Design	*Monofilament*
Specific gravity	*0.91 g/cm³*
Equivalent diameter	*0.75 mm*
Length	*50 mm*
Aspect ratio	*67*
Alkali resistance	*Excellent*
Absorption	*Nil*
Tensile Strength	*448 MPa*
Modulus of elasticity	*3643 MPa*
Chemical resistance	*Excellent*
Melting point	*160°C*
Ignition point	*590°C*

The research used chemical additives such as superplasticizer: 1. "Sika Techno 20S" - Sika with a specific gravity of 1060kg/m3, and the recommended dosage is 0.6 - 1.2%; 2. The accelerator "Master ROC SA 194" - BASF, with a specific gravity of 1040kg/m3, and the recommended dosage is 4 - 8%.

Four types of shotcrete samples were made. Concrete was made without polypropylene fibers with 5, 10 and 15 kg of polypropylene fibers. First, control concrete without fibers was made, followed by brushed shotcrete with the addition of 5, 10 and 15 kg of polypropylene fibers, respectively.

The mix design of shotcrete is given in Table 3.

A "wet process" was used to prepare the basic mix of shotcrete. Shotcrete is made on the concrete factory. Consistency by the slump test class S4 (180-230 mm) is required.

The transport of the basic concrete mixture to the shotcrete machine was done by automakers. Fresh concrete is pumped out of the concrete mixer trucks into the basket of the shotcrete machine, where by pressing the fresh concrete it is carried out to the nozzles where it is mixed with the accelerator, after which it is thrown out of the nozzle under great pressure and is deposited in several layers to the surface.

Table 3 - Shotcrete mix

Material		Mix mark			
		SC1-0kg	SC2-5kg	SC3-10kg	SC4-15kg
Cement (kg/m3)		440	440	440	440
Aggregate (kg/m3)	0/4mm – 65%	1088	1088	1088	1088
	4/8 mm – 35%	583	583	583	583
Superplasticizer (kg/m3)		4,4	4,4	4,4	4,4
Accelerator (kg/m3)		17,6	17,6	17,6	17,6
Water (kg/m3)		198	198	198	198
Polypropylen fiber (kg/m3)		0	5	10	15
w/c		0.45	0.45	0.45	0.45

3. RESULTS AND DISCUSSION

The consistency of the fresh basic mix design shotcrete was class S4 according to standard SRPS ISO 4103/1997.

For the testing of shotcrete for absorption energy according to SRPS EN 14488-5, slabs60x60x10cm were sampled according to SRPS EN 14488-1.

Samples of cube edge shapes d=100 mm were sampled for testing the compressive strength and tensile splitting strength. Sampling of plates in shotcrete cubes is shown in Figure 2.

Figure 2 - Samples for testing

Samples of shotcrete were placed into slab shaped metal molds with the dimensions of 60x60x10 cm and cube shaped metal molds dimensions d=100 mm, which were air-cured for the first 24h and then in water in ambient conditions until the moment of testing according to SRPS EN 12390-2. The slope stabilization with shotcrete is shown in Figure 3.

Figure 3 – Stabilization of the slope with shotcrete

Testing of concrete compressive strength and splitting tensile strength at the age of 28 days was carried out according to SRPS EN 12390-3 and SRPS EN 12390-6 standard. Bulk density of hardened concrete was tested according to SRPS EN 12390-7 standard and ranged from 2220 to 2260 kg/m^3. The test results are shown in Figures 4 as the mean of three tests.

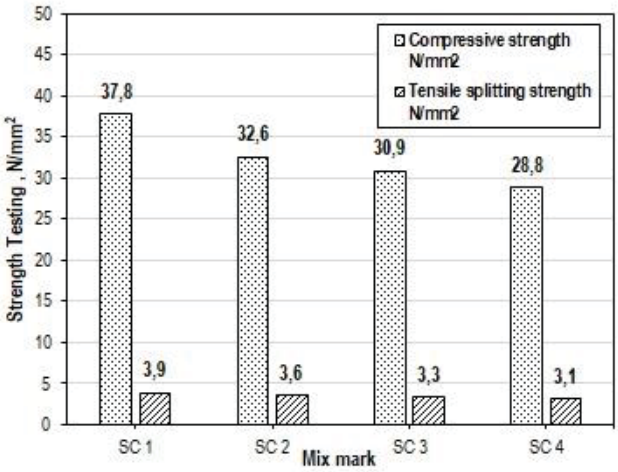

Figure 4 – Result testing compressive strength and splitting tensile strength at the age of 28 days

a) 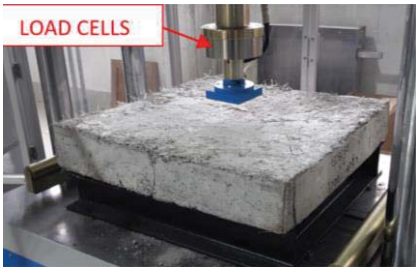

b)

Figure 5 –Disposition of testing Fig. a) and test finishing Fig b)

For the puncture testing of concrete slabs 600x600x100 mm, a digital hydraulic press with the range of 300kN was used. During testing, a steel frame of 500x500 mm was used. Under the slab, an inductive displacement meter LVDT is placed in the central part. Procedure of testing with the measuring equipment is shown in Figure 5.

A diagram load – deflection is shown in Figure 6.

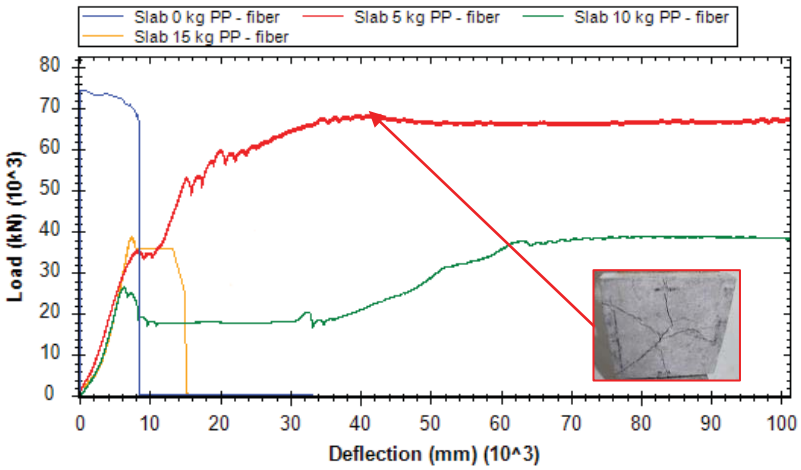

Figure 6 – Chart load / deflection during the examination of the slab made of fiber reinforced shotcrete

The obtained test results are shown in Table 5.

Table 5 – Test results for shotcrete slabs at the age of 28 days

Mix mark	*Results of testing's slabs*		
	Maximal load	*Deflection at maximal load*	*Energy at maximal load*
	kN	*mm*	*J*
SC1-0kg (Slab 0 - PPfiber)	*74.512*	*0.0018*	*48*
SC2-5kg (Slab 5 - PPfiber)	*68.550*	*4.1328*	*206559*
SC3-10kg (Slab10 - PPfiber)	*39.009*	*8.1015*	*206341*
SC4-15kg (Slab15 - PPfiber)	*38.829*	*0.7369*	*52513*

4. CONCLUSIONS

Based on the obtained diagram for the puncture testing of the slab for all four types of shotcrete, the following can be noticed:

1. Slab SC 1 - 0 kg, shotcrete without polypropylene fibers acheived the highest load compared to other concrete mixes but due to the lack of fibers; brittle fracture., fractures are formed

2. Slab SC 2 - 5kg, shotcrete with 5 kg of polypropylene fibers had the highest ductility. The fibers are well distributed and oriented in the cement matrix, the maximum force is 68.55 kN for a deflection of 4.13 mm.

3. Slab SC 3 - 10kg, shotcrete with 10 kg of polypropylene fibers have lower ductility compared to the SC 2 series. This result can be due to poor homogenization due to the increased content of polypropylene fibers, the maximum force is 39.0 kN for a deflection of 8.1 mm.

4. Slab SC 4 - 15kg, shotcrete with 15 kg of polypropylene fibers had a maximum force of 38.8 kN for a deflection of 0.7 mm. This lower result was obtained due to the weaker homogenization of the fibers in the cement matrix.

The results obtained by testing the compressive and tensile splitting strength indicate that the addition of fibers to the tested properties is only justified for the quantity of 5 kg of polypropylene fibers.

ACKNOWLEDGMENTS

The work reported in this paper is a part of the investigation within the research project TR 36017 "Utilization of by-products and recycled waste materials in concrete composites in the scope of sustainable construction development in Serbia: investigation and environmental assessment of possible applications" supported by the Ministry of Education, Science and Technological Development, Republic of Serbia. This support is gratefully acknowledged.

REFERENCES

[1] Muravljov M., Zakic D., Askrabic M., Gavrilovic D., Fizičko – mehanička svojstva torkret betona sa dodatkom sintetičkih vlakana namenjenog za tunelske obloge, Savremeni materijali i konstrukcije sa regulativom: 2016: p.1-10.

[2] Franzen, T., 1992. Shotcrete for underground support: a State-of-the-art report with focus on steel-fibre reinforcement. Tunn. Undergr. Sp. Tech. 7 (4), 383-391

[3] Hoek, E., Kaiser, P., Bawden, W., 2000. Support of Underground Excavation in Hard Rock. CRC Press, Boca Raton, Florida, USA.

[4] Malmgren, L., 2005. Interaction between Shotcrete and Rock-experimental and Numerical Study. PhD dissertation. Lulea University of Technology, Sweden.

[5] Ansell, A., 2010. Structural behaviour of shotcrete on irregular hard rock surfaces. In: Shotcrete: Elements of a System. CRC Press/Balkema, Leiden, The Netherlands.

[6] Austin, S., Robins, P., 1995. Sprayed Concrete: Properties, Design and Applications. Whittles Publishing, Caithness, Scotland.

[7] Matsumoto, Y., Nishioka, T., 1992. Theoretical Tunnel Mechanics. University of Tokyo Press, Tokyo, Japan.

ДГКС Друштво грађевинских конструктера Србије
ASES Association of Structural Engineers of Serbia
S-54
15. KONGRES
6-8. 9. 2018. Zlatibor

Dragan Nikolić[1], Snežana Mitrović[2], Goran Ćirović[3]

PROCENA MEHANIČKIH SVOJSTAVA UHPC

Rezime:

Tokom procesa hidratacije u cementnim kompozitima se formira nehomogena struktura, dok svojstva materijala u očvrslom stanju variraju iako se pri proizvodnji ne menjaju maseni udeli komponentnih materijala. Teorija grubih skupova predstavlja naprednu tehniku za tretiranje problema neizvesnosti, nepreciznosti i netačnosti i pogodna je za procenu dostizanja zahtevanih mehaničkih svojstava kompozita u ranim starostima. U radu su prikazani rezultati ispitivanja 12 projektovanih mešavina betona izuzetno visokih mehaničkih svojstava. Variran je vodovezivni faktor, sadržaj silikatne prašine i čeličnih vlakana. Izvršena je analiza parametara primenom gubih skupova u programskom paketu Rosetta i data su pravila za odlučivanje koja mogu biti od pomoći u procesu donošenja odluka o udelu komponentnih materijala u odnosu na zahtevana i postignuta mehanička svojstva.

Ključne reči: grubi skupovi, UHPC-ultra high performance concrete, procena meh. svojstava

ESTIMATION STRENGTH PROPERTIES OF UHPC

Summary:

During the hydration of cement, a heterogeneous structure is created within its composite materials and the properties of the material in a hardened state vary during the production period even though the mass proportion of the component materials in the concrete does not change. The rough set theory represents an advanced technique for treating the problems of uncertainty, ambiguity and inaccuracy, and it is suitable for assessing the attainment of the required mechanical properties of the composite based on its properties in early ages. This paper shows the results of tests completed on 12 mixtures of ultra high performance concrete. The water/binder ratio and the content of silica fume and steel fibers are varied. By applying rough sets in the program solution Rosetta, an analysis of the parameters is carried out and the rules are given for deciding which of them can help in the process of making a choice as to the proportions of the component materials in the concrete mixture in relation to the required and attained mechanical properties.

Key words: rough set, UHPC - ultra high performance concrete, estimation strength properties

[1] *PhD, High School of App. Sci. of Civil Eng. and Geodesy, Belgrade, nikolic@vggs.rs*
[2] *PhD, High School of App. Sci. of Civil Eng. and Geodesy, Belgrade, mitrozs@sezampro.rs*
[3] *PhD, High School of App. Sci. of Civil Eng. and Geodesy, Belgrade, cirovic@sezampro.rs*

1. INTRODUCTION

The development of modern civil engineering is based to a large extent on a permanent search for high quality materials and on bettering and perfecting the characteristics of existing materials. The aim of current research is the development of materials which have high mechanical properties, satisfactory resistance to a variety of aggressive agents (durability) and whose use can be justified economically [1,2]. Alongside this, in the research and development of materials in civil engineering, the generally accepted concept of sustainable development has a strong influence, which together with sociological and economic aspects includes saving energy, environmental protection and the preservation of unrenewable natural resources [3].

High and ultra high performance concrete came about at the end of last century through modification of the existing rules for deciding on the combination of component materials [4]. In some cases the characteristic strength of this concrete is over 200 MPa, depending on the regime applied, care of the samples and quantity of highly reactive material in the mixture [5,6]. With this, is its notably improved performance when applying pressure which induces tensile stress, also its stiffness and durability when compared with other types of concrete [7,8,9]. In France in 2002, based on many years of research, the first recommendations were made for the use of this type of composite [10].

The rough set theory is an advanced mathematical concept for dealing with inaccuracy, ambiguity and uncertainty in the analysis of data, which was introduced at Warsaw University in 1982 [11]. The problem of determination or assessment of strength in UHPC on the basis of testing the mechanical properties of concrete in early ages is characterised by an incomplete and insufficient body of information, and by virtue of this, falls into the domain where the rough set theory is highly applicable.

Since its initial introduction, the rough set theory has found an important role in expert systems, systems for supporting decision making, shape recognition and solving different problems in civil engineering [12,13]. By using these methods in soft programming Attoh-Okine introduced a system for supporting decision making in the repair and maintenance of road constructions [14]. Also, Kim,Y.M. et. al. suggested determining the categories of cracks in reinforced concrete structures [15].

This paper shows an analysis of experimental test results, with the purpose of showing that the use of rough sets can help in the decision making process, that is that on the basis of the mechanical properties of ultra high performance concrete in early ages, the mechanical properties of a composite 28 days old can be worked out. In order to calculate the relevant characteristics of the data in tables and to generate rules for classification, the software solution Rosetta was used [16]. The software is designed to support the process of gaining new knowledge, processing data and generating rules in the context of rough set theory. The experimental data shown in this study is part of a defended Master's thesis [17].

2. BRIEF OVERVIEW OF ROUGH SET

A basic assumption in rough set theory is that each item (object) in the discussion is associated with some particular information (data). This means that each object is displayed with the help of specific information about it. More objects which can be described by the

same information are similar to eachother, that is they cannot be different to each other with regard to the available information. Relations generated in this way are known as indiscernibility relations, and they represent the mathematical basis for the rough set theory.

The goal of achieving the mathematical formulation of a rough set begins with a data table. It is understood that the term attribute is used rather than the term criterium since the first term is much more general than the second. It is also understood that the data table is a quadruple data group:

$$S = (U, A, V, f) \tag{1}$$

where:
U – a finite set of objects
A – a finite set of attributes
For each attribute $a \in A$ there is a set Va of its values or assessments. Each attribute a determines the function f: $U \rightarrow V_a$. For each subset B of A, there is an indiscernibility relation I on U, marked as I(B) and thus defined as:

$$I(B) = \{(x, y) \in U \times U : f_a(x) = f_b(y), \forall a \in B\} \tag{2}$$

Let U be a finite set of objects – a universe and let X exist so that $X \subseteq U$, with $x \in X$. Binary relations B on U are introduced, that is the indiscernibility relation. Let B be a subset of A ($B \subseteq A$).

The following operations on sets are defined:
$B*(X)$ - a lower approximation of X is defined as follows:

$$B*X = \{x \in U : B(x) \subseteq U\} \tag{3}$$

$B^*(X)$ - an upper approximation of X defined as follows:

$$B^*X = \{x \in U : B(x) \cap X \neq 0\} \tag{4}$$

Boundary region of X is the set

$$BN_B(X) = B^*(X) - B*(X) \tag{5}$$

If the boundary region of X is an empty set:

$$BN_B(X) = 0 \tag{6}$$

the set is crisp (exact) with respect to B, and in the opposite case

$$BN_B(X) \neq 0 \tag{7}$$

the set X is rough (inexact) with respect to B.

3. EXPERIMENTAL PROGRAM

3.1. OVERVIEW

In the experimental program, only component materials available in Serbia were used. In previous laboratory tests the compatability of the cement with the chemical additives was confirmed. When making the mix, water from the town water supply was used.

In the experimental program, ordinary portland cement was used CEM I 52.5R, and as an aggregate, quartz sand with a granule size of 0-0.5mm was used. When testing its granulometric composition, 70.2% of the aggregate grains were between 0.2 and 0.4 mm. Enough polycarbosilane based superplasticizer was used to make it possible to have a very low water/binder ratio. As a mineral supplement, extra fine silica fume was added. Flat steel fibers were used (length/diamater=8/0.15 mm) with strain resistance ≈ 3000 N/mm^2. The steel fibers were coated with brass in order to increase durability and resistance to corrosion.

3.2. MIX PROPORTIONS

The experiment was carried out altogether on 12 different concrete mixtures. The composition of the mixtures is shown in Table 1. Each individual mixture was prepared three times in order to show the repeatability of the experiment results for each of the properties. The composition of the mixture was chosen on the basis of previous research in order to reach the compressive strength of ultra high performance concrete. The volume proportion of steel fibers moved within a range of 2.5 to 4.2%. All mixtures were prepared in a standard 5l cement and plaster mixer. The fresh mixture was poured into steel molds (4x4x16cm). Samples were pressed on a vibrotable at a frequency of 150 Hz.

Table 1 – UHPC mix proportions

No.	Cement [kg]	Aggregate [kg]	Silica fume [kg]	Additive [kg]	Steel fiber [kg]	Water	w/c*1	w/b*2
C1	850	1180	100	20.0	195	207.0	0.24	0.20
C2	850	1160	100	23.0	195	212.0	0.25	0.20
C3	950	1045	110	35.4	195	226.6	0.24	0.20
C4	850	1095	170	35.4	195	204.6	0.24	0.20
C5	900	950	200	34.6	330	198.4	0.22	0.18
C6	900	950	200	36.4	330	179.6	0.20	0.16
C7	850	1050	185	39.0	330	164.0	0.19	0.16
C8	1050	900	230	28.6	300	180.4	0.17	0.14
C9	900	1050	200	42.1	230	240.9	0.27	0.22
C10	850	1020	185	34.5	330	168.5	0.20	0.16
C11	850	1020	185	39.5	330	169.5	0.20	0.16
C12	850	1020	185	37.8	330	162.2	0.19	0.16

*1 – water/cement ratio, *2 – water/binder ratio

3.3. COMPRESSIVE AND FLEXURAL STRENGTH

The experiment was carried out on concrete in fresh and hardened states. All 12 mixtures were class consistency S1. The temperature of the concrete in a fresh state was measured at between 22 and 25°. The density of fresh concrete was from 2560 to 2630 kg/m3. Its flexural strength was determined through tests using prisms of 4x4x16 cm, and the compressive strength by a modified cube method (examination surface 4x4 cm). Table 2 shows the test results of the mechanical properties of concrete.

Table 2 – Experimental results

Concrete	Compressive strength [N/mm^2]			Flexural strength [N/mm^2]		
	2 days	7 days	28 days	2 days	7 days	28 days
C1	86.1	123.8	146.9	15.2	22.5	26.7
C2	82.4	113.1	136.3	17.1	23.3	23.9
C3	77.4	96.3	131.3	17.6	20.3	28.7
C4	82.3	128.1	148.2	14.7	24.8	29.5
C5	97.4	125.6	153.1	24.9	28.7	29.8
C6	95.3	125.6	155.0	21.8	24.3	25.9
C7	96.1	132.5	153.1	18.8	25.6	26.2
C8	93.9	123.8	154.4	16.8	21.1	21.9
C9	82.6	97.8	128.1	16.5	18.3	22.8
C10	83.9	96.9	146.9	18.9	23.6	32.6
C11	89.6	115.6	159.4	21.4	25.9	29.5
C12	78.5	93.8	170.9	19.2	25.3	30.1

4. DECISION ALGORITHM FOR ESTMATING CATEGORY OF STRENGTH PROPERTIES

As well as showing the mechanical properties, Table 3 also gives the values of the water/binder ratio and the volume proportion of steel fibers in the 12 concrete mixtures. The table represents a table of attributes and a decision table. The columns in the table are marked by the attributes (properties of the mixture), and the rows are marked by objects (the experimental mixtures), while the values in the table are the attribute values.

7 criteria were adopted for the evaluation of variant solutions:
- f_c^2: compressive strength at 2 days old
- f_s^2: flexural strength at 2 days old
- f_c^7: compressive strength at 7 days old
- f_s^7: flexural strength at 7 days old

- f_c^{28}: compressive strength at 28 days old
- f_s^{28}: flexural strength at 28 days old
- w/b: water/binder relationship
- C_{sf}: volume proportion of steel fibers in $1m^3$ of composite.

These criteria represent attribute conditions, and the solution applicable (or non-applicable) composition of the designed concrete mixtures represents the attribute decision. The values of the attributes expressed are numerical. For the required mechanical properties at 28 days old (compressive strength >150 N/mm^2 and flexural strength >25 N/mm^2), the concrete also needs to fulfill the necessary workability requirements in order for fresh concrete to be added.

Table 3 – Decision table

No.	f_c^2	f_s^2	f_c^7	f_s^7	w/b	C_{sf}	O
C1	86.1	15.2	123.8	22.5	0.20	2.4	no
C2	82.4	17.1	113.1	23.3	0.20	2.4	no
C3	77.4	17.6	96.3	20.3	0.20	2.4	no
C4	82.3	14.7	128.1	24.8	0.20	2.4	no
C5	97.4	24.9	125.6	28.7	0.18	4.0	yes
C6	95.3	21.8	125.6	24.3	0.16	4.0	yes
C7	96.1	18.8	132.5	25.6	0.16	4.0	yes
C8	93.9	16.8	123.8	21.1	0.14	3.7	yes
C9	82.6	16.5	97.8	18.3	0.22	2.8	no
C10	83.9	18.9	96.9	23.6	0.16	4.0	no
C11	89.6	21.4	115.6	25.9	0.16	4.0	yes
C12	78.5	19.2	93.8	25.3	0.16	4.0	yes

Discretization of the values of the attribute conditions was inspired by the need to describe numerical values in linguistic terms rather than precise values. Presentation of the data grouped in intervals secures more correct processing of the data as it reduces the influence of deviation of some of the data at particular intervals of the experimentally acquired values. In this way, part of the excess data can be identified and then removed. The values of the attribute conditions are divided into three intervals of equal length and shown in Table 4.

The question is often asked as to whether some of the data can be removed from the decision table on the condition that its basic characteristics are kept. Reductors represent a minimal subset of attributes which makes the same classification of elements of the universe possible as a complete set of attributes. In other words, attributes which do not belong to the reductors are excess in terms of of the classification of elements in the universe. Determining the reductions is an essential task in the rough set theory. A flexible set of algorithms for processing data is available in the software solution Rosetta. In this paper, a genetic algorithm reducer is used for reducing data and generating rules for decision making as an effective tool for finding the reduction of rough sets.

A presentation of the function and purpose of algorithms, and also a method of deciding on the minimal subset of attributes is given in detail in a study by Vinterbo and Øhrn [18].

Table 4 – Decision table after discretization

No.	f_c^2	f_s^2	f_c^7	f_s^7	w/b	C_{sf}	O
C1	1	0	1	0	1	0	no
C2	0	1	1	1	1	0	no
C3	0	1	0	0	1	0	no
C4	0	0	2	1	1	0	no
C5	2	2	2	2	1	2	yes
C6	2	2	2	1	0	2	yes
C7	2	1	2	2	0	2	yes
C8	2	0	1	0	0	1	yes
C9	1	0	0	0	2	1	no
C10	1	1	0	1	0	2	no
C11	1	2	1	2	0	2	yes
C12	0	2	0	2	0	2	yes

With:
fc2: [*, 82.5)→0; [82.5, 91.8) →1; [91.8, *)→2;
fs2: [*, 17.0) →0, [17.0, 19.1) →1, [19.1, *)→2;
fc7 [*, 105.5) →0, [105.5, 124.7) →1, [124.7, *)→2;
fs7 [*, 22.9) →0, [22.9, 25.1) →1, [25.1, *)→2;
w/b [*, 0.17) →0, [0.17, 0.21) →1, [0.21, *)→2;
Csf [*, 2.6) →0, [2.6, 3.9) →1, [3.9, *)→2;

The decision making rules from the first reduced groups of attributes { f_c^2, f_s^7} have the following form:

f_c^2 ([82.5, 91.8)) AND f_s^7 ([*, 22.9)) => no
f_c^2 ([*, 82.5)) AND f_s^7 ([22.9, 25.1)) => no
f_c^2 ([*, 82.5)) AND f_s^7 ([*, 22.9)) => no
f_c^2 ([91.8, *)) AND f_s^7 ([25.1, *)) => yes
f_c^2 ([91.8, *)) AND f_s^7 ([22.9, 25.1)) => yes (8)
f_c^2 ([91.8, *)) AND f_s^7 ([*, 22.9)) => yes
f_c^2 ([82.5, 91.8)) AND f_s^7 ([22.9, 25.1)) => no
f_c^2 ([82.5, 91.8)) AND f_s^7 ([25.1, *)) => yes
f_c^2 ([*, 82.5)) AND f_s^7 ([25.1, *)) => yes

On the basis of the given rules for decision-making, it is possible to evaluate whether the mechanical properties of the composite achieve the required values at 28 days old, and within the given parameters.

5. CONCLUSIONS

On the basis of early hardness, it is very important in the production process of prefabricated elements of composite materials with a cement matrix to anticipate whether recently produced elements fulfil the required quality standard. Concrete is a heterogenous material, as a consequence of which there can be a definite deviation in the compressive stength achieved at 28 days old, even though the elements are prepared from the same class and type of concrete.

This paper pointes out the importance of assessment of the hardness of ultra high performance concrete in relation to the required values due to a lack of research on this type of composite prepared with component materials available on the domestic market. In the experimental study, 12 mixtures were prepared in a laboratory with the purpose of showing that it is possible to produce cement composite material with extremely high mechanical properties with local materials.

By using rough sets, suggestions can be made to the decision maker as to possible problems in the production itself. The function of rough belonging has a probabilistic character, so with this kind of analysis, based on attributes that reflect measurable properties, conditions and experience as well as by using several groups of attributes, an objective decision can be made.

On the basis of experimental results it is possible to draw the following observations:

- It was shown that a compressive strength of over 150 MPa and a flexural strength of over 30 MPa can be achieved with component materials available on the domestic market without the use of hydrothermal processing. Getting ultra high performance concrete with a compressive strength of over 200 MPa is conditional on the use of concrete mixtures with notably higher quality cements which are not available on the domestic market and by using steam curing or autoclave curing.
- The experimental results were analysed by using rough sets and the decision making rules were presented, on the basis of which it is possible to work out whether the ultra high performance concrete fulfils the required properties primarily on the basis of the mechanical properties in early ages. This does not mean that the decision making results introduced do not apply to a composite made from other component materials, but they certainly differ depending on the quality of the composite materials used.
- It can be seen that mixtures with a water/binder ratio of over 0.2 cannot reach a compressive strength of over 150 MPa and what needs to be kept in mind is that designing the concrete mixtures for this type of composite is without the use of hydrothermal processing.
- The growth of the value of the fc/fzs ratio in relation to the age of the composite in this experimental research can only be seen when the volume proportion of steel fibers is increased. In figure 2, growth in the fc/fzs ratio at 28 days old compared with 2 and 7 days old can only be seen when using 4% of steel fibers in the concrete mixture.

ACKNOWLEGMENTS

This work was part of TR 36017 project and provided under financial support of Ministry of Education and Science, Republic of Serbia.

REFERENCES

[1] Balaguru P, Shah SP. Fiber Reinforced Cement Composites. New York: McGraw Hill, 1992.

[2] Bentur A, Mindess S. Fiber Reinforced Cementitious Composites. London, UK: Elsevier Applied Science, 1990.

[3] Marinkovic S,Radonjanin V, Malesev M, Ignjatovic I. Comparative environmental assessment of natural and recycled aggregate concrete. Waste Management, , doi:10.1016/j.wasman.2010.04.012 in press

[4] Skazlic M, Bjegovic D, Mrakovcic S. High performance fiber reinforced concrete. Građevinar, Croatia 2004; 56(2): 69-78.

[5] Yunsheng Z, Wei S, Sifeng L, Chujie J, Jianzhong L. Preparation of C200 green reactive powder concrete and its static–dynamic behaviors. Cement & Concrete Composites 2008; 30: 831–838.

[6] Yazıcı H, Yardımcı M, Yigiter H, Serdar Aydın S, Turkel S. Mechanical properties of reactive powder concrete containing high volumes of ground granulated blast furnace slag. Cement & Concrete Composites 2010; 32: 639–648.

[7] Cwirzen A, Penttala V, Vornanen C. Reactive powder based concretes: Mehanical properties, durability and hybrid use with OPC. Cement and concrete research 2008; 38:1217-1226.

[8] Yang SL, Millard SG, Soutsos MN, Barnett SJ, Le TT. Influence of aggregate and curing regime on the mehanical properties of ultra-high performance fibre reinforced concrete (UHPFRC). Cement and concrete research 2009;23:2291-2298

[9] Feylessoufi A, Tenoudji C, Morin V, Richard P. Early ages shrinkage mechanism of ultra-high performance cement-based materials. Cement and concrete research 2001; 21:1573-1579

[10] Ultra-High Performance Fibre-Reinforced Concrete. Interim Recommendations AFGC/SETRA working group, 2002

[11] Pawlak Z. Rough Sets. International Journal of Computer and Information Science, 1982; 11:341-356

[12] Cirovic G, Plamenac D. Rough sets – application in the construction industry. Serbia: Operational Research Society, 2005.

[13] Cirovic G, Cekic Z. Case-based reasoning model applied as a decision support for construction projects. Kybernetes – The International Journal of Systems & Cybernetics 2002; 31(6):896-908.

[14] Attoh-Okine N. Rough set application to data mining principles in pavement management database. J Comput Civil Eng ASCE 1997;11(4):231–237

[15] Kim YM, Kim CK, Lee JC. Rough set algorithm for crack category determination of reinforced concrete structures. Advances in Engineering Software 2009; 40: 202–211

[16] http://www.lcb.uu.se/tools/rosetta/, Rosetta software official web page

[17] Nikolic D. Optimisation of high strength concrete composition using rough set. Msce thesis. University of Banja Luka 2010.

[18] Vinterbo S, Øhrn A. Minimal approximate hitting sets and rule templates. International Journal of Approximate Reasoning 2000; 25(2):123–143.

[19] Neville AM**.** Properties of Concrete. New York: John Wiley and Sons, 1994, 3rd ed.

ДГКС Друштво грађевинских конструктера Србије
ASES Association of Structural Engineers of Serbia
S-55
15. KONGRES
6-8. 9. 2018. Zlatibor

Bojan Milošević[1], *Slobodan Ranković*[2], *Žarko Petrović* [3], *Marina Mijalković*[4]

PREGLED EKSPERIMENTALNIH ISPITIVANJA LINIJSKIH NOSAČA OD SAMOUGRAĐUJUĆEG BETONA

Rezime:

Poslednjih godina, nova tehnologija koja se naziva samougrađujući beton je postala popularna u građevinarstvu. Više eksperimentalnih istraživanja je sprovedeno u cilju utvrđivanja konstrukcijskog ponašanja armiranih greda od samougrađujućeg betona. Cilj ovog rada je da se stručnoj javnosti prikažu neki od rezultata sprovedenih eksperimentalnih istpitivanja u periodu od 2008 do 2018 godine. Pored toga, prikazani su i rezultati sopstvenog eksperimentalnog istraživanja kontinualnog grednog nosača na dva polja koji je izradjen od samo ugrađujućeg betona. Verifikacija eksperimentalno dobijenih rezultata sprovedena je primenom programskog paketa Abaqus.

Ključne reči: samougrađujući beton, linijski nosači, granična nosivost, Abaqus

OVERVIEW OF EXPERIMENTAL EXAMINATION OF LINEAR GIRDERS MADE OF SELF-COMPACTING CONCRETE

Summary:

In recent years, an emerging technology termed Self-Compacting Concrete (SCC) has become popular in construction industry. Many experimental tests are carried out to investigate the structural behaviour of SCC reinforced beams. The aim of this paper is to present some of the results of the conducted experimental investigations, which were performed in the period from 2008 to 2018. In addition, on the basis of its own experimental research, the results of the testing on two-span continuous beam made of SCC are presented. The verification of the experimentally obtained results was carried out using the Abaqus software package.

Key words: self-compacting concrete, linear girders, limit load, Abaqus

[1] *Prof. PhD, College of Applied Studies in Civil Engineering and Geodesy, University of Belgrade, Republic of Serbia, prodic_80@yahoo.com*
[2] *Assistant Prof. PhD, Faculty of Civil Engineering and Architecture, University of Niš, Republic of Serbia, slobodan.rankovic@gaf.ni.ac.rs*
[3] *Assistant Prof. PhD, Faculty of Civil Engineering and Architecture, University of Niš, Republic of Serbia, zarko.petrovic@gaf.ni.ac.rs*
[4] *Full Prof. PhD, Faculty of Civil Engineering and Architecture, University of Niš, Republic of Serbia, marina.mijlkovic@gaf.ni.ac.rs*

1. INTRODUCTION

Self-compacting concrete (SCC), as a relatively new material, represents an insufficiently researched area, both in terms of characteristics in fresh and hardened state. Self-compacting concrete (SCC) is a type of concrete that consolidates under its own weight without external compaction. The extremely fluid nature of SCC makes it appropriate to use in difficult conditions and in sections with congested reinforcement. The fresh, self-compacting concrete mixture poured into the formwork has the ability to completely fill the formwork under its own weight, even the smallest spaces between reinforcing bars reaching a sufficient level of compactness, while the hardened concrete has properties and durability as well as a conventional vibrated concrete.

The first recommendations for proper design of self-compacting concrete were published by EFNARC in 2002 (EFNARC, 2002). The European design commission composed of five European associations drafted the "The European Guidelines for Self Compacting Concrete" in 2005 (EFNARC, 2005). By the Technical Committee CEN/TC 104 “Concrete and related products” the standard EN 206-9:2010 was prepared, which was published by the European Committee for Standardization in February 2010 (EN 206-9:2010, 2010). This standard defining the rules for design of self- compacted concrete is an annex to the standard EN 206-1:2000 and it will become its integral part.

The paper presents a short referential review of the research conducted up to date in relation to construction of structural elements made from self-compacting concrete. Mechanical characteristics tests of self-compacting concrete in fresh and hardened state are presented as well as the tests carried out on continuous beams loaded with short-term static loading to failure. The continuous beams are made of self-compacting concrete, reinforced with reinforcement percentage (0,64%). The numerical analysis of continuous beams was carried out using the Abaqus software, and the obtained results were compared with the experimentally obtained ones. Based on the analysis and discussion of the obtained results, the possibility of applying EC2 regulations for the design of structural elements made of self-compacting concrete has been confirmed.

2. REVIEW OF RESEARCH CONDUCTED SO FAR

The paper first presents the results of some experimental research that was conducted in the period 2008-2018.

The impact of long-term load in beams made of self-compacting concrete (SCC) and their comparison with the results obtained in beams made of conventional normally vibrated concrete (NVC) was shown in one of the studies (Xiao et al., 2008). The program of testing included eight beams made of SCC and four girders made of NVC, in which the percentage of reinforcement, static system and load intensity was varied. Under the same environmental conditions, the shrinkage-time curve of self-compacting concrete is very similar to that of normal concrete while the deflection creep coefficient of SCC beams after 18 months is about 1.6, which is very close to NVC beams.

Among the first tests carried out was the experimental testing of the load bearing capacity of the simply-supported beam with reverse T cross-section in order to compare the characteristics of the beams made of conventional vibrated and self-compacting concrete. During the experiment, the development and width of the cracks, load-deflection relationship and failure modes were monitored. Almost identical characteristics of the beams made of vibrated and self-compacting concrete exposed to short-term static load were observed (Kumar et al., 2009).

Experimental testing of high-altitude beams made of self-compacting and vibrated concrete exposed to shear and bending effects was the subject of one of the conducted studies (Hassan et al., 2010). By varying the content of the large aggregate, the height of the beam, the percentage of longitudinal reinforcement, the appearance and development of cracks due to bending / shearing, load-deflection relationship and failure modes were monitored. It has been observed that the load capacity of beams made from self-compacting concrete is slightly lowerthan those of conventional vibrated concrete.

Structural performance of self-consolidating concrete used in reinforced concrete beams as well as the comparison between the experimental results and theoretical calculations based on the codes provisions were shown in paper (Sharifi Y., 2012). Six simply supported reinforced SCC beams were tested under four point bending with a pure moment region. Comparing the experimental and analytical results it was concluded that theoretical calculations used for reinforced beams with conventional concrete can be used for reinforced beams cast with self-consolidating concrete.

Testing of the reinforced, pre-stressed and composite simply-supported beams made of self-compacting concrete under loads applied at one-third points of the span (four-point load) is shown in paper (Cattaneo et al., 2012). Regarding the limit value of the bending moment as well as the moment-curvature relationship, the criteria defined by EC2 are satisfied.

In one of the rare studies dealing simultaneously with self-compacting and self-curing concrete (Vidivelli et al., 2013) twelve concrete mixtures with various replacements of constituent materials and addition of mineral and chemical admixtures were made and all the beams were tested as simply supported beams under the action of the centre single point load. The experimental results were compared with the predicted values of the flexural behaviour of beams at various stages, such as yield load, ultimate load and deflection through the ANN modelling. The predicted results of ANN compared with the experimental results were quite satisfactory.

The paper (Helincks et al. 2013) presented an experimental test program that was carried out to investigate the bond and shear performance of powdertype self-compacting concrete. In total, 72 pull-out specimens were tested, cast with different concrete mixtures and rebar diameters (8, 12, 16, and 20 mm). It was found that characteristic bond strength values of the SCC specimens were as high as or higher than those of the specimens with vibrated concrete. In order to study the shear behaviour, four-point bending tests were executed on a total of 102 SCC and NVC beams made with different reinforcement ratios (1.0%, 1.5%, and 2.0%) and tested with different shear span-to-depth ratios (from 1.5 to 3.0). The results of the experiments led to the conclusion that the bond strength of SCC beams is as high as or higher than the bond strength of NVC beams and the SCC beams showed equal or lower ultimate shear strength than the NVC test beams.

The behavior of beams made of conventional concrete under cyclic load is well known, while behavior of beams made from self-compacting concrete under cyclic load is still insufficiently tested. Experimental testing was carried out on a simply-supported beam with reverse T cross-section, exposed to the action of static and cyclic load at one-third points of the span (Korte et al., 2014). Deflections and strains as well as development and width of cracks were monitored, whereby the faster increase in strains and crack development were observed in the beams of self-compacting concrete.

In an experimental investigation (Biolzi et al., 2014) the shear strength and the fracture behavior of self-compacting reinforced concrete (RC) beams were investigated. Beams with and without shear reinforcement made with self-consolidating and normal vibrated concrete were tested in four-point bending tests. Comparisons with similar tests on normal vibrated concrete beams show that self-compacting concrete beams exhibit similar shear strength associated with a more brittle behavior.

One of the main drawbacks of self-compacting concrete is its cost due to higher amount of cement and chemical mixtures included in its composition. As an alternative to reducing costs, it is possible to replace a part of cement with by-products such as silicate dust, slag and others. In accordance with EFNARC recommendations, mixtures with ash, silicate dust and glass fibers were made (Aderhya et al., 2016). It has been observed that the ash mixture has a pronounced early strength, while the later age strength is increased in the mixture with silicate dust. The behavior of simply-supported beams made of self-compacting concrete with such mixtures was studied. Depending on the percentage of reinforcement of the beams, there is a ductile or brittle fracture, and the failure mode corresponds to theoretical settings that apply to conventional vibrated concrete.

In the paper (Dharmaraj R., Malathy R., 2016) the effect of corrosion inhibitor (Hexamine) in self-compacting concrete on both fresh and hardened concrete was presented. The replacement of cement with fly ash in self-compacting concrete for the M25 mix design was about 40%, with the presence of corrosion inhibitor with varying percentages viz., 0%, 1%, 2%, 3%, 4%, and 5%. The experimental programme consisted of the testing of two beam specimens, designed to assess the contribution of corrosion inhibitor (Hexamine) to the flexural capacity of the beam. It was observed that the addition of corrosion inhibitors does not influence the compressive strength of concrete and it was recommended to use 2% Hexamine mix which provides dominant strength to the self-compacting concrete. The increase in first crack load have been observed for beams with Hexamine 2% mix in comparison to the conventional beams.

Experimental testing of high two-span continuous beams loaded with two concentrated forces in the middle of each span is shown in the paper (Khatab et al., 2017). Tested beams were examined for shear effects depending on the quantity and position of the longitudinal reinforcement and stirrups. In all cases there were large diagonal cracks occurring between the medium support and the points in which the load was applied. Experimental results were compared with the recommendations given by ACI 318M-11, EC2, CSA A 234-04 as well as strut-and-tie model, with the results best matching with ACI 318M-11.

As self-compacting concrete is capable of flowing along the densely arranged reinforcement, its applications are investigated in the perforated beam exposed to bending in which an additional reinforcement was placed around the perforations (Gohar et al., 2017). The main parameters in this study were the shape of perforation (circular and oval) and

configuration of the reinforcement around the perforation. Some beams had a higher, and some had a lower failure force in relation to the control beam, with a change of the coefficient of ductility of beams which was not correlated with the limiting failure force.

A study of the flexural behaviour of non-prismatic beams made of self compacting concrete is shown in one of the papers (Sharik I., Daniel J., 2017). The paper focuses on investigating of the characteristics of M50 self-compacting concrete where cement is replaced with ground granulated blast furnace slag (GGBS) and Micro Silica (MS) with six different proportions. Using that concrete mixtures the beams with non uniform cross section were made and then flexural behavior of these beams were tested and compared with that of the conventional beam. The load carrying capacity of conventional beam was higher than in the case of the non-prismatic beams and the crankrod provided in the region of varying cross section prevents the formation of a shear crack.

This study proposes a finite element model to analyse two different SCC beams by using the computational platform, ABAQUS (L. Thompson Yaw, et al. 2017). Research is based on the validation of SCC beams that were experimentally in the KNUST structural engineering laboratory, there were two beams, loaded monotonically. The load-deflection curves of tested beams were primarily used for verification purposes, with theoretical code-based estimates serving as benchmark. Results indicated that the FEM model compared very well with the experimental responses observed in terms of deformation and load capacities at first crack and ultimate failure.

Dolatabad and Maghsoudi presented the results of an experimental study of six continuous un-bonded post-tensioned I beams (Yousef Askari Dolatabad, Ali-Akbar Maghsoudi, 2018). Self-compacting concrete with compressive strength of 90 MPa (HSSCC) as well as normally vibrating concrete with compressive strength of 93 MPa (HSNC) were used for making testing beams. All beams were pre-stressed in the same way, but with different reinforcement percentage by internal steel reinforcement. Based on the conducted research it was noticed that the increase in tendon stress at an ultimate state in HSSCC beams is lower than that of HSNC beams with almost the same concrete strength. The results indicate that the ACI model provides the smallest standard error of estimate so, the ACI model provides better estimates than the AASHTO model and the AASHTO model provides better estimates than BS for tested beams cast with two types of high strength vibrating and non-vibrating concrete.

In order to evaluate the load capacity of reinforced concrete deep beam, finite element study of the structural behaviour of reinforced self-compacting concrete deep beam was carried out using Abaqus finite element modeling tool (Akinpelu M. A., Adedeji A. A., 2018). The model is verified on the basis of experimental results taken from literature. The parametric effect of varied value: concrete compressive strength, vertical web reinforcement ratio and horizontal web reinforcement ratio on the diagonal cracking and ultimate load capacity as well as load-deflection response of deep beam were also evaluated. Based on the results of the study, it follows that the FE model is capable of simulating the entire loading response of a reinforced concrete deep beam with reasonable accuracy.

Based on the analysis of the experimental studies carried out so far on the application of self-compacting concrete for the construction of structural elements, it is noted that almost all tests were carried out on the simply-supported beams, except for one static system of the two-span continuous beam. Beams were examined both for bending and shearing, and their behavior under the effect of short-term static loading corresponds to the behavior of the beams

made of conventional vibrated concrete, as well as to the conditions defined by the regulations for constructions of conventional vibrated concrete.

3. EXPERIMENTAL INVESTIGATION

Experimental laboratory tests were conducted in two phases. The first phase included testing of physical-mechanical properties of the material as well as of mechanical properties of the self-compacting concrete made with river aggregate. The second phase included testing of continuous beam made from self-compacting concrete with river aggregate, under the action of short-termed test load up to failure. Geometrical properties of test specimens, arrangement and type of measuring instruments as well as the testing procedure were defined. Designing of continuous beam was conducted in compliance with the EC2 regulation.

All the mixture specimens which were tested were made from CEM I 42.5 R cement manufactured by HOLCIM. The rock powder used was obtained by milling limestone, and MC PowerFlow 1102, hyperplasticizer admixture was used for making mixtures.

In Table 1 were presented the results of concrete mixture tests during the Slump-flow test as well as density of all concrete mixtures.

Table 1 - Test results for concrete in the fresh state

Concrete	Density [kg/m^3]	Slump-flow test [cm]	t_{500} [s]	Water/cement ratio
SCC	2305	60,5	4,8	0,49

Compressive strength tests were conducted on the 150 mm side cubes, after 2, 7, 14 and 28 days, and the obtained results were presented in Table 2. Tensile splitting strength was determined after 28 days on the cylinders ∅150/300 mm in compliance with EN 12390-6. Determination of tangent and secant modulus of elasticity was performed after 28 days on the cylinders ∅150/300 mm in compliance with the standard EN 1992-1-1:2004, and the obtained mean values of tangent and secant modulus of elasticity are displayed in Table 2.

Table 2 - Test results for concrete in the hardened state

Concrete	Compressive strength [MPa]	Tensile strength [MPa]	Tangent modulus of elasticity [MPa]	Secant modulus of elasticity [MPa]
SCC	46.55	3,80	26,20	25,50

The tested continuous beam has rectangular cross-section, dimensions b/d=15/20 cm, of a total length 340 cm, with the span between supports of 160 cm. The girders are reinforced and use ribbed reinforcement RA 400/500–2, and the designed class of self-compacting concrete is C 30/37.

The load was applied using a hydraulic device, whereby the piston force of the test device was transferred to the beam in two points at the middle of both spans, (Fig. 1) in the controlled, so called “time mode”, with a constant increase of deflection in the function of time up to

failure, with the 0,02 mm/s (1,2 mm/min) deflection increase rate. During the test, global beam strain (deflections) in the function of load are monitored.

Slika 1 - Disposition of continuous beam in the testing phase

In Fig. 2 dependence between load and deflection is shown. The deflections of beams at low load have the same values. With the increase in load, yielding of reinforcement and appearance of cracks, there was a slight difference in the beam deflections girder.

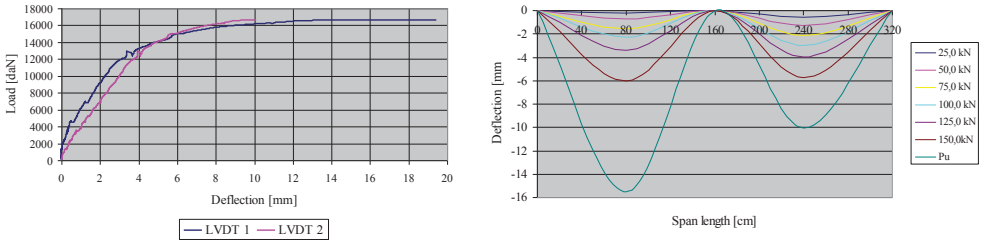

Slika 2 - Load-deflection correlation in the cross-sections I and II of the continuous beams, Graphical presentation of the elastic lines of the beam

The goal of the numerical analysis was verification of the potential of modeling continuous RC girders made from self-compacting concrete and verification of experimentally obtained result. The continuous girder was completely modeled, with simulation of the appropriate boundary conditions for the adopted static system (continuous girder with two spans) as well as of the applied load. In the characteristic cross-section III the finite element grid is denser, so the elements having dimensions 5x2x2 cm were adopted, while the remaining part of the continuous girder was modeled using elements having dimensions 10x2x2 cm. Concrete damaged plasticity model (CDP) was used for modeling of the reinforced concrete, implementing 3D Solid of the finite element C3D20, while T3D2 element was used for reinforcement modeling. Modeling of the continuous girder was performed based on the mechanical characteristics of self-compacting concrete which were determined in laboratory.

On the basis of the numerically determined values of deflections, a comparison was made with the results obtained by experimental tests, which is presented in Fig. 4.

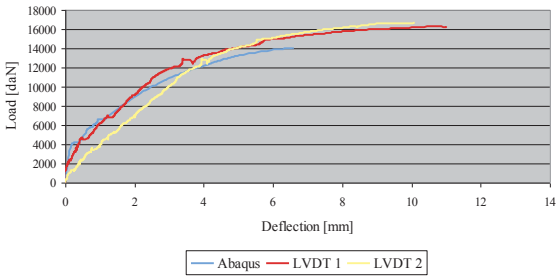

Slika 4 - Comparative load-deflection correlation diagrams in the cross-section I and cross-section II of the continuous beam obtained by experiments and ABAQUS

Comparison of numerically obtained results with the results obtained by experimental testing was made on the basis of diagram of dependence between load and deflection. Certain differences were found in the obtained results that are inevitable due to the idealization of the mechanical characteristics of beam materials and certain approximations in the numerical model.

4. CONCLUSION

Based on the analysis of the results of research so far conducted, related to the possible use self–compacting concrete for structural elements, the following conclusion can be drawn: The behavior of beams made of self-compacting concrete when exposed to bending and shear is similar to those made of conventional vibrated concrete. By comparing the experimentally obtained results with the recommendations given in EC2 and ACI, it has been observed that beams made of self-compacting concrete satisfied the criteria defined in the regulations for conventional vibrated concrete. The analysis using the finite element method was carried out using appropriate software packages, whereby verification was carried out to the model that can predict the response of the beams without experimental research. The finite element method is capable of simulating the response of the loaded reinforced concrete beams made of self-compacting concrete with a reasonable accuracy.

Based on the conducted experimental tests two sets of conclusions were carried out. The first group relates to a physical-mechanical properties of the self-compacting concrete with the river aggregate in the fresh and hardened state in which it has been observed that the self-compacting concrete meets the requirements defined by the following EFNARC and EN 206-9 regulations. The second group are conclusions regarding the limit state of the continuous beams, made with self-compacting concrete in which it has been observed that the beams fully comply with the criteria defined by EC2. Based on the conducted numerical analysis and comparison of the experimentally obtained relationship between the load and deflection, it can be noticed that in the first phase there is almost no deviation of the results, while with the increase in the intensity of the load in the phase from the appearance of the first crack and the occurrence of the yielding of steel there are almost insignificant deviations.

ACKNOWLEDGEMENT

This research is supported by The Ministry of Education, Science and technological development of the Republic of Serbia, within the framework of the projects Development and improvement of methods for analyses of soil-structure interaction based on theoretical and experimental research (TR 36028) and Development and implementation of a comprehensive approach to the design of new structures and safety evaluation of existing structures in order to reduce seismic risk in Serbia (TR 35043) for the period 2011-2018.

REFERENCES

[1] EFNARC, Specification and Guidelines for Self-Compacting Concrete, 2002, pp.32

[2] EFNARC, The European Guidelines for Self-Compacting Concrete Specification Production and Use, 2005, pp.66

[3] EN 206-9:2010, Additional rules for Self-Compacting Concrete (SCC), 2010, pp 27

[4] LIU Xiao-jie, YU Zhi-wu, JIANG Li-zhong: Long term behavior of self-compacting reinforced concrete beams, J. Cent. South Univ. Technol., 15, 2008, 423-428

[5] Kumar R., Kumar R., Kumar N.: In Situ Performance of Self-Compacting Concrete in T-Beams, Journal of Materials in Civil Engineering, 21(03), 2009, 103-109

[6] Hassan A. A. A., Hossain K. M. A., Kachemi M.: Strength, cracking and deflection performance of large-scale self-conolidating concrete beams subjected to shear failure, Engineering Structures, 32, 2010, 1262-1271

[7] Sharifi Y.: Structural Performance of Self-consolidating Concrete Used in Reinforced Concrete Beams, KSCE Journal of Civil Engineering, 16(4), 2012, 618-626

[8] Cattaneo S., Giussani F., Mola F.: Flexural behaviour of reinforced, prestressed and composite self-consolidating concrete beams, Construction and Building Materials, 36, 2012, 826-837

[9] Vidivelli B., Kathiravan T., Gobi T.: Flexural Behaviour of Self Compacting and Self Curing Concrete Beams, The Asian Review of Civil Engineering, 2 (2), 2013, pp. 1- 9

[10] Helincks P., Boel V., Corte W., Schutter G., Desnerck P.: Structural behaviour of powder-type self-compacting concrete: Bond performance and shear capacity, Engineering Structures, 48, 2013, 121–132

[11] Korte S., Boel V., Corte W., Schutter G.: Behaviour of fatigue loaded self-compacting concrete compared to vibrated concrete, Structural Concrete, 15(04), 2014, 575-589

[12] Biolzi L., Cattaneo S., Mola F.: Bending-shear response of self-consolidating and high-performance reinforced concrete beams, Engineering Structures 59, 2014, 399–410

[13] Aderhya S. V., Vennila A., Venkatasubramani R., Vidya S. V.: Flexural Behaviour of Reinforced Beam using Self-compacting Concrete, Int. Jou. Of Earth Sciences and Engineering, 09 (03), 2016, 533-548

[14] Dharmaraj R., Malathy Dr. R.: Flexural behaviour of reinforced self compacting concrete containing corrosion inhibitors, International Journal of Advanced Engineering Technology, 8 (2), 2016, 532-535

[15] Khatab T. A. M., Ashour F. A., Sheehan T., Lam D.: Experimental investigation on continuous reinforced SCC deep beams and Comparisons with Code provisions and models“ Engineering Structures, 131, 2017, 264-274

[16] Gohar S., Afefy M. H., Kassem M. N., Taher F. El-Din S.: Flexural performance of self-compacting concrete beams under repeated loading, J. Engineering Structures., 143, 2017, 441-454.

[17] Imran Sharik M., Joshua Daniel A.: To study the flexural behaviour of non-prismatic beams using self compacting concrete, Pak. J. Biotechnol., 14 (3), 2017, 377-381

[18] Lemuel Thompson Yaw, Jack Banahene Osei and Mark Adom-Asamoah.: On The Non-Linear Finite Element Modelling of Self-Compacting Concrete Beams, Journal of Structural and Transportation Studies, 2 (2), 2017, 1-18

[19] Yousef Askari Dolatabad, Ali-Akbar Maghsoudi,: Ultimate stress increase in unbonded tendons in post-tensioned indeterminate I-beams cast with high strength normal and self compacting concrete, Engineering Science and Technology, an International Journal, 21, 2018, 495–506

[20] Akinpelu M. A., Adedeji A. A.: Structural Response of Reinforced Self-Compacting Concrete Deep Beam using Finite Element Method, Journal of Soft Computing in Civil Engineering, 2-1, 2018, 36-61

[21] Milošević B.: Eksperimentalno-teorijska analiza graničnih stanja linijskih nosača od samougrađujućeg betona sa recikliranim agregatom, Građevinsko-arhitektonski fakultet Univerziteta u Nišu, Niš, 2016.

ДГКС Друштво грађевинских конструктера Србије
ASES Association of Structural Engineers of Serbia
S-56
15. KONGRES
6-8. 9. 2018. Zlatibor

Aleksandar Savić[1], Marina Aškrabić[2], Brankica Kovačević[3], Danijela Pavlović[4]

SVOJSTVA SCC MEŠAVINA SA KRUPNIM RECIKLIRANIM AGREGATOM

Rezime:

U radu su prikazani rezultati fizičko-mehaničkih ispitivanja betona sa krupnim recikliranim agregatom. Napravljene su četiri serije samougrađujućeg betona (Self-Compacting Concrete – SCC), sa upotrebom recikliranog agregata od betona (Recycled Concrete Aggregate – RCA) kao zamene za obe frakcije prirodnog krupnog agregata. Ove serije projektovane su uz primenu postupka mešanja iz dve faze (Two Stage Mixing Approach - TSMA) uz praćenje svojstava betona u svežem i očvrslom stanju. Sposobnost tečenja svežeg betona je praćena pomoću testa rasprostiranja sleganjem, a urađena su i ispitivanja uz pomoć V-levka i L-boksa. Utvrđene su vrednosti čvrstoća pri pritisku, kao i čvrstoće pri savijanju, cepanju i prionljivost (pull-off). Sve mešavine pokazale su zadovoljavajuća svojstva, što opravdava upotrebu recikliranog betona u svojstvu agregata za SCC betone.

Ključne reči: agregat od recikliranog betona, samougrađujući betoni, postupak mešanja

PROPERTIES OF SCC MIXTURES WITH COARSE RECYCLED AGGREGATES

Summary:

Paper presents the results of physical and mechanical testing of concrete mixtures prepared with recycled concrete aggregate. Four series of Self-Compacting Concrete (SCC) were made, with the use of recycled concrete aggregate (RCA), as a substitute for both natural coarse aggregate fractions. These series were designed using the Two Stage Mixing Approach (TSMA), and the properties of the obtained concrete mixtures in fresh and hardened state were recorded. Flowability of fresh mix was determined using slump flow test, while V-funnel and L-box tests were also performed. Compressive strength and also flexural, splitting and bond (pull-off) strength were determined. All the mixtures showed favourable properties, proving the possibility of the recycled concrete aggregate use for production of worthy SCC.

Key words: recycled concrete aggregate, self-compacting concrete, mixing method

[1]*Dr, dipl.inž.građ., doc., University of Belgrade, Faculty of Civil Engineering, Belgrade, savic.alexandar@gmail.com*
[2]*Mast.inž.građ., asist., University of Belgrade, Faculty of Civil Engineering, Belgrade, amarina@grf.bg.ac.rs*
[3]*Mast.inž.građ., brankica_ko@yahoo.com*
[4]*Mast.inž.građ., danijelapavlovic86@yahoo.com*

1 INTRODUCTION

Unquestionably, construction industry presents a branch of industry with significant environmental impact. Contemporary approach, in accordance with sustainable development postulates, integrates three main stages: a critical study as the first, followed by a thorough analysis as the second and, in the case that it is possible and practical, modernization by implementing the philosophy of sustainable development. In this regard, all activities of construction (planning, design, implementation, operation, duration and life expectancy, etc.) are constantly under review, providing more sustainable use of resources, promotion of energy efficiency and sustainability of buildings, with an emphasis on recyclable materials and minimizing waste. [1]

In general, concrete is one of the most commonly used material in the construction industry and the above considerations provide a significant impact on its current evolution. Conventional concrete is placed using vibrating equipment to provide reduction in entrained air content, eliminating the presence of caverns and weak spots on the contact with reinforcement bars and formwork (so-called Normal Vibrated Concrete - NVC).

Extrapolation of the concept of superplasticizers use in the direction of obtaining fluid consistency of concrete has led to the concept of self-compacting concrete (SCC) as well as to its application [2]. The development of new materials, the latest generation of superplasticizers based on polycarboxylate, that entered the wide use during the last decade of the 20th century, enabled the successful implementation of SCC. The definition of self-compacting concrete states that this concrete, without the use of mechanical means of placement (quite independently of the competence of workers engaged), fills all the corners of the formwork and the narrow spaces between the reinforcement bars (only under the influence of its own weight) so that, in the final stage, a compact concrete with higher durability is produced.

Having in mind the fact that for the production of 1 m^3 of concrete almost 1 m^3 of aggregate is utilized [3], a reduction in natural aggregate consumption represents a logical step towards implementation of sustainable development postulates in this production. Different kinds of recycled aggregate are made and experimented with, and C&D (construction and demolition) waste concrete (as recycled concrete aggregate – RCA) became one of the logical solutions to this problem [4].

The dominant disadvantage of RCA in comparison to the natural aggregate (NA), river gravel or crushed stone, is the so-called 'residual cement paste' that stays as part of RCA particles after crushing of C&D concrete. This is actually a part of the hardened cement paste around the NA aggregate particles in the original concrete being recycled. The main implication of the presence of this residual cement paste is higher water absorption of RCA compared with NA, and therefore fast and reliable measurement of water absorption becomes a very important segment in determination of aggregate properties before the production of new concrete [5].

Tam et al. [6] came up with a new mixing approach which they defined as the two stage mixing approach (TSMA) and experimentally observed that this technique for mixing of ingredient of concrete (consisting of new sequence of mixing ingredient) gives better compressive strength.

Regardless of the water absorption measurement, and the method applied to reduce the negative impact of this to the water to cement ratio in concrete, this parameter remains critical, especially when it comes to the production of SCC, which is, almost by default, sensitive to the water content, and the water content changes. Also, the aspect of mechanical properties reduction with the use of RCA amplifies when SCC with RCA is produced. It is of high importance to have recycled aggregate of high quality, in order to obtain favourable physical and mechanical properties of concrete. This is not always the case, having in mind that the C&D concrete waste does not necessarily have the needed properties.

2 EXPERIMENTAL PROGRAMME

2.1 SCOPE AND OBJECTIVE

The aim of this study was to investigate the influence of the coarse recycled concrete aggregate on physical and mechanical properties of self-compacting concrete mixtures, both in fresh and hardened state. Mixture of aggregate consisted of natural and recycled aggregate, divided in three standard fractions: I (0/4 mm), II (4/8 mm), and III (8/16 mm). For this purpose four different mixtures were prepared:

- Referent mixture, designated as SCC I, prepared with natural river aggregate,
- Mixture designated as SCC II, made with fraction II (4/8 mm) composed only of recycled concrete aggregate, and with natural river aggregate fraction III (8/16 mm),
- Mixture designated as SCC III, made with natural river aggregate fraction II (4/8 mm), and with fraction III (8/16 mm) composed only of recycled concrete aggregate,
- Mixture with both II and III fractions composed only of recycled concrete aggregate, designated as SCC IV.

Mixtures were defined using the principle of equal effective water/cement ratios. Mixtures containing recycled concrete aggregate had additional amount of water due to higher water absorption of this kind of aggregate. Also, two-stage mixing approach (TSMA) was used to improve the interface zone of the recycled concrete aggregate grains and cement paste in the concrete. Mixing technique was consistent with the algorithm shown in Figure 1.

The paper presents the comparison of different physical and mechanical properties of fresh and hardened mixtures. It was important to find out the scale in which the properties of concrete will degrade, due to the use of recycled concrete aggregate instead of natural aggregate, and also to investigate the recycled aggregate grain size as the parameter.

2.2 MATERIALS

Aggregates used for preparing the concrete mixtures were natural river aggregate, separated in three fractions and coarse recycled concrete aggregate, separated in two fractions. Fine aggregate (0/4 mm) of river origin was used in all the mixtures in the percent of 50.6% (860 kg/m^3) compared to mass of the aggregate. Second fraction (4/8 mm) was used in 32.2% (530 kg/m^3)and third fraction (8/16 mm) in 18.2% (310 kg/m^3).

Natural aggregate was standard, commercially available river gravel from the Danube river.

Recycled concrete aggregate was obtained from a demolished concrete sub-structure for tram rails in Vojvode Stepe street, Belgrade. At the moment of crushing, this concrete was

more than 30 years old. According to the performed tests class of original concrete was C35/45 at the moment of crushing. True density of recycled concrete aggregate was 2,425 g/cm^3, while it's water absorption equalled 3.4% for both fractions of recycled concrete aggregate [7,8].

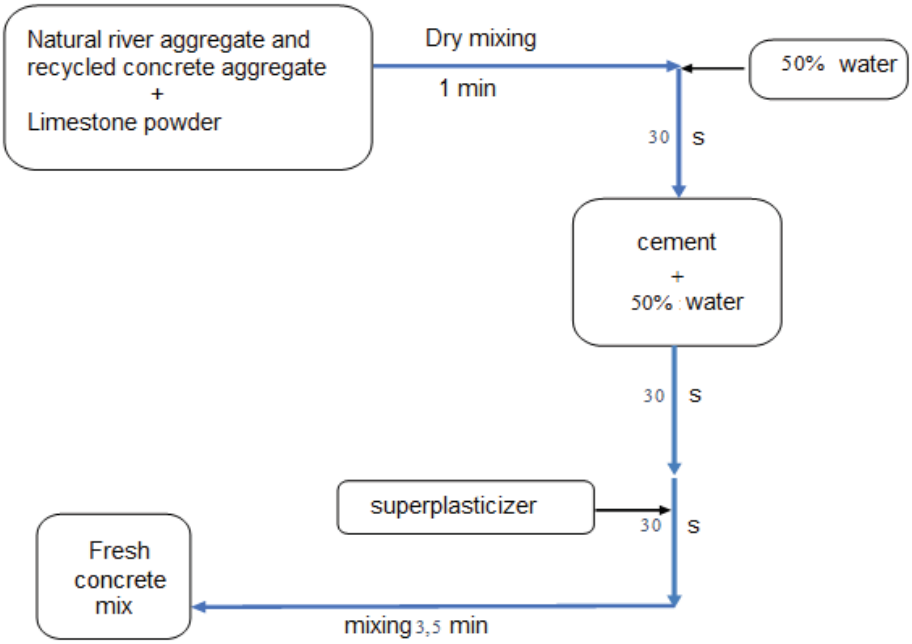

Figure 1 – Scheme of the TSMA used for preparation of concrete mixture

Limestone powder, produced by Granit peščar, Ljig was used. True density of limestone powder was 2,720 g/cm^3. Portland cement PC 20M (S-L) 42.5R, produced by Lafarge Beočin was used in all the mixes. True density of cement was 3.040 g/cm^3, with specific surface of 4240 cm^2/g.

Superplasticizer Cementol Hiperplast 463 produced by TKK, Srpenica, was also applied with density of 1.08 g/cm^3 [7,8].

2.3 MIXTURES

Composition of the four tested mixtures is presented in Table 1.

The quantities of the cement and limestone powder were held constant (380 kg/m^3 and 250 kg/m^3 respectively). These mixtures can be referred to as powder type mixtures with quantity of powder component of more than 550 kg/m^3. The quantities of the superplasticizer were also the same for all the mixtures, providing practically similar values of the slump flow. The fine aggregate fraction I (0/4 mm) was natural aggregate for all the mixtures.

Table 1 – Composition of mixtures (kg/m^3)

Mixture		SCC I	SCC II	SCC III	SCC IV
Cement		380	380	380	380
Limestone powder		250	250	250	250
Water		194	205	205	205
Natural river aggregate	I (0/4 mm)	860	860	860	860
	II (4/8 mm)	530	-	530	-
	III (8/16 mm)	310	310	-	-
Recycled concrete aggregate	II (4/8 mm)	-	530	-	530
	III (8/16 mm)	-	-	310	310
Superplasticizer		5.7	5.7	5.7	5.7

3 RESULTS AND DISCUSSION

Various tests of fresh and hardened concrete were performed in order to estimate the possibility of using recycled concrete aggregate within SCC mixtures. Flowability of fresh mix was determined using slump flow test [9], viscosity of concrete was tested using V-funnel [10] and flowability and passing ability were determined using L-box test [11]. Compressive strength as the most important property of concrete was measured after 1, 7 and 28 days. Tensile strength properties of concrete mixtures were estimated through several tests: flexural, splitting and bond strength. In addition, static and dynamic moduli of elasticity were obtained for all mixtures.

3.1 FRESH MIX PROPERTIES

Bulk densities of fresh mixes varied from 2352 kg/m^3 (mixture SCC IV) to 2386 kg/m^3 (mixture SCCII). Table 2 incorporates the following results: final flow diameter (SF) and time in which concrete sample reaches diameter of 500 mm (t_{500}), V-funnel time (t_v), hight ratio within L box (PA) and related time t_f.

According to limits defined in specifications and guidelines for SCC [12], concrete mix named SCC III belongs to SF3 class, while all the other mixtures had slump-flow diameter larger than the upper limit for this class (850 mm). Time t_{500}, measured during slump flow test, placed all the mixtures in VS2 class. These results show that all the mixtures had very good flowability. Differences between the properties of fresh mixtures were more noticeable when comparing their viscosity, through V-funnel test. Mixtures SCC I and SCC III belong to VF1 class, according to V-funnel test, while mixtures SCC II and SCC IV belong to VF2 class. It can be noted that the highest viscosity was obtained for mixtures with the highest amount of recycled concrete aggregate. These observations were confirmed with the time measured during the L-box test (t_f). The highest values for t_f were measured for the mixture SCC IV

followed by mixture SCC II. All the mixtures satisfy the condition for PA2 class in relation to the hight ratio results of the L-box test. No blocking effect was noticed for any of the mixtures.

Table 2 – Fresh mix properties

Property	*SCC I*	*SCC II*	*SCC III*	*SCC IV*
SF (mm)	*890*	*865*	*840*	*870*
t_{500} *(s)*	*2.0*	*2.1*	*2.3*	*2.5*
t_v *(s)*	*7.4*	*11.2*	*7.5*	*12.4*
PA (-)	*1.00*	*0.97*	*0.94*	*0.94*
t_f*(s)*	*3.8*	*5.1*	*4.1*	*7.1*

3.2 HARDENED CONCRETE PROPERTIES

Compressive strength was tested for all the mixtures after 1, 7 and 28 days. Tests were performed on the cubes (a=10 cm) according to the SRPS EN 12390-3:2018 [13], and results are presented in Figure 2.

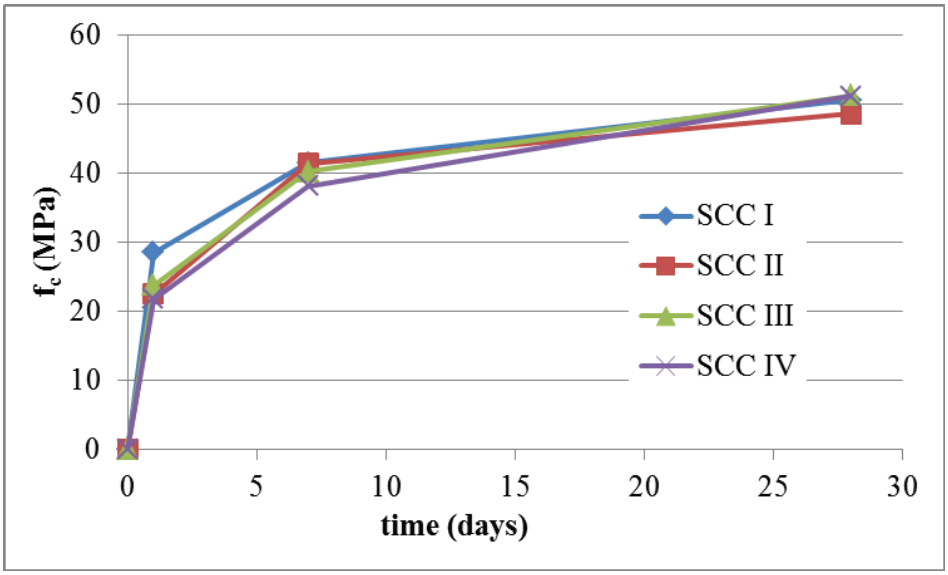

Figure 2 – Compressive strength of concrete mixtures at the ages of 1, 7 and 28 days

Compressive strengths of the studied series reached similar values at all ages. The biggest differences between the measured values can be noticed at the early ages (after 1 day). At this time the referent mixture, SCC I, had the highest value of compressive strength, followed by mixture SCC III that reached 83.5% of the strength of SCC I. Mixtures SCC II and SCC IV at

this point had very similar values, equalling 79.1% and 76.0% of the referent mixture strength. At the age of 28 days the differences were considerably smaller. Mixture SCC II had 5% lower strength than referent mixture, while mixtures SCC III and SCC IV reached approximately the same values as referent mixture (1% higher).

Tensile strength of concrete was indirectly tested at the age of 28 days using three different methods: flexural test [14], splitting test [15] and the bond test [16]. Flexural tests were performed on the prismatic samples, 12×12×36 cm as three point bending test. Splitting test was performed on the cubes (a=15 cm), while pull-off test was performed with metal plates (d=50 mm) that were glued using epoxy resin to the surface of concrete. Results of these tests are presented in Figure 3.

Most probably due to the better packing of the sharp-edged recycled aggregate grains, the highest flexural strength was reached for mixtures containing 100% of coarse recycled concrete aggregate (SCC IV) and the mixture where 100% of the III fraction was replaced by recycled concrete aggregate (SCC III). Similarly, these mixtures reached high values of splitting strength, namely 98.4% (SCC IV) and 94.4% (SCC III) of the referent mixture strength.

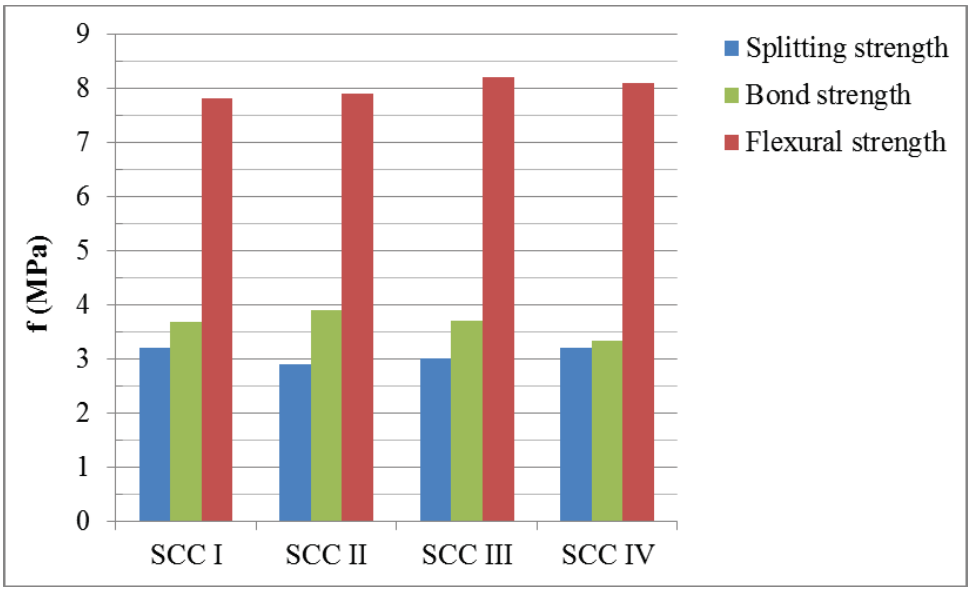

Figure 3 – Flexural, splitting and bond strength (pull-off) of concrete mixtures at 28 days

On the other hand, bond strength (determined by pull-off method) was highest for the mixture SCC II, where fraction II was replaced with recycled concrete aggregate, while the lowest bond strength was recorded for the mixture SCC IV. Flexural strength was 2.5 times higher than splitting strength of concrete for mixtures SCC I and SCC IV, while this ratio equalled 2.7 for mixtures SCC II and SCC III.

Dynamic and static modulus of elasticity were measured at the age of 28 days. As it was expected, dynamic modulus values were higher, but followed the same trend as static modulus values [17]. Dynamic modulus was measured using resonant frequency method [18], while

static modulus was measured according to SRPS EN 12390-13 [19]. Results of these tests are presented in Figure 4.

The highest modulus of elasticity was measured for referent mixture, as it was expected, but the mixture SCC III had almost identical values. Static modulus of elasticity for the other two mixtures was less than 5 % lower than the static modulus of the referent mixture. Dynamic modulus of elasticity was the lowest for the mixture SCC IV, which contained the highest content of the recycled concrete aggregate.

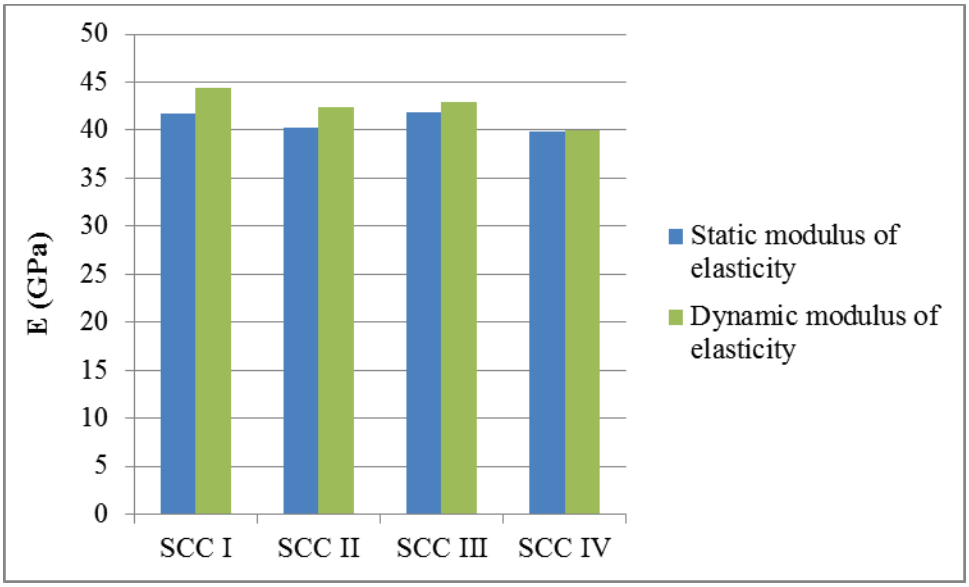

Figure 4 – Static and dynamic modulus of elasticity of concrete at the age of 28 days

4 CONCLUSIONS

In this paper, the influence of recycled concrete aggregate content on the fresh and hardened mix properties was investigated. Based on the results presented in the previous section, the following conclusions can be drawn:

- Mixtures with recycled concrete aggregate showed good flowability, but higher viscosity than referent mixture. This is especially the case for the mixtures SCC II (only fraction II consisted of recycled coarse aggregate) and SCC IV (where the total coarse aggregate consisted of recycled concrete aggregate). No blocking effect was noticed in any of the mixtures.
- Differences in compressive strength were the highest at the early age of mixtures. After 28 days compressive strength was very similar for all the mixtures, being highest for the mixture SCC III (1.4% higher than the strength of the referent mixture) and lowest for the SCC II (3.9% lower than the strength of the referent mixture).
- Flexural strength was the highest for the mixture SCC III, but the differences between the mixtures ranged from 2% to 5%.

- Splitting strength was the highest for the referent mixture, but the differences between this and the other three mixtures were lower than 10%.
- Static modulus of elasticity was equivalent for mixture SCC III and the referent mixture. Differences in comparison to the moduli of mixtures SCC II and SCC IV were lower than 5%.
- Dynamic modulus of elasticity reached higher values than static modulus, but followed the same trend.

Moreover, a note has to be made that there was no negative effect on the mechanical properties due to the presence of additional water for the SCC. Similar properties of all mixtures were achieved for both coarse aggregate fractions replacement, showing no significant differences when aggregate size is taken as a parameter, and this can be explained by the fact that this study was conducted with recycled aggregate of good properties and in laboratory conditions.

ACKNOWLEDGEMENTS

The work reported in this paper is a part of the investigation within the research project TR 36017 ‘‘Utilization of by-products and recycled waste materials in concrete composites in the scope of sustainable construction development in Serbia: investigation and environmental assessment of possible applications’’, supported by the Ministry of Science and Technology, Republic of Serbia. This support is gratefully acknowledged.

REFERENCES

[1] Savić, A: Investigation Of The Properties Of Fresh And Hardened Self-compacting Concrete With Mineral Additions Based On Industrial By-Products, Doctoral thesis, University of Belgrade, Faculty of Civil Engineering, Belgrade, 2015

[2] Jevtić, D.: Odabrana poglavlja iz savremenih materijala u građevinarstvu, Građevinski fakultet Univerziteta u Beogradu, 2017

[3] Radonjanin, V., Malešev, M., Marinković, S., Al Malty, A.E.S.: Green recycled aggregate concrete, Construction and Building Materials 47, 2013, 1503–1511

[4] Kisku, N., Joshi, H., Ansari, M., Panda, S.K., Nayak, S., Dutta, S.C.: A critical review and assessment for usage of recycled aggregate as sustainable construction material, Construction and Building Materials 131, 2017, 721–740,

[5] Tošić N., Savić A., Carević V. : A method for the continuous measurement of water absorption of coarse recycled aggregates, Association of Structural Engineers of Serbia, Symposium Zlatibor, 2016, 1023-1030

[6] Tam, V.W., Gao, X.F., Tam, C.M. : Microstructural analysis of RAC produced from two-stage mixing approach, Cement and Concrete Research, 35 (6), 2005, 1195-1203

[7] Kovačević, B.: Ispitivanje SCC betona sa delimičnom zamenom prirodnog agregata recikliranim, Master thesis, Faculty of Civil Engineering, Belgrade 2017.

[8] Pavlović, D.: Fizičko-mehanička svojstva SCC betona sa recikliranim agregatom, Master thesis, Faculty of Civil Engineering, Belgrade, 2017.

[9] SRPS EN 12350-8:2012, Testing fresh concrete - Part 8: Self-compacting concrete - Slump-flow test, Institute for standardization of Serbia, 2012.

[10] SRPS EN 12350-9:2012, Testing fresh concrete - Part 9: Self-compacting concrete - V-funnel test, Institute for standardization of Serbia, 2012.

[11] SRPS EN 12350-10:2012, Testing fresh concrete - Part 10: Self-compacting concrete - L box test, Institute for standardization of Serbia, 2012.

[12] Specification and guidelines for self-compacting concrete, European Federation of Producers and Applicators of Specialist Products for Structures, EFNARC, 2002

[13] SRPS ISO 4012:2000, Concrete -- Determination of compressive strength of test specimens, Institute for standardization of Serbia, 2000.

[14] SRPS EN 12390-5:2010, Testing hardened concrete - Part 5: Flexural strength of test specimens, Institute for standardization of Serbia, 2010.

[15] SRPS EN 12390-6:2012, Testing hardened concrete - Part 6: Tensile splitting strength of test specimens, Institute for standardization of Serbia, 2012.

[16] SRPS EN 1542:2010, Products and systems for the protection and repair of concrete structures - Test methods - Measurement of bond strength by pull-off, Institute for standardization of Serbia, 2010.

[17] Savić, A., Aškrabić, M.: Correlation between dynamic modulus of elasticity and compressive strength for self-compacting mortars, 6th International Congress of Serbian Society of Mechanics, Tara, Serbia, June 19-21, 2017, S4a 1-8

[18] SRPS U.M1.026:1993 Concrete - Determination of the dynamic modulus of elasticity and Poisson's ratio, Institute for standardization of Serbia, 1993.

[19] SRPS EN 12390-13:2015 Testing hardened concrete - Part 13: Determination of secant modulus of elasticity in compression, Institute for standardization of Serbia, 2015.

ДГКС Друштво грађевинских конструктера Србије
ASES Association of Structural Engineers of Serbia
S-57
15. KONGRES
6-8. 9. 2018. Zlatibor

Živko P. Cuckić [1], *Vesna Ž. Cuckić* [2], *Olga Cuckić* [3]

TEHNOLOGIJA NEZAVISNE NOSIVE RAMOVSKE KONSTRUKCIJE

Rezime:

Ovaj rad predstavlja tehnološki napredno i ekonomično rešenje za obnovu prostora i obnovu zgrada. Novi nezavisni nosivi okvir uključuje izgradnju horizontalnog proširenja i vertikalnog dodavanja. Na taj način se dodaju nova stambena područja.

Key words: nosivi okvir, nadogradnja konstrukcije

AUTONOMOUS LOAD-BEARING FRAMEWORK TECHNOLOGY

Summary:

This paper presents a technologically advanced and cost-effective solution for redevelopment of territories and renovation of buildings. A new autonomous load-bearing framework entails building horizontal extension and vertical addition. In that way a new residential areas is added.

Key words: load bearing framework, building upgrade, construction

[1] *MA Živko P. Cuckić, BSc in the field of Construction, Assistant Professor at the Department of the Surface Systems and Structural Dynamics at the Faculty of Civil Engineering in Priština, 1982-1987, Director of Binačka Morava from Gnjilane and the Regional Road Fund, completed his specialization studies for the Prefabrication in Prague, approved by the Academic Lubor Janda, an author of several Strategic Projects especially the ISG in New York City upon the Formation of free economic zones in Old Serbia, via cooperation between EU and Russia. The owner of the Company "Dadge International LLC", e-mail: dadge_serbia@yahoo.com*
[2] *Architect Vesna Ž. Cuckić, Technical Associate at Dadge International ltd. e-mail: vesnacuckic@yahoo.com*
[3] *Architect Olga Cuckić. Technical Associate at Dadge International ltd. e-mail: olja892@yahoo.com*

1. PROBLEM

Residential and commercial multi-storey building stock in the US/Canada market is rapidly aging, a gap is widening between its current condition and the requirements of modern dwelling standards (energy efficiency, convenience, internal engineering infrastructure, community space, recreational/ sports areas, playgrounds, parking space).

As an example, out of the 2,547 residential buildings that NYC Housing Authority manages 85% is 30 years and older (more than 50% of those is 50 years and older)

When the time for renovation comes, owners of property tend to minimize their investment (the rent increase can negatively affect their business). As a consequence in most cases problems gets swept under the rug.

2. CURRENT SOLUTION IN THE MARKET

There is a standard "demolish-then-build" solution: acquisition of property available in the market, demolition and then a new construction. Its disadvantages/difficulties:

- acquisition costs in locations attractive for investment tend to rise;
- scarce appropriate building stock that gets even less available because quality of construction had been significantly improved since the middle of the 20-th century;
- high capital costs;
- comparatively long project times;
- often far from being smooth processes of getting approvals from city authorities and consent from the local community

It does not make sense to demolish those buildings (structurally they are in a good condition) but it does make sense to renovate them and make capital repairs/ upgrade to the modern dwelling standards.

3. NEW – PROPOSED SOLUTION

Our proposed solution is a full renovation and extension of a building using our Autonomous (load) Bearing Framework technology ("ABF technology"). The ABF Technology entails building horizontal extension and vertical addition. The added new foundation around the existing building footprint consists of CFA (Continuous Flight Auger) piles supporting piers and columns. They form the base for autonomous bearing framework arising around the building to support a rigid platform that bridges over the existing building. The new superstructure construction and vertical enlargement rises from that level. Enlargement of building footprint depends on a site size, configuration and zoning requirements. With creation of new residential areas (available for rent or purchase) and public and commercial spaces, our solution ensures financial flows necessary for the maintenance and upgrade of infrastructure and neighborhood improvement. Monolithic poured concrete construction is suggested as a standard construction method for the ABF technology. Pictures on Fig. 1 presents ABF Technology visualized.

Figure 1 - Visualization of ABF technology

Left picture shows Existing building constructed in the 50s of the 20th century: no elevators, no central AC and ventilation, no fire protection system, obsolete appearance, low energy efficiency. Apartments need repairs/ upgrade.

Middle picture shows Phase I of Reconstruction. A new foundation added. Footprint consists of piles supporting piers and columns. They form the base for ABF arising around the building to support a rigid platform that bridges over the existing building. The new superstructure construction and vertical enlargement rises from that level.

Right picture shows Phase II (Final). A new energy efficient building with a modern appearance. Elevator(s) added, new HVAC, electrical, plumbing and fire protection systems, smart building management system installed focusing on energy management, fire detection system, CCTV, access control system and lighting controls.

Reconstruction of an "old" building using the ABF technology (Autonomous Bearing Framework) advantages:

• full renovation of an existing building that extends a building's lifespan at least to one hundred (100) years;

• renovation project can run without relocation of inhabitants and demolition of an "old" building significantly decreasing construction costs (up to 30%);

• high investment attractiveness of renovation project: creation of additional housing units (2.0-3.0 multiplier to existing units' number, depending on zoning requirements).

ABF Technology is unique in a sense that it captures all positive experience and goes far beyond compared to the secondary development projects that were carried out in several countries such as USA, Japan, Israel and Russia and used the same principle but different technical solutions.

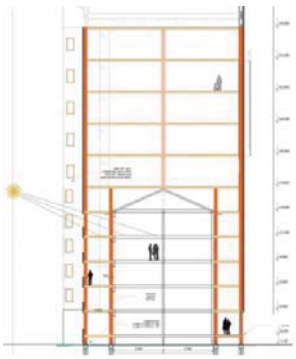

Figure 2 - Cross section of the building with ABF technology

Up-to-date it is the most technically advanced and cost-effective technology. The key features it ensures are:

1. Full constructive autonomy - no additional loads to the existing building and its foundation;
2. Full renovation or installation of new HVAC, electrical, plumbing, and fire protection systems;
3. Sustainable design solution (energy efficient and leak free building envelope, ventilated space);
4. Relocation of inhabitants optional;
5. Creation of additional public areas (community, retail, recreational spaces, playgrounds, parking spaces).

4. ADVANTAGES OF ABF TECHNOLOGY

In the midst of growing deficit of attractive for investment property the ABF technology makes it easier to find a property in an attractive location for expansion and building new sellable areas. It makes a renovation project attractive for investor (IRR=50% and higher) through creation of additional housing units (2.0-3.0 multiplier to existing units' number, depending on zoning requirements), decreased capital requirements, development cost reduced by 20% to 30% due to reduction of the development project's lead time and less stringent requirements for qualification of construction workers (poured concrete construction methods is well mastered by contractors in the US/ Canadian construction market). It increases possibilities to receive consent/ support of local communities with creation of new residential areas, public and commercial spaces, it ensures financial flows necessary for the maintenance and upgrade of infrastructure to the modern standards and significant improvement of the social environment in neighborhoods. Innovativeness of the ABF technology confirmed by virtue of PCT publication and patent application in the USA. In 2009 Mr. Norifumi Konakawa (Japan), a technology leader in secondary development, admitted that ABF Technology proved its technical superiority versus a number of Mr. Konakawa's patents related to building's renovation methods whereby an existing building is expanded and integrated into a new one. Figures 3-6 presents some examples of ABF technology.

Figure 3 - Visualization of ABF technology 2

Figure 4 - Visualization of ABF technology 3

Figure 5 - Visualization of ABF Technology 4

Figure 6 - Visualization of ABF Technology 5

5. CONCLUSION

• The renovation market in the USA/Canada seems to be multi-billion and has a potential to grow: currently the housing market has a shortage of affordable units and communities strive for economical and effective solutions to renovate and modernize existing properties and neighborhoods.

• Annual rate of renewal of the multi-storey building stock in the USA/ Canada (the number of buildings that were added to the building stock in a year less the number of buildings that were taken out) is about 1%. In other words, if 40% of buildings that are old enough it will take at least 40 years to replace them. Moreover during this time a significant part of the stock will continue critically aging.

• In the privately owned property market about 25-30% of properties have a considerable part of not-used buildable areas. It would makes sense to re-capitalize those properties via renovation based on the ABF technology in order to increase the buildable area available for rent or purchase to the maximum allowed by the zoning requirements.

• In the property market owned and managed by non-private investors NYC Housing Authority's example is notable: out of the 2,547 residential buildings that it manages 85% is 30 years and older (more than 50% of those is 50 years and older).

REFERENCES

[1] Prof. Krastavčević Momir, Montažni građevinski objekti, Beograd 1984.

[2] Prof. Gavrilović Predrag, Spojevi i veze montažnih betonskih zgrada, 1984

[3] Jiri Witzany, Konstrukce pozemnih staveb70, Praha 2003.

ДГКС Друштво грађевинских конструктера Србије
ASES Association of Structural Engineers of Serbia
S-58
15. KONGRES
6-8. 9. 2018. Zlatibor

Mirjana Malešev[1],Slobodan Šupić[2],Vlastimir Radonjanin[3],Mirjana Laban[4],Miroslava Radeka[5]

EKO GRADNJA – ODRŽIVO KORIŠĆENJE OTPADNIH MATERIJALA NASTALIH SAGOREVANJEM BIOMASE

Rezime:

Biomasa se u Srbiji delimično koristi kao izvor energije, ali pepeo, nastao sagorevanjem biomase, se uglavnom odlaže na deponije i zagađuje životnu sredinu. U okviru IPA projekta: Poljoprivredni otpad - izazovi i poslovne mogućnosti, započeto je istraživanje raspoloživosti različitih vrsta pepela koji nastaje sagorevanjem žetvenih ostataka u AP Vojvodini. Osnovna ideja projekta je uvođenje mogućnosti korišćenja biopepela u građevinarstvu kao sastavnog dela građevinskih objekata. Zamena cementa sa biopepelom, kao CO_2 neutralnim gorivom, smanjila bi negativan uticaj industrije betona na globalno zagrevanje, te dala mogućnost ekonomskog vrednovanja pepela kao novog proizvoda. Ovaj rad predstavlja osnovne ciljeve projekta, planirane aktivnosti i načine ekonomskog umrežavanja.

Ključne reči: biomasa, deponija, otpad, upotrebna vrednost, beton, novi proizvod

ECO BUILD - SUSTAINABLE USE OF WASTE MATERIALS FROM BIOMASS COMBUSTION

Summary:

Biomass is partially used as energy source in Serbia, but the ashes, generated by the combustion of biomass, are rather disposed on the landfill polluting the environment. Within IPA project: Agricultural Waste – Challenges and Business Opportunities, an investigation of the availability of different types of ash generated by the combustion of harvest residues in AP Vojvodina has begun. The main idea of the project is to introduce possibility of biomass ash use in civil engineering structures as integral part of construction. Substituting cement with the biomass ashes, as CO_2 neutral fuel, would reduce the impact on global warming and provide the possibility of economic valuation of ash as new product. This paper presents the basic goals of the project, planned activities and ways of economic networking.

Key words: biomass, landfill, waste, use-value, concrete, new product

[1] *PhD, Full Professor, University of Novi Sad Faculty of Technical Science*
[2] *MSc CE, University of Novi Sad Faculty of Technical Science*
[3] *PhD, Ass. Professor, University of Novi Sad Faculty of Technical Science*
[4] *PhD, Assoc. Professor, University of Novi Sad Faculty of Technical Science*
[5] *PhD, Full Professor, University of Novi Sad Faculty of Technical Science*

1. INTRODUCTION

Biomass is one of the largest renewable energy sources (RES) on a global level, as well as in Republic of Serbia. Although the biomass e-stock market has been recently established in the country, the biomass is much underrated and unused RES and Serbia belongs to top European countries by the amount of available, but unused biomass. The main reasons lie in: lack of experience (absence of projects in this field), transition issues of many industrial companies, low electricity tariff and poorly developed market for biomass fuel and biomass utilisation facilities.

In order to improve competitiveness of regional economy subjects and further develop business environment, from the aspect of sustainable biomass utilization, Faculty of Civil Engineering from Osijek and Faculty of Technical Sciences from Novi Sad started working on the IPA CBC project Agricultural Waste – Challenges and Business Opportunities (Eco Build). Low competitiveness, poor networking between enterprises, inadequate disposal of agricultural harvest residues – biomass are the main issues the project is dealing with.

One of the main outputs of the project is a cooperation network between: biomass providers (farmers), biomass users (industrial companies that use biomass as an energy source), and engineering companies (cement and concrete factories) that would use biomass waste – biomass ash as new construction material. Within this cycle, higher-education institutions will conduct research on possibilities of biomass ash application in cement-based composites/disseminate results, whereas enterprises and SMEs will provide biomass waste and learn how to manage it usefully. This paper presents the main ideas and objectives of the project.

2. BIOMASS AS RES IN SERBIA

The search for energy alternatives involving locally available and renewable energy sources (RES) is one of the main concerns of governments, scientists and business people worldwide. Biomass – the fourth largest energy source after coal, oil and natural gas - is the largest and most important renewable energy option nowadays and can be used to produce different forms of energy. Renewability and versatility are, among many other aspects, important advantages of biomass as an energy source. Moreover, compared to other RES, biomass resources are common and widespread across the globe.

Many countries have already adopted the goal of enhancing the role of renewable sources in their energy supplies. The Renewable Energy Directive [1] establishes an overall policy for the production of energy from RES in the EU, as it requires the EU to fulfil at least 20% of its total energy needs with renewables by 2020. The Republic of Serbia has, in accordance with the Directive and the Decision of Ministerial Council of the Energy community (10/18/2012), set itself ambitious goal of a 27% of RES in gross final energy consumption by 2020 [2]. One of the main ideas of the Directive is to reduce carbon dioxide (CO_2) global emission, as an unavoidable by-product of burning fossil fuels and its negative impact on global warming. In this sense, biomass appears to be the optimal choice, as it, when combusted, releases carbon dioxide which in turn is readily absorbed by plants, making it CO_2 neutral source. Figure 1

illustrates projection of the Government of Serbia to build capacities for electricity generation from renewable sources and the share of biomass and biogas power plants in the total projected power of power plants in the range from 2015 to 2030.

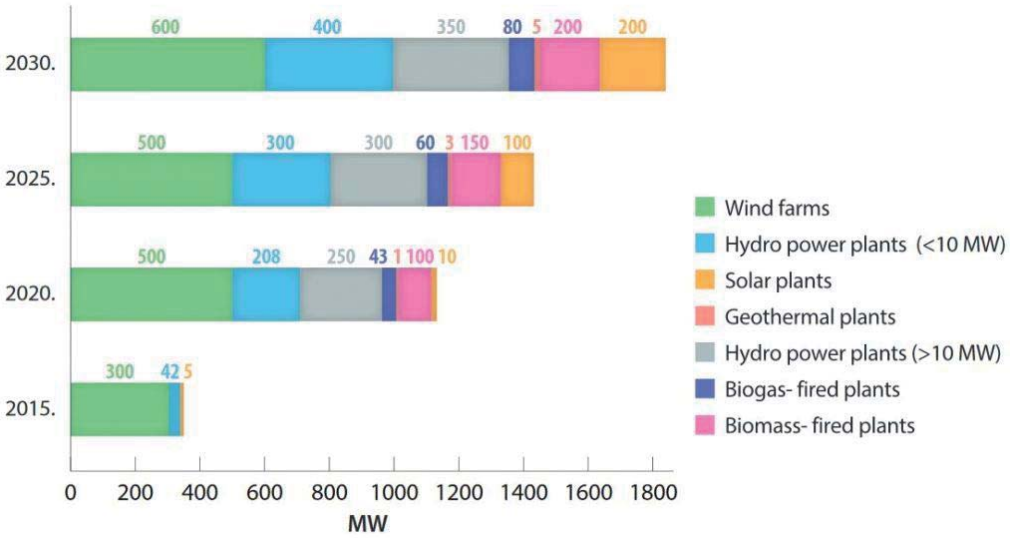

Figure 1 - Projection of the Government of Serbia to build capacities for electricity generation from renewable sources 2015-2030 [3]

Biomass includes biodegradable parts of wood industry by-products, wastes and residues of biological origin from agriculture (which includes plant and animal matter), as well as industrial and municipal waste. Biomass can be divided into:

- Biomass from forestry (unused wood, remains of stumps, semi-wild trees, etc.),
- Agricultural biomass (straw, leaves, parts of fruit trees, sugar cane, corn, etc.),
- Energy crops (beets, potatoes, trees, etc.),
- Biomass obtained from animal farms,
- Industrial waste (drinks industry, food industry, etc.),
- Municipal waste (paper and plant residues can be used as a source of biomass).

In Serbia, biomass resource is estimated at 3,405 million tons of oil equivalent which makes up 61% of the total potential of renewable energy resources. Most promising utilization options for biomass include space heating in households and buildings using biomass pellets or briquettes and co-firing or total replacement in district heating plants firing heavy oil or coal in south Serbia, where natural gas is not available yet, as well as use in the field of growing and processing of agricultural products, in frame of sustainable development of the agriculture. It is estimated that the total potential of biomass from agriculture in Serbia is about 12.5 million tons per year [4]. Table 1 provides an overview of the potential of biomass from agriculture in Serbia.

Table 1 – The energy potential of biomass from the residue of agricultural production in Serbia [4]

	Biomass	Biomass for combustion (25% of total, 103 t)	Low thermal power (MJ/kg)	Equivalent value of light heating oil (103 t)
1	Wheat straw	743,75	144	247,92
2	Barley straw	103,13	14,2	34,87
3	Oat straw	6,4	14,5	2,21
4	Rye straw	3	14	1
5	Corn	1787,5	13,5	574,55
6	Seed corn	21,56	13,85	7,11
7	Grain ear	357	14,7	124,95
8	Sunflower stem	200	14,5	69,05
9	Sunflower shell	30	17,55	12,54
10	Soya straw	80	15,7	29,9
11	Rapeseed straw	75	17,4	31,07
12	Stalks of hops	1,98	14	0,66
13	Stalks of tobacco	0,26	13,85	0,09
14	The remains of cutting in orchards	289,44	14,15	97,5
15	The remains of cutting in vineyards	71,55	14	23,85
16	Manure	110	23	60,24
	TOTAL:	3880,57	14,26	1317,51

By combustion of biomass, large quantities of biomass ash are generated. This ash represents a waste product, which is either disposed of in landfill, occupying valuable land and polluting the environment or recycled on agricultural fields or forest. Based on the physical, chemical and morphological properties, it is reported that biomass ash has a substantial potential for use as a pozzolanic mineral admixture and/or as an activator/binder in cement-based materials. Compared to coal fly ash, where significant research has already taken place and high use are already reported in several countries, commercial utilization of biomass ash is not so widely reported. The use of biomass ashes contributes to enhanced sustainability in the construction industry, as for every portion of replaced Portland cement there is an improvement in the environmental footprint of concrete, including a reduction in CO_2 emission. Moreover, recycling these materials as raw materials for another process reduces waste.

3. CROSS BOARDER COOPERATION FOR BIOMASS UTILIZATION

For all the reasons given in the previous chapter, Department for Materials and Structures, Faculty of Civil Engineering Osijek and Department of Civil Engineering and Geodesy, Faculty of Technical Sciences Novi Sad started working on IPA project Agricultural Waste – Challenges and Business Opportunities (Eco Build). Main idea of the project is creating the network between agriculture and industry, through scientific research and solve problem of waste disposal. Biomass is cheaper than commonly used types of fuel in industry, hence, by its use as energy source industry would benefit. Networking of industry and construction companies will introduce possibility of biomass ash (BA) use in civil engineering structures as integral part of construction, so their competitiveness would be improved. Project outputs include:

- Report on preparation and use of BA as building material;
- New, standardized BA products: eco-concrete, eco-mortar and stabilized earth;
- New teaching material for elective course on use of BA and
- Cooperation network for biomass and BA users and providers.

From the aspect of the methodology, the main approach is cross boarder (CB) cooperation through which skills, equipment, knowledge, science and research will jointly be used to address mentioned issues. Joint management and research team will ensure most efficient help when tackling common challenges. The main solution developed during the project will be a possibility of using biomass ashes (BA) in civil engineering as:

1. A mineral additive in concrete and mortar preparation and
2. A soil stabilization agent.

The knowledge collected in the project would be transferred from project partners to agriculturist (holders of biomass), industry (biomass users) and construction companies (users of biomass ashes) through round tables aiming to encourage cooperation of agriculturists and industry. Acknowledging the possibility of biomass ash application in civil engineering would give a new value to this type of waste and thus solve the problem of its disposal. The approach used in the project would solve the problem of biomass disposal entirely within the regions covered by the project and also develop new construction products/building materials that would make these regions recognizable and more competitive in building materials market.

The reasons why CB cooperation is truly needed to achieve project's objectives and results are:

- The regions participating in the project share the same problem of biomass from crop residues disposal and there is a mutual understanding of the urgency of solving it.
- Croatia as EU member is already required to achieve 20% of energy from renewable sources while Serbia as a candidate for EU membership is about to be required to do the same.

- As the awareness of the use of alternative fuels in industry and alternative materials in building construction is low to non-existent at both sides participating, the project aims to raise it especially within the target groups of local agriculturists, industrial and construction companies on how their mutual cooperation (without any additional investment) can contribute to improved competitiveness, economy and reduction of environmental risks relating to ash deposition in environment, unless re-used, in this way benefiting all mentioned.
- There are some real-life examples of biomass application in Serbian industry which will enable more proficient transfer of knowledge from industry in Serbia to industry in Croatia, as planned in the project through the planned dissemination of findings. The project deals with the creation of completely new and potentially very valuable types of construction products that are so far unexplored. Therefore, all the advantages and disadvantages of these ashes in building structures should be considered.

The entire project team consists of experts from different disciplines (civil and chemical engineers), each team member from different research background, capable to analyze the problem thoroughly only by working together with mutually benefit. In addition, the project partner from Serbia already conducted a preliminary research of locally available biomass ashes and the acquired knowledge would be transferred to the project partner.

4. ACTIVITIES AND RESULTS OF THE CBC

In broad terms, activities of this project can be classified as: research, networking/dissemination and preparation of laboratory product samples.

These activities will include following actions:

1. Joint research of biomass ashes as potentially building materials – The aim of this activity is to analyze biomass ashes as building material which will result in guidelines relevant for its further use. Detailed investigation will encompass characterization of biomass ashes through testing of chemical, physical and mechanical properties, testing of basic and durability properties of mortar, concrete and soil stabilization based on biomass ash, as well as basic properties of laboratory produced sample products. Based on all obtained results, possible application of biomass ashes in construction industry will be proposed and published in a form of report. Research will be conducted by Joint team.

2. Laboratory sample production of new, eco-concrete/mortar and stabilized soil – This activity will include practical demonstration of real-life application of tested biomass ashes in a form of production of laboratory samples of: 1. eco-concrete element, 2. eco-precast concrete element, 3. eco-mortar and 4. Eco stabilized earth. This will provide definite proof of practical use of biomass ash in construction businesses.

3. Creation of new teaching material for elective course on use of BA – In order to empower students, SMEs, agricultural subjects and construction businesses and provide them with new knowledge, skills and improve networking new course materials will be developed. This new course will become available to all interested parties. Materials will also be made available to regular students of both Faculties.

4. Creation of cooperation networks for biomass and BA users/providers – By including different target groups and connecting them in joint interest of recycling of agricultural waste,

this project will create new business cooperation network that will improve competitiveness as well as cross-border business cooperation.

Dissemination of results and findings will be done jointly and on both sides of programme area so that it is most proficient and covers largest possible area as well as the target group members.

Cross Boarder added value is environmental sustainability because project brings new approach in dealing with waste in environmental friendly and sustainable way. Higher education/research will conduct research/disseminate results; enterprises and SMEs will provide agricultural biomass waste and learn how to manage it usefully, produce prototype according to Report; learn about new technologies - become more competitive; business organizations will improve enterprise networking to become more competent, public will benefit from improved management of agricultural waste.

Sustainability of the main project outputs has been taken into account in the preparation process in a way that Report and teaching materials created for dissemination/education on use of BA in construction and industry will be used for future reference, research or similar waste management; samples of biomass ash mineral additive/soil stabilization agent and eco-concrete and mortar/stabilized soil will be kept at the Faculties as a teaching/demo materials for future reference and educational purposes in the new courses and newly created cooperation networks for biomass and BA users and providers will remain in place for future, thorough exploitation with support of Chambers of Commerce in Croatia and Serbia as well as experts from academia.

5. CONCLUSIONS

This paper presented IPA CBC project Agricultural Waste – Challenges and Business Opportunities (Eco Build) with the main idea to introduce possibility of biomass ash use in civil engineering structures as integral part of construction.

Biomass utilization can provide CO_2 offsets and reduce greenhouse gases and air pollutants, induced by concrete industry; help mitigate climate change; reduce risks to life and property and help provide a secure, competitive energy source. Shifting to a home-grown, renewable energy economy provides opportunities for growth and expansion, especially for rural communities as these renewable feed-stocks are directly connected to the land, primarily agricultural and forestry lands.

Developing options for creating value from biomass rather than consistently treating it as a disposal problem has significant economic and social values, including potentially improving air quality by reducing fire risks, reducing landfill costs, reducing reduction/removal costs, reducing fire suppression costs, and increasing public safety.

The great potential of biomass in Serbia and Croatia lies in the agricultural residues and wood biomass. Apart from these two sources of biomass, significant sources can be obtained from the waste of livestock production. The second group of biomass energy crops includes the plants that serve as raw material for biodiesel, bioethanol, etc. Biomass is partially used as energy source, but the ashes, generated by the combustion of biomass, are rather disposed on the landfill then further utilized.

Substituting cement in mortar and concrete, with the ashes provided from the combustion of biomass (ash containing Al, Ca, Fe, Mg, Na, P, Si), as CO2 neutral fuel, would reduce the

impact on global warming, give a new use-value and the possibility of economic valuation of ashes as a new product. All these effects would constitute a strong impetus for the creation of conditions for the integrated management of the use of large quantities of ash from biomass originating from agriculture in Serbia and Croatia.

ACKNOWLEDGEMENTS

The paper presents the part of research realized within the project "Theoretical and experimental research and improvement of educational process in civil engineering" conducted by the Department of Civil Engineering and Geodesy, Faculty of Technical Sciences, University of Novi Sad.

REFERENCES

[1] Directive 2009/28/EC of the European Parliament and of the Council of 23 April 2009 on the promotion of the use of energy from renewable sources

[2] https://www.energetskiportal.rs/en/regulations/legislation/strategies/, assessed on 16th June, 2018.

[3] Energy Sector Development Strategy of the Republic of Serbia for the period by 2015 with projections by 2030, assessed on 22th June, 2018.

[4] Brkić M, Janić T.: *Collection, storage and briquetting of biomass in agriculture, Proceedings from consultations: Significance and perspectives of biomass briquetting*, Ecological movement of Vojvodina, Faculty of Forestry, Belgrade, Federal Ministry for Science, Development and Environment, Vrnjačka Banja, (in serbian), 1996.

ДГКС Друштво грађевинских конструктера Србије
ASES Association of Structural Engineers of Serbia
S-59
15. KONGRES
6-8. 9. 2018. Zlatibor

Žarko Lazić[1], Lev Zaretsky [2], Gordana Broćeta[3], Marina Latinović[4]

VISOKO ADHEZIONO 10-ŽIČANO UŽE ZA PREDNAPREZANJE

Rezime:

Armasteel Llc, inženjerska kompanija u oblasti proizvodnje užadi za prednaprezanje, pokrenula je program razvoja novog tipa građevinskog čelika za prednaprezanje u formi 10-žičanog trougaonog užeta sa stabilnom strukturom i podužnim lučnim zavojima od tjemena užadi po obimu presjeka. Postavljena je hipoteza da bi se primjenom građevinskog čelika, opisanog oblika, moglo postići povećanje adhezije između užeta i betona, a time i tehnološka efikasnost u proizvodnji prednapregnutih betonskih elemenata. U radu su prikazani rezultati sopstvenih eksperimentalnih istraživanja. Ispitivanjem adhezije primjenjena je interno razvijena metoda ispitivanja i "pull-out" metoda, prema ASTM-u. Analizom rezultata pokazalo se da se primjenom 10-žičanih užadi dobija višestruko veća adheziona čvrstoća.

Key words: 10-žičano uže za prednaprezanje, „pull-out", adhezija, prednaprezanje.

HIGH BOND 10-WIRE PC STRAND

Summary:

Armasteel Llc, an engineering company in the field of steel reinforcement production for prestressed concrete, has launched a program for the development of a new type of pre-stressed steel in the form of a 10-wire triangular strand with a stable structure and longitudinal arches from the strand's edge points around the cross section. A hypothesis set up was that the use of the construction steel, with described form, could increase the adhesion between strand and concrete, and thus the technological efficiency in the production of prestressed concrete elements. The paper presents the results of own experiments. Testing adhesion, an internally developed test method is carried out and "pull-out" method, according to ASTM. Analysing the results, it was found that by applying 10-wire strands, a higher adhesion strength was obtained.

Key words: 10-wire PC strand, pull-out, adhesion, prestressing.

---

[1] *Phd student, MA, Structural engineering and materials laboratory IGM "KABAS", Vojvode Sinđelića 61, 74000 Doboj, B&H, zarko@igmkabas.com*
[2] *Phd, Armasteel Llc, 455000 Magnitogorsk, RUS, zaretsky1@yandex.ru*
[3] *Asst. prof., PhD, University of Banja Luka, Faculty of Architecture, Civil Engineering and Geodesy, Bulevar vojvode Stepe Stepanovića 77, 78000 Banja Luka, B&H, gordana.broceta@aggf.unibl.org*
[4] *Asst., MA, University of Banja Luka, Faculty of Architecture, Civil Engineering and Geodesy, Bulevar vojvode Stepe Stepanovića 77, 78000 Banja Luka, B&H, marina.latinovic@aggf.unibl.org*

1. INTRODUCTION

Armasteel Llc, an engineering company in the field of production of steel reinforcement for prestressed concrete, has launched a program for the development of a new type of pre-stressed steel in the form of a 10-wire triangular strand (1 + 6 + 3) with a stable structure and longitudinal arches from the strand's edge points to the cross section center.

1.1. ADVANTAGES AND DISADVANTAGES OF PC STRANDS

Prestressed concrete strands made of high carbon, cold drawn steel wires are the most commonly used reinforcement for precast span elements. The efficiency of this reinforcement type is based on the unique combination of properties: flexibility, unlimited length, lower expenses and low relaxation losses.

However, in spite of the economical and technological benefits, PC strands have not fully replaced the steel rebars ("mild steel") from the prestressed concrete elements. Lack of bond between strand and concrete is one of the main reasons for the fact that PC strand have not replaced fully "mild steel". PC strands have spiral structure which allows to move in helical direction longitudinally in its own imprint in the concrete, as a results, losing adhesion due to contraction of the strand cross section (Poisson coefficient).

Furthermore, the surface of standard 7-wire PC strands is similar to the cylinder, there are short and shallow grooves on the transition between the wires that forms concrete ribs. These ribs are usually rather weak to resist slipping of the strands under high capacity load.

Existing PC strands have quite large end slip, as shown at Figure 1. Considering this, prestressed concrete elements, have large zones without full input of prestressing force Figure 2. This means that beams cross section in shear span zone do not have maximum shear capacity, which would have if there is full input of prestressing force presented.

Figure 1 – Typical end slip of conventional 7-wire strand

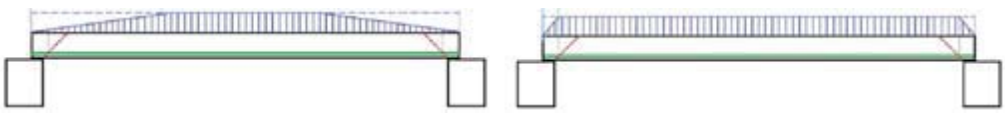

Figure 2 – Shematic view of prestressing force transfer length [6]

1.2. TECHNICAL SOLUTIONS FOR IMPROVEMENT OF BOND CONNECTION

Improvement of lower bond connection between conventional 7-wire strand and concrete is a challenge that many scientists have tried to solve. There were many different configurations of strands that have been offered from middle of the XX century to the present time.

All of these engineering solutions had serious imperfections. Some of them were non technological, impossible to be manufactured or to be applied, very expensive, with increased relaxation losses and decreased fatigue.

Zalialiutdinov and Latypova in 1977. [2] proposed solution to make longitudinally short segments with central wire of larger diameter Fig.3. There is also solution, from the same authors, with additional smooth curves [3].

Both of these strands have very high relaxation losses and elongations, that will in the end effect on the bond strength.

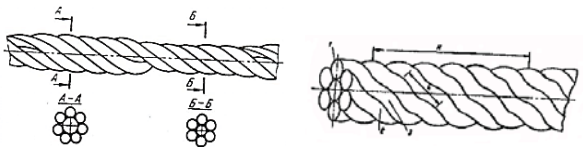

Figure 3 – Typical end slip of conventional 7-wire strand [2,3]

Solutions proposed could not pass a basic requirement for their use (bond connection with concrete), so they failed at the first stage.

2. NEW STRAND PROTOYPE

Idea for invention of prestressed reinforcement with improved technical properties, was borned in Magnitogorsk (RUS), where group of engineers, guided by this idea, decided to establish an engineering company called Armasteel Llc [6].

2.1. DEFINING REQUIREMENTS

There was defined the list of requirements that the product must meet:

- production and workability,
- high and stable bond connection with concrete,
- high and stable elasticity modulus,
- high fatigue resistance,
- prevention of strand jamming between previously laid strands,
- avoidance of adverse effects and
- guarantee of concrete flowing around all strands.

First five points means that configuration of strand must be simple and unchangeable along the whole length of the strand: spiral configuration, unchangeable relative positions and uninterrupted contact of wires, unchangeable direction and period of lay, same diameters of wires for uniform tempering.

2.2. BASIC DESIGN AND PROTOTYPE

Team from Magnitogorsk decided to improve and test one of forgotten ideas from 60's of XX century, so called "triangular" strand configuration. Idea mentioned above originaly was proposed by USSR's scientist I. C. Berinskiy in 1967 [1].

According to Berinskiy, in order to ensure the compactness of the structure (when constructing triangular strands with linear contact), that is made from wires of the same diameter during one technological operation, several basic conditions need to be provided:

- the wires of any concentric winding (spinning, bending) must be touched between one another and the wires adjoining winding,
- the wires must touch the entire length of the strand with the equal pitch for all windings.

Based on these assumptions, analytical dependence was made between the parameters of the two assembled wires, assuming that in the normal section (at 90° angles) of the strand, the wires will have an ellipsoidal shape.

Berinskiy wanted to present a calculation for strands that serve as a prestressed reinforcement. Figure 4, presents calculation scheme of strands cross section at a plane that is vertical respect to the axis, on which the wires with corresponding screwing (bending) are marked with numbers inside the circle. Thus for example, the 12-wire strand consists of strings 1, 2, and 3; 15-wire strand from 1, 2, 3, and 6; 18-wire strand of 1, 2, 3, and 5 and 21-wire strand of 1, 2, 3, 5 and 9.

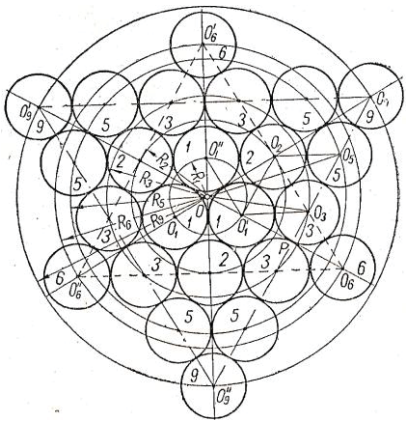

Figure 4 – Scheme of triangular strands for the proposed calculation method [1]

The strands of linear (straight) contact, in compacted wrap of any concentric windings must be touched by the wires of adjoining winding at the cross section and along its length of the strand, were will most significant strand profile have "triangular" shape:

$$O_1^{'}O_1^{''} = O_1^{'}O_2 = O_1^{'}O_3 = O_2O_3 = O_2O_5 = O_3O_5 = O_2O_6 = O_5O_9 = \delta \quad (1)$$

where $\delta -$ diameter of strand.

Marking

$$< O_1^{'}OO_3 = \beta_1; \quad (2)$$
$$< O_3OO_5 = \beta_2; \quad (3)$$
$$< O_5OO_2 = \beta_3, \quad (4)$$

it will be established that

$$\beta_1 = \beta_2 = \beta_3 = 60° . \quad (5)$$

Considering the triangles *O1'OO'', O1'OO2, O1'OO3, O3OO2, O6OO3, O3OO5, O5OO9* and merging the cosine theory with each of them, we get the output equality:

$$\delta^2 = R_1^2 + R_1^2 - 2R_1^2 cos120° ; \quad (6)$$

$$\delta^2 = R_1^2 + R_1^2 - 2R_1^2 cos120° ; \quad (7)$$

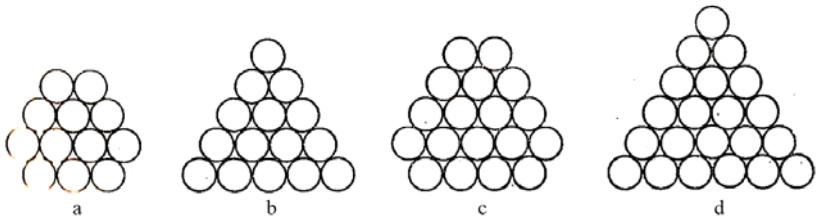

Figure 5 – Stable cross sectional planes of triangular prestressed strands: a) 12-wire, b) 15-wire, c)18-wire and d)21-wire [1]

Figure 5, shows possible cross sectional planes of "triangular" strands that can be used as prestressed reinforcement for prestressed concrete structures.

This "triangular" strand configuration can ensure some very important properties. For example it prevents longitudinally "movement" of the strand in the concrete mass.

However, these strands were not stable, because wires do not have supports in the direction of the tangent what caused that they moved from their original (initial) position, forming completely new configuration of the strand.

Furthermore, this strand could move along its own imprint in the concrete. This movement was destructive for the prestressed concrete elements.

These are reasons why Berinskiy's idea did not have an industrial application.

2.3. DEFINING APPLICABLE CONFIGURATION

Initialy it is decided that triangular strand need to have stable structure which will prevent stratification.

"1+6+3" strand configuration was chosen, because it was only possible combination of "triangular" spiral structure. To prevent movement in its own imprint in the concrete, it is decided to add a periodical profile to the external surface of wires.

This "triangular" strand had such a significant difference from its previous prototypes that it was considered as an independent invention (Figure 6) [6].

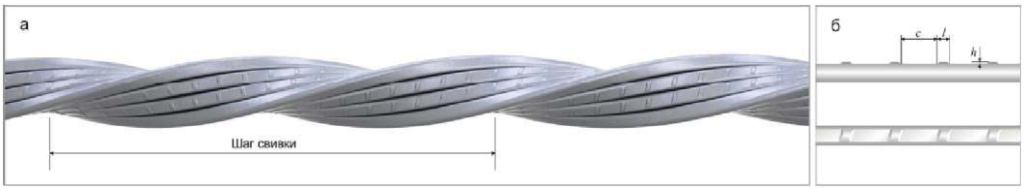

Figure 6 – Triangular strand with periodical profile on external surface: a) spinning step, b) periodical profile [6]

This innovative strands for its application needed specialized anchor grip, as it is shown on Figure 7.

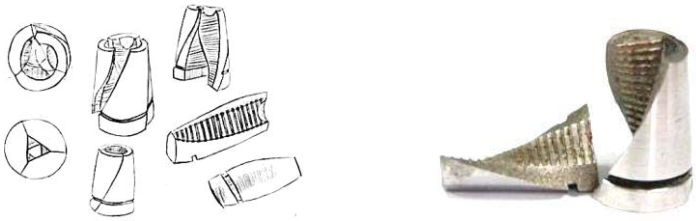

Figure 7 – Triangular strand's specialized anchor grip [6]

2.4. "TRIANGULAR" STRAND INTERACTION WITH CONCRETE

Interaction between strand and concrete first need to be tested on adhesion strength. Testing for determination of adhesion strength is so called "pull out" test.

The first attempt of "pull out" tests were realized in October 2014 at Chelyabinsk precast concrete plant No1 [4]. These samples of "triangular" 10-wire strand used in "pull out" tests were not stabilized, they were only processed by low temperature tempering, without tensioning, in one word, deadline was short and they were not fully completed.

The strands were pull out from 250x250 mm cubes made from concrete class of 50 MPa without any kind of reinforcement. Test was carried out on 4 specimens after 28 days (Figure 8):

- 2 specimens with conventional 7-wire strand with 9.3 mm diameter, 51 mm^2 cross section area and 140 mm bond length;
- 2 specimens with innovative 10-wire strand with 11.5 mm diameter, 53.5 mm^2 cross section area and 140 mm bond length;

Figure 8 – Specimens with "triangular" strand: a) first sample, b) second sample [4]

Table 1 – Results of "pull out" tests carried out in October 2014 at Chelyabinsk PCP [4]

Specimens	***Dimensions (mm)***	***Slip at… (kN)***	***Pull out force (kN)***
(1) 7-wire	*250x250*	*/*	*65*
(2) 7-wire	*250x250*	*20*	*43*
(1) 10-wire	*250x250*	*/*	*86*
(2) 10-wire	*250x250*	*/*	*92*

This test shows obvious advantage of "triangular" 10-wire PC strands and it was a big sign of potential high bond prestressed reinforcement of cold drawn wire.

The second attempt of "pull out" tests were realized in April 2018 at Structural engineering and materials laboratory IGM "Kabas" Doboj. Because of short period of time, early concrete strength and some technical deviations at the disposition of the test, results can be only considered as acquiring a prior knowledge of the next step.

This initial test is conceived in following order:

a) defining 3 types of conventional concrete mixtures
b) sampling concrete cubes 150x150x150 mm for testing compressive strengths for all 3 types of conventional concrete (3x specimens per type)
c) preparing molds and reinforcement for bond testing samples with defining accurate bond length of strand
d) sampling concrete prisms 150x150x300 mm for all 3 types of conventional concrete (3x specimens per type)
e) testing concrete compressive cube strength at 2, 7 and 28 days,
f) pull-out strand from concrete prisms at 7 and 28 days.

After 2 and 7 days specimens are tested to gain the first results about behaviour of concrete mixtures. This results are shown in Table 2.

Table 2 – Concrete compressive tests carried out in April 2018 at IGM "Kabas" Doboj

Concrete	***Samples***	***Dimensions (mm)***	***2 days***	***2 days***	***7 days***	***7 days***
			Force (kN)	***Stress (MPa)***	***Force (kN)***	***Stress (MPa)***
C20	*1*	*150x150x150*	*40,31*	*1,8*	*188,1*	*8,36*
	2	*150x150x150*	*40,23*	*1,8*	*191,7*	*8,52*
	3	*150x150x150*	*54,88*	*2,4*	*185,3*	*8,23*
C25	*1*	*150x150x150*	*98,42*	*4,4*	*361*	*16,04*
	2	*150x150x150*	*98,38*	*4,4*	*370,6*	*16,47*
	3	*150x150x150*	*100,10*	*4,4*	*373*	*16,60*
C30	*1*	*150x150x150*	*237,69*	*10,6*	*631,7*	*28,07*
	2	*150x150x150*	*228,05*	*10,1*	*600,2*	*26,67*
	3	*150x150x150*	*239,29*	*10,6*	*635*	*28,22*

Pull-out test has been carried out after 7 days. Table 3. below shows complete results of 18 specimens (3x per type of concrete for each 7-wire (9,3 mm) and 10-wire (11,5 mm)). On Figure 9, it is shown visual comparison of average F-s (force-slip) diagram in this test.

Table 3 – Pull out tests carried out in April 2018 at IGM "Kabas" Doboj

Concrete	***Samples***		***Wires (num.)***		***Pull out force (kN)***		***Pull out slip (mm)***	
			9.3	***11.5***	***9.3***	***11.5***	***9.3***	***11.5***
C20	*9.3-1*	*11.5-1*	*7*	*10*	*3,6*	*9,2*	*9,3*	*16,7*
	9.3-2	*11.5-2*	*7*	*10*	*4,7*	*11,7*	*17,9*	*26,1*
	9.3-3	*11.5-3*	*7*	*10*	*3,9*	*11,9*	*23,2*	*21,9*
C25	*9.3-1*	*11.5-1*	*7*	*10*	*13,4*	*15,3*	*23*	*28,1*
	9.3-2	*11.5-2*	*7*	*10*	*9,1*	*13,8*	*28,9*	*21,4*
	9.3-3	*11.5-3*	*7*	*10*	*8,1*	*11,4*	*27,9*	*24*
C30	*9.3-1*	*11.5-1*	*7*	*10*	*12,2*	*21,9*	*25,7*	*18,7*
	9.3-2	*11.5-2*	*7*	*10*	*17,3*	*15,6*	*30,7*	*18,8*
	9.3-3	*11.5-3*	*7*	*10*	*17,4*	*damaged*	*19,8*	*damaged*

As Table 3. and Figure 9 shows, 10-wire (11,5 mm) strand is obviously in any case superior in view of adhesion strength, instead of 7-wire strand (9,3 mm). This superiority is reflected as 20% higher pull-out strength than 7-wire strand, according to test that has been done.

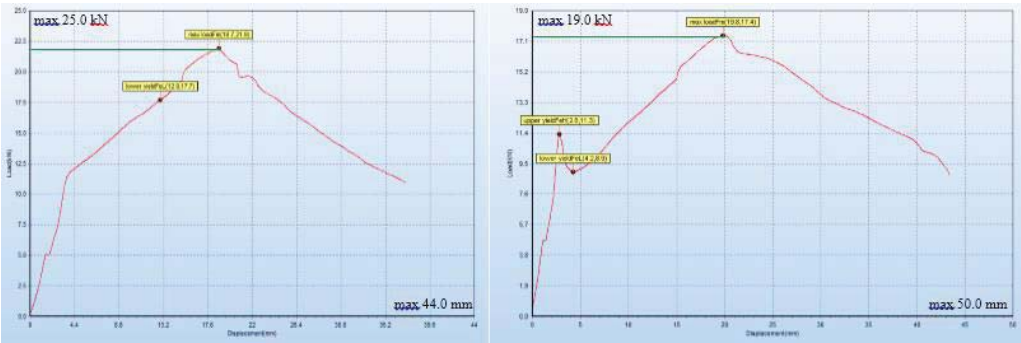

Figure 9 – Load-displacement diagram (Force-slip) shows: a-left) 10-wire strand (max F=21,9 kN) ; b-right) 7-wire strand (max F=17,4 kN)

Results in this tests should be taken with reserve, from that reason tested specimens were 7 days old and there were made some technical deviations (4 concentrated supports on surface to prevent bumpy surface). These imperfections were main reason of early cracking. Figure 9b shows those cracks, that are caused early dissipation of energy.

Figure 10 – Pull-out test: a-left) disposition with UTM (universal testing machine; b-right) cracks on testing side surface

The third attempt of "pull out" tests were realized in May 2018 at Armasteel company. These tests were done according to ASTM A1081 standard test method for evaluating bond of 7-wire steel prestressing strand [5].

Due to the lack of experience during the preparation and during the tests, there were some technical deviations, which are certainly sufficient to give a certain suspicion. Because of this results as previous "pull out" tests should be taken with some percentage of reserve.

Besides this, results shows superiority in favor of the "triangular" 10-wire strands, about 40% higher pull out force in comparison with conventional 7-wire strands.

It should be noted that ASTM method include tests with mortar, not with concrete [5].

3. CONCLUSION

Armasteel Llc, an engineering company in the field of steel reinforcement production for prestressed concrete, has launched a program for the development of a new type of pre-stressed steel in the form of a 10-wire triangular strand (1 + 6 + 3) with a stable structure and longitudinal arches from the strand's edge points around the cross section. A hypothesis set up was that the use of the construction steel, with described form, could increase the adhesion between strand and concrete, and thus the technological efficiency in the production of prestressed concrete elements. This paper presents the results of own experimental research in which the results of the application of newly produced 10-wire and conventional 7-wire strands are compared. In adhesion tests, an internally developed test method is carried out with reduced bond lengths on prismatic concrete specimens and "pull-out" method, according to ASTM, at the concrete age of 7 days.

By analysis of the results in all cases, it was found that by applying "triangular" 10-wire strands, a higher adhesion strength was obtained compared to the use of conventional 7-wire strands, but this must be taken with caution, because all tests have some imperfections which will have to be removed in forward steps.

So, with great certainty, it can be said that "triangular" 10-wire strand have much higher adhesion strength and that, with acquired current experience and knowledge from these tests, should be now precisely defined with sufficient reliability as ultimate.

This higher adhesion strength will give much smaller "end slip", namely it will reduce the force losses due to slipping and will significantly decrease transfer length what will directly effect the increase in shear capacity of the prestressed concrete element.

REFERENCES

[1] Berinskiy I.Z.: Steel trihedral strands for prestressed concrete constructions, Steel Ropes, collection of proceedings, Vol. 4, Kiev, USSR, pp.232-235, 1967.

[2] Latypov K.U. & Zalialiutdinov K.G.: Reinforcing strand. Author's certificate No. 580263, Moscow, USSR, 1977.

[3] Latypov K.U. & Zalialiutdinov K.G.: Reinforcing strand. Author's certificate No. 587187, Moscow, USSR, 1978.

[4] Zaretsky L.M. & Kharitonov W.A.: Trihedral 10-wire compacted strand. Concrete Plant International, No 1, pp. 148-152, 2017.

[5] American society for testing and materials: ASTM A1081 / A1081M-15, Standard test method for evaluating bond of seven-wire steel prestressing strand, ASTM International, West Conshohocken, PA, 2015.

[6] Armasteel Llc, www.armasteel.org, 455000 Magnitogorsk, RUS

ДГКС Друштво грађевинских конструктера Србије
ASES Association of Structural Engineers of Serbia
S-60
15. KONGRES
6-8. 9. 2018. Zlatibor

Aleksandar Radević[1], Jelena Dragaš[2], Vedran Carević[3], Dimitrije Zakić[4], Mladen Mladenović[5]

UTICAJ RAZLIČITIH USLOVA NEGE NA SVOJSTVA BETONA NA BAZI CEMENTA I VISOKOG SADRŽAJA LETEĆEG PEPELA

Rezime:

Istraživanje je imalo za cilj da se ispita uticaj različitih uslova nege na mehanička svojstva betona spravljenog sa visokim sadržajem letećeg pepela (HVFAC) u poređenju sa klasičnim betonom na bazi cementa (OPC). Primenjena su tri različita režima nege betona: nega u vodi, nega na vazduhu u laboratoriji i nega u standardnim laboratorijskim uslovima nakon premazivanja uzoraka sredstvom na bazi poliolefinske emulzije. Cilj je bio da se utvrdi uticaj ovakvih režima nege na razvoj čvrstoće pri pritisku i modula elastičnosti tokom vremena, kao i čvrstoća pri zatezanju (athezija) putem Pull-off metode i vodonepropustljivost betona. Uzorci negovani u vodi su imali najbolja mehanička svojstva, dok primena sredstva za negu nije imala značajniji uticaj na predmetna svojstva u poređenju sa uzorcima negovanim na vazduhu.

Ključne reči: OPC beton, HVFAC beton, uslovi nege, mehanička svojstva

THE INFLUENCE OF DIFFERENT CURING CONDITIONS ON CEMENT AND HIGH VOLUME FLY ASH CONCRETE PROPERTIES

Summary:

The research was conducted in order to evaluate the influence of different curing conditions on mechanical properties of high volume fly ash concrete (HVFAC) in comparison with the ordinary Portland cement concrete (OPC). Three different curing regimes were evaluated: standard water curing, standard laboratory air curing and curing in standard laboratory conditions using curing compound based on the polyolefin emulsion. The main objectives were to evaluate the influence of these curing regimes on the compressive strength and modulus of elasticity development over time, as well as the pull-off adhesion strength and water permeability of concrete. The samples cured in water had the highest mechanical properties, whereas the use of the curing compound did not significantly influence these properties compared with the samples cured in standard air conditions.

Key words: OPC concrete, HVFAC concrete, curing conditions, mechanical properties

[1]*Assistant professor, PhD, Faculty of Civil Engineering, University of Belgrade, aradevic@grf.bg.ac.rs*
[2]*Teaching Assistant, MSc, Faculty of Civil Engineering, University of Belgrade, jelenad@imk.grf.bg.ac.rs*
[3]*Teaching Assistant, MSc, Faculty of Civil Engineering, University of Belgrade, vedran@imk.grf.bg.ac.rs*
[4]*Associate Professor, PhD, Faculty of Civil Engineering, University of Belgrade, dimmy@imk.grf.bg.ac.rs*
[5]*Student, MSc, Faculty of Civil Engineering, University of Belgrade, mladen92mladen@gmail.com*

1. INTRODUCTION

In the modern age, a lot of human action is directed at the preservation of the environment. The construction industry is no exception to this trend. Relatively big effort is made in the identification of the negative effects that the use of different construction materials and processes have on the environment. The main focus of current research done in the material science field is oriented towards finding new alternatives to conventional construction materials by using waste and recycled materials. This is the reason why conventional cement concrete is being modified by the use of supplementary cementitious materials (mainly fly ash and slag) and recycled materials (mainly recycled concrete aggregate).

Since the 1930s, fly ash has been used as a partial replacement of clinker in Portland cement, or as an addition in concrete, mostly to limit the amount of early heat generation. The important benefit from the utilization of fly ash as a cement replacement is the reduction of carbon dioxide (CO_2) emissions from the Portland cement production. Approximately one ton of CO_2 is released for each ton of the Portland cement clinker [1]. A positive environmental effect of using fly ash in concrete is also obtained through the decrease of the amount of fly ash deposited in landfills and through the use of the waste material instead of natural resources for concrete production. It is for these reasons that today there is a general trend of replacing higher amounts of Portland cement in concrete.

In 1985, the Advanced Concrete Technology Group at CANMENT, Canada, started a project to develop structural high volume fly ash concrete (HVFAC) [2], [3]. HVFAC is usually defined as the concrete with more than 50% of fly ash in the total amount of cementitious materials. A large amount of research has been done regarding the physical and mechanical properties of HVFAC and in addition, work was also done on the evaluation of its material properties through the standards for cement concrete [4]. On the other hand, only a limited amount of research has been done so far regarding HVFAC structural properties.

Furthermore, the connection between HVFAC material properties testing and conditions in practical use must be evaluated for its safe application. One of the most important factors ensuring good performance of concrete is adequate curing. The mechanism of cement hydration and the influence of different curing types on physical and mechanical properties of conventional cement concrete are well known. However, the influence of different curing conditions on HVFAC has not been fully understood.

Pozzolanic material is usually defined as the material which will, in the presence of moisture, chemically react with calcium hydroxide $Ca(OH)_2$ at ordinary temperatures to form compounds possessing cementitious properties. At normal temperatures, the pozzolanic reaction is slower than the hydration of cement, so longer curing is needed for the full potential of fly ash to be reached [5]. It is generally recommended that HVFAC is moist cured for at least 7 days [6]. Adequate duration of moist curing helps the successful development of hydration and pozzolanic reaction, and increased curing temperatures can improve early age strengths [7]. However, results from the literature show that increased curing temperatures or steam curing, although helping the early age strength, can have adverse effect on the 28-day compressive strengths [8], [9]. In order to resolve the discrepancy of current results from literature, further studies are needed to determine the influence of different curing regimes on HVFAC properties.

This paper presents the research conducted in order to evaluate the influence of different curing conditions on HVFAC mechanical properties in comparison with the conventional cement concrete. Two types of concrete were made and tested: HVFAC and ordinary Portland cement concrete (OPC) designed to have the same workability and 28-day compressive strength for samples cured in water. Three curing conditions were chosen for the analysis: standard water curing (W), standard laboratory air curing (L) and curing in standard laboratory conditions using curing compound based on the polyolefin emulsion to coat the samples (C). The main objectives were to evaluate the influence of these curing regimes on the compressive strength and modulus of elasticity development over time as well as the pull-off adhesion strength and water permeability of both OPC and HVFAC samples.

2. MATERIALS AND CURING PROCEDURE

Both types of concrete were made with the same component materials (aggregate, cement and water) and the HVFAC mixture was designed to have 50% of fly ash in total cementitious materials mass.

All concrete mixtures were made using tap water and river aggregate obtained from "Elita-Cop" separated into three fractions (0/4 mm, 4/8 mm and 8/16 mm) using standard sieving method. Prior to sieving and mixing, the aggregate was dried in the oven until the constant mass was reached. The sieve analysis of used aggregate is presented in Figure 1. The density of used aggregate was 2673 kg/m^3, 2578 kg/m^3 and 2602 kg/m^3 for fractions 0/4 mm, 4/8 mm and 8/16 mm, respectively.

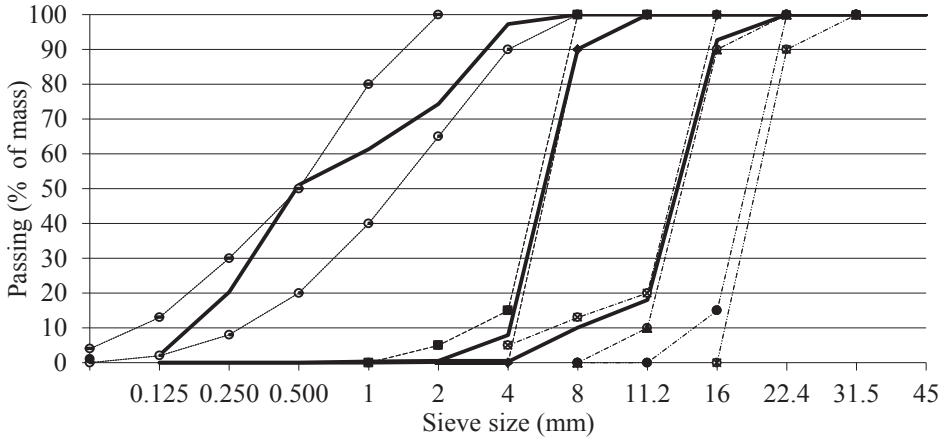

Figure 1 – Sieve analysis of aggregate

Portland composite cement CEM II (class PC 20M (S-L) 42.5R) produced by "Lafarge", Beočin was used for preparation of both concrete types. This type of cement contains additions (ground slag and limestone) up to 20% of the total mass, and there is no fly ash in the composition of cement. The specific gravity of cement was 3040 kg/m^3.

Fly ash was obtained from the "Nikola Tesla B" power plant in Obrenovac, Serbia. The average specific gravity of fly ash determined using the pycnometer method was 2075 kg/m^3.

The particle size distribution and chemical composition of fly ash are presented in Figure 2 and Table 1. In the last row of Table 1, the maximum allowed values of certain substances according to EN 450-1: 2012 [10] are presented. As it can be seen, the total quantity of SiO_2 + Al_2O_3 + Fe_2O_3 is higher than 70%. Figure 2 shows that the quantity of particles smaller than 45µm is higher than 12%. It can be concluded that the fly ash used in this research met the requirements of EN 450-1:2012 for the use of fly ash in concrete, and according to the ASTM-C618 [11] provisions could be classified as class F fly ash.

Table 1 – Chemical composition of fly ash (% of mass)

SiO_2	Al_2O_3	Fe_2O_3	TiO_2	CaO	MgO	Na_2O	K_2O	P_2O_6	SO_3	MnO	LOI
64.14	19.22	4.35	0.16	8.32	0.01	0.36	0.66	0.17	0.86	0.03	4.68
-	-	-	-	-	max 4	max 5	-	max 5	max 3	-	max 6

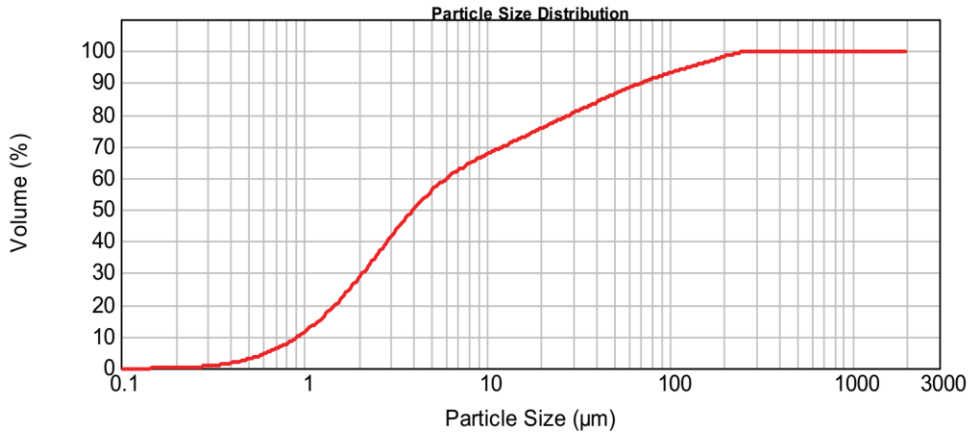

Figure 2 – Sieve analysis of fly ash

The concrete mix design was based on the absolute volume method. The mixing procedure began with mixing sand and coarse aggregate in a mixing pan for one min, then adding cement and fly ash and mixing for another minute. Water was added during the next 30 s, and the mixing continued for approximately 2.5 min. The mixture was used to cast 10 cm concrete cubes for compressive strength testing, 15·30 cm cylinders for testing the modulus of elasticity and 15 cm cubes for testing pull-off strength and water permeability. All samples were demoulded after 24 h. The values of the various properties reported in this paper represent the mean value of three measurements.

After mixing, all specimens were cast in steel moulds and the concrete was compacted using a vibrating table. The first group of specimens was demoulded after 24h and placed in water thank (W-samples). The second group (L-samples) was cured in standard laboratory air conditions (T=20±2°C, RH=60±5°C). Curing of the third group of samples was done using the curing compound based on the polyolefin emulsion (C-samples). Namely, immediately after casting into moulds, the uncovered concrete surface of the C-specimens was sprayed with the

liquid curing compound for preventing water loss in concrete. After the demoulding, the same spraying procedure was applied to all remaining surfaces.

As the target values, workability class S2 and compressive strength class C25/30 (MB30) were adopted for both OPC and HVFAC mixtures. All concrete samples which were made from either one of the two mixtures were additionally divided into three categories according to the applied curing procedure: OPC-W, OPC-L, OPC-C, HVFAC-W, HVFAC-L and HVFAC-C. The concrete mix design of OPC and HVFAC mixtures are presented in Table 2.

Table 2 – Concrete mix design

Mixture	*W/CM** *[-]*	*Water* *[kg/m^3]*	*Aggregate [kg/m^3]* *(0/4 mm)*	*(4/8 mm)*	*(8/16 mm)*	*Cement* *[kg/m^3]*	*Fly ash* *[kg/m^3]*
OPC	*0.614*	*175*	*835*	*557*	*464*	*285*	*0*
HVFAC	*0.488*	*195*	*838*	*503*	*335*	*200*	*200*

* *Water-to-cementitious materials ratio*

3. RESULTS AND DISCUSION

3.1. WORKABILITY AND CONCRETE DENSITY

Concrete workability was tested using the Abrams cone method according to EN 12350-2: 2010 standard. The average value of measured slump values was 7.0 cm for the OPC mixture, and 9.6 cm for the HVFAC mixture. The obtained values for the OPC and HVFAC mixtures corresponded to different workability classes, S2 and S3 respectively. From the engineering point of view it can be considered that the workability of these two types of concrete was not significantly different.

Concrete bulk density was tested according to EN 12350-2: 2010 standard. The average density for the OPC mixture was 2353 kg/m^3, and for the HVFAC 2260 kg/m^3. This reduction in density occurred due to a significantly lower density of fly ash compared with the cement and the lower amount of aggregate that was used in the HVFAC mixture.

3.2. COMPRESSIVE STRENGTH

Compressive strength was determined at the ages of 1, 3, 7, 28 and 114 days. The test was conducted in accordance with EN 12390-1:2010 standard. Figure 3 shows the development of compressive strength of both OPC and HVFAC mixtures cured at different regimes. At the age of 28 days, the samples cured in water had compressive strength of 38.7 MPa and 40.8 MPa for the OPC and HVFAC mixtures, respectively. Both of these values corresponded to the designed concrete class C25/30.

As expected, OPC samples stored in water had the highest compressive strength during all 114 days of testing. Also, it can be seen that the application of curing compound based on the polyolefin emulsion did not result in the preservation of the concrete compressive strength compared with samples cured in water. Moreover, the L-samples and C-samples had lower 28-day compressive strength compared with the water cured samples, for 20% and 15%, respectively. The decrease was even more pronounced at the age of 114 days: 39% and 30%

for the L-samples and C-samples, respectively. The use of the curing compound did not significantly influence the compressive strength compared with the samples cured in air (L-samples).

HVFAC samples cured in water had the highest 28-day compressive strength, similar like in the case of the OPC samples. The L-samples and C-samples had lower 28-day compressive strength compared with the water cured samples, for 23% and 29%, respectively. These differences were also higher at the age of 114 days: 34% and 36% lower compressive strength for the L-samples and C-samples compared with the W-samples, respectively.

The influence of different curing conditions on the compressive strength analysed in this study was similar for both OPC and HVFAC mixtures. At the age of 28 days the difference between the decrease of compressive strength between the W-samples and L-samples was up to 5% for both OPC and HVFAC mixtures. This difference was even more pronounced for C-samples that had up to 15% higher decrease in strength for HVFAC mixtures compared with the OPC ones.

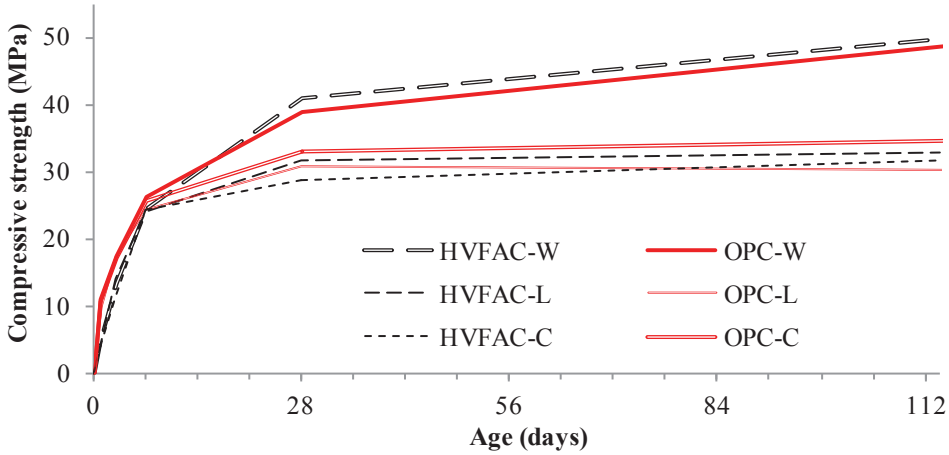

Figure 3 – Compressive strength development of differently cured OPC and HVFAC mixtures

The early age compressive strengths (before 7 days) of all OPC mixtures were higher compared with the HVFAC mixtures cured in the same way. This can be explained with the fact that the pozzolanic reaction needs time and takes place after the beginning of hydration, approximately at the age of 7–14 days or later [12], [13]. It can also be noticed that the influence of different curing conditions was less pronounced at early ages than in later ages, for both concrete types and especially for the OPC mixtures. This can be a consequence of the fact that all samples were stored in moulds for the first 24h and had enough water for early age strength development.

The compressive strength development over time was similar for corresponding OPC and HVFAC mixtures, as can be seen in Figure 3. This property of the selected OPC and HVFAC mixtures cannot be simply compared due to the different mix designs. However, it was expected that after 28 days the strength increase of OPC mixture should be lower than the HVFAC mixture; but, at that age a significant increase of strength was noticed for both OPC and HVFAC mixtures cured in water. A possible explanation can be found in the use of

blended cement that has slag as a pozzolanic material. In samples that had enough water (W-samples) a significant strength increase can be explained with the pozzolanic reaction that has developed in both HVFAC and OPC concretes. The extent of the pozzolanic reaction in HVFAC depends on the available $Ca(OH)_2$ and water content. Therefore, a lower strength gain of HVFAC mixture can be explained with relatively high fly ash amount and limited Portland cement amount.

It can generally be concluded that the influence of different curing conditions on the compressive strength was more pronounced in HVFAC mixtures compared with the OPC ones. For more specific conclusions, additional research is needed.

3.3. MODULUS OF ELASTICITY

The modulus of elasticity was tested at 3, 7 and 28 days. The test was conducted in accordance with SRPS U.M1.025:1983 standard. Figure 4 shows the effect of different curing conditions on the modulus of elasticity. Similar like in the case of compressive strength, the W-samples had the highest values of the modulus of elasticity at the age of 28 days.

For the OPC mixtures, the L-samples and C-samples had lower 7-day modulus of elasticity compared with the W-samples, for 16% and 11%, respectively. These differences were slightly higher at the age of 28 days: 17% and 16% lower modulus of elasticity for the L-samples and C-samples compared with the W-samples was obtained, respectively.

This difference was similar for HVFAC L-samples and lower for the C-samples. The L-samples and C-samples had lower 7-day modulus of elasticity compared with the water cured samples, for 15% and 2%, respectively. At the age of 28 days, these differences were also slightly higher: 16% and 6% lower modulus of elasticity for the L-samples and C-samples compared with the W-samples were obtained, respectively.

HVFAC had slower increase of modulus of elasticity in the first seven days compared with OPC samples. After 7 days, the increase was more pronounced for HVFAC, especially for the L-samples and C-samples.

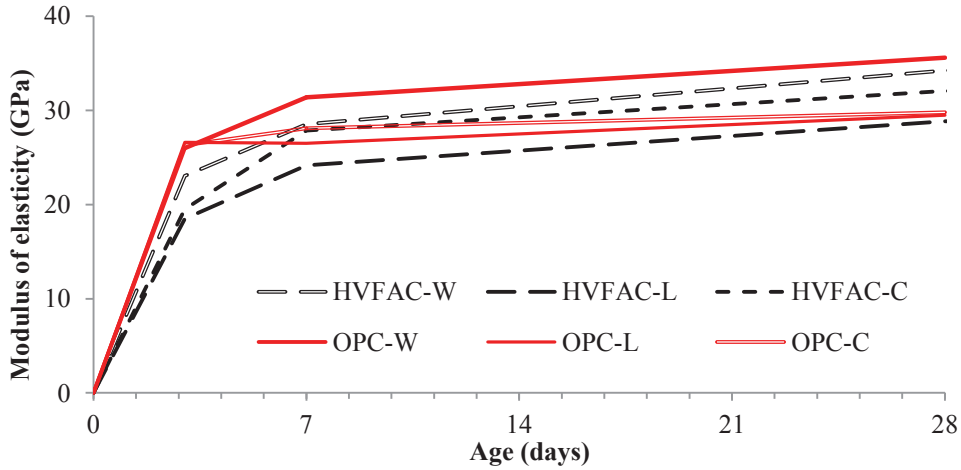

Figure 4 –Modulus of elasticity development of differently cured OPC and HVFAC mixtures

3.4. PULL-OFF TEST

For the purpose of defining the influence of different curing conditions on the concrete surface quality, the pull-off adhesion test was performed. The axial tensile force was applied until the fracture, using metal discs (50 mm in diameter and 30 mm thick), glued with an epoxy adhesive to the concrete surface. Testing was conducted in accordance with EN 1542:2010 standard, at the age of 28 days. The preparation of the samples consisted of drilling the 50 mm notch with a depth of 15±5 mm, and then cleaning the concrete surface before the metal disc gluing. Measured pull-off tensile strength values are given in Figure 5.

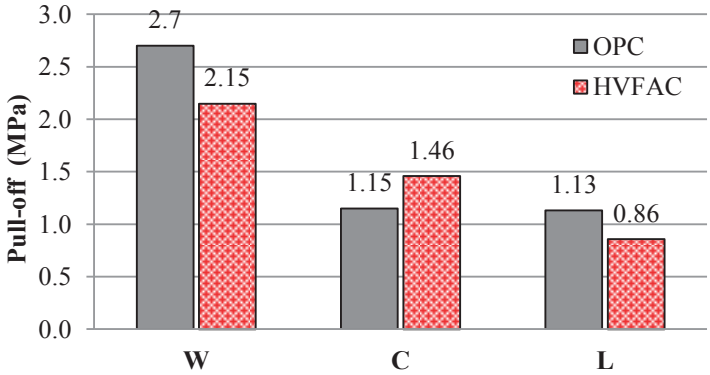

Figure 5 – Pull-off strength of OPC and HVFAC samples

It can be seen that for both types of concrete, the water-cured samples had significantly higher tensile strength compared with the L and C-samples. The tensile strength of OPC samples was 20% higher compared with the HVFAC samples even though the 28-day compressive strength was 5% lower for the OPC mixture.

Samples that were not cured in water had tensile strength lower than 1.5 MPa. No significant difference between the L and C-samples was noticed for both OPC and HVFAC mixtures.

3.5. WATER PERMEABILITY TEST

The testing of concrete water permeability was performed according to EN 12390-8: 2010 standard. Tested samples were exposed to water at a pressure of 500 kPa for 72 hours in the laboratory conditions (T=20±2°C and RH=60±5%). After being exposed to water pressure, the samples were broken and the maximum water penetration depth was measured. The obtained results are shown in Figure 6.

According to the presented results, it can be concluded that, in this particular case, the curing conditions had higher impact on the concrete water permeability than the used concrete type. HVFAC samples cured in water had lower water penetration than the OPC samples cured in the same way. According to SRPS U.M1.206:2013 standard, the OPC-W mixture corresponded to the waterproof class V-I, and the HVFAC-W to the waterproof class V-II. In the case of concrete specimens cured using the other two regimes, considerably higher water penetration depths were measured. Since the water penetration depths ranged from 9.2 cm to

13.4 cm, these concrete types cannot be classified as water-resistant concrete. The application of different curing conditions had a significant influence on the water permeability of both OPC and HVFAC mixtures.

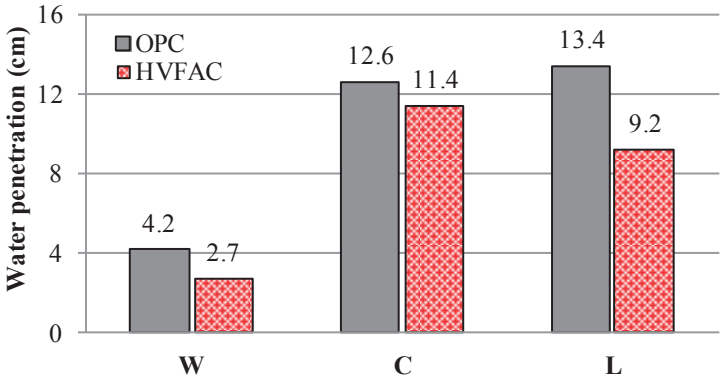

Figure 6 – Maximum depth of water penetration

4. CONCLUSION

In order to support the implementation and promotion of sustainable development and the importance of concrete curing conditions, different tests were conducted on the OPC and HVFAC mixtures. The main objectives were to evaluate the influence of three different curing regimes on the compressive strength and modulus of elasticity development over time as well as the pull-off adhesion strength and water permeability of both concrete types. Based on the presented results, the following conclusions can be made:

- Concrete samples cured in water had the highest compressive strength during all 114 days of testing and they were higher for up to 39% and 36% compared with other curing regimes for OPC and HVFAC, respectively.
- Compared with the water-cured samples, the modulus of elasticity was lower for L-samples and C-samples for both OPC and HVFAC mixture for up to 17%.
- For both types of concrete, the water-cured samples had significantly higher pull-off tensile strength compared with the L and C-samples. The tensile strength of the OPC samples was 20% higher compared with the HVFAC samples.
- The curing conditions had the most significant impact on the concrete water permeability. The OPC and HVFAC samples cured in water had the lowest water penetration, up to 30% of the specimen height. In the case of samples cured in other two ways, penetration depths ranged from 60% to 90% of the specimen height. HVFAC samples had up to 35% lower water penetration compared with the corresponding OPC samples.

Generally, the use of the curing compound did not significantly influence the concrete properties compared with the samples cured in standard air conditions.

ACKNOWLEDGEMENTS

The presented study is a part of the research financially supported by the Ministry of Education, Science, and Technological Development of the Republic of Serbia under the research projects TR 36048: "*Research on condition assessment and improvement methods of civil engineering structures in view of their serviceability, load-bearing capacity, cost effectiveness and maintenance*" and TR 36017: "*Utilization of by-products and recycled waste materials in concrete composites in the scope of sustainable construction development in Serbia: investigation and environmental assessment of possible applications*".

REFERENCES

[1] A. Bilodeau and V. M. Malhotra, "High-Volume Fly Ash System: Concrete Solution for Sustainable Development," *ACI Mater. J.*, pp. 41–47, 2000.

[2] N. Bouzoubaa and V. M. Malhotra, "Performance of Lab-Produced High-Volume Fly Ash Cements in Concrete," *Concr. Int.*, vol. 23, no. 4, pp. 31–35, 2001.

[3] V. M. Malhotra and P. K. Mehta, *High-Performance, High-Volume Fly Ash Concrete for Building Sustainable and Durable Structures*, Third Edit. Supplementary Cementing Materials for Sustainable Development Inc., Ottowa, Canada, 2005.

[4] J. Dragaš, N. Tošić, I. Ignjatović, and S. Marinković, "Mechanical and time-dependent properties of high-volume fly ash concrete for structural use," *Mag. Concr. Res.*, vol. 68, no. 12, pp. 632–645, 2016.

[5] S. H. Gebler and P. Klieger, "Effect of Fly Ash on the Durability of Air-Entrained Concrete," in *Proceedings of the 2nd International Conference on Fly Ash, Silica Fume, Slag, and other Natural Pozzolans in Concrete*, 1986, pp. 483–519.

[6] M. D. A. Thomas, "Optimizing the Use of Fly Ash in Concrete," *Portl. Cem. Assoc.*, p. 24, 2007.

[7] P. K. Mehta and O. E. Gjørv, "Properties of portland cement concrete containing fly ash and condensed silica-fume," *Cem. Concr. Res.*, vol. 12, no. 5, pp. 587–595, 1982.

[8] B. Liu, Y. Xie, and J. Li, "Influence of steam curing on the compressive strength of concrete containing supplementary cementing materials," *Cem. Concr. Res.*, vol. 35, no. 5, pp. 994–998, 2005.

[9] J. Payá, J. Monzó, M. V. Borrachero, E. Peris-Mora, and F. Amahjour, "Mechanical treatment of fly ashes - Part IV. Strength development of ground fly ash-cement mortars cured at different temperatures," *Cem. Concr. Res.*, vol. 30, no. 4, pp. 543–551, 2000.

[10] CEN, *EN 450-1: Fly ash for concrete — Part 1: Definition, specifications and conformity criteria*. Brussels: European Committee for Standardization, 2012.

[11] ASTM C618, "Standard Specification for Coal Fly Ash and Raw or Calcined Natural Pozzolan for Use in Concrete," West Conshohocken, Pennsylvania, 2015.

[12] L. Lam, Y. L. Wong, and C. S. Poon, "Degree of hydration and gel/space ratio of high-volume fly ash/cement systems," *Cem. Concr. Res.*, vol. 30, no. 5, pp. 747–756, May 2000.

[13] R. Siddique and P. Cachim, *Waste and Supplementary Cementitious Materials in Concrete: Characterisation, Properties and Applications*. Woodhead Publishing, 2018.

ДГКС Друштво грађевинских конструктера Србије
ASES Association of Structural Engineers of Serbia
S-61
15. KONGRES
6-8. 9. 2018. Zlatibor

Franc Sinur[1], Aljoša Šajna[2], Teja Török Resnik[3], Jakob Šušteršič[4]

BETONSKI KONTEJNER ZA ODLAGANJE NISKO I SREDNJE RADIOAKTIVNOG OTPADA

Rezime:

Ovaj rad predstavlja razvoj betonskog kontejnera i zahtjeve koji se moraju ispuniti radi odlaganja radioaktivnog otpada na niskom i srednjem nivoju. Kontejner za skladištenje je napravljen od samozbijajućeg betona visolih performancija (SCC-VP), koji obezbeđuju dugoročne mehaničke osobine i izuzetno nisko propustljivost tečnosti. Dalje, predstavljeni su rezultati SCC-VP testova, način izvođenja „drop-testa" u skladu sa odredbama ADR-a i analiza rezultata ovih ispitivanja.

Ključne reči: betonski kontejner, radioaktivni otpad, samozbijajući beton visokih performacija, „drop-test"

CONCRETE CONTAINER FOR DISPOSAL OF LOW AND INTERMEDIATE LEVEL RADIOACTIVE WASTE

Summary:

This paper presents the development of the concrete container and the requirements which have to be meet for disposal of low- and intermediate-level radioactive waste (LILW). The disposal container is made of self-compacting high performance concrete (SC-HPC), which provides long term mechanical properties and extremely low permeability for liquids. Further on, some results of SC-HPC tests, the method of carrying out the "drop-test" in accordance with the ADR provisions and the analysis of the results of these tests are presented.

Key words: concrete container, radioactive waste, self-compacting high performance concrete, drop test

[1] *Ph.D., IBE Consulting Engineers, Ljubljana, Slovenia, franc.sinur@ibe.si*
[2] *Ph.D., ZAG Slovenian National Building and Civil Engineering Institute, Ljubljana, Slovenia, aljosa.sajna@zag.si*
[3] *POMGRAD, Construction Company, Murska Sobota, Slovenia, teja.torok@pomgrad.si*
[4] *Ph.D., IRMA Institute for Research in Materials and Applications, Ljubljana, Slovenia, jakob.sustersic@irma.si*

1. INTRODUCTION

Low and intermediate level waste (LILW) is generated by the use of radioactive materials in medicine, science and industry, and in particular, they are the result of electricity generation at the Krško Nuclear Power Plant (NEK). Performance can be in gaseous, liquid or solid form. Waste materials should be properly processed and disposed of in the radioactive waste disposal site within the framework of the radioactive waste management process. The solution for the LILW disposal site at Vrbina, Krško is based on the established solutions for LILW disposal in the world, on previous domestic solutions and experiences, as well as on the solutions that were verified and defined in the procedure for placing the disposal site in space.

The LILW disposal site is designed as a facility in which all the activities required for the operation of the disposal site are carried out, and in particular for the disposal of radioactive waste. The LILW disposal site is dedicated to administrative and service activities, acceptance of waste, disposal of waste and ensuring the physical safety of the disposal site. The following facilities are planned in the area of the disposal site plateau: Administrative-service facility (ASF), Technological facility (TF), Storage silo with hall over the silo (Silo and Hall), Control Pool (CP).

All LILW waste will be inserted into single containers before disposal, which is considered one of most important element of the engineering multi-tier system. Storage containers ready for disposal will be transported to the disposal site in accordance with the provisions of the requirements for the transport of dangerous goods by road (ADR)[1]. Slovenia has implemented the ADR provisions [1] in national legislation through the Law on the Transport of Dangerous Goods (ZPNB)[2]. This precisely prescribes that containers for the transport of dangerous goods must be tested with a “drop test”.

In total, 950 containers of type N2d will be deposited, with a maximum permissible mass of 40 t. Containers deposited in the silo with the help of a portal crane and special grips. Empty spaces between containers and containers and the silo wall will be filled with filling concrete.

The main concreting authority for the development project and the holder of the Slovenian Technical Approval for the disposal container is ARAO – agencija za radioaktivne odpadke (Agency for Radwaste Management), Ljubljana. A large team of experts from IBE (LILW disposal site and container designer), Pomgrad (manufacturer of container prototype), ZAG and IRMA (co-operating Institutes in the project) participated in the development project of the disposal container. This paper, prepared by some individual representatives of all participants in the project, summarizes only the most important parts of the papers that were presented at the 15th Slovenian Colloquium on Concrete [3 – 6].

2. DISPOSAL CONTAINER

Concrete container as one of the most important elements of the engineering part of the multi-tier system for preventing the passage of radioactive substances from the disposal site to the environment acts as: (a) biological shield in the time before the disposal, (b) mechanical protection of LILW during storage and disposal, (c) the basic safety element during the transport and internal transport (displacement) of LILW in the container, (d) the basic criterion

of the profile in the process of preparing waste for disposal and (e) the central object of handling LILW in the area of the storage silo.

The most important and most specific container requirement is, in addition to the resistance and stability of all anticipated loads in the filling phase and the transport before the final disposal, also the durability in the expected life span of 300 years.

In view of the known environmental conditions to which containers will be exposed after disposal in the silo, the containers will be exposed to carbonization in the first phase (in the period 2020 – 2061), after the filling and closing the silo, and the abandonment of water pumping from 2062 onwards, the silo with containers exposed to underground water.

2.1. GEOMETRIC CHARACTERISTICS OF THE N2d CONTAINER

The basic geometry of the container was determined based on the installation of 4 TTC barrels. The N2d container is an upgrade of the N2b container, where it differs substantially only in the design of the cover and anchorage of the cover in the reinforced concrete container. The specific solutions of the container are given below and are result of the development of the container through the acquisition of the Slovenian Technical Approval. The detailed geometrical data of the container are given in Table 1. The disposal container is shown in graphic form the Figure 1. Figure 2 shows the anchoring of the cover in the reinforced concrete container.

Table 1 – Geometrical characteristics of container N2d

Parameter	***Unit***	***Value***
Geometric data on the container		
External dimensions		
Width	*m*	*1,95*
Length	*m*	*1,95*
Height	*m*	*3,30*
Chamfered outer edges of the walls (in both directions)	*m*	*0,20*
Internal dimensions – the bottom of the container		
Width	*m*	*1,49*
Length	*m*	*1,49*
Internal dimensions – top of the container		
Width	*m*	*1,55*
Length	*m*	*1,55*
Thickness of the bottom slab	*cm*	*23*
Wall thickness at the top	*cm*	*20*
Wall thickness at the bottom	*cm*	*23*
Geometric data on the cover – maximum dimensions		
Width	*m*	*1,66*
Length	*m*	*1,66*
Width of support	*cm*	*5,5*
Cover thickness	*cm*	*20*
Cover thickness above support	*cm*	*20*

Table 1 continued

Volume of the container		
Gross volume – external occupation of space	*m^3*	*12,28*
Net volume – after installation the cover	*m^3*	*6,31*
Mass		
Cover	*t*	*1,36*
Empty container with the cover	*t*	*14,92*
Maximum permissible nass of the full container	*t*	*40*

Section of the container

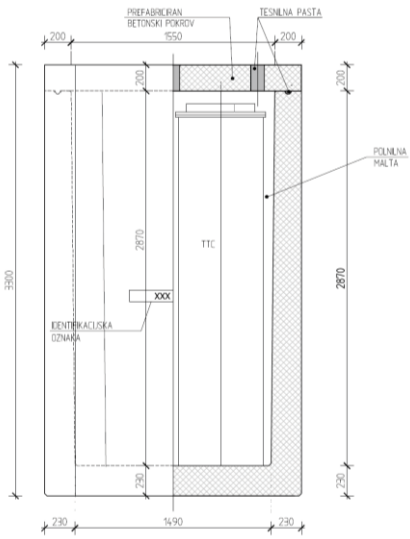

3D display of the container with reinforcement

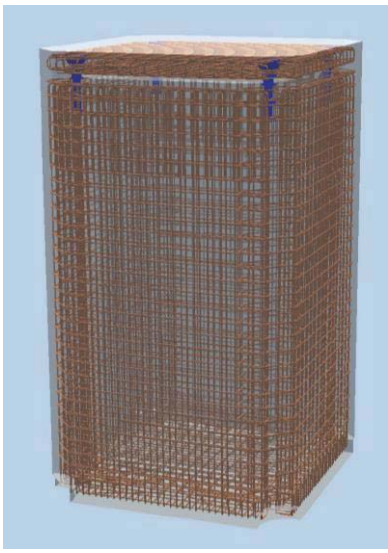

Container layout – bottom and cover

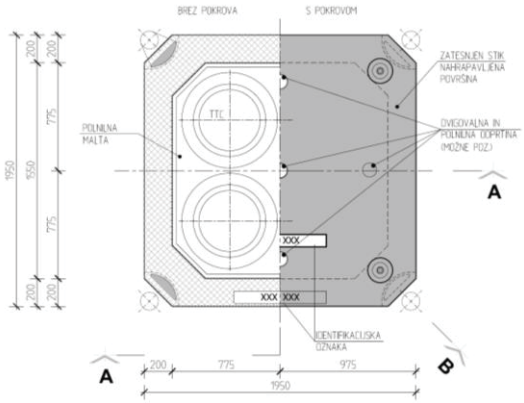

Figure 1 – Disposal container

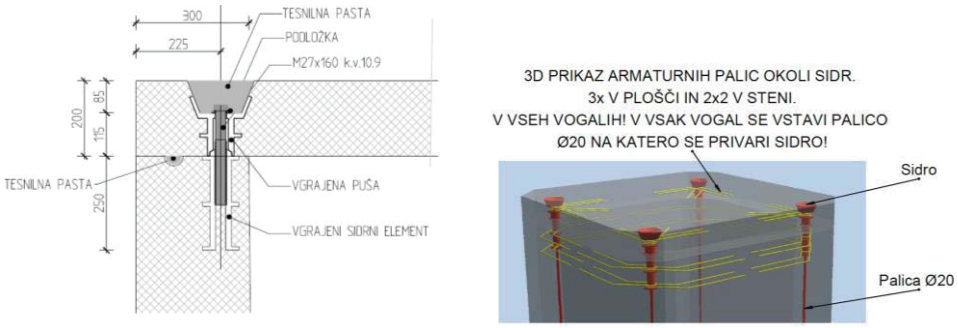

Figure 2 – Mode of anchoring of the cover

2.2. CHARACTERISTICS OF THE N2d CONTAINER

Essential characteristics are as follows:

- the container is lifted from the bottom – the steel structure with wheels is lowered from the top to the bottom of the container and hugs it, the swiveling legs turn in the prepared grooves on the underside of the container,
- the lifting from the bottom represents safer and more controlled lifting and lowering of the container,
- with the proposal lifting technique, we avoid the occurrence of tensile stresses in concrete during moving (lifting and lowering) of the container,
- at the bottom of the container, a circular recess is made on the outer corners for lifting legs (in this case the thickness of the biological shield, measured diagonally, is at least 20 cm),
- the required distance between containers with the lifting technique used is approximately 20 cm (due to the circumferential steel structure of the grippers and the turning hoist feet),
- the outer corners of the container are chamfered by 20 cm,
- inner corners are thickened – the thickness measurement is the setting of barrel in the corner, the filling options with the barrel remain unchanged,
- increased dimensions of the corners are used to anchor the concrete cover, extending over the entire container; anchoring is done via pre-inserted anchor elements in the corners of the container and the sleeve in the corners of the cover; the fixing is done by screwing the bolts over the sleeves into pre-installed anchoring elements in the corners of the container,
- a groove is formed on the top of the container wall and a pen is on the inside of the cover; the intermediate space between the groove and the pen is filled with seal mortar.

3. COMPOSITE MATERIALS OF THE CONTAINER

Three composite materials have been developed in the framework of the development project for the production od disposal container: (1) concrete for the production of reinforced concrete walls, bottom and cover of the container, (2) filler mortar to fill the empty spaces between the inserted barrels with LILW and the inner surface of the container, and (3) seal

mortar for sealing the intermediate space between the filler mortar and the inner surface of the cover and for sealing the contact between the cover and the top surface of the walls.

Within the framework of the project, the requirements for the properties of the basic materials used for the preparation of composites and for the properties of all three composites (concrete, filler and seal mortars) were determined. These requirements are set out in the Container Testing Program [7]. In order to obtain the Slovenian Technical Approval (STA), it was necessary to develop composites with properties that met all the requirements. The results of the tests given in the Container Testing, Measurement and Testing results [8] show that all requirements are met. The average results of the tests of concrete properties (Table 2), filler mortar (Table 3) and seal mortar (Table 4) are given in fresh and hardened state.

Table 2 – Average results of the tests of concrete properties

Slump-flow (SIST EN 12350-8:2010)	*680/710 mm*
Density of fresh concrete (SIST EN 12350-6;2009)	*2393 kg/m^3*
Air content (SIST EN 12350-7:2009, Chapter 5)	*2,0 %*
w/c ratio (SIST 1026:2008, D3)	*0,37*
Compressive strength 28 days (SIST EN 12390-3:2009)	*86,0 MPa*
Depth of penetration of water under pressure 28 days (SIST EN 12390-8:2009)	*3 mm*
Shrinkage 182 days (DIN 4227-Part 1)	*0,374 mm/m*
Freeze/thaw resistance up to 200 cycles (SIST 1026:2016, ND)	*101,0 %*
Modulus of elasticity 28 days (DIN 1048)	*42500 MPa*
Total porosity (EN 1936:2006)	*10,85 %*
Chloride content (SIST EN 206:2013, Chapter 5.2.8)	*0,070 %*

Table 3–Average results of the tests of filler mortar properties

Slump-flow (SIST EN 12350-8:2010)	*670/700 mm*
Density of fresh concrete (SIST EN 12350-6;2009)	*2301 kg/m^3*
Air content (SIST EN 12350-7:2009, Chapter 5)	*2,2 %*
w/c ratio (SIST 1026:2008, D3)	*0,41*
Compressive strength 28 days (SIST EN 12390-3:2009)	*86,4 MPa*
Depth of penetration of water under pressure 28 days (SIST EN 12390-8:2009)	*3 mm*
Chloride content (SIST EN 206:2013, Chapter 5.2.8)	*0,075 %*

Table 4–Average results of the tests of seal mortar properties

Fluidity (SIST EN 445:2008) - immediately	*13,4 sec*
- after 30 min	*15,4 sec*
Volume change (SIST EN 445:2008)	*1,3 %*
Compressive strength 28 days (EN 196-1)	*48,0 MPa*
Setting times (EN 196-3) – initial time	*115 min*
- final time	*207 min*

4. CONTAINER DROP-TEST

According to the requirements of ADR [1], the drop-test must be carried out in such a way that the container from the heigh of 30 cm freely descends to the ground, to the so-called target. The target must be from a solid material with a mass that is theoretically ten times the maximum mass of the container. For the purpose of specific investigations, Pomgrad prepared a test site in its plant in Lipovci whose volume of concrete foundation or target is approximately 150 m^3.

Three drop-tests were carried out for the purpose of developing and validating the adequacy of the container. The details are given in Table 5.

Table 5–Key data of drop-tests performed

Container No.	***Mass***	***Drop height***	***Position***
0	*39,6 t*	*approx. 30 cm*	*on the corner of the bottom*
1	*26,5 t*	*33 cm*	*on the corner of the bottom*
2	*40,0 t*	*30,5 cm*	*on the corner of the cover*

4.1. DROP-TEST NO. 1

During the test, the speed and movement of the container was measured before and after the collision. The speed and movement of the container were measured using the optical measurement system GOM Aramis HS with high speed Photron MiniUX 100 cameras. The capture of images took place at a speed of 500 images per second. The speed determined at the collision was 2,53 m/s.

Within the drop-test, a more detailed inspection and inventory of visible damage on the container after the test was performed. The container was oriented with a bottom slab down. It fell to the edge of the side surfaces 3 and 4 (Figure 3), which also show the relatively most damage.

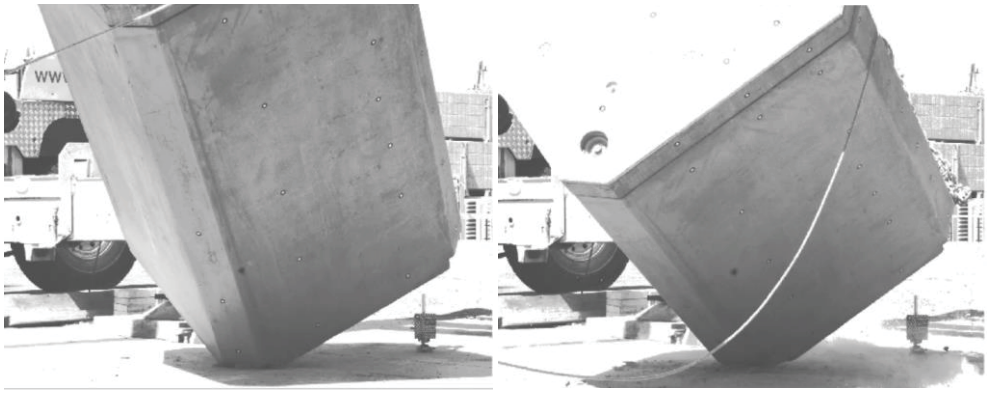

Figure 3 – Sequences of collision t = 0,33 s (left) and t = 1,0 s (right)

On the side surface 3 there are cracks with a width of up to 0,1 mm across the entire height of the surface. On the cover of the container on the right lower edge there is a chip of size about 30 × 4 cm (with a depth of up to 20 mm). In the lower right edge of the surface there is a chip depth of 42 to 65 mm.

On the side surface 4 there are two cracks with a width of up to 0,1 mm approximately 74 cm away from the right edge. On the left upper edge there is a chip of depth from 26 to 76 mm. In the lower left edge there is a chip depth of up to 22 mm. The edge in the lower right edge has a depth of up to 56 mm.

The measured damages were compared with the maximum permissible limits specified in the document [9]. All the damages measured are smaller than the permitted.

4.2. DROP-TEST NO. 2

Container no. 2 was dropped to the corner of the cover at an angle of 46,85°with respect to the vertical. The basic goal of the measurements in the tests was to provide reliable input data for checking and calibrating the numerical model of the container, especially the force in the screws, anchors and deformation of reinforcement.

The speed determined at the collision was 2,44 m/s. The hight of the drop and the speed at the are slightly lower that that of container 1, which is probably due to the fact that the load rope broken down gradually (i.e., in two steps), and the container was moved to a slightly lower position before the final drop.

The maximum force measured in the screws is 163,8 kN and is less than the designed screw load of 264,4 kN. Measurements indicate that the prestressing in the screws after the test did not change significantly (the difference in forces is less than 12 %), which means that the screws were not plastic deformed and that no major contact damage occurred.

The maximum measured deformation of the reinforcement is 490 μm/m, which is less that the deformation at the limit of the reinforcement creep (approx. 2000 μm/m).

Even in the container 2 (as with container 1) all the damages measured are smaller than the allowed ones.

5. CONCLUSION

On the basis of already established solutions, the first draft of the container and the requirements of the disposal site were prepared, which were based predominantly on safety analyses designed for the disposal site and on the basis of the requirements for the transport of dangerous goods on public roads. Based on the starting points, a final solution of the container was completed within the project team for the Slovenian Technical Approval, which meets all the requirements given in the project documentation.

REFERENCES

[1] European Agreement concerning the International Carriage of Dangerous Goods by Road (ADR); http://www.unece.org/trans/danger/publi/adr/adr2017/17contentse0.htlm.

[2] Zakon o prevozu nevarnega blaga (ZPNB), Ur.l. UPB1 33/06, 41/09, 97/10.

[3] Sinur F., Duhovnik B.: Odlagalni zabojnik za nizko- in srednjeradioaktivne odpadke. Zbornik gradiv in referatov 25. slovenskega kolokvija o betonih: Betoni z izboljšanimi lastnostmi, Ljubljana, IRMA, 2018, 53 – 60.

[4] Török Resnik T., Kavnik T.: Odlagalni zabojnik za odlaganje nizko in srednje radioaktivnih odpadkov (NSRAO): Izdelava prototipov zabojnikov in testiranje padcev zabojnikov. Zbornik gradiv in referatov 25. slovenskega kolokvija o betonih: Betoni z izboljšanimi lastnostmi, Ljubljana, IRMA, 2018, 61 – 68.

[5] Ercegovič R., Narobe G., Šušteršič J.: Kompoziti za izdelavo zabojnika za NSRAO. Zbornik gradiv in referatov 25. slovenskega kolokvija o betonih: Betoni z izboljšanimi lastnostmi, Ljubljana, IRMA, 2018, 69 – 78.

[6] Bohinc U., Robič S., Šajna A.: Preskus padca AB zabojnika za odlagališče NSRAO in vrednotenje poškodb. Zbornik gradiv in referatov 25. slovenskega kolokvija o betonih: Betoni z izboljšanimi lastnostmi, Ljubljana, IRMA, 2018, 79 – 88.

[7] Program testiranj zabojnikov, materialov in preskusov potrebnih za certificiranje zabojnika za NSRAO, Št.: NRVB-POM Program testiranj zabojnikov_1017, 2018.

[8] Rezultati testiranj zabojnikov, meritev in preskusov potrebnih za certificiranje zabojnika za NSRAO, Št.: NRVB-POM_Rezultati testiranj zabojnikov_2/18, 2018.

[9] Pristop izpolnjevanja ADR zahtev pri padcu zabojnika, Opis pristopa podprt z izračuni, NRVB---5G1610A5G1610B, IBE, Franc Sinur, Boštjan Duhovnik, Ljubljana, julij 2017.

ДГКС Друштво грађевинских конструктера Србије
ASES Association of Structural Engineers of Serbia
S-62
15. KONGRES
6-8. 9. 2018. Zlatibor

Zlatko Zafirovski[1], *Milorad Jovanovski*[2], *Vasko Gacevski*[3]

TEHNIČKE MERE ZA REHABILITACIJU U HIDROTEHNIČKOM TUNELU NA SASKA RIJECI – M. KAMENICA

Rezime:

Hidrotehnički tuneli predstavljaju izazovne konstrukcije sa stanovišta dizajna, izgradnje i održavanja. Obično su pod konstantnim dejstvom vode, zbog čega su skloni popravljanju i sanaciji. Funkcionalnost ovih vrsta tunela zavisi od odgovarajućih tehničkih mera koje su preduzete u njihovom ekspolatacionom periodu. Ovo uključuje znanje i stručnjake iz nekoliko naučnih oblasti. U ovom radu su prikazane neke od tehničkih mera za rehabilitaciju hidrotehničkog tunela na reci Sasa.

Key words: Hidrotehnički tunel; Analiza; Rehabilitacija; PLAXIS 3D

TECHNICAL MEASURES FOR THE REHABILITATION IN THE HYDROTECHNICAL TUNNEL ON SASKA RIVER – M. KAMENICA

Hydrotechnical tunnels represent challenging constructions from a design, construction and maintenance point of view. They are usually under constant effect of the water, which makes them prone to repairs and rehabilitation. The functionality of these kind of tunnels depends on the proper technical measures taken in their service period. This involves knowledge and experts from a few scientific areas. In this paper some of the technical measures for the rehabilitation of the hydrotechnical tunnel on Saska River are shown.

Key words: Hydrotechnical tunnel; Analysis; Rehabilitation; PLAXIS 3D

[1] *PhD, Civ. Eng., Assistant Professor, University „Ss. Cyril and Methodius“, Faculty of Civil Engineering – Skopje, zafirovski@gf.ukim.edu.mk*
[2] *PhD, Geo. Eng., Professor, University „Ss. Cyril and Methodius“, Faculty of Civil Engineering – Skopje, jovanovski@gf.ukim.edu.mk*
[3] *B.Sc., Civ. Eng., Teaching Associate, University „Ss. Cyril and Methodius“, Faculty of Civil Engineering – Skopje, vaskogacevski@yahoo.com*

1. INTRODUCTION

This tunnel is part of the mine for lead and zinc Sasa, which in one of the biggest and most famous mines in Macedonia, located in the eastern part of the country (Figure 1). It is approximately 12 km from the town Makedonska Kamenica at elevation of 1000 m.

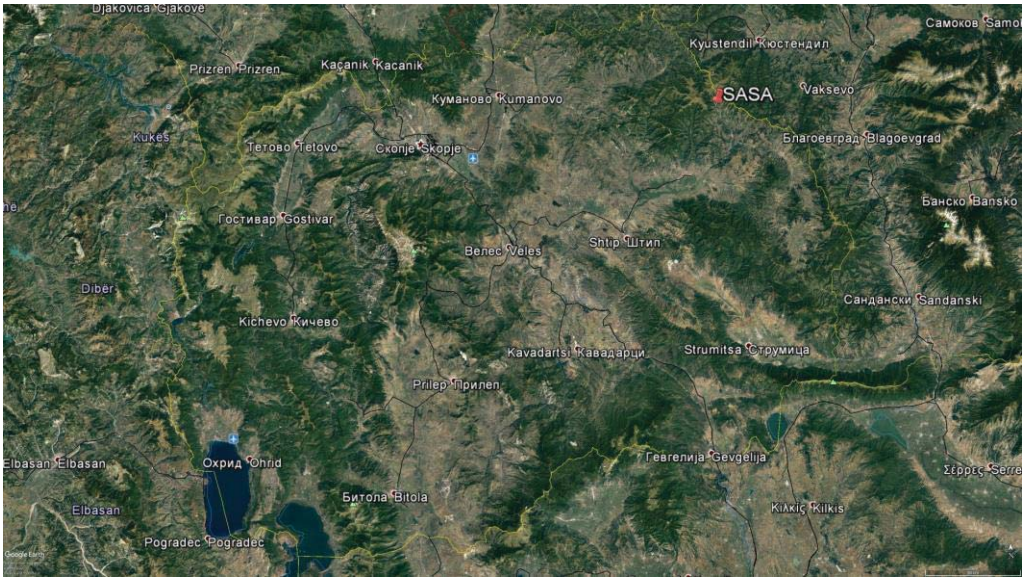

Figure 1 - Satellite view of the mine location (source: Google Earth)

1.1. GENERAL INFORMATION

The tunnel on Saska River is in function since 1971. It has a length of 1925 m with longitudinal slope of 5-7 %. The cross section varies in height and width (≈ 3 m) based on the geological composition and the support lining. Along the tunnel at a certain part are the tailings of the mine. The tailing are used for the disposal of the flotation pulp gained from the technological process of flotation of the minerals of lead and zinc. In the past three tailings have been realized, and another one is planned for the future exploitation period of the mine.

1.2. PREVIOUS REHABILITATIONS

There are several previous interventions made to this tunnel, that include: rehabilitation of the damaged concrete support lining, increasing durability and anti-corrosive protection of the concrete, injection of cracks and holes in the concrete and in the area between the rock and the concrete support, rehabilitation of the dilatation and the working joints, rehabilitation and protection of the invert arch, placement of additional shotcrete and rock bolts etc.

2. GEOLOGICAL AND GEOTEHNICAL PROPERTIES OF THE TERRAIN IN THE ZONE OF THE TUNNEL

The information for the geological condition of the terrain in the zone of the tunnel are collected from a few investigation stages, from which an appropriate base of geotechnical data was created.

2.1. LITHOLOGY

Present in the zone of the tunnel are the following natural and artificial compositions:

- Natural materials: gneiss rock, diluvial, proluvial and scree materials and alluvium (sandy gravel);
- Artificial materials: tailings sand (floatation pulp) and concrete from the tunnel support lining.

2.2. TECTONIC PROPERTIES

The character of the river valley and the condition and interaction of the represented rock masses indicate an intensive tectonic activity of this terrain in the geological past. The results from the investigations from which the faults and the fault zones where verified, also prove the complex tectonic condition of the terrain. The wider region belongs to zones with intensity of I = VIII° MCS (Mercali-Cancani-Sieberg). According to the national seismogenic sources the closest located area (berovsko-pehcevsko) is with expected intensity of I = XI° MCS, and expected magnitude of M = 7,5°.

2.3. ENGINEERING – GEOLOGICAL TYPES OF ROCK MASSES

There are two groups in which the represented rock masses in the zone of the tunnel can be divided:

- Strongly tied rock masses – represented by the gneisses which build the base of the terrain;
- Loose rock masses – represented by the alluvial sediments and the floatation pulp.

2.4. HYDROGEOLOGICAL PROPERTIES

The represented rock masses according to their hydrogeological function in the terrain assembly behave as collectors and isolators.

In the group of hydrogeological collectors belong the alluvial sediments and the flotation pulp (tailings).

In the group of hydrogeological isolators belong the strongly tied rock masses (gneisses).

2.5. GEOTECHNICAL CHARACTERISTICS OF THE ROCK MASSES

Most of the information's for the characteristics of the rock masses where obtained from the existing technical documentation.

- Gneisses: RQD=30 %, σ_p=30 MPa, c=300 KPa, φ=36°, γ=25 kN/m^3, ν=0.30, RMR= III class;

- Gravel: E=52000 kN/m^2, ν=0.28, c=0 KPa, φ=34°, γ=22.18 – 22.80 kN/m^3;
- Flotation pulp: c=0 KPa, φ=31°, γ=18 – 20.5 kN/m^3.

Figure 2 – Tunnel exit

3. CURRENT STATE OF THE TUNNEL

From the completely made analysis, the on-site inspection in the tunnel, and the overall results it has been noted that the hydrotechnical tunnel on Saska River can adequately perform its function.

However, due to the observed irregularities along the tunnel in terms of established and identified defects, it was recommended to apply measures with which the functionality of the tunnel construction would increase, and this would result in better condition and longer exploitation period for using the tunnel.

Mostly the irregularities refer to increased amount of water on the walls of the tunnel and some damages to the support lining. A specific defect which is present along the tunnel is the damage of the concrete invert. Along the length of the tunnel almost the entire bottom where the water flows is eroded and is some places a channel with a depth of over 20 cm was formed.

4. REHABILITATION SOLUTIONS AND ANALYSIS OF THE TUNNEL

The tunnel is divided in few sections:

- Parts with primary (rock bolts and reinforced shotcrete) and secondary support (reinforced concrete lining);
- Parts with only primary support (rock bolts and reinforced shotcrete);
- Parts with no support (only rock mass).

The rehabilitations solutions vary depending on the sections.

4.1. REHABILITATION OF THE TUNNEL SECTIONS WITH ONLY PRIMARY SUPPORT

Parts of the tunnel have only primary support (reinforce shotcrete d=20 cm and rock bolts La=2,5 m ap/an=1,25/1,25 m) and invert arch with no secondary support. For these segments multiple variant solutions where considered:

- Solution 1: Partial secondary support – pillars (reinforced concrete d=30 cm);
- Solution 2: Full secondary support above the invert (reinforced concrete d=30 cm);
- Solution 3: Rehabilitation of the invert with anchors, new reinforcement and new layer of concrete (d=20 cm).

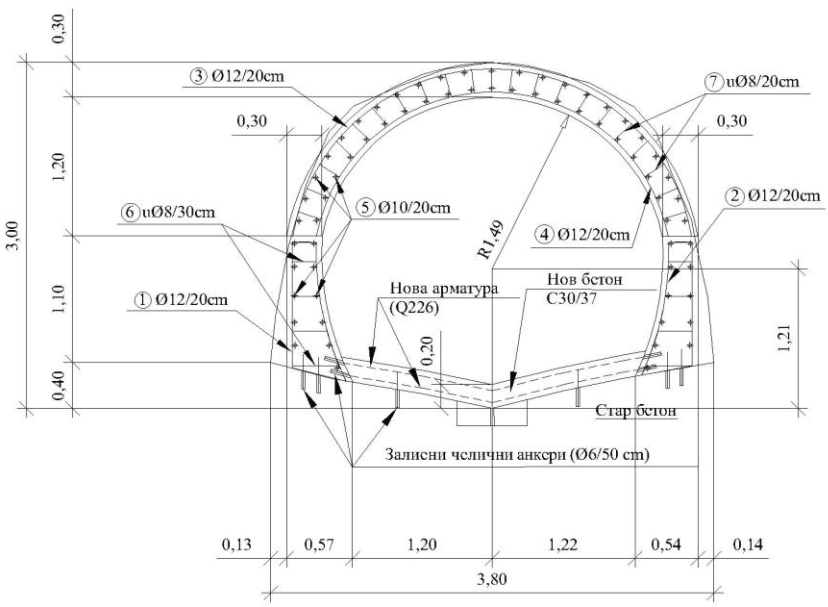

Figure 3 – Tunnel cross section with full secondary support

4.2. ANALYSIS OF THE TUNNEL SECTIONS WITH ONLY PRIMARY SUPPORT

The analysis was made for multiple variant solutions covering several stages:

- Solution 1: Analysis of the tunnel with the invert from reinforced concrete and primary support from reinforced shotcrete and rock bolts (for stability control);
- Solution 2: Analysis of the tunnel with the invert and pillars from reinforced concrete, as well as primary support from reinforced shotcrete and rock bolts;
- Solution 3: Analysis of the tunnel with primary and full secondary support (d=30 cm);
- Solution 4: Analysis of the tunnel with primary and secondary support, without the invert.

The analysis process was simulated in the numerical model in multiple phases:

- Phase 1: Initial stress condition in the massif before construction;
- Phase 2: Excavation of the tunnel and construction of the invert with the pillars;
- Phase 3: Pseudo-static analysis.

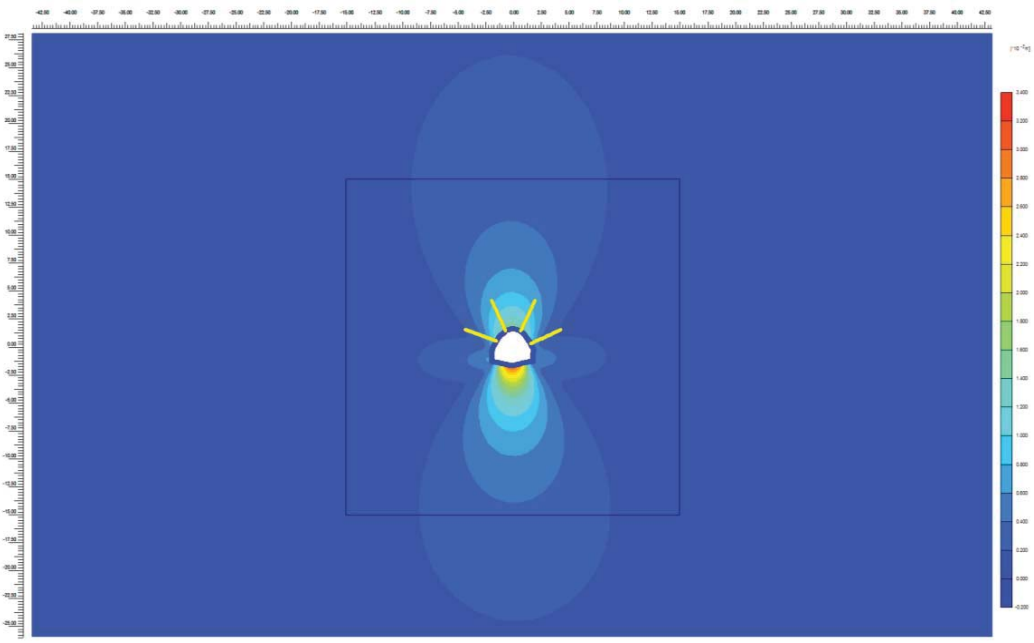

Figure 4 – Deformations of the local environment and the lining

The maximum deformations in the local environment are 3.24 mm. The results from the analysis show that the bigger static values occur in seismic conditions.

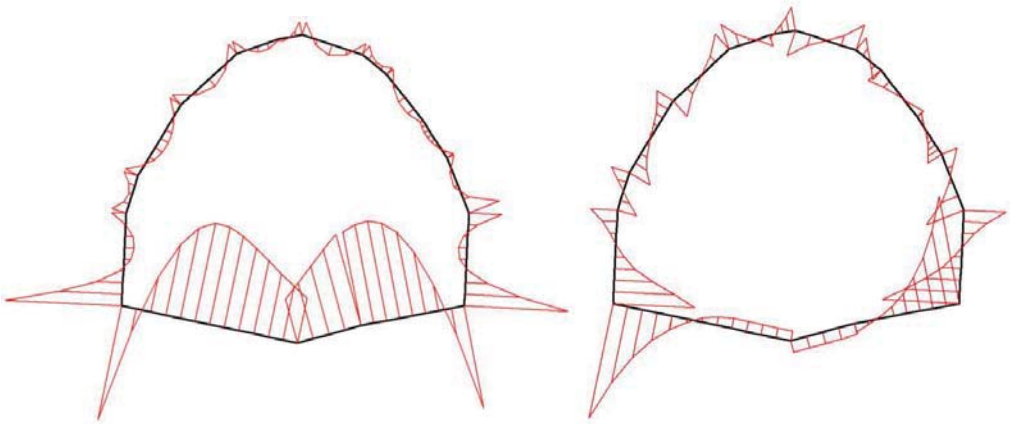

Figure 5 – Diagrams of bending moment (left) and transversal forces (right)

5. CONCLUSIONS

For proper exploitation and long lasting service life, the rehabilitation and maintenance is mandatory process for hydrotechnical tunnels. The rehabilitation solutions and analysis for the tunnel on Saska River shown in this paper are just part of the complexed process that enables the improvement of the tunnel construction bearing capacity and functionality. This process requires qualified experts from different scientific areas and adequate detailed information's regarding the local environment, previous conditions, rehabilitations and interventions and the current state of the tunnel.

REFERENCES

[1] Construction design of the "Saska" river diversion tunnel, stage II, Faculty of Civil Engineering, Skopje, 2006.

[2] Design of rehabilitation of the lining of the "Saska" river diversion tunnel from survey mark 1+200 to survey mark 1+717 and rehabilitation of the invert, Faculty of Civil Engineering, Skopje, 2003.

[3] As built design of the "Saska" river diversion tunnel (stage II), Faculty of Civil Engineering, Skopje, 2008.

[4] As built design of the injection works at the "Saska" river diversion tunnel, stage II, Geofluid, Skopje, 2007.

[5] Geodetic report on the surveys conducted for special purposes, Geomer, Delcevo, 2009.

[6] Partial – technical solution for the accompanying facility of the diversion collector "Velkovski stream" */shaft – diversion tunnel/* after raising the "New TSF" of Sasa mine – M. Kamenica – stage I, above elevation 990.0 m, Mine institute "Zavod PMS", Skopje, 2000.

[7] Construction report on completed activities aimed at rehabilitation of the damaged sections of collector no. 6 between survey marks 0+90 and 0+120 at the lead and zinc mine "Sasa" – M. Kamenica, RE-KO Inzenering, 2007.

[8] Main design on rehabilitation of a section of the "Saska" river diversion tunnel at survey mark 0+970 – 1+140.5, Civil Engineering institute "Makedonija", Skopje, 2005.

[9] Addenda to the main design on rehabilitation of a section of the "Saska" river diversion tunnel at survey mark 0+960 – 1+140.5 Civil Engineering institute "Makedonija", Skopje, 2006.

[10] Technical solution for rehabilitation of the "Saska" river diversion tunnel at survey mark 1+150 – 1+200 km./, beneath the new tsf of Sasa mine – M. Kamenica – stage I, Mining institute – Department for mineral processing, Skopje, 2002.

[11] Technical solution for rehabilitation of the "Saska" river diversion tunnel at survey mark 1+150 – 1+200 km. /tunnel type - v./ beneath the new tsf of Sasa mine – M. Kamenica – stage I, Mining institute – Department for mineral processing, Skopje, 2002.

[12] Main design for rehabilitation of the invert of "Saska" river diversion tunnel from km. 0+000 to km. 0+950, Faculty of Civil Engineering, Skopje, 2010.

ДГКС Друштво грађевинских конструктера Србије
ASES Association of Structural Engineers of Serbia
S-63
15. KONGRES
6-8. 9. 2018. Zlatibor

Liljana Dimevska[1], Meri Cvetkovska[2], Ana Trombeva Gavriloska[3], Marijana Lazarevska[4]

ANALIZA STAMBENIH ZGRADA PREMA NIJIHOVIM ARHITEKTONSKOM I TERMIČKIM KARAKTERISTIKAMA

Rezime:

Cilj ovog rada je arhitektonsko-gradjevinska analiza stanbenih zgrada u gradskoj četvrti u Skoplju, izgrađene nakon zemljotresa bez toplotne izolacije. Stanbeno naselje je izabrano zbog intenzivne izgradnje zgrada nakon zemljotresa 1963. Analiza uključuje: procenat učešća u ukupnoj izgradnji, godina, tip konstrukcije, površina objekta, broj stanova i stanara. Rezultati pokazuju da preko 76% stanbene površine pripada objektima sa niskom energetskom efikasnošću. Izvršena je komparativna analiza različitih tipova zgrada primenom softvera. Analizirani su najčešći tipovi zgrada u postojećem stanju i budućem scenariju sa poboljšanim toplinskim karakteristikama. Ako se sprovede adekvatna rekonstrukcija objekata, oni mogu poboljšati svoje energetske performanse i ispuniti kriterijume aktuelnih standarda za energetski efikasne zgrade.

Ključne reči: stambene zgrade, energetski efikasne zgrade, potrošnja energije

RESIDENTIAL BUILDINGS ANALYSIS ACCORDING TO THEIR ARHITECTURAL AND THERMAL CHARACTERISTICS

Summary:

The aim of this research is to carry out an architectural and structural analysis of the residential buildings in a selected city quarter of Skopje, built after the earthquake, with lack of thermal insulation materials. The analysis include: the percentage in total construction, year and type of construction, floor area, number of apartments and residents. The results show that over 76% of the floor area belongs to the type of buildings that have low energy efficiency characteristics. A comparative software analysis of the structural elements of the most common type of building was carried out on the existing condition and the future scenario with improved thermal characteristics. If proper renovation of these buildings is carried out, they can improve their energy performance, and meet the criteria for today's energy efficiency standards.

Key words: residential buildings; energy efficient buildings; energy consumption

[1] *Assist. Prof. M. arch, Faculty of Architecture, FON University, liljana.dimevska@fon.edu.mk*
[2] *Prof. PhD, Faculty of Civil Engineering, University "Ss. Cyril and Methodius", cvetkovska@gf.ukim.edu.mk*
[3] *Assoc. Prof. PhD, Faculty of Architecture, University "Ss. Cyril and Methodius", agavriloska@arh.ukim.edu.mk*
[4] *Assist.prof., PhD, Faculty of Civil Engineering, UKIM, Skopje, marijana@gf.ukim.edu.mk*

1. INTRODUCTION

As a result of the devastating earthquake in 1963, the housing stock of the capital City of Skopje was destroyed by 85%. Due to the crucial need for rapid construction of the residential buildings in order to provide home for the homeless people after the earthquake, more than 60% of the existing collective housing buildings in Skopje were built in the period between the 60s and the 80s of the 20th century. [1] According to the large consumption of energy, the residential buildings for collective housing, built after the earthquake, are classified as energy-inefficient buildings [8]. Today, many of these buildings are in the same condition as they were built then, and unfortunately they do not correspond to today's standards. Therefore, there is a need for urgent take-up of energy saving measures for these buildings [9].

The aim of this paper is to analyse the residential buildings of collective housing that were built in the period from 1963 to 1980 with lack of thermal insulation materials. The analysis involves: documenting the existing condition of those objects, and obtaining data about the percentage of their representation versus the new residential buildings in a typical residential neighborhood. The documented buildings are classified according to their architectural and building characteristics. The analysis was carried out in a typical residential district in Skopje, which has a large number of residential apartment building intensively built in the post-earthquake period which are in the same condition even today.

Firstly, a research about energy consumption in different sectors in the Republic of Macedonia was conducted, and after that the energy consumption in the housing stock of the City of Skopje was explored in order to inspect the representation of the residential sector and its role in the total heat and electricity consumption in the country and in the capital city as well. A classification of the residential buildings in Skopje was made according to the year of construction of the buildings and according to their thermal insulation materials. Thus, the buildings were categorized in several types of buildings, from which, the buildings with the weakest energy characteristics were further analysed. According to the results of the analysis, it might be concluded that over 70% of the total housing stock in the quarter belong to these energy - inefficient buildings, i.e. a serious share in the energy consumption. Therefore, the quarter is assessed as a neighborhood with great potential for energy efficiency.

2. ENERGY CONSUMPTION ANALYSES

2.1 ENERGY CONSUMPTION IN DIFFERENT SECTORS IN MACEDONIA

The Republic of Macedonia strives to reduce energy consumption by 20%, reduce emissions by 20%, and increase the percentage of energy produced from renewable sources by 20% in the gross final energy consumption. According to the State Statistical Office of the Energy Balance [3], the largest share in the total final energy consumption is 31.34% (543.35 ktoe), with the transport sector 29.72% (515.19 ktoe) followed by the residential sector with 26.21% (454.41 ktoe) and the commercial and public sector with 11.50% (199.35 ktoe). Moreover, it is stated that the consumption of final energy in the residential sector, i.e. the households, is 1473 kWh per resident, whereby the total consumption of electricity is the most frequent in the household sector, with 261.9 ktoe [2]. From these data it can be concluded that the residential sector takes serious representation of the total energy consumption. According

to the latest Third Energy Efficiency Action Plan of the Republic of Macedonia for energy consumption [3], it is estimated that in the residential and the tertiary sectors, the energy consumption in all buildings has the largest share in the final energy consumption, thus offering the greatest potential for energy efficiency.

2.2 ENERGY CONSUMPTION IN THE RESIDENTIAL SECTOR IN SKOPJE

The data on the total number of households within the city of Skopje, as well as the total area of the residential structure are in accordance with the statistics from the last census in the Republic of Macedonia in 2002 [5]. According to it [5], the total number of households in the city of Skopje in 2008 was 16,437, while the housing structure in the city covered a total area of 11,448,261 m^2. According to the data from the Statistical Office of the Republic of Macedonia [2], 1.275.724 MWh of electricity, i.e. 79.70 kWh/m^2 of specific electricity consumption was spent in the residential sector of the city of Skopje. The buildings in Skopje, depending on the construction period, are classified in four groups: Buildings constructed before 1963; Buildings constructed between 1965 and 1980, in accordance with the criteria for aseismic construction, with or without poor thermal insulation; Buildings constructed between 1980 and 1991, when the first Yugoslav standards, which required obligatory application of thermal insulation, appeared; Objects built from 1991 to the present, with the use of insulating materials according to today's standards for energy-efficient buildings [8].

Based on the conclusions from the above analysed data, there are some questions which might arise such as the following one: How should the correct procedures be taken in order to: reduce energy consumption, improve the energy efficiency of the residential sector of the city and reduce the air pollution? For this purpose, a typical residential area in Skopje was selected, and the buildings representing the settlement were analysed. The buildings, which, according to the above-mentioned classification, belong to a group of buildings built between 1965 and 1980 were further analysed in more detail.

3. ARCHITECTURAL AND STRUCTURAL ANALYSIS OF THE HOUSING STOCK IN A SELECTED RESIDENTIAL DISTRICT

3.1. SELECTING AND ANALYSING A TYPICAL RESIDENTIAL DISTRICT

The Municipality of Karpos, which today covers a large part of the Municipality of Idadija, is known as one of the most recent and attractive municipalities in Skopje, whose housing stock was mostly built in the period from 1965 to 1985 of the last century. The residential buildings were built in a similar architectural style, from a concrete structure system with very low energy efficiency. The required heating energy in the settlement is mostly supplied through the BEG - Central distributive heating system [2].

The analysis excludes objects of educational, administrative and commercial purpose, i.e. all objects whose main purpose is not housing. The results show that there are no buildings built before 1963 in the selected area, and that 76% of the buildings were built in the period from 1965 to 1980, whereby in the analysed settlement they are known as "Russian" and "Romanian" buildings. The analysis was performed in a selected city quarter known as Karpos 3, as a typical residential settlement, Figure 1.

Figure 1 - Plan of the analysed city quarter in the settlement Karpos 3, [Reproduced with the permission of the State Archive, City of Skopje]

The selected city quarter Karpos 3, compared to the other city quarters known as Karpos 1,2 and 4, occupies the largest area, with the largest representation of residential buildings. There are 72 buildings within the analysed city quarter, where 16 of them are public buildings and 56 of them are residential buildings for collective housing, from which it can be concluded that residential buildings dominate in the considering range. From the residential buildings compared to the year of construction, 43 of them were built from 1965 to 1980, 9 of them were built from 1980 to 1990 and 4 of them were built after 1990.

From Figure 2 which shows a chart with the percentage of the representation of the buildings in relation to the year of construction, it can be concluded that 76% of the residential buildings were built from 1963 to 1980, 17% were built in the period between 1980-1991, and just 7% from 1991 until now. There are no buildings before the earthquake in the selected area.

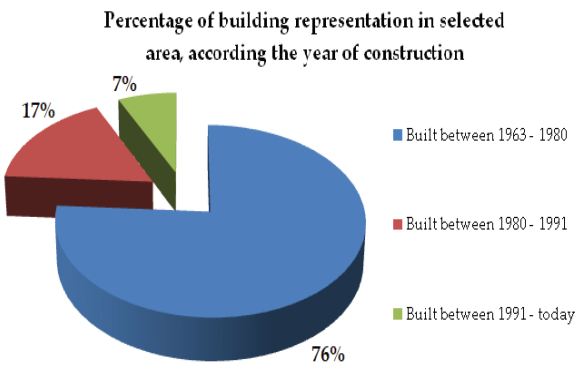

Figure 2 - Percentage of representation of buildings according the year of performance

3.2. CLASSIFICATION OF THE SELECTED BUILDINGS ACCORDING THEIR ARCHITECTURAL AND STRUCTURAL FEATURES

According to the fact that the residential sector has the greatest potential for energy savings, and that the buildings built up to the 1980s do not correspond to today's energy efficiency standards, it is established that in the selected residential area, such buildings account for over 70%. The further analysis was made on five types of buildings built from 1965 to 1980 which were marked as different types of buildings (type of building 1, 2, 3, 4, 5), Figure 3.

Figure 3. Classification of buildings built between 1965 and 1980 (part of the quarter where the analyzed buildings are situated), reproduced with the permission of the State Archive, City of Skopje],

In the selected quarter, 31 residential buildings are classified as type 1 and type 2 or "Russian" buildings and represent 72% of the total housing stock in the quarter, Figure 3. These buildings are known as prefabricated residential buildings of the type "Karpos", which were intensively constructed in 1963, according to the donation project from Russia. These buildings were built in the countries of the former Soviet Union, named as "Khrushchyovka", [7] and were designed as social architecture, i.e. they are very rational in their construction in terms of height of buildings, materials, size of apartments. Furthermore, this type of buildings can be divided into two subtypes that differ the number of apartments: type 1 and 2. The second type of buildings refers to the "Romanian'' towers, which are represented by 9 buildings. They can also be divided in two subtypes: type 3 and 4 according to the difference in their architectural solution. The third type of buildings are the so called "Experimental'' buildings, named as type 5, which are very similar to the first type according to their solution, and there are only 4 of these buildings in the quarter.

3.3. ARCHITECTURAL AND URBAN ANALYSIS OF THE SELECTED BUILDINGS

Depending on the type of the analysed buildings, there is a variation according to their height, module, type of apartments, etc. The "Russian'' buildings have 4 floors, the "Romanian'' buildings have 10 floors while the "Experimental'' ones have 6 floors. The adequate urban density of 20% in the quarter is achieved according to their height and floor area. Regarding their position, the buildings have a rectangular shape, a compact volume and their position is such that each building gets enough sun during the day, providing that no building casts a shadow on the adjacent ones.

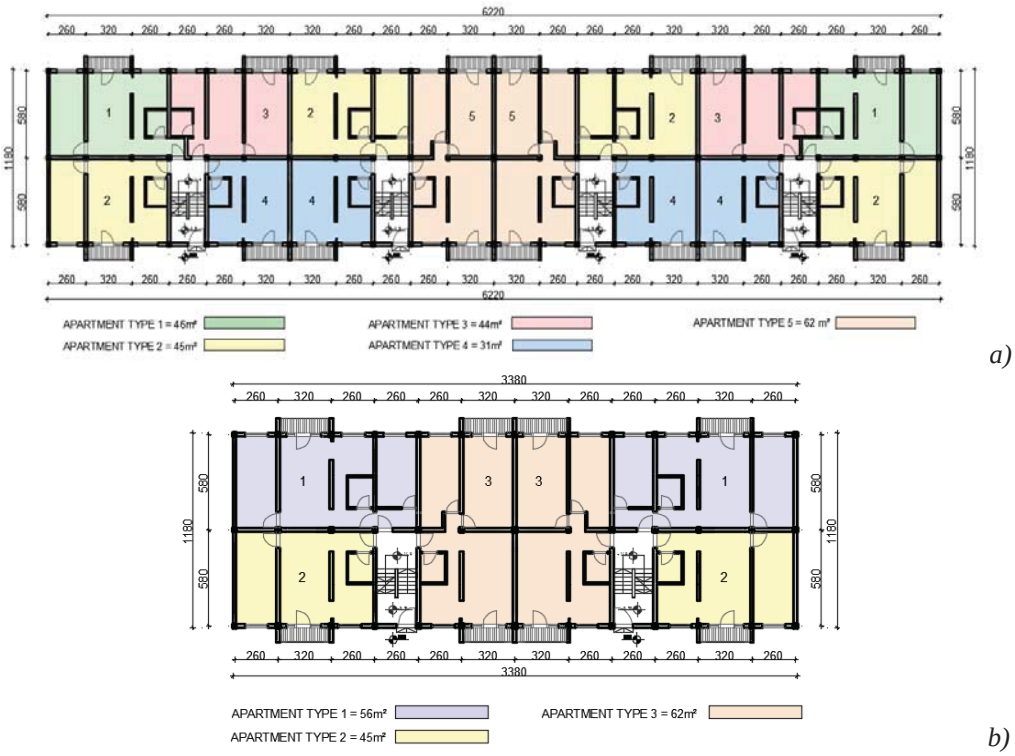

Figure 4 - Characteristic floor plan of a multi-storey "Karpos" type building: a) type 1; b) type 2, [reproduced with the permission of State Archive, City of Skopje]

Figure 4 shows the plan both types of "Russian" buildings, which tells the number, the type and the area of the apartments. Type 1 buildings contain 4 entrances, a total of 56 apartments, 16 of which are studios, 32 of them are two bedroom apartments and 8 of them are three bedroom apartments. Type 2 buildings have 2 entrances, a total of 24 apartments, 8 of which are studios, 8 of them are two-bedroom and 8 of them are three-bedroom apartments.

3.4. STRUCTURAL ANALYSIS OF THE SELECTED BUILDINGS

The use of prefabricated concrete elements for the performance of the structural system of type 1 and type 2 buildings, was derived from the need to provide the necessary space for housing for the shortest period of time. The massive structural system of supporting concrete walls does not offer the possibility of developing this type of objects vertically, which is why they have no more than four floors. These buildings are economical in their building materials, architectural design, with optimal windows and small terraces [7]. Buildings of type 3, 4 and 5 are built of skeleton reinforced concrete structural system, which allows the development of objects vertically, with more than ten floors. The external part of the buildings is made from bricks without the use of thermal insulation.

3.4.1. Massive building system with prefabricated concrete panel elements

The outer perimeter of the walls in prefabricated reinforced concrete elements are generally made of 3 layers, Figure 5 and 6:

- Exterior coat made from a concrete panel with finishing mortar with a thickness of 6 cm;
- Intermediate layer - thermal insulation from polystyrene with a thickness of 5 cm;
- Interior structural reinforced concrete panel with a thickness of 12-15 cm. [10]

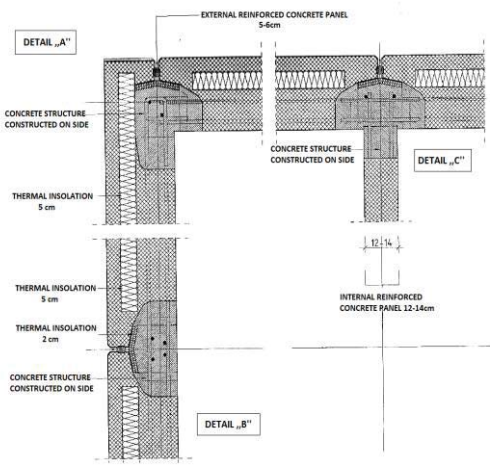

Figure 5 - An external and internal wall of an prefabricated concrete panel[10]

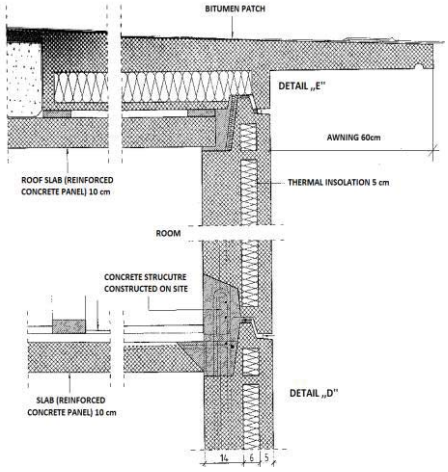

Figure 6 - An external wall, slab and roof of an prefabricated concrete panel [10]

The external panels are made from prefabricated reinforced concrete elements with a height of 260-270 cm (normal floor height), according to the dimensions of a structural field (260/580cm or 320/580cm). A three-layer panel with profiles and anchors for connecting the panels is produced with the technological integration process, Figure 5 and 6. The internal structural walls are usually performed as single-layer reinforced concrete panels with a thickness of 12-14 cm. The elements for the slabs are generally performed as single-layer reinforced concrete panels, with dimensions corresponding to a structural field, i.e. a constructive module (260-360cm in width and 260-580cm in length), Figures 6 and 7 [10].

4. METHODS AND RESULTS

4.1. RESULTS FROM THE ANALYSED RESIDENTIAL BUILDINGS (BUILT FROM 1963 TO 1980) IN THE SELECTED SETTLEMENT

According to the data for the examined buildings, obtained from the State Archives of the R. Macedonia, Department of the City of Skopje and according to the conducted survey with the tenants and residents of the buildings, the obtained results are shown in Table 1.

The five types of analysed buildings, are similar according to their position, shape and module, while the height varies from 4 to 10 floors. Accordingly, the number of apartments and tenants is different. Type 1 buildings contain 56 apartments or 151.2 tenants per building.

Table 1. Characteristics of residential buildings built 1965 -1980 in the selected settlement

Type of building	1	2	3	4	5
Description of the building	Russian building	Russian building	Romanian building	Romanian building	Experimental building
Year of construction	1963 - 1965	1963 - 1965	1965 - 1967	1966 - 1968	1964 - 1966
Number of buildings	18	13	5	3	4
Number of flats per building	56	24	60	40	24
Number of tenants per building[5]	151.2	64.8	162	108	64.8
Floor area (m²)	745	405	500	350	420
Number of stories	4	4	10	10	5
Shape of building	Rectangular	Rectangular	Rectangular	Rectangular	Rectangular
Type of construction and materials	Prefabricated reinforced concrete structural elements.	Prefabricated reinforced concrete structural elements	Reinforced concrete skeleton structure with masonry wall	Reinforced concrete skeleton structure with masonry wall	Reinforced concrete skeleton structure with masonry wall
Heating	Central city heating	Central city heating	Central city heating	Central city heating	Central city heating
Cooling	Air conditioner	Air conditioner	Air conditioner	Air conditioner	Air conditioner
Ventilation	Natural	Natural	Natural	Natural	Natural

There are 18 such buildings in the quarter with floor area of 745m^2 per building. They contain a total of 1008 apartments and 2721.6 tenants. The type 2 buildings have 24 apartments, 64.8 tenants and a floor area of 405m^2 per building. There are 13 buildings of this type. They contain a total of 312 apartments and 842.4 tenants. Type 3 buildings contain 60 apartments with 162 tenants with a floor area of 500m^2 per building. There are 5 such buildings and they contain a total of 300 apartments and 810 tenants. The type 4 buildings contain 40 apartments 108 tenants and area of 350 m^2 per building. There are 3 buildings of this type. They contain a total of 120 apartments and 324 tenants. The type 5 buildings have 24 apartments and 64.8 tenants and a floor area of 420m^2 per building. There are 4 buildings and they contain 96 apartments and 259.2 tenants. The results are summarised in Table 2. In the quarter, the residential buildings built from 1965 to 1980 contain 1836 apartments and 4957.2 tenants.

4.2. PARAMETRIC ANALYSIS OF THE THERMAL CHARACTERISTICS OF THE CURRENT SITUATION AND AN IMPROVED FUTURE SCENARIO

In the selected quarter, the largest consumers of energy are the “Russian buildings”. The main factors for the energy consumers are: poor thermal insulation in the outer walls, roof and ground floor slab; numerous thermal bridges, which occur as a disadvantage of prefabricated systems and wooden framed windows with single glazed glass. On the other hand, the orientation, the urban position, the ratio of buildings, the form and the volume, and solution of the apartments give great potential for energy efficiency. These buildings can be adequately renovated, and the intervention should be based on software analyses for improving energy efficiency. For this purpose, a software analysis was carried out in order to analyse the thermal

[5] *It is assumed that the average number of tenants in an apartment is 2.7 in accordance with the provisions of the PRPR [5], as well as the Rulebook for architectural standards and norms.*

characteristics of the materials used in typical “Russian’’ building. Subsequently, an improved scenario with a minimal and cost-effective intervention was made in order to meet the criteria for energy efficiency in accordance with today's standards.

4.3. METHODOLOGY OF EXAMINATING THE THERMAL CHARACTERISTICS

The envelope of a building is composed of its external walls, the openings, the roof and the floor slab structure. Analysis of the thermal characteristics of these structural elements was carried out in order to see the current energy efficiency situation, as well as the potential for further improvement in a typical “Russian’’ building type 1, Figure 4 (a). The analysis was performed with the KnaufTerm2PRO-M software. The calculation includes the following input parameters such as: location; position in relation to the exposure to wind; number of facades exposed to the wind; way of ventilating; type and purpose of the building; residential units; geometry, surface and volume of the casing, volume of the heated and ventilated space.

The minimum outdoor design temperature is taken to be 0ºC, the internal optimum project temperature is 20ºC, the external average temperature is 12.4ºC, the number of heating days is 170, the number of wet days is 60, the number dry days is 90, the number of heating days per the week is 7, the number of heating hours during the day is 24. The existing materials of the elements, were inserted in the calculation of the current state. This is shown in Figure 5 and 6. An additional layer of thermal insulation of 10 cm (extruded polystyrene XPS, as efficient and at the same time most economical variant) was added to the existing elements in the calculation of the improved scenario. These layers refer to the outer walls, the floor slab above the unheated space and the roof [10]. The windows in existing state are made by wooden frames and single-glazed glass, while in the improved scenario, they are six-chamber PVC frames with double-glazed low-emission glasses 4+12+4 (an economical, an efficient and the most commonly used variant). Different results were obtained in terms of the energy parameters such thermal transmittance or U value (W/ m²K) and thermal resistance or R value, R_{si}, R_{se} (m²K / W). These results are shown in Table 2 and Table 3.

4.4. COMPARISON OF THE THERMAL CHARACTERISTICS OF THE EXISTING AND FUTURE CONDITION OF THE BUILDING

After obtaining the thermal values through the software analysis of the structural elements of the existing and the future state of the building, a comparison was made between the two states. Figure 8 shows an intersection of an external wall with its layers and their thermal parameters in the existing condition, from which it can be clearly seen that the assembly of the wall does not satisfy the requirements for energy efficiency because its U value is 0,659 W/m²K and it’s bigger than U_{max}, which according to the Rulebook for energy efficient building, is not allowed to be more than 0.35 W/m²K for external walls, [9]. Figure 9 shows an intersection of an external wall with its layers and their energy parameters in a future improved scenario. A significant improvement of the thermal values can be noticed and the assembly can satisfy the energy efficiency requirements by adding a thermal insulation (10cm of XPS). In the improved scenario U value is 0.241 W/m² K, which is a smaller value than U_{max}. The same procedure is applied to other elements such as floor slab above basement, roof construction and windows. The results are shown in Tables 2 and 3.

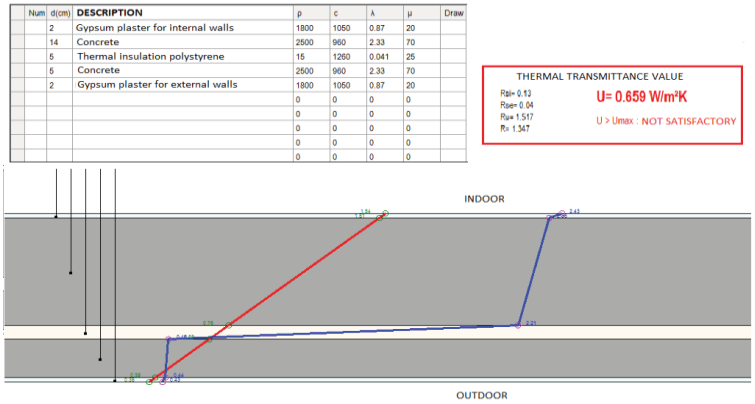

Num	d(cm)	DESCRIPTION	ρ	c	λ	μ	Draw
	2	Gypsum plaster for internal walls	1800	1050	0.87	20	
	14	Concrete	2500	960	2.33	70	
	5	Thermal insulation polystyrene	15	1260	0.041	25	
	5	Concrete	2500	960	2.33	70	
	2	Gypsum plaster for external walls	1800	1050	0.87	20	
			0	0	0	0	
			0	0	0	0	
			0	0	0	0	
			0	0	0	0	
			0	0	0	0	

Figure 8 - Thermal parameters of an external wall (an existing state)

Num	d(cm)	DESCRIPTION	ρ	c	λ	μ	Draw
	2	Gypsum plaster for internal walls	1800	1050	0.87	20	
	14	Concrete	2500	960	2.33	70	
	5	Thermal insulation polystyrene	15	1260	0.041	25	
	5	Concrete	2500	960	2.33	70	
	10	XPS d=10cm, thermal insulation	33	1500	0.038	50	
	2	Gypsum plaster for external walls	1800	1050	0.87	20	
			0	0	0	0	
			0	0	0	0	
			0	0	0	0	
			0	0	0	0	

Figure 9 - Thermal parameters of an external wall (an improved future scenario)

4.5. PARAMETRIC ANALYSIS RESULTS

The results summarised in Table 2. refer to the analysis of the structure assemblies at the existing condition of the building, from which it can be established that none of the assemblies fulfill the standards in accordance to the Rulebook for Energy performance of buildings, from which the maximal thermal transmittance coefficients in non-transparent (Umax) and in transparent structures (Uw max) are determined. Table 3 refers to a future scenario for improving the energy efficiency, where an additional thermal insulation on structural elements is added (explained in Figure 9). If the results from Table 2 and the ones from Table 3 are compared, it can be noticed that a significant improvement can be achieved with the additional layers of thermal insulation in the assemblies, as well as the change of windows, where all assemblies meet the criteria for energy efficiency in accordance with the Rulebook for Energy Efficiency of Buildings [9].

Table 2 .Thermal parameters of the structure elements in the current condition of the building

Main structural elements of the building	Building materials	Total width (cm)	Calcul. type	U value (w/m²k)	Umax (W/M²k)	R value (m²k/w)	Rsi value (m²k/w)	Rse value (m²K/W)	Sun permeab. factor (g)	Satisfactory level
External (façade) wall	Plaster 2cm, reinforced concrete wall 14cm, polystyrene 5cm, concrete wall 5cm, Exterior plaster 2cm	28	classic-EN6946	**0.659**	**0.35**	1.347	0.13	0.04	0	U > Umax not satisfactory
Ground floor slab structure	Parquet 2.2 cm, cement layer 5cm, reinforced concrete slab 10 cm, interior plaster 1.5 cm	18.7	classic-EN6946	**2.688**	**0.35**	0.202	0.13	0.04	0	U > Umax not satisfactory
Roof structure	Plaster 2cm, reinforced concrete slab 15cm, vapor membrane, airspace 20cm, wooden substructure 5cm, bitumen patch 0.07cm	42.57	classic-EN6946	**1.127**	**0.25**	0.717	0.13	0.04	0	U > Umax not satisfactory
Windows and doors	Wooden framed windows with single glazed glass	/	windows	**4.6**	**1.8**	0.217	0.13	0.04	0.87	U > Umax not satisfactory

Table 3. Thermal parameters of the structural elements in the future improved scenario

Main structural elements of the building	Building materials	Total width (cm)	Calcul. type	U value (w/m²k)	Umax (W/M²k)	R value (m²k/w)	Rsi value (m²k/w)	Rse value (m²K/W)	Sun permeab. factor (g)	Satisfactory level
External (façade) wall	Interior plaster 2cm, reinforced concrete wall 14cm, polystyrene 5cm,reinforced concrete wall 5cm, **XPS extruded polystyrene 10 cm**, exterior plaster 2cm	38	classic-EN6946	**0.241**	**0.35**	3.979	0.13	0.04	0	U < Umax Structure is satisfactory
Ground floor slab structure	Parquet 2.2 cm, cement layer 5cm, reinforced concrete slab 10 cm, **XPS extruded polystyrene 10 cm,** interior plaster 1.5 cm	28.7	classic-EN6946	**0.333**	**0.35**	2.834	0.13	0.04	0	U < Umax Structure is satisfactory
Roof structure	Interior plaster 2cm, **XPS extruded polystyrene 20 cm**, reinforced concrete slab 15cm, vapor membrane, airspace 20cm, wooden substructure 5cm, bitumen patch 0.07cm	62.57	classic-EN6946	**0.284**	**0.25**	3.349	0.13	0.04	0	U < Umax Structure is satisfactory
Windows and doors	Pvc window with six chamfered frame and low - e double glazed glass (4+12+4)	/	windows	**1.7**	**1.8**	0.588	0.13	0.04	0.4	U < Umax Structure is satisfactory

5. CONCLUSION

In the examined city quarter Karpos 3, the residential buildings problematic in terms of their energy efficiency, have a representation of 76%, i.e. 43 buildings built between 1965 and 1980. From the conducted analysis of buildings, it can be concluded that according to their form, architectural design, orientation and position of the buildings, they have great potential to become energy-efficient buildings. Software analysis was carried out in order to determine the existing energy features of the buildings, as well as predicting a future scenario for improving the energy efficiency consumption of these buildings. This paper, presents the principles of how to proceed correctly in order to find the most economical and the most effective energy saving solution for this type of urban districts, built with a large number of old and energy-inefficient buildings. The research data can be further used as input parameters in creating a calculative model, both for calculating real energy consumption and for creating improved scenarios for energy saving. The same model can also be implemented in the other settlements within the municipality of Karpos, where there are more buildings of the analysed type.

REFERENCES

[1] M. Tokoarev ,, 50 years of reconstruction and building of Skopje (1963-2013), historical and critical view of architecture'' (in Macedonian), Porta 3, 34-45, 25th of January 2013

[2] Action Plan for Sustainable Energy Development of the City of Skopje, (SEAP), (in Macedonian), Skopje, April, 2011, 35-36, 73-38;

[3] A. Kirov, K. Dimitrov, I. Sazdovski, A. Teskeredzik, P. Atanasovski, D. Angelkov, A. Dukovski, Third Action Plan for Energy Efficiency of the Republic of Macedonia for the period 2016-2018, (in Macedonian), June, 2016, 7-10, 39-41;

[4] Government of the Republic of Macedonia, Ministry of economy of the Republic of Macedonia, Second Action Plan for Energy Efficiency of the Republic of Macedonia for 2015, (in Macedonian), Skopje, April, 2014, 69-71;

[5] Agency for Spatial Planning, Annual Report on the implementation of the PRTR by 2014, (in Macedonian) 2015, Skopje 224-227;

[6] N. Gelevski, S. Naumovska, I. Sopov, „50 years since the earthquake in Skopje, Skopje ancient or modern", (in Macedonian), National University Library "St. Kliment Ohridski", Skopje, 2014, pp.183-193, ISBN 978-608-4658-31-3;

[7] Satu Paiho, Åsa Hedman, Rinat Abdurafikov, Ha Hoang, Mari Sepponen, Ilpo Kouhia, Malin Meinander, „Energy saving potentials of Moscow apartment buildings in residential districts'', VTT Technical Research Centre of Finland, Finland, June 2017, Vol. 66, 706 - 713 (2013) November issue;

[8] P. Nikolovski, CeProSARD, Energy efficiency controllers training, „Overview of typical measures for energy efficiency buildings improvement", (in Macedonian), 7th of June, 2014, Skopje, 2-9, 25-30 ISO 9001:2008 ISO 14001:2004;

[9] Ministry of economy of the Republic of Macedonia, Rulebook on Energy Performance of Buildings, (in Macedonian), 2016, Skopje, 61-63, 20130942263

[10] "Modern prefabricated building systems from prefabricated reinforced concrete elements and assemblies", (in Macedonian) internal script of Faculty of Architecture, St. Cyril and Methodius University, 2012, Skopje, personal communication.

ДГКС Друштво грађевинских конструктера Србије
ASES Association of Structural Engineers of Serbia
S-64
15. KONGRES
6-8. 9. 2018. Zlatibor

Marija Docevska[1], Leart Taravari[2], Jose Campos e Matos[3], Goran Markovski[4]

PLAN KONTROLE KVALITETA LUČNIH BETONSKIH MOSTOVA

Rezime:

Većina planova kontrole kvaliteta je orijentisana ka elementima, sa nedostatkom holističkog pristupa u proceni betonskih mostova. Bez uzimanja u obzir konstruktivnog sistema i bez povezivanja vrste, položaja i procesa oštećenja sa konstruktivnim sistemom, teško je utvrditi ključne pokazatelje učinka (pouzdanost, sigurnost itd.). Ovde je metodologija kontrole kvaliteta uspostavljena unutar VG3 COST Akcije 1406 implementirana u dve studije slučaja, lučni betonski most u Portugalu i Makedoniji, slične topologije. Primenjeni plan uzima u obzir pouzdanost, modele loma i osetljive zone. Korišćeni su vizuelni pregledi i izrađeni numerički modeli mostova. U obe studije slučaja primenjeni su različiti pristupi životnog ciklusa kako bi se kvalitativno procenili ključni pokazatelji učinka tokom vremena. Konačno, rezultati se upoređuju kako bi se pronašo najefikasniji scenario.

Ključne reči: plan kontrole kvaliteta, lučni betonski mostovi, osetljive zone, pouzdanost

QUALITY CONTROL PLAN OF ARCH CONCRETE BRIDGES

Summary:

Most of the quality control plans are element-oriented, facing with the lack of holistic approach in assessment of concrete bridges. Without considering the structural system and without linking the damage type, position and process with the type of structural system, it is hardly possible to derive key performance indicators (reliability, safety, etc.). Here, quality control methodology established within WG3 of COST Action 1406 was implemented into two case studies, concrete bridge located in Portugal and in Macedonia, both arch with similar topology. The applied quality control plan considers 'virgin' reliability, focuses on failure modes and related vulnerable zones. To consider all these aspects, results from visual inspections were used and numerical models of the bridges were built. In both case studies, different life time cycle approaches were applied to qualitativly evaluate different key performance indicators over time. Finally, the results are compared in order to find the most effective scenario.

Key words: quality control plan, arch concrete bridges, vulnerable zone, virgin reliability

[1]*MSc, Faculty of Civil Engineering-Skopje UKIM, Skopje, R.Macedonia, docevska@gf.ukim.edu.mk*
[2]*BSc, Faculty of Civil Engineering-Skopje UKIM, Skopje, R.Macedonia, leart1taravari@gmail.com*
[3]*PhD, Civil Engineering Department Minho University, Campus de Azurem, 4800-058 Guimaraes, Portugal, jmatos@civil.uminho.pt*
[4]*PhD, Faculty of Civil Engineering-Skopje UKIM, Skopje, R.Macedonia, markovski@gf.ukim.edu.mk*

1. INTRODUCTION

Quality control (QC) of bridges is differently implemented from country to country. However, most of them have the same basic approach consisting of inspection and rating of each bridge element separately. This element-oriented procedure is facing with a lack of holistic approach to the bridge assessment (Isailovic *et al.* 2018) . Without considering the structural system and linking the damage type, damage position and damage process with the type of structural system, it is hardly possible to derive key performance indicators. Additionally, the inspector should bear in mind all possible failure modes.

Applied QC plan considers the vulnerability of the structural system to the defects locations. It takes into consideration the 'virgin' reliability, focuses on failure modes and related vulnerable zones. A general approach for QC plans was already developed in the scope of WG3 for all types of structures and is now analyzed within the scope of arch bridges. In this paper, evolution in time of performance indicators of two existing arch bridges, in terms of reliability, safety, costs and availability, was performed qualitatively under no maintenance, corrective and preventative maintenance.

2. CASE STUDIES

In this section, a protocol for a quality control plan is used to demonstrate the methodology established in WG3 of COST Action TU1406. The research presented in this paper is performed during a short-term scientific mission at the University of Minho, Guimaraes, Portugal in March 2018. The quality control plan was performed in few steps:

- collecting the general data of the bridge (original drawings, construction year, inspection/intervention year, location, obstacle type, climate, exposure, etc.)
- comparison of current traffic load to traffic load model used for the previous calculation
- estimation of an initial 'virgin' reliability index β_0
- assessment of damage extend, intensity and identification of damage processes
- qualitative assessment of resistance reduction based on observed damages (rough assessment of resistance reduction on structural level (reliability))
- definition of various maintenance scenarios, evaluation of KPIs for all of them and comparison.

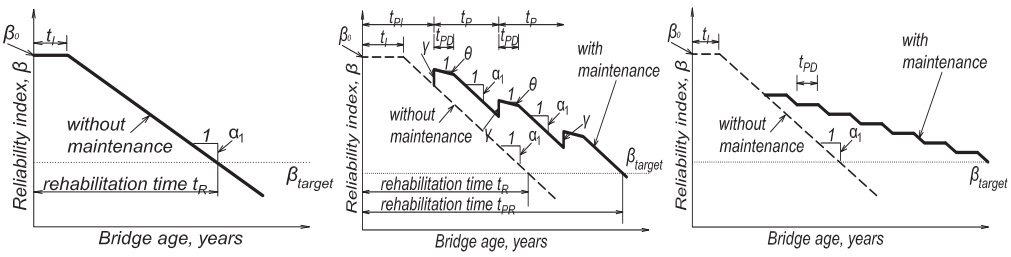

Figure 1. Degradation models for reliability index under no maintenance (left), corrective (middle) and preventative (right) scenario

Four different maintenance scenarios were considered: “running to failure” or “do-nothing and rebuild” scenario, corrective scenario, preventive scenario and hybrid scenario (corrective plus preventive) through application of linear degradation models for reliability index proposed by Frangopol (Frangopol *et al.* 2001) (Fig.1).

2.1. CASE STUDY 1 – ARCH CONCRETE BRIDGE LOCATED IN PORTUGAL

The first case study is arch concrete bridge located in Guarda district, Portugal. The subject bridge is one span open spandrel deck arch with total length of 24 m and rise of 4.65 m. General view of the bridge along with the longitudinal section and bridge location are shown on Fig.2. The subject bridge carries the regional road 324(ER) over the river Cro and consists of: two traffic lanes 2.53 m and 2.51 m, two safety strips 0.45m and 0.51 m and two sidewalks of 1.0 m width.

Figure 2. Side view of the bridge (left), longitudinal section (middle) and location (right)

In order to define possible failure modes and to link the vulnerable zones with the observed defects, it is necessary to define the bridge structural elements: deck slab (1), arch slab (2), arch abutment/springing (3), spandrel wall piers (4) and wall piers at the springing (5) (WG3 Report 2018).

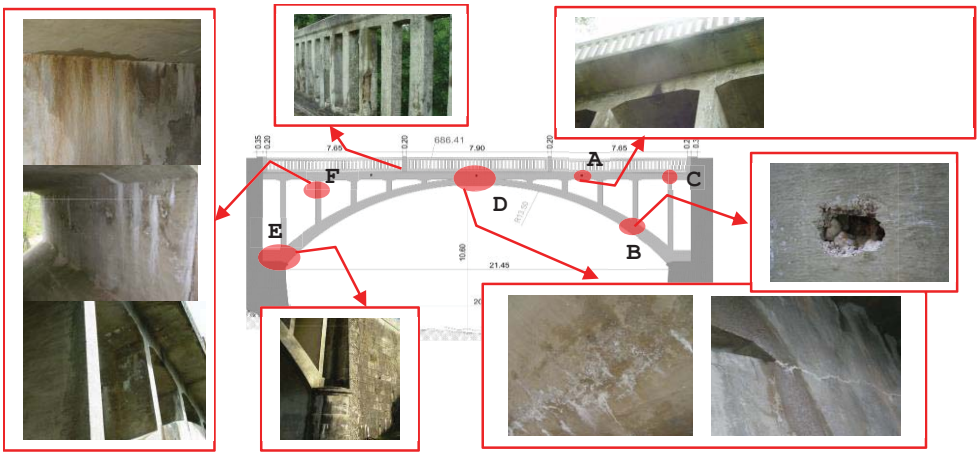

Figure 3. Subject bridge with appropriate labels of vulnerable zones and defects

Considering load bearing elements of the bridge, there are some regions which are highly vulnerable depending on a structural system. For such a structural system, the following vulnerable zones are defined: high moment regions (A, B, C, D), high compression regions (E, F), high deflection regions (D) and high compressive stress regions (E). They are acknowledged on Fig.3 where photos from visual inspection are also incorporated.

The protocol for performance bridge evolution enhanced by the anticipated failure modes is applied and presented in Table 1. Only findings related to vulnerable zones, regarding structural reliability and safety are listed in the table.

Table 1. The protocol

Failure mode	Vulnerable area	Element	Damage observations	Damage process	KPI	Performance value (1-5)	Overall rating
Bending failure	A	Deck	Efflorescence	Leaching	Symp.	/	**R=4 S=2**
		Deck	Wet spots	Water permeability	R	3	
	B	Arch	Surface cracks	Corrosion	R	3	
		Arch	Spalling	Corrosion	R	1	
		Arch	White spots	Carbonization	R	3	
	C	Deck	Efflorescence	Leaching	Symp.	/	
		Deck	White spots	Carbonization	R	3	
	D	Arch	Longitudinal crack	Structural damage	R	3	
		Arch	Surface cracks	Corrosion	R	3	
Compression failure	E	Arch	No damage	/	/	/	
	F	Walls	Surface cracks	Corrosion	R	4	
		Walls	Brown spots	Corrosion	R	3	
Falling from the bridge	/	Railing	Spalling	Corrosion	S	2	
	/	Railing	Cracks	Corrosion	S	2	

2.1.1. Semi-quantitative assessment of bridge reliability

For each scenario, qualitative evolution of the following KPIs was made: R-reliability, C-costs, A-availability and S-safety. The reference information needed to evaluate KPIs in time, is the evaluation performed on damage-free state of the bridge, so-called "virgin" state (WG3 Report 2018). Therefore, an initial reliability index β_0 was roughly calculated using Monte Carlo simulation and First Order Reliability Method (FORM) as the shortest distance from the origin in the n-dimensional space of reduced variables to the curve described by $g(R,S) = R - S = 0$.

Ultimate bending moment from the unfavourable load combination taken from the original design project is presented on the Fig.4 below. The axial force was low and therefore neglected.

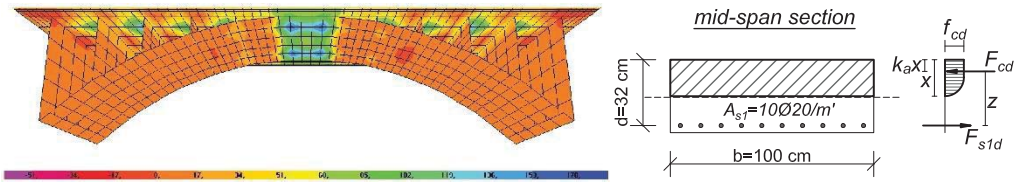

Figure 4. Ultimate bending moment from the unfavourable load combination

The bending moments at the supports are very low comparing with the bending moment at the midspan, showing that the system is simple supported. Therefore, the overall reliability of the bridge was obtained as the reliability of the midspan section of the arch (Nowak, Collins 2000). The limit state function for the bending failure mode is the following:

$$R = M_{Rd} = F_{s1d} \cdot d - F_{cd} \cdot k_a \cdot x = A_s \cdot f_{yd} \cdot d - f_{cd} \cdot \alpha_v \cdot x \cdot b \cdot k_a \cdot x$$

$$S = M_{sd} = 170\,kNm \tag{1}$$

$$g(R,S) = R - S = A_s \cdot f_{yd} \cdot d - f_{cd} \cdot \alpha_v \cdot x \cdot b \cdot k_a \cdot x - M_{sd} \tag{2}$$

Herein, the depth and width of the cross-section were considered as deterministic parameters, while M_{Sd}, A_S, f_{yd} and f_{cd} were considered as random variables. The values of the random variables are taken from the literature (Nowak, Collins 2000).

With both methods a value of 5.05 was obtained. On the basis of the report from the last visual inspection of the bridge, approximately 5% resistance reduction was assessed, since the last inspection was taken 5 years after repairing of the bridge and the bridge is in overall good condition. Therefore, the initial reliability index for the further analysis was reduced from 5.05 to the value of 4.90 using the abacus presented in WG3 report.

2.1.2. Evolution of KPIs for different maintenance scenarios

For each considered scenario, qualitative evolution of the following KPIs was made: R-reliability, C-costs, A-availability and S-safety. All KPIs are expressed on the scale of 1 to 5 (1-best, 5-worst) in order to generate 4-leg spider diagram.

'Running to failure' scenario

In this scenario, the bridge defects are developed until bridge failure and finally the bridge is replaced with a new structure. The effect of the essential maintenance action, like replacement of several deteriorated bridge components or replacement of the whole structure (like in this case), means that probability of failure (and therefore reliability index) should be set to its initial value (i.e., at t=0) (Neves).

Corrective scenario

First corrective (essential) maintenance action in this scenario was taken while the bridge is still in overall good condition (Reliability level 3). Identical corrective actions (for example: sub- and superstructure repairs, expansion joint and bearing replacement, drainage

improvement etc.) were assumed to be taken periodically over 13 years with a lower improvement in reliability ($\gamma = \frac{\beta_0^{'} - \beta_{state5}}{n} = \frac{4.90 - 2}{6} = 0.48$).

Preventive scenario

The effects of preventative maintenance actions (for example: deck sealing and applying over-layers, cleaning and lubricating bearings and expansion joints, cleaning bridge drainage system etc.) were modeled through a delay of a degradation process for a period of time t_{PD} immediately after application of the action, without any improvement in reliability index.
A hybrid scenario was also considered where preventative actions are performed between each two corrective actions. Comparison of the scenarios will be presented in Section 3.

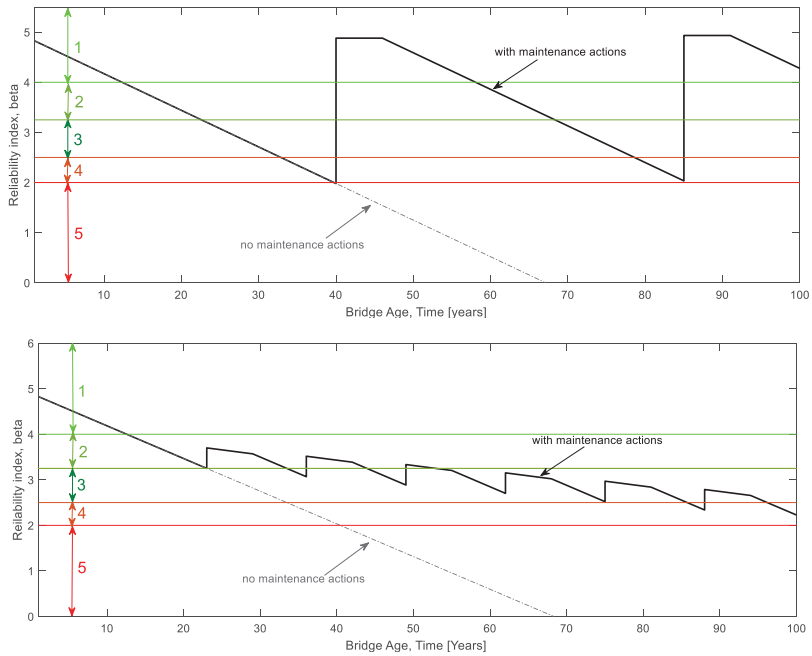

Figure 5. Semi-quantitative performance indicator for the "running to failure" (top) and corrective (bottom) scenario

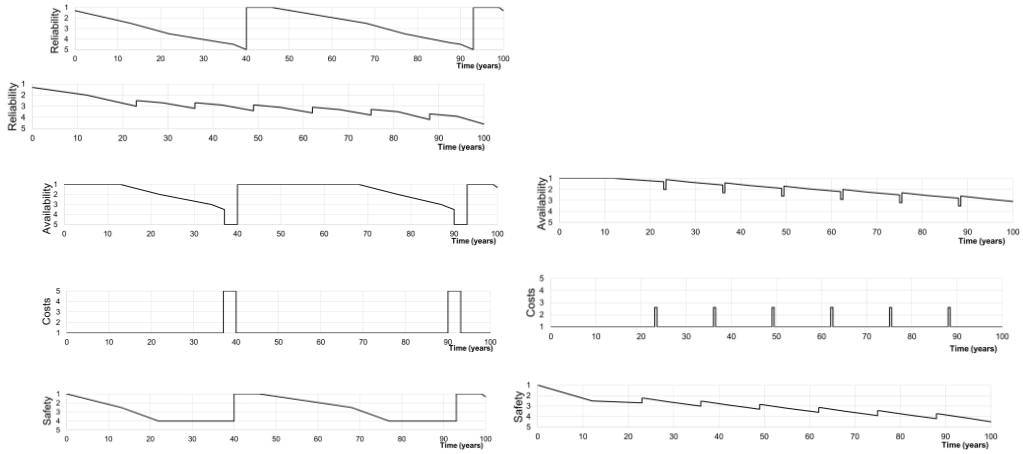

Figure 6. Evolution of qualitative KPIs for the "running to failure" (left) and corrective (right) scenario

2.2. CASE STUDY 2-ARCH CONCRETE BRIDGE LOCATED IN MACEDONIA

The second case study is fixed-end slab-type arch concrete bridge located in Macedonia, Section Katlanovo-Veles. Its central part (arch-type slab) has a span of L=54 m, and its approaching structures consist of three spans at the side of Skopje and five spans at the side of Veles, each with 6 m span (total length 17x6m=102m) (Fig.7). The project documentation of the bridge was not at disposal. Thus, taking into account the time period when the bridge has been constructed (year 1963), it could be concluded that the bridge has been designed in accordance with the "old" Technical regulations PTP-5 for loading of road bridges (issued 1948/1949). The bridge carries the National road M-1 (E-75) and its overall width is B=2x3.80 m + 2x0.60 m + 2x0.20 m = 9.20 m.

Figure 7. Sideview of the bridge(left), longitudinal section(middle) and location(right)

At the time of bridge inspection, considerable number of defects were observed (Fig.8): improper construction (A), inappropriate water drainage (B), very heavy damages due to corrosion of concrete and steel reinforcement of deck slab and longitudinal girders (B),

expressed process of carbonization on entire deck slab surface (B), insufficient or spalled concrete cover (A and B), cracks at the connection with the column (C), improper expansion joint (F), visible reinforcement due to missing parts of concrete on the railing parapets (E) and inappropriate concreting and segregation (A and D). Photos of the defects from visual inspection linked with the vulnerable zones of this bridge are shown on Fig.8.

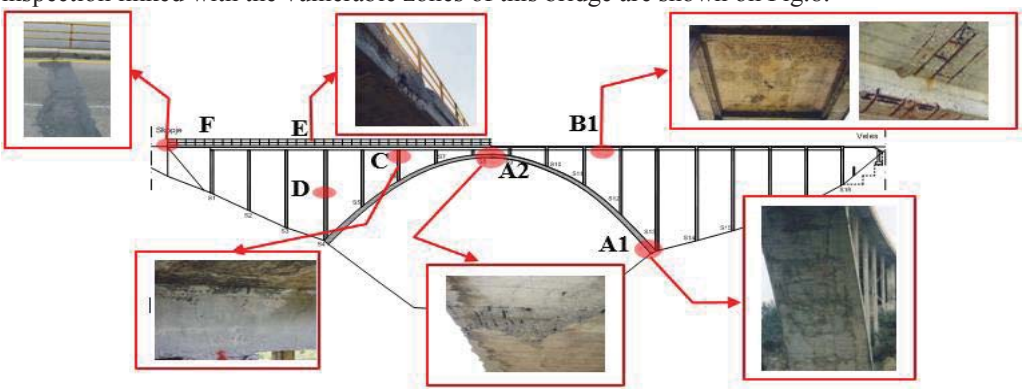

Figure 8. Subject bridge with appropriate labels and vulnerable zones

After inspection, the present condition of the bridge was estimated with index 4, meaning that heavy repairs are necessary. The protocol of performance bridge evolution is presented in Table 2.

2.2.1. Semi-quantitative assessment of bridge reliability

In order to obtain the initial reliability index of the arc-deck slab, numerical model of the bridge was built in Radimpex Software TOWER 7.0. The bridge was analysed according to current codes in Macedonia and according to "old" Technical regulations PTP-5 for live loads of road bridges. Since the arch slab is fixed-end slab, the overall reliability index was obtained considering the arch as a parallel system, meaning that for the overall system to fail, failure at mid-span and supports section is required (Novac and Collins, 2000).
The limit state function $g(R,S) = R - S = 0$ for the unfavourable failure mode (in this case bending failure) is the following:

$$R = M_{Rd} = F_{cd} \cdot z + F_{s2d} \cdot (d - a_2) - N_{sd} \cdot (\frac{d}{2} - a_1) \quad (3)$$

$$S = M_{sd}(\text{support}) = 1405\, kNm$$

$$S = M_{sd}(\text{midspan}) = 405 kNm$$

Table 2. The protocol

Failure mode	Vulnerable area	Element	Damage observation	Damage process	KPI	Performance value (1-5)	Overall raiting
Bending failure mode	A1	Arch-slab	Segregation	Poor construction	Sym p.	/	**R=4 S=3**
	A2	Arch-slab	Spalled concrete	Corrosion	R	2	
	B1	Deck slab	Brown spots	Corrosion	R	4	
	B1	Deck slab	Wet spots	Water permeability	R	4	
	B2	Girder	Spalled concrete	Corrosion	R	4	
	C	Column	Cracks	Structural	R	3	
	F	Exp.Joint	Longitudinal crack	Structural	R	3	
Compression failure mode	A1	Arch slab	Segregation	Poor construction	Sym p.	3	
	D	Piers	Segregation	Poor construction	Sym p.	/	
Falling from the bridge	/	Parapet	Spalled concrete	Poor construction	S	3	
	/	Railing	Rust	Corrosion	S	2	

Figure 9. Ultimate bending moment from the unfavourable load combination

The bridge overall reliability index using Monte Carlo and FORM, as well as, the approach with the parallel systems, was obtained 2.15 (since the bridge is originally designed according to old, less conservative codes for loads). According to the relation between qualitative and quantitative reliability scale proposed in WG3 Report, this bridge belongs to reliability level 4 ($\beta = 2 - 2.50$) where old bridges with major resistance reduction belong (WG3 report, 2018).
In order to juxtapose the bending moments and axial forces from the least favorable ultimate load combinations, as well as the load carrying capacity of the cross sections at the support and in the mid-span, M-N diagrams were constructed. From the diagrams, it was concluded that the M-N combinations from the least favorable ultimate load combinations are smaller than any critical M-N combination.

2.2.2. Evolution of KPIs for different maintenance scenarios

Two life time cycle approaches are shown to evaluate all key performance indicators considered for the bridge in the following 100 years.
In the first scenario (Reference – "Do nothing" scenario) (Fig.10 left) the bridge will be repaired and strengthened in the next years, since the reliability and availability for heavy vehicles are already limited. When the reliability reaches level 5, the bridge will be

reconstructed and thus inserts the reliability to level 1. In between, lack of any major repairs of superstructure was considered, except basic pavement repairs each 20 year. With this scenario, defects were developed up to the bridge failure. The cost of the reconstruction was assumed to be 1 Milion EUR (on the basis of the original project for the bridge reconstruction), big repairs 500 000 EUR and small (pavement) repairs 100 000 EUR.

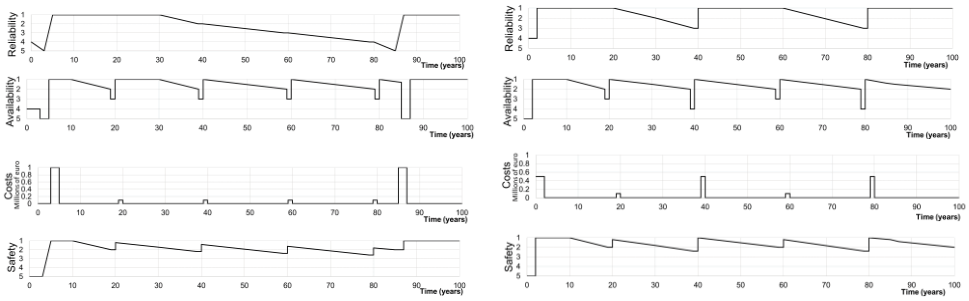

Figure 10. Evolution of the KPIs for the reference(left) and preventative(right) scenario

Second scenario (Fig.10 right) consists of set of bridge major rehabilitations each 40 year and minor rehabilitations (new top asphalt, new railing, etc.) every 20 years. In this scenario, denoted as preventative scenario, actions are taken while the bridge is still in overall good condition (Reliability level below 5). Since the price of the bridge repair is different to set the reliability to its initial value from different reliability levels (Neves, year), lower prices for major bridge rehabilitations are considered in this scenario in comparison with the previous one.

3 COMPARISON

Four-leg spider (Fig.11) was consructed for both case studies in order to compare all considered maintenance scenarios.

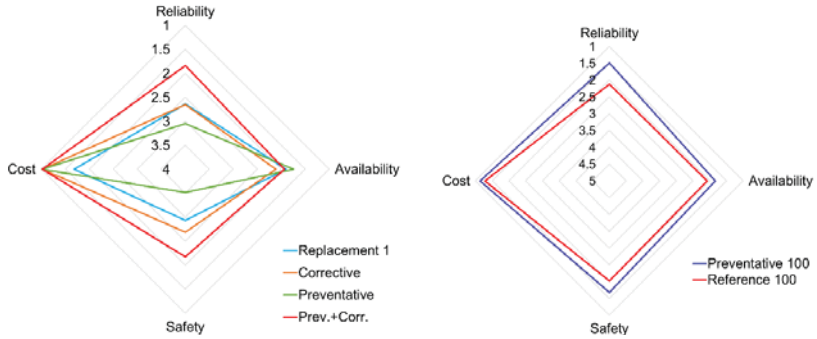

Figure 11. Four-leg spider diagram for the considered maintenance scenarios(left) and the second(right) case study

For the first case study, hybrid scenario is the most effective one with the largest spider area, while for the second case study the preventative scenario is more effective than the reference („do-nothing“ scenario) one.

4 CONCLUSION

The quality control plan established within the scope of WG3 of COST Action TU1406 was implemented here into two case studies, arch concrete bridge located in Portugal and in Macedonia. With the applied quality control plan, ‘virgin‘ reliability, anticipated failure modes and related vulnerable areas were taken into account, bringing some advantages in terms of other element-oriented quality control methodologies. With such a holistic approach, preventative maintenance and possible rehabilitation can be planned and optimized.

REFERENCES

[1] Hajdin, R.; Kusar, M.; Masovic, S.; Linneberg, P.; Amado, J.; Tanasic, N. WG3 Technical Report – Establishment of a Quality Control Plan. (Draft Version).

[2] Isanovic, D.; Hajdin, R.; Matos, J. 2018. Bridge Quality Control Using Bayesian Net, in Proc. of the 40th IABSE Symposium „Tomorrow‘s Megastructures“.

[3] Frangopol, D.; Kaller, M.; Noortwijk, J. 2004. Probabilistic Models for Life-Cycle Performance of Deteriorating Structures: Review and Future Directions, Prog. Struct. Engng. Mater. : 197-212.

[4] Frangopol, D.; Kong, J.; Gharaibeh, E.2001. Reliability-Based Life Cycle Management of Highway Bridges, Journal of Computing in Civil Engineering: 27-34.

[5] Nowak,A; Collins, K. 2000. Reliability of Structures. Tomas Casson. 255p.

[6] Neves, L. A. C.: Life-Cycle Analysis of Bridges Considering Condition, Safety and Maintenance Cost Interaction: Dissertation, University of Minho-Guimaraes. 20p.

ДГКС Друштво грађевинских конструктера Србије
ASES Association of Structural Engineers of Serbia
S-65
15. KONGRES
6-8. 9. 2018. Zlatibor

Srđan Živković[1], Marko Milošević[2]

DIJAGNOSTIKA STANJA ČELIČNOG MOSTA PREKO REKE MLAVE

Rezime:

Postojeći most preko reke Mlave, na putu za manastir Rukumija, predstavlja montažno – demontažnu čeličnu konstrukciju tipa „Bejli M-56“, sistema proste grede raspona 36,55 m i jednog dela proste grede raspona 9,10 m. Usled dejstva korozije, nastale dejstvom atmosferskih uticaja po svim elementima noseće strukture, došlo je do ozbiljnih oštećenja mosta. Primenom metoda bez razaranja utvrđen je stepen oštećenja poprečnih preseka elemenata u cilju izrade kontrolnog statičkog proračuna. Rezultati dobijeni dijagnostikom postojećeg stanja mosta obezbeđuju neophodne tehničke podloge za moguće varijantna rešenja sanacije mosta.

Key words: dijagnostika stanja, čelični mostovi, sanacija.

DIAGNOSTICS OF THE STATE OF STEEL BRIDGE OVER MLAVA RIVER

Summary:

The existent bridge over the Mlava river at the road to Rukumija monastery presents pre-fabricated military steel construction “Bailey M-56“type, simple beam system, with the range of 36,55 m and one simple beam part with the range of 9,10 m. Due to the effect of corrosion which has occurred due to atmospheric effects on all of the bearing construction elements, the bridge has been seriously damaged. Using the non-destructive method, the level of damage of cross-section elements has been determined, in order to create control static calculation. The results obtained during diagnostics of current bridge state create necessary technical surface for possible bridge rehabilitation solutions.

Key words: state diagnostics, steel bridges, rehabilitation

[1]*Assistant professor, PhD, Faculty of Civil Engineering and Architecture – University of Niš, srdjan.zivkovic@gaf.ni.ac.rs*
[2]*PhD student, Master in Civil Engineering, Innovation Center University of Niš, Faculty of Civil Engineering and Architecture – University of Niš, marko.milosevic@gaf.ni.ac.rs, marko.milosevic.mat@gmail.com*

1. SHORT DESCRIPTION OF THE EXISTENT STATE OF THE BRIDGE

The existent bridge over the Mlava river at the road to Rukumija monastery presents pre-fabricated military steel construction “Bailey M-56“type, simple beam system, with the range of 36,55 m and one simple beam part with the range of 9,10 m. “Bailey“system bridge construction presents temporary solution for vehicle transit and can by no means be considered as permanent solution, completely according to Technical instructions by manufacturers of „Bailey“ system from 1966. The project on the derived state of the bridge is non-existent.

Pre-fabricated bridge is created over an old wooden construction which parts haven’t been removed yet. Middle river column is made of steel piles that are pound in the ground, with unknown foundation depth, that represent the support at the spot of steel construction extension. Steel columns have the radius of 320 mm and are placed at the axial distance of 5530 mm. Coast columns are created by the “Bailey” system details, including non-standardized steel plates made of S.0361 steel and M20 screw bolts of 4.6. bolt grade. According to the field state, it has been noticed that coast columns haven’t been used by an older system and that predicted ramps, which are a standard part of “Bailey” bearing haven’t been created by standard procedure.

Larger bridge span consists of 12×3050 mm modules, height of 1550 mm, while smaller bridge span consists of 3×3050 mm modules. There are three transversal trusses made of I260 rolled profiles at each module set over the main trusses and longitudinal trusses made of I100 rolled profiles set on top of them. Upper and lower module zones present U100 rolled trusses while diagonals and fillings are made of I100 and U100 rolled profiles. Upper zone is connected to the side impacts brace at each module, while counter braking brace made of round steel Ø25 mm is located at the lower surface of each module. Above longitudinal trusses there have been made wooden mats that are 3÷5 cm thick. The width of carriageway construction is 4250 mm. Carriageway rails bumpers are steel trusses also of „Bailey“ licensed system. The connection between two modules is derived exclusively from two clinches that represent pinned connection both in lower and upper zone. The connection between transversal and main trusses at the lower zone is created mechanically, by the use of adhesion force created at the screws and with permanent interlock.

Static calculation by which the dimensioning is done is non-existant, hence, the type and intensity of load for which the bridge has been made remain unknown.

2. METHODOLOGY

Having in mind the corrosion effect due to atmospheric impact on almost all elements of bearing structure (Figure 6 – Figure 12) it is necessary to determine the level of cross-section reduction in order to approach the control static analysis.

Since all the bearing construction elements are made of steel, the applied methods were non-destructive:

- ultrasound method and
- magnetic flux method.

Control static calculation [2] from the determination of enlarged stress point for both transversal and longitudinal trusses has been conducted at the basis of conducted measurings (Figure 1, Figure 2, Figure 3) and maximum impact mapping (Figure 4, Figure 5). The control static calculation has been conducted for the vehicle load V300, regardless the fact that there has been entirely different, not applicable to current standards for vehicle transit over the bridge, load scheme at the moment of bridge construction.

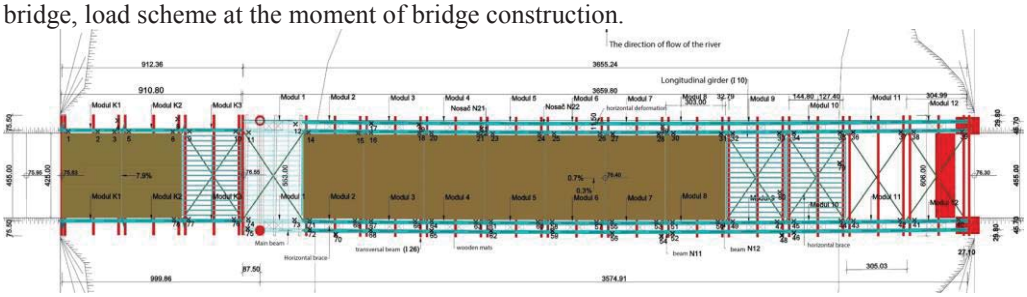

Figure 1 – The bridge disposition with measure spots positions

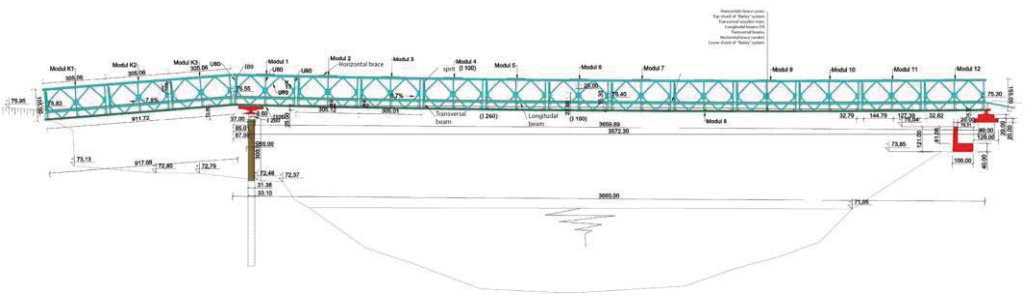

Figure 2 – Longitudinal section of the bridge with measure spots positions

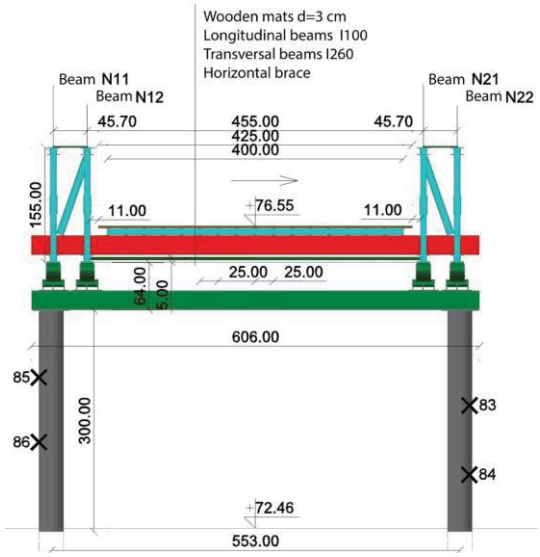

Figure 3 – Cross-section of the bridge with measure spots positions

3. BRIDGE DEFORMATIONS

Acoording to the recorded geometry of current existing state of the bridge, it is clearly noticable that there is a permanent vertical deflection that has formed due to bridge's own weight. It is ≈153 mm deep due to formed chainstitch at the main truss construction. Some deformations that are perpendicular to the main trusses surface have been noticed and they present a horisontal curve which deformation is ≈115 mm. The permanent vertical deflection has formed due to timely deformations and uncontrolled traffic load, including the loss of construction integrity due to corrosion and cross-sections reduction. Static system of "Bailey" system that is created from joints located at 3050 mm module distance and that by definition do not present a rigid construction should also be considered. The wind had additional effect on the horizontal deflection.

The general bearing state of both mobile and immobile bearings is such that effects caused by soil embank, salting out and local trees and undergrowth have made the deformations excessive.

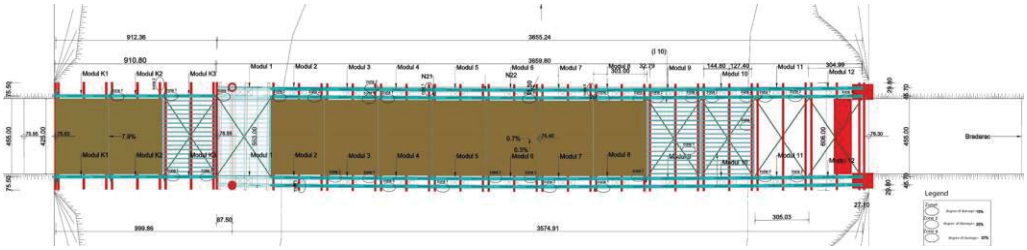

Figure 4 – The bridge disposition with damage zones

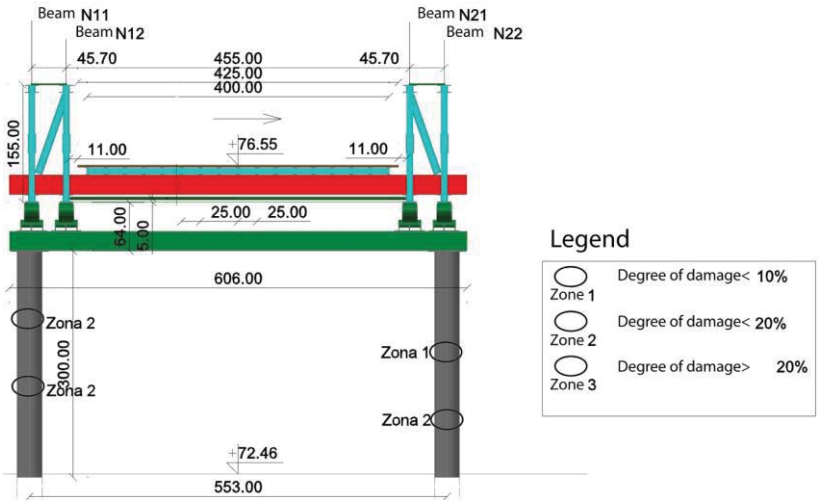

Figure 5 – Cross-section of the bridge with damage zones

4. CONCLUSION

According to conducted control static calculation [2], considering 1-3 damage zones and the forming of permanent deflection at approximately half the span with simultaneous horizontal bridge moving beyond the surface, it can be concluded that:

- the existent bridge hasn't been predicted for loads that correspond bridge crossing, according to Sl. list SFRJ 1/91,
- according to the conducted analysis on the effect of its own weight, maximum loads, with no fatigue coefficient participation, are approximately 48% of allowed stress for S.0361 steel. If the fatigue coefficient for the period from the moment of construction until today is considered, and which is in the range 1,20-1,30, it is clearly noticeable that engagement of reception sections equals 48% * 1,25 = 60% of maximum allowed stresses. Having in mind the fact that elements of different static length form the cross-section, we question the realistic dynamic impact coefficient.
    - Impact coefficient for the larger span:

$$K_d = 1{,}4 - 0{,}008 \cdot 36{,}0 = 1{,}112 \quad (1)$$

    - Impact coefficient for the smaller span:

$$K_d = 1{,}4 - 0{,}008 \cdot 9{,}0 = 1{,}328 \quad (2)$$

    - Impact coefficient of transversal trusses:

$$K_d = 1{,}4 - 0{,}008 \cdot 4{,}5 = 1{,}364 \quad (3)$$

- Impact coefficient of longitudinal trusses:

$$K_d = 1{,}4 - 0{,}008 \cdot 3{,}0 = 1{,}376. \quad (4)$$

From the given calculation it is clear that the biggest threat for superstructure elements lies on both transversal and longitudinal trusses, where the average impact coefficient mean 1,370.

- maximum measured permanent deflection created by bridge's own weight is $v_{max} = 153\,mm$, which gives ratio $36000\,mm/153\,mm = 235$, that is by far larger than allowed deflection $v_d = 36550\,mm/500 = 73\,mm$. From the given calculation it is clearly noticeable that the measured permanent deflection is approximately 100% larger than maximum allowed deflection;
- maximum measured permanent horizontal deformation equals 115 mm. This big horizontal movement can be explained by potential occurrence due to cumulative enlargement of horizontal movements due to enlarged crossing speed, the occurrence of horizontal and vertical vibrations combined with the damage of nodal connections at the bearing bridge construction;
- according to maximum exploitation of stress for other allowed values that are referring to the part of movement load, the stress value equals:

$$\sigma_d = 1600\,daN/cm^2 \cdot (1{,}0 - 0{,}60) = 640\,daN/cm^2 \quad (5)$$

It is considered that the vehicle of 10 t (which is approximately 5t by axle) maximum allowed load for bridge crossing. Other than that, the crossing speed must not be over 20 km/h.

Due to the value of dynamic impact coefficients for both transversal and longitudinal trusses, one of the recovery methods is embedding of longitudinal panels over the existing ones, in order to eliminate the impact coefficient and reduce the overall enlarged stress at dynamic load (5) of the bridge as a whole.

Figure 6 – The amount of corrosion at the bearing construction at the point of leaning of longitudinal trusses on transversal trusses

Figure 7 – General look of corroded transversal and longitudinal trusses

Figure 8 – The state of bearing construction at the point of river piles, view from the bottom

Figure 9 – The look of the bridge at the point of middle river piles

Figure 10 – Connection between the bearing construction of larger and smaller span with complete upper zone destruction

Figure 11 – Detail of connection between main bridge construction among larger and smaller span, the amount of corroding

Figure 12 – Corrosion of side impact reception intersection

REFERENCES

[1] B. Stipanić, D. Buđevac: Čelični mostovi, Građevinska knjiga, 1989.

[2] Institut za građevinarstvo i arhitekturu, Građevinsko-arhitektonski fakultet Univerziteta u Nišu: *Ekspertiza stanja mosta preko reke Mlave za manastir Rukumija*, 2014.

[3] M. Pržulj: Mostovi, Udruženje „Izgradnja“, 2014.

[4] J. Radić: Uvod u mostarstvo, Sveučilište u Zagrebu – Građevinski fakultet, 2009.

[5] Z. Marković: Granična stanja čeličnih konstrukcija prema Evrokodu, Akademska misao, 2014.

[6] V. Androić, M. Čaušević, D. Dujmović, I. Džeba, D. Markulak, B. Peroš: Čelični i spregnuti mostovi, IA Projektiranje, 2006.

[7] S. Živković, M. Milošević: Zbirka rešenih zadataka iz čeličnih konstrukcija prema Evrokodu. GAF, 2017.

ДГКС Друштво грађевинских конструктера Србије
ASES Association of Structural Engineers of Serbia
S-66
15. KONGRES
6-8. 9. 2018. Zlatibor

Slobodan Cvetković[1], *Ninoslav Milenković*[2]

MOST HERMANOS PATINO U GRADU SANTIAGO DE LOS CABALLEROS – POPRAVKA / OJAČANJE MOSTA

Rezime:

Tokom septembra 2015. godine, tim inženjera iz Srbije zajedno sa inženjerima firme Estrumet, pregledala je most Hermanos Patino koji se nalazi u gradu Santiago de los Caballeros, Dominikanska Republika. Viseći most prelazi reku Yaque, projektovan i izgrađen od strane US Steel International, otvoren za saobraćaj 1962. godine. Most je do današnjih dana popravljan nekoliko puta, poslednja intervencija je bila 2012. godine. Sve ove intervencije su nestručno izvedene, što se naročito ogleda u niveleti. Radovi na popravci mosta započeli su u aprilu 2017. godine, a završeni su krajem aprila 2018. godine.

Ključne reči: most, pregled, ugib, korozija, lančanica, sigurnost, ojačanje

HERMANOS PATINO BRIDGE IN SANTIAGO DE LOS CABALLEROS – BRIDGE REHABILITATION

Summary:

During September 2015, team of engineers composed of Serbian and Estrumet stuff made inspection of Hermanos Patino Bridge located in the city Santiago de los Cabaleros, Dominican Republic. The suspension bridge over Yaque River was designed and built by US Steel International, it was opened for traffic in 1962. During bridge service life, few rehabilitations have been done – last in 2012 year - none of them were taking care about bridge overall stability and bearing capacity. Alarm was made by local goverment when it was noticed that bridge elevation had negative camber. Based on bridge inspection results, C&N Consult and Mostprojekt prepared rehabilitation design for general reinforcing of the bridge, but reinforcing of local damages were prepared directly on the site. Rehabilitation works started in April 2017 and were finished at the end of April 2018.

Key words: bridge, inspection, negative camber, corrosion, catenary, safety, rehabilitation

[1] *dipl. građ. inž, C&N Consult doo Beograd, slobodacvetkovic@yahoo.com*
[2] *dipl. građ. inž, C&N Consult doo Beograd, ninoslaw@gmail.com*

1. INTRODUCTION

The bridge over Yaque river was designed and built by US Steel International, it was opened for traffic in 1962. It is classic suspension bridge with central span of 121920 mm and two side spans of 60960 mm. All spans are designed as simple span beams supported with catenary.

According available records, MOPS (owner) has no technical documentation for a.m. bridge. During bridge service life, few rehabilitations have been done – last in 2012 year. No available records about interventions made during rehabilitation works.

2. AVAILABLE TECHNICAL DOCUMENTATION

The team of ESTRUMET bridge inspectors tried to find any data about a.m. bridge as a part of the preparations for inspection. The following was found:

- Movie "Bridge for Yaque" made by US Steel International
- Photos of the bridge made in 2006 and 2015
- Old photos of the bridge (Internet)
- Surveying data (levels) – 24.07.2015
- Esterella references (2012 Repair Contractor):

"The renewed Hermanos Patino Bridge

The Santiago Hermanos Patino Bridge was built in 1962 by the American Steel and Export Company. It underwent a process of maintenance and renovation usually involving steel company "Ingenieria Estrella". The renovation of the bridge, which is one the city symbols, makes vehicular traffic and returns passers tranquility in one of the busiest Santiago area, contributing to the beauty of its historic center.

The work included the cleaning of the whole structure, metal plates, rivets and screws, and replacement of damaged rods under the direction of engineer Emmanuel Peña, "Ingenieria Estrella". Road repair consisted of a milling asphalt deteriorated up to 2 inches on the bridge and distributors. Also, sanitation of approach areas, earthwork and stabilization with soil cement, as well as the paving of 20,000 bridge square meters and approaches, vertical and horizontal signalization, and the renovation of the pedestrian areas, ropes and islets."

Puente Duarte in Santo Domingo was designed and constructed by same contractor – US Steel International. This bridge is very similar to Yaque Bridge, and analogy was used in order to get basic idea about the steel structure.

As opposite, on the old photos, the positive camber can be seen. It means that real deflection of the bridge, in center of the main span, is between 20 and 30 cm in upward direction.

The surveying data (2015) shows that bridge have negative camber:

- 28 cm for upstream girder, and
- 24 cm for downstream girder

Preparation for inspection included also fabrication of light cantilevered scaffolding which was equipped with wheels – it can be moved along pedestrian paths on the bridge. From this scaffolding, the bottom parts of the main girders, and part of bridge steel superstructure, can be reached. Preparation also included equipment for measuring DL forces in hangers. This

equipment was composed of existing elements that were in ESTRUMET storage and it had limited capacity.

Figure 1 - Bridge in urban surroundings

Figure 2 - Negative camber (deflection) reflected on bridge railings

3. INSPECTION OF THE BRIDGE

ESTRUMET, C&N Consult and Mostprojekt formed a team with 7 bridge engineers + supporting stuff, and a team for surveying works. Also, the necessary equipment was provided. The inspection of the bridge was done in period 8th – 12th September 2015.

3.1. INSPECTION OF THE DECK

Bridge has 4 traffic lines + pedestrian paths on the both sides. Pavement on the deck is asphalt on traffic lines and concrete on the pedestrian paths. Bridge has RC deck slab placed over steel stringers. Average thickness of the asphalt is 3-1/2“ (~8.9 cm) – measured in the areas near curbs as well as in the areas of traffic lanes. Average thickness of the concrete slab is 6 “ (~15.2 cm), measurement was taken through drilled hole. According available data, originally bridge had no additional pavement over RC deck. This fact is confirmed with shape of drainage outlets (grid is placed in the level of concrete), as well as with asphalt removal in the zone of expansion joints and with special treatment of top surfaces of the deck slab. Also, this fact was confirmed by analogy with Puente Duarte.

It means that additional DL is:
1.95 kN/m^2 (asphalt) + 0.5 kN/m^2 (steel reinforcement 2012) = 2.45 kN/m^2

3.2. INSPECTION OF HANGERS

All hangers are made of wire strand (outer diameter 1-3/4“ = 44.5 mm), with braking force ~ 180 tons (US) = 1600 kN.

Allowable force in hanger ~ 1600 / 2.5 = 640 kN

Zinc anchorage cones came out of the sockets for ~ 5 mm almost on every hanger. Under visual inspection, the hanger strands are OK.

Estimation:

DL hanger force (original design) ~ 435 kN

DL hanger force (site condition) ~ 435 + 7.6 x 7.2 x 2.45 = 569 kN

LL hanger force ~ 0.8 DL, ~ 0.8 x 435 = 348 kN (“old“ AASHTO)

Actual safety factor < 1600 / (569 + 348) = 1.74 << 2.5

During bridge inspection, it was tried to measure DL force in hangers, but installed device had failure at 510 kN. It means that a.m. estimation for forces in hangers is close to reality.

3.3. INSPECTION OF CATENARY STRANDS

The suspension system is formed with 12 spiral strands (outer diameter 2-3/8“ = 60.3 mm), with breaking force 340 US tons ~ 3000 kN. The strands are arranged in 4 vertical layers with 3 strands in each layer. Axis to axis distance of the strands are:

- 115 mm in horizontal, and
- 110 mm in vertical plane.

Allowable force in catenary: 12 x 3000 / 2.5 = 14400 kN.

At this moment, without detailed analyze of loads, we could not make any estimation what actual force in catenary was. Due to deflections of the bridge main girders, it was obvious that catenary was overloaded.

According visual inspection, the strands are OK – only few broken wires had been recorded. The clamps for hangers had not been opened during inspection, but some corrosion of the strands inside clamps was seen. The similar situation is with strands over saddles. Anchorages of strands are OK.

3.4. INSPECTION OF STEEL STRUCTURE

The bridge steel structure is extremely corroded, especially on upstream side – probably due to wind direction. During previous rehabilitation, corroded parts of steel members were replaced with new ones using welding. Also, some of the gusset plates are also replaced. This work had been done very unprofessional – nobody took care about actual force transferring. Many of a new steel elements ware found only with tack welds. All of these contributed to the unwilling deflections of the bridge. During construction works on the reinforcement of the steel structure, there was no consequent schedule for welding and welding parameters were not properly ordered. As result of such uncontrolled welding, the local deformations of steel members occurred and distribution of the stress due to DL is unpredictable. Many rivets lost heads due to corrosion. Most of them are replaced with A325 bolts during previous rehabilitation.

A.m. works on steel structure reinforcement (2012) will be main task for future rehabilitation of the bridge – the way how to include new steel reinforcement into DL transmission to bridge structure, as well as to execute rehabilitation works with limited traffic, is our main concern.

Measured hardness of the pin material: 178 HB
Tensile strength ~ 3.38 x 178 = 591 MPa
Measured hardness of the steel structure: 116 HB
Tensile strength ~ 3.55 x 116 = 412 MPa = 515 x 116 = 59740 psi

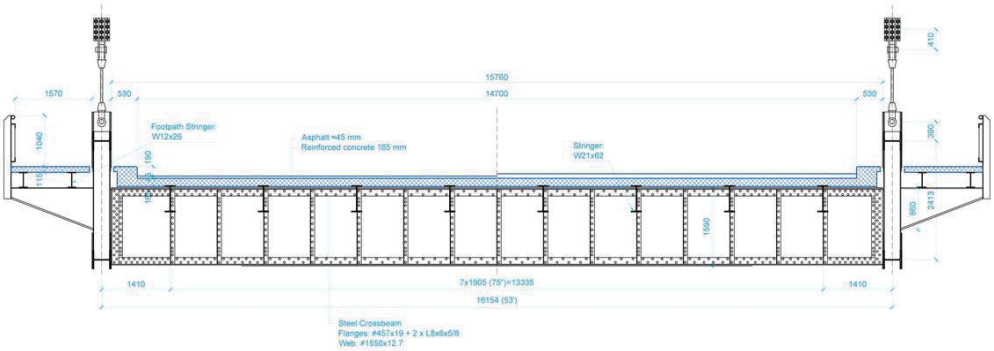

Figure 3 - Bridge cross section

4. SCOPE OF REHABILITATION DESIGN

In the next stage of this Project, we made rehabilitation design keeping traffic on the bridge (only 2 lanes) most of the time. The following activities were planned (based on the latest ASSHTO issue):

- Reinforcement of catenary installing additional cable stay system
- Making main girders (built as three independent simple span truss beams) continuous for axial loads
- Recovering of the original bridge elevation
- Making some hangers to be adjustable ones
- Reinforcement of the bridge steel structure due to existing structure condition, increased traffic load and very high wind and seismic loads
- Replacement of damaged rivets by fitted bolts
- Reinforcement of concrete deck using carbon composites
- Reinforcement of bridge substructure
- New pavement system and new expansion joints
- New corrosion protection for C5-I exposure according ISO 12944

5. BRIDGE REHABILITATION

The bridge rehabilitation works started on April 2017. Team of Serbian engineers joined to Estrumet team at the beginning of May. The works were finished at the end of April 2018.

It was obvious that bearing capacity of the catenary and main girder are jeopardized – catenary should be reinforced; main beams should be lifted in order to get positive camber and to compensate DL forces. We decided to design catenary reinforcement with stay all-threaded-high strength rods. The reason why we used rods instead cables was very aggressive

atmosphere, we were afraid that we cannot execute proper cable corrosion protection in the zone of wedges, the second reason was fact that Estrumet had all necessary equipment and experience for works with high-strength all-threaded rods.

Figure 4 - Tensioning of the stay rods – night work, bridge without traffic

Figure 5 - Tensioning of the catenary hangers

Before any tensioning of the stay rods, the strengthening of the main beam was done replacing corroded rivets (one by one) by fitted high-strength bolts and adding steel plates where necessary. We decided to joint new steel to existing one mainly by welding, taking into consideration welding schedule that can cause minimal damages to structural geometry and composition of existing steel. The reason why we designed welding on riveted bridge structure was fact that previously rehabilitation works already made a lot of damage to the existing steel structure. Most of these damages could not be repaired, only covered with new reinforcement. Eventual new small damages due to welding will cause neglectable influence on safety. This fact dictated the construction phases – as final result, reinforced bridge will have camber similar to the camber that it had at beginning of its service life.

Figure 6 - Bridge railings after rehabilitation works

Figure 7 - Bridge after rehabilitation

ДГКС Друштво грађевинских конструктера Србије
ASES Association of Structural Engineers of Serbia
S-67
15. KONGRES
6-8. 9. 2018. Zlatibor

Vlastimir Radonjanin[1], *Mirjana Malešev*[2], *Ivan Lukić*[3], *Slobodan Šupić*[4], *Vesna Bulatović*[5], *Olivera Bukvić*[6]

PROCENA STANJA DELA AB KONSTRUKCIJE TRAKTA D RTV NA MIŠELUKU U NOVOM SADU

Rezime:

Tokom bombardovanja 1999. godine, objekat „TV-Centar“ RTV na Mišeluku u Novom Sadu je u značajnoj meri oštećen, nakon čega je doneta odluka o rušenju svih nadzemnih etaža, dok je suterenska etaža zadržana u cilju rekonstrukcije i ponovne upotrebe. U cilju izrade projekta sanacije/rekonstrukcijem, urađen je detaljan vizuelni pregled i procena stanja predmetnog objekta. U ovom radu prikazani su rezultati procene stanja za Trakt D/4.

Key words: procena stanja, vizuelni pregled, defekti, oštećenja

ASSESSMENT OF RC STRUCTURE OF PART OF THE "TV-CENTER" RTV ON MISELUK IN NOVI SAD

Summary:

During the bombing in 1999, the "TV-Center" RTV on Miseluk in Novi Sad was significantly damaged, after which a decision was made to demolish all above ground levels, while the basement floor was retained for the purpose of reconstruction and re-use. In order to design the reconstruction/repair solutions, a detailed visual inspection and assessment of the condition of the object was done. This paper presents the results of the assessment of the condition for Part D/4.

Key words: assessment, visual inspection, defects, damages

[1] *PhD, Full Professor, University of Novi Sad Faculty of Technical Science*
[2] *PhD, Full Professor, University of Novi Sad Faculty of Technical Science*
[3] *PhD, Assoc. Professor, University of Novi Sad Faculty of Technical Science*
[4] *Ass. MSc CE, University of Novi Sad Faculty of Technical Science*
[5] *PhD, Assoc. Professor, University of Novi Sad Faculty of Technical Science*
[6] *Ass. MSc CE, University of Novi Sad Faculty of Technical Science*

1. INTRODUCTION

The building whose assessment was carried out and presented in this study includes the parts of the "TV-Center" RTV on Miseluk in Novi Sad. It is the basement part of the building, including tract "D" and tract "F", which remained after the demolition and removal of the structure damaged during the bombing in 1999. A schematic view of parts of building with adopted axes, for easier orientation and visual inspection, is given in Figure 1. This paper presents the results of the evaluation of the condition of the D/4 tract.

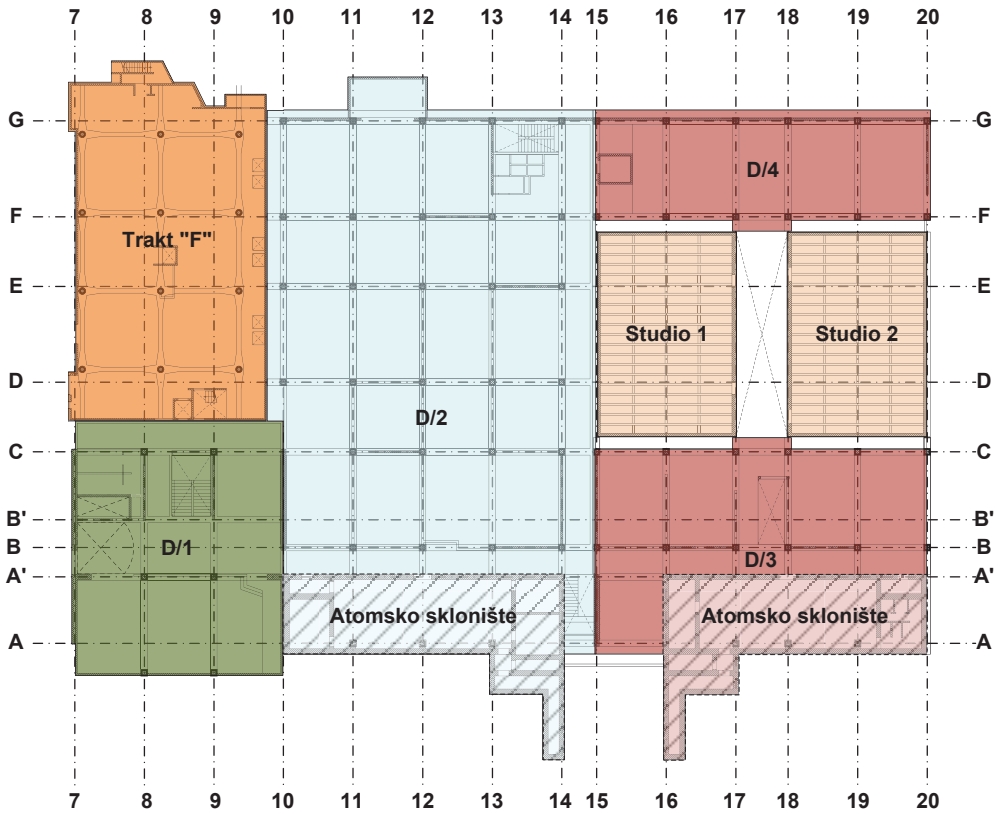

Figure 1 - Position of Tract D within the whole building

Tract D/4 was constructed as a RC construction with bearing colulmns of square cross-section (50/50cm) of raster in one direction 2x6.4m + 4.8m + 2x6.4m and 8.8m in the other direction, RC variable-height beams in the column support areas (b/h = 60/45 cm) and monolithic RC slabs thickness of 16 cm, load-bearing in two directions. Designed concrete class for floor structure, RC walls and pillars is C30/37 [1].

In order to determine the condition of the main reinforced concrete structure of the tract "D" and the tract "F" in the basement of the RTV building in Miseluk, the following activities were carried out:

- Review and analysis of available project documentation.
- Checking the dimensions of the structure and basic elements of RC structure.
- Detailed visual inspection with registration of characteristic defects and damages in the supporting structure, including technical description with the classification of detected defects and damages, graphic view and photo documentation of "recorded" defects and damage.
- Control of the deflections of selected structural elements.
- Subsequent determination of concrete compressive strength on concrete cores, which were taken from the selected elements of the RC structure.
- Analysis of all collected data.

2. VISUAL INSPECTION

Tract "D/4" includes the elements of the load-bearing structure in the groundfloor between the axis F-G / 15-20. For easier examination, the tract is divided into 5 fields (slabs), which are defined by the longitudinal and transverse axes. Within the tract, the visual inspection included:

- Top slab
- Peripheral and transverse beams
- Columns
- Walls

All the elements of the load-bearing RC structure were concreted on the spot (monolithic RC structure), where the intermediate RC slabs were constructed as semi-precast compound RC slabs, where precast RC slabs were used as a formwork and as the "lower part" of the RC floor structure which together with a monolithic slab, concreted on a precast RC board, makes a unique RC structure.

Some elements of the structure are painted with decorative paint or they have a cladding of ceramic tiles or plaster. The upper surface of RC panels above the basement could not be examined due to the existence of floor layers.

The visual inspection revealed the following defects and damages:

- insufficient thickness of the protective layer of concrete,
- visible reinforcement,
- corrosion of reinforcement,
- chemical corrosion of concrete – leaching of $Ca(OH)_2$, visible white deposits in the cracks or joints of precast RC slabs,
- cracks and fissures along the reinforcement bars,
- cracks and fissures caused by flexural failure,
- cracks and fissures in the places of stirrups,
- mechanical damages,
- traces of leakage,

- cracking, breaking of surface concrete layer,
- cracks caused by the technology of production, storage, transport and assembly of precast RC slabs.

Figure 2 shows the disposition of detected defects and damages.

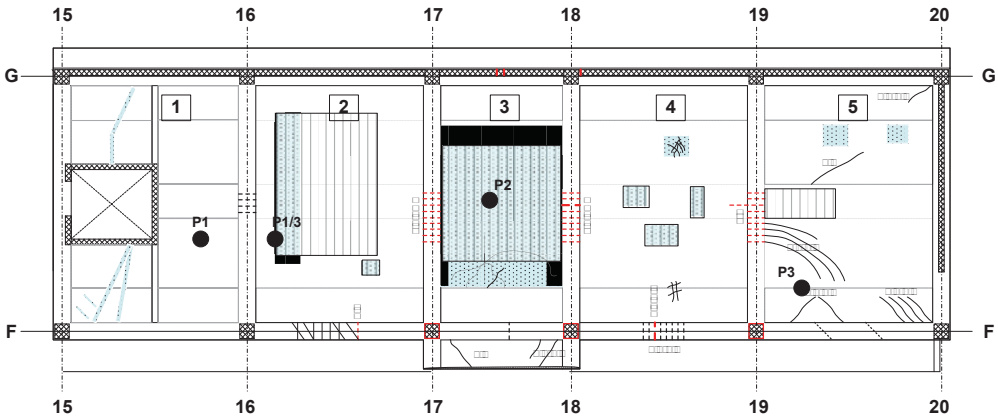

Figure 2 - Disposition of defects and damages for Tract „D/4“

2.1. RC SLAB

Visual inspection of RC slabs on the bottom side included all precast parts of the compound structure. The remaining monolithic part, which was concreted above the precast RC panels, could not be reached and assesed neither from the top, nor from the bottom. Characteristic defects and damages are given in Figures 3 and 4.

Figure 3 - Slab F-G/17-18: insufficient thickness of the protective layer of concrete, visible corroded reinforcement, wet cracks with traces of leaching of $Ca(OH)_2$

Figure 4 - Traces of leakage, thin fissures in the reinforcement zones, diagonal and slant cracks that are connected with cracks in the beam in axis 19

By analyzing the results of the visual inspection of the lower surfaces of RC slabs above the basement in the D/4 tract, it was concluded that the characteristic defects are: insufficient thickness of the concrete layer and visible reinforcement, while the characteristic damages are

the cracks caused by the production technology of precast RC slabs. Since preacst RC slabs (used as a formwork and as a "lower part" of the compound RC construction) were used for the construction of the floor structures, all the observed damages were registered on precast slabs, while the aseessment of the monolithic part of the RC slab was not possible to accura determine.

The insufficient thickness of the protective layer of concrete and the visible reinforcement were observed on all slabs, where the percentage distribution of defects on individual slabs varied from 10% (slab 4) to 75% (slab 3).

On all precast slabs, thin, shallow, net-like fissures were recorded, caused by sudden drying of the surface of the concrete after flushing. On the wet parts of the slabs, these cracks significantly aggravated visual inspection and detection of other types of cracks. On individual slabs there are slant cracks and cracks parallel to the axes (cracks that follow the direction of reinforcement), as well as diagonal and branched cracks. In the field 5, cracks spreading from from the beam in axis 19 into precast RC slab (cracked by flexural overload) were registered. Cracks that follow the position of the reinforcement are caused by corrosion of the reinforcement and are registered on four out of five slabs (slabs 2-5). Other registered cracks and cracks on precast slabs are most likely the result of storing, transporting and installing precast RC slabs.

Traces of leakage through fissures/cracks and moist areas were recorded on all tract slabs, with the surface area of these zones of 5% (slabs 1 and 5) up to 60% (slab 3). On slabs 2, 3 and 4, in the zones of the hole, intense water penetration was registered, resulting in the decay of the surface layer of concrete, and in these places the process of corrosion of the reinforcement advanced. Since water leakage and wetting are most pronounced in field 3, it can be assumed that there are deep fissures/cracks in this field on the monolithic slab.

2.2. RC BEAMS

Registered defects and damages are presented in Figures 5 and 6.

By analyzing the results of the visual inspection of the RC beams as part of the floor structure above the basement, in the part of the building "D/4" it was concluded that the defects (small protective layer, visible reinforcement) have local character, and the characteristic damages are cracks and fissures caused by bending.

RC beams were concreted on-site, together with the monolithic part of the slab. For concrete, wooden coatings were used, hence the concrete surfaces were uneven, with characteristic leakage of cement milk on the joint of the board - line segregation.

Cracks and fissures caused by bending are registered on 4 RC beams (17/F-G, 18/F-G, 19/F-G and F/18-19). The cracks are, in their vertical orientation, located in the central part of the beam. The width of the cracks on all beams ranges from 0.2 to 2 mm. Leaching of $Ca(OH)_2$ was observed in the zone of the crack, and the corrosion of the reinforcement was observed.

Cracks in the places of stirrups have local charterers and are registered on 4 RC beams.

In addition to the registered damages, large deflections were observed on RC beams 17/F-G, 18/F-G, 19/F-G and F/18-19. An analysis of deflections is given in Table 2.

Figure 5 – The beam in axes 17/F-G – Flexural cracks (0,3-2mm)

Figure 6 - The beam in axis 19/ F-G: Flexural cracks (1-2mm)

2.3. RC COLUMNS

Registered defects and damages are shown in Figures 7 and 8.

Figure 7 - Column F17 – Parallel cracks in the upper zone of the column, maximum width 4mm (side of the column to the axis E)

Figure 8 - Column F19 - Parallel cracks in the upper zone of the column, maximum width 4mm and crushing of concrete on the connection with the beam (side of the column to the axis 20)

Analyzing the results of the visual inspection of RC basement columns in tract D/4, it was concluded that defects in the form of insufficient thickness of the protective layer of concrete, concrete segregation and concrete honeycombing are locally present, and the characteristic damages are cracks and fissures due to bending.

The numbered defects were observed on 5/12 columns and are located predominantly in the upper zone of the column. The segregation zones and honeycombing are located in the joint zone with the beam, resulting from inadequate concreting and compacting of the concrete.

Flexural cracks are registered in the upper part of the columns F17, F18, F19 and G17, on the outside of the column and up to 4mm width. In addition to the mentioned cracks, on these columns, concrete crushing in the joint zone with the beam (on the opposite side of the column in relation to cracks and fissures) was registered, with the damage being the most severe on the column F19. These damages are due to the deformation of the beam in a rigid frame due to overload. In addition to the described cracks, cracks at the places of stirrups on these columns were recorded, as well.

2.4. RC WALLS

The visual inspection of the walls was difficult due to the cladding (ceramic tiles or mortar) and the paint they are covered with. The registered damages are shown in Figures 9 and 10.

Figure 9 – Wall in the axis G/17-18 – Two vertical cracks, approximately in the middle of the length of the wall, width of 0,1-0,2mm

Figure 10 - Wall in the axes G/18-19 and G/19-20 - Crack in the zone of the column

RC walls were concreted on the spot in a board formwork. On a wall G/18-19 by the column G/19, one thin crack (0.1-0.2mm) was detected, and on the wall G/17-18, approximately in the middle of the range, two parallel cracks (0.1- 0.2mm) and a crack width of approx. 2mm with column G/18 was detected. On all cracks, the denivelation of the walls on both sides of the cracks/fissures was observed.

On the part of the wall G/19-20 there is a hole, where the local corrosion of the reinforcement and the removal of the protective layer of concrete have been observed.

3. DEFORMATION ANALYSIS

Geodetic survey recorded the deformations of the structural elements which suffered significant damages with registered significant deflections. The deformations were recorded using an optical nivelir and a 1 mm ram with a laser distortion (Leica DISTO ™ D810 touch).

The values of the deflections measured on the floor structure of tract D/4 (15-20/FG) are given in Table 1. As this is load-bearing slab in two directions, a shorter direction was adopted for the deformation analysis (from axis 16 to axis 20), a span of 6.4m for the fields 16-17, 18-19 and 19-20, and 4.8m for the field 17-18. The values of the slabs' deflections are given in the

fields, where the mark "0" referes to the deflection by the beam in initial axis, and "1" the deflection by the beam in the axis at the end of the field. All the deflections are specified for each field separately (in relation to the adopted "zero point").

By analyzing the results of geodetic measurements, it can be concluded that 3 out of 4 analyzed fields do not meet the conditions for the deflection, with values up to 2.5 times higher than allowed. Since the cracks due to high tensile stress in concrete were not detected, and considering that thin precast RC plates were used as a formwork, it can be assumed that the defects are dominantly originating from the time of the building construction.

Table 1 – Values of deflections of RC slab of tract D/4 (F-G/15-20)

Field	Slab deflections in shorter direction (cm)			Slab deflection (cm)	Allowed deflections L/300 (cm)	u ≤ L/300 Fulfilled condition (Yes/No)
	0	1/2	1			
16-17/F-G	2,80	7,4	2,13	4,94	2,13	No
17-18/F-G	6,15	6,0	1,6	2,12	1,6	Yes
18-19/F-G	7,35	10,2	2,13	5,46	2,13	No
19-20/F-G	6,80	6,8	2,13	2,34	2,13	No

Pored ugiba ploča, zbog prslina i pukotina usled savijanja na pojedinim AB gredama, uočenih tokom vizuelnog pregleda, izmerene su i deformacije tih greda. Ugibi su mereni samo na sredini grede i prikazani su u tabeli 2. Dopuštena vrednost ugiba usvojena je kao L/300.

Table 2 – Values of deflections of RC slab of tract D/4 (F-G/15-20)

Field	Deflection (cm)	u ≤ L/300 = 2,93 cm Fulfilled condition (Yes/No)
16/F-G	1,4	Yes
17/F-G*	5,1	No
18/F-G*	5,3	No
19/F-G*	6,0	No
20/F-G	1,9	Yes
* The beam with visible flexural cracks		

By analyzing the values of the measured beam defections, it is estimated that they are approximately 2 times higher than allowed, and taking into account the data on the cracks on the beams and the associated columns, beams form the rigid frame with, it was concluded that the damages were caused by overload during bombing or during demolition of the building.

4. SUBSEQUENT TESTING OF COMPRESSIVE STRENGTH AND THICKNESS AND TYPES OF LAYERS OF FLOOR SLAB

In order to determine the compressive strength of concrete, the cores from the floor structure were taken. In addition to assessing the compressive strength, the extracted concrete core was used to determine the thickness of the RC slab as well as the type and thickness of the layers on it. In total, 4 concrete cores were extracted, three of which were used to determine the

strength. Due to the insufficient height of the core P1, which is required for the determination of the strength, the core P1/3 was subsequently taken. The results are given in Table 3.

Table 3 – Tract „D/4"(cores P1, P1/3, P2 and P3)

Layer	Span thickness (mm)	Average thickness (mm)	Compressive strength
Concrete screed	72-98	87.7	$f_{b,sr}$=49,1MPa $f_{b,min}$=40,3MPa
RC slab* + precast RC slab	123 +40	-	
RC slab + precast RC slab **	156-180	165.3	

* on one concrete core RC slab and precast RC slab are separated
** on three cored RC slab and precast RC slab are connected

5. ANALYSIS OF CONDITION OF LOAD-BEARING STRUCTURE

5.1. FLOOR STRUCTURE

The floor structure above the basement in the tract "D/4" is constructed as a semi-precast compound RC slab. In addition, precast RC slabs served as a formwork and as the "lower part" of the RC floor structure, which together with the monolithic slab, concreted on the precast RC board, makes a unique RC floor structure. The characteristic defects are insufficient thickness of the protective layer of concrete and visible reinforcement, and the characteristic damages are the cracks resulting from the production technology of precast RC slabs. Cracks that follow the position of the reinforcement are caused by corrosion of the reinforcement and are registered on 80% of the slabs. Traces of leakage through cracks/fissures and wet zones are not evenly distributed in the fields. Since water leakage and wetting are most pronounced in field 3, it can be assumed that there are deep cracks in this field on the monolithic slab.

By analyzing the results of the visual inspection of RC beams as part of the floor structure above the basement, in the part of the tract "D/4", it was concluded that the defects were of local character, and the characteristic damages are the cracks caused by flexural overload. The cracks are vertical, located in the central part of the beam, with a maximum width of up to 2mm, exceeding the value of the boundary width of the flexural crack and they are registered on 4 RC beams. The most damaged beam is the beam in the axis 19/F-G (fracture).

Based on the examination of the extracted concrete cores and the analysis of the data on the types and thicknesses of the layers, it was concluded that the floor structure was constructed as a semi-precast compound structure, consisting of precast RC slab with an average thickness of 4cm and RC monolithic slab with an average thickness of 12cm. Concrete built in the monolithic part of the floor structure meets the requirements for the projected concrete class.

By analyzing the results of geodetic measurements, it can be concluded that 3 out of 4 analyzed fields do not meet the conditions for the deflections, with values up to 2.5 times higher than allowed. Since the cracks due to high tensile stress in concrete were not detected, and considering that thin precast RC plates were used as a formwork, it can be assumed that the defects are dominantly originating from the time of the building construction. Measured beam thicknesses are approximately 2 times higher than allowed and taking into account the data on

the cracks on the beams and the associated columns, beams form the rigid frame with, it was concluded that the damages were caused by overload during bombing or during demolition.

5.2. RS COLUMNS AND RC WALLS

Analysis of the results of the visual inspection of RC columns showed that the defects, in the form of a segregation zone and a concrete honeycombing, are registered on 40% of columns. Cracks with a width of up to 4mm were registered in the upper part of the 4 elements, and they are caused by bending of the beam in a rigid frame due to overload. In addition to the cracks, crushing of concrete in the joint zone with the beam was detected, as well.

Within the "D/4" tract in the basement RC walls were plastered or covered with ceramic tiles, hence a visual inspection of the surfaces was difficult. Due to the described surface layers, the existence of defects is not registered, and two parallel vertical cracks (0.1-0.2mm) and one cracks with a width of about 2mm were recorded in two fields, with a slight denivelation of the walls on both sides of the cracks.

6. CONCLUSION

Based on the analysis of the condition of the RC structure (compound RC slabs and RC beams) above the basement in the section "D/4", it was concluded:

- The stability of the floor structure is endangered and the load-bearing capacity is reduced in the parts between the axis 16-20/F-G due to the presence of flexural cracks whose width exceeds the limit value.
- On the remaining part of the structure, stability is not compromised, but the load-bearing capacity of the slabs is questionable due to insufficient data on the degree of coupling of the precast and monolithic RC slab.
- Due to the penetration of water through cracks in the slabs to the interior of the basement, direct exposure to external influences, and due to the insufficient thickness of the protective layer of concrete, the durability is partially reduced, hence if measures are not taken to prevent water penetration and the closure of the building, durability will be significantly compromised in a short period of time.

Based on the analysis of the condition of the vertical RC elements (columns and walls) of the basement in the section "D/4", it was concluded:

- The stability of the frame structure is endangered and the load-bearing capacity is significantly reduced due to the presence of cracks in the upper parts of the columns.

ACKNOWLEDGEMENT

The paper presents the part of research realized within the project “Theoretical and experimental research and improvement of educational process in civil engineering” conducted by the Department of Civil Engineering and Geodesy, Faculty of Technical Sciences, University of Novi Sad.

REFERENCES

[1] Radonjanin V. et all: *Study on the assessment of the condition - The main load-bearing RC structure of the building Tract "D" and the building Tract "F" within the RTV on Miseluk in Novi Sad*, 2018, Novi Sad.

ДГКС Друштво грађевинских конструктера Србије
ASES Association of Structural Engineers of Serbia
S-68
15. KONGRES
6-8. 9. 2018. Zlatibor

Miloš Knežević[1], Ivana Tešović[2], Duško Lučić[3], Zlatko Zafirovski[4], Mladen Muhadinović[5]

REKONSTRUKCIJA ŽELJEZNIČKE PRUGE VIRPAZAR-BAR, U TUNELU "SOZINA" U CRNOJ GORI

Rezime:

U ovom radu dat je kratak pregled izvedenih radova na rekonstrukciji željezničke pruge u tunelu "Sozina" u Crnoj Gori. Izvođenje radova na rekonstrukciji u najdužem željezničkom tunelu na Balkanu, noću, u teškim uslovima rada, u trajanju od svega 4 časa i 30 minuta dnevno, su poseban inženjerski izazov, i u ovom radu je dat pregled problema na koje smo nailazili prilikom izvođenja radova. Radovi na izvođenju su otpočeli u februaru 2017. godine i završeni su u decembru 2017. godine.

Ključne reči: željeznica, Tunel "Sozina", rekonstrukcija

REHABILITATION OF THE RAILWAY TRACK VIRPAZAR-BAR, IN THE TUNNEL "SOZINA" IN MONTENEGRO

Summary

In this paper is given a brief overview of the performed works on rehabilitation of the railway track in the tunnel "Sozina" in Montenegro. Reconstruction works in the longest railway tunnel in the Balkans, at night, in difficult working conditions, lasting only 4 hours and 30 minutes per day, are a special engineering challenge, and this paper gives an overview of the problems we encountered during the work. Works on the construction commenced in February 2017, and are completed in December 2017.

Key words: *Railway, Tunnel "Sozina", rehabilitation*

[1] *Prof. PhD, Faculty of Civil Engineering, University of Montenegro, Podgorica, Montenegro, knezevicmilos@hotmail.com*
[2] *Civil Engineer, Institut za građevinarstvo doo Podgorica, Podgorica, Montenegro, ivanatesovic90@gmail.com*
[3] *Prof. PhD, Faculty of Civil Engineering, University of Montenegro, Podgorica, Montenegro, dusko.lucic.666@gmail.com*
[4] *Doc. PhD, Faculty of Civil Engineering, Ss. Cyril and Methodius University, Skopje, Macedonia, zafirovski@gf.ukim.edu.mk*
[5] *MSc, Faculty of Civil Engineering, University of Montenegro, Podgorica, Montenegro, mladenmuhadinovic@gmail.com*

1. INTRODUCTION

The Railway Vrbnica - Bar, the length of 169,2 km is a part of International railway Belgrade – Bar and Route 4 , which connects the port of Bar with trans - European corridors X and VII, for the Montenegrin economy it is the most important Traffic.

This section of open track is located in the Southern Region of Montenegro, on the railway line Vrbnica-Bar, between the railway station Virpazar (km 434+504,96) and station Sutomore (km 445+577,69), segment to the railway tunnel "Sozina", with entrance and exit parts, from km 439+032,00 to km 445+572,00. Location of tunnel "Sozina" is about 35 km from Podgorica, main Railway station in Montenegro. The works on rehabilitation are related to the track rehabilitation on section Virpazar-Sutomore in tunnel Sozina, from km 439+032.00.65 to km 445+572.00, in total length 6,54 km along the railway line Vrbnica-Bar.

Montenegro has received funds from the European Union for the implementation of the project "Rehabilitation Works on Section Virpazar-Sutomore, in Tunnel Sozina" for both Works and Supervision. The project is financed in accordance with the rules of the Regional Development Programme 2012-2013 Instrument for Pre-Accession Assistance (IPA). Rehabilitation works include civil, electrical and telecommunication works.

Execution of the works is carried out by JV Strabag AG Austria and Crnagoraput AD Podgorica, and Supervision of the works is carried out by Institut za građevinarstvo Ltd Podgorica. The Client is Directorate of Public Works Podgorica and the End Recipient is Railway Infrastructure of Montenegro. Value of the works is 4,083,891.36 € (excluding VAT). Contract is carried out in accordance with Fidic Red Book (1999 Edition). Execution of works (Commencement day) have started in February 2017 and has been finished in December 2017.

2. SCOPE OF WORKS

The designed solution for this section of single track and standard gauge, keeps the existing axis and the vertical alignment of the existing line and with the railway line electrified 25 kV, 50 Hz single-phased system, with the highest axle load of P max=25 t and 8 t/m' (UIC class D4), and v=80 km/h.. Total length of the railway line which has to be reconstructed is 6.540,21 m, from km 439+032,00 to km 445+572,00. The works are divided in following sections:

- works before the entrance to the tunnel, in length 18,46 m,
- works in the tunnel "Sozina", in length 6.170,60 m,
- works after the tunnel exit, in length 351,15 m.

Contract between Client and Contractor defines execution of following works:

- Replacement of wooden sleepers with concrete sleepers (concrete sleepers length 2,40 m, rails type 49E1, Fastening SKL14 type Vossloh (or equivalent), crushed siliceous stone for ballast;
- Mechanical excavation of existing ballast prism;
- Cleaning of drainage channels;
- Rehabilitation of the subsoil before the entrance in the tunnel (18,46 m) and part of the railway track after the tunnel exit (351,15 m);
- Electrical works include replacement of tunnel consoles, contact line wire, groundings and all electrical connections;

- Telecommunication works include replacing of cable channels and its covers, telephone metal boxes and extensions on rail STA cable.

Execution of works is organized every day during night, in duration 4 hours and 30 minutes.

3. SHORT DESCRPITION OF TECHNOLOGY FOR EXECUTION OF WORKS

In accordance with limited working conditions (very narrow tunnel profile and railway track closure in duration of 4 h and 30 minutes, it was very important that Contractor proposed maximal rational technology which reduces on minimum following parameters: percentage of manually work, time for execution of works and cost for works execution.

3.1. ORGANIZATION OF WORKS

Contractor has organized that site (storage offices, depony for new materials, depony for old sleepers and fastenings, offices for engineers, work train, machines) is positioned at the Station Virpazar. Depending of the time schedule, Contractor sometimes to storage machines has used 1st track in the Station Sutomore. Depony for old excavated ballast was positioned before the entrance in the tunnel and its position is very good, because of nearness of the local road in order excavated material can be used for embankment of local rural roads. Depending of the works that were executed and time schedule, Contractor has used railway track closure from Station Virpazar or Station Sutomore, in accordance with Traffic Instruction and Telegrams that has been issued by End Recipient – Railway Infrastructure of Montenegro. Execution of works is organized every day during night in duration 4 hours and 30 minutes.

3.2. MATERIALS

For rehabilitation works have been used following main materials: concrete sleepers l=240 cm (Rajshwellen Serbia), fastening (Rajshwellen Switzerland), Rails R260 (ArcelorMittal Poland), Rails R350HT (ArcelorMittal Spain), crushed stone aggregate (Mineralkop Montenegro), material for OCL (Integral doo Topola Serbia). Acceptance and Taking over of all materials has been organized in factories in presence of Contractor and Engineer representatives.

3.3. MECHANIZATION

For execution of the works, Contractor has used following main machines: Track motor vehicle, ballast cleaning machine, MFS wagons, ballast profiling machine, tamping machine, two way excavators, Hooper wagons, RGS wagons, gantry crane, loader, roller, truck, wrench machine, drilling machine, AT equipment, rail cutting machine, oxygen cutter, OCL TMV, Flat wagon with OCL equipment. Depending of the time schedule, Contractor engaged above mentioned machines.

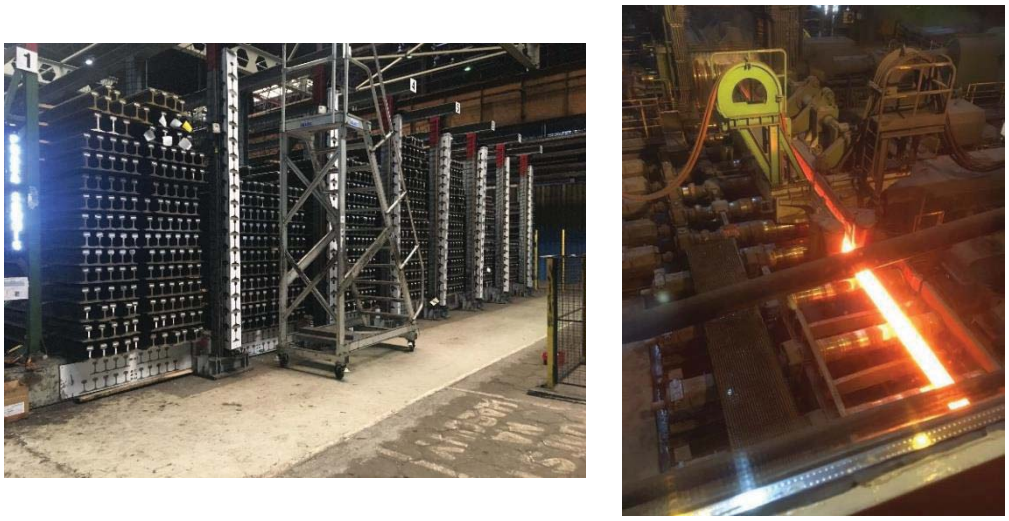

Fig. 1. Taking over of rails in the factory ArcelorMittal Poland

Fig. 2. Taking over of sleepers and fastening in the factory Rajshwellen Serbia

3.4. WORK SEQUENCES

Chorological order of basic working position regarding Civil Works:

1) Temporary relocation of cables and cable channels,
2) Cutting of rails in length up to 30 m,
3) Excavation of old ballast prism – first pass of ballast cleaning machine,
4) Cleaning of drainage channels,
5) Excavation of old ballast prism – second pass of ballast cleaning machine and first unloading of new crushed stone aggregate,
6) Dismantling of the existing track and laying of the new track, loading of new crushed stone aggregate and mechanical regulation of track,
7) Laying of new concrete cable channels,
8) Dismantling of the old track and sorting of material,
9) AT welding of the track,
10) Unloading of new crushed stone aggregate and mechanical regulation of track,
11) Laying of temporary dislocated TK cables,
12) Installation of devices against lateral track movement,
13) Unloading of new crushed stone aggregate and final mechanical regulation of track,
14) Installation of track signs,
15) Final profiling of the ballast prism,
16) Including track in CWR.

4. PROBLEMS DURING EXECUTION OF WORKS

As it is case at most of the projects, at early beginning of this project many problem arise. Problems are not problems if all participants in construction process: Contractor, Engineer, Client and End Recipient, all time during construction keep in mind that all have the same goal – to solve problems and finish project successfully.

At the beginning, it was founded a discrepancy between geodetic survey provided by the Client and actual situation at site. It was big problem because it meant that all designed coordinates in Main design of railway truck are not good. Most projects stop when Contractor realizes similar problem. We solved it in a way that Engineer instructed a Variation Order to the Contractor to develop new geodetic survey. After developing survey by Contractor, Engineer sent new geodetic survey to the responsible designer for railway track, and he changed design. Due to this problem there was no delay in the performance of works because while designer was changing design, the Contractor carried out preparatory works and works on cleaning of the ballast prism in the tunnel.

Also, at the beginning, although in tender documentation was defined that cable channels for telecommunication installations exist along the entire tunnel, we realized that there are no cable channels at site. Cables were mainly laid mainly through the ground, and due to the large presence of surface water at many places in the tunnel, mostly were laid in the water and mud. The Engineer instructed the Contractor Variation Order to purchase and install new concrete channels with covers throughout the tunnel.

After temporary relocation of telecommunication cables in the tunnel, the Contractor began with works on first mechanical excavation of the ballast prism. Because of the narrow tunnel profile, with already shortened knife of the ballast cleaning machine, it was often necessary more than 1 hour to adjust knife, which in the period of 4 hours and 30 minutes represents a

very long period. This was big problem for Contractor during mechanical excavation of the ballast prism, but it seemed there is no solution for this problem.

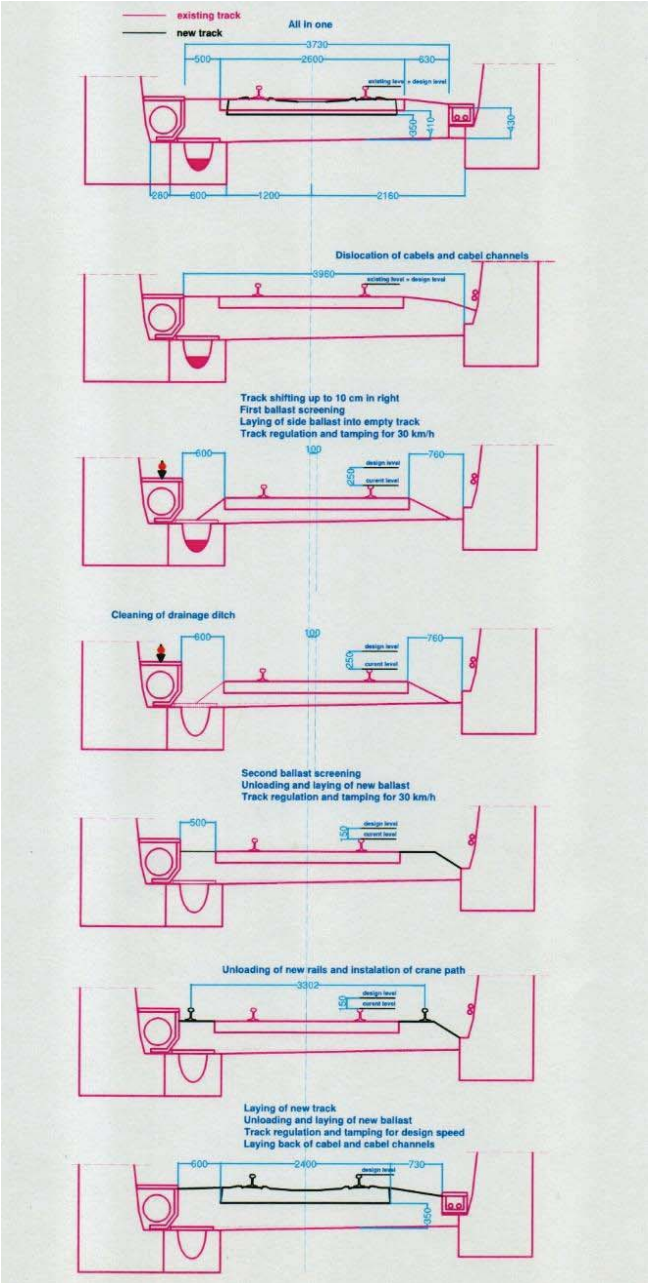

Fig. 3. Figure Work sequences shown throw tunnel cross section

Fig. 4. Telecommunication cables before start of works

Contract for execution of the works does not include the repair of the tunnel structure, and we believe it is not good engineering decision. During the execution of the works, at many places we found serious constructive damages of the tunnel structure, and a special problem is the large appearance of water in the form of a spring and leak from the tunnel lining, whose drainage from the railway track was not foreseen. Considering all these conditions and the fact that we can not repair tunnel structure at the moment, we decided to lay new concrete covers with openings on existing drainage channel in order to collect water from the railway track. At one place in the tunnel, a large amount of water, which we assume that has a flow from spring in the tunnel, can not be circumvented from the track, and unfortunately in one short part the track will be partly underwater.

We think that repair of the tunnel structure is necessary and we expect that repair will be realized in next couple of years. Unfortunately, because of bad planning of investments, in few years reconstruction of the tunnel structure will be performed in a tunnel where the railway track has been reconstructed shortly before, and it means repetition of many items from this Contract in few years.

Fig. 6. Huge amount of water in railway track

During mechanical excavation of the ballast prism, at three points in the tunnel we found the so-called "hunches", i.e. big cracks of the concrete invert slab, each in the lengths of cca 100 m. At that places, also deformed drainage channels were identified. These cracks are consequence of the Montenegrin Earthquake in 1979. This weak places were not treated by project documentation are were surprise for us at site, and again designer was required to adjust the position of the track level because of the new situation at site. Considering the fact that concrete sleepers should be installed along whole tunnel, at these weak points - "hunches", the thickness of the ballast prism below the sleeper is smaller than the minimum defined by regulations, and somewhere it is only 10 centimeters. Due to the small thickness of the ballast

prism, End Recipient would have a maintenance problem due to the crushing of the crushed stone aggregate at this places, and in order to make better situation than it could be, we decided to install concrete sleepers with rubber pads thickness 1 cm, where 1 cm thickness of the rubber pad compensate 5 cm thickness of the ballast prism. This solution can reduce bad impact of the cracked invert slab on the railway track in the exploitation. In this regard, we consider that installation of concrete sleepers in the tunnel is not a good solution. Wooden sleepers in this tunnel would be better solution that concrete sleepers, because of its smaller high when compare to concrete sleepers, and considering the fact that there is no change of humidity and temperature in the tunnel, the wooden sleepers are not exposed to cracking and rotting. This statement confirms the fact that existing wooden sleepers that have been dismantled from the tunnel, are mostly without cracks and End Recipient will use it for maintenance of other sections at railway.

Fig. 7. Cracks in concrete invert slab

Contract for execution of the works defines rehabilitation of the subsoil in length of 18.46 m. However, the geotechnical study found that in the length of 190 m before the entrance in the tunnel, it is necessary to repair the subsoil. From engineering point of view, it was unacceptable to repair just 18.46 m of bad subsoil and not whole section in length of 190 m. Engineer requested the Client to approve the signing of the Annex of the Contract for rehabilitation works of the subsoil in the length of 190 m before the tunnel entrance. The description of these works is not the subject of this paper. Therefore, it is very important that the Client before tendering process and signing the Contract with Contractor, very carefully choose the chainage of the section that will be repaired in order to get a good product in the end.

The general problem on the project was a very short period for execution of the works, which is during night rail track closure in duration of 4 hours and 30 minutes. In this short period, it is necessary that mechanization reach the site, which usually takes 45-60 minutes, and for the remaining time the Contractor has to carry out planned works, which is very short period and additionally complicates the execution of works and increases the investment. Of course, considering the daily volume of transport of goods and passengers from Podgorica to Bar by railway, attitude of Railway Infrastructure of Montenegro to provide such a short rail track closure is understandable.

Considering the tunnel length of 6,170.60 m, a special challenge was the implementation of health and safety measures at the site. We are very happy that the execution of works ended without serious injuries at work.

5. CONCLUSION

This project confirms that the dictum "A job well planned is a job half-finished" is true. With very good organization the Contractor shortened time necessary for execution of works from 12 to 8 months, which is a great success. Also, this project is a lesson to the Client that works that are going to be executed together with the scope should be carefully selected before tendering process. Before starting with the investment, it is very important to realistically consider all the problems that exist at the section that is going to be reconstructed.

Also, this project is yet another proof that the problem does not exist, if all participants in building process: Contractor, Engineer, Client and End Recipient, want to solve the problem and have the same goal which is a successful completion of the project for. Of course, occurrence of problems is normal, but problems should be solved, not increased or created.

REFERENCES

[1] Italferr S.p.a., Roma, Institut za istraživanja i projektovanje u privredi d.o.o. Budva, Institut za građevinarstvo d.o.o. Podgorica (2011). Main design for railway line track for Section Virpazar-Sutomore (km 434+504,96 – km 446+418,44).

[2] Institut za građevinarstvo d.o.o. Podgorica (2015). Annex of main design for rehabilitation of railway track Kolašin-Bar, Superstructure design of railway section Virpazar-Sutomore in tunnel Sozina, from km 439+032,00 to km 445+572,00.

ДГКС Друштво грађевинских конструктера Србије
ASES Association of Structural Engineers of Serbia
S-69
15. KONGRES
6-8. 9. 2018. Zlatibor

Doncho Partov[1], Petar Grekov[2], Vesselin Kantchev[3]

PREGLED UKOPANIH ARMIRANOBETONSKIH LUČNIH MOSTOVA I NJIHOVA PRIMENA U BUGARSKOJ

Rezime:

U ovom radu je predstavljena primena pojedinih konstruktivnih sistema za ukopane lučne armiranobetonske mostove sa prefabrikovanim betonskim elemenata za raspone od 10 do 20m. Predloženi sistemi uključuju lučne elemente za glavnu konstrukciju i zidne elemente koji podupiru zemlju oko glavne konstrukcije. Obično prelaze preko železničke pruge, ukupne dužine 25-40 m, u gradovima Češke, Slovačke, Brazila i Bugarske. Debljina prefabrikovanog luka je od 180 do 300 mm. Prikazane su glavne karakteristike i hipoteze proračuna ovakvih konstrukcija. Takođe, opisani su postupci proizvodnje prefabrikovanih elemenata i njihova montaža.

Ključne reči: prefabrikovani beton, lučni mostovi, konstruktivni siistem, interakcija tlo-konstrukcija

SURVEY OF THE BURIED REINFORCED CONCRETE ARCH BRIDGE AND ITS APPLICATION IN BULGARIA

Summary:

This paper presents the application of the some constructive systems for buried arch reinforced concrete bridges using precast concrete elements for a single span of between 10 - 20 meters. The proposed systems includes arch-shaped elements for the main structure and wall elements to retain the earth over this main structure. They are crossing usually over the railway line, with a total length of 25 - 40m, in the city of Czech Republic, Slovakia, Brazil and Bulgaria. The thickness of the precast arch is in the range between 180 and 300 mm. The main features and hypotheses used in the structural design are presented. The procedures used for the manufacture of the precast elements and onsite construction are also described.

Key words: precast concrete; arch bridges; constructive system; soil-structure interaction

[1] *Prof. Civ. Eng. D. Partov, PhD, 1373 Sofia, Suhodolska Str.175, Univ. Str. Eng. and Arch., partov@vsu.bg*
[2] *Assist. Prof. P.Grekov, PhD, 1373 Sofia, Suhodolska Str.175, Univ. Str. Eng. and Arch., petar_grekov@abv.bg*
[3] *Assoc. Prof. V. K. Kantchev, PhD,1373 Sofia, Suhodolska Str.175, Univ.Str. Eng. and Arch, kantchev@vsu.bg*

1 INTRODUCTION

According[16] arch bridges have been constructed around the world since thousands years ago. They acted as crossing between countries, cities or districts overpassing valleys or rivers. The exceptional performance of arch bridges have been recorded as early as 3000 B.C. by ancient Egyptians [2], 800 B.C. by the Assyrians [30], 100 B.C. by the Romans and 610 A.D. by the Chinese [17]. In this early century, the material for arch bridges consists of stone, wooden and masonry. Due to the materials' (stone and bricks) properties, thus, arches can withstand high compression force from the loading acted on the arches. Therefore, it is suitable to act as a compressive structure such as culvert, arch cross drain, etc. Due to discovering of Portland cement in 1824, concrete comprising of components such as cement, fine aggregate, course aggregate and water is fairly common in the arch bridge construction since 1830 [16]. During the last quarter of 19th Century and from early of 20th century, reinforced concrete (R.C.) was widely used for road and bridges. This resulted in longer span of concrete arches to 100m in 1912 [16]. Development of the concrete materials has apparently shown its increasing of strength of durability in concrete arch bridges. One of the current trend in construction work is to prefabricate concrete structure components. It has brought much contribution and convenience to the road and rail bridges. Precast concrete units are often is preferable solution for small bridge replacement due to their low initial cost, rapid installation and low maintainance [5]. This system consists of few major components. They are precast arch element, spandrel wall, foundation, wingwall and backfilling components. According [5, 24] currently the available of this system are BEBO Arch Bridge System (1965, Switzerland)[2]; Matiere Arch Bridge System (1983, France)[20]; TechSpan Arch Bridge System (1983, Spain)[21, 28]; NUCON Arch Bridge System (1995, United Kingdom)[29]; Concrete-Filled FRP Tube Arch Bridge System (2001,United States)[7]; Flexi-Arch Bridge System (2008, United Kingdom)[23]; Rivo CS-P Series Arch Bridge System (2008 Malaysia)[26]; Pearl Chain Arch Bridge System (2010 Denmark)[13]; and CONSPAN Arch Bridge System(2012, United St.)[22]; These systems have their own limited designed spans and are generally assembled from single-leaf, double-leaf or triple-leaf precast elements (Figure 1).

Figure 1. Precast arch segment types: (a) Single leaf; (b) Double leaf; (c) Triple leaf[5]

BEBO arches are a precast component bridging system that provides great strength in relatively light concrete shell structures. Experience shows backfilled reinforced concrete arch bridges are extremely durable and require little maintenance. Spans range from 3.66m to 31.0m, and are uniquely capable of ultra low-profile geometries with span-to-rise ratios as low as 10:1. The versatility of the system makes it attractive for a multitude of applicationsd(Fig.1a, Fig. 1b,). According[5] these systems' arch profile can be in circular, elliptical or parabolic in order to suit to structural and functional requirement of the specific project. Initially, simple reinforced concrete rectangular section is adopted by BEBO arch, Matiere arch, TechSpan arch and CON/SPAN arch (Fig. 1c).

Figure 1a,b,c. Precast arch segment types adopted by BEBO arch and CON/SPAN arch.

Simple rectangular section is easy for mould fabrication. However, the section becomes heavy and bulky for longer span arch with the increased thickness. Subsequent costs of handling, transporting and installation are also affected with the increased weight of the precast segments resulting in the necessity of heavier machineries and equipment. Since so, NUCON arch uses plain concrete NUCON blocks with own section as shown in Figure 2(b). Since the introduction of FRP, Concrete Filled FRP Tube arch applies the circular concrete section with FRP wrapped (Figure 2(c)). It is proven more durable. For Flexi-Arch System, it is similar to NUCON arch which uses solid rectangular segmental blocks section as shown in Figure 2(a)). Corrugated section which has been proven to have higher stiffness and substantial material saving is then developed by Rivo CS-P Series Arch System. Considering the segmental blocks concept and prestressing and post-tensioning technology, Pearl Chain Bridge System is developed. Figure 2(e) represents the Super-Light Deck section of Pearl Chain Bridge System.

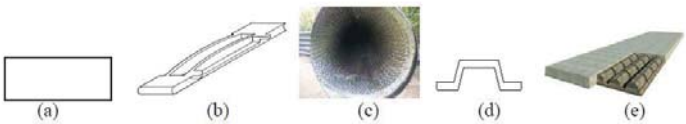

Figure 2. Arch Sections: (a) Rectangular Solid; (b) NUCON [29]; (c) Circular Concrete Filled FRP Tube [7]; (d) Corrugated [26]; (e) Pearl Chain Super-Light Deck [13]

According[5] by taking full advantage of precast technology and limitations, the following aspects have been taken into account in the conceptualization and development of the spandrel arch bridge system: functionality and aesthetics, arch profile development and foundation design, transportation arch panel, casting arch panel, de-moulding and stacking, site installation and on-site joint and backfilling process. The arch systems are designed to withstand the loading based on respective country's code of practice. They are modelled accordingly in design and analysis for all possible loading stages. Consideration of soil-structure interaction is also taken into account in the design analysis as to represent the soil behaviour to the arch structure. This consideration may optimize the design of arch panel as well.

2. BURIED ARCH BRIDGES INTEGRATED WITH SAND FILLING MATERIAL

2.1. PRINCIPLE OF INTERACTION WITH THE BACKFILL

According[24] the filling of the building is an important part of the construction of the Matière scrubbed structures to which it need to pay increased attention. It is important to know

that buried arch bridges are engineering structures built in the form of a shell surrounded by compacted soil. The effect of the cooperation between soil and ground is achieved through the phenomenon of a trumpet arch in the ground, which bring a relief of the shell. The backfill of a ground-shell construction is an essential carrying component[8, 25]. Ground-shell objects can be of a small, medium or large span. The intensity of the impact of soil on the carrying structure depends on the stiffness of the shell relative to the surrounding backfill. For this reason, ground-shell structures are divided into rigid and flexible ones. Rigid structures include objects made of low tensile strength materials (concrete, stone, brick). These are vaulted objects. Backfill around the shell is a construction material, so it must be properly designed and produced. At the stage of construction, backfill constitutes a significant *burden* on the shell structure, but in the end, thanks to the phenomenon of a trumpet arch, it increases the load capacity of the coating on the external load. According [24] for an overfilled arch structure, the fill represents more than a loading. Through its passive resistance, it also contributes to the load carrying capacity of the arch and thus becomes a structural part. This phenomenon is commonly known as soil-structure-interaction(Fig.3).

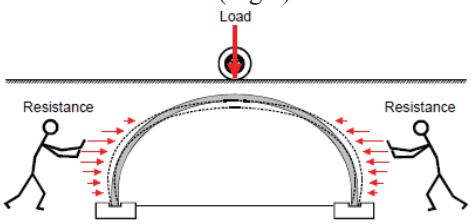

Figure 3. Soil- Buried Arch Structure- Interaction

The design of slender overfilled concrete arch structures was investigated extensively in the early 1960's by Swiss engineer Werner Heierli in connection with the construction of the Swiss Federal highway system. Heierli's design approach made wide use of soilstructure-interaction. In order to verify the results of his theoretical investigations, a first full-scale test was performed in 1965/1966 in a gravel pit near Zurich, Switzerland. The arch deformations were used to determine the lateral earth pressures for the different loading cases and to evaluate the soil-structure-interaction behavior(Fig.4a).

Figure 4a. Soil- Structure- Interaction Test, 1965, Switzerland

As a result of the successful experiment, the first so called "BEBO System" bridge was built in 1967 on Swiss Federal Highway Number 1. The soil-structure-interaction was investigated under conditions which included variations in overfill depths, degree of backfill compaction and the angle of internal friction of the backfill material. Prefabricated structures

are cross-sections of pipes, open and closed (type Matiere)(Fig.4b,c), parabolic (type Prefac), box (type Box-culvert and Opti-quadro), and frame (type CON/SPAN®).

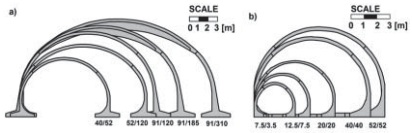

Figure 4b,c. Matiere arc type structure cross-section: a) opened, b) closed [24]

According[24] the Matiere-type structures are formed from prefabricated units of any number of segments with a width of 1 to 5 m. The composition of each segment includes two lower elements (walls) and one upper element (vault). A wide range of height and width of these structures allows to obtain a span of 22 m and a height of 10 m. Matiere structures exist in two cross-sectional forms – arc (Fig. 4b,c), and rectangular [27]. They are produced in spans of from 6 to 10 m [25]. *Taking into account backfill as stiffener of a structure at the design stage, it is possible to reduce the thickness of the elements. The object flexibility is achieved by a unique combination of upper and lower elements. It is a joint, where is no rigid connection between these elements. Additionally, the system allows to use prefabricated cornices and retaining walls.* This minimizes the amount of construction works and reduces the total time of the construction of a facility.

3. THE CONSTRUCTIVE SYSTEM MODULARCH® SYSTEM (ABM MOSTY) IN THE CZECH REPUBLIC

3.1. INTRODUCING IN THE MODULARCH® SYSTEM

Some possibilities of using arch systems Modularch® system (ABM Mosty) for small bridges in the abroad are presented in the following. Figures 4d,e shows some schemes, where single precast elements were used to span the entire opening in the Czech Republic[20]. Figures 2 and 3, shows a scheme with three precast elements, used in three crossing roads built in Czech Republic[5].

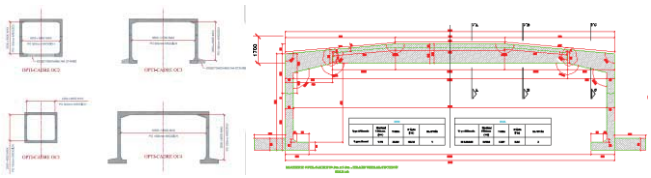

Figure 4d,e. Small span culverts with one precast concrete elements

According [24] patented Matière thin-walled, arched, thin-walled systems using interactiona back-up body, were developed in France in the early 1980s by Matière (founded in 1932). The aforementioned interaction with the appropriate backfill enables these structures to be designed as subtle, thus economically efficient. These are systems made of prefabricated, simply reinforced concrete panels. The first object made by Matière Modularch® was made in

1983. Perhaps the greatest proof of the success of these patented systems is the fact that over 15,000 Matière objects have already been built around the world in more than twenty countries where the system is properly licensed(ABM MOSTY)[20].

3.1.1. Application example: Reconstruction of bridge in Výškov in Bohemia 2

According[20] road bridge No: 250-011 in the "Ústecký Kraj" region converts the second class II road over double-track electrified railway Žatec – České Zlatníky. The bridge is situated close to the power plant in Výškov in Bohemia. The original construction of the bridge was made as a three-spans, prestressed -assembled beam construction of 30 m long beam I-73. The lower part of the bridge is made on monolithic RC columns with reinforced concrete bearing cantilever beams. And this very bottom part of the bridge was found to be very poor - grade VI. Damage was also caused by the insulating layers of the bridge, its bearings and bridges, where is the classical risk points of bridge structures of this type. The investor and the designer proceeded to implement a new bridge instead of costly reconstruction with uncertain results due to the very poor bottom structure. As a solution, an investor has chosen an (ABM Mosty) maintenance-free, buried construction(Fig.5 and Fig.6). These systems have no moving parts, ie. no bearings and no conclusions. The advantage of ABM systems is the possibility of realizing a load-bearing structure without limiting the operation of the over-ground infrastructure - whether road or, as in this case, a railway line. After design approval, a new bridge project from the prefabricated arched CM4 system was completed, combined with a 91 m^2 side panel and a 145 m^2 vault providing a clear opening of 15,3 m in width and 8,8 m in height. (Fig.5,6).

Figure 5. Large span buried bridge with three precast concrete elements during assembling

Figure 6. Large span buried arch bridge with three precast concrete elements in operation

3.1.2. Application example: Green Bridge in Slovakia

ABM Mosty has installed a new twin span arch over a busy motorway in Slovakia. The bridge reconnects the Alps and Carpathian Mountains allowing for the large wild animals safely migrate between the two territories thus maintain their genome diversity. The total length of the structure is 112,5m. The job was completely finished in February 2016(Fig.7).

Figure 7. Large span buried bridge with three precast concrete elements during assembling

3.1.3. Application example: arch bridge over Posna stream in Czech Republic

This arch bridge over Posna stream was replacing an existing small span frame with a new structure of 8m span. Interesting information about this bridge is that it has been designed wide enough to allow bats to fly through the structure following the stream. (Fig.8).

Figure 8. Small span buried bridge with three precast concrete elements during assembling

3.1.4. Application example: arch bridge in Liberec in Czech Republic

The existing stone arch was in bad condition after over 155 years of service so it has been decided the structure would be replaced by a new arch structure. The ABM precast arch was chosen as the best system in terms of durability (simply reinforced concrete) and speed of construction, which is critical item on any rail works(Fig.9).

Figure 9. Small ABM buried bridge with three precast concrete elements during assembling

3.1.5. Application example: arch bridge in Jaromer, in Czech Republic

The existing stone arch was in bad condition after over 145 years of service so it has been decided the structure would be replaced by a new arch structure. The ABM precast arch was chosen as the best system in terms of durability (simply reinforced concrete) and speed of construction, which is critical item on any rail works. (Fig.10).

Figure 10. Small ABM buried bridge with three precast concrete elements during assembling

4. THE CONSTRUCTIVE SYSTEM IN THE BRAZIL

According[11] the basic idea of the constructive system is to use precast arch-shaped elements placed on the cast-in-place concrete base. These vaults have protruding reinforcement in the crowning region to receive the cast-in-place concrete. The extreme vaults also have protruding reinforcements to make the connection to the other precast elements which work as retaining wall. The sequence of implementation for the construction process of small bridges is presented in Figure11[11,14,15].

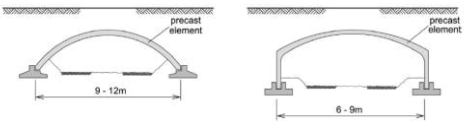

Figure 11. Large span culverts with one precast concrete elements [11]

The cast-in-place concrete in the arch crowning aims to: a) increase the cross section where there is a very high positive bending moment (which cause traction on the inner side of the arch) due to the concentrated load and b) improve the transversal distribution of live loads. Thus, this additional field work makes possible using precast concrete elements with small thicknesses. Figure 5 shows an alternative with two elements that can be used when it is necessary to get larger spans. This alternative can reach around 20 m span. Naturally, an adjustment must be made in precast elements and assembly requires more labour, beyond the need to link the crown(Fig.12).

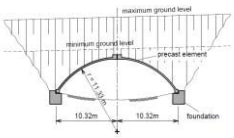

Figure 12. Large span culverts with two precast concrete elements used in three crossing road in Canada[11,12]

4.1. APPLICATION EXAMPLE: BRIDGE IN THE CITY- LOCATED IN NORTH-EASTERN OF BRAZIL

The application example was carried over a railroad in the north part of Teresina, a city located in North-eastern of Brazil[11]. Figure 6 shows the main parts of the construction geometry. The bridge has a width of 11,76m, being composed by 12 arches made with 24

precast elements and also by precast retaining walls of 0,33m thickness. The thickness of the precast arch is 180mm, reaching 300mm in the region of the arch crowning(Fig.13)[11].

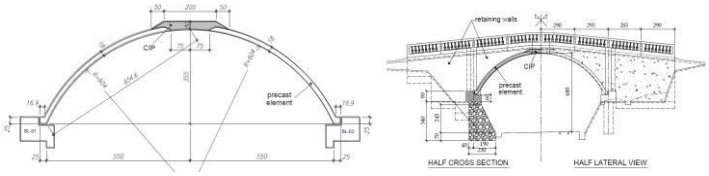

Figure 13. Bridge geometry and details

The elements were fabricated near the construction site using the resources of the contractor responsible for the construction. A mould made with bricks was used for precast arch which allowed moulding 4 elements simultaneously. Figures 14a,b,c shows details of arch elements fabrication. The weight of each precast elements was around 30kN.

a) b) c)

Figure 14a,b,c. Precast concrete arch: a) brick mould, b) casting, c) transportation[11]

Although the assembly and the connection between arch elements were expected to be made in the construction site, as shown in the Figure 14, the builder chose to make connection of precast elements near to the construction site. Thus, the shoring in construction site, which would be hard-working due to railway line, was eliminated. Figures 15a,b,c,d shows this construction step, where the elements corresponding to a complete arch were produced[11].

a) b) c) d)

Fig. 15a,b,c,d. Partial assembling: a) precast elements over the shoring, b) lateral view, c) view after connection and d) handling the complete arch

Figure 16 shows the finished bridge in operation. A more complete description of the work and the constraints can be seen in reference [27].

Figure 16. Finished Bridge in operation

5. APPLICATION OF THE CONSTRUCTIVE SYSTEM IN BULGARIA

5.1. APPLICATION EXAMPLE: ARCH BRIDGE OVER STRUMA RIVER

The following text will consist information about the large structures included in the first RW "Operational Program on Transport" financed project in Bulgaria – "ELECTRIFICATION AND RECONSTRUCTION OF THE RAILWAY LINE SVILENGRAD - TURKISH BORDER". General points (types of designed structures; general structure and technological characteristics of the bridges; issues that appeared during the construction process) will mentioned about the new structures, as well as the reconstructed ones along the existing railway track. The main contractor chose at this place to execute a fully prefabricated reinforced concrete structure and provide a **gauge** on an agricultural sub-basement. The design is based on the patented Matiere® system, made of thin-walled reinforced concrete. The main motive in choosing a structure was that the facility would be ready for 72 hours, which can be said to have been practically achieved(Fig.17)[19].

Figure 17. Railway bridge per km 300 948 - New bridge on the old route,[19]

5.2. APPLICATION EXAMPLE: ARCH BRIDGE BETWEEN TRIVODITZI AND NOVO SELO IN BULGARIA

The construction part will be implemented in such a way that the railway lines will intersect with the existing communication, which connects two settlements - Trivoditsi and Novo Selo. This intersection will take place at different levels, with a new overpass and a new bridge belonging to it. The new bridge is designed from prefabricated elements of the ABM CM4 91 construction. The construction consists of basic elements such as: two symmetrical prefabricated external walls and one prefabricated vault plate at the highest part. The bridge has a width of 15,290m, being composed by 8 arches made with 24 precast elements including also precast retaining walls of 0,600-0,350m thickness. The thickness of the precast arch is 350mm, reaching 350mm in the region of the arch crowning (Fig.18a,b).

a) b)

Fig.18a,b Bridge geometry and details and finished bridge in operation

6. FINAL REMARKS

The paper showed the feasibility of a constructive proposal for small bridges with structural arch system, employing precast concrete elements, highlighting the following points: a) Although constructive proposal would be best employed with elements fabricated in precast facilities, it presents practicability for precast concrete manufactured under site conditions and with very simple equipment; b) The constructive proposal showed to be flexible, enabling modifications to connect the precast elements out of the construction site, in order to not require shoring in situ; c) The assembly and cast-in-place concrete were made without difficulties[9,10,18].

7. CONCLUSION

For many years, the arch has been used as a safe, durable, economical and aesthetic structural form. Using modern construction materials and analysis tools, and taking advantage of the supportive action of compacted backfill, the arch bridge could be refined into a slender structure that can be prefabricated at a central plant and transported to the site for installation. Precast concrete components, manufactured under controlled conditions, reach a very high degree of strength and durability, and structures build from such components generally require very little maintenance. A major strong point of overfilled precast concrete arch bridge structures therefore is that they are designed and built to last. They withstand both the elements and time[1,3,4,6].

ACKNOWLEDGMENTS

The authors would like to thank to “REMING” Company in Sofia for Research Foment.

REFERENCES

[1] Armtec/Products and Services/Bridge Materials/BEBO Concrete Arches/Product Guide, No:07, 2011, pp.1-11.

[2] Bernini J., Fitzsimons N. & Heierli, W.: Overfilled Precast Concrete Arch Bridge Structures”. 16th Congress of International Association for Bridge and Structural Engineering (IABSE), Lucerne, 2000, pp. 380-387.

[3] Bernini J.: Overfilled Precast Concrete Arch Bridge Structures, BEBO of America, Inc. Zurich, Switzerland, 2000, pp.1-5.

[4] Chiou W.J. and Slaw, R.A.: Somerset County Bridge: a precast replacement solution. PCI Jouranl, Vol. 43, No 2, 1998, pp.22-30.

[5] Chong Yong Ong, Kok Keong Choong, Geem Eng Tan and Tai Boon Ong.: Trends and Development of Precast Concrete Closed Spandrel Arch Bridge Systems, Applied Mechanics and Materials, Vol. 802,2015, pp. 295-300.

[6] Chong Yong Ong, Kok Keong Choong, Geem Eng Tan and Tai Boon Ong.: Precast Concrete Closed Spandrel Arch Bridge System as Viable Alternative to Conventional Beam Bridge System, Applied Mechanics and Materials Vol. 802, 2015 pp. 261-266.

[7] Dagher H.J, Bannon D.J., Davids, W.G., Lopez-Anido R.A., Nagy E. & Goslin, K.: Bending Behaviour of concrete-filled tubular FRP arches for bridge structures, Construction and Building Materials, 2012, 37, pp 432-439.

[8] Drahorad M.: Buried Arch Reinforced Concrete Bridges – Superstructure Analysis with Respect to the Soil-Structure Interaction, Transaction of the VSB TU of Ostrava, CZ, CES, Vol.15, No 2, pp.29-36.

[9] El Debs M. K.: Precast concrete: fundaments and applications. EESC-USP, São Carlos. 2000,(in Portuguese: Concreto pré-moldado: fundamentos e aplicações).

ДГКС Друштво грађевинских конструктера Србије
ASES Association of Structural Engineers of Serbia
S-70
15. KONGRES
6-8. 9. 2018. Zlatibor

Dunja Radovanović[1], *Nenad Fric*[2]

TOPLO CINKOVANJE ČELIČNIH KONSTRUKICJA – MOGUĆNOSTI I OGRANIČENJA

Rezime:

Toplo cinkovanje predstavlja jedan od najčešće primenjivanih sistema zaštite čeličnih konstrukcija od korozije. U slučajevima u kojima nema ograničenja za primenu toplog cinkovanja, ovaj postupak je najekonomičnije rešenje jer se radi o trajnoj zaštiti od korozije koja ne zahteva održavanje u toku eksploatacije objekata. U ovom radu prikazan je sam postupak toplog cinkovana sa akcentom na njegovim specifičnostima, mogućnostima ali i ograničenjima. Posebna pažnja posvećenja je postupku pripreme konstrukcija za toplo cinkovanje kao i opisu prihvatljivog kvaliteta proizvoda nakon samog postupka. U radu su prikazane mogućnosti i kapaciteti svih cinkara u Srbiji i okruženju.

Ključne reči: toplo cinkovanje, čelične konstrukcije, zaštita od korozije

HOT-DIP GALVANIZING OF STEEL STRUCTURES – POSSIBILITIES AND LIMITATIONS

Summary:

Hot-dip galvanizing is one of the most commonly used systems for the corrosion protection of steel structures. In cases where there are no restrictions for the application of hot-dip galvanizing, this procedure is the most economical solution because it offers permanent protection against corrosion that does not require maintenance during the structure's exploitation. In this paper, we present the process of hot-dip galvanizing with an emphasis on its specificities, capabilities and limitations. Particular attention is paid to the process of preparing steel structures for hot-dip galvanizing as well as describing the acceptable quality of the finished product. The paper presents the possibilities and capacities of all hot-dip galvanizing companies in Serbia and in the region.

Key words: hot-dip galvanization, steel structures, corrosion protection

[1] *MSc, Civil Eng, Velesstroy Construction Company d.o.o, Belgrade, dunjaradovanovic5787@gmail.com*
[2] *PhD, Civil Eng, Assistant professor, Faculty of Civil Engineering University of Belgrade, fric@imk.grf.bg.ac.rs*

1. INTRODUCTION

Hot-dip galvanizing is a process in which a zinc coating or a zinc iron alloys coating is applied to steel structural elements. The process is carried out in hot-dip galvanizing baths.

In cases where there are no restrictions for the application of hot-dip galvanizing, this procedure is the most economical solution because it offers permanent protection against corrosion that does not require maintenance during the structure's exploitation.

Hot-dip galvanizing companies must perform their job in accordance with SRPS EN ISO 1461: 2013 [1] standard. It is most important standard about hot-dip galvanizing and it specifies the general properties of coatings and test methods for coatings applied on steel structural elements.

2. TECHNICAL REQUIREMENTS FOR HOT-DIP GALVANIZING OF STEEL STRUCTURES

Before hot-dip galvanization is performed, the customer is obliged to deliver to the contractor certain information related to their request. This information is defined by the standard SRPS EN ISO 1461: 2017 (Annex A) [1]. The information relates to the properties of the basic material that can affect the application of the coating, surface conditions of the interior parts of the construction that are not visible, special requirements related to the coating and other information.

Additionally, prior to beginning the works, the contractor is obliged to submit information related to the methods of applying the coating on uncovered areas. At the end of the process, the contractor should deliver a certificate of conformity and a certificate of job completion in accordance with quality standards, such as ISO 9001.

2.1. TECHNICAL OPENINGS ON STEEL STRUCTURAL ELEMENTS PREPARED FOR HOT-DIP GALVANIZING

Steel structural elements arrive at hot-dip galvanizing companies prepared in a certain way. At the start of the galvanizing process, all delivered elements must be measured on an industrial scale and, subsequently, stored in a proper manner. The minimum sizes of the technical openings (holes) must be in accordance with Table 1. The elements must have drilled holes (wells, cutouts, etc.) in accordance with the EN ISO 14713 [2] standard:

- openings for zinc input and air outlet from closed tubes and angles. They must be located at the bottom of the lower and upper points, as close as possible to the welds. If the structural element has holes that cannot be seen, the customer is obligated to submit a layout of the holes,
- openings for hanging. For simple elements up to 2500 mm in length, there is a single hanging point with a minimum distance of 20 mm from the edge. For elements longer than 8000 mm, more supporting points are necessary and they must be placed at 1500 mm from the end of the steel structural element to avoid its bending,

- irradiation openings, which are also used for closed surfaces between two plates, which are completely welded together (if the welded surface is larger than 2500 mm^2), to prevent explosion during hot-dip galvanizing. The opening can be on one or both plates.

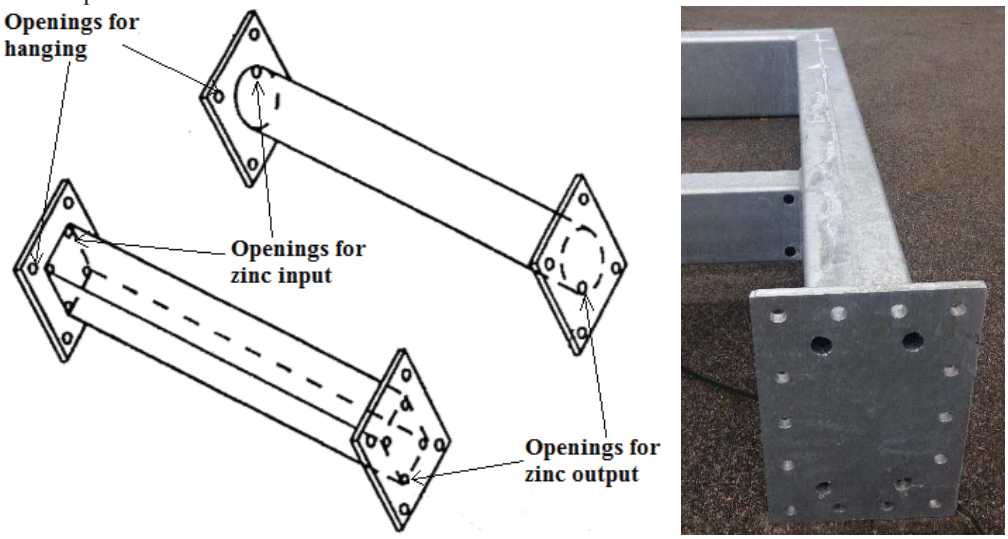

Figure 1 – Technical openings on steel structural elements [3]

The plates and stiffeners must be cut into critical areas where zinc accumulation would cause an explosion.

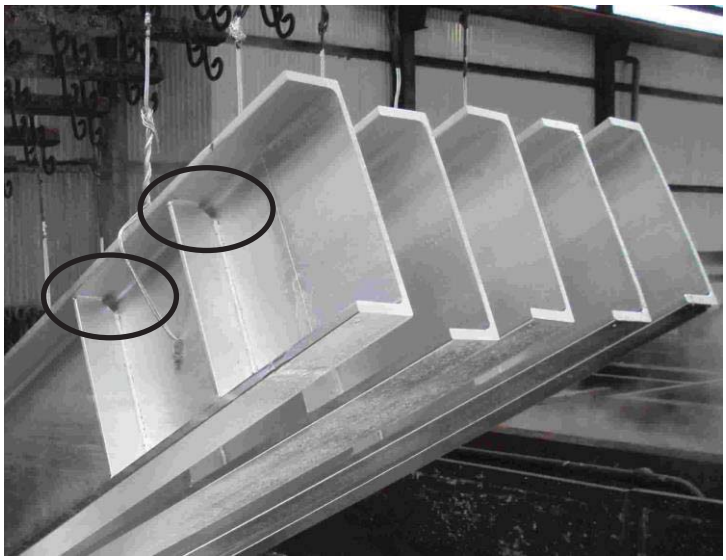

Figure 2 – Stiffeners cut in the critical areas [4]

Table 1 – Minimal diameter of technical openings [5]

Steel hollow sections – dimensions [mm]			Minimal diameter of the opening $Ø_{min}$ [mm]		
			Number of openings		
○	□	▭	1	2	4
15	15	20x10	6	-	-
20	20	30x15	8	-	-
30	30	40x20	10	8	-
40	40	50x30	12	10	-
50	50	60x40	16	12	10
60	60	80x40	20	12	10
80	80	100x60	20	16	12
100	100	120x80	25	20	12
120	120	160x80	25	20	16
160	160	200x120	32	20	16
200	200	260x140	32	20	16

2.2. PREPARATION OF STEEL SURFACES PRIOR TO HOT-DIP GALVANIZING

Applying effective corrosion protection is conditioned by the preparation of the steel surface, as the zinc reaction occurs only on a chemically clean surface. The chemical composition and condition of the surface of the base material (final appearance and roughness), the mass of the parts and the conditions during the application of the zinc coating can affect the thickness, texture, physical and mechanical properties of the coating [3].

No residual oil, grease, dirt or slag are allowed to remain on the surface; therefore, a series of procedures are used. At first, elements are degreased by immersion in an alkaline or acid solution, after which they are washed in water (rinsing). The second step is to immerse the elements in hydrochloric acid (which is at room temperature), which removes rust and slag from the rolling mill (pickling). Afterwards, the elements must be rinsed in water again. It is very important to note that the pickling process lasts between 20 and 90 min, which represents a bottleneck of the hot-dip galvanizing process, and the capacity of the plant depends on the number of baths with hydrochloric acid. The third and final step of the surface preparation in the galvanizing process (fluxing), consists of the elements' immersion in a 30% zinc ammonium chloride solution at 65–80 °C (flux solution). This removes any remaining oxides, welding slag, paint and heavy grease from the surface of the elements and provides better adhesion of zinc and base material and deposits a protective layer on the steel to prevent any further oxides from forming on the surface prior to immersion in the molten zinc. The cleaning process is shown schematically in Figure 3.

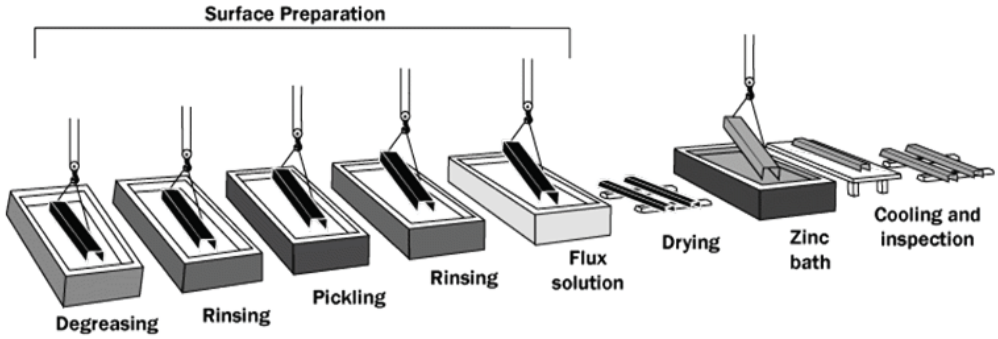

Figure 3 – Hot-dip galvanizing process [6]

3. HOT-DIP GALVANIZING TECHNOLOGY

After cleaning and rinsing of steel structural elements (which are hanging from bearing beams during the entire process) they are immersed in the bath with molten zinc. The molted zinc is at a temperature of around 450 °C because that is the temperature at which the metallurgical reaction between iron and zinc occurs. During the reaction, more ferro-zinc layers are formed. The initial reaction is very fast and the main protective layer is formed during this period, with the appearance of a large quantity of water vapour (Figure 4). After that, the reaction slows down and the thickness of the coating does not increase significantly any further, but the element is still immersed for a certain period. The process usually lasts about 4–5 min, but can take longer, e.g. for some elements in which zinc should penetrate into the interior.

Figure 4 – Hot-dip galvanizing process

When extracting from the tub, the bearing beam is raised at a certain angle due to zinc plating, and the workers remove excess zinc and slag from the surface of the melt. The galvanized element can be cooled either with water or air, after which a clear, luminous shine

appears. Additionally, this is an efficient way to inhibit undesirable reactions of the newly formed coating with the atmosphere.

3.1. DETERMINATION OF ZINC COATING THICKNESS

The length of effective corrosion protection is approximately proportional to the thickness of the coating. The thickness of the coating is usually determined by the thickness of the steel and can be determined according to Tables 2 and 3, given in EN ISO 1461:2013 [1], for centrifuged or non-centrifuged samples.

Table 2 – Minimum coating thickness and mass on samples that are not centrifuged [1]

Article and its thickness	Local coating thickness (minimum)[a] µm	Local coating mass (minimum)[b] g/m^2	Mean coating thickness (minimum)[c] µm	Mean coating mass (minimum)[b] g/m^2
Steel > 6 mm	70	505	85	610
Steel > 3 mm to ⩽ 6 mm	55	395	70	505
Steel ⩾ 1,5 mm to ⩽ 3 mm	45	325	55	395
Steel < 1,5 mm	35	250	45	325
Castings ⩾ 6 mm	70	505	80	575
Castings < 6 mm	60	430	70	505

Table 3 – Minimum coating thickness and mass on samples that are centrifuged [1]

Article and its thickness	Local coating thickness (minimum)[a] µm	Local coating mass (minimum)[b] g/m^2	Mean coating thickness (minimum)[c] µm	Mean coating mass (minimum)[b] g/m^2
Articles with threads:				
> 6 mm diameter	40	285	50	360
⩽ 6 mm diameter	20	145	25	180
Other articles (including castings):				
⩾ 3 mm	45	325	55	395
< 3 mm	35	250	45	325

Centrifugal zinc plating represents the immersion of elements in a prefabricated vessel, which, after forming the coating, rotates at a high speed and in this way removes excess zinc. It is used for hot-dip galvanizing elements with threads and other small parts.

If there are uncoated areas, they must not exceed 0,5 % of the total surface of the element and each uncoated area for renovation shall not exceed 10 cm^2. If uncoated areas are larger, the article containing such areas shall be re-galvanized, unless otherwise agreed between the customer and contractor. The coating thickness on the renovated areas shall be a minimum of 100 µm unless the customer purchaser advises the contractor otherwise, for example, when the galvanized surface is to be over-coated and the thickness for renovated areas is to be the same

as for the hot-dip galvanized coating. The coating on the renovated areas shall be capable of giving corrosion protection to the steel to which it is applied [1].

The first purpose of zinc coating is to protect steel from corrosion, while the outer appearance and aesthetics should be secondary. Roughness and smoothness are relative terms and are different when the elements are protected by zinc coating or mechanically purified, such as wires, tubes and sheets. In practice, it is not possible to determine the definition of appearance and finishing. However, appearance should be controlled from a distance of at least 1 m and the surface must be free of clumps, bubbles, rough and sharp places and uncoated surfaces.

The acceptance control may be performed by the customer or it will be performed on their behalf, before the product leaves the hot-dip galvanizing company. This control represents an assessment of the appearance of the coating on the product and measurement of the thickness of the zinc coating. Testing of zinc coating adhesion is usually not performed, unless otherwise agreed. The control sample for measuring the zinc layer thickness should be taken from the article or group of articles from a lot that is selected for sampling. The minimum number of articles from each inspection lot that forms the control sample shall be in accordance with Table 4 [1].

Table 4 – Minimum coating thickness and mass on samples that are not centrifuged [1]

Category	Size of significant surface area	Number of reference areas to be taken per article
a	$> 2\ m^2$	$\geqslant 3$
b	$> 100\ cm^2$ to $\leqslant 2\ m^2$	$\geqslant 1$
c	$> 10\ cm^2$ to $\leqslant 100\ cm^2$	1
d	$\leqslant 10\ cm^2$	1 on each of N articles
NOTE 2 m^2 = 200 cm × 100 cm; 100 cm^2 = 10 cm × 10 cm.		

4. CONCLUSIONS

The most important limitation for using hot-dip galvanizing as corrosion protection of steel structures are the dimensions of galvanizing baths. Very often, dimensions of steel structural elements are not limited by transport possibilities, but by galvanizing bath dimensions, so it is very important that the designers have good information about galvanizing possibilities in their country and region (Table 5). Sometimes, the limiting parameter are bearing beams and crane capacity (in cases of massive girders – welded or hot rolled) which can be up to 10 t (in MetalCinkara, Inđija) or number of baths with hydrochloric acid (e.g. in MetalCinkara there are 8 baths with hydrochloric acid).

Hot dip galvanized steel structural elements are not influenced by operating conditions (temperature, humidity, air quality, etc.), which is contrary to painted elements. The upper layer of steel consists only of zinc, but there is no demarcation line between the steel and zinc; rather, a gradual transition through a series of zinc-iron alloys. The protective coating is fused into the metal and can therefore provide much better protection than other coatings such as paint. While protection by paint may have to be re-processed every 5 or 6 years, protection by

galvanizing should last in excess of 30 years, even with exterior usage in coastal environments [7].

Table 5 – Bath dimensions in galvanizing companies in Serbia and region

Country	Company	Bath dimensions		
		Length [mm]	Width [mm]	Depth [mm]
Serbia	MetalCinkara, Inđija	13750	1700	3200
Serbia	Cinkara, Kruševac	9300	1400	3200
Serbia	Unipromet, Čačak	9500	1400	2800
Serbia-Kosovo	Galvazink, Prizren	8800	1300	2600
Bosnia and Herzegovina	Ibra, Tuzla	6000	700	2000
Bosnia and Herzegovina	Fabrika za pocinčavane, Srebrenica	7000	1200	1800
Bosnia and Herzegovina	SurTec Eurosjaj, Konjic	9000	1100	2900
Croatia	Italikacink, Lički Osik - Gospić	9200	1600	3000
Croatia	Kotlar, Đurđevac	3500	1400	2000
Croatia	Cinčaona Helena, Donja Zelina	6200	1200	2500
Croatia	Adriacink, Split	7500	1400	2800
Croatia	Dalekovod proizvodnja, Dugo Selo	12500	1700	2800
Slovenia	Pocinkovalnica, Celje	12600	1700	2900

ACKNOWLEDGMENT

The authors of this paper are grateful to the management and all employees of "MetalCinkara" company from Inđija (Republic of Serbia) for their hospitality during the factory visit, for given literature and selfless help in collecting the data necessary for writing this paper.

REFERENCES

[1] SRPS EN ISO 1461:2013: Hot dip galvanized coatings on fabricated iron and steel articles – Specifications and test methods

[2] SRPS EN ISO 14713-1:2017: Zinc coatings - Guidelines and recommendations for the protection against corrosion of iron and steel in structures - Part 1: General principles of design and corrosion resistance (ISO 14713-1:2017)

[3] Radovanović D.: Sistemi antikorozivne zaštite čeličnih konstrukcija sa primerom primene na industrijskom objektu, MSc Thesis, University of Belgrade, 2018.

[4] http://www.webforge.com.au/webforge/engineering/galvanizing, Available on 01.07.2018, 20:00h

[5] Vodič za inženjere i arhitekte: Potapanje toplim cinkovanjem, Metal-cinkara, d.o.o, April 2008.

[6] https://galvanizeit.org/hot-dip-galvanizing/what-is-hot-dip-galvanizing-hdg/hdg-process, Available on 01.07.2018, 19:00h

[7] https://www.rubbuk.com/rubb-quality-materials-and-processes/galvanizing-steel-framework/, Available on 01.07.2018, 19:30h

ДГКС Друштво грађевинских конструктера Србије
ASES Association of Structural Engineers of Serbia
S-71
15. KONGRES
6-8. 9. 2018. Zlatibor

Dunja Radovanović[1], *Nenad Fric*[2]

SISTEMI ANTIKOROZIVNE ZAŠTITE ČELIČNIH KONSTRUKCIJA PREMA STANDARDU EN ISO 12944

Rezime:

Veoma je važno zaštiti čelične konstrukcije od korozije obzirom da je osetljivost na koroziju jedan od dva najveća nedostataka čeličnih konstrukcija. Pored toplog cinkovanja, premazi su najčešće primenjivani sistem zaštite čeličnih konstrukcija od korozije. Oni su praktično nezamenljivi u slučajevima u kojima nije moguće primeniti toplo cinkovanje. U ovom radu prikazani su svi relevantni standardi sa naglaskon na standard SRPS EN ISO 12944 kao najznačajniji za primenu premaza. Objašnjeni su pojmovi kategorija korozivnosti sredine, načini i nivoi pripreme čeličnih površina, metode nanošenja i merenja debljine premaza kao i različite vrste premaza koje se mogu koristiti za antikorozivnu zaštitu čeličnih konstrukcija.

Ključne reči: čelične konstrukcije, korozija, premazi, priprema površina, metode nanošenja

STEEL STRUCTURE CORROSION PROTECTION SYSTEMS ACCORDING TO THE EN ISO 12944 STANDARDS

Summary:

It is very important to protect steel structures against the influence of corrosion since it is one of the two biggest defects of steel structures. In addition to hot-dip galvanizing, coating is the most commonly used system for the protection of steel structures against corrosion. It is practically irreplaceable in cases where use of the hot-dip galvanizing is not possible. In this paper all relevant standards, with emphasis on SRPS EN ISO 12944 as most important for coatings usage, are shown. Terms of corrosivity categories, methods and preparation grades of steel surfaces, methods for coatings applying and measurement of their thickness, as well as which coatings type can be used for corrosion protection of steel structures are explained.

Key words: steel structures, corrosion, coatings, preparation of surfaces, application methods

[1] *MSc, Civil Eng, Velesstroy Construction Company d.o.o, Belgrade, dunjaradovanovic5787@gmail.com*
[2] *PhD, Civil Eng, Assistant professor, Faculty of Civil Engineering University of Belgrade, fric@imk.grf.bg.ac.rs*

1. INTRODUCTION

It is very important to protect steel structures against the influence of corrosion since it is one of the two biggest defects of steel structures. Steel structures can be exposed to different influences if they are unprotected in the atmosphere or immersed (partially or completely) in water or buried in the soil. Therefore, it is necessary to be familiar with the rules as well as with the latest corrosion protection systems. In addition to hot-dip galvanizing, coating is the most commonly used system for the protection of steel structures against corrosion. It is practically irreplaceable in cases where use of the hot-dip galvanizing is not possible.

Standard SRPS EN ISO 12944: *Paints and varnishes - Corrosion protection of steel structures by protective paint systems* includes all measures for anticorrosive protection for painting and consissts of next parts:

- Part 1: General introduction
- Part 2: Classification of environments
- Part 3: Design considerations
- Part 4: Types of surface and surface preparation
- Part 5: Protective paint systems
- Part 6: Laboratory performance test methods
- Part 7: Execution and supervision of paint work
- Part 8: Development of specifications for new work and maintenance
- Part 9: Protective paint systems and laboratory performance test methods for offshore and related structures

In addition to this standard, it is also necessary to know other related ones, which deals with some specific parts od corrosion protection process (e.g. surface preparation, classification of environments etc):

- SRPS EN ISO 8501: Preparation of steel substrates before application of paints and related products - Visual assessment of surface cleanliness, Part 1 to Part 4
- SRPS EN ISO 8502: Preparation of steel substrates before application of paints and related products - Tests for the assessment of surface cleanliness, Part 1 to Part 12
- SRPS EN ISO 8503: Preparation of steel substrates before application of paints and related products - Surface roughness characteristics of blast-cleaned steel substrates, Part 1 to Part 5
- SRPS EN ISO 8504: Preparation of steel substrates before application of paints and related products - Surface preparation methods, Part 1 to Part 4.

2. CATEGORIES OF CORROSIVITY

The corrosion of steel structures at first depends on the environment in which it is located. The environment is described on the basis of:

- category of atmospheric corrosivity,
- category of the environment for constructions immersed in water or buried in the soil and
- data on specific corrosion strains.

For evaluation of the atmospheric corrosivity, the local environment and microsound are of the main importance. The location of the structure itself affects corrosion depending on whether the structure is exposed to atmospheric conditions, whether it is in a covered or indoor conditions. In the enclosed area, local corrosion can also occur as a result of condensation. In the case of structures exposed to atmospheric influences, there are a total of six categories of corrosivity and they are shown in Table 1.

Table 1 – Categories of corrosivity [1]

Atmosferic-corrosivity categories	
C1	Very low
C2	Low
C3	Medium
C4	High
C5 - I	Very high (industrial)
C5 - M	Very high (marine)

For water-immersed constructions, the type of water (sweet, salty or saturated) plays an important role, as well as other factors, such as the presence of plants or a higher concentration of oxygen that can accelerate corrosion. The influence of corrosion on structures buried in the soil is increased due to the presence of various organic and inorganic substances, water or oxygen. This type of corrosion is particularly harmful for linear systems such as pipelines, tunnels, tanks, because the content of oxygen or changes in groundwater level through the soil layers can be changed and cause the appearance of extreme shaft corrosion, also called pitting. The categories of corrosivity for structures immersed in water and buried in the soil are shown in Table 2.

Table 2 – Corrosivity categories for structures immersed in water or buried in soil [1]

Category	Environment	Examples of environment and structures
lm1	Fresh water	Structures in rivers or hydropower plants
lm2	Sea or brackish water	Port structures
lm3	Burial in soil	Subterranean containers, steel beams and similar structures

3. SURFACE PREPARATION

In order to ensure good adhesion of the basic coating as well as to reduce impurities and harmful substances that can cause corrosion, steel surface preparation depends on various factors such as the age of the structure and location, type and aggressiveness of the

environment, the condition of the existing coating system, the planned coating system and other.

Before cleaning the surface, the degree of rustling is determined, which is assessed in accordance with SRPS EN ISO 8501-1 [2]. This standard contains photographs, which classify surface states into 4 categories as shown in Table 3.

Table 3 – Rust grades [2]

Rust grades	Representative photographs	Descriotion
A		Steel surface largely covered with adhering mill scale but little, if any, rust
B		Steel surface which has begun to rust and for which the mill scale has begun flake
C		Steel surface on which the mill scale has rusted away of from which it can be scraped but with slight pitting visible under normal vision
D		Steel surface on which the mill scale rusted away and on which general pitting is visible under normal vision

3.1. SURFACE PREPARATION METHOD

As mentioned, before applying a protective coating system, the surface must be prepared, or cleaned from grease, oil, salt and other pollutants. This can be done in several different ways, such as mechanical cleaning and cleaning with hand tools, flame and water cleaning or with solvents and chemicals.

The most common and most effective way of cleaning is abrasive cleaning. It involves the cleaning of steel surfaces with the help of compressor which provides the air volume and pressure to move the abrasive media though the hose and blast nozzle until it hits the target surface. This process is known as "dry cleaning" and is environmentally unacceptable in view of the waste that remains after it, however, by introducing a water immediately after the abrasive, the piling up and dispersal of waste is eliminated [3].

Manual and machine cleaning involves the usage of various tools, brushes, scrapers, rotating wire brushes, vibrating hammers and others. When the usage or accumulation of

abrasive is not allowed, these procedures are generally applied, but it should be kept in mind that they give poorer effects in terms of cleaning the surface.

In the case of flame cleaning, rust and thick oxide layer produced by thermal treatment of steel are removed under the action of an oxygen-acetylene flame that is applied on the surface. After that, the surface is machined with mechanical brushes and dust and other dirt must be removed before painting.

3.2. PREPARATION GRADES OF STEEL SURFACES

Each degree of surface preparation is indicated by the appropriate lettering (which defines the preparation process) and the degree of cleaning from rust or previous coatings. Standard SRPS EN 8501-1 [2] contains photographs of reference samples, which are marked by the degree of rust, in addition to the degree of preparation.

Table 4 – Blast-cleaning preparation grades [2]

Category	Cleaning method	Surface description
Sa1	Easy abrasive blast cleaning	The surface after cleaning, without any magnification, must be free of visible traces of oil, grease and dirt, and rusts, incisors, coatings and foreign matter that are poorly adhered must be removed.
Sa2	Careful abrasive blast cleaning	The surface after cleaning, without any magnification, must be free of visible traces of oil, grease and dirt, and most of rust, honeycomb, coating and foreign matter must be removed. Any residual pollution must be firmly fixed.
Sa21/2	Very carefully abrasive blast cleaning	The cleaning area observed without magnification must be free of visible traces of oil, grease and dirt and must be free from rust, haze, coating and foreign matter. Any residual imprints of impurities can only be as bright spots in the form of strips or dots.
Sa3	Abrasive blast cleaning up to clean metal	The cleaning area observed without magnification must be free of visible traces of oil, grease and dirt and must be free from rust, haze, coating and foreign matter. The surface must have a uniform metallic glow.

Table 5 – Hand and power tool preparation grades [2]

Category	Cleaning method	Surface description
St2	Thorough hand and power tool cleaning	The surface after cleaning, without any magnification, must be free of visible traces of oil, grease and dirt, and rusts, incisors, coatings and foreign matter that are poorly adhered must be removed.
St3	Very thorough hand and power tool cleaning	The surface is cleaned just like St 2 only much more carefully and all the way until the metallic shine of the substrate is achieved.

Table 6 – Flame preparation grades [2]

Category	Cleaning method	Surface description
Fl	Flame cleaning	The surface after cleaning, observed without magnification, must be free from holes, rust, paint and foreign matter. Only traces of impurities in the form of shades of different colors must remain on the surface.

The described grades of preparation (Table 4, 5 and 6) are used for steel surfaces which did not contain coatings or which contained it, but provided that coating was removed to the extent that the degree of preparation was achieved.

Table 7 – Preparation grades after localized removal of previous coatings [4]

Category	Cleaning method	Surface description
PSa2	Careful localized abrasive blast cleaning	Coatings that adhere well do not touch. The same descriptions apply as for the standard preparation grades for the primary surface preparation. For comparison only images with the C or D standard SRPS EN 8501-1 [2] are used, with an equivalent degree of preparation and the choice depends on the intensity of the corrugated corrosion.
PSa21/2	Very carefully localized abrasive blast cleaning	
PSa3	Localized abrasive blast cleaning up to clean metal	
PSt2	Thorough localized hand and power tool cleaning	
PSt3	Very thorough localized hand and power tool cleaning	
PMa	Localized mechanical abrasion	It is carried out by using a disc with abrasive paper or rotating wire brushes in combination with a needle pistol. Same description of prepared surfaces as for PSa 21/2. Photos are contained in SRPS EN ISO 8501-2 [4].

Standard SRPS EN 8501-1 [2] contains 28 representative photographs with which steel surfaces should compare. Of the total, 4 photographs represent the degree of corrosion and they are taken from the German standard DIN 55928, and the other 24, which illustrate the degree of preparation of surfaces obtained in the 3 described ways, are taken from the Swedish standard SIS 055900: 1967. They are only printed in Sweden and only their application is allowed.

4. PROTECTIVE PAINT SYSTEMS

The process of painting or colouring is the most commonly used procedure. It does not require a specially trained manpower and can be applied to all types of objects or elements, regardless of the shape and complexity of the cross-section.

Systems consist of basic, intermediate and final coating layer. The primary coating purpose is to provide good adhesion to the metal surface (or old coating) and to protect the metal until the next coating is applied, as well as throughout the entire working life. The interlayer serves to reduce or completely prevent moisture penetration through the paint system and it must be compatible with the final coating. The final coating contributes to the protection against corrosion and gives the required colour.

4.1. DETERMINATION OF PAINT FILM THICKNESS

The thickness of the dry film (DFT) is important for the coating. It represents the thickness of the coating that remains on the surface after curing.

As a rule, the DFT is measured on the whole color system, and if it is found to be appropriate, the thickness of the dry film of the basic coating or other parts of the system can be measured individually.

The thickness of the dry film is measured in relation to the nominal thickness of the dry film (NDFT), which is defined as the determined thickness of the dry film for each coating or for the entire color system, which ensures the required lifetime. If the parties do not agree differently, the DFT must be at least 80% of the NDFT, and the individual values between 80% and 100% of the NDFT are acceptable only if the total mean value is greater than or equal to the nominal thickness of the dry film. The largest acceptable thickness of dry film is the thickness above which characteristics of the system are considered to be worse. In order to avoid this, the aim is to apply colors in a thin layers as thick layers can cause additional strains and failure of the system. It is recommended that the maximum acceptable thickness is at most three nominal thicknesses of the film [5].

Wet film thickness (WFT) can also be required to ensure that the subsequent thickness of the dry film is satisfied. The thickness of the wet film is measured using the instrument called „wet film comb“ (Figure 1). For a fast DFT calculation, WFT can be multiplied by 0,69.

Standard SRPS EN ISO 12944-5 [6] in its Appendix A gives different examples of color systems for certain corrosion categories, number of coating layers and dry film thickness values based on air-spray method of painting. When the paint is applied with a roller, brush, or other equipment, more layers are needed to obtain the appropriate thickness of the film.

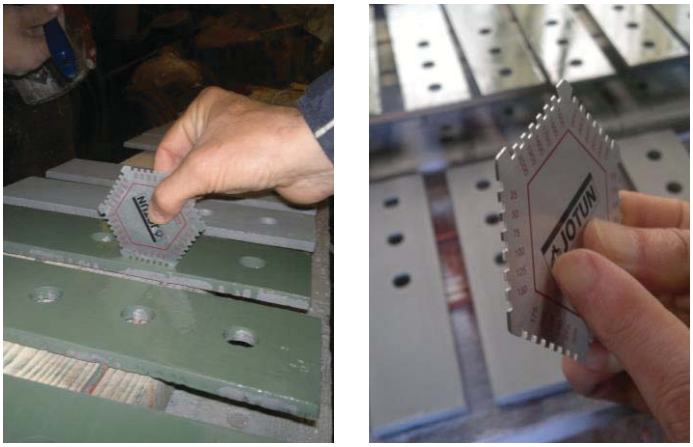

Figure 1 – Wet film comb usage [7]

4.2. PRINCIPLES AND APLICATION METHODS

Prior to selection of propriate protective painting system, investor defines the criteria that are of the greatest importance for him such as:

- warranty period and lifetime of the system,
- production technology,
- price and
- delivery speed.

Taking care of important criteria, SRPS EN ISO 12944-5 [6] standard can be used for selection of painting system. Standard specified painting systems by applying two basic principles:

- according to the binder used in the final coating, where the systems are given in the "sum table" - the usage is recommended when selecting the system based on the final coating, as well as to compare a lifetime of the color system for more than one category of corrosion , in case the category is not known
- according to the binder used for basic coating, where systems are shown only for one category of corrosion - it is suitable for the usage when the exact corrosion category of the medium to which the structure is exposed is known.

As an example a summary table for corrosivity category C2 is given (Table 8). The color systems shown in the table are just an example, since other systems with the same characteristics are also possible.

As a binder for basic and final coating can be used: AK - alkyd, AY - acrylic, PVC – polyvinyl-chloride, EP - epoxy, CR – chlorinated rubber and ESI – ethyl-silicate and PUR – polyurethane, aliphatic. Zinc (R) – zinc rich primer or misc – primers with miscellaneous types of anticorrosive pigment can be used for the base color type. If a zinc-rich color is used, the smallest content of zinc as a pigment in the non-volatile part of the paint must be 80% for both organic and inorganic binders. This quantity represents the basis for the life of basic colors with high zinc content.

Number of coating applications for each system and nominal thickness of dry film, which are defined by the standard, are shown in the Tabel 8.

Table 8 – Summary table for corrosivity category C2 [6]

Substrate: Low-alloy carbon steel Surface preparation: For Sa $2^1/_2$ from rust grade A, B or C only (see ISO 8501-1)										
System No.	Priming coat(s)				Subseq. coat(s)	Paint system		Expected durability		
	Binder type	Type of primer	No. of coats	NDFT [µm]	Binder type	No. of coats	NDFT [µm]	Low	Med	High
A.2.01	AK	Misc.	1	40	AK	2	80			
A.2.02	AK	Misc.	1-2	80	AK	2-3	120			
A.2.03	AK	Misc.	1-2	80	AK, AY PVC, CR	2-4	160			
A.2.04	AK	Misc.	1-2	100	-	1-2	100			
A.2.05	AY, PVC CR	Misc.	1-2	80	AY,PVC CR	2-4	160			
A.2.06	EP	Misc.	1-2	80	EP, PUR	2-3	120			
A.2.07	EP	Misc.	1-2	80	EP, PUR	2-4	160			
A.2.08	EP, PUR ESI	Misc.	1	60	-	1	60			

It is important to keep in mind that applied coatings within a single system must be compatible. It is not mandatory to have all coatings of one system from same origin, but as a precautionary measure, all coatings should be obtained from one manufacturer, whose recommendations need to be followed. It is necessary to choose either a coating system that would correspond to the degree of preparation that could be achieved, or the degree of preparation that corresponds to the purpose and type of the coating system.

For each system, it is defined the lifetime in relation to the category of corrosivity. The lifetime is the time that goes from coating to the first next major renewal. The term "lifetime" of the paint protection system should not be mixed with the warranty period. The warranty period is, as a rule, shorter than the lifetime, and it is defined in the administrative part of the contract. The prescribed lifetime can be short, medium and long, as shown in Table 9.

Table 9 – Lifetime of coating systems

Lifetime	Years	Label
Short	2 - 5	L
Medium	5 - 15	M
Long	> 15	H

5. CONCLUSIONS

One of the basic preconditions for achieving the required durability of steel structures is the adequate protection against corrosion. The technical regulations related to this subject are at a very high level and it can be said that all aspects of coating usage as a steel structure corrosion protection are covered by the applicable standards. On the other hand, there is a great number of experiences in practice where, as a result of ignorance of the standards, contractors easily accept the obligations to perform corrosion protection with a guaranteed lifetime which is not possible to achieve. This is especially pronounced in the case of the reconstruction and rehabilitation of existing structures where the surface is prepared "in situ", most often by hand tools. Although in such cases the best surface preparation is obtained by using sandblasting, this method is usually abandoned due to the high cost of protection that should prevent the spread of quartz in urban areas. As a consequence of this approach, corrosion occurs significantly before the expiration of the warranty period, which introduces the participants into the long and painstaking work of the continuous repair of the applied coating system. Also, coating systems can cost significantly depending of type, number and thickness of layers in the prescribed system. Contactor are very often forced to change their suppliers to provide compatibility of all layers in coating system so this must be taken in to account during the calculation of prices.

ACKNOWLEDGMENT

The authors of this paper are grateful to the management and all employees of "Jadran" company from Belgrade (Republic of Serbia) for their hospitality during the company visit, for given literature and selfless help in collecting the data necessary for writing this paper.

REFERENCES

[1] SRPS EN ISO 12944-2: *Paints and varnishes - Corrosion protection of steel structures by protective paint systems - Part 2: Classification of environments (ISO 12944-2:2017)*

[2] SRPS EN ISO 8501-1: *Preparation of steel substrates before application of paints and related products - Visual assessment of surface cleanliness - Part 1: Rust grades and preparation grades of uncoated steel substrates and of steel substrates after overall removal of previous coatings (ISO 8501-1:2007)*

[3] Radovanović D.: *Sistemi antikorozivne zaštite čeličnih konstrukcija sa primerom primene na industrijskom objektu*, MSc Thesis, University of Belgrade, 2018.

[4] SRPS EN ISO 8501-2: *Preparation of steel substrates before application of paints and related products - Visual assessment of surface cleanliness - Part 2: preparation grades of previously coated steel substrates after localized removal of previous coatings (ISO 8501-2:1994)*

[5] SRPS EN ISO 12944-7: *Paints and varnishes - Corrosion protection of steel structures by protective paint systems - Part 7: Execution and supervision of paint work (ISO 12944-7:2017)*

[6] SRPS EN ISO 12944-5: *Paints and varnishes - Corrosion protection of steel structures by protective paint systems - Part 5: Protective paint systems (ISO 12944-5:2018)*

[7] Fric N.: *Theoretical and experimental research of losses of pretension force in high strength bolts,* PhD Dissertation, University of Beograde, 2015.

ДГКС Друштво грађевинских конструктера Србије
ASES Association of Structural Engineers of Serbia
S-72
15. KONGRES
6-8. 9. 2018. Zlatibor

Nikola Tošić[1], Andrija Radović[2], Bogdan Šakić[3], Snežana Marinković[4]

DUGOTRAJNI UGIBI GREDA OD ZELENIH BETONA: ANALITIČKI I NUMERIČKI PRORAČUNI

Rezime:

Pouzdan proračun ugiba je jedan od komplikovanijih aspekata projektovanja armiranobetonskih elemenata. Svi proračunski modeli zahtevaju veliki broj eksperimentalnih rezultata za kalibraciju. U slučaju zelenih betona od otpadnih i recikliranih materijala, takvi rezultati nedostaju. Ovaj rad predstavlja rezultate primene analitičkih i numeričkih proračunskih modela za ugibe armiranih greda od betona sa prirodnim agregatom, betona sa recikliranim agregatom i betona sa velikim sadržajem letećeg pepela. Eksperimentalni rezultati na šest prostih greda su upoređeni sa predviđanjima dobijenim pomoću analitičkog modela iz *fib* Model Code 2010 i numeričkog modela formiranog u programu DIANA. Rezultati potvrđuju primenjivost ovih modela za proračun ugiba greda od zelenih betona.

Ključne reči: reciklirani agregat, leteći pepeo, greda, ugibi, Model Code, DIANA

LONG-TERM DEFLECTIONS OF GREEN CONCRETE BEAMS: ANALYTICAL AND NUMERICAL CALCULATIONS

Summary:

Reliably calculating the deflections is one of the more difficult aspects of the design of reinforced concrete members. All calculation models require a large number of experimental results for their calibration. Such results are lacking for beams made of green concretes with recycled and waste materials. This paper presents the results of applying analytical and numerical calculation models for predicting deflections of reinforced natural aggregate concrete, recycled aggregate concrete and high-volume fly ash concrete beams. Experimental results on six simply supported beams were compared with predictions obtained using the *fib* Model Code 2010 analytical model and a numerical model formulated using DIANA. Results confirm the applicability of these models in predicting deflections of green concrete beams.

Key words: recycled concrete aggregate, fly ash, beam, deflections, Model Code, DIANA

[1] *PhD, Teaching assistant, University of Belgrade, Faculty of Civil Engineering, ntosic@imk.grf.bg.ac.rs*
[2] *MSc, Research assistant, University of Belgrade, Faculty of Civil Engineering, andrijaradovic1@gmail.com*
[3] *BSc, Student, University of Belgrade, Faculty of Civil Engineering, bsakicbk@gmail.com*
[4] *PhD, Full professor, University of Belgrade, Faculty of Civil Engineering, sneska@imk.grf.bg.ac.rs*

1. INTRODUCTION

All modern design codes based on limit state theory distinguish between the ultimate limit state (ULS) behaviour, i.e. bending, shear, punching, etc., and serviceability limit state (SLS) behaviour, i.e. stresses, cracks and deflections, of reinforced concrete structures. The usual design procedure so far has been the design of a structure according to ULS and its subsequent verification for SLS. However, for several reasons, this is changing.

Over the past several decades, deflection control has been becoming increasingly important. The use of increasingly higher-strength concretes and reinforcements has led to a steady increase in average steel strain of reinforced concrete members, to which deflection is roughly proportional [1]. Combined with a reduction of the safety factors for steel strength, caused by increasingly controlled production, it could be argued that today, concrete structures are 'roughly four or five time more flexible than those designed 50 years ago' [1].

This trend has placed more and more emphasis on deflection control in order to avoid visible sag, impairment of structure functionality and avoid damage to partitions and finishes. However, the problem is that models for calculating deflections are far less reliable than those for calculating ULS, yet this is rarely realized by practicing engineers [2]. In comparison with ULS models, there are many sources of uncertainty for calculating deflections [2] such as actual load level compared with design load, concrete tensile strength, modulus of elasticity, shrinkage and creep variability, tension stiffening, ambient condition effects and loading age and load history. Prediction of deflection is especially difficult for reinforced concrete members since their stiffness changes over time due to cracking, shrinkage and creep. The traditional approach in the European tradition, has been to view a structure's behaviour as intermediate between two extremes—a completely uncracked state (state 1) and a fully cracked state (state 2)—and then interpolate between these two using a suitable empirical distribution coefficient [3]. This has been the dominant approach, used by practically all codes, whether they perform this interpolation on the level of curvatures or deflections as the *fib* Model Code 2010 and Eurocode 2 do [4,5], or at the level of moment of inertia, as ACI 318 does [6].

Another approach that is becoming increasingly present is the use of finite element analysis (FEA) through powerful software capable of incorporating all necessary nonlinearities in the design, e.g. ABAQUS, DIANA, ANSYS [1]. Such programs are fast approaching a point where they will become 'practical, every-day tools for design office engineers' [7].

Nonetheless, both these analytical and numerical approaches require large numbers of reliable experimental results in order to calibrate their model parameters and validate them. For traditional, natural aggregate concrete (NAC), such databases exist and have been used for these purposes [8,9]. However, for the emerging field of green concretes, i.e. concretes produced with recycled and waste materials, such experiments are scarce. Two of the most promising green concretes are recycled aggregate concrete (RAC) and high-volume fly ash concrete (HVFAC). Unfortunately, even though their ULS behaviour has been relatively well-tested [10–13], their behaviour under sustained loads has been tested only a limited number of times in the case of RAC [14,15] and never in the case of HVFAC.

The aim of this study is to assess to possibility of using well-established analytical and numerical models for the calculation of deflections of reinforced RAC and HVFAC beams and perform a comparison with experimental results from an existing study [16].

2. DEFLECTION CALCULATION MODELS

2.1. EXPERIMENT BEING MODELLED

As stated in the previous section, in order to calibrate and validate deflection prediction models, reliable experimental results are necessary and in the area of green concretes they are scarce. Because of this, an experimental programme was carried out at the University of Belgrade's Faculty of Civil Engineering by Tošić et al. [16], in which the long-term behaviour of reinforced NAC, RAC and HVFAC beams was tested under sustained load. The experimental results of the study have been previously published in detail [16,17] and only the most important information will be presented here.

Three concrete mixes were prepared: NAC, RAC with 100% coarse recycled concrete aggregate (RCA) and HVFAC with fly ash comprising 50% of total cementitious materials. The basic mechanical properties of the concretes are given in Table 1.

Table 1 – Mechanical properties of the concrete mixes

Concrete	f_{cm} (MPa)		E_{cm} (MPa)		f_{ctm} (MPa)	
	7 days	28 days	7 days	28 days	7 days	28 days
NAC	24.7	30.5	30100	32200	2.0	2.4
RAC	24.2	28.1	26200	30800	2.0	2.5
HVFAC	16.4	22.6	25200	28700	1.2	2.1

Six simply supported, 3.2 m-span beams were produced, two beams from each mix. The beams had a 160 x 200 mm cross-section and 2Ø10 mm bars as tensile reinforcement (with an effective depth of 169 mm) and 2Ø6 mm bars as compressive reinforcement, Figure 1. The beams were loaded in four-point bending in thirds of their span.

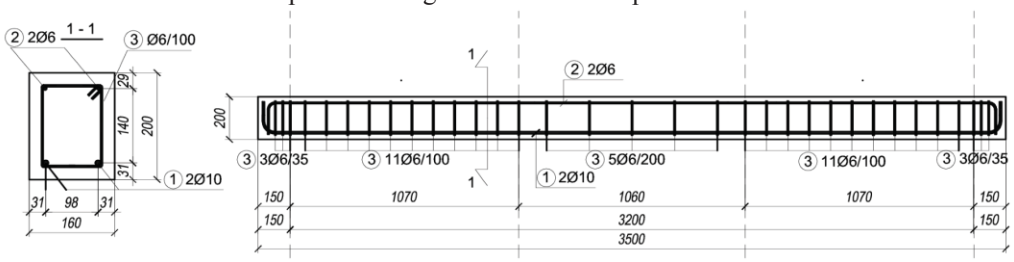

Figure 1 – Reinforcement layout of the beams

Constant stress-to-strength at loading age ratios, $\sigma_c/f_{cm}(t_0)$, were chosen for the beams: 0.6 for beams loaded after 7 days and 0.45 for beams loaded after 28 days. These ratios represent relatively higher stress levels for reinforced concrete structures, although not forbidden in practice, design of structural members according to ULS requirements can easily lead to high stress levels in service. However, such stresses (above 40–50% of compressive strength) do produce creep non-linearity [18] where the relationship between creep strain and stress

becomes non-linear. While these stress levels are high, they are still plausible in practice and codes such as Eurocode 2 and the *fib* Model Code 2010 have provisions for these cases [4,5].

On the beams, deflections were measured for 700 days using dial indicators. The applied bending moments on the beams and measured deflections are presented in Table 2.

Table 2 – Beam loads and measured deflections

Beam	M_{Ed} (kNm)	M_{Ed}/M_{cr}	M_{Ed}/M_{Rd}	$a(t_0)$ (mm)	$a(700)$ (mm)	$a(t_0)/a(700)$
NAC7	7.63	3.33	0.53	9.17	19.34	2.11
NAC28	6.84	2.49	0.48	8.11	17.22	2.12
RAC7	7.86	3.65	0.55	10.89	23.24	2.13
RAC28	6.36	2.45	0.44	6.23	15.52	2.49
HVFAC7	5.49	3.27	0.39	6.13	13.05	2.13
HVFAC28	5.35	2.59	0.38	4.04	9.48	2.20

Finally, shrinkage and creep were measured on accompanying 120 x 120 x 360 mm prisms for 700 days. However, creep was only measured on RAC and HVFAC specimens loaded after 7 and 28 days (RAC7, RAC28, HVFAC7 and HVFAC28) and not on NAC. The $\sigma_c/f_{cm}(t_0)$ ratios were the same as in the beams: 0.60 for RAC7 and HVFAC7 and 0.45 for RAC28 and HVFAC28. Table 3 presents the results on creep and shrinkage. It should be noted that the reported experimental creep coefficient, φ_{exp}, which represents the ratio of creep strain to initial strain, is actually the non-linear creep coefficient, i.e. is stress-dependent.

Table 3 – Beam loads and measured deflections

Beam	$\varepsilon_{cs}(700)$ (‰)	$\varphi_{exp}(700)$
NAC	0.680	–
RAC7	0.810	2.50
RAC28		2.69
HVFAC7	0.630	1.78
HVFAC28		1.75

2.2. ANALYTICAL APPROACH – *fib* MODEL CODE 2010

Analytical calculation of deflections in this study was performed using the *fib* Model Code 2010 model (MC2010) [4]. In its rigorous form, MC2010 is based on the interpolation of curvatures calculated in two states: state 1 (uncracked) and state 2 (fully cracked). The interpolation is performed at the cross-sectional level using a distribution coefficient ζ. For the case of pure bending, this distribution coefficient can be defined as

$$\zeta = \begin{cases} 1 - \beta \cdot \left(\frac{M_{cr}}{M}\right)^2 & \text{for } M \geq \sqrt{\beta} \cdot M_{cr} \\ 0 & \text{for } M < \sqrt{\beta} \cdot M_{cr} \end{cases} \tag{1}$$

where β is a coefficient accounting for the influence of the duration of loading or repeated loading and is taken as 1.0 for single short-term loading and 0.5 for sustained loads or multiple cycles of repeated loads [4]. Curvatures are then interpolated according to the following equation:

$$\left(\frac{1}{r}\right)_{eff} = \zeta \cdot \left(\frac{1}{r}\right)_2 + (1 - \zeta) \cdot \left(\frac{1}{r}\right)_1 \tag{2}$$

where $(1/r)_{eff}$ is the interpolated effective curvature, and $(1/r)_2$ and $(1/r)_1$ are curvatures in the fully cracked and uncracked states, respectively. The curvatures themselves are composed of a curvature due to load $(1/r)_{load}$ and curvature due to shrinkage $(1/r)_{cs}$:

$$\left(\frac{1}{r}\right)_n = K \cdot \frac{M \cdot l^2}{E_{c,ef} \cdot I_{i,n}} + \varepsilon_{cs} \cdot \alpha_e \cdot \frac{S_{i,n}}{I_{i,n}}; \;\; n = 1, 2 \tag{3}$$

where K is a coefficient depending on the static system (0.104 for a simply supported beam under uniformly distributed loading and 0.107 for a simply supported beam in four point bending in thirds of the span); $I_{i,n}$ is the moment of inertia of the transformed section in state 1 or 2; $S_{i,n}$ is first moment of area of the reinforcement about the transformed section's centroid (in state 1 or 2). The effect of creep is taken into account using the effective modulus $E_{c,ef}$:

$$E_{c,ef} = \frac{E_{cm}}{1 + \varphi_{cc}} \tag{4}$$

which also defines the modular ratio $\alpha_e = E_s/E_{c,ef}$ where E_s is the modulus of elasticity of reinforcement (may be taken as 200 GPa).

The shrinkage strain ε_{cs} in Equation (3) and creep coefficient φ_{cc} in Equation (4) can be calculated using the MC2010 shrinkage and creep models which will not be presented here in detail [4]. In this paper, curvatures were calculated in 50 cross-sections for each beam and a double numerical integration was performed to obtain deflections [2].

2.3. NUMERICAL APPROACH – DIANA

For a numerical calculation of deflections, the commercial software DIANA, developed by DIANA FEA (Delft, the Netherlands) was used. DIANA has been under development since 1972 and since then it has proven to be an extensive multi-purpose finite element software package DIANA includes extensive material models, element libraries and analysis procedures, based on the latest and the most advanced finite element analysis techniques.

In this study, the beams were modelled as plain stress elements, i.e. modelling was two-dimensional. For this purpose rectangular, 40 x 40 mm 4-node quadrilateral Q8MEM elements were chosen [19] with nodes at side endpoints , Figure 2. The beam supports and force application points were modelled with 60 x 60 mm steel plates also meshed with Q8MEM elements.

For modelling concrete, a smeared cracking approach was adopted. DIANA offers two distinct possibilities: a multi-directional fixed crack model which requires a separate choice of material models in compression and in tension, and a total strain model which requires the

input of a single stress–strain relationship [20]. In this study, the multi-directional fixed crack model was chosen. In compression, concrete was modelled as a linear-elastic material whereas in tension, the linear tension softening relation was chosen [20]. This relation requires the input of fracture energy G_F for which MC2010 also offers an expression [4]. Reinforcement was assumed to be linear-elastic.

Time effects, i.e. shrinkage and creep are compatible with this model and can be input directly in the form of previously calculated shrinkage and creep compliance (J_c) functions.

For the analysis, first the self-weight and imposed dead load are applied and then time steps are executed to calculate deflections over time. As the analysis procedure, the modified Newton-Raphson method was chosen [21].

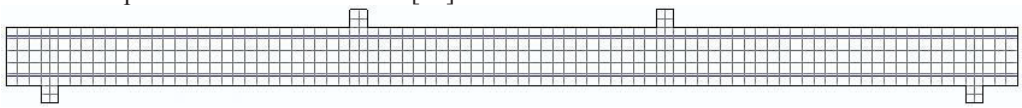

Figure 2 – Beam model in DIANA

3. RESULTS AND DISCUSSION

3.1. DEFLECTIONS CALCULATED USING MEASURED INPUT VALUES

In the first part of the analysis, in both the MC2010 and DIANA models, measured values of input parameters were used. Besides geometric and loading parameters, this included the compressive strength, modulus of elasticity, tensile strength, shrinkage strain and creep coefficient of the concretes. Since creep was not measured for NAC, beams NAC7 and NAC28 were not included in the analysis. Mechanical properties were taken from Table 2 and shrinkage strain and creep coefficient directly from measured results [22]. The only calculated/assumed values were 200 GPa for the modulus of elasticity of reinforcement and concrete fracture energy calculated using the MC2010 expression:

$$G_F = 73 \cdot f_{cm}^{0.18} \tag{5}$$

where compressive strength is entered in MPa and fracture energy is obtained in N/m.

This approach of using measured values for input parameters should provide an optimal assessment of the deflection model itself, eliminating further uncertainties that are introduced when input parameters are predicted from code expressions based on compressive strength. In other words, these results are expected to be in good agreement with experimental values if the models are adequate. The results for deflections are shown in logarithmic time scale in Figure 3 for RAC beams and Figure 4 for HVFAC beams.

The figures reveal interesting conclusions. First of all, with both DIANA and MC2010, deflections are better predicted for RAC than for HVFAC beams. For RAC beams the agreement between DIANA and MC2010 and experimental values of 'final' deflections (after 700 days) is within 10%. For all four beams, the agreement between the predictions by DIANA and experimental results is excellent, within 15% (the differences decrease over time). At the same time, the predictions by MC2010 do not fit experimental results equally well. In the case of RAC beams the initial deflections are overestimated by up to 10% and the difference decreases over time. However, for HVFAC, especially for beam HVFAC28, the overestimation is very significant: the initial deflection of beam HVFAC is overestimated by 145%.

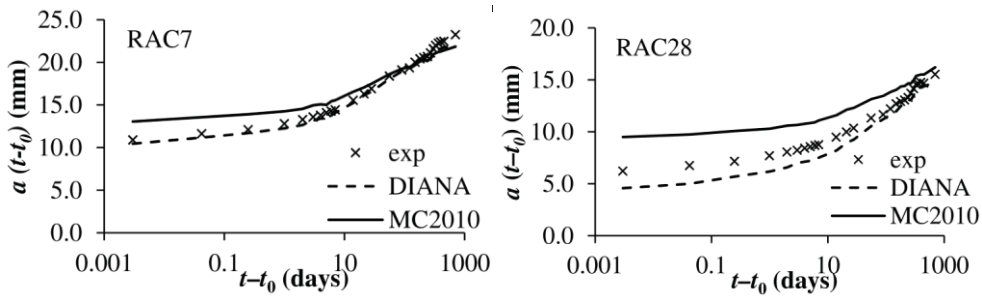

Figure 3 – Comparison of experimental and calculated RAC deflections (measured inputs)

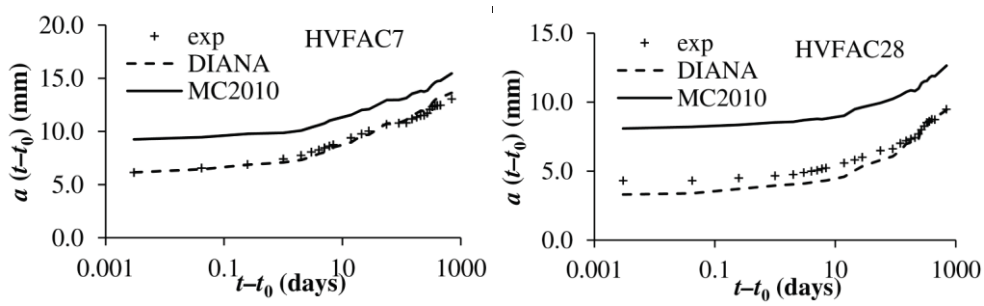

Figure 4 – Comparison of experimental and calculated HVFAC deflections (measured inputs)

These results reveal that tension stiffening, as it is modelled in the MC2010 analytical model, can be inadequate for predicting deflections of reinforced concrete beams, albeit with predictions on the safe side. Meanwhile, the smeared cracking approach with linear tension softening, modelled in DIANA, behaves excellently in predicting deflections of all the beams.

3.2. DEFLECTIONS CALCULATED USING CODE-PREDICTED INPUT VALUES

In this phase, instead of using measured values of input parameters, all of them (modulus of elasticity, tensile strength, shrinkage strain, creep coefficient, fracture energy) were predicted using MC2010 expressions based on compressive strength. In this case, deflections of NAC beams could be calculated. This approach has the effect of testing a wider range of a model's capabilities, not only its deflection model but also the quality of mechanical and time-dependent property predictions. Additionally, since standard MC2010 expressions would be used for RAC and HVFAC beams, they would reveal whether these expressions are also suitable for green concretes.

As the beams were loaded to high $\sigma_c/f_{cm}(t_0)$ ratios, non-linear creep effects had to be taken into account for stresses above $0.4f_{cm}(t_0)$ [4]. Above this limit, up to stresses equal to $0.6f_{cm}(t_0)$, the simplified non-linear creep coefficient given by MC2010 can be used [4]. In this study, the approach described by Tošić et al. [16] was used: after calculating the stress distribution after loading, the non-linear creep coefficient was applied to the part of the cross-section which surpassed the linear creep limit of $0.4f_{cm}(t_0)$ and the linear creep coefficient was applied to the remaining part of the cross-section.

The results for deflections are shown in logarithmic time scale in Figures 5, 6 and 7 for NAC, RAC and HVFAC beams, respectively.

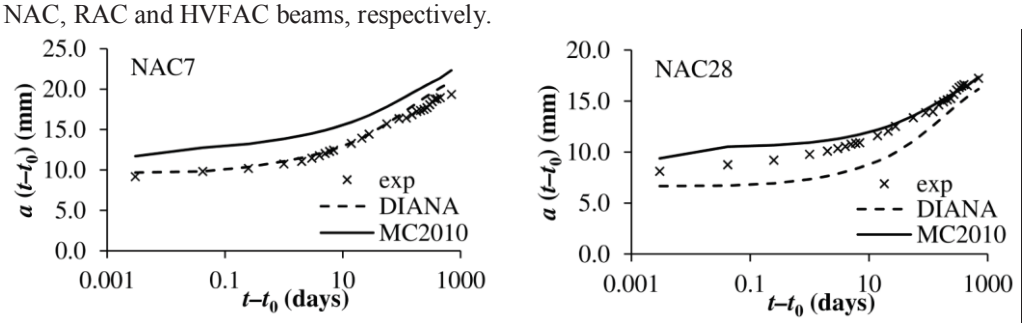

Figure 5 – Comparison of experimental and calculated NAC deflections (calculated inputs)

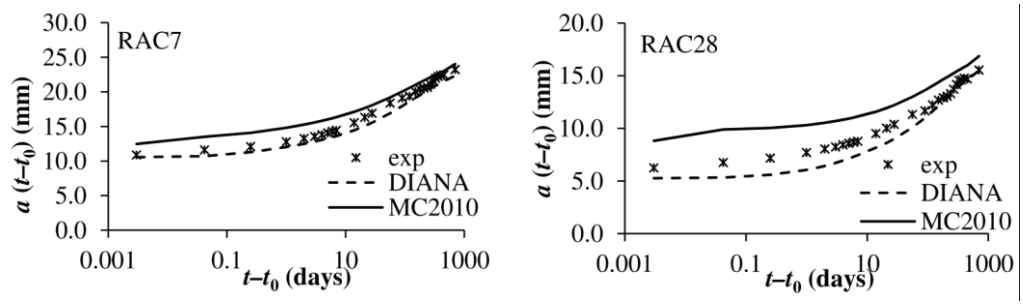

Figure 6 – Comparison of experimental and calculated RAC deflections (calculated inputs)

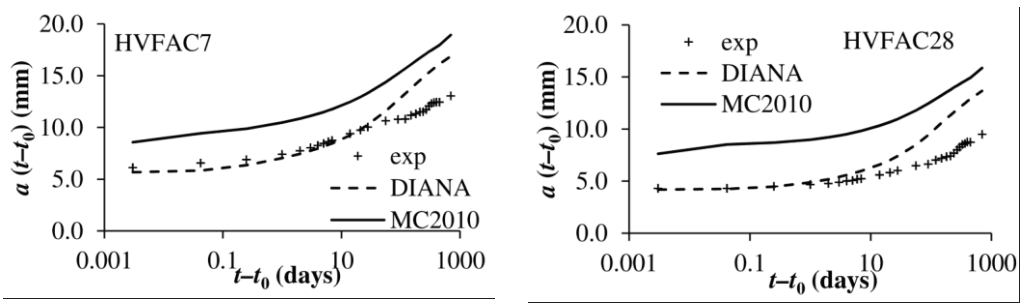

Figure 7 – Comparison of experimental and calculated HVFAC deflections (calculated inputs)

Figures 5, 6 and 7 reveal a different trend compared with Figure 3 and 4. When using measured values of input parameters, the DIANA model fit experimental deflections excellently, whereas when code-predicted input values are used, the prediction by DIANA show poorer agreement – for beams NAC7, RAC7 and RAC28 the agreement is still very good, however, for the remaining beams the deflections are either underestimated (NAC28) or they diverge from experimental values over time (HVFAC7 and HVFAC28). While the differences in the case of NAC and RAC beams are not so significant (up to 15%), for HVFAC beams the differences between DIANA predictions and experimental results are up to 44% (HVFAC28 after 700 days).

In the case of MC2010 predictions, the situation is similar, the predictions for NAC and RAC beams are again on the safe side (up to 30% in the case of initial deflections of beam NAC7); however, for HVFAC beams the differences are between 40% and 75%.

These results show that in this case, the use of code-predicted input parameters is suitable for NAC and RAC beams, probably with minor corrections needed for RAC beams, in accordance with previous studies [15]. However, for HVFAC beams, there seems to be a significant difference compared with NAC beams, probably at the level of tension stiffening, which requires a different model to be formulated for these concretes.

4. CONCLUSIONS

This study presented the results of analytical and numerical calculations of long-term deflections of NAC, RAC and HVFAC beams under sustained load and their comparison with experimental results. Based on the analyses carried out using the MC2010 analytical model and the DIANA numerical model, the following conclusions can be drawn:

- If experimentally obtained values of model input parameters are used (mechanical and time-dependent properties of concrete), very good agreement can be found with experimentally measured deflections of RAC and HVFAC beams in the case of the DIANA numerical model. In the case of the MC2010 analytical model, good agreement is found for RAC beams, whereas the deflections of HVFAC beams are significantly overestimated;
- If code expressions are used to calculate values of input parameters, the agreement between calculated and measured deflections decreases for all beams and for both the MC2010 and DIANA models, with DIANA still showing better results. While predictions for NAC and RAC beams are satisfactory, considering all sources of uncertainty, the deflections of HVFAC beams are significantly overestimated by both models, pointing to the need of formulating a new tension stiffening model for HVFAC.

ACKNOWLEDGEMENTS

The work reported in this paper is funded under grant TR 36017 by the Ministry for Education, Science and Technology, Republic of Serbia.

REFERENCES

[1] FIB Bulletin 52, Structural Concrete - Textbook on Behaviour, Design and Performance, International Federation for Structural Concrete (fib), Lausanne, 2010. doi:10.1017/CBO9781107415324.004.

[2] A.W. Beeby, S. Narayanan, Designer's guide to Eurocode 2: Design of concrete structures, Thomas Telford, London, 2005.

[3] A. Ghali, R. Favre, M. Eldbadry, Concrete Structures. Stresses and Deformation, Taylor & Francis, New York, 2002.

[4] FIB, fib Model Code for Concrete Structures 2010, International Federation for Structural Concrete (fib), Lausanne, 2013. doi:10.1002/9783433604090.

[5] EN 1992-1-1, Eurocode 2: Design of concrete structures - Part 1-1: General rules and rules for buildings, CEN, Brussels, 2004.

[6] ACI 318-11, Building code requirements for structural concrete (ACI 318-11) and commentary, American Concrete Institute, Farmington Hills, MI, 2011.

[7] FIB Task Group 4.4, Practitioner's guide to finite element modelling of reinforced concrete structures, FIB, Lausanne, 2008.

[8] B. Espion, Long-Term Sustained Loading Test on Reinforced Concrete Beams, Université Libre de Bruxelles Service Génie Civile, Brussels, 1988.

[9] B. Espion, P. Halleux, Long-Term Deflections of Reinforced Concrete Beams: Reconsideration of Their Validity, ACI Struct. J. 87 (1990) 232–236.

[10] A.B. Ajdukiewicz, A.T. Kliszczewicz, Comparative tests of beams and columns made of recycled aggregate concrete and natural aggregate concrete, J. Adv. Concr. Technol. 5 (2007) 259–273. doi:10.3151/jact.5.259.

[11] J. Pacheco, J. De Brito, D. Soares, Destructive Horizontal Load Tests of Full-scale Recycled Aggregate Concrete Structures, ACI Struct. J. 112 (2015) 815–826.

[12] J. Xiao, C.Q. Wang, J. Li, M. Tawana, Shake-table model tests on recycled aggregate concrete frame structure, ACI Struct. J. 109 (2012) 777–786.

[13] M. Arezoumandi, J.S. Volz, C.A. Ortega, J.J. Myers, Effect of total cementitious content on shear strength of high-volume fly ash concrete beams, Mater. Des. 46 (2013) 301–309. doi:10.1016/j.matdes.2012.10.031.

[14] A.M. Knaack, Y.C. Kurama, Sustained Service Load Behavior of Concrete Beams with Recycled Concrete Aggregates, ACI Struct. J. 112 (2015) 565–578. doi:10.14359/51687799.

[15] S. Seara-Paz, B. González-Fonteboa, F. Martínez-Abella, D. Carro-Lopez, Long-term flexural performance of reinforced concrete beams with recycled coarse aggregates, Constr. Build. Mater. 176 (2018) 593–607.

[16] N. Tošić, S. Marinković, N. Pecić, I. Ignjatović, J. Dragaš, Long-term behaviour of reinforced beams made with natural or recycled aggregate concrete and high-volume fly ash concrete, Constr. Build. Mater. 176 (2018) 344–358.

[17] N. Tošić, Behaviour of reinforced concrete beams made with recycled and waste materials under long-term loading, University of Belgrade, 2018.

[18] Z.P. Bažant, M. Jirasek, Creep and Hygrothermal Effects in Concrete Structures, Springer, Dordrecht, 2018.

[19] J. Manie, W.P. Kikstra, DIANA User's Manual - Element Library, Delft, 2017.

[20] J. Manie, W.P. Kikstra, DIANA User's Manual - Material Library, Delft, 2017.

[21] J. Manie, W.P. Kikstra, DIANA User's Manual - Analysis Procedures, Delft, 2017.

[22] N. Tošić, S. Marinković, I. Ignjatović, J. Dragaš, V. Carević, Experimental measurements on the behaviour of reinforced NAC,RAC and HVFAC beams under sustained loads, Mendeley Data, V1. (2017). doi:10.17632/86mvvjr65h.1.

ДГКС Друштво грађевинских конструктера Србије
ASES Association of Structural Engineers of Serbia
S-73
15. KONGRES
6-8. 9. 2018. Zlatibor

Slobodan Ranković[1], Bojan Milošević[2], Žarko Petrović[3], Marina Mijalković[4]

ISPITIVANJE OŠUPLJENIH PRETHODNONAPREGNUTIH ELEMENATA ZA MEĐUSPRATNE KONSTRUKCIJE

Rezime:

U rada su prikazani rezultati ispitivanja, pod uticajem probnog opterećenja, međuspratne konstrukcije od prethodnonapregnutih ošupljenih betonskih nosača spregnutih sa betonskom pločom livenom na licu mesta. Uporedno su dati i rezultati ispitivanja pojedinačnog ošupljenog nosača. Izvršena je uporedna analiza rezultata merenih globalnih deformacija (ugiba) u polovini raspona i lokalnih deformacija (dilatacija – napona) u konstruktivnim elementima (betonu nosača, betonu ploče i kablovima za prednaprezanje). Ispitivanje pod probnim opterećenjem vršeno je za uticaje eksploatacionog opterećenja i uticaje do postizanja traženog koeficijenta sigurnosti.

Ključne reči: Ošupljena betonska ploča, ispitivanje, sprezanje betona betonom

TESTING OF HOLLOWED PRESTRESSED ELEMENTS FOR FLOOR SLABS

Summary:

In the paper are presented the test results obtained under the impact of floor slabs made of pre-stressed hollowed concrete girders composed with the concrete slab cast in situ. Comparatively provided are the results of testing of an individual hollowed girder. A comparative analysis of results of the results measured by global deformations (deflections) at mid span and local deformations (strains-stresses) in the structural elements (girder concrete, slab concrete and pre-stressing cables) is performed. The examination under test load is performed for the service load impacts, and of the impacts until reaching the required safety coefficient.

Key words, Hollowed concrete slab, testing, concrete-concrete coupling

[1] *Assistant Prof. PhD, Faculty of Civil Engineering and Architecture, University of Niš, Republic of Serbia, slobodan.rankovic@gaf.ni.ac.rs*
[2] *Prof. PhD, College of Applied Studies in Civil Engineering and Geodesy, University of Belgrade, Republic of Serbia, prodic_80@yahoo.com*
[3] *Assistant Prof. PhD, Faculty of Civil Engineering and Architecture, zarko.petrovic@gaf.ni.ac.rs*
[4] *Full Prof. PhD, Faculty of Civil Engineering and Architecture, marina.mijlkovic@gaf.ni.ac.rs*

1. INTRODUCTION

Hollowed adhesively pre-stressed concrete elements for production of floor slabs have been manufactured according to a licensed technology in the production facilities in our country for many years. They are produced using the extrusion method with cable pre-stressing and cutting to pre-designed lengths. Considering the concrete designing requirements for construction of buildings and for locally available materials, there is a need for an experimental verification of their mechanical characteristics. The effects of composing of the prefabricated girders with in situ cast concrete are particularly important for making specific conclusions about bearing capacity and serviceability of the mentioned structure. On the basis of the manufacturer's request, in April this year an experimental analysis of floor slab made of the mentioned hollowed prefabricated elements and elements themselves was performed.

Characteristics of the HCS200 tested elements

Examination of the effects of test load was performed for a specific case of designing of floor slab of approximately 700 m^2 and for a useful load of 670 daN/m^2. The HCS 200 elements 120 cm wide and 20 cm high (thick) were tested, in the specific case the total lengths amounts to 766 cm. The class of concrete they are made of was C50/60. Confining was performed using cables Y1860 S7, (5∅12,5 + 2∅9,3 mm). The thickness of the slab being cast ("topping") over the element was d=6 cm. The geometrical characteristics and position of the cables are provided in the figures.

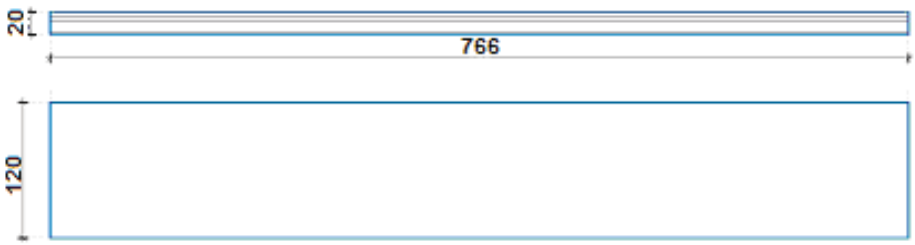

Figure 1 - Dimensions of the tested element HCS 200

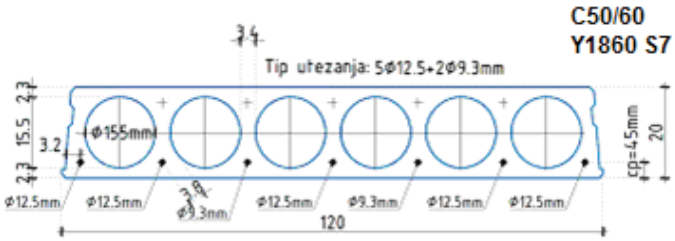

Figure 2 – Cross-section of the HCS 200 tested element

2. EXPERIMENTAL SETUP AND TESTING PROGRAM

Experimental setup

Regarding the real conditions in the service, which include composing of prefabricated elements with the slab cast in situ, the test load was performed on a slab produced in the same way. A platform was installed on which three HCS 200 elements were set, and joined by casting a top slab having thickness d=6 cm. The measurements were performed for the effects of the own weight of slab casting. The prefabricated elements having span of 766 cm were rested on the concrete cubs of 13 cm, so the free span was 740 cm, and the static span 753 cm. One (control) HCS 200 element for testing is set individually without casting a slab, and it had a role of a control (benchmark) element. Dynamical tests were also performed, for defining of dynamical parameters (frequency and damping), but being extensive, they are not presented here.

Types of load (static distributed load)

The test (replacement) load was applied using the concrete elements having the form of rectangular parallelepiped having dimensions (60/60/150 cm) which are used in construction of retaining walls. The weight of an individual element is 1300 kg. These elements are distributed in steps on the previously marked chessboard 1,2 m x 1,53 m. In the first phase was tested the impact of additional permanent load of g=420 daN/m2 and useful load of p=250 daN/m2, i.e. a total of q=670 daN/m2. In the second phase of testing of the safety coefficient, other concrete elements were also used until the required load was achieved (q=1,35g+1,50p). The testing procedure was conducted in compliance with the standard SRPS U.M1.047. The test load was applied in two phases.

Loading phases

In phase I (service load) on the elements of the floor slab, a maximum service load of q=700 daN/m^2 was applied in 4 steps. The load was retained for 16 hours, after which it was unloaded and residual values of stress and strain (deflections and dilatations) were read. During application of the load, a potential emergence of cracks in concrete was monitored. In phase II of the load (safety coefficient test phase) 135% of own weight and 150% of service load was applied. The load was applied in multiple steps with reading out of measured values on the instruments and monitoring of cracks emergence. Regarding that the own weight of the element was g=250 daN/m^2 and that of the concrete topping of d=6 cm was g=150 daN/m^2, i.e. the additional permanent load g_d=420 daN/m^2, and the useful load p=250 daN/m^2, the required load amounted to q_{potr}=(0,35×400+1,35×420+1,50×250) =1080daN/m^2. The total applied load was q_{max}=1130 daN/m^2. (8×1300 kg ×3).

Measuring

Global deformation of elements (deflections) under the test load are followed by measuring the vertical displacement at the mid span via inductive transducers (LVDT) whose parameter is 1/100 mm, and by measuring the inclination using clinometers with the parameter of 1,055". Measuring dilatations in steel cables and concrete was performed using strain gauges with the gauge length of 3 mm for steel and 50 mm for concrete with the parameter ($p=1\times10^{-6}$). Dilatations in concrete were measured on the top surface of prefabricated elements and on the top surface of newly cast concrete in order to define the composite effects along the height of a girder. Stresses were calculated for the known value of modulus of elasticity of the used

materials (steel and two types of concrete. Measurements were also performed for the effects of the own weight of the concrete slab cast in situ.

Arrangement of measuring locations and measuring instruments placed according to the principle of "surrounding cross-section" is presented in figure 3. The deflection at the mid span, deflection over support points, strains in pre-stressing cables, strains in concrete of prefabricated elements and strain in the concrete cast in situ were monitored.

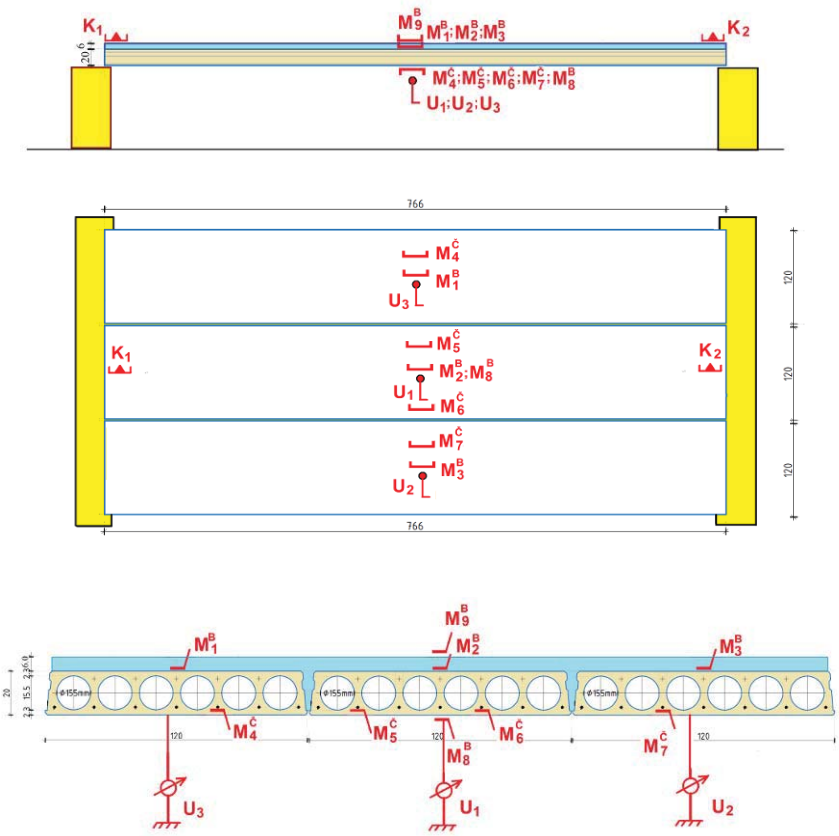

Figure 3 – Arrangement of measuring instruments during testing of floor slab made of HCS 200 elements.

3. TEST RESULTS

3.1. HCS 200 ELEMENTS COMPOSED WITH THE CONCRETE SLAB

I phase – Service load

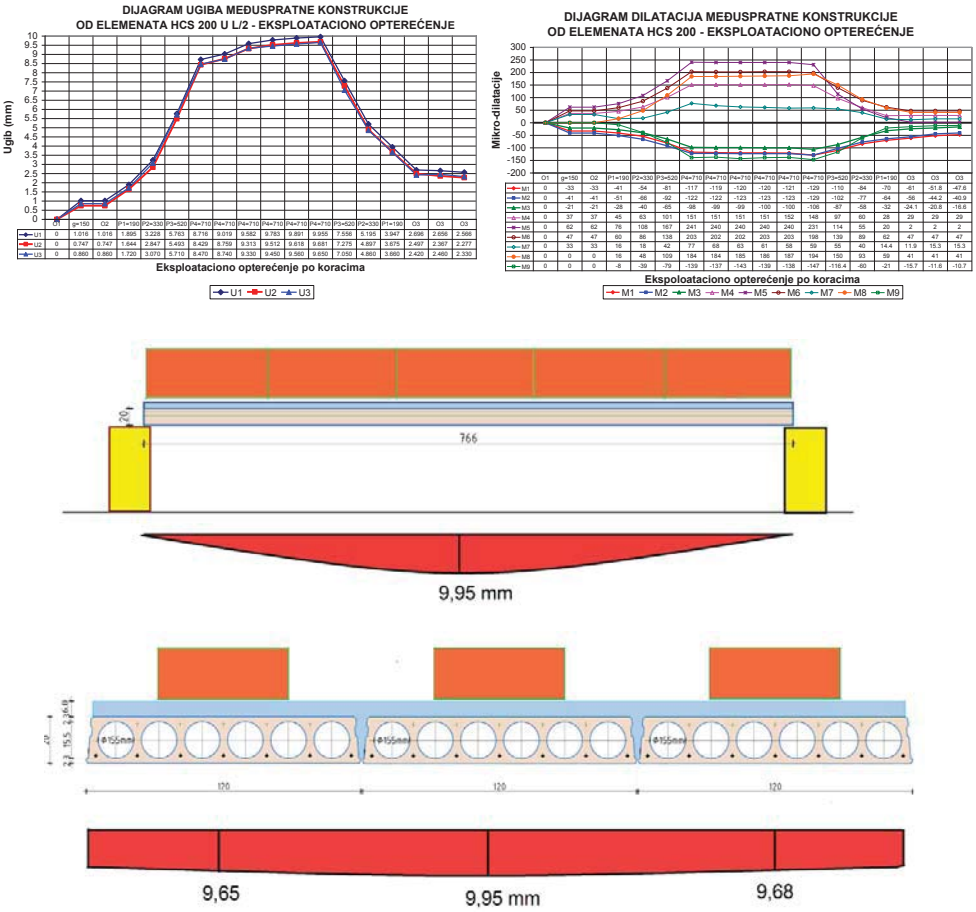

Figure 4 – Disposition of the tested floor slab in the service load phase, and values of maximum measured deflections (q=700 daN/m^2)

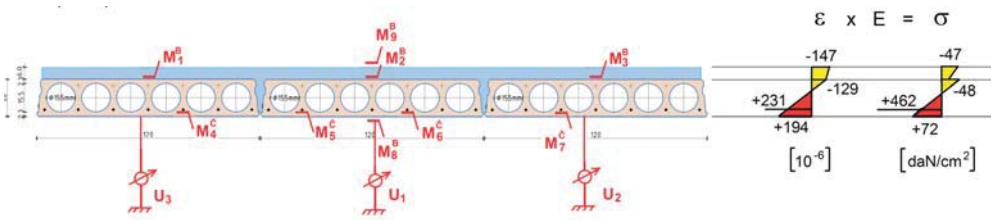

Figure 5 – Diagram of maximum of measured strains (stresses) under service load

3.2. INDIVIDUALLY LOADED HCS 200 ELEMENTI

I phase – Service load

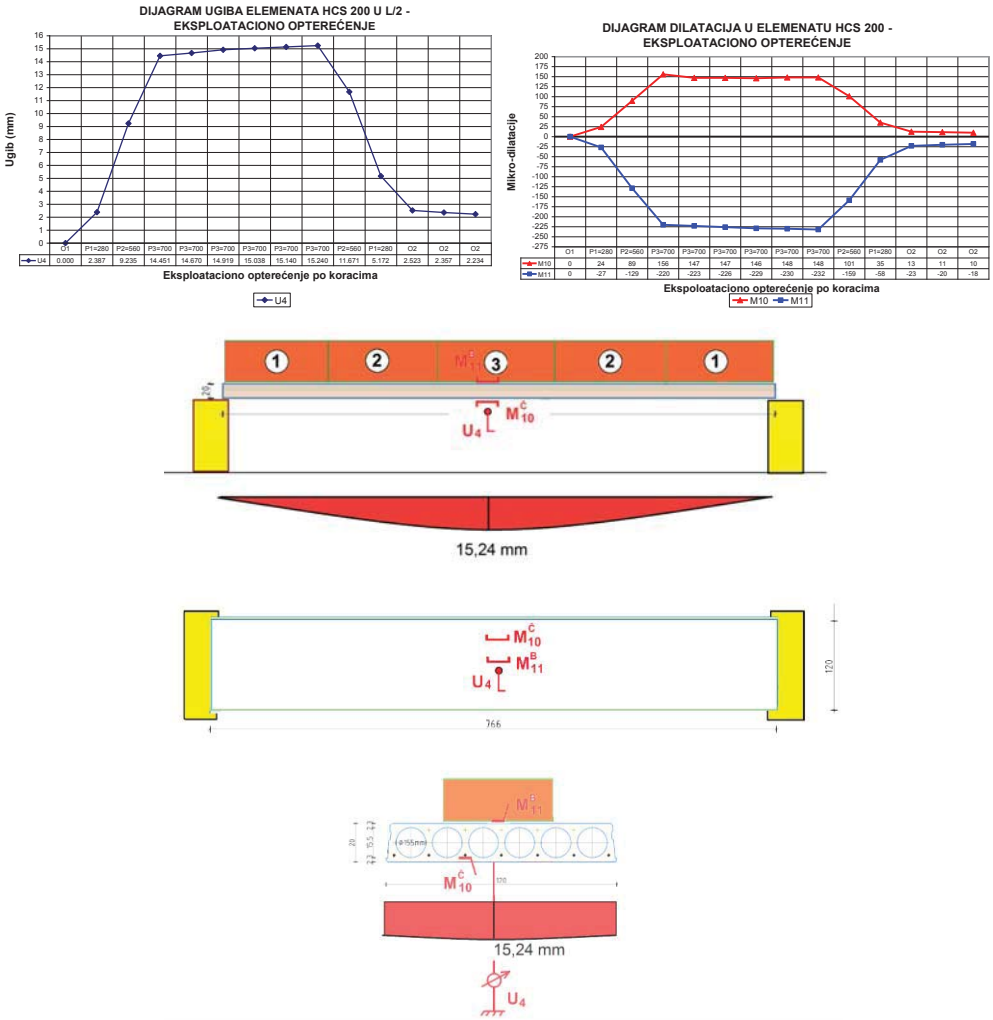

Figure 6 – Disposition of the tested floor slab in the service load phase, and values of maximum measured deflections (q=700 daN/m^2)

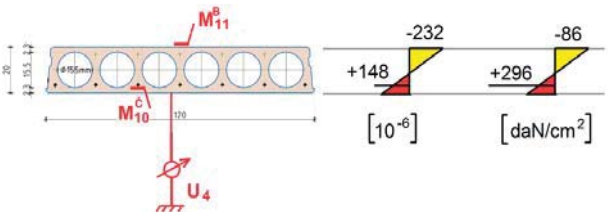

Figure 7 – Diagram of maximum of measured strains (stresses) under service load

4. ANALYSIS OF THE TEST RESULTS

Under service load (q=700 daN/m^2) of the floor slab with HCS 200 elements, using a comparative analysis of experimentally obtained results and calculation results obtained from the original software package of the license supplier, it was established that: 1) Maximum deflection in relation to the span is 1/842<*l*/200, 2) Residual deflection is 17%<20%, 3) Ratio of the calculated and maximum measured deflection is 2,66>1; 4) Measured strains in the cables are ε=+0,23‰ i.e. stress σ=+462 daN/cm^2; 5) Measured strains in the concrete element are ε=-0,13‰ i.e. stress σ=-48 daN/cm^2; 6) Measured strains in the cast slab concrete are ε=-0,15‰ i.e. stress σ=-47 daN/cm^2 and they are lower than the calculated and permitted values; 7) Failure coefficient is higher than the required safety coefficient at the load of q=1130 daN/m^2. There were no cracks emerging at the service load, while at safety coefficient, their maximum was δ=0,05 mm. Dynamic parameters, which are not discussed here were also satisfactory. By comparing the value of the deflection of the floor slab obtained by composing of the HCS200 prefabricated elements and the slab cast in situ, and of the loaded individual HCS 200 element, the results as in table 1 are obtained 1. From them, significance and efficiency of composing two concretes are evident, because the values of deformations are 171%, i.e. 347% lower for the action of composite structure. This directly affects bearing capacity and serviceability of the HCS200 elements.

Table 1- Deflections values at mid span

	Deflection at mid span (mm)		
	At service load q=700daN/m^2 (y_{exp})	At safety coefficient load q=1130daN/m^2 (y_S)	Calculated (y_{cal})
HCS 200+"topping"	8,93	17,97	23,80
HCS 200	15,24	62,30	64,40
η (%)	171	347	271

5. CONCLUSIONS

Based on the results of the measured values of deformations and their comparison with the calculated values, it is concluded that the floor structure from the HCS200 prefabricated hollowed concrete elements behaved quite stiffer, i.e. that the measured parameters are lower than the calculated ones. The reason is the higher efficiency of composition realized between the prefabricated elements and slab cast in situ, in comparison with the calculation assumptions. It is necessary to pay an additional attention to that bond and the increasing the degree of the composite, because increasing the bond at the interface of two concretes, even better results in terms of stiffness could be achieved, and indirectly in terms of bearing capacity of the structural system. In practice, in production, this bond is realized through making the upper surface of prefabricated concrete rough, that is, by friction. With additional connecting means, i.e. with a sort of connecting bolts, the bonding degree would be certainly higher. And the efficiency of the structure, i.e. its bearing capacity would be additionally improved. This

can be most evidently concluded based on measuring the obtained ratio of deformation of composed and non-composed HCS 200 girders (171%, i.e. 347% lower deflection).

6. PHOTO DOCUMENTS FROM THE TESTING

Photo 1 - Presentation of the test load on the floor slab for service load p_{exp} = 700 daN/m^2,(y_{max}=9,95 mm)

Photo 2 - Presentation of the test load on the floor structure for the realized safety coefficient q_{max}=1,35g+1,50p=1130 daN/m^2,(y_{max}=20,54 mm)

Photo 3 - Presentation of the test load on the HCS 200 element for service load p_{exp} = 700 daN/m^2 (y_{max}=15,14 mm)

Photo 4 – Presentation of the test load on the HCS 200 element for the realized safety coefficient q_{max}=1,35g+1,50p=1130 daN/m^2,(y_{max}=62,30 mm)

ACKNOWLEDGEMENT

This research is supported by The Ministry of Education, Science and technological development of the Republic of Serbia, within the framework of the projects Development and improvement of methods for analyses of soil-structure interaction based on theoretical and experimental research (TR 36028) and Development and implementation of a comprehensive approach to the design of new structures and safety evaluation of existing structures in order to reduce seismic risk in Serbia (TR 35043) for the period 2011-2018.

LITERATURA

[1] Izveštaj o ispitivanju br. IK 05/18: *Ispitivanje međuspratne konstrukcije od ošupljenih prethodnonapregnutih elemenata-HCS 200 i element-HCS 200*, GAF Niš, April 2018.

[2] Radojković, M.: Ispitivanje konstrukcija, Građevinska knjiga, Beograd, 1979

ДГКС Друштво грађевинских конструктера Србије
ASES Association of Structural Engineers of Serbia
S-74
15. KONGRES
6-8. 9. 2018. Zlatibor

Anka Starčev-Ćurčin[1], Andrija Rašeta[2], Mirjana Malešev[3], Danijel Kukaras[4], Đorđe Lađinović[5], Miloš Šešlija[6]

PROCENA NOSIVOSTI ARMIRANOBETONSKOG ZIDA DIMENZIONISANOG STRUT-AND-TIE METODOM

Rezime:

U ovom radu analizirana je nosivost armiranobetonskog zidnog nosača koji je dimenzionisan metodom pritisnutih štapova i zatega, tzv. Strut-and-Tie metodom. Metoda koristi ekvivalentni rešetkasti nosač kojim je modeliran zidni nosač. Automatsko određivanje Strut-and-Tie modela i dimenzionisanje armiranobetonskog ravanskog nosača urađeno je korišćenjem sopstvenog programa "ST method" u koji je implementirana Strut-and-Tie metoda. Procena nosivosti urađena je primenom nelinearne analize, u programu Abaqus, pri čemu je nosač izložen monotono rastućem statičkom opterećenju.

Ključne reči: procena nosivosti, Strut-and-Tie metoda, nelinearna analiza

STRENGTH ASSESSMENT OF THE REINFORCED CONCRETE WALL DESIGNED BY STRUT-AND-TIE METHOD

Summary:

In this paper the strength of the reinforced concrete wall is analyzed, which is designed by the method of compressed and tensioned elements, so-called Strut-and-Tie method. The method uses an equivalent truss to model the wall member. The automatic determination of the Strut-and-Tie model and design of the reinforced concrete plane member was done using self-developed "ST method" program, in which the Strut-and-Tie method is implemented. The strength assessment was made using the nonlinear analysis in the Abaqus commercial program, where the member is exposed to a monotonically increasing static load.

Key words: strength assessment, Strut-and-Tie method, nonlinear analysis

[1] *Assistant professor, PhD, University of Novi Sad, Faculty of Technical Sciences, astarcev@uns.ac.rs*
[2] *Assistant professor, PhD, University of Novi Sad, Faculty of Technical Sciences, araseta@uns.ac.rs*
[3] *Full professor, PhD, University of Novi Sad, Faculty of Civil Engineering, miram@uns.ac.rs*
[4] *Associate professor, PhD, University of Novi Sad, Faculty of Civil Engineering, danijel.kukaras@gmail.com*
[5] *Full professor, PhD, University of Novi Sad, Faculty of Technical Sciences, ladjin@uns.ac.rs*
[6] *Assistant, MSc, University of Novi Sad, Faculty of Technical Sciences, slavijasrb@gmail.com*

1. INTRODUCTION

Elements with a geometric and/or static discontinuity can be designed by the Strut-and-Tie method. The method can be applied to the entire member, but it is especially suitable in areas of complex path of internal forces. Basically, the Strut-and-Tie model represents an equivalent truss that consists of elements in compression - struts, and elements in tension - ties, and of the regions of their intersections, so-called, nodal zones, all of which have predefined dimensions. The principle of the method is that the concrete parts of the reinforced concrete element are replaced by struts, while the reinforcement is replaced with ties, [1], [2], [3] and [4].

The Strut-and-Tie model is well designed if the strengths of each compressed and tensioned element of the equivalent truss, as well as the strength of nodes are higher than the design requirements. The safety of the Strut-and-Tie approach depends on whether or not the stress limitations in the Strut-and-Tie model elements are defined according to the regulations. Also, the Strut-and-Tie models must be checked for their ultimate limit strength state.

The algorithmic approach of the Strut-and-Tie method gives the possibility of providing a software solution in the form of a program so that the application of the Strut-and-Tie model can be simplified as much as possible. In this paper, for the analysis purposes, the "ST method" program was used, in which the Strut-and-Tie method for the design of reinforced concrete plane members is implemented, [5] and [6].

In this paper the reinforced concrete wall member is analyzed and designed by means of the Strut-and-Tie method in the "ST method" program for which the strength assessment is done according to nonlinear static analysis in the Abaqus commercial program.

2. STRENGTH OF RC ELEMENTS DESIGNED BY STRUT-AND-TIE METHOD

Numerical and experimental tests indicate that reinforced concrete members that are designed by the Strut-and-Tie method have a higher strength than the designed one. In the continuation of this chapter the papers and their conclusions, that confirm this fact, are briefly described.

In the paper [7], the combinations of two different Strut-and-Tie models were used for design of four deep beams, with scaled sizes, simply supported, with a large hole as a geometric discontinuity and loaded with concentrated ultimate force. The goal of the research is to confirm the basic principles of Strut-and-Tie modeling by experimentally testing of a series of deep beams with a large opening, near the left support, designed by the Strut-and-Tie approach. By combining the two basic Strut-and-Tie models taken from the existing literature, four different reinforcement layouts were obtained. All models were tested by applying the load, with the same concentrated force, until failure. The behavior of the model was continuously monitored while the load was gradually increasing. Each model had its own crack pattern, strength capacity, displacement and failure mode. All samples endured a force greater than the design one on the basis of which the elements of the model were designed. This confirms that by choosing the Strut-and-Tie method as the design technique we obtain safer

structures and that the method is conservative. Experimental testing demonstrated the reliability and predictability of the Strut-and-Tie modeling technique.

The paper [8] presents the experimental results of a scaled simply supported deep beam, with a variable height and an opening. Four samples with same dimensions and loads, in the form of a concentrated force, were examined and, for each, different crack pattern was obtained. The obtained failure force was higher for all models when compared to the designed force which was used for the structural design of the model. This confirmed the conservative nature of the Strut-and-Tie method when used for the design of reinforced concrete members, especially ones with complex geometries. It was also confirmed that a real member can be modeled with several different models, but the choice of one solution can, for example, be influenced by the arrangement of the reinforcement, such as the orthogonal arrangement of reinforcing bars, due to the simpler execution of the reinforced concrete element.

Experimental results of the members with complex geometry, simply supported with reduced height and with an opening, which are designed using the Strut-and-Tie method are presented in the paper [9]. The test was done in two phases. In the first phase, six samples with a lower scaling value were tested. Five samples had the same geometry but different reinforcement arrangement, depending on the adopted Strut-and-Tie model. The last, sixth, sample was tested without reinforcement in order to determine the strength capacity of the element and to obtain the crack pattern, relying only on the tension strength of the concrete. In the second phase, two samples with the same load transfer scheme were tested as was in the first phase, but samples were scaled with a higher value. The expression was given in the paper that connects the scaling values of the first and second phases. One sample was reinforced and the other was not. When compared to the corresponding sample from the first phase, the crack pattern of the reinforced sample from the second phase was almost identical. Also, the proposed ratio of the scaling value of the samples of the first and second phases matched with the value of the failure load. In the samples of the first and second phases that were without reinforcement, the scaling values for the failure load value were not expected, as well as the crack pattern, i.e. the failure mode, what reiterated the unreliability of the behavior of the concrete element without reinforcement. This means that it is necessary for the reinforcement to allow tension to appear within the strut by placing it perpendicularly to the strut length what reduces the concrete contribution to the load bearing. The results showed that different Strut-and-Tie models can provide required strength capacity and safety of a reinforced concrete member, but the behavior of the element is significantly different, indicating the indeterminacy of the method. All reinforced concrete samples have higher load bearing capacity than the one required by the design technique.

In the paper [10], four deep beams of the same span, height and thickness were experimentally tested. The two beams had one asymmetrically arranged opening, in the lower left corner, near the support. The remaining two beams had two asymmetrically arranged openings, in the left lower corner and in the right upper corner of the member. All members were designed according to the Strut-and-Tie method. The various truss models adopted for the member design have influenced the different reinforcement layouts in the members. All members have sustained higher load than the design ones, which again indicates the indeterminacy of the Strut-and-Tie method. The results of the tests indicate the differences between the designed and the measured load values for all members, i.e. the measured strength values were higher.

3. NUMERICAL ANALYSIS

In this paper the reinforced concrete wall member wuth 6.1 m span, 3.8 m height and 50 cm thickness is analyzed. The member is a simply supported static beam system, loaded with two concentrated, ultimate limit, forces of 1600 kN located in the third of the span at the level of the upper edge of the member, Fig. 1. The characteristics of the applied materials are as follows: concrete C30/37 and the reinforcement B500C.

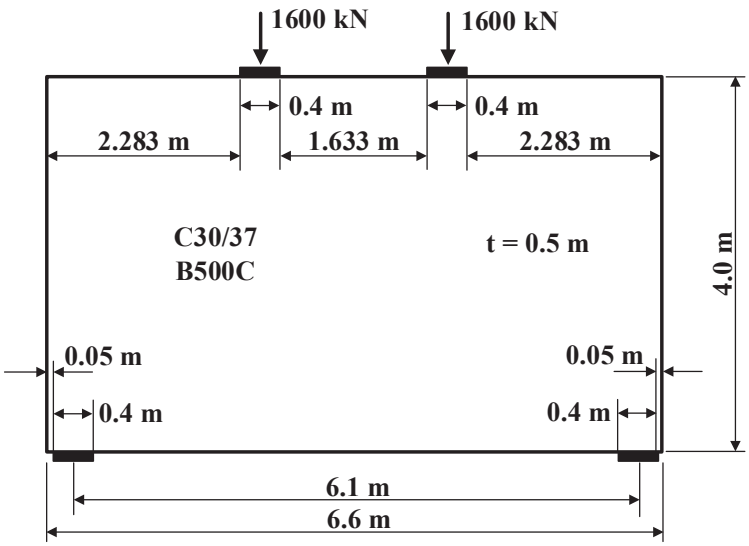

Figure 1 – Reinforced concrete wall member

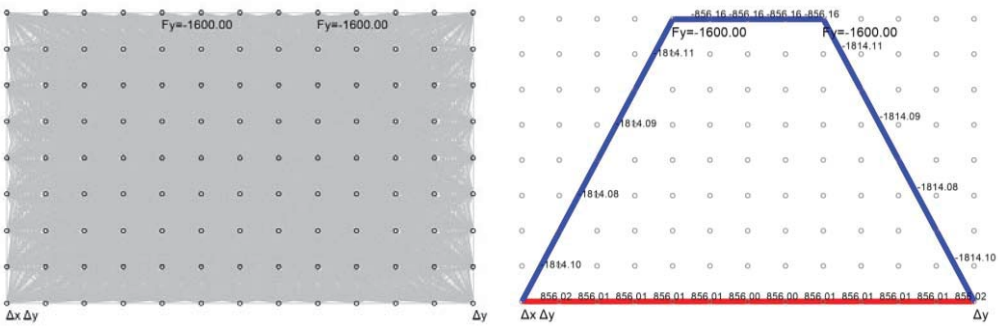

Figure 2 – Finite element mesh (left) and the Strut-and-Tie model (right)

The member is designed by the Strut-and-Tie method using the "ST method" program, [1] and [6]. The arrangement and quantity of the adopted reinforcement are shown in Fig. 1 The finite element mesh is shown in Fig. 2 left, and automatically defined Strut-and-Tie shape in the "ST method" program in Fig. 2 right. Fig. 3 shows the control of the stress state in the

nodes of the adopted Strut-and-Tie model, according to [6]. The final shape of the Strut-and-Tie model is shown in Fig. 4.

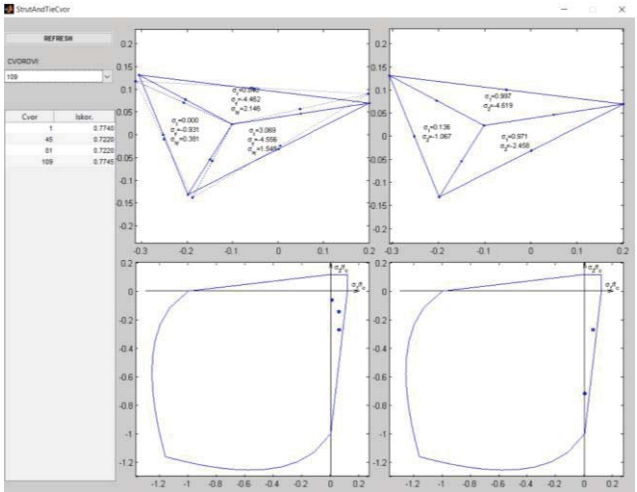

Figure 3 – Stress control in the Strut-and-Tie model nodes from "ST method" program

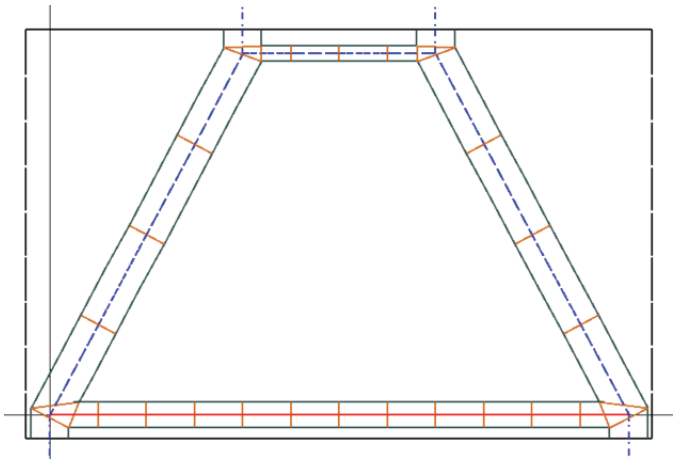

Figure 4 – The Strut-and-Tie model in the "ST method" program

Strength assessment of the reinforced concrete wall member is done by nonlinear static anaysis in commercial program Abaqus 2016. The member is exposed to a monotonically increasing static load. The concrete part of the member is modeled with CPS4R finite elements [11], with dimensions 50x50 mm. The reinforcement is modeled with truss finite elements T3D2 [11]. The bond between concrete and reinforcement is modeled without the possibility of slipping. The wall member model is shown in Fig. 5 left. The bilinear stress-strain relation is applied to the reinforcement, Fig. 5 right. The uniaxial stress-strain relations for concrete at compression and tension are shown in Fig. 6. Material nonlinearity in concrete is covered by

the application of the CDP (Concrete Damage Plasticity) model [11] with parameters: K_c=2/3, ψ=56°, σ_{bo}/ σ_{co}=1.16, ε=0.1 i μ=0. Parameters were adopted based on the recommendations given in [6] and [12].

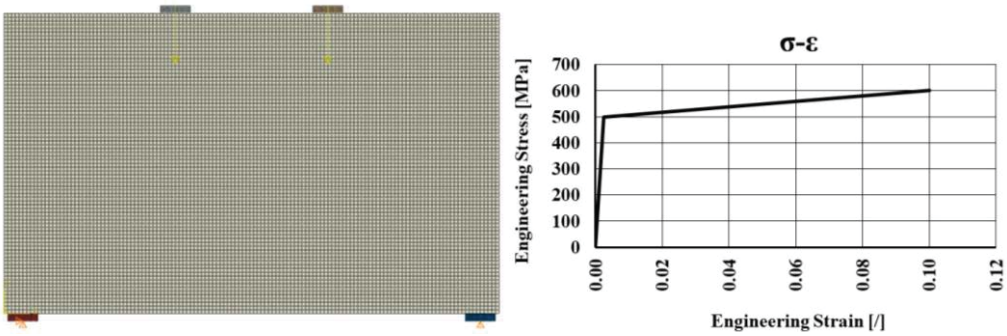

Figure 5 – The wall member model in Abaqus

The results of the analysis show that at the ultimate load of 2x1600 kN, the stress in the reinforcement is 103 MPa, at a load of 2x1995 kN the stress in the reinforcement is 438 MPa (the design yelding limit), and at a load of 2x2132 kN, the stress in the reinforcement is 500 MPa. At a load of 2x2132 kN, the results of nonlinear static analysis show that there was no crushing of concrete in the Strut-and-Tie elements.

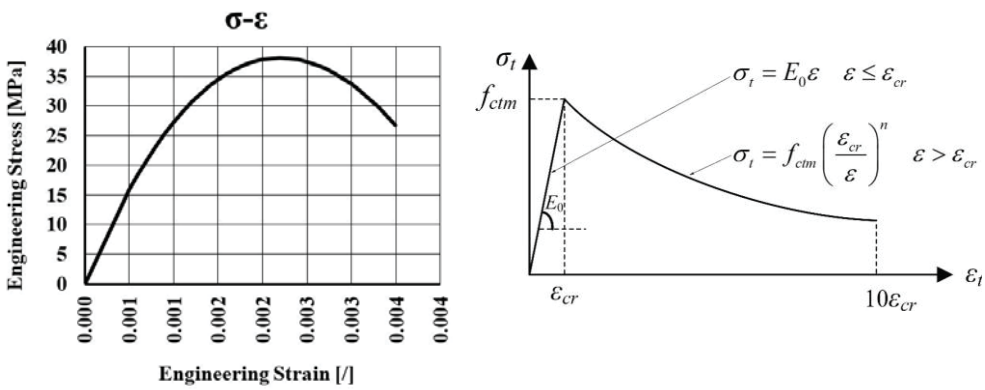

Figure 6 – The uniaxial stress-strain relations for concrete in compression (left) and tension (right)

With its shape, for the ultimate load of 2x1600 kN, the Strut-and-Tie model obtained in the "ST method" program follows the crack pattern of the concrete part of the member at tension, Fig. 7. Based on the analysis results, it is concluded that the load value at which the designed yielding value (438 MPa) has been reached is increased by 25% relative to the ultimate load value (2x1600 kN) based on which the member is designed. This strength reserve appears due to the fact that the designed Strut-and-Tie model determined by the "ST method" program is a truss member with constant cross-sections for struts and ties. On the other hand, the generated

Strut-and-Tie model in the real member, modeled in the Abaqus commercial program, has bottle-shaped struts with cross-sections that are actually larger than design sections and thus with lower stress levels than the design ones. In the ties of the Strut-and-Tie model, due to the adhesion between the concrete and the reinforcement, the tensile stress in the reinforcement is reduced. Also, when choosing the reinforcement, the usual practice is that, if the exact quantity of the required reinforcement cannot be adopted, it is chosen to be a little larger.

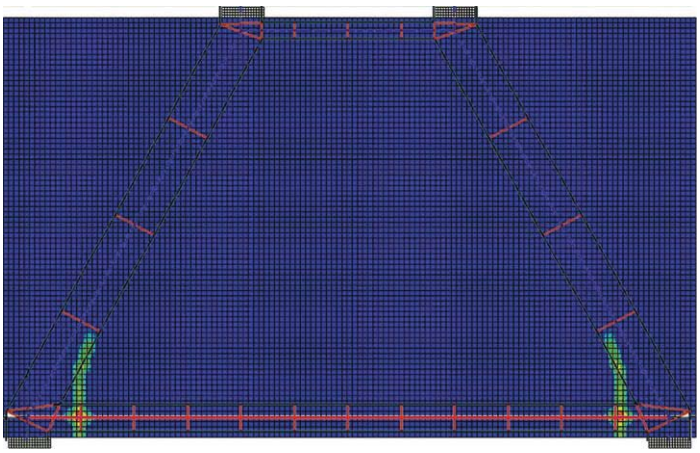

Figure 7 – Crack pattern in the member due to tension at load of 2x1600 kN

4. CONCLUSION

One way of overcoming discontinuity problems in members, in terms of discontinuity due to sudden changes in geometric and/or static properties, is the possibility of modeling a real reinforced concrete member with an equivalent truss system, which is basically a Strut-and-Tie method. Also, this method can also be used for design of the whole member.

In this paper a reinforced concrete wall member was analyzed which was previously designed by the Strut-and-Tie method in the "ST method" program. The strength assessment of the member is done by nonlinear static analysis.

Based on the results of the analysis, it is concluded that the designed yielding stress value in the reinforcement was achieved at a load of 2x1995 kN, which is 25% higher than the ultimate load (2x1600 kN). Based on this, it is concluded that there is a strength reserve relative to the ultimate limit state applied for the design of the member by the Strut-and-Tie method.

ACKNOWLEDGEMENT

The results presented in this paper are part of the research project TR 36043 "Development and application of a comprehensive approach to the design of new and safety assessment of existing structures for seismic risk reduction" financed by the Ministry of Education, Science and Technological Development of the Republic of Serbia.

REFERENCES

[1] Schlaich J., Schafer K., Jennewein M.: Toward a consistent design of structural concrete. Journal of the Prestressed Concrete Institute, PCI, Vol. 32, No. 3, May-June 1987, pp 74-150.

[2] Schlaich J., Schafer K.: Designs and detailing of structural concrete using strut and tie models. The Structural Engineer;Vol 69, No 6, 1991 , pp 113-125.

[3] Reineck K.H.: Examples for the Design of Structural Concrete with Strut-and-Tie Models, American Concrete Institute, 2002.

[4] International Federation for Structural Concrete (fib): Design examples for strut-and-tie models, Tecnical report prepared bz Working Party 1.1-3 in *fib* Task Group 1.1, Design Applications, ISBN 978-2-88394-101-4, 2011.

[5] Starčev-Ćurčin A., Rašeta A., Brujić Z.(2016): The program ST Method for determining the Strut-and-Tie models of RC plane members, Technical Gazette 23, 1(2016), pp 291-300, ISSN 1330-3651(Print), ISSN 1848-6339 (Online), DOI: 10.17559/TV-20140818132418.

[6] Starčev-Ćurčin A.: Optimizacija i analiza armiranobetonskih ravanskih nosača primenom metode pritisnutih štapova i zatega, PhD Thesis, University of Novi Sad, 2017.

[7] Maxwell B.S., Breen J.E.: Experimental Evaluation of Strut-and-Tie Model Applied to Deep Beam with Opening, ACI Structural Journal, V.97, No.1, January-February 2000, pp. 142-148.

[8] Chen B.S., Hagenberger M.J., Breen J.E.: Evaluation of Strut-and- Tie Modeling Applied to Dapped Beam with Opening, ACI Structural Journal, V.99, No.4, July-August 2002, pp. 445-450.

[9] Ley M.T., Riding K.A., Widianto, Bae S., Breen J.E.: Experimental Verification of Strut-and-Tie Model Design Method, ACI Structural Journal, V.104, No.6, November-December 2007, pp. 749-755.

[10] Brena S.F., Morrison M.C.: Factors Affecting Strength of Elements Designed Using Strut-and-Tie Models, ACI Structural Journal, V.104, No.3, May-June 2007, pp. 267-277.

[11] Abaqus 2016 Analysis Users Guide, © Dassault Systèmes, 2015.

[12] Lopez-Almansa F., Alfarah B., Oller S.: Numerical Simulation of RC Frame Testing With Damaged Plasticity Model Comparison With Simplified Models, Second Europen Conference on Erthquake Engineering And Seismology, Isntanbul, Aug. 25-29, 2014.

ДГКС Друштво грађевинских конструктера Србије
ASES Association of Structural Engineers of Serbia
S-75
15. KONGRES
6-8. 9. 2018. Zlatibor

Svetlana Kostić[1], Biljana Deretić-Stojanović[2]

DVA NUMERIČKA MODELA ZA NELINEARNU ANALIZU CFT STUBOVA

Summary:

U radu su prikazana dva linijska nelinearna konačna elementa koja se mogu koristiti za nelinearnu analizu CFT stubova. Prvi element je element koncentrisane plastičnosti zasnovan na materijalnom modelu generalisane plastičnosti, a drugi je fiber konačni element raspodeljene plastičnosti. Razmatrane su vrednosti parametara modela koji se koriste kod stubova kvadratnog i kružnog poprečnog preseka. Tačnost oba elementa je prikazana kroz poređenje sa rezultatima nekoliko eksperimenata dostupnih u literaturi.

Key words: nelinearna analiza, CFT stubovi, fiber konačni element, GP element

TWO NUMERICAL MODELS FOR NONLINEAR ANALYSIS OF CFT COULUMNS

Summary:

Two nonlinear 1D finite elements suitable for CFT column analysis are presented. The first element is the GP element that belongs to the concentrated plasticity elements and is based on the ideas of the generalized plasticity material model. The second element is the distributed plasticity force based fiber beam/column element. For both elements, selection of parameters is discussed for analysis of square and circular CFT columns. Accuracy of the two models is verified by comparison with experimentally available results.

Key words: nonlinear analysis, CFT columns, fiber finite element, GP element

[1] *doc., dipl. građ. ing, Građevinski fakultet Univerziteta u Beogradu,svetlana@grf.bg.ac.rs*
[2] *V.prof, dipl. građ. ing, Građevinski fakultet Univerziteta u Beogradu,biljads@grf.bg.ac.rs*

1. INTRODUCTION

Concrete filled steel tube columns (shortly, CFT) are nowadays widely used in modern engineering practice. They have improved performances over pure steel and concrete structures, because of higher stiffness and strength, increased ductility, better fire performance, etc. Since behaviour of these members is highly nonlinear, the numerical models should be able to take into account the nonlinear effects such as: nonlinear behaviour of steel and concrete, effects of concrete confinement, cracking of concrete, creep, shrinkage, etc.

To date, there are two main approaches in modelling CFT columns [1]. Firstly, there are models with continuum finite elements that are very accurate and are useful for detailed modelling of connections. Because of very high computational costs, they are not suitable for modelling whole structure. On the other side are 1D line elements that are less accurate, but are less computationally expensive. There are different formulations of these elements. Basically, all of them can be classified into a group of concentrated plasticity elements and the distributed plasticity elements. In concentrated plasticity elements, plastic deformations can be developed only at specific locations along the element usually placed at the element ends [1, 2]. On the other side, in distributed plasticity elements, plastic deformations may develop at several locations along the element length [3]. In this paper, use of the GP element that belongs to the concentrated plasticity elements and the fiber beam/column distributed plasticity element for modelling CFT column behaviour is discussed.

2. GP ELEMENT

The GP element is the concentrated plasticity element with two plastic hinges at element ends (Figure 1). Its formulation, i.e. relations between element basic forces and element end deformations are based on the relations of the generalized plasticity material model [4]. The element accounts for the interaction between axial forces and two bending moments about the principal axes of the cross section, gradual yielding of the cross section, the hardening (or softening) behavior and nonlinear geometry under large displacements. More details about the element formulation and the two element state determination algorithms can be found in [1, 2].

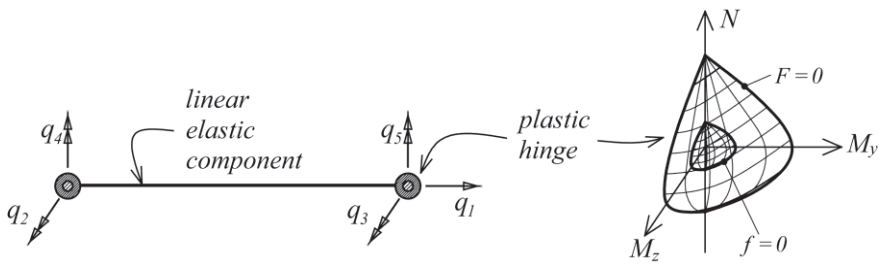

Figure 1 – GP finite element model

In order to use the GP element for modeling CFT columns, the following element parameters need to be appropriately chosen:

- yield function $\boldsymbol{f}$,
- element parameters β and δ
- elastic element stiffness,
- hardening parameters.

Yield finction f encloses the elastic region and serves as a boundary between inactive and active state of each plastic hinge. It has the following form:

$$f(\boldsymbol{q}, \boldsymbol{q_b}, \alpha) = \Phi(\boldsymbol{q} - \boldsymbol{q_b}) - H_i\alpha \tag{1}$$

where $\boldsymbol{q}$ are element basic forces, $\boldsymbol{q_b}$ are the basic forces that correspond to the center of the yield surface for the description of the kinematic hardening, α is the isotropic hardening variable and H_i is the isotropic hardening parameter. For 2D analysis, the following expressions for the function Φ are adopted:

$$\phi(n, m) = c_4m^2 + c_3n^2 + c_2n^2m^2 - c_1 \qquad \text{(for square section)} \tag{2}$$

$$\phi(n, m) = c_5m + c_4n^4 + c_3n^2 + c_2n - c_1 \qquad \text{(for circular section)} \tag{3}$$

where n and m have the following meaning

$$n = \frac{N - q_{bN} - \varphi N_0}{N_0} \text{ and } m = \frac{M - q_{bM}}{M_0} \tag{4}$$

and N is the section axial force, N_0 is the axial compression capacity, M is the bending moment, M_0 is the plastic moment capacity and q_{bN} and q_{bM} are components of the $\boldsymbol{q_b}$ vector. The parameter φ accounts for the shift of the yield surface of the composite section from the origin [1].

Parameter c_1 controls the size of the yield surface and is taken as equal to:

$$c_1 = \left(\frac{M_{ys}}{M_0} - 0.3\frac{N_{c0}}{N_0}\right)^2 \qquad \textit{(for monotonic loading)} \tag{5}$$

$$c_1 = 0.25\left(\frac{M_{ys}}{M_0} - 0.3\frac{N_{c0}}{N_0} + 0.1\right)^2 \qquad \textit{(for cyclic loading)} \tag{6}$$

The study [1] has shown that for analysis of CFT columns, the element parameters δ and β should be taken as $\delta=0.1$ and $\beta=1-c_1$.

Values of other parameters c_i can be found elsewhere [1, 5].

The elastic element axial stiffness is calculated as the sum of the elastic axial stiffness of the steel and concrete part of CFT section (E_s and E_c are elastic modulus of the steel and concrete, A_s and A_c are area of steel and concrete part of CFT section):

$$(EA)_{CFT} = E_sA_s + E_cA_c \tag{7}$$

The elastic element bending stiffness is calculated as the sum of the elastic bending stiffness of the steel and cracked concrete part of CFT section (I_s and I_c are moments of inertia of steel and concrete part of CFT section):

$$(EI)_{CFT} = E_sI_s + kE_cI_c \tag{8}$$

Coefficient k takes into account cracking of concrete and is taken as equal to 0.6.

The hardening parameters H_i and H_k depend on the values of material parameters.

3. FIBER ELEMENT

In this study, the force formulated fiber beam/column element is used [6], Figure 2. The element has proven to be very accurate for analysis of steel, concrete and composite structures.

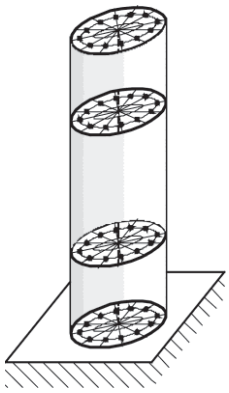

Figure 2 – Distributed plasticity fiber beam/column element

In order to use this element, the uniaxial constitutive relations for steel, concrete and reinforcement (if present) need to be assigned to points of the discretized cross section. Different material models can be used. This study use results of the study [7] where concrete part of the section is modelled with Chang & Mander material model [8]. Parameters of the model are concrete compressive strength f_c, concrete strain at maximum compressive strength ε_{cc}, initial elastic modulus E_c, tensile strength of concrete f_t, tensile strain at the maximum tensile strength ε_t and parameters that define the nonlinear branch of the curve x_p, x_n and r. The following values of parameters have shown to be good choice:

$$\sigma_l = \frac{2t(B-t)f_y}{(B-2t)^3} \qquad \text{(for square section)} \tag{9}$$

$$\sigma_l = \frac{2t\alpha_\theta f_y}{(D-2t)^3} \qquad \text{(for circular section)} \tag{10}$$

$$C = -2\frac{\sigma_l}{f_c} - 1.254 + 2.254\sqrt{1 + \frac{7.94\sigma_l}{f_c}} \tag{11}$$

$$\varepsilon_{c0} = \frac{(f_c)^{0.25}}{1150} \quad , \quad \varepsilon_{cc} = \varepsilon_{c0}(1 + 5(C-1)) \tag{12}$$

$$n = \frac{E_\varepsilon \varepsilon_{cc}}{C f_c} \ , \qquad r = \frac{n}{n-1} \tag{13}$$

$$f_t = 0.62\sqrt{f_c} \ , \qquad \varepsilon_t = \frac{2f_t}{E_c} \tag{14}$$

In Equation (9) B is the dimension of the square steel tube, D is the diameter of the circular steel tube, t is its thickness and f_y is yield strength of the steel tube.

For steel, the study presented in [7] has shown that Giuffre-Menegotto-Pinto model with isotropic hardening gives the best results. The parameters of the model are E_s (initial modulus of elasticity), f_y (yield stress), strain hardening ratio b. For parameters R_0, R_1 and R_2 the following values are adopted: R_0=15, R_1=0.925 and R_2=0.15.

4. NUMERICAL EXAMPLES

In this part of the paper, the results of analysis for few numerical examples of the two described models are compared with the experimental results. All numerical simulations are performed in FEDEASLab [9] and in OpenSEES [10].

4.1. TESTS WITH PROPORTIONAL MONOTNIC LOADING

Several tests with square and circular CFT columns are numerically investigated. The first group of tests are tests on simply supported beam exposed to eccentric monotonically increasing axial force (Figure 3).

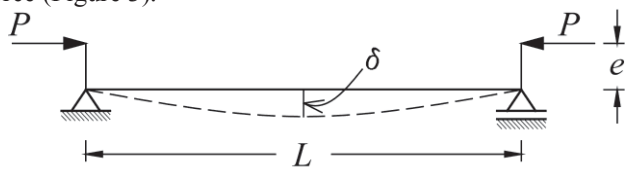

Figure 3 – Test setup for tests with proportional monotonic loading

Here, results of tests by Cederwall et al. [11] on square CFT columns and Matsui and Tsuda [12] on circular CFT columns are presented. Geometrical and material properties of the specimens are given in Table 1.

Table 1 – Geometrical and material properties of tests with proportional monotonic loading

Specimen	***B or D (mm)***	***t (mm)***	***L (mm)***	***e (mm)***	***f_c (MPa)***	***f_y (MPa)***
Cederwall 1	***120***	***5***	***3000***	***20.0***	***47***	***304***
Cederwall 2	***120***	***5***	***3000***	***20.0***	***46***	***438***
Cederwall 6	***120***	***8***	***3000***	***20.0***	***46***	***300***
Cederwall 7	***120***	***8***	***3000***	***20.0***	***47***	***376***
Matsui C121	***165***	***4.5***	***1982***	***20.7***	***32***	***414***
Matsui C123	***165***	***4.5***	***1982***	***62.0***	***32***	***414***

Results of the two numerical models are shown in Figure 4. As can be seen, both numerical models follow very well the experimentally obtained results.

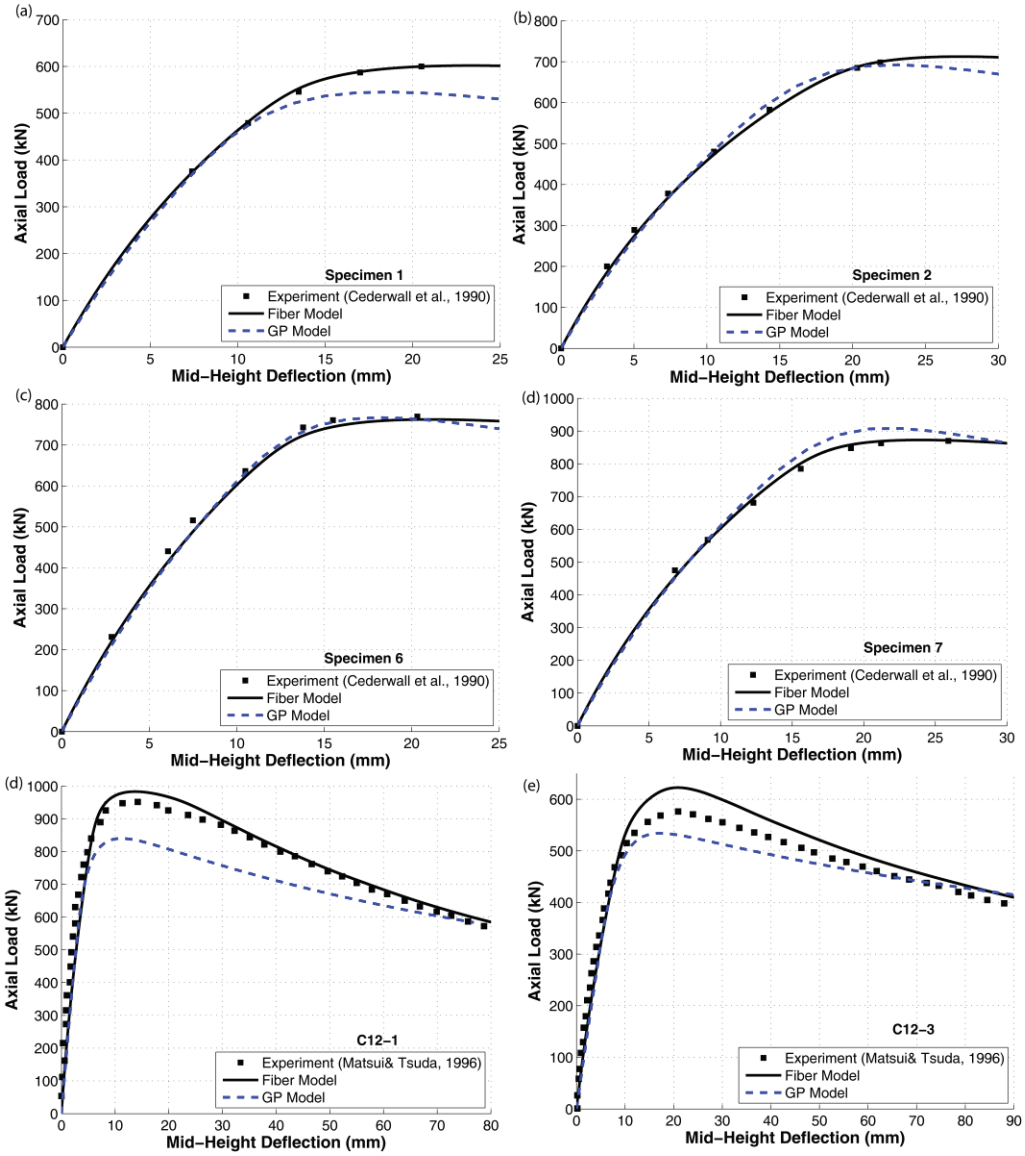

Figure 4 – Test setup for tests with proportional monotonic loading

4.2. TESTS WITH FOUR POINT LOADING – CIRCULAR CROSS SECTION

The second group of tests refers to tests by Wheeler and Bridge [13] on specimens with circular cross section, exposed to four point loading (Figure 5).

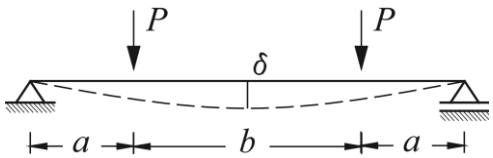

Figure 5 – Test setup for tests with proportional monotonic loading

Forces *P* are monotonically increasing. All specimens have thickness *t=6.4 mm* and yield stress of steel section f_y*=351 MPa*. Shear span *a* (Figure 5) is *1300 mm*, and bending span *b* is equal to *1200 mm*. Other test data are given in Table 2.

Table 2 – Geometrical properties for Wheeler and Bridge specimens

Specimen	***D (mm)***	***f_c (MPa)***
TBP002	***406***	***40***
TBP005	***456***	***48***

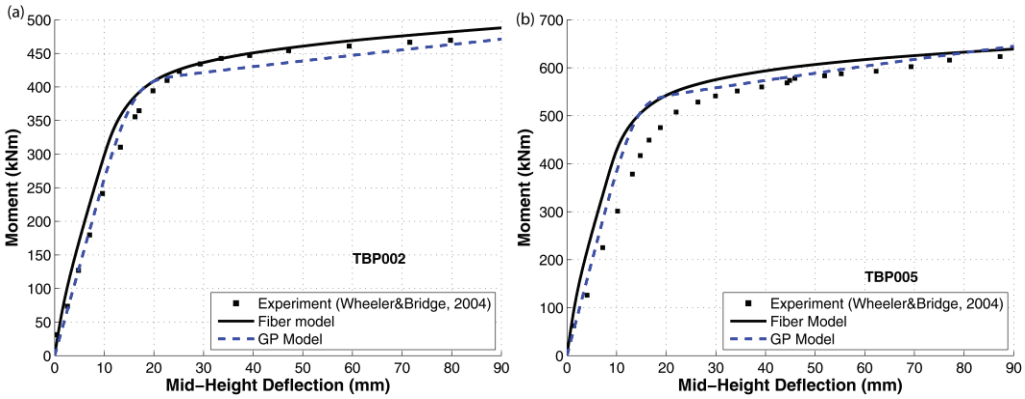

Figure 6 – Test setup for tests with proportional monotonic loading

Results from Figure 6, again, show high agreement between numerical and experimental results.

4.3. TESTS WITH CYCLIC LOADING – SQUARE CROSS SECTION

The last group of tests refers to the square CFT specimens subjected to the cyclic lateral displacements under constant axial force, tested by Sakino and Tomii [14], Figure 7.

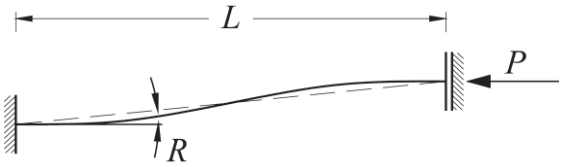

Figure 7 – Test setup for tests with proportional monotonic loading

Geometrical and material data for this test are: *B=100 mm*, *t=4.21 mm*, f_c = *20.36 MPa*, f_y*=290.27 MPa*. Results for specimen CIV3-2 are shown in Figure 8. Here, results of the GP model predicts well the ultimate strength, but strength degradation is better followed by the fiber model.

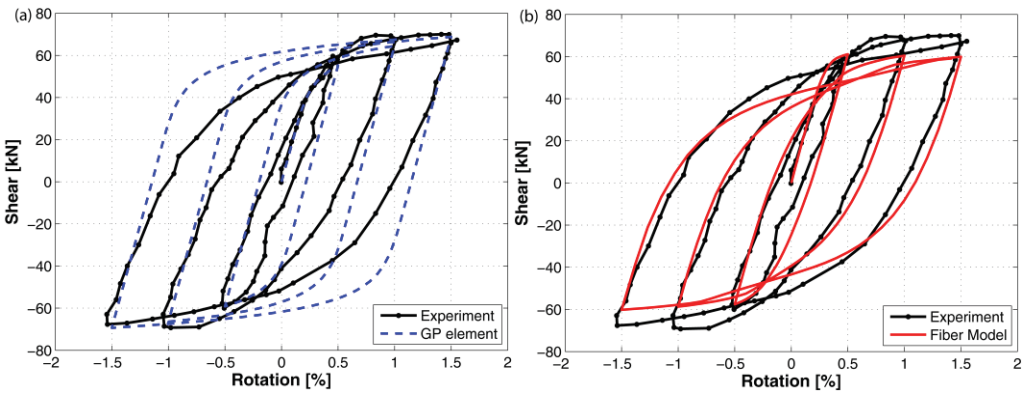

Figure 8 – Test setup for tests with proportional monotonic loading

5. ADVANTAGES AND DISADVANTAGES OF TWO NUMERICAL MODELS

Comparing the accuracy of two presented numerical models, it can be concluded that both elements offer high level of accuracy, but the fiber model is in slight advantage over the GP model. On the other side, considering computational efficiency, the GP element is in advantage over the fiber model since its computational time is about 6 times lower than the calculation time of the fiber element, when one element is used. For modelling whole structure, this difference increases to 10 or more times, which are significant savings [1]. Also, demands for computer memory are much lower for GP element since less parameters are saved during the state determination process.

Comparing the robustness of the element formulation, both elements have very powerfull algorithms with quadratic convergence.

Referring to the elements versatility, the fiber model is in advantage over the GP element for the following reasons:

- different cross section types can be easily implemented into the fiber model since it requires just different definition of the cross section; in GP element, the new expression

for the yield surface is needed; these expressions are available only for the most common cross section types
- in the fiber model residual stresses can be easily applied by assigning the initial stresses to the fibers, while in GP element it can be done indirectly by changing the size of the initial yield surface
- buckling of the steel tube can be easily implemented into the fiber model by modifying the definition of the steel material model, while in GP model it may be accounted for approximately by modifying the limiting surface
- by its formulation, the fiber model offers the possibility for plastic deformations to appear at any of the monitored cross sections; in the GP element plastic deformations may form only at element ends. Therefore, depending on the loading, some members may require more than one GP element per length.

6. CONCLUSIONS

Behaviour of CFT columns is highly nonlinear and an adequate numerical model needs to include the most significant of them. In this paper, two nonlinear 1D finite elements that are suitable for nonlinear analysis of CFT columns are presented. For each of them, parameters adjusted for analysis of circular and square CFT columns are given. Numerical results obtained using these two elements are compared with few experimentally available results. These results have shown that both elements possess high accuracy. Finally, advantages and disadvantages of the two models are discussed.

ACKNOWLEDGEMENT

The first author thanks the Ministry of Science of the Republic of Serbia for financial support under the project number TR36046.

REFERENCES

[1] Kostic, S.M., Filippou, F.C., and Deretic-Stojanovic, B.: Generalized plasticity model for inelastic RCFT column response Computers & Structures, vol.(168),no.((56-67), 2016.

[2] Kostic, S.M., Filippou, F.C., and Lee, C.-L.: An Efficient Beam-Column Element for Inelastic 3D Frame Analysis, in Computational Methods in Earthquake Engineering: Volume 2, M. Papadrakakis, M. Fragiadakis, and V. Plevris, Editors. Springer Netherlands: Dordrecht. (49-67) 2013.

[3] Kostic, S.M. and Filippou, F.C.: Section Discretization of Fiber Beam-Column Elements for Cyclic Inelastic Response Journal of Structural Engineering, vol.(138),no.(5), (592-601), 2012.

[4] Auricchio, F. and Taylor, R.L.: 2 Material Models for Cyclic Plasticity - Nonlinear Kinematic Hardening and Generalized Plasticity International Journal of Plasticity, vol.(11),no.(1), (65-98), 1995.

[5] Hatzigeorgiou, G.D.: Numerical model for the behavior and capacity of circular CFT columns, Part II: Verification and extension Engineering Structures, vol.(30),no.(6), (1579-1589), 2008.

[6] Taucer, F., Spacone, E., Fillippou, F. C.: A fiber beam-column element for seismic response analysis of reinforced concrete structures, UC Berkeley: Berkeley. 1993.
[7] Blagojevic, N., Kostic, S.M., and Stosic, S.: Fiber konačni element u nelinearnoj analizi kvadratnih spregnutih CFT stubova Građevinski materijali i konstrukcije, vol.(60),no.(1), (31-46), 2017.
[8] Chang, G.A. and Mander, J.B.: Seismic Energy Based Fatigue Damage Analysis of Bridge Columns: Part I-Evaluation of Seismic Capacity, Department of Civil Engineering, State University of New York: Buffalo, N.Y. 1994.
[9] Filippou, F.C.: FEDEAS: Nonlinear Static and Dynamic Analysis from Research to Practice, in ASCE Structures Congress XIV. 1996. Chicago: American Society of Civil Engineers.
[10] McKenna, F.: Object Oriented Finite Element Programming Frameworks for Analysis, Algorithms and Parallel Computing, University of California, Berkeley, CA. 1997.
[11] Cederwall, K., Engstorm, B., and Grauers, M.: High-Strength Concrete Used in Composite Columns, in 2nd Int. Symp. on Utilization of High-Strength Concrete. 1991. Detroit: American Concrete Institute (ACI).
[12] Matsui, C. and Tsuda, K.: Strength and Behavior of Slender Concrete Filled Steel Tubular Columns, in The second international symposium on civil infrastructure systems. 1996. Hong kong, China.
[13] Wheeler, A. and Bridge, R.Q.: The Behavior of Circular Concrete-Filled Thin-Walled Steel Tubes in Flexure, in The 5th International Conference on Composite Construction in Steel and Concrete. 2004. Mpumalanga, South Africa.
[14] Sakino, K. and Tomii, M.: Hysteretic behavior of concrete filled square steel tubular beam-columns failed in flexure Transactions of the Japan Concrete Institute, vol.(3),no.((439-446), 1981.

ДГКС Друштво грађевинских конструктера Србије
ASES Association of Structural Engineers of Serbia
S-76
15. KONGRES
6-8. 9. 2018. Zlatibor

Nikola Ivanović[1], Jelena Dobrić[2], Milan Spremić[3], Nina Gluhović[4], Jovana Milovanović[5]

NELINEARNA ANALIZA BOČNO-TORZIONOG IZVIJANJA U PROFILA OD ALUMINIJUMSKE LEGURE

Rezime:

Ovaj rad prikazuje komparativnu analizu granične nosvosti konstruktivnih elemenata od aluminijumske legure na bočno-torziono izvijanje implementrajući uticaje početnih geometrijskih imperfekcija. Rezultati nelinearne numeričke analize, koja je sprovedena u programu ABAQUS, se porede sa rezultatima dobijenim primenom metode za proračun elemenata na BTI date u EN 1999-1-1. Svrha analize je procena tačnosti pomenute računske metode, definisane od strane standarda, na primeru realnih Al elemenata U poprečnog preseka sa inicijalnim imperfekcijama kod kojih opterećenje ne deluje u centru smicanja.

Ključne reči: aluminijum, kritični moment, U profil, bočno-torziono izvijanje, imperfekcije

NON-LINEAR LATERAL BUCKLING ANALYSIS OF ALUMINIUM ALLOY CHANNEL BEAMS

Summary:

This research paper presents the comparative analysis of lateral-torsional buckling resistance of structural aluminium alloy members, accounting for the effects of initial geometrical imperfections. The results of non-linear numerical analysis, conducted using ABAQUS software, are compared with the results obtained by utilizing the procedure for calculation of LTB resistance suggested by EN 1999-1-1. The purpose of the analysis is the assessment of accuracy of the above-mentioned code-prescribed design method using the real Al channel-section members with initial imperfections on which the load does not act in the shear centre.

Key words: aluminium, critical moment, channel, lateral-torsional buckling, imperfections

[1] *MSc, Structural Engineer, DNEC d.o.o., Belgrade*
[2] *PhD, MSc, BSc, assistant professor, University of Belgrade, Faculty of Civil Engineering*
[3] *PhD, MSc, BSc, assistant professor, University of Belgrade, Faculty of Civil Engineering*
[4] *MSc, PhD student, University of Belgrade, Faculty of Civil Engineering*
[5] *MSc, Structural Engineer, Jaroslav Černi Institute for the Development of Water Resources, Belgrade*

1. INTRODUCTION

This paper has focus on comparison of lateral-torsional buckling resistances of channel-section aluminium alloy beams with initial geometrical imperfections, obtained by finite-element analysis and by applying the procedure for sections mono-symmetric with respect to their major axis, described in EN 1999-1-1 [4]. The Finite Element (FE) modelling for the linear lateral-torsional buckling analysis, which incorporates the information about the cross-sectional properties, material properties, FE mesh, member lengths and structural systems, as well as the position of the line load, is thoroughly explained in the research paper of Ivanović et al. [5]. In the aforementioned paper, authors stated the following conclusions:

- Equation for calculation of critical moment of beams with cross-sections symmetrical about the major principal axis, with load applied perpendicular to the major axis in the direction of the shear centre, is available in EN 1999-1-1, annex I [4]. However, this equation is found to be the same as the equation proposed by EN 1993-1-1 [2] for estimation of critical moment of beams with standard doubly-symmetric cross-sections, with load applied in the symmetry plane.
- The deviations between the FEM analysis values of the critical moment of the channel-section beams and the corresponding values calculated according to EN 1999-1-1 [4] range from 1% to 1.5%. The values of the critical moment obtained in accordance with EN 1999-1-1 [4] did not appear to be safe-sided compared with the FEM results.
- FEM analysis critical moment values are observed to be decreasing with the increase of horizontal eccentricity of the load; therefore, by extrapolating this discovery in the opposite direction, it is rationally concluded that the lateral-torsional buckling capacity would increase if the load is applied in the vertical plane passing through the shear centre. Considering relatively small deviations from the values calculated using the Code [4], it is assumed that the equation for critical moment could provide results with a certain safety factor relative to the FEM analysis values if the equation is modified in a manner which would include the effect of horizontal eccentricity of the load.

The question remains whether the design approach prescribed by EN 1999-1-1 [4] will be more rigorous than the FEM procedure, if non-linear features of the material and initial crookedness and twist are introduced in the analysis. This research was conducted with the objective to shed light on this issue and to bring the problem of lateral-torsional buckling of channel-section beams closer to understanding. It should be mentioned beforehand that the procedure adopted by EN 1999-1-1 [4], which addresses the calculation of lateral-torsional buckling capacity of real beams, is somewhat similar to that displayed in EN 1993-1-1 [2]. It is assumed that the reader is familiar with this procedure, thus no significant effort will be made in order to clarify it.

2. NON-LINEAR LATERAL-TORSIONAL BUCKLING ANALYSIS OF CHANNEL BEAMS WITH INITIAL IMPERFECTIONS

In the preceding research paper [5], Linear Buckling Analysis (LBA) is described, from which the values of elastic critical moments of the analysed channel-section aluminium alloy beams are obtained. LBA implies that the material is linearly elastic and that the examined members are ideally straight, in which case the value of the bending moment in the governing

section is increasing without lateral displacements until it reaches its critical value. The point on the Moment - Lateral Displacement diagram in which it occurs is called the bifurcation point, which, by definition, is a point where more than one equilibrium states coexist. This point is represented by M_{cr} in Fig. 1 and the determination of this point is one of the key problems of the theory of elastic stability. If member imperfections are introduced, the value of maximum moment will descend below the value of elastic critical moment. The maximum value of bending moment, in this scenario, represents lateral-torsional buckling capacity of a beam with initial imperfections (see Fig. 1).

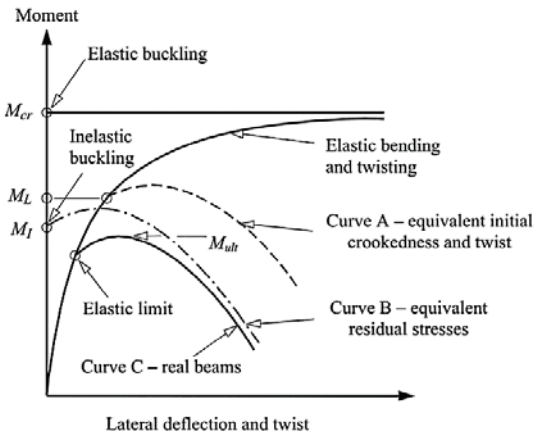

Figure 1 – Behaviour of beams with imperfections [7]

All that was said in the preceding research paper [5] regarding the FE models in terms of boundary conditions, geometry and FE mesh still holds. For the sake of clarity, cross-section with position of the loads, shear centre (S) and centroid (T), and the FE model are shown in Fig. 2. Load q1 from Fig. 2 represents the line load in the direction of the centroid, while load q2 represents the line load applied in the middle of the top flange.

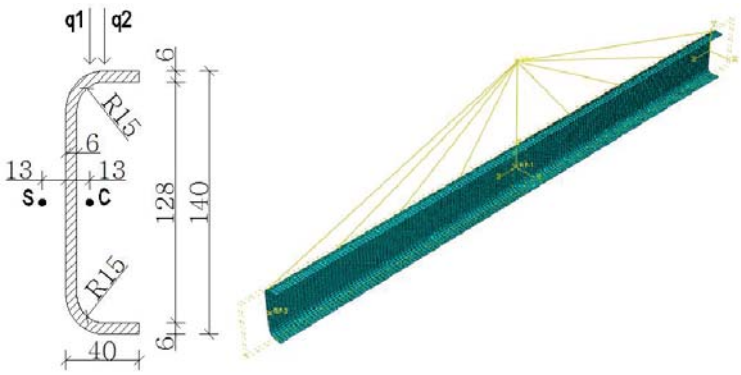

Figure 2 – Cross-section with load positions and FE model

The difference lies in the type of the analysis, which will be described here more precisely. The method of analysis which was used is the Explicit Dynamic Method (EDM). The first

option to be considered for the analysis of the members prone to exhibit large deformations caused by the loss of stability should be the Modified Riks Method [1]. However, this method is not known to be effective for the entire spectra of possible models, which was the case for this analysis, as well. However, one method, which has been proven to be satisfactory for the broader spectra of cases, including non-linear lateral buckling, is the EDM. When opting for this method, it should be borne in mind that it is essentially a dynamic method used to simulate static load and that the results are greatly dependent on, among other parameters, the time of the load application.

For the numerical analysis of elastic critical moment the entire stress-strain relationship is of little significance, acknowledging the fact that LBA demands only the value of modulus of elasticity. On the other hand, when analysing the bending capacity of a member as a whole, the stress-strain relationship is crucial, owing to the pronounced non-linearity of aluminium alloy EN-AW 6061-T6/T651, for it conditions the behaviour of the member subjected to stresses beyond the proportionality limit of the material, set as 120 MPa in the analysis [5]. In Annex E, EN 1999-1-1 [4], various types of stress-strain curve models are proposed: bilinear model with and without strengthening branch, trilinear model with and without strengthening branch, along with the continuous models (see Fig. 3).

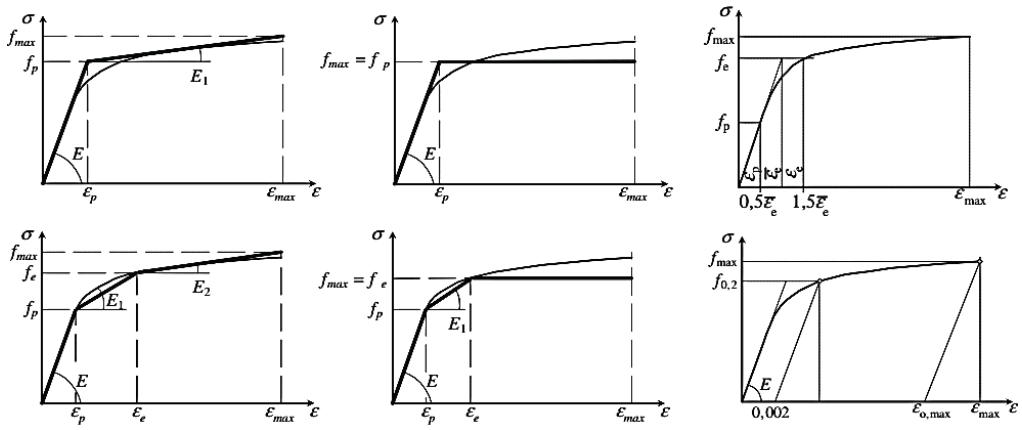

Figure 3 – Models of stress-strain curves suggested by EN 1999-1-1 [4]

Stress-strain model which was used is the continuous model in the form of σ=σ(ε), as described in E2.2.1, EN 1999-1-1 [4]. True stress-strain curve is then obtained as recommended in clause C.2, EN 1993-1-4 [3], in order to account for the "necking" phenomenon. After this transformation the stress-strain curve assumes the shape as shown in Fig. 4. From Fig. 4 it can be observed that the material demonstrates significant strengthening, which would not have been so pronounced hadn't the true values of the stresses and strains been employed. In ABAQUS software [1], the elastic behaviour of the material is governed by Hook's law; above the proportionality limit, which was set at 120 MPa, the plastic deformations commence. The non-linear material properties are taken into account by subtracting the value of elastic deformation, which is equal to the ratio of the stress and the modulus of elasticity, from the true values of strains.

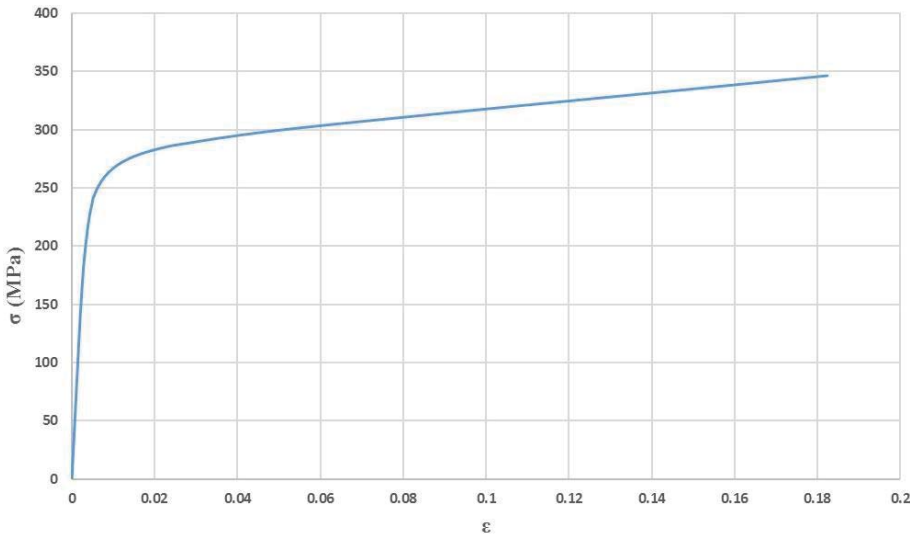

Figure 4 – True stress-strain curve

Stress-strain curve with true stress values from 120 MPa onward and with true values of irreversible strains, which for the stress value of 120 MPa have the value of 0, is imported in the software in a part where the inelastic material behaviour is to be defined.

Parameters which define the dynamic analysis have to be chosen carefully. One of the parameters which demonstrate great influence on the results is the time period. For the purpose of the analysis of the models described in the paper [5], the initial time period of 100 sec was adopted as the time in which the assigned load is applied gradually.

The method employed in obtaining the results demands definition of the partition in the mid-span, by which the governing cross-section is isolated. The function used for this purpose is Integrated Output with variable SOM, which defines the plot of total bending moment against time.

The imperfections were imported as the deformed shape of the models used for linear buckling analysis. The described members are relatively sensitive to imperfections, so that the first mode of lateral-torsional buckling is sufficient to trigger the reduction of the bending capacity below the value of the elastic critical moment. The first lateral-torsional buckling mode is comprised of two deformation components which are unfavourable from the stability standpoint: twist and lateral deflection. Taking into account the fact that the analysed members are formed by the process of extrusion, residual stresses, as well as the variations of material parameters along the cross-section can be neglected, as opposed to the case when the members are welded [6]. The amplitude value of initial imperfection, comprising both the twist and the bow imperfection, is chosen to be equal to the maximum manufacturing imperfection of L/750, in accordance with EN 1090-2, where L is the span length. The visual representation of initial geometric imperfection is shown in Fig. 5.

Figure 5 – Model without and with initial geometric imperfection

The applied load slightly exceeds the critical load obtained from LBA and it is equal to the critical load multiplied by 1.5.

The results obtained from EDA are presented as the plots of mid-span bending moment against the rotation of the support sections (see Fig. 6 – Fig. 8).

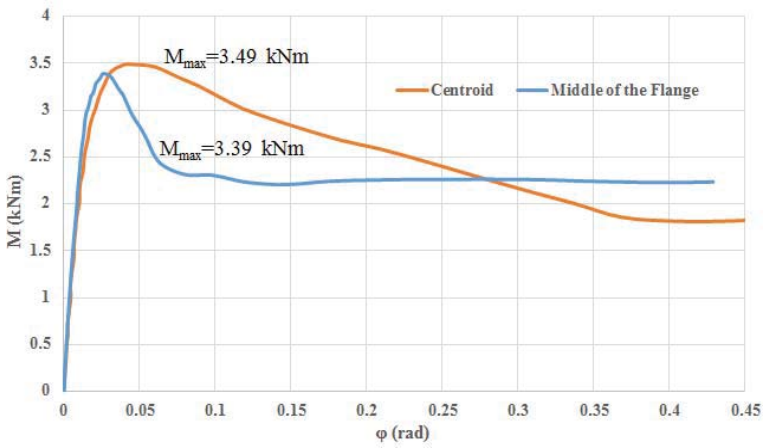

Figure 6 – Bending capacity of 1.5 m beams

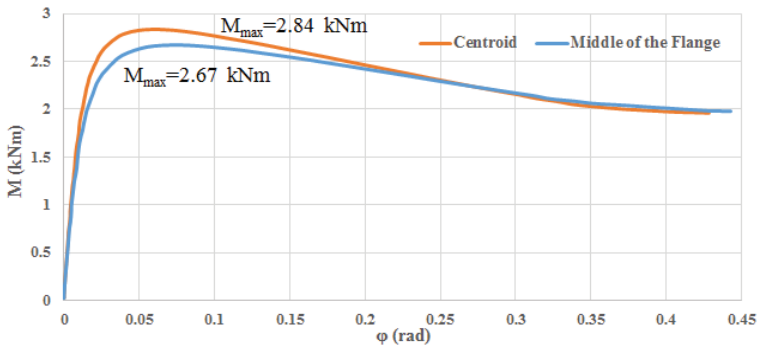

Figure 7 – Bending capacity of 2 m beams

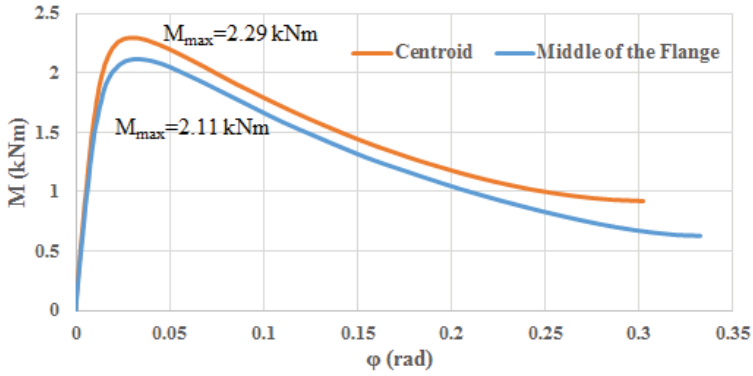

Figure 8 – Bending capacity of 2.5 m beams

In Fig. 9 the example model which has undergone inelastic deformations at the moment of failure is shown for the purpose of visual description. Von Mises stresses, expressed in MPa, are shown in the legend in the upper left corner.

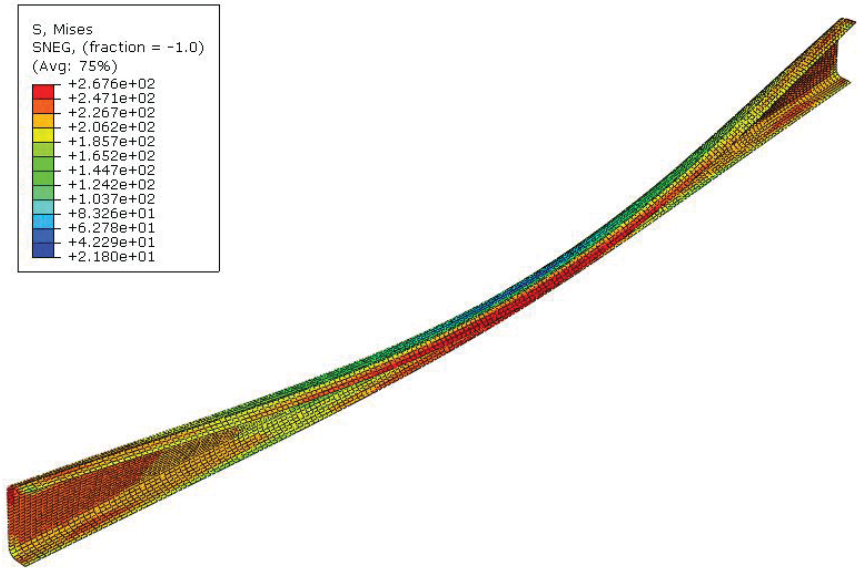

Figure 9 – Example model at the moment of failure

3. RESULTS AND DISCUSSION

The values of bending resistances of the analysed beams obtained from non-linear analysis in ABAQUS are compared in Table 1 with the values obtained using the design approach from Eurocode 9. The comparison includes different beams' spans and variation of load position related to cross-section geometry.

Table 1 – Comparison of bending resistances of the analysed beams

Span		1.5 m		2 m		2.5 m	
Load position		Centroid	Middle of the flange	Centroid	Middle of the flange	Centroid	Middle of the flange
Bending resistances (kNm)	*FEM*	3.49	3.39	2.84	2.67	2.29	2.11
	EC9	3.36	3.36	2.57	2.57	2.1	2.1
Deviation (%)		3.7	0.9	9.5	3.8	8.3	0.5

It can be concluded from the results presented above that the deviations of the values of bending resistances are generally larger than it is the case with the values of critical moments. Graphic comparison of these results is shown in Fig. 10 – Fig. 11.

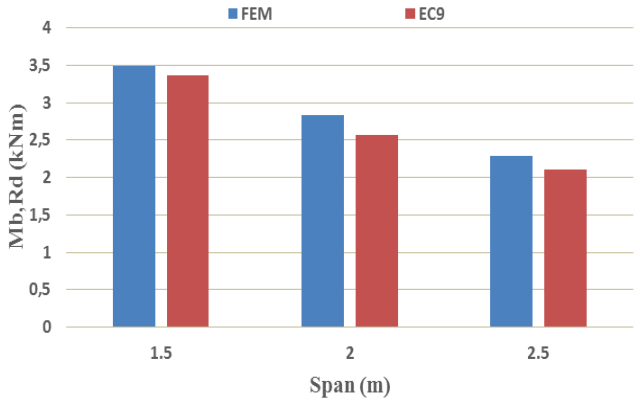

Figure 10 – Bending resistances for load applied in the centroid plane

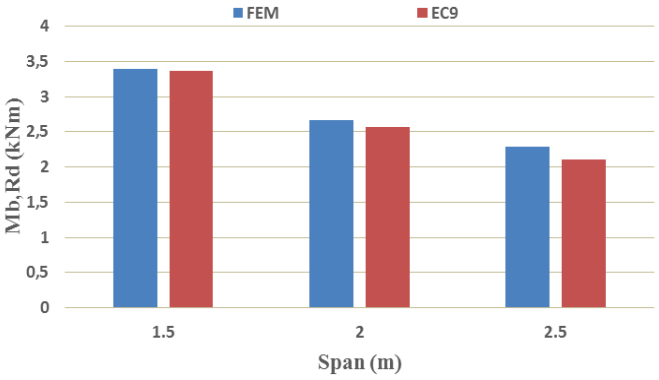

Figure 11 – Bending resistances for load applied in the middle of the flange

It can be noticed from Table 1, as well as from Fig. 10 and Fig. 11, that the values of bending resistances obtained in accordance with Eurocode 9 [4] appear to be safe-sided with respect to the values obtained by FEM analysis. This was not the case with the values of the critical moments, but the fact that the strengthening of the material is not included in the Eurocode design approach against lateral buckling should be appreciated, for it may contribute to this increase of bending capacity.

4. CONCLUSIONS

This paper focuses on the comparative analysis of lateral-torsional buckling capacity of structural channel-section aluminium alloy beams with initial imperfections. The results obtained using FEM analysis and design propositions provided in EN 1999-1-1 are compared and the following conclusions can be accentuated:

- Initial geometric imperfections are introduced in the FEM analysis as the first mode of lateral-torsional buckling scaled so that the amplitude value in the mid-span is equal to L/750, where L is the span length.
- The values of maximum bending moments in the mid-spans obtained by the means of FEM analysis deviate from the values calculated using the design recommendations available in EN 1999-1-1 by 0.5% to 9.5%
- The values of bending capacity of members with initial imperfections obtained using EN 1999-1-1 are shown to be on the safe side, as compared to the values obtained using FEM analysis. Therefore, with respect to the results from this and the preceding research paper [5] it is concluded here that overall lateral buckling resistance of examined aluminium alloy beams with initial imperfections is not overestimated by the Code [4].

REFERENCES

[1] Abaqus 6.12 Analysis User's Manual

[2] EN 1993-1-1:2005, Eurocode 3 – Design of steel structures – Part 1-1: General rules and rules for buildings

[3] EN 1993-1-4:2006, Eurocode 3 – Design of steel structures – Part 1-4: General rules – Supplementary rules for stainless steels

[4] EN 1999-1-1:2007, Eurocode 9 – Design of aluminium structures – Part 1-1: General structural rules

[5] Ivanović N., Marković Z., Dobrić J., Spremić M., Gluhović N.: *Numerical lateral buckling analysis of aluminium alloy beams with channel sections*, Symposium of Association of Structural Engineers of Serbia, 2016., Zlatibor, Serbia.

[6] Mazzolani, F., 2003, Aluminium structural design

[7] Trahair, N. S., Bradford, M. A., Nethercot, D. A., Gardner, L., 2007, The behaviour and design of steel structures to EC3

ДГКС Друштво грађевинских конструктера Србије
ASES Association of Structural Engineers of Serbia
S-77
15. KONGRES
6-8. 9. 2018. Zlatibor

Todor Vacev[1], Miloš Milić[2], Stepa Paunović[3], Ivan Nešović[2], Andrija Zorić[4]

PRIMENA NELINEARNE MKE ANALIZE NA LAMINATNE KONSTRUKCIJE NA PRIMERU REZERVOARA ZA VODU V=100 m^3

Rezime:

Projektovanje i izrada konstrukcija od različitih materijala poboljšanih karakteristika je omogućena napretkom industije u 20. veku. Kao najbolji materijali za upotrebu u agresivnim sredinama pokazali su se kompoziti. Kompoziti su materijali sastavljeni od dve ili više komponenti. Oni zadržavaju dobre, ali i loše osobine materijala od kojih se sastoje. Najveću primenu za izradu rezervoara za tečnosti i gasove ima armirani poliester. U radu je prikazana analiza horizontalnog, ukopanog, cilindričnog rezervoara za vodu sa torosferičnim dancima, izrađenog od poliestera, primenom nelinearne analize zasnovane na Metodi konačnih elemenata (MKE) i savremenih inženjerskih softvera.

Ključne reči: kompozitni materijal, poliester, rezervoar za vodu, MKE

APPLICATION OF NONLINEAR FEA ON LAMINATE STRUCTURES IN CASE OF A WATER TANK V=100 m^3

Summary:

The Design and manufacturing of structures made of different materials with improved characteristics is enabled by industrial advance in the 20th century. As best in aggressive environment appeared to be composites. Composites are materials consisted of two or more components. They keep both the good and the bad properties of the basic materials. Tanks for liquids and gases are mostly manufactured of reinforced polyester. The paper presents a structural analysis of a horizontal buried cylindrical water tank with torispherical ends, made of polyester, using nonlinear Finite Element Analysis (FEA) and advanced engineering software.

Key words: composite material, polyester, water tank, FEA

[1] *PhD, Associate prof., Faculty of Civil Eng. and Architecture, A. Medvedeva 14, Niš, Serbia, todor.vacev@gaf.ni.ac.rs*
[2] *M. Eng., teaching fellow, Faculty of Civil Eng. and Arch., A. Medvedeva 14, Niš, Serbia, milos.cicevac@gmail.com*
[3] *M. Eng., teaching fellow, Faculty of Civil Eng. and Arch., A. Medvedeva 14, Niš, Serbia, stepa.paunovic@gmail.com*
[4] *M. Eng., teaching fellow, Faculty of Civil Eng. and Arch., A. Medvedeva 14, Niš, Serbia, ivan.m.nesovic@gmail.com*
[5] *M. Eng., Assistant, Faculty of Civil Eng. and Architecture, A. Medvedeva 14, Niš, Serbia, azoric90@gmail.com*

1. INTRODUCTION

Polyester applied in structural engineering is a material consisted of the polyester resin as a binder, and glass fibres as a reinforcement. Polyester is resistent to a large number of inorganic and organic compounds, and it is stable on temperatures from -40^{0}C to +120^{0}C [1, 7], which makes it a material suitable for numerous structures.

Reinforced polyester is produced by adding of glass fibres and fine sand and mixing with the polyester binder, in layers of determined thickness. Reinforced polyester has density of 1,5-1,8 g/cm³, it is stable, and aging negligibly affects the physical and mechanical properties of the products made of it [1]. There are attempts to use coco instead of glass fibres as an reinforcement, which would made polyester a more ecological material [2].

Domain of application of the reinforced polyester is very large. It does not emit detrimental matters into water, so it may be used for open tanks for fishery [3]. Covering of structures with polyester may be used for improving of chemical resistance or mechanical strength.

Most of the polyester composite is produced by continual process of winding. Using this process the polymerization is developing under thermal influence from the inductively heated steel core and infrared radiation from the outer side, as well as by the heat release, because the reaction is exothermal (Fig. 1).

Figure 1 – Continual process of winding [4]

Pipes are produced pipes is from inside to outside, which enables an equal inner diameter and optimal hydraulic properties [4]. By this process, pipes with diameter ≤2400 mm can be made.

Table 1 – Structure of a polyester pipe wall [4]

Layer	Structure	Purpose
Inner	„C“ glass	Protection
Boundary	Cut glass fibre	Protection
Inner structural	Continual and cut glass fibre	Structural enforcement
Core	*Si* sand, cut and continual glass fibre	Durable hard core
Outer structural	Continual and cut glass fibre	Structural enforcement
Outer	„C“ glass	Protection

Besides the pipes, it is possible to produce elements where pipes are used as semifinished product. Thus, cutting the pipes at certain angle and joning them, one may obtain fittings [5], elbows etc. By closing of the pipe on one or both ends one may produce a tank or a silo [1].

Figure 2 – Horizontal tank made of polyester [1]

Tanks are made of reinforced polyester, and their purpose is storage and transport of liquids in food processing and chemical industry. If a constant liquid temperature is needed, the tanks may be insulated by polyurethane insulation. Tanks may be consisted of several segments, and the most often they consist of a cylindrical part and top/bottom ends. Because of the smooth inner surface of the poliester tank, it does not allow accumulation of deposits or lime [4].

2. MECHANICAL CHARACTERISTICS OF POLYESTER

Introducing of the polyester composites in civil and mechanical engineering resulted in a need for issuing necessary standards in this field. Currently, in Serbia do not exist standards which regulate design and manufacturing of structures made of polyester, so foreign standars are used [6, 7, 8]. The procedure applied in this paper is based on European codes [7], which define the tank design using classical methods of calculation. The classical design is based on the proof that the bearing capacity or strength of the structure is higher than the proposed influences.

First, it is necessary to determine the number of the lamina and their thickness. The lamina thickness depends on the percentual content of glass in the layer, glass density, and applied binder. The thickness is calculated as follows:

$$t_i = [1/\rho_g + (100 - m_g)/(m_g\, \rho_r)]\, 10^{-3} \qquad (1)$$

where:

t_i thickness of the i-th lamina in mm,
m_g percent of glass over mass in the i-th layer,
ρ_r density of the binder in the i-th layer,
ρ_g density of the glass in the i-th layer.

Beside the thickness of the single lamina, the standard [7] regulates the total thickness of the laminate - not less than *3 mm*. Also, the laminate should be symmetrical regarding the midplane, and overlapping of the layers should not be greater than *1/6* of the thickness of a single lamina.

Design of the reinforced polyester structure is based on critical dilatation under load, being different from the most usual steel, timber, and concrete structures, where stresses and deformations govern. For the reinforced polyester structures the dilatations are limited as:

$$\varepsilon_{ar} = 0{,}1\ \varepsilon_R \tag{2}$$

where:

ε_R dilatation at failure of the binder material with out fibre strengthening.

Reason for such limit is different beahaviour under load of the materials that make the composite. The binder material may reach its limit strength at dilatation lower than the glass fibres, so at overload the binder breaks, and the glass fibres take the bearing role. The composite breaks apart, which leads to the final failure of the structure. Also, these stuctures have small thickness, so it is necessary to check buckling stability. The standard [7] treats that case, too.

3. MODELING OF THE SOIL SURROUNDING THE TANK

The analysed tank is layed in a dugout pit on a layer of sand, and covered over by sand with thickness of 1.0 m, all according to manufacturer's guidelines [4]. Such method of mounting means that the tank does not lay on stiff supports, but the supporting is ellastically across the outer surface of the tank. Such supporting unavoidably implies some deformations. The solution for this problem can be found in the existing methods used for soil modeling.

The simplest soil model is proposed by Winkler [9], who provides the coefficient of the reaction of the ground. The model is used for modeling of foundation footings made of reinforced concrete, diaphragms [9], tunnels and surrounding rock mass (Fig. 3) [10] etc. In this model, the surrounding soil is substituted by a system of equal elastic and mutually independent springs, so the contact pressure and displacement in the connection are given by the following equation:

$$q_i = k_s\ w_i \tag{3}$$

where:

q_i contact pressure at location „i“,

k_s modulus of the soil reaction (coefficient of subgrade reaction),

w_i displacement of the structure at location „i“ perpendicularly to the contact surface.

There are several methods for determination of the coefficient of subgrade reaction. In this paper, for the purpose of modeling of a tank laid in sand, three methods were considered. Proposed relations are given in Table 2.

Table 2 – Coefficient of subgrade reaction according to various authors

Author	Expression	k_s [10^6 Pa/m]	C_{stiff} [10^3 N/m]
Selvadurai [11]	$k_s = E_s / B(1-\nu_s^2)$	12.35	148.20
Meyerhoff and Baike [12]	$k_s = 2\,E_s / B(1+\nu_s)$	18.99	227.88
Kloeppel and Glock [13]	$k_s = 0.65\,E_s / B(1-\nu_s^2)$	24.69	296.28

As one may notice from the equations, it is also necessary to know the Young's modulus of elasticity (E_s) and Poisson's coefficient (ν_s) for defining of the coefficient of subgrade reaction. Recommendations for compacted sand given by Bowles [14] were used (E_s=50 MPa, ν_s=0.35).

Besides that, in the equations is given the characteristic width of the structure (B), which is in this case equal to the diameter of a cylindrical part of the tank ($B = R_r = 3$ m).

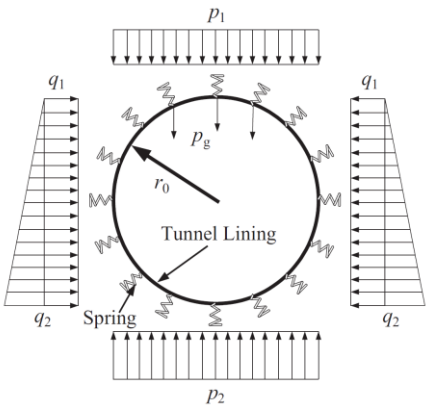

Figure 3 – Substitution of the soil surrounding the tunnel by fictive springs [10]

Contact pressure on structure acts via fictive members, set perpendicularly regarding the contact surface. The members transfer the compression force, but not the tension. The compression stiffness of the fictive members is determined based on the reaction coefficient:

$$C_{stiff} = k_s A \tag{4}$$

where:
A – corresponding area of the fictive member. In this case A=0.012 m^2.

4. STRUCTURAL MODELING AND ANALYSIS USING FEA

Advanced analysis of composite, as well as the other structures, is predominantly based on application of the FE Method and advanced software that enable including of the geometrical and material nonlinearity and use of complex material models, like the composites. Tedious classical calculation, based on the theory of shells and composites can be succesfully substituted by the mentioned advanced methodology, which will be shown here for a case of a horizontal cylindrical water tank with capacity of V=100 m^3, produced by numerous manufacturers.

The cylindrical shape of the tank results from the manufacturing technologyical, because it can be made by continual winding. Elements that close the cylinder, the ends, may be manufactured as flat, hemispherical, or torospherical, Fig. 4 [7]. The cylindrical shell, as a critical structural part regarding the stresses and stability, is commonly stiffened with rings, made also of polyester. Instead of it, one may apply metal stiffeners, but with merging the metal parts into the composite material, in order to achieve resistence to aggressive substance.

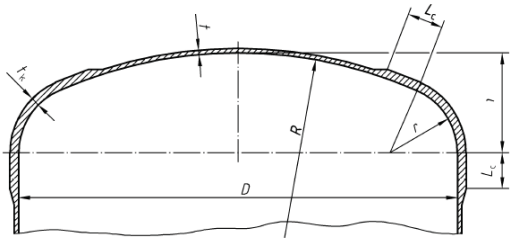

Figure 4 – Detail of a torispherical end [7]

Detailed recommendations for the dimensions of the structural detailing are given in the standard [7]. Thickening of the walls are performed (Fig. 4) in order to achieve the joining between the end and the cylinder. The joining is performed by butt glueing, with adding of some material on the outer side, as a strenghtening. Modeling of the lamina in the software [15] is realized according to the common manufacturing technology, and the aim of the analysis is verification of the strength and prudence of the structure.

Due to the symmetry of the structure and the load, an 1/4 of the structure is analysed. The tank is burried into the ground (sand), and based on that, fictive members across the whole perimeter of the tank are modeled. The members are finite elements of GAP type [15], which exclude transfer of tension forces.

The following load cases were analysed:

- self weight of the tank (G) + weight of the sand cover of height HN=1.00 m (S);
- self weight of the tank (G) + hydrostatic pressure, tank fully loaded (W) + weight of the sand cover of height HN=1.00 m (S).

The load from the soil can be determined using several theories and methods, all of them treating the problem in a very simple way. Here, the method of determination of the load perpendicular to bunker walls, given in the Eurocode for bunkers and silos [16] is applied:

$$p_n = \gamma\, z\, [\tan^2(45^0 - \varphi/2)\sin^2\alpha + \cos^2\alpha] \qquad (5)$$

where:

p_n - load perpendicular to bunker walls,
γ - density of sand ($\gamma = 14.0$ kN/m^3),
z - distance of the load point to the terrain surface,
φ - angle of internal friction for sand ($\varphi = 39^0$),
α - slope between the loaded surface and the horizontal surface.

Analysis is done as geometrically nonlnear for all values of the coefficient of subgrade reaction. Results for the load combination G+W+S are given in Table 3.

Table 3 – Characteristic results depending on the coefficient of subgrade reaction

Author	C_{stiff} [10^3 N/m]	Total displacement [10^{-3} m]	Equivalent dilatation [$^0/_{00}$]
Selvadurai	148.20	15.1	0.635
Meyerhoff & Baike	227.88	11.3	0.515
Kloeppel & Glock	296.28	9.6	0.448

Observing the results for the governing load combination (G+W+S) one may conclude that with the increase of the stiffness of the surrounding soil, the structure deformations decrease. The most unfavourable case of the stiffness is given by Selvadurai, so it was adopted for further presentation. The characteristic output data of the analysis are given as contour images. (Fig. 6-9). Total displacements and equivivalent dilatations are presented. The details of the end are given separately, as potential spots for eventual optimization.

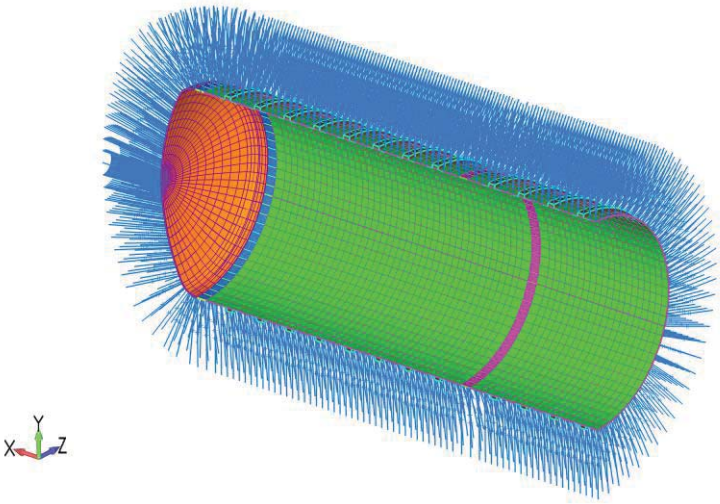

Figure 5 – Model of the structure, FE mesh and GAP elements

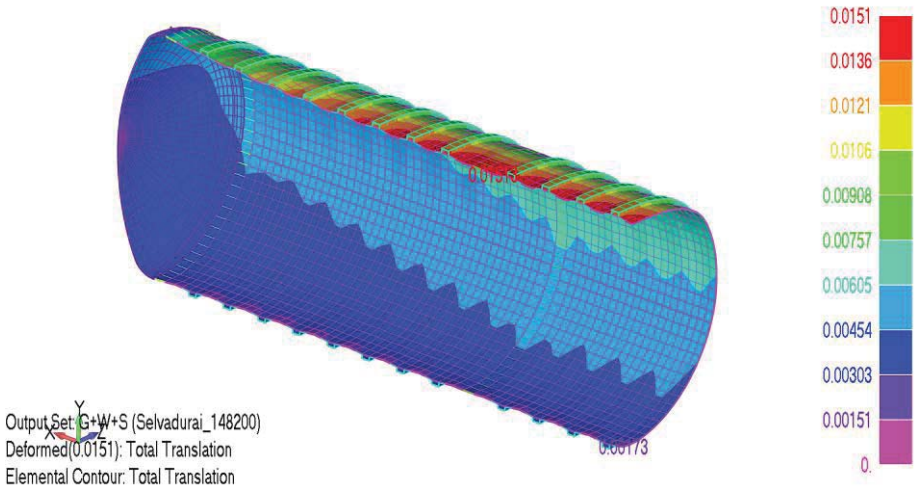

Figure 6 – Load G+W+S. Total deformations. Max. value: 15.1 mm

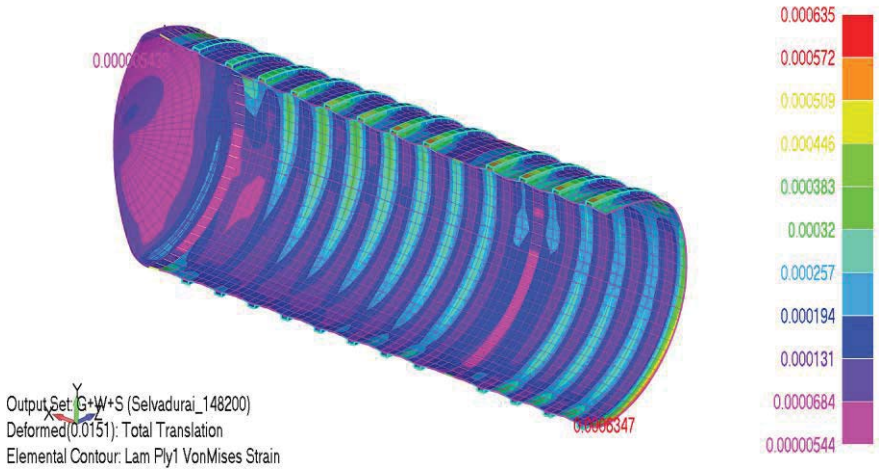

Figure 7 – Load G+W+S. Equivalent dilatations. Max. value: 0.635 ‰

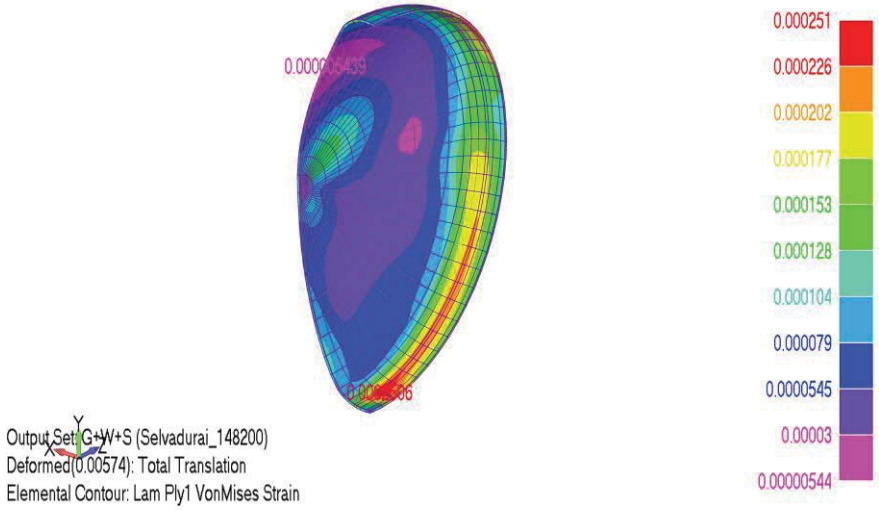

Figure 8 – Load G+W+S. Equivalent dilatations. Detail of the end. Max. value: 0.251 ‰

The equivalent dilatations are adopted as a basic criterion for the assessment of structure strength, according to the standard [7]. The question of the total displacements is not defined as a criterion for the assessment of structure in the mentioned standard, but it is nevertheless given as a comparative illustration of the behaving of the structure. Observations on the obtained results and on the complete analysis are given in the conclusions of the paper.

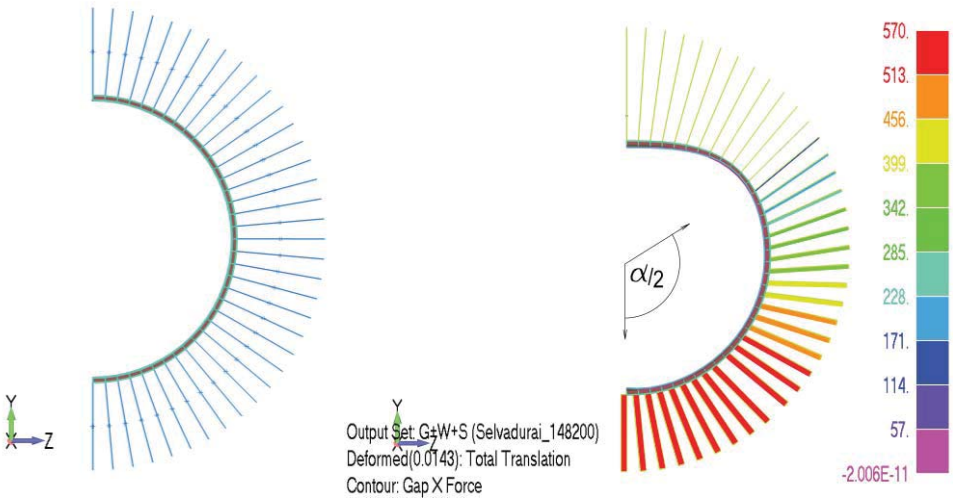

Figure 9 – Load G+W+S. Compression forces in the fictive members. Max. vrednost: 570 N

5. CONCLUSION

Modeling of the presented structure is a sythesis of the manufacturing technology, referent standards and the methodology given in the applied software. On a relatively simple example, which did not include all functional details of the structure (manholes, fitings for filling, emtying, and ventilation), it was shown that advanced modeling and analysis can precisely present distribution of deformations, dilatations, and other influences.

Load combination G+W+S is critical as for displacements, as well as for dilatations. This was expected, because in this case is present superposition of the high hydrostatic pressures inside in the lower part of the tank with high pressures from outside in the top part of the tank from the sand/earth cover.

Displacements of the structure, though not defined by codes, may be considered as relatively small and acceptable for this type of structure. Obtained dilatations are under allowed values, which means that the structure has satisfactory strength. Details of the end show that dilatations are significantly below the allowed values, so there is possibility for the optimization of the structure, i.e., reduction of thickness. Also, the number of the streghtening ribs could be reduced.

The standard [7] recommends that horizontal cylindrical tanks mounted on saddle supports should rest across a central angle of $\alpha = 120^0$. This may lead to the conclusion that modeling of a tank without soil simulation should be with supports that span this angle. In this paper the soil is substituted by GAP elements of specified stiffness, and they are compressed over the angle of $\alpha = 120*2 = 240^0$, which better describes the stress state in the soil that surrounds the tank.

Further analyses should include modeling of the voids, application of the contact analysis instead of the fictive members, and optimization. Also, according to the available technology of manufacturing, optimization may encompas the joining areas, that is, the strenghtening ribs recommended by the standard [7].

LITERATURE

[1] tehnikakb.rs/srl/proizvodi/

[2] Yousif, B. F., Ku, H.: Suitability of using coir fiber/polymeric composite for the design of liquid storage tanks, Materials & Design, Oxford, UK, 2012, 847-853.

[3] Kenneth, M.: Construction of Fiberglass Water Tanks, The Progressive Fish-Culturist, vol. 26, 2011, 91-92.

[4] poliesterpriboj.com/cevi-tehnologije

[5] dubaipipes.com/general.html

[6] Design recommendation for storage tanks and their supports with emphasis on seismic design, Architectural Institute of Japan, Tokio, Japan, 2010.

[7] EN 13121-3:2008+A1 - GRP tanks and vessels for use above ground - Part 3: Design and workmanship, European Committee for Standardization, Brussels, Belgium, 2010.

[8] BS 4994(1987) - Specification for the design and construction of vessels and storage tanks in reinforced plastics

[9] Prolovic, V: Foundation engineering, Faculty of Civil Engineering and Architecture, Niš, 2003. (in Serbian)

[10] Popović, B.: Tunnels, Građevinska knjiga, Belgrade, 1987.

[11] Zhang, D., Huang, H., Phoon, K. K., Hu, Q.: A modified solution of radial subgrade modulus for a circular tunnel in elastic ground, Soils and Foundations, vol. 54(2), 2014, 225-232.

[12] Selvadurai, A. P. S.: Elastic Analysis of Soil-Foundation Interaction, Developments in Geotechnical Engineering, Vol. 17, Elsevier Scientific Publishing Co., Amsterdam, 1979.

[13] Meyerhoff, G. G., Baike, L. D.: Strength of Steel Culvert Sheets Bearing Against Compacted Sand Backfill, Highway Research Board, Proceedings of the 42nd Annual Meeting, 1963.

[14] Kloeppel, K., Glock, D.: Theoretische und experimentelle untersuchungen zu den traglastproblemen biegeweicher, in die Evde eigenbetten Rohre. Publ. No. 10, Institut fuer Statik and Stahlbau, T. H. Darmstadt, Germany, 1970. (in German)

[15] Bowles, J., E.: Foundation Analysis and Design, 5th edition, McGraw-Hill Book Co, Singapore, 1997.

[16] FEMAP-NX NASTRAN – Software Manual

[17] BS EN 1993-4-1:2007 – Eurocode 3 – Design of steel structures – Part 4-1: Silos, British Standards Institution, London, UK, 2007.

ДГКС Друштво грађевинских конструктера Србије
ASES Association of Structural Engineers of Serbia
S-78
15. KONGRES
6-8. 9. 2018. Zlatibor

Koce Todorov[1], Ljupčo Lazarov[2]

OTPORNOST, KRUTOST I DUKTILNOST RAMOVA SA ZIDANOM ISPUNOM IZLOZENI BOČNOM OPTEREĆENJU

Rezime:

Zidana ispuna se karakteriše značajnom čvrstoćom i krutošću u svojoj ravnini i time može u velikoj meri promeniti ponašanje konstrukcija izloženih seizmičkim opterećenjima.
Da bi se istražio uticaj zidane ispune na ponašanje objekata izloženih bočnim opterećenjima, izvršena je obimna nelinearna statička analiza u ovom radu. Analizirano je šest armirano-betonskih ramova sa različitim brojem spratova, projektovani kao okviri bez ispune. U fazi procene karakteristike ramova, sve konstrukcije su nadopunjene zidanim panelima sa dve različite karakteristike čvrstoće i krutosti.
Dobijeni rezultati, izraženi u poređenju krive kapaciteta i degradacije krutosti, pokazuju značajan uticaj zidane ispune na čvrstoću, krutost i duktilnost analiziranih ramova.

Ključne reči: ramovi sa zidanom ispunom, nelinearna staticka analiza, degradacija krutosti

STRENGTH, STIFFNESS AND DUCTILITY OF MASONRY INFILLED FRAMES UNDER LATERAL LOADS

Summary:

Masonry infill is characterized with significant in-plane strength and stiffness and it can greatly alter the response of structures exposed to seismic loads.
In order to investigate the influence of masonry infill on the behaviour of structures exposed to lateral loads, an extensive nonlinear static analysis was performed. Six reinforced concrete frames with different number of storey, designed as bare frames were analysed. In the phase of assessment, all structures were updated with the presence of masonry infill panels with two different strength and stiffness characteristics.
The obtained results, expressed in terms of the comparison of capacity curves and stiffness degradation shows significant influence of masonry infill on the strength, stiffness and ductility of analased frames.

Key words: masonry infilled frames, nonlinear static analysis, stiffness degradation

---

[1] *Assistant Professor, Ss. Cyril and Methodius University in Skopje, Faculty of Civil Engineering, Skopje, Republic of Macedonia, todorov@gf.ukim.edu.mk*
[2] *Professor, Ss. Cyril and Methodius University in Skopje, Faculty of Civil Engineering, Skopje, Republic of Macedonia, lazarov@gf.ukim.edu.mk*

1. INTRODUCTION

Reinforced concrete frames with masonry infill are often used structural systems in construction practice worldwide. In this type of structures, the external and internal walls made of different materials, usually of ceramic blocks and bricks, are built as infill panels between reinforced concrete elements. Masonry infill is characterized with significant in-plane strength and stiffness and it can greatly alter the response of structures exposed to lateral loads. The infill panels increase the structural stiffness, strength and damping and act as a first line of defence in seismic activity, reducing the ductility demand and consequent damage of structural elements. However irregular distribution of infill in plane and along building height can lead to series of unfavourable effects (torsion effects, dangerous collapse mechanisms, soft or weak storey, variations in the vibration period, etc.). That is why different opinions about the influence of the infill on the seismic behaviour of the structures can be found in the scientific and expert community (Fardis and Panagiotakos 1997, Manfredi and al. 2012, Todorov 2014).

The presence of infill significantly changes the mechanism for lateral load redistribution. Thus, the predominant frame system, in which the elements are exposed to bending, is transformed into a predominant truss system whose elements are generally exposed to axial action (Murthy and Jain 2000). Although this is an undeniable fact, according to the usual design practice, the interaction between the infill and the frame structure is most often neglected. This can lead to significant errors in determining the stiffness, bearing capacity and ductility of the analysed structure, which can especially be emphasized in reinforced concrete frames with discontinuity in the distribution of the masonry infill to the height of the building.

2. DESCRIPTION OF ANALYSED STRUCTURES

In order to analyse the influence of the masonry infill on the behaviour of reinforced concrete frames, a series of nonlinear static analyses was conducted in this research. All analysed frames have been designed without taking into account the influence of the infill. In the phase of nonlinear assessment, all frames were additionally upgraded with the presence of masonry infill. Two different distribution of infill panels was analysed: fully infill frames (FI) and infilled frames with open first floor (OS). All numerical analyses were performed by the program SeismoStruct v6.0.

2.1. DESIGN PARAMETERS

In order to cover structures with different dynamic characteristics, six reinforced concrete plane frames with different number of storeys (n=2, 3, 5, 7, 10 and 13), in the following text marked as frames R1, R2, R3, R4, R5 and R6, are generated in this investigation. All analysed structures are designed as three bay plane frames with a span of 5m and a constant storey height of 3m. The frames are designed to represent the exterior frame of a reinforced concrete spatial frame structure, Figure 1. After the distribution of the surface load on the frames in both orthogonal directions, the beams of analysed frames were exposed to uniform load of 25kN/m' on the floors and 15kN/m' on the roof. At the beam – column joints additional concentrated forces, which represent the influence of the beams in the longitudinal direction, was applied. A

schematic representation of distribution of the gravity loads and the storey mass of the analysed frames is presented at Figure 1.

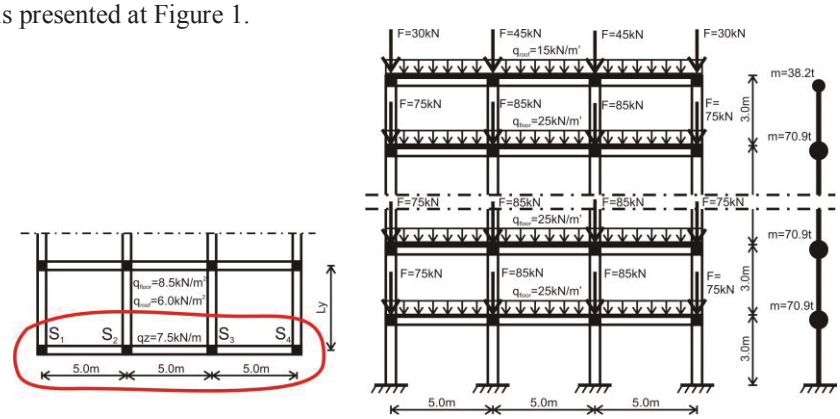

Figure 1. Schematic representation of analysed frame structures

2.2. MODELING ASSUMPTIONS

For the modelling of reinforced concrete elements, the model of distributed plasticity with the displacement based formulation of finite elements is used. Each structural element is divided at four subsections with different lengths. For the purpose of numerical integration, the cross sections in Gauss integration points are discretised with a triangular mesh of elements – fibres, with an optimal mesh density of about 100 fibres per cross-section. During the analysis, each fibre of cross-section is exposed to a uniaxial state of stress. Internal forces are obtained by numerical integration of stresses in the individual fibres. Mander's RC model for confined and unconfined concrete and Menegoto - Pinto steel model with the Monti - Nuti buckling rules for the longitudinal reinforcement was used to describe the stress - strain relationship in individual fibres. The nonlinear behaviour of masonry infill was modelled with the equivalent diagonal strut, using the model developed by Crisafulli (1997), Smyrou at al. (2011).

Nonlinear static analysis is performed for the action of constant gravity load, which represents the initial state of stress and deformation in the structural elements and for the action of a monotonically increasing lateral load, which represents the inertial seismic forces initiated by the action of the seismic impact. It's well known that results of the nonlinear static analysis are strongly depend from the pattern of distribution of the lateral force. Taking into account that in the frames with an open floor, the effective modal mass in the first mode shape is over 80% of the total mass for all frames, i.e. over 90% for frames R1 to R4 with a strong infill and for frames R1 to R3 with a weak infill, in the further analyses assumed distribution of the lateral load according to the first mode shape was used. This assumption is based on the fact that with the development of nonlinearities in the structural elements the participation of the effective modal mass of the dominant mode shape is usually increased. It should be noted that the distribution according to the first mode shape, determined for an undamaged structure, assumes the invariance of the mode shapes in function of the damage, which usually is not true. However, changes in mode shapes, due to the influence of material nonlinearity, are usually small and do not have a major impact on the results of nonlinear static analysis, although the changes in vibration periods due to a reduction in the horizontal stiffness can be significant.

2.3. ADAPTED FEATURES OF MASONRY INFILL

Masonry infill was defined with two different strength and stiffness characteristics, namely week infill (WI) and strong infill (SI). The weak infill is characterized by the compression strength in the diagonal direction fm=0.8MPa and a thickness of 15 cm., while the strong infill has a compression strength of 1.2MPa and a thickness of 25cm. An initial modulus of elasticity equal to 1500fm was adopted for both types of infill. The compression strength is reached at strains of 0.002, while complete degradation of the strength and stiffness of the infill occurs at ultimate strain of 1%. The secant modulus of elasticity, at the point of achievement of compression strength is equal to one third of the initial modulus of elasticity, Esec=500fm. For defining the characteristics of the shear spring in the used material model, the initial shear bond strength of the infill τo=0.3MPa and coefficient of friction μ=0.5 were adopted. The maximum shear strength τmax was limited to 0.6 MPa.

According to the adopted concept for modelling the masonry infill, a compression strut is characterising with variable area which reduction is a function of the reached axial strains. The initial area of compression strut is a product of the thickness of the infill and the width of the equivalent diagonal, for which a value of 20% of the length of the diagonal is adopted. When strains in infill reach the value $\varepsilon 1$=0.0005, the area of the diagonal begins to linearly decrease. At strain equal to 0.0063, its area is 50% of the initial. Stress – strain relationship for masonry infill, reduction of strut area and defined diagram lateral force – inter-storey drift for masonry infill panel are presented at Figure 2.

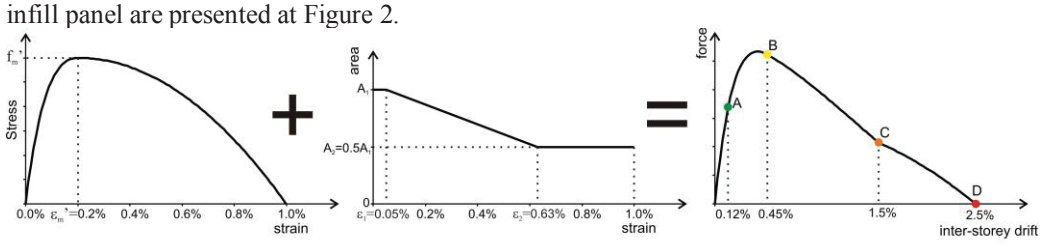

Figure 2. Stress – strain relationship for masonry infill, reduction of strut area and defined diagram lateral force – inter-storey drift for masonry infill panel

3. CAPACITY CURVES

The capacity curves for the analysed frames without and with masonry infill, determined for the distribution of the lateral load according to the first mode shape, are presented in Figure 3. On the vertical axis, the total base shear, expressed as a percentage of the total weight of the frame is displayed, while the horizontal axis shows the top displacements as a percentage of the total height of the frame (top drift). The curves are also marked by the points of appearance of the first plastic hinge in the structure, the points of formation of the mechanism, as well as the level of the design seismic force increased by 30%. The appearance of the first plastic hinge is defined by determination the step in the analysis when the strain of the longitudinal reinforcement in any section of the frame elements reached yield strains, which is 0.2%. The state of plastic mechanism formation is reached in the moment when plastic hinges occurs in at least two cross sections of all four columns of the considered frame.

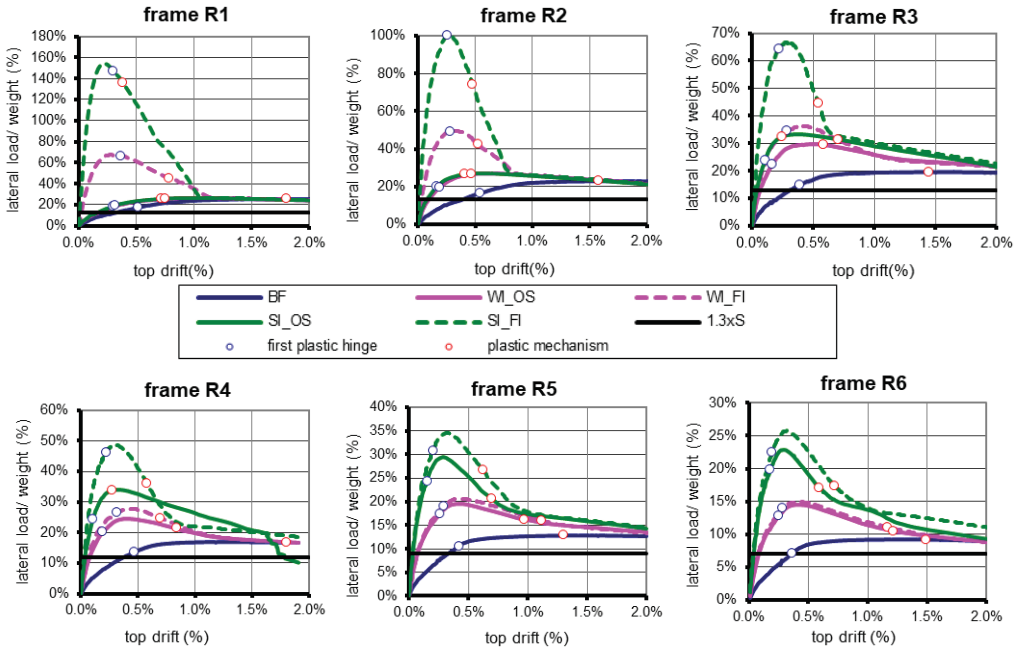

Figure 3 – Capacity curves of analysed frames

From the diagrams presented in Figure 3, it can be noticed that the masonry infill has favourable effects on the load bearing capacity of the analysed frames, by increasing the level of the lateral force that causes the appearance of the first plastic hinge, as well as, by increasing the maximum capacity of the frames. The ratio between the level of lateral force as well as the displacement at first plastic hinge for the infilled and bare frames is presented in Figure 4.

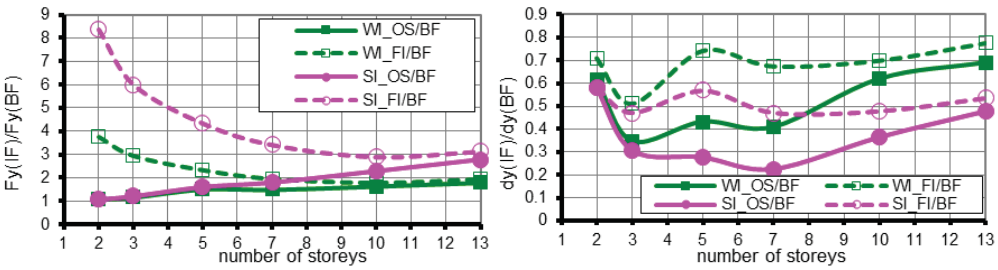

Figure 4 – Ratio of lateral loads and top displacements at occurrence of first plastic hinge for infilled and bare frames

Increasing the level of the lateral load at first plastic hinge in the infilled frames, compared to the bare frames, is a result of the redistribution of the internal forces due to the influence of the infill. Unlike the bare frames where the first plastic hinge occurs in the beam elements of the lower storeys, in the frames with an open first floor the first plastic hinge usually occurs in the support of one of the columns, Figure 6.

The ratio between the lateral load at appearance of the first plastic hinge in the frame with the open floor and the bare frame, increases with increasing the number of storeys. This ratio is greater in the high rise frames with strong infill compared to the infilled frames with weak infill. Unlike open storey frames, in frames with a continuous infill, the ratio between the yield force for the infilled and bare frames decreases with increasing a number of storeys. At the highest frame the lateral load at the first plastic hinge formation for frames with open ground floor and frames with continuous infill is almost the same, indicating that the impact of the infill absence in the first floor is reduced by increasing the number of storeys, making the frames with the open floor to behave approximately in the same way as the frames with a continuous infill. Unlike the level of lateral load, the top drift at yield decreases due to the presence of the infill. The infilled frames reach the yield strength at smaller top displacement compared to the bare frames, Figure 4. The yield displacements in frames with weak infill are greater than the displacements in the appropriate frames with strong infill. This ratio is quite small in the frames R1 and R2, and increases with increasing a number of storey.

Top drift and the level of the lateral force, expressed as a weight ratio, obtained at the moment plastic mechanism formation for the analysed frames are presented in Figure 5.

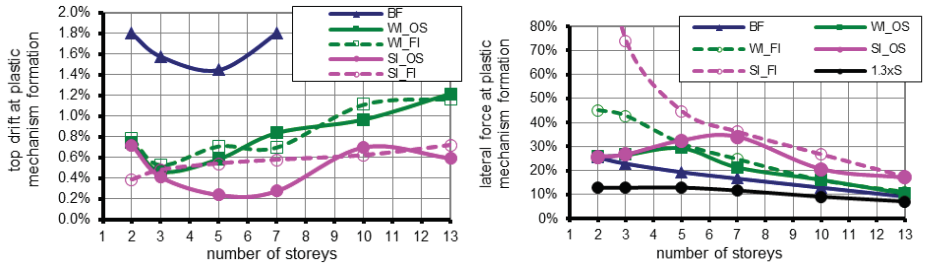

Figure 5 – Top drift and lateral force at the moment of plastic mechanism formation

The lateral force at the moment of plastic mechanism formation in low rise open storey frames is approximately the same as the lateral force in the respective bare frames, and is significantly less than the lateral force in the frames with continuous infill. With increasing a number of storey, the differences between open storey frames and frames with continuous infill are reduced, while the differences between bare frames and open storey frames increases. In all frames with continuous infill, and in the frames R5 and R6 with open ground floor, the level of lateral force at mechanism formation is less than the level of force at the beginning of the yield. At the bare frames, the top drift at the moment of plastic mechanism formation ranges from 1.45% to 1.8%, while at the infilled frames these displacements are 2 to 6 times smaller. On the bare frames the plastic mechanism is manifested through the formation of plastic hinges at the ends of the beams almost along the entire height of the frames, while in the infilled frames a plastic mechanism is expressed through a soft story mechanism formed by the appearance of plastic hinges at both ends of the columns on the ground floor, or through a combination of the formation of plastic hinges at the ends of the beams and columns on the lower storeys.

The state of occurrence of the first plastic hinge and the state of mechanism formation for the analysed frames is shown in Figure 6. The blue colour indicates an element in which the condition of the appearance of first crack is reached, red colour represent the sections in which the yield strain in tensile reinforcement are reached, with green colour a cross section at which

the ultimate strain in the concrete cover is achieved, while in the dark blue colour are marked sections in which strains reach values 0.8% in the concrete core, i.e. in the confined concrete.

Frame	condition	Bare frame (BF)	Open storey frame with week infill (WI_OS)	Fully infilled frame with week infill (WI_FI)	Open storey frame with strong infill (SI_OS)	Fully infilled frame with strong infill (SI_FI)
R1	yield		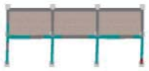	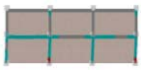	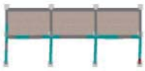	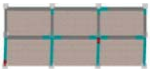
	mechanism		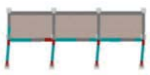	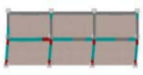	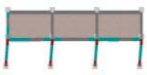	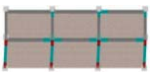
R2	yield	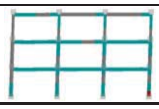	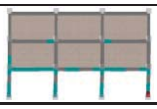	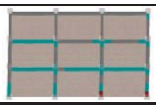	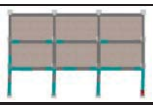	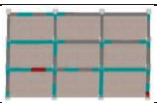
	mechanism	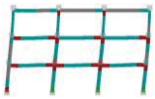	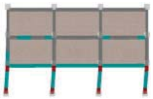	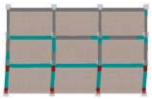	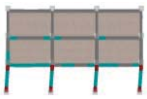	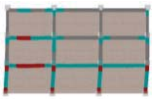
R3	First yield			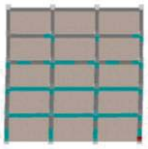	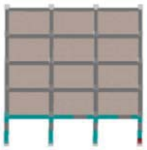	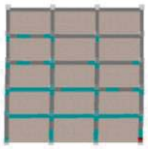
	mechanism	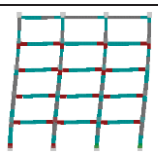	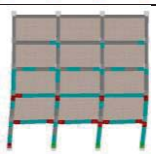	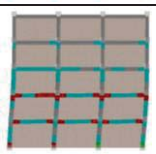	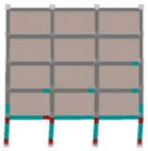	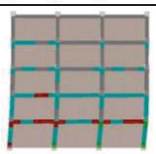
R4	First yield	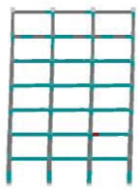	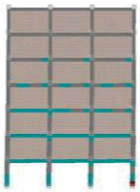	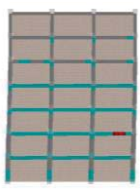	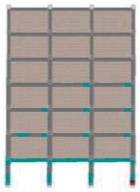	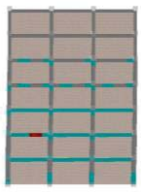
	mechanism	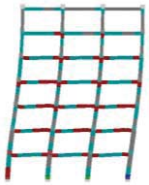	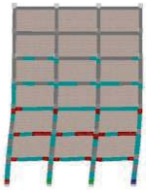	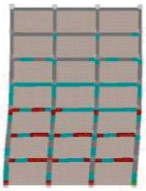	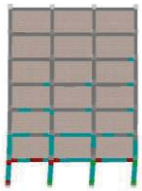	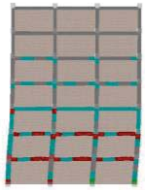

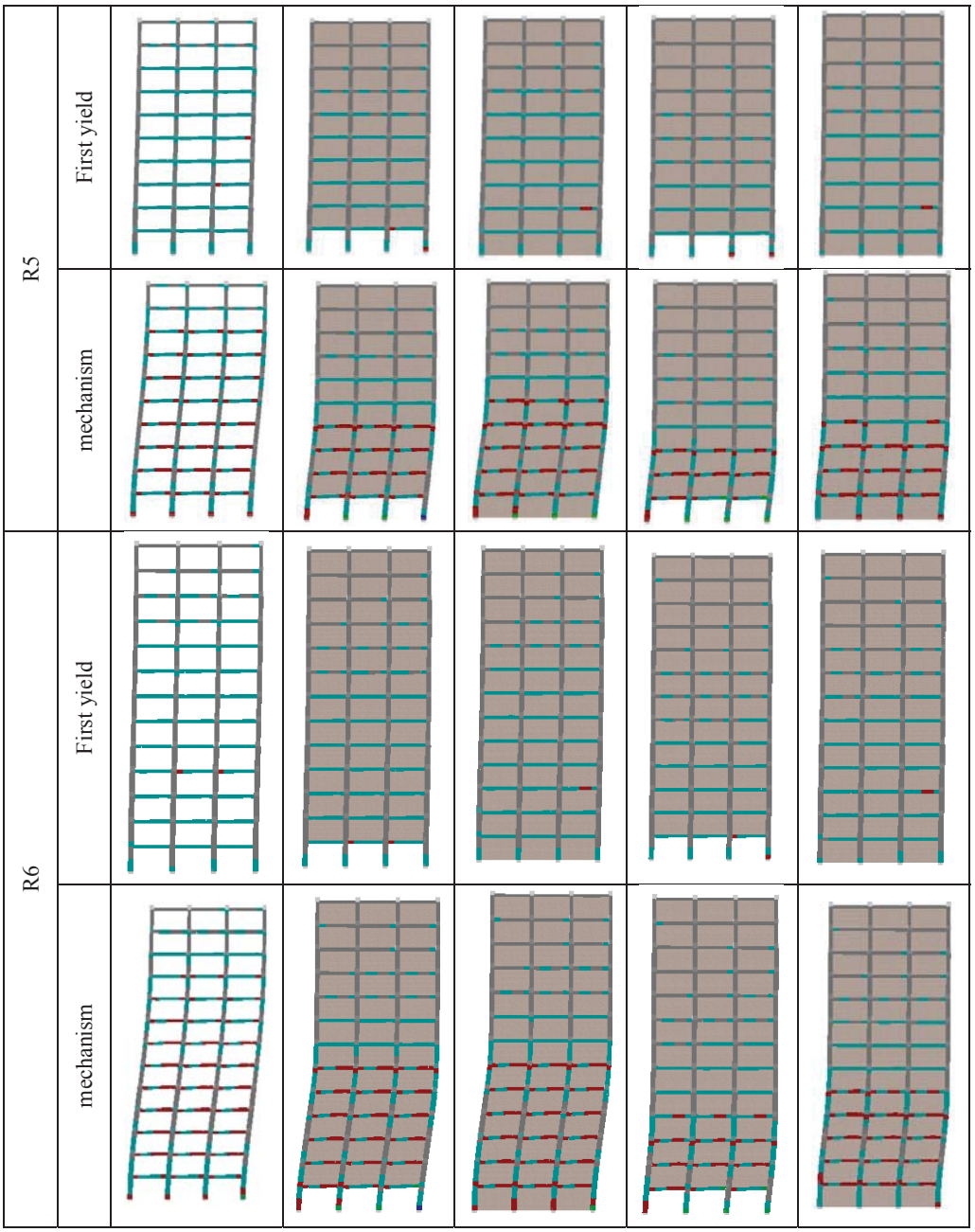

Figure 6 – Ooccurrence of the first plastic hinge and plastic mechanism formation for analyzed frames

4. STIFFNESS DEGRADATION

The linear analysis theory is based on the constant stiffness of the structure, regardless of the degree of deformation of the structural elements. However, with the cracks appearance in the reinforced concrete elements and in the masonry infill, as well as with the achievement of the yield strains in the reinforcement, the stiffness of the structure continuously degrades. The degree of degradation depends on the achieved deformation in the structural elements, which at global level are in function of the achieved lateral displacements. Figure 7 shows the ratio between the secant and the initial lateral stiffness in function of the achieved lateral top drift.

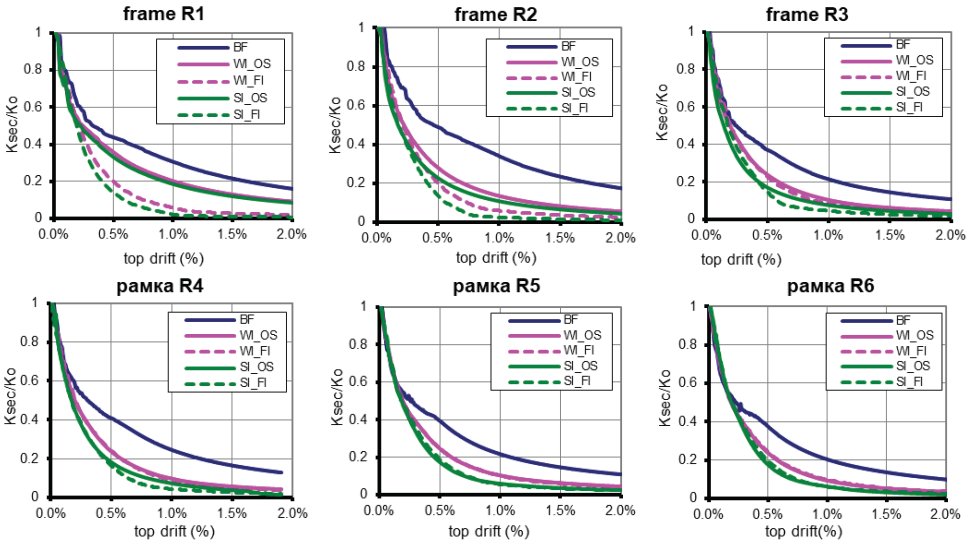

Figure 7 – Degree of stiffness degradation of analysed frames

The degree of degradation of the lateral stiffness of the bare and infilled frames is almost identical to the top drift in range from 0.1% to 0.15%, which is especially expressed at the higher frames. With the further increaseing of displacements, bare frames have a lower degree of degradation, compared to the infilled frames. The highest degree of degradation occurs in frames with a continuous infill over the entire height. Degree of degradation, almost does not depend on the number of storeys. At top drift equal to 0.5% of the total height, the secant stiffness with respect to the initial ranges from 38% to 50% in the bare frames, about 20% to 25% in the frames with an open ground floor and about 15 % to 25% in frames with continuous infill.

At the moment of the appearance of the first plastic hinge, and due to the effects of cracks in reinforced concrete elements, the secant stiffness of the bare frames ranges from 42% to 47% in relation to the initial stiffness. These values are 3% to 8% lower than the recommendations for stiffness reduction according to Eurocode 8 (EN 1998-1:2004). According to the obtained distribution of cracks through the structural elements, it can be noticed that the usual reduction of the stiffness is due to the appearance of cracks in the beam elements, in which the degree of cracks at the moment of first yield is significantly greater compared to the columns. This is especially expressed in the higher frames. The concept of

equal reduction of stiffness in all elements would have no greater impact on the global characteristics of the analysed structures, but it can have a significant impact on the redistribution of internal forces in structural elements with different degree of stiffness degradation.

5. CONCLUDING REMARKS

Presence of the masonry infill, its quality and irregular distribution in the height have a significant influence on the fundamental structural characteristics – stiffness, strength and ductility. Masonry infill significantly affects the level of the lateral load that causes the appearance of the first plastic hinge, as well as the bearing capacity of the frames. Due to the overstrength of the columns, as well as due to the modification in the lateral loads bearing mechanism, the frames with a masonry infill and open first floor have a greater bearing capacity compared to the bare frames. With increasing the number of storey, the ratio between the capacity of the bare frames and the infilled frames with open first floor increases. Unlike the increased capacity, the infilled frames show significantly smaller yield displacements and less ability to develop plastic deformations compared to the bare frames.

With the development of cracks in the reinforced concrete elements and in the masonry infill, as well as with the appearance of yielding in the reinforced concrete elements there is a permanent degradation of the stiffness at the reinforced concrete frames with and without masonry infill. Degree of degradation in frames with and without infill is approximately equal until top displacement ranging from 0.1% to 0.15% of the total height. With increasing a displacement, the frames with the infill show a faster degree of stiffness degradation compared to the bare frames. This tendency is more pronounced at frames with a stronger infill compared to those with weaker infill. The number of storey has insignificant effect on the degree of degradation of the stiffness of the analysed frames.

REFERENCES

[1] Fardis M.N., Panagiotakos T.B.: Seismic Design and Response of Bare and Masonry-Infilled Reinforced Concrete Buildings. Part II: Infilled Structures. Journal of Earthquake Engineering, 1(3), 1997, 475-503.

[2] Manfredi G., Ricci P., Verderame G.M.: Influence of Infill Panels and Their Distribution on Seismic Behavior of Existing Reinforced Concrete Buildings. Open Constr. Build. Technol. J., 6, 2012, 236-253.

[3] Murty C.V.R.., Jain S.K.: Beneficial Influence of Masonry Infill's on Seismic Performance of RC Frame Buildings, Proceedings of the 12th World Conference on Earthquake Engineering, New Zealand, 2000, Paper No. 1790.

[4] Smyrou E., Blandon C., Antoniou S., Pinho R., Crisafulli F.: Implementation and Verification of a Masonry Panel Model for Nonlinear Dynamic Analysis of Infilled RC Frames. Bulletin of Earthquake Engineering, 9(5), 2011, 1519-1534.

[5] Todorov K.: Seismic Performance of Masonry Infilled Reinforced Concrete Frames with Open First Storey. PhD thesis, Faculty of Civil Engineering, University Ss. Cyril and Methodius, Skopje, R. Macedonia, 2014.

ДГКС Друштво грађевинских конструктера Србије
ASES Association of Structural Engineers of Serbia
S-79
15. KONGRES
6-8. 9. 2018. Zlatibor

Stefan Kondić[1], *Jelena Dobrić*[2], *Nina Gluhović*[3]

PRORAČUN PEŠAČKE PASARELE PREMA EVROKODU 9

Rezime:

Primena aluminijumskih legura u građevinarstvu, zbog svojih brojnih prednosti, nalazi široku primenu za građenje različitih tipova konstrukcija. U ovom radu prikazan je proračun pešačke pasarele koja je izvedena od ekstrudiranih elemenata od aluminijumske legure EN-AW 6082 T6, sa posebno oblikovanim poprečnim presecima tako da omoguće primenu inovativnih spojnih sredstava. Prikazan je proračun i konstruisanje veza ekstrudiranih elemenata sa zavrtnjevima koristeći preporuke date u standardu CNR-DT 208/2011 za proračun konstrukcija od aluminijumskih legura. Takođe, u radu je dat proračun vibracija pešačke pasarele, kroz različite metode proračuna. Rezultati numeričke analize poređeni su sa preporukama iz različitih, trenutno dostupnih standarda i literature koji definišu kriterijume prihvatljivosti u pogledu vibracija pešačkih pasarela.

Ključne reči: pešačka pasarela, aluminijumske legure, vibracije, specijalne veze

DESIGN OF PEDESTRIAN BRIDGE ACCORDING TO EUROCODE 9

Summary:

Aluminum alloys, due to its numerous advantages, is widely used in the construction of various types of structures in civil engineering. Design of pedestrian bridge, entirely constructed of extruded elements made of aluminum alloy EN-AW 6082 T6 with cross sections designed to enable the use of innovative joints, is presented in this paper. The design and construction of special bolted joints is presented using the recommendations given in standard for design of aluminum structures CNR-DT 208/2011. Also, calculation of pedestrian bridge vibrations through different design methods is given here. Results of numerical analysis are compared with the recommendations from different currently available standards and literature referring to the comfort criteria of pedestrian bridge vibrations.

Key words: pedestrian bridge, aluminum alloys, vibrations, special joints

[1]*MSc Eng, stekond@yahoo.com*
[2]*PhD, Assistant professor, University of Belgrade Faculty of Civil Engineering, jelena@imk.grf.bg.ac.rs*
[3] *PhD student, Teaching assistant, University of Belgrade Faculty of Civil Engineering, nina@imk.grf.bg.ac.rs*

1. INTRODUCTION

In addition to the well-known advantages of aluminum alloys such as corrosion resistance, lower weight and high strength-to-weight ratio in comparison to the carbon steel, one of the greatest advantages of aluminum alloys is the great flexibility of the cross-sectional design that the extrusion process provides. The most important advantages of the extruded profiles are the improvement of the cross-sectional properties, the optimization of the structural behavior and the weight reduction. Moreover, extruded aluminum profiles allow usage of special joints, which, unlike the traditional joints, can be completely accomplished without the cross-sectional weakening that occurs when drilling holes, for example. However, the lower modulus of elasticity of aluminum alloys and lower overall weight of the structure leads to higher susceptibility of these structures to the serviceability requirements, such as deflection and vibrations. The application of extruded aluminum alloy profiles and special joints for construction of a novel type of pedestrian bridge is presented in this paper. Moreover, vibrations of this pedestrian bridge due to human walking are analyzed through numerical model and the results are compared with different standards.

2. NUMERICAL MODEL OF PEDESTRIAN BRIDGE

The numerical model of the analyzed pedestrian bridge was developed in 3D FEA software Dlubal RFEM 5 [1]. Analyzed pedestrian bridge is a lattice girder, spanning 30 m, with a 3.0 m structural height of lattice girder. Overall width of the pedestrian bridge is 3.3 m and height is approximately 6.50 m. Vertical lattice girders are supported by the vertical portal frames. Access of the pedestrians to the bridge is enabled with the stairs, pin connected to the vertical portal frames, on the both sides of the bridge.

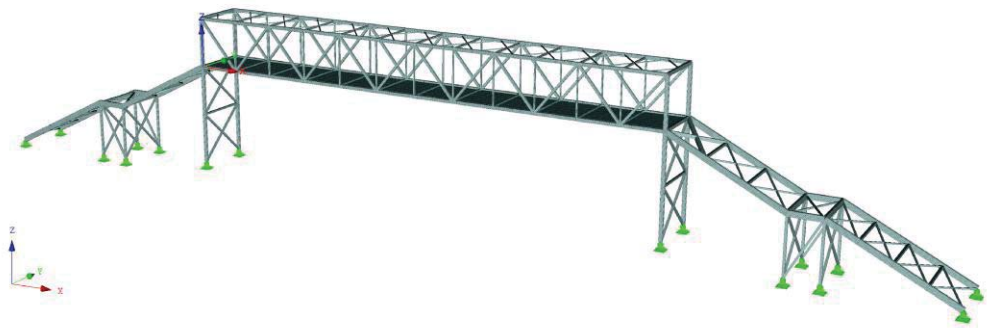

Figure 1 – Numerical model of pedestrian bridge

Pedestrian bridge deck consists of a deckplate and longitudinal stiffeners and is supported by the cross beams. Cross beams are pin connected to the vertical lattice structure, except at the position of vertical portal frames. Vertical portal frames are constructed from simply supported columns, vertical bracing and cross beams connected to the columns as moment resisting joint. Overall stability of the structure is accomplished using vertical and horizontal bracings, as

shown in Figure 1. Cross-sections of extruded aluminum alloy EN-AW 6082 T6 profiles which are used for construction of pedestrian bridge are shown in Figure 2a, and design resistance of cross-sections and structural members are defined according to recommendations given in EN 1999-1-1 [2]. Class of cross sections of all extruded profiles is three, except for the cross beams, which are the second class.

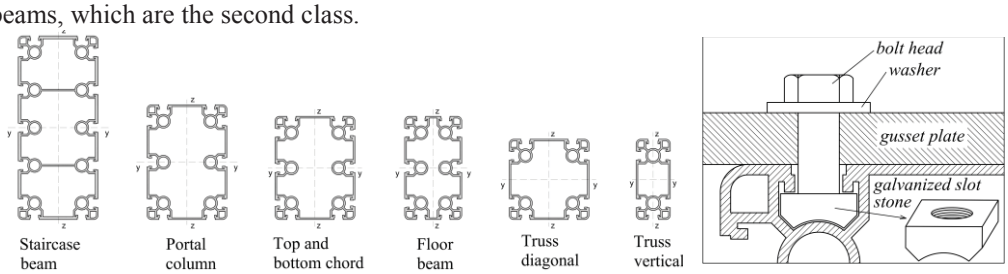

a) extruded cross sections *b) bolt-channel joint*

Figure 2 – Member cross-sections and a connection detail of aluminum alloy profiles

Most commonly used special joints are: snap-fit joints, screw port joints, and bolt-channel joints. Cross section of every single member of the pedestrian bridge is specifically designed to enable the use of bolt-channel joints, which are shown in Figure 2b. Bolt-channel joints are composed of galvanized slot stone, with thread which is positioned in the channels of the extruded profiles, and bolt with the washer, as shown in Figure 2b. Construction and design of this type of joint according to CNR-DT 208/2011 [3] is in detail explained in this paper.

3. DESIGN OF BOLT-CHANNEL JOINTS

Design resistance of bolt-channel joints, which is used for connection of extruded profiles of pedestrian bridge, shown in Figure 2a, was determined according to Italian Recommendations for aluminum structures CNR-DT 208/2011 [3]. CNR-DT 208/2011, Section IV [3] defines design recommendation for this type of joint. Design resistance is determined relative to the direction of the channel/slot axis. Instead of using partial safety factor for slip resistance γ_{M3}=1.25, which is used for the design of carbon steel joints, according to EN 1993-1-8 [4], CNR DT 208/2011 [3] defines partial safety factor γ_{M3}=1.5. The main symbols which represent the dimensions of different parts of bolt-channel joint, which are used in Eq. (1) to (3), are given in Figure 3.

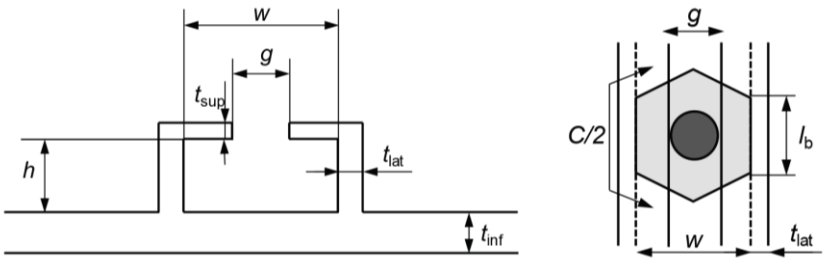

Figure 3 – Channel geometry and symbols used for design [3]

Slip resistance (bolt resistance for force acting parallel to the channel axis) should be calculated according to the Eq. (1):

$$F_{s,Rd} = \frac{n \cdot \mu}{\gamma_{M3}} \cdot F_{p,C} \tag{1}$$

where:

$F_{p,C}$ is bolt preloading force $F_{p,C} = 0.7 \cdot f_{ub} \cdot A_s$;

μ is friction coefficient;

n is the number of friction surfaces;

A_s is nominal stress area.

Shear resistance (bolt resistance for force acting transverse to the channel axis) should be calculated according to the Eq. (2):

$$F_{v,Rd} = \frac{1.2 \cdot l_b \cdot t_{lat} \cdot f_u}{\gamma_{M3}} \tag{2}$$

where:

l_b is contact length between the web of the channel and the bolt head;

t_{lat} is web thickness of the channel;

f_u is ultimate strength of the aluminum alloy.

Pull-out resistance of bolt should be calculated according to Eq. (3):

$$F_{o,Rd} = 1.2 \cdot \frac{g \cdot t_{sup} \cdot f_u}{\gamma_{M3}} \tag{3}$$

where:

g is width of channel opening;

t_{sup} is thickness of upper flanges;

f_u is ultimate strength of the aluminum alloy.

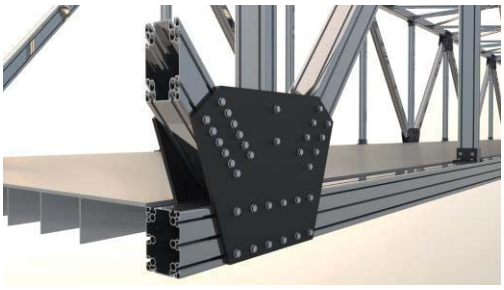

Figure 4 – Bottom chord and truss members connected using gusset plates

Figure 5 – Staircase beam and bottom chord connected to portal frame using angle plates

The bolt-channel joints of the analyzed pedestrian bridge used for the connections of different structural members are presented in Figure 4 and Figure 5. The main conclusions which are drawn from construction of this type of the joint is that relevant design resistance was always the slip resistance (design resistance in the channel axis direction), calculated according to Eq. (1). This particular resistance can be increased with the increase of bolt diameter and material properties of bolt. The shear resistance in perpendicular direction to that

of the channel, according to Eq. (2) and pull out resistance according to Eq. (3) depends on the geometry of the channel and can be significantly increased by the appropriate geometric modeling of the cross-section channel.

4. PEDESTRIAN INDUCED VIBRATIONS

4.1. DESIGN METHODS

Numerical analysis of natural frequencies and accelerations of a pedestrian bridge due to human walking was performed using a 3D FEA software Dlubal RFEM 5 [1], with add-on module RF-DYNAM Pro, which is used to model different types of dynamic loads, and is capable of time-history analysis [5].

Vertical forces due to human walking, applied to the numerical model of a pedestrian bridge, are divided into different sinusoidal oscillations by a Fourier transformation [6] and should be determined according to Eq. (4):

$$F(t) = \sqrt{N} \cdot G \cdot \left(1 + \sum_{j=1}^{3} a_j \cdot sin(2\pi \cdot j \cdot f_s \cdot t - \varphi_j)\right) \tag{4}$$

and horizontal component in transverse direction [7] according to Eq. (5):

$$F(t) = \sqrt{N} \cdot G \cdot \sum_{j=1/2}^{2} a_j \cdot sin(2\pi \cdot j \cdot f_s \cdot t) \tag{5}$$

where:

N	is the number of pedestrians;
G	is the self-weight of a single pedestrian, 0.80 kN;
f_s=2 Hz	is the step frequency;
a_j	is a factor for j^{th} harmonic fraction;
φ_j	is a shift of each harmonic function.

Table 1 - The values of the Fourier transformation coefficients [6], [7]

	Vertical component		Transverse component
j	α_j	φ_j	α_j
1	0.4+0.1·(f_s-2)/0.4	0	0.05
2	0.1	π/2	0.01
3	0.1	π/2	0.05
4	/	/	0.05

Values for different harmonics of Fourier transformation coefficients for vertical and transverse component of human walking force are given in Table 1. Pedestrian load which is applied to the numerical model of pedestrian bridge is given in Figure 6. For vibration analysis three design methods were used, two numerical FEA software based methods, and a response spectra method. Numerical methods are used for modeling of pedestrian load with or without the change of position over time (which we named *accurate* or the *simplified method*), while the *response spectra method* is based on the determination of the characteristic acceleration, which is the 95 % fractile of the maximum acceleration, for different pedestrian densities, according to recommendations from literature [7], [8].

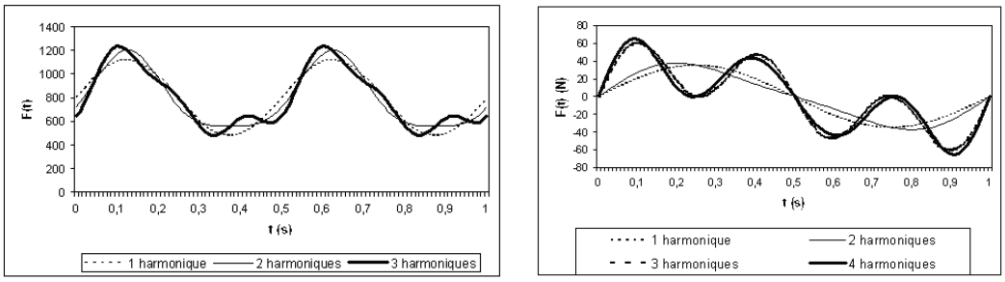

a) vertical component [7] *b) transverse component [7]*

Figure 6 –Pedestrian load applied on the numerical model of a pedestrian bridge (f_s*=2* Hz)

4.1.1. Accurate and simplified method for numerical modeling of pedestrain load

Numerical models of pedestrian walking are analyzed by two methods: accurate and simplified method. In accurate method, pedestrian walking is simulated by generating separate load cases and applying nodal loads for each position of the foot over the entire length of the bridge deck, followed by generating the corresponding time diagrams presented in Figure 7a. The step length of l_s=62.5 cm was selected so that the load was applied at the certain time interval at the middle of the bridge span.

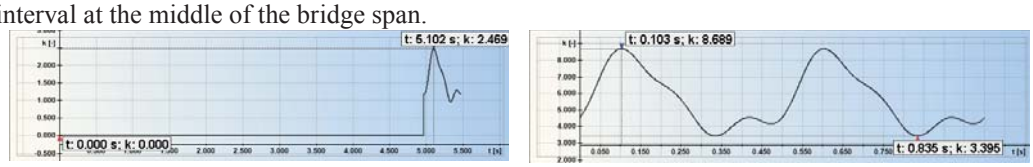

a) accurate method *b) simplified method*

Figure 7 –Pedestrian load applied on the numerical model of a pedestrian bridge

According to simplified method, pedestrian load is applied only in nodes where greatest displacement or acceleration is expected, and corresponding time diagram is given in Figure 7b. Assuming the pedestrian bridge is a simply supported beam, with 30 m span, accelerations are analyzed only in the middle of the span.

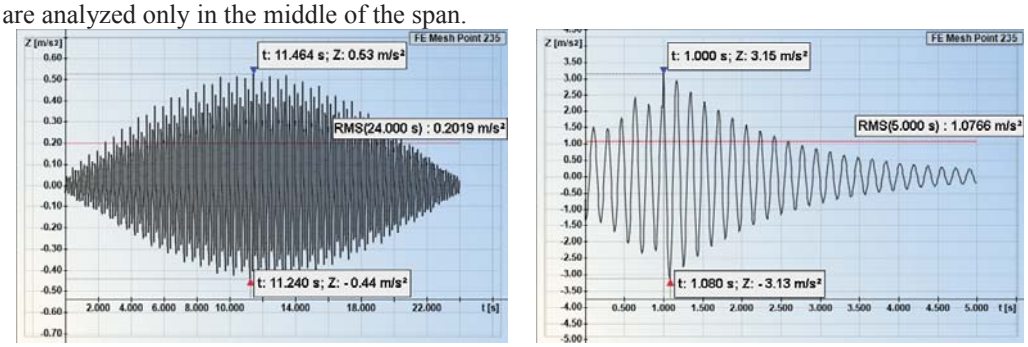

a) accurate method *b) simplified method*

Figure 8 – Accelerations of the pedestrian bridge deck at the middle of the span

Acclerations of the pedestrian bridge deck in the middle of the bridge span according to the two diffrenet methods of analysis are presented in Figure 8. As presented in Figure 8, simplified method gives higher values of maximal peak accelerations and root mean square acclerations, which are often used for comparison with the design recomendations.

4.1.2. Response spectra method

The aim of a spectral design method is to find a simple way to describe the stochastic loading and system response that provide design values with a specific confidence level [8]. This analysis method is developed as relatively simple order-of-magnitude calculation, which can be used in common engineering practice. However, considering that this design method should incorporate various types of bridge structures and stochastic nature of pedestrian walking, the results which are given by this design method should be on the safe side of the prediction. The maximum structure acceleration should be defined according to Eq. (6):

$$a_{\max} = k_{\mathrm{a},95\%} \cdot \sqrt{\frac{C \cdot \sigma_F^2}{m_{\mathrm{e,i}}} \cdot k_1 \cdot \xi^{k_2}} \tag{6}$$

where:

$k_{\mathrm{a},95\%}$	is the peak factor to transform the standard deviation of the response σ_{a} to the characteristic value $a_{\mathrm{max},95\%}$;
C	is constant describing the maximum of the load spectrum;
ξ	is damping ratio;
a_1, a_2, a_3	are constants which depends on the pedestrian loading density;
b_1, b_2, b_3	are constants which depends on the pedestrian loading density;
f_{i}	is natural frequency that coincides with the mean step frequency of the pedestrian stream;
σ_{F}^2	is variance of the acceleration response;
$m_{\mathrm{e,i}}$	is modal mass of the considered mode *i*.

Variables k_1 and k_2 should be calculated as a function of constants a and b and considered natural frequency of the structure, as presented in Eq. (7):

$$k_1 = a_1 \cdot f_i^2 + a_2 \cdot f_i + a_3 \qquad k_2 = b_1 \cdot f_i^2 + b_2 \cdot f_i + b_3 \tag{7}$$

Calculation procedure using Response spectra method is explained in detail in [7] and [8], with definition of all constants used in Eq, (6) and (7). Numerical analysis of pedestrian bridge accelerations is conducted using three presented analysis methods and the results of the numerical analysis are compared with design recommendations.

4.2. RESULTS OF ANALYSIS OF PEDESTRIAN BRIDGE VIBRATIONS

The criteria regarding pedestrian comfort and design recommendations are usually expressed by limits placed on the accelerations of the pedestrian bridge deck. The acceleration of the pedestrian bridge deck in the middle of the bridge span obtained by numerical analysis in Dlubal RFEM 5 software [1] and using the response spectra method are compared with design recommendations given in EN 1990 [9] and comfort criteria given in [7]. Although the effects of horizontal vibrations are also analyzed through numerical analysis, more interesting results, from the design point of view, were the ones due to vertical vibrations in the middle of the bridge span, which are presented in this paper.

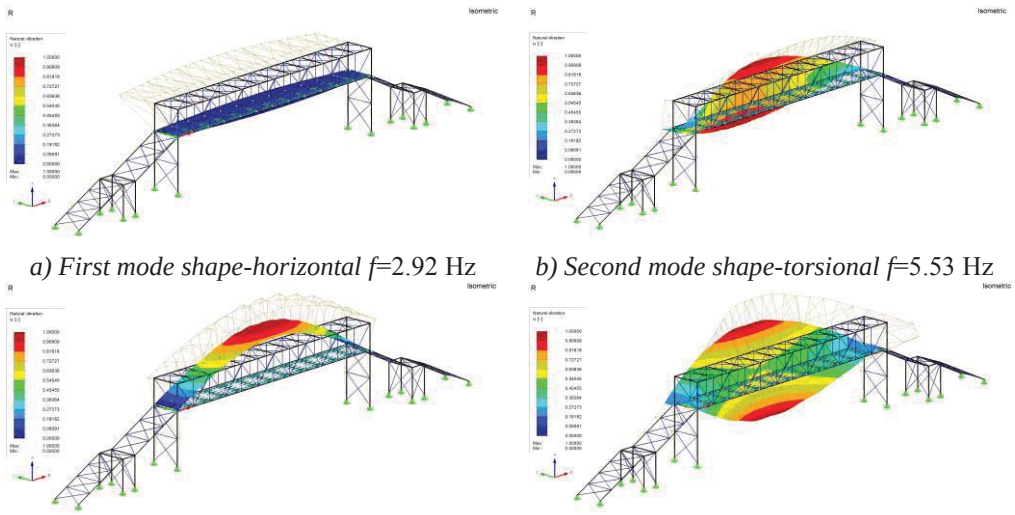

a) First mode shape-horizontal f=2.92 Hz *b) Second mode shape-torsional f=5.53 Hz*

c) Third mode shape-vertical f=5.65 Hz *d) Fourth mode shape-torsional f=8.90 Hz*

Figure 9 – Mode shapes and natural frequencies of pedestrian bridge

EN 1990 [9], defines limit values for accelerations in the vertical and horizontal direction, of 0.7 m/s^2 and 0.2 m/s^2, respectively, which should not be exceeded. Also, this standard defines conditions when it is necessary to perform a dynamic analysis depending on the range of natural frequencies for relevant modes. Dynamic analysis of structure should be performed when natural frequency of vertical mode shapes is less than 5 Hz and of horizontal mode shapes less than 2.5 Hz. Relevant mode shapes and natural frequencies of analyzed pedestrian bridge are shown in the Figure 9. As shown in Figure 9, natural frequencies of vertical and horizontal mode shapes are slightly higher than limiting values defined in EN 1990 [9].

Table 2 – Comfort classes of pedestrian bridge vibrations induced by human walking [7]

Comfort class	Degree of comfort	Acceleration level vertical	Acceleration level horizontal
CL1	Maximum	<0.5 m/s^2	<0.10 m/s^2
CL2	Medium	0.5 - 1.0 m/s^2	0.1 - 0.3 m/s^2
CL3	Minimum	1.0 - 2.5 m/s^2	0.3 - 0.8 m/s^2
CL4	Unacceptable discomfort	>2.5 m/s^2	>0.8 m/s^2

Comfort classes defined in [7] give a direct relation between horizontal and vertical accelerations of pedestrian bridge structure, as shown in Table 2. Comfort class should be defined based on the pedestrian bridge purpose and level of traffic over the bridge, and are classified form class 1 to class 4, which represent maximum comfort to unacceptable discomfort, respectively. Analysis which is presented in this paper includes different levels of pedestrian traffic density (from 0.15 to 1.50 pedestrians over one square meter) as given in Table 3.

Table 3 – Comparison of vertical accelerations of analyzed pedestrian bridge with design recommendations

		Bridge deck acceleration		Comparison with comfort classes [7]	Comparison with EN 1990 [9]
Design methods	Density [P/m^2]	a_{max} [m/s^2]	a_{RMS} [m/s^2]	a_{max} [m/s^2]	a_{max} [m/s^2]
RFEM Accurate	/	0.53	0.20	CL2	✓
RFEM Simplified	0.15	1.72	0.59	CL3	✗
	0.20	1.99	0.68	CL3	✗
	0.50	3.15	1.08	CL4	✗
	1.00	4.45	1.52	CL4	✗
	1.50	5.45	1.86	CL4	✗
Response spectra	0.15	$a_{d,vert}$=1.64 m/s^2		CL3	✗
	0.20	$a_{d,vert}$=1.90 m/s^2		CL3	✗
	0.50	$a_{d,vert}$=3.00 m/s^2		CL4	✗
	1.00	$a_{d,vert}$=3.17 m/s^2		CL4	✗
	1.50	$a_{d,vert}$=2.05 m/s^2		CL4	✗

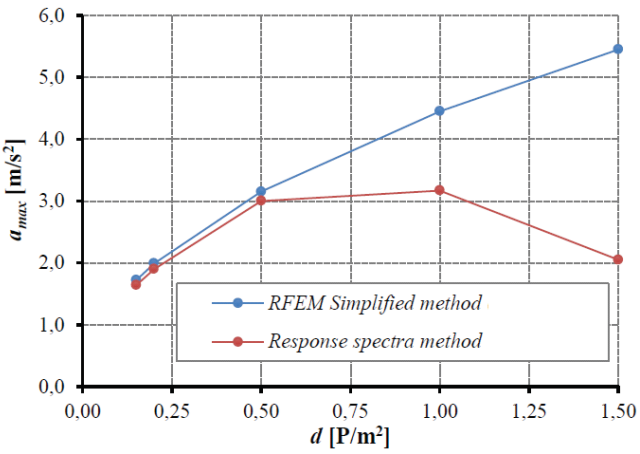

Figure 10 – Comparison of maximum vertical accelerations for different pedestrian traffic

As shown in Table 3, design recommendations which are given in EN 1990 [9] are satisfied only using the accurate numerical modeling of pedestrian loading in numerical analysis. Also, the accurate method of pedestrian load modeling resulted in fulfillment of the comfort criteria for the comfort class 2, which represent the medium comfort class. The simplified approach of pedestrian load modeling or calculation of vertical accelerations according to response spectra

leads to fulfillment of the comfort class 3 for the lower values of pedestrian traffic density (0.15 P/m^2 and 0.2 P/m^2). The higher values of pedestrian traffic density over the bridge span, leads to comfort class 4, which represent unacceptable discomfort.

Comparison of the maximal accelerations obtained from the numerical analysis using the simplified method with the results obtained from the response spectra method, is given in Figure 10. Note that the difference between the maximum acceleration values obtained from the two methods is small for densities of pedestrian traffic up to 0.5 P/m^2. However, the difference significantly increases for higher densities. This is due to the static nature of the pedestrian load for the high traffic densities, which the response spectra method takes into account.

Based on the comparison with the corresponding pedestrian bridge model made of the cold-formed steel profiles, it is obvious that the aluminum pedestrian bridge is much more sensitive to the pedestrian-induced vibrations. The acceleration that occurs is up to five times higher than that of similar carbon steel bridge **Error! Reference source not found.**, [11]. This is particular to the material used - the low damping, and the low weight of the pedestrian bridge made of aluminum which makes up only 45% of the total weight of the steel bridge.

5. CONCLUSION

The main objective of this paper was to investigate vibrations induced by pedestrian traffic in a novel aluminum pedestrian bridge, as well as to investigate the possibility of application of extruded profiles and special bolt-channel joints.

The implementation of extruded profiles and special joints appears to be a good solution in terms of optimizing the cross-sectional properties and avoiding the cross-sectional weakening at the joint location. Bearing capacity of a single bolt in special joints, although smaller than of the traditional joints of carbon steel, can be significantly increased by using a larger bolt diameter and by adjusting the geometry of the cross-section of the extruded profiles. Also, the lower weight of the aluminum alloy structure and the relatively simple assembly of the presented joints, results in a significantly easier and faster installation in comparison to the similar carbon steel structure.

EN 1990 [9] does not define precise recommendations for fulfillment of pedestrian bridge vibrations criteria. The upper bounds of the maximal accelerations, prescribed by the standard, can be satisfied only by a detailed numerical analysis and the accurate method of pedestrian load modeling, of the analyzed pedestrian bridge. The simplified method for pedestrian load modeling or calculation according to response spectra method leads to the higher values of vertical accelerations and medium or minimal comfort classes depending on pedestrian traffic density.

Response spectra method, considered to be relatively simple calculation procedure, can often lead to higher values of vertical accelerations or even unacceptable discomfort for pedestrians, especially in the case of structures made form light materials such as aluminum. Therefore, detailed numerical analysis is sometimes necessary in order to satisfy high comfort criteria and serviceability of the structure.

ACKNOWLEDGMENT

This investigation is the part of TR-36048 project supported by the Serbian Ministry of Education, Science and Technological Development.

REFERENCES

[1] Dlubal RFEM 5 Structural Engineering Software for Analysis and Design / http://www.dlubal.com (accessed 19.11.2016.)

[2] Eurocode 9 - Design of aluminium structures - Part 1-1: General structural rules, European Committee for Standardization (CEN), 2007.

[3] CNR-DT 208/2011 Istruzioni per la progettazione, l'esecuzione ed il controllo di strutture di alluminio, Consiglio Nazionale delle Ricerche, Roma, 2011.

[4] Eurocode 3 – Design of steel structures - Part 1 - 8: Design of joints, EN 1993-1-8, European Committee for Standardization (CEN), 2010.

[5] Schubert, G. and Niemeier, A: Time History Analysis Using RF-/DYNAM Pro - Walking and Running Across Pedestrian Bridge, [Video file], Retrieved from http://www.youtube.com/embed/7OxxsCEK41M?autoplay=1, 2015 (accessed 25.2.2018.)

[6] Bachmann, Hugo and Ammann, Walter J and Deischl, Florian and Eisenmann, Josef and Floegl, Ingomar and Hirsch, Gerhard H and Klein, Günter K and Lande, Göran J and Mahrenholtz, Oskar and Natke, Hans G and others: Vibration problems in structures: practical guidelines, Birkhäuser, 2012.

[7] Sétra, Footbridges: Assessment of vibrational behaviour of footbridges under pedestrian loading, Technical guide SETRA, Paris, France, 2006.

[8] Heinemeyer, Christoph and Butz, Christiane and Keil, Andreas and Schlaich, Mike and Goldack, Arndt and Trometer, Stefan and Lukic, M and Chabrolin, Bruno and Lemaire, Arnaud and Martin, Pierre-Olivier and others.: Design of lightweight footbridges for human induced vibrations, European Commission-JRC Scientific and Technical Reports, JRC, 2009.

[9] Eurocode 0 - Basis of structural design, EN 1990, European Committee for Standardization (CEN), 2010.

[10] Kruškonja J.: Resistance and serviceability analysis of steel footbridge structure according to EN 1993-1-3, MSc thesis, University of Belgrade, Faculty of Civil Engineering, 2018.

[11] Kruškonja J., Dobrić J., Gluhović N.: Resistance and serviceability analysis of steel footbridge structure according to Eurocode, 15. Congress of the Association of Structural Engineers of Serbia, Zlatibor, 6th-8th September, 2018.

ДГКС Друштво грађевинских конструктера Србије
ASES Association of Structural Engineers of Serbia
S-80
15. KONGRES
6-8. 9. 2018. Zlatibor

Fidan Salihu[1], Meri Cvetkovska[2], Ana Trombeva Gavriloska[3], Milivoje Milanović[4]

KOMPARATIVNA ANALIZA POŽARNE OTPORNOSTI KONTINUIRANIH AB PLOČA PRIMJENOM EUROKODA 2 I MKE

Rezime:

U radu su prikazani numerički rezultati požarne otpornosti kontinuiranih AB ploča, nosivih u jednom pravcu. Analiziran je uticaj procenta armiranja i raspona ploče. Analize su sprovedene pomoću programa SAFIR (2D Analiza). Požarna otpornost ploča je definisana primenom 'metode granične nosivosti'. Ova savremena metoda koja se koristi za proračun konstrukcija, koristi se i za definisanje požarne otpornosti. Prezentirani su i upoređeni rezultati dobijeni primenom 'uprošćene' proračunske metode, opisane u Eurocodu 2 dio 1.2, i primenom programa SAFIR.

Ključne reči: kontinuirana AB ploča, uprošćena proračunska metoda, MKE, požarna otpornost

COMPARATIVE ANALYSIS ON FIRE RESISTANCE OF ONE WAY CONTINUOUS RC SLABS ACCORDING TO EC2 AND FEM

Summary:

This paper presents the numerically achieved results for the fire resistance of one-way continuous reinforced concrete slabs. The effects of: reinforcement ratio and slab span are analyzed. The analyses were conducted by using the software SAFIR (2D Analysis). The fire resistance of the RC slabs was defined by 'ultimate strength design' criteria as used in all modern concrete design codes. Results obtained from 'simplified' calculation method for continuous slabs, described in Eurocode 2 part 1.2, and by using the software SAFIR are presented and compared in this paper.

Key words: Continuous RC slab, Simplified Calculation Method, FIM, fire resistance

[1]*Assist., MSc, Faculty of Civil Engineering and Architecture, University of Prishtina "Hasan Prishtina", salihufidan@gmail.com*
[2]*Prof., PhD, Faculty of Civil Engineering, University "Ss. Cyril and Methodius" (UKIM), Skopje, Republic of Macedonia cvetkovska@gf.ukim.edu.mk*
[3]*Assoc.prof., PhD, Faculty of Architecture, UKIM, Skopje, agavriloska@arh.ukim.edu.mk*
[4]*Assist.prof., PhD, State University in Novi Pazar, Department of Civil Engineering, Novi Pazar, Srbija, milanovicnp@gmail.com*

1. INTRODUCTION

The resistance of building members to the effects of fire is an important part of any structural and fire safety design. Floor slabs, as horizontal elements, have a very important role in providing bearing capacity, usability and stability of the building as a whole. Their proper selection and design, when they are exposed to different types of loads (mainly: permanent and variable), should provide stable and safe structure during the exploitation period.

In case of fire floor slabs do not have only **load bearing function**. In most cases they are used as elements for separating the fire compartment. Where compartmentition is required, the elements forming the boundaries of the fire compartment, including joints, shall be designed and constructed in such a way that they maintain their separating function during the relevant fire exposure [1]. This shall ensure, where relevant, that **integrity failure** does not occur, **insulation failure** does not occur, thermal radiation from the unexposed side is limited.

Does the floor structure meet the required fire resistance criteria mainly depends on: mechanical and thermal characteristics of the materials used for the construction; initial loading level; support conditions; dimensions of the cross section; steel ratio; concrete cover thickness and fire scenario.

The fire resistance of the continuous reinforced concrete solid slabs which have load bearing capacity only in one direction with different thickness and spans, used for the multistory residential buildings, is analyzed in this paper.

A durable structure shall meet the requirements of serviceability, strength and stability throughout its design working life, without significant loss of utility or excessive unforeseen maintenance. In fire conditions, as a result of a large number of real fire tests and corresponding numerical analyzes, it was found out that the moment of failure of the floor structure is always followed by significant deformation (deflection). If the structure is close to the limit state, after the cooling phase the residual deflections are so great that it cannot be used without significant rehabilitation. For these reasons, during the fire action, the deformation (deflection) of the slab is limited to prescribed value. According to the ISO standard, this limit value is L/30 (L is the span of the slab) [3].

This paper presents the numerically achieved results for the fire resistance of three solid RC slabs with different span. For comparison, all slabs were analysed as continuous slabs and were exposed to ISO standard fire from the bottom side, as most usual fire scenario. The RC slabs were constructed without thermal insulation at the bottom side of the slabs. Based on the numerically achieved results, certain conclusions that can be useful for achieving the prescribed fire resistance of these type of floor structures were obtained.

2. FIRE RESISTANCE OF ONE-WAY CONTINUOUS RC SLABS

Flexural continuity can improve the fire resistance of a bending member. A member with flexural continuity is a statically indeterminate member which would need to fail at more than one cross section to lose its load carrying capability. Slabs which are continuous over several supports have continuity which is beneficial in fire design, because collapse does not occur when the ultimate strength is reached at only one cross section.

In fire-exposed structures, the benefits of continuity allow load to be resisted in alternative ways through moment redistribution as heat-affected areas lose strength. The benefit are greatest in ductile concrete which can undergo large rotations at 'plastic hinges'. Additional benefits can occur in materials like reinforced concrete where the flexural strength may be different in positive and negative bending.

During definition the fire resistance of continuous slabs there should be taken into account that their continuity enables redistribution of forces (Figure 1). The temperature changes between lower fiber (heated) and upper (cooler) of cross section lead the tendency that slabs lift from the support, and because that is not possible, there appears negative reaction which causes increase of bending moment at internal support, hence bending moment at span decreases. This is favorable in terms of fire resistance due to the fact that heated reinforcement in lower fiber of the cross section unloads, in the account of support reinforcement, who remains unheated, or very little increases their temperature, therefore does not decrease the strength and deformation properties. Negative bending moment at support increases until the plastic hinge is formed. The first plastic hinge will occur at span, and almost at failure even in the support.

As the surface of the negative reinforcement increases, a large negative moment will be absorbed, and in this case, the smallest moment in the field will be obtained, but this is not always favorable. As large as the negative moment, the heated concrete in the lower compressed fiber area undergoes large strains in compression, which can lead to the fracture of the same and cause the slab failure. In order to eliminate this, it is recommended that the provided negative reinforcement should fulfill condition:

$$A_{s,prov} f_{sd,fi} / bd_{fi} f_{cd,fi} < 0.30 \qquad (1)$$

It can be shown that equation (1) checks that the depth of the compression zone a_f is not more than 35% (0.3/0.85) of the effective depth of the cross section d_f. This check is not necessary if there is significant longitudinal reinforcing in the compression zone.

Plastic hinge at span will occur when ultimate span moment will be reduced and will be equal to the positive moment from external loads (2):

$$M_{Ed,fi,span} = \frac{w_{Ed,fi} l x_1}{2} - \frac{w_{Ed,fi} x_1^2}{2} - \frac{M_{Ed,fi,\sup ort} x_1}{l} = M_{Rd,fi,Span} \qquad (2)$$

$$x_1 = \frac{l}{2} - \frac{M_{Ed,fi,\sup ort}}{w_{Ed,fi} l} \qquad (3)$$

If equation (3) substitutes in equation (2), obtains relation between external load and ultimate reduced positive moment and unreduced negative moment at support, respectively relationship from which fire resistance can be defined:

$$M_{Ed,fi,Suport} = \frac{w_{Ed,fi} l^2}{2} - w_{Ed,fi} l^2 \sqrt{\frac{2M_{Rd,fi,Span}}{w_{Ed,fi} l^2}} \le M_{Rd,fi,Suport} \qquad (4)$$

The position of the maximum mid-span moment of end span of slab is given by equation (5) as:

$$x_1 = \sqrt{\frac{2M_{Rd,fi,Span}}{l}} \tag{5}$$

and for interior span of continuous slab by equation (6) as: $x_1 = \frac{l}{2}$ (6)

A 'simplified' calculation method described in Eurocode 2 [1] was also used for the fire resistance analysis of the continuous RC slabs.

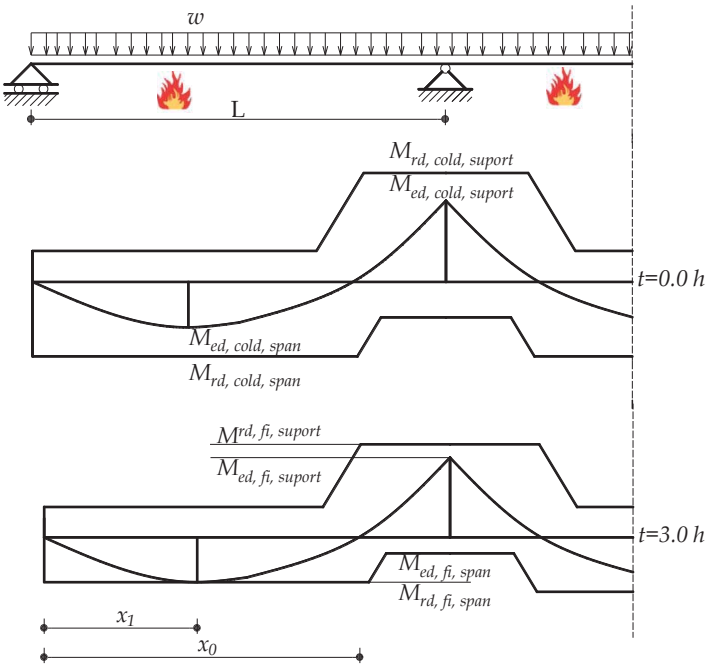

Figure 1 – Redistribution of bending moments in Continuous RC slab with three spans, exposed to fire from the bottom side

2.1. SIMPLIFIED CALCULATION METHOD FOR CONTINUOUS SLABS BY EUROCODE 2

This simplified method only applies where the loading is predominantly uniformly distributed and the design at ambient temperature has been based on linear analysis or linear analysis with limited redistribution. This method uses strength reduction factors based on Figure 4.2a, Curve 1 [1].

The moment of resistance $M_{Rd,fi,Span}$ of the section at the position of maximum sagging moment should be calculated for fire conditions in accordance with equation (7).

$$M_{Rd,fi,Span} = \frac{\gamma_s}{\gamma_{s,fi}} \times k_s(\theta) \times M_{Ed} \times \left(\frac{A_{s,prov}}{A_{s,req}}\right) \tag{7}$$

where

γ_s is the partial material factor for steel used in EN 1992-1-1

$\gamma_{s,fi}$ is the partial material factor for steel under fire conditions

$k_s(\theta)$ is a strength reduction factor of the steel for the given temperature (θ) under the required fire resistance. (θ) may be taken from Figure 4.2a, Annex A [1] for the chosen axis distance

M_{Ed} is the applied moment for cold design to EN 1992-1-1

$A_{s,prov}$ is the area of tensile steel provided

$A_{s,req}$ is the area of tensile steel required for the design at ambient temperature, according to EN 1992-1-1

$A_{s,prov} / A_{s,req}$ should not be taken as greater than 1.3.

In the absence of more rigorous calculations, the moment of resistance at supports for design for the fire situation may be calculated using equation (8).

$$M_{Rd,fi} = \frac{\gamma_s}{\gamma_{s,fi}} \times M_{Ed} \times \left(\frac{A_{s,prov}}{A_{s,req}}\right)\left(\frac{d-a}{d}\right)$$

(8) where

$\gamma_s, \gamma_{s,fi}, M_{Ed}, A_{s,prov}, A_{s,req}$ are as defined in equation (7).

a is the required average bottom axis distance given in Table 5.8, Column 3 for slabs [1].

Equation (8) is valid where the temperature of the top steel over the supports does not exceed 350°C for reinforcing bars and does not exceed 100°C for prestressing tendons.

3. SLAB ANALYSIS RESULTS

The following parameters, characteristics and conditions were assumed:

- The slabs were exposed to ISO 834 Standard fire only from the below side,
- A separate stripes wide b = 1 m were analysed,
- The temperature dependent physical and mechanical properties of the siliceous aggregate concrete (compressive strength f_{ck}=30Mpa) and the reinforcement (yield strength f_{yk}=400Mpa) were assumed according to EC2, part 1-2,
- Dead load G_1=1.5 kN/m^2 (excluding self weight),
- Live load Q=4.0 kN/m^2, $\psi_{2,1}$=0.6 (for category C)

All data about the slabs geometry and the intensities of the dead and live loads are given in Table 1.

As first case study the criterion Load bearing function (R) was analysed.

Table 1 – Slab geometry and load intensity

Slab	Span (m)	Thickness (cm)	Concrete cover (cm)	G_{slab} (kN/m^2)	G_1 (kN/m^2)	Q_1 (kN/m^2)	$p_{slab,cold}$ (kN/m^2)	$p_{slab,fire}$ (kN/m^2)
S_1	4	16	2.5	4	1.5	4	13.425	7.900
S_2	5	16	2.5	4	1.5	4	13.425	7.900
S_3	6	16	2.5	4	1.5	4	13.425	7.900

Example 1. For a continuous RC slab with known span, load, geometry and reinforcing, calculate flexural capacity under fire exposure, using Simplified Calculation Method [1].

Given information: L=4m Bottom cover c_0=25mm Top cover c_0=25mm

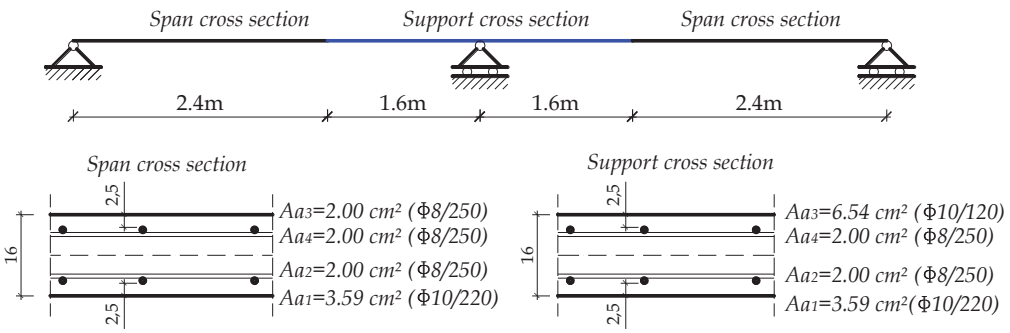

$$w_{Ed} = g_k \cdot \gamma_g + q_k \cdot \gamma_q = 5.5 \cdot 1.35 + 4 \cdot 1.5 = 13.425 kN/m$$

$$M_{Ed,span} = \frac{9}{128} w_{Ed} l^2 = 15.10 kNm \qquad M_{Ed,\sup} = \frac{w_{Ed} l^2}{8} = 28.85 kNm$$

$$w_{Ed,fi} = g_k \cdot \gamma_g + q_k \cdot \gamma_q = 5.5 \cdot 1.0 + 4 \cdot 0.6 = 7.9 kN/m$$

$$M_{Ed,fi,span} = \frac{9}{128} w_{Ed,fi} l^2 = 8.88 kNm \qquad M_{Ed,fi,\sup} = \frac{w_{Ed,fi} l^2}{8} = 15.8 kNm$$

<u>Check fire resistance after t=150 min</u>

<u>*Span*</u>

From Figure 4.2a, Annex A [1] for the chosen axis distance, for x=30mm → *θ=615 ºC*

Strength reduction factor of tension reinforcement, from Figure 4.2a, Curve 1 [1]:

$$k_{s(615°)} = 0.23 + (0.47 - 0.23)\frac{700 - 615}{100} = 0.434$$

$$M_{Rd,fi,Span} = \frac{\gamma_s}{\gamma_{s,fi}} \cdot k_s(\theta) \cdot M_{Ed,span} \cdot \left(\frac{A_{s,prov}}{A_{s,req}}\right) = \frac{1.15}{1} \cdot 0.434 \cdot 15.1 \cdot \frac{3.59}{3.41} = 7.93 < 8.88$$

→ <u>*Croos section fails*</u>

Support

The moment of resistance at support:

$$M_{Rd,fi,\sup} = \frac{\gamma_s}{\gamma_{s,fi}} \times M_{Ed} \times \left(\frac{A_{s,prov}}{A_{s,req}}\right)\left(\frac{d-a}{d}\right) = \frac{1.15}{1} \cdot 26.85 \cdot \frac{6.54}{6.28} \cdot \frac{13-4.75}{13} = 20.40 > 15.80$$

$$M_{Rd,fi} > M_{Ed,fi}$$

Moment redistribution

$$M_{Ed,fi,Suport}^{Red} = \frac{w_{Ed,fi} l^2}{2} - w_{Ed,fi} l^2 \sqrt{\frac{2M_{Rd,fi,Span}}{w_{Ed,fi} l^2}} \leq M_{Rd,fi,Suport}$$

$$M_{Ed,fi,Suport}^{Red} = \frac{7.9 \cdot 4^2}{2} - 7.9 \cdot 4^2 \sqrt{\frac{2 \cdot 7.93}{7.9 \cdot 4^2}} = 18.42 < 20.40 \rightarrow$$ *The condition is fulfilled*

Conclusion: The fire resistance of the slab is **R150**

The fire resistance for all case studies is given in Table 2.

Table 2 – Fire resistance of RC slabs

Slab	Steel ratio(%)		Fire resistance (min) Simplified calculation method	Fire resistance(min) Software SAFIR
	Span	Support		
S_1	0.224	0.408	R150	153
S_2	0.353	0.706	R150	159
S_3	0.543	1.013	R150	153

The results obtained by simplified calculation method [1] and the software SAFIR (2D Analysis) are presented and compared.

All the results for the analysed slabs are presented in Figures (2-6).

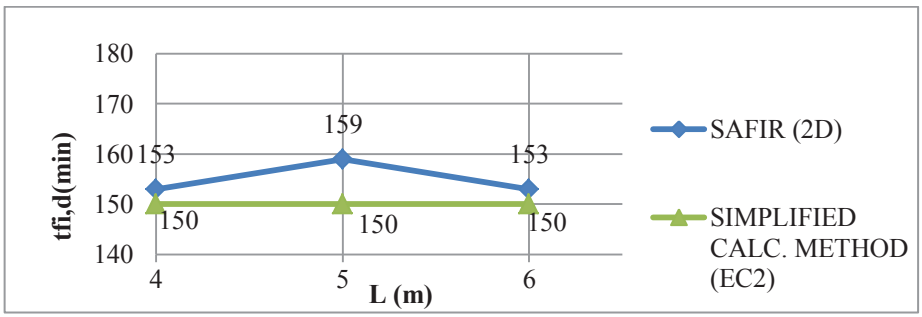

Figure 2 – Relation 'slab span-fire resistance' of one-way continuous RC slab and comparision of the results obtained with the simplified calculation method and the program SAFIR (2D Analysis)

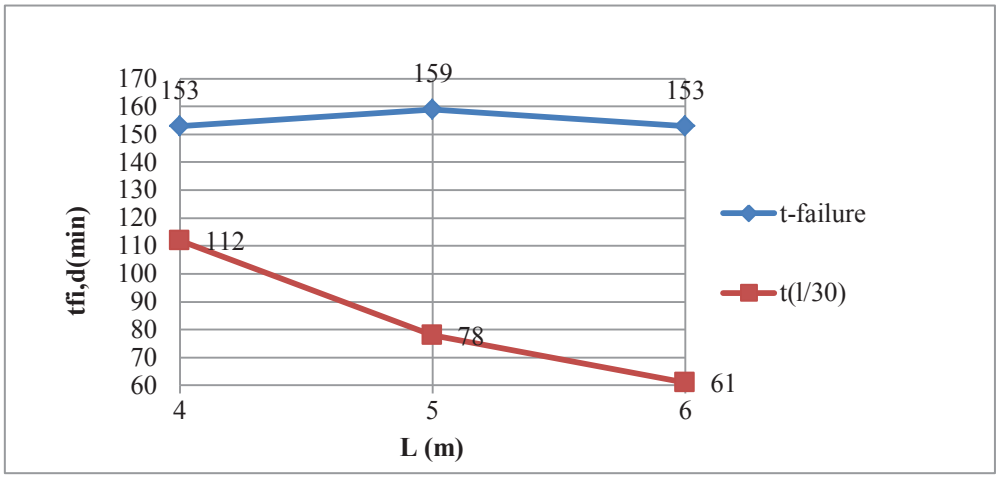

Figure 3 –Fire resistance of slabs at failure moment and allowable deflection

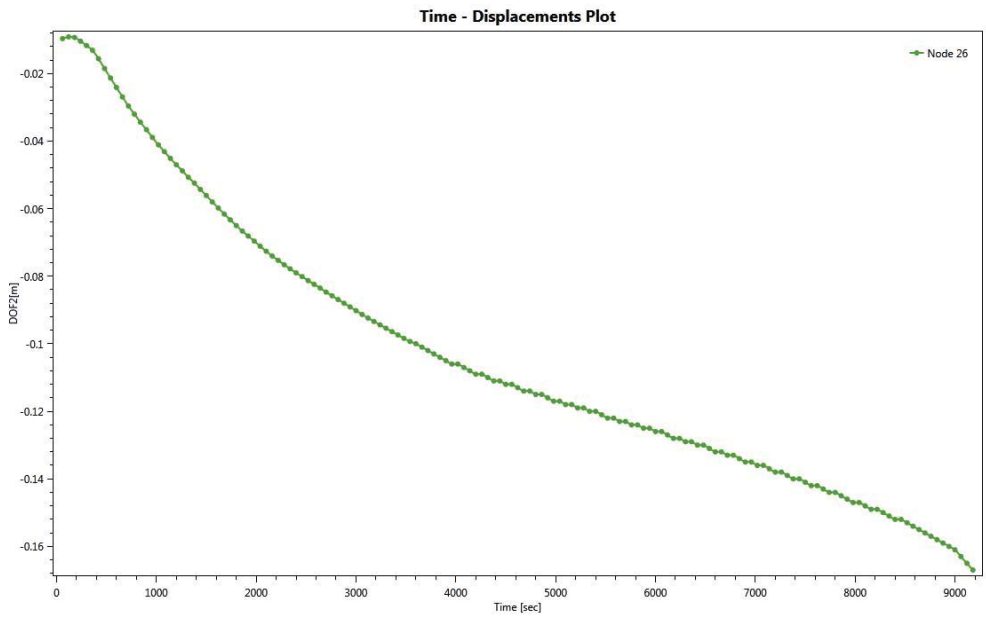

Figure 4 – Maximal span deflection versus time of slab with l=4m

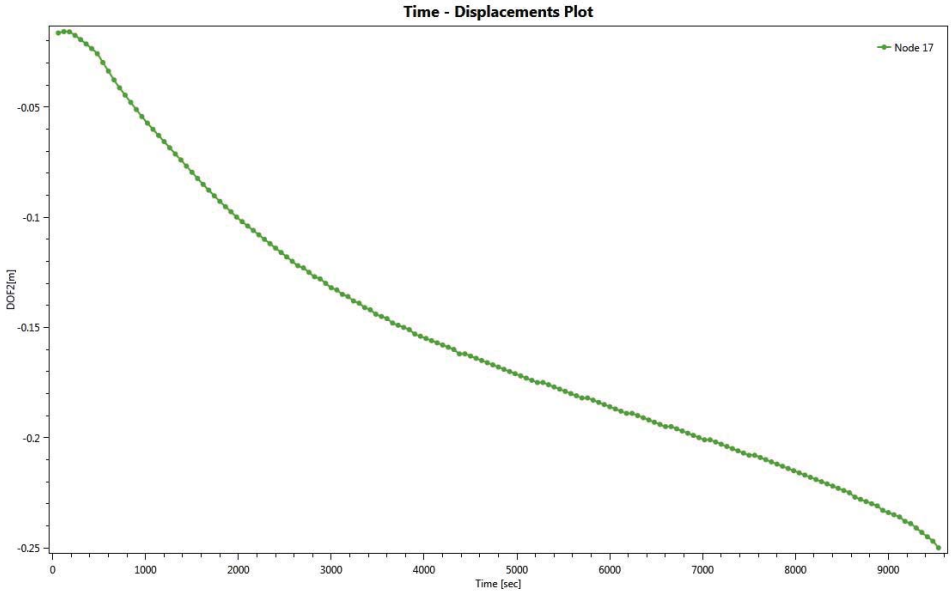

Figure5 – Maximal span deflection versus time of slab with l=5m

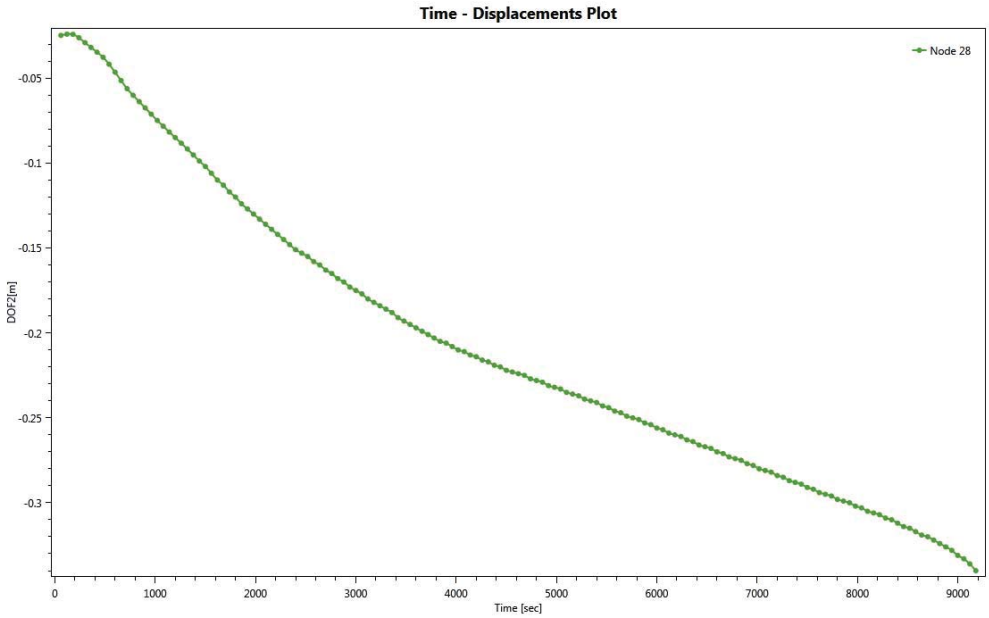

Figure 6 – Maximal span deflection versus time of slab with l=6m

4. CONCLUSIONS

The simplified calculation method (EN 1992-1-2, 2004), presented in this paper, is capable for defining the fire resistance of one-way continuous reinforced concrete slabs, exposed to fire from the bottom side. This method is simple for implementation, useful for single members and provides satisfactory results. The simplified procedures recommended in Eurocode 2, part 1-2, are helpful only for some orientation analysis and are always on the side of safety. The obtained results with software SAFIR, from 2D Analysis of one way continuous slabs, show a good agreement with Simplified Calculation Method [1].

The analysis presented in this paper show that reinforcement ratio has positive effect on increasing the fire resistance of RC slabs. By increasing the slab span, the fire resistance of the slabs is decreased from the aspect of achievement the limit state of deformations, but not from the aspect of fracture. Due to the higher reinforcement ratio of the slabs, the time-to-fracture has a higher value, especially when the reinforcement ratio is higher for the negative bending moment. The reason for that is the unheated negative reinforcement at the support that may accept the redistribution of the bending moments. But, the reinforcement ratio at the support should not be too high. In such case, for providing an equilibrium of internal forces, the heated concrete will be exposed to high compression stresses that may cause crushing of the concrete and the fire resistance will be lower, which is case with the slab with span of 6 m.

REFERENCES

[1] [1] EN 1992-1-2 (2004): Design of concrete structures - Part 1-2: General rules. Structural fire design

[2] Adam Levesque, “Fire Performance of Reinforced Concrete Slabs”, Master Thesis, Worcester Polytechnic Institute, May 2006

[3] Buchanan A., “Structural design for fire safety”, Wiley, New York, USA, (2001).

[4] Cvetkovska, M. (2002): Nonlinear Stress Strain Behaviour of RC Elements and Plane Frame Structures Exposed to Fire, Doctoral dissertation, Ss Cyril and Methodius University in Skopje, Macedonia

[5] Wang, G. (2006): "Performance of Reinforced Concrete Flat Slabs Exposed to Fire", Fire Engineering Report 06/2, University of Canterbury, Christchurch, New Zealand.

[6] Lim, L. (2003): "Membrane Action in Fire Exposed Concrete Floor Systems", *Doctoral dissertation,* Departament of Civil Engineering, University of Canterbury, Christchurch, New Zealand

ДГКС Друштво грађевинских конструктера Србије
ASES Association of Structural Engineers of Serbia
S-81
15. KONGRES
6-8. 9. 2018. Zlatibor

Jagoda Kruškonja [1], Jelena Dobrić[2], Nina Gluhović[3]

ANALIZA NOSIVOSTI I UPOTREBLJIVOSTI ČELIČNE PASARELE PREMA EVROKODU

Rezime:

Ovaj rad ukratko prikazuje analiizu nosivosti i upotrebljivosti čelične konstrukcije pešačke pasarele. Noseća konstrukcija, fomirana od hladno-oblikovanih profila, dimenzionisana je prema EN 1993-1-3. Analizirane su vibracije mosta i data komparatvna studija sa stanovišta različitih kriterijuma u pogledu komfora prema Evrokodu i prema SETRA/AFGC preporukama. Rad takođe poredi ponašanja čelične pešačke pasarele sa statički i konstruktivno ekvivalntnom pasarelom čiji je osnovni materijal Al legura.

Ključne reči: pasarela, hladno oblikovani profili, Evrokod, vibracije, klase komfora

RESISTANCE AND SERVICEABILITY ANALYSIS OF STEEL FOOTBRIDGE STRUCTURE ACCORDING TO EUROCODE

Summary:

This paper briefly presents resistance and serviceability analysis of steel footbridge structure. The main structural system consists of cold-formed members, which were designed according to EN 1993-1-3. Analysis of vibration of the footbridge structure was performed, including comparative study from the aspect of different criteria regarding the comfort according to Eurocode and SETRA/AFGC recommendations. Additionally, the paper compares behavior of steel footbridge with static and structural equivalent footbridge whose base material is aluminum alloy.

Key words: footbridge, cold-formed members, Eurocode, vibration, comfort classes

[1] *MSc Eng, jagodakruskonja@gmail.com*
[2]*PhD, Assistant professor, University of Belgrade Faculty of Civil Engineering , jelena@imk.grf.bg.ac.rs*
[3]*PhD student, Teaching assistant, University of Belgrade Faculty of Civil Engineering, nina@imk.grf.bg.ac.rs*

1. INTRODUCTION

Thin-walled cold-formed steel has growing base of application in civil engineering structures. The cold-formed steel members have been used for different building systems serving as purlins, wall girts, and the building covers. An essential feature of thin-walled elements is that cross-section local stability should be considered in their design, because it often contributes to their overall structural responses under load. Unlike the base part of European specification EN 1993-1-1 [1], where the design of structural element begins with the classification of cross sections, Eurocode for design of cold-formed structures EN 1993-1-3 [2] assumes that cross-section is slender and no full effective due to early elastic local buckling. For design of slender steel cold-formed structures, the effective-width concept is applied.

This paper presents structural analysis of steel footbridge. The lattice structural system was adopted for the main bearing structure including orthotropic steel decks for footpaths. The geometrical dimensions of the main pedestrian bridge structure are: span length is 30 m, width is 3,3 m and height is 3 m. All structural elements were designed as cold-formed members including open, press-braked sections and hollow cold-rolled sections. Figures 1-3 show adopted cross-sections of the man structural elements. The design resistance predictions for ultimate and serviceability limit states were calculate according to recommendations given in EN 1993-1-3 [2] and EN 1993-2 [3]. The base material is steel S355. Static and dynamic calculations were made using the Dlubal RFEM software program [4].

.

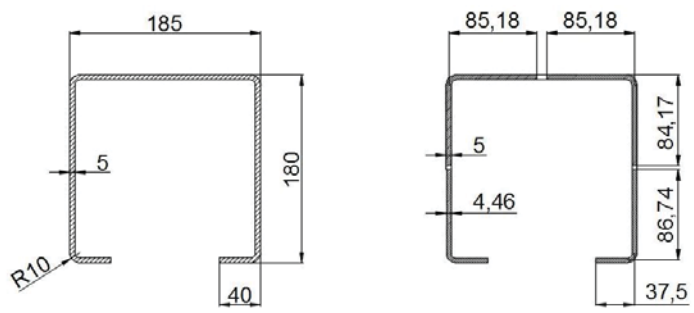

Figure 1 – Main truss chords, gross cross-section on the left, effective cross-section on the right

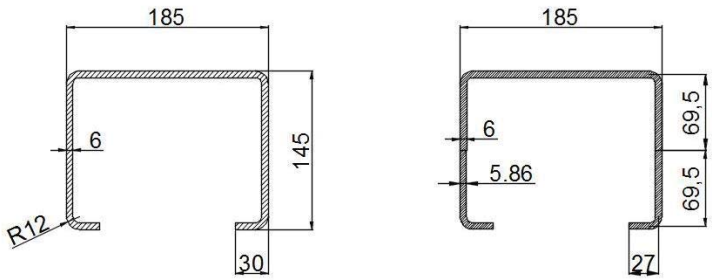

Figure 2 – Main truss diagonal, gross cross-section on the left, effective cross-section on the right

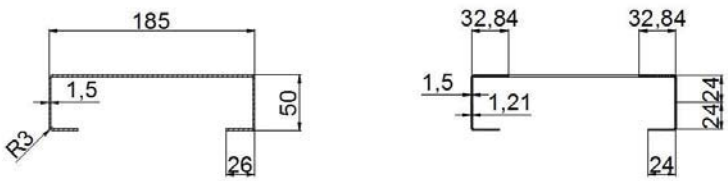

Figure 3 – Main truss vertical, gross section on the left, effective cross-section on the right

2. VIBRATIONS

2.1 EUROCODE PEDESTRIAN COMFORT CRITERIA (FOR SERVICEABILITY)

Eurocode 1990 [5] gives recommendations for Serviceability Limit States, which is, inter alia, related to vibration pedestrian bridges:

(1) The comfort criteria should be defined in terms of maximum acceptable acceleration of any part of the deck.

The following accelerations are the recommended maximum values for any part of the deck:

- 0,7 m/s^2 for vertical vibrations,
- 0,2 m/s^2 for horizontal vibrations due to normal use,
- 0,4 m/s^2 for exceptional crowd conditions.

(2) A verification of the comfort criteria should be performed if the fundamental frequency of the deck is less than:

- 5 Hz for vertical vibrations,
- 2,5 Hz for horizontal (lateral) and torsional vibrations.

2.2 COMFORT CLASSES AND ACCELERATION RANGES

The comfort classes for different acceleration ranges of the bridge recommended by this guideline are presented in the Table 1. In general, four comfort classes are distinguished. The given comfort classes and acceleration levels are values given by Charles and Hoorpah with reference to the SETRA/AFGC guidelines [9].

Table 1 – Definition of comfort classes and related acceleration ranges [6]

Comfort level	*Degree of comfort*	*Acceleration level vertical*	*Acceleration level horizontal* a_{limit}
CL1	*maximum*	*<0,5 m/s²*	*<0,10 m/s²*
CL2	*medium*	*0,50 - 1,00 m/s²*	*0,10 – 0,30 m/s²*
CL3	*minimum*	*1,00 – 2,50 m/s²*	*0,30 – 0,80 m/s²*
CL4	*unacceptable discomfort*	*>2,50 m/s²*	*>0,80 m/s²*

2.3 MODAL ANALYSIS

Modal analysis is done to check if Eurocode 1990 [5] requirements, which refer to the fundamental frequency, are satisfied. As results, modal analysis gives the characteristic mode shapes and corresponding frequency values necessary for vibration analysis.

Results obtained by modeling in the RFEM program are shown in Figures 4-6 [4]:

Figure 4 – First mode shape, horizontal f_1*=4,313Hz*

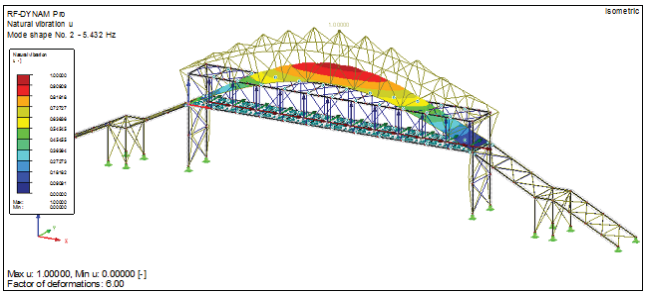

Figure 5 – Second mode shape, vertical f_2*=5,432Hz*

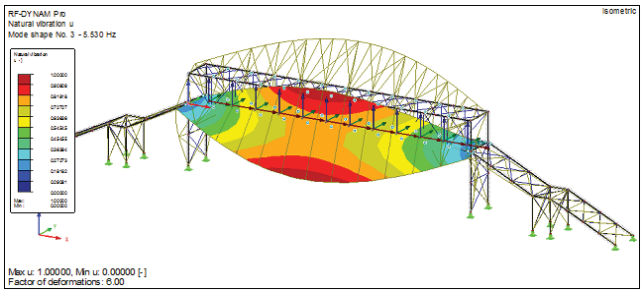

Figure 6 – Third mode shape, torsion f_3=5,530Hz

Authoritative node for the analysis of vertical vibration (Figure 7) was selected based on the maximum amplitude of the second mode shape (Figure 5), which is provided in the appropriate vertical direction. The first mode shape (Figure 4), in the horizontal direction, shows that no node in the zone of the lower belt of the bridge, i.e. the board on which the pedestrians are walking, has pointed out. So in the analysis of horizontal vibrations, the same node (Figure 7) is observed.

Since the research goal is to compare the vibration results of the steel bridge made from cold-formed members with an analog bridge made of aluminum, it was necessary to analyze the results of the node emphasized on Figure 8.

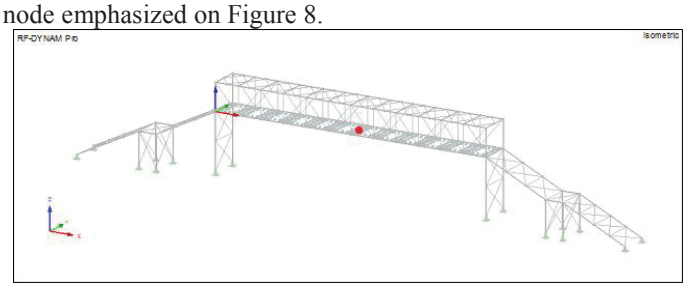

Figure 7 – Node 1 position in the mid of a span

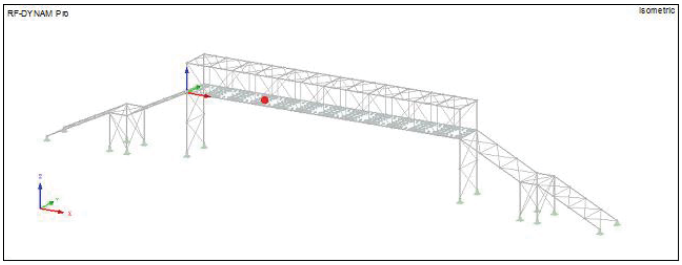

Figure 8 – Node 2 position in the quarter of a span

2.4 DESIGN – VIBRATIONS INDUCED BY PEDESTRIAN TRAFFIC

By observing the pedestrians while walking, it can be noted that each step represents a single impulse, while the steps during movement are a series of impulses moved along the path

and time. Assuming that the load of both feet is the same, and that it takes time for the foot to be fixed on a surface constant for a particular walk mode, the load induced by the stroke is periodic and can be divided into different sinusoidal oscillations using the Fourier transform [7]. Time history analysis has common use in dynamic analysis of the structures by software. A full and simplified Time history analysis in RFEM is considered.

Accurate – RFEM Time history analysis [8] covers simulation of the human movement to gain the response of the construction as the maximum acceleration.

For the vertical vibrations, Bachmann [8] represents the load of the human walk at a normal pace of 2 Hz (taking into account the first three harmonics) as:

$$F(t)=\sqrt{N}\cdot G\cdot\left(1+\sum_{j=1}^{3}\alpha_j\cdot\sin\left(2\pi\cdot j\cdot f_s\cdot t-\varphi_j\right)\right) \quad (1)$$

where:

$G=0{,}8$ kN	self-weight of one pedestrian
$N=4$	number of pedestrians (adopted 4 for natural frequencies $f > 2{,}4\ Hz$)
α_j	load component for j-th harmonic (Table 2)
φ_j	phase angle of the j -th harmonic (Table 2)
$f_s=2$ Hz	adopted frequency of walking

Table 2 – Fourier terms for the process of walking [8]

j	α_j	φ_j
1	*0,4+0,1 (f_s-0,2)/4*	*0,0*
2	*0,1*	*π/2*
3	*0,1*	*π/2*

The transverse component, corresponding to changing from one foot to the other when walking, occurs, therefore, at a frequency of half that of the frequency of walking (1 Hz for f_s= 2 Hz). Taking into account the first three harmonics, Fourier coefficients of lateral force components can be described as [9]:

$$F(t)=\sqrt{N}\cdot G\cdot\sum_{j=1/2}^{2}\alpha_j\cdot\sin(2\pi\cdot j\cdot f_s\cdot t) \quad (2)$$

where:

Table 3 – Components of load for j-th harmonics

j	α_j
1/2	*0,05*
1	*0,05*
3/2	*0,05*
2	*0,05*

For the application simplified analysis (RFEM No position dependency) [8], the same functions (1) and (2) are used to describe the human walk as in the RFEM Time history

analysis, but with different numbers of pedestrians (3) and without changing the position. The relevant nodes (Figures 7-8) and their reaction for different traffic densities are examined.

$$N = b \cdot L \cdot d \qquad (3)$$

where:

b=3,3 m is bridge width

L=30 m is span length

d is traffic density (Table 4)

Table 4 – Pedestrian traffic classes and densities [6]

Traffic class	*Density d (P=person)*	*Description*	*Characteristics*
TC1	*group of 15P d=15 P/bl*	*Very weak traffic*	*(b=width of deck; l =length of deck)*
TC2	*d=0,2 P/m²*	*Weak traffic*	*Comfortable and free walking, Overtaking is possible, Single pedestrians can freely choose pace.*
TC3	*d=0,5 P/m²*	*Dense traffic*	*Significantly dense traffic, Unrestricted walking, Overtaking can be intermittently inhibited.*
TC4	*d= 1,0 P/m²*	*Very dense traffic*	*Freedom of movement is restricted, Uncomfortable situation, obstructed walking, Overtaking is no longer possible.*
TC5	*d=1,5 P/m²*	*Exceptional dense traffic*	*Very dense traffic and unpleasant walking, Crowding begins, One can no longer freely choose pace.*

2.5 COMPARISON OF RESULTS

This section presents the comparative dynamic analysis between footbridge structural systems made from cold-formed sections presented in this paper, and aluminum alloy presented in study of Kondić [10-11]. Table 5 and 6 compare their vertical and horizontal fundamental frequency in accordance with EN 1990 [5] and SETRA guidelines [9], respectively.

It can be seen from Table 5 that, regarding to values of the vertical and horizontal fundamental frequency of both bridges, a verification of the comfort criteria is not needed according to EN 1990 [5].

Given used methods, there are quite big margins in obtained results - from the fact that, according to the first method, the steel bridge meets the comfort conditions according to the

requirements of EN 1990 [5] and provides maximum comfort according to the classification by SETRA guidelines [9], to the extent that, according to the third method nothing is fulfilled.

The vertical acceleration (Table 5) of the Aluminum Bridge (mass 12.6 t) is several times higher than the acceleration of the steel bridge (mass 27.9 t). The horizontal acceleration (Table 6) of the two bridges is approximately the same except for the Spectra response method.

Table 5 – Vertical acceleration results compared with EN 1990 comfort demand and Comfort level

	Cold-formed steel footbridge				*Aluminum alloy footbridge* [10]			
	Node 2 $a_{max,vert}$ *[m/s²]*	*Node 1* $a_{max,vert}$ *[m/s²]*	*Comfort level*	*EN 1990*	*Node 2* $a_{max,vert}$ *[m/s²]*	*Node 1* $a_{max,vert}$ *[m/s²]*	*Comfort level*	*EN 1990*
RFEM Time history analysis	*0,07*	*0,10*	*CL1*	√	*0,82*	*0,53*	*CL2*	*x*
RFEM No position dependency	-	-			-	-		
d=0,15	*0,36*	*0,60*	*CL2*	√	*1,71*	*1,72*	*CL3*	*x*
d=0,2	*0,42*	*0,69*	*CL2*	√	*1,97*	*1,99*	*CL3*	*x*
d=0,5	*0,66*	*1,10*	*CL3*	*x*	*3,12*	*3,15*	*CL4*	*x*
d=1,0	*0,93*	*1,55*	*CL3*	*x*	*4,42*	*4,45*	*CL4*	*x*
d=1,5	*1,14*	*1,90*	*CL3*	*x*	*5,41*	*5,45*	*CL4*	*x*
Response spectra method [6]	$a_{d,vert}$*[m/s²]*				$a_{d,vert}$*[m/s²]*			
d=0,15	*0,73*		*CL2*	*x*	*1,64*		*CL3*	*x*
d=0,2	*0,83*		*CL2*	*x*	*1,90*		*CL3*	*x*
d=0,5	*1,32*		*CL3*	*x*	*3,00*		*CL4*	*x*
d=1,0	*1,41*		*CL3*	*x*	*3,17*		*CL4*	*x*
d=1,5	*0,99*		*CL2*	*x*	*2,05*		*CL4*	*x*
Mass	*27,9 t*				*12,6 t*			
Vert. frequency	*5,43 Hz*				*5,65 Hz*			
Lat. frequency	*4,31 Hz*				*2,92 Hz*			

Table 6 – Horizontal acceleration results compared with EN 1990 comfort demand and Comfort level

	Cold-formed steel footbridge				*Aluminum alloy footbridge* [10]			
	Node 2 $a_{max,lat}$ *[m/s²]*	*Node 1* $a_{max,lat}$ *[m/s²]*	*Comfort level*	*EN 1990*	*Node 2* $a_{max,lat}$ *[m/s²]*	*Node 1* $a_{max,lat}$ *[m/s²]*	*Comfort level*	*EN 1990*
RFEM Time history analysis	*0.01*	*0.01*	*CL1*	√	*0,02*	*0,03*	*CL1*	√
RFEM No position dependency	-	-			-	-		
d=0,15	*0,03*	*0,04*	*CL1*	√	*0,03*	*0,05*	*CL1*	√
d=0,2	*0,03*	*0,05*	*CL1*	√	*0,04*	*0,05*	*CL1*	√
d=0,5	*0,05*	*0,08*	*CL1*	√	*0,06*	*0,09*	*CL1*	√
d=1,0	*0,07*	*0,11*	*CL2*	√	*0,08*	*0,12*	*CL2*	√
d=1,5	*0,09*	*0,14*	*CL2*	√	*0,10*	*0,15*	*CL2*	√
Response spectra method [6]	$a_{max,lat}$*[m/s²]*				$a_{max,lat}$*[m/s²]*			
d=0,15	*0,77*		*CL3*	*x*	*1,94*		*CL4*	*x*
d=0,2	*0,89*		*CL4*	*x*	*2,23*		*CL4*	*x*
d=0,5	*1,40*		*CL4*	*x*	*3,53*		*CL4*	*x*
d=1,0	*1,75*		*CL4*	*x*	*4,88*		*CL4*	*x*
d=1,5	*1,71*		*CL4*	*x*	*6,57*		*CL4*	*x*

3. CONCLUSION

EN 1990 [5] is stiff with only one limit of the required comfort. Classification of comfort in four levels is more practical.

According to the EN 1990 [5], no comfort check is necessary when the required limits demands of the bridge's fundamental frequencies are satisfied. In the case of a steel bridge, the validity of this condition is confirmed by the first most precise method, while in the case of Al bridge is not.

Response spectra method calculations are on the safe side and engineers should apply them to small objects, while for larger structures a more accurate software calculation should be used.

When comparing the result of vibrations of the pedestrian bridge from cold-formed steel members and aluminum, the results were less favorable for aluminum due to less weight.

ACKNOWLEDGMENT

This investigation is the part of TR-36048 project supported by the Serbian Ministry of Education, Science and Technological Development.

REFERENCES

[1] European Committee for Standardization CEN: EN 1993-1-1, Eurocode 3: Design of steel structures, Part 1-1: General rules and rules for buildings, 2005.

[2] European Committee for Standardization CEN: EN 1993-1-3, Eurocode 3: Design of steel structures, Part 1-3: General rules – Supplementary rules for cold-formed members and sheeting, 2006.

[3] European Committee for Standardization CEN: EN 1993-2, Eurocode 3: Design of steel structures, Part 2: Steel bridges, 2006.

[4] Dlubal RFEM, Structural Engineering Software for Analysis and Design, https://www.dlubal.com/en (visited may 2018.)

[5] European Committee for Standardization CEN: EN 1990, Eurocode 0 – Basis of structural design, Annex A2: A2.4.3.2 Pedestrian comfort criteria (for serviceability), 2006.

[6] European Commission, Research fund for Coal and Steel, Advanced load models for synchronous pedestrian excitation and optimized design guidelines for steel footbridges, 2008.

[7] Analiza graničnog stanja upotrebljivosti pešačkih mostova u pogledu vibracija indukovanih pešacima, doktorska disertacija, mr Marija Spasojević-Šurdilović, dipl.inž.građ, Univerzitet u Nišu, Građevinsko-arhitektonski fakultet, avgust 2013.

[8] Dlubal Webinar: Time History Analysis Using RF-/DYNAM Pro - Walking and Running Across Pedestrian Bridge, https://www.youtube.com/watch?v=7OxxsCEK41M (visited may 2018.)

[9] Technical guide, Footbridges Assessment of vibrational behavior of footbridges under pedestrian loading, Published by the Sétra, realized within a Sétra/Afgc (French association of civil engineering) working group, 2006.

[10] Analiza nosivosti i upotrebljivosti pešačke pasarele prema EN 1999-1-1, master rad, Stefan Kondić, dipl.inž.građ, Univerzitet u Beogradu, Građevinski fakultet, jun 2018.

[11] Kondić S., Dobrić J., Gluhović N.: Design of pedestrian bridge according to Eurocode 9, 15. Congress of the Association of the Structural Engineers of Serbia, Zlatibor, 6th-8th September, 2018.

ДГКС Друштво грађевинских конструктера Србије
ASES Association of Structural Engineers of Serbia
S-82
15. KONGRES
6-8. 9. 2018. Zlatibor

Marina Rakočević[1]

UTICAJ BROJA SLOJEVA I DEBLJINE PLOČE NA NAPONSKO DEFORMACIJSKO STANJE U TEORIJI SLOJEVA

Rezime:

U ovom radu prikazan je uticaj broja slojeva i debljine ploče na pomjeranja i napone kod slobodno oslonjenih slojevitih kompozitnih ploča opterećenih upravno na srednju ravan ploče. Naponsko deformacijska analiza zasnovana je na analitičkom rješenju jednačina teorije slojeva pri čemu su analizirane ploče sa antimetričnim rasporedom slojeva. Analizom tačnosti, konvergencije i stabilnosti primarnih i sekundatnih promjenljivih u radu su definisane granice primjene u zavisnosti od uticaja debljine ploče i broja slojeva.

Ključne riječi: teorija slojeva, ploča, sloj, pomjeranje, napon

AN INFLUENCE OF THE NUMBER OF LAYERS AND THE THICKNESS OF PLATE ON STRESS-STRAIN STATE IN A LAYERWISE PLATE THEORY

Summary:

This paper presents the influence of the number of layers and of the thickness of plate on the displacements and the stresses of simply supported rectangular laminated composite plates loaded perpendicularly to the middle plane. The stress-strain analysis are based on the analytical solution of equations in a layerwise theory where the plates, with an antisymmetric layer arrangement, are analyzed. The quantified limits in terms of the impact of the plate thickness and the number of layers on the accuracy, convergence and stability of primary variables and secondary variables have been analysed in the paper.

Key words: layerwise theory, plate, layer, displacement, stress

[1]*Associate professor, University of Montenegro, Faculty of Civil Engineering, Podgorica, Montenegro, marinara@ac.me*

1. INTRODUCTION

In the last decades, different mathematical models have been developed with the aim of determining the problems of composite beams, plates and shells in an appropriate manner. When determining the internal stress and strain state for abovementioned composite structures, depending on the desired accuracy, classical and contemporary theories are available. The classical theories are generally well known, and are based on the idea that the composite structure is considered as a whole of equivalent rigidity, while the contemporary theories tend to obtain the most accurate stress and strain change along the cross-section, and develop mathematical models that may include imperfections in the structure of the composite construction.

This paper takes into consideration the laminated composite plates made of layers of different materials and geometric characteristics. The basic element of the laminated composite plate is a layer or lamina which consists of a matrix and fibers embedded in the matrix. The fibers are a bearing element of a layer, while the role of the matrix is to protect fibers from external impact, to keep the fibers together and to make even distribution of influence on each fiber. The subject of the analysis is the laminated composite plates obtained by a combination of different cross-ply orientations, each of which comprises unidirectional fibers. Compared to the composite plate made of conventional materials, the composite plate made of modern materials has a significantly less weight and considerably better physical and mechanical characteristics.

This paper presents the analysis of simply supported rectangular laminated composite plates loaded perpendicularly to the middle plane using a computational method based on Reddy's Layerwise theory, [1-3]. The stress-strain analysis was based on the analytical solution of equations of the Layerwise theory, where the plates with an antisymmetric layer arrangement were analyzed. Each of the layers contains continuous fibers oriented in one of two mutually orthogonal directions.

This paper uses a mathematical model based on the theory called the Generalized Laminated Plate Theory (GLPT) developed by Reddy J.N. The equations for bending of simply supported rectangular laminated composite plates with orthogonal layers were solved in a closed form, using the Navier's solution, where discretization was made through the thickness of the plate. In this way, the three-dimensional problem of elasticity theory is reduced to the solution of differential equations with variable x and y in plane of the plate, and with the interpolation through the plate thickness by one-dimensional interpolation functions of coordinate z.

The quantified limits of the computational method in terms of the impact of plate thickness and the number of layers on the accuracy, convergence and stability of primary variables, component displacements, and secondary variables, component stresses, have been analysed in the paper.

2. THEORETICAL BACKGROUND

For the adopted coordinate system, the component displacements in the direction of the axes x, y and z are u, v and w respectively. The mathematical model of the layerwise theory is based on the assumptions of Reddy's Partial layerwise theory by introducing the following assumptions for displacements:

$$
\begin{aligned}
u(x,y,z) &= u(x,y) + U(x,y,z) \\
v(x,y,z) &= v(x,y) + V(x,y,z) \\
w(x,y,z) &= w(x,y)
\end{aligned}
\tag{1}
$$

where u(x,y),v(x,y) and w(x,y) are the displacements of the points in the middle plane of the plate, while U(x,y,z) and V(x,y,z) represent additional displacements which are assumed to be a sum of multiplication of unknown nodal displacements $u^J(x,y)$ and $v^J(x,y)$ (J=1,..,n, n-total number of the nodes through the thickness of the plate) and the one-dimensional linear interpolation functions $\psi J(z)$ along the independent layers:

$$
\begin{aligned}
U(x,y,z) &= \sum_{J=1}^{n} u^J(x,y)\psi^J(z) \\
V(x,y,z) &= \sum_{J=1}^{n} v^J(x,y)\psi^J(z)
\end{aligned}
\tag{2}
$$

Equation (2) reduces the three-dimensional problem to two-dimensional, whereby the interpolation function of one variable can be of any degree. The number of nodes, where the components of displacement are calculated, depends on the degree of 1D interpolation function, and its distribution through the thickness.

Figure 1 shows the assumed cross-sectional deformation in case when the interpolation function is linear.

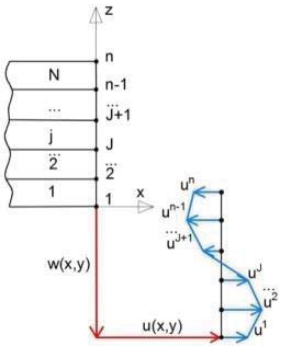

Figure 1 - Undeformed and deformed cross-section of the plate

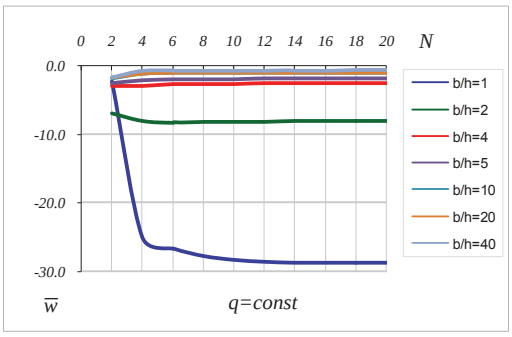

Fig.2: Change $(\bar{w},\ N)$ for different ratio b/h

The total number of nodes, in which node displacements are calculated, is n=N+1, where for the adopted linear interpolation the relation between the mark J for the node and the mark j for the layer is given with J=j+1. The mathematical model of the generalized layerwise theory is characterized by the case that the number of nodes does not have to be related to the number of

layers, i.e. the nodes may be arbitrarily selected. In accordance with the assumptions, this paper adopted the nodes at the ends of the layers. Due to the accepted discretisation by the thickness, this procedure is not purely analytical.

The simple supported laminate plate with dimensions *axb*, which consists of N orthotropic layers with the bearing direction oriented towards x and y axis of the coordinate system, is considered. For such orientation of the layers, based on the condition of orthogonality, it can be proved that $A_{16}=A_{26}=A_{45}=B^{J}_{16}=B^{J}_{26}=B^{J}_{45}=D^{IJ}_{16}=D^{IJ}_{26}= D^{IJ}_{45}=0$. Equations of the problem were obtained by applying the principle of virtual displacements, and are derived analytically using the double trigonometric series. From a system of 3+2n equations, it is possible to obtain the unknown coefficients of the trigonometric series, and then the displacements by using equations (1) and (2), [1-3].

Stresses in an arbitrary node are calculated from the constitutive equations, while the transverse stresses in the plane (x,z) and (y,z) are determined by using a particular semi-analytical method, while ensuring the continuity conditions on the connection of the layers. The additional conditions are zero shear stresses on the top and bottom of the plate.

3. ANALYSIS OF RESULTS

The laminated plates are loaded by uniformly distributed load q = const, and the layers have the equal thickness and the same material characteristics $E_1/E_2=25$; $E_2=1$; $G_{12}=G_{13}=0.5$; $G_{23}=0.2$; $\nu_{12}=\nu_{13}=0.25$.

Displacements and stresses are given in a dimensionless form:

$$\bar{w}=\frac{100E_2}{q\left(\frac{b}{h}\right)^3}w,\quad \bar{u}=\frac{100E_2}{q\left(\frac{b}{h}\right)^2}u,\quad \bar{\sigma}_{xx}=\frac{1}{q\left(\frac{b}{h}\right)^2}\sigma_{xx},\quad \bar{\sigma}_{yy}=\frac{1}{q\left(\frac{b}{h}\right)^2}\sigma_{yy},$$
$$\bar{\sigma}_{xy}=\frac{1}{q\left(\frac{b}{h}\right)}\sigma_{xy},\quad \bar{\sigma}_{xz}=\frac{1}{q\left(\frac{b}{h}\right)}\sigma_{xz},\quad \bar{\sigma}_{yz}=\frac{1}{q\left(\frac{b}{h}\right)}\sigma_{yz} \tag{3}$$

where:

a is plate length,
b is plate width,
h is plate thickness,
q is intensity of the distributed load.

The displacements and stresses were calculated in the following points:

$$\bar{w}(\frac{a}{2};\frac{b}{2};0),\quad \bar{u}(a;\frac{b}{2};0),\quad \bar{\sigma}_{xx}(\frac{a}{2};\frac{b}{2};0),\quad \bar{\sigma}_{yy}(\frac{a}{2};\frac{b}{2};z_2^{up}),$$
$$\bar{\sigma}_{xy}(a;b;h),\quad \sigma_{xz}(a;\frac{b}{2};z_2),\quad \sigma_{yz}(\frac{a}{2};b;z_{n-1}) \tag{4}$$

The convergence and stability of the solutions obtained by applying the calculation procedure [2] were considered by varying the number of layers from 2 to 20, by changing the thickness ratio of the plate b/h from 1 to 40 [3]. Figures 2 to 8 graphically show the obtained values.

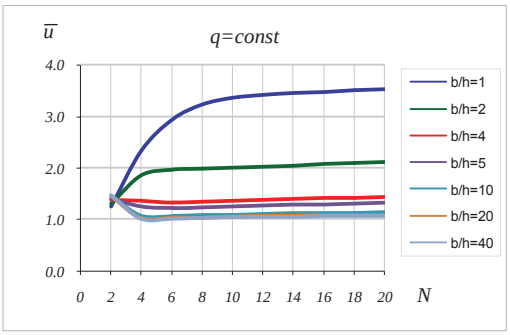

Figure 3 - Change $(\bar{u},\ N)$ *for different ratio b/h*

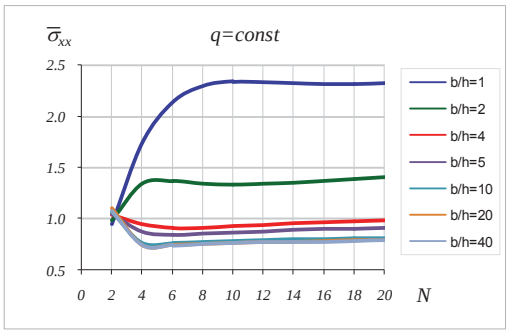

Figure 4 - Change $(\bar{\sigma}_{xx},\ N)$ *for different ratio b/h*

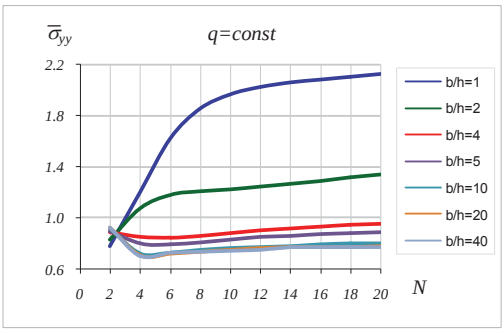

Figure 5 - Change $(\bar{\sigma}_{yy}, N)$ *for different ratio b/h*

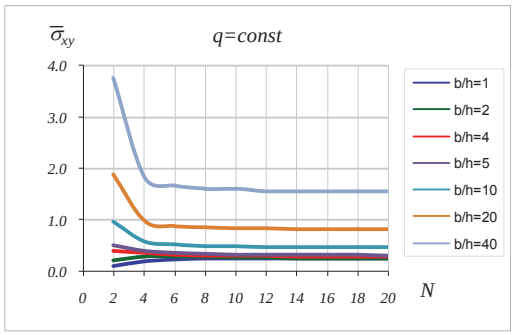

Figure 6 - Change $(\bar{\sigma}_{xy},\ N)$ *for different ratio b/h*

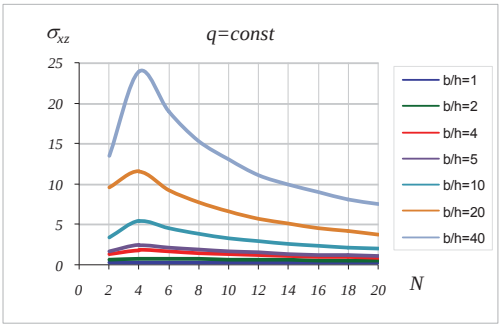

Figure 7 - Change (σ_{xz}, N) *for different ratio b/h*

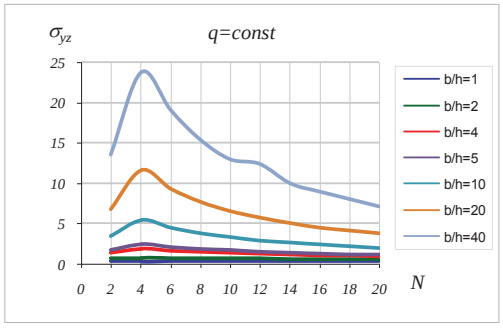

Figure 8 - Change $(\sigma_{yz},\ N)$ *for different ratio b/h*

4. CONCLUSION

Analyzing the effect of the number of layers on the deflection, it is noticed that, for thin and moderately thick plates, a sudden reduction of deflection is achieved by increasing the number of layers up to N = 6. Thereafter, the addition of new layers leads to a slight increase of the deflection. By increasing the number of layers in the thinner plates, there is no significant change in the component displacement $\bar{u}$ and normal stresses $\bar{\sigma}_{xx}$ and $\bar{\sigma}_{yy}$, while in the thicker plates of b/h<4, there is a significant change. Increasing the number of layers up to N = 4 in the thinner plates leads to a significant change in the dimensionless shear stresses comparing to the thicker plates. The change in shear stresses σ_{xz} and σ_{yz}, depending on the change in the number of layers, is more significant in the thinner than in the thicker plates.

REFERENCES

[1] Rakočević M.: Lamination - Theory and Application, Chapter 3: Bending of Laminated Composite Plates in Layerwise Theory, INTECHOPEN, Open access, 2018.

[2] Rakočević M., Popović S., Ivanišević N.: (2017) A computational method for laminated composite plates based on layerwise theory, Composites Part B, 122, 2017, 202-218.

[3] Rakočević M., Popović S.: Bending analysis of simply supported rectangular laminated composite plates using a new computational method based on layerwise theory, Archive of Applied Mechanics, 88(5) , 2018, 671-689

ДГКС Друштво грађевинских конструктера Србије
ASES Association of Structural Engineers of Serbia
S-83
15. KONGRES
6-8. 9. 2018. Zlatibor

Ana Trombeva-Gavriloska[1], Marijana Lazarevska[2], Meri Cvetkovska[3], Miloš Knežević[4]

NAPREZANJE U VEZNOM SLOJU KOD CFRP OJAČANE AB GREDE

Rezime:

Veliki broj postojećih AB konstrukcija pokazuju neadekvatne performanse u smislu smanjene nosivosti, što dovodi do potrebe za njihovim ojačanjem. Cilj rada je numerička analiza uticaja postojanja diskontinualne zone na ponašanje ojačane AB grede s CFRP trakom. U ovom radu veza izmedju AB grede i CFRP trake je modelirana primenom numeričkog vlaknastog modela baziranog na pomeranjima. Za opis zone diskontinuiteta predložen je jednostavni pristup koristeći modifikaciju originalnog konstituvnog zakona. Verifikacija implementirane modifikacije je analizirana preko prostiranja naprezanja u vezi pri maksimalnom opterećenju i pri istom optrećenju, za tri različita slučaja diskontinuiteta u veznom sloju.

Ključne reči: ojačanje, naprezanje u veznom sloju, CFRP

BOND STRESS DISTRIBUTION ALONG CFRP STRENGTHENED RC BEAM

Summary:

A large number of existing RC structures exhibit non adequate performance in terms of diminished bearing capacity and there is a need of post strengthening during their service life. The aim of the presented work was to numerically assess the influence of the presence of discontinuous zone upon overall response of the CFRP strengthened RC beam. In this paper the bond between reinforced concrete beam and CFRP plate has been modelled using a numerical displacement-based fibber model. A simple approach to the weak zone in the bond description is proposed, by using the modification of the original constitutive law for description of the bond. Verification of the implemented modification is analyzed using the bond stress distribution under ultimate load and equal load, for three different cases of discontinuous zone in the bond layer.

Key words: strengthening, bond stress distribution, CFRP

[1] PhD, Assoc. Prof. , Faculty of Architecture, Skopje, Macedonia, e-mail: agavriloska@arh.ukim.edu.mk
[2] PhD, Assist. Prof. , Faculty of Civil Engineering, Skopje, Macedonia, e-mail: marijana@gf.ukim.edu.mk
[3] PhD, Prof., Faculty of Civil Engineering, Skopje, Macedonia, e-mail: cvetkovska@gf.ukim.edu.mk
[4] PhD, Prof., Faculty of Civil Engineering, Podgorica, Montenegro, e-mail: knezevicmilos@hotmail.com

1. INTRODUCTION

Many reinforced concrete structures may exhibit non-adequate performance during their service life caused by the change of loading and environmental conditions. The factors which contribute either for decreasing of the bearing capacity or structural safety of the construction are: the effects of change in the environmental conditions, the increasing of the loads and the design of older structures, which may have been adequately compared with contemporary codes but are inadequate according to the current codes. These factors may decrease the bearing capacity or structural safety of the construction and impose the need of their strengthening. Strengthening of RC members is crucial if their flexural strength is not sufficient to maintain service functions, [1]. The load capacity of flexural loaded structural members can be increased by external additional reinforcement. The usage of externally bonded lighter, stronger and more durable FRP (fiber reinforced polymer) strips is one typical example of a retrofitting technique, which has been employed during the recent practice [2]. The utilization of FRP composite materials in rehabilitating structures is method that can greatly reduce maintenance requirements, increase strength, life safety and service life of concrete structures.

Experimental researches have shown that failure of the externally strengthened RC element occurs because of the loss of composite action between concrete and FRP strip. Furthermore, transferring of the stresses from the concrete to the external reinforcement is essential at structures reinforced by external FRP reinforcement. It is clear that the failure behavior of a plated beam can be very strongly influenced by the integrity of the bond between the plate and the concrete. The bond layer between reinforced concrete surface and FRP strip has the key role for the failure occurrence of the externally strengthened construction with loss of composite action. Practice shows that the inadequate execution of bonding process is the most important problem during the strengthening of reinforced concrete structures. This may lead to weakening of the bond layer in some position along the length of the plate and creating discontinuities within the bond layer. In such case significant changes of the bearing capacity of the strengthened element, which were not taken into account during the design procedure, can be observed. It is extremely difficult to evaluate the influence of these weak zones within the bond layer upon structural response of the strengthened beam.

For proper and accurate determination of the bearing capacity of the reinforced concrete structure strengthened with externally added FRP reinforcement, a model which can properly describe the stresses in the bond layer must be used [4]. The fibber model, with appropriate modifications, could be used for the analysis of the reinforced concrete elements strengthened with externally added FRP plates [5].

Therefore, the aim of the presented work was to numerically assess the influence of the presence of discontinuous zone upon overall response of the beam. The formulation is established on the basis of the model presented by Spacone [5] and the introduction of flexible bond between concrete and external FRP reinforcement. In this paper the bond between reinforced concrete beam and CFRP plate has been modelled using a numerical displacement-based fibber model. A simple approach to the weak zone in the bond description is proposed. Using the modification of the original constitutive law for description of the bond between the reinforced concrete beam and CFRP plate the discontinuous bond zone has been modelled.

Verification of the implemented modification is analyzed using the bond stress distribution along the externally strengthened reinforced concrete beam under ultimate load, for three different cases of discontinuous zone in the bond layer. Numerical analysis, which were carried out, show that the proposed modelling of the weak zone is appropriate.

2. NUMERICAL MODEL FORMULATION

The numerical model employed for the analysis of the externally strengthened reinforced concrete beam element is based on a fiber model. The two-node displacement-based reinforced concrete beam model, presented in Spacone and Limkatanyu [5], has been used.

Constitutive bond law between concrete and external FRP reinforcement is described by linear relation between displacement and shear stresses in the bond layer up to the maximal bond strength. In the original constitutive bond law slip occurs when the maximum bond shear stress is reached, which means that displacement is increasing while the corresponding shear stress is zero. For the purpose of the analysis presented in this paper a modification in the bond law was introduced. In order to model weak zone in the bond layer, maximal shear stress, τ_1, remained unchanged, while displacement at slip was significantly increased. By this modification a much more flexible bond is achieved compared to the perfectly bonded area. Comparison between the original and the modified constitutive bond law is shown in Figure 1.

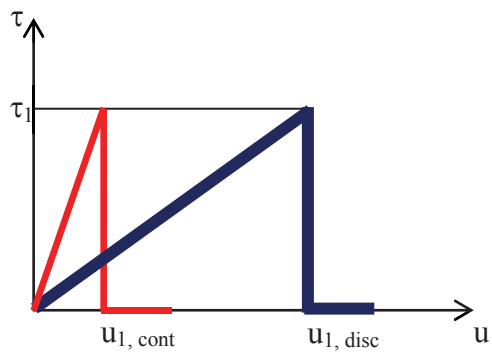

Figure 1- Modification of the original constitutive bond law

Numerical analyses were performed on reinforced concrete beams strengthened with CFRP strip with same geometrical characteristics as those tested and described by Zarnic [6]. A 3200 mm long reinforced concrete beam externally strengthened with CFRP strip was analysed. A beam element has 2900 mm span and cross section b/h=800/120 mm, strengthened with CFRP strip with 100 mm width and thickness of 1,2 mm. The reinforcement steel ratio was set to 0.04% and 6 mm diameter steel stirrups were placed at 100 mm intervals. Epoxy layer for plate bonding was modelled with thickness of 1 mm. The strengthened beam was subjected to four-point bending. Force F was acting at 960 mm from the bearings. Due to the symmetry of the case, only a half of the beam was considered for the numerical study. A representation of the beam geometry is shown in Figure 2.

A mesh of 57 elements was used to obtain response in terms of bond stress distribution between reinforced concrete element and CFRP strip, as well as tensile distribution in CFRP

strip. Numerical analyses were performed on two types of externally strengthened reinforced concrete elements. Reinforced concrete element externally strengthened with continuous bond between concrete substrate and CFRP strip was modeled as a referent sample. The second type of elements was modeled with discontinuous bond between concrete substrate and CFRP strip. Parametric analyses were carried out for three discontinuous bonds with different length. In all three cases discontinuous bond starts at 396 mm from the support. A distance of 346 mm from the start of the CFRP strip was selected in order to obtain sufficient anchors length of external reinforcement and to avoid peeling off forces. Finite nodes of the analyzed cases of were selected with progressive increasing of discontinuous bond. In the case of »d19_38«, finite node was selected near to the position where beam is subjected on bending force and in the case of »d19_50« the discontinuous bond was through the position of bending force.

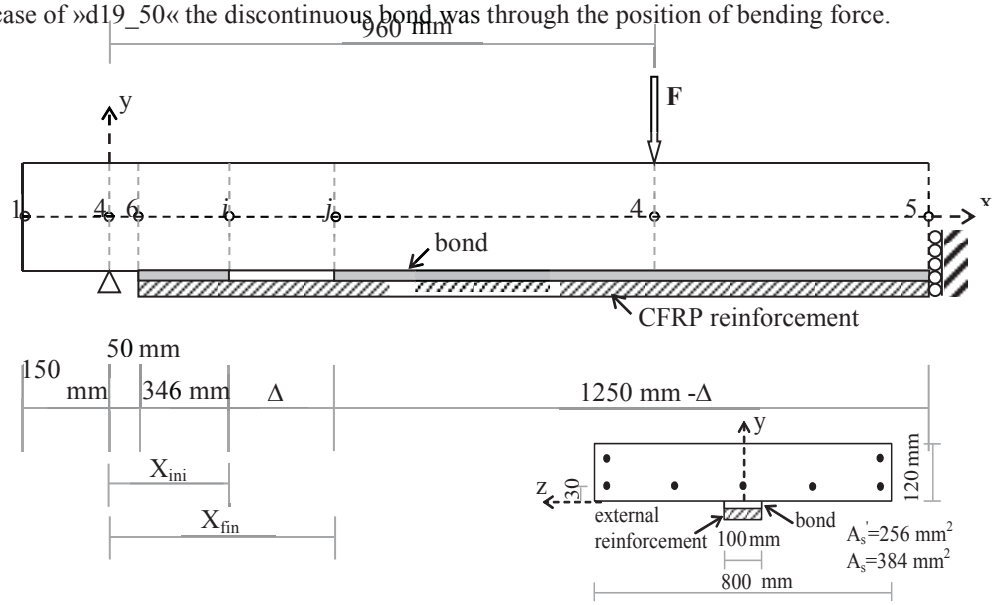

Figure 2- Geometry of the externally strengthened reinforced concrete beam with discontinuous bond

3. RESULTS AND DISCUSION

The perfect bond area in analyzed cases was described by values $u_{1,cont}$=0.0013 mm and τ_1=3.1 Mpa. In order to confirm the introduced modification in the bond law sensitivity analysis of the numerical model for selected values of increasing $u_{1,disc}$, employed for numerical modeling of the weak bond, was performed for all discontinuous zones.

Calculated bearing capacity of the referent sample with continuous bond was F_{ult}=56.4 kN, while the bearing capacity for the reinforced beam with discontinuous bond are summarized in Table 1 and graphically presented in Figure 3.

Table 1- Influence of the parameter $u_{1,disc}$ upon bearing capacity of strengthened beam

$u_{1,disc}$ [mm]	F_{ult} [kN]		
	»d19_26«	»d19_38«	»d19_50«
0.013	55.52	51.94	57.40
0.13	34.80	32.42	32.42
0.39	27.76	23.94	23.92
0.78	26.46	20.16	20.16
1.17	25.24	18.86	17.60
1.56	25.24	16.40	17.54

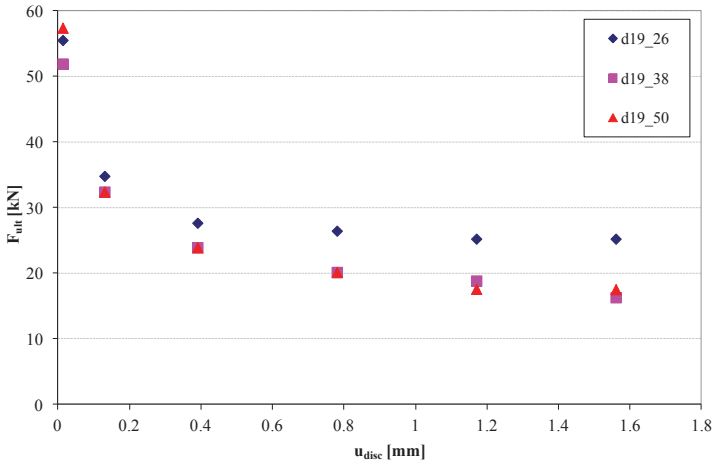

Figure 3- Modelling of discontinuous bond with different length Δ

From the Figure 3 could be concluded that for all three discontinuous zones the values of the calculated bearing capacity are decreasing and approaching to an asymptotic value when $u_{1,disc}$ is increasing. The results show that the modification introduced to the model is appropriate.

Figure 4 presents bond stress distribution along the externally strengthened beam for referent sample and for selected values of the parameter $u_{1,disc}$ for observed discontinuous zones under ultimate limit state.

Furthermore, analysis are caried out for selected values of the parametar $u_{1,disc}$ used in the modeling process of the weak bond zone upon the equal force of F=16,40 kN, Figure 4.

Bond stress distribution exhibits a sudden increase at the beginning of the plate, which phenomenon was also experimentally confirmed [6]. Further, additional peaks in bond stress distribution could be observed at both ends of the weak bond section and at the place where the beam is subjected on bending force. From the presented results could be concluded that with the increasing of the paramatar $u_{1,disc}$ the bond stress distribution decreases at the beginning of the CFRP strip and at the point where force acts. While at both ends of the weak bond section the bond stress distribution is approximately equal despite the value of parameter $u_{1,disc}$. It

could be concluded that bond stress distribution mainly depends on the change of the cross-section.

In the weak section bond stresses decrease as the parameter $u_{1,disc}$ increase and approach to zero, which meets our expectations and confirm that the modification of the bond-slip behavior for the weak part was appropriate and is in accordance with the actual situation.

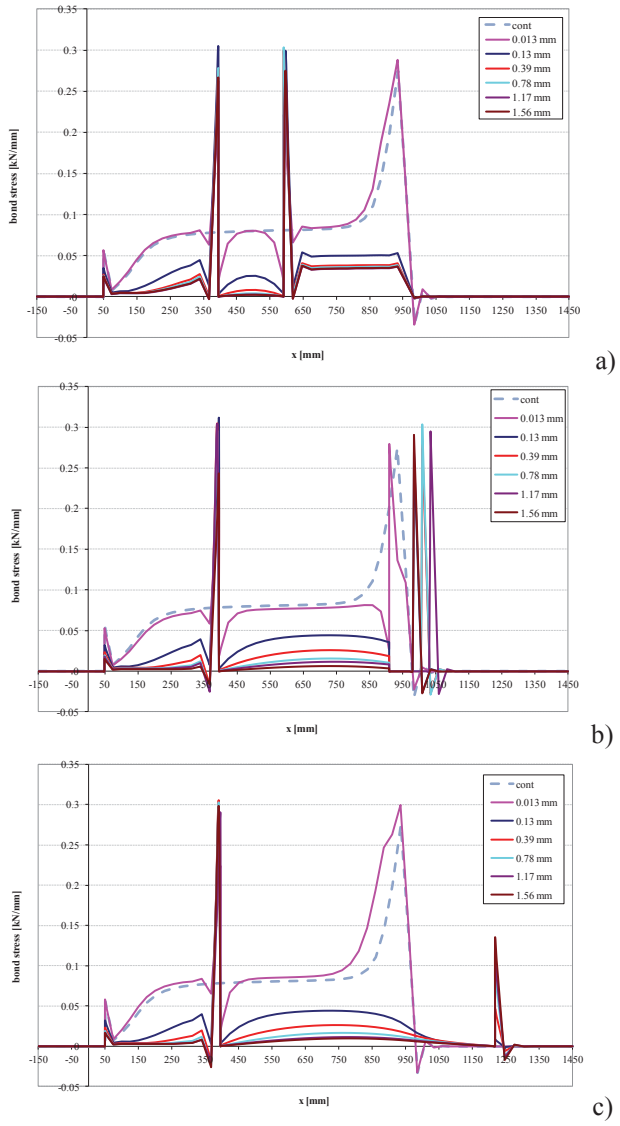

Figure 3- Influence of the parameter $u_{1,disc}$ to bond stress distribution for different length of discontinuous bond: a) »d19_26«; b) »d19_38«; c) »d19_50«

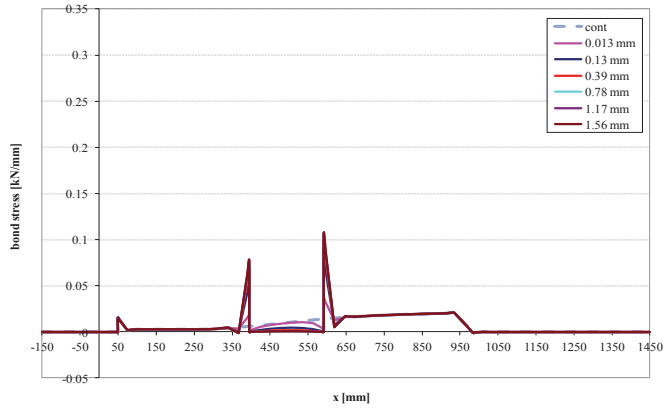

a)

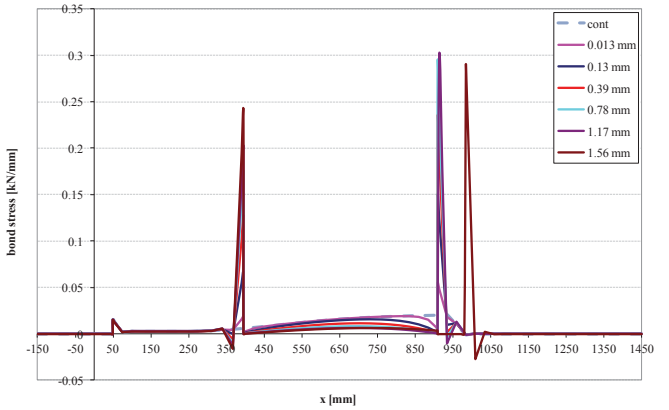

b)

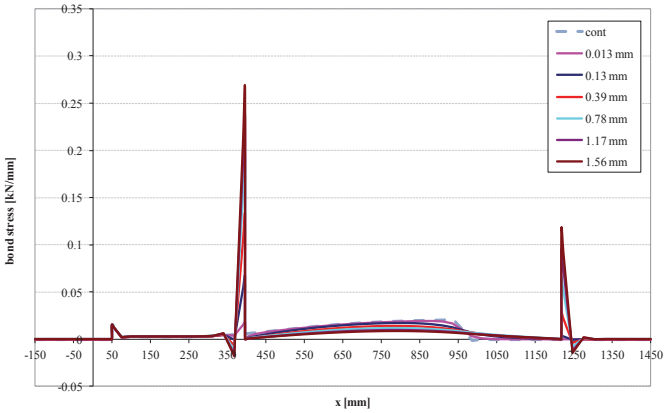

c)

Figure 4 Influence of the parameter $u_{1,disc}$ to bond stress distribution for different length of discontinuous bond under equal force: a) »d19_26«; b) »d19_38«; c) »d19_50«

4. CONCLUSIONS

Experimental researches had shown that failure of the externally strengthened structures subjected to flexure mainly depend on the bond between concrete and external reinforcement and occur by de-bonding of the external reinforcement. This has great importance especially in the case when the external reinforcement is improperly bonded to the RC beam. Improper execution may occur during the process of strengthening, and that could lead to appearance of weak zones in bond layer. The influence of substantially weaker bond on the behavior of the strengthened structure is very difficult to be evaluated, especially because it could not be taken into account in the design stage.

The modeling of the weak bond zone, as well as verification of the introduced modification of the numerical model, is presented in this paper. For the cases where the failure occurred due to de-bonding of the FRP plate, the numerical model used in the analysis has given excellent results in predicting the response of externally strengthened reinforced concrete beams. This also applies for the cases where improper execution of the bond could be crucial for the beam's bearing capacity. However, it should be mentioned that even though the loss of composite action is the main focus of this paper, the beam model which has been used in the simulations can be used for modeling of some other types of failures, such as CFRP tensile rupture and concrete crushing.

The local bond stress concentrations, due to changed cross-section, have negative influence on the quality of the bond between concrete substrate and FRP plate. The obtained results show that the bond stress distribution in the weak zone approach to zero when the value of the parameter $u_{1,disc}$ is increasing, which is in accordance with the actual situation.

REFERENCES

[1] Anania L, Badal A, Failla G. Increasing the flexural performance of RC beams strengthened with CFRP materials. Construction and Building Materials 2005; 19: 55–61.

[2] Ashour AF, El-Refaie SA, Garrity SW. Flexural strengthening of RC continuous beams using CFRP laminates. Cement & Concrete Composites 2004; 26: 765–775.

[3] Aprile A, et al. Role of Bond in RC Beams Strengthened with Steel and FRP Plates. J Struct. Engrg ASCE 2001; 127(12): 1445-1452.

[4] Chen J F, Teng JG. Anchorage Strength Models for FRP and Steel Plates Bonded to Concrete. Journal of Structural Engineering 2001; 127(7): 784-791.

[5] Spacone E, Limkatanyu S. Responses of Reinforced Concrete Members Including Bond-Slip Effects. ACI Structural Journal 2000; 97 (6): 831-839.

[6] Zarnic R, Gostic S, Bosiljkov V, Bokan-Bosiljkov V. Improvement of bending load-bearing capacity by external bonded plates. Proceeding of creating with concrete 1999, p. 433-442.

ДГКС Друштво грађевинских конструктера Србије
ASES Association of Structural Engineers of Serbia
S-84
15. KONGRES
6-8. 9. 2018. Zlatibor

Igor Gjorgjiev[1], *Marija Vitanova*[2]

IDENTIFIKACIJA PRIGUŠENJA ZA NOVE MOSTOVE NA AUTOPUTU TESTIRANE POD DINAMIČKIM OPTEREĆENJEM

Rezime:

U ovom radu je predstavljena identifikacija prigušenja i rezultati dobijeni na osnovu dijagnostičkih testova izvedenih merenjima ambijentalnih vibracija i dinamičkim opterećivanjem novih mostova. Cilj dijagnostičkog opterećivanja mostova je definisanje dinamičkih modalnih parametara. Dekompozicija frekventnog domena (FDD) korišćena je za dobijanje sopstvene frekvencije konstrukcije. Metod logaritamskog dekrementa primenjen je za izračunavanje koeficijenta prigušenja. Koeficijent prigušenja izračunat je u stanju slobodnih vibracija, pri čemu je most pobuđen dinamičnim opterećenjem. Pokriveno je nekoliko scenarija dinamičke pobude. Konstrukcija je vertikalno pobuđena kamionima različitih brzina. Dobijeni rezultati pokazuju da je prigušenje u vertikalnom pravcu zavisilo od brzine kamiona.

Ključne reči: Testiranje mostova, Dinamičko opterećenje, FDD, Koeficijent prigušenja

DAMPING IDENTIFICATION FOR NEW HIGHWAY BRIDGES TESTED UNDER DYNAMIC LOADING

Summary:

In this paper, damping identification and results obtained from diagnostic tests performed by ambient vibration measurements and dynamic loads on newly built bridge structures are presented. The objective of diagnostic loading of bridges is to define the dynamic modal parameters. Frequency Domain Decomposition (FDD) was used to obtain the natural frequency of the structure. The logarithmic decrement method was applied to calculate the damping coefficient. The damping coefficient was calculated in free vibration state where the bridge deck was excited by dynamic load. Several dynamic excitation scenarios were covered. The structure in vertical direction was excited by moving trucks with different speeds. The obtained results showed that the obtained damping in vertical direction for the tested overpasses depended on the speed of the trucks.

Key words: Bridge testing, Dynamic loading, Frequency Domain Decomposition, Damping coefficient

[1]*Associate Professor, PhD, "Ss. Cyril and Methodius" University, Institute of Earthquake Engineering and Engineering Seismology,igorg@iziis.ukim.edu.mk*
[2]*Assistant Professor, PhD, "Ss. Cyril and Methodius" University, Institute of Earthquake Engineering and Engineering Seismology,marijaj@iziis.ukim.edu.mk*

1. INTRODUCTION

Structural design relies on the ability of engineers to anticipate excitation and predict structural response. Vibration measurement is essential in developing an accurate model or confirming the design project and the construction process. It is also an essential segment in defining the safety of bridge structures. These measurements are performed on full scale structures exposed to exploitation loading. One of the methods of load testing is dynamic load testing where the superstructure is loaded by lorries passing along the bridge roadway with different speeds and over road bumps. An additional technique which is known as ambient vibration tests is also applicable in determining the structural modal parameters. Both methods can be used to obtain the modal parameters and the dynamic amplification factor.

Bridges are subjected to dynamic forces imposed by moving vehicles. All moving vehicles generate additional dynamic effects on bridges. Usually, they are indicated by dynamic amplification factors (DAF) introduced in the bridge design codes. The DAF of a bridge is defined as the maximum total load (including the dynamic part) effect divided by the maximum static load effect. The DAF is an important parameter in the design of the bridges and is to be taken into account by evaluation of the bridge load carrying capacity. The value of the DAF depends on many factors: the bridge span length and natural frequency, the vehicle speed, the structural dynamic characteristics and others.

After the action of the dynamic load or impact, the superstructure is in free vibration response. The response is completely determined by the properties of the structure, and its vibration can be understood by examining the structure's mechanical properties. The vibration testing methodology is based on the resonant concept where an impact or dynamic load is applied and the motion of the structure in free vibration is measured. This measure enables determination of the damping coefficient and the damped natural frequency. This methodology was also applied in the testing program for overpasses.

The paper presents a study of the dynamic amplification factors (DAF) obtained from the results of dynamic load tests of two bridges. The study of the DAF was carried out for bridges designed according to the Eurocodes. The dynamic properties of the bridges were obtained by loaded lorries passing along the bridge roadway with different speeds and over road bumps. The obtained values of the DAF were analysed and compared to the values from the performed analysis. Then the results from the analysis of the deck behaviour in vertical direction under free vibration were presented. The logarithmic decrement method was applied to calculate the damping coefficient. The damping coefficient was calculated for different vehicle speed. Finally, frequency domain decomposition (FDD) was used to obtain the natural frequency of the structure in vertical direction. Based on the performed dynamic testing for structures, it can be concluded that the dynamic amplification and the damping coefficient depend on the vehicle speed.

2. OBJECTIVES OF THE TESTS

Pursuant to the existing laws in the R. Macedonia, upon completion of the structure of each newly built bridge, prior to its putting into operation, it is necessary to perform a trial loading in accordance with MKS U.M1.046.

The objective of trial loading of bridges is to define whether the behaviour of the bridges under static and dynamic loads is correct. The objectives of trial loading are: - checking whether the bearing capacity and deformability of the built structure are in compliance with the results from the main and the working design; - checking of the quality of the works done, preciseness of manufacturing and geometry of elements; - checking of the quality of the built-in materials; - checking of the usability of the structure. Additionally to these tests, an ambient and free vibration tests are performed to obtain the natural frequencies and the damping coefficients in vertical direction.

3. DESCRIPTION OF THE TESTED BRIDGES

Both tested bridge structures represent monolith pre-stressed continuous slab systems with characteristics shown in Table 1. The bridges are monolithically connected to the piers and supported on elastomeric bearings by the abutments. The deck of the two overpasses is a solid prestressed concrete slab. The depth of the slabs is constant along the structure. The bridges are continuous over the piers and are monolithically connected to them. They are separated from the abutments by structural joints and supported by the abutments on two elastomeric bearings.

Table 1 – Geometry of the bridges

Bridge structure	*No. of spans*	*Length of structure [m]*	*Width of structure [m]*
1	2	48.6	6.0
2	2	34.0	8.4

The piers and the abutments of both structures are supported by a deep foundation. The piers are supported by four piles connected by an orthogonal pile cap. The abutments are supported by six piles positioned, at plan view, on each side of the abutment columns. The abutments are of a typical spill through type, consisting of three orthogonal columns of varying cross section. The deck slabs rest on plain elastomeric bearings above the abutments.

4. LOAD TESTING AND MEASURING INSTRUMENTS

The instrumentation used for measuring the static quantities of interest, strains and deflections in both mid-spans were measured together with the strains in the middle support (Fig. 1). Furthermore, continuous measurement of accelerations was also done. For measurement of strains, strain gages (SG) from KYOWA (Japan) were used, for measurement of displacement, displacement transducers (LP) from Micro-Epsilon (USA) were used. For measurement of accelerations, accelerometers from PCB (USA) were used. All quantities were measured continuously and in discrete times when the maximal values for characteristic

quantities were reached. Every cross section of interest was tested by use of two loading schemes (symmetrical and non-symmetrical).

Figure 1. Overpass 2 Testing of the bridge- Instalation of measuring instruments in the middle of span (left) and Measuring instruments: displacement transducers (LVDT) (right)

After completing the static loading on each bridge, the dynamic coefficient was determined experimentally. This was done by measuring the deformation at the mid point of one characteristic span. Firstly, the "static" deformation was measured (deformation under one static truck). After that, the track passed with the predefined speed of 10km/h, 20km/h and 30km/h over the measured span and, in this way, the "dynamic" deformation was measured. For better efficiency, an obstacle (metal plate with a thickness of 5cm) was set on the way of the moving truck so that it simulated impulse and enabled simulation of greater "dynamic" deformation (Figure 2).

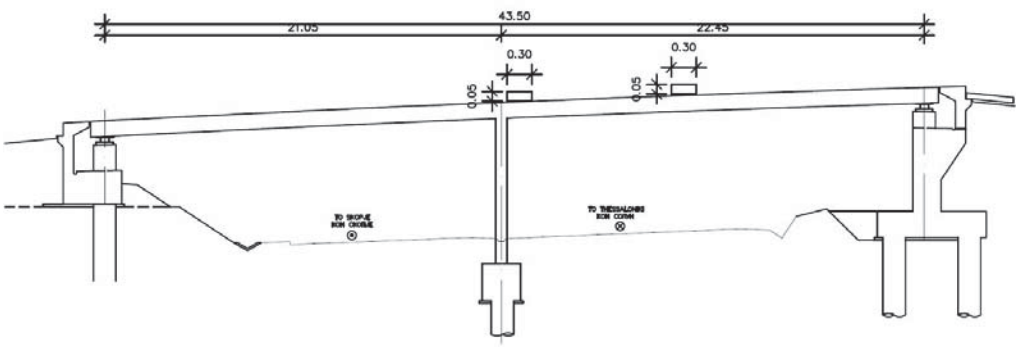

Figure 2. Overpass 2, Location of steel plates used for dynamic testing- longitudinal view

5. METHODS OF DAMPING IDENTIFICATION

5.1. LOGARITHMIC DECREMENT METHOD

The logarithmic decrement method for modal damping estimation is applicable in free vibration state, which can be simulated by forced vibration tests (FVT). In order to obtain the desired damping, the response of the structure to a harmonic force provided by the shakers is to be measured. After stopping the action force by switching off the shakers during excitation in resonant state, the decaying response of the structure should be measured. Having this measured, the decaying exponential curve that best fits the decaying amplitudes is obtained by performing a regression analysis (Figure 3).

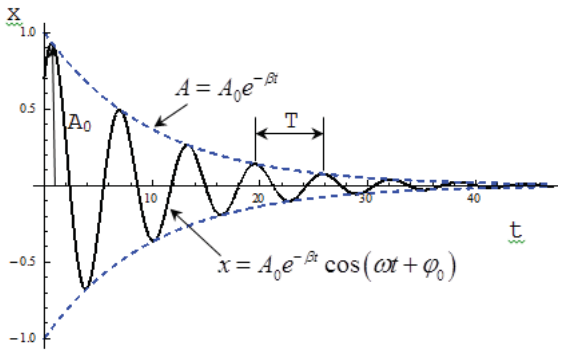

Figure 3. Logarithmic decrement method

The exponential function of the decaying curve that fits the amplitudes of the damped oscillation is defined by equation 1.

$$y = y_0 e^{-\xi \omega_n t} \tag{1}$$

where ξ represents the damping ratio, ωn is the oscillation angular frequency measured in rad/sec2 (f=ωn/2π), t is the time of the observation in seconds. From here, the value of the modal damping for the desired and measured mode of vibration is easily determined.

5.2. HALF-POWER BANDWIDTH METHOD

Upon obtaining the frequency response curves of the analyzed system, modal damping can be measured by using the half-power bandwidth method. This method consists of defining the resonant frequency and two nearby frequencies w1 and w2 located in the frequency spectrum (Figure 4) by application of equation 2:

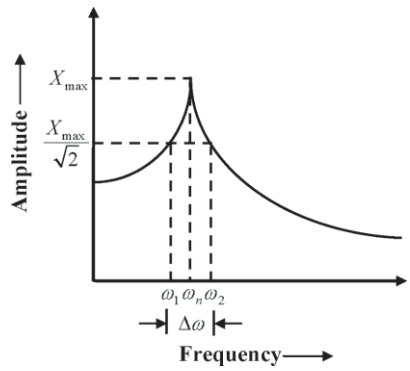

Figure 4. Half- power bandwidth method

$$X(\omega_1, \omega_2) = \frac{X(\omega_n)}{\sqrt{2}} \tag{2}$$

After defining the required frequency values (ω_n, ω_1 and ω_2) in the frequency spectra, the damping value can be calculated applying equation 3.

$$\xi = \frac{\omega_2 - \omega_1}{2\omega_n} \times 100\% \tag{3}$$

6. OBTAINED RESULTS

The fist dynamic test was performed where the superstructure was loaded by lorries passing along the bridge roadway with different speeds and over road bumps. During the investigations presented in this paper, only the vertical deformations in the midst of the span were analyzed and they are presented in Table 2. The values in the first row represent the vertical deformation under static loading. These values were obtained when the fully loaded truck was in the midst of the span. In the last three rows, the deformation obtained from the dynamic test with different speeds of the truck are presented. For OP1, the maximal displacement amplification factor was obtained for a speed of 10km/h, while for OP2, it was obtained for a speed of 40km/h. It can be seen that the vertical deformation is dependent on the truck speed.

Table 2. Dynamic deformation in the midst of spans

Result	*OP1*	*OP2*	*DAF-OP1*	*DAF-OP2*
"Static" deformation (mm)	*1.50*	*0.70*	*1.0*	*1.0*
"Dynamic" deformation (mm) - 10km/h	*1.90*	*-*	*1.26*	*-*
"Dynamic" deformation (mm) - 20km/h	*1.66*	*0.80*	*1.10*	*1.14*
"Dynamic" deformation (mm) - 30km/h	*1.71*	*-*	*1.14*	*-*
"Dynamic" deformation (mm) - 40km/h	*-*	*0.85*	*-*	*1.21*

The performed dynamic tests were additionally used to calculate the damping coefficient in vertical direction. The damping coefficient was calculated by use of the logarithmic decrement method for several different truck speeds. The truck speeds for OP1 were 10, 20 and 30km/h and the obtained damping coefficients were in the range of 1.16% to 1.56%. The values for OP1 are presented in Table 3. In the case of OP2, the truck speeds were 20 and 40km/h. For these speeds, the damping coefficients were 3.5% (Table 4).

Table 3. Damping coefficient for OP1

Instrument		*Damping [%]*		
Label	*Direction*	*10 [km/h]*	*20 [km/h]*	*30 [km/h]*
Acc1	*Z*	*1.16*	*1.23*	*1.56*

Table 4. Damping coefficient for OP2

Instrument		*Damping [%]*	
Label	*Direction*	*20 [km/h]*	*40 [km/h]*
Acc1	*Z*	*3.5*	*3.5*

The time histories of the recorded vertical acceleration in the midst of the span in free vibration motion for OP1 are presented in figure 7, while for OP2, they are presented in figure 5. The black line represents the recorded motion, while the green one represents the logarithmic decrement. The presented figures clearly show the differences in the vibration decay.

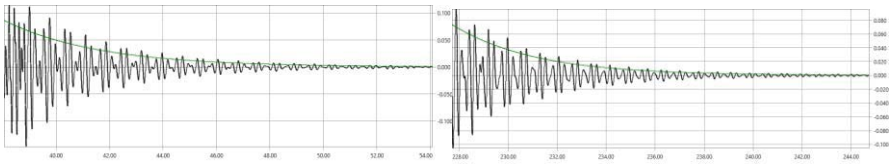

a) 10km/h *b) 20km/h*

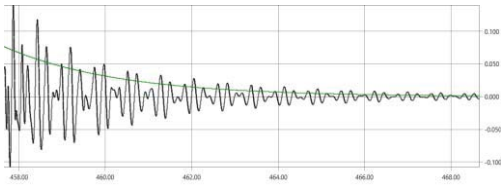

c) 30km/h

Figure 5. Free vibration and logarithmic decrement for OP1

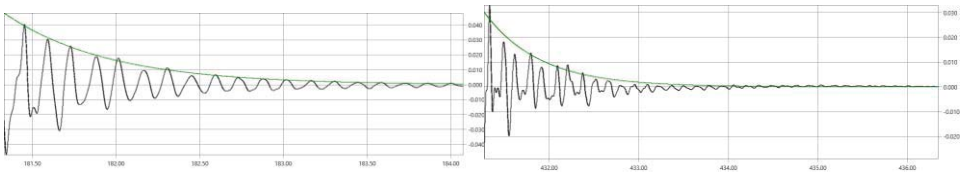

a) 20km/h *b) 40km/h*

Figure 6. Free vibration and logarithmic decrement for OP2

Finally, the results from measurements of ambient vibration are presented. In order to analyze the results, each of the estimated spectral density matrices was decomposes. The singular values of the spectral density matrices were calculated for OP1 and OP2 and are presented in figure 7. From the analyzed results, the first three natural frequencies for OP1 were obtained to amount to 3.91, 5.28 and 8.97Hz. For OP2, only one natural frequency amounting to 7.25Hz was obtained.

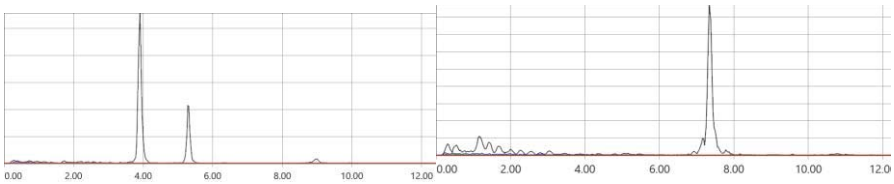

a) SVD for OP1 *b) SVD for OP2*

Figure 7. Singular values of the spectral density matrices

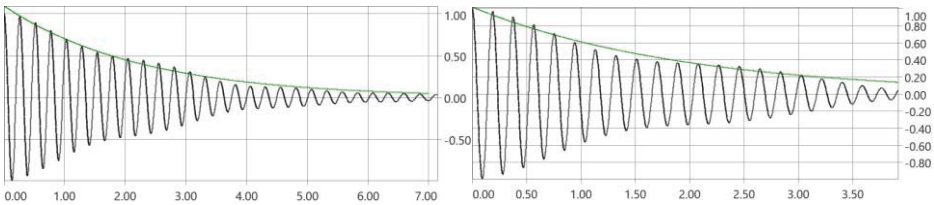

a) at 3.91Hz *b) at 5.28Hz*

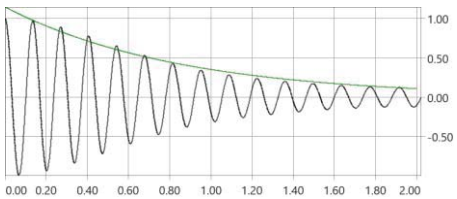

c) at 7.25Hz

Figure 8. Modal damping coefficient calculated for OP1 by EFDD

The modal damping was calculated by application of the half power method. For OP1, the modal damping coefficient calculated by enhanced frequency domain decomposition (EFDD) for the first mode shape was 1.79%, while for the second mode shape, it was 1.51%. For OP2, the modal damping coefficient was 2.56%.The inverse response function is presented in figure 8.

The damping coefficient calculated according to the half-power bandwidth method for OP1 at frequency 3.91 was 1.23%, while at frequency 5.28, it was 1.20%. For OP2, the damping coefficient at f=7.25 was 1.31%. The damping coefficient was calculated from the singular values of the spectral density matrices curve, figure 9 and figure 10.

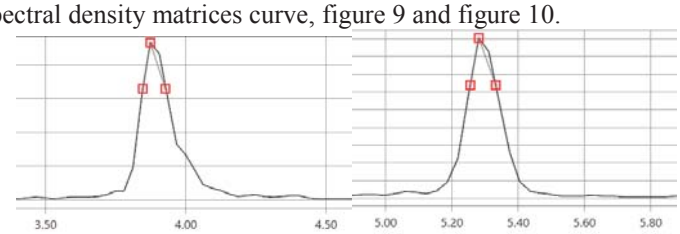

a) at 3.91Hz b) at 5.28Hz

Figure 9. Damping coefficient for OP1 obtained by the half power method.

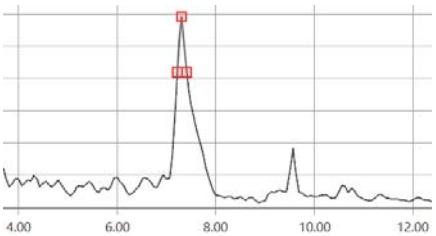

Figure 10. Damping coefficient for OP2 obtained at 7.25 Hz by the half power method.

7. CONCLUSIONS

Based on tests performed by trial dynamic loading of two overpasses and performed ambient measurements, the dynamic amplification factor and modal parameters were obtained. From the presented results, the following conclusions can be drawn:

- The strains in the deck indicated that the superstructure behaved in the linear elastic range for all the time of the testing.
- The total residual deformations upon completion of the testing, immediately after unloading, amounted to 0.7 mm for OP1 and 0.7 mm for OP2, which were less than the maximum allowed 1.26mm for OP1 and 0.78 mm for OP2.
- The first natural frequency in vertical direction was 3.91Hz for OP1, while for OP2, it was 7.25Hz.
- The obtained results showed that, for bridges designed according to the Eurocode, the dynamic amplification factor values for the deck were within 1.1–1.26 for OP1 and within 1.14-1.21 for OP2. The experimentally obtained mean dynamic coefficient at the vehicle speed

of 10km/h, 20km/h and 30km/h amounted to 1.17 for OP1 and 1.17 for OP2. The maximum computed design dynamic coefficient for all three bridges ranged within the limits anticipated in the project.

- It was established that DAF values strongly depended on the vehicle speed passing along the roadway surface. There was no exact correlation as to whether the DAF values were increased by lower or higher vehicle speed.
- The obtained damping of the structure for a speed of 10 km/h, 20 km/h and 30 km/h amounted to 1.16%, 1.23% and 1.56%, respectively, for OP1, and 3.5% for OP2.
- The damping coefficient calculated by enhanced frequency domain decomposition (EFDD) for OP1 was 1.7% for the first mode, while for the second mode, it was 1.5%. For OP2, it was 2.56.
- The damping coefficient calculated by the half power bandwidth method for OP1 was 1.23% for the first mode, while for the second mode, it was 1.2%. For OP2 it was 1.31.
- The calculated damping coefficients EFDD were closer to the damping values obtained by the free vibration test than those obtained by the half power bandwidth method.
- The analytically calculated damping coefficients were close to the realistic values of damping, which were obtained by impact tests. The ambient vibration testing can be used to estimate the damping coefficients with an acceptable accuracy.

REFERENCES

[1] Brady, S. P., O'Brien, J. O., Znidaric, A., 2006. Effect of Vehicle Velocity on the Dynamic Amplification of a Vehicle Crossing a Simply Supported Bridge, Journal of Bridge Engineering 11(2), pp. 241-249. doi:10.1061/(ASCE)1084-0702(2006)11:2

[2] Brownjohn, J.M.W., De Stefano, A., Xu, You-Lin, Wenzel, H. and Aktan, A.E. (2011). J. Civil Struct. Health Monit. Vibration-Based Monitoring of Civil Infrastructure: Challenges and Successes. 1:3-4, 79-95

[3] Bruls, A., Calgaro, J. A., Mathieu, H., Prat, M., 1996. “ENV1991 – Part 3: The Main Models of Traffic Loads on Bridges; Background Studies”, IABSE Colloquim, Delft, The . Delft: IABSE, pp. 215-228

[4] Cantieni, R., Dynamic Load Testing of Highway Bridges, IABSE Proceedings, P-75/84, Zürich, August 1984. (paper in proceedings)

[5] Cantero, D., González, A., O'Brien, E. J., 2009. “Maximum Dynamic Stress on Bridges Traversed by Moving Loads”, Proceedings of the ICE – Bridge Engineering 162(BE2), pp. 75-85. doi:http://dx.doi.org/10.1680/BREN.2009.162.2.75

[6] Kopacik, A., 2003. “Loading Tests of Highway Bridges in Slovakia”, 11th FIG Symposium on Deformation Measurements. Santorini: FIG, pp. 1-7.

[7] Halling, M.W., Muhammad, I., and Womack, K.C. (2001). J. Struct. Eng. Dynamic Field Testing for Condition Assessment of Bridge Bents. 127:2, 161-167

[8] Tian, Z., Zhang, L., Peng, T., 2008. “Load tests of Dongping Bridge in Foshan, China”, 17th Congress of IABSE Creating and Renewing Urban

[9] Structures, Chicago: IABSE, pp. 1-7 Wahab, M.M.A., and Roeck, G.D. (1998) J. Bridge Eng. Dynamic Testing of Prestressed Concrete Bridges and Numerical Verification. 3:4, 159-169

ДГКС Друштво грађевинских конструктера Србије
ASES Association of Structural Engineers of Serbia
S-85
15. KONGRES
6-8. 9. 2018. Zlatibor

Igor Gjorgjiev[1], *Borjan Petreski*[2], *Vlado Micov*[3]

EKSPERIMENTALNO ISPITIVANJE VEZE GREDA-STUB ZA PREFABRIKOVANE AB KONSTRUKCIJE

Rezime:

Ovo eksperimentalno ispitivanje predstavlja rezultate kvazi-statičke procedure testiranja veze greda-stub za prefabrikovane konstruktivne sisteme od armiranog betona. Testiranjem se određuje kapacitet nosivosti i deformabilnost određene veze u nelinearnom domenu. Dva identična modela stvarne veličine su podvrgnuta cikličnom opterećenju i ispitivanju do loma. Opterećenje se nanosi na prefabrikovani nosač-gredu koji potom prenosi silu na stub preko specifične veze. Utvrđeno je da veza prilikom testiranja ostaje neoštećena, a da lom nastupa usled gubitka nosivosti stuba.

Ključne reči: prefabrikovanje, beton, veza, kapacitet, eksperiment

EXPERIMENTAL STUDY OF BEAM-TO-COLUMN CONNECTION FOR PREFABRICATED RC STRUCTURE

Summary:

This experimental study presents the results from a quasi-static testing procedure of a beam-to-column connection for a prefabricated reinforced concrete structural system. The testing is performed for determination of the bearing capacity and deformability characteristics of the particular connection in the nonlinear domain. Two identical real-size models are subjected to cyclic loading and investigated until failure. The load is applied at the prefabricated truss-beam element which then transfers the forces in the column through the specific connection. It is established that the connection remains undamaged during the testing and the structural failure is governed by a failure in the column.

Key words: prefabricated, concrete, connection, capacity, experiment

[1] *Assoc. Prof., PhD, Institute of Earthquake Engineering and Engineering Seismology, University "Ss. Cyril and Methodius", igorg@iziis.ukim.edu.mk*
[2] *Ass., MSc, Institute of Earthquake Engineering and Engineering Seismology, University "Ss. Cyril and Methodius", borjan@iziis.ukim.edu.mk*
[3] *Prof., PhD, Institute of Earthquake Engineering and Engineering Seismology, University "Ss. Cyril and Methodius", micov@iziis.ukim.edu.mk*

1. INTRODUCTION

Prefabricated reinforced concrete structures provide advantages in terms of the time of erection, cost of the project, quality and safety control and sustainable construction. They are widely regarded as a high quality, economic and architecturally versatile technology offering a wide range of commercial and industrial needs [1]. However, their application in seismically active areas is rather limited, mainly due to scarce design guidelines as compared to those available for cast-in-place concrete structures [2].

Considering the past seismic performance of prefabricated structures, lack of mechanical connections between the structural elements cause the most severe damages and failures. The inability to transfer the horizontal earthquake-induced actions leads to the loss of support of beams [3]. The problem arises due to the use of friction connections and a very limited support width. Some precast structures show the failure of the connections even in cases in which pin beam-to-column connections are used, due to inadequate connection design [4]. On the other hand, the in-situ reinforced concrete moment-frame construction with monolithic beam-to-column connection shows substantially better quality during seismic excitations. Generally, the damage in the in-situ connections occurs if constructed without the use of modern details for ductile response [5].

The understanding on the behavior of the connection is important and can only be assessed by conducting experimental tests [6]. Experimentally, the precast connections demonstrate higher flexural strength than the monolithic connections subjected to static and cyclic loading. Their ductility and energy absorption is satisfactory and superior to the monolithic models investigated, as well [7]. The study presented in this paper examines the load capacity and deformability properties of a specific beam-to-column connection through quasi-static full-scale testing. The models are subjected to cyclic loading and examined in the nonlinear domain. The loading of the specimens is applied through the truss-beam elements which transfer the forces to the columns and foundations. Two identical models are investigated until failure and the behaviour of the particular connection is assessed by the output of the configured instrumentation. Afterwards, the test results in the form of force-displacement graphs, displacement and strain time-histories are presented and analysed. In the end, it is verified that the monolithic nature of the joint connection under the design loads is preserved throughout the testing procedure.

2. SPECIMEN DIMENSIONS AND DETAILING

In the beginning, detailed design for the beam-to-column connection model is performed in order to fulfil the primary goal of this study. It is aimed at designing the specimens for simulation of the realistic behaviour of the connection disregarding any possible error during the course of the experiment. The design is performed with the intention to prevent occurrence of failure in the connection under the maximum design load.

The testing specimen is designed to simulate the connection behaviour between a corner column, primary truss-beam and secondary truss-beam. It contains 4 structural elements: (1) foundation, (2) column, (3) secondary truss-girder and (4) primary truss-girder. The foundation

element is designed as a single footing with base dimensions of 200/120 cm and a 50 cm height. The column has a square cross-section with side length of 60 cm. Its connection with the foundation structure is monolithic. On the upper side of the column, a joint simulating realistic connection of a corner column and orthogonally connected primary and secondary truss-beams, is formed. The secondary beam-to-column connection is not a subject of this testing procedure and therefore its modelling is performed structurally with the real dimensions. Due to testing limitations, the main beam is constructed with one truss panel, even though it originally contains four. The dimensions of the top and bottom chord correspond to the real dimensions of the main truss. Figure 1 presents the base view of the model setup assembled for testing.

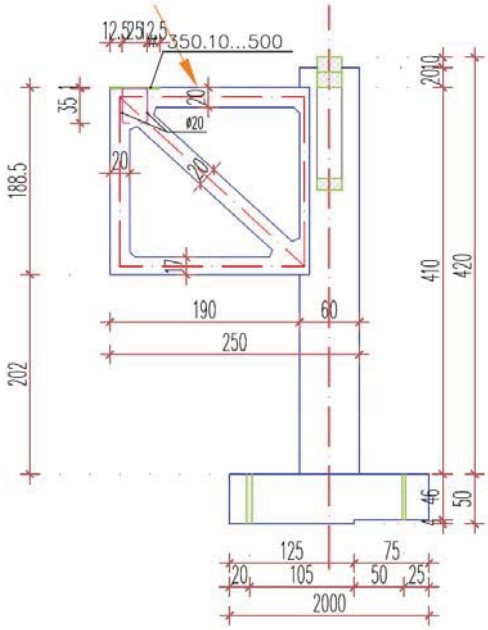

Figure 1 – Base view of the testing model

The reaction wall for the horizontal load is a stiff tapered cantilever bolted to a steel system. It is connected to the laboratory floor slab (strong floor) by means of large steel reinforcement bars crossing the slab and the steel elements. The four independent structural elements consisting the testing assembly (footing, column, secondary and primary truss) are designed separately. The footing is designed to withstand the maximum loading of the testing procedure. The column is primarily designed for maximum design loads and then checked for the ultimate loading of the testing procedure. The longitudinal reinforcement of the column consists of 12 bars with reinforcement ratio of approximately 1.3%. Closed stirrups of 8 mm diameter at 7.5 cm distance from centre to centre and additional 8 mm tie stirrups at 30 cm distance are used as transverse reinforcement of the column. As mentioned before, the secondary truss-beam is modelled structurally since it is not loaded during the experimental procedure. In contrast, the main truss is the element where the loading is applied and it should simulate transfer of the realistic loading to the connection of interest. Therefore, the elements of the main truss are

designed individually in order to be capable of supplying the necessary capacity. None of the constituent elements is prestressed, thus they are reinforced with longitudinal and transverse reinforcement.

The loading of the model is applied through hydraulic actuators connected to the primary truss-beam on the opposite side of the reaction walls. The upper side of the column is allowed to move laterally in the both orthogonal directions. As the model is investigated in horizontal arrangement, additional elements are implemented with the purpose of carrying the self-weight of the model. At the same time they enable free translation of the model. The connection between the upper side of the primary truss and the actuators is hinged allowing full transmission of the axial force. Hence, special connection incorporating a steel interface element is designed and shown in Figure 2.

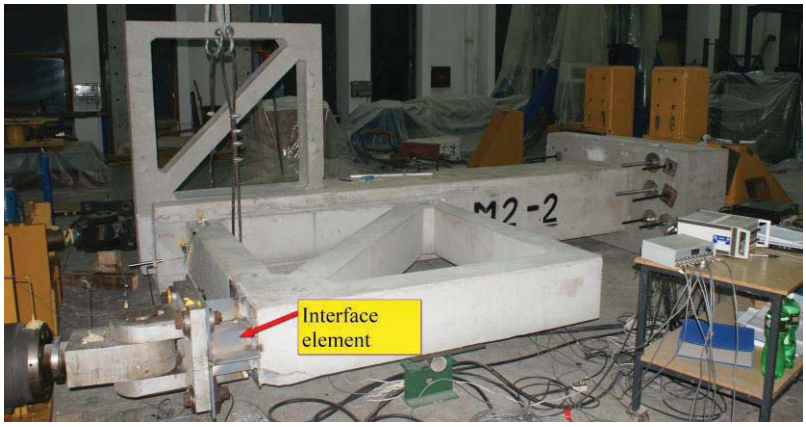

Figure 2 – View of the interface elements

3. TESTING PROCEDURE

The aim of this experimental testing is acquiring data for the capacity and deformability of the beam-to-column connection of a precast system composed of a column and a truss-beam. Two identical specimens are investigated within the experiment under increasing cyclic loading until failure of the elements.

The quasi-static testing is performed in the Dynamic Testing Laboratory of the Institute of Earthquake Engineering and Engineering Seismology in Skopje. For that purpose, specifically defined systems within the laboratory are engaged: multi component loading system for quasi-static testing, measurement and control system, data acquisition and data processing system.

3.1. INSTRUMENTATION SETUP

The instrumentation is composed of displacement transducers (LVDT) placed at pre-defined characteristic positions on the model, strain gauges (SG) that measure the strains in the reinforcement bars and a load cell which measures the applied force. Four sets of instruments are deployed on the investigated specimens depending on their placement and purpose.

Complete schematic of the instrumentation sets of the model is shown in Figure 3. Table 1 demonstrates the constituent instrumentation of each set.

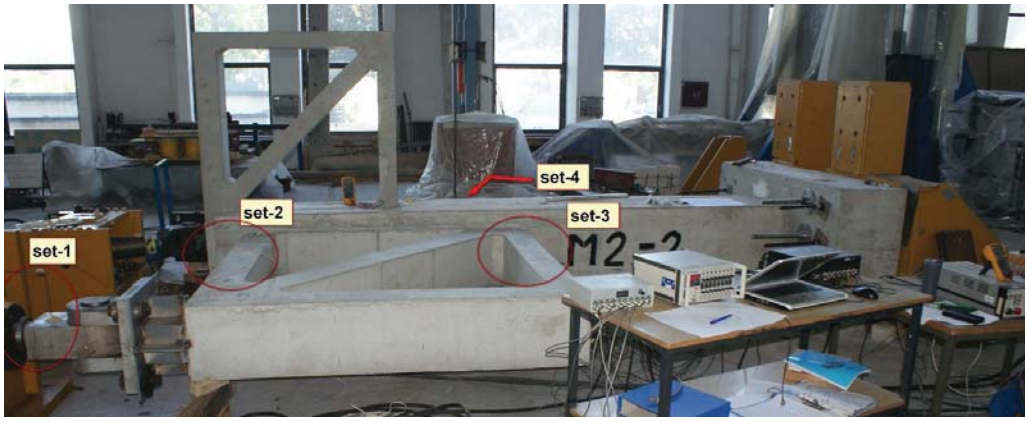

Figure 3 – Instrumentation setup by sets

Table 1 – List of instrumentation

Set	Instrument	Dimension	Unit
1	LC-1	force	kN
1	LVDT-1	displacement	mm
2	LVDT-2	displacement	mm
2	LVDT-4	displacement	mm
2	SG-1	strain	mm/mm
2	SG-2	strain	mm/mm
3	LVDT-3	displacement	mm
3	LVDT-5	displacement	mm
3	SG-3	strain	mm/mm
3	SG-4	strain	mm/mm
4	LVDT-6	displacement	mm
4	LVDT-7	displacement	mm
4	LVDT-8	displacement	mm

3.2. MODEL LOADING

The loading program of the testing procedure consists of a single test for obtaining the capacity of the beam-to-column connection by examination of the failure at the joint. The force

Fv is applied in cycles at the upper part of the truss (Fig. 4). It then produces moment of 1.9Fv in the connection joint and the specimen is subjected to collapse.

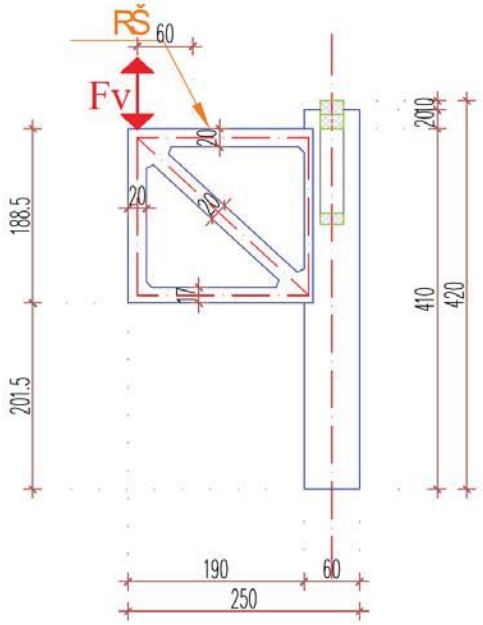

Figure 4 – Loading of the model

3.3. TEST RESULTS

The testing of the models is performed following a predefined load application program. A hydraulic actuator applies successive monotonic increase of the displacement amplitude at the end of the truss girder until the connection has reached nonlinearity. The force-displacement and moment-displacement graphs obtained from the varying displacement levels of the model are presented in Figure 5. It is observed that the yielding moment of the beam-to-column connection is evaluated at M=285kNm (Fig. 5a) and force applied is Fv=150kN (Fig. 5b).

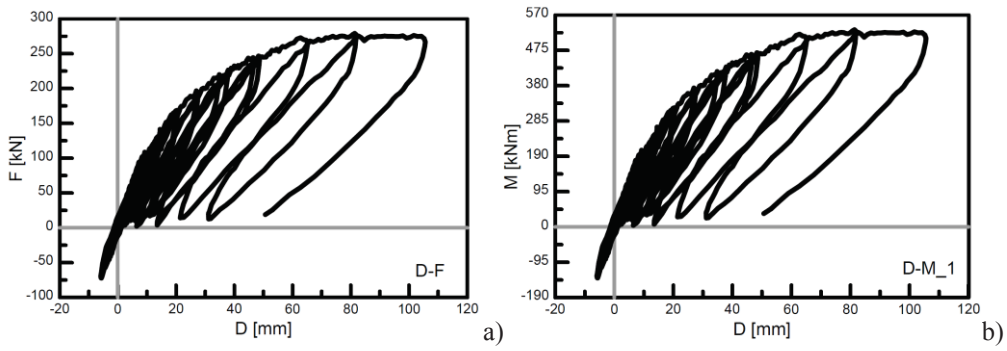

Figure 5 – a) Force-displacement b)Moment-displacement

Additionally, Figure 6 displays the time-history of the cyclic monotonic load, measured by the LC at the actuator.

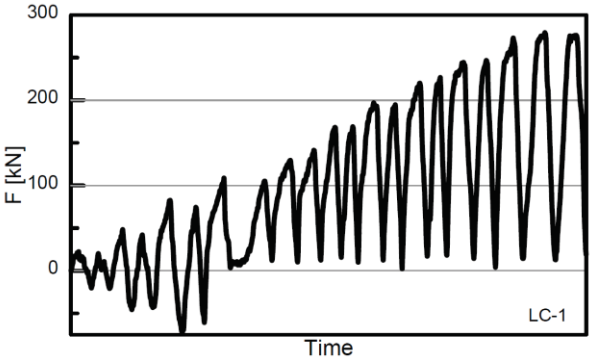

Figure 6 – Time-history of the applied cyclic load

Figure 7 exhibits the characteristic damage in the investigated model specimens after the completion of the experiment. The failure in the column that governs the failure mode of the structural system is firstly detected (Fig. 7a). Then, in Figure 7b, the connection investigated is displayed after the testing under M=540kNm (column failure point). From the observation, it is established that there are not any cracks visible and the connection is not damaged. That implies the compactness of the monolithic beam-to-column connection and its resistance to the applied loading.

a)

b)

Figure 7 – Damage observed at (a) column (b) connection.

4. REMARKS

This experimental study presents the procedure and results of a full-scale laboratory testing for capacity and deformability determination of characteristic connection joint. Specifically, testing of the realistic behaviour of a beam-to-column connection of a prefabricated reinforced concrete hall system has been performed. A connection that largely affects the behaviour of the structural system and governs the failure mode of the prefabricated structures during seismic events. The observed behaviour is summarized by the following remarks:

- Appearance of significant cracks in the column base is observed, under loading moment of 540kNm. Under the same moment value, damage in the beam-to-column connection is not detected.

- Hysteretic relationship for a critical cross-section of the column is presented in the form of force-displacement (Figure 5a) and moment-displacement graphs (Figure 5b).

- From the results obtained, it can be inferred that the failure firstly occurs in the column, denoting that monolithic connection between the column and the truss-beam is achieved.

- Due to the reaching of monolithic connection, there is no need for further structural interventions for improvement and strengthening of the joint.

5. CONCLUSIONS

The experimental results gained from the testing of the beam-to-column connection represent a useful database for the prefabricated concrete structures. Additionally, the testing results presented in this paper demonstrate the monolithic nature of the connection, its bearing capacity and deformability and its effect on the stability of the prefabricated reinforced concrete hall structures. The hysteretic diagrams obtained support the design procedure of the connection, providing beneficial data for the characteristic points of the structural response.

Benefitting the conclusions of this experimental study, further development in the analytical modelling and performance optimization of the beam-to-column connection can be achieved. The results obtained provide significant importance for analytical improvement of the constitutive and analytical models of the prefabricated structures.

REFERENCES

[1] Elliott K.S., Jolly C.: Multi-storey precast concrete framed structures, John Wiley & Sons, 2013.

[2] Alcocer S. M., Carranza R., Perez-Navarrete D., Martinez R.: Seismic tests of beam-to-column connections in a precast concrete frame, PCI journal, 47(3), 70-89, 2002.

[3] Belleri A., Brunesi E., Nascimbene R., Pagani M., Riva P.: Seismic performance of precast industrial facilities following major earthquakes in the Italian territory, Journal of Performance of Constructed Facilities, 29(5), 04014135, 2014.

[4] Magliulo G., Ercolino M., Petrone C., Coppola O., Manfredi G.: The Emilia earthquake: seismic performance of precast reinforced concrete buildings, Earthquake Spectra, 30(2), 891-912, 2014.

[5] Sezen H., Whittaker A. S.: Seismic performance of industrial facilities affected by the 1999 Turkey earthquake, Journal of Performance of Constructed Facilities, 20, 28-36, 2006.

[6] Blandon J. J., Rodriguez M. E.: Behavior of connections and floor diaphragms in seismic-resisting precast concrete buildings, PCI journal, 50(2), 56-75, 2005.

[7] Loo Y. C., Yao B. Z.: Static and repeated load tests on precast concrete beam-to-column connections, PCI journal, 40(2), 106-15, 1995.

ДГКС Друштво грађевинских конструктера Србије
ASES Association of Structural Engineers of Serbia
S-86
15. KONGRES
6-8. 9. 2018. Zlatibor

Ilda Kovačević[1], Sanin Džidić[2]

MOGUĆNOSTI PROIZVODNJE BETONA VISOKE ČVRSTOĆE U BOSNI I HERCEGOVINI

Rezime: U svijetu postoje brojne betonare i izvođači radova koji redovno proizvode, transportuju i ugrađuju beton visoke čvrstoće u prefabrikovane konstrukcije i konstrukcije koje se izvode na licu mjesta. Međutim, skoro da nema betonare u Bosni i Hercegovini koja ima iskustva sa proizvodnjom betona visoke čvrstoće. Ovo istraživanje se bavi betonskim mješavinama i mogućnostima proizvodnje betona visoke čvrstoće od raspoloživih domicilnih materijala u Bosni i Hercegovini. Eksperimentalno istraživanje potvrđuje da zaista postoje adekvatni uslovi i domicilni materijali od kojih je moguće proizvesti beton visoke čvrstoće i da postoje mogućnosti za proizvodnju ovog materijala u Bosni i Hercegovini.

Ključne riječi: *Beton visoke čvrstoće, Čvrstoća na pritisak, Mikrosilika, Superplastifikator*

POSSIBILITIES FOR PRODUCTION OF HIGH-STRENGTH CONCRETE (HSC) IN BOSNIA AND HERZEGOVINA

Summary: Worldwide, there are numerous concrete plants which routinely deal with production, transportation and casting of high–strength concrete in construction of both prefabricated and cast in situ structures. However, there is almost no concrete plant which produces high–strength concrete in Bosnia and Herzegovina. This research is about concrete mixtures and production of high–strength concrete with available domestic materials in Bosnia and Herzegovina. Experimental study conducted in this research resulted in confirmation that there are indeed adequate conditions and domestic constituents in Bosnia and Herzegovina able to produce high–strength concrete and there is a possibility for high–strength concrete production in Bosnia and Herzegovina.

Key words*: High-Strength Concrete, Compression Strength, Silica Fume, Superplasticizer*

[1] Ilda Kovačević, MA in Architecture, International BURCH University Sarajevo, Faculty of Engineering and Natural Sciencies, Department of Architecture, Sarajevo, Bosnia and Herzegovina, phone: +387-61-029-886, e–mail: ilda_kovacevic@hotmail.com
[2] Prof. dr. Sanin Džidić, Associate Professor, University of Bihać, Technical Faculty, Department of Civil Engineering and International BURCH University Sarajevo, Faculty of Engineering and Natural Sciencies, Department of Architecture, phone +387-61-905-480, e-mail: ninsa_d@hotmail.com

1. INTRODUCTION

High-strength concrete has been used as structural material for several decades in the world. Worldwide, there are numerous concrete plants which routinely deal with production, transportation and casting of high–strength concrete in construction of both prefabricated and cast in situ structures. However, there is almost no concrete plant which produces high–strength concrete in Bosnia and Herzegovina, and if examine experimental studies, there is also little or no tracks of concrete development in this direction. Thus, experimenting with high–strength concrete production in Bosnia and Herzegovina challenges capabilities and qualities of domestic materials.

This research is about concrete mixtures and production of high–strength concrete with available domestic materials in Bosnia and Herzegovina. This experimental study is shaped through the use of four different concrete mixtures; the first concrete mix was made as ordinary concrete consisting of aggregate, cement and water. The second one was basically the first mixture but with decreased W/C ratio and addition of superplasticizer. The last two mixtures were made with the addition of silica fume in 5 and 15 percent of total cementitious content in mixture, in order to increase the possibility of achieving higher compressive strengths comparable with common worldwide workable mixtures of silica fume high–strength concrete achieved by using superplasticiser. For each concrete mix, three concrete specimens were produced for further testing of hardened concrete.

2. CONSTITUENT MATERIALS

All materials used for the concrete mixtures examined in this research are domestic, and include aggregates from quarry "Džehveruša" near Cazin, cement of Heidelberg CEMENT Group in Kakanj, silica fume of BSI Metalleghe in Jajce, and water from water supply system and water source "Klokot" in Bihać. The only exception is superplasticizer which is a product of "SIKA Group", but also available on the market in Bosnia and Herzegovina.

Experimental study of this study focuses on compressive strength of hardened concrete, and all experimental phases are performed to meet EN 206 [26] and EN 12390 [22-25]. Since the goal is to produce high–strength concrete in Bosnia and Herzegovina out of domestic materials, this study aims to conclude whether this is possible or not with these specific materials. All experimental work is conducted in the laboratory of the Institute for Material Testing at the Faculty of Technical Studies, University of Bihać in Bosnia and Herzegovina

Cementitious material used for this study is Portland Cement CEM I 52. 5 N, produced in Cement Factory in Kakanj. Manufacturer, claims that Portland Cement (PC) CEM I 52. 5 N can be used as the cement for both plain concrete and reinforced concrete with high compressive strengths. This cement consists of 95–100% of Portland cement clinker, up to 5% of raw gypsum and minor additional substances. Presence of raw gypsum in PC CEM I 52.5 N, regulates setting time and accelerates it. CEM I 52.5 N enables greater compressive strengths at both early and later ages of concrete. Specific gravity of the CEM I 52.5 N is 3.18, and its grain size is approximately in rage from 5–30 μm. [29] Manufacturing process and product itself is

coordinated with the EN 197-1 [21] for cement, and is regularly inspected and approved by GIT Tuzla, Bosnia and Herzegovina and IGH Split, Croatia.

Aggregate used for this study is crushed dolomite from the quarry "Džehveruša" near Cazin, Bosnia and Herzegovina. High quality aggregate of "Džehveruša" is so far used for infrastructural projects (roadways, streets, curbs etc.) and as constituent material for structural concretes. Quarry "Džehveruša" can separate aggregate sizes up to the 31.5 mm, while sizes 0–4, 4–8, 8–16, 16–31.5, that remains at the last sieve are reselected and taken for secondary breaking and blasting.

Grading percentages in the quarry are as follows: size 0–4 takes 50 per cent of total aggregate capacity of "Džehveruša", size 4–8 takes 25 per cent, grain size of 8–16 takes 20 per cent, and finally grain size group 16–31.5 takes only 5 per cent of total aggregate capacity of the quarry "Džehveruša". Maximum aggregate size used for high–strength mixtures is 16 mm. Thus, this experimental study includes grain size groups 0–4, 4–8, 8–16 mm.

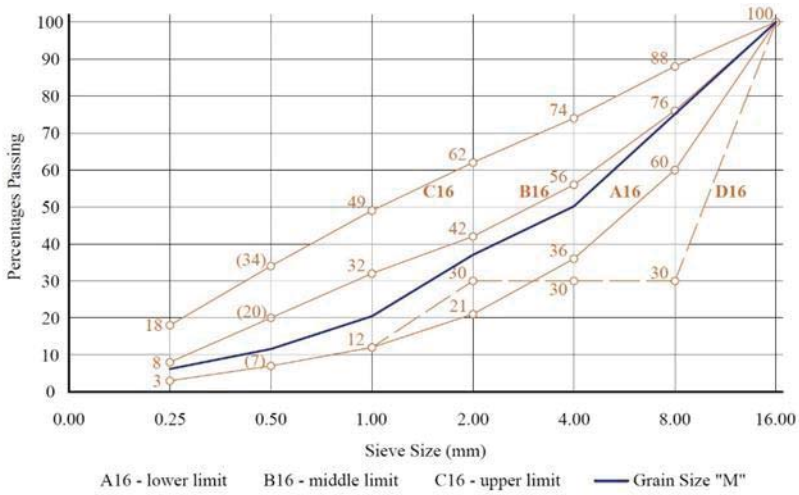

Figure 1 – Derived Grain Size Distribution Curve Fit into Area between the Limits Recommended by EN 206

Water used in this study is potable water from the Water Supply System in Bihać, from spring Klokot in Bihać. Its pH value is less than 7. This water is safe for human consumption, which means that it is clean and without any chemicals or other impurities that could bring undesired consequences for concrete mixtures, or develop harmful chemical reactions. Water is very important material in concrete mixtures, and it is a constituent which hydrate cement particles and creates binder paste. Water content in one cubic meter of concrete mixture may vary from 5 to 10 percent.

In high–strength concrete, water content is lower due to lower W/C ratios which are the practice in HSC proportioning. This study uses three different W/C ratios: first mixture uses 0.52, the following three use 0.35 and the last one uses 0.29. Lower W/C ratio means decreased water content in concrete mixtures, which leads to decreased workability of fresh concrete.

With ultra–low W/C ratio, it becomes impossible to lubricate all cement grains and fine particles of aggregate. To overcome the problem of low workability, common practice is the addition of superplasticizer in order to increase concrete workability and to lubricate all cement grains, fine aggregate particles and silica fume particles in the case of silica fume high–strength concrete.

Superplasticizer used in this study is SIKA product, "Plastocrete N". It is a brown liquid, chemical concrete admixture which is highly efficient plasticizer, lubricant and at the same time, a water–proofing agent. [30]

Advantage of "Plastocrete N" lies in improving concrete workability without increasing of the water presence in concrete mixture, what makes it excellent for concrete mixtures which require very low W/C ratio. Plastocrete's advantage is also its ability to reduce shrinkage and increase both durability and strength.

Silica fume (microsilica) used for this study is a by–product of silicon and ferrosilicon industries, manufactured by B.S.I. d.o.o., member of Metalleghe Group and European Silica Fume Committee, in Jajce, Bosnia and Herzegovina. Chemical analysis, shows that silica fume from Jajce, contains 96.2 per cent of SiO_2, and is fully amorphous material. Such properties satisfy general requirements proposed by Silica Fume Committee in order for silica fume to be suitable in high–strength concrete production.

For this study, mineral admixture silica fume is added to Concrete Mix 3 and Concrete Mix 4, in amount of 5 and 15 per cent of total mass of cementitious material used per m^3.

3. MIX DESIGNS

As earlier highlighted, four different concrete mix designs were prepared in this study. Mix design 1 is concrete mixture of cement, aggregate and water, with W/C ratio of 0.52 as used for ordinary concrete.

Table 1 - Mix Design 1 – Content of Constituents per m^3 and for Experimental Mixture

CONSTITUENTS	***per 1m^3***	***Trial mixture 3 cube specimens 15 cm x 15 cm x15 cm***
Cement	*450.00 kg*	*5.92 kg*
Water	*234.00 l*	*3.08 l*
W/C ratio	*0.52*	*0.52*
Aggregate 0 – 4 mm	*940.50 kg*	*12.78 kg*
Aggregate 4 – 8 mm	*395.00 kg*	*5.37 kg*
Aggregate 8 – 16 mm	*545.50 kg*	*7.41 kg*

Mix design 2 is a concrete mixture of cement, aggregate and water, with the use of superplasticizer "Plastocrete N". Superplasticizer is used in order to decrease water demand.

Table 2 - Mix Design 2 – Content of Constituents per m^3 and for Experimental Mixture

CONSTITUENTS	***per 1m^3***	***Trial mixture 3 cube specimens 15 cm x 15 cm x 15 cm***
Cement	*450.00 kg*	*5.92 kg*
Water	*157.50 l*	*2.07 l*
W/C ratio	*0.35*	*0.35*
Aggregate 0 – 4 mm	*940.50 kg*	*12.78 kg*
Aggregate 4 – 8 mm	*395.00 kg*	*5.37 kg*
Aggregate 8 – 16 mm	*545.50 kg*	*7.41 kg*
Superplasticiser – 0.5%	*22.5 kg*	*0.023 kg*

Mix design 3 is a concrete mixture of cement, aggregate, water and superplasticizer, with the addition of silica fume of 5 percent of total mass of cementitious material used per cubic metre. With concrete mixture containing silica fume, more adequate term is W/B (water/binder) ratio or W/C + SF (water/cement + silica fume) ratio rather than W/C (water/cement) ratio. In this specific case, W/C+SF is kept 0.35. Thus, water content increased when compared to previous mix designs due to addition of silica fume.

Table 3 - Mix Design 3 – Content of Constituents per m^3 and for Experimental Mixture

CONSTITUENTS	***per 1m^3***	***Trial mixture 3 cube specimens 15 cm x 15 cm x 15cm***
Cement	*450.00 kg*	*5.92 kg*
Water	*164.00 l*	*2.16 l*
W/C+SF ratio	*0.35*	*0.35*
Aggregate 0 – 4 mm	*940.50 kg*	*12.78 kg*
Aggregate 4 – 8 mm	*395.00 kg*	*5.37 kg*
Aggregate 8 – 16 mm	*545.50 kg*	*7.41 kg*
Superplasticizer – 0.5%	*2.25 kg*	*0.023 kg*
Silica Fume – 5%	*22.5 kg*	*0.290 kg*

Mix design 4 is a concrete mixture of cement, aggregate, water, superplasticizer with addition of silica fume of 15 percent of total mass of cementitious material used per cubic meter. This mixture is designed with the lowest W/C+SF ratio by decreasing water content and increasing percentage of silica fume. Thus, designed W / C+SF ratio is 0.29.

Table 4 - Mix Design 4 – Content of Constituents per m^3 and for Experimental Mixture

CONSTITUENTS	***per 1m^3***	***Trial mixtures 3 cube specimens 15 cm x 15 cm x 15cm***
Cement	*450.00 kg*	*5.92 kg*
Water	*150.10 l*	*1.98 l*
W/C+SF ratio	*0.29*	*0.29*
Aggregate 0 – 4 mm	*940.50 kg*	*12.78 kg*
Aggregate 4 – 8 mm	*395.00 kg*	*5.37 kg*
Aggregate 8 – 16 mm	*545.50 kg*	*7.41 kg*
Superplasticizer – 0.5%	*2.25 kg*	*0.023 kg*
Silica Fume – 15%	*67.5 kg*	*0.880 kg*

4. PRODUCTION AND CURING OF CONCRETE SPECIMENS

Production of concrete specimens for this study was done in accordance to the EN 12390-2 [23]. All selected materials, or constituents for these experimental concrete specimens are approved by European standards; if not approved by licence, their properties are in accordance with standard requirements for constituents.

Figure 2 - Specimens after the Compaction were Left for 24 Hours in Moulds

According to EN 12390-2, curing may take place fully under water or in chamber with ≥ 95 percent of humidity and constant temperature of 20 ˚C ± 2 ˚C, which proved to be very hard to achieve. For this experimental study, all specimens were marked and submerged into clean potable water and left curing for the next 28 days.

Figure 3 - Curing of Concrete Specimens Fully under the Water

5. COMPRESSIVE STRENGTH TESTING

Hardened concrete testing is standardized by EN 12390. EN 12390 – Testing hardened concrete – Part 3: Compressive strength of test specimens [31] states that specimens are loaded to failure in a compression testing machines conforming EN 12390 – 4 [25].

According to European standard for concrete specification, performance, production and conformity – EN 206: 2014, compressive strength should be expressed as $f_{c,cyl}$ for cylindrical specimen and $f_{c,cube}$ for cubical specimen. Annex B of EN 206 states identifying criteria for compressive strength at the table B.1. Unless it is specified, otherwise specimens are tested at 28 day of curing, according to the EN 206. However, it is possible to test specimens for compressive strength earlier or later than 28 days.

Table 5 - Identify Criteria for Compressive Strength [26]

Number n of test results for compressive strength from the defined volume of concrete	***CRITERION 1***	***CRITERION 2***
	Mean of n results (f_{cm}) N/mm^2	*Any individual test result (f_{ci}) N/mm^2*
1	*Not applicable*	$\geq f_{ck} - 4$
2 to 4	$\geq f_{ck} + 1$	$\geq f_{ck} - 4$
5 to 6	$\geq f_{ck} + 2$	$\geq f_{ck} - 4$

Concrete strength was identified by compression testing machine. After the specimens were taken out of the water, they were wiped in order to remove the surface water. Before placing

specimen at the compression machine, specifications including mass, dimension and geometry of each specimen were recorded and checked for any potential inaccuracies.

After they were checked, specimens were carefully positioned at the centre of the compression testing machine, in order to prevent possible unsatisfactory failures of cube specimens.

As previously mentioned, hardened concrete testing is standardized by EN 12390. EN 12390 – Testing hardened concrete – Part 3: Compressive strength of test specimens [24] states that specimens are loaded to failure in a compression testing machines conforming EN 12390 – 4 [25].

Figure 4 - Compression Testing Machine and Concrete Cube Specimen at the Moment of Failure

Figure 5, shows common shape of test cube specimen failure in testing of hardened concrete at the compression testing machine. Best way to explain cracking and failure of specimens at the peak of applied loading is to state that four exposed sides were cracking uniformly, while top and bottom sides remained with small or no cracking and damages.

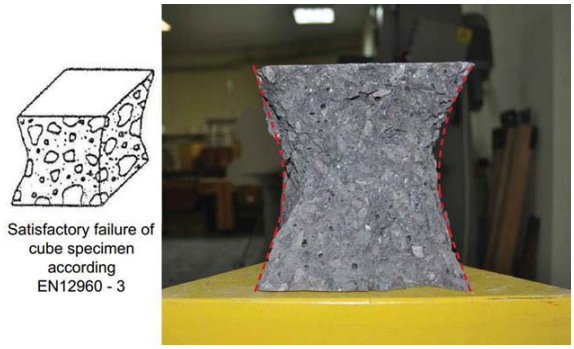

Figure 5 - Example of Satisfactory Failure of the Cube Specimen according to EN12960 – 3 (left) and the Actual Failure of One Cube Specimen from Study (right)

6. TEST RESULTS

During the testing, the following results on concrete compression strength were obtained:

Mix Design 1: cement, water, aggregate;

Date of casting: 8th August 2017 Date of testing: 5th September 2017

Table 6 - Results of Testing Hardened Concrete Specimens of Mix Design 1

MIX DESIGN 1	***Age of specimen***	***Mass of specimen***	***Area***	***Maximum force at the failure***	***Compressive strength***
	days	***kg***	***mm²***	***kN***	***MPa***
Specimen 1	*28*	*8.580*	*22500*	*1110*	*49.33*
Specimen 2	*28*	*8.520*	*22500*	*1020*	*45.33*
Specimen 3	*28*	*8.460*	*22500*	*1100*	*48.89*
Mean Value		*8.520*		*1076.67*	*47.85*

According to the criteria stated in BAS EN 206:2014, Annex B, Table B1, Mix Design 1 is classified as concrete class C 35/45. As concrete specimens are produced in cubic shape, for determination of concrete class characteristic compressive strength (f_{ck}) value is 45 MPa.

Mix Design 2: cement, water, aggregate, superplasticizer 0.5%;

Date of casting: 22nd August 2017 Date of testing: 19th September 2017

Table 7 - Results of Testing Hardened Concrete Specimens of Mix Design 2

MIX DESIGN 2	***Age of specimen***	***Mass of specimen***	***Area***	***Maximum force at the failure***	***Compressive strength***
	days	***kg***	***mm²***	***kN***	***MPa***
Specimen 1	*28*	*8.730*	*22500*	*1424*	*63,30*
Specimen 2	*28*	*8.730*	*22500*	*1370*	*60.89*
Specimen 3	*28*	*8.610*	*22500*	*1275*	*56.67*
Mean Value		*8.690*		*1356.33*	*60.30*

According to the criteria stated in BAS EN 206:2014, Annex B, Table B1, Mix Design 2 is classified as concrete class C 45/55. For determination of concrete class characteristic compressive strength (f_{ck}) value is 55 MPa.

Mix Design 3: cement, water, aggregate, superplasticizer 0.5% and SF 5%;

Date of casting: 22nd August 2017 Date of testing: 19th September 2017

Table 8 - Results of Testing Hardened Concrete Specimens of Mix Design 3

MIX DESIGN 3	***Age of specimen***	***Mass of specimen***	***Area***	***Maximum force at the failure***	***Compressive strength***
	days	***kg***	***mm²***	***kN***	***MPa***
Specimen 1	*28*	*8.675*	*22500*	*1540*	*68.44*
Specimen 2	*28*	*8.610*	*22500*	*1610*	*71.55*
Specimen 3	*28*	*8.730*	*22500*	*1588*	*70.58*
Mean Value		*8.672*		*1579.33*	*70.20*

According to the criteria stated in BAS EN 206:2014, Annex B, Table B1, Mix Design 3 is classified as concrete class C 55/67. As concrete specimens are produced in cubic shape, for determination of concrete class characteristic compressive strength (f_{ck}) value is 67 MPa.

Mix Design 4: cement, water, aggregate, superplasticizer 0.5% and SF 15%

Date of casting: 22nd August 2017 Date of testing: 19th September 2017

Table 9 - Results of Testing Hardened Concrete Specimens of Mix Design 5

MIX DESIGN 5	***Age of specimen***	***Mass of specimen***	***Area***	***Maximum force at the failure***	***Compressive strength***
	days	***kg***	***mm²***	***kN***	***MPa***
Specimen 1	*28*	*8.620*	*22500*	*1926*	*85.56*
Specimen 2	*28*	*8.610*	*22500*	*1450*	*64.40*
Specimen 3	*28*	*8.630*	*22500*	*1818*	*80.80*
Mean Value		*8.620*		*1731*	*76.92*

According to the criteria stated in BAS EN 206:2014, Annex B, Table B1, Mix Design 4 is classified as concrete class C 55/67. As concrete specimens are produced in cubic shape, for determination of concrete class characteristic compressive strength (f_{ck}) value is 67 MPa.

7. CONCLUSION

After experimental research conducted, the following conclusions can be expressed:

Concrete technology in Bosnia and Herzegovina is backwards when compared to the world's concrete technology. Routinely accomplished concrete structures in the rest of the world are still in laboratories or don't exist at all in Bosnia and Herzegovina;

Experimental study conducted in this research resulted in confirmation that there are indeed adequate conditions and domestic constituents in Bosnia and Herzegovina able to produce high–strength concrete and there is a possibility for high–strength concrete production in Bosnia and Herzegovina;

This study explored the influence of superplasticizer and silica fume on hardened concrete properties–referring to characteristic compressive strength. For experimental purposes of this study, four different concrete mixtures were designed and each was produced in three cube specimens, with dimensions of 15 x 15 x 15 cm. Aggregate composition and content of cement remained equal for every single mixture, while variations were delivered through addition of superplasticizer and different contents of silica fume, with a decrease of water content and with that, a decrease of W/C ratio. Process of production, curing, and testing was done in accordance to BAS EN 206: 2014 and BAS EN 12390 Parts 1, 2, 3 and 4 at the Institute for Material Testing at the Faculty of Technical Sciences, University of Bihać. Use of superplasticizer reduced the W/C ratio from 0.52 to 0.35 and showed noticeable rise in concrete compressive strength after 28 days. Use of superplasticizer and decreased W/C ratio remained for the next two mixtures; addition of silica fume in 5 percent of total cementitious content was added to increase compressive strength of concrete Mix Design 3. Thus, such mixture resulted with the first designated class of high–strength concrete according to BAS EN 206. Last concrete mixture in this study contained 15 percent of silica fume and showed the highest compressive strength when compared to the rest of the mixtures, as expected; criteria in BAS EN 206: 2014, Annex B, Table B1, classified this mix as, the first designated class of high–strength concrete C 55/67;

By implementing background theory from qualitative researches and standards into the experimental analyses, this study provided all arguments which could accelerate and increase development of concrete technology in Bosnia and Herzegovina, and at the same time enhance the high quality of domestic constituent materials necessary for concrete technology development;

Further research needs to be focused to mixing and proportioning of the various concrete mixtures, with more mix tests and continuing testing of properties through concrete specimens for high-strength concrete;

Through experimental analyses, this research study proved that there is an ability and opportunity for high–strength concrete production in Bosnia and Herzegovina. As long as concrete is described as the mixture of raw materials, and artificially produced new material, there are numerous "what ifs" to be consider and to questions of what would give the best possible results. Therefore, future work may refer to types and locality of raw material by

focusing on aggregate type, or its chemical, physical and mechanical properties. Cement, water, silica fume and superplasticizer are already those of the best quality in the area of Bosnia and Herzegovina. Thus, in the future work, aggregate types included in high–strength concrete mix designs may be chosen from other parts of Bosnia and Herzegovina;

Also, future work may rely on economic analyses by comparing the use of conventional normal strength concrete and high–strength concrete, amount of raw material used, mixed materials and costs through specific equal study cases, with the same architectural and structural designs, but with different structural materials.

REFERENCES

[1] Annadurai A, Ravichandran A, 2014, "Development of Mix Design for High Strength Concrete with Admixtures", IOSR Journal of Mechanical and Civil Engineering (IOSR-JMCE), e-ISSN: 2278-1684,p-ISSN: 2320-334X, Volume 10, Issue 5, pp 22 - 27;

[2] Bajramović E, Džidić S, 2017. "Accredited Laboratories in Process of Introducing Construction Products to EU Market", Book of Proceedings of the 3rd International Scientific and Professional Conference "SFERA 2017- Concrete Technologies", organized by SFERA doo Mostar, Faculty of Civil Engineering of the University "Džemal Bijedić" Mostar, Faculty of Civil Engineering of the University of Mostar, Faculty of Architecture and Civil Engineering of the University of Niš and Faculty or Technology of the University of Tuzla, March 23-24, 2017, Mostar, Bosnia and Herzegovina, pp 100 - 105;

[3] Caldarone M. A, 2009. "High-Strength Concrete - A Practical Guide", Taylor & Francis Group, London and New York, UK and USA, ISBN10: 0-415-40432 (hbk), ISBN 13: 978-0-415-40432-7 (hbk);

[4] Džidić S, 2015. "Otpornost betonskih konstrukcija na požar", International BURCH University Sarajevo, Bosnia and Herzegovina, ISBN 978-9958-834-47-9; COBISS.BH-ID 22444550;

[5] Džidić S, Kozlica S, Ćehić E, 2016. "Experiences in Testing of Compressive Strength of Concrete during Construction of Waste Water Collection and Treatment Plant in Bihać according to BAS EN 206:2014", Book of Proceedings of the 12th International Scientific and Professional Conference on Contemporary and Theory and Practice in Construction, University of Banja Luka Faculty of Architecture, Civil Engineering and Geodesy, December 7-8, 2016, Banja Luka, Bosnia and Herzegovina, ISBN 978-99976-663-3-8, UDK 69:71/72(082)(0.034.2) 624(082)(0.034.2), COBISS.RS-ID 6340024, pp 495 - 502;

[6] Džidić S, Okugić H, Bajramović E, 2017, "Studije o betonu 2016-2017; International BURCH University Sarajevo, Bosnia and Herzegovina, CIP 624.012.4, ISBN 978-9958-834-57-8, COBISS.BH-ID 24495622 ;

[7] Eilzer W, Stockmann R, Weigel F, 2003. "Planung und Ausführung der Muldebrücke Glauchau in Hochleistungsbeton B85", 13. Dresdner Brückenbausymposium. Dresden, Germany, pp 139 – 154;

[8] Felić A, Haračić E, 2015. “Studija ekonomske opravdanosti eksploatacije dolomita "Džehveruša" Cazin", EDA, Rad Putevi, Bihać, Bosna i Hercegovina;

[9] Kovačević I, Džidić S, 2018, “High-Rise Buildings–Structures and Materials”, International BURCH University Sarajevo, March 2018, Sarajevo, Bosnia and Herzegovina, ISBN I978-9958-834-58-5; COBISS.BH-ID COBISS.BH-ID 24904454;

[10] McCormac J. C, Brown R.H, 2014. “Design of Reinforced Concrete”, 9th Edition, ACI 318-11 Code Edition, John Wiley & Sons, Inc. USA, SBN: 978-1-118-12984-5, ISBN: 978-1-118-43081-1 (BRV);

[11] Portland Cement Association, 1994. “High-Strength Concrete”, Concrete Technology Today, Volume 15, Number 1, March 1994, 5420 Old Orchard Road, Skokie, Illinois 60077-1083, USA;

[12] Ramesh D, Murali S, Balaji S, Ganesan V. 2015. “Design of High-Strength Concrete Mix 60 and Investigation of its Strength”, International Journal of Innovative Research in Science, Engineering and Technology, Vol. 4, Issue 10, October 2015, ISSN (Online): 2319-8753, ISSN (Print): 2347-6710, pp 10157 -10161,

[13] Rashid M. A, Mansur, M. A, 2009. “Considerations in Producing High-Strength Concrete.” Journal of Civil Engineering (IEB), 37(1) (2009), pp 53 - 63;

[14] Rogić V, Šaravanja K, Dasović D, 1986. “Tehnologija dobivanja i istraživanja betona visokih marki sa amfornom mikrosilikom i superplastifikatorima - beton sa mikrosilicom (BSM).”, XIII Kongres Jugoslavenskog društva za visoke brane. Mostar, Univerzitet Džemal Bjedić u Mostaru, Zbornik radova Mostar, Jugoslavija, pp 43 – 65;

[15] Sivakumar N, Muthukumar S, Sivakumar V, Gowthaw D, Muthuraj V, 2014. “Experimental Studies on High-Strength Concrete by Using Recycled Coarse Aggregate”, International Journal of Engineering And Science Vol. 4, Issue 01 (January 2014), ISSN(e): 2278-4721, ISSN (p):2319-6483, pp 27 - 36;

[16] Skazlić M, Tomičić I, 2006. “Arimiranobetonski elementi od betona visokih čvrstoća naprezani savijanjem”, GRAĐEVINAR 58 (2006) 8, Journal of the Croatian Association of Civil Engineers, Zagreb, Croatia, ISSN 1333-9095, pp 631 - 640;

[17] Tuppinger H, Amlacher H, 2002. “Hochleistungsbeton im Brückenbau”, Montanuniversität Leoben, Lehrstuhl für Gesteinshüttenkunde, Lieserbrücke, 9851, Austria;

[18] Umar H. M, Naseer S, Sohail M. R, Hussain M, 2014, “Experimental Study on Strength of Concrete using Silica Fumes as Supplementary Cementitious Material“, First International Conference on Emerging Trends in Engineering, Management and Sciences, December 29-30, 2014 Peshawar, Pakistan;

[19] Wu D, Sofi M, Mendis P, 2010. “High-Strength Concrete for Sustainable Construction”, Proceedings of the International Conference on Sustainable Built Environment, (ICSBE-2010), University of Moratuwa, Society for the Promotion of Science, Kandy, Japan, pp 434 – 442.

STANDARDS

[20] BAS EN 12350-2:2010, Testing fresh concrete – Part 2: Slump – test, Institut za standardizaciju Bosne i Hercegovine, Istočno Sarajevo, Bosna i Hercegovina;

[21] BAS EN 197-1:2013, Cement - Part 1: Composition, specifications and conformity criteria for common cements, Institut za standardizaciju BiH, Istočno Sarajevo, Bosna i Hercegovina;

[22] BAS EN 12390-1:2013, Testing hardened concrete - Part 1: Shape, dimensions and other requirements for specimens and moulds, Institut za standardizaciju BiH, Istočno Sarajevo, Bosna i Hercegovina;

[23] BAS EN 12390-2:2010, Testing hardened concrete - Part 2: Making and curing specimens for strength tests, Institut za standardizaciju BiH, Istočno Sarajevo, Bosna i Hercegovina;

[24] BAS EN 12390-3:2010, Testing hardened concrete - Part 3: Compressive strength of test specimens, Institut za standardizaciju BiH, Istočno Sarajevo, Bosna i Hercegovina;

[25] BAS EN 12390-4:2003, Testing hardened concrete - Part 4: Compressive strength - Specification for testing machines, Institut za standardizaciju BiH, Istočno Sarajevo, Bosna i Hercegovina;

[26] BAS EN 206:2014 Concrete - Specification, performance, production and conformity, Institut za standardizaciju Bosne i Hercegovine, Istočno Sarajevo, Bosna i Hercegovina;

[27] BAS EN 933 Tests for geometrical properties of aggregates, Institut za standardizaciju Bosne i Hercegovine, Istočno Sarajevo, Bosna i Hercegovina;

[28] BAS EN 934-2+A1:2013 Admixtures for concrete, mortar and grout - Part 2: Concrete admixtures - Definitions, requirements, conformity, marking and labelling, Institut za standardizaciju Bosne i Hercegovine, Istočno Sarajevo, Bosna i Hercegovina.

INTERNET RESOURCES

[29] http://www.kakanjcement.ba/

[30] https://egy.sika.com/dms/getdocument.get/b4245150-*e1f5.../Plastocrete®%20-N.pdf*

ДГКС Друштво грађевинских конструктера Србије
ASES Association of Structural Engineers of Serbia
S-87
15. KONGRES
6-8. 9. 2018. Zlatibor

Marija Todorović[1], Boško Stevanović[2], Ivan Glišović[3], Tijana Stevanović[4]

OJAČANJE ZAVRTNJIMA LEPLJENIH LAMELIRANIH DRVENIH NOSAČA SA REDUKOVANOM VISINOM PRESEKA

Rezime:

Redukcija visine drvenih nosača kod oslonaca znatno umanjuje nosivost grede. U ovom radu je predstavljeno eksperimentalno ispitivanje lepljenih lameliranih nosača sa redukovanom visinom kod oslonaca opterećenih na savijanje, sa i bez ojačanja. Kao ojačanje upotrebljeni su zavrtnji za drvo, postavljeni pod uglovima od 90° i 45° u odnosu na podužnu osu nosača. Neojačni nosači su doživeli lom usled otvaranja pukotine i njene propagacije. Ove pukotine su rezultat prekoračenja napona zatezanja upravno na vlkana drveta i smičućeg napona. Ispitivanje je pokazalo da se upotrebom zavrtanja može povećati kapacitet nosivosti i deformabilnosti posmatranih nosača.

Ključne reči: zasek, lepljeno lamelirano drvo, zavrtnji, ojačanje, eksperimentalno ispitivanje

END-NOTCHED GLULAM BEAMS REINFORCED WITH SCREWS

Summary:

Notches made at the ends of timber beams significantly decrease load carrying capacity of a structural member. This paper presents an experimental research on bending behaviour of end-notched glulam beams, with and without reinforcement. Screws for timber were used as reinforcement, positioned at angles of 90° and 45° to the longitudinal beam axis. The unreinforced beams failed due to crack opening and its propagation. Cracks that appeared in the notch details resulted from excessive tensile stresses perpendicular to grain and shear stresses. This study shows that reinforcing the beams at the notched ends can improve their load carrying capacity and deformability.

Key words: notch, glulam, screws, reinforcement, experimental investigation

[1] *Assistant, MSc, Faculty of Civil Engineering, University of Belgrade, todorovicm@grf.bg.ac.rs*
[2] *Full professor, PhD, Faculty of Civil Engineering, University of Belgrade, bole@imk.grf.bg.ac.rs*
[3] *Assistant professor, PhD, Faculty of Civil Engineering, University of Belgrade, ivang@imk.grf.bg.ac.rs*
[4] *Assistant, MSc, Faculty of Civil Engineering, University of Belgrade, tstevanovic@grf.bg.ac.rs*

1. INTRODUCTION

Notched solid timber and glued laminated timber (glulam) beams are very common in structural engineering practice. Notches represent a weak spot in a structure, and it is advisable to avoid them. However, there are various reasons for beam notching, the most common one being limitation in construction height at the supports, and others such as: stabilization of structural elements against lateral buckling, intersection of members and joint details [1]. Adequate design of notched beams is necessary in these cases.

The load carrying capacity of timber beams is considerably reduced as a result of stress concentration around the notch. Notches made on the tension side induce tensile stresses perpendicular to grain which, accompanied by shear stresses, can cause longitudinal splitting typically starting at the notch corner (Figure 1). Cracks are unattractive appearance from aesthetic point of view, but are also very dangerous from structural perspective because crack propagation as the load level increases can lead to a failure of a beam. Reinforcement of such members is a cost-effective alternative for enhancing the load carrying capacity of structures in service.

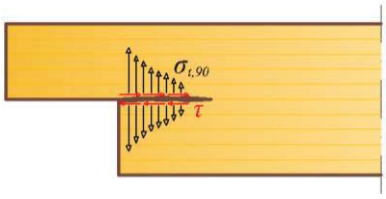

Figure 1: Stress concentration at the notched end of a beam

The stress state at a crack can be described by different fracture modes. Mode 1 is a tensile opening mode characterized by separating of crack surfaces in the direction that is perpendicular to them - Figure 2(a). Mode 2 represents in plane shear mode where crack surfaces slide one over the other - Figure 2(b). The combination of the previous two modes is a mixed mode fracture, as shown in Figure 2(c). Although both stresses (shear and tension perpendicular to grain) appear, crack opening is an apparent failure mechanism of a notch and it is caused by tension perpendicular to grain. Therefore, Mode I fracture is the most common failure mode of end-notched timber beams [2]. However, shear component usually exists and it should be also taken into consideration.

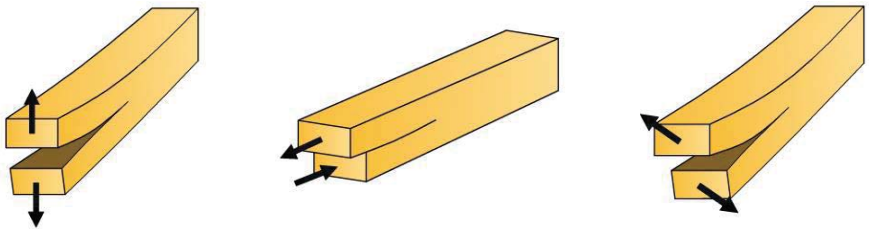

a) Mode 1 fracture *b) Mode 2 fracture* *c) Mixed mode fracture*

Figure 2: Fracture modes [1]

Notched ends of beams should be reinforced so as to avoid brittle failure and increase load carrying capacity of the beams. There are various types of strengthening techniques which are mainly based on preventing the expected cracks. Parameters such as ease of installation, invisibility of reinforcement, simplicity of design approach and cost are all important for determining the strengthening method. Different types of elements (rods [3], screws [4,5], plates and sheets [6]) and materials (wood-based materials, steel, advanced composite materials like carbon or glass fibre based polymers [7]) have been successfully used as reinforcement of notched timber beams.

In the past decades, many researchers have dealt with notched timber beams and it is obvious that notched beam strengthening and repair represents a very important topic in the field of timber structural design. In the PhD thesis Jockwer [1] gave a thorough analysis of different design approaches of both unreinforced and reinforced notched beams. Franke, Franke and Harte [8] dealt with methods for repair of structural performance of timber beams, including the ones with notches. In paper Oudjene et al. [9] presented a numerical approach for modelling both unreinforced and reinforced notched beams. Dietsch [10] talked about the necessity of new design approaches of strengthened timber beams, including strengthening of notches, and implementation of these in a new section of Eurocode 5 [11], emphasizing the importance of adequate analytical design.

This paper presents experimental results of end-notched glulam beams that were reinforced with screws. Screws are economic and time-efficient solution for reinforcement and they can be easily applied [12], which is the reason why they were chosen in this study. Five unreinforced and ten reinforced end-notched glulam beams were tested in bending to the point of failure, with two different reinforcement schemes considered. The results in terms of load-deformation relationship, failure mode, ultimate load carrying capacity and stiffness were compared between tested beam series. The conclusions on effectiveness of screws as a reinforcement method were made.

2. EXPERIMENTAL TESTING

The experimental research was conducted at the Laboratory of Structures, Faculty of Civil Engineering, University of Belgrade. Five unreinforced (Series U) and ten reinforced (Series R) notched glulam beams were tested in bending to the point of failure. Unreinforced beams were used as a control series. Reinforcing was performed with screws. Five reinforced beams had screws installed perpendicular to beam axis (Series R-s90) and five had screws positioned at an angle of 45° to beam axis (Series R-s45).

The glulam beams were made from spruce timber classified in the strength class C22 according to EN 338 [13]. Before the tests were performed, the beams were conditioned at a temperature of T = 20±2º C and a relative humidity of RH = 65±5 %. After testing, moisture content was measured in each beam using a digital hygrometer at different locations. The moisture content in tested beams varied between 11.0 % and 11.9 %.

The overall length of the beams was 4000 mm and the cross section was 100 x 220 mm. Each beam was composed of seven 32 mm thick laminations. At the notched ends, the height of the beams was reduced to 110 mm (by half) and the length of notches was 250 mm. The reinforcement selected in this study was traditional wood screws (Figure 3) with a diameter 10 mm and length of 200 mm for Series R-s90 and 250 mm for Series R-s45. Threaded part of screws was 125 mm and 160 mm, respectively. According to the manufacturer the steel grade

of screws was 5.6. Two screws in one row were positioned near the both notched ends of the beams. The requirements for minimal screw edge distances and spacing were satisfied while keeping the reinforcement as close as possible to the notch corners.

Figure 3: Screws used as reinforcement

All beams were subjected to bending test in accordance with EN 408 [14]. The beams were tested to failure under monotonic load in four-point bending configuration over a simply supported span of 3750 mm. The distance between two loading points was 1350 mm, while the distance from the loading points to the supports was 1200 mm. The specimens were supported on roller bearings at the ends. Roller bearings were also used at the load application points. The effects of local indentation at both the load application and support positions were minimized by placing steel plates.

A schematic illustration of the bending test configuration for Series U, Series R-s90 and Series R-s45 is shown in Figure 4, while Figure 5 shows experimental test set-up.

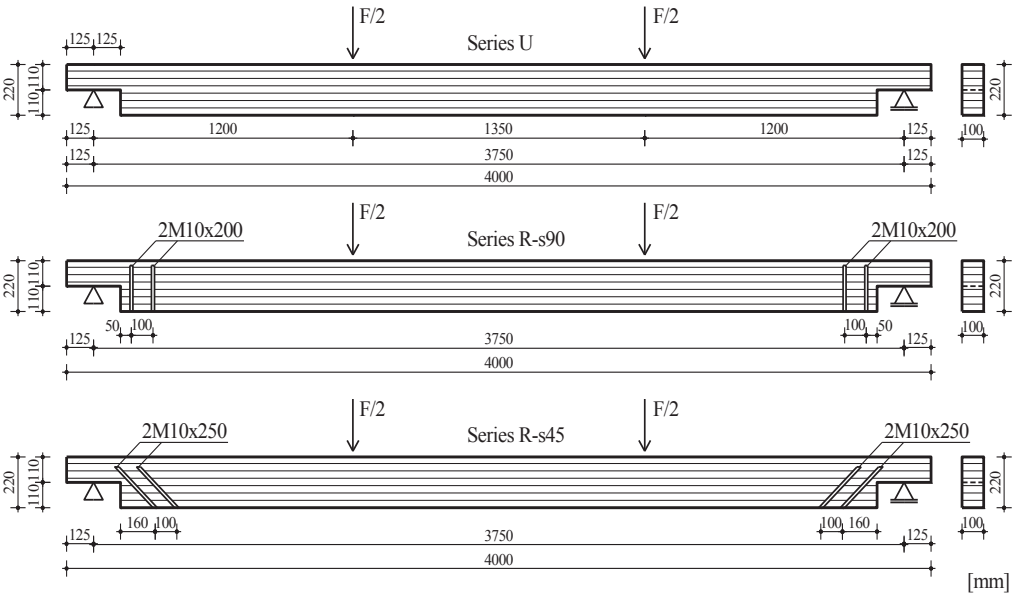

Figure 4: Geometry and loading of the beams

When considering the specimens that were going to be reinforced special attention was put into inserting the screws. The preparation of Series R specimens is shown in Figure 6. The holes for screws were pre-drilled very carefully to a diameter of 8 mm, with approximately drilling length of 200 mm and 250 mm. The screws were inserted using a moment wrench.

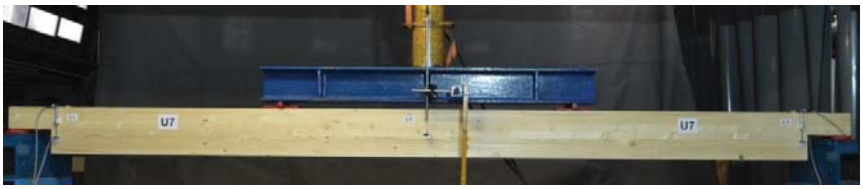

Figure 5: Experimental test set-up

Figure 6: Preparation of reinforced specimens

The load was applied monotonically until failure using a hydraulic jack and recorded with a compression load cell. The load was transformed from one point to two points with a steel beam. Monotonic static load was applied at a stroke-controlled rate of 4 kN per minute so as to cause the failure of the unreinforced beams in approximately 5 minutes. The reinforced beams were tested with the same load rate in order to ensure a fair comparison of test results. The failure of the reinforced beams was achieved in about 10 minutes.

Linear variable differential transducers (LVDTs) were used for the measurement of mid-span deflection of the beams as well as the measurement of crack opening in notch details. The deformation data from LVDTs and corresponding load data from a loading cell were recorded by a computerized data acquisition system. Self-weight of hydraulic jack and steel beam were added to the recorded load. This additional load was 1.3 kN.

3. RESULTS AND DISCUSSION

3.1. LOAD-DEFLECTION BEHAVIOUR AND FAILURE MODES

The load-deflection behaviour to failure of tested beams is shown in Figures 7 and 8.

The effects of the notches on the mechanical properties of glulam beams are significant. All tested beams with unreinforced notches (Series U) exhibited linear load-deflection behaviour until the point of failure. Beams failed at the notch details due to excessive tensile stress perpendicular to grain, as it is shown in Figure 9. Crack opening (Mode 1 fracture) at the notch corner was the obvious failure mechanism of unreinforced notched beams. However, crack shearing (Mode 2 fracture) also had a considerable influence. Due to brittle nature of wood behaviour in tension and in shear, failure of Series U beams was sudden without warning signs. Prior to ultimate load, only very little crack opening was observed. After the development of initial crack at the notch corner, uncontrollable crack growth occurred. This led to a separation of the cross-section in two parts (upper and lower). The crack path was generally clear and straight.

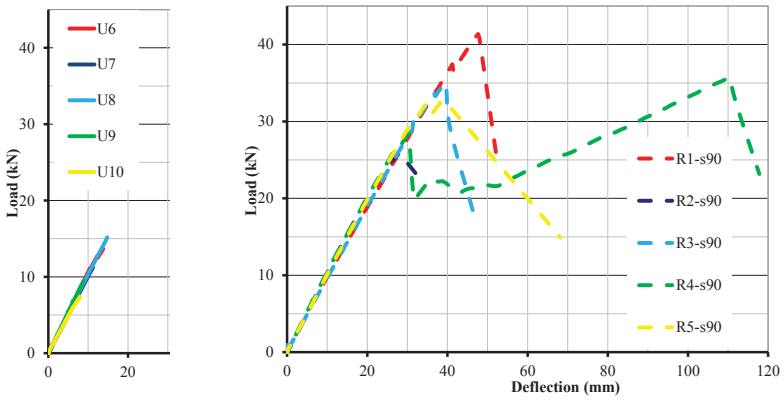

Figure 7: Load-deflection curves for Series U and Series R-s90 beams

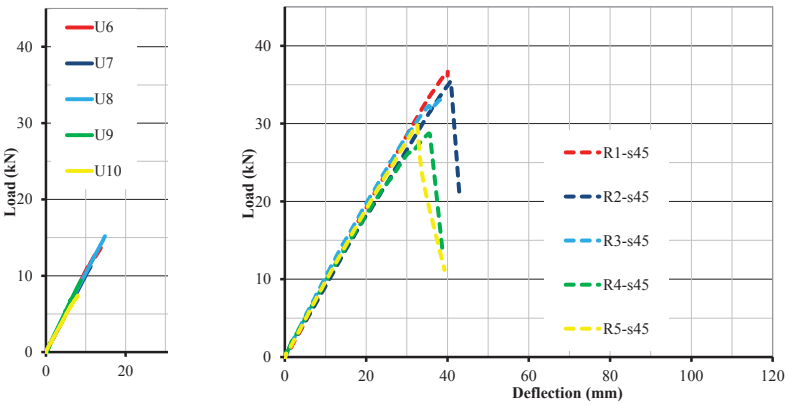

Figure 8: Load-deflection curves for Series U and Series R-s45 beams

Figure 9: Typical failure mechanism of Series U beams

Reinforced notched beams (Series R) essentially experienced linear behaviour up to the point of failure. Nine out of ten beams failed in a brittle way. One of the beams had a drop in the load carrying capacity, but continued to carry the load until failure was reached. Although ultimate load was improved, the reinforcement wasn't enough to change the failure mode from combined tensile perpendicular to grain and shear to bending failure. Figure 10 shows typical failure of reinforced beams.

Figure 10: Typical failure mechanism of reinforced beams – Series R

Despite the reinforcement intervention, initial cracking of the notch corner cannot be prevented. It can be seen that crack initiation started at relatively low loads. This can be explained by the very small deformation capacity of wood before the tensile strength perpendicular to grain is exceeded. Excessive crack opening was limited by the reinforcement. With further loading the stable crack growth was accompanied by sharing of the crack. At failure, unstable crack growth occurred and crack shearing increased considerably. It can be assumed that the shear failure was dominant failure mechanism. In most cases, failure was accompanied by withdrawal of the screws.

At the notch corner vertical reinforcement screws were subjected to combined loading parallel and perpendicular to the shear plane. There were clear plastic deformations in the reinforcement indicating that plastic hinge was formed in the fracture region in the case of these beams. The idea of inclined screws was to load the reinforcement axially (in tension), the direction in which they demonstrate the highest stiffness. Therefore, Series R-s45 beams were expected to have much higher load carrying capacity, but due to insufficient anchorage length of the screws, they failed even earlier than the beams from Series R-s90. Since conventional screws require pre-drilled holes for installation, better results could be achieved with self-tapping screws for reinforcing and strengthening procedures of timber structures.

3.2. LOAD CARRYING CAPACITY, DEFORMABILITY AND STIFFNESS

The results of experimental tests in terms of load carrying capacity, deformability and stiffness for the three series of beams are given in Table 1. The ultimate load was taken as a maximum force, which caused the failure of the beams. The mid-span deflection was taken as the value that corresponded to the ultimate load. The bending stiffness was calculated from liner part of the load-deflection curve of each beam, using the mid-span deflection equation for four-point bending:

$$EI = \frac{1}{48}\frac{3F(3l^2 - 4c^2)c}{2\Delta w} \tag{1}$$

where E = modulus of elasticity, I = moment of inertia, $\Delta F/\Delta w$ = slope of load-deflection curve between 10 % and 40 % of ultimate load, l = beam span, c = distance between support and load application point.

Comparisons in relation to ultimate load, mid-span deflection and bending stiffness for the reinforced beams (Series R-s90 and Series R-s45) and unreinforced beams (Series U) are also reported in Table 1.

Table 1 – Experimental results

Beam	**Ultimate load F (kN)**	**Mid-span deflection for ultimate load w (mm)**	**Bending stiffness EI (kNmm^2 x 10^8)**
Series U			
U6	15.0	13.8	9.03
U7	12.7	12.1	8.85
U8	16.7	15.1	9.55
U9	10.7	8.8	9.91
U10	8.7	8.0	8.60
Average	12.8	11.5	9.19
SD	3.2	3.1	0.53
CV	25.2	26.6	5.8
Series R-s90			
R1-s90	42.7	47.7	8.46
R2-s90	29.8	27.8	10.46
R3-s90	36.3	39.7	8.63
R4-s90	37.0	110.4	9.32
R5-s90	34.0	39.2	9.14
Average	35.9	52.9	9.20
SD	4.7	32.9	0.79
CV	13.0	62.1	8.5
Comparison to Series U (%)	180.5	360	-
Series R-s45			
R1-s45	38.0	40.1	9.01
R2-s45	36.7	40.8	8.29
R3-s45	34.6	38.9	9.19
R4-s45	30.0	59.1	8.54
R5-s45	31.1	32.6	8.83
Average	34.1	42.3	8.77
SD	3.5	9.9	0.36
CV	10.1	23.5	4.1
Comparison to Series U (%)	166.4	267.8	-

The unreinforced notched beams (Series U) had an average ultimate load of 12.8 kN. The load carrying capacity of the beams was considerably reduced due to presence of notches. Introduction of reinforcement at the notched ends of the beams resulted in improvement in load carrying capacity. The reinforced beams obtained an average ultimate load of 35.9 kN and

34.1 kN, for screws positioned at the angles of 90° and 45°, respectively. All reinforced beams showed an increase in ultimate load when compared to the loads recorded for the beams without reinforcement. This increase was 180.5 % and 166.4 %. Unreinforced notched beams completely lost their load carrying capacities after the first crack developed. On the other hand, reinforced beams continued to carry the load after initial cracking. However, insufficient anchorage length didn't allow for the reinforced beams to fail in bending, since the withdrawal of the screws occurred before the beams reached the load carrying capacity of beams without notches.

The reinforced beams underwent large deformations before the failure when compared to the unreinforced ones. Average measured mid-span deflection at ultimate load was 52.9 mm, 42, 3 mm and 11.5 mm for beams of Series R-s90, Series R-s45 and Series U, respectively. At failure, the reinforced beams exhibited in average 3.6 – 4.6 times larger mid-span deflections. Hence, screws helped improve the ductility of the beams.

All the beams had similar bending stiffness values. This was expected since the applied reinforcement wasn't meant to improve the bending stiffness. Series R-s45 had a bit lower value which can be explained by the variability in timber properties that generally exists when this material is in question.

4. CONCLUSIONS

The experimental procedure performed in this research included bending tests of 15 notched glulam beams to the point of failure (five unreinforced beams and ten reinforced ones). The screws were selected as reinforcement. The effects of reinforcing were evaluated in terms of load-deflection behaviour, failure mode, ultimate load carrying capacity and stiffness of reinforced beams, which were compared to the unreinforced notched beams. Following conclusions were drawn:

- Notched glulam beams when subjected to bending failed due to stress concentration at the notch corner. The load carrying capacity of these beams is defined by excessive crack opening. Brittle failure mechanism is typical for unreinforced notched beams.
- Initial cracking of the notch corner cannot be prevented by the reinforcement. However, by using reinforcement at the notches failure is delayed significantly.
- The reinforcement prevents excessive crack opening at the notch corner. Nevertheless, final failure of the reinforced notches due to excessive crack growth is caused by crack shearing.
- Reinforcing intervention of notched glulam beams with screws increases the load carrying capacity and deformability.
- At the notch corner, reinforcement screws perpendicular to beam axis are subjected to combined parallel and perpendicular to the crack loading. Hence, reinforcement with high strength and stiffness in both directions is required to achieve the best reinforcing effect.
- Reinforcement screws inclined at an angle of 45° to beam axis are dominantly loaded in the axial direction. Special attention should be paid to the anchorage length of these screws.
- Generally, self-tapping screws are recommended to be used instead of the pre-drilled screws.

This research gives an insight in reinforcing possibilities of notched timber members. It can be a good basis for further investigation of the effectiveness of other types of reinforcement like carbon or glass fibre based polymer bars. Also, results obtained from tests can be useful in developing appropriate analytical design models for notched timber beams.

REFERENCES

[1] Jockwer R.: Structural Behaviour of Glued Laminated Timber Beams with Unreinforced and Reinforced Notches, PhD Thesis, ETH, Zurich, Switzerland, 178, 2014.

[2] Smith I., Landis E, Gong M.: Fracture and Fatigue in Wood. John Wiley & Sons, Ltd., 2003.

[3] Steiger R., Serrano E., Stepinac M., Rajčić V., O'Neill C., McPolin D., et al.: Strengthening of timber structures with glued-in rods. Construction and Building Materials, 97, 2015, 90–105.

[4] Bejtka I., Blass H. J.: Self-tapping screws as reinforcements in beam supports. International Council for Research and Innovation in Building and Construction, CIB-W18/39:1–13, 2006.

[5] Dietsch P., Brandner R.: Self-tapping screws and threaded rods as reinforcement for structural timber elements - A state-of-the-art report. Construction and Building Materials, 97, 2015, 78–89.

[6] André A.: Benefits of strengthening timber with fibre-reinforced polymers. PhD Thesis, Chalmers University of Technology, Gothenburg, Sweden, 54, 2011.

[7] Schober K. U., Harte A. M., Kliger R., Jockwer R., Xu Q., Chen J. F.: FRP reinforcement of timber structures. Construction and Building Materials, 97, 2015, 106–18.

[8] Franke S., Franke B., Harte A. M.: Failure modes and reinforcement techniques for timber beams – State of the art. Construction and Building Materials, 97, 2015, 2–13.

[9] Oudjene M., Tran V., Meghlat E., Ait-Aider H.: Numerical Models for Self-Tapping Screws as Reinforcement of Timber Structures and Joints. In: Proceedings of World Conference on Timber Engineering - WCTE 2016, Austria, 2016.

[10] Dietsch P.: Reinforcement of Timber Structures – a New Section for Eurocode 5. In: Proceedings of World Conference on Timber Engineering - WCTE 2016, Austria, 2016.

[11] European Committee for Standardization: Eurocode 5: design of timber structure. Brussels, 2004.

[12] Blass H., Bejtka I.: Reinforcements perpendicular to the grain using self-tapping screws. In: Proceedings of 8th World Conference on Timber Engineering, 2004, 1001-1006.

[13] European Committee for Standardization: EN 338: Structural timber - Strength classes. Brussels, 2009.

[14] European Committee for Standardization: EN 408: Timber structures - Structural timber and glued laminated timber - Determination of some physical and mechanical properties, Brussels, 2010.

ДГКС Друштво грађевинских конструктера Србије
ASES Association of Structural Engineers of Serbia
S-88
15. KONGRES
6-8. 9. 2018. Zlatibor

Dragan Manojlović[1], Tatjana Kočetov Mišulić[2], Aleksandra Radujković[3]

METODA TEŽINSKIH OSTATAKA U ANALIZI SPREGNUTOG SISTEMA DRVO-BETON

Rezime:

Za analizu kompozitnih sistema drvo-beton spregnutih mehaničkim spojnim sredstvima mogu se primeniti pojednostavljen "γ" postupak dat u EN 1995 ili numeričke metode zasnovane na varijacionoj ili diferencijalnoj formulaciji. U ovom radu je predstavljena primena Galerkinove metode u analizi spregnutog sistema drvo-beton. Izbor probnih funkcija koje opisuju problem elastičnog sprezanja kao i njihov uticaj na konačne rezultate je analiziran u radu. U cilju upoređenja dobijenih rezultata sprovedena je analiza prema analitičkom rešenju i pojednostavljenom "γ" postupku. Na osnovu predloženih numeričkih modela, za uporednu analizu sa eksperimentalnim podacima, izabran je model koji najbolje opisuje problem elastičnog sprezanja.

Ključne reči: Galerkinova metoda, spregnuti sistem drvo-beton, numerička analiza

WEIGHTED RESIDUAL METHOD IN ANALYSIS OF TIMBER CONCRETE COMPOSITE SYSTEM

Summary:

For design of mechanically coupled composite timber-concrete systems the simplified "γ-procedure" adopted in EN 1995 or numerical methods based on variation or differential formulation could be applied. This paper presents the Galerkin's method in the analysis of the TCC system. The selection of trial functions that describe the problem of elastic composite action as well as their influence on the final results was analyzed. For comparison of the obtained results, analyzes were performed according to analytical solution and the "γ" method. On the basis of the proposed numerical models, a model that best fits the problem of elastic coupling was chosen for further comparative analysis with the experimental data.

Key words: Galerkin's method, timber-concrete composite system, numerical analysis

[1]*Ass., BSc, MSc, PhD student, Faculty of Technical Sciences, University of Novi Sad, manojlovic.dragan@uns.ac.rs*
[2]*Ass. Prof., PhD, Faculty of Technical Sciences, University of Novi Sad, tanya@uns.ac.rs*
[3]*Ass. Prof., PhD, Faculty of Technical Sciences, University of Novi Sad, leksa@uns.ac.rs*

1. INTRODUCTION

Since the composite structures made by different materials and methods of joining have reached very high level of application in the construction industry in last several decades, there is a demand for their more precise analysis and design. It is known that the type of used fasteners influence the most the overall behaviour of the coupled structures. Because of that, it is of crucial importance how to introduce the problem of the connection behaviour between coupled materials into the analysis and design.

Composite timber-concrete systems (TCC), where mechanical fasteners are usually used as coupling means, generally have certain slip in coupling zone due to the external load. The level of joint stiffness depend on type of used fasteners, their distances, way of shaping, installation etc. However, when mechanical couplings are used, the partial (elastic) composite action occurs, so the interlayer slip in the connection between timber and concrete members must be considered for the calculation of TCC cross-sections using the partial coupling theory.

The theory of partial (elastic) composite action is based on the corresponding assumptions of the theory of elasticity and takes into account the interlayer slip in the connection at their calculation. The differential formulation of the problem is a complex method of calculation for engineering practice, so due to necessary simplification, several approximate methods have been developed.

The widely spread "gamma" method, adopted in EN 1995-1 [1], is based on the effective stiffness of the composite system and on the theory of elastic coupling, taking into account the conservative effect of the distribution of forces within the girders, and so far most fully covers all the parameters that affect the behaviour of TCC. Also, for the calculation of composite systems, it is possible to apply various approximate methods based on the variation [3] or the differential formulation. To define them, it is necessary to know the differential formulation of the problem in order that methods could be applied. Depending on the problem formulation, the most commonly used are the methods of the residuum or the variation method [4].

Of particular importance are those methods in which the assumption of a solution in the form of approximate or trial functions is used as the starting point. One of those methods, which is used as the baseline for the formulation of the finite element method (FEM), is the residual method. There are various variants of the residual methods, that differ one from the other in the choice of weight functions. The Galerkin's method of weighted residuals, as the basis of FEM, is more general than Ritz method in the same way as the principle of virtual work is more general than the principle of minimum potential energy. The method is specific in choice of weight functions as trial ones, that have to be selected as approximation of required solution.

This paper presents the Galerkin method in the analysis of the TCC system. The selection of trial functions that describe the problem of elastic composite action as well as their influence on the final results was analyzed. For comparison of the obtained results, analyzes were performed according to analytical solution [5] and the "gamma" method [1]. All analyzes were performed using MATLAB software [2]. On the basis of the proposed numerical models, a model that best describes the problem of elastic coupling was chosen for further comparative analysis with the experimental data [6].

2. GOVERNING EQUATION OF TCC SYSTEM

If the composite timber-concrete simply supported beam system with uniformly distributed load *q(x)* without an external axial force is observed, the problem of partial composite action could be represented with differential equation of the second order in the function of the axial force in the concrete with the following expression:

$$N_b'' - \alpha^2 N_b = \beta M_x \tag{1}$$

where are:

$$\alpha^2 = k\left(\frac{1}{A_b E_b} + \frac{1}{A_d E_d} + \frac{r^2}{(EI)_0}\right) \tag{2}$$

$$\beta = \frac{k \cdot r}{(EI)_0} \tag{3}$$

M_x - the moment of the fully composite section ($k \to \infty$),
k - the slip modulus [N/m^2],
r - the distance between centroid of flange and web elements.

Also, the problem of the TCC beam could be expressed through the differential equation of the fourth order in function of vertical displacement:

$$w'''' - \alpha^2 w'' = \frac{\alpha^2 M_x}{(EI)_\infty} - \frac{M_x''}{(EI)_0} \tag{4}$$

where:

$$(EI)_\infty = \frac{\alpha^2 (EI)_0}{\alpha^2 - \beta_r} = E_d I_d + E_b I_b + \frac{r^2 E_d A_d E_b A_b}{E_d A_d + E_b A_b} \tag{5}$$

EI is the bending stiffness (0 and ∞ denote the properties for non-composite and fully composite beams, respectively).

Solving the differential Equations (1 or 4) is a complex task, especially for different load cases and/or boundary conditions. In the literature, analytical solutions for different load cases and support conditions could be found. According to [5], analytical solutions for axial force *N*, interlayer slip force T_s and vertical displacement *w*, for a simply supported beam system and continuous load, are given by the equations (6-8).

Axial force $$N_x = \frac{\beta}{\alpha^2} M_x \left[1 - 2\frac{\cosh \alpha \frac{l}{2} - \cosh \alpha (\frac{l}{2} - x)}{x(l-x)\alpha^2 \cosh \alpha \frac{l}{2}}\right] \tag{6}$$

Slip force $$T_s = \frac{\beta}{\alpha^2} T_x \left[1 - \frac{\sinh \alpha (\frac{l}{2} - x)}{(\frac{l}{2} - x)\alpha \cosh \alpha \frac{l}{2}}\right] \tag{7}$$

Vertical displacement

$$w(x) = w_\infty(x) + \frac{q \cdot \beta \cdot r}{\alpha^6 \cdot EI_0} \cdot f(x) \tag{8}$$

$$w_\infty(x) = \frac{q \cdot L^4}{24 \cdot EI_\infty} \cdot \left(\frac{x}{L}\right) \cdot \left(1 - 2 \cdot \left(\frac{x}{L}\right)^2 + \left(\frac{x}{L}\right)^3\right)$$

$$f(x) = \left(\frac{\cosh\left(\alpha \cdot \left(x - \frac{L}{2}\right)\right)}{\cosh\left(\alpha \cdot \frac{L}{2}\right)} + \frac{x \cdot L \cdot \alpha^2}{2} - \frac{x^2 \cdot \alpha^2}{2} - 1\right)$$

A demonstration of the qualitative change of the axial force N i.e. slip force T_s in TCC system is shown in Figure 1.

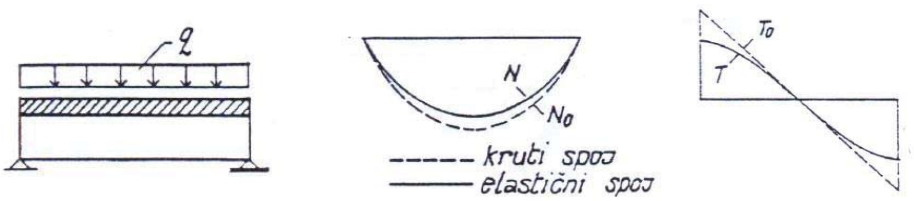

Figure 1- A demonstration of qualitative change of the axial i.e. slip forces in TCC [5]

3. PROBLEM FORMULATION IN WEAK FORM

A physical problem was observed in the domain Ω, which can be 1D to 3D, defined with a differential equation:

$$L(\overline{\boldsymbol{u}}) - \boldsymbol{f}_\Omega = 0 \tag{9}$$

where are:

L - corresponding linear differential operator,

$u(x)$ - unknown function of the problem, that depends on the coordinate x within the space Ω, where the functions $u(x)$ satisfy the given boundary conditions at the boundaries of the domain Ω,

f_Ω – given force term in domain Ω.

The unknown function of the problem $u(x)$ is approximated with the approximate function $\bar{u}(x)$ (14), where the approximate function $\bar{u}(x)$ satisfies the boundary conditions upon the displacements (essential conditions), but does not have to satisfy the conditions by forces (natural conditions). As $\bar{u}(x)$ is approximate solution of the equation (9), the residue or residuum is obtained:

$$L(\overline{\boldsymbol{u}}) - \boldsymbol{f}_\Omega = \boldsymbol{R}(\overline{\boldsymbol{u}}) \neq 0 \tag{10}$$

Since equation (9) is a system of equations i.e. a matrix equation, than the residue $R(\bar{u})$ is a vector. Of course, if $\bar{u}(x)$ would be the exact solution, then the residue vector $R(\bar{u})$ would be equal to the zero vector. The idea behind the method is to reduce the residue vector to the zero

vector "in the average sense". Because of that, linearly independent weight functions $W(\bar{u})$ are introduced with the condition that the integral of the scalar product of the weight function vector and the residual vector within the domain Ω is equal to zero:

$$\int_{\Omega} \boldsymbol{W}^T(\overline{\boldsymbol{u}}) \cdot \boldsymbol{R}(\overline{\boldsymbol{u}}) \cdot d\Omega = \int_{\Omega} \boldsymbol{W}^T(\overline{\boldsymbol{u}}) \cdot (L(\overline{\boldsymbol{u}}) - \boldsymbol{f}_{\Omega}) \cdot d\Omega = 0 \tag{11}$$

The scalar product of the two vectors is equal to zero if these vectors are mutually orthogonal. Accordingly, the integral equation (11) is a condition of the orthogonality of the residual vector to the selected vector of weight functions.

Residue methods consist of finding functions $\bar{u}(x)$ for which the integral equation (11) will be satisfied. If the equation (11) is satisfied for any weight functions vector, then the residue vector will approach the zero vector.

In this way, the approximate solution $\bar{u}(x)$ approximates the exact solution u(x). All solutions $\bar{u}(x)$ that satisfy (9) must satisfy (11) regardless the choice of weight functions. The dimension of the weight functions vector corresponds to the number of unknown coefficients c_m of the considered problem.

As one of the basic variants of the residual method, which adopts weight functions as trial functions for which the required solution is approximated, is Galerkin's method [4].

Based on the differential equations of the elastic coupling (1 or 4) and the conditions (11), it is possible to define the following relations for determining the problem of the TCC girder trough the axial force in the concrete or trough displacements for the case of a TCC beam loaded with continuous load q, according to fallowing expressions:

$$\int_0^L \Phi_m(x) \cdot \left[\frac{d^2 N_b}{dx^2} - \alpha^2 N_b - \beta M_x\right] \cdot dx = 0 \quad , \quad m = 1,2, \dots, n \tag{12}$$

$$\int_0^L \Phi_m(x) \cdot \left[\overline{w}'''' - \alpha^2 \overline{w}'' - \frac{\alpha^2 M_x}{(EI)_\infty} + \frac{M_x''}{(EI)_0}\right] \cdot dx = 0 \quad , \quad m = 1,2, \dots, n \tag{13}$$

An integral formulation that implicitly contains a differential equation of the problem is called a weak formulation (12 or 13) that expresses the conditions and relations that must be satisfied in the average, or in an integral sense.

Since the differential equation of the problem is of even order ($2r = 4$), it is possible to reduce the required order of derivation in the trial functions by partial integration of the expression (11) from $r = 4$ to $r = 2$. By partial integration of expressions (12 or 13) is achieving that selected trial functions must satisfy only the essential conditions, that have to be satisfied by the selection of trial functions themselves, while the force conditions are already included in the very formulation of the partial integration problem.

By solving the integrals, a system of n equations by unknown coefficients c_m is obtained and an approximate solution for the required function $u(x)$ could be derived by determination of coefficients c_m.

4. APPROXIMATION OF THE SOLUTION – TRIAL FUNCTIONS

The unknown function *u(x)* of problem's differential equation has to be approximated by the approximate solution $\bar{u}$ (14), that could be represented as a superposition of products of known base functions Φ_m and unknown coefficients c_m.

$$\bar{u} = \sum_{m=1}^{n} c_m \cdot \Phi_m \tag{14}$$

where are:

Φ_m - set of chosen linearly independent functions $\Phi_m(x_m)$,

c_m - unknown parameters, constants or functions to be determined.

Suitable, and therefore, most often, trial functions are polynomials or trigonometric functions. The choice of trial functions Φ_m is arbitrary, but the quality of the solution largely depends on one's own. Therefore, qualitative knowledge of the nature of the solution is very useful in order to avoid the wrong choice of functions that in their form represent a rough deviation from the analytical solution.

Trial functions should satisfy the following conditions:

- to be continuous and differentiable till the necessary order,
- in addition to essential, they also have to satisfy natural boundary conditions,
- to correspond qualitatively by the form to the analytical solution,
- to be complete, e.g. in the case of polynomials of a certain degree, all members of the lower degrees should also be included.

Based on the well-known solutions from the literature (6) and (8), as well as on the qualitative flow of the solution (Fig. 1), three functions (hyperbolic, sinusoidal and polynomial functions) were selected for trial functions in this paper.

The adopted trial functions describe the law of the change of the axial force *N*, slip forces T_s *(N')* and displacement *w* along the composite girder and qualitatively correspond to the solutions (Fig. 1). By means of expressions (15, 16 and 17), selected trials for *N* or *w* are given, while on Fig. 2 the shape of the function and its first derivative along the beam are shown.

1. Hyperbolic function: (15)

$$\bar{u}(x) = c_1 \cdot \Phi_1(x) = c_1 \cdot \left(\frac{\cosh\left(x - \frac{L}{2}\right)}{\cosh\left(\frac{L}{2}\right)} + \frac{x \cdot L}{2} - \frac{x^2}{2} - 1 \right)$$

2. Sinusoidal function: (16)

$$\bar{u}(x) = c_1 \cdot \Phi_1(x) = c_1 \cdot \sin\left(\frac{\pi \cdot x}{L}\right)$$

3. Polynomial function: (17)

$$\bar{u}(x) = c_1 \cdot \Phi_1(x) = c_1 \cdot \left(\frac{x}{L}\right) \cdot \left(1 - 2 \cdot \left(\frac{x}{L}\right)^2 + \left(\frac{x}{L}\right)^3\right)$$

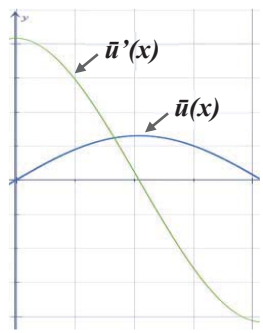

Figure 2 – Trial function and its first derivative

5. NUMERICAL EXAMPLES AND VERIFICATION OF THE RESULTS

For the numerical analysis, the same timber-concrete composite floor structure previously used for analysis by Ritz' method [3], is also considered for analysis with Galerkin's method. The disposition of the elements and fasteners, as well as their dimensions and properties of the applied materials, are shown in Fig. 3. The floor structure consists of a glulam beams that are coupled with concrete slab by vertically arranged dowel type fasteners.

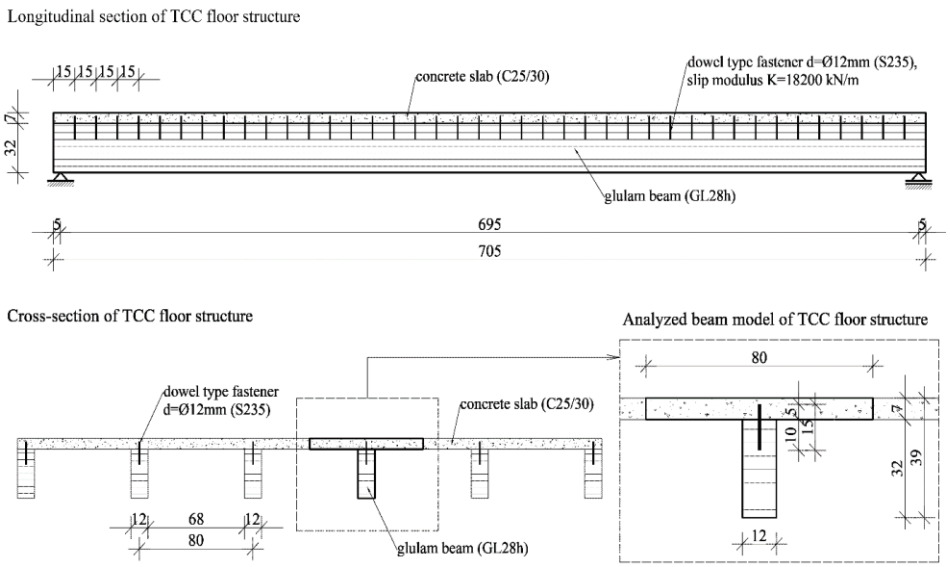

Figure 3 - Analyzed model of the timber-concrete composite floor structure [3]

Based on the selection of trial functions for deflection *w(x)* and axial force *N(x)*, the following variant models are defined.

Models of group A, where the unknown function in weak form formulation (12) is *N*:

- Model N-HIP – for trial function of axial force *N(x)*, the hyperbolic functions was adopted by the given expression (15),
- Model N-SIN – for trial function of axial force *N(x)*, the sinusoidal functions was adopted by the given expression (16),
- Model N-POL – for trial function of axial force *N(x)*, the polynomial functions was adopted by the given expression (17).

Models of group B, where the unknown function in weak form formulation (13) is *w*:

- Model w-HIP – for trial function of deflection *w(x)*, the hyperbolic functions was adopted by the given expression (15),
- Model w-SIN – for trial function of deflection *w(x)*, the sinusoidal functions was adopted by the given expression (16),
- Model w-POL – for trial function of deflection *w(x)*, the polynomial functions was adopted by the given expression (17).

Based on the Galerkin method, several subprograms/codes for the analysis of TCC structures are written in MATLAB 2014 [2]. On the basis of performed analysis for variant models (group A and group B), the deviations (in percents) of obtained results to analytical solution are shown in Fig. 4 and 5. Calculated deviations are given for vertical displacements (w), moments (M_1, M_2), axial forces (N_1, N_2) and stresses (σ_1 i σ_2) for the cross-section of concrete/timber element (top and bottom) in the middle of the beam span. The percentage differences of the maximum shear forces (F_s) in connectors and the maximum slip force (T_s) values at the concrete-timber contact in support zones are shown too. Beside the analysis of variant models, the simplified "γ-procedure" was also performed in order of comparison with analytical solution.

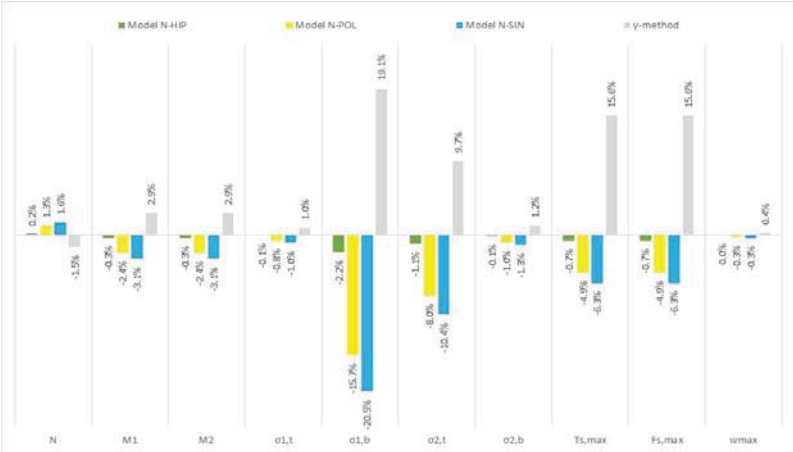

Figure 4 - Deviations of the variant models of group A in relation to the analytical solution

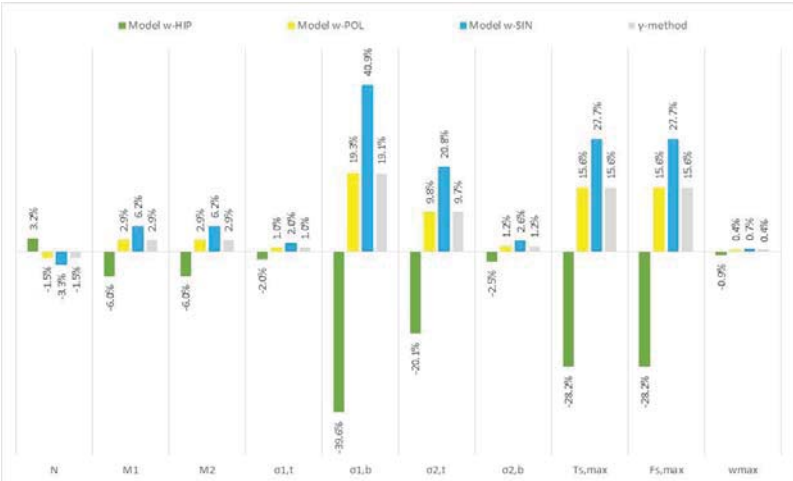

Figure 5 - Deviations of the variant models of group B in relation to the analytical solution

Observing the deviations of all models, it can be noticed that in the models of group A there are smaller differences in relation to the analytical solution than in the models of group B.

Analysis of results obtained by different trial functions for the approximate solution of the normal force N shows that a minimal deviation occurs when a hyperbolic function is adopted, and the maximum one if it is the sinusoidal function. The models N-POL and N-SIN have significant deviations in stresses ($\sigma_{1,b}$ and $\sigma_{2,t}$) even up to 21%, and minor deviations in the slip and shear forces (T_s and F_s) up to 6.5%. All values are smaller than those obtained by analytical solutions. Comparing the Group A models with results of the "γ" method, none of the models has greater deviations in absolute sense, but it can be noticed that the N-POL and N-SIN models give smaller values.

Analysis of results obtained by different trial functions for the approximate displacement w solution shows that a minimal deviation occurs if the polynomial function is adopted, and the maximum one if it is a hyperbolic function. The w-HIP and w-SIN models have significant deviations in stresses ($\sigma_{1,b}$ and $\sigma_{2,t}$) even up to 41%, and for slip and shear forces (T_s and F_s) even up to 28%. Model w-HIP shows significantly smaller values comparing to analytical. By comparing the models of group B with results of the "γ-method", it can be seen that the best match with the "γ-method" has the w-POL model.

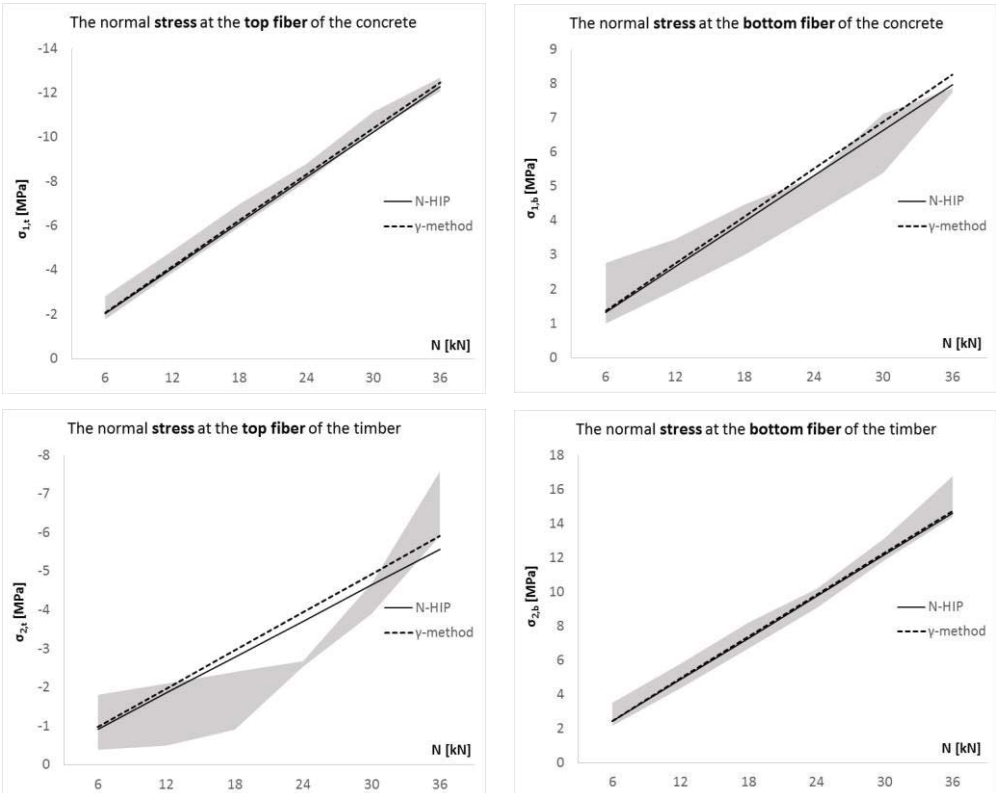

Figure 6 – Comparative analysis of numerical model N-HIP and experimental data

As the N-HIP model describes the problem of TCC partial composite action on the best way, this model was applied for comparative analysis with experimental test results of TCC (EP1 and EP2) beams [6], where mechanical fasteners were used. The diagrams in Figure 6 show the stresses in cross-section of constitutive elements of TCC beams in the middle of the span, in relation to force intensity throughout loading phases (F = 6, 12, 18, 24, 30 and 36 kN). The shaded surfaces represent the envelopes of the results obtained from experiments for beams EP1 and EP2, while the full and dashed lines represent the results of the numerical analysis by N-HIP model and by "γ-method" respectively. Considering the stresses ($\sigma_{1,b}$ and $\sigma_{2,t}$) on the contact of two materials, deviations from the experimental results can be noticed, significantly for $\sigma_{2,t}$ at loads F =18 and 24 kN. A good match with experimental results on the top and bottom sides of the cross-section as well as in bottom of the concrete slab is obvious.

6. CONCLUSION

Based on the presented analysis using the Galerkin's method, it can be concluded that the selection of trial functions and baseline unknowns (w and N) in problem formulation has the major influence on the final effect values. Also, the qualitative knowledge of solution nature can significantly contribute to the errors' reduction. In presented analysis the proposed N-HIP model qualifies as most appropriate in order to solve the problem of partial coupling.

As the presented formulation in the FEM is quite usual form, the Galerkin method could be successfully applied for definition of a composite FE for partially timber-concrete composite systems, thereby enabling an efficient engineering tool in practice.

ACKNOWLEDGMENTS

The work has been done within the scientific research project TR 36043 "Development and application of a comprehensive approach to the design of new and safety assessment of existing structures for seismic risk reduction in Serbia", which is funded by the Ministry of Science of Serbia.

REFERENCES

[1] EN 1995-1. (2008): *Eurocode 5: Design of timber structures - Part 1-1: General – Common rules and rules for buildings*, CEN, Brussels.

[2] MATLAB R2014a (2014): *MathWorks Inc. The Language of Technical Computing*.

[3] Manojlović D., Radujković A., Kočetov Mišulić T. (2017): *Application of Ritz method in analysis of timber-concrete composite system*, 17. International Symposium MASE, Ohrid, Faculty of Civil Engineering, pp. 721-728.

[4] Reddy J. N. (2002): *Energy Principles and Variational Methods in Applied Mechanics*, 2nd Edition, John Wiley & Sons, Inc., New York, pp. 608.

[5] Stevanović B. (1994): *Analiza spregnutih nosača od drveta i betona*, Magistarska teza, Građevinski fakultet Univerziteta u Beogradu, Beograd, 119 str.

[6] Stevanović B. (2004): *Eksperimentalna i teorijska analiza spregnutih nosača drvo-beton izvedenih mehaničkim spojnim sredstvima*, Materijali i konstrukcije 47, str. 29-46.

ДГКС Друштво грађевинских конструктера Србије
ASES Association of Structural Engineers of Serbia
S-89
15. KONGRES
6-8. 9. 2018. Zlatibor

Vladimir Živaljević[1], *Mitar Đogo*[2], *Dušan Kovačević*[3]

MKE ANALIZA DINAMIČKOG ISPITIVANJA ŠIPA U JEDNOLIČNOM I VIŠESLOJNOM GLINOVITOM TLU

Rezime:

Šipovi su elementi konstrukcije temelja koji se često koriste u slučajevima fundiranja u zemljištu slabe nosivosti kako bi se smanjilo sleganje konstrukcije. Zbog prirode njihove izgradnje, kontrola kvaliteta je ograničena. Stoga, izračunavanje nosivosti šipova je jedan od ključnih koraka u projektovanju konstrukcije temelja na šipovima. Dinamičko ispitivanje šipova probnim opterećenjem podrazumeva procenu nosivosti šipova na bazi merenja sile i brzine u zoni vrha šipa usled aksijalne udarne sile. U ovom radu analizirano je dinamičko ispitivanje šipa i njegovo numeričko modeliranje metodom konačnih elemenata. Analiziran je slučaj šipa u glinovitom tlu.

Ključne reči: šipovi, dinamički test, probno opterećenje, MKE analiza

FEM ANALYSIS OF THE DYNAMIC TEST BY LOAD OF THE PILE IN UNIFORM AND MULTILAYER CLAY SOIL

Summary:

Piles are foundation elements that are often used in cases of foundation in soil of low bearing capacity to reduce the settlement of the structure. Due to the nature of their construction, quality control is limited. Therefore, calculation of the bearing capacity of piles is one of the key steps in pile foundation design. Dynamic pile load testing implies assessment of the pile bearing capacity based on the measurement of the force and velocity near the top of the pile due to the axial impact force. In this paper a dynamic pile load testing and its numerical modelling using the finite element method was analysed. The soil type that was analysed was a clay soil.

Key words: pile foundation, dynamic test by load, FEM analysis

[1] *Master of Civil Engineering, Department of Civil Engineering and Geodesy, Faculty of Technical Sciences, University of Novi Sad, zivaljevic.vladimir@uns.ac.rs*
[2] *Prof. Dr. of Civil Engineering, Department of Civil Engineering and Geodesy, Faculty of Technical Sciences, University of Novi Sad, mitar@uns.ac.rs*
[3] *Prof. Dr. of Civil Engineering, Department of Civil Engineering and Geodesy, Faculty of Technical Sciences, University of Novi Sad, dusan@uns.ac.rs rs*

1 INTRODUCTION

Piles are foundation elements that are often used in cases of foundation in soil of low bearing capacity to reduce the settlement of the structure. The load can be transmitted through the piles to the ground via pile base and pile sheath.

Due to the nature of their construction, quality control is limited. Therefore, calculation of the bearing capacity of piles is one of the key steps in pile foundation design. In general, there are three ways of determining the bearing capacity of the floating piles:

- theoretical methods based on the physical-mechanical properties of the soil,
- static or dynamic load testing of piles and
- methods based on the dynamic data obtained during pile driving.

Dynamic pile load testing implies assessment of the pile bearing capacity based on the measurement of the force and velocity near the top of the pile due to the axial impact force. The impact force is applied using a drop weight system, where a falling mass is allowed to fall freely from a certain height. Load application is instant, and the impact force should be large enough to achieve sufficient pile settlement, which will fully mobilize the bearing capacity of the pile [1].

In this paper a dynamic pile load testing and its numerical modelling using the finite element method of a 32m long concrete pile with a foundation depth of 30m was analysed. To give a more realistic representation of the actual in-situ conditions, the extension of 2m above the ground was formed. This makes connections of measuring sensors accessible. The soil type that was analysed is a clay soil. What is more, two different soil configurations were analysed.

2 PILE DYNAMIC TEST BY LOAD

Pile dynamic test by load implies assessment of the pile bearing capacity based on the measurement of force and velocity near the top of the pile due to the axial impact force. Primarily, two types of pile dynamic testing can be distinguished - testing with the use of conventional pile driving hammers and testing with the use of a drop weight system designed specifically for testing purposes. In this paper the emphasis will be put on a dynamic test with the use of drop weight system.

A dynamic test by load can be applied to any type of pile regardless of the construction method and is increasingly used for dynamic testing of drilled piles and caissons. These tests are particularly important for high-capacity piles (over 2,5 MN [2]), for which static test by load is very expensive or physically difficult to perform (e.g. over water).

The application of dynamic testing is carried out by letting the mass fall from a certain height to the top of the pile, creating a dynamic stress wave during the impact that moves to the base of the pile. The impact force of the ram (drop weight) should be large enough for pile to achieve sufficient settlement, which will fully mobilize the bearing capacity of the pile. This implies that one of the most important requirements for dynamic pile testing is the application of a ram of adequate weight, especially in cases of testing of high-capacity piles, and in cases where the pile is located in the soft soil (in order to achieve proper settlement with the purpose of activating the maximum resistance of the soil). The recommendation of some authors [2] is

that the mass of the falling ram (in tons) is at least 0,1-0,2% of the required bearing capacity of the pile (in kN). By combining the results of this test method with the results of pile static test by load, the accuracy of determining the actual pile bearing capacity can be increased.

A typical system of drop weight consists of four components:

- a frame and/or a guide for drop weight (ram),
- ram,
- mechanism for the release of ram and
- impact plates with or without cushion.

A pair of accelerometers and a pair of strain gauges are attached to the top of the pile on the opposite sides for the needs of dynamic measurements, at a distance of at least one diameter from the upper surface of the pile. These sensors are connected to instruments (PDAs - Pile Driving Analyzers) that process and display test data and results. Accelerometers are used to record the acceleration at the point of measurement providing, based on expression (1), the calculation of velocity with time (v(t)). The strain (ε(t)) is measured between two fixed points, which provides the calculation of the stress at the measurement point, i.e. the force with time (F(t)). This calculation approach assumes the uniformity of strain (ε_t), and hence the stresses in the pile's cross-section, knowledge of the area of the cross-section (A_p) and the modulus of elasticity of the material of the pile (E_p).

$$v(t)=\int a_{cc}(t)dt \tag{1}$$

$$F(t)=\varepsilon(t)\cdot A_p\cdot E_p \tag{2}$$

The main sources of difficulties of dynamic measurements are related to construction, impact of the ram, pile resistance and measuring point and can be classified as follows:

- nonuniform element geometry,
- poor concrete quality on the outer surfaces,
- a drop of a falling ram at an angle relative to the surface and axis of the pile and
- high friction resistance at the top of the pile.

3 PARAMETRIC STUDY

Analysis of two different configurations was conducted in this paper. The aim of the parametric study was to examine the effects of the soil profile changes. Table 1 gives the outline of configurations with dynamic modulus of elasticity of soil layers.

Table 1 – Soil profile and dynamic modulus of elasticity according to test configuration

Configuration	Soil profile	Soil modulus of elasticity (MPa)
A	Clay – medium	27,5
B	Clay – soft	22,0
		24,6
	Clay – medium	27,2
		29,8
	Clay - stiff	32,4
		35,0

The soil dynamic modulus of elasticity (E_{dyn}) was determined according to [3].

The soil type that had been analysed in configuration A is a clay soil of medium density. Configuration B study the behaviour of piles in the multilayer clay soil. In this configuration the soil profile consists of 6 layers of clay, such that the upper layers have lower elastic modules than the lower ones.

Figure 1 shows both soil configurations, and for each one gives the dynamic modulus of elasticity (E_{dyn}), the Poisson coefficient (η), the angle of internal friction (φ), cohesion (c), and the bulk density (γ) for each of the soil layers.

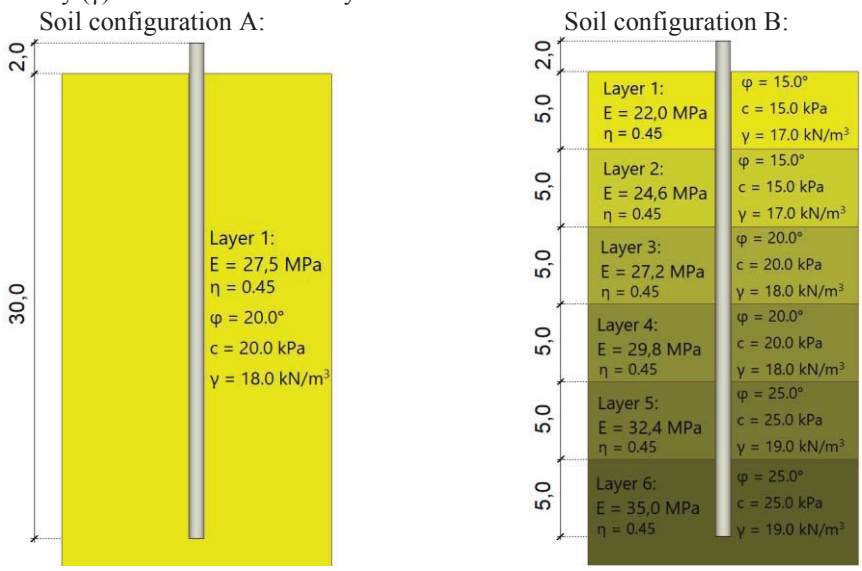

Figure 1 – Soil configurations and characteristics

4 FEM MODELLING AND ANALYSIS

Numerical modelling of pile dynamic load testing was done using the FEM software Midas GTS NX©, which is aimed for analysis of structure-soil interaction.

The geometry of the model can be very decently discretized using various geometry tools, which enable the definition various 3D shapes over which a mesh of FE is generated. The FEs are further attributed the characteristics of the material and/or some other characteristics that adequately describe the behaviour of the model. The FEM model considered in this paper is spatial (3D). The rendered view of cross section of numerical model is given on the Figure 2.

The considered pile element is modelled using concrete material with the Young's modulus of elasticity of 30GPa. The length of the pile is 32m. The model covers the soil "half-space" prism, with dimensions 40x40x60m. These dimensions provide enough distance from the pile to the edge of the half-space in order make analysis results far enough from the pile negligible.

The soil types that had been analysed are given in Table 1 and Figure 1. For the modelling of concrete pile and soil 3D hexahedral FEs were used. Material behaviour of pile and soil is assumed to be linear-elastic. The dynamic calculation includes a time-history analysis for a

time interval of 100ms. The dynamic force acting on the pile is of a pulse character and is given by the Equation (3):

$$F_{dyn}=F_{stat} \cdot f(t) \tag{3}$$

where F_{stat} is a static value of force and f(t) is a function that describes a change in the force intensity depending on the time, Figure 3.

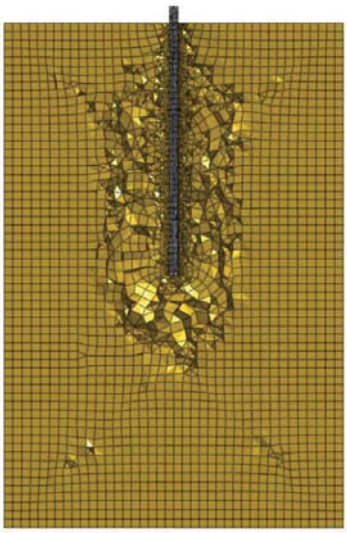

Figure 2 - Rendered view of cross section of numerical model (configuration A)

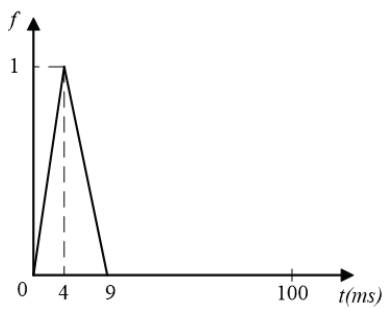

Figure 3 - Time function of force intensity

The change in the force in time is defined so that the function linearly changes the value from 0 to 1 in the interval from 0ms to 4ms, and in the interval from 4ms to 9ms the function value decrease from 1 to 0. After this period, the function has a zero value, which represents the interval in which the dropping mass is in the air after bouncing off of pile surface after the impact. The peak intensity of the dynamic force is determined using analytical methods. As an orientation value, the values of the nominal pile bearing capacity determined by theoretical methods based on the physical-mechanical properties of the soil given in [4] were used to obtain the same settlement as the settlement due to the impulse force.

5 RESULT ANALYSIS

Results of dynamic analyses are shown in the form of figures and diagrams. Diagrams show the values of the settlement of pile top and base (m) and the calculated velocity (m/s) at the four nodes along the pile's cross-section radius (center, 0,1m, 0,3m and 0,5m from the pile's axis - Figure 4) in function of time.

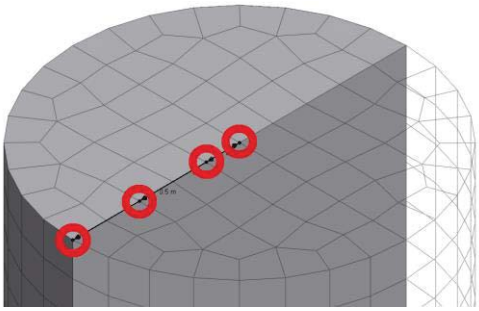

Figure 4 - Display of nodes along the radius of a pile's cross-section for a more detailed view of results

5.1. CONFIGURATION A

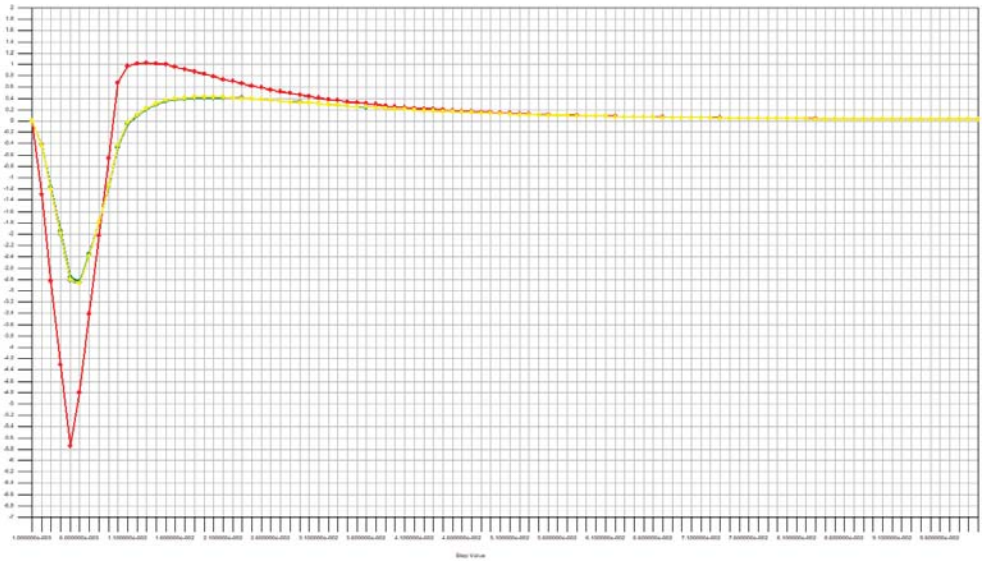

Figure 5 - Velocities (m/s) for time interval 0ms-100ms (central node (red curve), 0,1m (yellow curve), 0,3m (green curve) and 0,5m (blue curve) from the pile's axis)

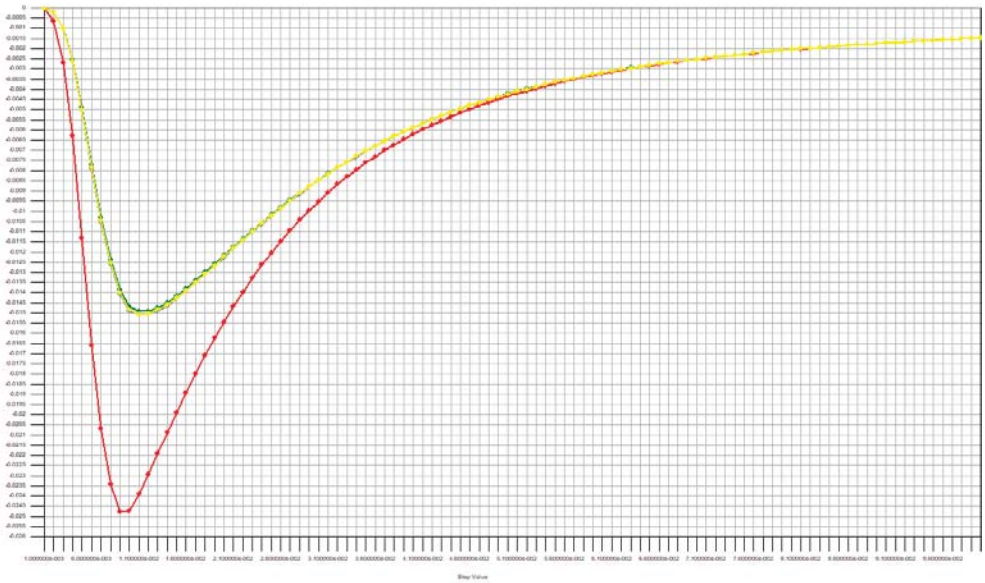

Figure 6 – Settlement of the top of the pile (m) for time interval 0ms-100ms (central node (red curve), 0,1m (yellow curve), 0,3m (green curve) and 0,5m (blue curve) from the pile's axis)

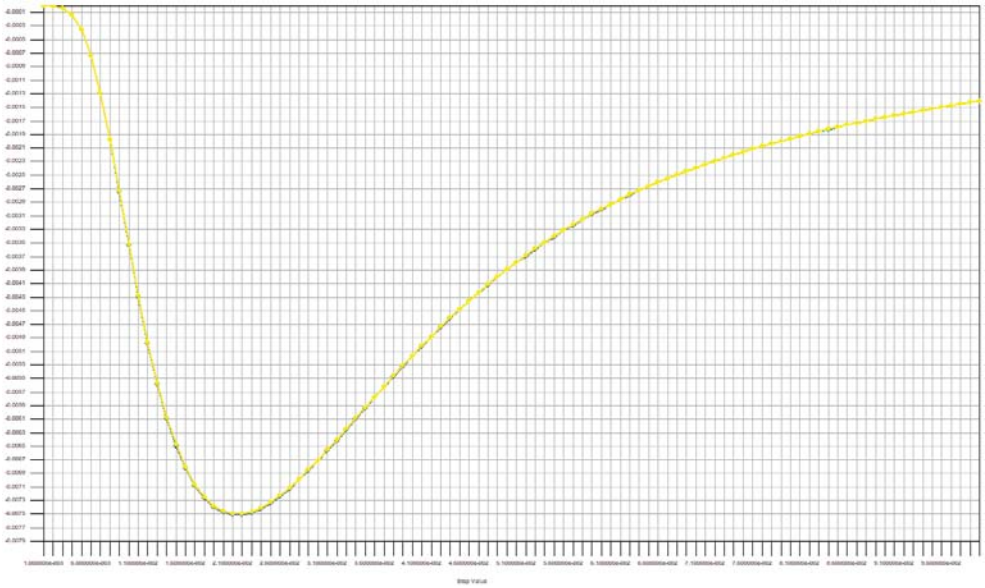

Figure 7 - Settlement of the base of the pile (m) for time interval 0ms-100ms (central node (red curve), 0,1m (yellow curve), 0,3m (green curve) and 0,5m (blue curve) from the pile's axis)

Figures 5 and 6 show a large difference between the value of the results in the same time increments at different curves in the initial phase of the analysis. Since these figures show the results on the top surface of the pile, the reason for this phenomenon lies in the fact that the impulse force is modelled as a nodal load and as such is applied in the central node of the upper surface of the pile. Therefore, the high velocity and settlement peaks in the loaded node should be taken with the reserve and in the analysis of the results the priority should be given to the results referring to the points located at a certain distance from the loaded node (in this case at 0,1m, 0,3m and 0,5 m from the center point) since the values of the results in the same time increments on these curves are almost identical.

In Figure 7, which represents the pile base settlement, settlement values in all increments, on all curves (i.e. at all points along the radius of the lower surface of the pile) are roughly equal. Therefore, it can be concluded that the stress concentration at a sufficient distance from the loaded node does not affect the results of the analysis. By comparing Figures 6 and 7, it can be noticed that the peaks of settlement curves of the base and the top of the pile are "translated" for 11ms. This phenomenon indicates the time necessary for the stress wave from the moment of impact to cover the distance from the top to the base of the pile.

The maximum settlement of the top of the pile is $s_{t,max}$=15,0mm and occurs at the time increment t=10ms (the center point is exempted). The maximum settlement of the base of the pile is $s_{b,max}$=7,51mm and occurs at the time increment t=21ms. The maximum calculated peak velocity is $v_{t,max}$ =2,8m/s (the center point is exempted).

5.2. CONFIGURATION B

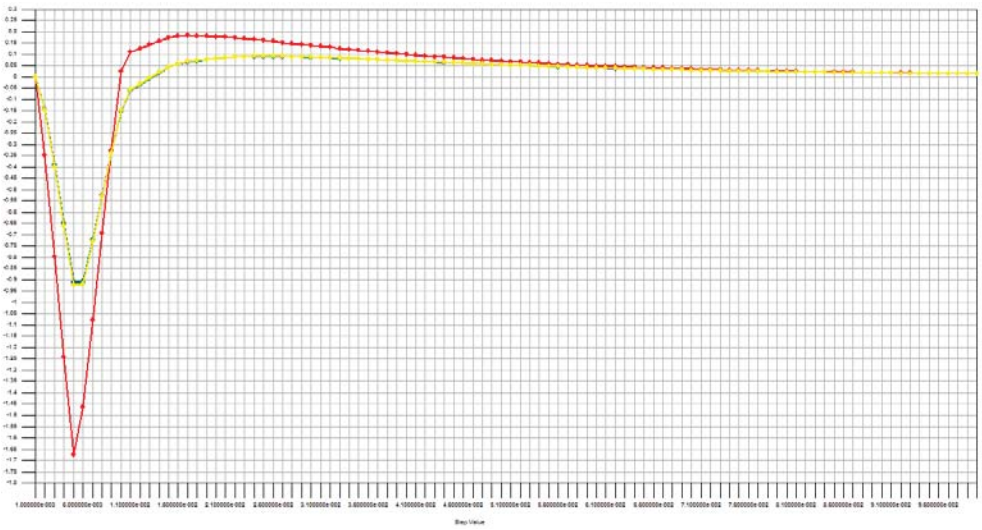

Figure 8 - Velocities (m/s) for time interval 0ms-100ms (central node (red curve), 0,1m (yellow curve), 0,3m (blue curve) and 0,5m (green curve) from the pile's axis)

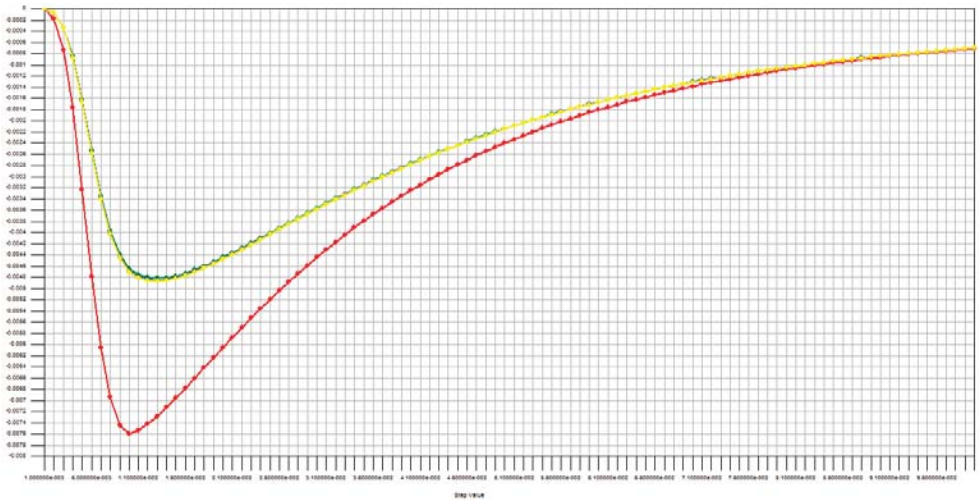

Figure 9 – Settlement of the top of the pile (m) for time interval 0ms-100ms (central node (red curve), 0,1m (yellow curve), 0,3m (blue curve) and 0,5m (green curve) from the pile's axis)

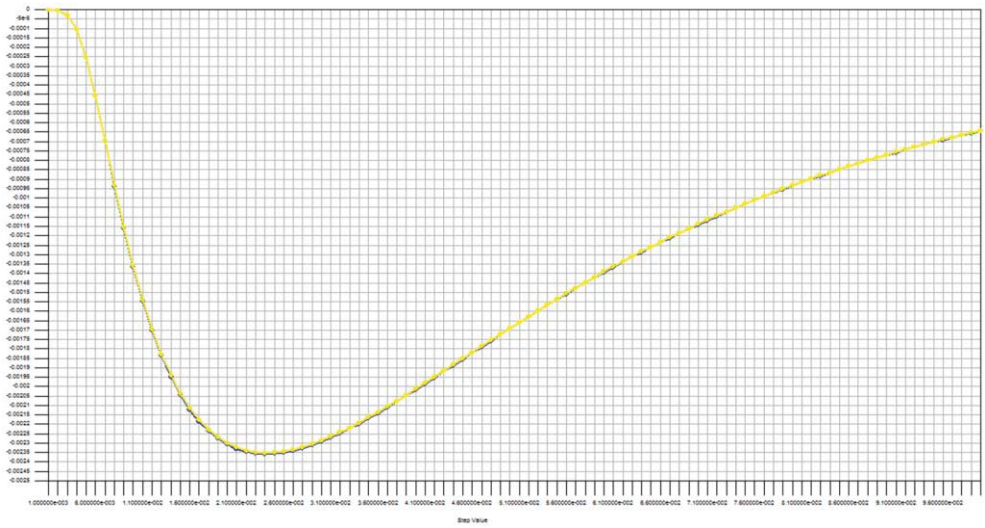

Figure 10 - Settlement of the base of the pile (m) for time interval 0ms-100ms (central node (red curve), 0,1m (yellow curve), 0,3m (blue curve) and 0,5m (green curve) from the pile's axis)

The maximum settlement of the top of the pile is $s_{t,max}$=4,9mm and occurs at the time increment t=13ms (the center point is exempted). The maximum settlement of the base of the pile is $s_{b,max}$=2,4mm and occurs at the time increment t=24ms. The maximum calculated peak velocity is $v_{t,max}$ =0,9m/s (the center point is exempted). Lower values of settlement in this test

configuration are the consequence of the use of higher damping value in this case than in previous test configuration.

6 CONCLUSIONS

Dynamic analysis of two configurations of pile dynamic test by load were carried out, aiming to simulate the pile dynamic test by load. These test configurations differed from each other in the soil profile. After analysing the results of the dynamic calculation, the following conclusions were made:

- In the case of an uniform soil profile the large difference between the value of the results in the loaded node and nodes along the radius of the pile in the same increments of time should be taken with reserve because the impulse force was modelled as a nodal and as such was applied in the central node of the upper surface of the pile. Hence, during the analysis of the results the priority should be given to the results referring to the points located at a certain distance across the crss-section radius from the loaded node.
- Values of settlement in all increments are at all points along the radius of the lower surface of the pile equal. Therefore, it can be concluded that the stress concentration does not affect the results of the analysis at a sufficient distance from the point of load. The maximum settlement of the base and the top of the pile values are “translated” for 11ms, indicating the time necessary for the stress wave from the moment of impact to reach from the top to the base of the pile.
- In the case of a multilayer soil profile, the same conclusions can be applied as in the case of uniform soil profile. In this case, a different value of the relative damping coefficient was considered. Due to the higher damping value, the calculated values of velocities and settlement are lower than in the case of a uniform clay soil profile.

ACKNOWLEDGEMENTS

The presented paper has been done within the scientific research project TR 36043 "Development and application of a comprehensive approach to the design of new and safety assessment of existing structures for seismic risk reduction in Serbia", which is funded by the Ministry of Science of Serbia.

REFERENCES

[1] https://www.uml.edu/docs/SW%202004_Paikowsky_color_tcm18-106946.pdf (Accessed 27 November 2017)

[2] M. Schallert, O. Klingmüller, Dynamic load testing of large scale piles – offshore and onshore, Gesellschaft für Schwingungsuntersuchungen und dynamische Prüfmethoden mbH, Mannheim, Germany, 2012.

[3] Đ. Uzelac, Roadway structures, Faculty of Technical Sciences, Novi Sad, Serbia, 2015

[4] S. Stevanovic, Foundation I (in Serbian), Scientific book, Belgrade, 1989.

ДГКС Друштво грађевинских конструктера Србије
ASES Association of Structural Engineers of Serbia
S-90
15. KONGRES
6-8. 9. 2018. Zlatibor

Doncho Partov[1], V . K. Kantchev[2], Ch. P. Stoyanov[3]

ANALIZA PRERASPODELE MOMENTA SAVIJANJA IZNAD OSLONCA KONTINUALNOG SPREGNUTOG NOSAČA KORIŠĆENJEM INTEGRALNIH JEDNAČINA VOLTERRA

Rezime:

Rad prikazuje numeričku analizu promene napona usled tečenja u statički neodređenom spregnutom čelično-betonskom nosaču. Za određivanje preraspodele momenta savijanja iznad oslonca kontinualnog spregnutog nosača usled njegovog sleganja u odnosu na vreme "*t*", izveden je sistem dve nezavisne Volterra integralne jednačine drugog reda na osnovu teorije viskoelastičnog tela Arutyunyan–Trost-Bažant. Ispituje se primer sa predloženim modelom. Funkcije tečenja su definisane na osnovu predloga "CEB-FIP" modela 2010. Modul elastičnosti betona E_c (t) pretpostavlja se da je konstantan u vremenu *"t"*.

Ključne reči: relaksacija, numerička analiza, statički neodređen spregnuti nosač

ANALYSIS OF THE RELAXATION OF A BENDING MOMENT OVER THE SUPPORT IN A CONTINUOUS COMPOSITE BEAM USING INTEGRAL EQUATIONS OF VOLTERRA

Summary:

The paper presents numerical analysis of the stress changes due to creep in statically indeterminate composite steel-concrete beam. For determining the relaxation of a bending moment, aroused over the support due to its settlement, in a continuous composite steel-concrete beam, with respect to time "*t*", system of two independent Volterra integral equations of the second kind have been derived, on the basis of the theory of the viscoelastic body of Arutyunyan–Trost-Bažant. Example with the model proposed is investigated. The creep functions is suggested by the "CEB-FIP" models code 2010. The elastic modulus of concrete $E_c(t)$ is assumed to be constant in time "*t*".

Key words: relaxation, numerical analysis, indeterminate composite steel-concrete beam

[1] *Prof. Civ. Eng. D. N. Partov, PhD, 1373 Sofia, Suhodolska Str.175, Univ. Str. Eng. and Arch., partov@vsu.bg*
[2]*Assoc. Prof. V. K. Kantchev, PhD,1373 Sofia, Suhodolska Str.175, Univ.Str. Eng. and Arch, kantchev@vsu.bg.*
[3]*Eng.Ch.P.Stoyanov, Msc, PhD student,1373 Sofia,Suhodolska Str.175,Univ.Str.Eng. and Arch, ing4040@abv.bg*

1. INTRODUCTION

Steel-concrete composite beams are wide spread form of construction in both buildings and bridges, (Cosenza –Zandonini 1999[14]; Oehlers and Bradford 1999[21]; Wang 2002[31], Johnson 2004[19]; Folić and Zenunović 2009[17]; Vayas and Iliopoulos 2014[30], Dujmović, Androić, and Lukačević, 2015[16]). One of the very serious problem in the steel-concrete composite beams is to determine, their time-varying behaviour under sustained service loads, which drawn the attention of engineers who were dealing with the problems of their design more than 60 years. Creep have a considerable impact upon the performance of composite beams, causing increased deflection as well as affecting stress distribution. In general, time-dependent deformation of concrete regarding creep phenomena may severely affect the serviceability, durability and stability of structures. Creep analysis of composite structures is normally performed on the basis of the linear theory of viscoelasticity for aging materials. A large number of practical problems concerning the influence of creep effect on the reliability and durability of concrete and composite structures can be solved exactly, through the four fundamental theorems of this theory, as demonstrated by the (Chiorino, 2010,2014)[12,13]. These compact formulations are particularly suitable for codes and technical guidance documents (CEN 2004a, CEN 2004b)[10,11], and helpful in the global assessment of creep induced structural effect in the preliminary design stages, as well as in the control of the output of the detailed numerical investigations and safety checks. The investigation of creep effect in composite steel-concrete beams has been an important task for engineers since the first formulation of the mathematical model of linear viscoelasticity(Bažant, 1975 and Branson,1977)[4-9]. In this paper it is analyzed the time dependent behavior of statically indeterminate composite steel-concrete beam with respect to rheological properties of concrete according to world code provisions: Eurocode2 (Comité Européen de Normalisation [CEN] 2004a[10,11].

2. GENERAL DATE

2. 1. STRUCTURAL ANALYSIS OF CONTINUOUS COMPOSITE BEAMS

2.1.1. Advantages and disadvantages

Continuous composite beams possess most of the advantages of continuous steel beams, namely: *Good structural behavior*. When the beam is loaded, it operates through positive field and negative bearing moments. Both are smaller than in a simple beam with the same opening. The deformed axis of the beam has positive and negative sections. The latter contribute to the reduction of beam deflections. The deformed axis of the beam is smooth. Discontinuity is only at both ends, where by loaded structure arise *kink* in the longitudinal profile of the roadway. *Lower construction height*. Compared to the simple beam, the structural height of the continuous beam is reduced by 20-30% due to the decrease in the maximum value of the bending moments. The reduced construction height implies less wind load on the bridges. Compared to the simple beam, the bearings are reduced by approximately half. *Continuous*

composite beams also have the advantages of composite systems consisting of: Reduced construction steel consumption. When the road plate is steel orthotropic, the consumption of structural steel for it is 40-45% of the total cost. A disadvantage of continuous composite beams is the disadvantage of all continuous systems, that they are influenced by supports movements. Another disadvantage of the continuous composite beams is their sensitivity to negative moments. These moments suggest a tension in the concrete slab, which can not be absorbed and the slab cracks. *Simplified construction technology***:** Steel beams have simplified design details. As a result, labor costs have been greatly reduced. *Various methods of construction*: Continuous beams allow a variety of ways to mount the steel part, as in most cases temporary supports are not required because the construction can be self-supporting.

2.2.AREA OF APPLICATION

Continuous composite beams are used for small openings of 10-30 m in the form of slabs with embedded profiles as well as for larger openings 30-60m for beams of conventional construction.

2.3. CONSTRUCTIVE SCHEMES AND STRUCTURAL FORMS

Continuous composite beams are made in two or more spans. If there are no terrain or geological complications, it is recommended that the spans of three or more spans constructions represent 70-80% of the internal length. Beams can be of constant and variable height. The variable is achieved by polygonal or curvilinear execution of the lower belt. If the assembly technology is a longitudinal launching, it requires a constant height beam. For composite beams the variable height is more suitable because in the cross sections the concrete slab does not participate in the assumption of the negative bending moments (this does not concern to the longitudinal reinforcement in it) and in order to increase the bearing capacity of the steel section it is desirable to increase the height his.

3. CONTINUOUS BEAMS REGARDING THE CREEP OF CONCRETE

3.1. PHILOSOPHY OF THE CHANGE IN THE VALUES OF THE BENDING MOMENT IN THE-SECTION OF THE BEAM, DUE TO CREEP OF CONCRETE

It is known that in statically indeterminate beams, positive (in the fields) and negative bending moments occur over the beams' supports. It is known that the reinforced concrete slab, acting as a top flange on the beam, can withstand tensile stresses over the supports of the beams at certain small limits. Usually, tensile stresses in concrete are exhausted by the influence of concrete shrinkage or temperature differences. In the area of the negative moments, by dimensions of the composite beams, it is usually necessary to ignore the composite actions between the two materials(concrete and steel) and to dimension only the steel section so, that it only takes the negative bending moment. In other cases, prestressing is done in the concrete slab in order to use the effective width of the reinforced concrete slab, with the prestressing having to be such, that after the corresponding concrete creep losses in the most unfavorable load combinations, it is not the compressive tension in the plate exceeded.

Other differences between statically **indeterminate** and **determinate** composite steel - concrete beams lie in their different behavior, taking into account the rheological properties of concrete. In case the external load on the simple beam is constant throughout its length, due to the occurrence of creep of the concrete, begin the distributions of the stresses through the height of the cross section of the beam, while keeping the external moment constant in each cross section of the beam. By statically **indeterminate** beams, as a result of the creep of concrete, bending moments along the beam change. In the statically **indeterminate** composite beams, the value of the support moment depends on the distribution of the bending stiffness EI along the beam. As a result of creep, it is known that the elastic modulus of concrete is conventionally assumed to decrease: $E_{\varphi} = E_c / 1 + \varphi.$ This acceptance unambiguously dictates the change in bending stiffness of the ideal composite cross-section, with the exception of a beam with a constant cross-section. The change of bending stiffness in the individual cross sections of the beam is different and therefore the bending moment diagram along the beam changes. For these reasons, stresses in any cross section in statically indeterminate beams change in a more complicated way. Not only is the redistribution of stresses in height of the cross-section of the beams, but also a change in the values of the external moment in the cross-section of the beam, causing redistributions of the internal stresses in the beam. *As a result of creep in time* $t > 0$*: we get a new elastic beam line, that resembles the original elastic line in time* $t = 0$. The mutual angle of rotation of two adjacent cross sections over the support in time will equally be zero. From this reason, as a result of the creep of the concrete over the internal supports of the beam from an external load, no further stress state will occur; i.e. no new bearing reactions will occur in a statically indeterminate construction. Therefore, the study of statically indeterminate composite steel-concrete constructions will be performed in the same procedure as in the simply supported beams, i. e. in elastic stages (Fig.1), which show the influence of creep process in statically indeterminate composite beam (upon: bending moment diagrams; down: deflection in the composite beam).

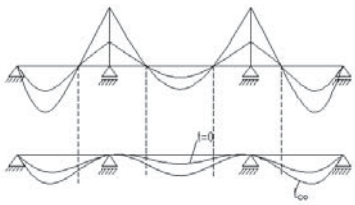

Figure 1. Influence of creep process

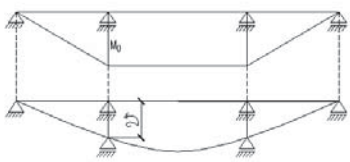

Figure 2. Settlement of Supports- creep process

The above considerations are, however, only valid for composite beams with the same cross sections over the entire length of the structure: i.e: EI = const. It is claimed that with different flexural stiffness of the structure along the length, the impact of creep is not so noticeable and that the studies made show slight differences, about 2% -3%, for examination: with or without the creep of the concrete. Quite differently, the question arises in the study of statically indeterminate composite steel-concrete structures subjected to uneven support,s settlement, shrinkage of concrete, temperature changes, under conditions of course, in the direct influence of concrete creep. Let's look at what is the behavior of a composite beam

when preloading the construction by settlement of the beam support. Let this decrease be with the value ϑ: which corresponds to the bending moment diagram: M_o (Fig.2), which show the influence of creep process in statically indeterminate composite beam by settlement of support:(upon: Bending moment diagrams; down: deflection in the composite beam). Let us reapply the rule, that the elastic line of the beam arosed after the creep of the concrete, will be similar to the elastic line resulting from the settlement of the support. The curvature of the elastic line as a result of creep of the concrete will be in linear relation to the curvature of the initial beam axis. In this case, the stressed state in the continuous beam, in the initially created elastic line, however, lacks "inflection points" which, on the one hand, allow to meet the criteria of resemblance to the elastic line as a result of creep the concrete and, on the other hand, to satisfy the condition of zero mutual rotation of two adjacent cross sections over the support. In order to fulfill these conditions, we must assume that the elastic line of the structure in the creep process of the concrete does not change. In other words, "in terms of" the concrete slab, the creep will be flowing, as she is connected to an endlessly rigidity steel disc. This formulation predetermines the decrease in the stress value in the beam (its relaxation), which is obtained therein as a result of the creep of the concrete. This analysis is a description of the problem associated with the opposite task of creep, namely: the relaxation of stresses in a concrete element. In such an element subjected to the deformation (resulting in certain stresses in it), which after insertion is maintained with special devices at its original values, a decrease in stresses in the concrete element begins to occur. In other words, stresses due to creep of concrete begin to decrease, i.e to relax. In a few examples of the subject, it is solve to creep into statically indeterminate beams, subjected to prestressing by settlement their supports. The solution was carried out using the reduced modulus of elasticity $E_{ci} = E_c / 1 + 1,1\varphi$. This approach leads to acceptable results for practice. We can also solve differential equations according to the (Dischinger theory,1939)[15], using an approximate solution that is based on the precondition for an endlessly stiff steel beam.

3.2. CALCULATION OF STATICALLY INDETERMINATE INTERNAL FORCES IN CONTINUOUS COMPOSITE BEAM

The main task in the calculation of continuous composite steel- concrete beams is the determination of statically indeterminate forces and moments. After their determination using the rules in structural mechanics, bending moments and shear forces can be determined in an arbitrary cross section of the beam. The exact calculation of the static indeterminate forces in the continuous beams (supporting moments), taking into account the rheological properties of the concrete, leads to a system of interdependent differential equations according to the theory of Dischinger or (Rüsch-Jungwirth,1976)[27]. By putting into practice the theory of the viscous-elastic body of (Maslov,1941)[20]-(Arutyunyan,1952)[3]–(Alexandrovskii,1966)[2]-(Trost-Zerna,1967)[29,32]-(Prokopovich,1978)[26] (Bažant,2000)[7,8], for concrete creep (see: EC 2), it is possible to develop a modern computational mathematical model based on the theory of the integral equations of Volterra and AAEMM of Bažant. On the basis of our experience and the algorithms developed for statically determinable composite beams, modern solutions to the problem so formulated can be obtained.

4. RELAXATION OF A SUPPORTS MOMENT IN COMPOSITE BEAM

4.1. GENERAL DATE

In statically indeterminate composite steel-concrete beams, a new equilibrium state arises in the case of a kinematic changes of the construction. This phenomenon can be observed by the settlement of an internal support, or by impact of forced mounting movement of the support in order to introduce prestressing in the building structure. Thanks to the visco-elastic character of the concrete, redistribution of the internal sectional forces in the beam has begun, for which a mechanic- mathematical model is constructed. It is known that in the case of composite beams, with a constant moment of inertia along its length, the new elastic line induced by the settlement of the support remains unchanged at time t. This fact has been proven in the study of a homogeneous concrete beam by settlement of the support. This practical example is evidenced by the presence of the second theorem by G. Colonnetti(1941)[12,13]. From the point of view of hereditary mechanics, it is a purely relaxing process in which the deformation introduced remains constant during the instantaneous settlement of the support. Thus, the deformation introduced in the composite beam construction creates in it a stress state, expressed by the internal forces in the composite structure. In the preserved form of the elastic line after the lowering of the support and the emergence of the new support moment $M_B = 3(EI/l^2).\Delta$: in time there is no change in the curvature of the steel beam, which unconditionally imposes the condition: $M_{st,\varphi} = 0$.

4.2. EXAMPLE ACCORDING EC4: CONTINUOUS BEAM BY THE SETTLEMENT OF AN INTERNAL SUPPORT

Let us try to apply this theory to a continuous composite steel-concrete beam with three supports, subjected to settlement of mean supports, in which we import by lowering of the mean support with $\Delta = 22,58cm$, a prestressing moment with a value: $M_0 = \Delta 3E_{st}I_i / l^2 = 11050kNm$ *(Fig.3).*

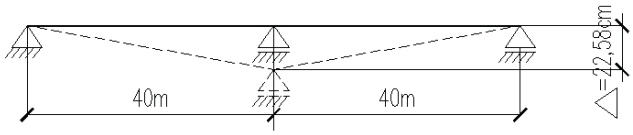

Figure 3. Statically indeterminate composite steel-reinforced concrete structures subjected to kinematic support,s settlement

Let,s a continuous composite steel- concrete beams with three supports has two equal openings equal to 40 m. The cross-section of the bridge beam is as follows in millimeters: bottom flange: -60x500; stem: -12x2000; upper flange: 20x300; thickness of reinforced concrete slab: 200mm; effective plate width: 3000 mm(Fig.4)[29].

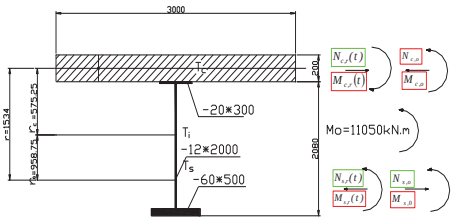

Figure 4: Composite beam

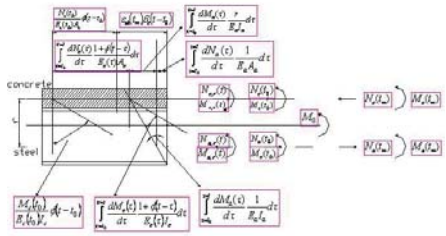

Figure 5. Mechanic-Mathematical model

To simplify the calculations, we assume that the cross section of the bridge is the same throughout its length. The geometric characteristics of the combined cross-section over time, excluding creep, are as follows: $I_i = 12425000cm^4$; $I_i = 200000cm^4$; $A_{st} = 600cm^4$; *n=6,0;* $W_{1,i} = 1104117cm^3$; $W_{2,i} = 1568448cm^3$; $W_{3,i} = 261441cm^3$; $W_{4,i} = 77426cm^3$. Using the knowledge to determine the particular cross-section forces in the individual components of the composite beam: concrete and steel, we obtain: $M_{st,0} = (I_{st} / I_i).M_0 = 317,25Mpm$. The result is the same as when calculating the settlement at the steel beam only, using the structural mechanics formula:. $M_0 = (\Delta.3E_{st}I_{st})/l^2 = 317,164Mpm$; $M_{c,0} = (I_c / nI).M_o = 2,964Mpm$; $N_{st,o} = -N_{c,o} = (A_{st}.r_{st} / I_i).M_0 = 511,58Mp$.

The preload stresses in the composite construction in the time: $(t = 0)$ will be equal to:

$\sigma_{1,c} = -110500000/1104117 = -100,079daN/cm^2$; $\sigma_{2,c} = -110500000/1568448 = -70,45daN/cm^2$;

$\sigma_{3,st} = -110500000/261441 = -422,65daN/cm^2$; $\sigma_{4,st} = 110500000/77426 = +1427,2daN/cm^2$;

As a result of creep, the moment of the support will relax, as in time $(t = \propto)$ and it will get the value: $M_{t=\propto} = M_{t=0}.I_{i,t=\propto} / I_{i,t=0} = 1105.7724369/12425000 = 686,956Mpm$ .When calculating the stresses in the time $(t = \propto)$, the cross-sectional resistance moments will be obtained *by the modulus ratio*:.*By:* $E_{ci} = E_c / 1 + 1,1\varphi = 350000/1 + 11.2 = 109375daN/cm^2$, $n = E_a / E_{c,i} = 19,2$

The geometric characteristics of the composite beams in the time $(t = \propto)$, taking into account creep, are as follows: $I_i = 7724369cm^4$;*n=19,20;* $W_{1,i} = 1337734cm^3$; $W_{2,i} = 1632178cm^3$; $W_{3,i} = 85009cm^3$; $W_{4,i} = 65944cm^3$.

$\sigma_{1,c} = -68695600/1337734 = -51,352daN/cm^2$ $\sigma_{2,c} = 68695600/1632178 = -42,088daN/cm^2$;

$\sigma_{3,st} = -68695600/88009 = -780,552daN/cm^2$; $\sigma_{4,st} = 68695600/65944 = 1041,726daN/cm^2$;

The results show that creep causes a significant reduction in the initial stressess (40%-48,0%) in the composite beam as a result of settlement of central support by 22,58 cm.

5. INVESTIGATION OF A CONTINUOUS BEAM BY SETTLEMENT OF THE SUPPORT USING INTEGRAL EQUATION OF VOLTERRA

In this paper the authors treat the investigation of the stress-strain state of a continuous composite beam by settlement of supports regarding the creep of concrete, which has been described with the functions of the "CEB-FIP" models code 2010. Till now, these functions have been applied in the EC4 to calculate the stress-strain state of composite constructions in time t using the "Effective Modulus Method"(EMM). In order to answer some of the issues discussed on the pages of the international journals about the advantages and disadvantages of the integral and algebraized concept of expressing the process of creeping the concrete over time as scientific concepts, a new mechano-mathematical integral model for determination of the forces in statically indeterminate composite steel-composite constructions, in case of settlement of the supports, taking into account the influence of concrete creep, according to the model of **"CEB-FIP" models code 2010.**

5.1. BASIC ASSUMPTION AND MATERIAL CONSTITUTIVE RELATIONSSHIP

The main hypotheses in the elastic analysis of composite steel-concrete sections with stiff (rigid) shear connectors are assumed as in the previous papers[22-25] as following: **a)** Bernoulli's concerning plane strain of cross-sections (Preservation of the plane cross section for the two elements considered compositely); **b)** No vertical separation between parts, in other words identical vertical displacement at the slab-beam interface is assumed; **c)** The connection system is distributed continuously along the axis of the beam; **d)** The cross sections are free to deform (because they belong to statically determinate structures); **e)** Concrete is not cracked $\sigma_c \leq (0.4 \div 0.5)R_c$; **f)** For the service load analysis of these cross sections the stress levels are small and, therefore , linear elastic behaviour may be assumed for the steel beam, in another words Hooke's law applies to steel as well as to concrete under short-time loads; **g)** For the concrete part, the strain can be considered as a linear functional of the previous stress history alone. This linearity implies the principle of superposition, which states that strain response due to stress increments applied at different times may be added. **h)** In the range of service ability loads concrete behaves in a way allowing to be treated as a linear viscoelastic body. **i)** According to our proposal, the influence of the development of the bending moment $M_{c,r}(t)$ in the concrete member, upon the redistribution of the normal force of concrete $N_{c,r}(t)$ can be neglected; **j)** For the service load analysis no slip and uplift effects occurs between the steel and concrete; **k)** A single theory of interaction ignoring shear lag effects is considered. With another word we can say that shear lag phenomenon of the deck slab is considered by using the appropriate effective slab width(Šmerda, Křistek, 1988)[28].

5.2. BASIC EQUATION OF EQUILIBRIUM

Let us denote both the normal forces and the bending moments in the cross-section of the plate and the girder after the loading in the time $t = 0$ with $N_{c,0}$, $M_{c,0}$, $N_{a,0}$, $M_{a,0}$ and with $N_{c,r}(t)$, $M_{c,r}(t)$, $N_{a,r}(t)$, $M_{a,r}(t)$ a new group of normal forces and bending moments, arising

due to creep and shrinkage of concrete. For a composite bridge girder with $J_c = \frac{A_c(nI_c)n}{A_s I_s} \leq 0.2$ according to the suggestion of (Sonntag 1951) we can write the equilibrium conditions in time *t* as follows:

$$N_{c,r}(t) = N_{a,r}(t); \tag{1}$$

$$M_{c,r}(t) + N_{c,r}(t)r = M_{a,r}(t); \text{which don't arise;} \tag{2}$$

Due to the fact that the problem is a twice internally statically indeterminate system, the equilibrium equations (1), (2) are not sufficient to solve it. It is necessary to produce two additional equations in the sense of compatibility of deformations of both steel girder and concrete slab in time *t* (Fig.5).

5.3. SOLVING THE PROBLEM WITH SETTLEMENT OF THE SUPPORT USING THE INTEGRAL EQUATIONS

Using the mathematical formulas for expressing creep according to the Eurocode 2 model, for determining of the internal forces in the statically indeterminate composite beam in time "t", a system of two independent integral equations of the second order of Volterra will be derived. The solution will be made using our knowledge of the study of the distribution of forces from the concrete slab to the steel beam, as by an constant external moment. The difference will only consist in the fact, that while in the cross-section of the simple beam the sum of the internal forces, during the creep process, will again be equal to the external constant bending moment, then by the settlement of support, the aroused external moment will relax, i.e. decreases. Its value will be obtained as the particular cross-section forces, aroused as a result of the creep of concrete, transformed into a bending moment, must be removed from the moment over the support, obtained from its settlement. The assignment of the task is as follows: the resulting momentum due to the sudden displacement of the support starts to decrease. For this purpose, the particular cross-section internal forces in concrete and steel are determined at time t = 0. They decrease in $t = \propto$ to a certain value. The values obtained are in equilibrium and it is possible to determine the resultant moment over the support in the beam. The same Volterra equations are recorded as in simple beams, taking into account the absence of a moment in the time over the support: $M_{st,\varphi} = 0$, because the task is considered in the light of the second Colonnetti theorem, which hypothesis is transformed into the adoption of an endlessly stiff steel beam, in the process of creep, that explane the proposition, that elastic line of the beam does not change, but only the affin is moved in relation to the initial shape, i.e. no change in curvature and which makes the condition for: $M_{st,\varphi} = 0$. Note: For the instant support settlement, account must be taken of the behavior of the system subject to the second Colonnetti, where the component**:** $M_{a,r}(t) = 0$**.** Considering the above, the relaxation in the instant displacement of the support can be covered by the emergence of a new, equilibrated group of cross-section forces in time $t = \propto$, as follow in next text.

5.4 DERIVING OF THE GENERALISED MECHANIC-MATHEMATICAL MODEL USING INTEGRAL EQUATION

Using the mentioned approach in [22-25] for constant elasticity module of concrete for assessment of normal forces $N_{c,r}(t)$ and bending moment $M_{c,r}(t)$ two linear integral Volterra equations of the second kind are derived.

$$N_{c,r}(t)=\lambda_N\int_{t_0}^{t}N_{c,r}(\tau)\frac{d}{d\tau}\left[\left[1+\phi_{RH}\beta(f_{cm})\beta(\tau)\beta_c(t-\tau)\right]\right]d\tau++\lambda_N(t)N_{c,0}\phi_{RH}\beta(f_{cm})\beta(t_0)\beta_c(t-t_0) \quad (3)$$

$$M_{c,r}(t)=\lambda_M(t)\int_{t_0}^{t}M_{c,r}(\tau)\frac{d}{d\tau}\left(\left[1+\phi_{RH}\beta(f_{cm})\beta(\tau)\beta_c(t-\tau)\right]\right)d\tau+\lambda_M(t)M_{c,0}\phi_{RH}\beta(f_{cm})\beta(t_0)\beta_c(t-t_0) \quad (4)$$

Where $\lambda_N=\left[1+E_cA_c/E_aA\right]^{-1}=0,375$. In each of these equations the functions: $N_{c,0}\phi_{RH}\beta(f_{cm})\beta(t_0)\beta_c(t-t_0)$; $M_{c,0}\phi_{RH}\beta(f_{cm})\beta(t_0)\beta_c(t-t_0)$; $\frac{d}{d\tau}\left[1+\phi_{RH}\beta(f_{cm})\beta(\tau)\beta_c(t-\tau)\right]$ are given and $\lambda_M=1$. The final result of the of the prestressed moment over the support after its relaxation is obtained by subtracting the work from the relaxed normal force multiplied by the shoulder to the center of gravity of the composite beam and the value of the relaxed moment in the concrete slab.

$$M(t=\infty)=M_0-N_{c,r}(t_\infty).r-M_{c,r}(t_\infty)=1105000-239862,3.1,534-2200,7=7348,50kNm.>6869,56kNm(EMM).$$

5.5 NUMERICAL METHOD OF SOLUTION

The integral equations (3) and (4) are weakly singular Volterra integral equation of the second kind. To solve (c) and (4) we use the method called product trapezoidal rule (Atkinson,1997)[4].

6. NUMERICAL EXMPLE

The two methods presented in the previous paragraph is now applied to a continuous composite steel-concrete beam with three supports, subjected to settlement of mean supports, whose cross section is shown in Fig. 4. The following parameters are chosen according EC2 model[1].

$h_0=2AC/u=\frac{2.3000.200}{3000+3000}=200\ mm$; $\beta_H=150\left[1+(1.2*80/100)^{18}\right]h_0/100+250=693,881<1500;$;

$\beta(f_{cm})=\left.\frac{5.3}{(f_{cm}/10)^{0.5}}\right|_{f_{cm}=30}=3.06$; $\beta(t_0)=\left.\frac{1}{0.1+(t_0)^{0.2}}\right|_{t_0=28}=0,488449545$; $\phi_{RH}=1+\left.\frac{1-RH/100}{0.46\sqrt[3]{(h_0/100)}}\right|_{RH=80,h_0=200}=1,3451$;

$\phi_0=\phi_{RH}\beta(f_{cm})\beta(t_0)=2,0104$; $\beta_c(36500-28)=0,9943$; $\phi_{t=36500}=\phi_0\beta_c(36500-28)=2,01.0,99=1,99=2,0$;

$\beta(\tau)=\frac{1}{0.1+(\tau)^{0.2}}$; $\beta_c(t-\tau)=\left[\frac{t-\tau}{\beta_H+(t-\tau)}\right]^{0.3}$.

$$E_c=3,5.10^4\ MPa,\ E_a=2,1.10^5\ MPa,\ A_c=6000\,cm^2,\ A_a=600\,cm^2, n=\frac{E_a}{E_c}=6,00$$

$$I_c=200000\,cm^4,\ I_a=3567300\,cm^4,\ r_c=57,525\,cm,\ r_a=95,875\,cm,\ r=153,4\,cm,$$

602

$$A_i=1600\,cm^2,\ I_i=12425000\,cm^4.M_0=11050\,kNm),\ N_{c,o}=N_{a,o}=\frac{A_a}{I_i}r_a.M_o=5115,90\,kN,$$

$$M_{c,o}=29,644\,kNm; M_{a,o}=\frac{I_a}{I_i}M_o=3172,528kNm,$$

6.1. NUMERICAL SOLUTION USING INTEGRAL EQUATION OF VOLTERRA

In fig. 6a,b it is shown the values of normal forces and bending moments in time $t \propto$ equal 100 years. A numerical method for time-dependent analysis of composite steel-concrete sections according EC2[1,18] models is develop using MATLAB code and numerical algorithm, which was successfully applied to a continuous composite steel-concrete beam. For a good accuracy of the time values, the numerical results are presented on logarithmic time scales. The choice of the length of time step(one day) of the proposed numerical algorithm is based on numerous numerical experiments with different steps. So we conclude that good results can be achieved from practical point of view with one day step. For our purpose we consider a period of about 36500 days(100 years).

7. STRESS HYSTORIES IN SUPPORT SECTION OF THE BEAM ACCORDING THE RECEIVED NUMERICAL RESULTS

In the concrete plate the normal component: $N_c(t_0)$ and the bending moment: $M_c(t_0)$ decrease by effect of creep. In the steel beam, only the normal component $N_a(t_\infty)$ arise, which increase the total negative stresses in the upper flange of the beam and decrease the total positive stress in the bottom flange of the beam. The decrease of the stresses in concrete slab is accompanied by a gradual migration of stresses from the concrete slab to the steel beam. Consequently, the stress history in the composite beam becomes the most interesting aspect of this study. These graphs also shows how important is the age of concrete by the process of the relaxation. Considering the value of the normal component: $N_c(t_0)$ and the bending moment: $M_c(t_0)$ we see that they decrease more for young concrete and a little for old one. Above all the influence of concrete age at loading time t_0 is significant only when its values are very low (i.e. with young concrete).

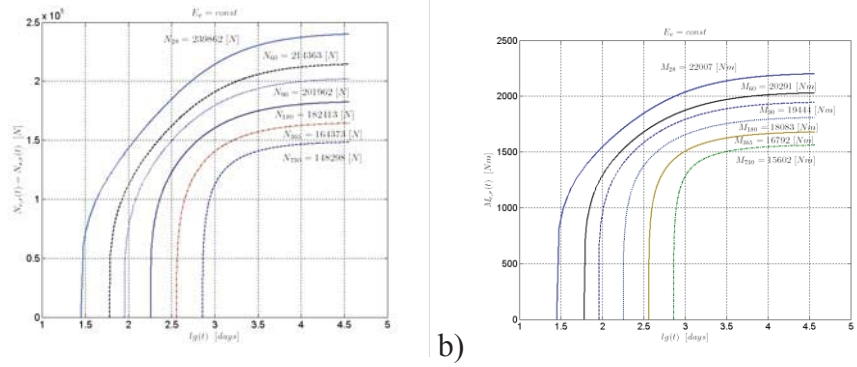

Figures 6a,b. Normal forces $N_{c,r}(t) = N_{a,r}(t)$ *,and bending moments* $M_{c,r}(t)$ *in time:* $t_\infty = 36528 - 337230$ *days, when relaxation begin in time* t_o *= 28, 60, 90, 180, 365 and 730 days*

7.1. STRESS HISTORIES IN SUPPORT SECTION OF THE BEAM ACCORDING RECEIVED NUMERICAL RESULTS

The stresses in upper and lower fibres of concrete plate and steel beam we obtain in time t_0 using the formulae which is known from the engineering discipline (strength of material) as follows(see point 4.2.1):

$$\sigma_{c,0}^{up} = -(M_0 / nI_i).z_{c,up} = -100,08 daN/cm^2, \quad \sigma_{c,0}^{down} = -(M_0 / nI_i).z_{c,doun} = -70,442 daN/cm^2$$

$$\sigma_{a,0}^{up} = -(M_0 / I_i).z_{a,up} = -422,657 daN/cm^2 \quad \sigma_{a,0}^{down} = (M_0 / I_i).z_{a,doun} = 1427,16 daN/cm^2$$

The stresses in upper and lower fibres of concrete plate and steel beam we obtain in time t_∞ ,during the creep process, using the formulae as follows:

$$\sigma_{c,r}^{up}(t_\infty) = \frac{N_{c,r}(t)}{A_c} + \frac{M_{c,r}(t)}{I_c} z_{c,up} = \frac{239862,3}{6000} + \frac{220070}{200000}.10 = 50,98055 daN/cm^2 \; ; \; \sigma_{c,r}^{down}(t_\infty) = \frac{N_{c,r}(t)}{A_c} - \frac{M_{c,r}(t)}{I_c} z_{c,down} = \frac{239862,3}{6000} - \frac{220070}{200000}.10 = 28,97355 daN/cm^2$$

$$\sigma_{a,r}^{up}(t_\infty) = -\frac{N_{a,r}(t)}{A_a} = -\frac{239862,3}{600} = -399,7705 daN/cm^2 \; ; \; \sigma_{a,r}^{down}(t_\infty) = -\frac{N_{a,r}(t)}{A_a} = -\frac{239862,3}{600} = -399,7705 daN/cm^2$$

The stresses in upper and lower fibres of concrete plate and steel beam we obtain in time t_∞ , after finishing of the creep process, using the formulae as follows:

$$\sigma_c(t_\infty)^{up} = -100,08 + 50,98055 = -49,09945 daN/cm^2 \; ; \; \sigma_c(t_\infty)^{down} = -70,442 + 28,973 = -41,46845 daN/cm^2$$

$$\sigma_a(t_\infty)^{up} = -422,657 - 399,7705 = -822,4275 daN/cm^2 \; ; \; \sigma(t_\infty)^{down} = 1427,16 - 399,7705 = 1027,3895 daN/cm^2 ;$$

where: z_c and z_a – distance from the mass center of concrete plate and steel beam to their upper and lower fibres.

8. CONCLUSION

The results obtained by numerical method, using the integral equation of Volterra, on the basis of the theory of the viscoelastic body of Maslov- Arutyunyan–Trost-Bažant and according the creep functions, suggested by the "CEB-FIP" models code 2010[1], are comparable with the results obtain by the the EMM of the EC4, based on the Dischinger proposal(see tables: 1 and 2).

Table 1. Level of stresses of composite beams according Integral equation of Volterra and CEB MC90-99

Stress in time t_0	t_0 = 28 days	*Stress in time* t_∞	t_∞ = 36500 days
M_0 *(kNm)*	*11050*	M_0 *(kNm)*	*11050*
$n_0 = \frac{E_a}{E_{cm}}$	*6,00*	$n_L = n_0(1+\psi_L\phi_t)$ $\psi_L = 1,1$	*19,20*
$\sigma_c^{up} = -\frac{N_{c,0}}{A_{c,0}} - \frac{M_{c,0}}{I_c} z_{c,up}$ *(MPa)*	*-10,0085*	$\sigma_{c,r}^{up}(t_\infty) = -\frac{N_{c,r}(t)}{A_c} + \frac{M_{c,r}(t)}{I_c} z_{c,up} = 5,098055$ *MPa)*	*-4,909945*

Continuous of Table 1. Level of stresses of composite beams according Integral equation of Volterra and CEB MC90-99

$\sigma_c^{down} = -\frac{N_{c,0}}{A_{c,0}} + \frac{M_{c,0}}{I_c} z_{c,d}$ (MPa)	-7,0441	$\sigma_{c,r}^{down}(t_\infty) = -\frac{N_{c,r}(t)}{A_c} - \frac{M_{c,r}(t)}{I_c} z_{c,d} = 2,897355$ (MPa)	-4,146845
$\sigma_a^{up} = \frac{N_{a,0}}{A_{a,0}} - \frac{M_{a,0}}{I_a} z_{a,up}$ (MPa)	-42,2663)	$\sigma_{a,r}^{up}(t_\infty) = -\frac{N_{a,r}(t)}{A_a} = -39,97705$ (MPa)	-82,24275
$\sigma_a^{down} = \frac{N_{a,0}}{A_{a,0}} + \frac{M_{a,0}}{I_a} z_{a,d}$ (MPa)	143,20)	$\sigma_{a,r}^{down}(t_\infty) = -\frac{N_{a,r}(t)}{A_a} = -39,97705$ (MPa)	102,73895

Table 2. Level of stresses of composite beams according EC4 and EMM of Dischinger

Stress in time t_0	t_0 = 28 days	Stress in time t_∞	t_∞ = 36500 days
M_0 (kNm)	M_0 =11050	M_∞ (kNm)	M_∞ =6869,56
$n_0 = \frac{E_a}{E_{cm}}$	6,00	$n_L = n_0(1+\psi_L\phi_t)$ $\psi_L = 1,1$	19,20
$\sigma_c^{up} = M / W_{i,y,c,up} / n_0$ (MPa)	-10,008	$\sigma_c^{up} = M / W_{i,y,c,up} / n_L$ (MPa)	-5,1352
$\sigma_c^{down} = M / W_{i,y,c,d} / n_0$ (MPa)	-7,0442	$\sigma_c^{down} = M / W_{i,y,c,d} / n_L$ (MPa)	-4,2088
$\sigma_a^{up} = M / W_{i,y,a,up}$ (MPa)	-42,2663	$\sigma_a^{up} = M / W_{i,y,a,up}$ (MPa)	-78,0552
$\sigma_a^{down} = M / W_{i,y,a,d}$ (MPa)	143,20	$\sigma_a^{down} = M / W_{i,y,a,d}$ (MPa)	104,1726

,

ACKNOWLEDGMENTS

The authors would like to thank to "Ministry of Education" in Sofia for Research Foment.

REFERENCES

[1] ACI Committee 209,: Guide for Modelling and Calculating Shrinkage and Creep in Harden Concrete(ACI 209.2R-08)," American Concrete Institute, Farmington Hills, MI, 2008,45pp.

[2] Alexandrovskii S.V.: Analysis of Plain and Reinforced Concrete Structures for Temperature and Moisture Effects (with Account of Creep) (in Russian), Stroyizdat, Moscow, 1966, 443 pp.

[3] Arutyunian N. Kh.: Some Problems in the Theory of Creep, Techstroizdat, Moscow, (French transl., Eyrolles 1957, English transl., Pergamon Press 1966), 1952, 319 pp.

[4] Atkinson E. K.: The Numerical Solution of Integral Equations of the Second Kind, Cambridge University Press, Cambridge, UK, 1997, 572 pp.

[4] Bažant Z. P.: Theory of Creep and Shrinkage in Concrete Structures: A Précis of Recent Developments, Mechanics Today, Vol.2, Pergamon Press, New York, 1975, pp. 1-93.

[5] Bažant Z. P.:, Editor , Mathematical Modeling of Creep and Shrinkage of Concrete, John Wiley & Sons, 1988, 459 pp.

[6] Bažant Z. P., Xi, Y. P., Baweja, S. and Carol, I.: Preliminary guidelines and recommendations for characterizing creep and shrinkage in structural design codes, Proceedings. of the 5th International RILEM Symposium on Creep and Shrinkage of Concrete (Barcelona), Z. P. Bažant and I. Carol eds., E&FN Spon, London, UK, 1993, pp.805-829.

[7] Bažant Z. P. and Baweja, S.: Creep and Shrinkage Prediction Model for Analysis and Design of Concrete Structures: Model B3, Adam Nevile Simposium : Creep and Shrinkage –Structural design Effects, SP-194, A. Al-Manasereer, ed., American Concrete Institute, Farmington Hills, MI, 2000, pp.1-84.

[8] Bažant Z. P.: Criteria for Rational Prediction of Creep and Shrinkage of Concrete, Adam Neville Symposium: Creep and Shrinkage – Structural Design Effects, SP-194, A. Al-Manaseer ed., American Concrete Institute, Farmington Hills, MI, pp. 2000, 237-260.

[9]Branson D. E.: 1977, Deformation of Concrete Structures, McGraw Hill Book Co., New York, 1977, 546 pp.

[10] Comité Européen de Normalisation (CEN): Eurocode 2: Design of Concrete Structures-Part 1-1: General Rules and Rules for Buildings, European Standard BS EN 1992-1-1: 2004, European Committee for Standardization (CEN), Brussels, Belgium, 2004a, 227 pp.

[11] Comité Européen de Normalisation (CEN): Eurocode 4: Design of Composite Steel and Concrete Strucures-Part 1-1:General Rules and Rules for Buildings, European Standard BS EN 1994-1-1: 1994, European Committee for Standardization (CEN), Brussels, Belgium, 2004b, 118 pp.

[12] Chiorino M. A., Sassone M., Bigaran D., Casalegno C.: Effects of Creep and Shrinkage on the Serviceability Limit State, Proceedings of Symposium, Concrete Sructures-Stimulators of Development, Dubrovnik, May, 2007, pp.623-632.

[13] Chiorino M. A.: Analysis of structural effects of time-dependent behavior of concrete an internationally harmonized format, Proceedings of III All-Russia Int. Conference "Concrete and Reinforced Concrete –Glance in Future", Moskow,12-14 May, 2014, Russian ,pp. 324-337, English, 2014, pp. 338-350.

[14] Cosenza E., Zandonini R.: Composite Construction. Structural Engineering Handbook, C. Wai-Fah,ed.,CRC Press, Boca Raton, FL., 1999, pp. 1-122.

[15] Dischinger F.: Elastische und Plastische Verformungen der Eisenbetontragwerke und Insbesondere der Bogenbrücken, Der Bauingenieur, Vol.20, 1939, pp. 53-63, 286-94, 426-37, 563-72.

[16] Dujmović D., Androić B., Lukačević I.: Composite structures according to Eurocode 4, Wilhelm Ernst & Sohn Verlag fur Architektur und Technische Wissenschaften, GmbH& Co. KG, Berlin, Germany, 2015,890 pp.

[17] Folić R., Zenuvović D.: Composite Structures of Steel and Concrete, Faculty of Technology Science, Novi Sad, Serbia, 2009, 362 pp.

[18] Jirasek M., Bažant Z. P.: Inelastic Analysis of Structures, Wiley and Sohns, LTD, Hoboken, NJ, 2002, 732 pp.

[19] Johnson R. P.: Composite Structures of Steel and Concrete, Blackwell, Oxford, UK, 2004, 230 pp.

[20] Maslov G. N.: Thermal Stress States in Concrete Masses, with Account of Concrete Creep (in Russian), Izvestia NIIG, 28, 1941, pp 175-188.

[21] Oehlers D., Bradford M.: Elementary behavior of composite steel and concrete stuctural members, Oxford, Butterworth-Heinemann, 1999, 279 pp.

[22] Partov D., Kantchev V.: Time-dependent analysis of composite steel-concrete beams using integral equation of Volterra, according EUROCODE-4, Engineering Mechanics, V. 16, No 5, 2009, pp. 367-392.

[23] Partov D., Kantchev V.: Numerical analysis of composite steel-concrete section using integral equation of Volterra, Central. European Journal of Engineering, Vol.1, No.3, pp. 2011a, 316-331.

[24] Partov D., Kantchev V.: Level of creep sensitivity in composite steel-concrete beams, according to ACI 209R-92 model, comparison with EUROCODE-4(CEB MC90-99), Engineering Mechanics, Vol. 18, No. 2, 2011b, pp. 91-116.

[25] Partov D., Kantchev V.: Gardner and Lockman model in Creep analysis of composite steel-concrete section, ACI Structural Journal, Vol.111, No. 1, (January-February), 2014, pp. 59-69.

[26] Prokopovich I. E.: Fundamental study on application of linear theory of creep, (In Russian),Vyssha shkola, Kiev, 1978, 143 pp.

[27] Rüsch H., Jüngwirth D.: Berücksichtigung der Einflüsse von Kriechen und Schwinden des Betons auf das Verhalten der Tragwerke, Werner Verlag, 1976, Düsseldorf.

[28] Šmerda Z., Křistek Vl.: Creep and Shrinkage of Concrete Elements and Structures, Elsevier, New York, 1988, 296 pp.

[29] Trost H.: Zur Berechnung von Stahlverbundträgern im Gebrauchszustand auf Grund neuerer Erkentnisse des viskoelastishen Ferhaltens des Betons, Der Stahlbau, Vol.37, H11, 1968, pp.321-331.

[30] Vayas I., Iliopoulos A.: Design of steel-concrete Composite Bridge to Eurocodes, CRC Press, Taylor&Francis Group, Boca Raton, FL., 2014, 576 pp.

[31] Wang C. Y.: Steel and Composite Structures, Behaviour and Design for Fire Safety,Taylor and Francis Group, London, UK, 2002, 352 pp.

[32] Zerna W., Trost H.: Rheologische Beschreibung des Werkstoffes Beton, Beton und Stahlbetonbau, Vol. 62, H.7, 1967, pp. 165-170.

ДГКС Друштво грађевинских конструктера Србије
ASES Association of Structural Engineers of Serbia
S-91
15. KONGRES
6-8. 9. 2018. Zlatibor

Isidora Jakovljević[1], Saša Kovačević[2], Nenad Marković[3]

ELASTIČNA KRITIČNA SILA PLOČA I LIMENIH NOSAČA POD DEJSTVOM LOKALIZOVANOG OPTEREĆENJA

Rezime:

Određivanje elastične kritične sile (sile izbočavanja) predstavlja važan elemenat u određivanju granične nosivosti limenih nosača prema Evrokodu za proračun čeličnih konstrukcija. U radu se daje analiza kritične sile izolovane ploče koja odgovara rebru I nosača za različite granične uslove kao i kritične sile samog I nosača. Dati su zaključci o njihovoj vezi. Upoređene su eksperimentalno određene granične nosivosti I nosača sa vrednostima prema Evrokodu, za modele korišćene u ovoj analizi.

Ključne reči: izbočavanje ploča, izbočavanje I nosača, lokalizovano opterećenje

BUCKLING OF PLATES AND PLATE GIRDERS SUBJECTED TO PATCH LOAD

Summary:

The determination of the elastic critical load (buckling load) is an important element of the assessment of the ultimate load of plate girders. An analysis of the critical load of a plate corresponding to the web of an I-girder for different boundary conditions and the critical load of the I-girder itself is given in the paper. Conclusions regarding their correspondence are given. Also, experimentally determined ultimate loads of I-girders are compared with values according to Eurocode for the models used in this analysis.

Key words: plate buckling, plate girder buckling, patch loading

[1]*PhD student, teaching assistant, University of Belgrade, Faculty of Civil Engineering, isidora@imk.grf.bg.ac.rs*
[2]*M.Sc., School of Mechanical and Materials Engineering, Washington State University, Pullman, WA 99164, USA, sasa.kovacevic@wsu.edu*
[3]*PhD, assistant professor, University of Belgrade, Faculty of Civil Engineering, nenad@grf.bg.ac.rs*

1. INTRODUCTION

The stability problems and ultimate load behavior of steel plate girders have attracted a lot of attention during the last decades. The behavior of the plate girder (welded I-girder) subjected to patch load or partially distributed load on the flange in the plane of a web, without a vertical (transverse) stiffener bellow the load was also intensively investigated. This problem has got the importance with a general trend to avoid vertical stiffeners except at supports and also in the case of moving loads. Except for crane girders loaded by crane wheels, a remarkable realistic load case in which this situation arises is the launching phase of multi-span steel plate girder bridges during construction over temporary or permanent supports.

In the analysis of the behavior of the patch loaded girder the attention is directed towards the distribution of the local direct stresses under the load in the web, the elastic critical load of the web panel and the ultimate load of the girder. For the development of design procedures, the ultimate load is of a great importance. The research workers in many countries have investigated theoretically and experimentally this problem over the last fifty years. Even an increasing number of experimental results and laborious theoretical work has not offered a complete insight into the problem and intensive researches in various segments of this problem are still ongoing worldwide.

In the initial phases of investigations, attempts were made to relate the ultimate load to the elastic critical (buckling) load [1], [2], [3]. Very soon it was found that generally, it was not possible. Also, analytical procedures were not successfully applied, as the problem is very complex, depending on many interrelated parameters. As a corollary, a majority of the suggested solutions were of empirical nature, based on experimental researches. The development of computer programs based on the finite element (FE) method and increased capabilities of computers enabled the development of "numerical experiments" that are nowadays widely applied.

With the development of Eurocodes for the design of civil engineering structures, a new approach was applied to harmonize solutions of the patch load problem with other stability problems. The main points in the determination of the ultimate patch load are elastic critical load, yield load, and resistance function. The determination of the elastic critical (buckling) load got again the importance, as it is needed for the determination of the slenderness parameter.

The solution applied in Eurocode for steel structures [4] uses simplified expressions for the buckling coefficients. Together with some other simplifications and uncertainties, it gives very often rather conservative values for the ultimate load.

The investigation of patch load is carried out at the Faculty of Civil Engineering University of Belgrade within an international cooperation, initially in the eighties, with the University of Cardiff (with T. M. Roberts) and with the Czech Academy of Sciences in Prague (with M. Skaloud), and in last period with the Faculty of Civil Engineering University of Montenegro in Podgorica (with D. Lucic and his collaborators).

The results obtained in the experimental research [5] compared with the procedures applied in Eurocode had shown [6] significantly conservative results given by Eurocode. An attempt is made in this paper to give some improvements to that procedure.

Elastic critical load for an isolated web plate for different boundary conditions is compared with an elastic critical load of an I-girder. Moreover, the experimentally determined ultimate

load is compared with the procedure as currently given in Eurocode, as well as with the suggested correction for the determination of the elastic critical load (that includes taking into account the distribution length of an applied patch load).

Nowadays, numerical analysis techniques are widely used in research involving structural steel and in analyses and designs of steel structures and elements. The FE method based numerical analysis is the most popular computational tool in this field and it has been successfully applied in many papers regarding the critical load of plate girders under different loading conditions. The commercial multi-purpose FE analysis software Abaqus was used for the numerical analysis [7]. In order to get a better insight into the problem, geometry and loading of the girders were considered according to those applied in the accompanying experimental research [5].

2. ELASTIC CRITICAL LOAD

Introductory it was stated that the purpose of this paper is the comparison of the elastic critical loads for an isolated web plate, varying boundary conditions, with critical loads of an I-girder. The two plates schematically presented in Figure 1, labeled as *Model 1* with an aspect ratio a/h_w=1 and *Model 2* with an aspect ratio a/h_w=2 (a=1000 mm), were investigated. The web plate thickness was t_w=4 mm. The length of an applied uniform load s_s was varied. The degree of freedom 2 is only constrained in the vertical edges while the degree of freedom 3 is constrained in all edges. Three different cases were analyzed: (a) simply supported plate with no additional constraints, (b) plate simply supported on the vertical and clamped on the horizontal edges (degree of freedom 4 is constrained), (c) plate clamped along all edges (degree of freedom 5 is constrained in the vertical edges and the degree of freedom 4 in the horizontal edges). For the sake of brevity, through the rest of the paper, these cases will be marked as SS, CS, and CC, respectively. In the same vein, the two models of an I–girder according to the previously described Model 1 and Model 2 are displayed in Figure 2. The flange width and thickness was set to 120 mm and 8 mm, respectively. The boundary conditions are according to the experimental procedure described in [5]. The considered material for all cases is homogenous with an elastic modulus of E=210 GPa and Poisson's ratio of ν=0.3.

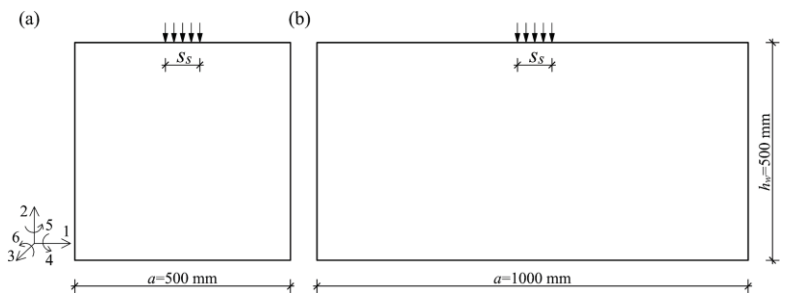

Figure 1 – Plate under patch load: (a) Model 1; (b) Model 2

For the FE analysis, a general-purpose four-node quadrilateral shell element with reduced integration and six degrees of freedom per node S4R from the Abaqus element library was

used. According to the mesh convergence study performed only on the isolated web plate of Model l, the adopted finite element size is 5 mm for all numerical runs. The variation of the buckling coefficient due to change of finite element size in the case of Model 1 for a simply supported plate is graphically presented in Figure 3(a). The results of the calculated elastic critical load are presented using the non-dimensional buckling coefficient k_f and tabulated in Table 1 and 2 for Model 1 and Model 2, respectively. Conclusively, it may be stated that they show a good agreement with the corresponding values found in the literature [8–14]. The buckling coefficient depends on boundary conditions, loading type and an aspect ratio a/h_w. On the other hand, it is not influenced by plate thickness or material properties. However, for a different plate thickness applied on a simply supported plate of Model 1, a slight variation in the results could be noticed, as charted in Figure 3(b).

Another sensitivity of the buckling coefficient is pictured in Figure 4. A simply supported plate model is analyzed when the degree of freedom 2 was constrained along the vertical edges, *i.e.* the edge support is set as previously described, and point supports are applied in the lower corners of the plate. In the case of Model 2, this change of boundary conditions does not affect the value of k_f. On the contrary, in the case of Model 1 and a longer uniform load, the difference in the results comes up to 25 %. Expectedly, the boundary conditions do not play a decisive role for higher aspect ratios since the applied load is localized and for an aspect ratio $a/h_w \geq 2$ their influence is negligible.

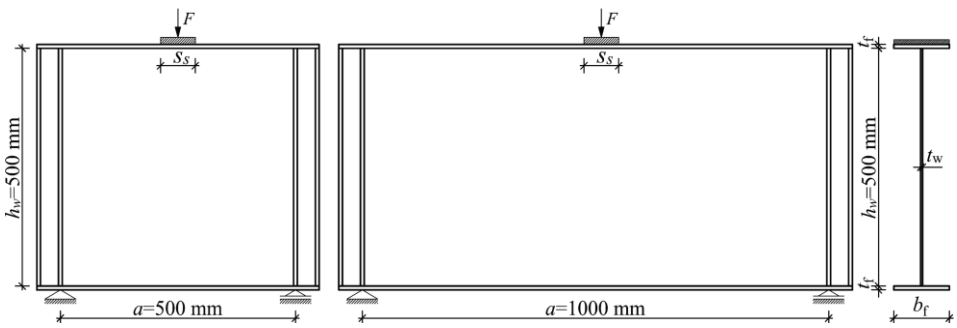

Figure 2 – Model 1 and Model 2 for I–girders

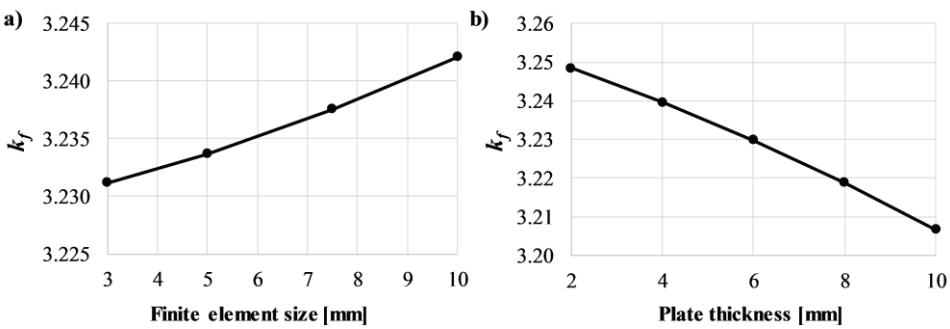

Figure 3 – Variation of the buckling coefficient due to change of: (a) FE size; (b) plate thickness

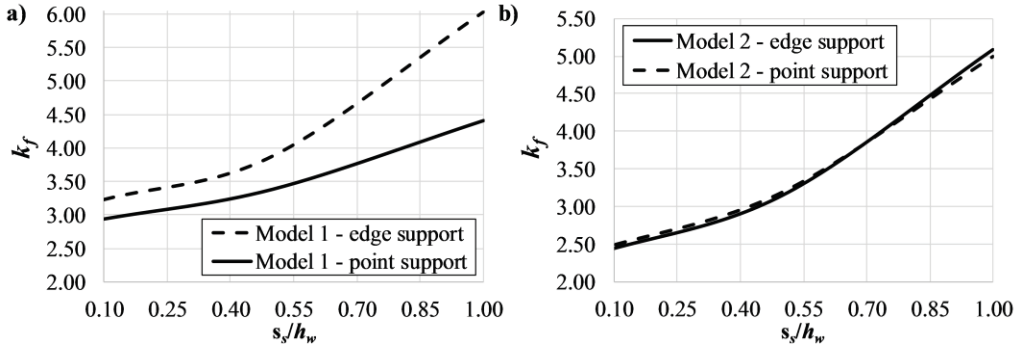

Figure 4 – Buckling coefficient for the plate supported on the vertical edges and for the plate with point supports in the corners

3. RESULTS AND DISCUSSION

The aim of this chapter is to highlight the obtained numerical results of the buckling coefficient considering an isolated web plate and I–girder. The results for all described numerical models are listed and discussed thoroughly. Furthermore, a new model for the determination of the buckling coefficients, as a function of patch load length, is presented. The purpose of the proposed model is to improve the ultimate load calculated using the procedure given in Eurocode. At the end of this section, detailed conclusions are given along with recommendations for further investigations.

Table 1 and Table 2 shows a comparison summary of the numerical results and the buckling coefficients obtained by Eurocode while a graphical representation is shown in Figure 5. One can instantaneously see that the SS plate for both models and for all lengths of an applied patch load gives extremely low values of the critical loads. Introducing the clamped constraint on the horizontal edges (CS plate) the k_f values are improved but still too far below the k_f of the I–girder, especially for Model 1.

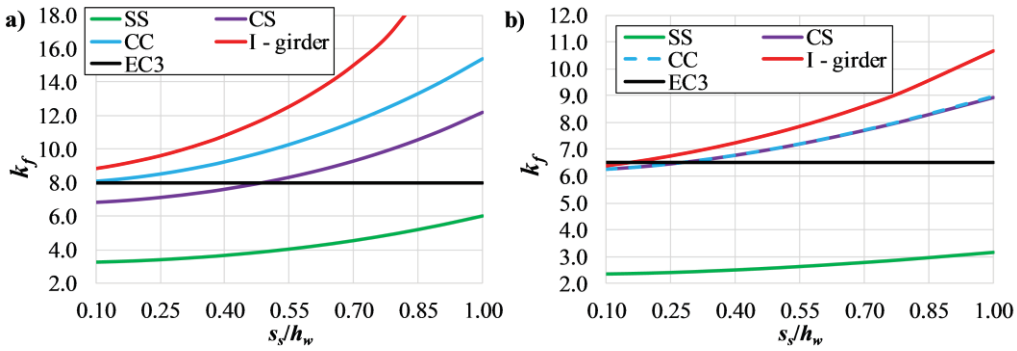

Figure 5 – Comparison of the buckling coefficient for: (a) Model 1; (b) Model 2

On the other hand, it can be noticed that the buckling coefficients for the I–girder are well-captured with the CC plate for shifted values of s_s. Consequently, it may be possible to obtain the buckling coefficient of plate girders by considering a clamped web plate. It is interesting to speculate on whether the values for the CC plate can be related to the values of an I-girder for different geometries and how they are connected.

It is noteworthy to observe another interesting point regarding the clamped boundary conditions for large values of s_s. It is clear from Figure 5 that the rigid transversal stiffeners (see Figure 2) influence the buckling coefficient more than clamped constraint whereas for small values of s_s their influence is not present since the load is localized. Additionally, the clamped constrain on the vertical edges (the difference between the CC and CS plate) reveals the fact that constrained rotations along these edges do not have an influence on the buckling coefficient for an aspect ratio $a/h_w \geq 2$, as stated before. Conversely, they influence the buckling coefficients with a uniform factor for an aspect ratio $a/h_w=1$ (Model 1) for all values of s_s. A further parametric study should be made in order to make an airtight conclusion about this boundary condition and its influence on the buckling coefficient.

Table 1 – Buckling coefficients for different boundary conditions for Model 1

s_s [mm]	s/a	s/h_w	k_f				
			SS	CS	CC	I–girder	EC3
0	0.00	0.00	3.20	6.78	8.00	8.61	8.00
25	0.05	0.05	3.21	6.80	8.02	8.69	8.00
50	0.10	0.10	3.23	6.85	8.10	8.85	8.00
75	0.15	0.15	3.27	6.92	8.21	9.06	8.00
100	0.20	0.20	3.32	7.02	8.35	9.32	8.00
125	0.25	0.25	3.38	7.13	8.53	9.61	8.00
150	0.30	0.30	3.46	7.27	8.74	9.96	8.00
175	0.35	0.35	3.54	7.44	8.98	10.36	8.00
200	0.40	0.40	3.64	7.62	9.26	10.81	8.00
250	0.50	0.50	3.88	8.07	9.91	11.90	8.00
300	0.60	0.60	4.18	8.62	10.70	13.27	8.00
350	0.70	0.70	4.54	9.29	11.64	15.01	8.00
400	0.80	0.80	4.97	10.10	12.73	17.37	8.00
450	0.90	0.90	5.47	11.05	13.98	21.60	8.00
500	1.00	1.00	6.04	12.17	15.41	31.95	8.00

As a further comparison between the I-girder and CC plate, the first buckling mode for Model for these two cases is juxtaposed. It can be seen in Figure 6 that the buckled shape for Model 1 for an isolated plate subjected to patch load length s_s=210 mm and the buckled shape of an I- girder subjected to patch load length s_s=100 mm correspond to each other, both numerically and graphically, due to the fact that the flange plate enables spreading the loading length into the web. Therefore, based on these results for the CC plate and I–girder, we can conclude that the buckling coefficients of an I-girder under patch loading can be determined considering an isolated web plate. For instance, for this particular case of Model 1 of the web plate and I–girder the values of buckling coefficient are shifted by patch load length of 115 mm for the cases $s_s/h_w \leq 0.5$ and approximately equal, *i.e.* $k_{f,girder}(s_s)=k_{f,plate}(s_s+115\text{ mm})$. Supposedly, this approximation is influenced by aspect ratio and for Model 2 the shifted length is notably less (approximately around 60 mm). It must be emphasized that the shifted lengths are not equally distributed for all patch load lengths and in order to draw a better conclusion about their influence, further analyses considering smaller patch load lengths rates should be performed.

Table 2 – Buckling coefficients for different boundary conditions for Model 2

s_s [mm]	s/a	s/h_w	k_f				
			SS	CS	CC	I–girder	EC3
50	0.05	0.10	2.37	6.24	6.25	6.38	6.50
100	0.10	0.20	2.40	6.36	6.37	6.61	6.50
150	0.15	0.30	2.45	6.54	6.54	6.90	6.50
200	0.20	0.40	2.51	6.77	6.77	7.23	6.50
250	0.25	0.50	2.59	7.04	7.04	7.63	6.50
300	0.30	0.60	2.68	7.35	7.35	8.08	6.50
350	0.35	0.70	2.78	7.70	7.71	8.60	6.50
400	0.40	0.80	2.90	8.08	8.09	9.20	6.50
500	0.50	1.00	3.15	8.93	8.96	10.65	6.50
600	0.60	1.20	3.44	9.86	9.94	12.56	6.50
700	0.70	1.40	3.78	10.85	11.03	15.17	6.50
800	0.80	1.60	4.16	11.92	12.24	19.00	6.50
900	0.90	1.80	4.60	13.11	13.56	25.20	6.50
1000	1.00	2.00	5.08	14.47	15.00	47.26	6.50

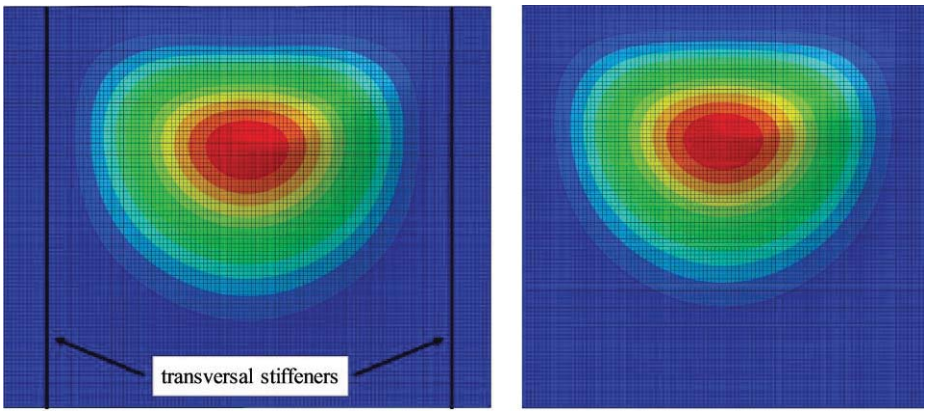

Figure 6 – First buckled shape for Models 1: (a) I–girder; (b) isolated web plate

According to our analysis of the buckling coefficients for the I–girder, a close fit can be established for the k_f values using high order polynomials. However, keeping in mind the simplicity of the design procedure in Eurocode a first or second order polynomial is desirable. For example, the following general form gives a good approximation for the k_f values of the I–girder:

$$k_f = \alpha s_s^2 + \beta s_s + \gamma$$

where:

α, β and γ are unknown constants. For these investigated cases of the I–girders, the constants are α=4.7·10^{-5}, β=2·10^{-3}, γ=8.7, α=1.8·10^{-5}, β=0 and γ=6.5 for Model 1 and Model 2, respectively. A graphical comparison of the numerically obtained buckling coefficient of the and I–girder and coefficients approximated by the proposed expressions is shown in Figure 7. One should bear in mind that these values for the constants are determined only for the analyzed geometries. A detailed parametric study is necessary in order to obtain a general expression as a function of geometric parameters, *i.e.* thickness of the web and flange, flange width, etc.

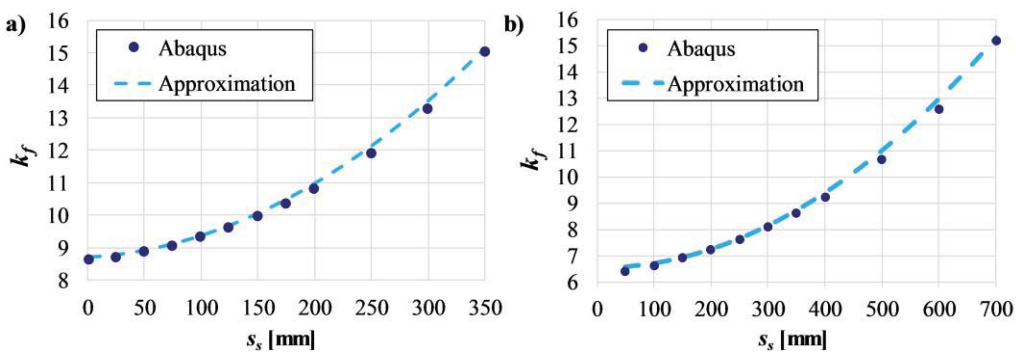

Figure 7 – Abaqus vs. proposed expressions for the k_f values for: (a) Model 1; (b) Model 2

Values of the experimentally obtained ultimate loads and corresponding ultimate loads according to the procedure applied in Eurocode with k_f given in Eurocode (not dependent on the loading length s_s) are pictorially compared in Figure 8. Noticeably, the ultimate loads calculated by Eurocode are considerably lower than the experimentally obtained ultimate loads and the difference is more pronounced for higher patch load lengths.

In order to improve the results from Eurocode, we propose a new model for the determination of k_f. The model includes the calculation of the buckling coefficient as a function of patch load length while the procedure for obtaining the ultimate load is the same as in Eurocode. The new values obtained by this improved model are also presented in Figure 8. One can immediately see that better values are produced by the proposed model. A salient feature of the suggested model is a simple correction regarding only the buckling coefficient while the ultimate loads are improved, especially for longer patch load lengths. However, in order to elucidate the influence of the length of patch load on buckling coefficient and to make a straightforward connection with an isolated web plate considering different geometries of an I–girder, further analyses are required.

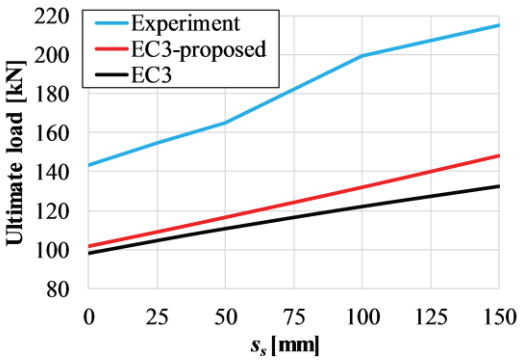

Figure 8 – Comparison of the ultimate load by different approaches

In a nutshell, the presented model enabled a fruitful background for parametric analyses and producing an erroneous number of numerical tests that can be used, in order to better determine the ultimate loads of plate girders using the buckling coefficients. Furthermore, since the ultimate loads are still too far below the experimentally obtained ultimate loads, the present model can be also exploited in order to improve different elements currently present in the design procedure in Eurocode, *i.e.* the effective loaded length.

REFERENCES

[1] Lagerqvist, O.: Patch loading–Resistance of steel girders subjected to concentrated forces, Ph.D. Thesis, Department of Civil and Mining Engineering, Division of Steel Structures, Luleå University of Technology, 1994:159D, Luleå, 1995.

[2] Girkmann K.: Stability of the webs of plate girders taking account of concentrated loads, International Association of Bridge and Structural Engineering, Final Report, 1936, 610-614.

[3] Zetlin L.: Elastic instability of flat plates subjected to partial edge loads, Proceedings of American Society of Civil Engineers (ASCE), Vol. 81, No. 795, 1955, 1-24.

[4] Eurocode 3 (EC3): Design of steel structures. Part 1–5: General rules–Supplementary rules for planar plated structures without transverse loading. EN1993-1-5; 2006

[5] Marković N.: Izbočavanje limenih nosača pod dejstvom lokalnog opterećenja, Doktorska disertacija (Ph.D. Thesis in Serbian), Univerzitet u Beogradu, Građevinski fakultet u Beogradu, 2003.

[6] Perović M., Marković N., Ćorić B.: Uticaj lokalnog opterećenja limenih nosača i novi propisi za proračun konstrukcija u Evropi, Zbornik radova, Internacionalni naučno-stručni skup Gradjevinarstvo–nauka i praksa, Žabljak, 20-24 februara 2006, Knjiga 1, 495-500

[7] Abaqus Simulia. Dassault Systemes. 2016

[8] White R. M, Cottingham W.: Stability of plates under partial edge loadings, Proceedings of American Society of Civil Engineers (ASCE), Journal of the Engineering Mechanics Division EM5, 85, 1962, 67-86.

[9] Khan M. Z, Johns K. C., Hayman B.: Buckling of plates with partially loaded edges, Proceedings of American Society of Civil Engineers (ASCE), Journal of the Structural Division, 103, ST3, 1977, 547-58.

[10] Rockey K. C., Bagchi D. K.: Buckling of plate girder webs under partial edge loadings, International Journal of Mechanical Sciences, 12, 1970, 61-76.

[11] Ren T., Tong G. S.: Elastic buckling of web plates in I-girders under patch and wheel loading, Engineering Structures, 27, 2005, 1528-1536.

[12] Galea Y.: Seuil de bifurcation d'équilibre d'un panneau non raidi soumis à des charges transversales agissant dans son plan, Constr. Métallique, Technique et applications, 1984, 1, 1-19.

[13] Graciano C., Lagerqvist O.: Critical buckling of longitudinally stiffened webs subjected to compressive edge loads, Journal of Constructional Steel Research, Volume 59, Issue 9, 2003, 1119-1146.

[14] Shahabian F., Roberts T. M.: Buckling of slender web plates subjected to combinations of in-plane loading, Journal of Constructional Steel Research, Volume 51, Issue 2, 1999, 99-121.

ДГКС Друштво грађевинских конструктера Србије
ASES Association of Structural Engineers of Serbia
S-92
15. KONGRES
6-8. 9. 2018. Zlatibor

Isidora Jakovljević[1], *Zlatko Marković*[2], *Jelena Dobrić*[3]

NUMERIČKA EVALUACIJA FLEKSIONOG IZVIJANJA NAKNADNO TERMIČKI OBRAĐENIH I HLADNOOBLIKOVANIH STUBOVA ELIPSASTOG POPREČNOG PRESEKA

Rezime:

Šuplji profili elipsastog poprečnog preseka se od skora mogu naći na tržištu. U važećem Evrokodu za čelične konstrukcije EN 1993-1-1, ne postoje odredbe koje se odnose na elipsaste preseke. Cilj ovog rada je predstaviti komparativnu analizu ponašanja hladnooblikovanih i naknadno termički obrađenih aksijalno pritisnutih stubova elipsastog poprečnog preseka. Analizirani su zglobno oslonjeni stubovi različitih vitkosti, uključujući uticaj početnih geometrijskih imperfekcija. Nelinearno ponašanje materijala modelirano je na osnovu rezultata testova na zatezanje prikazanih u prethodnim ispitivanjima. Dobijeni numerički rezultati pokazuju slično ponašanje pri izvijanju za sve stubove veće vitkosti, dok u slučaju manjih vitkosti, izvijanje hladnooblikovanih elemenata odgovara nižim krivama izvijanja.

Ključne reči: krive izvijanja, elipsasti šuplji profili, fleksiono izvijanje, numerička analiza

NUMERICAL EVALUATION OF FLEXURAL BUCKING OF HOT-FINISHED AND COLD-FORMED EHS COLUMNS

Summary:

Elliptical hollow sections (EHS) have been recently introduced to the construction market. However, in the current Eurocode standard for steel structures EN 1993-1-1, there are no design criteria defined for EHS. The aim of this paper is to present a comparative numerical analysis of behaviour of cold-formed and hot-finished EHS columns exposed to flexural buckling under pure axial compression. Pin-ended columns of various slendernesses without lateral restrains and with incorporated geometrical imperfections are analysed. Material nonlinear behaviour is included through experimental tensile test results adopted from previous researches. According to obtained numerical results, similar buckling behaviour is observed for both hot-finished and cold-formed columns of higher slenderness, while in the lower slenderness region, cold-formed compressed members tend to lower buckling curves.

Key words: buckling curves, elliptical hollow sections, flexural buckling, numerical analysis

[1]*Teaching assistant, PhD student, Faculty of Civil Engineering, University of Belgrade, isidora@imk.grf.bg.ac.rs*
[2]*Full professor, PhD, Faculty of Civil Engineering, University of Belgrade, zlatko@imk.grf.bg.ac.rs*
[3]*Assistant professor, PhD, Faculty of Civil Engineering, University of Belgrade, jelena@imk.grf.bg.ac.rs*

1. INTRODUCTION

Square, circular and rectangular hollow sections have been widely used in construction for the last few decades. However, elliptical hollow sections (EHS) have only recently been introduced to the construction market. Comparing to circular hollow sections (CHS), EHS of the same area have greater bending capacity around the major axis of inertia. The other advantage of EHS is their aesthetic appearance, therefore they are used in exposed steelwork. In the past years, elliptical hollow sections are implemented as columns in the Zeeman building at the University of Warwick (2003), in the Barajas airport building in Madrid (2004) and the Cork airport in Ireland (2006), then as supporting members for a glass façade in the Heathrow airport building in London (2007) and as an arches of the pedestrian Society bridge in Scotland (2005) [1].

However, in the current Eurocode standard for steel structures EN 1993-1-1 [2], there are no design criteria defined for EHS. Recent studies investigated behaviour of elliptical cross-sections under axial compression [3], bending [4] and combined actions [5]. A procedure for elliptical cross-section classification is proposed [6] and research of flexural buckling of EHS columns has been performed [7]. However, mentioned studies were exclusively focused on hot-finished hollow sections. The other option for tubular element production is cold-forming. Considering different fabrication processes in the case of cold-forming than in the case of hot-finishing method, and as an effect, different material properties, dissimilar behaviour of hot-finished and cold-formed structural members is expected.

The process of cold-forming is conducted at ambient temperature by compressing and squeezing steel sheets through set of rollers. In order to produce a tube section, steel sheets are afterwards welded. Additional rolling could be performed in order to get elliptical shape from circular section. Hot-finishing process consists of the same procedures as cold-forming, but with an addition of subsequent heat treatment in a furnace. It is noted that mentioned hot-finishing process differs from hot-forming process. The latter one does not include any rolling in ambient conditions, but only at temperatures above the material re-crystallization temperature, which means that the whole manufacturing process is conducted at elevated temperatures. Although hot-finished and hot-formed sections are often treated equally in design, recent research shows that their mechanical properties are actually different [8].

The aim of this paper is to present comparative numerical analysis of behaviour of cold-formed and hot-finished EHS columns exposed to flexural buckling under pure axial compression. As less common in the market, hot-formed sections are not included into this research. Numerical modelling is performed in the finite element software package ABAQUS [9]. Pin-ended columns with different slenderness, both hot-finished and cold-formed are analysed under axial loading. Geometrical properties of column cross-sections are adopted according to EHS products that could be found on a market nowadays [10]. Material nonlinear behaviour is included through experimental tensile test results presented in previous researches [7,11,12].

2. NUMERICAL ANALYSIS

The flexural buckling study presented in this paper analyses elliptical hollow sections of geometry corresponding to hot-finished sections manufactured by Tata Steel [10], with an aspect ratio of two. In order to avoid the influence of local buckling occurrence, it is decided to analyse sections of the class 1, 2 or 3 [2]. Limiting slenderness value for class 4 was calculated through equivalent diameter, according to equations proposed by Gardner and Chan [6]. The adopted cross-section for analysis is EHS of overall dimensions 150x75 mm and wall thickness of 5 mm.

Four different numerical column models were developed, with member lengths of 700, 1500, 2300 and 3100 mm, as it was performed in experimental research of flexural buckling of hot-finished EHS columns done by Chan and Gardner [7]. Therefore, a range of nondimensional column slenderness of the importance for describing buckling curves is included. Columns are pin-ended and, as only buckling about minor axis is simulated, there were no lateral supports added along the column height.

Numerical simulations are performed in the finite-element software package ABAQUS [9]. Finite elements implemented in numerical models are shell elements S4R with reduced integration and with six degrees of freedom per node. Uniform mesh density is chosen with finite element size of 7.5 mm, adopted according to mesh convergence study.

In the first step of numerical simulation, Eigenvalue analysis is conducted in order to determine buckling modes. Secondly, the modified Riks method is used for simulating the member behaviour in plastic stress domain, accounting material and geometrical nonlinearities.

Shapes of overall and local imperfections are incorporated in the model through corresponding buckling modes obtained in Eigenvalue analysis and by setting adequate imperfection amplitudes. According to recommendations given in EN 1993-1-5 [13], the advised value of geometric imperfection amplitude for numerical simulation is 80 % of fabrication tolerance. For out of straightness of circular hollow section, the fabrication tolerance is 1/500 of member length [14,15]. However, for numerical analysis performed in this research, the imperfection is applied through half-sine wave function with the amplitude of 1/1000 of member length, as well as it was done by Chan and Gardner in numerical parametric study and that showed the best agreement with experimental results [7]. Based on Chan's and Gardner's experimental research of the elliptical section compressive resistance [3], the local imperfection magnitude is applied as 1/100 of section thickness.

Material properties of cold-formed and hot-finished steel sections are taken into account through results of tensile coupon tests that are conducted in experimental investigations of elliptical and oval hollow sections. Quach and Young [11] obtained stress-strain curves for material coupons taken from different parts of section along a perimeter, for both cold-formed and hot-finished EHS. In the case of hot-finished sections, insignificant differences in material behaviour of the flattest coupons and corner coupons are observed. Contrary, material properties of cold-formed sections are not uniform throughout elliptical perimeter – corner coupons have greater yield stress and tensile strength, but smaller ductility. This is due to the manufacturing process, as curved parts of section were subjected to local cold bending. In the research of hot-finished EHS done by Chan and Gardner [7], only coupons from the flattest portion of section were tested. Similarly, when cold-formed oval hollow sections were investigated by Zhu and Young [12], only mechanical properties of flat coupons are obtained.

The summation of all stress-strain curves implemented in numerical models in this research is presented in Figure 1 and in the following list:

- hot-finished coupon (HF) tested by Chan and Gardner [7],
- hot-finished coupon (HF) tested by Quach and Young [11],
- cold-formed coupon (CF) from the flattest part of section tested by Quach and Young [11],
- cold-formed coupon (CF) from the most curved part of section tested by Quach and Young [11],
- cold-formed coupon (CF) from the flat part of oval hollow section tested by Zhu and Young [12].

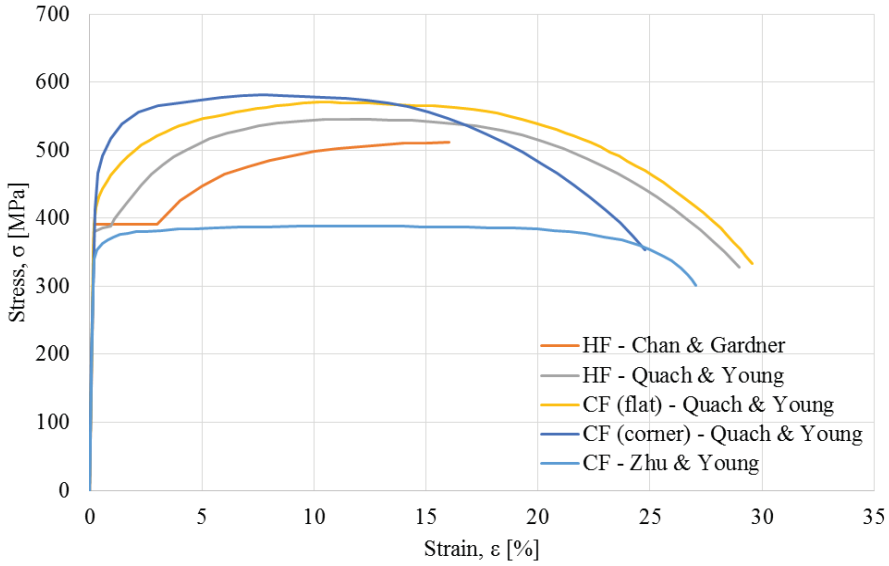

Figure 1 – Stress-strain curves for hot-finished and cold-formed steel sections

It could be observed from Figure 1 that the shape of the material stress-strain curve is different for cold-formed and hot-finished sections. Cold-formed sections exhibit gradual yielding behaviour with enhanced material properties, whereas hot-finished sections have sharp yielding stress–strain curves. The feature of the latter one is a yield plateau with noticeable yield stress f_y, while for cold-formed sections, the value of yield stress f_y is not obvious and 0.2 % proof stress $f_{0.2}$ needs to be determined. Behaviour of hot-finished steel better fits the behaviour of virgin steel material. Contrary, a cold-forming process causes a change in the stress–strain dependency of the basic material. However, even for the presented two hot-finished EHS, the lengths of the yield plateaus differ. This is due to the difference in manufacturing process after cold-rolling, as hot-finished sections tested by Chan and Gardner were exposed to the temperature of 900 ˚C, while for EHS tested by Quach and Young, heat treatment was performed at the temperature of approximately 750˚C.

The part of a stress-strain curve which shows the importance for simulation of flexural buckling is the part before reaching the material strength f_u. Therefore, the material curve

obtained by Chan and Gardner is presented in Figure 1 in the same way as it is given in their research, without post ultimate material behaviour.

In order to incorporate material properties into the numerical model, except defining Young's modulus and Poisson's ratio for elastic analysis, it was necessary to define true stress and true plastic strain for describing plastic behaviour of material. It is done according to the following relations as specified in Abaqus user's manual [9]: $\sigma_{true} = \sigma(1+\varepsilon)$ and $\varepsilon_{true,pl} = \ln(1+\varepsilon) - \sigma_{true}/E$, where E is Young's modulus.

Residual stresses usually arise due to cooling effects after hot-finishing, employed welding processes or by the prevention of springback introduced during manufacturing operations. Measurement of residual stresses in elliptical hollow sections is done by Law and Gardner for hot-finished members [16] and by Quach and Young for both hot-finished and cold-formed EHS [11]. Experimental results show that residual stresses in hot-finished sections are significantly smaller than those in cold-formed sections. During a production process, cold-formed sections are exposed to plastic deformation, so after elastic unloading, residual stress is induced. During heat treatment, a considerable amount of residual stress in hot-finished sections is released, as at elevated temperatures yield stress and Young's modulus decrease [8]. However, in this paper residual stresses are not explicitly included in the numerical analysis, according to numerical models developed by Chan and Gardner [7] and Zhu and Young [12].

3. RESULTS AND DISCUSSION

According to EN 1993-1-1 [2], the value of member buckling resistance N_b is obtained by multiplying the cross section resistance N_c with the buckling reduction factor χ, defined as:

$$\chi = \frac{1}{\Phi + \sqrt{\Phi^2 - \lambda^2}} \leq 1$$

where:

$\Phi = 0.5\,[1 + \alpha\,(\lambda - 0.2) + \lambda^2]$,

α is an imperfection factor,

λ is a nondimensional slenderness.

For cross sections of class 1, 2 or 3, a nondimensional slenderness is given by:

$$\lambda = \sqrt{\frac{A \cdot f_y}{N_{cr}}} = \frac{L_{cr}}{i \cdot \pi}\sqrt{\frac{f_y}{E}}$$

where:

L_{cr} is a buckling length for the considered buckling plane,

i is a radius of gyration for the corresponding axis,

A is a cross sectional area,

N_{cr} is an elastic critical buckling load.

The value of an imperfection factor depends on the flexural buckling curve. There are five buckling curves defined in EN 1993-1-1 [2], as presented in Figures 2 and 3. In the case of hollow sections, the choice of a buckling curve depends on the material yield strength and on the fabrication process. For hot-finished hollow sections of steel grade S235 to S420, a buckling curve is defined as *a*, while for cold-formed sections, it is *c*.

Results of flexural buckling analysis are presented through dependence between a buckling reduction factor, equal to a normalised compressive column resistance N_b/N_c, and a nondimensional slenderness. The value of a buckling resistance is obtained as an ultimate load reached during axial compression of a member, while other parameters as nondimensional slenderness and a cross section resistance are calculated, by using proper geometrical properties and material yield stress obtained from a stress-strain curve.

Figure 2 sums up all results of numerical simulations of flexural buckling behaviour from the application of five different material curves. For columns of nondimensional slenderness greater than 1.5, it could be observed that all spots lie in-between curves *a* and a_0. As the slenderness tends lower, the variation of results is greater. Therefore, for columns of the nondimensional slenderness lower that 0.5, results for cold-formed EHS lie above the curve *c*. Contrary, results for hot-finished specimens lie above the curve *a*. By increasing slenderness, buckling of cold-formed members fits higher curves. However, results for studied hot-finished EHS for all range of slenderness correspond to *a* and a_0 buckling curves.

It is noticed that results conducted by using material curves given by Quach and Young for flat and corner coupons do not significantly differ. However, the differences in flexural behaviour of members with applied cold-formed material properties of Quach and Young and of Zhu and Young are more noticeable. It could be explained by the different shape of material curves, which is observed by comparing a ratio between 0.2 % proof stress and a tensile strength. Although, it is outlined that material coupons tested by Zhu and Young are not taken from elliptical, but from oval sections, which makes an application of such input data in the specific problem of EHS flexural buckling questionable.

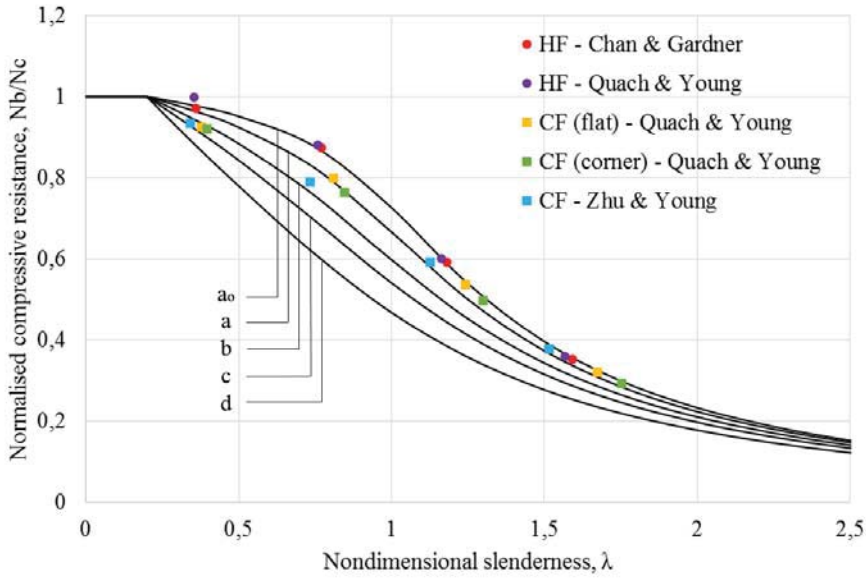

Figure 2 – Normalised FEA results and column buckling curves

It is worth noting that during analysis, it is observed that the influence of the applied local imperfection of 1/100 of plate thickness was negligible, even in the case of the shortest column model. As the section adopted for analysis is stocky and does not belong to the class 4, the outcome is not surprising.

In Figure 3, results are shown which are obtained by using material properties of hot-finished EHS from Chan's and Gardner's research. For comparison, experimental results of column tests of flexural buckling about major and minor axis of inertia, published by Chan and Gardner [7]' are also presented. By numerical simulation performed in this investigation it is not intended to verify any experimental results, as there are no input data for such analysis. Due to the lack of an exact measured initial geometrical imperfections along elliptical perimeter and column length, as well as due to the other effects during testing, there is variation in presented test and numerical results. However, in both cases there is a trend of following the highest buckling curves.

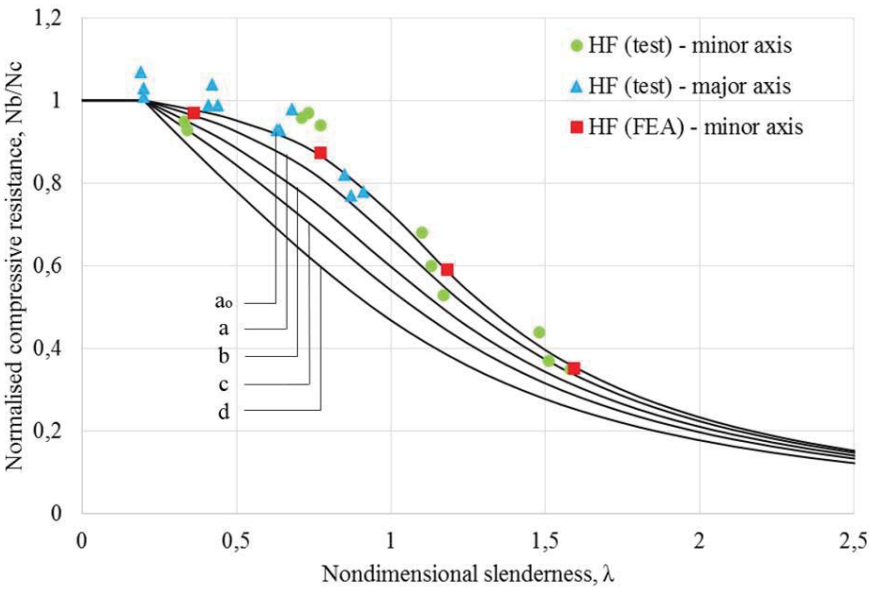

Figure 3 – Normalised FEA results and test results for hot-finished EHS [7]

Chan and Gardner [7] recommended that buckling curves defined for SHS, RHS and CHS hot-finished columns for buckling about both major and minor axis could also be applied to EHS columns. As all spots presenting buckling of investigated hot-finished members about minor axis lie above the buckling curve defined for hollow sections, the obtained results suit to the mentioned proposal of Chan and Gardner. Talking about cold-formed sections, the same conclusion could be made for columns of a lower slenderness. However, one should be aware of the example of slender columns where such propositions lead to safe-sided results in design.

4. CONCLUSIONS

This paper presents numerical evaluation of flexural buckling of elliptical hollow sections. Column models of hot-finished and cold-formed sections are made. Overall and local imperfections are included in simulation with amplitudes of 1/1000 of member length and 1/100 of plate thickness, respectively. Material properties are applied through results of tensile coupon tests presented in other researches of EHS. Only buckling about minor axis of inertia is analysed.

Obtained numerical results for hot-finished and cold-formed members are compared. In the range of higher slenderness, when buckling happens in the elastic stress domain before reaching the yielding stress, similar behaviour is observed for cross sections produces in both ways. Contrary, for a lower slenderness, cold-formed members tend to lower buckling curves than hot-finished ones. It is concluded that compressive capacities of columns are highly dependent on their material properties, especially in non-linear stress-strain domain.

Comparing buckling curves given in EN 1993-1-1 to the numerical results for EHS, it is noticed that in the lower slenderness area, results fit curves *a* and *c*, which are defined for hot-finished and cold-formed hollow sections of the specified steel grades. However, in the higher slenderness region, buckling of all models correspond to the curve *a*. Therefore, if adopting the same curve for all cold-formed members, design predictions might be conservative.

REFERENCES

[1] Chan T.M., Gardner L., Law K.H.: Structural design of elliptical hollow sections: a review, Proceedings of the Institution of Civil Engineers - Structures and Buildings, 163, 2010, 391–402.

[2] EN1993-1-1: Eurocode 3: Design of steel structures. Part 1-1: General rules and rules for buildings, CEN, 2005.

[3] Chan T.M., Gardner L.: Compressive resistance of hot-rolled elliptical hollow sections, Engineering Structures, 30, 2008, 522–532.

[4] Chan T.M., Gardner L.: Bending strength of hot-rolled elliptical hollow sections, Journal of Constructional Steel Research, 64, 2008, 971–986.

[5] Gardner L., Chan T.M., Abela J.M.: Structural behaviour of elliptical hollow sections under combined compression and uniaxial bending, Advanced Steel Construction, 7, 2011, 86–112.

[6] Gardner L., Chan T.M.: Cross-section classification of elliptical hollow sections, Steel and Composite Structures, 7, 2007, 185–200.

[7] Chan T.M., Gardner L.: Flexural Buckling of Elliptical Hollow Section Columns, Journal of Structural Engineering ASCE, 135, 2009, 546–557.

[8] Zhang X.Z., Liu S., Zhao M.S., Chiew S.P.: Comparative experimental study of hot-formed, hot-finished and cold-formed rectangular hollow sections, Case Studies in Structural Engineering, 6, 2016, 115–129.

[9] Abaqus: CAE 6.13-4, 2013.

[10] Tata Steel: Celsius® 355 EHS, 2018.

[11] Quach W., Young B.: Material Properties of Cold-Formed and Hot-Finished Elliptical Hollow Sections, Advances in Structural Engineering, 18, 2015, 1101–1114.

[12] Zhu J.H., Young B.: Design of cold-formed steel oval hollow section columns, Journal of Constructional Steel Research, 71, 2012, 26–37.

[13] EN1993-1-5: Eurocode 3 : Design of steel structures. Part 1-5: Plated structural elements, CEN, 2006.

[14] EN10210-2: Hot finished structural hollow sections of non-alloy and fine grain steels. Part 2: Tolerances, dimensions and sectional properties, CEN, 2006.

[15] EN10219-2: Cold formed welded structural hollow sections of non-alloy and fine grain steels. Part 2: Tolerances, dimensions and sectional properties, CEN, 2006.

[16] Law K.H., Gardner L.: Lateral instability of elliptical hollow section beams, Engineering Structures, 37, 2012, 152–166.

ДГКС Друштво грађевинских конструктера Србије
ASES Association of Structural Engineers of Serbia
S-93
15. KONGRES
6-8. 9. 2018.Zlatibor

Nina Gluhović[1], *Milan Spremić*[2], *Zlatko Marković* [3]

NAJNOVIJE ISTRAŽIVANJE DUKTILNOSTI PERFORIRANIH MOŽDANIKA

Rezime:

Značajna primena "Perfobond" moždanika u spregnutim konstrukcijama od čelika i betona rezultirala je razvojem potpuno nove grupe spojnih sredstava, označenih kao perforirni moždanici. Geometrija perforiranih moždanika osim na nosivost značajno utiče i na duktilnost spojnog sredstva. Duktilnost moždanika koja direktno zavisi od geometrije konektora definiše ponašanje smičućeg spoja. Početni rezultati istraživanja duktilnosti perforiranih moždanika dobijeni su na osnovu numeričkih modela koji su kalibrisani rezultatima eksperimentalnih ispitivanja ovog tipa moždanika. U radu su dati rezultati napredne numeričke analize na osnovu kojih je prikazana veza između duktilnosti i geometrije moždanika.

Key words: perforirani moždanici, smičući spoj, duktilnost, numerička analiza

RECENT RESEARCH ON DUCTILITY OF PERFORATED SHEAR CONNCTORS

Summary:

Significant implementation of "Perfobond" shear connectors in construction of composite steel-concrete structures resluted in development of entirely new type of shear connectors, denoted as perforated shear connectors. Except the shear resistance of this type of shear connector, the overall behaviour of shear connection is strongly influenced by shear connector geometry. Ductility of shear connector, which is strongly influenced by connector's geometry, defines the behaviour of shear connection. The results of resent research on ductility of perforated shear connectors are obtained from numerical models which are calibrated with results of experimental investigation of this type of shear connector. The results of extensive numerical analysis were used for definition of direct relation between connector's ductility and geometry and presented in this paper.

Key words: perforated shear connectors, shear connection, ductility, numerical analysis

[1]*PhD student, Teaching Assistant, Faculty of Civil Engineering University of Belgrade, nina@imk.grf.bg.ac.rs*
[2]*PhD, Assistant Professor, Faculty of Civil Engineering University of Belgrade, spremic@imk.grf.bg.ac.rs*
[3]*PhD, Professor, Faculty of Civil Engineering University of Belgrade, zlatko@imk.grf.bg.ac.rs*

1. INTRODUCTION

The new type of shear connector which was developed in order to improve fatigue resistance of shear connectors in composite bridge construction was Perfobond Rib shear connector. This type of shear connector was developed in the 80s by German company Leonhardt, Andrea and Partners in designing the Third Caroni Bridge in Venezuela and shown in Figure 1a. The Perfobond Rib shear connector was developed as flat rectangular steel plate perforated with a series of holes. The connection between shear connector and top flange of steel beam is obtained by welding. The holes in the shear connector are spaced closely, and the diameter of the holes should be large enough to obtain enhancement of the concrete. Series of holes and embedded concrete volume form a series of concrete dowels which act in shear. Steel reinforcement may or may not be positioned in the Perfobond Rib holes, as shown in Figure 1b, which influence different behavior of shear connection.

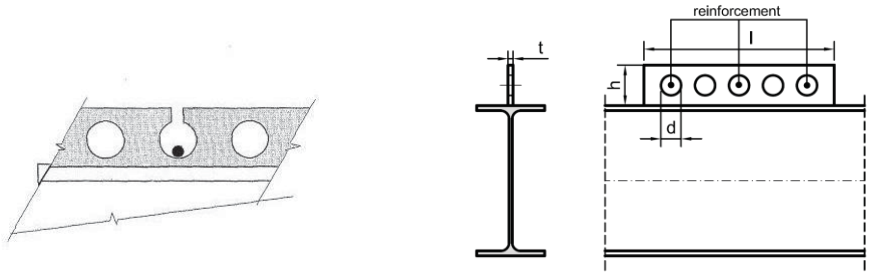

a) Leonhardt's Perfobond Rib [1] *b) position of reinforcement in Perfobond*

Figure 1 – Perfobond shear connector

Development of a new group of shear connectors, which are currently denoted as perforated shear connectors, is the results of the massive application of this type of connector in different type of structures. Figure 2 presents perforated shear connectors with holes in two rows, puzzle connector and T-perfobont connectors.

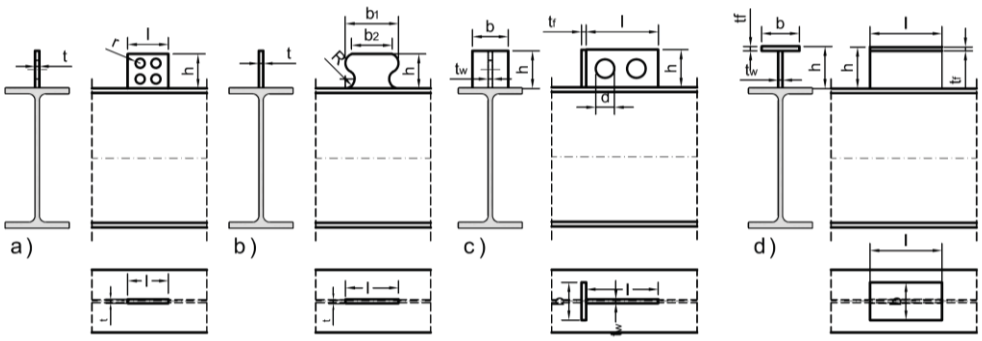

Figure 2 – Different types of perforated shear connectors

Development of different types of perforated shear connectors is followed with their experimental investigation through standard push-out tests according to EN 1994-1-1 [2]. Various geometry of perforated shear connectors shown in Figure 2, resulted in different sheer connection behaviour. Comparison of shear resistance and ductility of headed studs and perforated shear connectors' through numerical and experimental analysis is given by Spremić et al. [3]. Comparison is performed trough development of numerical models based on the experimental investigation of perforated shear connectors performed by Vianna et al. [4]. Investigation of perforated shear connectors given in [3] is extended and recent research on ductility of this type of shear connectors is presented in this paper.

2. NUMERICAL FE MODELS

Based on the experimental results, referred to Vianna et al. [4], the FE models was developed using the ABAQUS-Explicit dynamic solver [5] for quasi-static analysis. Non-uniform mass scaling was used. Quarter of the real experimentally investigated specimens for two types of perforated shear connectors was modelled using double vertical symmetry conditions, as shown in Figure 3. Calibration is performed for two push-out specimens, denoted as P-2F-120 (without reinforcement) and P-2F-AR-120 (with reinforcement), and results are presented by Spremić et al. [3].

For calibration of the material models of steel and concrete in ABAQUS [5] results from standard material tests presented in [4] were used. The isotropic plasticity model was used for the perforated shear connector for steel S355 and reinforcement with implementation of ductile damage and the shear damage models offered in ABAQUS [5].

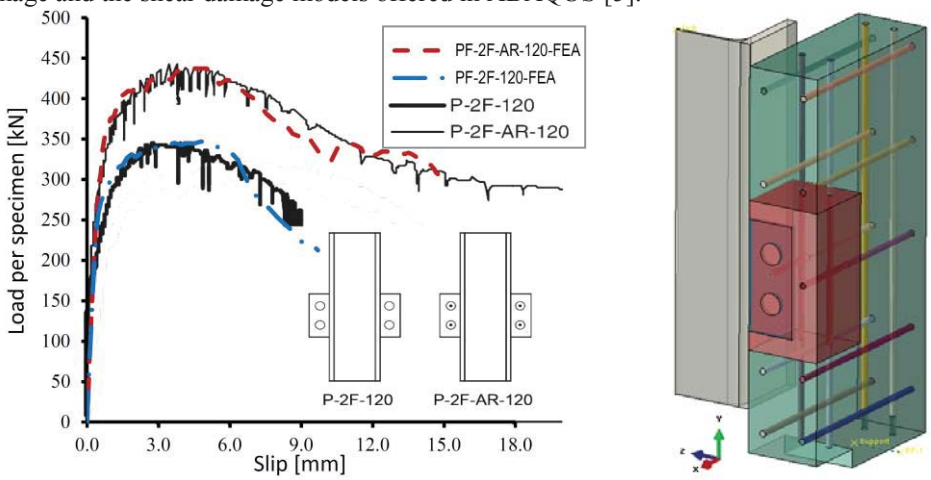

a) load – slip curve after calibration *a) FE model [3]*

Figure 3 – Calibration of numerical models

Concrete damage plasticity model was used for the concrete part of the specimen. The stress-strain curve was defined according to EN 1992-1-1 [6] up to the strain of ε_{cu1} = 3.5 ‰ with modulus of elasticity E_{cm} = 37000 N/mm^2 which correspondent to concrete C50/60 used

in the experimental investigation [4]. For the strain ε_c> 3.5 ‰ the stress-strain curve for concrete is defined according to Pavlovic et al. [7]. The general contact interaction with friction was used for concrete and steel parts of numerical model. Displacement controlled failure loading, according to recommendations given in EN1994-1-1 [2] is applied in reference point at the top of the steel profile web.

3. PARAMETRIC STUDY

In parametric study presented in this paper three different parameters were analyzed in order to find indicative parameters for behavior of shear connection with perforated shear connectors. FE model validated upon push-out experiment for PF-2F-120 specimen presented in [3] is used for the parametric study. Specimen denoted with PF-2F-120-FEA is conducted with perforated shear connector with two holes with 35 mm diameter and 6 mm thickness. Total length and height of perforated shear connector is 180 mm and 76.2 mm, respectively. Through parametric study height of concrete slab, diameter of hole and thickness of shear connector is varied. Therefore, in further figures results of numerical model P-2F-120-FEA (without reinforcement), calibrated with the experimental results is used for development other numerical models with different perforated shear connector geometry. Numerical models with larger concrete slab depth, larger whole diameter and larger shear connector thickness are denoted with PF-2F-h=160mm, PF-2F-120-d=45mm and PF-2F-120-t=8mm, respectively.

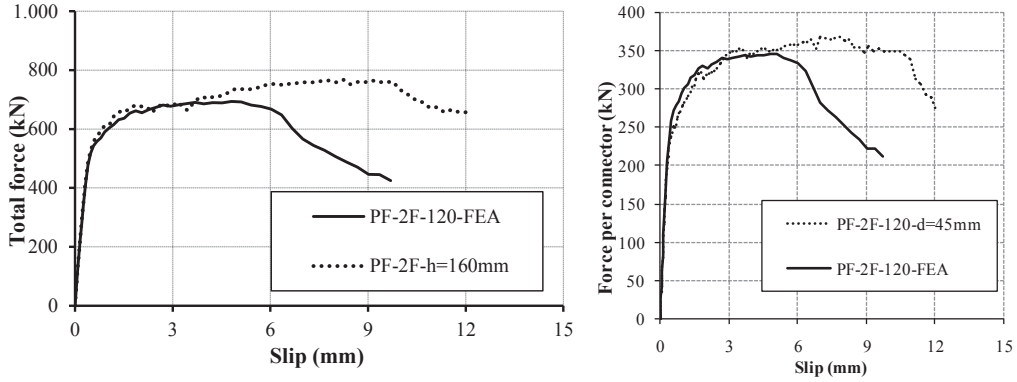

a) influence of slab depth *b) influence hole diamater*

Figure 4 – Influence of concrete slab depth and hole diameter

The concrete slab depth influence on ductility and resistance of perforated shear connector is analysed firstly, and presented in Figure 4a. Enlargement of concrete slab depth from 120 mm to 160 mm for specimen which is used for parametric analysis and explained before, influenced significantly on ductility which is increased for 60%. Ultimate shear force for whole specimen is enlarged from 693.7 kN for specimen with concrete slab depth of 120 mm to 767.0 kN for specimen with larger concrete slab depth. This represent enlargement of approximately 10 %. On the other side, slip to failure which represents slip for 90% of ultimate force on descending part of the force-slip curve, is enlarged from 6.6 mm to 10.7 mm.

The second parameter which was analysed in parametric study is hole diameter. The comparison is made for behaviour of two shear connections, one with perforated shear

connector with 35 mm hole diameter (PF-2F-120-FEA) and the second one with 45 mm hole diameter (PF-2F-120-d=45 mm), both for 6.0 mm thickness of shear connector and 120 mm concrete depth. The results are given in Figure 4b. Enlargement of diameter hole for 10 mm resulted in small change of ultimate shear resistance, approximately 7 %, but in much larger change of ductility. Slip to failure is increased for approximately 60% and amounts 10.89 mm. Therefore, similar ductility increase is achieved with enlargement of hole diameter and concrete slab depth for the same thickness of shear connector.

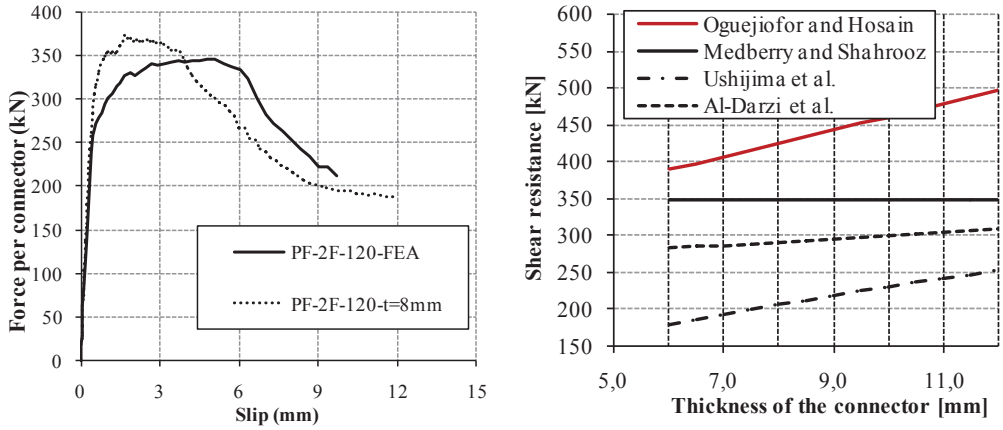

a) influence of connector thickness *b) predictive values of shear resistance*

Figure 5 – Influence of shear connector thickness

Further, through parametric study, influence of the shear connector thickness on shear connection behaviour is analysed for concrete slab depth of 120 mm. Behaviour of shear connection for two thicknesses, 6.0 and 8.0 mm are analysed and presented in Figure 5a. Enlargement of perforated shear connector thickness for 2 mm resulted in approximately 8% higher ultimate shear resistance. Also, slip to failure for thicker perforated shear connector is now 4.07 mm which is less than limit value given in EN1994-1-1 [2] for ductile shear connectors.

Different authors developed the predictive expressions for shear resistance of perforated shear connectors in function of different parameters, number of holes and their diameter and material properties of steel and concrete. These expressions are given in [4] and also presented in form of diagrams in Figure 5b. As shown in Figure 3 and Figure 5, for ultimate shear resistance obtained from experimentally investigated specimen PF-2F-120 and it's numerical model, the closest prediction is achieved with expression according to Medberry and Shahrooz [4]. Also, according to this expression, ultimate shear resistance is not influenced by thickness of shear connector. Moreover, ultimate shear resistance obtained from numerical analysis for thickness of 8 mm does not show close agreement with any of predictive values given in Figure 5b. Therefore, further development of predictive expressions for ultimate shear resistance of perforated shear connectors should include experimental investigation, but also extensive parametric study based on numerical FE models.

According to EN 1994-1-1 [4], shear connectors should be classified as ductile if the slip to failure is larger than 6.0 mm. Slip in shear connection is the effect of plastic deformation of the studs' shank. The compassion of perforated shear connectors' deformation, obtained from parametric study is given in Figure 6 and Figure 7. Also, the results of FE analysis of perforated connector's ductility are presented in Table 1 and Table 2. Deformation of connectors is calculated as the difference between the displacements in force direction of the top of the connectors and the connector's root.

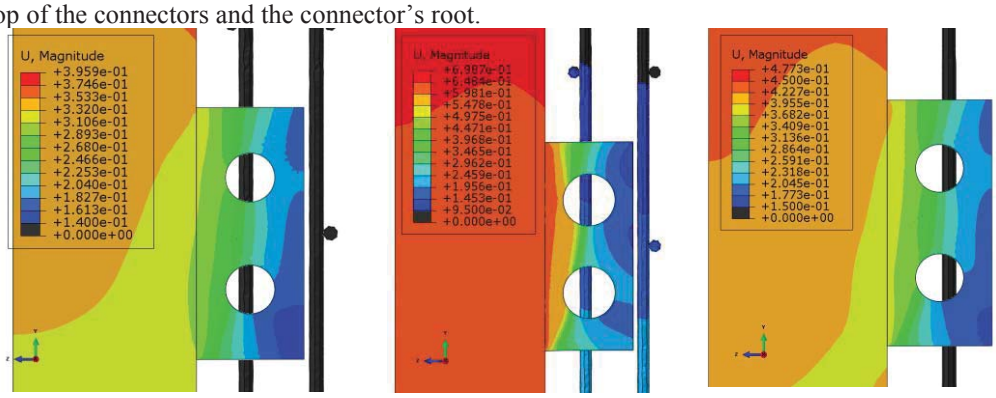

a) PF-2F-120-FEA *b) PF-2F-120-d=45mm* *c) PF-2F-h=160mm*

Figure 6 – Deformation of perforated shear connectors at the shear load correspondent to SLS

Figure 6 presents the comparison of deformation of different types of perforated shear connectors at the load which represent approximately 70% of ultimate shear force, which can be considered as loading level corresponding to serviceability limit state. The same comparison for 6.0 mm slip is given in Figure 7. Even at the shear load value which corresponds to serviceability limit state the initial cracks in concrete was occurred for all specimens.

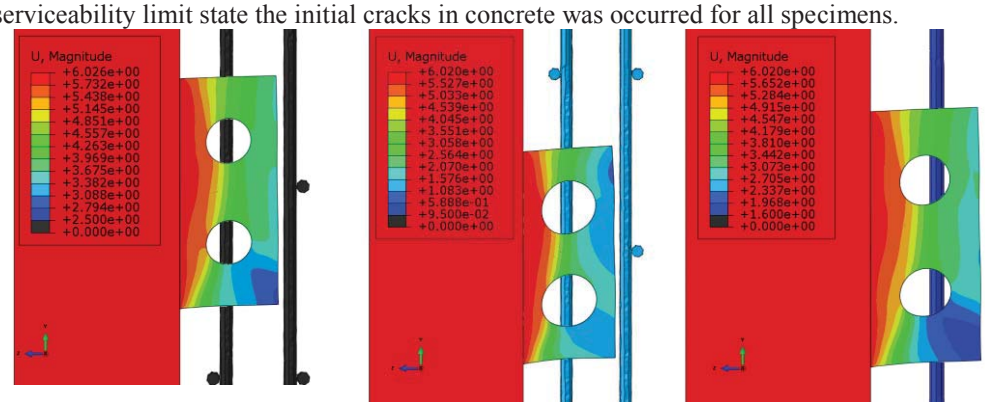

a) PF-2F-120-FEA *b) PF-2F-120-d=45mm* *c) PF-2F-h=160mm*

Figure 7 – Deformation of perforated shear connectors at the 6.0 mm slip

According to values presented in Table 1 deformation of perforated shear connector obtain similar values for two specimens PF-2F-120-FEA and PF-2F-h=160mm, and amounts 3.00 and 3.21 mm, respectively for shear load correspondent to SLS. This slip is the result of the

connector deformation and has the similar values considering that the same perforated connector is used for both specimens, and only the concrete slab depth is changed. Another part of total slip of 6.00 mm is the result of the concrete failure. As shown previously, total slip to failure of whole specimen is increased for 60 % as a result of concrete slab height enlargement. Results for 96% of ultimate shear force for the same two specimens are given in Table 2. Higher concrete slab resulted in higher deformation of perforated shear connector which is now larger than 6 mm.

Table 1 –Deformation of perforated connector

Specimen	slip at 70% ULS shear load			6.0 mm slip		
	$U2_{root}$ [mm]	$U2_{top}$ [mm]	$U2_{top}-U2_{root}$ [mm]	$U2_{root}$ [mm]	$U2_{top}$ [mm]	$U2_{top}-U2_{root}$ [mm]
PF-2F-120-FEA	0.33	0.16	0.14	6.00	3.00	3.00
PF-2F-120-d=45 mm	0.38	0.12	0.26	6.00	1.50	4.50
PF-2F-h=160mm	0.39	0.16	0.23	6.00	2.79	3.21

Table 2 –Deformation of perforated connector at 96% ULS shear load

Specimen	slip at 96% ULS shear load		
	$U2_{root}$ [mm]	$U2_{top}$ [mm]	$U2_{top}-U2_{root}$ [mm]
PF-2F-120-FEA	8.00	4.50	3.50
PF-2F-h=160mm	9.99	3.50	6.49

Enlargement of hole diameter form 35 mm to 45 mm, resulted in significantly enlargement of connector deformation. Deformation of connector with larger hole diameter (specimen PF-2F-120-d=45 mm) is enlarged for 50 % approximately, but also limited to 4.5 mm, as shown in Table 1. Therefore, analysed perforated shear connector cannot be classified as ductile, considering that deformation of connector obtained through FE analysis is significantly influenced by connector geometry and specimens layout.

4. CONCLUSION

From the parametric study presented in this paper, following conclusions can be drawn:

- Behavior of shear connection with perforated shear connectors is in direct relation with connector's geometry and depth of the slab. Different properties of perforated shear connectors, such as thickness or diameter hole can significantly influence the ultimate shear resistance and ductility.
- Initial cracks in concrete were occurred for all specimens even at the shear load value which corresponds to serviceability limit state. Failure of concrete is leading failure mode. Shear resistance of connection is in direct relation with shear bearing resistance of concrete slab.

- Thickness of connector has influence to shear resistance and ductility of connection. Higher shear resistance of this type of connector leads to lover slip value at ultimate shear load.
- Ductility of connection can be significantly improved adopting the perforated connector with larger diameter of hole.
- Connector with approximately 30% larger diameter of hole, 45 mm hole instead 35 mm hole, has similar shear resistance and 50% larger value of connector deformation.
- Higher concrete slab resulted in larger deformation of shear connector at loads which represent 96% of ultimate shear force and contributes to the larger ductility od shear connection.
- Considering obtained slip to failure for the analysed specimens with perforated shear connectors and their deformation, approximately 4.5 mm slip is the result of the connector deformation and another part is the result of the concrete failure. Therefore, it can be concluded that for certain specimen's layout, or even for different material properties of the concrete, this type of shear connector cannot be considered as ductile.

ACKNOWLEDGMENT

This investigation is the part of TR-36048 project supported by the Serbian Ministry of Education, Science and Technological Development.

REFERENCES

[1] Klaiber F. W., Wipf T. J., Reid J. R., Peterson M. J.: Investigation of Two Bridge Alternatives for Low Volume Roads, Volume 2 of 2, Concept 2: Beam in Slab Bridge, Iowa Department of Transportation, College of Engineering Iowa State University, April 1997.

[2] EN1994-1-1: Eurocode 4 - Design of Composite Steel and Concrete Structures. Part 1-1: General Rules end Rules for Buildings, Brussels, Belgium: European Committee for Standardization (CEN), 2004.

[3] Spremić M., Gluhović N., Marković Z., Dobrić J., Filipović A.: Comparison of headed studs with perfobon shear connectors – experimental and numerical analysis, Eurosteel 2017 Conference, Denmark, Proceedings of Eurosteel 2017, 2237-2246.

[4] Vianna J. Da C., S. A. L de Andrade, P. C. G. da S. Vellasco, Costa-Neves L. F.: Experimental study of Perfobond shear connectors in composite construction, Journal of Constructional Steel Research, 81, 2013, 62-75.

[5] ABAQUS User Manual. Version 6.12. Providence, RI, USA: DS SIMULIA Corp, 2012.

[6] EN1992-1-1: Eurocode 2 - Design of concrete structures. Part 1-1: General rules and rules for buildings. Brussels, Belgium: European Committee for Standardization (CEN), 2004.

[7] Pavlović M., Marković Z., Veljković M., Buđevac D.: Bolted shear connectors vs. Headed studs behaviour in push-out tests, Journal of Constructional Steel Research 88, 2013 134-149.

ДГКС Друштво грађевинских конструктера Србије
ASES Association of Structural Engineers of Serbia
S-94
15. KONGRES
6-8. 9. 2018. Zlatibor

Aljoša Filipović[1], Jelena Dobrić[2], Zlatko Marković[3], Dragan Buđevac[3], Nenad Fric[2]

EXPERIMENTAL INVESTIGATION OF COMPRESSED STAINLESS STEEL ANGLE COLUMNS

Summary:

This paper presents experimental program of ongoing scientific-research project that deals with behaviour analysis of compressed stainless steel columns with equal angle sections and which is being performed at University of Belgrade, Faculty of Civil Engineering. The project includes three types of steel products, hot-rolled, laser-welded and cold-formed members and two stainless steel grades, austenitic and lean-duplex alloys. The experiment covered all relevant tests: tensile coupon tests, stub-column tests and overall buckling tests of slender columns. Equal angle specimens of different overall slenderness were tested to determine both linear and nonlinear structural responses and failures, including flexural and torsional-flexural effects and the influences of the width-to-thickness ratios of the legs.

Key words: stainless steel, angle, compression, experiment, buckling, resistance

EKSPERIMENTALNO ISPTIVANJE PRITISNUTIH STUBOVA L PRESEKA OD NERĐAJUĆEG ČELIKA

Rezime:

Ovaj rad prikazuje eksperimentalni program tekućeg naučno-istraživačkog projekta koji se bavi analizom ponašanja pritisnutih stubova od nerđajućeg čelika ravnokrakog L poprečnog preseka, koji se sprovodi na Građevinskom Fakultetu, Univerzitetu u Beogradu. Projekat uključuje tri tipa čeličnih proizvoda, vruće-valjane, laserski-zavarene i hladno-oblikovane elemente i dve legure nerđajućeg čelika, austenitnu i niskolegiranu dupleks leguru. Eksperimentom su obuhvaćeni svi relevantni testovi: standardni testovi materijala na zatezanje, ispitivanje kratkih stubova na pritisak i ispitivanje globalne stabilnosti vitkih stubova. Uzorci ravnokrakog L poprečnog preseka različite vitkosti su testirani u cilju analize linearnog i nelinaernog konstruktivnog odgovora i oblika loma, uključujući efekte fleksionog i torziono-fleksionog izvijanja kao i uticaje vitkosti elemenata poprečnog preseka.

Ključne reči: nerđajući čelik, ugaonik, prtisak, eksperiment, izvijanje, nosivost

[1] *PhD student, University of Belgrade, Faculty of Civil Engineering, afilipovic@grf.bg.ac.rs*
[2] *Assistant professor, PhD, University of Belgrade, Faculty of Civil Engineering*
[3] *Full professor, PhD, University of Belgrade, Faculty of Civil Engineering*

1. INTRODUCTION

Single angle members exposed to compression have a traditional application in civil engineering mostly as members of different latticed structures or built-up columns. If these structures are in aggressive or urban environments, numerous stainless steel alloys may be beneficially utilized due to their corrosion resistance, attractive appearance, low maintenance requirements, good strength, toughness and fatigue properties.

Even though the geometry of angle section is simple, due to its asymmetry and distance between shear centre and centroid, the determination of the compressive capacity of angle columns may be complex. Furthermore, the angle members are usually eccentrically connected at their ends through one leg that introduce biaxial flexural deformation and consequently affect their ultimate structural responses. In general, failure of the centrically compressed angle member occurs due to flexural buckling about the minor principal axis of the cross-section or flexural–torsional buckling depending on its material response, cross-section slenderness, overall slenderness and boundary conditions.

The design of centrically compressed stainless steel angle members is not currently covered with European codified procedure. The lack of experimental data in this structural field results with the fact that the current design provisions in EN 1993-1-4 [1] rely solely on assumed analogies with the equivalent carbon steel members. Clause 5.4.1 [1] allows the use of appropriate provisions given in EN 1993-1-1 [2] and EN 1993-1-3 [3] for design of compressed stainless steels members but with modifications given in clause 5.4.2. However, the analytical method in clause 5.4.2 does not explicitly state the values of neither imperfection factor nor limiting slenderness for stainless steel angles in relevant buckling plane depending both on manufacturing process and steel grade. Exceptions from this rule are generally designated cold formed open sections. Thus, this kind of approach can lead to misconceived design practice since it does not offer clear response at the important issue related to application of corresponding design curve for reliable and safe prediction of buckling resistance of compressed stainless steel angle member.

An analytical method for design of centrically compressed members given in EN 1993-1-4 [1] is based on the Perry-Robertson equations and the linear expression for the imperfection parameter $\eta = \alpha(\bar{\lambda} - \bar{\lambda}_0)$. The influences of structure imperfections on the predicted flexural-buckling resistance is implicitly accounted for by employing an imperfection factor α associated with the appropriate buckling curve depending on the cross-section shape and manufacturing process. Besides, EN 1993-1-1 [2] stated additional rules for design single angle columns that are connected at their ends trough one leg by bolts or by welding. The procedure introduces an empirical equation for the non-dimensional effective slenderness ratio to account for both the end eccentricity and the end restraints.

Over the past two decades, significant attention has been paid to aspects of the potential use of stainless steel for construction purposes. However, none of the performed investigations was aimed at the buckling response of stainless steel angle columns. In order to fill this gap, the scientific-research project is being conducted at the University of Belgrade, Faculty of Civil Engineering. The project covers investigative and experimental work with the aim of acquiring further knowledge to facilitate the development of design procedures for compressed stainless

steel angles. The research focuses on different material and geometrical parameters of the selected stainless steel equal angles produced from austenitic and lean-duplex stainless steel alloy. To assess impacts of the initial imperfections on column compressive resistance that caused by different manufacturing procedures, three types of angle products are included: cold-formed, hot-rolled and laser-welded sections. Hence, the important innovative content of the project relates to extension of the scope of the current codified procedures in EN 1993-1-4 [1] not only to conventional angle profiles but also to the contemporary products such as the laser-welded angles. To determine both elastic and non-elastic ultimate responses including flexural and torsional-flexural modes and effects of cross-section slenderness, the equal angle specimens are selected to cover whole overall slenderness range.

2. EXPERIMENTAL TESTING

This paper describes a part of performed experimental investigation including material tests and overall buckling tests of slender pin-ended columns, addressing their flexural buckling capacity about the minor principal axis. The experiment aims at understanding the effects of the material nonlinearity, structural imperfections and cross-section slenderness on the ultimate behaviour of stainless steel angle columns.

Figure 1 – Specimens used in experiment

The test specimens are equal stainless steel hot-rolled, laser-welded and cold-formed angle products, as shown in Fig. 1. The basic material of hot-rolled and laser-welded specimens is the most commonly used austenitic stainless steel grade EN 1.4301 (X5CrNi18-10). The cold-

formed specimens are press-braked from flat strips of lean-duplex stainless steel EN 1.4162 (X2CrMnNiN21-5-1) as slender angle sections.

According to EN 1993-1-4 [1], the hot-rolled and laser-welded specimens are classified as semi-compact sections while cold-formed angles satisfy requirements for slender sections. The buckling behaviour of members in both linear and non-linear stress domain is achieved through the careful selection of the range of member overall slenderness. The scale of the tested members corresponds to the real structural elements which have use in civil industry. Considering type of steel product, cross-sections' dimensions and specimens' lengths, the total number of 48 specimens are divided into 12 tested series, each includes four repeated tests. The sectional geometric parameters of each tested product are illustrated in Fig. 2, while Table 1 summarizes the nominal geometrical dimensions of the specimens including overall slenderness ratio about minor principal axis.

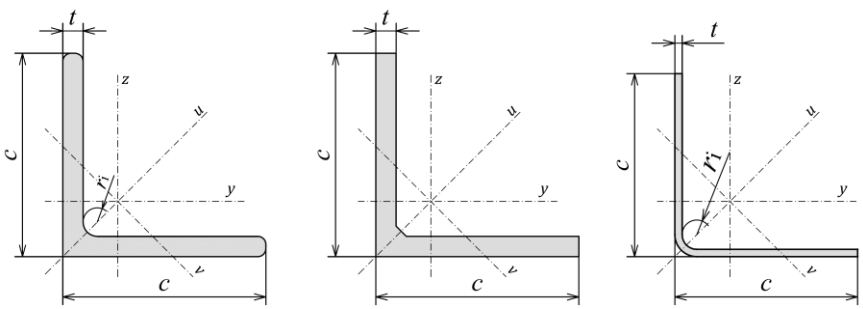

(a) hot-rolled angle *(b) laser-welded angle* *(c) cold-formed angle*

Figure 2 - Cross-sections of the angle specimens

Table 1 - Nominal geometry and slenderness ranges of specimens in the experiment

Designation of specimen series	Stainless steel grade	Stainless steel product	Specimen geometry			Slenderness ratio λ_v	Number of repeated tests
			Leg width c (mm)	Thickness t (mm)	Length L (mm)		
AHR 100	EN 1.4301	Hot-rolled	100	10	500	26	4
					1500	77	4
					2500	128	4
AHR 60	EN 1.4301	Hot-rolled	60	6	800	70	4
					2000	170	4
ALW 100	EN 1.4301	Laser-welded	100	10	500	25	4
					1500	76	4
					2500	127	4
ALW 60	EN 1.4301	Laser-welded	60	6	800	68	4
					2000	172	4
ACF 80	EN 1.4162	Cold-formed	80	4	1000	65	4
					2000	130	4

The specimens' geometry was controlled by direct mechanical measuring to determine the variation between the actual and nominal specimen dimensions.

The experimental data are used to establish qualitative data base through numerical simulations of experiments and to perform a quantitative numerical parametric study to enable accuracy assessment of buckling curves given in EN 1993-1-1 [2] for design of stainless steel angle columns.

2.1 MATERIAL PROPERTIES

The investigation is concentrated on the austenitic stainless steel grade EN 1.4301 and lean-duplex grade EN 1.4162 that typically used in structural applications.

Three coupons were longitudinally cut from both legs of hot-rolled and laser-welded specimens, respectively (see Fig. 3). To asses anisotropy of stainless steel and consider influence of cold working on the material response of the final press-braked sections, two test series are carried out. The first series included six flat coupons taken from the flat steel sheets in both longitudinal and transverse roll direction. The second series included three flat coupons longitudinally cut from the legs and two corner coupons used within the boundary of the internal radius of the cross-section's corner region of press-braked angle specimen. All coupons were cut by a water jet cutter to decrease heating of material during their preparation. The coupons were tested in accordance with EN ISO 6892-1 [4]. Tensile testing of coupons was performed at the University of Belgrade, Faculty of Technology and Metallurgy. The tests were carried out on the Shimadzu Universal Testing Machine AG-Xplus. Fig. 4 shows the setup for tensile coupon test.

Figure 3 – Location of coupons from hot-rolled and laser-welded angle specimens

The tests provided engineering stress–strain curves and determined the most important material properties: yield strength f_y used as 0.2% proof stress $f_{0.2}$, ultimate tensile strength f_u, strain corresponding to the ultimate tensile strength ε_u, total strain at fracture ε_f and modulus of elasticity E. The obtained engineering stress–strain curves and the mean values of the key material properties for hot-rolled angles are provided in Fig. 5. It can be seen from Fig. 5 that austenitic stainless steel EN 1.4301 exhibits a rounded nonlinear stress–strain relationship with gradual yielding and almost twice higher ductility than the typically used carbon steels. The

results also showed that the measured yield strengths of austenitic stainless steel exceed the nominal value stated in EN 10088-2 [5] with difference of 40 %.

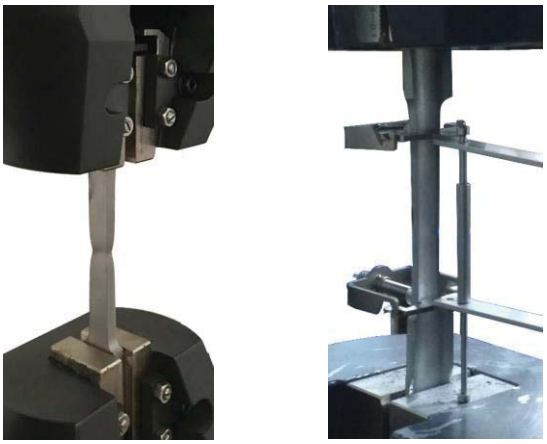

(a) flat coupon *(b) corner coupon*

Figure 4 – Tensile test setup

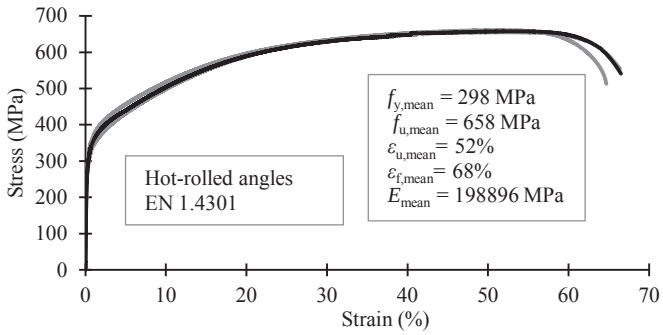

Figure 5 – Engineering stress-strain curves for hot-rolled angles

2.2 MEASUREMENT OF GEOMETRIC IMPERFECTIONS

The initial geometric imperfections of real structural elements introduce bending from the onset of loading and therefore strongly affect the ultimate buckling response of a column. To measure geometric imperfections, a laser measurement system with Leica Absolute Tracker AT930 was used. The fields of geometric imperfections were obtained by laser scanning the specimen at leg multiplanes and registering the individual scans into the same final global coordinate system. The colour distributions of scanned segments are based on deviation from nominally expected dimensions. One of benefits of used laser measuring system is the determination of deviation between the centroid axes of element with real geometry and its equivalent element with idealized nominal geometry. Dimensional variations that may be

considered as cross-section's imperfections lead to initial curvature of the centroid axis and contribute to changes in the strength and flexural rigidity of the structural element. Three types of overall geometric imperfections were identified from the measurement points: measurements normal to minor axis – bow imperfections, measurements normal to major axis – camber imperfections and twist imperfections. Fig. 6 shows the laser measurement system, example of three-dimensional geometric imperfection scans and types of overall geometric imperfections.

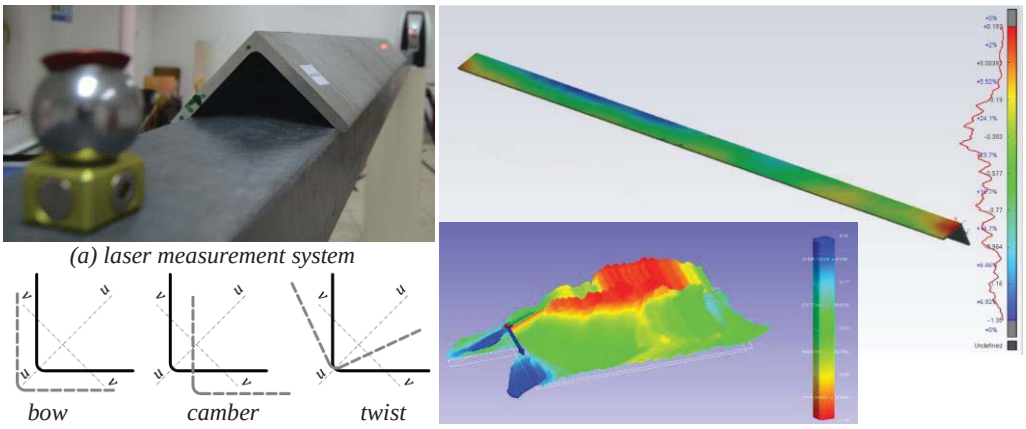

(a) laser measurement system

(b) overall imperfections

(c) imperfection colour distribution of scanned segments

Figure 6 – Method for measuring initial geometric imperfections of angle specimens

2.3 BUCKLING TESTS

The buckling tests of specimens were carried out at the Laboratory for Testing of Structures at the Institute for Testing of Materials in Belgrade. The specimens were tested under concentric compression loading using a hydraulic testing machine with fixed plates and a capacity of 5000 kN. All tests were performed monotonically using displacement control with a proper loading rate not exceeding 0.01 mm/s up to the maximum load capacity, and then continued up to approximately 70% of the maximum load before stopping the test.

Taking into account the specific geometry of angle section, direction of its principle axis and distance between section's shear centre and centroid, to provide pin-ended boundary conditions during testing was challenging. Hence, the lubricated spherical steel supported plates were utilized to provide a rotation about minor principle axis during the test. In the test set-up, the specimens were carefully aligned to ensure that the load application points at each end would be at the centroid of the angle section. After the alignment of the specimen in the testing machine, the ram of the actuator was moved slowly toward the specimen until the base plate was in full contact with the bottom specimen's end having a small initial load of approximately 3 kN. At this load, all instrumentation was adjusted for measuring the axial load, lateral deflections and axial strains.

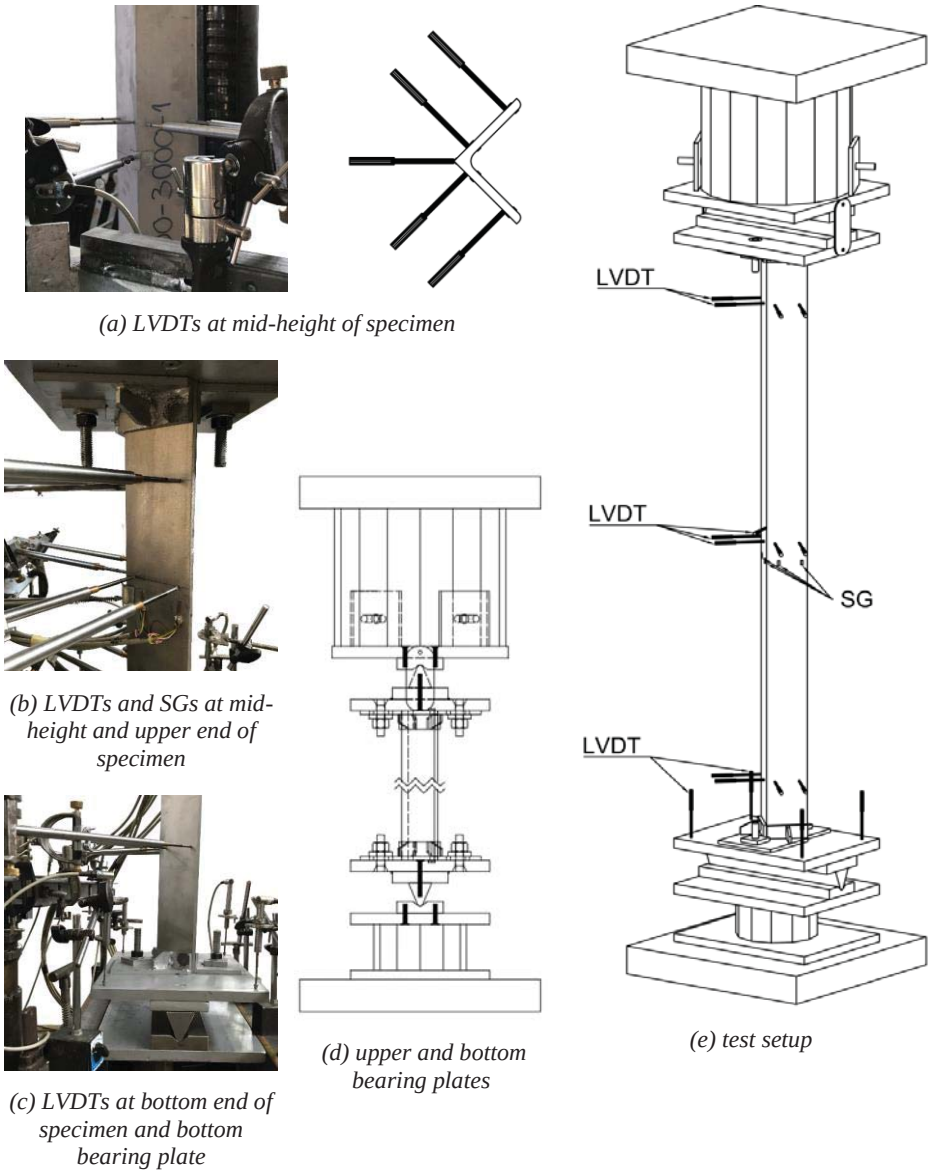

(a) LVDTs at mid-height of specimen

(b) LVDTs and SGs at mid-height and upper end of specimen

(c) LVDTs at bottom end of specimen and bottom bearing plate

(d) upper and bottom bearing plates

(e) test setup

Figure 7 – Instrumentation layout and test setup

The critical cross-section was expected to be at or near the mid-height of the column, thus the lateral movements and axial strains were therefore measured at this sections for all tested columns. To record both flexural and torsional movements of the specimen cross-sections, four longitudinal displacement transducers (LVDTs) were attached perpendicular to each leg at

mid-height and near to the ends of specimens. The displacement in the expected buckling plane perpendicular to minor principal axis was also measured with additional LVDT at the mid-height of specimens. Besides, four LVDTs were mounted on the bottom bearing plate to record its rotations and displacements. Axial strains were monitored by strain gauges (SGs) attached around the perimeter surface of the cross-section at the specimens' mid-height.

A calibrated load cell C6A Force Transducer was used to measure the applied load. A data acquisition system was used to record the applied load, LVDTs and strain gauge readings during the tests. Fig. 7 shows the detailed instrumentation layout and test setup.

(a) local buckling columns of low slenderness

(b) flexural buckling columns of intermediate slenderness

(c) flexural buckling columns of high slenderness

Figure 8 – Typical failure modes of the selected angle specimens

The obtained experimental results clearly showed different ultimate structural responses of angle columns with pin-ended boundary conditions. Depending of the overall slenderness ratios, width-to-thickness ratios of the legs and initial eccentricity conditions, the specimens failed in flexural, torsional-flexural, and coupled flexural/torsional-flexural modes. The local buckling failure characterized by distortion of the cross-section was dominant mode for hot-rolled and laser-welded specimens in the low slenderness range (λ_v = 25). In the intermediate slenderness range (λ_v = 76), the inelastic flexural buckling about minor principal axis was notified for the same stainless steel angle products. Contrary, the overall compressive capacity of the cold-formed angles (λ_v = 65) was limited by the capacity of the individual section elements. The failure mode was interaction of the local and overall flexural buckling. The

largest number of the most slender hot-rolled and laser welded angle specimens (λ_v = 170) had pure flexural buckling about minor axis. In the case of cold-formed stainless-steel angles (λ_v = 130), it was observed that the influence of section slenderness on the ultimate flexural buckling response is not explicitly evident. Typical deformed shapes of the selected specimens after buckling are shown in Fig. 8.

3. CONCLUSIONS

The presented ongoing project is planned as a pre-normative research aiming to propose initial criteria for design of compressed structural members with equal angle-sections for the next version of EN 1993-1-4. Following the extensive experimental programme supported by theoretical and numerical analysis, buckling curves referred to different manufactured performances of angle members will be developed. By providing the integration of gained outcomes in the Eurocode 3, this project will generate a wider range of economic benefits for manufacturers, users and designer across the European construction industry.

ACKNOWLEDGEMENTS

This investigation is supported by the Serbian Ministry of Education, Science and Technological Development through the TR-36048 project. The authors are grateful to chair of the Eurocode Working Group for EN 1993-1-4 Nancy Baddoo, to companies Montanstahl ag Switzerland, Armont SP Belgrade, Institute for Testing of Materials Belgrade, Institute for Materials and Structures Faculty of Civil Engineering University of Belgrade, Vetroelektrane Balkana Belgrade, ConPro Novi Sad, Energoprojekt Industrija PLC Belgrade, Vekom Geo Belgrade, CO-designing Belgrade, Peri Oplate Belgrade, North Engineering Subotica, Amiga Kraljevo, Mašinoprojekt kopring PLC Belgrade, Sika Belgrade, DvaD Solutions Belgrade and Soko Inžinjering Belgrade for their support.

REFERENCES

[1] Eurocode 3, Design of Steel Structures – Part 1-4: General Rules – Supplementary Rules for Stainless Steels, Including Amendment A1, CEN, Brussels, Belgium, 2015 EN 1993-1-4:2006+A1:2015.

[2] Eurocode 3, Design of Steel Structures – Part 1-1: General Rules and Rules for Buildings EN 1993-1-1, CEN, Brussels, Belgium, 2005.

[3] Eurocode 3, Design of Steel Structures – Part 1-3: General rules — Supplementary Rules for Cold-formed Members and Sheeting EN 1993-1-3, CEN, Brussels, Belgium, 2006.

[4] EN ISO 6892-1, Metallic materials – tensile testing, Part 1: Method of Test at Room Temperature. European Committee for Standardization, CEN, Brussels, 2009

[5] EN 10088-1:2005, List of stainless steels – EN 10088-2:2005: Technical delivery conditions for sheet/plate and strip of corrosion resisting steels for general purposes; EN 10088-3:2005: Stainless steels, Technical delivery conditions for semifinished products, bars, rods and sections for general purposes, CEN, Brussels, 2005.

ДГКС Друштво грађевинских конструктера Србије
ASES Association of Structural Engineers of Serbia
S-95
15. KONGRES
6-8. 9. 2018. Zlatibor

Vlastimir Radonjanin[1], *Mirjana Laban*[2], *Mirjana Malešev*[3], *Slobodan Šupić*[4]

POBOLJŠANJE OTPORNOSTI ZAPADNOG BALKANA NA HAZARDE IZGRADNJOM KAPACITETA U VISOKOM OBRAZOVANJU

Rezime:

U poslednjih nekoliko godina, broj i ozbiljnost prirodnih i antropogenih katastrofalnih događaja, kao i požara, značajno su povećani. Potrebno je poboljšati otpornost društava zapadnog Balkana na ove opasnosti uvođenjem novih studijskih programa i kurseva doživotnog učenja u obrazovanju. Projektni predlog "Znanje za otporno društvo - K-FORCE" je izabran za finansiranje u okviru ERASMUS+ programa - izgradnja kapaciteta u visokom obrazovanju. U radu su prikazani rezultati ankete koja je obavljena među mladima u WBC-u, kako bi se istražio nivo kulture sigurnosti i zajednički nivo razumevanja rizika u njihovom okruženju.

Ključne reči: otporno društvo, omladina, kultura sigurnosti, visoko obrazovanje

IMPROVING WESTERN BALKANS' RESILIENCE TO HAZARDS BY BUILDING CAPACITY IN HIGHER EDUCATION

Summary:

In the last few years, the number and severity of natural and anthropogenic catastrophic events, as well as fires, were significantly increased. It is necessary to improve the resilience of the Western Balkan societies to these events by introducing new study programs and lifelong learning courses in education. The project proposal Knowledge FOr Resilient society – K-FORCE was selected for funding under ERASMUS+ programme Capacity Building in Higher Education. The paper presents the results of survey done among the youth in WBC in order to investigate the level of safety culture and mutual level of understanding the risks in their environment.

Key words: resilient society, youth, safety culture, higher education.

[1] *PhD, Full Professor, University of Novi Sad, Faculty of Technical Sciences, Novi Sad*
[2] *PhD, Ass. Professor, University of Novi Sad, Faculty of Technical Sciences, Novi Sad*
[3] *PhD, Full Professor, University of Novi Sad, Faculty of Technical Sciences, Novi Sad*
[4] *MSc CE, University of Novi Sad, Faculty of Technical Sciences, Novi Sad*

1. INTRODUCTION

In the past decades the number of natural and anthropogenic disasters and fires has shown a significant growth in the Western Balkans (WB). Human losses, extensive damages to the urban areas, negative environmental impact and further weakening of the regional economy are some of indicators of increasing vulnerability. The WBs are highly prone to natural hazards and to the impacts of climate change. Furthermore, within the last 15 years most of the nations in the region newly gained their independence following a regional conflict and have undergone major structural changes. The newly independent nations and their urban areas sustain inadequate institutional capacities and have significant socio-economic and spatial vulnerabilities, increasing their risk to disasters initiated by natural hazards [1]. Preliminary surveys, targeted to identify the problem origin, indicated that competences, knowledge and skills of the existing staff in the field of Disaster Risk Management and Fire Safety Engineering (DRM&FSE) are insufficient to solve its growing problems, as they acquire knowledge and skills from other engineering disciplines. Knowledge and skills shortages in this sector are already being identified by great interest shown after 2014 flood in the WB, while the expected climate change and hazard events expansion will only exacerbate the situation. The recent devastating floods in the WBC region, notably in Serbia and Bosnia and Herzegovina in 2014, confirmed that most countries of this region continue to have difficulties integrating risk reduction into public investment planning, urban development, spatial planning and management and social protection. With the impact of climate change, combined with changes in land-use patterns, risks of disasters will further increase in the coming years.

Within the expanding emergency sector labour market, an urgent demand is expected for more educated and trained staff, as well as for continuing education in DRM&FSE field. There is a rising need for multidimensional approach and interdisciplinary engineering competences. Considering before mentioned, in WB region, available education is becoming insufficient and unsustainable without further modernization. In order to improve the resilience of the region to hazards, it is necessary to provide the required number of experts in the field of DRM&FSE. The concept of resiliency should be an integral part of disaster preparedness. Resiliency emphasizes the capacity of human recourses, infrastructure, operations, and even social systems to respond to and recover from extreme events. A special emphasize should be placed on building countries' financial resilience that would, jointly with knowleable humane resources, enhance preparedness to disaster risks. The growing cost and frequency of natural catastrophes and their implications for economic growth and development have led to a concern over the level of public awareness and education relative to large-scale catastrophes and disaster risk reduction measures. Public awareness and education of disaster risk reduction are, in particular, increasingly acknowledged as important components of effective risk management of natural catastrophes [2].

2. ENHANCING KNOWLEDGE AND EDUCATION IN DISASTER RISK MANAGEMENT

In recent years the number and severity of natural and manmade disasters has significantly increased. In addition, future disaster will be extreme and more complex with far-reaching and longer-term consequences as a result. Consequently, Decision No 1313/2013/EU on a Union Civil Protection Mechanism emphasizes an integrated approach to disaster management as

increasingly important [3]. To become resilient society, it is necessary to implement the EU Civil Protection Mechanism at a regional level and intensively cooperate and communicate, for which a new skilled young workforce is required. According to European Parliament Resolution Community approach on the prevention of natural and manmade disasters, prevention has a crucial significance for protection against disasters, requiring a further action. Reaching the prevention objectives and carrying out prevention actions, improving the disaster risk knowledge base and facilitating the sharing of knowledge, best practices and information, were defined as the first ranked action to take. Education and training (ET 2020) lie at the heart of the Europe 2020 strategy (ET 2020) to exit the recession and establish the foundations for future knowledge-based growth and social cohesion. The same goal is promoted in multiple EU documents, e.g.: European and Mediterranean Major Hazards Agreement (EUR-OPA), South East Europe 2020 Strategy – Jobs and Prosperity in the European Perspective (SEE 2020 Strategy) and Supporting growth and jobs – an agenda for the modernization of Europe's higher education systems COM (2011) 567 final.

The above listed are common objectives and goals both for EU and WB region, considering the on-going European integration process in the Balkans. The resilience improvement by developing higher education (HE) is in compliance with WB countries' national HE strategies and action plans, as well as national strategies in the field of fire protection and emergency.

Resilience to natural hazards should be a core element in the design of development programs. We need to better understand how and where we are vulnerable to disasters, and how best to manage the risks we face. Informed, knowledgeable and educated citizens and public authorities, with the human and financial resources to back them up, are the key to successful disaster risk management planning and implementation [4].

3. STATE AND DEVELOPMENT PERSPECTIVES OF DRM&FSE HIGHER EDUCATION IN WESTERN BALKANS

Within civil protection in Western Balkans Region, disaster risk reduction and disaster management need to be treated as a matter of priority, particularly in the light of the severe floods in 2014.

In July 2015 Serbia became the 33rd participating state in the EU Civil Protection Mechanism. Serbia will have to accomplish a countrywide risk assessment and assessment of its risk management capabilities.

The floods in the south of the country in February 2015 showed the need for Albania to further strengthen its capacity in this sector. As regards civil protection, the 2014-2018 national strategy for disaster risk reduction and civil protection has not been adopted yet.

Bosnia and Herzegovina expressed its interest in becoming a member of the EU Civil Protection Mechanism in 2014 and concluded a protocol on cooperation and establishment of a point of contact with the mechanism. Further coordination and cooperation efforts and further preparations for joining the mechanism are needed.

Western Balkans' higher education needs to respond and to educate and train young people for the sector that will significantly grow as these countries need to fulfil Chapter 27 requirements according to EU Enlargement Strategy.

Climate change, fast urbanization and new technologies, in interaction with irresponsible human activities, cause the need for multidisciplinary and interdisciplinary engineering competences, knowledge and skills. Considering these, available HE is insufficient and

unsustainable at regional level without modernization and further development. The brief analysis of available bachelor, master and doctoral study programs in the field of Disaster Risk Management was conducted on the regional and European level [5]. WB countries included in this research were Serbia, Bosnia and Herzegovina, Albania, Macedonia, and Croatia.

The research showed that there is an insufficient number of master degree programs in WB region to ensure sustainable and uniform capacity building in human resources in this area, and academic bachelor studies are implemented only at University of Novi Sad, Faculty of Technical Sciences in Serbia. A similar program does not exist even in neighbouring European countries, and the current situation in HE in this field is not self-sustainable, because there are no doctoral programs to ensure future researching staff. Number of graduates is insufficient for regional or national needs. Consequently, there is a need for experts who are competent to operate in all phases of the catastrophic events and that are able to solve problems in the field. Also, there is a need for education of competitive experts who will be able to create a sustainable financial plan for disaster preparedness and preventive measures, according to regional economy recourses. At this moment, existing HE programs do not meet the mentioned WB countries' needs for qualified staff. In order to improve regional resilience to hazards and capability for regional cooperation in risk prevention and response, it is necessary to provide the required number of multidisciplinary experts by modernizing and developing HE at the regional HEIs in subject field. Aim is to build regional-based disaster preparedness and a culture of safety and resilience at all levels. The WB HEI needs to assess the level and quality of HEIs capacity (infrastructure, facilities, laboratories, workforces etc.) in this field and to identify the key competences, knowledge and skills necessary for contemporary practice and future needs. A master study programs should be developed to satisfy various criteria, according to regional needs for resilient society, such as the shift from reactive to proactive actions and developing a culture of prevention. Based on the above, the project proposal Knowledge FOr Resilient society – K-FORCE was successfully prepared by University of Novi Sad in cooperation with 11 HEIs from Denmark (DTU, AAL), Sweden (LU), Slovakia (UNIZA), FYR Macedonia (UKIM), Bosnia and Herzegovina (UBL, UNTZ), Albania (UT, EPOKA), Serbia (VTSNS) and 5 non-academic partners (Protection and Rescue Directorate of the Republic of Macedonia, National Fire Safety Association of Republic of Serbia, European Youth Parliament Serbia, Ministry of Security of Bosnia and Herzegovina: Protection and Rescue Sector and Sector for International Cooperation and European Integrations and Union of chambers of commerce and industry of Albania). The K-FORCE project proposal has been selected for funding in ERASMUS+ program Capacity Building in Higher Education – EAC/A04/2015. The three years period of the project realization will start in October 2016. The project goals answering to above-mentioned issues will be achieved through development of innovative master studies implemented in six HEIs in the region and PhD studies implemented at UNS, Faculty of Technical Sciences (FTS) as well as through continual knowledge improvement of staff already working in this field through newly developed LLL courses. It will help harmonization of new programs content with the region's needs. Final goal is to produce capable experts, able to withstand difficult requirements of today and tomorrow.

4. FUTURE EDUCATION ASPIRATIONS ASSESSMENT

The Youth Safety Culture survey was conducted as part of the Knowledge for Resilient Society (K-FORCE) project (http://kforce.uns.ac.rs/) funded by the European Union under the Erasmus+ scheme to asses future education aspirations of youth.

The primary target group was set as High School and University students from Albania, Bosnia and Herzegovina and Serbia. The survey itself was characterised as a mass survey aiming to have as many subjects (answers) as possible, with the questions being simple and easy to understand for young people from different backgrounds.

Survey was drafted by European Youth Parliament Serbia (EYP Serbia) and contained three sections:

- previous experience in the field of DRM&FSE,
- safety culture and personal stances and
- future education aspirations.

Subject classification was proposed in regards to the subjects' country and city of residence, age, level of current education (High School or University) and field of education. The survey took between 5 and 10 minutes to fill out and was anonymous.

A total of 1462 subjects gave their responses to the survey. Because of missing information, invalid responses or other reasons, 98 responses were deemed invalid and the data analysis was done on 1364 subjects that filled out the survey completely and correctly.

Some of the comprehensive results, regarding youth future education aspirations are given in the tables below. For each question, possible answers are listed and the number of subjects which gave that answer is specified below it, as well as the percentage that this number represents to the total number of subject who answered that question.

Table 1 - Sample characteristics

Total subjects:						1364
By country of residence:						
Albania	Bosnia and Herzegovina	Serbia	Croatia			
486	469	396	13			
35.6%	34.4%	29.1%	0.9%			
By current education:						
University student	High School student	Not enrolled				
978	370	16				
71.7%	27.1%	1.2%				
By area of education:						
Engineering and Technology	Humanities and Social Sciences	General High School studies	Natural Sciences	Arts	Medical Sciences	Not enrolled
664	272	204	183	24	10	7
48.7%	19.9%	15.0%	13.4%	1.8%	0.7%	0.5%

Table 2 - Future education aspirations of respondents

I had a chance to learn about disaster risks and fire safety as part of my High School/University curriculum or during a lecture organised at my School/University.				
Yes		No		
562		802		
41.2%		58.8%		
If yes, in what context?				
I had a complete course concerning this.	I had a part of a course concerning this.	I attended one lecture.		
75	246	241		
13.3%	43.8%	42.9%		
I had a chance to learn about disaster risks and fire safety outside of my School/University.				
Yes		No		
839		525		
61.5%		38.5%		
If yes, in what context?				
I am a member of an organization that addresses these issues.	I attended an open lecture.	I heard about it during a conference/seminar.	I read an article.	
38	148	124	675	
4.5%	17.6%	14.8%	80.4%	
I would be interested in studying Disaster Risk Management or Fire Safety at University.				
1	2	3	4	5
404	251	296	212	201
Mean value:	2.67	Median:	3	
I would be interested in obtaining a Master's degree in Disaster Risk Management and Fire Safety.				
1	2	3	4	5
579	283	227	143	132
Mean value:	2.24	Median:	2	
I would attend an elective course in Disaster Risk Management and Fire Safety (if one existed) at my University.				
1	2	3	4	5
239	238	309	269	309
Mean value:	3.12	Median:	3	

Continuous of Table 2 - Future education aspirations of respondents

I would attend a free course in Disaster Risk Management and Fire Safety.				
1	2	3	4	5
131	135	311	333	454
Mean value:	3.62	Median:	4	

Aim of the survey was to acquire preliminary data about the existing interest among youth for future K-FORCE project activities. According to the preliminary data there is a promising number of students hat would be interested to attend a course or are interested in studying Disaster Risk Management or Fire Safety at University. The information from the conducted survey will be used to better develop and implement curricula in the field of DRM&FSE at partner Universities in Albania, Bosnia and Herzegovina and Serbia.

5. A BRIEF INSIGHT INTO NEW STUDY PROGRAMS

DRM&FSE subject area refers to multidisciplinary and interdisciplinary disciplines. Curricula include subjects from various academic disciplines, with Engineering and engineering trades as the dominant academic discipline, Environmental protection, Architecture and Construction, Civil Protection, Fire Science, Rescue studies, Climatology, Hydrology, Seismology and Economy as well as other disciplines (Health, Sociology).

The implementation of interdisciplinary DRM&FSE study programs in the field of Technical Sciences will enable continuation of the studies for a number of different profiles of engineering undergraduates, as well as continual education of professionals by offering LLL courses. Introduction of a novel interactive ICT platform for staff, student and workers' training will enable preparation of real-life case studies.

These programs support the creation and dissemination of Open Educational Resources in diverse European languages. Study programs, learning material offered by Flexible ICT learning platform, LLL courses, Glossary of DRM&FSE key words and terms, as well as an On-line Library will be available in English and regional languages (Serbian, Albanian and Bosnian).

Educational ICT based laboratories created in WB HEIs with interoperability capabilities and on-line library will provide national, regional and international case studies, integrated risk methodology assessment, hazard, risk and vulnerability regional cross-border mapping and results publications. That will insure continuous common regional problem based approach and compatibility of knowledge and skills, also aligned with contemporary trends in DRM&FSE field. Interdisciplinary, multi-language and ICT based both higher and continuous education approach insures regional and international cooperation will allow the exchange of knowledge and the mobility of students, teachers and workers, and strengthens national and regional capacities in EU integrations. Teaching methods improvement and modern ICT use in the education process will coincide with higher education development in the EU. This is especially true in knowledge about best available practices, EU legislation, practical laboratory skills and consequent harmonization with EU curricula.

Within implementation process, European HEIs will have crucial role. They will be responsible for knowledge transfer and experience sharing in including scientific research into education, thus securing curriculum quality from the start. They will steer the content of

curriculum and syllabi, define student-centred learning and teaching methods, share case studies for capstone-type subjects and advice on best usage of modern ICT in the education process. Compliance of the regional study program with similar programs, developed in the EU countries, strengthens the capacity of individual countries and the region as a whole in the process of European integration. Therefore, the brief analysis of available master and doctoral study programs in HEIs in the field of Disaster Risk Management and Fire Safety Engineering was done on the European level (Gencer 2014).

It was found that the majority of the most advanced engineering study programs in this field are available in Sweden at Lund University, Denmark at Danish Technical University and Aalborg University, Great Britain at University of Edinburgh and in FYR Macedonia at Ss. Cyril and Methodius University in Skopje. All of the studies are established in a close connection to Faculties and Departments of Civil Engineering. There are also fully developed study programs, at all three levels in Slovak Republic, at Faculty of Special Engineering, University of Žilina.

As Risk Management and Fire Safety education are not widely found in WB HEIs' curricula, the transfer of know-how of European HEIs to WB HEIs is special valuable, and response to the need for enhanced staff expertise which can underpin new curriculum modernization or development in a way to meet standards developed in EU.

Cooperation with the European HEIs and their contribution is crucial for new programs quality due to knowledge sharing, experience transfer in the fields of scientific research and education, particularly in developing similar programs and modules and assistance in defining needs for program content and teaching methods improvement and modern ICT and computer technology use in the education process coinciding with higher education development in the EU.

6. EXPECTED IMPACT OF MODERNIZED AND NEWLY DEVELOPED STUDY PROGRAMS

It is expected that modernized and newly developed study programs will contribute to resilience improvement of societies in several ways.

Firstly, students will be educated within an interdisciplinary and problem-solving framework, through acquiring theoretical, practical and applicable knowledge, skills and competences, according to National qualifications framework and European qualifications framework, WB countries' needs and EU trends, which will be well recognized by the national and regional labor market. Students on other HEIs study programmes will gain basic or improved knowledge of DRM&FSE issues, consequently resulting in raised awareness among student population.

Implemented programs will enable regional and international mobility of students and teachers from WB and their horizon broadening in this specific field.

Teaching staff will have opportunity to upgrade their teaching experience, capacity to pass on the knowledge updated with novel trends in both the field and teaching tools and methodology. Teaching staff in other disciplines will be able to foster their knowledge and capacity to introduce and interconnect DRM&FSE issues into their disciplines. Non-profit NGOs will have opportunity to realize their own visions and missions in building national and regional capacities for safe and prospective WB societies, on the path towards EU. Professionals in DRM&FSE area will expand and upgrade their knowledge and skills through

LLL courses. Public bodies and administration in charge for civil protection will improve qualification structure and better act as liaison between the emergency sector and scientific and education institutions as well as liaison between educational institutions and stakeholders from the emergency sector.

Employees in various industrial sectors will have an open access to created On-line Library, ICT portal and LLL courses database, through which they can gain knowledge on various DRM&FSE issues, thus raising their awareness about fires and disasters.

7. CONCLUSIONS

Natural disasters devastate lives and livelihoods across the world and slow down the development progress achieved through many decades of hard work. Consequently, the fiscal and economic pressure of developing countries, such as WB, having to deal with the adverse effects on natural disasters is increasing. Numerous human casualties, significant material damage and negative environmental impact of natural and manmade disasters and fires in the WB are the warning calling for change of approach to these issues. There is a need to raise awareness about disaster risks and their potential financial consequences. Raising public awareness regarding natural catastrophic risk and risk reduction strategies is a key component in the promotion of a culture of safety within nations' borders and beyond. Increased resilience and sustainable development requires a more proactive approach to tackle risk at its roots.

Resilient societies are based on knowledge and training, as well as preparedness. Building synchronized regional capacities in higher education in Disaster Risk Management and Fire Safety Engineering, according to regional needs and contemporary trends, is a first step towards building resiliency of our region. Acquired knowledge in the field of Disaster Risk Management and Fire Safety Engineering will provide the base for building a resilient society. It is necessary to build countries' own, consistent and compatible capacities in this educational field, which will enable a uniform level of required knowledge and skills.

ACKNOWLEDGEMENTS

The paper presents the part of research realized within the project "Theoretical and experimental research and improvement of educational process in civil engineering" conducted by the Department of Civil Engineering and Geodesy, Faculty of Technical Sciences, University of Novi Sad.

REFERENCES

[1] Gencer E.: A Compendium of Disaster Risk Reduction Practices in Cities of the Western Balkans and Turkey: A Review of Selected Cities Participating in UNISDR's "Making Cities Resilient: My City Is Getting Ready!" Campaign, 2004.

[2] Stocktaking Report on Risk Awareness And Education on Natural Catastrophes. (2008).OECD.

[3] Decision of the European Parliament and of the Council (2013). Official Journal of the European Union.

[4] Disaster Risk Assessment and Risk Financing: A G20 / OECD Methodological Framework (2012). OECD.

[5] Laban M., Radonjanin V., Milanko V., Draganić S.: Knowledge FOr Resilient Society - K-FORCE Project Proposal Submission, Call for Proposal EAC/A04/2015 KA2 – Cooperation for Innovation and the Exchange of Good Practise - Capacity Building in the Field of Higher Education, 2015.

ДГКС Друштво грађевинских конструктера Србије
ASES Association of Structural Engineers of Serbia
S-96
15. KONGRES
6-8. 9. 2018. Zlatibor

Ranko Babić[1], *Lidija Babić*[2] *Radomir Folić*[3]

NOVO REŠENJE PORTALA TUNELA ZA BRZE ŽELEZNICE

Rezime:
Uvodni deo rada sadrži neke opservacije o aerodinamici vozova visokih brzina (VVB), posebno interakciju VVB-tunel, što je detaljno razmotreno u sklopu soničnih udara. Dat je opširan pregled prethodnih istraživanja i inženjerskih ostvarenja usmerenih ka smanjenju uticaja ovog efekta na životnu sredinu, pre svega u vidu štitnika na portalima tunela. Oslanjajući se na optimalno profilisan ulaz tunela i na analogiju sa sličnim akustičkim strukturama predložena je nova konfiguracija štitnika, uz razmatranje tehnoloških aspekata u smislu ekonomičnih oplata.

Ključne reči: udarni talas, buka VVB, sonični udar, rog zvučnik, trenje graničnog sloja

NEW DESIGN OF TUNNEL HOODS FOR HIGH SPEED TRAINS

Summary:
In introductory part of paper we gave some observations about high speed train (HST) aerodynamics with concern on interaction HST-tunnel, which is described in detail, particularly the phenomenon of sonic boom. An extensive survey of prior research and engineering work aimed at mitigating environmental influence of this effect is given, mainly regarding tunnel hoods. Relying on optimally flared tunnel entrance and making analogy with similar acoustic structures we proposed a new configuration of tunnel hood, considering technological aspects through cost-effective concrete formworks.

Key words: shock wave, HST noise, sonic boom, horn loudspeaker, skin friction

[1] *Dr, University of Pristina, Faculty of Technical Sciences, Knjaza Miloša 7, Kosovska Mitrovica, Serbia,* ranko.babic@pr.ac.rs
[2] *Dr, University of Pristina Faculty of Technical Sciences, Knjaza Miloša 7, Kosovska Mitrovica, Serbia*,lidija.babic@pr.ac.rs
[3] *Dr, University of Novi Sad, Faculty of Technical Sciences, Trg D. Obradovica 6, Novi Sad, Serbia*,folic@uns.ac.rs

1. INTRODUCTION

Tunnels are inevitable parts of railway line because the request of track mild curvature cannot consistently follow terrain topography, particularly for high speed railways (HSR) [1, Fig.4], where track curvatures should have greater amounts [2]. The reason is tolerable acceleration (passenger comfort and prevention of load displacement) [3]. Therefore, HSR does not adapt itself to terrain topography, but the terrain to itself. HSR imposes new criteria for tunnel design and operation, not inherent to conventional railways. Serious aerodynamic effects appear within tunnel and in HST-tunnel interaction, which limit the maximum allowed train velocity for a given tunnel cross-section area, and influence the traction energy consumption. Pressure rise at the moment of train entering and unsteady aerodynamic field around the train are essential to know, in order to optimally choose tunnel configuration and undertake measures of pressure reliefs [4, 5, 6].

2. SOME ISSUES OF TRAIN (OPEN AIR) AERODYNAMICS

Today's HST convey passengers and goods with speeds of 350 km/h, or 400 km/h and more in near future, so one can travel from city centre to city centre almost at airline speeds. HST can compete with air travel at distances up to 700 km, offering 1,300 seats per train, with exclusive comfort, twice as many as the largest planes [7]. As the air drag increases with the square of speed, to keep the HST energy efficient it should be aerodynamically efficient. Soon as HSR entered operation (Japan, Shinkansen line, 210 km/h, 1964), the cab front of HST was shaped like a jet airliner, to decrease air drag, accounting for more than 50 % of total resistance. Rounded nose seemed likely to help, and it sat the pattern for years ahead [8].

Simple borrowing the nose shape from airliner to the fast trains does not match essential difference in aerodynamics: one flies through the free space, the other is "flying" on the ground, air density at 10,000 m and at the ground, air density dependence of temperature (density at □7ºC increases air drag by 10 % from that one at +20ºC, at sea level). With 1.2 kg mass of 1m^3 of "empty" air, a HST, with lateral dimensions e.g. WxH=3.4x4.2 m^2, running at 380 km/h (105.5 m/s), encounters 1,808 kg of air each second.

The air is, simultaneously, static and dynamic medium: it conveys the perturbation by the sound speed while the molecules just oscilate and actually remains at their places (static). It is also a compressible fluid. An object, moving through the air must literally cut through masses of air, putting them away to pass that portion of space. A conical (system of) wave front(s) is formed around the object, which angle is determined by the ratio of object and sound speeds.

Moving in open-air, HST generates a highly turbulent slipstream, to which complexity adds the presence of ground. The factor "ground" acts in combination with train length [9].

The size ratio, defined as R=max(W, H)/L, where W, H, L are width, height and length of airliner fuselage or HST, reaches 120 for HSTs of 400 m lenght (with lateral approximative dimensions WxH=3x4 m^2), while airliners are between 8□-12. We compared HSTs Shinkansen N700, Zefiro 380, CRH380A, AGV, Velaro, Talgo, TGV, with airliners (two and four jet engines) A318, A321, A340, A380, B737, B747, Il96, An148, MC21.

Although a raw parameter (not concerns shapes of nose and tail), it is a good measure for skin friction figure, prevailing component of HST air drag.

Boundary layer, formed by streamlined train nose, gradually turns out into turbulent diverging flow along the train.

Sharp noses generate thinner boundary layer along the train sides and also a steep rise of slipstream velocity in near wake region. For more rounded nose, faster boundary layer growth is observed while less vigorous flow occurs near wake region. Slipstream velocity magnitude decreases with height from the ground [9].

Viscous shear stress on train surface is produced due to different velocity layers in boundary layer, the integral force of which in the direction opposite to running train forms the total friction drag of the train [10, Fig.8].

It would be interesting to systematize profiles of HST noses since 1964 to nowadays, to survey the evolution of engineers' views about HST aerodynamics.

The track curvature can be also an aerodynamic factor as curved train involves additional flow effect in respect to its straight geometry. We think it is worth studying. The HST of 400 m length, running at 380 km/h along the curved section of track with horizontal radius 5872 m [3] is laterally concave for 3.46 m.

Topographic irregularities (wrinkles, ditches, cuttings etc.) [4], not to speak about overpasses, underpasses, tunnels, wind shields, buildings, premises, facilities, further complicate aerodynamic field around HST.

The smooth train body itself makes turbulent slipstreams, not to speak about all protrusions, edges, holes, on that smooth body (generated by wheels, bogies (turbulences), inter-car gaps, pantographs, etc.), causing the noise of the HST, which rises with speed [11]. By new pantograph aerodynamics its noise was considerably decreased: owl wing inspired solution - wingraph [11], or placing it in car roof box [12], aerodynamically shielded.

The already described turbulent pressure field around HST is stationary, determined only by train movement. Cross wind makes fundamentally new picture of train aerodynamics [5], [13-15], and even at moderate yaw angles questions the train/nose shape, if designed primarly for axial flow. We would refer to that "questioning" with the ratio defined as e.g. $(v_T/v_W)\sin\alpha$, where v_T is train speed, v_W wind speed, α yaw angle. Cross wind issues will not be considered in this paper although the train nose, profiled for side wind factor, obviously has not the optimal shape for tunnel effects relaxation.

3. MAIN PROCESSES IN HST-TUNNEL INTERACTION

In tunnel, the airflow is confined between the train and tunnel walls, and causes increase of drag, which depends on many factors, where the blockage ratio (areas of train S_{tr} and tunnel S_{tu} cross section) $B = S_{tr}/S_{tu}$ is the most important one [16, 17, 20]. Entry of HST into tunnel generates sharp pressure transients, heard as sonic boom at exit, as the most audible HST sound effect. This shock wave starts its propagation, at speed of sound, along the tunnel. Reaching the exit it produces blasting sound called sonic boom [18, 19]. But the picture is not that simple.

Creation of shock wave in tunnel begins well before the train nose enters the tunnel opening [9, 19, 20]. This pressure wave first enters the tunnel portal. Its configuration can be seen in e.g. [20], [21]. Then comes the main and the steepest portion of shock wave, caused by train

nose entering the tunnel aperture. The propagating pressure wave induces a forward flow in tunnel, as an headwave of the train, and a backward one, through the annular gap between the tunnel wall and the train wall [16]. Primary wave gradient is followed by a further, less steep increase of the pressure due to friction on the train and tunnel walls, respectively, caused by the entry of the train body [18]. The slipstream velocity may be significantly affected by the space size between the train side and the tunnel walls [23]. Compressive slope of the shock wave is terminated by the entry of the HST tail, causing a rarefaction transient [18]. These pressure transients, greater than those in open are can cause passenger discomfort, especially in poorly-sealed trains [9].

The induced slipstream velocities depends on train speed, blockage ratio, train length, tunnel length, the roughness of the train and the tunnel walls, and on the initial air speed in the tunnel. The effect increases with a longer train [16].

The emerged pressure impulse propagates along the tunnel at sound speed, or with relative speed in respect to train (Δv=340 - 70 m/s = 270 m/s, for tunnel speed of 250 km/h) and will produce sonic boom well in advance, before the train appears at the tunnel exit (3.4 s for tunnel of 300 m). Sonic boom is greater for slab track rather than for ballasted track [9].

Although the pressure change is small (2% or 3% of the atmospheric pressure for train speed >250 km/h), giving the name micro-pressure wave, its steep gradient is what causes blast effect, together with generation area, power and masses inserted into the wave.

Apart from sonic boom as outward effect of pressure impulse, there is a inward one - reflection of shock wave from the opposite tunnel portal, as negative, i.e. rarefaction wave. At its way back it encounters moving train and partially reflects from that discontinuity in tunnel, and partly passes toward the entrance from where it produces a subsequent, weaker, sonic boom outside, and a new rarefaction wave inside. The result is a very complex interference of propagating transients, giving a changing pressure distribution along the tunnel [4], [22], especially if the tunnel is double track [23].

Here we would point out that the rarefacted wave encounters not a brick wall but a fast moving obstacle where a impulsive Doppler effects takes place, changing not the sound frequency but its gradient.

In double track tunnel the flow velocity distributions in front of the train are essentially symmetrical with the train centreline, whereas along the annular region, between the train sides and the tunnel walls, with the space much narrower on one side of the train than on the other, is quite non-symmetrical. At the train rear, the boundary layer is separated from the tail head to generate numerous vortices, which subsequently shed into the near-wake flow and cause large fluctuations in the wake region. The unbalanced development of the boundary layer on both sides of the train causes the unbalanced development in the trailing vortex, which is clearly offset from the train centerline [22].

HST noise that originates from discontinuities at train body are enhanced at tunnel entrance. They are reduced by combination of measures: shields for aerodynamic shadowing of protruding equipment at train roof, coverings for bogies and interbogie space, gaps between the cars etc. But HST whooshes are simply unavoidable because of HST size and speed at intermediate stops and settlements near the railway which it passing by at full speed.

As the air drag gains step rise and prolonges along the whole tunnel, the train slows down before the enter to avoid unnecessary energy consumption.

In general, the interaction between tunnel and train makes the whole pressure field much more complicated compared to that one in open air [22].

4. MEASURES FOR SONIC BOOM MITIGATION

At early days of HSR Japan's engineers were witnesses of sonic booms echoing over populated areas around tunnel openings. Mountinuous character of Japan means many bridges (700,000) [24], and, hence, many tunnels. Japan is densly populated (arithmetic density 350 p/km^2, effective density 1164.15 p/km^2), so each opening has its numerous audience. The similar situation is in EU28, populated with 117 p/km^2 [25]. Therefore, the problem was pretty serious.

The principal way to mitigate the effect is to decrease the pressure gradient, which is proportional to the amplitude of the sonic boom. As HSTs should keep their velocity also in tunnels, it is attained by prolonging train nose and widening tunnel entrance. Trumpet-like tunnel entrance softens the sharp (block) discontinuity at tunnel opening. The length of flared tunnel entrance in combination with train speed will give desired gradient. It is related to expenses for additional construction works and it is possible for new tunnels only. Existing tunnels get elongations called hoods, which approximate trumpet-shaped entrance by one or two steps [26, 27, 28]. Oblique tunnel portals also produce obvious mitigation effect. A hat oblique tunnel portal combined with a buffer structure with top holes is particularly effective [29].

An optimally flared tunnel portal causes the pressure to rise linearly across the front of the compression wave generated by an entering HST. The interaction of train nose with successive changes in portal diameter produces a `rippling' of the pressure wave profile. The amplitude of these fluctuations depends on the length of the train nose and on the number of cylindrical sections, and suggest that an ideally flared portal is well approximated by a stepped-portal fabricated from three or four sections [26].

Hoods with sharp edges also deserve our attention [30, 31]. Such solutions, besides oblique tunnel portals, we find as aesthetically acceptable to fit into landscape (e.g. tunnel St. Gotthard).

Tunnel with Helmholtz resonators is another principal solution, interesting as a basis for similar solutions [32].

Our proposal of hood shape relies on the optimally, trumpet-like flared tunnel entrance, proposed in [26] (Fig.1, 1-4). It is possible to accomplish for new tunnels, but it is not cost-effective because of complex formworks and changed tunnel statics at the entrance, nevertheless hill slope at that place can be declined to reduce the load on tunnel concrete skirt.

We find an analogy between that shape and the horn of outdoor loudspeaker or megaphone [33], [34], [35, Fig.10], as presented on Fig.1-5.

A significant question arises while considering the optimal shape of tunnel ending, better to say endings, since the same structures should exist at both tunnel ports because of bilaterality of railway traffic. In that case a primary shock wave, generated by train entry, would be amplified by exit port, acting as loudspeaker.

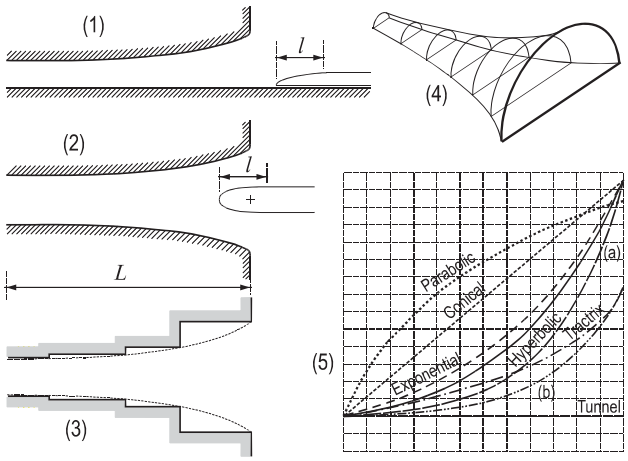

Figure 1. (1) and (2) Geometry of optimally flared tunnel entrance with HST, lateral and top view. (3) Step cylindrical approximation of ideal tunnel port (adapted from [26]). (4) 3D wire skeleton of tunnel port. (5) Profiles of horn of outdoor loudspeaker: (a) optimal tunnel profile normalised to conical, exponential and hyperbolic forms; (b) the same, to tractrix horn profile (adapted from [33], [35]).

By this simple analogy to loudspeaker horn shape we find amplifying function of optimally flared tunnel ending. It is for outward action of such tunnel mouth. For inward action, i.e. train entry, specific form of wavefront from rushing train will excite the optimally flared tunnel entrance as described in [26]. We would say that such effect of horn-like tunnel entrance, i.e. the decrease of pressure gradient, stems from Bernoulli Equation: pressure transient of Δt_1 and with velocity v_1 at the widest cross section will attain duration $\Delta t_2 > \Delta t_1$ at the narrowest cros section because of velocity increase $v_2 > v_1$.

5. CONCLUSION - THE CONCEPT OF PROPOSAL

Actually, hood is an extension of the tunnel. In [26] it is proposed optimal shape of tunnel mouth. We noticed discrepancy with [28] regarding the issue of optimal form. For existing tunnels, hoods of such, optimal, form, also would not be cost-effective since they imply complicated formworks.

Sliding formwork is advisable. To use a set of coaxial cylindrical sections that together approximate the ideal flared geometry [26], requests several different sliding formworks, which is also costly approach. Very similar situation would be for conical form, as better approximation of hyperbolic shape. What has left is cylindrical hood as a technically acceptable solution.

Cylindrical reinforced concrete structure hood is simply to build, by slip formwork. Holes on the hood are particularly effective. Our idea is to cross optimal flare and cylindrical, technically acceptable hood. It can be attained by triangle slits along the hood, as shown on Fig. 2. Cylindrical shape with such openings, stretching along the whole hood, simulate converging geometry which acts as a horn. The best shape would have slits but statics of the

structure calls for bridged edge of hood (Fig.2). Alternative form includes openings arranged to make an equivalent of triangle slit.

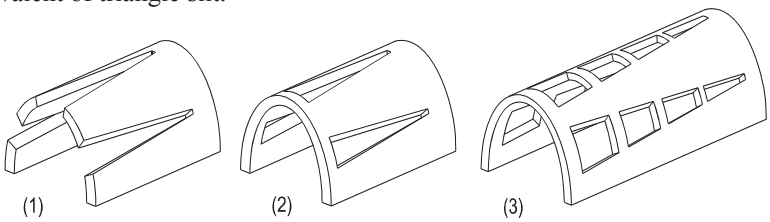

Figure 2. (1) Converging shape of hood is emulated by longitudinal slits. (2) To improve statics of hood extensions edge bridges are added. (3) Cage configuration with perforation creates the surface static system

ACKNOWLEDGEMENT

The research described in this paper was financially supported by the Ministry of Education and Sciences of Republic of Serbia within the Project TR 36043. This support is gratefully acknowledged

REFERENCES

[1] S. Hodas, "Design of Railway Track for Speed and High-speed Railways", Procedia Engineering, Vol. 91, 2014, pp. 256-261.

[2] M. Lindal, "Track geometry for high-speed railways", Royal Institute of Technology, Stockholm, 2001.

[3] D. J. Vermeij, "Design of high speed track", http://heronjournal.nl/45-1/3.pdf

[4] C. Baker, "A review of train aerodynamics Part 1 – Fundamentals", The Aeronautical Journal, 2014, vol 118, no. 1201.

[5] C. Baker, "A review of train aerodynamics Part 2 – Applications", The Aeronautical Journal, 2014, vol 118, no. 1202.

[6] C. Baker, "The flow arround high speed trains", VI International Colloquium on Bluff Bodies Aerodynamics & Applications, Milano, Italy, July, 20-24 2008.

[7] http://www.bombardier.com/en/media/newsList/details.40976-bombardier-highlights-high-speed-expertise-at-seminar-in-china.bombardiercom.html

[8] http://the-contact-patch.com/book/rail/r1416-aerodynamics-and-the-moving-train

[9] S. Faramehr, "Aerodynamic of the Trains in Tunnels" (PhD, Superv.: H. Hemida), September 2014 (http://etheses.bham.ac.uk/5468/1/Faramehr14PhD.pdf)

[10] Y. Wang, Y. An, Y. Chen, "Aerodynamic simulation of high-speed trains based on the Lattice Boltzmann Method (LBM)", Science in China Series E Technological Sciences, vol. 51, no. 6, p. 773-783, 2008/06/01

[11] "The Return of Dr. Eiji Nakatsu and Biomimicry", 02/08/2017, (http://www.cadalyst.com/%5Blevel-1-with-primary-path%5D/return-dr-eiji-nakatsu-and-biomimicry-32250)

[12] A. Orellano, "Aerodynamics of high speed trains , Vehicle aerodynamics lecture", Stockholm, KTH, May 12th, 2010, Bombardier

[13] S. Krajnovic, "Novel development in numerical simulations for aerodynamics of high-speed trains", 20th Nordic Seminar on Computational Mechanics, Gothenburgh, Sweden, Nov. 23-24, 2001,

[14] B. Diedrichs, "Aerodynamic calculations of crosswind stability of a high-speed train using control volumes of arbitrary polyhedral shape", VI International Colloquium on Bluff Bodies Aerodynamics & Applications, Milano, Italy, July, 20-24 2008

[15] T. Liu et al, "A CFD analysis of the aerodynamics of a high-speed train passing through a windbreak transition under crosswind", Engineering Applications of Computational Fluid Mechanics, 12:1, 137-151, 2018, DOI: 10.1080/19942060.2017.1360211

[16] J. Novák, "Single train passing through a tunnel", European Conference on Computational Fluid Dynamics, ECCOMAS CFD 2006, Netherlands, 2006

[17] T. Gilbert et al, "Aerodynamics of high-speed trains in confined spaces", The Seventh International Colloquium on Bluff Body Aerodynamics and Applications (BBAA7), Shanghai, China; September 2-6, 2012

[18] H. Sockel, "Aerodynamic effects caused by a train entering a tunnel", PAMM (Proceedings of Applied Mathematics and Mechanics), Vol. 1, Issue 1, Section 9.2, p. 268–269, March 2002

[19] Z. Jiang et al, "Investigation of Shock-Wave Generation by a High-Speed Train Running into a Tunnel", Mathematical analysis laboratory record, vol. 993, 1997, p. 26-34,

[20] J. Choi, K. Kim, "Effects of nose shape and tunnel cross-sectional area on aerodynamic drag of train traveling in tunnels",Tunneling and Underground Space Technology, Vol. 41, March 2014, Pages 62-73

[21] (http://www.sciencedirect.com/science/article/pii/S088677981300196X)

[22] http://acustica.ing.unibo.it/Researches/train/train.htm

[23] T. Kanazawa, "High-Speed Train-Tunnel Interactions", (http://www.ms.t.kanazawa-u.ac.jp/~fluid/staff/yang/train.html)

[24] M. Fu, P. Li, X. Liang, "Numerical analysis of the slipstream development around a high-speed train in a double-track tunnel", 2017, PLoS ONE 12(3): e0175044. https://doi.org/10.1371/journal.pone.0175044.

[25] "Road Maintenance in Japan: Problems and Solutions", Ministry of Land, Infrastructure, Transport and Tourism 2013, Japan

[26] http://ec.europa.eu/eurostat/tgm/table.do?tab=table&init=1&language=en&pcode=tps00003&plugin=1

[27] A. Winslow, M.S. Howe, "Stepwise approximation of an optimally flared tunnel portal", Journal of Sound and Vibration, Vol. 280, Issues 3-5, 23 February 2005, p. 983-995

[28] M. Iida, K. Kikuchi, T. Fukuda, "Analysis and Experiment of Compression Wave Generated by Train Entering Tunnel Entrance Hood", JSME International Journal, Series B, Vol. 49, No. 3, 2006

[29] D. Uystepruyst, M. William-Louis, F. Monnoyer, "3D numerical design of tunnel hood", arXiv:1511.06264v1 [physics.flu-dyn] 19 Nov 2015, (https://arxiv.org/pdf/1511.06264)

[30] L. Zhang et al, "Oblique tunnel portal effects on train and tunnel aerodynamics based on moving model tests", Journal of Wind Engineering and Industrial Aerodynamics, Vol. 167, August 2017, p. 128-139

[31] A. Winslow, M. Howe, M. Iida, "Influence of a Scarfed Portal on the Compression Wave Generated by a High-Speed Train Entering a Tunnel", SAGE Journals, Journal of Low Frequency Noise, Vibration and Active Control, Dec 1, 2005 (http://journals.sagepub.com/doi/abs/10.1260/026309205776232817)

[32] X. Xiang, L. Xue, B. Wang, "Aerodynamic Effects of Inclined Portals on the Initial Compression Wave Generated by a High-Speed Train Entering a Tunnel", Journal of Fluids Engineering, Voll. 137, Issue 12, Aug 04, 2015

[33] J. Tebbutta et al, "Numerical investigation on an array of Helmholtz resonators for the reduction of micro-pressure waves in modern and future high-speed rail tunnel systems", Journal of Sound and Vibration, Vol. 400, 21 July 2017, p. 606-625

[34] Bjørn Kolbrek, "Horn Theory: An Introduction, Part 1", audioXpress (https://www.grc.com/acoustics/an-introduction-to-horn-theory.pdf)

[35] J. Dinsdale, "Horn loudspeaker design", Wireless World, March 1974 (http://www.audioheritage.org/vbulletin/attachment.php?attachmentid=50940&d=1302885851&usg=AOvVaw2vFwmfepIqPZ3t9YMPtQKi)

[36] V. Phan, "The Icon Horn Loudspeaker", Nov 2014 (on http://digitalcommons.calpoly.edu/cgi/viewcontent.cgi?article=1253&context=mesp)

[37] (websites accessed for update on Jan 10, 2018)

ДГКС Друштво грађевинских конструктера Србије
ASES Association of Structural Engineers of Serbia
S-97
15. KONGRES
6-8. 9. 2018. Zlatibor

Predrag Popović[1]

ŠTA SMO NAUČILI OD VELIKIH KOLAPSA MOSTOVA

Rezime:

Veliki kolapsi ili havarije mostova su oni u kojima je došlo do gubitaka života ili velikih ekonomskih gubitaka. Uzroci kolapsa tokom izgradnje većih mostova su proračun koji nije uzeo u obzir sve terete u procesu gradnje, nestabilnost privremenih podupirača i neadekvantna bočna ukrućenja. Uzroci kolapsa mostova koji su godinama u upotrebi su bili zamor i krti lom čelika, pogrešan proračun, neadekvatno održavanje, povećani tereti, podlokovanje oslonaca požar i udar vozila u elemente mosta. Analize nekih od kolapsa su rezultirale u promenama načina projektovanja i održavanja mostova i promenama kodova. Te promene bi trebale do budu preventivne umesto reaktivne.

Ključne reči: kolaps, havarija, most, privremeni podupirači, zamor, održavanje

LESSONS LEARNED FROM MAJOR BRIDGE COLLAPSES

Summary:

Major bridge failures or collapses involve loss of life and/or adverse economic impact. The collapses during the construction are caused by failure to adequately account for loading conditions during the construction and are due to unstable temporary supports and inadequate lateral bracing. Failures after the bridge had been in-service for a number of years were caused by fatigue and brittle fracture, improper design, inadequate mainenance, application of loads larger than design loads, scour of foundations, fire, and vehicular impact. Some of these collapses resulted in changes in our approach to design and construction practices and changes in design codes. Changes to current practices should be deliberate and not reactionary.

Key words: collapse, failure, bridge, temporary shoring, fatigue, maintenance

[1] *M. Sc., Senior Principal & Vice President, Wiss, Janney Elstner Associates, Inc., Northbrook, IL, USA*

1. INTRODUCTION

Over the years there were instances of major bridge collapses that received the attention of the public and the engineering community, and resulted in examination of design and construction practices. Some of these also resulted in changes in our approach to design and construction of the bridges.

The collapses could be chronologically divided into those before the construction of the bridge is completed, and those that happened after the bridge had been in service for a number of years. Failures during the construction are usually caused by not adequately accounting for loading conditions during construction. Failures after the bridge had been in service for a number of years are usually because of improper design, inadequate maintenance, application of loads larger than for which the bridge was designed, scour of foundations, fire, and vehicular impact.

2. BRIDGE COLLAPSES DURING CONSTRUCTION

During the construction of a bridge, very often its components are not self-supporting and may require temporary shoring and bracing while the bridge is being erected. That may include vertical shoring tower supports (Figure 1) to carry self-weight of the bridge before the bridge is completed. These towers have to be designed and built to safely also carry lateral and longitudinal loads like wind and impact of construction loads. Shoring towers are usually not designed for these lateral loads but only for anticipated vertical loads. Lateral loads applied at the top of the tower and on the exposed area of the tower have to be transferred to the ground to eliminate bending stresses for which the tower was not designed.

To equalize the loads in each of the legs of the shoring towers, a system of steel grillages is built in the top of the tower, as shown in Figure 2.

Figure 1. Shoring towers

Figure 2. Transfer of load from bridge girders to shoring tower

That system has to be stable both for vertical and horizontal loads that will be applied to it. Figure 3 shows the conditions of the transfer beams that are not stable for longitudinal loads from the bridge superstructure.

Figure 3. Unstable elements at the top of bridge shoring tower

To transfer the loads to the ground, the foundations of temporary towers have to be adequate to transfer the loads within the allowable capacity of the soil and with acceptable settlement. Figure 4 shows failures of foundations of temporary shoring towers due to inadequate strength of concrete footings, and Figure 5 is a view of a collapsed bridge. During the construction of a segmental concrete bridge, the erection truss supports were not designed to support longitudinal loads due to friction of the wheels of the moveable crane resulting in the collapse shown in Figure 6.

Figure 4. Failure of footings for temporary shoring tower

Figure 5. Collapsed bridge due to uneven settlement of temporary supports

Figure 6. Collapsed erection truss

During demoliton of an old steel bridge, the fascia girder was being removed by picking it up with two cranes on barges, one on each end (Figures 7 and 8).

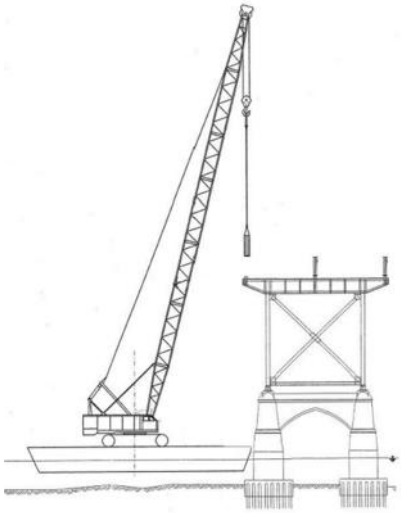

Figure 7. Removal of fascia girder from the bridge

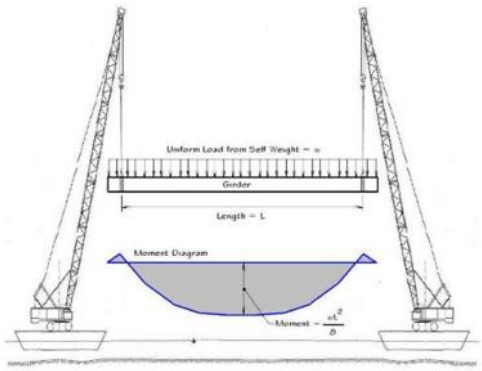

Figure 8. Pick-up points for the fascia girder

When the existing floor beams were cut to free the fascia girder from the rest of the bridge, the weight of the girder was transferred at each end to a crane (Figure 9). However, since the girder was not adequately laterally braced, it buckled under its own weight and collapsed. The two cranes also collapsed and the operator of one crane was killed (Figure 10).

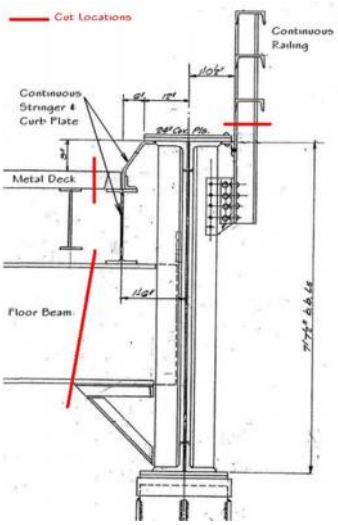

Figure 9. Cutting the connections of fascia girders

Figure 10. Collapsed girder and barges

Figure 11 shows another example of a collapsed bridge during its construction. Longitudinal steel girders were being erected and were temporarily braced laterally with steel frames. A new construction superintenent on the project saw one of the cross frames begin to buckle and decided to replace it prior to checking how tight the remaining cross frame connections were. Removal of this one cross frame resulted in long unbraced length of a girder which caused the girder to buckle and the whole structure to collapse.

Figure 11. Collapsed bridge girders during construction

3. COLLAPSES OF COMPLETED BRIDGES

In December 1967, a two-lane eye-bar suspension bridge built in 1928 collapsed under heavy rush hour traffic (46 fatalities). The bridge was 450 meters long with a main span of about 215 meters (Figure 12). It collapsed due to stress corrosion cracking and subsequent brittle fracture of an eye-bar in one of the non-redundant suspension chains.

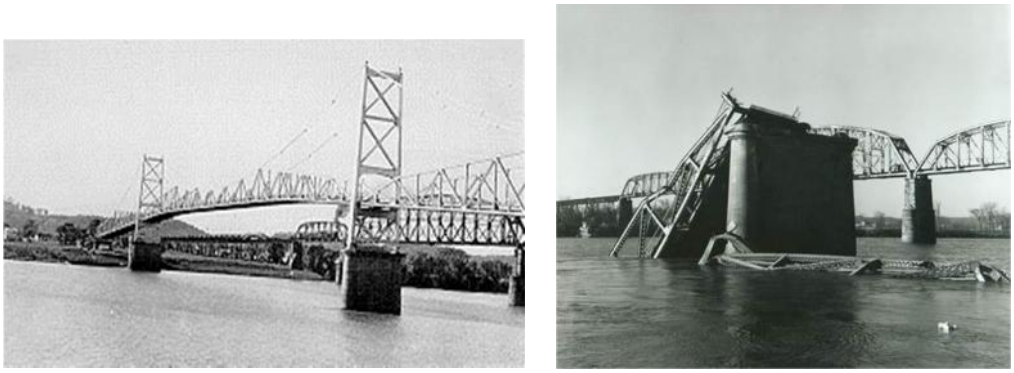

Figure 12. Eye-bar suspension bridge

A review of this collapse resulted in improvements in U.S. bridge practices. New rules mandated regular periodic inspections of all bridges carrying public roads (1970). There was a recognition of the importance of Fracture Critical Members (FCMs), i.e. tension members whose failure is expected to result in collapse or inabilty of a bridge to perform. Improvements were made in material toughness, detailing and construction requirements for FCMs in steel bridges (1978 and 1985).

Examples of fatigue failures are shown in Figures 13 and 14.

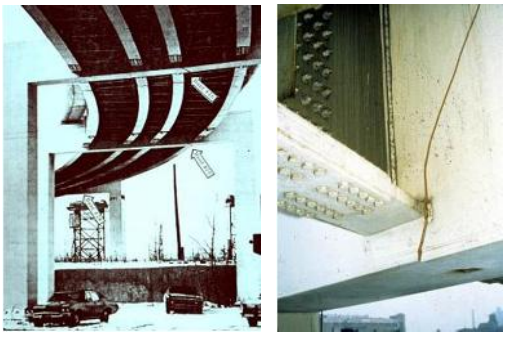

Figure 13. Rapid transit bridge

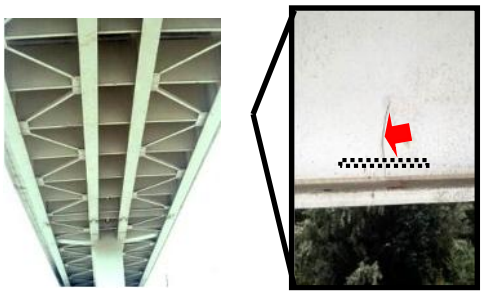

Figure 14. Highway bridge

In 2007, a 40-year old and 325 meter long steel truss bridge collapsed (13 fatalities). Figures 15 and 16 show the bridge before and after collapse. A subsequent investigation determined that a concrete overlay was placed in the 1970s increasing bridge dead load by about 15% and that construction at the time of the collapse resulted in an additional increase in

bridge load. However, the main cause of the collapse was the error in design of a gusset plate that resulted in its thickness being only one-half of what was required.

Figure 15. Truss bridge before

Figure 16. Collapssed truss bridge

In 1987, a multi-span bridge collapsed due to scour of the footing of one of the concrete piers (10 fatalities). A deep concrete foundation was undermined by scour, which resulted in its overstress and fracture and the collapse of three spans of the bridge (Figures 17 and 18).

Figure 17. Collapsed bridge

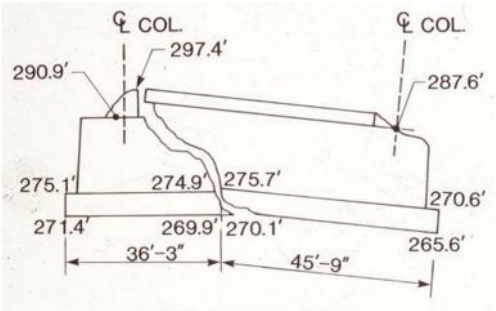

Figure 18. Settlement and fracture of foundation

In 1983, a suspended span of a long steel bridge collapsed (3 fatalities). The main steel girders in the collapsed span were supported at their ends by pin and hanger detail (Figures 19 and 20). The investigation of the collapse determined that the main cause was poor maintenance of the bridge and unrepaired deterioration. The bridge deck drains were covered over during a repaving project 10 years before the collapse, and water and road salts drained through the expansion joints at hanger locations causing hangers to corrode. Pack rust built-up pushed the hanger at one girder end off pin. The increased load in the remaining hanger bar led to its fatigue and brittle fracutre.

Figure 19. Collapse of suspended span

Figure 20. Remaining corroded hanger

The recent collapse of the Morandi Bridge in Genoa, Italy, is another example of a collapse of a bridge structure many years after it was constructed. An investigation has just started and the exact cause of the collapse has not yet been determined at the time this paper was written.

4. CONCLUSIONS

Major bridge collapses result in loss of life and large economic impact. Investigating these collapses we learn about their causes and try to apply this knowledge to improve bridge design and construction practices. A collapse due to steel fatigue and brittle fracture forced us to look at our design codes and change the design criteria for fracture critical steel members. Failures due to scour of bridge foundations caused us to institute regular periodic inspections of underwater bridge foundations. Failures due to unrepaired deterioration forced us to change the mainenance practices and to conduct more rigorous periodic isnpections of bridges.

The case histories listed in these articles were, in addition to the author, investigated by engineers from the author's firm and their contribution is gratefully acknowledged.

ДГКС ASES

CONGRESS SPONSORS

Civil engineering solutions
with state-of-the-art technology

For any bridge construction worldwide – you can at all times rely on PERI.

For over 45 years, PERI has been a competent partner of numerous construction companies and contractors all over the world. In the field of bridge construction, PERI's formwork and scaffolding systems as well as PERI's engineering expertise point the way ahead in the today's construction industry. These solutions positively influence construction procedures and thereby improve the results on the building site. PERI engineers constantly strive to optimise construction procedures and to take advantage of remaining efficiency potential.

Learn more about PERI systems and solutions on our website.

NIS, Pančevo

Sa prometom od 1,48 milijardi evra u 2017. godini PERI je najveći svetski proizvođač i isporučilac sistemskih oplata i skela za sve vrste betonskih radova. Ovaj koncern zapošljava preko 8700 ljudi u više od 70 zemalja na svim kontinentima.

Tunel Manajle

Airport City, Beograd

TC Galerija, Beograd

Gradite uspešno sa firmom PERI

Ekonomični sistemi oplata i skela za sve vrste betonskih radova

PERI®

PERI oplate d.o.o.
Oplate Skele Inženjering
Zmaja Ognjenog Vuka 2
22310 Šimanovci, Srbija
Tel. +381 (0)22 408 200
Fax +381 (0)22 408 250
office@peri.rs
www.peri.rs

ŠIRBEGOVIĆ

betonske konstrukcije za cijelu Regiju

U proteklih 25 godina kompanija **Širbegović** je izgradila preko 9,5 miliona m^2 prostora i time stekla imidž vodeće građevinske kompanije u Regiji kada su u pitanju betonske konstrukcije. Sjedište kompanije **Širbegović** nalazi se u Gračanici, Bosna i Hercegovina, sa podružnicama u Srbiji i Hrvatskoj. Osnovna djelatnost kompanije je projektovanje, inženjering te proizvodnja, transport i montaža prefabrikovanih armirano-betonskih i prednapregnutih konstrukcija koje imaju široku primjenu u izgradnji komercijalnih objekata, infrastrukture kao i stambenih objekata.

Kompanija **Širbegović** preko 25 godina nudi tehnički razvijena rješenja visokog kvaliteta, uz maksimalno uvažavanje estetsko-funkcionalnog aspekta objekata nastojeći da pronađe ravnotežu između arhitekture i građevinarstva i da uvijek bude u koraku sa vremenom odgovarajući na najraznovrsnije zahtjeve kupaca.

Kvalitet, brzina izvođenja radova, mogućnost gradnje kompleksnih objekata, iskustvo u pronalaženju tehničkih rješenja, maksimalno poštivanje rokova i cjelovita ponuda aduti su koji stvaraju ključnu konkurentnu prednost kompanije Širbegović.

Tokom dosadašnjeg poslovanja kompanija Širbegović je izgradila preko 4500 objekata, odnosno preko 9,5 miliona m^2 prostora i time zasluženo postala jedna od vodećih građevinskih kompanija na regionalnom tržištu kada su u pitanju betonske konstrukcije. Instalirani proizvodni kapaciteti se prostiru na 150.000 m^2 zemljišta i više od 35.000 m^2 objekata te omogućavaju izgradnju cca 800.000 m^2 betonskih konstrukcija godišnje.

Bitno je naglasiti da je kompanija Širbegović prva u Bosni i Hercegovini ispunila zahtjeve evropskih normi kojim se obezbjeđuje i dokazuje kvalitet betonskih konstrukcija.

Standardi o kvaliteti koji važe u EU su integralni dio proizvodnje, te sa njima rade i na tržištima na kojima nije obavezno da se primjenjuju.

To se prije svega odnosi na tržište Bosne i Hercegovine, Srbije i Crne Gore gdje ovi standardi još uvijek nisu stupili na snagu.

Osim toga kompanija **Širbegović** je od instituta IGH dobila certifikat kojim se potvrđuje vrhunska kvaliteta prefabrikovane konstrukcije i posebno visoki razredi čvrstoće, što je i potvrđeno razredom tlačne čvrstoće betona MB70 (C55/67) koji je postao uobičajena proizvodnja.

Ovo je prvi certifikat u regiji sa ovako visokim čvrstoćama betona, čime je kompanija Širbegović postavila nove standarde kvaliteta.

KVALITET JE NAŠ PRIORITET

- NORMA EN 13369:2013
- NORMA EN 206:2013
- NORMA EN 1168:2005+A3:2012
- NORMA EN 13225:2013
- NORMA EN 14992:2007+A1:2012
- NORMA EN 14991:2007
- DBV/ BDZ UPUSTVO ZA VIDNI BETON

- **BETONSKE KONSTRUKCIJE**
- **EU NORME**
- **IZGRAĐENIH 7 MILIONA m²**

OSNOVANO / ESTABLISHED SINCE 1990.

Prefabrikacija je savremeni sistem gradnje kod kojeg se konstruktivni elementi objekta proizvode serijski u fabrici, a potom transportuju do mjesta gradnje gdje se vrši montiranje objekta. Prednapregnute olakšane ploče (PPS) su montažni konstruktivni elementi sa kontinuiranim unutrašnjim šupljinama koje umanjuju težinu elemenata i stvaraju efikasan nosivi presjek. Riječ je o jedinstvenom proizvodu, raznolike primjene, sa garancijom velike vrijednosti u odnosu na ulaganje. Ove ploče mogu bez oslonca da premoste raspone do 19 metara.

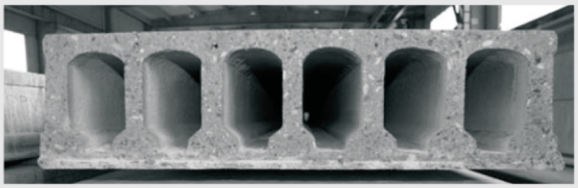

VIZIJA:
"Brzo i sigurno uz primjenu savremenih tehnologija."

Namjera kompanije **Širbegović** je ostati lider na tržištima na kojima djeluje i dalje se širiti na tržištu EU, te sve više jačati brend **Širbegović.** Tržišni udio planira povećavati ulaganjem u kvalitet, širenjem ponuda i usluga te jačanjem odnosa sa kupcima, čije će zadovoljstvo ostati primarni cilj poslovne politike.

Kompanija Širbegović planira i dalje razvijati transparentnost komuniciranja i saradnje sa projektantima i generalnim izvođačima, te stalno povećavati produktivnost putem inovacija i moderniziranja cjelokupne organizacije i korporativnog imidža.

Gračanica 75 320
Branilaca grada bb
Bosna i Hercegovina
T: 00387 35 700 000
F: 00387 35 700 979
E: info@sirbegovic.com
www.sirbegovic.com

Zaštitni premazi

Aditivi za betone i maltere / Superplastifikatori

Aditivi za betone i maltere / Aditivi za vodonepropusnost

ADING
sastojak svake građevine

PROIZVODNI PROGRAM

- Aditivi za betone i maltere
- Smese za zalivanje
- Reparacija betona
- Industrijski i sportski podovi
- Kitovi
- Hidroizolacije
- Zaštitni premazi
- Protivpožarni materijali
- Građevinska lepila
- Smese za izravnavanje
- Dekorativni premazi i malteri
- Proizvodi za građevinarstvo

www.ading.rs

Adresa: Nehruova 82, 11070 Novi Beograd ; Tel/Fax: + 381 11 616 05 76 ; email: ading@ading.rs

ARMONT
LICA KONSTRUKCIJA

West 65, Beograd

BOSCH, Pećinci

Budućnost je bliže nego što mislimo. Budućnost je danas. Vizija budućnosti kompanije Armont, zasniva se na pomeranju granica mogućeg.

Inovativni materijali, konstrukcije projektovane i izrađene po specifičnim zahtevima svakog pojedinačnog projekta, samo su deo onoga što čini da Armont svojim tehničko-tehnološkim dostignućima danas stvara rešenja budućnosti.

Od planiranja i projektovanja do izrade i montaže, kreativna rešenja projektnog biroa Armont mudro korespondiraju sa narastajućim potrebama i novim standardima gradnje.

Kako estetskim, tako i funkcionalnim rešenjima, Armont konstantno postavlja nove standarde gradnje. Budućnost više ne izgeda tako daleko i nedostižno.

Svojim projektima, poput Pupinove Palate u Novom Sadu, Armont jasno prikazuje svoju viziju - sada, više ništa nije nemoguće.

ARMONT SP
LICA ZGRADA

www.armont.biz

120 GODINA
FABRIKE CEMENTA POPOVAC

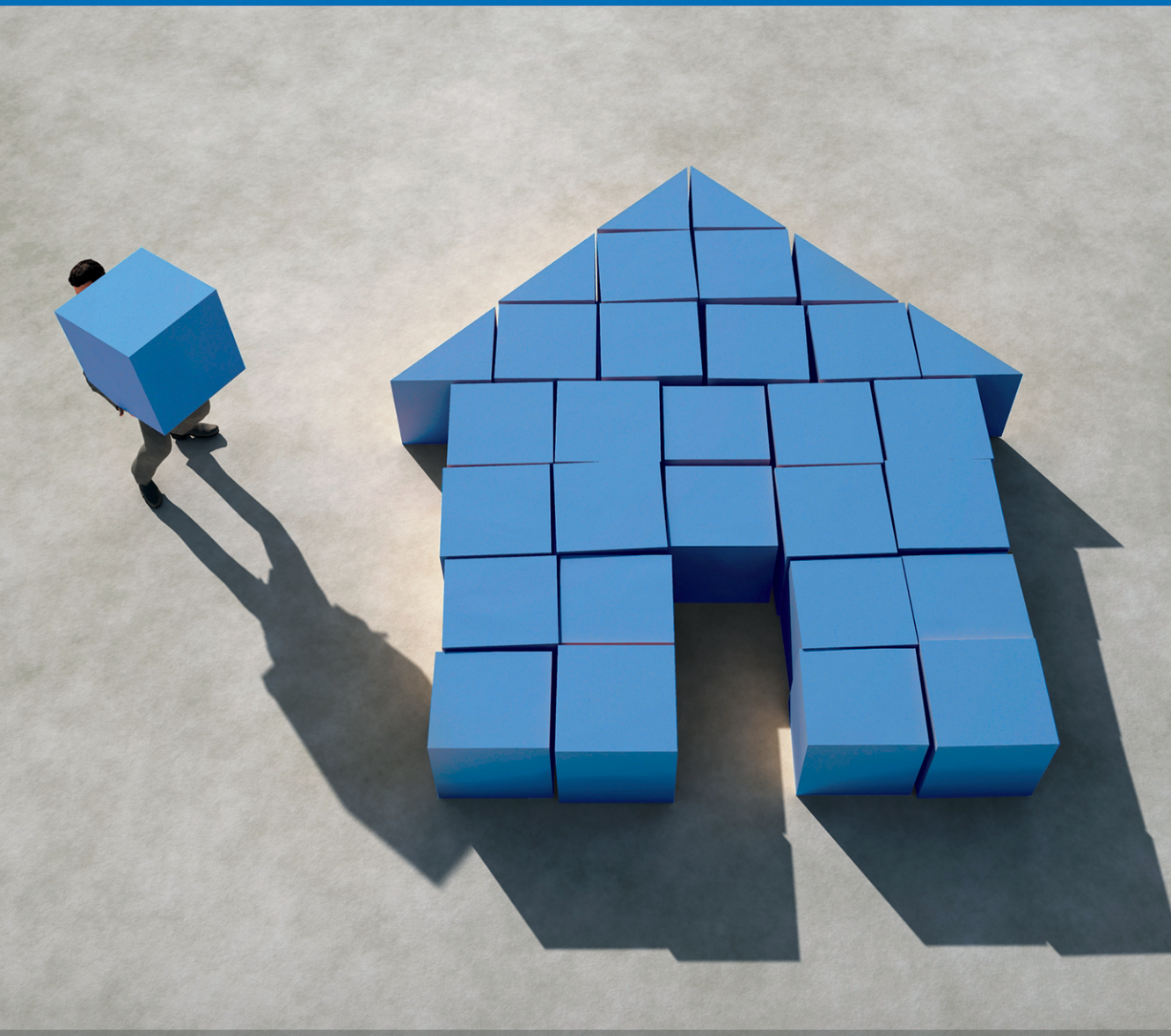

Fabrika cementa u Popovcu osnovana je daleke 1898. godine. Milioni tona cementa koje smo proizveli u proteklih 120 godina iskorišćeni su širom naše zemlje u bezbroj objekata bez kojih bi bilo teško zamisliti moderan život. Kuće, putevi, mostovi, fabrike, tuneli, stambene i poslovne zgrade, hidroelektrane i brojne druge građevine ostaju i opstaju zahvaljući kvalitetu naših proizvoda. Fabrika cementa Popovac danas je deo CRH Grupe, jednog od najvećih proizvođača građevinskih materijala u svetu.

ENERGOPROJEKT

SRPSKI BREND, SVETSKI KVALITET!

Energoprojekt | Bulevar Mihaila Pupina 12 | Beograd, Srbija

www.energoprojekt.rs

MONTAŽNE ARMIRANO BETONSKE KONSTRUKCIJE

Beton je jedan od najrasporostranjenijih građevinskih materijala. Osim što ima veliku oblikovnu moć, veliku nosivost na pritisak i krutost, beton je takođe veoma isplativ materijal. Prefabrikovane armirano betonske konstrukcije imaju izrazito dobre protivpožarne osobine. Proizvode se u zatvorenom prostoru i nude čitav niz različitih tehničkih rešenja visokih estetskih i funkcionalnih vrednosti.

U pogonima **MARTINI GRADNJE** odvija se i proces prednaprezanja konstruktivnih elemenata, kojim se pre svega postiže bolja nosivost i stabilnost svakog pojedinačnog elementa. Prefabrikovana betonska konstrukcija sastoji se od temelja, stubova, greda, međuspratnih ploča, krovnih nosača i zidnih panela. Ovim se omogućava građenje različitih objekata upotrebom relativno malog broja tipskih elemenata, proizvedenih u fabrici u velikim serijama. Proizvodnja ne zavisi od vremenskih uslova i može se odvijati tokom cele godine.

U niz objekata koji se mogu izraditi prefabrikovanim betonskim elementima spadaju: industrijski objekti, logistički centri, višespratni tržni centri i garaže, hoteli, stambene i upravne zgrade, kao i mnogi drugi.
Martini Gradnja je u mogućnosti da sa svojim stručnim timom, a na osnovu projektnog zadatka, klijentu ponudi svoje tehničko rešenje objekta. Shodno zahtevima investitora, prefabrikovani elementi se mogu prilagoditi već postojećem projektu.

MARTINI
GRADNJA D.O.O.

peikko group

50 years

1965-2015

SISTEMSKA REŠENJA KONSTRUKCIJE

U SVAKOM DETALJU

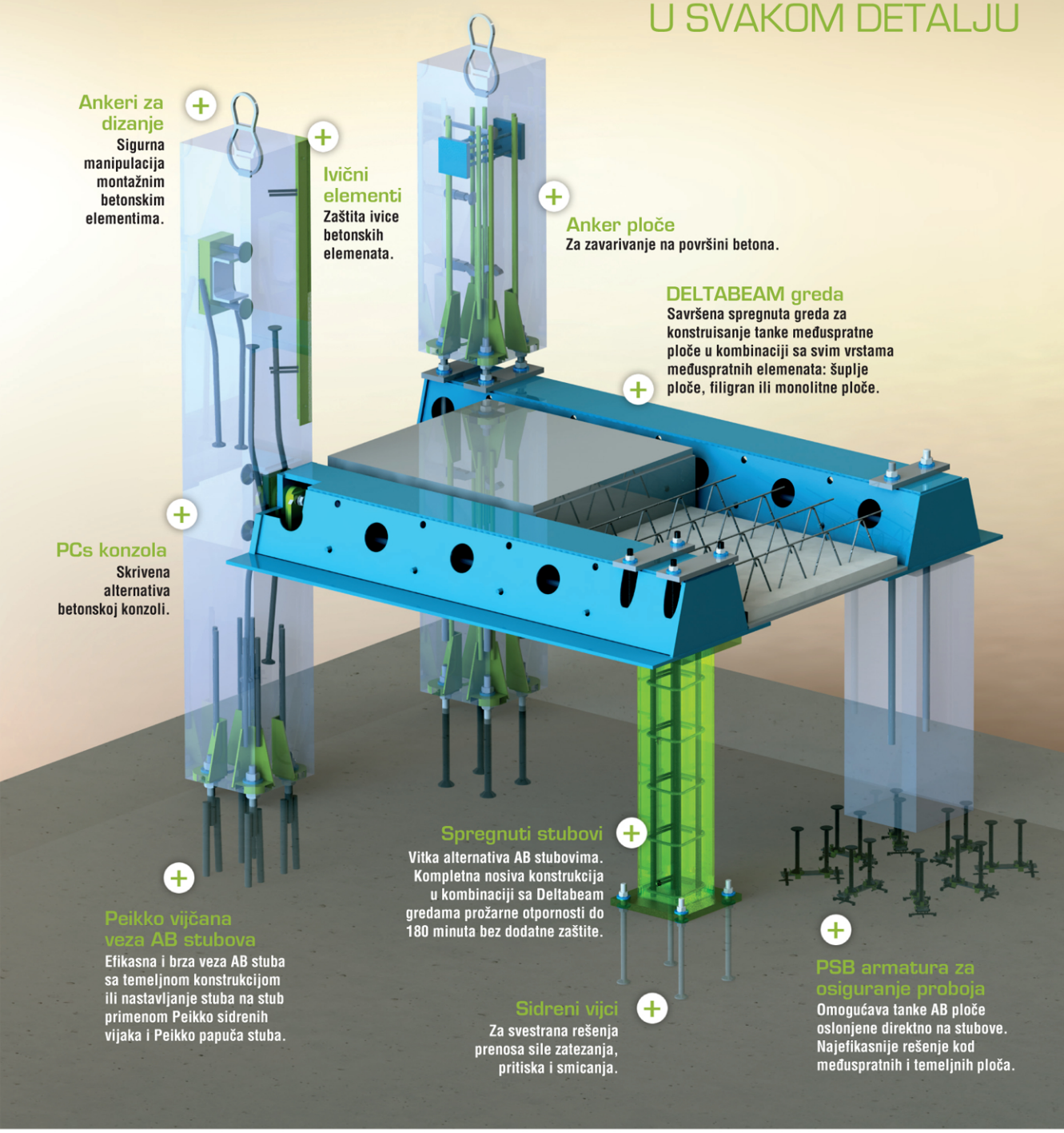

SVE NA JEDNOM MESTU!

Postojanje i neprestano napredovanje kompanije *Put Inženjering* traje duže od dve decenije. Apsolutna posvećenost i predanost fer poslovanju vremenom su rezultirale proširenjem proizvodnog kapaciteta, poslovnim uspehom i ostvarivanjem jakih veza sa saradnicima i klijentima. Prisutni smo na građevinskom tržistu na poljima niskogradnje, visokogradnje i hidrogradnje. Imamo zaokruženu proizvodnju, od kamenoloma, preko fabrike betona do proizvodnje i montaže prefabrikovanih AB konstrukcija.

PROIZVODNJA BETONA:

- Dve stacionarne fabrike betona
- Mobilna baza

Ukupan kapacitet proizvodnje betona je 200 m^3/h

KAMENOLOM:

Proizvodnja kamenog agregata raznih frakcija. Kpacitet postrojenja je 300 t/h.

PROIZVODNJA PREFBRIKATA:

- AB montažne konstrukcije (temelji, čašice, stubovi, krovni nosači)
- Prednapregnute šuplje ploče
- Nosači za mostovske konstrukcije
- *Betonblock* kocke za izradu potpornih i pregradnih zidova
- *New Jersey* zaštitne ograde
- Betonska galanterija

VISOKOGRADNJA

- Proizvodnja i montaža prefabrikovanih betonskih konstrukcija
- Izrada temelja i temeljnih greda
- Obrada armature u sopstvenom armiračkom pogonu
- Izgradnja objekata po sistemu ključ u ruke

NISKOGRADNJA

- Sve vrste iskopa
- Ugradnja ivičnjaka, kanalica, raster ploča, behatona, rigolica
- Asfaltiranje
- Izgradnja mostova i propusta
- Izvođenje kanalizacionih mreža i kolektora
- Pobijanje *Larssen* talpi za obezbeđenje terena

TRANSPORT

- Automikseri za prevoz betona
- Kiperi
- Damperi za teške uslove rada
- Pumpe za beton
- Kamioni, tegljači i specijalne prikolice za transport vangabaritnog tereta težine do 60t
- Autodizalice nosivosti od 35,40 i 70 tona

Put Inženjering je na izgradnji koridora kroz Srbiju učestvovao kao izvođač radova na tunelima Predejane i Manojle, Bancarevo i Progon. Radovi su obuhvatali iskop tunela i ulaznih portala, izvoz materijala i osiguranje puteva *Larssen* talpama. Od maja 2012. god. isporučili smo oko 53000m^3 specijalnih vrsta betona za potrebe izgradnje tunela Bancarevo.

PUT INŽENJERING

Preduzeće za proizvodnju, niskogradnju i transport

Knjaževačka bb, 18000 Niš, Srbija

Tel. 018 215 355, 575 574; fax 018 576 600

www.putinzenjering.com

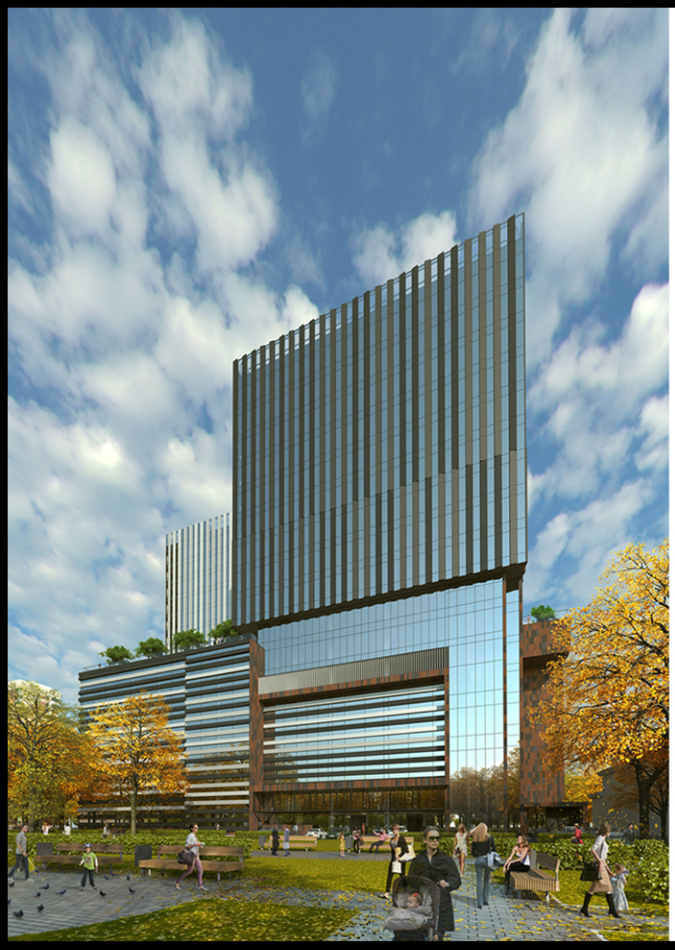

ЦЕНТРОПРОЈЕКТ

Захумска 26 11000 Београд Тел: +381 11 2422 318, Факс: +381 11 2404 645
Макензијева 51, 11000 Београд Тел: +381 11 2684 655, +381 11 2686 856 Факс: +381 11 2684 608
www: centroprojekt-doo.com Email: cp@centroprojekt-doo.com

Firma je izgradila visok renome i ime poznato stručnoj javnosti na izuzetnom kvalitetu svojih konstrukterskih rešenja. Ljudske resurse firme predstavljaju iskusni i mladi inženjeri, timski dobro organizovani i sposobni da odgovore na sve izazove, dajući inspirativna i precizna rešenja koja stvaraju razliku za naše klijente, korisnike i društvo u celini.

Oblasti u kojima se DEL ING naročito ističe su: mostogradnja, zgradarstvo, industrijsko građevinarstvo, upravljanje projektima, konsalting.

Zadovoljstvo naših partnera i klijenata koji nam se stalno vraćaju su naša najbolja preporuka.

DEL ING

Sedište: 11070 Beograd, Ompladinskih brigada 43.
Poslovne prostorije: 11030 Beograd, Jastrebovljeva 25.
Tel/Fax: +381 11 3541573, +381 11 3549289
e-mail: office@deling.rs web: www.deling.rs

ENERGOPROJEKT ENTEL

Privrženost kvalitetu i kodeksima dobre poslovne prakse omogućili su da ENERGOPROJEKT ENTEL već više od šest decenija bude sinonim za pouzdanog i profesionalnog partnera u oblastima:

PROIZVODNJE I PRENOSA ELEKTRIČNE I TOPLOTNE ENERGIJE | OBNOVLJIVIH IZVORA ENERGIJE
PROIZVODNJE I TRANSPORTA PITKE VODE | TRETMANA OTPADNIH VODA
PRERADE I TRANSPORTA NAFTE I GASA
INFORMACIONIH I KOMUNIKACIONIH TEHNOLOGIJA
ZAŠTITE ŽIVOTNE SREDINE

Naše poslovne aktivnosti sprovodimo uvek u skladu sa najvišim standardima savremenog inženjerstva, rukovodeći se korporativnim sloganom
UVEK MEĐU NAJBOLJIMA

MI SMO MAPEI. GRADIMO **BUDUĆNOST** VEĆ **80** GODINA.

Osnovana 1937, kompanija **Mapei** je proslavila važan jubilej prošle godine: **80 godina** profesionalizma i stručnosti u građevinskoj industriji. Od **najsavremenijih arhitektonskih kompleksa** i projekata najveće tehničke složenosti do **velikih javnih radova** i **sportskih objekata**, od najprestižnijih **muzeja** do **graditeljskog nasleđa**, od infrastrukture do domova u kojima živimo, Mapei materijali sreću se na gotovo **svim najvećim i najpoznatijim projektima današnjice.**

www.mapei.rs
MAPEI®

PIRAMIDA

... drvene konstrukcije velikih raspona
t. 022 639 205 f. 022 611 081
e. sm.piramida@neobee.net
web. www.piramidasm.rs

asaibelik D.O.O.

ISOQAR REGISTERED
UKAS MANAGEMENT SYSTEMS
ISO 9001; ISO 14001; OHSAS 18001

ASA IBELIK D.O.O.
Milana Rakića br. 48
11000 Beograd
011/3830-953
011/3830-954
mail: office@asaibelik.rs
PIB: 104842335
MB: 20250151

asmec consultants d.o.o.
CONSULTING ENGINEERS AND PROJECT MANAGERS

Kontakt

Asmec Consultants d.o.o
Višnjićeva 19
11000, Beograd, Srbija
tel: +381-11-3284046
www.asmecbg.com

Kompanija DNEC je osnovana sa ciljem da pruži specijalističke projektantske usluge u oblasti građevinarstva kao i opšte konsultantske usluge.

- Projektovanje konstrukcija u zgradarstvu
- Projektovanje mostova
- Projektovanje konstrukcija u niskogradnji i infrastrukturi
- Konsultantske usluge iz oblasti inžinjeringa
- Tehnička podrška i nadzor tokom izvođenja projekta
- Procena trenutnog stanja i sanacija konstrukcije
- Rehabilitacija i ojačavanje postojećih konstrukcija

exbc
STRUCTURAL STEEL

PROJEKTOVANJE, PROIZVODNJA I MONTAŽA ČELIČNIH KONSTRUKCIJA

Beograd
Jurija Gagarina 32A/III
tel./fax: +381 11 2284 200

Novi Sad
Bulevar Jovana Dučića 33/III
tel./fax: +381 21 6319 780

info@exbc.rs
www.exbc.rs

KOLAREVIĆ

Mi poznajemo tajnu drveta...

www.kolarevic.co.rs

Metal cinkara

TOPLO CINKOVANJE ČELIČNIH KONSTRUKCIJA

"Metal-cinkara" d.o.o.

Vojvode Putnika bb

22320 Inđija, Srbija

Telefon: 022/215 00 60, 063/381910

Mail: prodaja@metalcinkara.co.rs

BUILDING TRUST

STRUČNOST KOJOJ MOŽETE DA VERUJETE

Kompanija Sika nudi stručne savete i podršku klijentima, od koncepta, preko dizajna i detalja, do praktične primene i uspešne instalacije na gradilištu.

Sika vam pruža sveobuhvatna saznanja kroz najsavremeniju tehničku stručnost i globalno praktično iskustvo u primeni gotovih, pripremljenih rešenja za repariranje, poboljšanje i ojačanje postojećih građevinskih konstrukcija.

To podrazumeva potpuno kompatibilne proizvode i integrisane sisteme koji odgovaraju potrebama gotovo svakog projekta, a čiji je kvalitet dokazan na velikim i malim projektima širom sveta u tradiciji dugoj preko 100 godina.

ДГКС
Друштво грађевинских конструктера Србије

ASES
Association of Structural Engineers of Serbia